Volume 3

HANDBOOK OF IMMUNOHISTOCHEMISTRY AND IN SITU HYBRIDIZATION OF HUMAN CARCINOMAS

MOLECULAR GENETICS: LIVER AND PANCREATIC CARCINOMAS

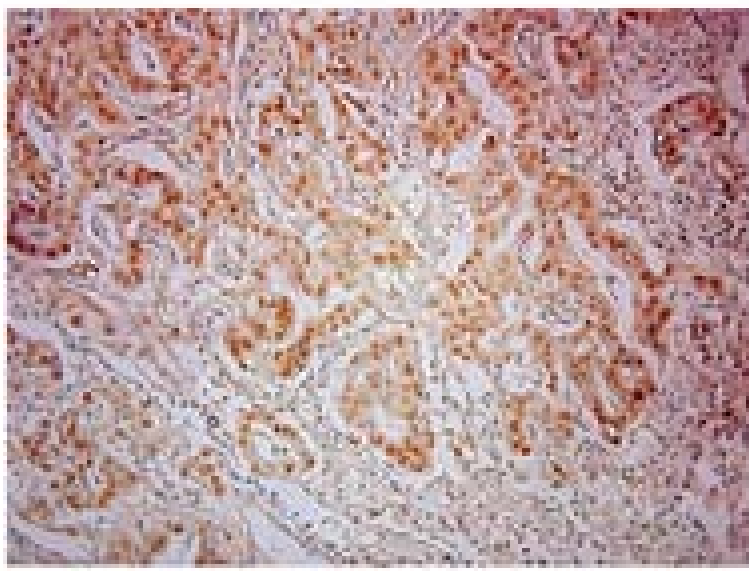

Edited by M.A. HAYAT

Handbook of Immunohistochemistry and *in situ* Hybridization of Human Carcinomas, Volume 3

Handbook of Immunohistochemistry and *in situ* Hybridization of Human Carcinomas

Edited by M.A. Hayat

Volume 1
Molecular Genetics; Lung and Breast Carcinomas

Volume 2
Molecular Pathology, Colorectal Carcinoma, and Prostate Carcinoma

Volume 3
Molecular Genetics, Liver Carcinoma, and Pancreatic Carcinoma

Volume 4
Molecular Genetics, Gastrointestinal Carcinoma, and Ovarian Carcinoma

Handbook of Immunohistochemistry and *in situ* Hybridization of Human Carcinomas, Volume 3

Molecular Genetics, Liver Carcinoma, and Pancreatic Carcinoma

Edited by

M.A. Hayat
Distinguished Professor
Department of Biological Sciences
Kean University
Union, New Jersey

ELSEVIER
ACADEMIC
PRESS

Amsterdam • Boston • Heidelberg • London • New York • Oxford
Paris • San Diego • San Francisco • Singapore • Sydney • Tokyo

Elsevier Academic Press
30 Corporate Drive, Suite 400, Burlington, MA 01803, USA
525 B Street, Suite 1900, San Diego, California 92101-4495, USA
84 Theobald's Road, London WC 1X 8RR, UK

This book is printed on acid-free paper.

Library of Congress Cataloging-in-Publication Data
Application submitted.

British Library Cataloguing in Publication Data
A catalogue record for this book is available from the British Library

ISBN: 0-12-088404-6

For all information on all Elsevier Academic Press publications visit our Web site at www.books.elsevier.com

Printed in China
05 06 07 08 09 10 9 8 7 6 5 4 3 2 1

To

molecular geneticists/clinical pathologists

Contents

Authors and Coauthors of Volume 3

Geunghwan Ahn
Department of Pathology, Samsung Medical Center, Sung Kyun Kwan University, School of Medicine, 50 Ilwon-Dong, Kangmam-ku, Seoul 135-710, Korea

Taku Aoki
Division of Hepato-Biliary-Pancreatic and Transplantation Surgery, Department of Surgery, Graduate School of Medicine, University of Tokyo, Tokyo 113-8655, Japan

Frank Bergmann
Institute of Pathology, University of Heidelberg, Im Neuenheimer Feld 110, 69120, Heidelberg, Germany

Alexander Berndt
HELIOS Clinic Erfurt, Institute of Pathology, Nordhauser Str. 74, D-99089 Erfurt, Germany

Dionissis S. Bonikos
Department of Radiology and Radiotherapy, University of Patras Medical School, Rion, Patras 26500, Greece

Habib Boukerche
Department of Pathology, Columbia University, College of Physicians and Surgeons, 630 West, 168th Street, New York, NY 10032

Markus W. Büchler
Department of General Surgery, University of Heidelberg, Im Neuenheimer Feld 110, 69120 Heidelberg, Germany

George G. Chen
Department of Surgery, Prince of Wales Hospital, The Chinese University of Hong Kong, Shatin, N.T., Hong Kong

Mi Sun Choi
Department of Pathology, Asan Medical Center, University of Ulsan College of Medicine, Seoul, Korea

Marcia M. Clayton
Room 222 Alumni Hall, Department of Pathology and Cell Biology, Thomas Jefferson University, 1020 Locust Street, Philadelphia, PA 19107

Steven W. Cole
School of Dentistry, Division of Oral Biology and Medicine, Dental Research Institute, 10833 Le Conte Avenue, 73-017 CHS, Los Angeles, CA 90095

William B. Coleman
Department of Pathology and Laboratory Medicine, Curriculum in Toxicology, UNC Lineberger Comprehensive Cancer Center, University of North Carolina School of Medicine, Chapel Hill, NC 27599

Regine Dahse
HELIOS Clinic Erfurt, Institute of Pathology, Nordhauser Str. 74, D-99089 Erfurt, Germany

Odile David
Department of Pathology and Laboratory Medicine, Tulane University School of Medicine, SL 79, 1430 Tulane Avenue, New Orleans, LA 70112-2699

Ming Dong
Department of Pancreatico-Biliary Surgery, First Affiliated Hospital, China Medical University, Shenyang, 110001, P.R. China

Hiroshi Egami
Department of Surgery II, Kumamoto University Medical School, Honjo 1-1-1, Kumamoto 8608556, Japan

Hiroshi Egusa
School of Dentistry, Division of Oral Biology and Medicine, Dental Research Institute, 10833 Le Conte Avenue, 73-017 CHS, Los Angeles, CA 90095

Irene Esposito
Institute of Pathology, University of Heidelberg, Im Neuenheimer Feld 110, 69120 Heidelberg, Germany

Manel Esteller
Cancer Epigenetics Laboratory, Molecular Pathology Program, Spanish National Cancer Center (CNIO), Madrid 28220, Spain

Mark A. Feitelson
Room 222 Alumni Hall, Department of Pathology and Cell Biology, Thomas Jefferson University, 1020 Locust Street, Philadelphia, PA 19107

Paul B. Fisher
Department of Pathology, Columbia University, College of Physicians and Surgeons, 630 West, 168th Street, New York, NY 10032

Helmut Friess
Department of General Surgery, University of Heidelberg, Im Neuenheimer Feld 110, 69120 Heidelberg, Germany

Toshio Fukusato
Department of Surgery, Gunma University, Graduate School of Medicine, 3-39-15 Showa-Machi, Maebashi 371-8511, Japan

Toru Furukawa
Department of Molecular Pathology, Tokyo University School of Medicine, 2-1 Seiryo-machi, Aoba-ku, Sendai, 980-8575, Japan

Charalambos Gogos
Department of Internal Medicine, University of Patras Medical School, Rion, Patras 26500, Greece

Weida Gong
Department of G. I. Medical Oncology-426, University of Texas MD Anderson Cancer Center, Houston, TX 77030

Xin-Yuan Guan
Department of Clinical Oncology, The University of Hong Kong, Rm 109, School of Chinese Medicine Bldg., 10 Sassoon Road, Hong Kong

Kejian Guo
Department of Pancreatic-Biliary Surgery, First Affiliated Hospital, China Medical University, Shenyang, 110001, P.R. China

Yoshihiko Hamamoto
Department of Surgery II, Yamaguchi University School of Medicine, 1-1-1 Minami-Kogushi, Ube, Yamaguchi 755-8505, Japan

M.A. Hayat
Department of Biology, Kean University, 1000 Morris Avenue, Union, NJ 07083

George Hemstreet
Department of Pathology and Laboratory Medicine, David Geffen School of Medicine, University of California at Los Angeles, 10833 Le Conte Ave., Los Angeles, CA 90095

Akira Horii
Department of Molecular Pathology, Tokyo University School of Medicine, 2-1 Seiryo-machi, Aoba-ku, Sendai, 980-8575, Japan

Suyun Huang
Department of G. I. Medical Oncology-426, The University of Texas MD Anderson Cancer Center, Houston, TX 77030

Norio Iizuka
Department of Surgery II, Yamaguchi University School of Medicine, 1-1-1 Minami-Kogushi, Ube, Yamaguchi 755-8505, Japan

Hiroshi Imamura
Division of Hepato-Pancreatic-Biliary Surgery, Department of Surgery, Tokyo University Graduate School of Medicine, 7-3-1 Hongo, Bukyo-ku, Tokyo 113-8655, Japan

Satoshi Inoue
Division of Hepato-Biliary-Pancreatic and Transplantation Surgery, Department of Surgery, Graduate School of Medicine, University of Tokyo, Tokyo 113-8655, Japan

Cristine Kalogeropoulou
Department of Radiology and Radiotherapy, University of Patras Medical School, Rion, Patras 26500, Greece

Dong-chul Kang
Department of Pathology, Columbia University, College of Physicians and Surgeons 630 West, 168th Street, New York, NY 10032

Chrisoula Karatza
Department of Internal Medicine, University of Patras Medical School, Rion, Patras 26500, Greece

Dionissios Karavias
Department of Surgery, University of Patras Medical School, Rion, Patras 26500, Greece

Dimitrios Kardamakis
Department of Radiology and Radiotherapy, University of Patras Medical School, Rion, Patras 26500, Greece

Noriko Kimura
Department of Pathology and Laboratory Medicine, Tohoku Rosai Hospital, 21-3-4 Dainohara Aoba-ku Sendai, 981-8563, Japan

Gunter Kloppel
First Department of Pathology, Showa University School of Medicine, 1-5-8 Hatanodai, Shinagawa-ku, Tokyo 142-8555, Japan

Stefanie Knob
Department of Surgery, University-Hospital, Mannheim, University of Heidelberg, 68135 Mannheim, Germany

Paul Komminoth
Department of Pathology, University Hospital of Zürich, Schmelzbergstrasse 12, CH-8091 Zürich, Switzerland

Hartwig Kosmehl
HELIOS Clinic Erfurt, Institute of Pathology, Nordhauser Str. 74, D-99089 Erfurt, Germany

Fumiki Kushihata
First Department of Surgery, Ehinme University, School of Medicine, 5333 SW 75th Street #GG193, Gainesville, FL 32608

Paul B.S. Lai
Department of Surgery, Prince of Wales Hospital, The Chinese University of Hong Kong, Shatin, N.T., Hong Kong

Sze-Hang Lau
Department of Clinical Oncology, The University of Hong Kong, Rm 109, School of Chinese Medicine Bldg., 10 Sassoon Road, Hong Kong

Zhaorui Lian
Department of Pathology and Cell Biology, Room 222 Alumni Hall, Thomas Jefferson University, 1020 Locust Street, Philadelphia, PA 19107

Fan Lin
Department of Laboratory Medicine, MC 01-31, Geisinger Medical Center, 100 N. Academy Avenue, Danville, PA 17822

Wilma L. Lingle
Tumor Biology Program, Mayo Clinic, Rochester, MN 55905

Jie Liu
Department of Pathology and Cell Biology, Room 222 Alumni Hall, Thomas Jefferson University, 1020 Locust Street, Philadelphia, PA 19107

Thomas Makatsoris
Department of Radiology and Radiotherapy, University of Patras Medical School, Rion, Patras 26500, Greece

Masatoshi Makuuchi
Division of Hepato-Biliary-Pancreatic and Transplantation Surgery, Department of Surgery, Graduate School of Medicine, University of Tokyo, Tokyo 113-8655, Japan

Marie-Pierre A. Mathoulin-Portier
Biopathology Department, Institut Paoli-Calmettes, 232 Bd. Sainte Marguerite, 13009 Marseille, France

Juanita L. Merchant
Department of Surgery, Prince of Wales Hospital, The Chinese University of Hong Kong, Shatin, N.T., Hong Kong

Ute M. Moll
Department of Pathology, State University of New York at Stony Brook, Stony Brook, NY 11794

Genevieve M. Monges
Biopathology Department, Institut Paoli-Calmettes, 232 Bd. Sainte Marguerite, 13009 Marseille, France

Toshio Morohoshi
First Department of Pathology, Showa University School of Medicine, 1-5-8 Hatanodai, Shinagawa-ku, Tokyo 142-8555, Japan

Hans Konrad Müller-Hermelink
Institute of Pathology, University of Wurzburg, D-97080 Wurzburg, Germany

Tetsuhiro Nakano
Department of Surgery, Gunma University, Graduate School of Medicine, 3-39-15 Showa–Machi, Maebashi 371-8511, Japan

Marco Niedergethmann
Department of Surgery, University-Hospital, Mannheim, University of Heidelberg, 68135 Mannheim, Germany

Ichiro Nishimura
School of Dentistry, Division of Oral Biology and Medicine, Dental Research Institute, 10833 Le Conte Avenue, 73-017 CHS, Los Angeles, CA 90095

Yilmaz Niyaz
P.A.L.M. Microlaser Technologies AG, Am Neuland 9-12, D-82347 Bernried, Germany

Young Lyun Oh
Department of Pathology, Samsung Medical Center, Sung Kyun Kwan University, School of Medicine, 50 Ilwon-Dong, Kangmam-ku, Seoul 135-710, Korea

Nobuyuki Ohike
First Department of Pathology, Showa University School of Medicine, 1-5-8 Hatanodai, Shinagawa-ku, Tokyo 142-8555, Japan

Susumu Ohwada
Department of Surgery, Gunma University, Graduate School of Medicine, 3-39-15 Showa Machi, Maebashi 371-8511, Japan

Masaaki Oka
Department of Surgery II, Yamaguchi University School of Medicine, 1-1-1 Minami Kogushi, Ube, Yamaguchi 755-8505, Japan

Makoto Osanai
Cancer Research Laboratories, Botterell Hall 3F, Room 357, Queen's University, Kingston Ontario K7L 3N6, Canada

Jingbo Pan
Department of Pathology and Cell Biology, Room 222 Alumni Hall, Thomas Jefferson University, 1020 Locust Street, Philadelphia, PA 19107

Aurel Perren
Department of Pathology, University Hospital of Zürich, Schmelzbergstrasse 12, CH-8091 Zürich, Switzerland

Theodore Petsas
Department of Radiology and Radiotherapy, University of Patras Medical School, Rion, Patras 26500, Greece

Monika Pilichowska
Department of Hematopathology, Brigham and Women's Hospital, Harvard Medical School, Boston, MA, 02115

Stefan Post
Department of Surgery, University-Hospital, Mannheim, University of Heidelberg, 68135 Mannheim, Germany

Jian Yu Rao
Department of Pathology and Laboratory Medicine, David Geffen School of Medicine, University of California at Los Angeles, 10833 Le Conte Ave., Los Angeles, CA 90095

Enrique Rengifo-Calzado
Center of Molecular Immunology, 216th St. and 15th Ave. Atabey, Playa, P.O. Box 16040, Havana, Cuba

Santiago Ropero
Cancer Epigenetics Laboratory, Molecular Pathology Program, Spanish National Cancer Center (CNIO), Madrid 28220, Spain

Thomas Rüdiger
Institute of Pathology, University of Wurzburg, D-97080 Wurzburg, Germany

Mika Sakaki
Department of Pathology, University of Tokushima School of Medicine, 3-18-15 Kuramoto-cho, Tokushima 770-8503, Japan

Jeffrey L. Salisbury
Tumor Biology Program, Mayo Clinic, Rochester, MN 55905

Toshiaki Sano
Department of Pathology, University of Tokushima School of Medicine, 3-18-15 Kuramoto-cho, Tokushima 770-8503, Japan

Norio Sawabu
Department of Internal Medicine and Medical Oncology, Cancer Research Institute, Kanazawa University, 13-1 Takaramachi, Kanazawa 920-8641, Japan

Karin Schütze
P.A.L.M. Microlaser Technologies AG, Am Neuland 9-12, D-82347, Bernried, Germany

David Seligson
Department of Pathology and Laboratory Medicine, David Geffen School of Medicine, University of California at Los Angeles, 10833 Le Conte Ave., Los Angeles, CA 90095

Neda Slade
Department of Pathology, State University of New York at Stony Brook, Stony Brook, NY 11794

Dong Eun Song
Department of Pathology, Asan Medical Center, University of Ulsan College of Medicine, Seoul, Korea

Gregg Staerkel
Department of Pathology, The University of Texas MD Anderson Cancer Center, Houston, TX 77030

Zao-zhong Su
Department of Pathology, Columbia University, College of Physicians and Surgeons, 630 West 168th Street, New York, NY 10032

Ming-Hong Tai
Department of Medical Education and Research, Kaohsiung Veterans General Hospital, 386 TaChung 1st Road, Kaohsiung 813, Taiwan

Xiaodong Tan
Department of Surgery II, Kumamoto University Medical School, Honjo 1-1-1, Kumamoto 860-8556, Japan

Andrea Tannapfel
Institute of Pathology, University of Leipzig, Liebigstraβe 26, 04103 Leipzig, Germany

Takayoshi Toyota
Department of Medicine, Tohoku Rosai Hospital, Japan Labor and Welfare Organization, Sendai, Japan

Henry Tsai
Department of Pathology and Laboratory Medicine, David Geffen School of Medicine, University of California at Los Angeles, 10833 Le Conte Ave., Los Angeles, CA 90095

Athanassios C. Tsamandas
Department of Pathology, University of Patras Medical School, Rion, Patras 26500, Greece

N. Lale Tufan
Department of Pathology and Cell Biology, Room 222 Alumni Hall, Thomas Jefferson University, 1020 Locust Street, Philadelphia, PA 19107

Alicia Viloria-Petit
Samuel Lunenfeld Research Institute, 1070-600 University Avenue, Toronto, ON M5G 1X5, Canada

Yi Wang
Department of Clinical Oncology, The University of Hong Kong, Rm 109, School of Chinese Medicine Bldg., 10 Sassoon Road, Hong Kong

Hiroyuki Watanabe
Department of Internal Medicine and Medical Oncology, Cancer Research Institute, Kanazawa University, 13-1 Takaramachi, Kanazawa 920-8641, Japan

Jota Watanabe
First Department of Surgery, Ehinme University, School of Medicine, 5333 SW 75th Street #GG193, Gainesville, FL 32608

Akira Watanuki
Department of Surgery, Gunma University, Graduate School of Medicine, 3-39-15 Showa-Machi, Maebashi 371-8511, Japan

Aileen Wee
Department of Pathology, National University of Singapore, National University Hospital, 5 Lower Kent Ridge Road, Singapore 119074

David T.W. Wong
School of Dentistry, Division of Oral Biology and Medicine, Dental Research Institute, 10833 Le Conte Avenue, 73-017 CHS, Los Angeles, CA 90095

Keping Xie
Department of G. I. Medical Oncology-426, The University of Texas MD Anderson Cancer Center, Houston, TX 77030

Hisafumi Yamada-Okabe
Department of Surgery II, Yamaguchi University School of Medicine, 1-1-1 Minami-Kogushi, Ube, Yamaguchi 755-8505, Japan

Kazuto Yamazaki
Department of Pathology, Teikyo University, Ichihara Hospital, 3426-3 Anesaki, Ichihara, Chiba, 299-0111, Japan

Yun Yen
City of Hope National Medical Center, 1500 E. Duarte Road, Duarte, CA 91010

Eunsil Yu
Department of Pathology, Asan Medical Center, University of Ulsan College of Medicine, Seoul, Korea

Zuo-Feng Zhang
Department of Pathology and Laboratory Medicine, David Geffen School of Medicine, University of California at Los Angeles, 10833 Le Conte Ave., Los Angeles, CA 90095

Jianming Zhao
Department of Pathology, University Hospital of Zürich, Schmelzbergstrasse 12, CH-8091 Zürich, Switzerland

Xiaofeng Zhou
School of Dentistry, Division of Oral Biology and Medicine, Dental Research Institute, 10833 Le Conte Avenue, 73-017 CHS, Los Angeles, CA 90095

Vassiliki Zolota
Department of Pathology, University of Patras Medical School, Rion, Patras 26500, Greece

Foreword

According to mortality data from the National Center for Health Statistics, approximately 1,334,100 new cases of cancer will have been diagnosed and 556,500 people will have died from cancer in the United States by the end of 2003. Although the number of cancer-related deaths has been on the decline since 1992, the incidence has increased over the same period. This increase is largely the result of the implementation of improved screening techniques that have in turn been made possible by advances in immunochemical diagnostic testing. As immunochemical techniques, such as *in situ* hybridization (ISH) and immunohistochemistry (IHC), continue to be refined, their use in improving patient care through research and improved methods of diagnosis is becoming ever more valuable.

The ISH technique is a well-established approach for identifying the organization and physical position of a specific nucleic acid within the cellular environment, by means of hybridizing a complementary nucleotide probe to the sequence of interest. The use of deoxyribonucleic acid (DNA) and ribonucleic acid (RNA) as probes to assay biological material has been in use for approximately 30 years. However, advances in ISH have led to a replacement of radioactive detection by more adaptable colorimetric and fluorescent fluorescence *in situ* hybridization methods for the interrogation of nuclei; metaphase chromosomes; DNA fibers; patient tissue; and, most recently, deriving information from patient samples using DNA microarrays. Technologic advances, including array comparative genomic hybridization, spectral karyotyping, and multicolor banding, have provided a refinement in the study of genome organization and chromosomal rearrangements. In addition, ISH using RNA has allowed for a determination of the expression pattern and the abundance of specific transcripts on a cell-to-cell basis. Advances in DNA and RNA ISH have migrated from the research setting and are becoming routine tests in the clinical setting, permitting examination of the steps involved in tumorigenesis, which would not have been possible by the use of classical cytogenetic analysis.

Since the introduction of monoclonal antibodies, IHC has developed into a vital tool that is now extensively used in many research laboratories as well as for clinical diagnosis; IHC is a collective term for a variety of methods, which can be used to identify cellular or tissue components by means of antigen–antibody interactions. Immunostaining techniques date back to the pioneering work by Albert Coons in the early 1940s, using fluorescein-labeled antibodies. Since then developments in the techniques have permitted visualization of antigen–antibody interactions by conjugation of the antibody to additional fluorophores, enzymes, or radioactive elements. Because there is wide variation in tissue types, antigen availability, antigen–antibody affinity, antibody types, and detection methods, it is essential to select antibodies almost on a case-to-case basis. The consideration of these factors has led to the identification of several key antibodies that have great utility in the study and diagnosis of tumors.

The scientific advances in the field of IHC have necessitated rapid developments in microscopy, image capture, and analytical software to objectively quantify results. These cutting-edge experimental systems have already produced many significant differences between cancers that might not have been distinguished by conventional means.

The focus of these volumes is the use of ISH and IHC to study the molecular events occurring at the DNA, RNA, and protein levels during development and progression of human carcinomas. Continued investment of time and expertise by researchers worldwide has contributed significantly to a greater understanding of the disease processes. Because the technical requirements for many immunohistochemical techniques are quite demanding and the methodology itself poses many pitfalls, the step-by-step methods provided in these volumes will serve as an excellent guide for both clinical and basic researchers studying human malignancies.

Simon Hughes
Ontario Cancer Institute
Princess Margaret Hospital
Toronto, Canada

Preface to Volume 3

One of the primary objectives of this volume is the same as that of Volumes 1 and 2—that is, discussion of procedures of immunohistochemistry (IHC) and *in situ* hybridization (ISH), including fluorescence *in situ* hybridization (FISH), as they are used in the field of pathology, especially cancer diagnosis. The practical importance of the antigen retrieval protocol in IHC was realized in 1991, and since then it has been used routinely in pathology laboratories. Many chapters in this volume contain the details of this protocol, although not all antigens require antigen retrieval for their detection. In this volume, IHC, ISH, and FISH of two major carcinomas (hepatocellular and pancreatic) are presented. Lung and breast carcinomas were discussed in Volume 1, and colorectal and prostate carcinomas were detailed in Volume 2. Other major cancers will be discussed in Volume 4.

Hepatocellular carcinoma (HCC) is a common cause of worldwide morbidity and mortality, representing the fifth most common cancer worldwide. It shows a marked geographic variation in incidence, being very prevalent in Asia and Africa but less common in the West. In Asia and Africa the incidence of the disease is ~30% per 100,000 individuals per year. In North America and Europe the annual incidence of HCC is less than five cases per 100,000 people. More than 300,000 new cases per year are diagnosed worldwide, and mean 5-year survival is less than 5%. The HCC recurrence rate is ~50% at 1 year after potentially curative resection, and the overall survival rate after resection is only 35–50%. Identification of highly sensitive tumor markers will improve the early detection of HCC. A large number of such markers are discussed in this volume.

Pancreatic cancer is a devastating disease with a very poor prognosis, and it continues to have one of the highest mortality rates of any malignancy. Each year, as an average, 28,000 patients are diagnosed with pancreatic cancer, and nearly all of them will die of the disease. The 5-year survival rate of patients with ductal adenocarcinomas of the pancreas is 4%, which is one of the lowest of any neoplasm. This disease is devastating because the vast majority of patients are diagnosed at an advanced stage of disease that is incurable with existing therapy. Currently no tumor markers are known that provide reliable screening for pancreatic cancer at an earlier, potentially curable stage, although some markers are being clinically tested. A large number of markers for pancreatic cancer are discussed in this volume.

Another objective of this volume is the discussion of the role of molecular genetics (molecular pathology, molecular medicine, and molecular morphology) to understand and achieve correct diagnosis and therapy in neoplastic diseases. Cancer is ultimately a genetic disease, and as such, the focus of much cancer research has been directed toward understanding which and how many oncogenes are activated and which tumor-suppressor genes become dysfunctional in human malignancies.

The elucidation of the genetic events underlying the initiation and progression of malignancy has been hampered by limitations inherent in both *in vitro* and *in vivo* methods of study. The limitation of an *in vitro*–based system is that genetic information obtained from cell lines may not accurately represent the molecular events occurring in the actual tissue milieu from which they were derived. However, *in vivo* genetic analysis is limited because of the inability to procure pure populations of cells from complex, heterogeneous tumor tissue. The development and use of molecular-based therapy for human malignancies will require a detailed molecular genetic analysis of patient tissue, including resolving the two previously mentioned limitations.

Molecular genetics/pathology has the advantage of assessing genes directly. Knowledge of the genetic basis of disease will, in turn, allow more specific targeting of the cause, rather than only the symptoms of the disease. The time is overdue to apply our knowledge of molecular genetics, in conjunction with IHC, FISH, and histology, to diagnostic, therapeutic, and prognostic decisions.

Genetic information will improve the prognosis used to monitor both the efficacy of treatment and

disease recurrence. Molecular markers, largely from tumors but also from the germline, have great potential for diagnosis, for directing treatment, and as indicators of the outcome. The role of mutations in cancer is emphasized because the characteristics of the tumor depend on the mutations that lead to their emergence. Widespread molecular testing is the future for clinical practice. Indeed, methods of molecular testing of tumors are well established and are discussed in this and other volumes of this series of handbooks.

Unfortunately, clinical practice has lagged behind the current knowledge of research in molecular genetics. Both technicians and pathologists need to be aware of the importance of molecular pathology testing. Somatic mutations are rarely performed, although some histopathology and cytogenetics laboratories have done limited testing, such as chromosomal rearrangements in lymphoma. Molecular testing should be regarded as a means of complementing, rather than replacing, established methods such as IHC and FISH.

It was challenging to bring some semblance of order to the vast body of information in the field of molecular genetics (molecular pathology), which has become available primarily in scientific journals during the past decade. The contributions by expert molecular geneticists and clinical pathologists in each of their disciplines to this volume have made it possible to accept this challenge.

The range of methods to examine genetic abnormalities has widened enormously, and many new and powerful molecular, immunohistochemical, and ISH techniques have become available. These include the detection of mutations using the polymerase chain reaction (PCR), reverse transcription-PCR, differential display of gene expression, deoxyribonucleic acid (DNA) sequencing, and comparative genomic hybridization on genomic microarrays to detect gene amplifications and detentions on a genomewide basis. Other relevant techniques include serial analysis of gene expression, suppression substractive hybridization, rolling circle amplification, Southern Blot hybridization, specific cloned probes, and flow cytometry.

Various signal amplification approaches have also been introduced to increase the sensitivity, accompanied by reduced nonspecific background staining, of IHC. Similarly, the conventional PCR method has been improved through quantitative real-time PCR. Standard ISH has been improved by its modifications such as FISH and chromogenic ISH. Most of the aforementioned methods are discussed in Volumes 1–3, and the remaining will be presented in Volumes 4–6.

Pathologists are well advised to adapt to modern therapeutic shifts (i.e., morphologic interpretation needs to be combined with molecular diagnostic modalities). The latter protocols can provide a second level of testing that is particularly useful for the analysis of neoplasms for which histologic and immunophenotypic data are inconclusive. We already are down a path that has the potential to alter oncology clinical practice. Therapies are beginning to move toward specific molecular targets. My hope, through these volumes, is to expedite the translation of molecular genetics into clinical practice.

Each chapter is comprehensive and stands alone in terms of determination of cancer diagnosis, so the reader does not have to scour multiple places in the book or outside sources. A literature review of the subject matter from the early 1990s to the present is also included in most chapters. The results of most methods are shown by including a color photomicrograph that contains useful immunohistochemical and/or FISH diagnostic information; these illustrations facilitate the interpretation of the results obtained. Each chapter is organized logically, providing an introduction, materials required (including reagents, antibodies, apparatuses, and commercial sources), results, and discussion. The procedures are explained in a detailed step-by-step fashion so that the reader can use them without additional references. Advantages and limitations of the methods used for cancer diagnosis are also presented.

There are several reasons for the limited use of molecular genetics in clinical practice. One reason is the high cost of establishing facilities for molecular techniques; another is our comparatively meager understanding of the nature of many diseases, including cancer. Although equipment for molecular testing is available, some investment is needed. Another reason is the dearth of clinician–scientist training programs, resulting in limited clinician–scientists. Also, an inequity in pay exists between those working in clinical practice and research faculty. Accordingly, the difference in pay may be a disincentive for choosing a full-time career in medical research. The length of time (8 years as an average) to receive the MD/PhD is probably also a barrier in the development of new clinician–scientists. Also, many clinician–scientist trainees are married or in stable relationships, and personal time for family life and children is increasingly important to them. Narrowing the gap in income between clinical practitioners and full-time medical researchers would provide a positive incentive for this profession.

I am indebted to the authors of the chapters for their promptness and appreciate their dedication and hard work in sharing their expertise with the readers. In most cases the protocols presented were either introduced or refined by the authors and are routinely used in their clinical pathology laboratories. The methods presented offer much more detailed information than is available in scientific journals. Because of its relatively

recent emergence from the research laboratory, many molecular pathology protocols are still found in scientific journals and have not appeared in a book. Each chapter provides unique individual practical knowledge based on the expertise of the author. As with all clinical laboratory testing, the results obtained should be interpreted in conjunction with other established and proven laboratory data and clinical findings.

This volume has been developed through the efforts of 112 authors and coauthours representing 12 countries. The high quality of each manuscript made my work as the editor an easy one. The authors were gracious and prompt. This volume is intended for use in research and clinical laboratories by medical technicians and pathologists, especially in the field of oncology. This volume and other volumes of the series will also be of interest and help to teachers and medical students.

I am thankful to the Board of Trustees of Kean University and Dr. Dawood Farahi for recognizing the importance of completing this project. I appreciate the cooperation extended to me by Dr. Jasna Markovac, and I am grateful to Elizabeth McGovern for her expert help in preparing this volume.

M.A. Hayat
October 2004

Prologue

We possess scientific and industrial knowledge in new biotechniques, including human genetic technologies. However, ethical and social implications of these advances must be addressed. Such concerns are especially relevant in some of the applications of genetic engineering, such as pharmacogenetics; gene therapy; predictive diagnostics, including prenatal genetic diagnosis, therapeutic cloning, and cloning of humans and other animals; human tissue banking and transplanting; and patenting of inventions that involve elements of human origin including stem cells. Bioethics should be a legitimate part of governmental control or supervision of these technologies. Scientific and industrial progress in this field is contingent on the extent to which it is acceptable to the cultural values of the public. In addition, in medical research on human subjects, considerations related to the well being of the human subject should take precedence over the interests of science and industry. Any form of discrimination against a person based on genetic heritage is prohibited.

M.A. Hayat

Selected Definitions

Ablation: Ablation consists of the removal of a body part or the destruction of its function.

Adenocarcinoma: Adenocarcinoma is a malignant neoplasm of epithelial cells in a glandular or glandlike pattern.

Adenoma: Adenoma is a benign epithelial neoplasm in which the tumor cells form glands or glandlike structures. It does not infiltrate or invade adjacent tissues.

Adjuvent: Adjuvent is a substance that nonspecifically enhances or potentiates an immune response to an antigen; something that enhances the effectiveness of a medical treatment.

Affinity: Affinity is a measure of the bonding strength (association constant) between a receptor (one binding site on an antibody) and a ligand (antigenic determinant).

Allele: Allele is one of two or more alternative forms of a single gene locus. Different alleles of a gene have unique nucleotide sequences, and their activities are all concerned with the same biochemical and developmental process, although their individual phenotypes may differ. An allele is one of several alternative forms of a gene at a single locus that controls a particular characteristic.

Alternative Splicing: Genes with new functions often evolve by gene duplication. Alternative splicing is another means of evolutionary innovation in eukaryotes, which allows a single gene to encode functionally diverse proteins (Kondrashov and Koonin, 2001). In other words, the alternative splicing refers to splicing the same pre-messenger ribonucleic acid (pre-mRNA) in two or more ways to yield two or more different protein products. Alternative splicing can produce variant proteins and expression patterns as different as the products of different genes. Alternative splicing either substitutes one protein sequence segment for another (substitution alternative splicing) or involves insertion or deletion of a part of the protein sequence (length difference alternative splicing). Thus, alternative splicing is a major source of functional diversity in animal proteins. Many types and large numbers of proteins are required to perform immensely diverse functions in a eukaryote.

Lack of correlation between the complexity of an organism and the number of genes can be partially explained if a gene often codes for more than one protein. Individual genes with mutually alternative exons are capable of producing many more protein isoforms than there are genes in the entire genome. A substantial amount of exon duplication events lead to alternative splicing, which is a common phenomenon. Indeed, alternative splicing is widespread in multicellular eukaryotes, with as many as one (or more) in every three human genes producing multiple isoforms (Mironov *et al.,* 1999). Alternative splicing is a ubiquitous mechanism for the generation of multiple protein isoforms from single genes, resulting in the increased diversity in the proteomic world.

Amplification: Amplification refers to the production of additional copies of a chromosomal sequence, found as intrachromosomal or extrachromosomal DNA. Amplification is selective replication of a gene to produce more than the normal single copy in a haploid genome.

Anaplasia: Anaplasia results in the regression of cells and tissues to an undifferentiated state (dedifferentiation) in most malignant neoplasms.

Aneuploidy: Aneuploidy is the abnormal condition in which one or more whole chromosomes of a normal set of chromosomes either are missing or are present in more than the usual number of copies. Aneuploidy refers to not having the normal diploid number of chromosomes.

Annealing of DNA: Annealing of DNA is the process of bringing back together two separate strands of denatured DNA to re-form a double helix.

Antibody: Antibody (immunoglobulin) is a protein produced by B lymphocytes that recognizes a particular foreign antigenic determinant and facilitates clearance of that antigen; antigens can also be carbohydrates and even DNA.

Antigen: An antigen is a foreign substance that binds specifically to antibody or T-cell receptors and elicits an immune response.

Antigenic Determinant: Antigenic determinant is the site on an antigenic molecule that is recognized and bound by antibody.

Apoptosis: Apoptosis is the capacity of a cell to undergo programmed cell death. In response to a stimulus, a pathway is triggered that leads to destruction of the cell by a characteristic set of reactions. Failure to apoptose allows tumorigenic cells to survive and thus contributes to cancer.

Avidity: Avidity is referred to as the functional binding strength between two molecules such as an antibody and an antigen. Avidity differs from affinity because it reflects the valency of the antigen–antibody interaction.

Carcinoma: Carcinoma is one of various types of malignant neoplasm arising from epithelial cells, mainly glandular (adenocarcinoma) or squamous cells. Carcinoma is the most common cancer and displays uncontrolled cellular proliferation, anaplasia, and invasion of other tissues, spreading to distant sites by metastasis. The origin of carcinoma in both sexes is skin; in men it originates in the prostate, and in women it originates in the breast. The most frequent carcinoma in both sexes is bronchogenic carcinoma.

cDNA (Complementary Deoxyribonucleic Acid): mRNA molecules are isolated from cells, and DNA copies of these RNAs are made and inserted into a cloning vector. The analysis of that cloned cDNA molecule can then provide information about the gene that encoded the mRNA. The end result is a cDNA library.

Chromosomal Aberration: Chromosomal aberration is a change in the structure or number of chromosomes. The variation from the wild-type condition is either chromosome number or chromosome structure. Four major types of aberrations are deletions, duplications, inversions, and translocations. Variations in the chromosome number of a cell give rise to aneuploidy, monoploidy, or polyploidy.

Chromosomal Instability: Chromosomal instability is defined as an increased rate of chromosome aberrations, in contrast to microstallite instability, which induces alterations of DNA repeat sequences but no changes in chromosome number or structure. Chromosomal instability is associated with aggressive tumor behavior and poor prognosis.

Clinical Guidelines: Clinical guidelines are statements aimed to assist clinicians in making decisions regarding treatment for specific conditions. They are systematically developed, evidence-based, and clinically workable statements that aim to provide consistent and high-quality care for patients. From the perspective of litigation, the key question has been whether guidelines can be admitted as evidence of the standard of expected practice or whether this would be regarded as hearsay. Guidelines may be admissible as evidence in the United States if qualified as authoritative material or a learned treatise, although judges may objectively scrutinize the motivation and rationale behind guidelines before accepting their evidential value (Samanta *et al.,* 2003). The reason for this scrutiny is the inability of guidelines to address all the uncertainties inherent in clinical practice. However, clinical guidelines should form a vital part of clinical governance.

Clones: A clone is a group of cells that are genetically identical to the original individual cell.

Codon: A codon is a three-base sequence in mRNA that causes the insertion of a specific amino acid into polypeptide or causes termination of translation.

Concatemers: Concatemers are DNAs of multiple genome length.

Constitutive Gene: A constitutive gene is a gene whose products are essential to normal cell functioning, no matter what the life-supporting environmental conditions are. These genes are always active in growing cells.

Constitutive Mutation: Constitutive$^-$ mutation is a mutation that causes a gene to be expressed at all times, regardless of normal controls.

Cytokines: Cytokines are a group of secreted low molecular weight proteins that regulate the intensity and duration of an immune response by stimulating or inhibiting the proliferation of various immune cells or their secretion of antibodies or other cytokines.

Deletion: Deletion is a mutation involving a loss of one or more base pairs; a chromosomal segment or gene is missing.

Dendritic Cell: A dendritic cell is a type of antigen-presenting cell that has long membrane processes (resembling dendrites of nerve cells) and is found in the lymph nodes, spleen, thymus, skin, and other tissues.

Determinant: The determinant is the portion of an antigen molecule that is recognized by a complementary section of an antibody or T-cell receptor.

Diagnosis: Diagnosis means the differentiation of malignant from benign disease or of a particular malignant disease from others. A tumor marker that helps in diagnosis may be helpful in identifying the most effective treatment plan.

DNA Methylation: Genetic mutations or deletions often inactivate tumor-suppressor genes. Another mechanism for silencing genes involves DNA methylation. In other words, in addition to genetic alterations, epigenetics controls gene expression, which does not involve changes of genomic sequences. DNA methylation is an enzymatic reaction that brings a methyl

group to the 5th carbon position of cystine located 5′ to guanosine in a CpG dinucleotide within the gene promoter region. This results in the prevention of transcription. Usually multiple genes are silenced by DNA methylation in a tumor. DNA methylation of genes, however, is not common in normal tissues. Gene methylation profiles, almost unique for each tumor type, can be detected in cytologic specimens by methylation-specific polymerase chain reaction (Pu and Clark, 2003).

In the human genome, ~80% of CpG dinucleotides are heavily methylated, but some areas remain unmethylated in GC-rich CpG island (Bird, 2002). In cancer cells, aberrant DNA methylation is frequently observed in normally unmethylated CpG islands, resulting in the silencing of the function of normally expressed genes. If the silencing occurs in genes critical to growth inhibition, the epigenetic alteration could promote tumor progression resulting from uncontrolled cell growth. However, pharmacologic demethylation can restore gene function and promote death of tumor cells (Shi *et al.,* 2003).

ELISA: An Enzyme-linked immunosorbent assay in which antibody or antigen can be quantitated by using an enzyme-linked antibody and a colored substance to measure the activity of the bound enzyme.

Encode: Encode refers to containing the information for making an RNA or polypeptide; a gene can encode an RNA or a polypeptide.

Epigenetics: Epigenetics can be defined as the study of mitotically and/or meiotically heritable changes in gene function that cannot be explained by changes in DNA sequence. Epigenetic change means an alteration in the expression of a gene but not in the structure of the gene itself. Processes less irrevocable than mutation fall under the umbrella term "epigenetic." Known molecular mechanisms involved in epigenetic phenomenon include DNA methylation, chromatin remodeling, histone modification, and RNA interference. Patterns of gene expression regulated by chromatin factors can be inherited through the germ line (Cavalli and Paro, 1999). The evidence that heritable epigenetic variation is common raises questions about the contribution of epigenetic variation to quantitative traits in general (Rutherford and Henikoff, 2003).

Epitope: An epitope is the antigenic determinant or antigen site that interacts with an antibody or T-cell receptor.

Exon–Intron: An exon is the region of a gene that is ultimately represented in the gene's mature transcript, in both the DNA and its RNA product. Eukaryotic genes contain noncoding sequences (introns) embedded into coding sequences (exons). The introns are removed (splicing) following transcription of DNA into RNA.

Familial Trait: A familial trait is a trait shared by members of a family.

FISH: Fluorescent *in situ* hybridization is a technique of hybridizing a fluorescence probe to whole chromosome to determine the location of a gene or other DNA sequence within a chromosome.

Gastritis: Gastritis refers to the inflammation, especially mucosal, of the stomach.

Gene: A gene is the basic unit of heredity and contains the information for making one RNA and, in most cases, one polypeptide.

Gene Cloning: Gene cloning means generating many copies of a gene by inserting it into an organism (e.g., bacterium) where it can replicate along with the host.

Gene Expression: Gene expression is the process by which gene products are made.

Gene Family: A gene family consists of a set of genes whose exons are related; the members were derived by duplication and variation from some ancestral genes.

Gene Mutation: A gene mutation is a heritable alteration of the genetic material, usually from one allele form to another. A gene mutation is confined to a single gene.

Gene Therapy: Gene therapy is defined as a therapy in which a gene(s) or gene-transducer cells are introduced to the patient's body for a therapeutic or gene-marking purpose. Gene therapy by definition is not necessarily a molecular targeting therapy, but the reason for the high expectations is that new mechanisms of cancer cell targeting can be integrated into the therapy.

Genetic Code: Genetic code is the set of 64 codons and the amino acids (or terminations) they stand for. Genetic code is the correspondence between triplets in DNA (or RNA) and amino acids in protein.

Genetic Mapping: Genetic mapping determines the linear order of genes and the distances between them.

Genome: The genome is the total amount of genetic material in a cell. In eukaryotes it is the haploid set of chromosomes of an organism.

Genomic Instability: It takes many years to get a cancer. Approximately 20 years may elapse from the time of exposure to a carcinogen to the development of a clinically detectable tumor. During this time, tumors are characterized by genomic instability, resulting in the progressive accumulation of mutations and phenotypic changes. Some of the mutations bypass the host regulatory processes that control cell location, division, expression, adaptation, and death. Genetic instability is manifested by extensive heterogeneity of cancer cells within each tumor.

Destabilized DNA repair mechanisms can play an important role in genomic instability. Human cells may use at least seven different repair mechanisms to deal with DNA lesions that represent clear danger to survival and genomic stability. For example, homologous recombination repair, nonhomologous end-joining, and mismatch repair mechanisms normally act to maintain genetic stability, but, if they are deregulated, genomic instability and malignant transformation might occur (Pierce *et al.,* 2001). Also, because the human genome contains ~500,000 members of the *Alu* family, increased levels of homologous/homologous recombination events between such repeats might lead to increased genomic instability and contribute to malignant progression (Rinehart *et al.,* 1981).

In addition, BCR/ABL oncogenic tyrosine kinase allows cells to proliferate in the absence of growth factors, protects them from apoptosis in the absence of growth factors, or external survival factors, and promotes invasion and metastasis. The unrepaired and/or aberrantly repaired DNA lesions resulting from spontaneous and/or drug-induced damage can accumulate in BCR/ABL-transformed cells, which may lead to genomic instability and malignant progression of the disease (Skorski, 2002).

Genomic Library: The genomic library is a set of clones containing DNA fragments derived directly from a genome, rather than from RNA. It is the collection of molecular clones that contain at least one copy of every DNA sequence in the genome.

Genotype: The genotype is the combined genetic material inherited from both parents; also the alleles present at one or more specific loci. In other words, the genotype is the allelic constitution of a given individual.

Germline: The germline is the unmodified genetic material that is transmitted from one generation to the next through the gametes.

Germline Mutations: Mutations in the germline of sexually reproducing organisms may be transmitted by the gametes to the next generation, giving rise to an individual with the mutant state in both its somatic and germline cells.

G1 Phase: G1 phase is the period of the eukaryotic cell cycle between the last mitosis and start of DNA replication.

G2 Phase: G2 phase is the period of the eukaryotic cell cycle between the end of DNA replication and the start of the next mitosis.

Haploinsufficiency: Although classically tumor-suppressor genes are thought to require mutation or loss of both alleles to facilitate tumor progression, for some genes, haploinsufficiency, which is loss of only one allele, may contribute to carcinogenesis.

Hepatitis: Hepatitis consists of inflammation of the liver caused by viral infection or toxic agents.

Heterozygous: Heterozygous refers to a diploid organism having different alleles of one or more genes. As a result, the organism produces gametes of different genotypes.

Humoral Immunity: Humoral immunity is the immunity that can be transferred by antibodies present in the plasma, lymph, and tissue fluids.

Hybridization: Hybridization is the pairing of complementary RNA and DNA strands to give an RNA–DNA hybrid. In other words, pairing of two complementary single stranded nucleotides according to the base pairing rules: cytosine with quinine and adenine with thymine.

Immunotherapy: Immunotherapy involves delivering therapeutic agents conjugated to monoclonal antibodies that bind to the antigens at the surface of cancer cells. Ideal antigens for immunotherapy should be strongly and uniformly expressed on the external surface of the plasma membrane of all cancer cells. Many solid neoplasms often demonstrate regional variations in the phenotypic expression of antigens. These regional differences in the immunophenotypic profile within the same tumor are referred to as intratumoral heterogeneity. Therapeutic agents that have been used include radioisotopes, toxins, cytokines, chemotherapeutic agents, and immunologic cells.

Kaposi's Sarcoma: Kaposi's sarcoma is a multifocal malignant neoplasm that occurs in the skin and lymph nodes. It consists of cutaneous lesions reddish to dark blue in color, found commonly in men older than 60 years of age or in patients with AIDS.

Laser-Capture Microdissection: Tissue heterogeneity and the consequent need for precision before specimen analysis present a major problem in the study of disease. Even a tissue biopsy consists of a heterogenous population of cells and extracellular material, and analysis of such material may yield misleading or confusing results. Cell cultures can be homogenous but not necessarily reflect the *in vivo* condition. Therefore, a strategy is required to facilitate selective purification of relevant homogenous cell types.

The technology of laser-capture microdissection allows extraction of single cells or defined groups of cells from a tissue section. This technique is important for characterizing molecular profiles of cell populations within a heterogeneous tissue. In combination with various downstream applications, this method provides the possibility of cell-type or even cell-specific investigation of DNA, RNA, and proteins (Mikulowska-Mennis *et al.,* 2002).

Library: A library is a set of cloned fragments together representing the entire genome.

Ligand: A ligand is a molecule recognized by a receptor structure.

Loss of Heterozygosity: Loss of one copy of a chromosomal region is termed loss of heterozygosity (LOH). In the majority of cases in which the gene mutation is recessive, tumor cells often retain only the mutated allele and lose the wild-type one. This loss is known as LOH.

Lymph: Lymph is the intercellular tissue fluid that circulates through the lymphatic vessels.

Lymphadenopathy: Lymphadenopathy is the enlargement of the lymph nodes.

Lymph Nodes: Lymph nodes are small secondary lymphoid organs containing populations of lymphocytes, macrophages, and dendric cells, which serve as sites of filtration of foreign antigens and activation of lymphocytes.

Lymphokines: Lymphokines is a generic term for cytokines produced by activated lymphocytes, especially T cells, that act as intercellular mediators of the immune response.

Lymphoma: Lymphoma is a cancer of lymphoid cells that tends to proliferate as solid tumors.

Malignant: Malignant tumors have the capacity to invade and alter normal tissue.

Marker (Biomarker): A marker is a mutated gene or its product that serves as a signpost at a known location in the genome.

Metastasis: Initially tumor growth is confined to the original tissue of origin, but eventually the mass grows sufficiently large to push through the basement membrane and invade other tissues. When some cells lose adhesiveness, they are free to be picked up by lymph and carried to lymph nodes and/or may invade capillaries and enter blood circulation. If the migrant cells can escape host defenses and continue to grow in the new location, a metastasis is established. More than half of cancers have metastasized by the time of diagnosis. Usually it is the metastasis that kills the person rather than the primary (original) tumor.

Metastasis itself is a multistep process. The cancer must break through any surrounding covering (capsule) and invade the neighboring (surrounding) tissue. Cancer cells must separate from the main mass and must be picked up by the lymphatic or vascular circulation. The circulating cancer cells must lodge in another tissue. Cancer cells traveling through the lymphatic system must lodge in a lymph node. Cancer cells in vascular circulation must adhere to the endothelial cells and pass through the blood vessel wall into the tissue. For cancer cells to grow, they must establish a blood supply to bring oxygen and nutrients; this usually involves angiogenesis factors. All of these events must occur before host defenses can kill the migrating cancer cells.

If host defenses are to be able to attack and kill malignant cells, they must be able to distinguish between cancer cells and normal cells. In other words, there must be immunogens on cancer cells not found on normal cells. In the case of virally induced cancer circulating cells, viral antigens are often expressed, and such cancer cells can be killed by mechanisms similar to those for virally infected tissues. Some cancers do express antigens specific for those cancers (tumor-specific antigens), and such antigens are not expressed by normal cells.

As already stated, metastasis is the principal cause of death in individuals with cancer, yet its molecular basis is poorly understood. To explore the molecular difference between human primary tumors and metastases, Ramaswamy and Golub (2002) compared the gene-expression profiles of adenocarcinoma metastases of multiple tumor types to unmatched primary adenocarcinomas. They found a gene-expression signature that distinguished primary from metastatic adenocarcinomas. More importantly, they found that a subset of primary tumors resembled metastatic tumors with respect to this gene-expression signature. The results of this study differ from those of most earlier studies in that the metastatic potential of human tumors is encoded in the bulk of a primary tumor. In contrast, some earlier studies suggest that most primary tumor cells have low metastatic potential, and cells within large primary tumors rarely acquire metastatic capacity through somatic mutation (Poste and Fidler, 1980). The emerging notion is that the clinical outcome of individuals with cancer can be predicted using the gene profiles of primary tumors at diagnosis.

Methylation: DNA methylation (an epigenetic change) in mammals occurs at the cytosine residues of cytosine guanine (CpG) dinucleotides by an enzymatic reaction that produces 5-methylcytosine (5-mc). In other words, methylation of normal unmethylated CpG islands in gene promoter regions is an important method for silencing tumor-suppressor genes. Methylation results in transcriptional inactivation of several tumor-suppressor genes in human cancer and serves as an alternative for the genetic loss of gene function by deletion or mutation.

One of the first alterations of DNA methylation to be recognized in neoplastic cells was a decrease in overall 5-mc content, referred to as genomewide or global DNA hypomethylation. Despite the frequently observed cancer-associated increases of regional hypermethylation, the prevalence of global DNA hypomethylation in many types of human cancers suggests that such hypomethylation plays a significant and fundamental role in tumorgenesis.

Microsatellite: A microsatellite is a short DNA sequence (usually 2–4 bp) repeated many times in tandem.

A given microsatellite is found in varying lengths, scattered around a eukaryotic genome.

Mitogen: Mitogen is a substance (e.g., a hormone or growth factor) that stimulates cell division.

Molecular Genetics: Molecular genetics is a subdivision of the science of genetics, involving how genetic information is encoded within the DNA and how the cell's biochemical processes translate the genetic information into the phenotype.

Monitoring: Monitoring means repeated assessment if there is an early relapse or other signs of disease activity or progression. If early relapse of the disease is identified, a change in patient management will be considered, which may lead to a favorable outcome for the patient.

Monoclonal Antibody: Monoclonal antibodies are homogeneous antibodies produced by a clone of hybridoma cells.

mRNA Splicing: mRNA splicing is a process whereby an intervening sequence between two coding sequences in an RNA molecule is excised and the coding sequences are ligated (spliced) together.

Multifactorial Trait: A multifactorial trait is a trait influenced by multiple genes and environmental factors. When multiple genes and environmental factors influence a trait, it is difficult to find a simple relationship between genotype and phenotype that exists in discontinuous traits.

Mutagens: A mutagen is any physical or chemical agent that significantly increases the frequency of mutational events above the rate of spontaneous mutation.

Mutant: A mutant is an organism (or genetic system) that has suffered at least one mutation.

Mutation: Mutation is the original source of genetic variation caused, for example, by a change in a DNA base or a chromosome. Mutation is a permanent change in the sequence of DNA.

Neoplasia: Neoplasia refers to the pathologic process that causes the formation and growth of an abnormal tissue.

Neoplasm: A neoplasm is an abnormal tissue that grows by cellular proliferation faster than normal and continues to grow.

Oligonucleotide: An olignucleotide is a short piece of RNA or DNA.

Oncogene: An oncogene is a gene that transforms a normal cell to a tumorous (cancerous) state. Products of oncogenes are capable of causing cellular transformations. Oncogenes derived from viruses are denoted v-onc, whereas their cellular counterparts, or proto-oncogenes, are denoted c-onc.

Pancreatitis: Pancreatitis refers to the inflammation of the pancreas. It can be caused by alcoholism, endocrine diseases, pregnancy, drug effects, or abdominal injury; it can be hereditary, viral, parasitic, allergic, or immunologic.

PCNA: PCNA is a proliferating cell nuclear antigen.

Penetrance: Penetrance is the frequency (expressed as a percentage) of individuals who are phenotypically affected among persons of an appropriate genotype. A trait may show incomplete penetrance or complete (full) penetrance.

Phenotype: A phenotype is the observed biochemical, physical, or morphologic characteristics of an individual. The phenotype is the physical manifestation of a genetic trait, resulting from a specific genotype and its interaction with the environment. Genes give only the potential for the development of a particular phenotypic characteristic; the extent to which that potential is realized depends not only on interactions with the other genes and their products but also on environmental influences.

Polymerase Chain Reaction: The polymerase chain reaction (PCR) method is used to selectively and repeatedly replicate defined DNA sequences from a DNA mixture. The starting point for PCR is the DNA mixture containing the DNA sequence to be amplified and a pair of oligonucleotide primers that flank that DNA sequence.

Polymorphism: Polymorphism refers to the simultaneous occurrence in the population of genomes showing allelic variations, which are seen either in alleles producing different phenotypes or, for example, in changes in DNA affecting the restriction pattern. A polymorphic locus is any locus that has more than one allele present within a population. It is the occurrence of two or more alternative genotypes in a population at a higher frequency than what could be maintained by recurrent mutations. Single nucleotide polymorphism (SNP) is the variation in the DNA sequence limited to a single base pair.

Prognosis: Prognosis is defined as the prediction of how well or how poorly a patient is likely to fare in terms of response to therapy, relapse, survival time, or other outcome measures.

Prophylactic-Prophylaxis: Prophylactic-prophylaxis is prevention of disease or of a process that can lead to disease. It is the use of an antigenic (immunogenic) agent to actively stimulate the immunologic mechanism or the administration of chemicals or drugs to members of a community to reduce the number of carriers of a disease and to prevent others from contracting the disease. Alternatively, use of an antiserum from another person or animal to provide temporary protection against a specific infection or toxic agant can be tried.

Proteomics (Proteome): Proteomics facilitates making inventory of all proteins encoded in the genome of an organism and analysis of interaction of

these proteins. One of the primary goals of this technology is to describe the composition, dynamics, and connections of the multiprotein modules that catalyze a wide range of biological functions in cells. This technique provides exhaustive information on biochemical properties in living systems such as level of protein expression, posttranslational modifications, and protein–protein interactions.

Protooncogene: A protooncogene is the normal counterpart in the eukaryotic genome to the oncogene carried by some viruses. In other words, a protooncogene is a gene which, in normal cells, functions to control the normal proliferation of cells and which, when mutated or changed in any other way, becomes an oncogene.

PSA (Prostate Specific Antigen): PSA is a marker for early detection of prostate cancer.

***PTEN*:** The *PTEN* gene is phosphorylase and tensin homologue detected on chromosome 10. It is a tumor-suppressor gene that can be inactivated by mutation or genetic deletion and/or by epigenetic changes, including methylation. *PTEN* is involved in several types of human cancers and cancer cell lines, including brain, endometrium, prostate, breast, skin, colorectal, ovarian, and oral squamous cell carcinomas and leukemia, melanoma, and lymphoma.

Repressor Gene: A repressor gene is a regulatory gene whose product is a protein that controls the transcriptional activity of a particular operon.

Sarcoma: Sarcoma is a connective tissue neoplasm that is usually highly malignant. It is formed by proliferation of mesodermal cells.

Sarcomatoid: Sarcomatoid is a neoplasm that resembles a sarcoma.

Screening: Screening is defined as the application of a test to detect disease in a population of individuals who do not show any symptoms of their disease. The objective of screening is to detect disease at an early stage, when curative treatment is more effective.

Serial Analysis of Gene Expression (SAGE): SAGE is an approach that allows rapid and detailed analysis of thousands of transcripts. The LongSAGE method (Saha *et al.,* 2002) is similar to the original SAGE protocol (Velculescu *et al.,* 1995), but it produces longer transcript tags. The resulting 21 bp consists of a constant 4-bp sequence representing the restriction site at which the transcript has been cleaved, followed by a unique 17-bp sequence derived from an adjacent sequence in each transcript. This improved method was used for characterizing ~28,000 transcript tags from the colorectal cancer cell line DLD-1. The SAGE method was also used for identifying and quantifying a total of 303,706 transcripts derived from colorectal and pancreatic cancers (Zhang *et al.,* 1997).

Metastatic colorectal cancer showed multiple copies of the *PRL-3* gene that was located at chromosome 8q24.3 (Saha *et al.,* 2001). Several genes and pathways have been identified in breast cancer using the SAGE method (Porter *et al.,* 2001). The SAGE method is particularly useful for organisms whose genomes are not completely sequenced because it does not require a hybridization probe for each transcript and allows new genes to be discovered. Because SAGE tag numbers directly reflect the abundance of the mRNAs, these data are highly accurate and quantitative. For further details, see Part II, Chapter 6 by Dr. Ye in Volume I of this series.

Signal Transduction: Signal transduction describes the process by which a receptor interacts with a ligand at the surface of the cell and then transmits a signal to trigger a pathway within the cell. The basic principle of this interaction is that ligand binding on the extracellular side influences the activity of the receptor domain on the cytoplasmic side. The signal is transduced across the membrane. Signal transduction provides a means for amplification of the original signal.

Somatic Mutation: A somatic mutation is a mutation occurring in a somatic cell and therefore affecting only its daughter cells; it is not inherited by decedents of the organism.

Specificity: Specificity is the capacity for discrimination between antigenic determinants by antibody or lymphocyte receptor.

Splicing: Splicing is the process of linking together two RNA exons while removing the intron that lies between them.

Suppressor Gene: A suppressor gene is a gene that suppresses mutations in other genes. The effects of a mutation may be diminished or abolished by a mutation at another site. The latter may totally or partially restore a function lost because of a primary mutation at another site. A suppressor mutation does not result in a reversal of the original mutation; instead, it masks or compensates for the effects of the primary mutation.

Transcription: Transcription is the process by which an RNA copy of a gene is made.

Transduction: Transduction refers to the use of a phage (or virus) to carry host genes from one cell to another cell of a different genotype.

Transgenic Animals: Transgenic animals are created by introducing new DNA sequences into the germline via addition to the egg.

Tumor Markers: Tumor markers are molecular entities that distinguish tumor cells from normal cells. They may be unique genes or their products that are found only in tumor cells, or they may be genes or gene products that are found in normal cells but are aberrantly expressed in unique locations in the tumor

cells, or are present in abnormal amounts, or function abnormally in response to cellular stress or to environmental signals (Schilsky and Taube, 2002). Tumor markers may be located intracellularly (within the nucleus, in the cytoplasm, or on the membrane), on the cell surface, or secreted into the extracellular space, including into the circulation. Tumor markers usually are used for monitoring and detecting early response in asymptomatic patients. For example, tissue-based estrogen receptor and HER-2/*neu* amplification/overexpression markers in breast cancer have been validated to predict response to therapy in breast cancer. Other examples are prostate-specific antigen (PSA), which is a marker for early detection of prostate cancer, and carcinoembryonic antigen, which is used for detecting colon cancer.

Viral Oncogene: A viral oncogene transforms a cell it infects to a cancerous state.

Wild-Type: A term used to indicate the normal allele or the normal genotype. It is a strain, organism, or gene of the type that is designated as the standard for the organism with respect to genotype and phenotype.

Xenograft: Xenograft refers to transferring a graft or tissue from one species to another.

References

Bird, A. 2002. DNA methylation patterns and epigenetic memory. *Genes Dev. 16*:6–21.

Cavalli, G., and Paro, R. 1999. Epigenetic inheritance of active chromatin after removal of the main transactivator. *Science 286*:955–958.

Kondrashov, F.A., and Koonin, E.V. 2001. Origin of alternative splicing by tandem exon duplication. *Hum. Mol. Genet. 10*:2661–2669.

Mikulowska-Mennis, A., Taylor, T.B., Vishnu, P., Michie, S.A., Raja, R., Horner, N., and Kunitake, S.T. 2002. High quality RNA from cells isolated by laser capture microdissection. *Biotechniques 33*:1–4.

Mironov, A.A., Fickett, J.W., and Gelfand, M.S. 1999. Frequent alternative splicing of human genes. *Genome Res. 9*:1288–l293.

Pierce, A.J., Stark, J.M., Araujo, F.D., Moynahan, M.E., Berwick, M., and Jasin, M. 2001. Double-strand breaks and tumorigenesis. *Trends Cell Biol. 11*:S52–S59.

Porter, D.A., Krop, I.E., Nasser, S., Sgroi, D., Kaelin, C.M., Marks, J.R., Riggins, G., and Polyak, K. 2001. A sage (serial analysis of gene expression) view of breast tumor progression. *Cancer Res. 611*:5697–5702.

Poste, G., and Fidler, I.J. 1980. The pathogenesis of cancer metastasis. *Nature 283*:139–146.

Pu, R.T., and Clark, D.P. 2003. Detection of DNA methylation. Potential applications to diagnostic cytopathology. *Acta. Cytol. 47*:247–252.

Ramaswamy, S., and Golub, T.R. 2002. DNA microarrays in clinical oncology. *J. Clin. Oncol. 20*:1932–1941.

Rinehart, F.P., Ritch, T.G., Deininger, P., and Schmid, C.W. 1981. Renaturation rate studies of a single family of interspersed repeated sequences in human deoxyribonucleic acid. *Biochemistry 20*:3003–3010.

Rutherford, S.L., and Henikoff, S. 2003. Quantitative epigenetics. *Nat. Genet. 33*:6–8.

Saha, S., Bardelli, A., Buckhaults, P., Velculescu, V.E., Rago, C., St. Croix, B., Romans, K.E., Choti, A., Lengauer, C., Kinzler, K.W., and Vogelstein, B. 2001. A phosphate associated with metastasis of colorectal cancer. *Science 294*:1343–1345.

Saha, S., Sparks, A.B., Rago, C., Akmaev, V., Wang, C.J., Vogelstein, B., Kinzler, K.W., and Velculescu, V.E. 2002. Using the transcriptome to annotate the genome. *Nat. Biotechnol. 19*:508–512.

Samanta, A., Samanta, J., and Gunn, M. 2003. Legal considerations of clinical guidelines: Will NICE make a difference? *J. R.Soc. Med. 96*:133–138.

Schilsky, R.L., and Taube, S.E. 2002. Introduction: Tumor markers as clinical cancer test—are we there yet? *Sem. Oncol. 29*:211–212.

Shi, H., Maier, S., Nimmrich, I., Yan, P.S., Caldwell, C.W., Olek, A., and Huang, T.H. 2003. Oligonucleotide-based microarray for DNA methylation analysis: Principles and applications. *J. Cell. Biochem. 88*:138–143.

Skorski, T. 2002. BCR/ABL regulates response to DNA damage: The role in resistance to genotoxic treatment and in genomic instability. *Oncogene 21*:8591–8604.

Velculescu, V.E., Zhang, L., Vogelstein, B., and Kinzler, K.W. 1995. Serial analysis of gene expression. *Science 270*:484–487.

Zhang, L., Zhou, W., Velculstein, V.E., Kern, S.E., Hruban, R.H., Hamilton, S.R., Vogelstein, B., and Kinzler, K.W. 1997. Gene expression profiles in normal and cancer cells. *Science 276*:1268–1272.

Classification Scheme of Human Cancers

- Leukemias
  - Acute lymphoid leukemia (ALL)
  - Acute myeloid leukemia (AML)
  - Chronic myeloid leukemia (CML)
  - Other and unspecified leukemia (Other Leuk)
    - Other and unspecified lymphoid leukemias
    - Other and unspecified myeloid leukemias
    - Other specified leukemias, NEC

- Lymphomas
  - Non-Hodgkin's lymphoma (NHL)
    - Non-Hodgkin's lymphoma, specified subtype
    - Non-Hodgkin's lymphoma, subtype not specified
  - Hodgkin's disease (HD)
    - Hodgkin's disease, specified subtype
    - Hodgkin's disease, subtype not specified

- Central nervous system (CNS) and other intracranial and intraspinal neoplasms (CNS tumors)
  - Astrocytoma
    - Specified low-grade astrocytoma
    - Glioblastoma and anaplastic astrocytoma
    - Astrocytoma not otherwise specified
  - Other gliomas
  - Ependymoma
  - Medulloblastoma and other primitive neuroectodermal tumors (Medulloblastoma)
  - Other and unspecified malignant intracranial and entraspinal neoplasms (Other CNS)
    - Other specified malignant intracranial and intraspinal neoplasms
    - Unspecified malignant intracranial and intraspinal neoplasms
  - Nonmalignant intracranial and intraspinal neoplasms
    - Specified nonmalignant intracranial or intraspinal neoplasms
    - Unspecified intracranial or intraspinal neoplasms

- Osseous and chondromatous neoplasms, Ewing's tumor, and other neoplasms of bone (bone tumors)
  - Osteosarcoma
  - Chondrosarcoma
  - Ewing's tumor
  - Other specified and unspecified bone tumors (Other bone tumors)
    - Other specified bone tumors
    - Unspecified bone tumors

- Soft-tissue sarcomas (STS)
  - Fibromatous neoplasms (Fibrosarcoma)
  - Rhabdomyosarcoma
  - Other soft-tissue sarcomas
    - Other soft-tissue sarcomas
    - Unspecified soft-tissue sarcomas

- Germ-cell and trophoblastic neoplasms (germ-cell tumors)
  - Gonadal germ-cell and trophoblastic neoplasms
  - Germ-cell and trophoblastic neoplasms of nongonadal sites
    - Intracranial germ-cell and trophoblastic tumors
    - Other nongonadal germ-cell and trophoblastic tumors

- Melanoma and skin carcinoma
  - Melanoma
  - Skin carcinoma
- Carcinomas (except of skin)
  - Carcinoma of thyroid
  - Other carcinoma of head and neck
    - Nasopharyngeal carcinoma
    - Carcinoma of other sites in lip, oral cavity, and pharynx
    - Carcinoma of nasal cavity, middle ear, sinuses, larynx, and other ill-defined sites in head and neck
  - Carcinoma of trachea, bronchus, lung, and pleura
  - Carcinoma of breast
  - Carcinoma of genitourinary (GU) tract
    - Carcinoma of kidney
    - Carcinoma of bladder
    - Carcinoma of ovary and testis
    - Carcinoma of cervix and uterus
    - Carcinoma of other and ill-defined sites in GU
  - Carcinoma of gastrointestinal (GI) tract
    - Carcinoma of colon and rectum
    - Carcinoma of stomach
    - Carcinoma of liver and ill-defined sites in GI tract
  - Carcinomas of other and ill-defined sites not elsewhere classified (NEC)
  - Adrenocortical carcinoma
  - Other carcinomas NEC
- Miscellaneous specified neoplasms NEC
  - Embryonal tumors NEC
    - Wilms' tumor
    - Neuroblastoma
    - Other embryonal tumors NEC
  - Other rare miscellaneous specified neoplasms
    - Paraganglioma and glomus tumors
    - Other specified gonadal tumors NEC
    - Myeloma, mast cell tumors, and miscellaneous reticuloendothelial neoplasms NEC
    - Other specified neoplasms NEC
- Unspecified malignant neoplasms NEC

Birch, J.M., Alson, R.D., Kelsey, A.M., Quinn, M.J., Babb, P., and McNally, R.J.Q. 2002. Classification and incidence of cancers in adolescents and young adults in England 1979–1997. *Br. J. Cancer 87*:1267–1274.

I

Molecular Genetics

1

Quality Assurance in Immunohistochemistry

Thomas Rüdiger and Hans Konrad Müller-Hermelink

Introduction

Histopathology is widely applied as a fast, simple, and inexpensive method to classify neoplastic diseases. Histopathologic diagnoses form the basis for both patient treatment and clinical research, and pathologists are judged by the quality (i.e., reproducibility) of their diagnoses. Pathology as a specialty relies on the pattern recognition expertise of individual pathologists, a skill that may be subjective. Histologic criteria are often ill defined, frequently controversial, and inconsistently present in the spectrum of a disease (Taylor, 1994). Nonexperts may have problems recognizing subtle criteria in rare tumors, and most specific analyses of tumor classification may result in a significant interobserver discrepancy even among experts.

Special stains, such as periodic acid-Schiff (PAS) or reticulin, provide more objective information and have traditionally been applied to discriminate features not revealed on hematoxylin and eosin (H&E)–stained sections. Immunohistochemistry (IHC) can specifically detect individual epitopes and thus can discriminate cell types and their differentiation states with unique accuracy. It was first applied to histologic slides in the 1940, and the first paraffin sections were stained in 1974. More recently years, technical developments have made IHC the major ancillary technique in diagnostic pathology. These include antigen retrieval, availability of a broad range of primary antibodies working on paraffin sections, and sensitive detection systems (Chan, 2000; Hayat, 2002).

From a systematic viewpoint, IHC has greatly helped to better define or redefine entities and has made pathology more accurate (Taylor, 1994). Some entities, such as anaplastic large-cell lymphoma, were defined only after a specific antibody (CD30) allowed to distinguish them from very similar tumors, e.g., carcinomas. The analysis of transformation pathways of tumors has permitted the recognition of clinicopathologic entities and base classifications on tumor biology. For instance, the reliable distinction of mantle cell lymphoma from other indolent non-Hodgkin lymphomas was the basis to recognize its aggressive clinical course and to adapt therapeutic approaches.

From a more practical point of view, some specific differential diagnoses (e.g., non-Hodgkin lymphoma versus carcinoma) showed an error rate of 40% before IHC was applied (Wick *et al.,* 1999), and disagreement among pathologists about difficult but important diagnostic decisions was greater than 25% (Taylor, 1994). Recent advances in patient care, which are based on sentinel biopsies, have taken advantage of IHC in the search

Handbook of Immunohistochemistry and *in situ* Hybridization of Human Carcinomas, Volume 3: Molecular Genetics, Liver Carcinoma, and Pancreatic Carcinoma

for micrometastases. Although the chance to detect very small tumor foci on H&E staining alone is very low, IHC allows detection of single keratin-positive cells. This may convert H&E-negative to immunohistochemically positive sentinel lymph nodes in up to 10% of cases (Pargaonkar *et al.,* 2003). Even if the prognostic value of such recognized keratin-positive cells has yet to be formally established, the reliable detection of any keratin-positive cells is very reassuring for clinicians who base their therapeutic decisions on the report on the sentinel biopsy.

Thus, IHC has allowed increased diagnostic sensitivity, reliability, and reproducibility of diagnoses rendered by the pathologist. It is now widely applied as an immediate aid to diagnosis in a wide range of settings (Table 1). It is used to solve problems in the differential diagnosis and allows a diagnosis to be rendered on specimens formerly regarded as inadequate. To some extent, it may compensate for morphologic experience and skill. In addition, it may be useful to determine the likely origin of carcinomas (Chan, 2000). Of growing importance is the need for IHC to provide prognostic information for biology-based therapeutic approaches.

Initially, IHC served to obtain more accurate information from histologic specimens. With growing possibilities, expectations from IHC have also increased.

Now, the diagnosis, prognostic judgment, and therapy are based on IHC to such an extent that patient care is influenced by the reliability of immunohistochemical stains (O'Leary, 2001). To be confident in their results it is therefore necessary to perform quality controls on IHC itself. Initially a tool for quality control, IHC has now become its subject.

Definitions

As defined by the College of American Pathologists, quality assurance is a process of ensuring that all pathology services involved in the delivery of patient care are carried out in a manner appropriate to maintain excellence (Taylor, 1994). It is thus more an intention than a system, and it is placed in the hands of board-certified pathologists and their certified laboratories (O'Leary, 2001; Taylor, 1998a).

Table 1. Applications of Immunohistochemistry

▲ Histogenesis and differential diagnosis of neoplasms
▲ Likely site of origin in adenocarcinomas
▲ Quality assurance in sentinel lymph-node biopsies
▲ Definition of transformation pathways
▲ Detection of microorganisms
▲ Prognostic and predictive markers

Quality control is the aggregate of processes and techniques so derived as to detect, reduce, and correct deficiencies in the analytic process (Taylor, 1994). It comprises all actions taken to ensure that histopathologic diagnoses are reliable and contain all information needed to guide treatment.

Principles of Quality Control in Immunohistochemistry

How do the previous rather general descriptions relate to IHC? Reproducibility is of utmost importance to rely therapeutic decisions on pathologic diagnoses. This comprises both an intraobserver aspect on a day-to-day basis and an interobserver aspect among different pathologists. Categories that cannot be reproducibly classified are better lumped together in classifications of disease, as some categories of peripheral T-cell lymphomas have been. Because neoplasms are increasingly classified according to their immunophenotype, therapeutic decisions depend on the result of an immunohistochemical test. It is the pathologist's task to ensure that the results are reliable. Regarding IHC as a laboratory method, its quality represents its reliability, which depends on its sensitivity, specificity, and reproducibility (Rhodes *et al.,* 2001).

Because of some of the inherent characteristics of IHC, quality control is difficult to formalize. IHC is a complex technique; it therefore may be helpful to take a closer look at its different applications. Basically there are two different settings in which IHC contributes to the diagnostic workup of a neoplasm:

- First, a panel of antibodies may be used to support a classification of a neoplasm or to provide additional arguments in a differential diagnosis. The different antibodies applied in the panel control each other. Additionally, IHC is performed in the context of morphology and other ancillary studies, a context that also validates its results.
- In a second setting, specific molecules are targets of therapy. Response to therapy directly depends on the expression or overexpression of its target molecule in a neoplasm. To provide a rationale for treatment, the specific molecule is identified by IHC. Classically, this application comprises the detection of hormone receptors in breast carcinoma but more recently includes molecules targeted by antibodies (Herceptin) or specifically designed drugs (Glivec). Failure to demonstrate these molecules will probably exclude the patient from a treatment option. It is important to note that no controls by morphology or other tests are available,

rendering the reliability of the immunohistochemical test crucial for the patient.

These two major aspects of IHC give rise to different expectations of quality control, a fact taken into account by the regulations of the Food and Drug Administration (FDA), the authority that deals with the quality of therapeutic tests in the United States (Taylor, 1998b). Most immunohistochemical reagents are applied for diagnostic purposes and are recognized as special stains that are adjunct to conventional histopathologic examination. These are now classified as Class I devices. They do not have a significant history of false or misleading claims or risks to the patient associated with their inherent characteristics. Therefore, they are exempt from premarket notification to the FDA.

In contrast, immunostains that are not directly confirmed by routine histopathologic controls but that do have accepted scientific validation are Class II. Such devices generate a separate result that stands alone without direct histopathologic internal and external controls, and the manufacturer must submit performance claims for FDA approval. For new immunohistochemical stains that may provide independent information, the manufacturer will be required to follow the full Class III submission requirements with valid scientific evidence to support the new intended uses.

By this reclassification of immunohistochemical test systems as analyte-specific reagents, the burden of analysis of performance characteristics is shifted to the user. The individual laboratory and not the manufacturer has the ultimate responsibility for the quality of staining (Hsi, 2001). A laboratory that uses IHC should therefore be able to determine and document analytic and performance characteristics of a given test by using appropriate controls.

Although both applications have their own aspects of quality assurance, they both require reliable immunohistochemical stains. Therefore, first we review issues of quality control in the different technical steps of IHC, and then we discuss the individual aspects of both applications in detail. Much of the information presented here is based on our experience in a busy immunohistology laboratory, mainly in the field of hematopathology. This experience is necessarily subjective and biased, but as much as possible we have supported our opinion by published data.

Technical Aspects of Individual Steps of Immunohistochemistry

Performing IHC in a routine laboratory means a continuous struggle against the inherent perfidies of the method. Most laboratories have experience with immunohistochemical stains that perform well, suddenly deteriorate, and become difficult to interpret for no apparent reason. Quality control allows detection and correction of these problems.

The interpretability of a slide depends on certain steps:

- Acquisition and fixation of the specimen.
- Antigen demasking.
- Quality of the primary antibody.
- Sensitivity of the detection system.

IHC is a complex technique, and great variations of the method have been published. Different ways lead to interpretable results. There is probably no single protocol that allows optimum results for all antibodies, and most laboratories have introduced changes to the recipes published or suggested by the manufacturers. Sensitivity and specificity of IHC may vary dramatically with changes of the protocol (O'Leary, 2001). As a method, IHC therefore does not easily lend itself to standardization, and it may not be practical to attempt to standardize protocols across laboratories. However, it should be possible to standardize protocols within one laboratory.

Internal quality assurance comprises all measures taken to maintain the standard of immunohistochemical staining on a daily basis within a laboratory. It includes staining intensity, uniformity and sensitivity, and background and counterstaining; low intensity and nonspecific background staining are the major problems (Maxwell and McCluggage, 2000). Pathologists should follow the "total test strategy" (Shi *et al.,* 2001; Taylor, 2000), i.e., focus on each and every aspect of the whole procedure of IHC. This includes a defined approach to specimen acquisition, fixation, reagent validation, staining protocols, and interpretation. Still, the regular use of appropriate controls may allow collective validation of all technical aspects of IHC.

Fixation and Antigen Demasking

The performance of immunohistochemical staining is greatly influenced by specimen acquisition and fixation, steps that may be difficult to control because they are usually not in the hands of the pathologist but of the surgeon. If fixation is delayed for more than 30 min, epitopes may be poorly preserved. To ensure optimal penetration of the fixative, large specimens should be incised before fixation, especially when encapsulated. Fixation time may also influence IHC: both too short fixation and lengthy fixation for more than 24 hr may diminish IHC performance (Hayat, 2002; Werner *et al.,* 2000). Most tests purchased and methods published have

been optimized for specimens fixed in neutral-buffered formalin, and antigen demasking may not be effective after alcoholic fixation (Shi *et al.,* 1997) or fixation in B5 or Bouin's solution. In addition, after alcoholic formalin fixation false-positive results may be achieved, for example, with the HercepTest (Jacobs *et al.,* 1999).

Fixation must be standardized in some settings intending to provide quantitative results, because standardized specimen size and fixation protocols are required in the FDA-approved HercepTest. Referral centers, however, cannot trust that all material they receive is fixed identically.

Formalin fixation leads to cross-linking of proteins and therefore masks epitopes to which antibodies might bind. This process is partially reverted by methods of antigen demasking. In the past, numerous methods have been suggested, but diverse procedures may yield different degrees of antigen demasking. Initially, enzyme pretreatment was widely used, a process that was difficult to control, with a narrow optimum range between suboptimal demasking and overdigestion. A major step forward was the introduction of a heat-induced antigen retrieval, which is easily performed and effective for most antibodies (Taylor *et al.,* 1994).

Antigen retrieval crucially influences the performance of IHC; it can convert low staining intensity to high, and negative to positive (Shi *et al.,* 1996). Altered staining patterns with antigen retrieval may make existing literature on antigen expression obsolete, and the clinical interpretation of immunohistochemical stains and their consequences should no longer be based on preantigen retrieval data (Shi *et al.,* 2001). Prior to antigen retrieval, only 25% (9/36) estrogen receptor–positive tumors (with biochemical assays) could be detected by IHC (Cohen *et al.,* 1989). It has been identified as the single most important step for optimum staining results when compared to different primary antibodies and detection systems (Mengel *et al.,* 2002; von Wasielewski *et al.,* 2002). Therefore, much effort should be spent on the optimization of antigen retrieval, a work that may be more rewarding than changing dilutions of primary antibodies or detection systems.

To calibrate protocols of heat-induced antigen retrieval, both temperature and time of heating are of utmost importance (Joshi *et al.,* 2003). In addition, the pH of the retrieval fluid rather than its chemical constituents seems to be important. The best antigen-retrieval technique cannot be accomplished by changing any one of these parameters in isolation, and therefore a "test battery" may be applied to identify a protocol that gives maximum retrieval (Hsi, 2001; Shi *et al.,* 1998).

Because antigen retrieval lacks a firm theoretic basis of action there is no way to predict the behavior of a particular antibody (Hayat, 2002, Hsi, 2001; Pileri *et al.,* 1997). The method of heating may also influence the performance. In our laboratory, heating with a pressure cooker has proved more reliable and reproducible than microwave heating, confirmed by the fact that reproducible results on estrogen receptors have been achieved in 54% with pressure-cooker heating but only in 34% with microwave heating in a large interlaboratory study (Rhodes *et al.,* 2001). Probably, the higher temperature reached because of excess pressure contributes to the better retrieval, and a loss of maximum temperature by a few degrees results in lower staining index of normal germinal centers for Ki-67. In addition, overboiling does not generally occur, which makes the method easier to handle than microwave pretreatment. In a large, family-size pressure cooker, up to 150 slides can be "cooked" simultaneously.

A rational approach to antigen retrieval may aim for the maximum level of retrieval, the condition in which epitopes previously "masked" by formalin fixation have been retrieved to the fullest extent possible (Shi *et al.,* 1996). In a routine laboratory, however, it may not be practical to individualize antigen retrieval for every antibody. Too many and too elaborate protocols may be poorly adhered to; thus the level of retrieval must compromise with practicality. We therefore keep the heating temperature and time at the same level and test every antibody with different pH and at different dilutions (Table 2). Some authors have reported favorable experience with EDTA (ethylenediamine tetraacetic acid) solution at pH 8.0 (Pileri *et al.,* 1997). To be consistent, we apply antigen retrieval to all antibodies because the performance of antibody did not diminish after antigen retrieval compared to no pretreatment.

Antibodies and Detection Systems

A wide range of primary antibodies used with paraffin-embedded material and different detection systems are now available from different manufacturers. In interlaboratory studies, no primary antibody clones or detection systems have been found superior to others regarding hormone receptors (Rhodes *et al.,* 2000b) and overall performance (Rüdiger *et al.,* 1997).

Within the last decade, much work has been done to standardize the product specifications, which not only include technical details regarding specificity but also information about appropriate controls (Taylor, 1992). Guidelines are generally most stringent for primary antibodies, but there is little standardization for detection assays and the interpretation of results. Constraints to standardize tests in IHC have resulted in manufacturers increasingly offering prediluted primary antibodies, a development that makes most staining easier but

Table 2. Antigen retrieval applied in our laboratory

Citrate buffer (pH 5.5)	Optimal for most antibodies, including 34βE12, ACTH, AmyloidA, AE1/3, AFP, Actin, Alk-1, bcl-2, α-1Antitrypsin, bcl-6, BNH-9, Calcitonin, Calretinin, Cam5.2, CD3, CD4, CD5, CD8, CD15, CD20, CD23, CD30, CD31, CD34, CD52, CD56, CD57, CD79a, CD99, CD117, CD45, CD45R0, CEA, ChromograninA, CK5/6, CK7, CK8, CK10/13, CK19, CK20, CMV, Desmin, EMA, Gastrin, GFAP, GlycophorinA, HbcAg, HbsAg, Her2/neu, HMB45, HSV1, HSV2, ICSAT, Inhibin, Insulin, Immunoglobulin light and heavy chains
Citrate buffer (pH 7.0)	CD10
DAKO target retrieval solution	CD1a, CD21, CD25, CD35, CD38, CD61, CD103, CyclinD1, Heppar
Tris buffer (pH 10)	CD27

eliminates the possibility to vary dilutions to achieve optimum staining.

Unlike detection systems, antigen retrieval makes a difference regarding staining intensity (Rhodes *et al.,* 2000b). The newly introduced automated stainers have marginally improved overall staining, generally leading to a greater staining intensity and cleaner background. As a disadvantage, IHC is more readily available, and inconsistencies may result from a lack of understanding of the IHC, trouble shooting, and quality control because of the reliance on prepackaged reagents and automates (Maxwell and McCluggage, 2000).

Validation of New and Modified Immunohistochemical Assays

Because the individual laboratory has the ultimate responsibility for the quality of staining, new antibodies should be validated within a laboratory before routine use. There are no formal guidelines for how to validate new antibodies. They have to be validated both technically and interpretationally. To ensure maximum sensitivity of the stain we apply a "test battery," changing antigen retrieval methods and dilutions. All specimens are cooked in a pressure cooker for 5 min after the temperature has reached its maximum (121°C). If best results are achieved with a dilution different from that suggested by the manufacturer, more dilutions are tested to achieve optimum performance (Table 3). Antibodies that do not stain reliably should not be applied for routine diagnostics.

Interpretative validation requires that diagnoses should not be based on an antibody the pathologist is not acquainted with; such cases should be referred to an expert instead. For antibodies established in the literature, 10 positive and negative controls are sufficient to validate their staining performance (Hsi, 2001). However, if antibodies are new or there is little available information about them, more numerous cases may be necessary to understand the staining characteristics and the antibody's value in certain differential diagnoses. For antibodies that are rarely used or do not stain consistently, collaboration with other laboratories that have more experience with them in the diagnosed field should be sought.

Interpretation of Stains

IHC has some inherent problems that should be considered in interpreting its results. Generally, it may

Table 3. The "test battery" applied in our laboratory to define optimum staining performance of new antibodies. Results in the table refer to the signal/noise ratio, and the respective antibody would be further investigated for lower dilutions with Citrate (pH 5.5) and target retrieval solution

	Citrate (pH 5.5)	Citrate (pH 7.0)	Tris (pH 10.0)	Target retrieval solution
1/2 suggested dilution	+ +	_	_	+ +
Suggested dilution	+ +	_	_	+ +
2X suggested dilution	+	(+)	_	+

be difficult to localize the signal to individual cells, especially if the tumor has a highly heterogeneous composition or forms a minor part of the infiltrate. For example, Schmincke's carcinoma may easily remain undetected in a lymph node, even after IHC, if a keratin stain is not performed (Rüdiger *et al.,* 2002). Poorly fixed or overdigested specimens are especially problematic in this regard. In general, positive results should be regarded as more significant than negative ones, because failure to perform an expected staining may be the result of biological and technical reasons. Biological reasons may include alternative splicing, posttranslational modifications, or lysosomal breakdown of proteins that then are not detected (Kopolovic and Wolman, 1996). In addition to deficiencies in the technical staining procedure, antigens may decay if paraffin slides are stored over a long time before IHC is performed. Endogeneous biotin activity may also be retrieved by antigen retrieval, which will lead to granular cytoplasmic reactions (Hsi, 2001).

Because of its inherent characteristics of multistep detection, immunohistochemical reactions are not generally stochimetric (O'Leary, 2001). In contrast to flow cytometry with directly labeled antibodies, the signal strength may not be in linear correlation with the amount of antigen existing at a particular location. For example, no correlation is found in prostate carcinoma between serum prostate-specific antigen (PSA) levels (corrected for tumor volume) and tissue PSA expression (Weir *et al.,* 2000). Thus, every quantitation in IHC may be inexact (Gehrig *et al.,* 1999).

It may be an arbitrary decision what strength or percentage of staining is regarded as positive (Kopolovic and Wolman, 1996) and where to evaluate or score an inhomogeneously stained slide. Major differences, especially when scoring *Her2/neu* or *p53* expression, may result from different thresholds used by different observers. Binary assessments of positive versus negative are reliable only at the extremes of high and absent staining. Cases with intermediate staining are variably interpreted and should thus be validated by repeated staining or by different methods (McShane *et al.,* 2000).

Controls

The interpretation of any immunostaining is greatly facilitated by applying appropriate controls to monitor its overall performance. Nothing is more reassuring than an internal positive control that has undergone the whole process from tissue acquisition to processing and storage as well as the immunostain itself together with the tissue analyzed. Fortunately, such controls are available for many antibodies in most tissues. Failure of internal controls to stain adequately may include both negativity in cells expected to express the antigen analyzed and positivity in cells known to be negative for the respective antibody. The respective staining should be rejected and possibly repeated. Naturally, no conclusions whatsoever should be drawn from such a slide.

If not available, external controls can be used, among which suitable tissues must be selected. However, for many antibodies, apart from some specific keratins, an appendix cross-section will provide at least some reactive cells in a defined morphologic localization (Table 4). For a few antibodies, such as HER2/neu and Alk1, normal tissue controls may not be available. Tissue microarrays (Chan *et al.,* 2000; Hsu *et al.,* 2002; Packeisen *et al.,* 2002), cell lines (Wick and Swanson, 2002), and the newly developed short constrained peptides (Sompuram *et al.,* 2002) may serve as ubiquitous positive controls.

There is no general reference standard regarding external controls, but some principles should be observed. Tissues selected as positive controls should not react strongly because an intermediately or weakly reacting control is more sensitive to deficiencies in performance of the immunostaining. In routine practice, nuclear antibodies (Ki-67 protein or hormone receptors) are very sensitive to decreasing efficacy of antigen retrieval and detection. External controls reflect only a part of the procedure they undergo together with the test specimen. They are sensitive only to analytic errors and are not likely to reflect the preanalytic conditions encountered in the laboratory (O'Leary, 2001; Sompuram *et al.,* 2002). To control for the impact of tissue processing in parallel, a stain for vimentin may be applied (O'Leary, 2001), and this is probably the most important information that can be derived from this stain against this almost ubiquitous cell skeleton component. Moreover, unless cut on the same slide as the test tissue, an external control cannot prove whether the correct primary antibody was applied to the respective slide.

Negative controls can be eliminated because they are invariably present in all specimens. In addition, because immunostains are commonly ordered in the form of a panel on an individual case, the different stains can provide information on whether the tissue shows nonspecific staining as manifested by a similar pattern being observed in disparate antibodies (Chan *et al.,* 2000).

If deficiencies are suspected, different controls may help define the step responsible (Table 5).

The histopathologic report should include all data including antibody clone, staining pattern, and controls used.

Table 4. External controls for selected, frequently applied antibodies

Antibody	Controls	
34βE12	Tonsil	Squamous epithelium
Actin	Appendix	Smooth muscle, vessels
AE 1/3	Appendix	Epithelium
AFP	Liver	
Alk-1	Tumor only	
bcl-2	Appendix	Extrafollicular B-cells
bcl-6	Appendix	Follicular B-cells
BerEP-4	Appendix	Epithelium
BNH-9	Appendix	Vessels
Calcitonin	Thyroid	
Calretinin	Mesothelia	
Cam5.2	Appendix	Epithelium
CD 10	Appendix	Follicular B-cells
CD 117	Appendix	Mast cells
CD 15	Appendix	Granulocytes
CD 1a	Thymoma	Lymphocytes
CD 21	Appendix	Follicular dendritic cells
CD 23	Appendix	Follicular dendritic cells
CD 3	Appendix	T-cells
CD 30	Appendix	Plasma cells, isolated extrafollicular B-cells
CD 31	Appendix	Vessels
CD 34	Appendix	Vessels
CD 35	Appendix	Follicular dendritic cells
CD 38	Appendix	Plasma cells
CD 4	Appendix	T-cells (subset)
CD 5	Appendix	T-cells
CD 52	Appendix	All lymphocytes
CD 56	Brain	
CD 79a	Appendix	B-cells
CD 8	Appendix	T-cells (subset)
CD20	Appendix	B-cells
CD45	Appendix	Lymphocytes
CD57	Appendix	Intrafollicular T-cells (subset)
CD99	Thymus	Lymphocytes
CEA	Appendix	Epithelia
Chromogranin A	Appendix	Crypt epithelia
CK 10/13	Tonsil	Epithelia
CK 19	Appendix	Epithelia
CK 20	Appendix	Epithelia
CK 5/6	Tonsil	Epithelia
CK 7	Lung	
Cytomegalovirus	Positive case	
Cyclin D1	Internal	Few endothelia
Desmin	Appendix	Muscle
EMA	Appendix	Epithelia
Gastrin	Stomach antrum	Crypt epithelia
Glycophorin A	Internal	Erythrocytes
Hbc	Positive case	
Hbs	Positive case	
Heppar	Liver	
Her 2 neu	Breast carcinoma	With known overexpression
HMB 45	Skin	Melanocytes
Immunoglobulins	Appendix	Plasma cells
Insulin	Pancreas	Islands

Table 5. Effects of the most common deficiencies in IHC and steps to correct them.

Control Performance	Reason for Deficiency	Confirmation	Steps to Be Taken
Low signal in all antibodies/ all cases	Antigen retrieval detection system	Low proliferation index in germinal centers	Check buffer pH; temperature detection system batch; irregular pipetting, especially in automated stainers
Low signal in one antibody/ many causes and controls	Antibody dilution too high	External controls, especially tissue that formerly reacted	Redilute antibody, check batch
Low signal in all antibodies/ one case	Fixation	Check on H&E	Rebiopsy may be required if IHC is essential
Antibody with peculiar staining	Wrong antibody pipetted on the slide, error in antibody dilution	Controls	Redilute antibody
High background	Blocking serum from a species against which the detection system is directed, slides dried out	Staining product cannot be related to individual cells	Restain

External Quality Assurance

External measures of quality assurance supplement the internal quality assurance. An individual pathologist or laboratory should gauge their assay performance against that achieved by a larger number of other laboratories. The results achieved in the external tests are accurate predictors of in-house laboratory performance. External or institutional quality assurance has a long history in pathology. Programs on surgical pathology, IHC, and cytopathology have been operational in the College of American pathologists for almost two decades (Kraemer, 1989). Their IHC proficiency-testing program (Taylor, 1994) serves as an external test of performance in interpretation on external tissues. It also includes continuing medical education and laboratory inspection programs (O'Leary, 2001).

Generally, the external proficiency testing programs have led to more homogeneous results in the staining. In earlier years staining performance was also monitored, for example, for kappa light chains and a variety of other antigens (Reynolds, 1989). Initially, more than 50% of the laboratories failed to achieve acceptable results, but 42% improved on subsequent trials. More current trials, especially in the United Kingdom with participants from all over Europe, have concentrated on hormone receptors and Her2/*neu* expression in breast carcinoma (Rhodes *et al.,* 2001; Rhodes *et al.,* 2002). Multitissue array technology may well be applied economically to test a range of different reactivities for an antibody (Mengel *et al.,* 2002; von Wasielewski *et al.,* 2002). A major point of discussion of external quality control programs is that assays optimized for use on in-house material cannot be expected to produce results of the same quality on external material. Addressing this question for hormone receptors, Rhodes *et al.* found IHC results on external quality assurance tumors to be correlated to in-house performance (Rhodes *et al.,* 2000b).

Most studies on quality assurance have centered on the sensitivity and specificity of immunohistochemical staining for defined antibodies, but few data are available about the diagnostic use of IHC in different laboratories. In a study embracing the whole process of diagnostic IHC, the final diagnosis was not correlated significantly to externally judged staining quality. This does not suggest that sensitivity and specificity were not an issue but that other steps of immunohistochemistry, namely the selection of antibodies and conclusions drawn from the stains, may be even more problematic in diagnostic IHC at present (Rüdiger *et al.,* 2002).

All these external quality control programs allow only the detection of deficiencies in performance. To master the complex IHC, regular workshops and continuing medical education are of great help. Also, reasonable applications of IHC in the differential diagnosis of tumors are discussed in this volume.

Class II Applications

As outlined earlier, a limited but rapidly growing number of immunohistochemical tests is applied to detect target molecules for specific therapies and serves as an immediate basis for therapeutic decisions. For such antibodies the result cannot be directly confirmed by morphology, and standardization is therefore of utmost importance (Taylor, 1998a). The detected molecules usually relate to pathways of carcinogenesis and thus provide a basis for specific treatment. Their biological basis is reviewed in other chapters in this volume. Hormone receptors show classical application of IHC

to guide therapy based on the staining of an antibody, which cannot be validated by morphology. Similarly, herceptin, a monoclonal antibody against the Her2/neu molecule, is only indicated if the carcinoma overexpresses the molecule, which is usually caused by an amplification of the respective gene. Glivec is a tyrosin kinase inhibitor that was originally developed for the treatment of chronic myelogeneous leukemia but may also be effective in gastrointestinal stroma tumors expressing c-kit. Patients with solid tumors who might benefit from this therapy are identified by immunostaining for CD117 (c-kit). Because such medications offer a new perspective to specifically and effectively treat neoplasms with fewer side effects, they will be increasingly developed in the future.

Even if the prognostic value of a marker is good, it can be masked if not measured reproducibly for clinical trials, and some differences reported in outcome may stem from different staining or different scoring systems (McShane *et al.,* 2000). A reasonable balance must be found between sensitivity and specificity to accurately predict patients likely to benefit from targeted treatment (Rhodes *et al.,* 2000c). An ideal test should capture all possible treatment candidates with a high positive predictive value, should be agreed on among different observers, and should be carried out easily. Thus, the test must fulfill all the requirements of a true clinical laboratory assay for prognostic or predictive markers, prerequisites that are not easily met by immunohistochemical assays (Rhodes *et al.,* 2001).

Estrogen and Progesterone Receptors

Hormone receptor detection in breast carcinoma is a prerequisite for antihormone (tamoxifen) treatment: 50–60% of estrogen receptor positive but only 5% of negative breast carcinomas respond to a hormone treatment. Being originally based on enzyme immunoassays, the gold standard for hormone receptors has transmutated to IHC, which is more sensitive, specific, and economical (Zafrani *et al.,* 2000). As a morphology-based method IHC allows distinguishing between reactivity originating from the tumor itself and activity originating from reactive tissues.

Despite very good results in unicentric studies, hormone receptor expression is still not measured reproducibly: In a U.K. NEQUAS (National External Quality Assessment Scheme) study including 200 laboratories in 26 countries, reproducible results over a 2-year period could only be achieved in 24 of 66 laboratories. Of the laboratories, 80% could demonstrate receptor positivity in medium- and high-expressing tumors, but only 37% revealed it in low-expressing tumors (Rhodes *et al.,* 2000c). The latter low-expressing tumors are problematic in all studies (Mengel *et al.,* 2002; von Wasielewski *et al.,* 2002). Compared to these tumors sent to the laboratories externally, their pass rate on in-house tumors was 81–97% (Rhodes *et al.,* 2000c). However, there was a significant positive correlation between performance in both external and in-house tumors of the study. Underachievement was usually the result of overall staining sensitivity but neither of scoring nor the assay system used. The variability between laboratories increased if the participants used their own threshold values. Because there was also a significant correlation between the assay sensitivity and the reported frequency of receptor positivity (Rhodes *et al.,* 2000a), as a minimum requirement of quality control the latter should be noted in every institution and steps should be taken if it is too low (Table 6).

Her2/*neu*

The Her2/*neu* molecule is a growth factor receptor that distinguishes tumors of different biology among those that are discovered at a low stage. It identifies the harbingers of aggressive biological potential and is predictive of the outcome of a therapy with monoclonal antibodies raised against this molecule.

To guide therapy, there is no single best method, but IHC seems to hold most promise because of its cost, convenience, and biological relevance (Thomson *et al.,* 2001; Wisecarver, 1999). The HercepTest was developed in a unique attempt to prospectively standardize the methods (Rhodes *et al.,* 2002). The FDA-approved protocol for testing extends to all aspects from specimen size to the technical performance of antigen retrieval, scoring, and controls in a need to address the issues of limited standardization of the technical procedures. In such an FDA-approved highly standardized test, adherence to the approved protocol is an important issue, and, any deviation invalidates its FDA-approved status (Tubbs and Stoler, 2000).

The reproducibility and sensitivity of Her2/neu scoring was addressed in several external quality assurance trials. Comparing different primary antibodies (Press *et al.,* 1994) and detection systems, in some

Table 6. Frequency of positive results for hormone receptors in breast carcinoma in larger studies (Rhodes *et al.,* 2000a; Zafrani *et al.,* 2000)

Estrogen receptor	Progesterone receptor	%
+	+	55
+	–	20
–	+	3
–	–	22
+		59–78
	+	52–71

studies a performance similar to HercepTest could also be achieved with other primary antibodies (A0485, TAB250) and detection systems (Thomson *et al.,* 2001). The HercepTest has been criticized because of its high false-positive rate, which means a low positive predictive value (Pauletti *et al.,* 2000). When the HercepTest scoring system is adhered to strictly and the delivered cell line controls perform as expected, agreement is excellent. It gives more than 80% appropriate results, and the level of agreement in laboratories using HercepTest was significantly greater than that achieved by laboratories using other methods. The latter laboratories improved significantly on repletion; therefore, ongoing external measures may have the potential to provide a level of standardization equivalent to or even greater than the HercepTest alone (Rhodes *et al.,* 2002).

If systems other than the HercepTest are used, the critical steps are antigen retrieval and dilution of the primary antibody. In our experience, the HercepTest antigen retrieval system is laborious and does not result in maximum retrieval, which can be balanced by the dilution of the primary antibody if other systems are used.

In contrast to the hormone receptors, scoring is also a major issue in Her2/neu interpretation. It is questionable whether the scoring criteria of the HercepTest can also be applied for other protocols and different cut-off levels (60% instead of 10% cells with positive membranes) have been proposed (Vincent-Salomon *et al.,* 2003). Certain details of scoring, however, should be considered: only membrane staining may be scored, whereas cytoplasmic staining should not be regarded as positive. Also any staining of normal epithelia should lead to a rejection of the case and repetition of the stain (Thomson *et al.,* 2001). Therefore, slides analyzed for Her2/neu should contain neoplastic and nonneoplastic tissue, the latter as internal negative control.

Other Molecules

New approaches in the use of monoclonal antibodies and specifically tailored molecules (e.g., against tyrosinkinases) suggest that the number of molecules against which specific therapies are available will increase in the future and IHC will be increasingly applied to select patients for these therapies. A molecular substaging of disease may even be allowed by IHC and information may be added to existing staging procedures (Joshi *et al.,* 2003). However, all prognostic and predictive markers first have to be validated in clinical studies before they can be used in general practice. "The din and clatter of clinicians requesting the use of prognostic and predictive markers that have not been carefully evaluated in appropriate clinical studies must be perceived as the noise, not the signal, of good medical care" (Swanson, 1999).

Validation of Tests

Naturally, tests detecting molecules for therapeutic decisions have to be, and usually are, validated by independent methods. This validation may be clinical, against a gold standard (if this is available), or by interlaboratory variability (Wick and Mills, 2001). Ideally, it would be based on the response to therapy; however, this may not be practical because it may take years to perform all the necessary clinical studies. Other techniques to detect the protein or different aspects of the same biological process may serve for comparison.

To detect hormone receptors, radioimmune assays were originally the method of choice; however, IHC is more practical, not only because of its easier handling but also because, being based on morphology, it allows neoplastic cells to be distinguished from reactive cells. Cases that are positive for the radioimmune assays but negative for IHC may be so because of poor fixation, delayed handling, or sampling errors in the assay (Gehrig *et al.,* 1999).

The protein expression measured by IHC may also be compared to the messenger ribonucleic acid (mRNA) expression as measured by reversed-transcription-polymerase chain reaction (RT-PCR) (Dall *et al.,* 1995). Differences may result from concealed epitopes after fixation, posttranslational modification, or block of protein expression; in the latter case IHC would probably give the more valid result. Again, IHC allows correlation expression to tumor cells.

In the case of HER-2/neu expression, IHC may be calibrated with the aid of fluorescence *in situ* hybridization (FISH) (see Volume I of this series). Cases with 3+-overexpression in the HercepTest also show an amplification of the corresponding gene by FISH studies and respond to therapy. Cases with weak expression (1+/2+) should be validated with FISH. Low-score results are variably predictive of gene amplification, and there is a high inter-observer variability (Thomson *et al.,* 2001). Up to 42% of cases with score 2, which is also regarded as positive, may not be amplified (Roche and Ingle, 1999).

FISH studies and IHC assess different aspects of the HER2/neu gene in breast cancer, namely amplification versus overexpression, and it is not yet clear whether gene amplification or protein overexpression is the better predictor for clinical outcome and clinical response.

Studies have also been performed to assess the concordance of different antibodies to FISH studies, which give different results from different investigators. In one study on 254 breast cancers, HercepTest showed

a lower concordance to the FISH than other antibodies, namely TAB250 and CD11 (O'Malley *et al.,* 2001), in others, a better one compared to e2-4001 (Hoang *et al.,* 2000).

Immunohistochemistry as an Ancillary Technique in Diagnostic Pathology

Despite the growing importance of the previously mentioned applications of IHC to predict responses to specific therapies, most immunohistochemical staining is performed to characterize or classify poorly differentiated neoplasm. Some tumors, especially in hematopathology, are defined mainly according to their immunophenotype, and IHC is thus indispensable for their diagnosis. In this regard, IHC remains an ancillary technique that has to be understood in the context of morphologic studies. The major risk to the patient is not a poor performance of the immunohistochemical staining but the failure to perform the appropriate staining as part of the diagnostic workup. Antibodies and reagents for diagnostic purposes are classified by the FDA as Class I devices because they have no significant history of false or misleading claims or risks associated with their inherent characteristics (Taylor, 1998a).

The problems in diagnostic IHC are not so much the technical performance of the staining but rather lie at the interface between classical histology and IHC, namely to choose antibodies and conclude from a set of tests to a diagnosis, which is an integration of all available data (Rüdiger *et al.,* 2002). The process goes far beyond technical questions and includes additional steps. (An external quality control study, performed by the German Association of Pathologists, focused on the integration of IHC into the diagnostic process). Special emphasis was placed on the interface between IHC and morphologic methods as well as on the conclusions drawn from individual staining. An interesting result of this study was that the technical performance of individual staining was not decisive, and so correct diagnosis was reached in only a minority of cases. However, morphologic results obtained and information on the antibody specificity and the conclusions drawn from staining patterns were important.

Table 7 outlines steps that do not strictly refer to the technical aspects of IHC.

In most cases, the differential diagnosis based on the H&E-stained sections was of utmost importance to reach the correct final diagnosis. This included diagnoses that were based on morphology and only substantiated by IHC. Some difficult cases also fell into this category if appropriate markers were not available to prove the diagnosis by IHC. As an example, a keratin-negative metastasis originating from the adrenal was diagnosed based on the H&E section. In another group of cases, the correct selection of antibodies to solve a differential diagnostic problem was decisive. In a few cases the conclusions drawn from correctly interpreted staining were most important (e.g., to know the distribution of single keratins CD7 and CK20 in normal tissues to distinguish a primary gall bladder carcinoma from a metastasis of colonic carcinoma).

Table 7. Steps of diagnostic immunohistochemistry

▲ Formulation of a tentative diagnosis/differential diagnosis
▲ Selection of appropriate primary antibodies to solve the question
Technical steps
▲ Interpretation of every staining
▲ Conclusions for the diagnosis
▲ Final diagnosis as an integration of all available information

It is concluded from this study that for diagnostic purposes, currently the major problems are not technical aspects but the proficiency of the pathologist to select antibodies for certain differential diagnoses and to draw conclusions from the pattern of staining. Thus, the selection of an appropriate staining should be an integral part of quality assurance in IHC to solve a diagnostic problem taking the capabilities and limitations of the laboratory into account. This underlines the importance of continuing medical education and workshops to share knowledge about staining characteristics and the diagnostic value of commonly used antibodies.

Cost-Benefit Analysis in Immunohistochemistry

The cost of IHC should also be addressed, although there is no formal cost-benefit analysis of IHC. The benefits of pathologic tests are difficult to identify and quantify in understandable terms, and the cost-effectiveness thresholds are controversial. It is not settled whether there are limits above which services should not be provided (Raab, 2000).

It may be difficult to prove that correct diagnoses have a direct beneficial effect on patient outcome. This is probably true only if differential therapies are available that are effective for at least one of the diseases in question (Wick *et al.,* 1999). With the exception of hematologic malignancies, IHC has a limited role in altering the clinical course on oncology cases. Although some questions may seem crucial intuitively, they may have little impact on the outcome, especially if there is no effective therapy for any of the tumor types in question and identical treatment will be applied anyway.

The prognosis for "poorly differentiated neoplasms" such as melanoma or primitive neuroectodermal tumor has not changed substantially with the advent of IHC. In metastatic tumors of unknown origin, there are no truly site-specific treatments, with the exception of breast carcinoma. Prognostic information directly linked to IHC may be spurious at present; however, with the introduction of more specific therapeutic approaches it may become more important, especially if patients are selected based on the performance of the single antibody.

Cost effectiveness can also be related to an increase in diagnostic certainty, which usually is a great clinical demand (Raab, 2000). IHC is an inexpensive technique when compared to other clinical investigations. Based on theoretical models, IHC would therefore still be cost effective even if it was rarely efficious. Thus, it is considerably undervalued, especially if it can save numerous clinical investigations in the detection of a primary tumor in metastatic cancer. Based on models, IHC would be cost effective even if the cost were 5–10 times as much as it currently costs in the United States (Raab, 2000).

To work cost effectively, it is important to formulate differential diagnoses based on the conventional staining and to select individual antibodies to answer the differential diagnosis in question rather than using a large panel of different antibodies in every case. Clearly, studies are needed that address the impact of IHC (and of other ancillary methods and referral centers) on patient outcome and to build up evidence regarding its cost efficiency.

Another topic in cost containment is the repetition of outside IHC in referral centers. In a study by Wetherington *et al.* there was a nonconcordance in testing in about one-fifth of the cases (21.2%) and IHC resulted in a significant change in diagnoses in 18% of 186 cases (Wetherington *et al.,* 2002). Reasons may be manifold but are partially subjective. Pathologists are used to the staining characteristics in their own laboratories and may not feel confident evaluating outside slides. Additionally, appropriate controls to validate the sensitivity and specificity may not be available.

In conclusion, there are some good approaches to quality control in IHC, but because of its widespread use, patients have too much to lose to allow diagnostic IHC to continue much longer as a *laissez-faire* discipline. More elaborate and individual therapeutic approaches have raised a need for greater objectivity (Taylor, 1994). We are still far from our colleagues in laboratory medicine with regard to the validation of our diagnoses. Future years will probably bring the exclusive use of validated methods only for IHC to the absolute exclusion of others. Also, measures have to be taken to further validate assay results by demonstrating consistency over time, by calibrating results quantitatively, and by introducing duplicate tests for the more serious applications. Currently, IHC exists as an adjunctive morphologic method that is not consistently validated by other objective methods such as *in situ* hybridization or PCR.

In the future, certified reference material and appropriately standardized and validated control reagents may replace the standardization of each and every step of the immunohistochemical test. If the controls for a specific test are validated and mandated, the reagents and platforms do not need to be mandated as long as they produce the desired results (Moskaluk, 2002).

The success of quality assurance schemes strongly depends on the willingness of pathologists to commit themselves to the guidelines (Sweep and Geurts-Moespot, 2000). Upcoming demands for more specialized technologists and administrative oversight as well as for technical and informational infrastructure to satisfy the requirements for procedural collaboration and technical documentation. By validating immunohistochemistry like this, expenses will increase and in the end prompt many laboratories to refer specimens needing IHC to specialized centers (Wick and Mills, 2001).

References

Chan, J.K. 2000. Advances in immunohistochemistry: Impact on surgical pathology practice. *Semin. Diagn. Pathol. 17*:170–177.

Chan, J.K., Wong, C.S., Ku, W.T. and Kwan, M.Y. 2000. Reflections on the use of controls in immunohistochemistry and proposal for application of a multitissue spring-roll control block. *Ann. Diagn. Pathol. 4*:329–336.

Cohen, C., Unger, E.R., Sgoutas, D., Bradley, N., and Chenggis, M. 1989. Automated immunohistochemical estrogen receptor in fixed embedded breast carcinomas. Comparison with manual immunohistochemistry on frozen tissues. *Am. J. Clin. Pathol. 92*:669–672.

Dall, P., Heider, K.H., Sinn, H.P., Skroch-Angel, P., Adolf, G., Kaufmann, M., Herrlich, P., and Ponta, H. 1995. Comparison of immunohistochemistry and RT-PCR for detection of CD44v-expression, a new prognostic factor in human breast cancer. *Int. J. Cancer 60*:471–477.

Gehrig, P.A., Van Le, L., Olatidoye, B., and Geradts, J. 1999. Estrogen receptor status, determined by immunohistochemistry, as a predictor of the recurrence of stage I endometrial carcinoma. *Cancer 86*:2083–2089.

Hayat, M.A. 2002. *Microscopy, Immunohistochemistry and Antigen Retrieval Methods.* New York, NY Kluwer/ Plenum Publishers.

Hoang, M.P., Sahin, A.A., Ordonez, N.G., and Sneige, N. 2000. HER-2/neu gene amplification compared with HER-2/neu protein overexpression and interobserver reproducibility in invasive breast carcinoma. *Am. J. Clin. Pathol. 113:*852–859.

Hsi, E.D. 2001. A practical approach for evaluating new antibodies in the clinical immunohistochemistry laboratory. *Arch. Pathol. Lab. Med. 125*:289–294.

Hsu, F.D., Nielsen, T.O., Alkushi, A., Dupuis, B., Huntsman, D., Liu, C.L., van de Rijn, M., and Gilks, C.B. 2002. Tissue microarrays

are an effective quality assurance tool for diagnostic immunohistochemistry. *Mod. Pathol. 15*:1374–1380.

Jacobs, T.W., Gown, A.M., Yaziji, H., Barnes, M.J., and Schnitt, S.J. 1999. Specificity of HercepTest in determining HER-2/neu status of breast cancers using the United States Food and Drug Administration-approved scoring system. *J. Clin. Oncol. 17*:1983–1987.

Joshi, M.B., D'Amico, T.A., and Harpole, D.H., Jr. 2003. Molecular biologic substaging of stage I NSCLC through immunohistochemistry performed on formalin-fixed, paraffin-embedded tissue. *Methods Mol. Med. 75*:369–388.

Kopolovic, J., and Wolman, M. 1996. Reasons underlying discrepancies in results between immunohistochemistry and molecular biology. *Eur. J. Histochem. 40*:177–180.

Kraemer, B.B. 1989. Quality assurance activities of the College of American Pathologists. *Acta. Cytol. 33*:434–438.

Maxwell, P., and McCluggage, W.G. 2000. Audit and internal quality control in immunohistochemistry. *J. Clin. Pathol. 53*:929–932.

McShane, L.M., Aamodt, R., Cordon-Cardo, C., Cote, R., Faraggi, D., Fradet, Y., Grossman, H.B., Peng, A., Taube, S.E. and Waldman, F.M. 2000. Reproducibility of p53 immunohistochemistry in bladder tumors. National Cancer Institute, Bladder Tumor Marker Network. *Clin. Cancer Res. 6*:1854–1864.

Mengel, M., von Wasielewski, R., Wiese, B., Rüdiger, T., Müller-Hermelink, H.K., and Kreipe, H. 2002. Inter-laboratory and inter-observer reproducibility of immunohistochemical assessment of the Ki-67 labelling index in a large multi-centre trial. *J. Pathol. 198*:292–299.

Moskaluk, C.A. 2002. Standardization of clinical immunohistochemistry: Why, how, and by whom? *Am. J. Clin. Pathol. 118*:669–671.

O'Leary, T.J. 2001. Standardization in immunohistochemistry. *Appl. Immunohistochem. Mol. Morphol. 9*:3–8.

O'Malley, F.P., Parkes, R., Latta, E., Tjan, S., Zadro, T., Mueller, R., Arneson, N., Blackstein, M., and Andrulis, I. 2001. Comparison of HER2/neu status assessed by quantitative polymerase chain reaction and immunohistochemistry. *Am. J. Clin. Pathol. 115*:504–511.

Packeisen, J., Buerger, H., Krech, R., and Boecker, W. 2002. Tissue microarrays: A new approach for quality control in immunohistochemistry. *J. Clin. Pathol. 55*:613–615.

Pargaonkar, A.S., Beissner, R.S., Snyder, S., and Speights, V.O., Jr. 2003. Evaluation of immunohistochemistry and multiple-level sectioning in sentinel lymph nodes from patients with breast cancer. *Arch. Pathol. Lab. Med. 127*:701–705.

Pauletti, G., Dandekar, S., Rong, H., Ramos, L., Peng, H., Seshadri, R., and Slamon, D.J. 2000. Assessment of methods for tissue-based detection of the HER-2/neu alteration in human breast cancer: A direct comparison of fluorescence *in situ* hybridization and immunohistochemistry. *J. Clin. Oncol. 18*:3651–3664.

Pileri, S.A., Roncador, G., Ceccarelli, C., Piccioli, M., Briskomatis, A., Sabattini, E., Ascani, S., Santini, D., Piccaluga, P.P., Leone, O., Damiani, S., Ercolessi, C., Sandri, F., Pieri, F., Leoncini, L., and Falini, B. 1997. Antigen retrieval techniques in immunohistochemistry: Comparison of different methods. *J. Pathol. 183*:116–123.

Press, M.F., Hung, G., Godolphin, W., and Slamon, D.J. 1994. Sensitivity of HER-2/neu antibodies in archival tissue samples: Potential source of error in immunohistochemical studies of oncogene expression. *Cancer Res. 54*:2771–2777.

Raab, S.S. 2000. The cost-effectiveness of immunohistochemistry. *Arch. Pathol. Lab. Med. 124*:1185–1191.

Reynolds, G.J. 1989. External quality assurance and assessment in immunocytochemistry. *Histopathology 15*:627–633.

Rhodes, A., Jasani, B., Balaton, A.J., Barnes, D.M. and Miller, K.D. 2000a. Frequency of oestrogen and progesterone receptor positivity by immunohistochemical analysis in 7016 breast carcinomas: Correlation with patient age, assay sensitivity, threshold value, and mammographic screening. *J. Clin. Pathol. 53*:688–696.

Rhodes, A., Jasani, B., Balaton, A.J., and Miller, K.D. 2000b. Immunohistochemical demonstration of oestrogen and progesterone receptors: Correlation of standards achieved on in house tumours with that achieved on external quality assessment material in over 150 laboratories from 26 countries. *J. Clin. Pathol. 53*:292–301.

Rhodes, A., Jasani, B., Barnes, D.M., Bobrow, L.G., and Miller, K.D. 2000c. Reliability of immunohistochemical demonstration of oestrogen receptors in routine practice: Interlaboratory variance in the sensitivity of detection and evaluation of scoring systems. *J. Clin. Pathol. 53*:125–130.

Rhodes, A., Jasani, B., Balaton, A.J., Barnes, D.M., Anderson, E., Bobrow, L.G., and Miller, K.D. 2001. Study of interlaboratory reliability and reproducibility of estrogen and progesterone receptor assays in Europe. *Am. J. Clin. Pathol. 115*:44–58.

Rhodes, A., Jasani, B., Anderson, E., Dodson, A.R., and Balaton, A.J. 2002. Evaluation of HER-2/neu immunohistochemical assay sensitivity and scoring on formalin-fixed and paraffin-processed cell lines and breast tumors: A comparative study involving results from laboratories in 21 countries. *Am. J. Clin. Pathol. 118*:408–417.

Roche, P.C., and Ingle, J.N. 1999. Increased HER2 with U.S. Food and Drug Administration-approved antibody. *J. Clin. Oncol. 17*:434.

Rüdiger, T., Höfler, H., and Müller-Hermelink, H.K. 1997. Ringversuch Immunhistochemie der Universitätsinstitute für Pathologie in Deutschland. *Pathologe 18*:262–272.

Rüdiger, T., Höfler, H., Kreipe, H.H., Nizze, H., Pfeifer, U., Stein, H., Dallenbach, F.E., Fischer, H.P., Mengel, M., von Wasielewski, R., and Müller-Hermelink, H.K. 2002. Quality assurance in immunohistochemistry: Results of an interlaboratory trial involving 172 pathologists. *Am. J. Surg. Pathol. 26*:873–882.

Shi, S.R., Cote, R.J., Yang, C., Chen, C., Xu, H.J., Benedict, W.F., and Taylor, C.R. 1996. Development of an optimal protocol for antigen retrieval: A 'test battery' approach exemplified with reference to the staining of retinoblastoma protein (pRB) in formalin-fixed paraffin sections. *Pathology 179*:347–352.

Shi, S.R., Cote, R.J., Young, L.L., and Taylor, C.R. 1997. Antigen retrieval immunohistochemistry: Practice and development. *J. Histotechnol. 20*:145–154.

Shi, S.R., Cote, R.J., Chaiwun, B., Young, L.L., Shi, Y., Hawes, D., Chen, T.Y., and Taylor, C.R. 1998. Standardization of immunohistochemistry based on antigen retrieval technique for routine formalin-fixed tissue sections. *Appl. Immunohistochem. 6*:89–96.

Shi, S.R., Cote, R.J., and Taylor, C.R. 2001. Antigen retrieval immunohistochemistry and molecular morphology in the year 2001. *Appl. Immunohistochemistrv Mol. Morphol. 9*:107–116.

Sompuram, S.R., Kodela, V., Zhang, K., Ramanathan, H., Radcliffe, G., Falb, P., and Bogen, S.A. 2002. A novel quality control slide for quantitative immunohistochemistry testing. *J. Histochem. Cytochem. 50*:1425–1434.

Swanson, P.E. 1999. Labels, disclaimers, and rules (oh, my!). Analyte-specific reagents and practice of immunohistochemistry. *Am. J. Clin. Pathol. 111*:445–448.

Sweep, C.G., and Geurts-Moespot, J. 2000. EORTC external quality assurance program for ER and PgR measurements: Trial

1998/1999. European Organisation for Research and Treatment of Cancer. *Int. J. Biol. Markers 15*:62–69.

Taylor, C.R. 1992. Report of the Immunohistochemistry Steering Committee of the Biological Stain Commission. Proposed format: Package insert for immunohistochemistry products. *Biotech. Histochem. 67*:323–338.

Taylor, C.R. 1994. An exaltation of experts: Concerted efforts in the standardization of immunohistochemistry. *Hum. Pathol. 25*:2–11.

Taylor, C.R., Shi, S.R., Chaiwun, B., Young, L., Imam, S.A., and Cote, R.J. 1994. Strategies for improving the immunohistochemical staining of various intranuclear prognostic markers in formalin-paraffin sections: Androgen receptor, estrogen receptor, progesterone receptor, p53 protein, proliferating cell nuclear antigen, and Ki-67 antigen revealed by antigen retrieval techniques. *Hum. Pathol. 25*:263–270.

Taylor, C.R. 1998a. Report from the Biological Stain Commission: FDA issues final rule for classification/reclassification of immunochemistry (IHC) reagents and kits. *Biotech. Histochem. 73*:175–177.

Taylor, C.R. 1998b. FDA issues final rule for classification/reclassification of immunochemistry reagents and kits. *Appl. Immunohistochemistry 6*:115–116.

Taylor, C.R. 2000. The total test approach to standardization of immunohistochemistry. *Arch. Pathol. Lab. Med. 124*:945–951.

Thomson, T.A., Hayes, M.M., Spinelli, J.J., Hilland, E., Sawrenko, C., Phillips, D., Dupuis, B., and Parker, R.L. 2001. HER-2/neu in breast cancer: Interobserver variability and performance of immunohistochemistry with 4 antibodies compared with fluorescent *in situ* hybridization. *Mod. Pathol. 14*:1079–1086.

Tubbs, R.R., and Stoler, M.H. 2000. The quality of Her-2/Neu predictive immunohistochemistry: Something FISHy? *Mod. Pathol. 13*:1–3.

Vincent-Salomon, A., MacGrogan, G., Couturier, J., Arnould, L., Denoux, Y., Fiche, M., Jacquemier, J., Mathieu, M.C., Penault-Llorca, F., Rigaud, C., Roger, P., Treilleux, I., Vilain, M.O., Mathoulin-Pelissier, S., and Le Doussal, V. 2003. Calibration of immunohistochemistry for assessment of HER2 in breast cancer: Results of the French multicentre GEFPICS study. *Histopathology 42*:337–347.

von Wasielewski, R., Mengel, M., Wiese, B., Rüdiger, T., Müller-Hermelink, H.K., and Kreipe, H. 2002. Tissue array technology for testing interlaboratory and interobserver reproducibility of immunohistochemical estrogen receptor analysis in a large multicenter trial. *Am. J. Clin. Pathol. 118*:675–682.

Weir, E.G., Partin, A.W., and Epstein, J.I. 2000. Correlation of serum prostate specific antigen and quantitative immunohistochemistry. *J. Urol. 163*:1739–1742.

Werner, M., Chott, A., Fabiano, A., and Battifora, H. 2000. Effect of formalin tissue fixation and processing on immunohistochemistry. *Am. J. Surg. Pathol. 24*:1016–1019.

Wetherington, R.W., Cooper, H.S., Al-Saleem, T., Ackerman, D.S., Adams-McDonnell, R., Davis, W., Ehya, H., Patchefsky, A.S., Suder, J., and Young, N.A. 2002. Clinical significance of performing immunohistochemistry on cases with a previous diagnosis of cancer coming to a national comprehensive cancer center for treatment or second opinion. *Am. J. Surg. Pathol. 26*:1222–1230.

Wick, M.R., Ritter, J.H., and Swanson, P.E. 1999. The impact of diagnostic immunohistochemistry on patient outcomes. *Clin. Lab. Med. 19*:797–814, vi.

Wick, M.R., and Mills, S.E. 2001. Consensual interpretive guidelines for diagnostic immunohistochemistry. *Am. J. Surg. Pathol. 25*:1208–1210.

Wick, M.R., and Swanson, P.E. 2002. Targeted controls in clinical immunohistochemistry: A useful approach to quality assurance. *Am. J. Clin. Pathol. 117*:7–8.

Wisecarver, J.L. 1999. HER-2/neu testing comes of age. *Am. J. Clin. Pathol. 111*:299–301.

Zafrani, B., Aubriot, M.H., Mouret, E., De Cremoux, P., De Rycke, Y., Nicolas, A., Boudou, E., Vincent-Salomon, A., Magdelenat, H., and Sastre-Garau, X. 2000. High sensitivity and specificity of immunohistochemistry for the detection of hormone receptors in breast carcinoma: Comparison with biochemical determination in a prospective study of 793 cases. *Histopathology 37*:536–545.

2

Methodology of Microarray Data Analysis

Xiaofeng Zhou, Hiroshi Egusa, Steven W. Cole, Ichiro Nishimura, and David T.W. Wong

Introduction

Microarrays have revolutionized biological research by allowing researchers to study the expression of thousands of genes simultaneously for the first time (DeRisi *et al.,* 1996; Schena *et al.,* 1995). Although biomedical investigators have quickly adopted this powerful new research tool, accurate analysis and interpretation of the data have presented an immense challenge in the fields of statistical science and data mining. To make matters worse, microarray technology has rapidly expanded from simply a ribonucleic acid (RNA) expression profiling method to many different applications, including genome-wide single nucleotide polymorphism (SNP) genotyping (Lindblad-Toh *et al.,* 2000a; Lindblad-Toh *et al.,* 2000b; Mei *et al.,* 2000), comparative genomic hybridization (CGH) (Albertson and Pinkel, 2003; Pollack *et al.,* 1999), and various types of protein arrays (Cahill and Nordhoff, 2003). A variety of data analysis tools have been developed to accommodate the various applications for microarray analysis. In this article, we survey some common analytical strategies for expression analysis, which can be potentially adapted to most microarray applications.

The major steps involved in microarray data analysis are as follows: 1) microarray image acquisition and raw data generation, 2) data normalization and transformation, 3) classification and exploratory data analysis, and 4) post-analysis follow-up and validation. The first step, microarray image acquisition and raw data generation, is heavily platform dependent. Regardless of the approach chosen, the arrays are scanned after hybridization. Independent grayscale images, typically 16-bit tiff (tagged information file format) files, are generated for each sample to be analyzed. Image analysis software is then used to identify arrayed spots and measure the relative fluorescence intensities for each element. There are many commercial and freely available software packages for image quantitation. (Go to microarray.genetics.ucla.edu/public/softwarelinks for a list of microarray analysis software.) Although there are differences between various imaging softwares, most give high-quality, reproducible measures of hybridization intensities.

For the purpose of our discussion, we will ignore the particular microarray platform used, the type of measurement reported (mean, median, or integrated intensity for various complementary deoxyribonucleic

Handbook of Immunohistochemistry and *in situ* Hybridization of Human Carcinomas, Volume 3: Molecular Genetics, Liver Carcinoma, and Pancreatic Carcinoma

acid [cDNA] microarray, or the average difference for Affymetrix GeneChips), the background correction performed, or spot-quality assessment and trimming used. As our starting point, we will assume that for each biological sample we assay, we have a high-quality measurement of the intensity of hybridization for each gene element on the array.

Microarray Data Normalization and Transformation

The hypothesis underlying microarray analysis is that the measured intensity for each gene element on the array represents its relative expression level. Biologically relevant expression patterns usually are compared between different states on a gene-by-gene basis. However, before the expression levels can be compared appropriately, a number of transformations must be carried out on the data to eliminate questionable or low-quality measurements and to adjust the measured intensities to facilitate comparisons (Quackenbush, 2002).

Expression Ratios

Most microarray experiments investigate the relative differences in gene expression, and a straightforward approach to this problem involves screening genes based on the ratio of their expression intensity across samples. Although ratios provide an intuitive measure of expression changes, they have the disadvantage of treating up- and down-regulated genes differently. Genes that up-regulated by a factor of 2 have an expression ratio of 2, whereas those down-regulated by the same factor have an expression ratio of (–0.5). The most widely used alternative transformation of the ratio is the logarithm base 2, which has the advantage of producing a continuous spectrum of values and treating up- and down-regulated genes in a similar fashion: $\log_2(1) = 0$, $\log_2(2) = 1$, $\log_2(1/2) = -1$, $\log_2(4) = 2$, $\log_2(1/4) = -2$, and so on. This log transformation treats the expression ratios (or their reciprocals) symmetrically, so that a gene up-regulated by a factor of 2 has a $\log_2$(ratio) of 1, a gene down-regulated by a factor of 2 has a $1\log_2$(ratio) of −1, and a gene expressed at a constant level (with a ratio of 1) has a $\log_2$(ratio) equal to zero. Most statistical analyses of differential expression rely on log-transformed intensity values. Log transformation should only be carried out after noise-suppression measures are taken (because measurement error is often linear in the original assay metric but not in the logfold change metric).

Normalization

A critical step for microarray data analysis is normalization, which adjusts the individual hybridization intensities to balance them appropriately so that meaningful biological comparisons can be made. There are a number of reasons why data must be normalized, including unequal quantities of starting RNA, differences in labeling, hybridization, or detection efficiencies between the fluorescent dyes used, and systematic biases in signal measurement accuracy and sensitivity. Conceptually, normalization is similar to adjusting expression levels measured by northern analysis or quantitative real-time polymerase chain reaction (PCR) relative to the expression of one or more housekeeping genes whose levels are assumed to be constant between samples. Many approaches have been used for microarray normalization, including total intensity-based normalization, Lowess normalization, model-based normalization, linear regression analysis (Chatterjee and Price, 1991), log centering, rank invariant methods (Tseng *et al.,* 2001), and ratio statistics (Chen *et al.,* 1997; Chen *et al.,* 2002). We will describe the three most commonly used methods here: total intensity-based normalization, Lowess normalization, and model-based normalization.

Total Intensity-Based Normalization

Total intensity-based normalization is the most common normalization approach, and it is based on several simple assumptions. The first is that we are starting with equal quantities of RNA for the two (or more) samples to be compared. Given that there are millions of individual RNA molecules in each sample, we will assume that the average mass of each molecule is approximately the same, and that, consequently, the number of molecules in each sample is also the same. The second assumption is that the arrayed elements represent a random sampling of the genes in the genome. This is important because we will also assume that the arrayed elements randomly interrogate the two RNA samples. If the arrayed genes are selected to represent only those we know will change, then we will likely oversample or undersample the genes in one of the samples being compared. If the array contains a large enough assortment of random genes, we do not expect to see such bias. This is because for a finite RNA sample, when representation of one RNA species increases, representation of other species must decrease. Consequently, approximately the same number of labeled molecules from each sample should hybridize to the arrays; therefore, the total hybridization intensities summed over all elements in the arrays should be the same for each sample.

There are many variations for this type of normalization, including scaling the individual intensities so that the mean or median intensities are the same within a single array or across arrays or using a select subset of the arrayed genes rather than the entire collection. One common approach is z-transformation, which not only equalizes the mean of each array but also equalizes the magnitude of variability of individual probe values about that mean. A variant of this approach is to analyze data in the context of an analysis of variance (ANOVA) statistical model that explicitly estimates and removes such differences (Kerr *et al.,* 2000; Kerr and Churchill, 2001). Some investigators also normalize observations of each gene to have the same mean (and standard deviation). This type of normalization is implicit in the use of Pearson correlation coefficients as a "similarity measure" for class discovery analyses. However, for reasons discussed in the following, normalization within genes can actually decrease the signal-to-noise ratio in the dataset as a whole. If gene-specific normalizations are applied, it is critical to ensure that they do not have the effect of equating large biological changes with random noise.

Lowess Normalization

The advantage of Lowess normalization is that it takes systematic biases into consideration. Lowess normalization assumes that the dye bias is dependent on spot intensity. Several reports have indicated that the $\log_2$(ratio) values can have a systematic dependence on intensity (Yang *et al.,* 2002a; Yang *et al.,* 2002b), which most commonly appears as a deviation from zero for low-intensity spots. The easiest way to visualize intensity-dependent effects, and the starting point for the Lowess analysis described here, is to plot the measured $\log_2(R_i/G_i)$ for each element on the array as a function of the $\log_{10}(R_i*G_i)$ product intensities (R-I plot), where G_i and R_i are the measured green and red intensities for the array element in a two-color microarray assay. This "R-I" plot can reveal intensity-specific artifacts in the $\log_2$(ratio) measurements. Locally weighted linear regression (Lowess) analysis has been proposed (Kepler *et al.,* 2002; Yang *et al.,* 2002a; Yang *et al.,* 2002b) as a normalization method that can remove such intensity-dependent effects in the $\log_2$(ratio) values.

Model-Based Normalization

Another popular form of normalization is model-based normalization (model-based expression analysis), which applies a theoretical statistical model to raw fluorescence intensity data in an attempt to infer the true quantity of biological signal (e.g., messenger RNA, or mRNA, concentration). The D-Chip statistical software (Li and Wong, 2003) pursues this approach with high-density oligonucleotide data. Model-based normalization takes into account both global differences across arrays and individual characteristics of the set of probes measuring a specific mRNA target on each array to estimate the true target quantity and remove noise.

All types of normalization are aimed at increasing the signal-to-noise ratio by removing extraneous sources of variance such as instrumentation noise or systematic individual differences across sample donors in biological characteristics. However, no normalization is guaranteed to succeed in this mission, and some methods can actually decrease the signal-to-noise ratio if applied recklessly. It is easy to determine whether normalization has been helpful. If the normalized data show greater consistency across replicates than do the original expression values, normalization has achieved its goals. To determine whether consistency has increased, one can simply compute a correlation between replicate measures for the same experimental condition. In differential expression studies (discussed later), analysis seeks to identify *differences* in gene expression across conditions, and a successful normalization would increase the correlation between measures of that difference across replicate observations. Standardizing data within genes is an example of a normalization that can sometimes decrease the signal-to-noise ratio in the dataset as a whole because this method can equate the magnitude of variation in genes showing only small amounts of absolute variability (likely resulting from noise) with those showing very significant biological changes. Another problem that can arise in normalization is the loss of resolution, particularly at the low end of the expression spectrum in which the majority of genes reside. Excessive normalization can prevent statistical analyses from discovering changes even when they are clearly present in the original data and independently verifiable by nonmicroarray technologies (Cole *et al.,* 2003). Thus all normalizations should be reviewed to ensure that they have succeeded in increasing the signal-to-noise ratio.

Array Element Filtering

If one examines several representative R-I plots, it becomes obvious that the variability in the measured $\log_2$(ratio) values increases as the measured hybridization intensity decreases. This is not surprising because relative error increases at lower intensities, where the signal approaches background. One solution is to use only array elements with intensities with a statistically significant difference from the background. If we measure the average local background near each array

element and its standard deviation, we would expect 95.5% confidence that good elements would have intensities more than two standard deviations above the background. By keeping only array elements that are significantly above the background, we can increase the reliability of measurements. However, this approach may sometimes be too conservative and can needlessly exclude data from analysis. Another solution is to directly estimate the lower bound of reliability in a data set and then raise all values below that level up to this new "floor" value. This approach suppresses noise without excluding data. Software is now available for finding reliability floors (Cole *et al.,* 2003).

A different problem can occur at the high end of the intensity spectrum, where the array elements saturate the detector used to measure fluorescence intensity. Once the intensity approaches its maximum value, comparisons are no longer meaningful because the array elements become saturated and intensity measurements cannot go higher. There are a variety of approaches to deal with this problem as well, including eliminating saturated pixels in the image-processing step or setting a maximum acceptable value ("ceiling") for each array element. Again, software is available for estimating ceiling values based on observed data (Cole *et al.,* 2003).

Classification and Exploratory Data Analysis

The classification and exploratory data analysis is the most challenging step for extracting reliable and interpretable biological information from tens of thousands of microarray data points. Many different statistical approaches have been proposed for carrying out this critical step, but no single approach is appropriate for all purposes. Which strategy is most effective depends heavily on the goals of analysis.

The most common study objectives can be subgrouped into three categories: class comparison, class prediction, and class discovery (Simon *et al.,* 2003). Class comparison, or differential expression analysis, is the comparison of gene expression in different groups of samples. The major characteristic of class comparison studies is that the classes being compared are defined independently of the expression profiles. The specific objectives of such a study are to determine whether the expression profiles are different between the classes and, if so, to identify the differentially expressed genes. One example of a class comparison study is the comparison between gene expression profiles in breast cancer patients with and without germline BRCA1 mutations (Hedenfalk *et al.,* 2001).

Class prediction studies are similar to class comparison studies in that the classes are predefined. However, in class prediction studies, the emphasis is on generating an expression-based multivariate function (referred to as the predictor) that accurately predicts the class membership of a new sample on the basis of the expression levels of key genes. Such predictors can be used for guiding many clinical decisions, such as risk assessment, diagnostic testing, prognostic stratification, and treatment selection. Many studies include both class comparison and class prediction objectives.

Class discovery is fundamentally different from class comparison or class prediction in that no classes are predefined. Usually the purpose of class discovery in cancer studies is to determine whether discrete subsets of a disease entity can be defined on the basis of gene expression profiles. This purpose is different from determining whether the gene expression profiles correlate with some already-known diagnostic classification. Examples of class discovery are the studies by Bittner *et al.* (Bittner *et al.,* 2000) that examined gene expression profiles for advanced melanomas and by Alizadeh *et al.* (Alizadeh *et al.,* 2000) that examined the gene expression profiles of patients with diffuse large B-cell lymphoma. Often the purpose of class discovery is to identify clues regarding the heterogeneity of disease pathogenesis.

Statistical methods will be described here for all three objective categories, class comparison, class prediction, and class discovery.

Class Comparison

One approach for class comparison commonly used in the early microarray studies was a simple fold difference approach, in which a gene is declared to have changed significantly if its average expression level varies by more than a constant factor, typically twofold, between different groups of biological samples (Schena *et al.,* 1995). This approach was replaced quickly with more sophisticated approaches simply because such a "twofold rule" is unlikely to yield optimal results. A factor of 2 can have quite different significance and meaning in different regions of the spectrum of expression levels, especially at the very high and very low ends. In a noisy environment, 2000/1000 or 2/1 can have a quite different significance. Small random fluctuations are much more likely to produce a change from 1 to 2 than from 1000 to 2000.

Another method of identifying differentially expressed genes is to use a t-test, a test for a difference between two means based on t distribution. The significance analysis of microarrays (SAM) is one such implementation

using a t-test (Tusher *et al.,* 2001) (www-stat.stanford.edu/~tibs/SAM/index.html). SAM identifies genes with statistically significant changes in expression by assimilating a set of gene-specific t-tests. Each gene is assigned a score on the basis of its change in gene expression relative to the standard deviation of repeated measurements for that gene. Genes with scores greater than a threshold are deemed potentially significant. SAM uses permutations of the repeated measurements to estimate the percentage of genes identified by chance, the false discovery rate (FDR). The threshold can be adjusted to identify smaller or larger sets of genes, and FDRs are calculated for each set. As demonstrated by the study of Tusher *et al.* (2001) SAM outperforms the fold difference–based approach for identifying genes with true changes in expression (Figure 1).

One potential problem with the t-test for array data, however, is that the repetition numbers are often small because experiments remain costly or tedious to repeat. It is difficult to obtain accurate estimates of the standard deviation of individual gene measurements based on only a few measurements. However, it has been observed that an overall reciprocal relationship exists between variance and gene expression levels and that genes expressed at similar levels exhibit similar variance (Hatfield *et al.,* 2003). Therefore, it is possible to use this prior knowledge in a Bayesian statistical framework to obtain more robust estimates of variance for any gene by examining the expression levels of other genes in the same expression neighborhood within a single experiment (Baldi and Long, 2001; Long *et al.,* 2001). This approach supplements the weak empirical estimates of single-gene variances across a small number of replicates, with more robust estimates of variance obtained by pooling genes with similar expression levels. The CyberT program is an example of this regulated t-test implementation (www.igb.uci.edu). The alternative is to use a strict frequentist approach, in which the estimate of the standard deviation is compromised by the limited number of measurements of each gene that is typical of DNA microarray experiments.

All approaches based on the t-test assume that the investigator is seeking genes with a large signal-to-noise ratio, in the sense that the magnitude of change between conditions is large relative to the magnitude of variability among observations from the same conditions (this is exactly the quantity measured by a t-test statistic). However, many biologists are not so concerned with signal-to-noise ratios *per se* as with the likelihood that a specified change will be reproducible in future experiments. For example, consider a gene showing a 3-fold, 30-fold, and 300-fold increase across three replicated comparisons of healthy and tumor tissue.

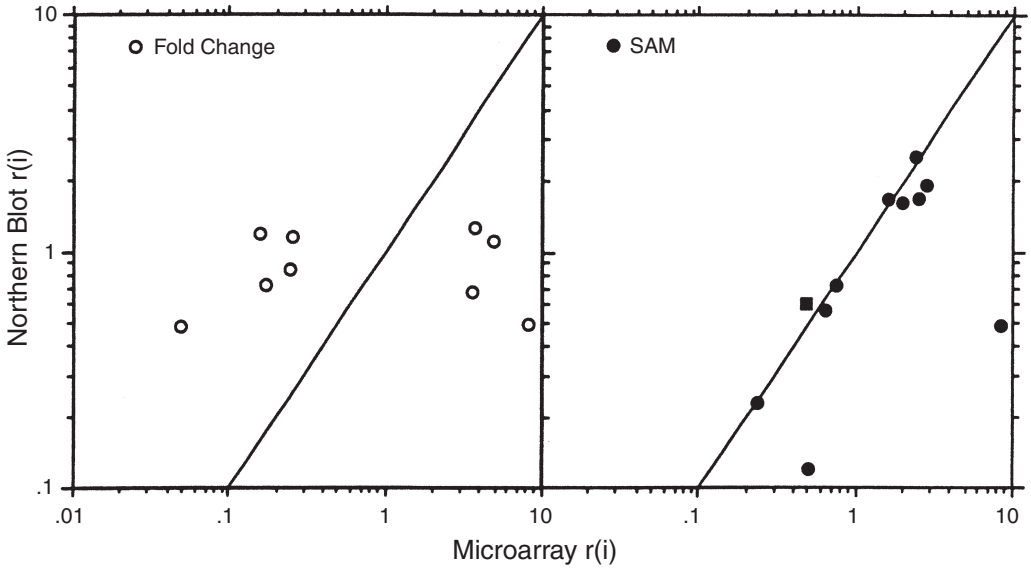

Figure 1. Performance comparison of fold difference approach and t-test–based approach (SAM) for class comparison. Genes showing significant changes between treated and untreated samples were identified by either fold change method or SAM (significance analysis of microarrays). Northern Blots were performed on those genes to validate the fold changes for the identified genes. The expression ratio of treated and untreated samples for each gene was calculated separately using Northern Blot data and microarray data. These ratios were plotted for genes identified by the fold change method (*left*) and SAM (*right*). The straight lines indicate the position of exact agreement between Northern Blot and microarray results. From Tusher *et al.,* 2001.

Most biologists would be very interested in this gene because it consistently shows a large change in expression. However, the magnitude of variability in the change (noise) is very large, and a t-test would not identify this gene as showing statistically significant change (because the average signal is large, but the noise is even larger, so the signal-to-noise ratio is comparatively small). Many microarray data sets do in fact show this sort of qualitiative consistency in the absence of quantitative consistency. To capture qulitatively consistency change that show high variability across samples, one approach is to estimate the lower bound of expected change rather than the mean change (as estimated by the t-test). Instead of using signal-to-noise ratios to distinguish reliable changes from noise, one implementation of this approach used raw fluroscence intensity changes to determine which fold-change results are trustworthy (Cole *et al.,* 2003). This approach captures differentially expressed genes more efficiently than do other methods based on the t-test and related signal-to-noise measures, and it thus reduces the likelihood that biologically significant changes in expression will be overlooked by statistical analyses.

Class Prediction

Class prediction refers to the assignment of particular tumor samples to already-defined classes, which could reflect current states or potential future outcomes. Because it is likely that these predictions will affect clinical decisionmaking, these studies must be performed with statistical rigor and reported clearly with unbiased statistics. One of the most common errors in microarray analysis is the use of cluster analysis and simple fold-change statistics for class prediction and class comparison (Simon *et al.,* 2003). Although cluster analysis is appropriate for class discovery, it is generally not effective for class comparison or class prediction. Cluster analysis is considered an unsupervised method because no information about sample grouping is used. The distance measures are generally computed with regard to the complete set of genes represented on the array that are measured with sufficiently high signals or with regard to all genes that show meaningful variation across the sample set. Because relatively few genes may distinguish any particular class, the distances used in cluster analysis will often not reflect the influence of these relevant genes. This feature accounts for the poor results often obtained in attempting to use cluster analysis for class prediction studies. It is more appropriate to use a supervised method (i.e., one that makes distinctions among the specimens on the basis of predefined class label information) than an unsupervised method, such as cluster analysis (Simon *et al.,* 2003). Supervised class prediction is usually based on the assumption that a collection of differentially expressed genes is associated with class distinction.

The first step toward constructing the class predictor (or classifier) is to select the subset of informative genes. Various class comparison methods described in the previous section can be used here. Once the informative genes are defined, the relative weights correlating to the individual predictive strengths will be assigned to these informative genes. Many methods have been developed for defining a multivariate predictor (Dudoit *et al.,* 2002). A commonly used strategy is based on linear combinations of the weighted intensity measurements of the informative genes (Golub *et al.,* 1999; Radmacher *et al.,* 2002). This procedure uses a fixed set of "informative genes" and makes a prediction on the basis of the expression level of these genes in a new sample. For example, in the study by Golub *et al.,* this weighted votes approach was used to predict patients with acute myeloid leukemia (AML) or acute lymphoblastic leukemia (ALL) (Golub *et al.,* 1999) (Figure 2). Each informative gene casts a "weighted vote" for one of the classes, with the magnitude of each vote dependent on the expression level in the new sample and the degree of that gene's correlation with the class distinction. The votes are summed to determine the winning class, as well as "prediction strength" (PS), which is a measure of the margin of victory that ranges from 0 to 1. The sample is assigned to the winning class if PS exceeded a predetermined threshold and is otherwise considered uncertain.

One alternative method to assign weights related to the individual predictive strengths of these informative genes is to use a dimension reduction technique such as principal components analysis or partial least squares on the informative genes and to base the prediction on the resulting factors (Khan *et al.,* 2001; Nguyen and Rocke, 2002; West *et al.,* 2001). In a careful comparison of alternative class prediction tools, Dudiot and colleagues demonstrated that relatively simple strategies such as linear discriminant function analysis (linear regression) or diagonal discriminant function analysis (similar to the weighted voting scheme outlined earlier) generally outperform more complex and intensive statistical techniques (Dudoit *et al.,* 2002).

Validation of the prediction model is essential because the prediction model generated by supervised methods is invariably more accurate for the data set used to generate the model than it would be with new data. Methods for obtaining unbiased estimates of a

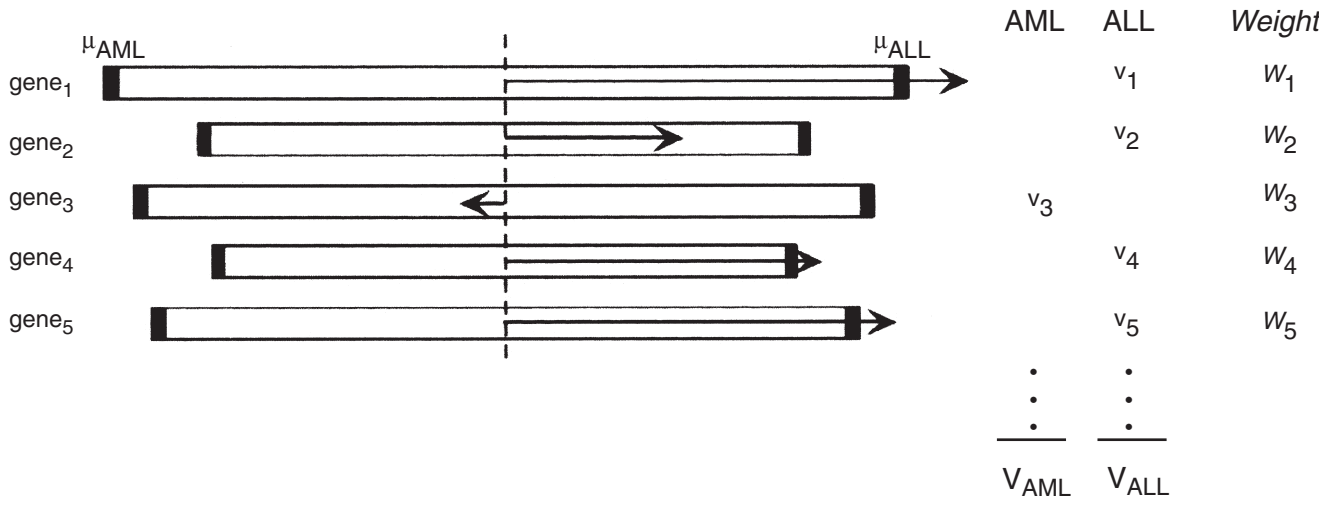

Figure 2. Prediction of acute myeloid leukemia (AML) or acute lymphoblastic leukemia (ALL) using "weighted votes." A set of informative genes is first identified that are more highly correlated with the AML–ALL class distinction than would be expected by chance. The prediction of a new sample is based on "weighted votes" of this set of informative genes. Each gene (g_i) votes for either AML or ALL, depending on whether its expression level x_i in the sample is closer to μ_{AML} or μ_{ALL} (which denote, respectively, the mean expression levels of AML and ALL in a set of reference samples). The magnitude of the vote is $w_i v_i$, where w_i is a weighting factor that reflects how well the gene is correlated with the class distinction and $v_i = |X_i - (\mu_{AML} + \mu_{ALL})/2|$ reflects the deviation of the expression level in the sample from the average of μ_{AML} and μ_{ALL}. The votes for each class are summed to obtain total votes V_{AML} and V_{ALL}. The sample is assigned to the class with the higher vote total, provided that the prediction strength exceeds a predetermined threshold. The prediction strength reflects the margin of victory and is defined as $(V_{win} - V_{lose})/(V_{win} + V_{lose})$, where V_{win} and V_{lose} are the respective vote totals for the winning and losing classes. From Golub *et al.,* 1999.

predictor's error rate include leave-one-out cross-validation or application to an independent data set. By using these techniques, it is possible not only to evaluate the possibility of overfitting the predictor but also to compare various prediction methods and to assess which are less prone to overfitting.

Class Discovery

A general question facing researchers is how to organize observed data into a meaningful structure. For example, biologists need to organize the different species of animals before a meaningful description of the differences between animals is possible. According to the modern system used in biology, humans belong successively to the primates, the mammals, the amniotes, the vertebrates, and the animals. In this classification, the higher the levels of aggregation, the less similar the members in the respective class. Humans have more in common with all other primates (e.g., apes) than they do with the more "distant" members of the mammals (e.g., dogs), etc. This classification structure is a cluster, which can be applied for class discovery. For the purpose of class discovery based on microarray data, clustering is defined as grouping together objects (genes or samples) with similar properties (Eisen *et al.,* 1998). This can also be viewed as the reduction of the dimensionality of the system. Clustering is not a new technique; many algorithms have been developed for it, and many of these algorithms have been applied to microarray studies for class discovery. Examples of using clustering techniques for class discovery include the studies by Bittner *et al.* (2000) that examined gene expression profiles for advanced melanomas and by Alizadeh *et al.* (2000) that examined the gene expression profiles of patients with diffuse large B-cell lymphoma. The two major styles of clustering algorithms, hierarchical and *k*-means clustering, and self-organizing maps have all been used for clustering expression profiles.

Hierarchical Clustering

Hierarchical clustering is an agglomerative approach in which the closest elements in the data set are joined to form groups, which are further joined until the process has been carried to completion, forming a single hierarchical tree. This method is also referred to as joining or tree clustering. Once the tree is constructed, the data can be partitioned into any number of clusters by cutting the tree at the appropriate level.

The process of hierarchical clustering proceeds in a simple manner. First, the pairwise distance matrix is calculated for all genes to be clustered. Second, the

distance matrix is searched for the two most similar genes or clusters; initially each cluster consists of a single gene. This is the first true stage in the "clustering" process. If several pairs have the same separation distance, a predetermined rule is used to decide between alternatives. Third, the two selected clusters are merged to produce a new cluster that now contains at least two objects. Fourth, the distances are calculated between this new cluster and all other clusters. There is no need to calculate all distances because only those involving the new cluster have changed. Last, steps 2–4 are repeated until all objects are in one cluster.

Three common options for hierarchical clustering are single linkage, average linkage, and complete linkage. These options differ in their definition of the distance between two clusters. Single linkage defines the distance between clusters as the minimum distance over all pairs. Average linkage takes the average distance over all pairs, and complete linkage uses the maximum distance over all pairs. Each of these options will produce slightly different results, as will any of the algorithms if the distance metric is changed. Single linkage often produces large, elongated clusters (Butte and Kohane, 2000). Complete linkage finds small, compact clusters that do not exceed some diameter threshold. The threshold value is determined by the level at which the tree is cut. Average linkage is sometimes used as a compromise between the other two options and gives acceptable results typically for gene-expression data (Eisen *et al.,* 1998). Figure 3 shows an example of hierarchical clustering on 31 melanoma samples. This hierarchical dendrogram demonstrates that 19 samples are tightly clustered at the bottom of the dendrogram in the area of highest similarity, which may represent a subset of melanoma (Bittner *et al.,* 2000).

One alterative type of hierarchical clustering, the two-way clustering, is particularly interesting. The hierarchical clustering usually focuses on cases (patients) or variables (genes). It turns out that the clustering of both may yield useful results. For example, imagine a study in which a researcher has generated microarray data on differential expressed genes (variables) for a group of patients with cancer (cases). The researcher may want to cluster cases (patients) to detect clusters of patients with similar syndromes. At the same time, the researcher may want to cluster variables (genes) to detect clusters of measures that appear to tap similar physical abilities. A good example of using this two-way clustering is illustrated in the study on tumor and normal colon tissues by Alon *et al.* (1999).

Hierarchical clustering has become one of the most widely used techniques for class discovery based on gene-expression data because it is a simple process and the result can be easily visualized (Eisen and Brown, 1999). The first report by Wen *et al.* (1998) uses clustering and data-mining techniques to analyze large-scale gene-expression data. This report is significant in that it shows how integrating results obtained by using various distance metrics can reveal different but meaningful patterns in the data. Eisen *et al.* (1998) also make an elegant demonstration of the power of hierarchical clustering in the analysis of microarray data.

However, there are several problems with the ability to adequately describe the data. The decision to include a pair of genes in the same cluster is based only on a specific distance between them (introduced to quantitatively characterize the degree of coregulation), and any such decision is final. The local nature of this decision rule often inhibits the algorithm's ability to find a global structure. Also, the hierarchical trees are more suited for the description of real hierarchical relationships (e.g., evolutionary processes), although there is no evidence for the existence of such relationships in the biological functions of different genes. The expression vector that represents the cluster might no longer represent any of the genes in the cluster as the clusters grow in size. Consequently, as clustering progresses, the actual expression patterns of the genes themselves become less relevant. In addition, if a bad assignment is made early in the process, it cannot be corrected. Furthermore, the resulting structure is complex and there is no general agreement on how to choose the location for cutting the tree.

An alternative, which avoids these artifacts, is to use a divisive clustering approach, such as *k*-means or self-organizing maps, to partition data (either genes or experiments) into groups that have similar expression patterns.

k-Means Clustering

If there is advance knowledge about the number of clusters that should be represented in the data, *k*-means clustering is a good alternative to hierarchical methods. The *k*-means algorithm (Herzel *et al.,* 2001; Tavazoie *et al.,* 1999) is a nonhierarchical clustering technique (a divisive clustering approach). In this clustering technique, objects are partitioned into a fixed number (k) of clusters, so that the clusters are internally similar but externally dissimilar.

The *k*-mean clustering algorithm is a conceptually simple three-step process but can be computationally intensive. In the first step, the algorithm randomly assigns all training data to one of k clusters (where k is specified by the user). In the second step, the mean intercluster and intracluster distances are calculated. The third step is an iterative step, and its goal is to minimize the mean intercluster distances, maximize intracluster distances, or both, by moving data from

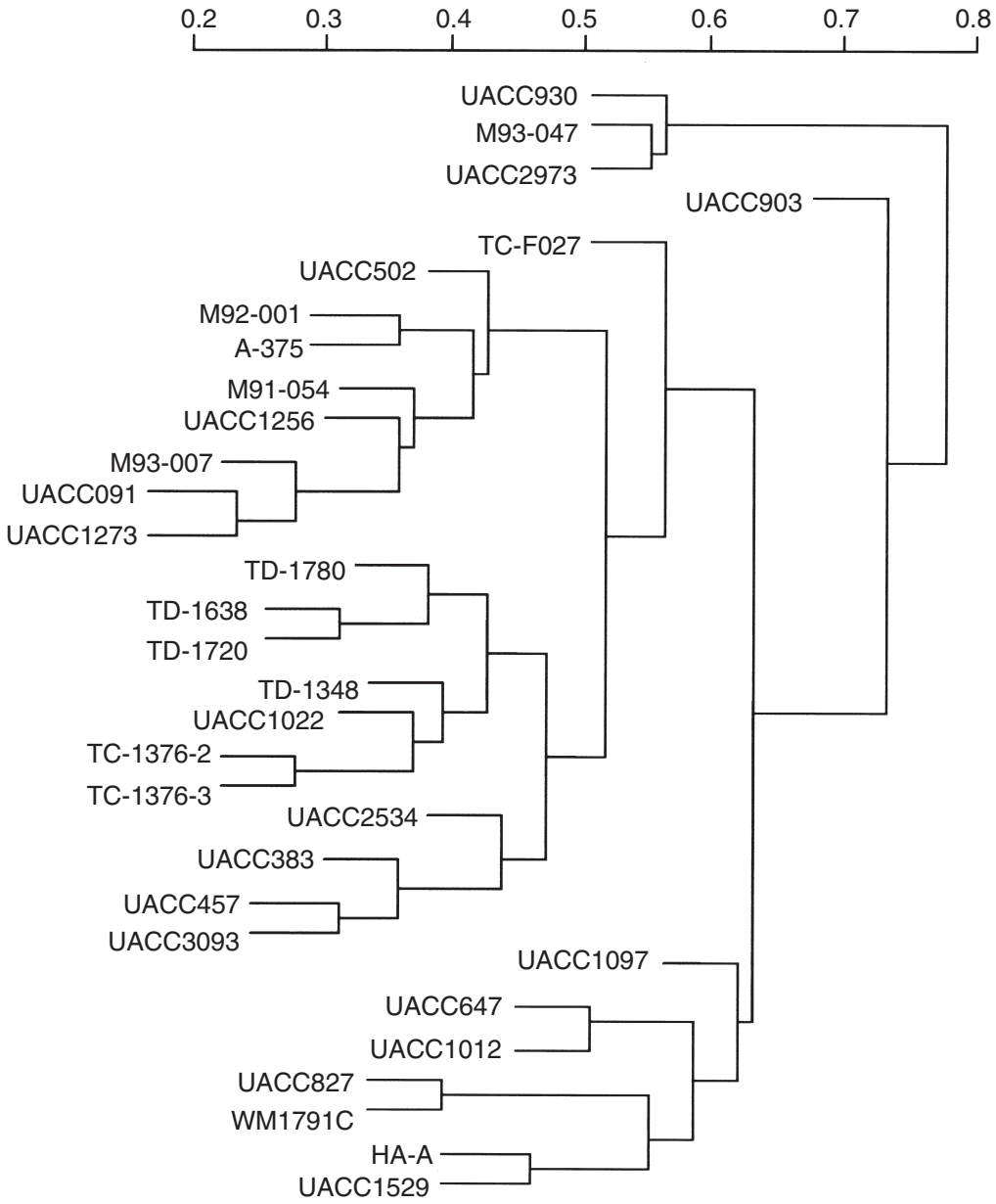

Figure 3. Hierarchic clustering dendrogram on 31 cutaneous melanoma samples based on overall expression pattern measured by microarray analysis. From Bittner *et al.,* 2000.

one cluster to another. In each iteration, one piece of data is moved to a new cluster where it is closest to the mean vector of the new cluster. After each move, new expression vectors for the two affected classes are recalculated. This process continues until any further move would increase the mean intercluster means (expression variability for each cluster) or reduce intracluster distances.

An advantage of the *k*-means algorithm is that, because of its simplicity, it can be used in a variety of applications. For instance, a recent variant of the *k*-means clustering algorithm designed specifically for the assessment of gene spots (on the array images) is the work of Bozinov and Rahnenfuhrer (2002). This technique is based on clustering pixels of a target area into foreground and background clusters. *k*-means clustering is particularly useful with techniques such as principal component analysis (PCA). PCA allows a visual estimation of the number of clusters represented in the data. This can be used to specify *k* and to group genes (or experiments) into related clusters.

The major disadvantage of this method is that the number *k* is often not known in advance. Another potential problem with this method is that, because each

gene is uniquely assigned to some cluster, it is difficult for the method to accommodate a large number of stray data points, intermediates, or outliers. Additional concerns about the algorithm have to do with the biological interpretation of the final clustered data from the algorithm. Despite these difficulties, *k*-means clustering results often show more stability across repeated experiments than do other class discovery tools.

Self-Organizing Maps

A self-organizing map (SOM) is a neural-network–based divisive clustering approach (Kohonen, 2001). Neural networks are analytic techniques modeled after the processes of learning in cognitive systems and the neurologic functions of the brain. Neural networks use a data "training set" to build rules capable of making predictions or classifications on data sets. A SOM assigns genes to a series of partitions on the basis of the similarity of their expression vectors to reference vectors that are defined for each partition. It is the process of defining these reference vectors that distinguishes SOMs from *k*-means clustering. Before initiating the analysis, the user defines a geometric configuration for the partitions, typically a two-dimensional rectangular or hexagonal grid. Random vectors are generated for each partition, but before genes can be assigned to partitions, the vectors are first "trained" using an iterative process that continues until convergence occurs so that the data are most effectively separated.

First, random vectors are constructed and assigned to each partition. Second, a gene is chosen at random, and, using a selected distance metric, the reference vector that is closest to that gene is identified. Third, the reference vector is then adjusted so that it is more similar to the vector of the assigned gene. The reference vectors that are located nearby on the two-dimensional grid are also adjusted so that they are more similar to the vector of the assigned gene. Fourth, steps 2 and 3 are iterated several thousand times, decreasing the amount by which the reference vectors are adjusted and increasing the stringency used to define closeness in each step. As the process continues, the reference vectors converge to fixed values. Finally, the genes are mapped to the relevant partitions depending on the reference vector to which they are most similar.

Several groups have used SOMs to investigate patterns in gene expression data (Golub *et al.,* 1999; Tamayo *et al.,* 1999; Toronen *et al.,* 1999). SOMs have the distinct advantage that they allow *a priori* knowledge to be included in the clustering process. In choosing the geometric configuration for the clusters, the user is effectively specifying the number of partitions into which the data is to be divided. Tamayo *et al.* propose that SOMs are ideally suited for exploratory data analysis, allowing one to impose partial structure on the clusters (in contrast to the rigid structure of hierarchical clustering, the strong prior hypotheses used in Bayesian clustering, and the nonstructure of *k*-means clustering) and facilitating easy visualization and interpretation (Tamayo *et al.,* 1999).

The most prominent disadvantage of the SOM approach is that it is difficult to know when to stop the algorithm. If the map is allowed to grow indefinitely, the size of the SOM is gradually increased to a point where clearly different sets of expression patterns are identified. Therefore, as with *k*-means clustering, the user has to rely on some other source of information, such as PCA, to determine the number of clusters that best represents the available data. For this reason, Sasik and his colleagues believe that SOM, as implemented by Tamayo *et al.* (1999), is essentially a restricted version of *k*-means (Sasik *et al.,* 2001).

Underlying all the class discovery techniques presented here is the problem of the "basis" for clustering. Class discovery tools group genes (or cases) based on a similarity score quantifying the consistency between each gene's profile of expression across cases (or each case's profile of expression across genes) and that profile of expression for all other genes (or cases). The definition of this similarity score profoundly affects the eventual "solution" derived by class discovery algorithms, but there is no clear consensus on which similarity metric is most appropriate. Broadly speaking, there are two basic possibilities. One is a "scalefree" representation that standardizes the mean and variance of data from each gene (or case) before comparing that scalefree profile with all other scalefree profiles. In many class discovery programs, a Pearson or Separman correlation coefficient is used by default as the similarity metric, and this implicitly invokes the scalefree approach. Under this approach, random noise can be inflated to a magnitude comparable to significant biological changes unless careful noise suppression is applied before analysis. Because microarrays survey so many genes, although comparatively few are expressed in any given sample, there is ample opportunity for noise to generate spurious results that subsequently detract from the replicability of results. The alternative is to retain information about the variance of observations on each gene, in which case noise influences are effectively reduced, but the eventual class discovery solution is dominated by the distinction between highly expressed genes and those expressed at low levels. Most researchers have used the scalefree approach, but this approach will produce reliable classes only if noise is fully suppressed before analysis (e.g., by floor/ceiling

analyses). Even then, general class definitions may be stable, but the specific genes included in each class can vary substantially across repeated experiments.

Postanalysis Follow-Up and Validation of Microarray Data

Validation is essential for microarray-based experiments. It has been proposed that at least two important questions need to be considered when evaluating microarray data (Chuaqui *et al.,* 2002). First, is the microarray data valid? Second, do the data or the model systems based on those data fundamentally describe the phenomenon being investigated? The postanalysis validation will serve as the quality-check step and provide feedback information for refining the model system generated based on microarray data.

Validation of the Experimental Data

Validation of the microarray expression data is essential. Some researchers have considered performing the data validation step even before advanced data analysis (such as classification and exploratory data analysis), so that only the validated data will be used for classification. However, in most microarray studies, validation before classification involves a lot more genes than does validation after the classification. This is because the classification step is a data reduction step that only keeps the highly informative genes that contribute to the classification. There are two approaches for independent confirmation of microarray data: *in silico* analysis and laboratory-based analysis. The *in silico* approach has been reviewed previously; it compares array results with information available in the literature and in public or private expression databases and provides the opportunity to validate data without further experimentation (Chuaqui *et al.,* 2002).

Laboratory-based validation provides independent, experimental verification of gene-expression levels and typically begins with the same samples that were studied in the microarray experiment. The methodology used varies depending on the scientific question, but commonly used techniques include quantitative reverse transcription (RT)–PCR, Northern Blot, ribonuclease protection assay, and *in situ* hybridization or immunohistochemistry using tissue microarrays. Quantitative RT-PCR is the choice of many for quantitatively measuring specific mRNAs because, once established, the method is fast, accurate, reproducible, and relatively inexpensive and requires a minimal amount of starting template (Rajeevan *et al.,* 2001; Walker, 2002).

Validation of the Model Generated from Microarray Data

Many gene-expression profiling studies in human cancers attempt to build predictors (prediction models) of patient prognosis and response to therapy (Rosenwald *et al.,* 2002; Shipp *et al.,* 2002). Because it is likely these predictors will provide information that could affect clinical decisionmaking, such studies must be performed with statistical rigor and be reported clearly and with unbiased statistics. All predictors should be validated. If cross-validation is used to estimate prediction accuracy, then the entire model-building process, including the selection of informative genes, should be repeated in each cross-validation training set. If a separate sample group is used for validation, the sample size should be sufficiently large to provide meaningful confidence intervals for prediction accuracy.

Looking Ahead

The use of microarray and other global-profiling technologies has led to a significant number of exciting new biological discoveries and important correlations between gene-expression patterns and disease states. Never before could a small sample of RNA from two different conditions reveal so much information at the transcriptional level. Microarray technologies have also provided high-throughput platforms for genomewide SNP genotyping (Lindblad-Toh *et al.,* 2000a; Lindblad-Toh *et al.,* 2000b; Mei *et al.,* 2000) and CGH for detecting DNA copy number abnormality (Albertson and Pinkel, 2003; Pollack *et al.,* 1999). At the protein level, there have also been great advances in expression quantification through micro-ELISA (enzyme-linked immunosorbent assay) protein arrays (Huang *et al.,* 2001; Tam *et al.,* 2002), dual-labeling displays of protein expression on an array (Clontech, Inc.), or protein chips in combination with MALDI (matrix-assisted laser desorption/ionization) mass spectrometry for protein identification (Ciphergen, Inc.). Contemporary molecular biologists are endowed with powerful new tools to explore the genome and proteome of many species for both basic biological analyses and the discovery of new disease influences or drug targets.

Nonetheless, it is important that investigators continue to optimize statistical methodologies and to develop new approaches to produce accurate and valid data. In particular, much more attention needs to be paid to the external validity of the results produced by microarray data analysis tools. When a statistical tool identifies a difference, or a cluster of related genes, how often does this indication hold up in subsequent

validation studies? Most current statistical approaches to microarray data have only been presented with examples of application, but no quantitative evaluation of their accuracy with regard to external verification is available. Alternative class prediction tools have been compared in terms of their predictive accuracy, and similar comparisons are sorely needed for class discovery and differential expression analyses. Another issue requiring further study is the balance between false-positive and false-negative errors. External validation studies have suggested that many differential expression analyses of microarray data overlook true differences even when they are present in the data (false-negative results). An important topic for future research is whether development of more sensitive, noise-resistant algorithms might enhance the information yield from massively parallel microarray measurement. We probably are still a long way from a satisfactory solution to the problems. With its potential to quantitatively determine expression levels of a large number of genes in parallel, microarray technology holds the promise of becoming an extremely valuable tool in basic biological sciences and clinical diagnostics. However, its ultimate utility will depend critically on whether the search for efficient statistical methods meets with success.

References

Albertson, D.G., and Pinkel, D. 2003. Genomic microarrays in human genetic disease and cancer. *Hum. Mol Genet. 12 Suppl 2*:R145–152.

Alizadeh, A.A., Eisen, M.B., Davis, R.E., Ma, C., Lossos, I.S., Rosenwald, A., Boldrick, J.C., Sabet, H., Tran, T., Yu, X., Powell, J.I., Yang, L., Marti, G.E., Moore, T., Hudson, J., Jr., Lu, L., Lewis, D.B., Tibshirani, R., Sherlock, G., Chan, W.C., Greiner, T.C., Weisenburger, D.D., Armitage, J.O., Warnke, R., Levy, R., Wilson W., Grever, M.R., Byrd, J.C., Botstein, D., Brown, P.O., and Staudt, L.M. 2000. Distinct types of diffuse large B-cell lymphoma identified by gene expression profiling. *Nature 403*(6769):503–511.

Alon, U., Barkai, N., Notterman, D.A., Gish, K., Ybarra, S., Mack, D., and Levine, A.J. 1999. Broad patterns of gene expression revealed by clustering analysis of tumor and normal colon tissues probed by oligonucleotide arrays. *Proc. Natl. Acad. Sci. USA 96*(12):6745–6750.

Baldi, P., and Long, A.D. 2001. A Bayesian framework for the analysis of microarray expression data: Regularized t-test and statistical inferences of gene changes. *Bioinformatics 17*(6):509–519.

Bittner, M., Meltzer, P., Chen, Y, Jiang, Y, Seftor, E., Hendrix, M., Radmacher, M., Simon, R., Yakhini, Z., Ben-Dor, A., Sampas, N., Dougherty, E., Wang, E., Marincola, F., Gooden, C., Lueders, J., Glatfelter, A., Pollock, P., Carpten, J., Gillanders, E., Leja, D., Dietrich, K., Beaudry, C., Berens, M., Alberts, D., and Sondak, V. 2000. Molecular classification of cutaneous malignant melanoma by gene expression profiling. *Nature 406*(6795):536–540.

Bozinov, D., and Rahnenfuhrer, J. 2002. Unsupervised technique for robust target separation and analysis of DNA microarray spots through adaptive pixel clustering. *Bioinformatics 18*(5): 747–756.

Butte, A.J., and Kohane, I.S. 2000. Mutual information relevance networks: Functional genomic clustering using pairwise entropy measurements. *Pac. Symp. Biocomput.* 418–429.

Cahill, D.J., and Nordhoff, E. 2003. Protein arrays and their role in proteomics. *Adv. Biochem. Eng. Biotechnol. 83*:177–187.

Chatterjee, S., and Price, B. 1991. *Regression Analysis by Example.* John Wiley & Sons, New York.

Chen, Y., Dougherty, M.L., and Bittner, M.L. 1997. Ratio-based decisions and the quantitative analysis of cDNA microarray images. *J. Biomed. Optics 24*:364.

Chen, Y. Kamat, V., Dougherty, E.R., Bittner, M.L., Meltzer, P.S., and Trent, J.M. 2002. Ratio statistics of gene expression levels and applications to microarray data analysis. *Bioinformatics 18*(9):1207–1215.

Chuaqui, R.F., Bonner, R.F., Best, C.J., Gillespie, J.W., Flaig, M.J., Hewitt, S.M., Phillips, J.L., Krizman, D.B., Tangrea, M.A., Ahram, M., Linehan, W.M., Knezevic, V., and Emmert-Buck, M.R. 2002. Post-analysis follow-up and validation of microarray experiments. *Nat. Genet. 32 Suppl*:509–514.

Cole, S.W., Galic, Z., and Zack, J.A. 2003. Controlling false-negative errors in microarray differential expression analysis: A PRIM approach. *Bioinformatics 19*(14):1808–1816.

DeRisi, J., Penland, L., Brown, P.O., Bittner, M.L., Meltzer, P.S., Ray, M., Chen, Y., Su, Y.A., and Trent, J.M. 1996. Use of a cDNA microarray to analyse gene expression patterns in human cancer. *Nat. Genet. 14*(4):457–460.

Dudoit, S., Fridlyand, J., and Speed, T. 2002. Comparison of discrimination methods for the classification of tumors using gene expression data. *J. Am. Stat. Assoc. 97*:77–87.

Eisen, M.B., and Brown, P.O. 1999. DNA arrays for analysis of gene expression. *Methods Enzymol. 303*:179–205.

Eisen, M.B., Spellman, P.T., Brown, P.O., and Botstein, D. 1998. Cluster analysis and display of genome-wide expression patterns. *Proc. Natl. Acad. Sci. USA 95*(25): 14863–14868.

Golub, T.R., Slonim, D.K., Tamayo, P., Huard, C., Gaasenbeek, M., Mesirov, J.P., Coller, H., Loh, M.L., Downing, J.R., Caligiuri, M.A., Bloomfield, C.D., and Lander, E.S. 1999. Molecular classification of cancer: Class discovery and class prediction by gene expression monitoring. *Science 286*(5439):531–537.

Hatfield, G.W., Hung, S.P., and Baldi, P. 2003. Differential analysis of DNA microarray gene expression data. *Mol. Microbiol. 47*(4):871–877.

Hedenfalk, I., Duggan, D., Chen, Y, Radmacher, M., Bittner, M., Simon, R., Meltzer, P., Gusterson, B., Esteller, M., Kallioniemi, O.P., Wilfond, B., Borg, A., and Trent, J. 2001. Gene-expression profiles in hereditary breast cancer. *N. Engl. J. Med. 344(*8):539–548.

Herzel, H., Beule, D., Kielbasa, S., Korbel, J., Sers, C., Malik, A., Eickhoff, H., Lehrach, H., and Schuchhardt, J. 2001. Extracting information from cDNA arrays. *Chaos 11*(1):98–107.

Huang, J.X., Mehrens, D., Wiese, R., Lee, S., Tam, S.W., Daniel, S., Gilmore, J., Shi, M., and Lashkari, D. 2001. High-throughput genomic and proteomic analysis using microarray technology. *Clin. Chem. 47*(10):1912–1916.

Kepler, T.B., Crosby, L., and Morgan, K.T. 2002. Normalization and analysis of DNA microarray data by self-consistency and local regression. *Genome Biol. 3*(7):RESEARCH0037.

Kerr, M.K., and Churchill, G.A. 2001. Experimental design for gene expression microarrays. *Biostatistics 2*(2):183–201.

Kerr, M.K., Martin, M., and Churchill, G.A. 2000. Analysis of variance for gene expression microarray data. *J. Comput. Biol. 7*(6):819–837.

Khan, J., Wei, J.S., Ringner, M., Saal, L.H., Ladanyi, M., Westermann, F., Berthold, F., Schwab, M., Antonescu, C.R., Peterson, C., and Meltzer, P.S. (2001). Classification and diagnostic prediction of cancers using gene expression profiling and artificial neural networks. *Nat. Med. 7*(6): 673–679.

Kohonen, T. 2001. *Self-Organizing Maps*. Springer, Berlin, Heidelberg, New York.

Li, C., and Wong, W.H. 2003. DNA-Chip Analyzer (dChip). In *The Analysis of Gene Expression Data: Methods and Software*. Springer, New York.

Lindblad-Toh, K., Tanenbaum, D.M., Daly, M.J., Winchester, E., Lui, W.O., Villapakkam, A., Stanton, S.E., Larsson, C., Hudson, T.J., Johnson, B.E., Lander, E.S., and Meyerson, M. 2000a. Loss-of-heterozygosity analysis of small-cell lung carcinomas using single-nucleotide polymorphism arrays. *Nat. Biotechnol. 18*(9):1001–1005.

Lindblad-Toh, K., Winchester, E., Daly, M.J., Wang, D.G., Hirschhorn, J.N., Laviolette, J.P., Ardlie, K., Reich, D.E., Robinson, E., Sklar, P., Shah, N., Thomas, D., Fan, J.B., Gingeras, T., Warrington, J., Patil, N., Hudson, T.J., and Lander, E.S. 2000b. Large-scale discovery and genotyping of single-nucleotide polymorphisms in the mouse. *Nat. Genet. 24*(4): 381–386.

Long, A.D., Mangalam, H.J., Chan, B.Y., Tolleri, L., Hatfield, G.W., and Baldi, P. 2001. Improved statistical inference from DNA microarray data using analysis of variance and a Bayesian statistical framework. Analysis of global gene expression in Escherichia coli K12. *J. Biol. Chem. 276*(23): 19937–19944.

Mei, R., Galipeau, P.C., Prass, C., Berno, A., Ghandour, G., Patil, N., Wolff, R.K., Chee, M.S., Reid, B.J., and Lockhart, D.J. 2000. Genome-wide detection of allelic imbalance using human SNPs and high-density DNA arrays. *Genome Res. 10*(8):1126–1137.

Nguyen, D.V., and Rocke, D.M. 2002. Tumor classification by partial least squares using microarray gene expression data. *Bioinformatics 18*(1):39–50.

Pollack, J.R., Perou, C.M., Alizadeh, A.A., Eisen, M.B., Pergamenschikov, A., Williams, C.F., Jeffrey, S.S., Botstein, D., and Brown, P.O. 1999. Genome-wide analysis of DNA copy-number changes using cDNA microarrays. *Nat. Genet. 23*(1):41–46.

Quackenbush, J. 2002. Microarray data normalization and transformation. *Nat. Genet. 32 Suppl*:496–501.

Radmacher, M.D., McShane, L.M., and Simon, R. 2002. A paradigm for class prediction using gene expression profiles. *J. Comput. Biol. 9*(3):505–511.

Rajeevan, M.S., Vernon, S.D., Taysavang, N., and Unger, E.R. 2001. Validation of array-based gene expression profiles by real-time (kinetic) RT-PCR. *J. Mol. Diagn. 3*(1):26–31.

Rosenwald, A., Wright, G., Chan, W.C., Connors, J.M., Campo, E., Fisher, R.I., Gascoyne, R.D., Muller-Hermelink, H.K., Smeland, E.B., Giltnane, J.M., Hurt, E.M., Zhao, H., Averett, L., Yang, L., Wilson, W.H., Jaffe, E.S., Simon, R., Klausner, R.D., Powell, J., Duffey, P.L., Longo, D.L., Greiner, T.C., Weisenburger, D.D., Sanger, W.G., Dave, B.J., Lynch, J.C., Vose, J., Armitage, J.O., Montserrat, E., Lopez-Guillermo, A., Grogan, T.M., Miller, T.P., LeBlanc, M., Ott, G., Kvaloy, S., Delabie, J., Holte, H., Krajci, P., Stokke, T., and Staudt, L.M. 2002. The use of molecular profiling to predict survival after chemotherapy for diffuse large-B-cell lymphoma. *N. Engl. J. Med. 346*(25):1937–1947.

Sasik, R., Hwa, T., Iranfar, N., and Loomis, W.F. 2001. Percolation clustering: A novel approach to the clustering of gene expression patterns in Dictyostelium development. *Pac. Svmp. Biocomput.* 335–347.

Schena, M., Shalon, D., Davis, R.W., and Brown, P.O. 1995. Quantitative monitoring of gene expression patterns with a complementary DNA microarray. *Science 270*(5235): 467–470.

Shipp, M.A., Ross, K.N., Tamayo, P., Weng, A.P., Kutok, J.L., Aguiar, R.C., Gaasenbeek, M., Angelo, M., Reich, M., Pinkus, G.S., Ray, T.S., Koval, M.A., Last, K.W., Norton, A., Lister, T.A., Mesirov, J., Neuberg, D.S., Lander, E.S., Aster, J.C., and Golub, T.R. 2002. Diffuse large B-cell lymphoma outcome prediction by gene-expression profiling and supervised machine learning. *Nat. Med. 8*(1):68–74.

Simon, R., Radmacher, M.D., Dobbin, K., and McShane, L.M. 2003. Pitfalls in the use of DNA microarray data for diagnostic and prognostic classification. *J. Natl. Cancer Inst. 95*(1):14–18.

Tam, S.W., Wiese, R., Lee, S., Gilmore, J., and Kumble, K.D. 2002. Simultaneous analysis of eight human Th1/Th2 cytokines using microarrays. *J. Immunol. Methods 261*(1–2):157–165.

Tamayo, P., Slonim, D., Mesirov, J., Zhu, Q., Kitareewan, S., Dmitrovsky, E., Lander, E.S., and Golub, T.R. 1999. Interpreting patterns of gene expression with self-organizing maps: Methods and application to hematopoietic differentiation. *Proc. Natl. Acad. Sci. USA 96*(6):2907–2912.

Tavazoie, S., Hughes, J.D., Campbell, M.J., Cho, R.J., and Church, G.M. 1999. Systematic determination of genetic network architecture. *Nat. Genet. 22*(3):281–285.

Toronen, P., Kolehmainen, M., Wong, G., and Castren, E. 1999. Analysis of gene expression data using self-organizing maps. *FEBS Lett. 451*(2):142–146.

Tseng, G.C., Oh, M.K., Rohlin, L., Liao, J.C., and Wong, W.H. 2001. Issues in cDNA microarray analysis: quality filtering, channel normalization, models of variations and assessment of gene effects. *Nucleic Acids Res. 29*(12):2549–2557.

Tusher, V.G, Tibshirani, R., and Chu, G 2001. Significance analysis of microarrays applied to the ionizing radiation response. *Proc. Natl. Acad. Sci. USA 98*(9):5116–5121.

Walker, N. J. (2002). Tech.Sight. A technique whose time has come. *Science 296*(5567):557–559.

Wen, X., Fuhrman, S., Michaels, G.S., Carr, D.B., Smith, S., Barker, J.L., and Somogyi, R. 1998. Large-scale temporal gene expression mapping of central nervous system development. Proc. *Natl. Acad. Sci. USA 95*(1):334–339.

West, M., Blanchette, C., Dressman, H., Huang, E., Ishida, S., Spang, R., Zuzan, H., Olson, J.A., Jr., Marks, J.R., and Nevins, J.R. 2001. Predicting the clinical status of human breast cancer by using gene expression profiles. *Proc. Natl. Acad. Sci. USA 98*(20):11462–11467.

Yang, l.V., Chen, E., Hasseman, J.P., Liang, W., Frank, B.C., Wang, S., Sharov, V., Saeed, A.I., White, J., Li, J., Lee, N.H., Yeatman, T.J., and Quackenbush, J. 2002a. Within the fold: Assessing differential expression measures and reproducibility in microarray assays. *Genome Biol. 3*(11):research0062.

Yang, Y.H., Dudoit, S., Luu, P., Lin, D.M., Peng, V., Ngai, J., and Speed, T.P. 2002b. Normalization for cDNA microarray data: A robust composite method addressing single and multiple slide systematic variation. *Nucleic Acids Res. 30*(4):e15.

3

Microarray-Based Gene Expression Analysis of Defined Tumor Areas

Regine Dahse, Alexander Berndt, and Hartwig Kosmehl

Introduction

The completion of the human genome project and the recent development of novel, highly sensitive, high-throughput techniques have now afforded the opportunity to perform a comprehensive molecular characterization of normal, premalignant, and tumor cells.

Among the most powerful tools for identifying carcinogenesis-associated genes and dissecting regulatory patterns are high-density arrays of oligoncleotides or complementary deoxyribonucleic acids (cDNAs). Arrays work by hybridization of labeled DNA or ribonucleic acid (RNA) to DNA molecules attached on a glass or plastic surface. Nucleic acid arrays (often called microarrays, gene-chip arrays, or simply "chips") are generally produced by either robotic spotting of nucleic acids (polymerase chain reaction [PCR] products, plasmids, or oligonucleotides) onto a glass slide or *in situ* synthesis of oligonucleotides using photolithography. As a result of technical achievements, arrays with more than 25,000 different oligonucleotide probes or 10,000 different cDNAs per square centimeter can now be produced.

One of the most important applications for DNA microarrays is the study of differential gene expression. Differences in gene expression are responsible for morphologic differences and are indicative of cellular responses to environmental stimuli. Knowing where, when, and to what extent a gene is expressed is central to understanding the biological role of its encoded protein. Therapeutic targets can be identified by determining which genes are up-regulated in different tumor types, and candidate genes can be intentionally overexpressed in model systems to identify downstream target genes and to explore signaling pathways.

Gene expression analysis using microarrays requires the development and successful implementation of a variety of laboratory strategies. Cell cultures and cell lines would provide pure cell populations that could be studied under defined conditions. However, because of the lack of interaction with the stromal microenvironment, gene expression patterns of cultured tumor cells do not reflect the status of the primary tissue. Direct molecular examination of tumors is limited by the inherent heterogeneity of primary tissues containing an admixture of various cell populations with different gene expression patterns. Laser-based microdissection

Handbook of Immunohistochemistry and *in situ* Hybridization of Human Carcinomas, Volume 3: Molecular Genetics, Liver Carcinoma, and Pancreatic Carcinoma

of defined areas from histologic tumor sections has recently gained importance as a tool to obtain purified cell populations from complex primary tissues.

Another major problem that has to be overcome in gene expression analysis is efficiently obtaining high-purity and high-quality RNA from limited amounts of starting material such as microdissected tissue areas, small biopsies, or fine-needle aspirates.

There are different methods for preparing labeled material for the array-based gene expression analysis. The RNA can be labeled directly or by ligation to an RNA molecule carrying biotin; labeled nucleotides can be incorporated into cDNA during or after reverse transcription; or cDNA can be generated that carries a T7 promoter at its 5′ end for RNA *in vitro* amplification and subsequent incorporation of labeled nucleotides into complementary RNA (cRNA). The relative messenger RNA (mRNA) abundance in two samples (such as normal versus tumor cell, premalignant lesion versus tumor, primary tumor cell versus metastatic cell) can be assessed by monitoring the differential hybridization of the two samples to the sequences on the array. Two different fluorescent dyes (usually the red-fluorescent dye Cyanine 5 and the green fluorescent dye Cyanine 3) are used to label CDNA from two different conditions, which is then mixed in equal proportions and competitively cohybridized to an array. After hybridization of the labeled samples, the arrays are scanned at two different wavelengths, and the quantitative fluorescence image is used to detect the relative transcript abundance for each condition. Quantitative estimates of the number of transcripts per cell can be obtained directly by averaging the signal from multiple probes; mRNAs present at a few copies (relative abundance of about 1:100,000) to thousands of copies per cell can be detected, and changes as subtle as a factor 1.3 to 2 can be detected if replicate experiments are performed. Array experiments generate large and complex multivariate data sets, and some of the challenges do not lie in generating the data but in the development and handling of computational and statistics tools to analyze the large data amounts.

MATERIALS AND METHODS

Laser Microdissection

Identification of differentially expressed genes from defined tumor areas such as the tumor–host interface requires separating tumor and normal cells, thereby maintaining the tissue architecture and RNA integrity.

Laser microdissection instruments enable the user to define the region of a stained tissue slide to excise. The cells of interest are isolated from their surroundings with a clearcut gap by laser microdissection. Laser treatment does not impair DNA, RNA, or protein recovery. The selected cell cluster or even single cells are transferred directly into a collection tube.

Several systems for cell microdissection are available that mainly vary in the principle of how to capture the dissected cells, in system configuration, and in applications. Some systems offer the possibility of working with cells straight from a culture dish. Most allow the user to avoid touching the specimen by catapulting or dropping the laser-dissected cells straight into a capture tube.

The instruments include an inverted microscope and either an infrared laser (PixCell II from Arcturus Engineering, Mountain View, CA; Clonis from Bio-Rad, Hercules, CA), or ultraviolet laser (PALM Microbeam from PALM Bernried, Germany; Leica AS LMD from Leica Microsystems of Wetzlar, Germany; and μCUT from MMI Heidelberg, Germany). Several different tissue-capture techniques are offered. The widely approached PixCell II uses a disposable cap, which is placed over the target tissue area on a slide. The caps are lined with thermoplastic film that forms a protrusion when hit by a laser pulse. The protrusion closes the gap between tissue and film, so that lifting the cap will remove the target cells, leaving them attached to the cap. The μCUT cuts around the tissue of interest, which is mounted on special membrane-covered slides, and an adhesive layer in a collection cap to capture the sample is used during the collection process. Capture using a special film is not the only way to collect an excised specimen. The PALM MicroBeam uses a technology called laser pressure catapulting (LPC) where a "photonic cloud" provides an energy pulse, which catapults the excised specimen into a microfuge tube cap in an entirely noncontact manner without encroachment of adjacent unwanted areas.

Thin (7–8 μm) tissue sections are mounted on regular glass slides or on glass surfaces with a supporting membrane. This membrane (such as PALMs MOMeNT membrane) maintains tissue architecture and supports the dissection and catapulting of larger cell areas.

For paraffin-embedded specimens, coating with some tissue-adhesive such as Poly-L-lysine might be advisable prior to specimen application on a membrane.

For any microdissection, an optimized staining and fixation protocol is needed that provides acceptable morphology despite the optical losses from stained frozen sections without coverslips. It should preserve the RNA integrity:

1. Fix for 1 min at room temperature in absolute ethanol or for 3 min in ice-cold acetone.
2. Rehydrate by dipping in 95%–70%–50% ethanol (dilutions with diethyl pyrocarbonate (DEPC water).

DEPC water is prepared by adding DEPC to a final concentration of 0.1% to deionized distilled water. Autoclave for 1hr, open the autoclave door briefly to release steam, and leave overnight in the turned off but hot autoclave to decompose residual DEPC.

Bake all glassware for at least 4 hr at 250°C, and use fresh staining solutions to work under ribonuclease-free conditions as much as possible.

3. Stain for 15 sec in hematoxylin, dip in DEPC water.
4. Apply blueing reagent for 30 sec.
5. Stain for 10 sec in eosin Y, and rinse briefly in DEPC water.
6. Dehydrate by dipping in 50%–70%–95% ethanol (dilutions with DEPC water).
7. Dip for 1 min in xylene.
8. Air-dry for 10 min. The slides are now ready for microdissection.

For subsequent RNA extraction, the microdissected cells should be captured in lysis buffer from the selected RNA isolation method or in RNA stabilization solution (RNAIater, Ambion Inc., Austin, TX). In RNAlater, RNA is stable for 1 day at 37°C, 1 week at 25°C, 1 month at 4°C, or indefinitely at –20°C (as declared by the manufacturer).

Laser Microdissection in Two-Dimensional Coculture Models as a Novel Tool to Study Tumor-Stroma Interactions

Cellular adhesion, migration, and invasion are essential processes in tumor progression. These processes include actions by tumor cells as well as by the stromal microenvironment. In the last few years it has become evident that tumor cell behavior and progression is affected by tumor stroma, including peritumoral fibroblasts. *In vitro,* tumor cell–stromal fibroblast interaction can be studied by two-dimensional and three-dimensional coculture models (Sacks, 1996). In conventional two-dimensional coculture systems, the different cell types are grown together in glass slide–based chambers with medium. Immunohistochemical detection at the protein level can be easily performed; however, for gene expression analysis the cell compartments have to be dissociated and sorted.

Here we present a technique for coculturing and separating fibroblasts and carcinoma cells (Figure 4). It is based on cell cocultivation on a 1.35-µm thin membrane combined with laser capture microdissection of the cell compartments after rapid immunolabeling. Laser capture microdissected tumor and stroma cells from the presented membrane-based coculture model can be used for gene expression profiling and DNA-based analysis (Dahse *et al.,* 2002). Isolation of amplifiable DNA from the microdissected cells can be performed with standard procedures. Analysis of RNA

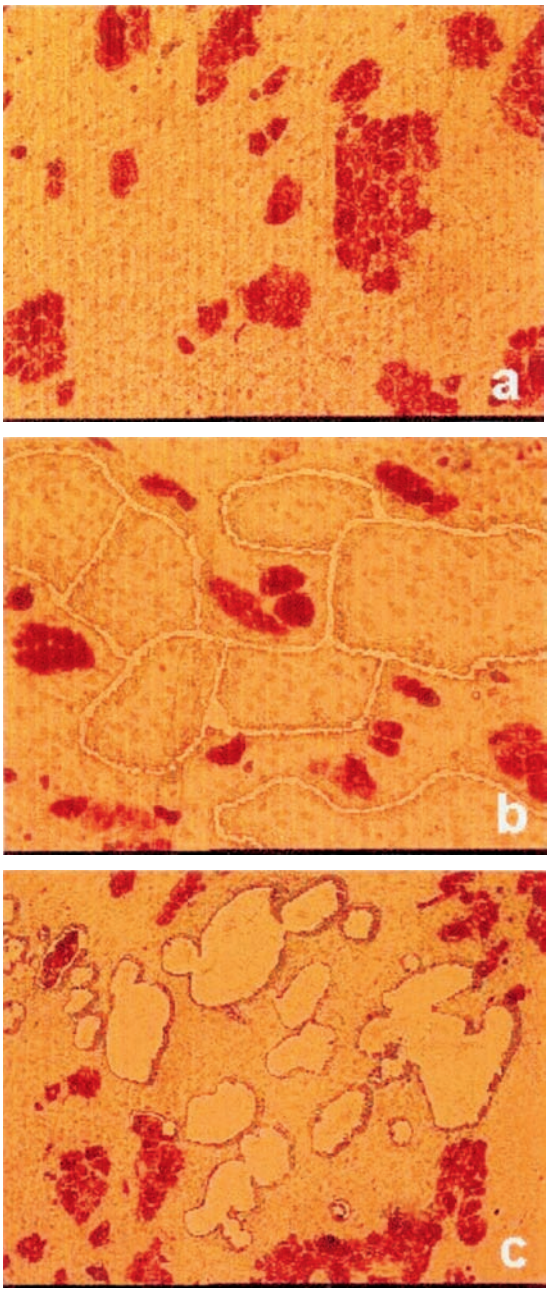

Figure 4. Coculture-laser capture microdissection. **A** represents a survey of the two-dimensional membrance coculture model. The tumor cell areas are immunostained with the laminin gamma2 chain antibody GB3. For better visualization, fibroblasts are counterstained with hematoxylin. Fibroblasts **(B)** or immunostained tumor cells **(C)** are microdissected with the laser beam. The laser tracks are clearly visible, and the precision of the procedure enables the dissection of the area of interest without cross contimation.

molecules is more troublesome and can be a major limiting step for downstream applications because of loss of RNA quality and quantity during RNA sample preparation from a limited number of immunostained cells. It is advisable to use a total-RNA extraction protocol for limited amounts of starting material, as described in Chapter 2.

Two-Dimensional Coculture of Tumor Cells and Fibroblasts

1. About 5×10^4 fibroblasts (such as human fibroblast cell line hTERT-BJ1, CLONTECH Laboratories Inc., Palo Alto, CA) are allowed to adhere to 2×2 cm membrane fragments floating in cell culture medium (IMDM, 10% FCS and 80 µg/ml gentamycin; Invitrogen GmbH, Karlsruhe, Germany). The special 1.35-µm thin membrane (PALM, GmbH, Bernried, Germany) has been originally developed for the mounting of histologic tissue sections on regular glass slides for the so-called MicroBeam-MOMeNT technique (microdissection of membrane-mounted native tissues) mainly to hold the microdissected area or specimen together during the catapulting procedure with the PALM MicroBeam System. The fibroblasts are cultured until showing a subconfluent monolayer on the upper side of the membrane. The membrane does not influence cell growth. Differences in growth behavior and cell morphology between cultivation on cell culture slides and cultivation on the membrane were not observed.

2. Overlay with 5×10^4 carcinoma cells and coculture for 6–10 days.

Rapid Immunostaining for the Detection of Tumor Cell Compartments

1. Fix the coculture membranes for 1 min in 70% ethanol and transfer to RNAse-free glass slides. After flattening and air-drying, fix the membranes with rubber cement. To identify the tumor cell compartment, immunolabeling for the laminin gamma2 chain can be performed, a marker that is expressed only in epithelial tumor cells. A modified immunostaining protocol based on the ChemMate Detection Kit AP/red (Dako A/S, Glostrup, Denmark) is used that allows identification of the tumor cells and maintenance of the DNA and RNA integrity for subsequent analysis. Alternatively, other established tumor cell markers such as cytokeratine can be used.

2. Incubate the slides with the fixed membranes for 10 min at room temperature with the anti-gamma2 chain antibody GB3 (Harlan Sera-Lab Limited, Leicestershire, UK) at a concentration of 60 µg/ml diluted in Antibody Diluent Solution (ZYMED Laboratories Inc., San Francisco, CA) supplemented with 1 u/µl RNAse inhibitor (Roche, Mannheim, Germany). After rinsing three times in RNAse-free phosphate buffer saline (PBS), perform detection of the primary antibody using the ChemMate Detection Kit AP/red according to the manufacturer's instructions. The incubation time of the secondary biotinylated antibody and the alkaline phosphatase conjugated streptavidin inhibitor should be shortened to 5 min at room temperature. All reagents are supplemented with 1 u/µl RNAse inhibitor.

3. Monitor the color development microscopically.

4. After rinsing in DEPC water, dehydrate the slides in 75%–95%–100% ethanol and dry in a fume hood.

5. For counterstaining, a short protocol with hematoxylin can be used, but it is not mandatory for visualization.

The slides are now ready for microdissection. For subsequent RNA extraction, the microdissected cell compartments should be captured in lysis buffer from the selected RNA isolation method or in RNA stabilization solution (RNAlater, Ambion Inc.).

RNA Extraction

A primary limitation of any probe design for microarray hybridization is the amount of total RNA (T-RNA) or poly (A) RNA that can be obtained from small samples as microdissected tissue areas. Previous studies demonstrated 50,000 to 200,000 cells (Mahadevappa and Warrington, 1999) or 50 ng–1 µg T-RNA (Gonzalez *et al.,* 1999) feasible for generating samples for hybridization of microarrays for gene expression profiling. In an effort to reduce the amount of starting material, it was shown that T-RNA can be used as a template for cDNA synthesis (Ohyama *et al.,* 2000).

In this chapter, an optimized T-RNA isolation protocol for limited amounts of starting material is presented that combines a guanidinium thiocyanate–based denaturation with a modified RNA precipitation and purification protocol (Dyanov and Dzitoeva, 1995).

1. Prepare a denaturation solution from the Micro RNA Isolation Kit (Stratagene, La Jolla, CA) according to manufactur's guidelines. Add 200 µl solution per microdissection sample, invert carefully, and incubate for 10 min at 37°C and for 5 min on ice.

2. Add 20 µl 2 M sodium acetate, 220 µl phenol, and 60 µl chloroform:isoamylethanol to each sample; vortex for 30 sec and incubate for 5 min on ice; spin at maximum speed (14,000 rpm) for 8 min at 4°C.

3. Remove the aqueous supernatant completely into a new tube, add 1 µl glycogen as a carrier and 3 volumes of ice-cold ethanol, mix slowly, and incubate for 20 min at −20°C.

4. Spin at maximum speed for 30 min at 4°C, remove the supernatant, and wash the tiny pellet with 75% ethanol. Spin again for 6 min, remove the alcohol, and air-dry the pellet at room temperature.

5. Resuspend the pellet in 16 µl DEPC-treated water. Add 1 µl ribonuclease inhibitor RNasin (Promega, Madison, WI), 2 µl 10X DNase enzyme buffer and 1 µl Rnase-free DNase, and incubate for 45 min at 37°C.

6. Extract the RNA with an equal volume of phenol:chloroform, spin at 6000 rpm for 10 min, and repeat the extraction with chloroform: isoamylethanol (24:1). Attention: if there is very little supernatant after phenol–chloroform extraction, skip the chloroform–isoamylethanol extraction step.

7. Remove the supernatant completely into a new tube, and add 1 µl glycogen as a carrier, 0.1 volume 3 M sodium acetate pH 5.4, and 3 volumes ice-cold ethanol. Mix slowly and incubate for at least 30 min at −70°C.

8. After centrifugation (10 min at maximum speed), wash the pellet twice in 70% ethanol, air-dry it briefly, and resuspend it in 10 µl DEPC-treated water.

The total-RNA pellet is stored at −70°C.

Hybridization Probe Preparation

To obtain the quantities of RNA essential for gene expression profiling and to generate hybridization probes from small microdissected samples, linear RNA *in vitro* amplification is required. T7 RNA polymerase-based linear amplification relies on attaching a T7 promoter sequence to the oligo(dT) primer used for synthesis of the first cDNA strand. After second-strand cDNA synthesis, amplified RNA (aRNA) is generated using T7 RNA polymerase and the double-stranded cDNA as targets for linear amplification (Eberwine *et al.,* 1992; Luo *et al.,* 1999). By adding a procedure called template switching to the protocol (Wang *et al.,* 2000), the amplification of low-abundance RNA is optimized and allows an amplification factor up to 500 per round.

For the RNA *in vitro* amplification protocol described herein, 10 µl TRNA sample is needed from the RNA extraction protocol explained previously.

1. First- and second-strand cDNA synthesis

▲ To initiate first-strand cDNA synthesis, use the SUPERSCRIPT Choice System (Gibco BRL). To 10 µl T-RNA add 1 µl 25 µM T7-oligo $(dT)_{15}$ primer: 5′ AAA CGA CGG CCA GTG AAT TGT AAT ACG ACT CAC TAT AGG CGC 3′ (Wang *et al.,* 2000), Denaturate at 70°C for 5 min, and anneal at 42°C for 3 min. Add 1 µl 25 µM template switch primer: 5′ AAG CAG TGG TAT CAA CGC AGA GTA CGC GGG 3′ (Wang *et al.,* 2000). Add 4 µl first strand reaction buffer, 2 µl dithiothreitol (DTT), 2 µl 10 mM dNTPs, 1 µl RNasin, and 1 µl Superscript II reverse transcriptase from the SUPERSCRIPT Choice kit according to Gibco guidelines. Incubate for 1 hr at 42°C.

▲ Perform second-strand cDNA synthesis with the Advantage cDNA PCR Kit (BD Biosciences Clontech, Palo Alto, CA). Add 106 µl DEPC-treated water, 15 µl Advantage PCR buffer, 3 µl 10 mM dNTPs, 1 µl RNase-H (Gibco BRL), and 3 µl Advantage cDNA Polymerase. Use the following cycling conditions: 2 min at 37°C, 3 min at 94°C, 3 min at 65°C, and 30 min at 75°C.

▲ Extract the resulting cDNA in two steps with phenol:chloroform:isoamylethanol followed by ethanol and 0.1 µg glycogen as a carrier. Wash the pellet twice in 75% ethanol. Resuspend it in 16 µl DEPC-treated water, and wash it twice in a Microcon YM100 spin column (Millipore, Billerica, MA).

2. Transcription and linear amplification

▲ Perform transcription of the ds-cDNA into aRNA with the T7 Megascript Kit (Ambion Inc.). To 16 µl double-stranded (ds)-cDNA add 4 µl reaction buffer; 1 µl ATP, GTP, CTP, and UTP, and 4 µl transcription enzyme mix (all included in the T7 Megascript Kit). Add DEPC-treated water to 40 µl. Incubate at 37°C for 10 hr or overnight to improve the yield of aRNA.

▲ Perform aRNA recovery. Extract the RNA with an equal volume phenol:chloroform, spin at 6000 rpm for 10 min, and repeat the extraction with chloroform:isoamylethanol (24:1). Be careful: If there is very little supernatant after phenol–chloroform extraction, skip the chloroform–isoamylethanol extraction step. Remove the supernatant completely into a new tube; add 1 µl glycogen as a carrier, 0.1 volume 3 M sodium acetate pH 5.4, and 3 volumes 20°C ethanol. Mix slowly and incubate for at least 30 min at −70°C. After centrifugation (10 min at $13{,}000 \times g$), wash the aRNA pellet twice in 70% ethanol, air-dry it briefly, and resuspend it in 15 µl DEPC-treated water.

This aRNA is now the template for the next dsDNA synthesis with random hexamers in the first-strand and T7-oligo-(dT) primer in the second-strand synthesis. Again, use the SUPERSCRIPT Choice System (Gibco BRL).

- To 15 µl aRNA add 2 µl random hexamer primer (1 mg/ml), 5 µl first-strand buffer, 2 µl 10 mM dNTP, 2 µl 10 mM DTT, and 1 µl Rnasin. Incubate at 65°C for 10 min, add 2 µl Superscript enzyme, and incubate at 42°C for 1 hr.
- Perform second-strand cDNA synthesis with the T7-oligo-(dT) primer as described before with the Advantage cDNA PCR Kit (BD Biosciences Clontech). Add 106 µl DEPC-treated water, 15 µl Advantage PCR buffer, 3 µl 10 mM dNTPs, 1 µl RNase-H (Gibco BRL), and 3 µl Advantage cDNA Polymerase. Use the following cycling conditions: 2 min at 37°C, 3 min at 94°C, 3 min at 65°C, and 30 min at 75°C.
- Extract the resulting cDNA as explained previously (two steps with phenol:chloroform: isoamylethanol followed by ethanol, wash it twice in a Microcon YM100 spin column), and use it as a template for the next transcription step into secondly amplified RNA (aaRNA) with the T7 Megascript Kit (Ambion). To 16 µl ds-cDNA add 4 µl reaction buffer; 1 µl dATP, dGTP, dCTP, and dUTP; and 4 µl transcription enzyme mix. Add DEPC-treated water to 40 µl. Incubate at 37°C for 10 hr or overnight.
- Perform aaRNA recovery as described. Extract the RNA with an equal volume phenol:chloroform, spin at 6000 rpm for 10 min, and repeat the extraction with chloroform:isoamylethanol (24:1). Again, be careful: If there is very little supernatant after phenol–chloroform extraction, skip the chloroform–isoamylethanol extraction step. Remove the supernatant completely into a new tube; add 1 µl glycogen as a carrier, 0.1 volume 3M sodium acetate pH 5.4, and 3 volumes 20°C ethanol. Mix slowly and incubate for at least 30 min at −70°C. After centrifugation (10 min at 13,000 × *g*), wash the aaRNA pellet twice in 70% ethanol and air-dry it briefly. Resuspend the pellet in 10 µl DEPC-treated water. Keep at −70°C until labeling.

3. Labeling

- Denaturate the aaRNA for 5 min at 65°C.
- Perform labeling in a reverse transcription (RT) reaction using 1.5 µl nucleotides (2 mM each) without dTTP, 1.2 µl dTTP (2 mM), 1.5 µl Cy5-dUTP (Amersham Biosciences), 6 µl first-strand buffer, 3 µl 0.1 M DTT, 10 µl random hexamer primer (1 mg/ml), and 2 µl Superscript II enzyme, all from SUPERSCRIPT Choice System (Gibco BRL). Alternatively, Cy3-dUTP can be incorporated. Add DEPC-treated water to 40 µl.
- Incubate for 1 hr at 42°C, add another 1.5 µl enzyme, and incubate again for 1 hr.
- Spin briefly and add 0.5 µl Rnase-H (5 U/µl). Incubate 20 min at 37°C.
- Purify the labeled cDNA by washing twice with DEPC-treated water in a Microcon YM30 spin column. Keep it at −20°C until hybridization.

Both Cy3 and Cy5 are photosensitive, and the exposure to light during labeling, hybridization, washing, and scanning procedures should be minimized. Cy-labeled nucleotides should be aliquoted into single-use, light-proof tubes and stored at −20°C. All reactions should be carried out in foil-wrapped tubes, and all hybridizations and washes should be done in foil-wrapped containers.

Hybridization

The aim in any hybridization is to obtain high specificity while minimizing background and to give reproducible, high-quality hybridization results.

Aminosilane-coated slide arrays bind DNA with high efficiency. Before hybridization, the free amine groups on the slide must be blocked, otherwise non-specific binding of labeled cDNA to the slide can deplete the probe and produce high background. Finally, hybridization conditions and wash must be optimized to provide high specificity and to minimize cross-hybridization.

1. Prehybridization

- Prepare prehybridization buffer containing 5X SSC (made from 20X SSC (Saline-Sodium citrate): 3 M sodium chloride/0.3 M sodium citrate × 2 H_2O), 0.1% SDS (sodium dodecyl sulfate) and 1% bovine serum albumin.
- Place slide arrays into a Coplin jar, fill with prehybridization buffer, and incubate at 37°C for 60 min.
- Meanwhile, prepare 2X hybridization buffer containing 50% formamide, 10X SSC, and 0.2% SDS.
- Wash the slides by dipping three times in distilled water at room temperature. Air-dry. Slides should be used immediately for hybridization.

2. Hybridization

- Combine 5 µl of purified, labeled probe with 20 µl 2X hybridization buffer and add 1 µl COT1-DNA (20 mg/ml) to block nonspecific hybridization. Denature 10 min at 95°C and cool on ice.

- Apply the mix to a prehybridized microarray slide, cover with a coverslip, and seal with rubber cement.
- Incubate at 37°C for 16–20 hr or overnight. Prewarm wash solutions at 40°C overnight.

3. Wash

- Place the array slide into a 50 ml tube with 40°C 2X SSC/0.1% SDS and shake gently so that coverslip falls off.
- Place the array slide into a Coplin jar with 40°C 2X SSC/0.1% SDS and wash twice for 5 min.
- Agitate in 40°C warm 0.1X SSC/0.1% SDS for 5 min.
- Agitate in 40°C warm 0.05X SSC for 5 min.
- Dip two times in distilled water and allow to air-dry.

Data Analysis

Differential gene expression is assessed by scanning the hybridized arrays using a confocal laser scanner capable of interrogating both the Cy3- and Cy5-labeled probes. Data from each fluorescence channel is collected and stored as a separate image. Image processing involves three steps. First, the spots representing the arrayed genes must be identified and distinguished from spurious signals that can arise as a result of precipitated probe or other hybridization artifacts or contaminants. The second step in analysis of the array images is the estimation of background. Following spot identification and local background determination, the background-subtracted hybridization intensities for each spot must be calculated using the median or the mean intensity for each spot. Following image processing, the data generated for the arrayed genes must be analyzed further before differentially expressed genes can be identified. The first step in this process is the normalization of the relative fluorescence intensities in each of the two scanned channels. Normalization is necessary to adjust for differences in labeling and detection efficiencies for the fluorescent labels and for differences in the quantity of starting RNA from the two samples examined in the assay. These problems can cause a shift in the average ratio of Cy5 to Cy3, and the intensities must be rescaled before an experiment can be properly analyzed.

The normalization strategies that can be used are based on some underlying assumptions regarding the data, and the strategies used for each experiment should be adjusted to reflect both the system under study and the experimental design (Hegde *et al.,* 2000). A useful approach has been described by Chen *et al.* (2001). They assume that some subset of housekeeping genes exists and that for these, the distribution of transcription levels should have some mean value and standard deviation independent of the sample. In this case, the ratio of measured Cy5 to Cy3 ratios for these genes can be modeled and the mean of the ratio can be adjusted to 1. Following normalization, data usually are analyzed to identify genes that are differentially expressed. Most published studies have used a post normalization cutoff of twofold up- or down-regulation to define differential expression. Clustering analysis is commonly used for interpreting microarray data, allowing a visual representation of complex data and a method for detecting similarity between experiments (gene ratios). This means the analysis calculates the average distance between each point in a cluster and all the points in a neighboring cluster. The two clusters that are closest to each other are connected to form the higher order cluster. These data are represented as a dendrogram (tree graph) with the closest branches of the tree representing genes with similar gene expression patterns.

CONCLUSION

Microarray technology is a powerful technology that will substantially increase the speed at which differential gene expression can be analyzed and gene functions are elucidated. To fulfil these expectations, improvements of the technology with respect to reproducibility, sensitivity, cost, and speed will be needed. The problems of sample collection, experimental procedure, and data analysis should not be underestimated. An independent verification method as a follow-up to the array results should also be considered, such as RT-PCR, Northern or Western Blot analyses, or *in situ* hybridization.

Ideally, microarray studies, limited to the mRNA level, should be accompanied by analyses at the protein level. Proteomics, large-scale complex analysis of the proteins that are present in a cell, is developing rapidly. Both technologies are complementary while focusing on different steps of the same process—the expression of genetic information into functional molecules.

The further development and use of arrays may be comparable to that seen for computers, which started as exclusive and expensive tools and then moved quickly to become routine in daily activities. It is expected that with further technical improvements and more widespread accessibility, array-based methods will become an integral part of a clinical laboratory.

References

Chen, J., Zhong, Q., Wang, J., Cameron, R.S., Borke, J.L., Isales, C.M., and Bollag, R.J. 2001. Microarray analysis of Tbx2-directed gene expression: A possible role in osteogenesis. *Mol. Cell Endocrinol. 177*:43–54.

Dahse, R., Berndt A., Haas, K., Hyckel, P., Böhmer, P., Uwe Claussen U., and Kosmehl, H. 2002. Coculture-LCM: Laser capture microdissection in 2-D coculture models as a tool to study tumor-stroma-interactions. *Biotechniques 33*:474–476.

Dyanov, H.M., and Dzitoeva, S.G. 1995. Isolation of DNA-free RNA from a very small number of cells. *Biotechniques 18*:558–560, 562, 564.

Eberwine, J., Yeh, H., Miyashiro, K., Cao, Y., Nair, S., Finnell, R., Zettel, M., and Coleman, P. 1992. Analysis of gene expression in single live neurons. *Proc. Natl. Acad. Sci. USA 89*: 3010–3014.

Gonzalez, P., Zigler, J.S., Epstein, D.L., and Borras, T. 1999. Identification and isolation of differentially expressed genes from very small tissue samples. *Biotechniques 26*:884–892.

Hegde, P., Qi, R., Abernathy, K., Gay, C., Dharap, S., Gaspard, R., Hughes, J.E., Snesrud, E., Lee, N., and Quackenbush, J. 2000. A concise guide to cDNA microarray analysis. *Biotechniques 29*:548–556.

Luo, L., Salunga, R.C., Guo, H., Bittner, A., Joy, K.C., Galindo, J.E., Xiao, H., Rogers, K.E., Wan, J.S., Jackson, M.R., and Erlander, M.G. 1999. Gene expression profiles of laser-captured adjacent neuronal subtypes. *Nat. Med. 5*:117–122.

Mahadevappa, M., and Warrington, J.A. 1999. A high-density probe array sample preparation method using 10- to 100-fold fewer cells. *Nat. Biotechnol. 17*:1134–1136.

Ohyama, H., Zhang, X., Kohno, Y., Alevizos, I., Posner, M., Wong, D.T., and Todd R. 2000. Laser capture microdissection-generated target sample for high-density oligonucleotide array hybridization. *Biotechniques 29*:530–536.

Sacks, P.G. 1996. Cell, tissue and organ culture as *in vitro* models to study the biology of squamous cell carcinomas of the head and neck. *Cancer Metastasis Rev. 15*:27–51.

Wang, E., Miller L.D., Ohnmacht G.A., Liu, E.T., and Marincola, F.M. 2000. High-fidelity mRNA amplification for gene profiling. *Nat. Biotechnol. 18*:457–459.

4

Tissue Microarray and Quantitative Fluorescence Image Analysis in Tumor Biomarker Analysis

Henry Tsai, George Hemstreet, David Seligson, Zuo-Feng Zhang, and Jian Yu Rao

Introduction

Cancer development is the result of alterations of numerous genes and signaling pathways; many of the changes are subtle and quantitative in nature. Traditional immunohistochemical analysis is a popular approach for detecting protein level expression abnormalities. However, it suffers from low sensitivity and, at best, is semi-quantitative in nature; thus it may not be reliably used to detect low level changes. Fluorescence-based approaches such as immunofluorescence or fluorescence *in situ* hybridization (FISH), although clearly more sensitive and quantitative, are in general unpopular among pathologists because they are difficult to evaluate and suffer from the quenching effect of the staining. However, recent developments of automatic fluorescence-based imaging technologies, coupled with more stable fluorescence dyes and nanocrystals, have revived the hope of quantitative measurement of protein level expression in cells and tissues in a fully automatic and robust fashion. This is particularly true with the recent development of another high-throughput technology; tissue microarray (TMA) discussed in this volume. Merging fluorescence-based analysis with TMA permits large-scale studies of tissue samples from a variety of patients with different stages and grades of disease. These studies, together with clinical data, are necessary to better evaluate for the diagnostic, prognostic, and therapeutic importance of cancer gene candidates, which is the central core of cancer biomarker analysis.

Tissue microarray-based quantitative fluorescence image analysis (TMA-QFIA) is a method in which protein markers on TMA sections are labeled by immunofluorescence using tyramide signal amplification and measured by a quantitative fluorescence detection system. The QFIA system was developed by Dr. George P. Hemstreet's laboratory and was initially used to analyze cells in urine samples to detect bladder cancer (Bonner *et al.,* 1998; Rao *et al.,* 1993). Subsequently, it has been used for the study of other types of cancer including esophageal (Hu *et al.,* 1998)

Handbook of Immunohistochemistry and *in situ* Hybridization of Human Carcinomas, Volume 3: Molecular Genetics, Liver Carcinoma, and Pancreatic Carcinoma

and breast cancer (Rao *et al.,* 1998). It provides a unique solution in biological analysis through its ability to quantify proteins or nucleic acids in individual cells in relation to their morphology and in association with other cells. Analysis problems such as expression heterogeneity and the potentially varied component cell types found in tissue samples can be effectively addressed by the ability of QFIA to assess the concentrations of individual proteins or the presence of targeted nucleic acid sequences within single cells.

The QFIA technique has two parts: quantitative fluorescence and image analysis. Quantitative fluorescence means that the intensity of a fluorescent signal emitted from cells labeled with fluorescent molecular probes is proportional to the concentration of target biomolecule within cells. The process of quantitatively labeling cells is often referred to as "biophysical cytochemistry" (West, 1970). Image analysis is used to isolate the signal from specific cells within a heterogeneous cell mixture or subcellular locales within cells and processes the signal to extract quantitative information from the microscopic images of cells quantitatively labeled with fluorochromes. The principle of QFIA is similar to flow cytometry in that cellular targets are labeled by direct or indirect fluorescence hybridization or immunofluorescence techniques, and the fluorescence intensities are measured to reflect the concentration of the marker. However, the technique differs from flow cytometry in that the image of the target object is available for examination. It also differs from traditional immunocytochemistry or immunohistochemistry (IHC) in offering true quantitation (Nibbering *et al.,* 1985) and provides several other advantages. First, it detects rare events, yet it also measures the expression patterns (mean) of a given marker in a population of cells. Second, it allows the evaluation of multiple biomarkers simultaneously on the single-cell basis using a limited number of cells. Furthermore, as an image-based technique, it also allows the simultaneous analysis of the morphologic appearance of a cell in conjunction with biomarker expression. These properties make QFIA an ideal technique for the study of molecular and biochemical changes in cytologic and tissue materials that are limited in quantity, such as tissue array analysis.

In this chapter we describe the preparation and quantitative labeling of cells, instrumentation needed for image analysis, and quality control of biomarker analysis to yield consistent analyses over time. We also show an example of TMA-QFIA analysis on BRCA1 expression in ovarian cancer. Finally, we briefly introduce some new developments in the area of fluorescence-based analysis.

MATERIALS

Tissue Microarray

1. Histologic slides of interest.
2. Paraffin tissue blocks corresponding to the chosen slide(s) with adequate remaining tissue (donor block).
3. Tissue arrayer containing an X-Y precision guide controlled through digital micrometers. Two thin-walled stainless steel coring needles are mounted to the unit on a swinging turret (Beecher Instruments, Silver Spring, MD).
4. A blank paraffin (recipient) block.
5. Microtome.
6. An adhesive-coated tape system (Instrumedics, Hackensack, NJ).

Quantitative Fluorescence Image Analysis Reagents

1. 10X Modified 3-[Morpholino]-2 hydroxypropanesulfonic acid (Sigma, St. Louis, MO) (MOPSO) buffer: 298.2 g KCl, 450.8 g MOPSO, 3630 ml double-distilled water. Dissolve thoroughly. Freeze in 400 ml aliquots (measured accurately).
2. Buffer (enough for 8 L of QFIA Fixit): Thaw 400 mL aliquot of 10X modified MOPSO buffer. Combine with 3600 ml deionized double-distilled water, 14.74 g dipotassium ethylenediamine tetraacetic acid (EDTA), and 0.8 g sodium azide. Dissolve thoroughly, and adjust pH to 6.5 with KOH.
3. Buffered-filtered saline (BFS, 1 L): 9.0 g sodium chloride, 980 ml double-distilled water, and 20 ml Buffer B (add after warming until crystals dissolve). Adjust pH to 7.0 with Buffer A, filter, and refrigerate. Discard after 1 week.
   a. Buffer A (0.1 M citric acid): 5.25 g citric acid and 250 ml double-distilled water. Refrigerate.
   b. Buffer B (0.2 M dibasic sodium phosphate): 7.1 g anhydrous sodium phosphate (dibasic) and 250 ml double-distilled water. Refrigerate.
4. Immunofix (modified Saccomanno fixative): 20 ml polyethylene glycol 1540 (Union Carbide), 516 ml 95% EtOH, and 464 ml BFS. Melt polyethylene glycol (PEG) at 60°C. Prepare 50% EtOH solution. Add stirring bar and begin stirring. Slowly add 20 ml of the melted PEG to the stirring ethanol solution. Let stir 1 hr. Store at room temperature.
5. 10X MOPSO/NaCl: Combine and stir thoroughly 233.76 g NaCl, 45.08 g MOPSO, and 4000 ml double-distilled water. Freeze in 400-ml aliquots (measured accurately). Use for Hoechst dye only (Hoechst working solution).

6. MOPSO/EDTA: Thaw 10X MOPSO/NaCl. Combine 400 ml 10X MOPSO/NaCl with 3600 ml double-distilled water, and add 14.88 g sodium EDTA. Dissolve thoroughly, adjust pH to 6.8, and filter. Freeze in approx 500-ml aliquots. Use for Hoechst dye only.

7. Hoechst 33258 (Molecular Probes, Eugene, OR) working solution (10 IJM alcoholic Hoechst, 40.0 ml): 0.2 ml Hoechst stock solution (0.2 mM), 29.3 ml MOPSO/EDTA (pH 6.8), and 10.5 ml 95% EtOH.

Immunofluorescence-Labeling Hardware and Image Analysis Hardware

1. The particular labeling system we used in our previous study was a BioGenex system (Model 6000, San Ramon, CA). Other systems can be used as well.
2. Leica DM RXA 2 microscope with a computer-controlled stage.
3. Hamamatsu Orca ER 1394 B/W charge-coupled devices (CCD) camera.
4. IBAS image analysis system (Roche Image Analysis Systems, Elon College, NC).
5. ImagePro Plus image capture and analysis software.

METHODS

Tissue Microarray

1. Amass histologic slides from completed pathologic diagnostic case evaluations based on the tumor pathology (type, grade, stage, etc.) and patient clinical criteria (demographics, surgical procedure, follow-up data, etc.) of interest.
2. Pathologically review the slides and choose representative ones.
3. Clearly mark histologic regions of interest directly on each slide.
4. Collect and evaluate paraffin tissue blocks corresponding to the chosen slide(s) for archival condition and for the adequacy of the remaining tissue.
5. Fix a blank paraffin (recipient) block to the tissue arrayer.
6. Punch a 0.5-mm diameter tissue core in the recipient paraffin block with the first needle, leaving a hole.
7. Using the histologic slide as a visual guide, "punch" the matching desired region on the donor block with a 0.6-mm inner diameter coring needle.
8. Transfer the resulting paraffin tissue core to the predetermined hole in the recipient paraffin block.
9. Repeat this process stepwise in closely neighboring regions in a grid pattern, resulting in the creation of a tissue microarray. Up to 500 cores can be arrayed on a standard-sized (22 mm × 35 mm) histologic block in a fixed and reproducible fashion.
10. Cut the arrayed block on a microtome, typically in 4–8-mm thick sections, depending on the anticipated assays.
11. An adhesive-coated tape system (Instrumedics, Hackensack, NJ) is useful in maintaining array formatting in the transfer of cut ribbons to the glass slides.
12. From 100 to 300 usable individual sections usually can be prepared in this manner, providing abundant array slides for numerous separate studies.

Quantitative Fluorescence

1. Deparaffinize and rehydrate the paraffin-embedded TMA sections (4-mm thick), followed by heat-antigen retrieval in 0.01 M citrate buffer (pH 6.0) for 25 min.
2. Cool at room temperature for 15 min.
3. Perform the assay using an automatic staining machine (Model 6000; BioGenex, San Ramon, CA). We used a three-step immunofluorescence procedure using the tyramide signal amplification labeling protocol (NEN Life Science Products, Boston, MA) and Texas Red as a fluorochrome to label the target protein of interest.
4. Incubate slides sequentially with protein blocking solution (30 min), avidin and biotin blocking solutions (10 min each), primary antibody (30 min), biotin-conjugated mouse anti-human IgG (1:200 for 30 min), streptavidin-HRP (1:100 for 30 min), tyramide amplification reagent (1:50 for 7 min), and streptavidin-Texas Red (1:500 for 30 min), with multiple washes between these steps.
5. Dual-label slides with Hoechst 33258, which is a highly specific DNA staining solution.
6. Place stained slide on a QFIA stage (Marzhauser Precision Stage).
7. Scan slide.

Image Analysis

A custom-designed software was developed with the following unique features:

1. Automatically scan each spot in tissue array.
2. Capture and store images of each spot.
3. Present each achieved image on the screen to allow manual selection of areas of interest (epithelial cells) using a light pen.
4. Convert light intensity of fluorescence into digital signals for feature extraction.
5. Built-in background subtraction mechanisms as detailed previously (Rao *et al.,* 2002).

Quality-Control Measures

1. Instrument calibration (test and adjust to a standard).

Implementation of measurement protocols requires that the analytical systems accurately represent the spatial and light-intensity characteristics of the targeted events, which include the following:

a. Spatial calibration against a stage micrometer.

b. Stability of the mercury lamp output over time.

c. Greyscale response versus relative luminosity.

d. Greyscale response versus weak and strong emission representing the low and high end of the greyscale response:

1. Wave-length emission bands of biomarker labels.

2. Standard-intensity beads or nanocrystals, ranging from very low luminous output to high output.

3. Compare the low end and high end of the greyscale response range for each instrument in each core.

4. Determine acceptable response range differences that produce the same biomarker values for standard cell lines.

2. Measurement standardization.

a. Detailed, standard measurement protocols for each biomarker or biomarker combination.

b. Background slides to correct for sample autofluorescence and nonspecific fluorescence labeling.

c. Cell standards for high and low biomarker content.

d. Acquisition of measurements within the dynamic range (8 bit, 12 bit, or 16 bit) of the light sensor (camera or pmt).

e. Specimen preparation and storage.

f. Replication of specimen measurement.

g. Measured events per measurement cycle.

RESULTS AND DISCUSSION

In this section, a proof of concept study is briefly described to demonstrate the TMA-QFIA approach. In the study, oncoprotein BRCA1 expression in ovarian tumor (borderline, low-grade, and high-grade) and nontumor samples were evaluated on TMA sections. The BRCA1 oncoprotein has been known to be difficult to measure by traditional IHC on paraffin sections. Thus a side-by-side comparison of TMA-QFIA with traditional IHC might be useful to determine whether QFIA-based analysis is superior to traditional approaches in detecting subtle protein level changes. In the end, we will briefly discuss the potential of new and enhanced procedures for biomarker measurement by fine-tuning the use of established technologies and applying new technologies.

BRCA1 Expression in Ovarian Cancer TMA by QFIA

In setting up an experiment using QFIA, we usually use cell lines to simulate actual clinical samples to first optimize antigen retrieval, antibody concentrations, and other assay variables. For instance, in demonstrating BRCA1 protein expression in papillary serous ovarian cancers, we used several cell lines with various levels of expression of BRCA1 to be served as standard controls (Rao *et al.,* 2002) and made an embedded cell block for each cell line following standard tissue-processing protocols. A test array was developed from these cell blocks. Cell lines are especially useful for comparing results of QFIA with the Western Blot for concordance. Keep in mind, however, that QFIA results may be more sensitive than Western Blot analysis in detecting subtle expressional abnormalities. For instance, in our control cell lines, whereas the Western Blot analysis showed similar level of expression of BRCA1 in 3AO and MLV3 cells, the TMA-QFIA analysis actually demonstrated a higher expression of BRCA1 in MLV3 cells, a benign serous cystadenoma cell line, than 3AO, a poorly differentiated carcinoma cell line. This finding was more consistent with the previous observation of a decreased BRCA1 expression in high-grade ovarian cancers (Zheng *et al.,* 2000).

A test array was built from specimens from 16 patients with sporadic papillary serous ovarian cancers (nine high-grade, five low-grade, and two borderline lesions), and three noncancer controls, as well as three cell lines (MLV3, MLV5, and 3AO). The results showed that BRCA1 labeling was modest in benign epithelial cells of the ovarian surface and fallopian tube. However, it was increased significantly in 6 of 7 borderline and low-grade tumors and decreased significantly in 8 of 9 of the high-grade tumors, compared to the corresponding normal epithelial cells derived from the fallopian tube (Figure 5). This finding confirmed reports that BRCA1 expression is altered during the ovarian carcinogenic process, probably by epigenetic mechanisms (Baldwin *et al.,* 2000; Zheng *et al.,* 2000).

When feasible, carrying out conventional IHC on the same array may yield interesting information. Several issues should be considered when one compares the results obtained from TMA-QFIA and manual categoric IHC. The first important difference with IHC is that a wide range of perceived intensity values

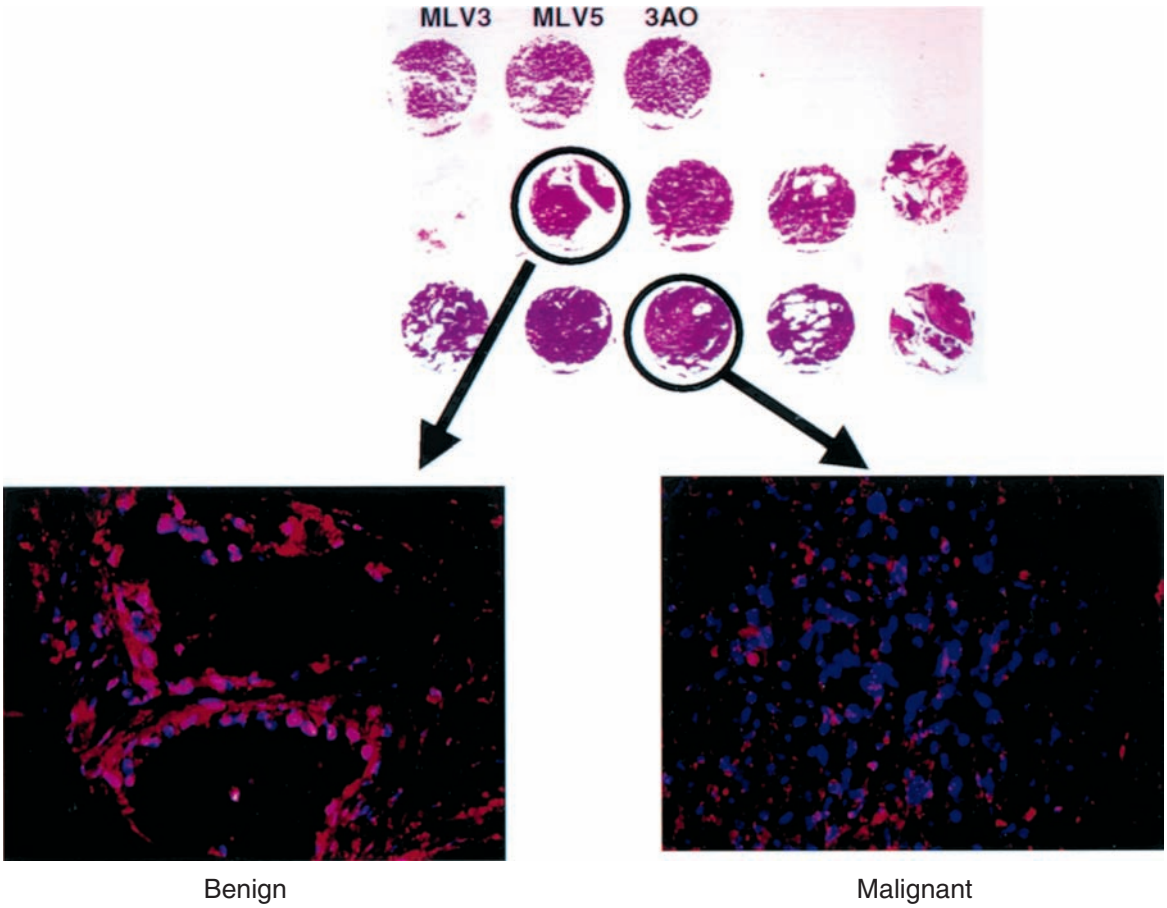

Figure 5. Representative images of BRCA1 with immunofluorescence-based quantitative fluorescence image analysis (400X) and immunohistochemistry labeling (200X) in benign and malignant cores are shown.

are grouped into a limited range of scoring categories. For example, in our study, tissue spots with an IHC score of 1 had TMA-QFIA mean fluorescence intensity as measured by average gray mean (AGM) values ranging from 30 up to 110. Also, within a case, the maximal IHC static range covered from 44 to 101 AGM. Thus, information may be lost as the result of the IHC categoric grouping. In addition, "gray zones" of scoring between categories (such as between 0–1 and 1–2) add to scoring ambiguities.

The second issue is the sensitivity of detection. In our experience, the TMA-QFIA appears to be more able to detect subtle expression abnormalities that are not detectable by manual IHC. For example, using IHC analysis, many high-grade cases would fall in the normal IHC range. However, using QFIA, all high-grade tumors fell in a region significantly below the normal range, as expected. This is further exemplified by findings from the adjacent dysplastic lesions in which a heterogeneous BRCA1 expression pattern can be detected by QFIA but not by IHC analysis. Overall, three out of four dysplastic lesions adjacent to high-grade tumor tissue also showed a significantly decreased expression by QFIA compared with the normal range; but, using IHC analysis, the majority were in the normal range.

Finally, another advantage that TMA-QFIA provides is an objective, instrument-based measurement, whereas manual IHC analysis is subjective and prone to intraobserver and interobserver variations. All these factors may contribute to the differences in the observations made using TMA-QFIA and IHC analysis, particularly for detecting changes at the low end of the target protein expression level and QFIA spectrum (i.e., AGM < 50) and for detecting subtle changes of expression.

In summary, as expected, the QFIA and IHC results showed similar trends among groups; however, IHC failed to detect significant differences between the field adjacent to the tumor and control samples, which was

the most intriguing finding picked up by QFIA. Compared to the corresponding fallopian tube epithelium, BRCA1 was significantly increased ($P < 0.05$ by student t-test) in the fields of 3 of 5 low-grade tumors and 3 of 7 high-grade lesions but decreased ($P < 0.05$ by student t-test) in the fields of remaining 4 of 7 high-grade lesions. This again suggested that QFIA analysis was more sensitive than IHC in detecting subtle quantitative expression abnormalities. Our finding from the adjacent fields suggested that alteration of BRCA1 expression is a common and probably an early event in the carcinogenic process for some papillary serous ovarian cancers. In addition, a similar pattern of decreased expression of BRCA1 in both the tumor and the adjacent field supports the hypothesis that some high-grade tumors may develop directly as a result of epigenetically driven inactivation of BRCA1 expression in the field.

New Technologies Associated with Fluorescence-Based Analysis

Fluorescent Nanocrystals

The commercialization of fluorescent nanocrystals offers advantages over organic dyes (Rosenthal 2001; Sukhanova *et al.,* 2002). Fluorescent nanocrystals are nanometer-sized particles of semiconductor materials, e.g., cadmium selenide (CdSe), engineered with a coating shell, e.g., zinc sulfide (ZnS) that eliminates nonradiative relaxation pathways, thus improving quantum yield and reducing photodegradation. Additionally, coating shells tune excitation/emission characteristics, confer desired physicochemical features, and enable labeling of biomolecules. Fluorescent nanocrystals are commercially available in a wide range of emissions, as nonderivatized core shells that may be cast into self-assembled films for instrument calibration, and as streptavidin- or carboxyl-derivatized core shells that may be coupled with primary or secondary antibodies. The photostability of these crystals makes possible nondegraded time-lapsed measurements (e.g., to evaluate excitation lamp stability). In our future study, EviFluors (Evident Technologies; Troy, NY), tuned at 490-nm, 540-nm, and 605-nm emissions and exhibiting sharp spectra with half-maximum bandwidths of 30 nm or less, will replace fluorescent dye conjugates used in our previous studies (Birckbichler *et al.,* 2000; Hemstreet *et al.,* 2000). These nanocrystals are matched to our imaging systems for high-energy excitation and efficient transmission and discrimination of emitted light (i.e., each label has its own high-pass luminance channel in each imaging system). In addition, complementary advances in the development of tunable microscope filters (Lequime *et al.,* 2002) allow separation and quantification of up to 40 fluorescent probes in a single cell. We anticipate the availability of software supporting a wide range of CCD cameras and an upgrade of our camera-based imaging systems to tunable filters.

Mercury-Xenon versus Mercury Vapor Lamp

Light output stability of the fluorescence excitation lamp is fundamental to high-quality measurements by QFIA, and variability in the output of the mercury (Hg) vapor lamp is a significant source of error. Stability is evaluated in terms of fluctuation or short-term variation and drift or long-term variation in light output. Mercury vapor lamps used in fluorescence microscopy usually have life spans of 300 hours, and as they approach the end of their life span, at 200 hours, exhibit output fluctuations primarily as a result of "discharge point shift" caused by cathode fatigue. In addition, electrode wear and sputtering produce "lamp blackening" a primary cause of output drift. Mercury-xenon lamps (Hamamatsu Photonics K.K., Japan) incorporate a barium iodide–impregnated cathode that exhibits virtually no wear over time; consequently, these lamps exhibit remarkable stability and have extended life spans of 1000 to 2000 hr.

Mercury-xenon lamp housings are cumbersome, however, and have not been adapted to microscope systems. Simple adaptation of the Hg lamp housing for the Hg-xenon lamp is not feasible because of significant differences in lamp configuration and electrical requirements. Orientation of the anode and cathode is reversed in the two lamps. The ignition trigger for the Hg-xenon is 10–20 K volts higher than that of the Hg lamp and requires significantly more electrical insulation. The power supply of the Hg lamp provides constant voltage, whereas that of the Hg-xenon provides constant current; thus different power supplies are needed. Hg-xenon lamp technology is advancing rapidly, and it is anticipated that soon a new generation of lamps will be integrated into microscope systems.

In conclusion, the TMA protocol is designed as a platform for analyzing large numbers of tissues in a high-throughput manner. Our study shows the potential application of combining TMA with QFIA for measuring protein expression *in situ,* particularly for the detection of subtle expression abnormalities that may not be detectable by traditional IHC methods. The automated image capture and fluorescence-based measurement algorithm of TMA-QFIA should translate from small-scale studies to studies involving large numbers of samples and presents significant technologic advances toward fully automated protein expression analysis.

References

Baldwin, R.L., Nemeth, E., Tran, H., Shvartsman, H., Cass, I., Narod, S., and Karlan, B.Y. 2000. BRCAI promoter region hypermethylation in ovarian carcinoma: A population-based study. *Cancer Res. 60*:5329–5333.

Bonner, R., Hurst, R., Rao, J., and Hemstreet, G.P. 1998. Instrumentation, accuracy and quality control in development of quantitative fluorescence image analysis. In M. Hanausek and Z. Walaszek (Eds.), *Tumor Marker Protocols, Methods in Molecular Biology Series 14*:181–205.

Birckbichler, P.J., Bonner, R.B., Hurst, R.E., Bane, B.L., Pitha, J.V., and Hemstreet, G.P., III. 2000. Loss of tissue transglutaminase as a biomarker for prostate adenocarcinoma. *Cancer 89*:412–423.

Hemstreet, G.P., III, Bonner, R.B., Hurst, R.E., Bell, D., and Bane, B.L. 2000. Abnormal G-actin content in single prostate cells as a biomarker of prostate cancer. *Cancer Detect. Prev. 24*:464–472.

Hu, N., Taylor, P.R., Rao, J.Y., and Hemstreet, G.P. 1998. Quantitative Fluorescence Image Analysis (QFIA) of esophageal balloon cytology smears and subsequent development of esophageal and gastric cardia cancer in Linxian, China. *Cancer Epidemiol. Biomarkers Prev. 7*:59–64.

Lequime, M., Parmentier, R., Lemarchand, F., and Amra, C. 2002. Toward tunable thin-film filters for wavelength division multiplexing applications. *Appl. Opt. 41*:3277–3284.

Nibbering, P.H., Leijh, P.C., and Van Furth, R. 1985. A cytophotometric method to quantitate the binding of monoclonal antibodies to individual cells. *J. Histochem. Cytochem. 33*:453–459.

Rao, J., Hemstreet, G.P., Hurst, R., Bonner, R., Jones, P., Min, K., and Fradet, Y. 1993. Alterations in phenotypic biochemical markers in bladder epithelium during tumorigenesis. *Proc. Natl. Acad. Sci. 90*:8287–8291.

Rao, J., Apple, S., Jin, Y.S., Hemstreet, G.P., and Nieberg, R. 1998. Single cell multiple biomarker analysis in archival fine needle aspiration specimens: Quantitative fluorescence image analysis of DNA ploidy, p53 and G-actin as breast cancer biomarkers. *Cancer Epidemiol. Biomarkers Prev. 7*:1027–1033.

Rao, J., Seligson, D., and Hemstreet, G.P. 2002. Protein expression analysis using quantitative flourescence image analysis on tissue microarray slides. *Biotechniques 32*:924–926.

Rosenthal, S.J. 2001. Bar-coding biomolecules with fluorescent nanocrystals. *Nat. Biotechnol. 19*:621–622.

Sukhanova, A., Venteo, L., Devy, J., Artemyev, M., Oleinikov, V., Pluot, M., and Nabiev, I. 2002. Highly stable fluorescent nanocrystals as a novel class of labels for immunohistochemical analysis of paraffin-embedded tissue sections. *Lab. Invest. 82*:1259–1261.

West, S.S. 1970. The microscope, spectra, and automated analysis. *Clin. Chem. 16*:643–650.

Zheng, W., Luo, F., Lu, J.J., Baltayan, A., Press, M.F., Zhang, Z.F., and Pike, M.C. 2000. Reduction of BRCAI expression in sporadic ovarian cancer. *Gynecol. Oncol. 76*:294–300.

5

Identification of Differentially Expressed Genes Using Rapid Subtraction Hybridization: Detailed Methodology for Performing Rapid Subtraction Hybridization

Dong-chul Kang, Zao-zhong Su, Habib Boukerche, and Paul B. Fisher

Introduction

Temporal modulations in gene expression represent primary determinants of the wide array of physiologic alterations occurring in cells during processes such as aging; differentiation; development; cell proliferation; and disease development and progression, including neurodegeneration and cancer (de la Monte *et al.,* 1995; Heller *et al.,* 1997; Jiang and Fisher, 1993; Shelton *et al.,* 1999; Zhang *et al.,* 1997). Based on this consideration, defining the spectrum of genes displaying differential expression concomitant with alterations in cellular physiology is paramount in comprehending these complex processes at the molecular level. Traditionally, subtraction hybridization has been used to identify and clone genes displaying differing expression kinetics (Sagerström *et al.,* 1997). However, the initially described subtractive complementary deoxyribonucleic acid (cDNA) library protocols were time consuming, labor intensive, and technically demanding and required a large amount of starting material, which mandated the development of improved subtraction hybridization schemes (Jiang and Fisher, 1993; Sagerström *et al.,* 1997).

During the past decade, advancements in polymerase chain reaction (PCR) and sequencing techniques have

Handbook of Immunohistochemistry and *in situ* Hybridization of Human Carcinomas, Volume 3: Molecular Genetics, Liver Carcinoma, and Pancreatic Carcinoma

enabled development of diverse methods to identify differentially expressed genes that can substitute or improve subtracted cDNA library analysis. These include differential ribonucleic acid (RNA) display (DDRT-PCR) (Liang *et al.,* 1995), reciprocal subtraction differential RNA display (RSDD) (Kang *et al.,* 1998), representational difference analysis (RDA) (Hubank and Schatz, 1994), RNA fingerprinting by arbitrarily primed PCR (RAP-PCR) (McClelland and Welsh, 1994), rapid subtraction hybridization (RaSH) (Jiang *et al.,* 2000; Kang *et al.,* 2002a), suppression subtractive hybridization (Diatchenko *et al.,* 1996; Diatchenko *et al.,* 1999), and serial analysis of gene expression (SAGE) (Velculescu *et al.,* 1995). Microarrays of combinatorial gene matrix oligonucleotides and cDNAs have also been used to detect alterations in gene expression (Schena *et al.,* 1995; Schena *et al.,* 1996). With the plethora of methods currently available, researchers now have numerous options for defining differential gene expression. Choosing the correct approach is based on suitability for specific experimental demands, which take into account factors including cost, labor, time, and amount of starting material. This latter problem, limited starting material, is no longer an insurmountable obstacle with the availability of PCR as well as the ability to amplify cRNA by *in vitro* transcription (Kacharmina *et al.,* 1999; Jiang *et al.,* 2000). In general, whereas construction and evaluation of subtracted cDNA libraries, DDRT-PCR, and RSDD are labor intensive, drawbacks to SAGE and microarray analyses include high cost and the need for preexisting databases of identified genes, respectively.

Theoretically, it is now possible to develop a complete "transcriptional map" that encompasses the entire repertoire of gene expression changes occurring during complex physiologic alterations in target cells and organisms. Unfortunately, no single currently available cloning approach can achieve this objective. Instead, a combination of multiple schemes, including cDNA library subtraction, DDRT-PCR, RSDD, SAGE, and microarray analyses, may be required. Moreover, the need for multiple approaches is reinforced by the observation that different sets of genes are identified using the various approaches applied to the same experimental system. The reason for the selective biases of the different approaches is not currently known.

To simplify and accelerate efforts to clone differentially expressed genes, Jiang *et al.,* (2000) developed the RaSH approach. This scheme combines PCR amplification, conventional subtractive hybridization, and ligation-driven selection of subtracted cDNAs. Proof-of-principle for the RaSH approach was obtained by analyzing the temporal changes of gene expression occurring during induction of terminal differentiation in human melanoma cells treated with interferon-beta (IFN-β) plus mezerein (MEZ) (Figure 5). In RaSH, cDNA samples are restriction-digested with frequent cutters such as *Dpn*II to an average size of 256 bp to improve hybridization efficiency. Moreover, restriction digestion of tester cDNA only prior to hybridization enables selection and cloning of tester-unique cDNAs by direct ligation of hybridization mixtures to corresponding sites in the plasmid vector. Thus, RaSH reduces the amount of starting materials required for conventional subtraction hybridization by one tenth by using PCR and obviates the need to separate and clone subtracted cDNA species into plasmid vector or bacteriophage, a nontrivial, technically demanding step in subtractive cDNA library construction (Jiang and Fisher, 1993; Sagerström *et al.,* 1997). In addition, RaSH uses reverse Northern Blot hybridization for further rapid confirmation of differential expression of RaSH clones (Huang *et al.,* 1999a; Kang *et al.,* 1998). This unique assortment of preexisting subtractive cDNA library protocols and innovative steps in the RaSH method significantly simplifies conventional subtractive cDNA library approaches resulting in a cost-efficient, fast, and highly efficacious system for performing subtraction hybridization. Since its inception, RaSH has enabled the cloning of genes displaying altered expression in the context of melanoma growth and differentiation, human immunodeficiency virus (HIV)-1 resistance in T-cells and HIV-1–infected and tumor necrosis factor (TNF-α)–treated human fetal astrocytes (Simm *et al.,* 2001; Su *et al.,* 2002; Su *et al.,* 2003a; Su *et al.,* 2003b). These successful applications of RaSH highlight the potential of this approach for diverse applications in multiple model systems.

In this chapter, we provide a detailed protocol for subtracted cDNA library construction by RaSH. Additional methods, including reverse Northern and Northern Blot hybridization, which are part of the RaSH approach, are described in detail elsewhere (Huang *et al.,* 1999a; Kang *et al.,* 1998). For basic molecular biology techniques a good reference source is Sambrook and Russell (2001).

MATERIALS

1. Oligo dT cellulose (Invitrogen).
2. Oligo $dT_{12\text{-}18}$ primer (0.5 mg/ml, Invitrogen).
3. Reverse transcriptase: Superscript RT II (200 U/μl, Invitrogen).
4. 10 mM dNTP Mix (Amersham-Pharmacia).
5. RNase inhibitor (10 U/μl).

6. *Escherichia coli* DNA polymerase I (10 U/µl, Invitrogen).
7. 10X second-strand buffer (Invitrogen).
8. *E. coli* ribonuclease (RNase) H (2 U/µl, Invitrogen).
9. *E. coli* DNA ligase (10 U/µl, Invitrogen).
10. *Dpn*II (New England BioLabs).
11. *Xho*I (New England BioLabs).
12. T4 DNA ligase (400 U/µl, New England BioLabs).
13. Taq DNA polymerase (5 U/µl, Invitrogen).
14. Centricon YM-50 (Amicon).
15. pCR II vector.
16. TE: 10 mM Tris-HCl pH 8.0, 1 mM EDTA.
17. Tris-saturated phenol (pH 8.0).
18. Chloroform.
19. 5 M NaCl.
20. Hybridization buffer: 50 mM Tris-HCl, pH 7.5, 0.2% sodium dodecyl sulfate (SDS), 0.5 M NaCl and 40% deionized formamide.
21. Competent cells: One Shot (Invitrogen).
22. Primers:
    XDPN18: CTGATCACTCGAGAGATC
    XDPN14: CTGATCACTCGAGA
    XDPN12: GATCTCTCGAGT
    T7 promoter primer
    M13 reverse primer

METHODS

1. **Tester and driver cDNA synthesis.**

1 µg poly A^+ RNA in d.w.	12 µl
Oligo $dT_{12\text{-}18}$ (0.5 mg/ml)	2.5 µl

Heat the mixture 70°C for 5 min and quench onice. Add the following and incubate at 37°C for 1.5 hr.

5X first-strand buffer	5 µl
10 mM dNTP mix	1.25 µl
0.1 M dithiothreitol (DTT)	2.5 µl
RNase inhibitor	0.5 µl
Superscript RT (reverse transcriptase) II (200 U/µl)	1.25 µl
	25 µl

Proceed to second-strand synthesis by addition of the following directly to reverse transcription reaction and incubation at 16°C for 3 hr.

d.w.	144.75 µl
10 mM dNTP mix	3.75 µl
10X second-strand buffer	20 µl
E. coli DNA polymerase I (10 U/µl)	5 µl
E. coli RNase H (2 U/µl)	0.85 µl
E. coli DNA Ligase (10 U/µl)	0.65 µl
	200 µl

Extract synthesized cDNA with phenol/chloroform.

Add 1/10 volume of 5 M NaCl and 2 volumes of ethanol.

Incubate at −80°C for 1 hr to overnight.

Precipitate cDNA by microcentrifugation and wash with 70% ethanol 2×.

Resuspend in 10 µl Tris Ethylenediaminetetraacetic acid (TE).

2. *Dpn*II restriction digestion for both tester and driver cDNAs.

Assemble the 50 µl reaction mixture as follows and incubate at 37°C for 4 hr.

cDNA	10 µl
d.w.	30 µl
10X *Dpn*II buffer	5 µl
DpnII (10 U/µl)	5 ml

Make up the volume to 100 µl with TE, extract, and precipitate digested cDNA as explained previously.

3. Adaptor ligation.

Assemble the ligation mixture as follows.

Dpn II-digested cDNA plus d.w.	16 µl
100 mM XD-14	4 µl
100 mM XD-12	4 µl
10X ligase buffer	3 µl

Heat at 55°C for 1 min and gradually cool down to 14°C for 1 hr.

Add 3 µl T4 DNA ligase (400 U/µl).

Incubate at 14°C overnight.

Dilute the reaction to 100 µl with TE.

4. Amplification of cDNA libraries.

Assemble PCR reaction mixture as follows. You need 20 PCR reactions for each library.

d.w.	164 µl
10X PCR buffer	20 µl
25 mM $MgCl_2$	8 µl
20 mM dNTPs	4 µl
2 mg/ml XD-18	1 µl
cDNA ligation mixture	2 µl
Taq DNA polymerase (5 U/µl)	1 µl
	200 µl

PCR parameters are as follows:
72°C for 6 min
20–25 cycles of the following:
1 min at 94°C.
1 min at 55°C.
2 min at 72°C.

Pool the PCR reactions and purify the PCR product with Centricon YM-50. (*PCR purification kit can substitute Centricon YM-50.*)

Ethanol precipitate as in section 1 and resuspend in TE to 1 µg/µl, if necessary.

5. *Xho* I digestion of tester cDNA.

Incubate the following restriction digestion reaction at 37°C for 4 hr.

20 µg tester cDNA	
10X *Xho*I buffer	10 µl
d.w.	up to 90 µl
*Xho*I (20 U/µl)	10 µl
	100 µl

Extract and precipitate digested cDNA as explained. Resuspend DNA with TE at 1 mg/ml.

6. Subtraction hybridization

a. Mix 0.1 µg *Xho*I-digested tester cDNA with 3 µg driver cDNA. *(Driver amount can be controlled by the desired ratio of subtraction)*.

b. Ethanol precipitation as in section 1.

c. Resuspend the cDNA mixture in 10 µl hybridization buffer.

d. Boil for 5 min and gradually cool down to 42°C.

e. Overlay with mineral oil to prevent evaporation.

f. Incubate at 42°C for 48 hr.

g. Extract the hybridization mixture with phenol/chloroform as section 1.

h. Ethanol precipitation as in section 1. No need for addition of NaCl in this step.

i. Resuspend in 20 µl of TE buffer.

7. Subtracted cDNA cloning.

a. Plasmid (pCR II) is prepared by *Xho*I digestion followed by calf intestinal alkaline phosphatase treatment and gel purification.

b. Assemble ligation reaction as follows and incubate 14°C overnight.

Subtracted cDNAs	2.5 µl
XhoI-digested pCR II vector	1 µl
10X Ligation buffer	1 µl
d.w.	up to 9 µl
T4 DNA ligase	1 µl
	10 µl

c. Transform competent cells (Shot-1) with ligation mixture.

8. PCR amplification of cDNA inserts for screening.

a. Grow 0.5 ml overnight culture.

b. Assemble PCR reaction.

Overnight culture	1 µl
d.w.	39.3 µl
10X buffer	5 µl
50 mM $MgC1_2$	1.5 µl
10 mM dNTP mix	1 µl
10 µM T7 promoter primer	1 µl
10 µM M13 Reverse Primer	1 µl
Taq DNA polymerase (5 U/µl)	0.2 µl
	50 µl

c. PCR as follows.

3 min at 95°C
35 cycles of
  1 min at 95°C
  1 min at 55°C
  1.5 min at 72°C
1 cycle of 72°C 10 min

RESULTS AND DISCUSSION

The RaSH protocol consists of three steps: 1) preparation of driver and tester cDNAs, 2) subtractive cDNA hybridization, and 3) cloning tester-specific cDNAs into plasmid vectors (Figure 6) (Jiang *et al.,* 2000; Kang *et al.,* 2002a). cDNAs from tester and driver are digested by frequent cutters to small fragments in average 256 bp to facilitate efficient subtraction hybridization. After ligation of double-stranded DNA to adaptors that provide primer sites and cloning restriction enzyme sites, the cDNA fragment is minimally amplified by PCR to obtain cDNA libraries. Subtractive hybridization is performed at a variable ratio of driver and tester cDNAs, of which only tester cDNAs were digested by cloning restriction enzyme (*Bam*HI or *Xho*I). Whereas the restriction site of the common tester cDNA is masked by hybridization with driver cDNA, the restriction site of the unique tester cDNA remains available for ligation into correspondingly digested vector, facilitating separation and cloning tester-specific cDNAs. Reverse Northern Blot hybridization further confirms differential expression of RaSH-cloned genes (Jiang *et al.,* 2000; Simm *et al.,* 2001; Su *et al.,* 2002; Su *et al.,* 2003a; Su *et al.,* 2003b).

RaSH uses PCR to minimize the quantity of RNA required for the subtraction procedure. However, because differential gene expression can be normalized by excessive PCR, the number of PCR cycles is limited to maintain the original composition of RNA as much as possible. In fact, within the suggested number of amplification cycles, we could identify genes whose expression changed as little as threefold, which is comparable with other subtraction protocols that do not use PCR (Jiang *et al.,* 2000; Su *et al.,* 2002). PCR amplification in the RaSH protocol can be distinguished from PCR used in suppression subtractive hybridization (SSH; Diatchenko *et al.,* 1996), because the two methods are fundamentally different. Whereas PCR is the tool of subtraction in SSH in which amplification of commonly expressed genes is suppressed by panhandle-forming primers, PCR in RaSH is used for simply securing cDNA samples for subtraction

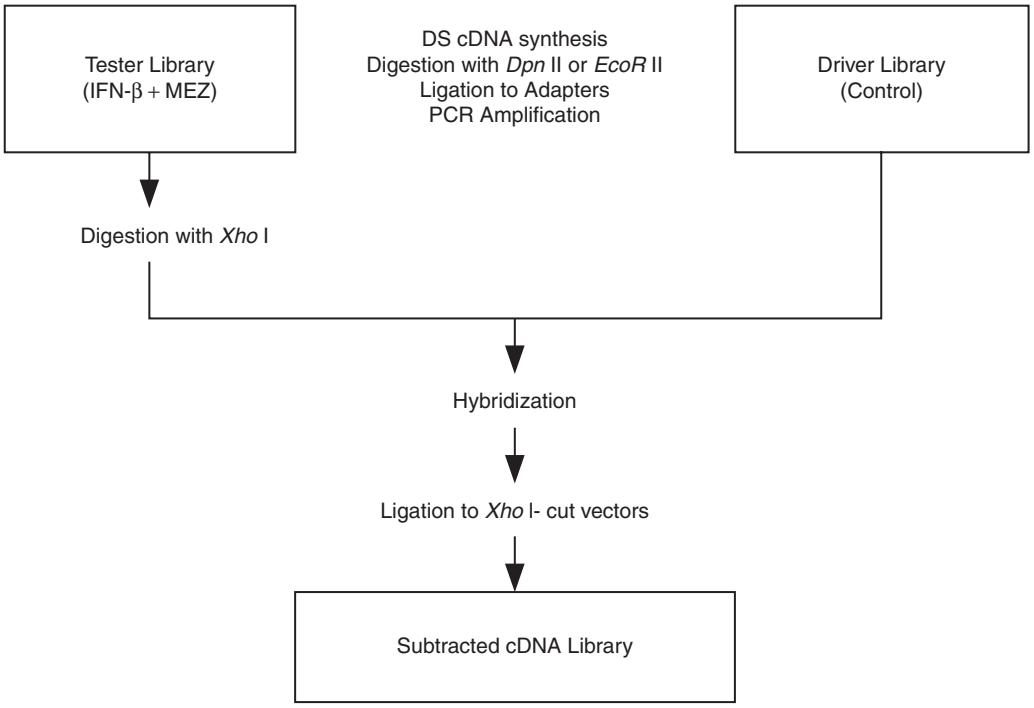

Figure 6. An overview of the rapid subtraction hydridization (RaSH) protocol. The RaSH scheme involves construction of tester interferon (IFN)-β + mezerein (MEZ) and driver (control) HO-1 libraries followed by digestion of only the tester library with *Xho*I. Following hybridization, differentially expressed sequences are cloned into *Xho*I-digested vectors, resulting in a subtracted complementary deoxyribonucleic acid (cDNA) library enriched for *mda* genes displaying elevated expression. RaSH can also be used to produce a subtracted cDNA library enriched for genes down-regulated during terminal differentiation by alternating tester and driver. (From Jiang *et al.,* 2000.)

hybridization. Selection of differentially expressed genes in RaSH is achieved by ligation of unmasked cohesive ends on unhybridized cDNAs to corresponding restriction enzyme–cleaved vector. Thus, RaSH does not require repeated steps of hybridization and PCR as does SSH, which can potentially distort the original messenger RNA (mRNA) composition, and also introduce unwanted PCR artifacts.

RaSH was first applied to identify differentially expressed genes during terminal differentiation of human melanoma cells (Fisher *et al.,* 1985; Jiang and Fisher, 1993; Jiang *et al.,* 1993). A combination treatment of HO-1 human melanoma cells with IFN-β and the antileukemic reagent MEZ undergo terminal differentiation defined by profound morphologic changes, irreversible growth arrest, and subsequent apoptosis (Fisher *et al.,* 1985; Kang *et al.,* 2002b). RNA samples are collected at 2, 4, 8, 16, and 24 hr after treatment to encompass the spectrum of temporal changes in gene expression (Huang *et al.,* 1999a; Jiang and Fisher, 1993). To determine the effect of cDNA size, two different restriction enzymes that yield average DNA fragments of ~256 bp (*Dpn*II) or 512 bp (*Eco*RII) were used in construction of RaSH libraries (*Dpn*-sLib and *Eco*R-sLib, respectively). Screening ~10% of each RaSH library resulted in 25 (*Dpn*-sLib) and 17 (*Eco*R-sLib) distinct cDNA clones at a redundancy rate of 1.44 and 1.64, respectively. The redundancy of individual clones increased with the size and abundance of the transcript. The enrichment effect of the RaSH subtraction protocol was calculated by comparison of cDNA amount of fibronectin and leukemia inhibitory factor (LIF) before and after subtraction by Southern Blot hybridization (Figure 7). The enrichment factor for fibronectin was 75-fold in *Dpn*-sLib and 6-fold in *Eco*R-sLib, whereas the enrichment factor for LIF was 544-fold in *Dpn*-sLib and 96-fold in *Eco*R-sLib. Thus, in general, redundancy is lower and enrichment is higher in *Dpn*-sLib than in *Eco*R-sLib. It is interesting that only three cDNA species are common between the two libraries. The underlying reason for the recognition of different genes in the RaSH-dervied *Dpn*-sLib versus the RaSH-dervied *Eco*R-sLib is not currently known, but it could reflect the fact that only ~10% of the two libraries were screened for differentially expressed genes or, alternatively, the

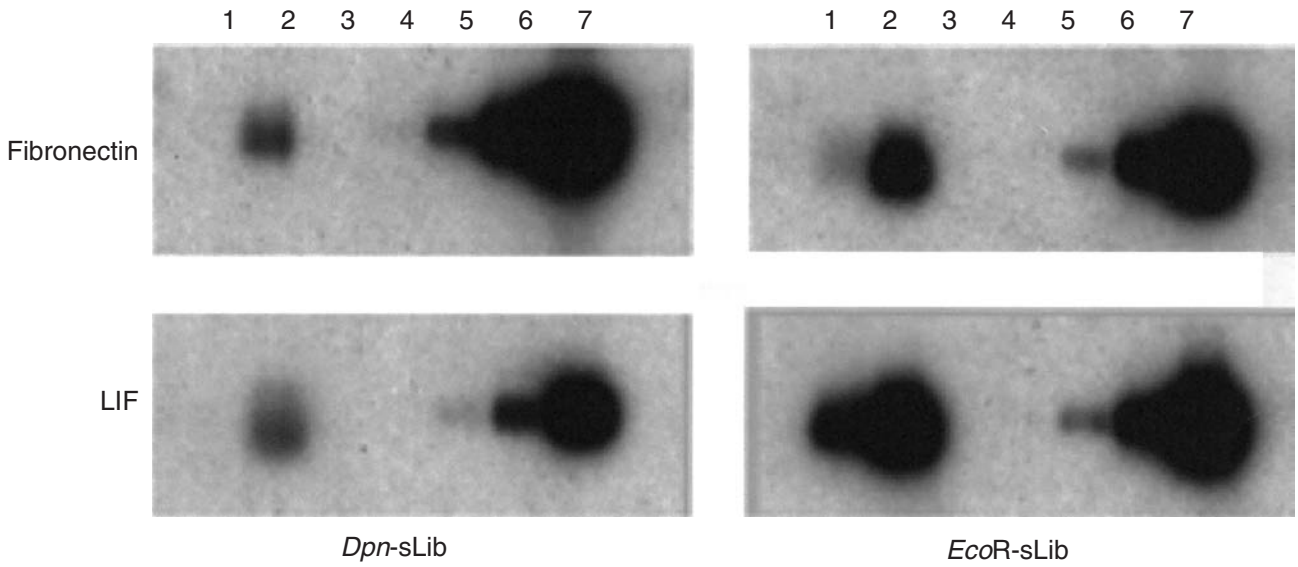

Figure 7. Determination of the subtraction efficiency for fibronectin and leukemia inhibitory factor (LIF) fragments in RaSH libraries. The relative amount of fibronectin and LIF fragments in polymerase chain reaction (PCR) libraries was determined by comparison of the signal intensity of fibronectin and LIF in specified complementary deoxyribonucleic acid (cDNA) libraries (*Dpn*-sLib and *Eco*R-sLib) with the signal intensity of defined amounts of the cDNA fragments by Southern Blot hybridization. Lane 1, 100 ng PCR-cDNA library from untreated cells; lane 2, 100 ng PCR-cDNA library from interferon-β + mezerein treated cells; lanes 3 to 7, increasing amounts of cDNA fragments of fibronectin and LIF (0.001, 0.01, 0.1, 1, and 10 ng, respectively). PhosphorImager (Molecular Dynamics) scanning determined hybridized signal intensity. Subtraction efficiency was determined by comparison of relative signal intensity of the molecules in cDNA libraries before and after subtraction. (From Jiang *et al.,* 2000.)

availability of restriction sites for each enzyme might contribute directly to differential gene identification (Jiang *et al.,* 2000; Kang *et al.,* 2002a).

In RaSH, the cDNA is fragmented by frequent cutting restriction enzymes to facilitate hybridization kinetics for identifying differentially expressed genes. However, the theoretical numbers of fragments that increase based on the size of transcript might be directly proportional to redundancy, as indicated by the high occurrence of relatively long transcript genes, such as fibronectin and LIF (Jiang *et al.,* 2000; Kang *et al.,* 2002a). By using two restriction enzymes, which recognize sites with different frequencies, it should be possible to define the relationship between theoretical fragment numbers and relative occurrence rate. Unexpectedly and for unknown reasons, the *Dpn*-sLib (average 256 bp cutting) manifested less redundancy than *Eco*R-sLib (average 512 bp cutting). However, enrichment was significantly higher in the *Dpn*-sLib than in the *Eco*R-sLib by a factor of ~7 -to ~16-fold. In addition, representation judged from gene diversity was also higher in the *Dpn*-sLib. *Dpn* II generates shorter DNA fragments than *Eco* RII on average, which may improve hybridization kinetics, decrease probability of nonspecific hybridization, or both. A library of shorter fragments from *Dpn* II digestion would also be more representative because of better PCR efficiency and less dependence on sequence context. Therefore, the *Dpn*-sLib is preferred to the *Eco*R-sLib with respect to redundancy rate, enrichment efficacy, and library representation.

Previous approaches to identify melanoma differentiation associated (*mda*) genes included random clonal selection, high-throughput microarray screening of arrayed cDNAs, and random isolation followed by differential screening of clones from subtracted cDNA libraries constructed from RNA samples collected during the induction of differentiation of human melanoma cells by IFN-β + MEZ (Huang *et al.,* 1999a; Huang *et al.,* 1999b; Jiang and Fisher, 1993). These studies provided important baseline data for evaluating the efficiency of the RaSH procedure. Subtracted cDNA library analysis by random selection, high-throughput microarray screening, and differential screening identified 23 from 70, 112 from 1000, and 65 from 400 cDNA clones, respectively, which manifested altered expression during terminal differentiation, suggesting an average 20% hit rate. In contrast, 50% of 64 colonies randomly picked from the two RaSH libraries (32 from each) appeared differentially

expressed in reverse Northern Blot hybridization, and 89% of the reverse Northern positive clones displayed altered gene expression in Northern Blot analysis (Jiang *et al.,* 2000). Thus, RaSH produces an ~45% hit rate, which is approximately twofold higher than conventional subtractive cDNA libraries constructed from this same model system. Moreover, whereas the average redundancy of RaSH is calculated at 1.52, that of subtractive cDNA library is 1.92. In these contexts, the lower redundancy and the higher hit rate for differentially expressed genes in the RaSH library in comparison with the subtractive cDNA library clearly demonstrates the value of RaSH over conventional methods. Additionally, the simplified protocol for separating and cloning subtracted cDNAs when using RaSH is also a strong point of this strategy over conventional subtractive cDNA library procedures.

Two potential problems encountered with RaSH can be easily addressed (Kang *et al.,* 2002a). Although the majority of RaSH clones contain a single cDNA, multiple cDNAs (two in most cases) can be connected in tandem and inserted into a single clone. Multiple inserts can be identified by restriction analysis, checking for the presence of a restriction site used in library construction. Alternatively, introducing a secondary enzyme site in the cloning step will prevent incorporation of multiple inserts into the cloning vector. Moreover, introduction of secondary enzyme sites can also enhance cloning efficiency by preventing vector self-ligation. Additional problems that can arise in the RaSH procedure involve restriction enzyme fragmentation of specific cDNAs. Because any part of a gene can be inserted into a RaSH clone, two parts of an unknown gene can be mistakenly interpreted as distinct cDNA species. Modification to immobilize the 3′-end using biotinylated oligo dT in reverse transcription could be used to remedy this problem.

Recently, RaSH has been applied for reciprocal subtraction to clone both up- and down-regulated genes associated with HIV-1 resistance and during neurodegeneration associated with damage to astrocytes following infection with HIV-1 or treatment with TNF-α. When applied to cloning differentially expressed genes in HIV-sensitive versus HIV-resistant T-cell variants, RaSH identified 11 elevated genes and 6 down-regulated genes in HIV-resistant T-cell variants (Simm *et al.,* 2001). In addition, 15 astrocyte elevated genes and 10 astrocyte suppressed genes have been identified following HIV-1 infection into human fetal astrocytes by reciprocal application of RaSH (Su *et al.,* 2002; Su *et al.,* 2003b). In another application of RaSH, 8 metastasis elevated genes, including 2 novel genes, were identified that display elevated expression in human melanoma cells that have the capacity to induce high levels of metastasis in athymic nude rats versus poorly metastatic variants (Boukerche *et al.,* 2004). The simplicity of the RaSH protocol facilitates reciprocal subtraction approaches. These examples clearly emphasize the utility of RaSH as a simple and efficient way to clone differentially expressed genes in diverse biological systems.

In summary, the RaSH approach represents a validated methodology for efficiently identifying and cloning genes of potential interest with tremendous upside potential. This strategy has already been used to identify genes associated with and potentially regulating cell growth and differentiation, apoptosis, and susceptibility to HIV-1 infection in T-cells and during damage to astrocytes following infection with HIV-1 or treatment with neurotoxic agents, such as TNF-α (Jiang *et al.,* 2000; Simm *et al.,* 2001; Su *et al.,* 2002; Su *et al.,*2003a; Su *et al.,* 2003b). In principle, RaSH can be applied to any biological system in which the end point is identifying differentially expressed genes. This includes, but is not limited to, characterizing differentially regulated genes involved in growth control, response to DNA damaging and chemotherapeutic agents, cellular response to virus infection, terminal differentiation, development, aging, neurodegeneration, apoptosis, tumorigenesis, metastasis, and cancer suppression. Based on its simplicity, robustness, and proven efficiency, RaSH will be a method of choice for defining relevant changes in gene expression occurring during complex physiologic changes in cells.

Acknowledgments

The present research was supported in part by National Institutes of Health grants CA35675, CA97318, CA98712, GM06888 and NS31492; the Samuel Waxman Cancer Research Foundation; and the Chernow Endowment. P.B.F. is the Michael and Stella Chernow Urological Cancer Research Scientist in the Departments of Pathology and Urology, College of Physicians and Surgeons of Columbia University and a SWCRF Investigator.

References

Boukerche, H., Su, Z.-Z., Kang, D.-C., and Fisher, P.B. 2004. Identification and cloning of genes displaying elevated expression as a consequence of metastatic progression in human melanoma cells by rapid subtraction hybridization. *Gene 343*:191–201.

de la Monte, S.M., Ng, S.C., and Hsu, D.W. 1995. Aberrant GAP-43 gene expression in Alzheimer's disease. *Am. J. Pathol. 147*:934–946.

Diatchenko, L., Lau, Y.F., Campbell, A.P., Chenchik, A., Moqadam, F., Huang, B., Lukyanov, S., Lukyanov, K., Gurskaya, N., Sverdlov, E.D., and Siebert, P.D. 1996. Suppression subtractive hybridization: A method for generating differentially regulated or tissue-specific cDNA probes and libraries. *Proc. Natl. Acad. Sci. USA 93*:6025–6030.

Diatchenko, L., Lukyanov, S., Lau, Y.F., and Siebert, P.D. 1999. Suppression subtractive hybridization: A versatile method for identifying differentially expressed genes. *Methods Enzymol. 303*:349–380.

Fisher, P.B., Prignoli, D.R., Hermo, H., Jr., Weinstein, I.B., and Pestka, S. 1985. Effects of combined treatment with interferon and mezerein on melanogenesis and growth in human melanoma cells. *J. Interferon Res. 5*:11–22.

Heller, R.A., Schena, M., Chai, A., Shalon, D., Bedilion, T., Gilmore, J., Woolley, D.E., and Davis, R.W. 1997. Discovery and analysis of inflammatory disease-related genes using cDNA microarrays. *Proc. Natl. Acad. Sci. USA 94*:2150–2155.

Huang, F., Adelman, J., Jiang, H., Goldstein, N.I., and Fisher, P.B. 1999a. Differentiation induction subtraction hybridization (DISH): A strategy for cloning genes displaying differential expression during growth arrest and terminal differentiation. *Gene 236*:125–131.

Huang, F., Adelman, J., Jiang, H., Goldstein, N.I., and Fisher, P.B. 1999b. Identification and temporal expression pattern of genes modulated during irreversible growth arrest and terminal differentiation in human melanoma cells. *Oncogene 18*:3546–3552.

Hubank, M., and Schatz, D.G. 1994. Identifying differences in mRNA expression by representational difference analysis of cDNA. *Nucleic Acids Res. 22*:5640–5648.

Jiang, H., and Fisher, P.B. 1993. Use of a sensitive and efficient subtraction hybridization protocol for the identification of genes differentially regulated during the induction of differentiation in human melanoma cells. *Mol. Cell. Differ. 1*:285–299.

Jiang, H., Kang, D.C., Alexandre, D., and Fisher, P.B. 2000. RaSH, a rapid subtraction hybridization approach for identifying and cloning differentially expressed genes. *Proc. Nad. Acad. Sci. USA 97*:12684–12689.

Jiang, H., Su, Z.-Z., Boyd, J., and Fisher, P.B. 1993. Gene expression changes associated with reversible growth suppression and the induction of terminal differentiation in human melanoma cells. *Mol. Cell. Differ. 1*:41–66.

Kacharmina, J.E., Crino, P.B., and Eberwine, J. 1999. Preparation of cDNA from single cells and subcellular regions. *Methods Enzymol. 303*:3–18.

Kang, D.C., Jiang, H., Su, Z.-Z., Volsky, D.J., and Fisher, P.B. 2002a. RaSH-Rapid subtraction hybridization. In Lorkowski, S., and Cullen, P., (eds) *Analysing Gene Expression*, Germany: Wiley-VCH Verlag GmbH, 206–214.

Kang, D.C., Gopalkrishnan, R.V., Wu, Q., Jankowsky, E., Pyle, A.M., and Fisher, P.B. 2002b. *mda*-5: An interferon-inducible putative RNA helicase with double-stranded RNA-dependent ATPase activity and melanoma growth-suppressive properties. *Proc. Natl. Acad. Sci. USA 99*:637–642.

Kang, D.C., LaFrance, R., Su, Z.Z., and Fisher, P.B. 1998. Reciprocal subtraction differential RNA display: An efficient and rapid procedure for isolating differentially expressed gene sequences. *Proc. Natl. Acad. Sci. USA 95*:13788–13793.

Liang, P., Bauer, D., Averboukh, L., Warthoe, P., Rohrwild, M., Muller, H., Strauss, M., and Pardee, A.B. 1995. Analysis of altered gene expression by differential display. *Methods Enzymol. 254*:304–321.

McClelland, M., and Welsh, J. 1994. DNA fingerprinting by arbitrarily primed PCR. *PCR Methods Appl. 4*:S59–65.

Sagerström, C.G., Sun, B.I., and Sive, H.L. 1997. Subtractive cloning: Past, present, and future. *Ann. Rev. Biochem. 66*:751–783.

Sambrook, J., and Russell, D. 2001. *Molecular Cloning: A Laboratory Manual,* 3rd ed. Cold Spring Harbor, NY: Cold Spring Harber Laboratory Press.

Schena, M., Shalon, D., Davis, R.W., and Brown, P.O. 1995. Quantitative monitoring of gene expression patterns with a complementary DNA microarray. *Science 270*:467–470.

Schena, M., Shalon, D., Heller, R., Chai, A., Brown, P.O., and Davis, R.W. 1996. Parallel human genome analysis: Microarray-based expression monitoring of 1000 genes. *Proc. Natl. Acad. Sci. USA 93*:10614–10619.

Shelton, D.N., Chang, E., Whittier, P.S., Choi, D., and Funk, W.D. 1999. Microarray analysis of replicative senescence. *Curr. Biol. 9*:939–945.

Simm, M., Su, Z., Huang, E.Y., Chen, Y., Jiang, H., Volsky, D.J., and Fisher, P.B. 2001. Cloning of differentially expressed genes in an HIV-1 resistant T cell clone by rapid subtraction hybridization, RaSH. *Gene 269*:93–101.

Su, Z.Z., Kang, D.C., Chen, Y., Pekarskaya, O., Chao, W., Volsky, D.J., and Fisher, P.B. 2002. Identification and cloning of human astrocyte genes displaying elevated expression after infection with HIV-1 or exposure to HIV-1 envelope glycoprotein by rapid subtraction hybridization, RaSH. *Oncogene 21*:3592–3602.

Su, Z.Z., Chen, Y., Kang, D.C., Chao, W., Simm, M., Volsky, D.J., and Fisher, P.B. (2003a) Customized rapid subtraction hybridization (RaSH) gene microarrays identify overlapping expression changes in human fetal astrocytes resulting from HIV-1 infection or TNF-α treatment. *Gene 306*:67–78.

Su, Z.Z., Kang, D.C., Chen, Y., Pekarskaya, O., Chao, W., Volsky, D.J., and Fisher, P.B. (2003b). Identification of gene products suppressed by HIV-1 infection or gp120 exposure of primary human astrocytes by rapid subtraction hybridization. *J. NeuroVirol. 9*:372–389.

Velculescu, V.E., Zhang, L., Vogelstein, B., and Kinzler, K.W. (1995). Serial analysis of gene expression. *Science 270*:484–487.

Zhang, L., Zhou, W., Velculescu, V.E., Kern, S.E., Hruban, R.H., Hamilton, S.R., Vogelstein, B., and Kinzler, K.W. 1997. Gene expression profiles in normal and cancer cells. *Science 276*:1268–1272.

6

Noncontact Laser Microdissection and Pressure Catapulting: A Basic Tool in Genomics, Transcriptomics, and Proteomics

Yilmaz Niyaz and Karin Schütze

The Force of Focused Light: An Introduction

Accurate analyses in modern molecular biomedical sciences rely on the capability of pure sample preparation. Therefore, cellular dissection and micromanipulation techniques have become important in genomic, transcriptomic, and proteomic research. Among various options for specimen capture, only the PALM laser microdissection system (PALM MicroBeam; P.A.L.M. Microlaser Technologies AG, Bernried, Germany) enables the transfer by means of focused laser light, which allows noncontact sample preparation—a paramount prerequisite for pure sample generation.

This microdissection and capture system is based on the patented laser pressure catapulting (LPC) technology, in which sample transfer from the objective plane toward a collection device is solely driven by a laser-induced transportation process. In principle, a pulsed nitrogen laser is coupled through the epifluorescence path into an inverted microscope and focused to a micron-sized spot via the objective lenses. By this means the microscope known as an opto-analytical device has become a most versatile micromanipulation tool: Selected specimen of differing origins can be first laser microdissected and thereafter ejected directly into a capture device only by the force of focal light. Thus the PALM micromanipulation system has no physical or mechanical contact to the specimen, so the risk of contamination or infection of the isolated probes is minimized.

Depending on the nature of the specimen, laser microdissection may be performed before catapulting to clear the surroundings of the selected specimen, warranting the homogeneity of the isolated sample. Noncontact laser microdissection and sampling of specimen as small as subcellular compounds, e.g., filaments or parts of chromosomes, and up to the capture of single cells or entire tissue areas are frequently performed in numerous research institutes or industrial laboratories throughout the world. The focused laser light is used to cut out

Handbook of Immunohistochemistry and *in situ* Hybridization of Human Carcinomas, Volume 3: Molecular Genetics, Liver Carcinoma, and Pancreatic Carcinoma

selected samples or to specifically ablate unwanted material. The nonfocused laser light still pervades the sample, but laser wavelength of 337 nm (ultraviolet A, or UVA) neither affects the viability of the living specimen nor does it destroy the biological information of cells or tissues. Thus, subsequent molecular genetic analyses can be easily carried out immediately after transfer of the catapulted material into an appropriate reaction vial. In addition, the same laser system can be used to microinject drugs or genetic material into living cells without harming their viability, enabling genetic engineering without mechanical tools, disturbing chemical agents, or perturbing viral vectors (Schütze *et al.,* 2003). With this unique combination of microsurgery and catapulting, the noncontact extraction of specific tissue or single cells has become one of the most interesting techniques for functional genomics and proteomics because the catapulted samples are surely derived from a morphologically defined origin.

History and Principle of Laser Cutting and Laser Pressure Catapulting

Since the 1960s, when laser technology was invented, many scientists have been able to demonstrate the applicability of lasers in cell biology and the suitability of the applied laser wavelength to living objects. This is proved by many laboratories where focused lasers are used for induced fusion or ablation of selected specimen (Schütze *et al.,* 2003).

Although the principle of laser ablation was discovered in 1986 (Srinivasan), the first application describing UVA laser microdissection of tissue slices was already published in 1976 by Meier-Ruge *et al*. Since then a multitude of new applications using laser-assisted microsurgery and microinjection have been carried out.

Laser microsurgery of cytoplasmic strands and cytoplasmic streaming within cells and protoplasts was one of the first experiments using cutting lasers, whereas the first laser microdissection of human chromosomes was reported in 1986 by Monajembashi *et al*.

The laser-assisted cellular fusion succeeded first with cells of a tumor cell line and with protoplasts, which led to the use of lasers in developmental analysis (Connolly, 2001; Heel and Dawkins, 2001; Matsunaga *et al.,* 1999).

As an extension of the work of Meier-Ruge *et al*. (1976), microdissection was used to isolate single renal cells from freeze-dried sections for subsequent genetic analysis (Kubo *et al.,* 1995). This enabled the separation of selected cell areas, resulting in the ability of analyzing single cells. For example, in forensic medicine, single specimens of suspect material from different sources (i.e., fingerprints, sperms from fabrics and vaginal smears after sexual abuse, cells attached to hairs, etc.), can be isolated by laser micromanipulation to be used as evidence.

Even subcellular resolution can be achieved with laser microdissection, e.g., single cell nuclei (Thalhammer *et al.,* 2000), chromosomes, polar bodies (Clement-Sengewald *et al.,* 2002), and cellular organelles (Meimberg *et al.,* 2003).

Furthermore, the combination of laser microdissection and laser trapping using UVA laser microbeam and NIR (near infrared) Optical Tweezers (PALM CombiSystem) enables interesting experiments in the field of cell and developmental biology such as blastomer fusion, sperm manipulation, laser zona drilling to facilitate fertilization; assist embryo hatching; and enables polar body isolation for preimplantation analysis (Clement-Sengewald *et al.,* 2002).

Laser-assisted microinjection with the UV-laser was established for the implementation of drugs or genetic material into living cells without interfering with mechanical, chemical, or viral processes. This allows genetic engineering or gene therapy in a highly selective and pure manner. Furthermore, if the laser hole is poked directly into the nuclear area of the cell, the genetic material is efficiently incorporated into the nuclear DNA, and expression can be verified a few days later using selection media, staining procedures, or expression reporters. Subsequently, Tirlapur and König (2002) presented the use of infrared femtosecond laser for microinjection as an innovative tool.

Laser Microdissection

The pulsed (3 ns) UVA laser beam used for laser microdissection and pressure catapulting (LMPC) is routinely focused to ≈1 μm in diameter when passed through the 40X objective; it affects the sample at high-energy density (≈ 1 MW/cm^2). This condensed UV radiation ($\lambda = 337$ nm) within the focal spot causes excitation within and between molecules by a mechanism not fully understood. The energy transfer is sufficient to break the molecular bonds, resulting in fragmentation of the radiated matter without any mechanical contact. Thus, at the focal point of the laser beam unwanted material is photofragmented into atoms and small molecules—a phenomenon that is called "ablative photodecomposition" or "cold ablation." However, because this cutting is a photochemical and fast process devoid of heat transfer, adjacent material is not harmed (Srinivasan, 1986).

The dispersed, nonfocused UVA laser light, being out of the range of the peak absorption wavelengths for deoxyribonucleic (DNA), ribonucleic acid (RNA), or proteins, does not interfere with biological material.

Therefore, these molecules can be routinely isolated from the specimen for downstream analyses and applications (Schütze *et al.,* 2003), or living cells can be captured for subsequent cultivation or cloning (Mayer *et al.,* 2002; Stich *et al.,* 2003). Numerous publications in the field of cell and developmental biology or from assisted human fertilization procedures have proved the safety of 337 nm nitrogen laser–based microsurgery and microdissection.

Laser Pressure Catapulting

After the ablation procedure has cleared the surroundings, the selected area is usually ejected from the object plane with a single laser shot. It is assumed that the laser-induced photodecomposition entails the formation of a locally restricted microplasma, yielding gaseous ejection, which drives microdissected samples out of the plane while expanding. The dissected sample is travelling with high speed (≈25 m/sec) along the front of the gaseous stream, and therefore it is transported for several millimeters against gravity directly into the capture device positioned within the laser beam. This LPC technology marks the breakthrough in modern laser capture methods and enables the entire noncontact preparation of pure and homogeneous samples in a fast and elegant way with the possibility of automation for higher throughput. Since the invention of LPC much research has been done using either direct catapulting or the combination of microdissection and catapulting (LMPC). Pieces of chromosomes, cell organelles, single cells, and large cell areas having a diameter of more than a millimeter have been catapulted using different objective magnifications for various downstream applications (Imamichi *et al.,* 2003; Lahr, 2000; Lehmann *et al.,* 2000). Even living cells or entire small organisms (e.g., *Caenorrhabditis elegans*) have survived this unique catapulting procedure. At present, only the LMPC technology is able to microdissect and catapult viable cells. The LMPC process has no detrimental effects on these isolated cells because they routinely proliferate after a short reconvalescence period (Stich *et al.,* 2003). A custom-made petri dish, the PALM DuplexDish, facilitates the microdissection and capture of living cells.

Sample Features and Specimen Preparation

Virtually any biological sample is suitable for noncontact laser microdissection and laser pressure catapulting. No restrictions have yet been reported regarding the origin of the selected specimen or the applied preparation and staining procedures. Routinely stained and fixed, paraffin-embedded specimens and frozen sections have been successfully processed with the LMPC technology. The only known exception is the freezing medium OCT in cryo-preserved specimen, which must be removed before laser application because this substance interferes with laser cutting.

Depending on the nature of the sample, catapulting may be performed directly, as is the case for cytocentrifuged specimens, single cells, or homogeneous tissue areas. However, tissue preparations are usually inhomogeneous and consist of a mixture of different cell types. To avoid contamination with unselected material, it is advisable to perform laser microdissection before catapulting to obtain pure samples.

The laser cuts a clear gap between selected and nonselected regions. Within the narrow laser cut all biological material is destroyed and the risk of contaminating the captured specimen is minimized. In the immediate surroundings of the cut, the cells remain intact and are perfectly suitable for subsequent genetic or proteomic analysis (Burgemeister *et al.,* 2003). If there are unwanted structures or cells within a selected area, they also may be selectively destroyed by laser ablation before catapulting.

Because tissue sections for laser microdissection or catapulting cannot be routinely embedded and coverslipped, their morphology sometimes appears quite different when compared with embedded tissue sections. Several approaches to improve specimen visualization have been tried using various embedding materials (Micke *et al.,* 2004). However, the convenience of substance application as well as its suitability for subsequent genetic or proteomic analysis is important. For improved visualization, the PALM LiquidCoverGlass has proved to be the most useful solution of various tested materials. Besides the improvement of visualization, this fluidic cover preserves RNA integrity in laser-microdissected tissue sections. Possibly, the application of LiquidCoverGlass shields the dried section from environmental humidity and therefore impedes ribonuclease (RNase)-activity, thus allowing prolonged sample capture time.

PALM AdhesiveTubes provide additional improvement of visualization of the specimen morphology, simultaneously allowing the harvest of laser-captured material without applying buffer *a priori* because within this sticky collection cap the catapulted specimen adheres by itself. This prevents evaporation and thus the danger of crystallization of salty buffers.

Several protocols for sample preparation and numerous downstream application techniques have been developed during the past few years of laser micromanipulation and microdissection (Lorkowski and Cullen, 2003; Schütze *et al.,* 2002; Westphal *et al.,* 2002). With the manifold application possibilities (Figure 8), various accessories were developed to improve sample handling and specimen visualization and to speed up

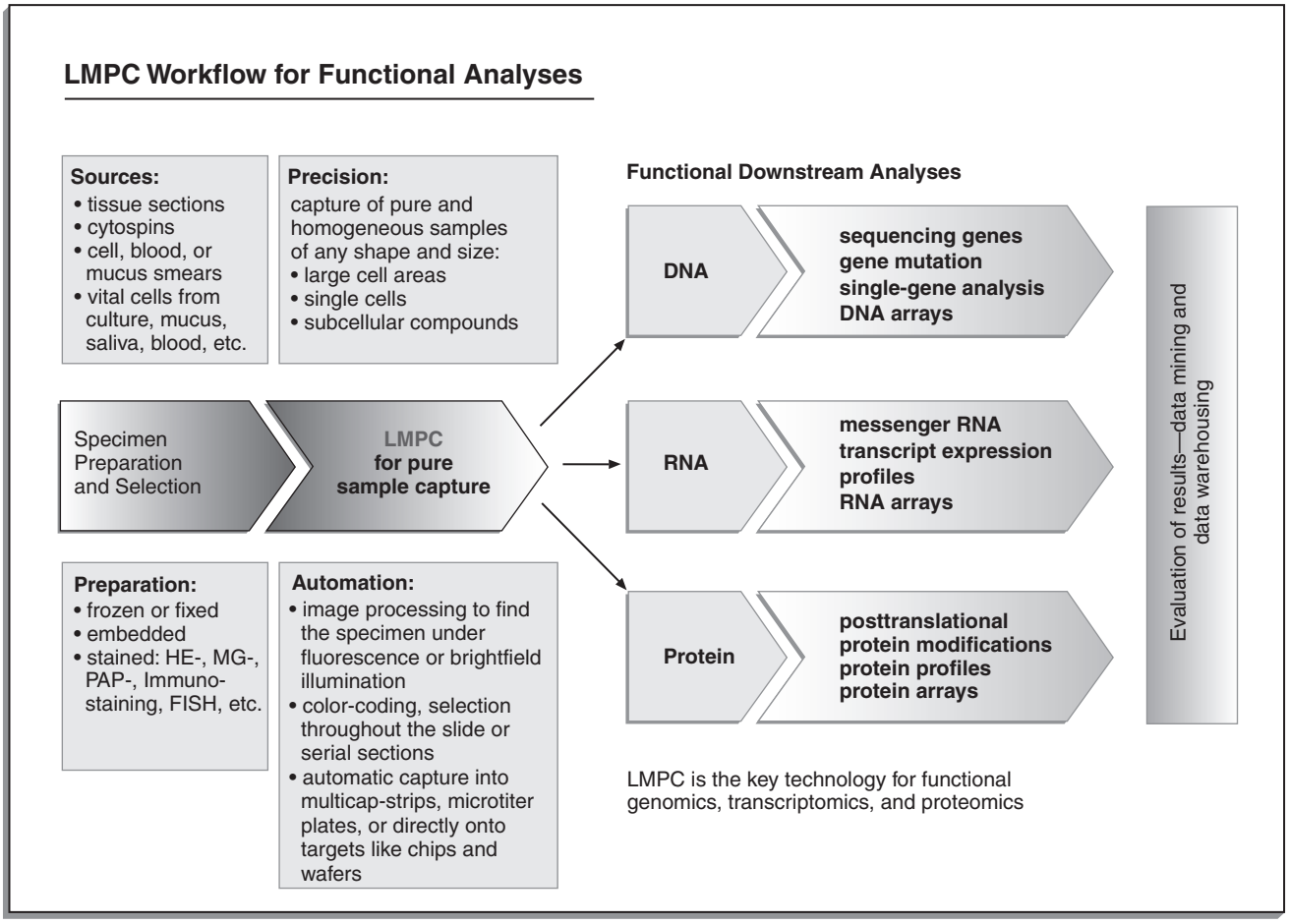

Figure 8. Laser microdissection and pressure catapulting (LMPC) workflow for functional analyses. Workflow and possible field of applications using the LMPC technology.

subsequent analysis. Special membrane-spanned object slides for cell or tissue preparation, double-membrane culture wells for the capture of living cells, and customized microfuge caps or microtiter plates for improved or higher throughput laser capture as well as continuously actualized protocols for sample treatment are available through P.A.L.M. Microlaser Technologies AG (www.palm-microlaser.com).

Glass-Mounted Specimen

When the sample is mounted directly on glass, without using the LPC membrane, the laser can catapult only small portions of material with each shot. When larger areas from a routinely glass-mounted tissue section need to be collected with multiple laser shots, numerous tissue flakes within the collection cap will result. However, the collected material is pure because it is catapulted solely from the selected area and thus derived from a morphologically defined origin. Direct catapulting from glass is recommended for cytocentrifuged specimens, small cell clusters, and pooled single cells.

Membrane-Mounted Specimen

To preserve morphology, the specimen should be mounted on a thin membrane spanning a routine glass slide. The LPC membrane serves as a backbone, which holds the selected tissue area close together and facilitates the capture of large tissue areas; tedious specimens; or fragile samples such as cell smears, very small cells, cell nuclei, and chromosomes. The laser first operates around the selected area following the preselected line and cuts the specimen and the underlying membrane. With the catapult shot of the laser, the entire selected area is ejected out of the object plane and catapulted directly into the collection vial, preserving the specimen morphology. In this manner, large areas of up to 1 mm in diameter, single cells, subcellular components,

and fragments of chromosomes can be collected independent of their shape and character. Comparison of samples catapulted from membrane-mounted versus glass-mounted tissue has shown that there is no significant difference in subsequent molecular analysis (Schütze *et al.,* 2003).

Membrane-mounted slides can also be used for cell cultivation. Cells grown on the surface of the membrane can be fixed before they are catapulted. It is also possible to catapult membrane-grown living cells and capture them alive (Schütze *et al.,* 2003). Two different kinds of membranes are available that differ in their chemical composition and laser-cutting behavior. The PEN (polyethylene–naphthalate) membrane is recommended for use with tissue sections, critical single cells, cell smears, blood smears, and mucus smears, whereas the POL (polyester) membrane is recommended for laser ablation prior to cutting to avoid contamination with nonselected material (e.g., chromosomes, chromosomal parts, filaments, cell organelles, etc.).

Specimens that barely adhere to the membranous surface require pretreatment of the membrane by means of irradiation with UVC light or applying chemical compounds that change the membrane from a strong hydrophobic to a more hydrophilic nature (e.g., polylysine). Specimens that vigorously move need immobilization within two sheets of LPC membranes. This so-called "sandwich-prep" is also recommended for conserving a minimum of humidity on the specimen so it will not dry out. The procedure of catapulting can be performed in the manner described earlier (Schütze *et al.,* 2002).

Technical Setup of the PALM MicroBeam System

The PALM MicroBeam is equipped with a pulsed nitrogen laser coupled into an inverted research microscope. Laser microdissection is possible with several objective magnifications from 5X to 100X. The cutting size of the implemented laser depends on the focal diameter of the beam. This focus results from the wavelength and beam quality of the laser, the magnification and numerical aperture (n.a.) of the applied objective, and the specimen's absorbance behavior used for microdissection. For best focusing results, a laser of high beam quality and an objective with n.a. greater than 1 is required. Higher aperture objectives, e.g., a 100X oil immersion objective (n.a. = 1.3), are necessary for minimum cutting size of less than 700 nm (Thalhammer *et al.,* 2000), enabling microdissection and microsurgery even of single nuclei, filaments, chromosomes, or chromosomal parts. The precise cutting of the PALM MicroBeam System is supported by an extremely precise (positioning better than 1 µm) motorized microscope stage (PALM RoboStage).

Modern detection methods are often based with fluorescence techniques. The PALM MicroBeam can optionally be equipped with features for fluorescence microscopy. Thus, LMPC is possible under simultaneous fluorescence observation. To reduce bleaching of the fluorescent dye to an absolute minimum, the screen-freeze mode of the RoboSoftware creates a screen shot of the fluorescent sample. Thus, the fluorescence illumination can be switched off because it is not needed for the subsequent microdissection and catapulting process.

PALM RoboSoftware for Automated Microdissection and Catapulting

The controlling software of the PALM MicroBeam system is the so-called "RoboSoftware," managing the motion of the motorized microscope, the motorized microscope stage, the motor-driven laser energy and laser focus settings, and finally the optional fluorescence equipment. An intuitive graphical user interface for all functions for microdissection and catapulting process facilitates the daily work.

The RoboSoftware includes automated process routines as well as additional functions. A wide palette of drawing tools for marking the incision path in preselection mode enables the outlining and color-coding of up to 100 independent target areas over the entire slide or even from different slides after serial sectioning. These selected target areas are listed in an "element list" protocol, which allows target grouping and experimental scheduling. Saving of the selected elements with respect to a reference position in personal files allows the relocation of the stored elements on each individual slide. Different laser functions are available to process the preselected and outlined specimens (Schütze *et al.,* 2002) (Figure 9).

For glass-mounted preparations:

- **AutoLPC** enables the automated catapulting of larger areas from glass-mounted preparations. With glass-mounted preparations only a small amount of cellular material can be transported with each single shot. Therefore, larger areas have to be catapulted with multiple shots. The distance between the single shots and the LPC-pattern depends on the tissue characteristics and can be preselected in the setup menu.
- Only **LPC** dot-marked specimens are catapulted. This function is of special benefit for cytocentrifuged specimens, but it is also used to isolate individual cells within a histologic preparation or to individually catapult precut membrane-mounted specimens.

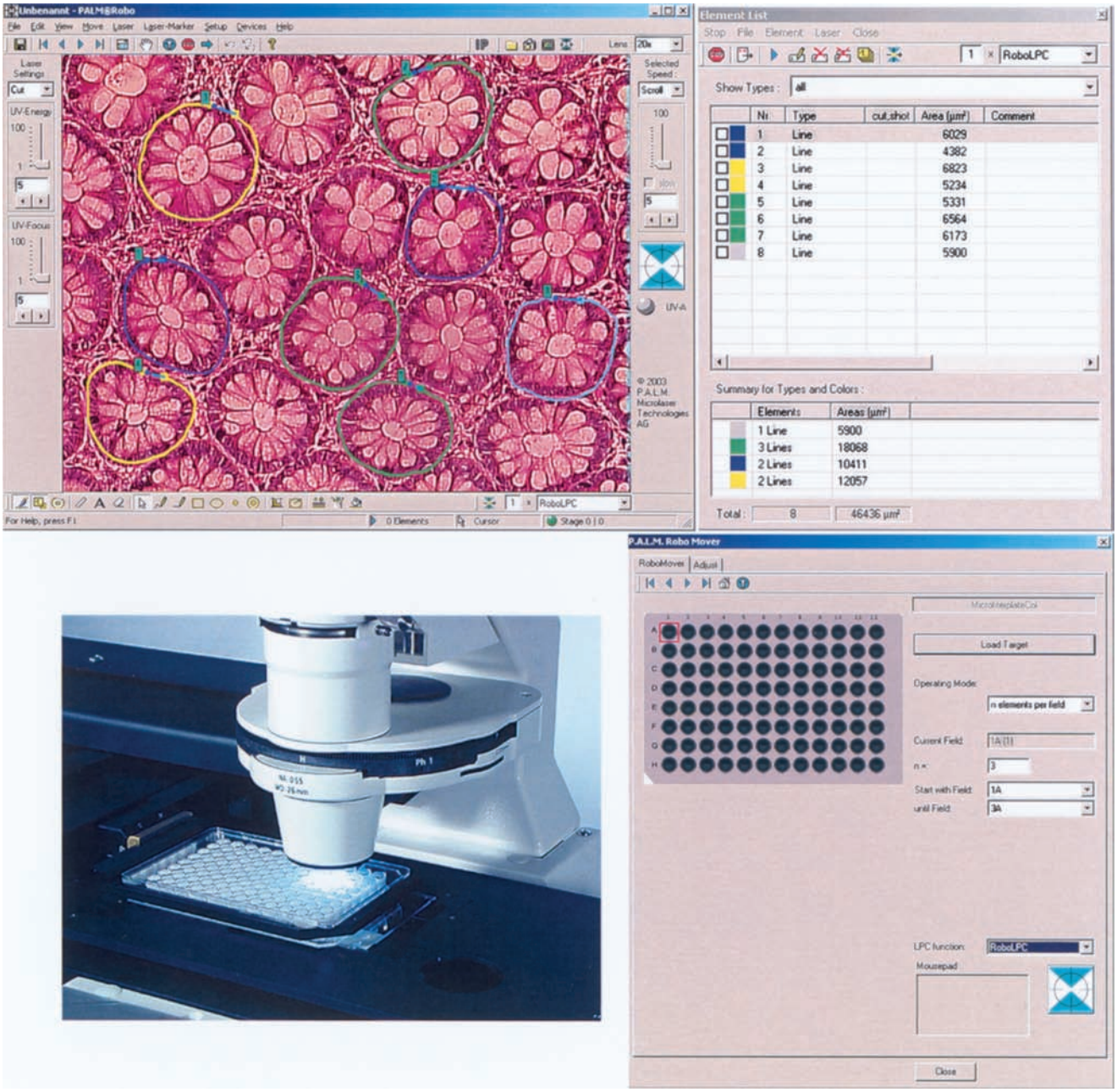

Figure 9. RoboSoftware and Overlay for RoboMover. In the upper left, areas of interest are selected either manually or via image-analysis software. The selected elements are displayed at the element list (*upper right*). Depending on the kind of the selected collection device, the RoboMover panel (*lower right*) shows schemes of the corresponding target. Either from here or via the element list, collecting can be started or complex experiments can be predesigned for subsequent automatic laser microdissection and pressure catapulting performance. The insert at the lower left shows the RoboMover platform on the PALM MicroBeam.

- With the use of **CloseCut&AutoLPC**, critical preparations can be isolated before AutoLPC to avoid contamination with neighboring tissue. Thus, pure sample preparations can be obtained.
- The **AutoCircle** allows automated circumcutting of a dot-marked specimen with a preset diameter and immediately catapulting it from its center. This function is recommended for single cells only.

For membrane-mounted preparations:

- In the **cut** mode, the laser cuts solely along the predrawn line. If **CloseCut** is selected, the user does not need to fulfill the drawing line around

a specimen because the computer will automatically do so and cutting will be performed accordingly. This yields a clearcut gap between the selected and nonselected material.

- **RoboLPC** allows cutting and catapulting in a single automated procedure. It is possible only for use with membrane-mounted specimens. The outlining is automatically cut up to a small connection bridge from which the entire area is immediately catapulted with one single laser shot. The size of the connecting bridge can be preselected from the laser setup menu. Within the cutting line all biological material is ablated. Thus, pure sample preparation is possible without danger of contamination.

The list of elements (Figure 9) is the main tool for summary and display of the outlined samples and corresponding area measures, the color-dependent sorting of the outlined areas, and laser activation. Choosing from the colored chart, the computer will microdissect or catapult only elements showing the particular chosen color. In this manner sorting is facilitated and laser capture becomes quick and easy. This technology, therefore, is important for high-throughput analysis and is necessary for proteomics and DNA array technology (Figure 8).

Automated Cell Recognition

The high degree of automation realized in the latest generation of PALM MicroBeam systems can be augmented by image-analyzing software modules allowing automated fast-scanning functions for specimen identification and image processing. Coupled with any of these software modules, the MicroBeam system is able to scan, detect, isolate, and finally capture the specimen of interest, e.g., fluorescent-labeled rare cells, metaphases, or fluorescence *in situ* hybridization treated cells in a fully automated manner (Figure 10). Identified targets are automatically saved in an on-screen review gallery and can easily be relocated and evaluated by the user before the LMPC process through the software interface between the image processing software and the RoboSoftware. In this way, the fully automated detection of fluorescence-labeled cells is correlated with quantitative occurrence rates, which are calculated by assessing the total number of cells in bright field during the scanning of the selected area.

With a second software module, under brightfield illumination different imaging software rulesets are created, which allow quick access to a high number of pure and homogeneous cell materials for array applications and analyses. This way, routinely stained samples are automatically detected. Positively recognized areas are outlined and transferred to the element list of the PALM MicroBeam, and marked areas are subsequently extracted automatically by the appropriate laser functions. These efficient detection algorithms are trained by PALM to achieve integrated, interactive classifiers for optimized recognition and accurate results (Figure 11).

RoboMover and RoboStage II

A fully robotic unit called "RoboMover" functions as a multipurpose collection device, with adapters for simple caps of microfuge tubes, entire tubes, multicap strips, and microtiter and multiwell plates and feeds analytical biochips (e.g., MALDI, SELDI or PCR-analyses), guided by the entries in the element list (Figure 9). This way, complex experimental setups can be planned and processed automatically. The highly automated sample capture device is supported by the second generation of RoboStage. This newly developed stage allows travel of large distances in x/y directions with high-accuracy relocation of selected areas and allows collection of samples from various object dishes fitting into versatile customized holders, such as DuplexDishes, three MembraneSlides, etc., which are all compatible with this stage. Successful sample capture can easily be controlled with the "cap-check" function of the RoboStage II.

Special software features enable linking of serial sections to simultaneously manage up to three slides (e.g., for serial sections of a sample). Here, on the leading slide (i.e., first slide) areas of interest can be outlined by the user and displayed at the linked subset of the following serial sections. The selected areas can individually be addressed and adjusted to their actual shapes, which may differ as a result of torsions occurring during sectioning.

This fully automated generation of samples by noncontact LMPC process for subsequent analyses vastly increases the throughput in routine and research laboratories. Noncontact laser microdissection and catapulting allows the largely automated and highly reliable capture of thousands of cells within a short time, thus enabling higher throughput specimen sampling (Figure 8).

Applications of PALM MicroBeam: Overview and Outlook

Laser microdissection and laser catapulting will also supplement functional proteomic studies correlating protein profiles with morphologically relevant features. Laser catapulting is either performed into routine vials or microtiter plates, from which the specimens are

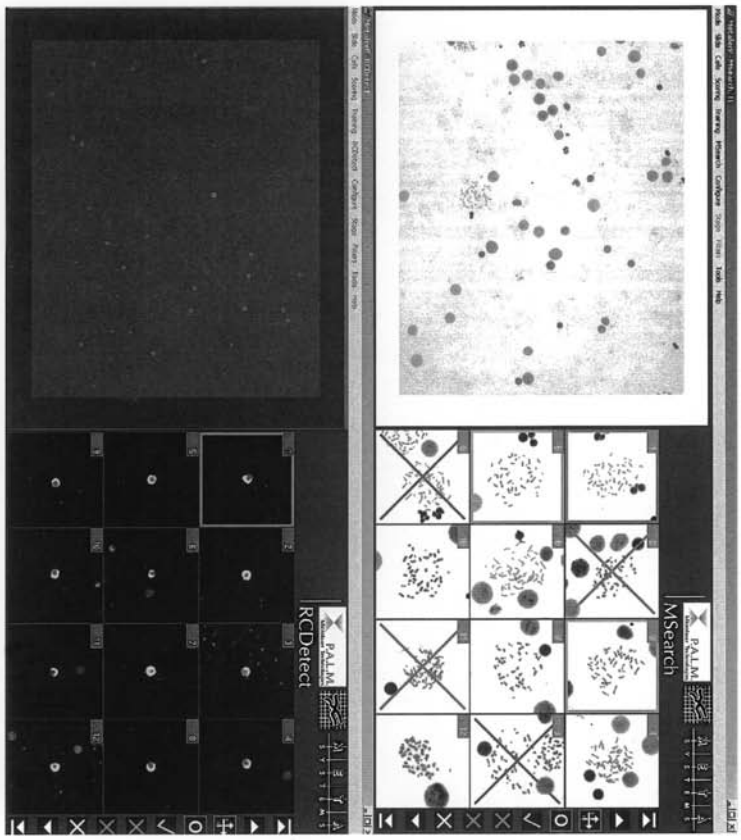

LMPC selected specimen

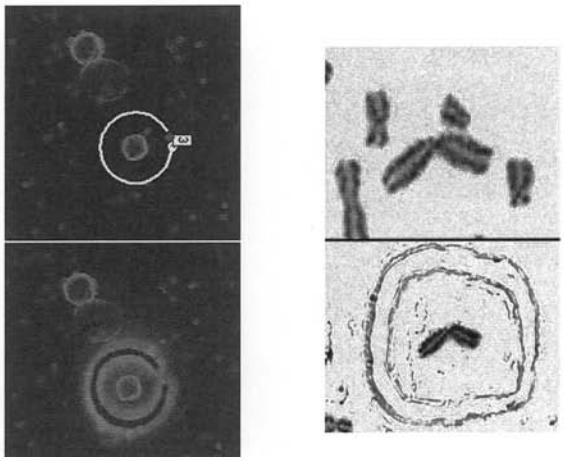

Figure 10. Automated image processing and laser microdissection and pressure catapulting (LMPC) function. The MicroBeamIP system recognizes spread chromosomes (*right panels*) or rare cells (*left panels*) automatically via pretrained classifiers. These detected samples can subsequently be isolated via LMPC.

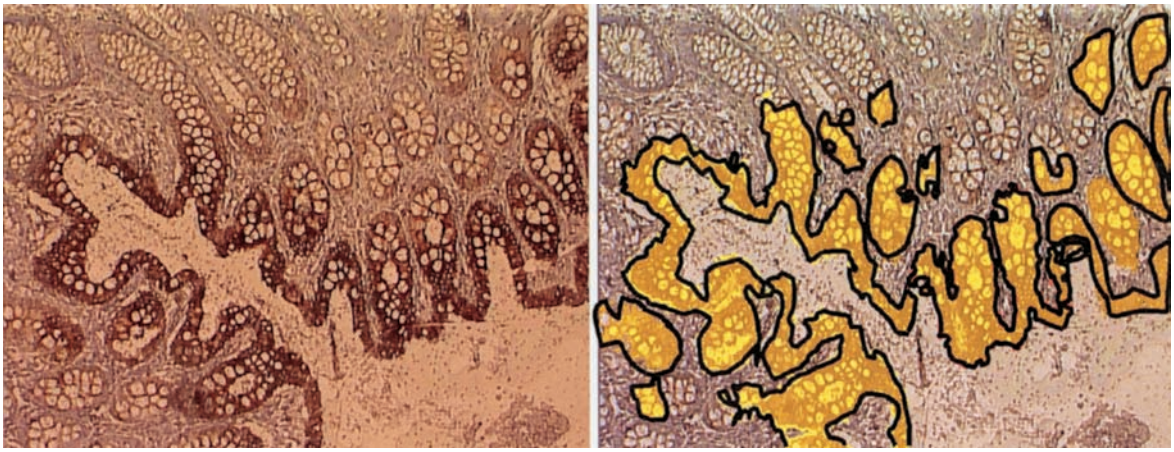

Figure 11. Automated shape recognition. A software module enables the automatic detection of cells out of a given tissue region (left versus right). Area presentation and outlining rules are especially programmed by P.A.L.M., which clearly speeds up the harvesting of large number of cells for array applications or functional proteomic experiments.

dissolved and subsequently picked up to be transferred to the corresponding surfaces, or it could be catapulted directly onto these surfaces (e.g., microarray wavers). Direct catapulting with no mechanical interference will save time, prevent the danger of losing a specimen during pipetting, and minimize contamination with unwanted material. Even the manufacturing of biomolecule arrays by catapulting liquid amounts from a liquid layer onto a glass slide is feasible. In summary, this versatile laser micromanipulation and microdissection system is the state-of-the-art tool, essential when pure sample generation is required throughout the entire field of modern molecular research and medical analyses.

Acknowledgment

We thank Dr. R. Burgemeister for discussions and information. Furthermore, we thank Dr. Bernd Sägmüller and Dr. Rainer Gangnus for providing Figures 9 and 10.

References

Burgemeister, R., Gangnus, R., Haar, B., Schütze, K., and Sauer, U. 2003. High quality RNA retrieved from samples obtained by using LMPC (laser microdissection and pressure catapulting) technology. *Pathol. Res. Pract. 199*:431–436.

Clement-Sengewald, A., Buchholz, T., Schütze, K., Berg, U., and Berg, F. 2002. Noncontact, laser-mediated extraction of polar bodies for prefertilization genetic diagnosis. *J. Assist. Reprod. Gen. 19*:183–194.

Connolly, C. 2001. Laser ablation reveals sexual attraction mechanism in flowers. *Biophot. Int. 8*:61–63.

Heel, K., and Dawkins, H. 2001. Laser microdissection and optical tweezers in research. *Today's Life Sci. 13*:42–48.

Imamichi, Y., Koebernick, K., and Wedlich, D. 2003. Prospects for tissue-specific analysis of gene expression in Xenopus embryos through laser-mediated microdissection of histological sections. *Pathol. Res. Pract. 199*:381–389.

Kubo, Y., Klimek, F., Kikuchi, Y., Bannasch, P., and Hino, O. 1995. Early detection of Knudson's two-hits in preneoplastic renal cells of the Eker rat model by the laser microdissection procedure. *Cancer Res. 55*:989–990.

Lahr, G. 2000. RT-PCR from archival single cells is a suitable method to analyze specific gene expression. *Lab. Invest. 80*:1477–1479.

Lehmann, U., Glöckner, S., Kleeberger, W., von Wasielewski, R., and Kreipe, H. 2000. Detection of gene amplification in archival breast cancer specimens by laser-assisted microdissection and quantitative real-time polymerase chain reaction. *Am. J. Pathol. 156*:1855–1864.

Lorkowski, S., and Cullen, P., eds. 2003. Tissue microdissection techniques. In: *Analysing Gene Expression,* Weinheim, Germany: Wiley-VCH.

Matsunaga, S., Schütze, K., Donnison, I., Grant, S., Kuroiwa, T., and Kawano, S. 1999. Technical advance: Single pollen typing combined with laser-mediated manipulation. *Plant J. 20*:371–378.

Mayer, A., Stich, M., Brocksch, D., Schütze, K., and Lahr, G. 2002. Going in vivo with laser microdissection. *Methods Enzymol. Series: Laser Capture Microscopy 356*:25–33.

Meier-Ruge, W., Bielser, W., Remy, E., Hillenkamp, F., Nitsche, R., and Unsold, R. 1976. The laser in the Lowry technique for microdissection of freeze-dried tissue slices. *Histochem. J. 8*:387–401.

Meimberg, H., Thalhammer, S., Brachmann, A., Müller, B., Eichacker, L., Heckl, W., and Heubl, G. 2003. Selection of chloroplasts by laser microbeam microdissection for single-chloroplast PCR. *BioTechniques 34*:1238–1243.

Micke, P., Bjørnsen, T., Scheidl, S., Bemoulin, J., Östman, A., Ponten, F., Bittinger, F., Lindahl, P., and Busch, C. 2004. A fluid cover medium provides superior morphology and preserves RNA integrity in tissue sections for laser microbeam microdissection. *J. Pathol. 202*:130–138.

Monajembashi, S., Cremer, C., Cremer, T., Wolfrum, T., and Greulich, K. 1986. Microdissection of human chromosomes by a laser microbeam. *Exp. Cell Res. 167*:262–265.

Schütze, K., Becker, B., Bernsen, M., Bjoernsen, T., Brocksch, D., Bush, C., Clement-Sengewald, A., van Dijk, M., Friedemann, G., Heckl, W., Lahr, G., Lindahl, P., Mayer, A., Nilsson, S., Scheidl, S., Stich, M., Stolz, W., Takemoto, M., Thalhammer, S., Vogt, T., and Burgemeister, R. 2002. Tissue microdissection In: D. Bowtell and J. Sambrook (eds.): *DNA Microarrays (A Molecular Cloning Manual) CSHL Press, New York*; Part 1: Manual dissection and laser capture microdissection:307–313; Part 2: Laser pressure catapulting:331–356.

Schütze, K., Burgemeister, R., Clement-Sengewald, A., Ehnle, S., Friedemann, G., Lahr, G., Sägmüller, B., Stich, M., and Thalhammer, S. 2003. Non-contact live cell laser micromanipulation using PALM microLaser systems; *P.A.L.M. Scientific Edition No. 11 Life Cell Manual*.

Srinivasan, R. 1986. Ablation of polymers and biological tissue by ultraviolet lasers. *Science 234*:559–565.

Stich, M., Thalhammer, S., Burgemeister, R., Friedemann, G., Ehnle, S., Lüthy, C., and Schütze, K. 2003. Live cell catapulting and recultivation. *Pathol. Res. Pract. 199*:405–409.

Thalhammer, S., Kölzer, A., Frösner, G., and Heckl, W. 2000. Laser-based isolation of cells and cell clusters for virus specific PCR analysis. *Eur. Biophys. J. 29*:12D–5.

Tirlapur, U.K., and König, K. 2002. Targeted transfection by femtosecond laser. *Nature 418*:290–291.

Westphal, G., Burgemeister, R., Friedemann, G., Wellmann, A., Wernert, N., Wollscheid, V., Becker, B., Vogt, T., Knüchel, R., Stolz, W., and Schütze, K. 2002. Noncontact laser catapulting: A basic procedure for functional genomics and proteomics. *Methods Enzymol. 356*:80–99.

7

DNA Methylation Analysis of Human Cancer

Santiago Ropero and Manel Esteller

Introduction

The inheritance of information based on gene expression levels is known as epigenetics, as opposed to genetics, which refers to information transmitted on the basis of gene sequence. The main epigenetic modification in mammals, particularly in humans, is the methylation of cytosine nucleotide residue. Cytosine methylation occurs after deoxyribonucleic acid (DNA) synthesis, by enzymatic transfer of a methyl group from the methyl donor S-adenosylmethionine (SAM) to the carbon-5 position of cytosine. This enzymatic reaction is performed by one of a family of enzymes called DNA methyl transferases (DNMTs). This rarely discussed nucleotide is crucial for many biological processes, and its disturbance has been associated with the following diseases (Robertson and Wolffe, 2000):

- Autism, in which, in Rett syndrome, there are mutations in the methyl-binding protein MeCP2
- Autoimmunity, in which patients with lupus suffer severe degrees of DNA hypermethylation
- Neurologic diseases, in which the methylation of the fragile X mental retardation-1 (*FMR*) gene is the catalyst of the disorder of the same name
- Atherosclerosis, in which protective cardiovascular genes are aberrantly hypermethylated
- Immunodeficiency, in which patients with ICF (immunodeficiency, centromere instability, and facial anomalies) have mutations in a major DNA methyltransferase
- Cancer risk, in which germline variants of the methyl-metabolism genes affect DNA methylation patterns (Paz *et al.,* 2002)
- Human imprinting, such as the aberrant methylation patterns in Beckwith-Wiedemann and Prader-Willi/Angelman syndromes
- Animal cloning, as a result of which poor Dolly and her look-alikes have problems in establishing their appropriate DNA methylation patterns.

Nothing escapes DNA methylation. It also plays a key role in cancer, as we discuss later in this chapter.

In mammalian cells DNA methylation occurs at the 5-position of cytosine within the CpG dinucleotide. Approximately 70% of the CpG dinucleotides in the mammalian genome are methylated, but the distribution of CpGs in vertebrate genomes is not uniform. Most of the genome is actually quite depleted of CpGs, a phenomenon termed CpG suppression (Bird, 1986). Most CpG sites in these areas are methylated during embryogenesis and remain methylated throughout the life span of the cells (Brandeis *et al.,* 1993). By contrast, ~1% of the genome is composed of CpG-rich regions

Handbook of Immunohistochemistry and *in situ* Hybridization of Human Carcinomas, Volume 3: Molecular Genetics, Liver Carcinoma, and Pancreatic Carcinoma

termed CpG islands (Bird, 1986). These CpG islands are usually unmethylated in all normal tissues and frequently span the 5′ end (promoter, untraslated region, and exon 1) of a number of genes.

Methylation of promoter CpG islands is associated with a closed chromatin structure and transcriptional silencing of the associated genes. We can find certain CpG islands normally methylated in at least four cases: imprinted genes, X-chromosome genes in women, germline-specific genes, and tissue-specific genes (reviewed in Baylin *et al.,* 1998). Genomic or parental imprinting is a process involving acquisition of a closed chromatin state and DNA hypermethylation in one allele of a gene (e.g., a growth suppressor gene) early in the male and female germline that leads to monoallelic expression. A similar phenomenon of reducing the gene dosage can also be invoked with regard to the methylation of CpG islands in one X-chromosome in women, which renders these genes inactive. Finally, although DNA methylation is not a widely used system for regulating "normal" gene expression, and we certainly have more complex and specialized molecular networks to achieve this aim, sometimes DNA methylation does accomplish this purpose (e.g., *MAGE* and *LAGE* gene families, the gene expression of which is restricted to the male or female germline and which are not later expressed in any adult tissue) (De Smet *et al.,* 1999). A more polemic case may be postulated for the classical tissue-specific genes; some of them contain CpG islands, whereas others contain only a few CpG dinucleotides scattered throughout in their 5′ regulatory region. Methylation has been postulated as one mechanism to silence these tissue-specific genes in those cell types where they should not be expressed. A well-characterized example of this type of regulation is provided by the methionine adenosyltransferases 1A and 2A in the rodent setting (Torre *et al.,* 2000). However, it is still not clear if this type of methylation is secondary to a lack of gene expression resulting from the absence of the particular cell type–specific transcription factor or is the main force behind the transcriptional tissue-specific silencing.

One question that remains to be answered is the significance of DNA methylation in areas outside the CpG islands. A possible explanation is that DNA methylation is used as a mechanism to repress parasitic DNA sequences (Yoder *et al.,* 1997). Our genome is littered with transposons and endogenous retroviruses acquired throughout the human history. These parasitic sequences, which account for more than 35% of the genome, can be controlled by direct transcriptional repression mediated by several host proteins; it is possible, however, that the main line of defense against expression of these sequences is inactivation through DNA methylation of their promoter regions. With time, this process has the potential to destroy many transposons.

The Significance of DNA Methylation in Cancer

The phenomenon mentioned earlier changes substantially when cells become cancerous. Three major phenomena occur in cancer affecting methylation patterns: 1) there is an increase in the activity of the methylating enzymes in the malignant cells; 2) there is a global hypomethylation of the genome if we compare a tumoral versus a normal cells (this is mainly the result of a generalized demethylation in the CpGs scattered in the body of the genes); and 3) there are local and discrete regions that suffer an intense hypermethylation. Other epigenetic aberrations observed in cancer cells can be described as loss of imprinting (LOI) events; epigenetic lack of the repression of intragenomic parasites; and the appearance of genetic defects in chromatin-related genes. These are unique but interrelated features.

Global Genomic Hypomethylation

One of the first reports linking aberrant DNA methylation to cancer was published by Lapeyre and Becker (1979), who determined by high-performance liquid chromatography (HPLC) the 5-methylcytosine content from normal rat liver and hepatocellular carcinomas induced in rats by acetyl aminofluorene or diethylnitrosamine. The carcinogen-induced cancers displayed a decrease in overall genomic methylation of about 20–40% compared to normal liver. Presently, we know that the malignant cell can have 20–60% less genomic 5-methylcytosine than its normal counterpart (Esteller *et al.,* 2001a). The loss of methyl groups is accomplished from various sources, but mainly by hypomethylation of the "body" (coding region and introns) of genes demonstrated, for example, in the cases of gamma-globin, gamma-cristallin, alpha-chorionic gonadotropin, *H-Ras*, and the *c-myc* genes and through demethylation of repetitive DNA sequences (reviewed in Ehrlich, 2000), which accounts for 20–30% of the human genome.

Three mechanisms can be invoked to explain the contribution of DNA hypomethylation to carcinogenesis: chromosomal instability, reactivation of transposable elements, and LOI. Undermethylation of DNA might favor mitotic recombination leading to loss of heterozygosity and promoting karyotypically detectable rearrangements. Additionally, extensive demethylation

in centromeric sequences is common in human tumors and may play a role in aneuploidy. Supporting this postulate, it has been shown that murine embryonic stem cells nullizygous for the DNA methyltransferase 1 (*DNMT1*) gene exhibit significantly elevated rates of genetic deletions (Chen *et al.,* 1998) and that patients with germline mutations in the other DNA, methyltransferase (*DNMT3b*), have numerous chromosome aberrations (Xu *et al.,* 1999). Hypomethylation of the malignant cell DNA can also reactivate intragenomic parasitic DNA: loss of methylation has been observed in L1 (long interspersed nuclear elements, *LINES*) and Alu (recombinogenic sequences) repeats in cancer cells (Alves *et al.,* 1996; Florl *et al.,* 1999; Thayer *et al.,* 1993; Yoder *et al.,* 1997). These and other previously silent transposons may now be transcribed and may even "move" to other genomic regions where they can disrupt normal cellular genes. Finally, the loss of methyl groups can affect imprinted genes. The best-studied case affects the *H19/IGF-2* locus in chromosome 11p15 (reviewed in Feinberg 1999), where the disturbance of methylation may cause overexpression of an antiapoptotic growth factor (*IGF-2*) and loss of a transformation-suppressing ribonucleic acid (RNA; *H19*) in certain childhood tumors.

Gene Hypermethylation in Human Cancer

CpG islands associated with tumor suppressor genes are unmethylated in normal tissues but often become hypermethylated during tumor formation. Growing evidence suggests that *de novo* methylation of CpG islands induces the silencing of associated tumor suppressor genes and may in fact be a critical step during tumor formation. The particular genes that are hypermethylated in tumor cells are strongly specific to the tissue of origin of the tumor (Esteller *et al.,* 2001). We have recently described a profile of hypermethylation among various primary human tumors (Esteller *et al.,* 2001a); however, we do not currently know why some genes become hypermethylated in specific tumors and others, with similar properties (e.g., a typical CpG island), a history of loss of expression in other tumor types, and the absence of mutations remain free from methylation. We can hypothesize, as has been done previously with genetic mutations, that silencing of a particular gene may confer a survival advantage in some situations. The genes that undergo abnormal methylation in their 5′-CpG island in human cancer cover the whole spectrum of pathways involved in tumorogenesis from cell cycle and apoptosis to DNA repair and invasiveness ability. Tumor suppresor genes that contain highly methylated CpG islands in tumor cells affect cell cycle ($p16^{INK4a}$, $p15^{INK4b}$, *Rb*, $p14^{ARF}$), DNA repair (*BRCA1, hMLH1, MGMT*), cell adherence (*CDH1, CDH13*), apoptosis (*DAPK, TMS1*), carcinogen metabolism (*GSTP1*), hormonal response (*RARB2, ER*), etc. Table 8 shows the most relevant hypermethylated genes in human cancer reported so far, their function, chromosomal localization, and tumor profile (Esteller, 2002).

Clinical Significance of DNA Methylation in Tumors

It is a growing hope that enumeration of the molecular alterations in cancer, particularly with respect to DNA changes, will lead to the development of new strategies for assessing cancer risk status, achieving the earliest tumor detection, monitoring prognosis, and instituting more accurate tumor staging along with the monitoring of prevention strategies. The detection of hypermethylated promoter region CpG islands may offer one of the most promising approaches to these goals. DNA methylation changes have been reported to occur early in the carcinogenesis and therefore are potentially good indicators of existing disease (Laird, 1997) and even of risk assessment for the future development of disease.

Four major cancer clinical areas can benefit from hypermethylation-based markers, as illustrated in Figure 12. They include neoplasm detection, tumor behavior, prediction of response to treatment, and therapies that target methylated tumor suppressor genes.

DNA Methylation as a Sensitive Biomarker for Tumor Detection

A delicate profile of CpG islands hypermethylation occurs in human tumors. The growing list of genes inactivated by promoter region hypermethylation provides an opportunity to examine the patterns of inactivation of such genes among different tumors. Usually one or more genes are hypermethylated in every tumor type. However, the profile of promoter hypermethylation for the genes differs for each cancer type providing a tumor type, and gene-specific profile. For example, gastrointestinal tumors (colon and gastric) share a set of genes undergoing hypermethylation characterized by $p16^{INK4a}$, $p14^{ARF}$, *MGMT, APC,* and *hMLH1,* whereas other aerodigestive tumor types, such as lung, head, and neck, have a different pattern of hypermethylated genes including *DAPK, MGMT,* $p16^{INK4a}$ but not *hMLH1* or $p14^{ARF}$. Similarly, breast and ovarian cancers show methylation of certain genes, including *BRCA1, GSTP1,* and $p16^{INK4a}$ (see Table 8). This gene hypermethylation profile of human cancer is

Table 8. Selected Genes That Undergo CpG Island Hypermethylation in Human Cancer

Gene	Function	Location	Tumor Profile	Consequences
p16^{INK4a}	Cyclin-dependent kinase inhibitor	9p21	Multiple types	Entrance in cell cycle
p14^{ARF}	*MDM2* inhibitor	9p21	Colon, stomach, kidney	Degradation of *p*53
p15^{INK4b}	Cyclin-dependent kinase inhibitor	9p21	Leukemia	Entrance in cell cycle
hMLH1	DNA mismatch repair	3p21.3	Colon, endometrium, stomach	Frameshift mutations
MGMT	DNA repair of 06-alkyl-guanine	10q26	Multiple types	Mutations, chemosensitivity
GSTP1	Conjugation to glutathione	11q13	Prostate, breast, kidney	Adduct accumulation?
BRCA1	DNA repair, transcription	17q21	Breast, ovary	Double strand breaks?
p73	p53 homologue	1p36	Lymphoma	Unknown (Cisplatin?)
LKB1/STK11	Serine/threonine kinase	19p13.3	Colon, breast, lung	Unknown
ER	Estrogen receptor	6q25.1	Breast	Hormone insensitivity
PR	Progesterone receptor	11q22	Breast	Hormone insensitivity
AR	Androgen receptor	Xq11	Prostate	Hormone insensitivity
RARβ2	Retinoic acid receptor β2	3p24	Colon, lung, head and neck	Vitamin insensitivity?
RASSF1	Ras effector homologue	3p21.3	Multiple types	Unknown
VHL	Ubiquitin ligase component	3p25	Kidney, hemangioblastoma	Loss of hypoxic response?
Rb	Cell cycle inhibitor	13q14	Retinoblastoma	Entrance in cell cycle
THBS-1	Thrombospondin-1, antiangiogenic	15q15	Glioma	Neovascularization
CDH1	E-cardherin, cell adhesion	16q22.1	Breast, stomach, leukemia	Dissemination
HIC-1	Transcription factor	17p13.3	Multiple types	Unknown
APC	Inhibitor of β-catenin	5q21	Aerodigestive tract	Activation β-catenin route
COX-2	Cyclooxygenase-2	1q25	Colon, stomach	Anti-inflamatory resistance?
SOCS-1	Inhibitor of JAK/STAT pathway	16p13.13	Liver	JAK2 activation
SRBC	*BRCA1*-binding protein	1p15	Breast, lung	Unknown
SYK	Tyrosine kinase	9q22	Breast	Unknown
RIZ1	Histone/protein methyltransferase	1p36	Breast, liver	Aberrant gene expression?
CDH13	H-cadherin, cell adhesion	16q24	Breast, lung	Dissemination?
DAPK	Proapoptotic	9q34.1	Lymphoma, lung, colon	Resistance to apoptosis
TMS1	Proapoptotic	16p11	Breast	Resistance to apoptosis
TPEF/HPP1	Transmembrane protein	2q33	Colon, bladder	Unknown

Esteller M. 2002. CpG island hypermethylation and tumor suppressor genes: A booming present, a brighter future. *Oncogene 21*:5427–5440.

consistent with the data of particular "methylotypes" proposed for single tumor types. In this way, it is possible to use the CpG island hypermethylation of tumor suppressor genes as tumor markers. One obvious advantage over genetic markers is that mutations occur at multiple sites and can be of very different types. In contrast, promoter hypermethylation occurs within the same region of a given gene in each form of cancer; thus, we do not need to test the methylation status first to assay the marker in serum or a distal site. Furthermore, the detection of hypermethylation is a "positive" signal that can be accomplished in a galaxy of normal cells, whereas certain genetic changes, such as loss of heterozygosity and homozygous deletions, will not be detected within a background of normal DNA.

If we wish to use these epigenetic markers in the real world, we will need to use quick, easy, nonradioactive, and sensitive ways of detecting hypermethylation in CpG islands of tumor suppressor genes, such as the

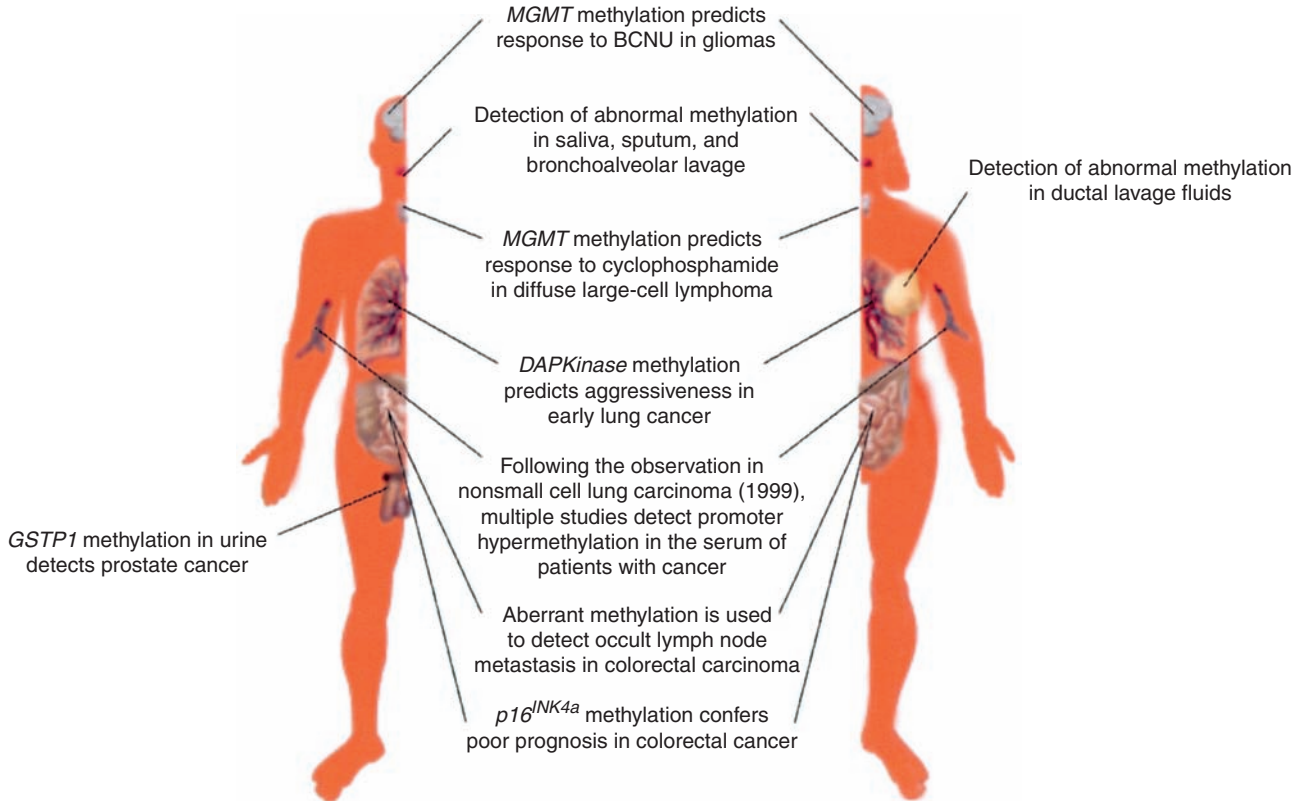

Figure 12. Examples of the translational use of DNA hypermethylation as a biomarker in the management of cancer patients.

methylation-specific polymerase chain reaction (PCR) technique (MSP) (Herman *et al.,* 1996). In this respect, CpG island hypermethylation has been used as a tool to detect cancer cells in all types of biological fluids and biopsies: broncoalveolar lavage (Ahrendt *et al.,* 1999), lymph nodes (Sanchez-Cespedes *et al.,* 1999), sputum (Palmisano *et al.,* 2000), urine (Cairns *et al.,* 2001), semen (Goessl *et al.,* 2000), ductal lavage (Evron *et al.,* 2001), and saliva (Rosas *et al.,* 2001). An exciting new line of research was also initiated in 1999 when we showed that it was possible to screen for hypermethylated promoter loci in serum DNA from patients with lung cancer (Esteller *et al.,* 1999a). Following our observation, many studies have corroborated the feasibility of detecting CpG island hypermethylation of multiple genes in the serum DNA of a broad spectrum of tumor types (Grady *et al.,* 2001; Kawakami *et al.,* 2000; Sanchez-Cespedes *et al.,* 2000), some of them even using semiquantitative and automated methodologies. Thus, DNA hypermethylation has proved its versatility over a wide range of tumor types and environments.

DNA Methylation as a Prognostic/ Predictor Factor

Clinical outcome is affected by many factors, some of which are a function of the genetic composition and health status of the patient, whereas others are inherent to the malignancy itself. It is important to distinguish between predictive markers, which are associated with the relative sensitivity to specific therapeutics strategies, and prognostic markers, which are associated with treatment-independent factors such as the growth rate and metastatic behavior of the malignancy. Both of these types of stratification markers are of clinical value and can assist physicians in their choice of treatment.

As examples of DNA methylation markers of poor prognosis, we can mention that the death-associated protein kinase (*DAPK*) and *p16*^{INK4a} hypermethylation have been linked to tumor virulence in patients with lung or colorectal cancer (Esteller *et al.,* 2001c; Tang *et al.,* 2000). Additional candidates awaiting analysis to determine their relation to enhanced metastasizing or angiogenic activity in primary tumors

include the aberrant methylation of E-cadherin (*CDH1*), H-cadherin (*CDH13*), and thrombospondin-1 (*THBS-1*), respectively.

With respect to the use of DNA methylation as predictive factors, the most compelling evidence is provided by the methylation-associated silencing of the DNA repair *MGMT* in human cancer. The MGMT protein (O^6-methylguanine DNA methyltransferase) is directly responsible for repairing the addition of alkyl groups to the guanine (G) base of the DNA. This base is the preferred point of attack in the DNA of several alkylating chemotherapeutic drugs, such as BCNU (1,3-bis(2-chloroethyl)-1-nitrosourea), ACNU (1-(4-amino-2-methyl-5-pyrimidinyl)methyl-3-(2-chloroethyl)-3-nitrosourea), procarbazine, streptozotocin, or temozolamide. Thus, our reasoning was that tumors that had lost *MGMT* as a result of hypermethylation (Esteller *et al.,* 1999b) would be more sensitive to the action of these alkylating agents because their DNA lesions could not be repaired in the cancer cell and therefore this would lead to cell death. We have presented evidence for the principle of this hypothesis, and *MGMT* promoter hypermethylation effectively predicts a good response to chemotherapy, greater overall survival, and longer time to progression in patients with glioma treated with BCNU (carmustine), (Esteller *et al.,* 2000a) (Figure 13).

Cases similar to that described for *MGMT* can be cited for other DNA repair and detoxifier genes that also undergo aberrant DNA methylation. For example, the response to cisplatin and derivatives may be a direct function of the methylation state of the CpG island of *hMLH1* (Plumb *et al.,* 2000); the response to adriamicine may be related to the methylation status of *GSTP1* (Tew and Ronai, 1999), and the response to certain DNA-damaging drugs could be a function of the state of *BRCA1* hypermethylation (Esteller *et al.,* 2000b; Lafarge *et al.,* 2001). Contrary evidence has also been presented. An old foe of cancer treatment, the *MDR-1* gene (multidrug resistance-1), can undergo reactivation by demethylation in certain malignancies (Kusaba *et al.,* 1999), although more studies are necessary to clarify this issue. I strongly encourage all the studies that address these issues because they may have a direct impact on clinical cancer treatment.

Finally, gene inactivation by promoter hypermethylation may be the key to understanding the loss of hormone responsiveness of many tumors. The inefficacy of the antisteroids, estrogen–progesterone–androgen related compounds such as tamoxifen, raloxifene, and flutemide, in certain breast, endometrial, and prostate cancer cases may be a direct consequence of the methylation-mediated silencing of their respective cellular receptors (*ER, PR,* and *AR* genes).

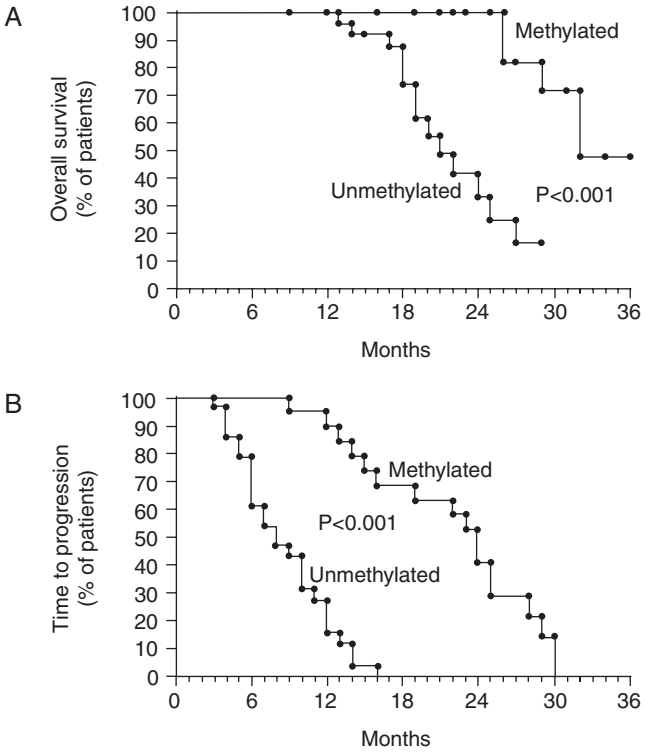

Figure 13. Overall survival (A) and time to the progression of disease (B) among patients with gliomas treated with carmustine, according to the methylation status of the *MGMT* promoter. (Esteller, M., Garcia-Foncillas, J., Andion, E., Goodman, S.N., Hidalgo, O.F., Vanaclocha, V., Baylin, S.B., and Herman, J.G. 2000a. Activity of the DNA repair gene MGMT and the clinical response of gliomas to alkylating agents. *New. Engl. J. Med. 343*:1350–1354.)

DNA Methylation as a Therapeutic Target

It is increasingly apparent that many important genes can be inactivated in association with promoter hypermethylation in a single type of cancer and even in the same patient's tumor. Given that this transcriptional repression is a potentially reversible process, reactivation of the involved genes can be considered as a possible therapeutic target, and this concept is receiving increasing attention. In fact, for several years we have been able to reactivate hypermethylated genes *in vitro* using demethylating agents such as 5-azacytidine or 5-aza-2-deoxicytidine (Decitabine) (Baylin *et al.,* 2001). One obstacle to the transfer of this technique to human primary cancers is lack of specificity of the drugs used (Villar-Garea and Esteller, 2003). These drugs inhibit the DNMTs and cause global hypomethylation, and we cannot reactivate solely the particular gene we wish to. New chemical inhibitors of DNA methylation are being introduced, such as procainamide,

which provide us with more hope, but the nonspecificity problem persists. If we consider that only tumor suppressor genes are hypermethylated, this would not be a great problem. However, we do not know if we have disrupted some essential methylation at certain sites, and global hypomethylation may be associated with even greater chromosomal instability (Chen *et al.,* 1998). Another drawback is the toxicity to normal cells, a phenomenon that was observed with the first higher doses used. However, these compounds and their derivatives have been used in the clinic with some therapeutic benefit, especially in hematopoietic malignancies (Schwartsmann *et al.,* 1997; Wijermans *et al.,* 1997). However, it is known that DNA methylation and regulation of histone deacetylase (HDAC) activity function together to inappropriately silence gene expression in cancer. The simultaneous inhibition of both processes may be the most efficacious approach to reactivating key genes for therapeutic purposes. This approach might allow the use of lower doses of DAC, thus more specifically inhibiting DNMT without other effects, while also realizing the ability of HDAC inhibition to up-regulate gene expression in the absence of dense promoter methylation level.

These new findings have proved very attractive to several pharmacologic and biotechnical companies, and they are now studying how to accomplish demethylation of cancer cells using novel approaches, such as antisense constructs or ribozymes, against the DNMTs. Nevertheless, we are still left with the problem of nonspecificity. Other companies tackle the problem using gene therapy–like strategies in which we reactivate a targeted methylated gene specifically, but the studies are still in their infancy. Thus, a great deal of the promise remains to be fulfilled.

METHODS

Although global genomic DNA methylation might have an important role in carcinogenesis, its measurement in cancer cells has little to offer as a molecular marker, either in sensitivity or in information content. Conversely, methylation levels at individual CpG dinucleotides are useful for quantifying differences at important regulatory sequences. Two alternatives are currently used to study the distribution of 5-methylcytosine residues in particular DNA sequences: nonbisulfite and bisulfite methods. The first relies on the use of methylation-sensitive restriction endonucleases combined with Southern Blot analysis or PCR detection, which sometimes means that results are limited to cleavage sites. This problem can be avoided by the bisulfite modification of the DNA, which comprises a wide range of techniques that allow the quantitative and accurate determination of the methylation status of the allele and even at the cell population level. All bisulfite-associated methods require PCR amplification of the bisulfite-modified DNA, and differences in methylcytosine patterns are displayed by methylation-dependent primer design (MSP), in conjunction with methylation-sensitive restriction endonucleases (combined bisulfite restriction analyses, or COBRA), genomic sequencing, and other approaches. Some of them even provide quantitative data about the average proportion of methylated and nonmethylated alleles in a population.

As a general rule, CpG island methylation first should be studied in great detail in cancer cell lines where the amount of material is not limited. The cell lines will also allow us to develop the demethylation and reexpresion experiments using 5-azacytidine or 5-aza-2-deoxycytidine. In the case of primary tumors, techniques that allow the screening of a large number of samples, such as MSP (Herman *et al.,* 1996), will be very useful, although other techniques can also be applied if a more quantitative estimate is desired.

Quantification of Global Methylation

Levels of methylcytosine occurrence in the genomic DNA can be measured by high-performance separation techniques or by enzymatic or chemical means. When separation devices are available, high-performance capillary electrophoresis (HPCE) may be the best choice because it is faster, cheaper, and more sensitive than HPLC (Fraga *et al.,* 2000; Fraga *et al.,* 2002a). By means of labeled antimethylcytosine antibodies, DNA methylation can be monitored in metaphase chromosomes; in hetero/euchromatin; and, most importantly, on a cell-by-cell basis within the same sample. The latter alternative, which generally yields qualitative results, is of great interest in cancer research because it can reveal methylation differences between normal and tumor tissues in the same sample.

HPLC-Based Methods

Relative methylcytosine contents of genomic DNA can be analyzed by chemical hydrolysis to obtain the total base composition of the genome and subsequent fractionation and quantification of hydrolysis products using HPLC technologies. The degree of DNA methylation of several samples has been quantified by this method, but at least 2.5 μg DNA are generally required to quantify 5-methylcytosine with a low standard deviation for replicate samples. Sensitivity of the system can be increased with mass spectrometry detection, which

has a detection limit 10^6 times the limit of absorption spectroscopy detectors.

HPCE-Based Methods

The development of HPCE techniques has given rise to an approach to research that has several advantages over other current methodologies used to quantify the extent of DNA (Fraga *et al.,* 2002a; Fraga and Esteller, 2002b). This method is faster than HPLC (taking less than 10 min per sample) and is also reasonably inexpensive because it does not require continuous running buffers and displays a great potential for fractionation (theoretically up to 10^6 plates). Approximately 1 methylcytosine in 200 cytosine residues can be detected by this method using 1 μg genomic DNA. To increase sensitivity, laser-induced fluorescence (LIF) and mass spectrometry detectors should be used.

Analyses of Genomewide Methylation by Chemical or Enzymatic Means

As previously stated, quantifying the degree of DNA methylation by HPLC or HPCE requires access to sophisticated equipment that is not always available. The radioactive labeling of CpG sites using the methyl-acceptor assay has been developed to address this problem, but, among the technique's other drawbacks, it can only monitor CpG methylation changes, and so CpNpG methylation cannot be detected. This method uses bacterial SssI DNA methyltransferase to transfer tritium-labeled methyl groups from SAM (S-adenosyl-L-[methyl-^{3}H]methionine) to unmethylated cytosines in CpG targets. The data obtained from a scintillation counter are used to calculate the number of methyl groups incorporated in the DNA.

In situ Hybridization Methods for Studying Total Cytosine Methylation

Global DNA methylation can also be quantified by methylcytosine-specific antibodies (Miller *et al.,* 1974). An important advantage of this approach is that it may be carried out on a cell-by-cell basis rather than in a heterogeneous population. Apart from classical immunoassay detection, approaches that involve quantifying the retention of radiolabeled DNA by polyclonal antibodies on nitrocellulose filters, immunoprecipitation, gel filtration, and visualization under the electron microscope, cytosine methylation can also be detected in metaphase chromosomes and in chromatin using monoclonal antibodies combined with fluorescence staining. An alternative to fluorescence detection is to connect a colored enzyme-dependent reaction.

Nonbisulfite Methods

The most widely used methods for studying DNA methylation patterns of specific regions of DNA with no base modifications are based on the use of methylation-sensitive and methylation-insensitive restriction endonucleases (MS-REs) (Cedar *et al.,* 1979). One of the restriction enzymes of the isoschizomer pair is able to cut the DNA only when its target is unmethylated, whereas the other is not sensitive to methylated cytosines. The most common isoschizomers used are the Hpa II/Msp I pair. Although these pairs of enzymes can cleave hemimethylated DNA, they do not distinguish between cytosines methylated at different positions in the pyrimidinic ring (Butkus *et al.,* 1987). However, there are several restriction enzymes that recognize the localization of the methyl group (McClelland *et al.,* 1994).

Once DNA has been digested with methylation-sensitive endonucleases, identification of the methylation status of a gene can be accomplished by Southern Blot hybridization or PCR procedures. In the former, digestion products are separated by gel electrophoresis, transferred to a nitrocellulose filter, and hybridized with a radiolabeled probe (Maniatis *et al.,* 1982). When DNA digestion is accomplished by methylation-sensitive nucleases, the obtaining of a larger DNA fragment than expected indicates methylation at one or both restriction targets that flank the homologous region of the DNA. An mC-positive will be detected when at least 10% of the DNAs present that modification as a result of their hybridization sensitivity.

When the amount of tissue is limiting, detection of cytosine methylation can be achieved by PCR, which requires less than 10 ng DNA, whereas Southern hybridization generally needs up to 10 μg DNA. Furthermore, a methylcytosine-positive can be detected when only 0.1% of the DNA molecules present such base modification (Kutueva *et al.,* 1996). PCR primers must correspond to flanking sequences of the restriction targets, so that the absence of methylation is revealed in the presence of a PCR band (Singer-Sam *et al.,* 1990). Nonbisulfite methods for the quantification of DNA methylation patterns are simple and rapid and can be used for any known-sequence genomic DNA region. These methods are extremely specific, but their limitation to specific restriction sites reduces their value.

Bisulfite Methods

The analysis of DNA methylation changed completely with the introduction of sodium bisulfite conversion of genomic DNA. The differential rates at

which cytosine and 5-methylcytosine are deaminated by sodium bisulfite to yield uracil and thymine in conjunction with PCR amplification and sequencing provides us a method to find specific methylated sequences.

Bisulfite converts all cytosines to uracil, except those that are methylated, which are resistant to modification and remain as cytosine (Furuichi *et al.,* 1970). This reaction constitutes the basis for discriminating between methylated and unmethylated DNA. Bisulfite modification of DNA can be followed by several methods, including sequencing, methylation-specific PCR, combined bisulfite restriction assays, and others. In general, each modification leads to greater sensitivity and resolution or contributes to the development of a novel perspective on the results. All of them work with PCR, which, among other advantages, is suitable for analyzing paraffin-embedded tissues and scarce purified DNA.

Bisulfite Modification of DNA

MATERIALS

- Sodium bisulfite 3 M (pH 5)
- Hydroquinone 20 mM
- Sodium hydroxide 3 M
- Wizard DNA purification resin (Promega)
- Isopropanol 80%
- Ethanol (70% and absolute)
- Ammonium acetate 10 M

PROCEDURE

- Dilute 1 µg of DNA in 50 µl, mix with 5.7 µl of NaOH 3 M, and incubate at 37°C for 15 min. This first step is for DNA denaturation because only cytosines that are located in single strands are susceptible to bisulfite modification.
- Add 33 µl of hidroquinone 20 mM and 530 µl of sodium bisulfite, both freshly prepared, and incubate at 50°C for 16–17 hr.
- Purify modificated DNA using the Wizard DNA purification resin according to the manufacturer (Promega), and elute in 50 µl of mili Q water.
- Complete the modification by adding 5.7 µl of NaOH 3 M, and incubate at 37°C for 20 min.
- Add 17 µl of ammonium acetate 10 M, 1 µl glycogen 10 mg/ml, and 3 volumes of absolute ethanol, and incubate overnight at −70°C to precipitate the modified DNA.
- Centrifuge at 12000 rpm at 4°C for 20 min, discard the supernatant, wash the pellet with ethanol 70%, and centrifuge in similar conditions.
- Discard the supernatant, and dry the pellet in a speed vacuum.
- Resuspend the pellet in 25 µl of mili Q water.

Bisulfite Sequencing

Sequencing bisulfite-altered DNA is the most straightforward means of detecting cytosine methylation. In general, after denaturation and bisulfite modification, double-stranded DNA is obtained by primer extension and the fragment of interest is amplified by PCR (Clark *et al.,* 1994). Methylcytosine may then be detected by standard DNA sequencing of the PCR products (Figure 14). The most important aspect of sequencing bisulfite-modified DNA is the primers design. Three factors need to be considered in the design of PCR primers for sequencing bisulfite-modified DNA:

- Bisulfite-converted DNA strands are no longer complementary, so primer design must be customized for each DNA chain.
- Primers should cover several cytosines that are not part of the CpG dinucleotides in the original sequences and are therefore converted to uracils by bisulfite. Inclusion of such bases in the primer design helps to avoid amplification of any residual unconverted DNA.
- Primers should not cover any potential sites for DNA methylation (CpG dinucleotides).

This method provides us with methylation maps of a single DNA molecule (Figure 14). The main disadvantage of bisulfite sequencing is that it is not useful for the screening of a large number of clinical samples.

Methylation-Specific PCR

MSP is the most widely used method of DNA methylation. It has had a significant impact on the burgeoning field of cancer epigenetics by making DNA methylation analysis accessible to a wide number of laboratories. Bisulfite sequencing is particularly useful for the quantitative or detailed analysis of 5-methylcytosine distribution, whereas MSP excels at the sensitive detection of particular methylation patterns.

The differences between methylated and unmethylated alleles that arise from sodium bisulfite treatment are the basis of MSP (Herman *et al.,* 1996) and are especially valuable in CpG islands as a result of the abundance of CpG sites. Primer design is a critical and complex component of the procedure. Bisulfite-converted DNA strands are no longer complementary, so primer design must be customized for each DNA chain. After chemical modification, two sets of primers should be designed. One primer set (U) will anneal to

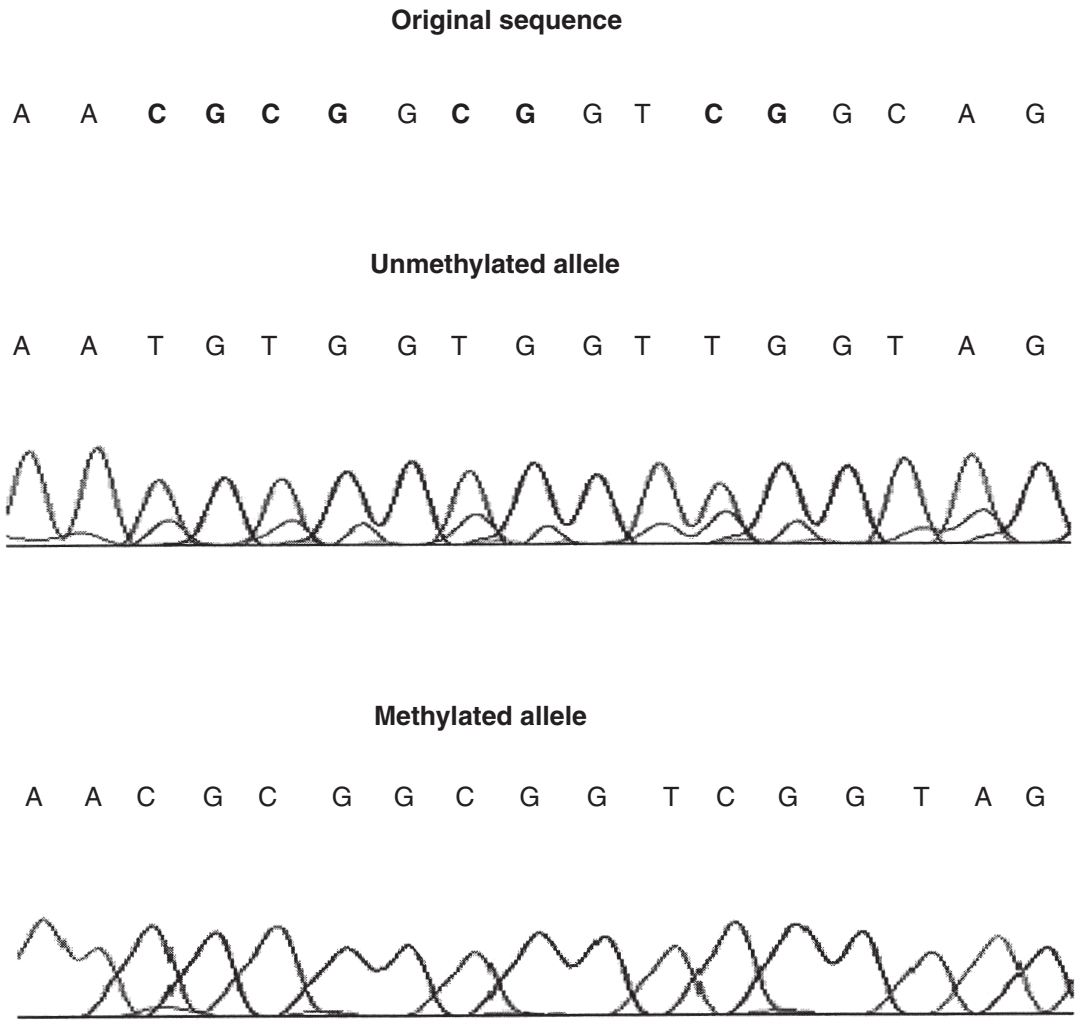

Figure 14. Methylation maps of a single DNA molecule obtained by direct sequencing of Bisulfite-modified DNA.

unmethylated DNA that has undergone a chemical modification, and second primer set (M) will anneal with methylated DNA that has undergone chemical modification. Thus, methylation patterns of all sequences must be determined in separate reactions. To optimize the PCR amplification step, the following critical requirements must be considered when designing the primers:

- The annealing temperature of both primers must be similar and always between 55°C and 65°C.
- The PCR product should be between 80 and 175 bp to allow the assessment of methylation patterns in limited region and to facilitate the application of this technique to samples, such as paraffin blocks, where amplification of larger fragments is not possible.
- Each primer should contain at least two CpG pairs.
- The sense primer should contain a CpG pair at its 3′ end.
- To avoid false-positive results (amplification of unmethylated, unmodified DNA), primers should contain non-CpG cytosines.

The main advantages of MSP are that it is a very sensitive method, permitting the analysis of small and heterogeneous samples, it can be used on paraffin-embedded samples, it is specific for relevant CpG sites, and it avoids the use of restriction enzymes and resultant problems associate with incomplete enzymatic digestion. However, MSP tends to be a more qualitative, rather than a quantitative, accurate method.

Because of its versatility, MSP has been widely proposed as a rapid and cost-effective tool of use in the study of CpG island hypermethylation in human cancer

(Figure 15). For example, MSP has been successfully used to evaluate the responsiveness of human cancer patients to alkalating agents (Esteller *et al.,* 2000a; Esteller *et al.,* 2002) or to detect tumoral DNA in the serum of patients with cancer (Esteller *et al.,* l999a) (see Figure 15).

Combined Bisulfite Restriction Analysis

The COBRA method consists of a standard sodium bisulfite PCR treatment followed by restriction digestion and a quantitation step (Xiong and Laird, 1997). The DNA amplification products of specific loci, previously modified by bisulfite, are digested with restriction enzymes that distinguish methylated from unmethylated sequences so that the degree of DNA methylation is linearly correlated with the relative amounts of digested and undigested products. The BstU I case may illustrate this point: its cleavage site (CGCG) is resistant to bisulfite modification when it is methylated but is transformed to TGTG when it is unmethylated. Thus, DNA cleavage after bisulfite treatment only occurs if the restriction target is methylated, and, moreover, cleavage products are proportional to the degree of methylation of the analyzed sequence. The average relative proportions of digestion products can be quantified by hybridization with 5′ end-labeled oligos and Phosphorimager detection. In contrast to MSP, PCR primers should not contain CpG pairs to avoid discrimination between different methylated templates. In general, this approach can be used when absolute percentages of methylated and unmethylated alleles are required to guarantee the final diagnosis. The major drawback is that BstU I will also cut if unconverted. Therefore the use of this enzyme can lead to overestimation of methylation, so that checking conversion state with enzymes such as Hpa II is needed (Jackson *et al.,* 2000). This is a specific and quantitative method but requires a complete chemical modification of DNA and cannot analyze all DNA sequences because it is confined to restriction targets.

Fluorescence-Based Real-Time Quantitative PCR Analysis

Sodium bisulfite modification creates methylation-dependent sequence differences in the genomic DNA. Fluorescence-based PCR is then performed using locus-specific PCR primers flanking an oligonucleotide probe with a 5′ fluorescent reporter dye (FAM) and a

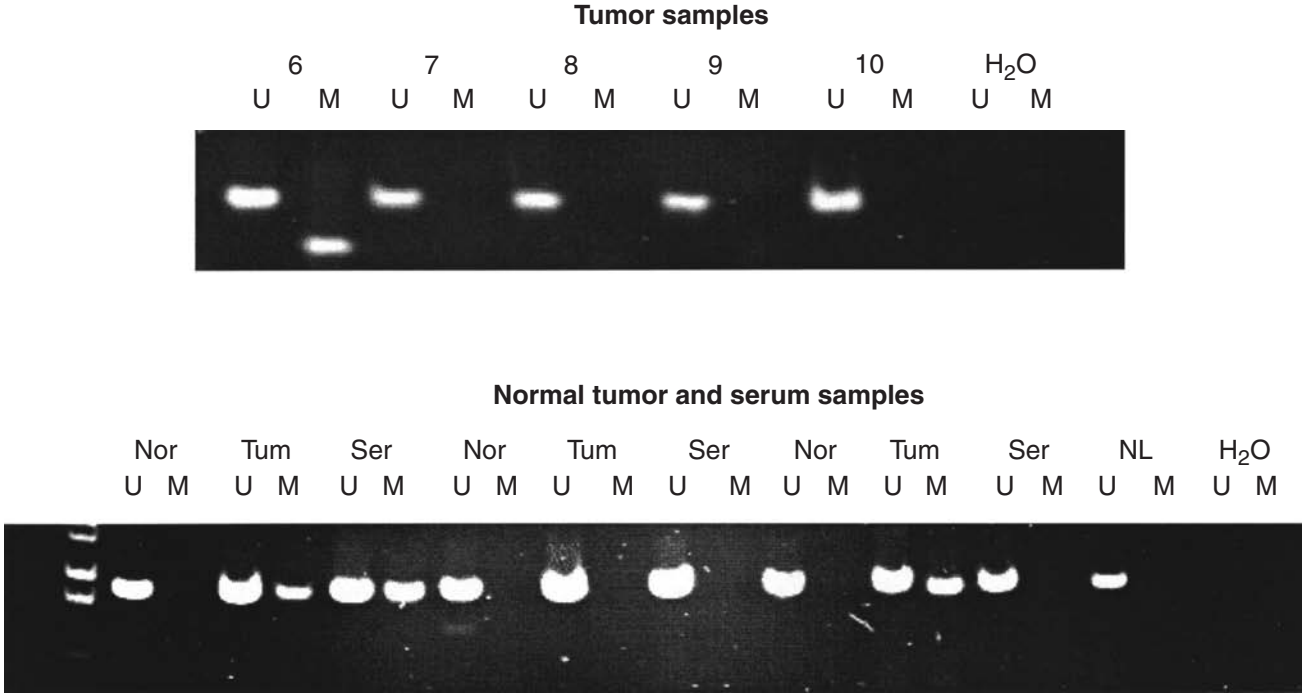

Figure 15. Analysis of the methylation status of a specific gene by methylation specific PCR (MSP) in tumor and serum samples. (Esteller, M., Sanchez-Cespedes, M., Rosell, R., Sidransky, D., Baylin, S.B., and Herman, J.G. l999a. Detection of aberrant promoter methylation of tumor suppressor genes in serum DNA from non-small cell lung cancer patients. *Cancer Res. 59*:67–70.)

3′ quencher dye (TAMRA). The 5′ to 3′ nuclease activity of DNA polymerase cleaves the probe and releases the reporter, whose fluorescence can be detected by the laser detector of the detection system (Eads *et al.,* 2000; Lo *et al.,* 1999). The most striking advantage of real-time quantitative PCR analysis is its potential to allow the rapid screening of hundreds to thousands of samples and its sensitivity, making it possible to detect a single methylated allele in 10,000 unmethylated alleles. Unlike other techniques, this assay is completed at the PCR step, without the need for further gel electrophoretic separation and hybridization. The drawbacks of this method are that it requires expensive hybridization probes and calibration curves must be generated in each setting.

Acknowledgments

We thank Dr. Michel Herranz for his help in the drawing of the figures.

References

Ahrendt, S.A., Chow, J.T., Xu, L., Yang, S.C., Eisenberger, C.F., Esteller, M., Herman, J.G., Wu, L., Decker, P.A., Jen, J., and Sidransky, D. 1999. Molecular detection of tumor cells in bronchoalveolar lavage fluid from patients with early stage lung cancer. *J. Nat. Cancer Inst. 91*:332–339.

Alves, G., Tatro, A., and Fanning, T. 1996. Differential methylation of human LINE-1 retrotransposons in malignant cells. *Gene 176*:39–44.

Baylin, S.B., Herman, J.G., Graff, J.R., Vertino, P.M., and Issa, J.P. 1998. Alterations in DNA methylation: A fundamental aspect of neoplasia. *Adv. Cancer Res. 72*:141–196.

Baylin, S.B., Esteller, M., Rountree, M.R., Bachman, K.E., Schuebel, K., and Herman, J.G. 2001. Aberrant patterns of DNA methylation, chromatin formation and gene expression in cancer. *Hum. Mol. Genet. 10*:687–692.

Bird, A.P. 1986. CpG-rich islands and the function of DNA methylation. *Nature 321*:209–213.

Brandeis, M., Ariel, M., and Cedar, H. 1993. Dynamics of DNA methylation during development. *Bioessays 15*:709–713.

Butkus, V., Petrauskiene, L., Maneliene, Z., Klimasauskas, S., Laucys, V., and Janulaitis, A. 1987. Cleavage of methylated CCCGGG sequences containing either N4-methylcytosine or 5-methylcytosine with MspI, HpaII, SmaI, XmaI and Cfr9I restriction endonucleases. *Nucleic Acids Res. 15*:7091–7102.

Cairns, P., Esteller, M., Herman, J.G., Schoenberg, M., Jeronimo, C., Sanchez-Cespedes, M., Chow, N.H., Grasso, M., Wu, L., Westra, W.B., and Sidransky, D. 2001. Molecular detection of prostate cancer in urine by GSTP1 hypermethylation. *Clin Cancer Res. 7*:2727–2730.

Cedar, H., Solage, A., Glaser, G., and Razin, A. 1979. Direct detection of methylated cytosine in DNA by use of the restriction enzyme MspI. *Nucleic Acids Res. 6*:2125–2132.

Chen, R.Z., Pettersson, U., Beard, C., Jackson-Grusby, L., and Jaenisch, R. 1998. DNA hypomethylation leads to elevated mutation rates. *Nature 395*:89–93.

Clark, S.J., Harrison, J., Paul, C.L., and Frommer, M. 1994. High sensitivity mapping of methylated cytosines. *Nucleic Acids Res. 22*:2990–2997.

De Smet, C., Lurquin, C., Lethe, B., Martelange, V., and Boon, T. 1999. DNA methylation is the primary silencing mechanism for a set of germ line- and tumor-specific genes with a CpG-rich promoter. *Mol. Cell. Biol. 19*:7327–7335.

Eads, C.A., Kanenberg, K.D., Kawakami, K., Saltz, L.B., Blake, C., and Shibata, D. 2000. Methyllight: A high-throughput assay to measure DNA methylation. *Nucleic Acid Res. 28*, e32.

Ehrlich, M. 2000. DNA hypomethylation and cancer. In: Ehrlich, M., (ed) *DNA Alterations in Cancer: Genetic and Epigenetic Changes,* Natick, MA: Eaton Publishing, 273–291.

Esteller, M., Sanchez-Cespedes, M., Rosell, R., Sidransky, D., Baylin, S.B., and Herman, J.G. 1999a. Detection of aberrant promoter methylation of tumor suppressor genes in serum DNA from non-small cell lung cancer patients. *Cancer Res. 59*:67–70.

Esteller, M., Hamilton, S.R., Burger, P.C., Baylin, S.B., and Herman, J.G. 1999b. Inactivation of the DNA repair gene O^6-methylguanine-DNA methyltransferase by promoter hypermethylation is a common event in primary human neoplasia. *Cancer Res. 59*:793–797.

Esteller, M., Garcia-Foncillas, J., Andion, E., Goodman, S.N., Hidalgo, O.F., Vanaclocha, V., Baylin, S.B., and Herman, J.G. 2000a. Activity of the DNA repair gene MGMT and the clinical response of gliomas to alkylating agents. *New. Engl. J. Med. 343*:1350–1354.

Esteller, M., Silva, J.M., Dominguez, G., Bonilla, F., Matias-Guiu, X., Lerma, E., Bussaglia, E., Prat, J., Harkes, I.C., Repasky, E.A., Gabrielson, E., Schutte, M., Baylin, S.B., and Herman, J.G. 2000b. Promoter hypermethylation is a cause of BRCA1 inactivation in sporadic breast and ovarian tumors. *J. Natl. Cancer Inst. 92*:564–569.

Esteller, M., Fraga, M.F., Guo, M., Garcia-Foncillas, J., Hedenfalk, I., Godwin, A.K., Trojan, J., Vaurs-Barriere, C., Bignon, Y.J., Ramus, S., Benitez, J., Caldes, T., Akiyama, Y., Yuasa, Y., Launonen, V., Canal, M.J., Rodriguez, R., Capella, G., Peinado, M.A., Borg, A., Aaltonen, L.A., Ponder, B.A., Baylin, S.B., and Herman, J.G. 2001a. DNA methylation patterns in hereditary human cancer mimics sporadic tumorigenesis. *Hum. Mol. Genet. 10*:3001–3007.

Esteller, M., Corn, P.G., Baylin, S.B., and Herman, J.G. 2001b. A gene hypermethylation profile of human cancer. *Cancer Res. 61*:3225–3229.

Esteller, M., Gonzalez, S., Risques, R.A., Marcuello, E., Mangues, R., Germa, J.R., Herman, J.G., Capella, G., and Peinado, M.A. 2001c. K-ras and p16 alterations confer poor prognosis in human colorectal cancer. *J. Clin. Oncol. 19*:299–304.

Esteller, M. 2002. CpG island hypermethylation and tumor suppressor genes: A booming present, a brighter future. *Oncogene. 21*:5427–5440.

Esteller, M., Gaidano, G., Goodman, S.N., Zagonel, V., Capello, D., Botto, B., Rossi, D., Gloghini, A., Vitolo, U., Carbone, A., Baylin, S.B., and Herman, J.G. 2002. Hypermethylation of the DNA repair gene O(6)-methylguanine DNA methyltransferase and survival of patients with diffuse large B-cell lymphoma. *J. Nat. Cancer Inst. 94*:26–32.

Evron, E., Dooley, W.C., Umbricht, C.B., Rosenthal, D., Sacchi, N., Gabrielson, E., Soito, A.B., Hung, D.T., Ljung, B., Davidson, N.E., and Sukumar, S. 2001. Detection of breast cancer cells in ductal lavage fluid by methylation-specific PCR. *Lancet 357*:1335–1336.

Feinberg, A.P. 1999. Imprinting of a genomic domain of 11p15 and loss of imprinting in cancer: An introduction. *Cancer Res. 59*:1743s–1746s.

Florl, A.R., Lower, R., Schmitz-Drager, B.J., and Schulz, W.A. 1999. DNA methylation and expression of LINE-1 and HERV-K

provirus sequences in urothelial and renal cell carcinomas. *Br. J. Cancer 80*:1312–1321.

Fraga, M.F., Rodriguez, R., and Canal M.J. 2000. Rapid quantification of DNA methylation by high performance capillary electrophoresis. *Electrophoresis 14*:2990–2994.

Fraga, M.F., Uriol, E., Borja Diego, L., Berdasco, M., Esteller, M., Canal, M.J., and Rodriguez, R. 2002a. High-performance capillary electrophoretic method for the quantification of 5-methyl 2′-deoxycytidine in genomic DNA: Application to plant, animal and human cancer tissues. *Electrophoresis 23*:1677–1681.

Fraga, M.F., and Esteller, M. 2002b. DNA methylation: A profile of methods and applications. *Biotechniques 33*:632–649.

Furuichi, Y., Wataya, Y., Hayatsu, H., and Ukita, T. 1970. Chemical modification of tRNA-Tyr-yeast with bisulfite: A new method to modify isopentenyladenosine residue. *Biochem. Biophys. Res. Commun. 41*:1185–1191.

Goessl, C., Krause, H., Muller, M., Heicappell, R., Schrader, M., Sachsinger, J., and Miller, K. 2000. Fluorescent methylation-specific polymerase chain reaction for DNA-based detection of prostate cancer in bodily fluids. *Cancer Res. 60*:5941–5945.

Grady, W.M., Rajput, A., Lutterbaugh, J.D., and Markowitz, S.D. 2001. Detection of aberrantly methylated hMLH1 promoter DNA in the serum of patients with microsatellite unstable colon cancer. *Cancer Res. 61*:900–902.

Herman, J.G., Graff, J.R., Myohanen, S., Nelkin, B.D., and Baylin, S.B. 1996. Methylation-specific PCR: A novel PCR assay for methylation status of CpG islands. *Proc. Natl. Acad. Sci. USA 93*:9821–9826.

Jackson, P., Millar, D., Kingsley, E., Yardley, G., Ow, K., Clark, S., and Russell, P.J. 2000. Methylation of a CpG island within the promoter region of the KAI1 metastasis suppressor gene is not responsible for down-regulation of KAI1 expression in invasive cancers or cancer cell lines. *Cancer Lett. 157*:169–176.

Kawakami, K., Brabender, J., Lord, R.V., Groshen, S., Greenwald, B.D., Krasna, M.J., Yin, J., Fleisher, A.S., Abraham, J.M., Beer, D.G., Sidransky, D., Huss, H.T., Demeester, T.R., Eads, C., Laird, P.W., Ilson, D.H., Kelsen, D.P., Harpole, D., Moore, M.B., Danenberg, K.D., Danenberg, P.V., and Meltzer, S.J. 2000. Hypermethylated APC DNA in plasma and prognosis of patients with esophageal adenocarcinoma. *J. Natl. Cancer Inst. 92*:1805–1881.

Kusaba, H., Nakayama, M., Harada, T., Nomoto, M., Kohno, K., Kuwano, M., and Wada, M. 1999. Association of 5′ CpG demethylation and altered chromatin structure in the promoter region with transcriptional activation of the multidrug resistance 1 gene in human cancer cells. *Eur. J. Biochem. 262*:924–932.

Kutueva, L.I., Ashapkin, V.V., and Vanyushin, B.F. 1996. The methylation pattern of a cytosine DNA-methyltransferase gene in *Arabidopsis thaliana* plants. *Biochem. Mol. Biol. Int. 40*:347–353.

Lafarge, S., Sylvain, V., Ferrara, M., and Bignon, Y.J. 2001. Inhibition of BRCA1 leads to increased chemoresistance to microtubule-interfering agents, an effect that involves the JNK pathway. *Oncogene 20*:6597–6606.

Laird, P.W. 1997. Oncogenic mechanism mediated by DNA methylation. *Mol. Med. Today 3*:223–229.

Lapeyre, J.N., and Becker, F.F. 1979. 5-methylcytosine content of nuclear DNA during chemical hepatocarcinogenesis and in carcinomas which result. *Biochem. Biophys. Res. Comm. 87*:698–705.

Lo, Y.M., Wong, I.H., Zhang, J., Tein, M.S., Ng, M.H., and Hjelm, N.M. 1999. Quantitative analysis of aberrant P16 methylation using real-time quantitative methylation-specific polymerase chain reaction. *Cancer Res. 59*:3899–3903.

Maniatis, T., Fritsch, E.F., and Sambrock, J. 1982. *Molecular Cloning: A Laboratory Manual.* Cold Spring Harbor Laboratory Press: Cold Spring Harbor, NY.

McClelland, M., Nelson, M., and Raschke, E. 1994. Effect of site-specific modification on restriction endonucleases and DNA modification methyltransferases. *Nucleic Acids Res. 22*:3640–3659.

Miller, O.J., Schnedl, W., Allen, J., and Erlanger, B.F. 1974. 5-Methylcytosine localised in mammalian constitutive heterochromatin. *Nature 251*:636–637.

Palmisano, W.A., Divine, K.K., Saccomanno, G., Gilliland, F.D., Baylin, S.B., Herman, J.G., and Belinsky, S.A. 2000. Predicting lung cancer by detecting aberrant promoter methylation in sputum. *Cancer Res. 60*:5954–5958.

Paz, M.F., Avila, S., Fraga, M.F., Pollan, M., Capella, G., Peinado, M.A., Sanchez-Cespedes, M., Herman, J.G., and Esteller, M. 2002. Germ-line variants in methyl-group metabolism genes and susceptibility to DNA methylation in normal tissues and human primary tumors. *Cancer Res. 62*:4519–4524.

Plumb, J.A., Strathdee, G., Sludden, J., Kaye, S.B., and Brown, R. 2000. Reversal of drug resistance in human tumor xenografts by 2′-deoxy-5-azacytidine-induced demethylation of the hMLH1 gene promoter. *Cancer Res. 60*:6039–6044.

Robertson, K.D., and Wolffe, A.P. 2000. DNA methylation in health and disease. *Nat. Rev. Genet. 1*:11–19.

Rosas, S.L., Koch, W., da Costa Carvalho, M.G., Wu, L., Califano, J., Westra, W., Jen, J., and Sidransky, D. 2001. Promoter hypermethylation patterns of p16, O6-methylguanine-DNA-methyltransferase, and death-associated protein kinase in tumors and saliva of head and neck cancer patients. *Cancer Res. 61*:939–942.

Sanchez-Cespedes, M., Esteller, M., Hibi, K., Cope, F.O., Westra, W.H., Piantadosi, S., Herman, J.G., Jen, J., and Sidransky, D. 1999. Molecular detection of neoplastic cells in lymph nodes of metastatic colorectal cancer patients predicts recurrence. *Clin. Cancer Res. 5*:2450–2454.

Sanchez-Cespedes, M., Esteller, M., Wu, L., Nawroz-Danish, H., Yoo, G.H., Koch, W.M., Jen, J., Herman, J.G., and Sidransky, D. 2000. Gene promoter hypermethylation in tumors and serum of head and neck cancer patients. *Cancer Res. 60*:892–895.

Schwartsmann, G., Fernandes, M.S., Schaan, M.D., Moschen, M., Gerhardt, L.M., Di Leone, L., Loitzembauer, B., and Kalakun, L. 1997. Decitabine (5-Aza-2′-deoxycytidine; DAC) plus daunorubicin as a first line treatment in patients with acute myeloid leukemia: Preliminary observations. *Leukemia 11 Suppl. 1*:S28–31.

Singer-Sam, J., Grant, M., LeBon, J.M., Okuyama, K., Chapman, V., Monk, M., and Riggs, A.D. 1990. Use of a HpaII-polymerase chain reaction assay to study DNA methylation in the Pgk-1 CpG island of mouse embryos at the time of X-chromosome inactivation. *Mol. Cell. Biol. 10*:4987–4989.

Tang, X., Khuri, F.R., Lee, J.J., Kemp, B.L., Liu, D., Hong, W.K., and Mao, L. 2000. Hypermethylation of the death-associated protein (DAP) kinase promoter and aggressiveness in stage I non-small-cell lung cancer. *J. Natl. Cancer. Inst. 92*:1511–1516.

Tew, K.D., and Ronai, Z. 1999. GST function in drug and stress response. *Drug Resist. Updat. 2*:143–147.

Thayer, R.E., Singer, M.F., and Fanning, T.G. 1993. Undermethylation of specific LINE-1 sequences in human cells producing a LINE-1-encoded protein. *Gene 133*:273–277.

Torre, L., Lopez-Rodas, G., Latasa, M.U., Carretero, M.V., Boukaba, A., Rodriguez, J.L., Franco, L., Mato, J.M., and Avila, M.A. 2000. DNA methylation and histone acetylation of rat methionine adenosyltransferase 1A and 2A genes is tissue-specific. *Int. J. Biochem. Cell. Biol. 32*:397–404.

Villar-Garea, A., and Esteller, M. 2003. DNA demethylating agents and chromatin-remodelling drugs: which, how and why. *Curr. Drug. Metabol. 4*:11–31.

Wijermans, P.W., Krulder, J.W., Huijgens, P.C., and Neve, P. 1997. Continuous infusion of low-dose 5-Aza-2′-deoxycytidine in elderly patients with high-risk myelodysplastic syndrome. *Leukemia 11*:1–5.

Yoder, J.A., Walsh, C.P., and Bestor, T.H. 1997. Cytosine methylation and the ecology of intragenomic parasites. *Trends Genet. 13*:335–340.

Xiong, Z., and Laird, P.W. 1997. COBRA: A senitive and quantitative DNA methylation assay. *Nucleic Acid Res. 25*:2532–2534.

Xu, G.L., Bestor, T.H., Bourc′his, D., Hsieh, C.L., Tommerup, N., Bugge, M., Hulten, M., Qu, X., Russo, J.J., and Viegas-Pequignot, E. 1999. Chromosome instability and immunodeficiency syndrome caused by mutations in a DNA methyltransferase gene. *Nature 402*:187–191.

8

Antiepidermal Growth Factor Receptor Antibody: Immunohistochemistry

Alicia Viloria-Petit and Enrique Rengifo-Calzado

Introduction

The epidermal growth factor receptor (EGFR) was the first sequenced (Downward *et al.,* 1984) and cloned (Ullrich *et al.,* 1984) member of a family of four structurally related glycoproteins, referred to as "the type I receptors." These include EGFR/ErbB-1/HER-1, HER-2/neu/ErbB-2, HER-3/ErbB-3, and HER-4/ErbB-4, all four transmembrane receptors, three of which possess intrinsic tyrosine kinase activity (Yarden and Sliwkowski, 2001).

EGFR-type receptors are normally expressed, although at different levels, in epithelial, mesenchymal, and neuronal tissue and play fundamental roles during the development of skin, neural, and cardiac tissue and in the maintenance of adult organs such as the heart and the skin (reviewed in Yarden and Sliwkowski, 2001). Alterations in the expression of at least two members of this family (EGFR and HER-2) as well as several of their specific ligands have been found in a broad spectrum of human cancers (Salomon *et al.,* 1995).

The EGFR was originally identified as the human homolog of the avian c-*erb*B protein, which was also found to be similar to the deduced amino acid sequence of the v-*erb*B oncogene of the avian erythroblastosis virus (Downward *et al.,* 1984). The human EGFR is located in chromosome 7p13-p l2 and encodes messenger ribonucleic acid (mRNA) species of 10 and 5.6 kb. The final product is a 1186-amino acid long, 170-kDa protein, consisting of 1) a 621-amino acid extracellular (EC) region, which is glycosilated and has two cysteine-rich subdomains, between which the ligand binding region is located; 2) a 23-amino acid hydrophobic transmembrane domain; and 3) a 542-amino acid cytoplasmic domain that contains the highly conserved tyrosine kinase (Salomon *et al.,* 1995; Ullrich *et al.,* 1984). This enzymatic activity is now known to be activated through at least two interconnected mechanisms: 1) the binding of specific ligand to the EC domain and 2) transphosphorylation by other members of the family (particularly HER-2 and HER-4), and presumably other intracellular kinases, e.g., Src (Prenzel *et al.,* 2001; Yarden and Sliwkowski, 2001). The former is the best-documented mechanism.

EGFR-activating ligands include epidermal growth factor (EGF), transforming growth factor-alpha (TGF-α), amphiregulin, heparin binding EGF (HB-EGF), betacellulin, and epiregulin. Binding of ligand promotes dimerization and autophosphorylation of the receptor, which in turn increases the tyrosine kinase

Handbook of Immunohistochemistry and *in situ* Hybridization of Human Carcinomas, Volume 3: Molecular Genetics, Liver Carcinoma, and Pancreatic Carcinoma

catalytic activity and results in phosphorylation of several tyrosine residues in the C-terminus (Yarden and Sliwkowski, 2001). These phosphorylated tyrosines serve as docking sites for several adaptor and signal transducer proteins, which initiate a variety of signaling pathways resulting in cell proliferation, differentiation, survival, migration, adhesion, and transformation (Arteaga, 2002). Signal transducer pathways induced by activated EGFR include phospholipase C-γ-1 (PLC-γ-1), mitogen-activated protein kinase (MAPK), phosphatidylinositol-3-kinase (PI3K), the stress activated protein kinases (SAPK/JNK), and the signal transducers and activators of transcription (STAT), among others (Grünwald and Hidalgo, 2003; Prenzel *et al.,* 2001). The specific signaling pathway activated as well as the potency of the signaling output depends on the type of activating ligand and the cellular levels of the homologous co-receptors (HER-2, HER-3, and HER-4), all of which can form heterodimers with EGFR (Yarden and Sliwkowski, 2001).

Oncogenic activation of EGFR occurs as a result of overexpression and/or mutation. Overexpression rarely occurs (with certain exceptions) by gene amplification, but rather results from changes in molecular mechanisms regulating gene expression (Salomon *et al.,* 1995) and is often accompanied by ligand overexpression (Arteaga, 2002; Salomon *et al.,* 1995). The co-expression of EGFR and ligands at tumor sites allows for EGFR activation via autocrine/paracrine mechanisms (Arteaga, 2002). Overexpression of EGFR has been observed in squamous carcinomas of the skin as well as carcinomas of the head and neck, esophagus, lung, pancreas, liver, colon, kidney, bladder, breast, cervix, ovarian, prostate, and brain (Herbst and Langer, 2002; Nicholson *et al.,* 2001; Salomon *et al.,* 1995). In some of these cancers (e.g., head and neck, ovarian, bladder, cervical, and esophageal) EGFR overexpression has been definitely linked to poor prognosis (Nicholson *et al.,* 2001). In addition, mutant, deleted variants of EGFR have also been found in gliomas and, to a lesser extent, in breast, ovarian, and lung carcinomas (Pedersen *et al.,* 2001). The most common and best known of these truncated EGFRs is frequently found in glioblastoma and is referred to as EGFRvIII. This receptor lacks most of the extracellular portion and possesses constitutive kinase activity, strongly associated with the transformed phenotype (Pedersen *et al.,* 2001).

In support of the crucial role that EGFR-driven signal transduction pathways have in cell transformation and cancer progression, interruption of this signaling with various EGFR inhibitors has been shown to inhibit tumor cell proliferation both *in vitro* and *in vivo*, i.e., in animal tumor models (Arteaga, 2002; Grünwald and Hidalgo, 2003). These observations coupled with 1) the ability to identify EGFR-overexpressing human tumors in patient tissue, 2) the association of EGFR with poor prognosis in a significant number of common malignancies, and 3) the lack of a vitally important physiologic role of the EGFR in the adult (except for skin and intestine homeostasis) have all suggested EGFR as a rational target for molecular therapeutic strategies (Arteaga, 2002). For this reason, a number of approaches have been developed over the last two decades to inhibit EGFR signaling, the main of which include the generation of monoclonal antibodies (MAbs) and small molecule inhibitors (SMIs) of the tyrosine kinase activity.

As a result of its cell surface localization, the EGFR is naturally accessible to the action of MAbs. Most currently available antibodies recognize the receptor ectodomain, compete for ligand binding, and induce EGFR dimerization as well as down-regulation at the cell surface (Arteaga, 2002). An immediate biological consequence of such antibody–receptor interaction is the inhibition of ligand-induced EGFR signaling, which may lead to cell cycle arrest and/or cell death (Crombet-Ramos *et al.,* 2002; Wu *et al.,* 1995; Wu *et al.,* 1996), as well as the down-regulation of EGFR-regulated molecules involved in crucial processes such as cell migration and tumor angiogenesis (Arteaga, 2002; Grünwald and Hidalgo, 2003), both of which are essential for tumor progression. In addition to blockade of autocrine EGFR signaling, it has been suggested that EGFR-directed antibodies might recruit Fc-receptor–expressing immune effector cells leading to antibody-dependent cellular cytotoxicity (ADCC) and immune-mediated tumor eradication. Such a mechanism has indeed been demonstrated to be essential for the activity of the Food and Drug Administration (FDA)–approved HER-2-directed antibody Herceptin/Trastuzumab (Genentech, Inc.) (Clynes *et al.,* 2000), which is currently used for the treatment of HER-2–overexpressing breast cancers. However, in the case of EGFR-directed antibodies, this mechanism, although existent, appears to be less relevant (Crombet-Ramos *et al.,* 2002; Fan *et al.,* 1993). EGFR-directed MAbs, which are undergoing clinical testing, include IMC-C225/Erbitux/Cetuximab (ImClone Systems Inc. and Bristol-Myers Squibb Co., currently in phase III), h-R3/TheraCIM (CIMAB S.A. and YM BioSciences Inc., phase II and III), ABX-EGF (Abgenix Inc., phase II), MDX-447 (Merck KGaA and Medarex Inc., phase II), and EMD 7200 (Merck KGaA, phase I) (Grünwald and Hidalgo, 2003). Of these, IMC-C225 is the most clinically advanced. In general, antibodies are convenient for treatment because they have a relatively long life (8 days or longer), are highly selective and specific, have a good side-effect profile, and yield no apparent exacerbation of

chemotherapy and radiation toxicity. Some drawbacks of MAbs are that they may not necessarily penetrate large tumors, or into the central nervous system; they are inactive against truncated forms of the receptor (at least those binding to the EC domain of EGFR); and there is no oral formulation (Herbst and Langer, 2002).

The SMIs, unlike MAbs, block EGFR activity by competing for the Mg-adenosine triphosphate (ATP) binding site of the catalytic domain of the EGFR tyrosine kinase, inhibiting receptor autoactivation and downstream signaling (Arteaga, 2002). The low molecular weight of these inhibitors, in theory, makes it easier to penetrate the tumor but also reduces their half-life *in vivo,* which could be considered a disadvantage as compared with MAbs. However, they can be administered orally, which makes them highly suitable for chronic therapy. SMIs currently in clinical development include ZD1839/Iressa/Gefitinib (AstraZeneca, phase III), OSI-774/Tarceva/Erlotinib (OSI Pharmaceuticals, phase III), CI-1033 (Pfizer, phase I), EKB-569 (Wyeth-Ayerst, phase I), PKI-166 (Novartis, phase I), and GW2016 (Glaxo-Smith-Kline, phase I) (Arteaga, 2002; Grünwald and Hidalgo, 2003). The last three compounds have demonstrated "dual" activity against both EGFR and HER-2 kinases (Grünwald and Hidalgo, 2003).

The achievement of clinically significant response rates using targeted therapies in many cases relies on the ability to select patients for treatment on the basis of tumor expression of the targeted protein. For a growing list of solid tumors, the expression of target molecules is now routinely measured by immunohistochemical staining of tissue sections from surgical biopsies (Spaulding and Spaulding, 2002). A good example is the assessment of HER-2 status in biopsies from patients with metastatic breast cancer, which is routinely done by immunohistochemistry (IHC), accompanied by fluorescent *in situ* hybridization (FISH), which, in conjunction, can detect HER-2 overexpression resulting from gene amplification and therefore serve to select those patients who might benefit from treatment with Herceptin/Trastuzumab, a specific humanized MAb directed against the extracellular domain of HER-2 (Konecny and Slamon, 2002).

The ability to detect the target molecule *in situ* in a biopsy specimen is critical for histologic methods of diagnosis. Detection of proteins in biopsies by IHC requires the preservation and, in some cases the unmasking of antibody binding sites after the tissue has been fixed. Characterization of the protein with regard to normal tissue distributions, cellular compartmentalization, and the range of expression levels in the tumor to be treated are also essential to the interpretation of the diagnostic IHC. If the therapy is directed to an overexpressed molecule, a cutoff between normal and overexpression must also be established. Finally, optimized assay parameters must also be rigorously validated to ensure comparable results between laboratories (Spaulding and Spaulding, 2002).

With the advent of EGFR-directed therapies, clinical trials are increasing the use of IHC screening strategies for EGFR expression, to select patients who are likely to respond to the therapy. The use of IHC in this context has several advantages. First, unlike HER-2, EGFR overexpression is rarely the result of gene amplification. With the exception of 30% of gliomas (Libermann *et al.,* 1985) and human squamous carcinoma cell lines (Yamamoto *et al.,* 1986), most EGFR-overexpressing tumors have elevated levels of the receptor in the absence of gene amplification (Salomon *et al.,* 1995). For this reason, EGFR amplification as determined by FISH is unlikely to be a useful diagnostic tool. However, the fact that IHC allows the detection of overexpressed protein and can be achieved in sections derived from paraffin blocks makes it a very suitable method. In many cases, surgical specimens from tumors are only available in the form of paraffin blocks, and the practice of archiving such specimens can, in some cases, obviate the needs for subsequent biopsies. In addition, the preservation of morphologic details in such fixed tissues is valuable for complete histopathologic diagnosis information, which can be used in combination with the EGFR status for diagnostic and prognostic purposes. This is not the case for other methods such as Northern and Western blotting and reverse transcriptase polymerase reaction (RT-PCR), which are extractive procedures that, although offering a quantitation advantage, destroy the cell and tissue architecture (Spaulding and Spaulding, 2002).

Clinical trials designed to test safety and efficacy of EGFR inhibitors are currently validating the use of IHC for the screening and selection of patients to undergo EGFR-directed therapy. For example, ImClone Systems Inc. used an EGFR IHC test developed at DakoCytomation (Carpinteria, CA), termed "the pharmDx EGFR IHC assay," to screen and select patients for a phase II trial of IMC-C225 in irinotecan-refractory colorectal cancer (Spaulding and Spaulding, 2002). Similarly, the Center for Molecular Immunology (CIM) in Havana, Cuba, developed an immunohistochemical assay using Ior egfR-3 (also known as DiaCIM or m-R3), the murine counterpart of their humanized anti-EGFR, h-R3 (also known as TheraCIM, produced by CIMAB S.A. and YM BioSciences Inc.) antibody, to screen and select patients for several clinical trials of hR3 (Crombet *et al.,* 2002; Crombet *et al.,* 2003; Crombet-Ramos *et al.,* 2001).

Ior egfR-3/m-R3 was initially developed at the CIM using standard hybridoma technology, after immunization of BALB/c mice with a purified fraction of human

placenta enriched in EGFR (Fernández *et al.,* 1992). The antibody recognizes EGFR with high affinity ($K_D = 10^{-9} - 10^{-10}$ M), inhibiting *in vitro* and *in vivo* proliferation of EGFR overexpressing cell lines (Crombet-Ramos *et al.,* 2002; Fernández *et al.,* 1992). As a result of its EGFR-blocking capability and antitumor activity, Ior egfR-3 entered phase I clinical trials in Cuba. However, it was discontinued because of the development of human anti-mouse antibodies (HAMA) (Crombet *et al.,* 2001). In addition, $^{99\text{-m}}$Technetium-labeled Ior egfR-3 was also used for immunoscintigraphic imaging studies, in which it showed an overall sensitivity of 84.2% for detection of primary tumors, metastasis, and recurrence of different epithelial neoplasms (Ramos-Suzarte *et al.,* 1999). Ior egfR-3 has been humanized to improve its immunologic effector functions in humans and reduce HAMA response (Mateo *et al.,* 1997). Humanization was achieved by grafting the complementary determining regions of Ior egfR-3/m-R3 into a human IgG_1 framework. The humanized antibody thus generated—termed h-R3—also binds EGFR with high affinity ($K_D = 10^{-9}$) and specificity, blocks growth factor binding and receptor activation, and inhibits subsequent signal transduction and cellular events including proliferation and cell survival (Crombet-Ramos *et al.,* 2002). In addition, both Ior egfR-3/m-R3 and h-R3 have the capability of detecting EGFR in formalin-fixed, paraffin-embedded tissue (Cedeño *et al.,* 1999; Fernández *et al.,* 1992; Rengifo *et al.,* 1999), a quality lacking in other currently available therapeutic EGFR-directed MAbs, e.g., IMC-C225 (Spaulding and Spaulding, 2002). The MAb h-R3 is currently under clinical testing in Cuba and Canada.

So far, the results with h-R3 in squamous carcinomas of the head and neck suggest that a highly significant percentage (>50%) of the EGFR-overexpressing population selected for the trials responded to h-R3 in combination with radiotherapy (Crombet-Ramos *et al.,* 2001; Winquist *et al.,* 2002). Evidence of cellular effects, including a significant reduction in tumor cell proliferation as well as tumor angiogenesis, were observed in several of the responding patients (Crombet-Ramos *et al.,* 2001), as similarly shown in preclinical studies (Crombet-Ramos *et al.,* 2002). The expression level of EGFR is routinely measured by IHC (using Ior egfR-3) in the ongoing phase II and III clinical trials with h-R3.

The clinical development of EGFR inhibitors has illustrated the difficulties and challenges associated with the validation of novel targeted drugs. Phase II and III trials had already been completed for several of the inhibitors, including IMC-C225 and ZD 1839 (Iressa). In some cases, the results have been negative, as, for example, in the phase III trials INTACT 1 and INTACT 2, in which Iressa was tested in patients with lung carcinoma, in combination with preestablished chemotherapeutic drugs, including cisplatinum and gemcitabine, or paclitaxel and carboplatin (reviewed in Raben *et al.,* 2003). No advantage of adding Iressa was observed as compared to chemotherapy alone. In another case, an inappropriate study design prevented the results from being validated (Randal, 2002). A common problem with the trials seems to be the lack of a reliable method for the selection of patients to be likely to respond to EGFR-directed therapy. The original hypothesis, which established that only patients who overexpressed EGFR would benefit from the treatment, was based only on preclinical data suggesting a relationship between the level of expression of EGFR and its susceptibility to the inhibitors (Bishop *et al.,* 2002; Motoyama *et al.,* 2002). Nevertheless, the results from several other preclinical studies also suggested that EGFR alone was not sufficient to predict the response of cell lines to EGFR inhibitors, and other factors, such as constitutive activation of downstream signaling pathways (Bianco *et al.,* 2003), the presence of activating ligand, and the relative expression of EGFR versus other members of its family (Motoyama *et al.,* 2002), have been shown to influence the cellular response to EGFR inhibitors in preclinical models (reviewed in Grünwald and Hidalgo, 2003). In addition, tumors that might look negative for EGFR expression, e.g., those expressing the truncated form of EGFR, EGFRvIII (which is not recognized by EGFR-specific antibody directed against the EC domain), could indeed possess an overactive EGFR and respond to some type of EGFR inhibitors, e.g., the SMI OSI-774, directed against the kinase domain (Iwata *et al.,* 2002). These data suggest that a useful pharmacodiagnostic marker for EGFR inhibitors should incorporate various elements pointing to an unequivocal EGFR overactivity, as well as to an EGFR dependence in downstream signaling pathways. In this regard, the development and validation of immunohistochemical methods to measure the actual activation of EGFR and of key, EGFR-driven signaling pathways could be of great relevance. For these reasons, we believe that the screening for EGFR expression, although useful, is not sufficient, and determination of EGFR activity by phosphospecific antibodies should also be included as a marker for patient selection. In addition, the determination of phosporylated EGFR before and after the administration of an EGFR inhibitor can also be useful to determine the optimal dose of the inhibitor and the actual response to the therapy, as suggested by general observations obtained with IMC-C225, OSI-774, and ZD1839, which suggested a linear relationship

between target inhibition and anti-tumor activity (Albanell *et al.,* 2002; Bishop *et al.,* 2002; Pollack *et al.,* 1999; Shin *et al.,* 2001).

In the following section we describe methods established by others and us for the immunohistochemical determination of EGFR (using Ior egfR-3) and phosphorylated (active) EGFR—using commercially available phospho-EGFR specific antibodies—in both paraffin and frozen tissue sections. These methods have been validated by their use in several preclinical and clinical studies, including clinical trials, and are suggested for their use in routine assessment of EGFR in human tumor samples.

MATERIALS AND METHODS

Protocol for Frozen Sections

1. Acetone.
2. Aqueous mounting medium for 3-amino-9-ethylcarbazole (AEC) (e.g., Dako glycergel C 563; Aqua Poly/Mount from PolySciences Inc.; GVA-Mount from Zymed Laboratories, Inc.). For 3,3′-diaminobenzidine tetrahydrochloride (DAB), use either aqueous or organic (e.g., Cytoseal 60 or Canadian Balsam) mounting medium.
3. Antibody diluting buffer: phosphate buffer saline (PBS), 1% bovine serum albumin (BSA), 0.02% sodium azide.
4. Biotinylated secondary antibody (e.g., anti-rabbit for sc-03 antibody, or anti-mouse for Ior egfR-3). Dako E 354 recommended for Ior egfR-3.
5. Blocking solution: 1.5% normal serum in PBS. Ideally, the serum must be from the same species used to obtain the secondary antibody.
6. Counterstain: Mayer's hematoxylin.
7. Coverslips.
8. Cryomolds (Tissue-Tek) for tissue freezing.
9. Delicate task wipers (e.g., Kimwipes EX-L, Kimberly-Clark).
10. Distilled and bidistilled water.
11. Dry ice or liquid nitrogen.
12. Dulbecco's PBS: 100 mg anhydrous calcium chloride, 200 mg potassium chloride, 200 mg monobasic potassium phosphate, 100 mg magnesium chloride·$6H_2O$; 8 g sodium chloride, and 2.16 g dibasic sodium phosphate·$7H_2O$; bring volume to 1 L with bidistilled water, pH 7.4.
13. EGFR-directed primary antibody (e.g., EGFR (1005)/sc-03, Santa Cruz Biotechnology, Inc; or Ior egfR-3, CIMAB S.A.).
14. Humidified chamber.
15. Hydrogen peroxide, 1% in PBS (optional). Prepare just before use.
16. Hydrophobic pen (e.g., PAP PEN, Daido Sangyo Co., Ltd).
17. Optimum cutting temperature (OCT) frozen section medium (e.g., Stephens Scientific).
18. Peroxidase substrate: AEC or DAB. AEC kit (Zymed Laboratories, Inc.) recommended.
19. Positively charged (e.g., ProbeOn Plus, Fisher-Biotech) slides. Alternatively, poly-L-lysine- or chrome alum-coated slides could be used.
20. Streptavidin-peroxidase (e.g., ABComplex, DAKO K 355, diluted 1:100 in PBS; or ready-to-use reagent from Zymed Laboratories Inc.).
21. Tris buffered saline (TBS): 50 mM Tris-HCl (pH 7.4), 150 mM NaCl. To prepare weight 2.4 g Tris and 8.76 g NaCl; bring volume to 1 L with bidistilled water, pH 7.4.

Tissue Freezing and Sectioning

1. Obtain fresh tumor tissue that does not exceed 5 mm in diameter.
2. Immerse in precooled PBS or, alternatively, saline solution (NaCl 0.9%). Keep on ice until freezing (ideally, maximum of 1 hr).
3. Discard PBS and place the tissue in the center of a cryomold previously covered with a drop of OCT embedding medium. Cover/embed tissue with OCT (avoiding bubbles) and either shock-freeze in liquid nitrogen or freeze slowly on dry ice. Cover molds with plastic wrap and store at −70°C.
4. Bring molds to cryostat chamber temperature for about 30 minutes before sectioning.
5. Cut tissue sections of 5 μm and place on positively charged or chrome alum-coated slides.
6. Air-dry tumor sections for a minimum of 1 hr. After this, slides could be stored at −70°C (in desiccated slide box wrapped in aluminum foil) or immediately fixed in ice-cold acetone for 10 min.
7. Air-dry fixed sections and store at −70°C (as described in **Step 6**). If you wish, fixed sections can be immediately stained.

Staining Procedure

1. If stored at −70°C, tissue section slides must be warmed to room temperature before unwrapping. Then air-dry. Fix 10 min in ice-cold acetone, if stored unfixed.
2. Rinse the slides twice in TBS pH 7.4, 5 min each.
3. Optional: quench endogenous peroxidase with 1% hydrogen peroxide in PBS for 10 min at room temperature.
4. Wash in PBS 3×, 5 min each.
5. Draw a circle around each tissue section using a hydrophobic pen. This keeps solutions on the tissue area for the required incubation time.

6. To block unspecific binding, cover sections with 1.5% normal serum in PBS (50 µl to 100 µl per section) and incubate in humidified chamber for 1 hr at room temperature. Ideally, serum is derived from the species in which the secondary antibody was produced (e.g., rabbit serum when using a rabbit anti-mouse secondary).

7. Incubate the slides with Ior egfR-3 for 60 min at room temperature. (Other commercially available EGFR-directed antibodies, e.g., sc-03, could be used.) Use PBS/BSA to prepare optimal dilution (see Notes). Recommended dilution for Ior egfR-3: 5 µg/ml (Cedeño *et al.,* 1999).

8. Discard primary antibody and wash in TBS 3×, 10 min each.

9. Remove the excess of TBS around the tissue section with delicate absorbent paper (e.g., Kimmwipe), but do not allow the section to dry.

10. Incubate the slides for 30 min with biotinylated rabbit anti-mouse (for Ior egfR-3; e.g., Dako E 354 diluted 1:100) or goat anti-rabbit (if using sc-03; e.g., ready-to-use reagent from ZYMED) at room temperature.

11. Rinse and dry excess TBS as in **Steps 8** and **9**.

12. Incubate for 30 min with streptavidin-peroxidase (e.g., ABComplex/HRP, DAKO K 355 diluted 1:100 in TBS) at room temperature.

13. Rinse as in **Steps 8** and **9**.

14. Incubate sections with peroxidase substrate solution (AEC recommended) for 10 min at room temperature. Follow reaction under microscope.

15. Rinse with distilled water.

16. Counterstain with Mayer's hematoxylin (1–3 min depending on freshness of reagent).

17. Wash out excess hematoxylin with tap water.

18. Optional: to intensify the blue in the hematoxylin, immerse slides in PBS for 30 sec.

19. Rinse with distilled water, then air-dry.

20. Mount coverslips with an aqueous mounting medium (for AEC or DAB) or with organic medium (DAB). See "Materials" for details.

Controls: Positive and negative control sections should be included.

Positive Controls

Frozen sections of any one of the following specimens:

1. Normal human skin: Strong staining in keratinocytes in basal layers of epidermis (100% of normal cells), outer root sheath of hair follicles, and accessory (eccrine and sebaceous) glands can be observed.

2. EGFR-positive ductal infiltrating breast carcinoma. Strong staining in more than 90% of neoplastic cells is observed (Cedeño *et al.,* 1999).

3. Head and neck tumor. As a rule, the cell membrane in these carcinomas stains quite intensely and uniformly (Spaulding and Spaulding, 2002).

4. A431 human squamous skin carcinoma xenografts in mice. Strong membrane/cytoplasmic staining observed in more than 90% of tumor cells.

Negative Controls

1. Use antibody-diluting buffer alone instead of monoclonal primary antibody. No specific reaction should occur on the negative slide.

2. If possible, use an isotype-matching immunoglobulin G (IgG) control of the same species in which the primary antibody was produced.

Evaluation of EGFR Expression

+++ More than 90% of the tumor cells show a strong staining compared with the positive control.
++ Between 70% and 90% of the tumor cells show staining compared with the positive control.
+ Less than 70% of the tumor cells show staining compared with the positive control.
− Less than 25% of the tumor cells show staining.

Notes:

1. Do not allow tissue sections to become dry at any stage in this protocol.

2. Keeping slides in a humidified chamber can minimize loss of solutions as a result of evaporation during incubations.

3. Optimal concentration of primary antibody depends on the type of antibody, as well as type of tumor tissue. It has to be determined by titration.

Protocol for Paraffin-Embedded Tissues

The same materials listed for cryosections protocol with the exception of numbers 1, 5, 8, 11, 15, 17. In addition, the following reagents are required:

1. 0.4% pepsin in 0.1 N hydrochloric acid.

2. 1 mM ethylenediamine tetra-acetic acid (EDTA), pH 8.0 (optional, see "Antigen Retrieval" for details).

3. 1.5% hydrogen peroxide in methanol. Light sensitive; prepare right before use.

4. Blocking solution: 5% horse serum in PBS.

5. Coplin jars, heat resistant with screw caps (optional, only if using heating for antigen retrieval).

6. Ethanol (100% and 95%).

7. Microwave (optional, see protocol for details).

8. Xylene.

Preparation of Slides

1. Obtain 5-µm sections from paraffin-embedded tumor tissue blocks. Adhere them to chrome alum-coated or poly-L-lysine coated slides.

2. Heat-fix the section slides at 60°C for at least 2 hr.

Paraffin Removal and Rehydration of Sections

1. De-wax the slides in three changes of Xylene.
   Xylene I ——————— 15 min.
   Xylene II ——————— 10 min.
   Xylene III ——————— 5 min.

2. Place the slides in 100% ethanol 2× and then in 95% ethanol, 5 min each.

3. Block endogenous peroxidase activity by immersing slides in a 1.5% H_2O_2-methanol solution for 30 min.

4. Rinse the slides gently with running tap water for 15 min (avoid a direct jet, which can wash off or loosen the sections).

5. Rinse with distilled water for 10 min.

6. Place the slides in TBS for 5 min.

Antigen Retrieval

Pepsin Pretreatment (for Ior egfR-3) is as follows:

1. Drain excess TBS, dry area around tissue with a Kimwipe, and encircle the section using a hydrophobic pen.

2. Incubate sections with 0.4% pepsin in 0.1 N hydrochloric acid at 37°C, 30 min.

3. Rinse gently in tap water, then in TBS for 5 min.

An alternative method for antigen retrieval is as follows:

1. Place slides inside Coplin jar, fully filled with 1 mM EDTA (pH 8.0). Using a microwave, heat sections in 1 mM EDTA (pH 8.0) for 1 min at full power, then heat for 14 min at medium power.

2. Cool slides for 20 min at room temperature.

3. Wash in distilled water 3×, 5 min each.

Staining Procedure

1. Incubate sections with 5% horse serum in PBS (blocking solution), 1hr at room temperature (previously, encircle sections with hydrophobic pen).

2. Drain blocking solution and incubate the slides with primary anti-human EGFR antibody for 2 hr at 37°C (for Ior egfR-3, dilute antibody in PBS/BSA at 20 to 150 µg/ml, depending on tissue type [Fernández *et al.,* 1992; Rengifo *et al.,* 1999].) Alternatively, sections can be incubated at 4°C overnight (as for sc-03 antibody, recommended concentration: 1–5 µg/ml).

3. Wash sections in TBS 3×, 5 min each.

4. Remove excess TBS from around the tissue section with Kimwipe. Incubate the slides for 30 min at room temperature with biotinylated secondary antibody at the appropriate dilution in PBS/BSA (e.g., rabbit anti-mouse immunoglobulins (Dako) diluted 1:100 for for egfR-3; or ready-to-use biotinylated goat anti-rabbit antibody, ZYMED, for sc-03).

5. Rinse the slides as in **Step 3**.

6. Incubate the slides for 30 min at room temperature with streptavidin-peroxidase (e.g., ABComplex/HRP K 355 from Dako diluted 1:100 in TBS; or ready-to-use streptavidin-peroxidase from ZYMED).

7. Rinse the slides as in **Step 3**.

8. Incubate sections with peroxidase substrate (AEC or DAB) solution for 10 min at room temperature.

9. Rinse the slides with distilled water.

10. Counterstain with Mayer's Hematoxylin, wash and dry as for **Steps 16–19** of frozen sections protocol.

11. Mount coverslips with an aqueous mounting medium for AEC. For DAB, use either organic or aqueous-based medium. Dehydrate DAB-stained slides before mounting with organic medium. Dehydration can be achieved by two successive washes in 95% ethanol, for 10 sec each, followed by two successive washes in 100% ethanol, 10 sec each, and finally two successive washes in xylene, 10 sec each.

12. Air-dry mounted slides before examining under light microscopy.

Controls

Positive and negative, paraffin-embedded control sections should be included. See suggested controls in protocol for frozen sections.

Evaluation of EGFR Expression

As suggested for staining of cryosections.

Immunostaining of Phosphorylated EGFR in Formalin-Fixed, Paraffin-Embedded Tissues

Same as specified in the previous "Materials" section (including optionals), with the exception of number 1. In addition, include phospospecific anti-EGFR antibody.

Note: Antibodies directed against tyrosine residues involved in the activation of either MAPK or PI3K pathways, both of which are crucial for the downstream cellular effects of receptor activation, are recommended (e.g., antibody #2234: Tyr1068; Cell Signaling Technology, Inc.).

Staining Procedure

1. Deparaffinize sections as for "Paraffin Removal and Rehydration of Sections" **Steps 1** and **2**.

2. Rehydrate by placing the sections in two washes of distilled water, 5 min each.

3. Wash sections in PBS for 5 minutes.

4. For antigen unmasking: heat sections in 1 mM EDTA (pH 8.0) for 1 min at full power, then at medium power for 14 min. Always keep slides fully immersed in buffer during the whole heating time. Cool slides at room temperature for 20 min.

5. Wash sections in distilled water, 3×, 5 min each.

6. Incubate sections in 1.5% hydrogen peroxide in methanol for 10 min.

7. Wash in distilled water, 2×, 5 min each.

8. Wash sections in PBS for 5 min.

9. Drain PBS excess, dry the area around the slide with delicate tissue, encircle section with hydrophobic pen, and incubate with blocking solution (5% horse serum in PBS) for 1 hr at room temperature.

10. Remove blocking solution and incubate with primary, anti-phospho-EGFR antibody overnight at 4°C. Recommended dilution for antibody #2234 (Cell Signaling Inc.) 1:50 in BSA/PBS.

11. Discard antibody solution and wash sections in PBS 3×, 5 min each.

12. Add secondary antibody (e.g., ready-to-use biotinylated goat anti-rabbit (ZYMED). Incubate for 30 min at room temperature.

13. Remove secondary antibody and wash sections as in **Step 11**.

14. Incubate sections with streptavidin-peroxidase complex for 10–30 min at room temperature (e.g., ready-to-use reagent, ZYMED; ABComplex, Dako).

15. Remove streptavidin-peroxidase complex and wash as in **Step 11**.

16. Add peroxidase substrate (AEC or DAB), and incubate for a maximum of 10 min at room temperature. Monitor reaction under microscope.

17. As soon as color develops, discard substrate solution and immerse slides in distilled water.

18. Counterstain with hematoxylin, as for **Steps 16–19** of the "Staining Procedure" for frozen sections.

19. Mount coverslips with aqueous mounting medium, if using AEC. If using DAB, dehydrate sections as for **Step 11** of the "Staining Procedure" for paraffin embedded tissues and mount using organic medium (e.g., Cytoseal 60).

Immunostaining of Phosphorylated EGFR in Frozen Sections

1. As for the first section, except for numbers 5 and 21. In addition, include a specific p-EGFR anti-EGFR antibody. Clone 74 (Transduction Laboratories) or anti-pEGFR #2234 (Cell Signaling Technology, Inc.) recommended.

Tissue Freezing and Sectioning

As for first section.

Staining Procedure

1. If previously stored at −70°C, warm up sections at room temperature before unwrapping.

2. Fix in ice-cold acetone for 10 min, then air-dry.

3. Wash slides in PBS 2×, 5 min each.

4. Block sections with 1% BSA in PBS for 20 min at room temperature.

5. Incubate with primary, anti-p-EGFR antibody dilute in BSA/PBS for 1 hr at room temperature. Recommended concentration for clone 74:10 µg/ml.

6. Wash with PBS 3×, 5 min each.

7. Proceed as for steps 9–20 of the "Staining Procedure" for frozen sections. Use PBS instead of TBS. Wash for 5 min, instead of 10 min.

Notes:

1. This protocol can be modified to use a fluorescein isothiocyanate (FITC)-conjugated secondary antibody for immunofluorescence, as reported by Saga and Jimbow (2001). If using Clone 74 as a primary, FITC-labeled anti-mouse IgG (Vector Laboratories) gives satisfactory results (Saga and Jimbow, 2001).

2. When using immunofluorescence, an anti-fade reagent is recommended for mounting coverslips. This is important to avoid fading of fluorescence over time. We recommend Prolong Antifade Kit (Molecular Probes, Inc.) for this purpose.

RESULTS AND DISCUSSION

EGFR Detection in Frozen Sections

The protocol described in the first section of Materials and Methods has been used for immunostaining of EGFR in different frozen human samples, including normal fetal and adult tissue, as well as tumors (Cedeño *et al.,* 1999).

All fetal tissues evaluated with Ior egfR-3 showed positive staining for EGFR. These included the following: epithelium of the skin (+++), stomach (+++), small (+++) and large (+++) intestine, gray substance of the cerebellum (++) and the brain (++), cortex of the adrenal glands (++), liver (++/+++), spleen (++), glomerulus (+) and tubules (++) in the kidney, pancreas (++/+++), heart (+), and prostate (+). As an example, Figure 16A shows membrane staining of EGFR in frozen sections of human fetal small intestine.

Evaluation of EGFR in adult frozen human tissue yielded the following results: skin: epidermis (+++), hair follicles (+++), accessory glands (+++); esophagus: epithelium (+++), glands (+++); stomach: epithelium (+); small intestine: crypts (++); colon: crypts (++); lung: basal cells of respiratory epithelium (+++), alveolar epithelium (−); pancreas: exocrine pancreas (−), islet cells (−); liver: hepatocytes (++); breast: ductal cells (++), stroma (−); genitourinary system: kidney (+/−), bladder (++), prostate (+++), ovary(−); nervous system: brain (+/−), cerebellum (++); lymphoid system: thymus (−), tonsils (−), spleen (−); cardiovascular system: heart (−), veins (−), arteries (−); muscle (−); endocrine system: thyroid (−), adrenal gland (+/−) (Cedeño *et al.,* 1999; Cedeño M. and Rengifo E.,

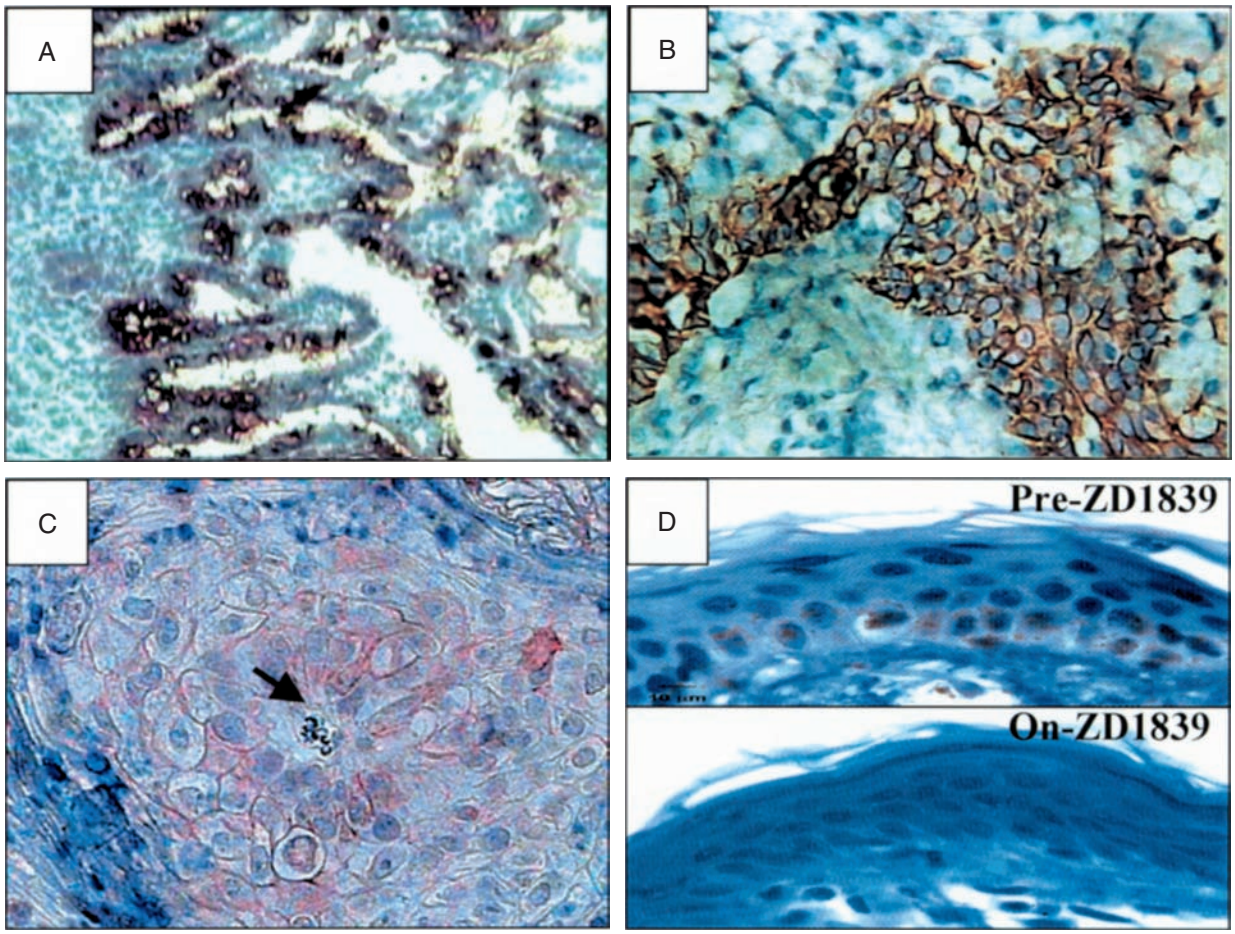

Figure 16. Immunostaining of total and phosphorylated epidermal growth factor receptor (p-EGFR) in human tissue. **A:** EGFR expression in cryosections of fetal small intestine as detected by Ior egfR-3 and diaminobenzidine (DAB), 5X magnification. **B:** Highly positive (+++) expression of EGFR in a formalin-fixed, paraffin-embedded section from a mucoepidermoid carcinoma of the lung. Note intense recognition of the plasma membrane of all epidermoid neoplastic cells (Ior-egfR-3, DAB). Magnification: 25X. **C:** Membrane and cytoplasmic localization of activated EGFR (Antibody 2234, Cell Signalling, Inc., substrate: 3-amino-9-ethylcarbazole) in paraffin sections of A431 tumor xenografts. Of note is the usual localization of the activated receptor in tumor cells located in close proximity to blood vessels (*arrow*). Magnification: 20X. **D:** lmmunostaining of activated EGFR (Chemicon antibody) in paraffin-embedded skin biopsies from patients undergoing therapy with the small molecule inhibitor of EGFR, ZD 1839/lressa (AstraZeneca). Activated receptor was detected in the basal layer of keratinocytes of the interfollicular epidermis previous to the treatment (Pre-ZD 1839), whereas it was absent in skin samples from patients undergoing therapy (On-ZD1839). This result was taken as a proof of drug activity. Reproduced from Albanell *et al.,* 2002.

unpublished observations). The symbol +/–, which was not described in the Materials and Methods section, represents staining that was questionable or rather weak.

Gene expression and protein localization are differentially regulated during the life span of an organism. In the case of EGFR, the general distribution in human tissues has been found to be similar in the fetus and adult (Damjanov *et al.,* 1986; Wakeling *et al.,* 1998), particularly in terms of localization, as detected by IHC. In epithelial cells, EGFR has been found to localize mainly in the cell membrane, at the basal-lateral region (Chailler and Ménard, 1999). Our data are in general agreement with this notion. We also observed a wide distribution of the receptor in many different epithelial cell types in the fetus and a more restricted distribution in adult tissue. Various studies have demonstrated variation in the expression of EGFR at different fetal ages (Oliver *et al.,* 1988). In some tissues, EGFR expression decreases as the fetus matures, becomes mild or absent in the adult, and increases again during malignant transformation (Leav *et al.,* 1998). Prostate and pancreas epithelium are good examples of such a phenomenon (Hormi and Lehy, 1994; Leav *et al.,* 1998; Salomon *et al.,* 1995).

For instance, in an immunohistochemical study performed by Hormi and Lehy (1994) in the fetal pancreas, it was observed that the endocrine cells are the ones that express EGFR in the fetus, but the immunostaining weakens as the fetal age increases. As can be seen in our study, the adult pancreas is negative for EGFR, which agrees with the notion that EGFR expression in human pancreas is lost by the time of birth. However, different from, and perhaps complementary to, the study by Hormi and Lehy, our analysis of a 19-week-old fetus showed that EGFR expression persists at this stage but only in the nonendocrine epithelial cells.

While looking in parallel at other fetal tissues, our results seemed in general agreement with what has been previously reported. For example, we found the expression of EGFR to be more intense in the tubules of the cortex and medulla when examining fetal kidney, as reported by Bernardini *et al.* (1996). Similarly, in the gut, we observed gross, intense staining in the base of both the crypts and intestinal villus, which fades away toward the superficial (upper region) crypt epithelium. This pattern has been extensively reported and relates to the high proliferation that constantly occurs at the base of the crypts (Chailler and Ménard, 1999). Taken together the results suggest that Ior egfR-3 is a validated antibody for EGFR detection in frozen sections of human tissue.

EGFR Detection in Paraffin Sections

The protocol described in the second section of Materials and Methods has been used for the staining of EGFR in tumor samples for diagnostic and prognostic purposes (Crombet *et al.,* 2002; Crombet-Ramos *et al.,* 2001; Rengifo *et al.,* 1999). A study conducted by the CIM, Havana, Cuba, used this protocol to evaluate EGFR overexpression, its co-expression with EGF, and their correlation with histopathologic features in lung cancer. It was observed that EGFR was more often overexpressed in nonsmall cell lung carcinoma (NSCLC) as compared to small cell lung carcinoma (SCLC). As an example, Figure 16B shows a strongly positive membrane staining for EGFR observed in a mucoepidermoid NSCLC (Ior egfR-3 [Rengifo *et al.,* 1999]). Approximately two-thirds of the NSLCs evaluated showed this intense staining, and EGF was often co-expressed with EGFR in these tumors (Rengifo *et al.,* 1999). Nevertheless, co-expression of EGFR and EGF did not appear to be of independent prognostic value as compared with established histopathologic features in NSCLC.

Elevated levels of EGFR and/or its ligands have been commonly identified in multiple cancer types, in which autocrine activation of EGFR appears to promote solid tumor growth (Nicholson *et al.,* 2001; Salomon *et al.,* 1995). The prognostic value of EGFR has been found to be strong in head and neck and ovarian cancer, among others, but in the lung it remains controversial (Meert *et al.,* 2002; Nicholson *et al.,* 2001). EGFR overexpression has been documented in NSCLC (mainly in the squamous type) and, to a much lesser extent, in SCLC (Meert *et al.,* 2002). In NSCLC, co-expression of EGFR and its ligand, TGF-α, has been observed in all histologic types, and it is frequent in the early stage but fails to exhibit a significant impact in overall survival (Rusch *et al.,* 1997). These findings, in agreement with ours, suggest that the EGFR/ligand autocrine/paracrine loop may be more important for lung tumor formation than for tumor progression (Rusch *et al.,* 1993). Clinical trials using EGFR-targeted agents have shown that only a small subset of patients with NSCLC seem to benefit from the therapy (Bunn and Franklin, 2002; Raben *et al.,* 2003). The true prognostic and therapeutic significance of EGFR could be overshadowed by the lack of proper markers of EGFR activation as well as downstream signaling. Identifying and validating predictive factors, which could be used to select patients with disease likely to respond to EGFR inhibitors, is becoming strictly necessary.

Detection of Phosphorylated (Active) EGFR

The protocol described in the third section of Material and Methods has been validated in our laboratory to prove the activated status of EGFR in EGFR-overexpressing A431 squamous cell carcinoma human tumor xenografts (Figure 16C) in immunocompromised animals, as well as the *in vivo* inactivation of the receptor after treatment of animals with EGFR-blocking agents. We recommend the use of this protocol in parallel to EGFR staining to justify EGFR targeting in clinical settings as well as to prove inactivation of the target during EGFR-targeted therapy. In this regard, a similar protocol in which a different p-EGFR antibody (Chemicon) was used had given satisfactory results demonstrating the inactivation of the EGFR after treatment of patients with various types of cancer with the small molecule inhibitor ZD1839/Iressa (Albanell *et al.,* 2002). Immunostaining was performed in skin biopsies obtained from a significant number of patients included in two phase I clinical trials of ZD1839 performed in 16 different centers worldwide (Albanell *et al.,* 2002; Figure 16D). Another p-EGFR antibody used in paraffin sections with good results includes clone 74 (BD Transduction Laboratories) (Moroni *et al.,* 2001).

As demonstrated by the aforementioned results, the protocols described for the detection of total and

phosphorylated/activated EGFR (p-EGFR) in human tumors have been validated by other laboratories and ours. However, although the detection of EGFR can be considered a common practice in the selection of patients to undergo EGFR-directed therapy, using either MAbs or SMIs (reviewed in Grünwald and Hidalgo, 2003), the value of the immunohistochemical determination of p-EGFR as an additional diagnostic and prognostic marker is still under testing. Preclinical studies suggested that IHC of p-EGFR can be a trustable marker to prove target (EGFR) inactivation, but a reduction in the levels of p-EGFR does not necessarily translate into inactivation of signaling pathways downstream of EGFR (e.g., PI3K/Akt and MAPK). It is the inactivation of these pathways that ultimately drives the anti-tumor activity of the EGFR inhibitors, including their anti-proliferative, proapoptotic, and anti-angiogenic effects (Arteaga, 2002; Grünwald and Hidalgo, 2003). To exemplify this point, experiments performed in Dr. Arteagas' laboratory at Vanderbilt University have shown that EGFR overexpressing cell lines that possess a mutant PTEN protein have constitutive high levels of phosphorylated/activated Akt, which are not reduced on treatment with EGFR inhibitors. This is despite the fact that EGFR inhibitors block the activation/phosphorylation of their target, as shown by a reduction in the levels of p-EGFR following exposure of the cells to the inhibitors (Bianco *et al.,* 2003). PTEN is a phosphatase that dephosphorylates the position D3 of phosphatidylinositol-3,4,5 trisphosphate (PI-3-P), a product of PI3K activity. The phosphorylated site D3 of PI-3-P recruits the plecstrin homology domain of Akt to the cell membrane, and it is therefore involved in the activation of Akt, downstream of PI3K. For this reason PTEN acts as a natural inhibitor of the PI3K/Akt pathway and is considered a tumor suppressor gene as a result of its demonstrated loss of function in several malignancies (Smith *et al.,* 2001; Whang *et al.,* 1998). Because a reduction in the activity of Akt seems to be essential for the antiproliferative an proapoptotic effects of EGFR inhibitors in many instances, cell lines with an overexpressed and overactive EGFR, but that also have a mutant, inactive PTEN, are naturally resistant to EGFR-directed therapy both *in vitro* and *in vivo* (Bianco *et al.,* 2003).

In agreement with the aforementioned notion, some EGFR-overexpressing cell variants, which exhibited resistance to EGFR-targeted therapy, have been observed to possess overactive PI3K, independent of EGFR activity. This has been the case for a naturally resistant cell line obtained from a glioblastoma (Chakravarti *et al.,* 2002), as well as for several variant cell lines resistant to EGFR-targeted therapy obtained from EGFR-overexpressing human tumor xenografts in mice. The latter were generated after continuous treatment of the tumor-bearing animals with the SMI ZD1839/Iressa, during which several of the initially responding xenografts became refractory to EGFR blockade. Apart from hyperphosphorylated Akt, which was not affected by EGFR inhibition *in vitro,* constitutively active (phosphorylated) MAPK was also observed in these resistant variants, but only the hyperactivation of PI3K was shown to be responsible for the resistant phenotype (Arteaga, C.L., personal communication). Taken together, these results suggest that the determination by IHC of both activated MAPK and PI3K, as determined with primary antibodies directed against the phosphorylated forms of MAPK and Akt (a downstream target of PI3K), respectively, should be included as part of the panel of molecular markers used to select patients for EGFR-directed therapy. The inactivation of these targets in response to EGFR blockade would be useful to determine drug activity and its correlation with patient response, proven that both pretreatment and posttreatment tumor samples were available.

The feasibility of using serial tumor biopsies for the determination of EGFR activity has already been shown in clinical studies with EGFR inhibitors, such as a phase I trial of IMC-C225 MAb performed in patients with head and neck cancer. In this study EGFR activity was determined by an enzymatic assay performed on extracts of tumor tissue (Shin *et al.,* 2001). Nevertheless, it must be kept in mind that in some less accessible tumors, or in cases in which tumor tissue necrosis could make it difficult to obtain optimal biopsy material, assessing tumor tissue may be impossible. An alternative way to overcome this problem is suggested by studies undertaken by Albanell and co-workers, in which a series of IHC stainings were performed in serial skin biopsies obtained from patients with cancer who were undergoing treatment with the SMI of EGFR ZD1839/Iressa (Albanell *et al.,* 2002). Among the molecular markers determined in this study were the phosphorylation/activation status of EGFR and its downstream-signaling pathways MAPK and STAT3, as well as some markers of the cellular effects of the inhibitor. These included cell proliferation, as measured by staining of Ki-67, which is a marker of "cycling" cells, and cell death, as determined by terminal deoxynucleotidyl transferase (Tdt)-mediated dUTP nick end labeling (TUNEL) staining. In addition, cell growth inhibition was indirectly measured by IHC of the cyclin-dependent kinase (CDK) inhibitor p27, whose up-regulation has been shown to be a consistent response to EGFR inhibitors, which appears to be essential for their anti-proliferative activity (Busse *et al.,* 2000). Among the positive findings

obtained in this study was a significant decrease in p-EGFR and p-MAPK observed in the skin of patients after treatment with ZD1839/Iressa. This suggested that the target (EGFR) was reached, and this resulted in the inhibition of the activity of downstream pathways (MAPK), at least in the skin of the patients (Albanell *et al.,* 2002). Reduction in EGFR signaling also seemed to parallel an increase in both the levels of the CDK inhibitor p27 and the percentage of apoptosing cells, as well as a decrease in cell proliferation (Albanell *et al.,* 2002). These results are consistent with what has been previously observed after exposure of EGFR-overexpressing tumor cells to various types of EGFR inhibitors both *in vitro* and *in vivo* (Busse *et al.,* 2000; Crombet-Ramos *et al.,* 2002). Problems encountered in the study of Albanell *et al.* include the lack of a dose-response effect in terms of the blockade of EGFR activity and the fact that there is no available data on the correlation between the IHC and the clinical response of the patients to the therapy. The former, as suggested by the authors, could be attributed to the doses of ZD1839 used in the study, which were all higher than 100 mg/day, a dose that has been previously shown to cause optimal receptor inhibition (Albanell *et al.,* 2002). Another important point to add with regard to this type of study is that the possible correlation between the molecular effects of the inhibitor in the skin and those that might occur in the tumor itself still remains to be determined. Studies of this matter are essential to establish whether skin biopsies would be useful in predicting the potential benefits of EGFR-directed treatment modalities, either early or later on during the course of the therapy.

CONCLUSIONS

Monoclonal antibodies directed against the EC domain or epitopes specific to the phosphorylated/activated form of EGFR, and that have the ability to detect the receptor in frozen or formalin-fixed, paraffin-embedded tissue samples, are useful pharmacodiagnostic tools for most EGFR-overexpressing tumors. When used in conjunction, these antibodies allow for a more accurate selection of those patients who might benefit from EGFR-directed therapy. Additionally, p-EGFR–specific antibodies are useful to establish the actual inactivation of the target during the course of treatment with a particular EGFR inhibitor. However, because the inactivation of EGFR cannot predict the subsequent blockade of downstream signaling pathways (the inactivation of which is ultimately required for the anti-tumor activity of the inhibitor), IHC of reliable markers accounting for the inactivation of key, EGFR-driven signal transduction pathways (e.g., PI3K/Akt) should also be included. Finally, the determination of markers of cell proliferation and cell death (apoptosis) by IHC is also recommended to obtain final proofs of the inhibitor biological activity.

References

Aida, S., Tamai, S., Sekiguchi, S., and Shimizu, N. 1994. Distribution of epidermal growth factor and epidermal growth factor receptor in human lung: Immunohistochemical and immunoelectron-microscopic studies. *Respiration 61*:161–166.

Albanell, J., Rojo, F., Averbuch, S., Feyereislova, A., Mascara, J., Herbst, R., LaRusso, P., Rischin, D., Sauleda, S., Gee, J., Nicholson, R., and Baselga, J. 2002. Pharmacodynamic studies of the epidermal growth factor receptor inhibitor ZD1839 in skin from cancer patients: Histopathologic and molecular consequences of receptor inhibition. *J. Clin. Oncol. 20*:110–124.

Arteaga, C. 2002. Overview of epidermal growth factor receptor biology and its role as a therapeutic target in human neoplasia. *Semin. Oncol. 29* (5 Suppl.14):3–9.

Bernardini, N., Bianchi, F., Lupetti, M., and Dolfi, A. 1996. Immunohistochemical localization of the epidermal growth factor, transforming growth factor alpha, and their receptor in the human mesonephros and methanephros. *Dev. Dyn. 206*:231–238.

Bianco, R., Shin, I., Ritter, C., Yakes, F., Basso, A., Rosen, N., Tsurutani, J., Dennis, P., Mills, G., and Arteaga, C. 2003. Lost of PTEN/MMCA1/TEP in EGF receptor-expressing tumor cells counteracts the antitumor action of EGFR tyrosine kinase inhibitors. *Oncogene 22*:2812–2822.

Bishop, P., Myers, T., Robey, R., Fry, D., Liu, E., Blagosklonny, M., and Bates, S. 2002. Differential sensitivity of cancer cells to inhibitors of the epidermal growth factor receptor family. *Oncogene 21*:119–127.

Bunn, P., Jr., and Franklin, W. 2002. Epidermal growth factor receptor expression, signal pathway and inhibitors in non-small cell lung cancer. *Semin. Oncol. 29* (5 Suppl.14):38–44.

Busse, D., Doughty, R., Ramsey, T., Russell, W., Price, J., Flanagan, W., Shawver, L., and Arteaga, C. 2000. Reversible G_1 arrest induced by inhibition of the epidermal growth factor receptor tyrosine kinase requires up-regulation of $p27^{KIP1}$ independent of MAPK activity. *J. Biol. Chem. 275*:6987–6995.

Cedeño, M., Rengifo, Ch., Guarnalusse, R., Cuesta Tedeño, M., Salazar, S., Rengifo, E., and Rodriguez, T. 1999. Evaluación inmunohistoquímica del AcM humanizado hR3 en tejido normal, tumores pulmonares y mamarios [Abstract 56]. *Rev. Esp. Oncol. 22* (Suppl.1):20.

Chailler, P., and Ménard, D. 1999. Ontogeny of EGF receptors in the human gut. *Front. Biosci. 4*:87–101.

Chakravarti, A., Loeffler, J., and Dyson, N. 2002. Insulin-like growth factor receptor I mediates resistance to anti-epidermal growth factor receptor therapy in primary human glioblastoma cells through continued activation of phosphoinositide 3-kinase signaling: *Cancer Res. 62*:200–207.

Clynes, R., Towers, T., Presta, L., and Ravetch, J. 2000. Inhibitory Fc receptors modulate *in vivo* cytoxicity against tumor targets. *Nat. Med. 6*:443–446.

Crombet, T., Osorio, M., Cruz, T., Figueredo, R., Koropatnick, J., Rengifo, E., Torres, O., Pérez, R., and Lage, A. 2002. Use of the anti-EGFR antibody h-R3 in combination with radiotherapy in

the treatment of advanced head and neck cancer [Abstract 53]. *Proc. Am. Soc. Clin. Oncol. 21*:14a.

Crombet, T., Torres, L., Neninger, E., Catalá, M., Solano, M., Perera, A., Torres, O., Iznaga, N., Torres, F., Pérez, R., and Lage, A. 2003. Pharmacological evaluation of humanized anti-epidermal growth factor receptor, monoclonal antibody h-R3, in patients with advanced epithelial-derived cancer. *J. Immunother. 26*:139–148.

Crombet, T., Torres, O., Neninger, E., Menendez, A., Stevenson, A., Ramos, M., Torres, F., Figueredo, R., Veitia, I., Iznaga, N., Pérez, R., and Lage, A. 2001. Phase I clinical evaluation of a neutralizing monoclonal antibody against epidermal growth factor receptor. *Cancer Biother. Radiopharm. 16*:93–102.

Crombet-Ramos, T., Rak, J., Pérez, R., and Viloria-Petit, A. 2002. Antiproliferative, antiangiogenic and proapoptotic activity of h-R3: A humanized anti-EGFR antibody. *Int. J. Cancer 101*:567–575.

Crombet-Ramos, T., Torres, L., Solano, M., Cruz, T., Osorio, M., Rengifo, E., Catalá, M., Neninger, E., Perera, A., Torres, O., Pérez, R., and Lage, A. 2001. Pharmacological and clinical evaluation of the humanized anti-EGFR monoclonal antibody, h-R3, in patients with advanced epithelial carcinoma [Abstract 1012]. *Proc. Am. Soc. Clin. Oncol. 20*:254A.

Damjanov, I., Mildner, B., and Knowles, B. 1986. Immunohistochemical localization of the epidermal growth factor receptor in normal human tissues. *Lab. Invest. 55*:588–592.

Downward, J., Yarden, Y., Mayes, E., Scrace, G., Totty, N., Stockwell, P., Ullrich, A., Schlessinger, J., and Waterfield, M. 1984. Close similarity of epidermal growth factor receptor and v-*erb-B* oncogene protein sequences. *Nature 307*:521–527.

Fan, Z., Masui, H., Altas, I., and Mendelsohn, J. 1993. Blockade of epidermal growth factor receptor function by bivalent and monovalent fragments of 225 anti-epidermal growth factor receptor monoclonal antibodies. *Cancer Res. 53*:4322–4328.

Fernández, A., Spitzer, E., Pérez, R., Boehmer, F., Eckert, K., Zschiesche, W., and Grosse, R. 1992. A new monoclonal antibody for detection of EGF-receptors in Western blots and paraffin-embedded tissue sections. *J. Cell Biochem. 49*:157–165.

Grünwald, V., and Hidalgo, M. 2003. Developing inhibitors of the epidermal growth factor receptor for cancer treatment. *J. Natl. Cancer Inst. 95*:851–867.

Herbst, R., and Langer, C. 2002. Epidermal growth factor receptor as a target for cancer treatment: The emerging role of IMC-C225 in the treatment of lung and head and neck cancers. *Semin. Oncol. 29* (Suppl.4):27–36.

Hormi, K., and Lehy, T. 1994. Developmental expression of transforming growth factor-alpha and epidermal growth factor receptor proteins in the human pancreas and digestive tract. *Cell Tissue Res. 278*:439–450.

Iwata, K., Provoncha, K., and Gibson, N. 2002. Inhibition of mutant EGFRvIII transformed cells by tyrosine kinase inhibitor OSI-774 (Tarceva) [Abstract 79]. *Proc. Am. Soc. Clin. Oncol. 21*.

Konecny, G., and Slamon, D. 2002. HER2 testing and correlation with efficacy of trastuzumab therapy. *Oncology 16*:1576–1578.

Leav, I., McNeal, J., Ziar, J., and Alroy, J. 1998. The localization of transforming growth factor alpha and epidermal growth factor receptor in stromal and epithelial compartments of developing human prostate, hyperplastic, dysplastic and carcinomatous lesions. *Hum. Pathol. 29*:668–675.

Libermann, T., Nusbaum, H., Razon, N., Kris, R., Lax, I., Soreq, H., Whittle, N., Waterfield, M., Ullrich, A., and Schlessinger, J. 1985. Amplification, enhanced expression and possible rearrangement of EGF receptor gene in primary human brain tumors of glial origin. *Nature 313*:144–147.

Mateo, C., Moreno, E., Amour, K., Lombardero, J., Harris, W., and Perez, R. 1997. Humanization of a mouse monoclonal antibody that blocks the epidermal growth factor receptor: Recovery of antagonistic activity. *Immunotechnology 3*:71–81.

Meert, A., Martin, B., Delmotte, P., Berghmans, T., Lafitte, J., Mascaux, C., Paesmans, M., Steels, E., Verdebout, J., and Sculier, J. 2002. The role of EGF-R expression on patient survival in lung cancer: A systematic review with meta-analysis. *Eur. Respir. J. 20*:975–981.

Moroni, M., Veronese, S., Schiavo, R., Carminati, O., Sorensen, B., Gambacorta, M., and Siena, S. 2001. Epidermal growth factor receptor and activation in nonseminomatous germ cell tumors. *Clin. Cancer Res. 7*:2770–2775.

Motoyama, A., Hynes, N., and Lane, H. 2002. The efficacy of ErbB receptor-targeted therapeutics is influenced by the availability of epidermal growth factor-related peptides. *Cancer Res. 62*:3151–3158.

Nicholson, R., Gee, J., and Harper, M. 2001. EGFR and cancer prognosis. *Eur. J. Cancer 73* (Suppl.4):S9–S15.

Oliver, A. 1988. Epidermal growth factor receptor expression in human foetal tissues is age-dependent. *Br. J. Cancer 58*:461–463.

Pedersen, M., Meltorn, M., Damstrup, L., and Poulsen, H. 2001. The type III epidermal growth factor receptor mutation. Biological significance and potential target for anti-cancer therapy. *Ann. Oncol. 12*:745–760.

Pollack, V., Savage, D., Baker, D., Tsaparikos, K., Sloan, D., Moyer, J., Barbacci, E., Pustilnik, L., Smolarek, T., Davis, J., Vaidya, M., Arnold, L., Doty, J., Iwata, K., and Morin, M. 1999. Inhibition of epidermal growth factor receptor-associated tyrosine phosphorylation in human carcinomas with CP-358,774: Dynamics of receptor inhibition and anti-tumor effects in athymic mice. *J. Pharmacol. Exp. Ther. 291*:739–748.

Prenzel, N., Fisher, O., Streit, M., Hart, S., and Ullrich, A. 2001. The epidermal growth factor receptor family as a central element for cellular signal transduction and diversification. *Endocr. Relat. Cancer 8*:11–31.

Ramos-Suzarte, M., Rodriguez, N., Oliva, J., Iznaga-Escobar, N., Perera A., Morales, A., González, N., Cordero¸ M., Torres, L., Pimentel, G., Borron, M., González, J., Torres, O., Rodriguez, T., and Pérez, R. 1999. 99mTc-labelled antihuman epidermal growth factor receptor antibody in patients with tumors of epithelial origin: Part III. Clinical trials safety and diagnostic efficacy. *J. Nucl. Med. 40*:768–775.

Raben, D., Helfrich, B., Ciardiello, F., and Bunn, P. 2003. Understanding the mechanism of action of EGFR inhibitors in NSCLC: What we know and what we do not know. *Lung Cancer 41* (Suppl.1):15–22.

Randal, J. 2002. Erbitux trial flawed from the beginning, committee finds. *J. Natl. Cancer Inst. 94*:1824–1825.

Rengifo, E., Guarnalusse, R., Salazar, S., Cuesta Tedeño M., Rodriguez, T., and Rengifo, E. 1999. Coexpression del factor de crecimiento epidermico y su receptor en carcinomas pulmonares incluidos en parafina [Abstract 55]. *Rev. Esp. Oncol. 22* (Suppl.1):19.

Rusch, V., Baselga, J., Cordon-Cardo, C., Orazem, J., Zaman, M., Hoda, S., McIntosh, J., Kurie, J., and Dmitrovsky, E. 1993. Differential expression of the epidermal growth factor receptor and its ligands in primary non-small cell lung cancers and adjacent benign lung. *Cancer Res. 53* (Suppl.10):2379–2385.

Rusch, V., Klimstra, D., Venkatraman, E., Pisters, P., Langenfeld, J., and Dmitrovsky, E. 1997. Overexpression of the epidermal growth factor receptor and its ligand transforming growth factor

alpha is frequent in respectable non-small cell lung cancer but does not predict tumor progression. *Clin. Cancer Res. 3*:515–522.

Saga, K., and Jimbow, K. 2001. Immunohistochemical localization of activated EGF receptor in human eccrine and apocrine sweat glands. *J. Histochem. Cytochem. 49*:597–601.

Salomon, D., Brandt, R., Ciardiello, F., and Normanno, N. 1995. Epidermal growth factor-related peptides and their receptors in human malignancies. *Crit. Rev. Oncol. Hematol. 19*:183–232.

Shin, D., Donato, N., Perez-Soler, R., Shin, H., Wu, J., Zhang, P., Lawhorn, K., Khuri, F., Glisson, B., Myers, J., Clayman, G., Pfister, D., Falcey, J., Waksal, H., Mendelsohn, J., and Hong, W. 2001. Epidermal growth factor receptor-targeted therapy with C225 and cisplatin in patients with head and neck cancer. *Clin. Cancer Res. 7*:1204–1213.

Smith, J., Tachibana, I., Passe, S., Huntley, B., Borell, T., Iturria, N., O'Fallon, J., Schaefer, P., Scheithauer, B., James, C., Buckner, J., and Jenkins, R. 2001. PTEN mutation, EGFR amplification, and outcome in patients with anaplastic astrocytoma and glioblastoma multiforme. *J. Natl. Cancer Inst. 93*:1246–1256.

Spaulding, D., and Spaulding, B. 2002. Epidermal growth factor receptor expression and measurement in solid tumors. *Semin. Oncol. 29* (Suppl.14):45–54.

Ullrich, A., Coussens, L., Hayflick, J., Dull, T., Gray, A., Tam, A., Lee, J., Yarden, Y., Libermann, T., Schlessinger, J., Downward, J., Mayes, E., Whittle, N., Waterfield, M., and Seeburg, P. 1984. Human epidermal growth factor receptor cDNA sequence and aberrant expression of the amplified gene in A431 epidermoid carcinoma cells. *Nature 309*:418–425.

Wakeling, E., Abu-Amero, S., Stainer, P., Preece, M., and Moore, G. 1998. Human EGFR, a candidate gene for the Silver-Russell syndrome, is biallelically expressed in a wide range of fetal tissues. *Eur. J. Hum. Genet. 6*:158–164.

Whang, Y., Wu, X., Suzuki, H., Reiter, R., Tran, C., Vessella, R., Said, J., Isaacs, W., and Sawyers, C. 1998. Inactivation of the tumor suppressor PTEN/MMAC1 in advanced human prostate cancer through loss of expression. *Proc. Natl. Acad. Sci. USA 95*:5246–5250.

Winquist, E., Abdenour, N., Sicheri, D., Ganguly, P., Venkatesan, V., Schneider, K., MacKinnon, J., and Laurie, S. 2002. A phase I dose escalation study of a humanized monoclonal antibody to EGFR (hR3) in patients with locally advanced squamous cell cancer of the head and neck (SCCHN) treated with radiotherapy (RT) [Abstract 926]. *Proc. Am. Soc. Clin. Oncol. 21*:232a.

Wu, X., Fan, Z., Masui, H., Rosen, N., and Mendelsohn, J. 1995. Apoptosis induced by an anti-epidermal growth factor receptor monoclonal antibody in a human colorectal carcinoma cell line and its delay by insulin. *J. Clin. Invest. 95*:1897–1905.

Wu, X., Rubin, M., Fan, Z., DeBlasio, T., Soos, T., Koff, A., and Mendelsohn, J. 1996. Involvement of p27KIP1 in G1 arrest mediated by an anti-epidermal growth factor receptor monoclonal antibody. *Oncogene 12*:1397–1403.

Yamamoto, T., Kamata, N., Kawano, H., Shimizu, S., Kuroki, T., Toyoshima, K., Rikimaru, K., Nomura, N., Ishizaki, R., and Pastan, I. 1986. High incidence of amplification of the epidermal growth factor receptor gene in human squamous carcinoma cell lines. *Cancer Res. 46*:414–416.

Yarden, Y., and Sliwkowski, M. 2001. Untangling the ErbB signalling network. *Nature Rev. 2*:127–137.

9

PTEN and Cancer

Odile David

Introduction

The gene *PTEN/MMAC1/TEP1* (Phosphatase and Tensin homolog deleted on chromosome TEN/Mutated in Multiple Advanced Cancers/TGFβ [transforming growth factor beta] regulated and Epithelial cell–enriched Phosphatase) is a tumor suppressor whose importance in human malignancies is becoming increasingly recognized (Cantley *et al.,* 1999; Di Cristofano *et al.,* 2000). The *PTEN* gene is located on chromosome 10q23.3 and encodes a dual-specificity phosphatase that negatively regulates the phosphoinositol-3-kinase/Akt cell survival pathway and mediates cell cycle arrest and apoptosis (Zhou *et al.,* 2002). Mutations of *PTEN* have been shown to play a prominent role in glioblastomas (Haas-Kogan *et al.,* 1998), breast (Pérez-Tenorio *et al.,* 2002), endometrial (Latta *et al.,* 2002), and prostate (Grünwald *et al.,* 2002) carcinomas. The precise role of PTEN in tumorigenesis with respect to tumor progression and metastasis as well as the mechanisms of PTEN inactivation appear to be varied and cell-type dependent (Fernandez *et al.,* 2002). For example, in a PTEN-null PC3 prostate cancer cell line, adenoviral infection of wild-type *PTEN* results in decreased metastatic potential without significantly altering tumor size (Davies *et al.,* 2002).

In most systems PTEN inactivation is believed to be a late event in tumorigenesis. However, in endometrial carcinomas, the most thoroughly studied tumor system with respect to PTEN and the one with the most extensive clinical studies, PTEN inactivation is thought to occur as an initiating event (Sun *et al.,* 2001). Mutations of *PTEN* have been reported in endometrial hyperplasias with and without cytologic atypia, resulting in the hypothesis that loss of PTEN function predisposes endometrial cells to neoplastic transformation (Latta *et al.,* 2002). Such mutations have been reported in 18–55% of premalignant endometrial lesions (Latta *et al.,* 2002) and in 50–83% of endometrial adenocarcinomas (An *et al.,* 2002). Immunostaining for PTEN is becoming increasingly warranted, and in some pathology laboratories it is performed routinely in clinical endometrial carcinoma specimens. Preservation of PTEN tumor suppressor function, as demonstrated by PTEN-positive immunostaining, has been shown to be a significant independent prognostic indicator of favorable survival in patients with advanced endometrial carcinoma (Kanamori *et al.,* 2001). Mutations in the *PTEN* gene appear to be infrequent in other common gynecologic malignancies (Tashiro *et al.,* 1997).

The *PTEN* gene was first identified in 1997 by three different groups simultaneously. This discovery was preceded by the discovery that there was a susceptibility gene for Cowden syndrome, an autosomal dominant syndrome in which patients develop multiple hamartomas and are at increased risk of breast, thyroid, and endometrial malignancies (Dahia, 2000). This susceptibility gene was mapped to 10q22-q23. The PTEN gene was mapped to 10q23 (Bonneau *et al*., 2000; Waite *et al.,* 2002). Besides its role in carcinogenesis, PTEN plays an

Handbook of Immunohistochemistry and *in situ* Hybridization of Human Carcinomas, Volume 3: Molecular Genetics, Liver Carcinoma, and Pancreatic Carcinoma

important role in the control of tissue growth, as demonstrated in experiments in *Drosophila,* and of mammalian brain development, as demonstrated in mouse models. In *PTEN*-null mice, neuronal cell bodies were enlarged, resulting in enlarged brain volume, particularly cerebellar (Beckman *et al.,* 2002).

The *PTEN* gene encodes a 403-amino acid polypeptide whose main substrates are inositol phospholipids generated by the inactivation of PI3 kinase (Myers *et al.,* 1998; Vivanco *et al.,* 2002). It has a C-terminal noncatalytic regulatory domain that contains three phosphorylation sites, at Ser380, Thr382, and Thr383, which regulate its stability and biologic activity (Torres *et al.,* 2001). Novel phosphorylation sites more recently discovered by mass spectrometric methods have also been reported. The mechanism of action of the PTEN protein product appears to be inhibition of the phosphorylation of Akt by PI3 kinase, thereby inhibiting cell survival (Cantley *et al.,* 1999). Numerous mutations of the *PTEN* gene have been identified (Bonneau *et al.,* 2000). Certain *PTEN* mutations in endometrial cancers have been associated with favorable prognosis (Minaguchi *et al.,* 2001; Risinger *et al.,* 1998), and *PTEN* promoter methylation has also been implicated in the development of endometrial carcinoma (Salvesen *et al.,* 2001). In a lung cancer cell line, overexpression of PTEN has been shown to inhibit invasion (Hong *et al.,* 2000). Although the frequency of *PTEN* gene mutations in lung cancer remains controversial, the protein itself is recognized as an important tumor suppressor (Kandasamy *et al*., 2002; Kohno *et al.,* 1998).

The PTEN gene product is an integral antagonist of the PI3 (phosphatidylinositol 3)-kinase pathway. PI3-kinase activation results in the generation of PIP3 (phosphatidylinositol 3,4,5, triphosphate) at the cytoplasmic membrane. PIP3 then acts as a second messenger that activates numerous downstream pathways that promote cell survival. One of the most important downstream proteins activated by PIP3 is Akt, which will be discussed in detail later in this chapter because of the important and clinically relevant relationship between Akt and PTEN. One of several PIP3 phosphatases, PTEN antagonizes the prosurvival effects of the PI3 kinase pathway and promotes apoptotic activity. PTEN seems to be the PIP3 phosphatase that is most potently involved in oncogenesis; it is a 3′-position lipid phosphatase that converts PIP3 to PIP2. It is interesting that another known PIP3 phosphatase, SHIP1, is a 5′-position phosphatase but knockout models in mice demonstrate a much weaker carcinogenic phenotype than in PTEN knockout mice (Vivanco *et al.,* 2002).

It would be remiss to discuss PTEN without mentioning its relationship with Akt, a signal transduction protein that has anti-apoptotic activity and whose activation is inhibited by PTEN. The PTEN protein product is expressed in inverse proportion to phosphorylated Akt in endometrial and breast cancer cell lines (Kanamori *et al.,* 2001; Weng *et al.,* 2001) and in mouse embryonic fibroblasts (Stambolic *et al.,* 1998). This relationship has important implications for our understanding of carcinogenensis and for the development of novel and effective anti-neoplastic agents.

Akt, also known as PKB (protein kinase B) and rac (*r*elated to protein kinase *a* and *c*), is a cytosolic signal transduction protein that plays an important role in the cell survival pathway (Hutchinson *et al.,* 2001). It is recruited to the plasma membrane by PI3 kinase, where it is phosphorylated by PDK1 and by a second as-yet-unidentified kinase. More specifically, Akt contains an amino-terminal plecstrin homology domain that binds phosphorylated lipids at the membrane in response to activation of PI3 kinases. Akt is activated by phospholipid binding and activation loop phosphorylation at Thr308 by PDK1 and also by phosphorylation within the C-terminus at Ser473 (Alessi *et al.,* 1996). Phosphorylation at the Thr308 site appears to be necessary and sufficient. Activated Akt may be found in the cell nucleus, although its exact function there is unknown.

Activated Akt promotes cell survival by inhibiting apoptosis by means of phosphorylating and thereby inactivating targets, which include members of the bcl-2 family, caspase 9, and forkhead transcription factors (Brunet *et al.,* 1999), among others. Activated Akt has been shown to negatively regulate the Ras-Raf-MAP kinase pathway via phosphorylation and inactivation of Raf at Ser259 (Zimmermann *et al.,* 1999). This is of particular significance in lung cancer because of the relatively high mutation rates of k-ras in non–small cell lung cancer (NSCLC) (Huncharek *et al.,* 1999). It has also been shown that in NSCLC cell lines, phosphorylation of Akt by PI3 promotes cell survival, and inhibition of PI3 permits apoptosis (Kandasamy *et al.,* 2002). This has also been demonstrated in murine mammary tissue (Hutchinson *et al.,* 2001). In addition, the influence of Akt on the p53-mediated apoptotic pathway has been demonstrated (Sabbatini *et al.,* 1999), as has the effect of p53 on Akt (Bachelder *et al.,* 1999). Akt is believed to up-regulate expression of mdm2, thereby promoting ubiquitination of p53 and decreased apoptosis; p53 has been shown to inhibit alpha 6 beta 4 integrin survival signaling by promoting the caspase 3–dependent cleavage of Akt.

Akt has been found to play a role in the survival of cancer cells in breast, prostate, ovary, and brain tissue (Campbell *et al.,* 2001; Davies *et al.,* 1999; Hutchinson *et al.,* 2001). It has also been shown to confer

chemoresistance in NSCLC cell lines treated with topotecan (Nakashio *et al.,* 2000) and etoposide, CDDP (cisplatin), paclitaxel, gemcitabine, and trastuzumab (Herceptin) (Brognard *et al.,* 2001) as well as breast cancer cell lines treated with trastuzumab (Cuello *et al.,* 2001). In a series of investigations conducted by Brognard *et al.* (2001) at the National Cancer Institute, constitutive Akt/PKB activity was demonstrated in 16 of 17 NSCLC cell lines by maintenance of S473 phosphorylation with serum deprivation. Akt activation was PI3-kinase–dependent and promoted survival; the PI3 inhibitors LY294002 and wortmannin inhibited Akt phosphorylation and increased apoptosis in cells with constitutively active Akt but not in cells without constitutively active Akt.

To test whether Akt activity promoted therapeutic resistance, LY294002 was added with individual chemotherapeutic agents or irradiation. LY294002 greatly potentiated chemotherapy-induced apoptosis in cells with high constitutive Akt levels but did not significantly increase chemotherapy-induced apoptosis in cells with low constitutive Akt levels. Combined with radiation in cells with active Akt, LY294002 additively increased apoptosis and inhibited clonogenic growth. These results were reproducible in transiently transfected Akt mutants. Transfecting dominant-negative Akt decreased Akt activity and increased basal apoptosis as well as chemotherapy and irradiation-induced apoptosis only in cells with high Akt/PKB activity. Conversely, transfecting constitutively active Akt into cells with low Akt/PKB activity increased Akt activity and attenuated chemotherapy and irradiation-induced apoptosis. By these methods, Akt was identified as a constitutively active kinase that promotes survival of NSCLC cells. It was concluded that modulation of Akt activity by pharmacologic or genetic approaches alters the cellular responsiveness to therapeutic modalities usually used to treat patients with NSCLC (Brognard *et al.,* 2001).

The relationship between PTEN and Akt has been well established in numerous studies. In 2002, Kandasamy *et al.* showed a relationship between Akt activation and PTEN mutation in NSCLC. Their group demonstrated that TRAIL (**t**umor necrosis factor–**r**elated **a**poptosis-**i**nducing **l**igand) did not induce apoptosis in some NSCLC cells. These cells were shown to be resistant to TRAIL because of the phosphatidylinositol 3′-kinase (PI3-K)-dependent activation of Akt/PKB. The expression of phospho-Akt varied at the functional level but not at the messenger ribonucleic acid (mRNA) level in NSCLC cells. Akt induced cell survival in NSCLC cells by blocking the Bid cleavage, upstream of cytochrome c release in the mitochondrial-dependent apoptotic pathway. The use of PI3-K inhibitors, wortmannin or LY294002, downregulated the active Akt and reversed cellular resistance to TRAIL. In addition, genetically altering Akt expression by transfecting dominant-negative Akt sensitized NSCLC cells to TRAIL. Conversely, transfection of constitutively active Akt into cells that expressed low, constitutively active Akt increased TRAIL resistance. Alternately to this approach, transfection with PTEN promoted sensitivity to TRAIL, whereas a PTEN mutant (PTEN-G129E) at the catalytic site was inactive in dephosphorylating active Akt. They concluded that loss of PTEN activity or overexpression of PI3-K–dependent Akt/PKB activity promoted the survival of NSCLC cells and furthermore that modulation of Akt activity by combining pharmacologic drugs or genetic alterations of the Akt expression may induce cellular responsiveness to TRAIL (Kandasamy *et al.,* 2002).

Thus, strong evidence is emerging in the basic science literature that PTEN and Akt are signal transduction proteins that figure prominently in mechanisms of carcinogenesis and chemoresistance. Ultimately, understanding the role of PTEN and members of the PI3-kinase pathway and its effectors in cancer will drive the development of targeted tumor-specific therapies.

It is important to know whether the antibody being applied to determine presence or absence of the PTEN protein detects total protein, i.e., active and inactive forms, as compared to only the active form (nonphosphorylated PTEN) or only the inactive form (phosphorylated PTEN). Pathology laboratories that routinely stain endometrial cancers to offer enhanced prognostic information generally use antibodies against the active form of PTEN. The PTEN antibody from Cascade Bioscience (Winchester, MA) is commonly used with reliable results. This antibody detects only the intact form of PTEN. It does not detect phosphorylated PTEN (phosphoPTEN). The antibody from Cascade Bioscience is a mouse monoclonal immunoglobulin G (IgG) that reacts with human and mouse PTEN.

A standardized scheme for interpretation of results of immunostaining of tumors with the PTEN antibody has not been developed. Generally results are interpreted as absence or presence of PTEN. As discussed earlier, absence of PTEN expression indicates PTEN inactivation and is common in endometrial adenocarcinomas. Loss of PTEN is considered an early event in endometrial carcinoma and has been demonstrated in precursor lesions such as complex hyperplasia with atypia as well as in histologically normal endometrial tissue (Mutter *et al.,* 2000). Loss of PTEN expression is considered a negative prognostic indicator in endometrial adenocarcinomas (Kanamori *et al.,* 2001).

In the research setting it is useful to know the activation state of the PTEN protein. If PTEN is present

but only in the phosphorylated form (phosphoPTEN), it is inactive and nonfunctional as a tumor suppressor. It would be interesting to know what percentage of tumors in which PTEN expression appears to be absent actually demonstrate inactivation of the PTEN protein rather than mutations in the *PTEN* gene. This is a question that the development of proteomic techniques may eventually be able to answer.

A phosphoPTEN-specific protein is available from CellSignaling Technology (Beverly, MA). This antibody has been used with success in our laboratory on a series of NSCLCs retrieved from the files at the Tulane University Hospital Pathology Department. Of 16 cases, 14 demonstrated strong expression of phosphoPTEN, implying inactivation of this important tumor suppressor. In the 14 positive cases, staining was generally diffuse and cytoplasmic as well as nuclear (Figure 17). For further details on expected staining patterns and interpretation of stained tissues, see the Results and Discussion section.

Although there are many upstream signals that may promote phosphorylation of the PTEN protein, the result of loss of PTEN expression is a diminished cellular capacity for apoptosis by unregulated activation of the PI3-kinase dependent signaling cascade, which promotes cell survival, most centrally through the Akt pathway, as discussed earlier.

MATERIALS AND METHODS

PTEN: Cascade BioScience

This antibody detects the nonphosphorylated form of PTEN.

MATERIALS

1. Xylene.
2. 100% Reagent alcohol.
3. 95% Reagent alcohol.
4. 80% Reagent alcohol.
5. Distilled ionized (DI) water.
6. Dako buffer: PBS with Tween × 10 stock, 1 part stock 9 parts distilled water.
7. 3% Hydrogen peroxide.
8. Anti-Human PTEN (clone 6H2.1) Antibody, dilute 1:100 in Dako antibody diluent.
9. Dako serum-free protein block.
10. Secondary antibody Dako LSAB2 link system.
11. Tertiary antibody Dako LSAB2-StreptAvidin.
12. Dako diaminobenzidine (DAB) chromogen substrate.
13. Counter-stain Gills II hematoxylin.
14. DakoAutostainer instrument (optional).

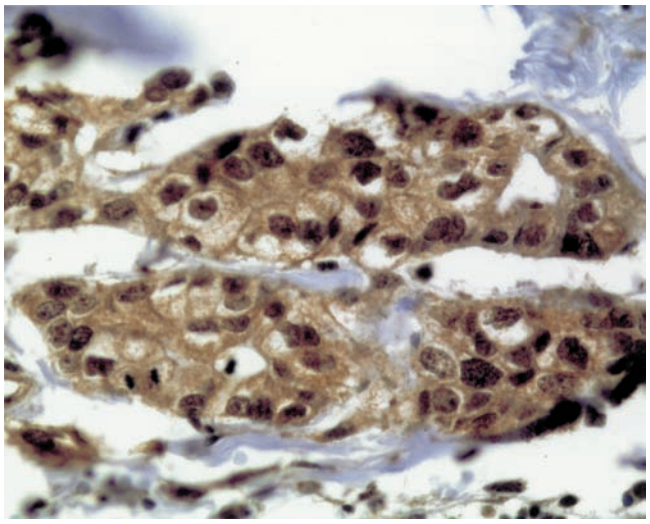

Figure 17. Formalin-fixed paraffin-embedded human primary pulmonary adenocarcinoma demonstrating diffuse strong nuclear and cytoplasmic membrane staining. Staining within a tumor is often homogeneous rather than patchy if PTEN is present. Cytoplasmic staining is often diffuse rather than membranous. (pPTEN Antibody CellSignaling. 400X mag).

METHODS

1. Paraffin-embedded tissue is cut at 4–5 μm and placed in a water bath with a temperature of 39°C.
2. Sections are picked up and placed on Superfrost Plus slides.
3. The slides are allowed to dry overnight and then placed in a 60°C oven and baked for 1 hr.
4. Tissue sections are deparaffinized and rehydrated through xylene and grades of reagent alcohol.
   - ▲ Xylene: three changes for 5 min each.
   - ▲ 100% EtOH: two changes for 5 min each.
   - ▲ 95% EtOH: one change for 5 min.
   - ▲ 70% EtOH: one change for 5 min.
   - ▲ Distilled water: one change for 5 min.
5. Dako Autostainer (These steps may also be performed manually)
   - ▲ Slides are loaded into the stainer.
   - ▲ Slides are placed in 3% hydrogen peroxide for 5 min.
   - ▲ Slides are then rinsed in phosphate buffer saline (PBS) with Tween.
   - ▲ Dako serum-free protein block is applied for 5 min.
   - ▲ Protein block is blown off.
   - ▲ Antihuman PTEN (clone 6H2.1): Antibody diluted 1:100 in Dako antibody diluent and applied for 90 min.
   - ▲ Primary antibody is rinsed off with buffer.

- Secondary antibody Dako LSAB2 link system is applied for 30 min.
- Slides are rinsed with TBS.
- Tertiary antibody Dako LSAB2 is applied for 30 min.
- Slides are rinsed with TBS (Tris buffered saline).
- Dako DAB chromogen substrate is applied for 1 min.
- Slides are rinsed with TBS.
- Slides are rinsed 2× with distilled water.
- Slides are stained for 1 min with counterstain GillsII hematoxylin.
- Slides are dehydrated with three changes of 100% EtOH for 5 min each.
- Slides are placed in three changes of xylene for 5 min each.
- Slides are coverslipped using Permount.

Note: The manual protocol from Cascade Bioscience is also effective.

PhosphoPTEN: Cell Signaling Technology

MATERIALS

1. Xylene.
2. 100% Reagent alcohol.
3. 95% Reagent alcohol.
4. 80% Reagent alcohol.
5. Distilled water.
6. Quenching solution: 20 ml 3% hydrogen peroxide and 180 ml methanol.
7. Dako target retrieval S1700 solution.
8. Dako buffer: PBS with Tween × 10 stock, 1 part stock 9 parts distilled water.
9. 3% Hydrogen peroxide.
10. Phospho-PTEN (Ser380/Thr382/383) Antibody: dilute 1:100 in Dako antibody diluent.
11. Dako serum-free protein block.
12. Secondary antibody Dako LSAB/Plus link system.
13. Tertiary antibody Dako LSAB/Plus.
14. Dako DAB chromogen substrate.
15. Counterstain Gills II hematoxylin.
16. Steamer or rice cooker.

METHODS

1. Paraffin-embedded tissue is cut at 4–5 μm and placed in a water bath at 39°C.
2. Sections are picked up and placed on Superfrost Plus slides.
3. The slides are allowed to dry overnight then placed in a 60°C oven and baked for 1 hr.
4. Tissue sections are deparaffinized and rehydrated through xylene and grades of reagent alcohol.
   - Xylene: three changes for 5 min each.
   - 100% EtOH: two changes for 5 min each.
   - 95% EtOH: one change for 5 min.
   - 70% EtOH: one change for 5 min.
   - DI water: one change for 5 min.
5. Antigen retrieval (95°C steamer)
   - Place slides in room temperature quenching solution (20 ml 3% hydrogen peroxide to 180 ml methanol) for 5 minutes (quenching of endogenous peroxidase).
   - Place slides in running water for 5 min.
   - Heat Dako target retrieval S1700 solution to 95°C then place slides in solution.
   - Bring the temperature back up to 95°C and leave slides in the solution for 20 min.
   - Take the container out of the steamer, open the lid of the container, and let sit for 20 min.
   - Rinse slides in deionized water.
6. Dako Autostainer
   - Slides are loaded into the stainer.
   - Slides are placed in 3% hydrogen peroxide for 5 min.
   - Slides are rinsed in PBS with Tween.
   - Dako serum-free protein block is applied for 5 min.
   - Protein block is blown off.
   - Phospho-PTEN (Ser380/Thr382/383) Antibody diluted 1:100 in Dako antibody diluent is applied for 90 min.
   - Primary antibody is rinsed off with buffer.
   - Secondary antibody Dako LSAB/Plus link system is applied for 30 min.
   - Slides are rinsed with TBS.
   - Tertiary antibody Dako LSAB/Plus is applied for 30 min.
   - Slides are rinsed with TBS.
   - Dako DAB chromogen substrate is applied for 1 min.
   - Slides are rinsed with TBS.
   - Slides are rinsed 2× with distilled water.
   - Slides are stained for 1 min with counterstain Gills II hematoxylin.
   - Slides are dehydrated with three changes of 100% EtOH for 5 min each.
   - Slides are placed in three changes of xylene for 5 min each.
   - Slides are coverslipped using Permount.

Note: The manual protocol provided in the CellSignaling Technology Product Information Sheet and on the CellSignaling Web site is also effective, although it requires overnight incubation.

A pilot study of phosphoPTEN expression in 14 NSCLCs was undertaken by our laboratory using the Materials and Methods outlined here. Blocks of

formalin-fixed paraffin-embedded archival NSCLCs were retrieved from the files at Tulane University Health Sciences Center. Sections were cut at 4 μm. Similar sections from control blocks of endometrial carcinomas and infiltrating ductal carcinomas of the breast were also prepared. Sections were stained for phosphoPTEN as well as phosphoAkt, p53, and raf. Antigen retrieval was performed by cooking the deparaffinized slides in a commercial rice cooker in preheated 95°C Dako target retrieval solution. After cooling and washing, slides were loaded onto a DakoAutostainer instrument. The slides were treated with 3% H_2O_2 endogenous block for 5 min and then serum-free Dako protein block for 5 min. Primary antibodies were applied at dilutions of 1:100 for phosphoAkt and phosphoPTEN, 1:40 for p53, and 1:50 for raf. Incubation time was 90 min. Secondary antibody (Dako LSAB + Link system) was applied for 30 min. Tertiary antibody (Dako LSAB + Streptavidin HRP) was applied for 30 min. Dako DAB chromogen substrate was applied until light-brown staining was seen (approximately 30 sec). Two runs were performed. In each run there were sections from the control blocks of endometrial carcinomas and infiltrating breast carcinoma as well as negative internal controls consisting of nonneoplastic lung tissue for each NSCLC. PhosphoAkt and phosphoPTEN staining was nuclear and cytoplasmic. Raf staining was cytoplasmic; p53 staining was nuclear. Intensity scoring was performed by counting 100 cells and grading the intensity of staining for each cell on a scale from 0 to 4 and then adding the results so that the maximum intensity score is 400 and the minimum is 0 (Miyamoto *et al.,* 1993). For example, 50 cells × 4 + 20 cells × 3 + 15 cells × 2 + 10 cells × 1 + 5 cells × 0 = 200 + 60 + 30 + 10 + 0 = 300. This score was independently generated two times per sample. Independent scores were within 40 points for each sample. For each sample the average of the two scores was taken. Results are discussed in the following section.

RESULTS AND DISCUSSION

It is well accepted that archival tissue presents special challenges when applying immunohistochemical techniques (Miller *et al.,* 2000; Montero *et al.,* 2003). Duration of fixation, nature of fixative, and other processing conditions including adequacy of tissue dehydration and paraffin block storage conditions are all factors that affect antigen preservation. The conditions prior to, during, and after fixation are often unknown. When considering antigens that are phosphorylated, it becomes even more important to know how quickly the tissue was placed in fixative after being removed from the patient or laboratory animal because dephosphorylation may occur *ex vivo.* These variables, among others, highlight the need for strict control over conditions for handling tissue specimens.

The expected pattern of immunostaining with any of the PTEN antibodies is both cytoplasmic and nuclear (see Figure 17). Although PTEN is a cytoplasmic protein and phosphorylation occurs in the cytoplasm, nuclear staining is also consistently observed in various cell lines and tissue types. The role of PTEN in the nucleus is poorly understood. It is interesting that PTEN has been shown to cross-talk with p53 to enhance transcriptional regulation and apoptotic activity (Mayo *et al.,* 2002). The significance of nuclear staining with PTEN is unclear. Nonetheless, in our study of NSCLCs (methodology discussed earlier), staining was indeed both cytoplasmic and nuclear. Staining was diffuse and consistent throughout the tumors that expressed phosphoPTEN. The same pattern was observed in endometrial and breast carcinomas used as positive controls.

The phosphoPTEN antibody from CellSignaling is polyclonal and was produced by immunizing rabbits with a synthetic phospho-Ser380 peptide corresponding to residues surrounding Ser380 of human PTEN. Nuclear and cytoplasmic staining is expected. The phosphoPTEN antibody detects PTEN only when phosphorylated at Ser380. In our study, we chose to use phosphoPTEN rather than total PTEN so that we could be certain of the activation state of this protein. PhosphoPTEN is inactive and incapable of inhibiting phosphorylation of PI3 kinase. That is, phosphoPTEN is ineffective as a tumor suppressor and as an inhibitor of Akt survival signaling. Antibodies against total PTEN identify both nonphosphorylated PTEN and phosphoPTEN, thereby producing results difficult to analyze with respect to pAkt. If total PTEN is expressed synchronously with pAkt in a tumor, questions remain: would this result mean that PTEN is mutated, in a phosphorylated form, or simply present as a bystander in cellular signaling activity? Using the phosphorylated form permits more insight into the pathway. If pAkt expression correlates with pPTEN expression, as our preliminary data suggest, then a new hypotheses may be generated, namely that in NSCLC, Akt activation occurs when PTEN is inactivated.

Quantitation of staining can be performed by the usual methods, either visually or by computer-assisted image analysis. This task is facilitated because generally a tumor is either mostly positive or completely negative. Tumors generally do not show scattered positive cells. Results may be expressed as a percentage of tumor cells positive. Staining intensity may be

reported, although this parameter does not seem to be of significance.

For research purposes, we used a combined intensity score, originally reported by Miyamota *et al.* (1993), and described here on p. 98. This system is most useful for comparing positive samples. An alternative scoring system that is well accepted is somewhat more subjective but is practical, given that PTEN staining is generally homogenous. An overall score of 0,1,2, or 3 is assigned as follows.

0: No appreciable staining in tumor cells
1: Barely detectable staining in cytoplasm, nucleus, or both, as compared with stromal elements
2: Readily appreciable brown staining distinctly marking the tumor cell cytoplasm or tumor cell nucleus, or both
3: Dark brown staining in tumor cells completely obscuring the cytoplasm or nucleus, or both

This scoring system has been reported previously (Freitas *et al.,* 2003) for purposes of statistical analysis, we consider scores of 0 or 1 to be negative, and scores of 2 or 3 to be positive. We have successfully used this system to relate expression of pAKt to survival outcome in patients with lung cancer (David *et al.,* 2004).

The PTEN antibodies seem to work best in tumors in which PTEN expression has already been extensively studied. Although we developed the phosphoPTEN antibody to investigate NSCLCs, this antibody works most reliably in endometrial carcinomas and glioblastomas.

In the pilot study of NSCLCs undertaken by our laboratory, we demonstrated that archival formalin-fixed NSCLCs are amenable to immunohistochemical staining with antibodies against both phosphoPTEN and phosphoAkt (CellSignaling Technology) as well as p53 and raf (Dako, Carpinteria, CA). Fourteen recent archival formalin-fixed, paraffin-embedded NSCLCs were retrieved from the files. Sections were cut for H&E (hematoxylin and eosin) staining to confirm the presence of NSCLC. All 14 samples had internal controls consisting of nonneoplastic lung tissue. Additional sections were cut for immunostaining. The p53 antibody was a D07 clone. Nuclear staining was expected. The phosphoAkt antibody was produced by immunizing rabbits with a synthetic phospho-Ser473 peptide corresponding to residues surrounding phosphorylation site Ser473 of human Akt. Nuclear and cytoplasmic staining was expected.

Raf is a downstream effector inhibited by Akt and was included to validate the methodology. Cytoplasmic staining was expected. The mitogen-activated protein kinase, c-raf is the main effector recruited by guanosine triphosphate (GTP)-bound ras so as to activate the MAP kinase pathway. Binding of raf to 14-3-3 is required for c-raf kinase activity and also blocks the ability of phosphatases to inhibit c-raf. 14-3-3 binds to c-raf at two phospho-serine residues: Ser259 and Ser621. Mutation of Ser259 to alanine constitutively activates raf kinase activity, but mutation of Ser621 to alanine results in an inactive kinase. The kinase or kinases that phosphorylate these serine residues have not been fully elucidated. However, Akt-mediated phosphorylation of Ser259 has been shown *in vivo* to inhibit raf kinase activity (Zimmermann *et al.,* 1999).

The results of our pilot study of NSCLCs showed that 12 of 14 NSCLCs demonstrated parallel expression of phosphoAkt and phosphoPTEN, supporting the hypothesis that in NSCLC, Akt activation (i.e., phosphorylation) occurs when PTEN is inactivated (i.e., phosphorylated). The average difference in Miyamoto scoring for phosphoAkt and phosphoPTEN for the 12 tumors was 50 points. The 2 discrepant tumors showed strong phosphoAkt staining and weak pohosphoPTEN staining. Of the 12 tumors, 8 demonstrated nuclear staining for p53 with average scores of 220. There was no correlation between p53 staining and either phosphoAkt or phosphoPTEN staining. All of the 14 NSCLCs demonstrated raf expression, validating antigen preservation in the tissues studied. The average raf score was 280. These results suggest that further investigation with larger numbers of samples is warranted to elucidate the role of PTEN in regulating cell survival mediated by Akt in NSCLC. These results were presented in poster form at the American Association of Cancer Research meeting in San Francisco (April 2002).

CONCLUSION

The clinical significance of PTEN, an increasingly important and seemingly ubiquitous tumor suppressor, is most apparent in endometrial adenocarcinomas. Mutations are frequent in both preneoplastic and neoplastic endometrial lesions. Many different mutations have been identified. Promoter methylation and microsatellite instability have also been implicated as mechanisms of PTEN inactivation, which seems to be an early event in endometrial carcinogenesis. More significantly, loss of the PTEN protein product may be identified by routine immunohistochemical techniques and is considered an unfavorable prognostic indicator. The role of PTEN in other tumor systems with respect to tumor progression and metastasis appears to be varied and cell-type dependent.

The role of the PTEN protein product, a dual-specificity phosphatase, is negative regulation of the PI3 kinase/Akt cell survival pathway. More specifically,

PTEN phosphorylates PI3 at the 3′ position, thereby preventing the activation of numerous downstream pathways, which would otherwise promote cell survival. There may, of course, be other as-yet-unelucidated mechanisms of action.

Concerning immunohistochemical techniques related to the identification of PTEN protein products, it is important to distinguish between antibodies that detect total PTEN (both phosphorylated and unphosphorylated forms), unphosphorylated PTEN (the active form) and phosphorylated PTEN (the inactive form). Antibodies against total PTEN are available but have not proved reliable by routine immunohistochemical techniques. The phosphorylated PTEN antibody is more commonly applied in experimental settings to elucidate mechanisms of tumorigenesis or cell development. The nonphosphorylated PTEN antibody is more commonly applied in clinical settings, generally for endometrial carcinomas and glioblastomas. In this context staining is generally performed to detect loss of PTEN expression, which is generally a poor prognostic indicator. Staining is generally diffuse in tumors that express PTEN and completely negative in tumors in which PTEN expression is lost. Positive staining is cytoplasmic, either membranous or diffuse, and nuclear, although the function of PTEN in the nucleus is unknown. The most important clinical application of PTEN immunohistochemistry is to gain prognostic information about preneoplastic and neoplastic endometrial lesions.

References

Alessi, D.R., Andjelkovic, M., Caudwell, B., Cron, P., Morrice, N., Cohen, P., and Hemmings, B.A. 1996. Mechanism of activation of protein kinase B by insulin and IGF-1. *EMBO J. 15*:6541–6551.

An, H.J., Lee, Y.H., Cho, N.H., Shim, J.Y., Kim, J.Y., Lee, C., and Kim, S.J. 2002. Alteration of PTEN expression in endometrial carcinoma is associated with down-regulation of cyclin-dependent kinase inhibitor, p27. *Histopathology 41*:437–445.

Bachelder, R.E., Ribick, M.J., Marchetti, A., Falcioni, R., Soddu, S., Davis, K.R., and Mercurio, A.M. 1999. p53 inhibits alpha 6 beta 4 integrin survival signaling by promoting the caspase 3-dependent cleavage of AKT/PKB. *J. Cell. Biol. 147*:1063–1072.

Beckman, S., Stambolic, V., and Mak, T. 2002. PTEN function in mammalian cell size regulation. *Curr. Opin. Neurobiol. 12*:516–522.

Bonneau, D., and Longy, M. 2000. Mutations of the human PTEN gene. *Hum. Mutat. 16*:109–122.

Brognard, J., Clark, A.S., Ni, Y., Dennis, P.A. 2001. Akt/protein kinase B is constitutively active in non-small cell lung cancer cells and promotes cellular survival and resistance to chemotherapy and radiation. *Cancer Res. 61*:3986–3997.

Brunet, A., Bonni, A., Zigmond, M.J., Lin, M.Z., Juo, P., Hu, L.S., Anderson, M.J., Arden, K.C., Blenis, J., and Greenberg, M.E. 1999. Akt promotes cell survival by phosphorylating and inhibiting a Forkhead transcription factor. *Cell 96*:857–868.

Campbell, R.A., Bhat-Nakshatri, P., Patel, N.M., Constantinidou, D., Ali, S., Nakshatri, H. 2001. Phosphatidylinositol 3-kinase/AKT-mediated activation of estrogen receptor alpha: A new model for anti-estrogen resistance. *J. Biol. Chem. 276*:9817–9824.

Cantley, L.C., and Neel, B.G. 1999. New insights into tumor suppression: PTEN suppresses tumor formation by restraining the phosphoinositide 3-kinase/AKT pathway. *Proc. Natl. Acad. Sci. USA 96*:4240–4245.

Cuello, M., Ettenberg, S.A., Clark, A.S., Keane, M.M., Posner, R.H., Nau, M.M., Dennis, P.A., and Lipkowitz, S. 2001. Down-regulation of the erbB-2 receptor by trastuzumab (herceptin) enhances tumor necrosis factor-related apoptosis-inducing ligand-mediated apoptosis in breast and ovarian cancer cell lines that overexpress erbB-2. *Cancer Res. 61*:4892–4900.

Dahia, P.L. 2000. PTEN, a unique tumor suppressor gene. *Endocr. Relat. Cancer 7*:115–129.

David, O., Jett, J., LeBeau, H., Dy, G., Hughes, J., and Friedman, M. 2004. PhosphoAkt overexpression in non-small cell lung cancer confers significant stage-independent survival disadvantage. *Clin. Cancer Res. 10*:6860–6871.

Davies, M.A., Kim, S.J., Parikh, N.U., Dong, Z., Bucana, C.D., and Gallick, G.E. 2002. Adenoviral-mediated expression of MMAC/PTEN inhibits proliferation and metastasis of human prostate cancer cells. *Clin. Cancer Res. 8*:1904–1914.

Davies, M.A., Koul, D., Dhesi, H., Berman, R., McDonnell, T.J., McConkey, D., Yung, W.K., and Steck, P.A. 1999. Regulation of Akt/PKB activity, cellular growth, and apoptosis in prostate carcinoma cells by MMAC/PTEN. *Cancer Res. 59*:2551–2556.

Di Cristofano, A., and Pandolfi, P.P. 2000. The multiple roles of PTEN in tumor suppression. *Cell 100*:387–390.

Fernandez, M., and Eng, C. 2002. The expanding role of PTEN in neoplasia: A molecule for all seasons? *Clin. Cancer Res. 8*:1904–1914.

Freitas, S., Moore, D.H., Michael, H., and Kelley, M.R. 2003. Studies of apurinic/apyrimidic endonuclease/ref-1 expression in epithelial ovarian cancer: Correlations with tumor progression and platinum resistance. *Clin. Cancer Res. 9*:4689–4694.

Grünwald, V., DeGraffenried, L., Russel, D., Friedrichs, W.E., Ray, R.B., and Hidalgo, M. 2002. Inhibitors of mTOR reverse doxorubicin resistance conferred by PTEN status in prostate cancer cells. *Cancer Res. 62*:6141–6145.

Haas-Kogan, D., Shaley, N., Wong, M., Mills, G., Yount, G., and Stokoe, D. 1998. Protein kinase B (PKB/Akt) activity is elevated in glioblastoma cells due to mutation of the tumor suppressor PTEN/MMAC. *Curr. Biol. 8*:1195–1198.

Hong, T.M., Yang, P.C., Peck, K., Chen, J.J., Yang, S.C., Chen, Y.C., and Wu, C.W. 2000. Profiling the downstream genes of tumor suppressor PTEN in lung cancer cells by complementary DNA microarray. *Am. J. Respir. Cell. Mol. Biol. 23*:355–363.

Huncharek, M., Muscat, J., and Geschwind, J.F. 1999. K-ras oncogene mutation as a prognostic marker in non–small cell lung cancer: A combined analysis of 881 cases. *Carcinogenesis 20*:1507–1510.

Hutchinson, J., Jin, J., Cardiff, R.D., Woodgett, J.R., and Muller, W.J. 2001. Activation of Akt (protein kinase B) in mammary epithelium provides a critical cell survival signal required for tumor progression. *Mol. Cell. Biol. 21*:2203–2212.

Kanamori, Y., Kigawa, J., Itamochi, H., Shimada, M., Takahashi, M., Kamazawa, S., Sato, S., Akeshima, R., and Terakawa, N. 2001. Correlation between loss of PTEN expression and Akt phosphorylation in endometrial carcinoma. *Clin. Cancer Res. 7*: 892–895.

Kandasamy, K., and Srivastava, R.K. 2002. Role of the Phosphatidylinositol 3′-kinase/PTEN/Akt Kinase pathway in tumor necrosis factor-related apoptosis-inducing ligand-induced apoptosis in non–small cell lung cancer cells. *Cancer Res. 62*:4929–4937.

Kohno, T., Takahashi, M., Manda, R., and Yokota, J. 1998. Inactivation of the PTEN/MMAC1/TEP1 gene in human lung cancers. *Genes Chromosomes Cancer 22*:152–156.

Latta, E., and Chapman, W.B. 2002. PTEN mutations and evolving concepts in endometrial neoplasia. *Curr. Opin. Obstet. Gynecol. 14*:59–65.

Mayo, L.D., and Donner, D.B. 2002. The PTEN, Mdm2, p53 tumor supressor-oncoprotein network. *Trends Biochem. Sci. 27*:462–467.

Miller, R.T., Swanson, P.E., and Wick, M.R. 2000. Fixation and epitope retrieval in diagnostic immunohistochemistry: A concise review with practical considerations. *Appl. Immunohistochem. Mol. Morphol. 8*:228–235.

Minaguchi, T., Yoshikawa, H., Oda, K., Ishino, T., Yasugi, T., Onda, T., Nakagawa, S., Matsumoto, K., Kawana, K., and Taketani, Y. 2001. PTEN mutation located only outside exons 5, 6, and 7 is an independent predictor of favorable survival in endometrial carcinomas. *Clin. Cancer Res. 7*:2636–2642.

Miyamoto, K.K., McSherry, S.A., Dent, G.A., Sar, M., Wilson, E.M., French, F.S., Sharief, Y., and Mohler, J.L. 1993. Immunohistochemistry of the androgen receptor in human benign and malignant prostate tissue. *J. Urol.* 149:1015–1019.

Montero, C. 2003. The antigen-antibody reaction in immunohistochemistry. *J. Histochem. Cytochem. 51*:1–4.

Mutter, G.L., Lin, M.C., Fitzgerald, J.T., Kum, J.B., Baak, J.P., Lees, J.A., Weng, L.P., and Eng, C. 2000. Altered PTEN expression as a diagnostic marker for the earliest endometrial precancers. *J. Natl. Cancer Inst. 92*:924–930.

Myers, M.P., Pass, I., Batty, I.H., Van der Kaay, J., Stolarov, J.P., Hemmings, B.A., Wigler, M.H., Downes, C.P., and Tonks, N.K. 1998. The lipid phosphatase activity of PTEN is critical for its tumor supressor function. *Proc. Natl. Acad. Sci. USA 95*:13513–13518.

Nakashio, A., Fujita, N., Rokudai, S., Sato, S., and Tsuruo, T. 2000. Prevention of phosphatidylinositol 3′-kinase-Akt survival signaling pathway during topotecan-induced apoptosis. *Cancer Res. 60*:5303–5309.

Pérez-Tenoria, G., and Stål, O. 2002. Activation of AKT/PKB in breast cancer predicts a worse outcome among endocrine treated patients. *Br. J. Cancer 86*:540–545.

Risinger, J.I., Hayes, K., Maxwell, G.L., Carney, M.E., Dodge, R.K., Barrett, J.C., and Berchuck, A. 1998. PTEN mutation in endometrial cancers is associated with favorable clinical and pathologic characteristics. *Clin. Cancer Res. 4*:3005–3010.

Sabbatini, P., and McCormick, F. 1999. Phosphoinositide 3-OH kinase (PI3K) and PKB/Akt delay the onset of p53-mediated, transcriptionally dependent apoptosis. *J. Biol. Chem. 274*: 24263–24269.

Salvesen, H.B., MacDonald, N., Ryan, A., Jacobs, I.J., Lynch, E.D., Akslen, L.A., and Das, S. 2001. PTEN methylation is associated with advanced stage and microsatellite instability in endometrial carcinoma. *Int. J. Cancer 91*:22–26.

Stambolic, V., Suzuki, A., de la Pompa, J.L., Brothers, G.M., Mirtsos, C., Sasaki, T., Ruland, J., Penninger, J.M., Siderovski, D.P., Mak, T.W. 1998. Negative regulation of PKB/Akt-dependent cell survival by the tumor suppressor PTEN. *Cell 95*:29–39.

Sun, H., Enomoto, T., Fujita, M., Wada, H., Yoshino, K., Ozaki, K., Nakamura, T., and Murata. Y. 2001. Mutational analysis of the PTEN gene in endometrial carcinoma and hyperplasia. *Am. J. Clin. Pathol. 115*:32–38.

Tashiro, H., Blazes, M.S., Wu, R., Cho, K.R., Bose, S., Wang, S.I., Li, J., Parsons, R., and Ellenson, L.H. 1997. Mutations in PTEN are frequent in endometrial carcinoma but rare in other common gynecological malignancies. *Cancer Res. 57*:3935–3940.

Torres, J., and Pulido, R. 2001. The tumor suppressor PTEN is phosphorylated by the protein kinase CK2 at its C terminus. Implications for PTEN stability to proteasome- mediated degradation. *J. Biol. Chem. 276*:993–998.

Vivanco, I., and Sawyers, C.L. 2002. The phosphatidylinositol 3-Kinase AKT pathway in human cancer. *Nat. Rev. Cancer 2*:489–501.

Waite, K.A., and Eng, C. 2002. Protean PTEN: Form and function. *Am. J. Hum. Genet. 70*:829–844.

Weng, L., Brown, J., and Eng, C. 2001. PTEN induces apoptosis and cell cycle arrest through phosphoinositol-3-kinase/Akt-dependent and -independent pathways. *Hum. Mol. Genet. 10*:237–242.

Zhou, X.P., Loukola, A., Salovaara, R., Nystrom-Lahti, M., Peltomaki, P., de la Chapelle, A., Aaltonen, L.A., and Eng, C. 2002. PTEN mutational spectra, expression levels, and subcellular localization in microsatellite stable and unstable colorectal cancers. *Am. J. Pathol. 161*:439–447.

Zimmermann, S., and Moelling, K. 1999. Phosphorylation and regulation of Raf by Akt (protein kinase B). *Science 286*:1741–1744.

10

The Role of *p53* and *p73* Genes in Tumor Formation

Ute M. Moll and Neda Slade

Gene Architecture of the p53 Family

The *p53* gene controls a powerful stress response by integrating upstream signals from many types of deoxyribonucleic acid (DNA) damage and inappropriate oncogenic stimulation, all of which lead to p53 activation. Activated p53 elicits apoptosis; cell-cycle arrest; and, in some circumstances, senescence, thereby preventing the formation of tumors. Hence, loss of p53 function is a preeminent finding in most human cancers, whether directly through mutation of p53 (the most common mechanism), impaired nuclear retention of p53, loss of the upstream activator p14ARF, or amplification of the p53 antagonist HDM2.

In 1997 two novel family members were identified and termed p73 (Kaghad *et al.,* 1997) and p63 (Osada *et al.,* 1998; Schmale and Bamberger, 1997). Based on their remarkable structural similarity with p53, p63 and p73 generated instant excitement and expectations about their biological functions. Several years later we have unearthed striking similarities but also surprising diversities. Both genes give rise to proteins that have 1) entirely novel functions and 2) p53-related functions. Moreover, the p53-related functions are either of a p53-agonistic or antagonistic nature. Both p63 and p73 share more than 60% amino acid identity with the DNA-binding region of p53 (and even higher identity amongst themselves), including conservation of all DNA contact and structural residues that are hotspots for p53 mutations in human tumors. In addition, p73 shows 38% identity with the p53 tetramerization domain and 29% identity with the p53 transactivation domain. In vertebrates, the p73 and p63 genes are ancestral to p53 and possibly evolved from a common p63/p73 archetype (Kaghad *et al.,* 1997; Yang *et al.,* 1998).

In contrast to the simple gene structure of TP53, which is highly conserved from mollusk to human, the structures of the TP 63 and TP 73 genes are complex (Figure 18). The three most conserved domains in all three genes are the N-terminal transactivation domain (TA), the central DNA-binding domain (DBD), and the C-terminal oligomerization domain (OD). The TP53 gene has a single promoter that encodes a single protein of 393 amino acids (human p53). In contrast to TP53, TP63 and TP73 have two promoters, P1 in the 5′UTR upstream of the noncoding exon 1 and P2 located within the 23-kb spanning intron 3. The P1 and P2 promoters produce two diametrically opposed classes of proteins: those containing the transactivation domain (TAp63, TAp73) and those lacking it (ΔNp63 and ΔNp73). The latter two occur in the human and mouse. In addition, alternative exon splicing of the P1

Handbook of Immunohistochemistry and *in situ* Hybridization of Human Carcinomas, Volume 3: Molecular Genetics, Liver Carcinoma, and Pancreatic Carcinoma

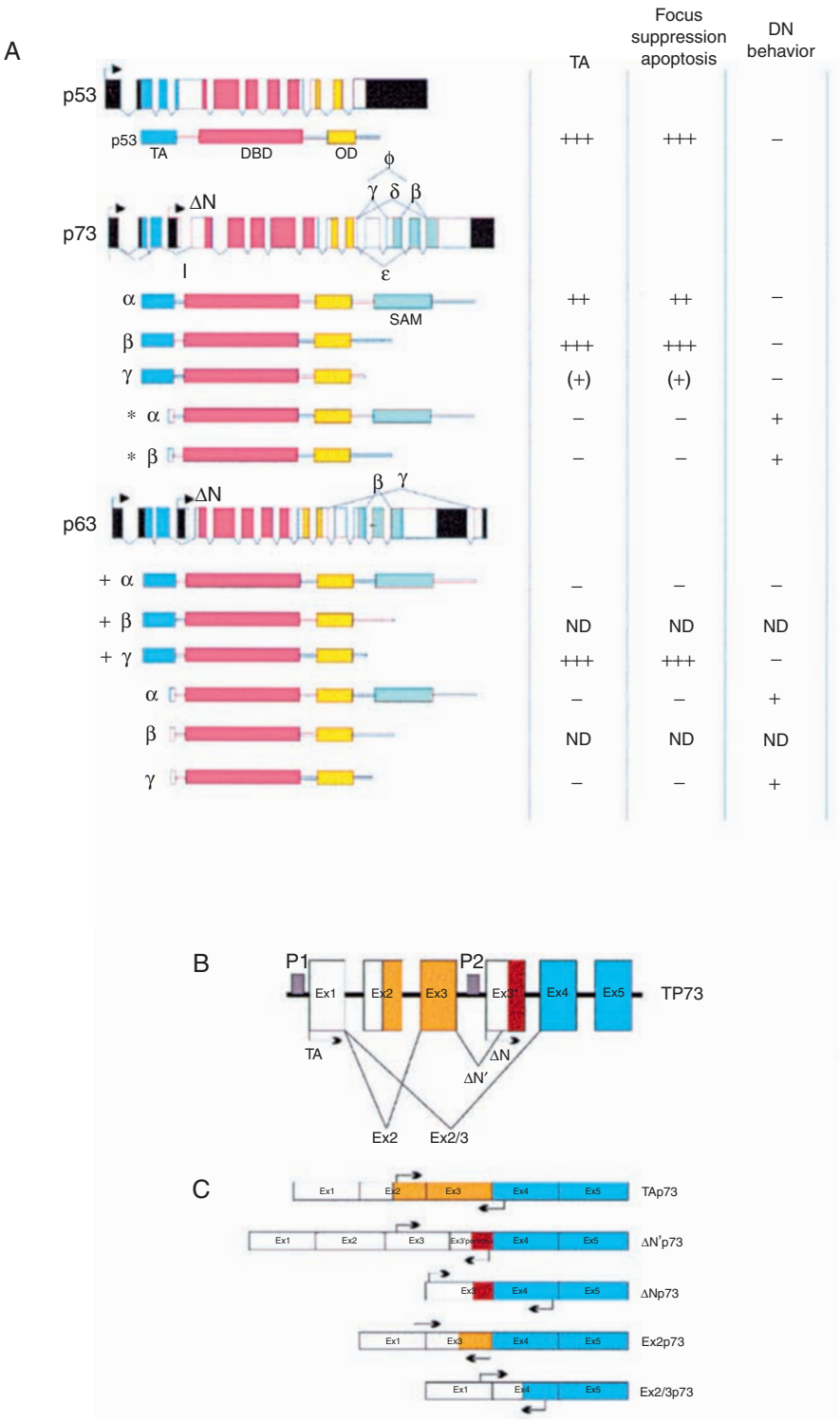

Figure 18. For legend, see opposite page.

Figure 18. **A:** Gene Architecture of the p53 family. In contrast to the simple structure of the p53 protein, which harbors the transactivation domain (TA), the DNA-binding domain (DBD), and the oligomerization domain (OD) as the three major modules, the products of TP73 and TP63 are complex and contain a C-terminal sterile alpha motif (SAM) domain in the alpha version. Both genes contain two promoters. The P1 promoter in the 5′ UTR region produces full-length proteins containing the TA domain, whereas the P2 promoter produces TA-deficient proteins with dominant-negative functions toward themselves and toward p53. In addition, extensive C-terminal splicing and, in the case of TP73 additional N-terminal splice variants of the P1 transcript, further modulate the p53-like functions of the TA-proteins (see columns). **B, C:** The complete set of N-terminal transcripts encoding TAp73 and four different ΔTAp73 isoforms. **B:** Gene architecture of the N-terminus of *TP73*. The transactivation-competent TAp73 and the splice forms Ex2p73, Ex2/3p73, and ΔN′p73 are all generated from the P1 promoter, whereas the P2 promoter in Intron 3 produces the transactivation deficient ΔNp73, starting with the unique exon 3′. Arrows indicate transcriptional start sites. **C:** Positions of the reverse transcription-polymerase chain reaction primer pairs for the various p73 isoforms used to measure all isoforms in tumor tissue: *white,* untranslated sequences; *yellow,* transactivation domain; *red,* exon 3′ derived coding sequences; *blue,* DNA-binding domain; *green,* translated (but nonproductive sequence) of ΔN′p73 that undergoes a premature stop in the 5′ UTR of exon 3′. The star indicates the used second translational start site in ΔN′p73. In ΔNp73, Ex2p73, and Ex2/3p73 translational start sites are indicated by colored borders.

transcripts of TP73 give rise to other isoforms lacking the transactivation (Kaghad *et al.,* 1997) domain (e.g., ΔN′p73, Ex2Delp73 and Ex2/3Delp73) (Fillippovich *et al.,* 2001; Ishimoto *et al.,* 2002). It is important that the ΔNp73 and ΔN′p73 transcripts encode the *same* protein (as a result of the use of a second translational start site because of an upstream premature stop in ΔN′p73) (Ishimoto *et al.,* 2002). TA proteins mimic p53 function in cell culture including transactivating many p53 target genes and inducing apoptosis, whereas (the collectively called) ΔTA proteins act as dominant negative inhibitors of themselves and of other family members *in vivo* in the mouse and in transfected human cells (Pozniak *et al.,* 2000; Yang *et al.,* 1998). Strikingly, squamous cell carcinoma of the skin produces high levels of ΔNp63α. Moreover, the TP63 locus is contained within a frequently amplified region in this cancer type (Hibi *et al.,* 2000). Furthermore, ΔNp73 is the predominant TP73 product in the developing mouse nervous system and is required to counteract the proapoptotic action of p53 (Pozniak *et al.,* 2000; Yang *et al.,* 2000) (see later in this chapter).

Additional complexity is generated at the C-terminus: TP73 and TP63 undergo multiple C-terminal splicings of exons 10–14, skipping one or several exons. So far nine transcripts were found for TP73, called α, β, γ, δ, ε, ζ, η, η1, and φ (α being full length) and three for TP63, called α, β, and γ. The p73 isoforms φ, η, and η1, lack the second C-terminal transactivation domain and the tetramerization domain encoded by exon 10. In some C-terminal isoforms, exon splicing also leads to unique sequences because of frameshifts. For TP63, three isotypes (α, β, and γ) are made. Splicing of different "tails" further modulates the p53-like function of TA proteins, although they do not appear to vary much in their role in tumorigenesis. Structurally, the γ forms of TP73 and TP63 most closely resemble p53, harboring just a small C-terminal extension beyond the last 30 amino acid stretch of p53. Surprisingly, however, whereas TAp63γ is as powerful as p53 in transactivation and apoptosis assays (Yang *et al.,* 1998), TAp73γ is rather weak. The α forms of TP73 and TP63 contain an additional highly conserved SAM (sterile alpha motif), which are protein interaction modules found in a wide variety of proteins implicated in development. The crystal and solution structure of p73 SAM agree with each other and feature a five-helix bundlefold that is characteristic of all SAM domain structures (Chi *et al.,* 1999; Wang *et al.,* 2001). Other SAM-containing proteins are the ETS transcription factor TEL (translocation-ETS-leukemia) that plays a role in leukemia, the polycomb group of homeotic transcription factors, and the ephrin receptors, among others. There are also functional differences between TAp73α and TAp63α. Whereas TAp73α is comparable to p53 in transactivation and apoptosis assays, TAp63α is very weak (Yang *et al.,* 1998). The reason for this difference is not obvious from the structure and remains unclear. In general, more structure-function analysis is needed to understand why and how C-terminal variations influence function.

In summary, by using alternate exon splicing and an alternative promoter, TP73 and TP63 genes can generate an impressive modular complexity by combining a specific "head" with a particular "tail." In practice, this means that our understanding of their biological roles will greatly depend on knowing which forms are expressed under what circumstances.

TP63 and TP73 Play Important Roles in Development and Differentiation

Both genes play important and, despite their structural similarity, surprisingly unique roles in mouse and human development. This is powerfully revealed by the striking developmental phenotypes of p63- and p73-deficient mice (Mills *et al.,* 1999; Yang *et al.,* 1999; Yang *et al.,* 2000) and is in contrast to p53-null mice, which are highly tumor prone but lack a developmental phenotype.

TP63 expression is essential for limb formation and epidermal morphogenesis (integument, tongue) including the formation of adnexa. Animals that are p63 null show severe limb truncations or even absence of limbs as well as craniofacial malformations. They also fail to develop skin, prostate, and mammary glands (a skin adnexa). Reminiscent of the knockout phenotype in mice, heterozygous germline mutations of p63 in humans cause the rare autosomal-dominant developmental disorders EEC (ectrodactyly, ectodermal dysplasia, facial clefts) and AEC (ankyloblepharon ectodermal dysplasia clefting, Hay-Wells syndrome). The p63 mutations found in patients with EEC are typically missense mutations within the DNA-binding domain. These EEC mutations inhibit DNA binding of the TAp63 forms. Conversely, EEC mutations in ΔNp63 proteins cause a loss of their dominant-negative properties toward p53 and TAp63γ (Celli *et al.,* 1999). The p63 mutations associated with AEC are in the SAM domain and the mutant cannot interact with apobec-1-binding protein-1 (ABBP-1). Without this interaction there is no alternative splicing of the K-SAM isoform of FGFR-2 that leads to the inhibition of epithelial differentiation and accounts for the AEC phenotype (Fomenkov *et al.,* 2003). It is important to note that basal cells of normal human epithelium including the epidermis strongly express p63 proteins, predominantly the ΔNp63 isotype (Yang *et al.,* 1998) but lose them as soon as these cells withdraw from the stem cell compartment (Pellegrini *et al.,* 2001). Consistent with this notion, keratinocyte differentiation is associated with the disappearance of ΔNp63α (Nylander *et al.,* 2000; Parsa *et al.,* 1999; Westfall *et al.,* 2003), whereas the expression of p53 target genes p21 and 14-3-3σ, mediating cell cycle arrest, increase. Together, these data clearly establish a fundamental role of p63 in keratinocyte stem cell biology and the apical ectodermal ridge of the limb bud (Pellegrini *et al.,* 2001). Whether this role is the likely one in stem cell self-renewal or in stem cell differentiation into stratified epithelium remains a matter of controversy (Mills *et al.,* 1999; Yang *et al.,* 1999). What appears clearer is that p63 is probably not simply required for the proliferative capacity of stem cells because their immediate progeny, the TAC cells, are equally proliferative but have already lost p63 expression (Pellegrini *et al.,* 2001). Expression of p63 is indispensable for the differentiation of a transitional urothelium (Urist *et al.,* 2002). Consistent with this notion, p63 is expressed in normal bladder urothelium and lost in most invasive bladder cancers.

TP73 also has distinct developmental roles. TP73 expression is required for neurogenesis of hippocampal structures, for pheromonal signaling, and for normal fluid dynamics of cerebrospinal fluid and the respiratory mucosa (Yang *et al.,* 2000). The hippocampus is central to learning and memory and continues to develop throughout adulthood. The basis of hippocampal dysgenesis in p73-deficient mice is the selective loss of large bipolar neurons called Cajal-Retzius (CR) cells. CR neurons co-express p73 and the secretory glycoprotein reelin, which is essential for neuronal migration into the cortex (Yang *et al.,* 2000). In addition, p73 null mice suffer from hydrocephalus, probably as a result of hypersecretion of cerebrospinal fluid by the choroid plexus and from purulent but sterile excudates of the respiratory mucosa. Moreover, the animals show abnormal reproductive and social behavior, which in rodents is governed by pheromone sensory pathways and regulated by the vomeronasal organ, which normally expresses high levels of p73. The predominant form in the developing mouse brain is ΔNp73 (Pozniak *et al.,* 2000; Yang *et al.,* 1998). Moreover ΔNp73 is the *only* form of p73 found in mouse brain and the sympathetic superior cervical ganglia in neonatal mice. It plays an essential anti-apoptotic role *in vivo,* and is required to counteract p53-mediated neuronal death during the normal "sculpting" of the developing mouse neuronal system (Pozniak *et al.,* 2000). Withdrawal of nerve growth factor (NGF), an obligate survival factor for mouse sympathetic neurons, leads to p53 induction and p53-dependent cell death. Conversely, NGF withdrawal leads to a *decrease* of ΔNp73. It is important, that sympathetic neurons are *rescued* from cell death after NGF withdrawal when ΔNp73 levels are maintained by viral delivery. These data put ΔNp73 downstream of NGF in the NGF survival pathway.

In tissue culture models, p73 also plays a role in differentiation of several cell lineages. Expression of TP73 increases during retinoic acid–induced and spontaneous differentiation of neuroblastoma cells (Kovalev *et al.,* 1998). Moreover, expression of specific C-terminal isoforms correlate with normal myeloid differentiation. p73α and β are associated with normal myeloid differentiation, whereas p73 γ, δ, ε, and θ are associated with leukemic blasts (Tschan *et al.,* 2000). This suggests

a p73-specific differentiation role that is not shared by p53 or p63.

The p53 gene has an important developmental role in early mouse embryogenesis, as revealed when the autoregulatory feedback loop with MDM2 is removed and p53 levels remain uncontrolled. Nevertheless, in stark contrast to TP63 and TP73 null mice, TP53 null mice make it through development with essentially no problems (with the exception of rare exencephaly in females). A commonly offered explanation is that p53 functions are covered by redundant p63 and p73 functions. The finding that ΔN isoforms, rather than TA isoforms, are the predominant proteins of TP63 and TP73 during development could be viewed as evidence for the important *in vivo* role of ΔN isoforms during development because, conversely, p53 cannot substitute for those forms. Of note, p73-deficient mice lack *spontaneous* tumor formation, even after a 2-year observation period (Yang *et al.,* 2000). Although the tumor rate after mutagenic challenge or the tumor rate of double p53/p73 null mice is currently unknown, this result is another clear difference between p53 and the other family members. It indicates that if TP73 and TP63 do have a role in tumor formation, it might be a complex one that is probably not revealed by simply eliminating the entire gene.

Expression of the p73 gene occurs at very low levels in all normal human tissues studied, making detection difficult. p63, mainly its ΔN form, occurs at higher levels and is readily detectable at the protein level. Expression of p63 is restricted to the nuclei of basal cells of normal epithelia (skin, esophagus, tonsil, prostate, urothelium, ectocervix, vagina) and to certain populations of basal cells in glandular structures of prostate, breast, and bronchi (Yang *et al.,* 1998). Specifically, p63 is expressed in myoepithelial cells of the breast, a specific marker for those cells in normal breast tissue (Ribeiro-Silva *et al.,* 2003a). The expression of p63 in prostate is restricted to basal cells and is used in the diagnosis of prostate cancer (Davis *et al.,* 2002).

Transcriptional and Apoptotic Activity of p63 and p73

Many functional parallels are found among p53, TAp73, and TAp63 and between ΔNp73 and ΔNp63. When ectopically overexpressed in cell culture, p73α and β closely mimic the transcriptional activity and biological function of p53. Both p73β and p73α, to a lesser extent, bind to canonical p53 DNA-binding sites and transactivate many p53-responsive promoters. In reporter assays, p73-responsive promoters include well-known p53 target genes involved in anti-proliferative and proapoptotic cellular stress responses such as p21WAF1,14-3-3σ, GADD45, BTG2, PIGs, ribonucleotide reductase p53R2, and IGFBP3. Bax transactivation is controversial. TAp73α and β also induce MDM2. Conversely, ectopic p73 overexpression leads to transcriptional repression of VEGF, analogous to the ability of p53 to transcriptionally suppress VEGF. Although there are probably still dozens of common targets that have not yet been described or discovered, it will be important to identify p63/p73-preferred or p63/p73-specific targets. For example, 14 novel target genes that are differentially regulated by various p53 family members were identified in 2003 (Chen *et al.,* 2003). In summary, there are common and perhaps preferred target genes for each p53 family member and its isoforms.

The domains of p73β (the most potent form in transactivation and growth arrest) necessary for inducing cell cycle arrest are the TA domain, the DNA-binding domain, and the tetramerization domain. However, unlike p53, p73-mediated apoptosis does not require the PXXP region or the entire C-terminal region. It is interesting that PXXP motifs, although dispensable for p73 apoptotic function, render p73 inactive in transactivation when deleted (Nozell *et al.,* 2003).

A surprising "essential cooperativity" among family members for transcriptional function has been found. In response to DNA damage, induction of p21/WAF (mediating cell cycle arrest) occurred normally in $p63^{-/-}$ and $p73^{-/-}$ single-null mouse embryo fibroblasts (MEFs) and in $p63/p73^{-/-}$ double-null MEFs. However, in double-null MEFs, the induction of bax, Noxa, and PERP genes (thought to mediate apoptosis) was suppressed. Chromatin immunoprecipitation assays (ChIP) confirmed that there is no binding of p53 to the bax, PERP, and NOXA promoters in the absence of p63 and p73, whereas, conversely, p63 still binds to them in $p53^{-/-}$ single-null MEFs. These data demonstrate that both p63 and p73 are essential for p53-induced apoptosis (Flores *et al.,* 2002).

Ectopic p73 promotes apoptosis in human tumor cell lines independent of their p53 status. Potency differences exist among the C-terminal isoforms. Overexpression of p73α, β, and δ suppresses focus formation of p53-deficient Saos-2 cells, whereas p73γ fails or suppresses only very poorly (De Laurenzi *et al.,* 1998; Ishida *et al.,* 2000; Jost *et al.,* 1997). Similarly, TAp63α lacks significant transcriptional and apoptotic ability, whereas TAp63γ is very potent in both (Yang *et al.,* 1998). However, cells overexpressing TAp63γ, TAp63α, ΔNp63α, and ΔNp63γ showed poor or no detectable apoptosis compared to overexpressed p53 or p73α (Dietz *et al.,* 2002). Using gene profiling via microarrays, ΔNp63α and TAp63α regulate a broad

spectrum of genes with diverse roles in cellular function but possess opposing regulatory effects toward each other (Wu *et al.,* 2003).

Regulation of p73 and p63 Protein Stability and Transcriptional Activity

Proteasomes are mediating the turnover of p73 proteins. In contrast to p53, however, this degradation is not mediated by MDM2. The molecular basis for the MDM2 resistance of p73 is region 92-112 of p53, which is absent in p73 and confers MDM2 degradability to p53 (Gu *et al.,* 2000). The p73 protein is also resistant to human papilloma virus (HPV) E6, which together with E6-AP mediates hyperactive degradation of p53 in HPV-infected cells (Balint *et al.,* 1999; Marin *et al.,* 1998). On a transcriptional level, however, the negative feedback regulation between the two genes is preserved. MDM2 is transcriptionally activated by p73 and, in turn, negatively regulates the transcriptional ability of p73, just as it functions toward p53 (Dobbelstein *et al.,* 1999). However, the mechanism is again distinct from that of p53. The binding to MDM2 causes the disruption of physical and functional interaction with p300/CREB (cyclic adenosine monophosphate response element binding factor)-binding protein (CBP), by competing with p73 for binding to the N-terminus of p300/CBP (Zeng *et al.,* 1999). Degradation of p73 might be linked to SUMO-1 (small ubiquitin-related modifier) (Minty *et al.,* 2000). The novel NEDD4-related E3 ubiquitin ligase NEDL2 was identified in 2003 to bind to p73 via its PY motif in the C-terminal region (Nakagawa *et al.,* 2003). However, p53, which lacks the PY motif, does not bind to NEDL2. Overexpression of NEDL2 results in the ubiquitination of p73; however, rather than mediating degradation, it enhances the steady-state level of p73 as well as its ability to transactivate p53/p73-responsive promoters. The differential binding of NEDL2 to p53 family members is thus another factor that might contribute to their functional divergence.

We determined the individual half-lives of all N-and C-terminal isoforms and found they differ only moderately. However, when coexpressed in various cell types, TAp73α/β proteins become markedly stabilized by ΔNp73α/β but are rendered functionally inactive. This is mediated via hetero-oligmerization by the transdominant ΔNp73. In contrast, p53 protein fails to accumulate via ΔNp73 co-expression. In the ongoing debate whether TAp73 is a relevant tumor suppressor, this suggests that increased TAp73 protein levels should be interpreted with caution when levels are the only criteria that can be used to deduce TAp73 activity, as is the case in primary tumors where functional studies are not possible (Slade *et al.,* 2004).

Proteasome inhibitors also stabilize overall levels of p63. In an additional family twist, however, the stability of ΔNp63 isoforms may also be regulated independently of proteasomes and, in fact, may be promoted by physical complex formation with wild-type p53. A protein–protein complex between ΔNp63α and p53, mediated by both DNA-binding domains, can form in cells. Moreover, p53 overexpression reveals p53-dependent degradation of ΔNp63 via a caspase-1 specific pathway (Ratovitski *et al.,* 2001). A check-and-balance system may exist: whereas ΔNp63 is a transcriptional inhibitor of p53, p53 is a stability inhibitor of ΔNp63. This relationship also points toward another level of intimate functional cross-talk among p53 family members, a theme that will surface again and again. Unlike p53 and p73, p63 does not bind to MDM2 at all (Dohn *et al.,* 2001). In summary, the respective E3 ubiquitin ligases for p63 and p73 remain to be identified.

Role of p73 and p63 in Tumors

p73 Is Not a Classic Knudson-Type Tumor Suppressor

The p73 gene maps to chromosome 1p36.33, which frequently undergoes loss of heterozygosity (LOH) in breast and colon cancer, neuroblastoma, and melanoma. This fact, in conjunction with the functional similarity to p53, originally led to the proposal that p73 is a tumor-suppressor gene (Kaghad *et al.,* 1997). Genetic data on most cancer types—with the notable exception of leukemias and lymphomas—however, exclude p73 as a *classic* Knudson-type tumor suppressor, which by definition is targeted to undergo loss of expression or function during tumorigenesis. To date, in a total of more than 1100 primary tumors, loss-of-function mutations in p73 are rare (0.6%). Moreover, imprinting of the p73 locus, initially thought to be an epigenetic explanation to satisfy the two-hit hypothesis (because it would only require one hit of LOH against the transcribed allele), is rather uncommon and, if present, varies from tissue to tissue and person to person and does not correlate with p73 expression levels (Kovalev *et al.,* 1998; Nomoto *et al.,* 1998; Tsao *et al.,* 1999; Zaika *et al.,* 1999). In fact, in lung, esophageal, and renal carcinoma, the second p73 allele is specifically *activated* in tumors (loss of imprinting) (Cai *et al.,* 2000; Mai *et al.,* 1998). As an additional difference from p53, p73 protein fails to be inactivated by most of the major viral oncoproteins that inactivate p53, namely SV40 T antigen and Ad E1B 55 kD. For HPV E6, although clearly not inducing p73 degradation, controversy exists whether E6 of low- and high-risk

strains inactivates the transcription function of p73 (Park *et al.,* 2001; Prabhu *et al.,* 1998). However, *some* viral protein products do target p73, and p73 transcriptional activity is inhibited by Ad E4orf6 and by HTLV 1 Tax. Similarly, p63 also fails to interact with SV40 T antigen and the HPV E6 protein.

Alteration of p73 Expression in Human Cancer

Surprisingly, work from our lab and others on multiple primary tumor types and cell lines showed that the most common cancer-specific alteration is *overexpression* of various isoforms of wild-type TP73, rather than a loss of expression. This suggests that TP73 plays an oncogenic role in tumorigenesis. The exception to this picture seems to be lymphoid malignancies. Although overexpression of p73 gene was found in B-cell chronic lymphocytic leukemia (Novak *et al.,* 2001) and during differentiation of myeloid leukemic cells (Tschan *et al.,* 2000), TP73 has been found to be transcriptionally silenced in some lymphoblastic leukemias and lymphomas resulting from hypermethylation (Corn *et al.,* 1999).

To date, significant prevalence of p73 overexpression has been found in a dozen different tumor types including tumors of breast, neuroblastoma, lung, esophagus, stomach, colon, and bladder; ovarian cancer; ependymoma; liver cancer; cholangiocellular carcinoma, chronic myeloid luekemia (CML) blast crisis, acute myelogenous leukemia colon carcinoma; and head and neck squamous carcinoma (associated with distant metastasis) (Moll *et al.,* 2001). Most studies measure overexpression of full-length p73 messenger ribonucleic acid (mRNA) (TAp73) by reverse transcription-polymerase chain reaction (RT-PCR), but a few studies also measure overexpression of TAp73 protein(s). For example, we found overexpression of TAp73 transcripts (5- to 25-fold) in 38% of 77 invasive breast cancers relative to normal breast tissue and in 5 of 7 breast cancer cell lines (13- to 73-fold) (Zaika *et al.,* 1999). Likewise, we found overexpression of TAp73 transcripts in a subset of neuroblastoma (8- to 80-fold) and in 12 of 14 neuroblastoma cell lines (8- to 90-fold) (Kovalev *et al.,* 1998). A close correlation between p73 mRNA levels and protein levels was shown (e.g., in ovarian carcinoma cell lines) (Ng *et al.,* 2000). In 193 patients with hepatocellular carcinoma, 32% of tumors showed detectable (high) p73 by immunocytochemistry and *in situ* hybridization, whereas all normal tissue had undetectable levels (low) (Tannapfel *et al.,* 1999). Of note, primary tumors and tumor cell lines with p73 overexpression tend to simultaneously overexpress a complex profile of shorter C-terminal splice variants (p73γ, δ, ε, and ϕ), whereas the normal tissue of origin is limited to the expression of p73α and β (Zaika *et al.,* 1999). It is important that, patients with high global p73 protein expression had a worse survival than patients with undetectable levels (Tannapfel *et al.,* 1999).

There is an emerging sense that the dominant-negative ΔTAp73 isoforms—rather than TAp73—might be *the* physiologically relevant components of tumor-associated p73 overexpression, functionally overriding an often concomitant increase in TAp73 expression. Of note, many of the early p73 overexpression studies in human cancers did not use primer pairs or antibodies specific for TAp73 and therefore determined the total p73 level derived from all isoforms. Therefore, up-regulation of ΔTAp73 forms likely contributed to the elevated total "p73" levels previously found in human cancers. This conjecture is based on the fact that, so far, only a few studies on a limited number of tumors focused on the expression of ΔTAp73, yet highly prevalent, tumor-specific up-regulation of ΔNp73 has already been found in six studies. These are in breast carcinoma, gynecologic cancers, hepatocellular carcinoma, and neuroblastoma (Casciano *et al.,* 2002; Concin *et al.,* 2004; Stiewe *et al.,* 2002a; Zaika *et al.,* 2002). In a study of 100 ovarian carcinomas, we found that ΔN′p73 transcripts are overexpressed in 95%, and TAp73 was concomitantly up-regulated in 35% (Concin *et al.,* 2004). In hepatocellular carcinoma TAp73 and ΔTAp73 are up-regulated compared to normal liver (Stiewe *et al.,* 2002b). In another study on various gynecologic cancers, we found that ΔNp73 is overexpressed in 73% of cases, compared to the patients' matched normal tissues of origin (Zaika *et al.,* 2002). Moreover, 31% of 52 breast cancers overexpressed ΔNp73 compared to normal breast tissue (Zaika *et al.,* 2002). In the first clinical study on the impact of ΔNp73 expression in human cancer, ΔNp73 was found to be an independent prognostic marker for reduced progression-free and overall survival in patients with neuroblastoma (Casciano *et al.,* 2002).

Alteration of p63 Expression in Human Cancer

The analysis of p63 in primary tumors indicates similar lack of mutations but up-regulation of dominant negative forms. For example, no p63 mutations were found in 47 bladder cancers (Park *et al.,* 2000) or in 68 squamous cell carcinomas of the head and neck (Weber *et al.,* 2002). Only 1 missense mutation (Ala148Pro) out of 66 various human tumors and 2 missense mutations in 35 tumor cell lines were found (Osada *et al.,* 1998).

The human TP63 gene is located on chromosome 3q27-28 within a region that is frequently amplified in squamous cell carcinomas. Some lung cancers and

squamous cell carcinomas of the head and neck show p63 overexpression associated with a modest increase in TP63 copy numbers (Hibi *et al.,* 2000). (The authors therefore named the amplified locus Amplified In Squamous carcinoma, AIS). It is important to note that, although many AIS isoforms are produced in those tumors, the majority are dominant-negative ΔNp63 forms (mainly p40 AIS). The p40AIS isoform acts like an oncogene in nude mice and in Rat1a focus formation assays (Hibi *et al.,* 2000). Similar findings exist in nasopharyngeal carcinoma (NPC), which almost always has functional wt p53. In 25 primary NPCs, *all* tumor cells overexpressed predominantly ΔNp63, which in normal nasopharyngeal epithelium is limited to proliferating basal and suprabasal cells (Crook *et al.,* 2000). In esophageal squamous cell carcinoma ΔNp63 is the major isotype expressed throughout. In contrast, in normal esophagus, p63 staining is restricted to the basal and suprabasal cell layers (Choi *et al.,* 2002). Thus, the maintenance of the ΔNp63 isoforms in squamous cancers may contribute to keeping the cells in a stem cell–like phenotype, thereby promoting tumor growth. However, ΔNp63α (also known as chronic ulcerative stomatitis protein, or CUSP) is frequently undetectable in cutaneous lesions such as basal cell carcinoma, basal cell nevus syndrome, and nevus sebaceous, in contrast to normal skin where it is strongly expressed in basal cells (Dellavalle *et al.,* 2002).

In prostate, p63 staining is a reliable marker of basal cells (Weinstein *et al.,* 2002) and stains positively in basal cell hyperplasia; however, prostatic adenocarcinoma, devoid of basal cells, is negative. This can be used clinically for differential diagnosis (Urist *et al.,* 2002).

Up-regulation of ΔNp63 was also found in 30 out of 47 bladder cancers (Park *et al.,* 2000). Interestingly, TAp63 was concomitantly down-regulated in 25 of those 47 tumors. However, another study on 160 bladder transitional cell carcinomas (TCC) examined this relationship more closely. Whereas 93% of low-grade papillary superficial tumors expressed p63, only 68% of intermediate- and high-grade superficial tumors were positive. Moreover, there was a striking drop to 16% when tumors progressed in stage from superficial to invasive. Thus, loss of p63 in TCC occurs with a progressive loss of urothelial differentiation associated with stage and grade (Urist *et al.,* 2002). This was confirmed by Koga and colleagues in 2003. p63 is expressed in myoepithelial cells of ducts in the breast (Ribeiro-Silva *et al.,* 2003a), in a minority of breast carcinoma (mainly ductal carcinomas), rarely in carcinoma *in situ,* and is not expressed in invasive carcinoma (Ribeiro-Silva *et al.,* 2003a). However, lack of p63 expression cannot be used as a reliable marker of invasiveness in breast ductal carcinoma *in situ* (Ribeiro-Silva *et al.,* 2003b). In less-differentiated gastric carcinoma p63 is highly expressed in both TA and ΔN forms, suggesting that it can promote neoplastic growth in gastric epithelium (Tannapfel *et al.,* 2001).

Upstream Components That Signal to p73 and p63

The p73 gene is able to mediate death stimuli from three different tumor surveillance pathways *in vivo*: oncogenes, DNA damage, and T-cell receptor hyperactivation.

p73 is activated to mediate apoptosis by cellular and viral oncogenes. We and others have established that the cellular and viral oncogenes E2F1, cMyc, and E1A can induce and activate the endogenous TAp73α and β proteins for target gene transactivation, apoptosis, and growth suppression in p53-deficient human tumor cells (Irwin *et al.,* 2000; Zaika *et al.,* 2001). E2F1 is a direct transcriptional activator because it binds to several E2F1-responsive elements within the P1 promoter of TP73 (Irwin *et al.,* 2000; Stiewe and Putzer, 2000). It does not activate the TP63 promoter, suggesting that this promoter is devoid of an E2F1 response element (Irwin *et al.,* 2000). Because oncogene deregulation of E2F1 and c-Myc are one of the most common genetic alterations in human tumors, these findings might provide a physiologic mechanism for TAp73 overexpression in tumors. Taken together, these data establish another important link between p73 and human cancer.

Moreover, during E2F1-mediated apoptosis in primary MEFs a striking nonadditive cooperation between wild-type p53 and p73 exists (Irwin *et al.,* 2000). Although wt MEFs show 77% apoptosis after forced E2F1 expression, $p53^{-/-}$ MEFs (containing p73) and $p73^{-/-}$ MEFs (containing p53) *both* show reduced killing ability after forced E2F1 expression with 12% and 15%, respectively. This excessively weakened killing ability of $p73^{-/-}$ MEFs, despite the presence of wt p53, is consistent with an important *synergistic* but independent signal emanating from TAp73 that cooperates with p53 to induce oncogene-triggered death in a tumor surveillance pathway.

An E2F1–p73 pathway mediates cell death of circulating peripheral T cells induced by T-cell receptor activation. Normal peripheral T cells undergo apoptosis after hyperstimulation of their T-cell receptors. This cell death pathway is mediated via the E2F1–p73 pathway (Lissy *et al.,* 2000). Consistent with this notion, E2F1 null mice exhibit a marked disruption of lymphatic homeostasis with increased numbers of T cells and splenomegaly, suggesting that p73 plays a role in tumor surveillance pathways of lymphoid cells

(Field *et al.,* 1996). Moreover, the p73 gene is transcriptionally silenced in acute lymphoblastic leukemia and Burkitt's lymphoma as a result of hypermethylation (Corn *et al.,* 1999). This appears to be restricted to lymphoid tumors, since neither other hematopoietic malignancies nor solid tumors show p73 hypermethylation (Corn *et al.,* 1999). Interestingly, in radiation-induced T-cell lymphomas of the mouse, the p73 locus undergoes LOH in 33% of the cases (Herranz *et al.,* 1999). Thus, in lymphoid tumors p73 shows some genetic features of a classic tumor suppressor gene. EGR-1, an immediate early gene that is activated by mitogens in quiescent postmitotic neurons, induces apoptosis in neuroblastoma cells. This apoptosis seems to be mediated by p73, which is elevated in cells overexpressing EGR-1 (Pignatelli *et al.,* 2003).

Very scant data are available on the activation of p63 by oncogenes. Both the epidermal growth factor receptor (EGFR) and p63 are overexpressed in a significant number of head and neck squamous cell carcinoma (HNSCC). A pharmacologic inhibitor of EGFR in a HNSCC line led to a decrease in p63 levels, suggesting that p63 is a downstream target of EGFR signaling (Matheny *et al.,* 2003).

Both p73 and p63 are activated to mediate apoptosis by a spectrum of DNA damage. Endogenous p73 is activated for apoptosis in response to cisplatin, taxol, and γ-IR in a pathway that depends on the tyrosine kinase c-abl (Agami *et al.,* 1999; Gong *et al.,* 1999; Yuan *et al.,* 1999), supporting the theory that DNA damage signals are channeled through c-abl to p73. Hence, one would predict that p73-deficient cells should have defective DNA damage checkpoint controls. This seems to be borne out by the observation that p53/p73 double-null MEFs are more resistant to killing by cisplatin and taxol than p53 single-null MEFs (Flores *et al.,* 2002). Endogenous p73 protein is also rapidly induced by Camptothecin treatment, etoposide, cisplatin, and doxorubicin (Bergamaschi *et al.,* 2003). Thus, DNA-damage–dependent activation of p73 might be partly responsible for p53-independent apoptosis.

Mechanisms of Transdominance: Heterocomplex Formation and Promoter Competition

We and others demonstrated physical interaction between oncogenic and anti-oncogenic family members as one of two mechanisms for their transdominant interference with the suppressor functions of wt p53 and TAp73 (Nakagawa *et al.,* 2002; Stiewe *et al.,* 2002a; Zaika *et al.,* 2002). Mixed protein complexes were found between endogenous ΔNp73α or β and wt p53, TAp73α, or TAp73 β in primary human tumors, cultured human tumor cells, and mouse neurons. The stoichiometric ratio of TA/ΔNp73 could be a determinant in tumor formation. The slightest decrease in this ratio might be sufficient to convert TAp73 from a tumor suppressor to an oncogene.

Concerning p53 mutants, physical interactions between certain—but not all—human p53 mutants and TAp73 or TAp63 proteins were found in coimmunoprecipitation assays, and these interactions correlate with functional transdominance. In contrast, complexes between wild-type p53 and p73 are not observed in mammalian cells (Di Como *et al.,* 1999). Unexpectedly, protein contact occurs between the DBD of mutant p53 and the DBD plus oligomerization domain of p73 (Strano *et al.,* 2000) rather than between the respective oligomerization domains. In cotransfections, mixed heterocomplexes were shown between p53 mutants p53Ala143, p53Leu173, p53His175, p53Cys220, p53Trp248, or p53Gly281 and TAp73 α, α, γ, and δ or TAp63. Physiologic complexes were found in five tumor cell lines between endogenous mutant p53 and p73 (Marin *et al.,* 2000; Strano *et al.,* 2000). Functionally, formation of such stable complexes leads to a loss of p73- and p63-mediated transactivation and proapoptotic abilities. Interestingly, the Arg/Pro polymorphism at codon 72 of mutant p53 is a biological determinant for binding and inactivation of p73, with 72R mutants of p53 being inhibitory, whereas 72P mutants are not (Bergamaschi *et al.,* 2003; Marin *et al.,* 2000).

This inhibition mirrors the ability of many transdominant missense p53 mutants to abrogate wild-type p53 function. It suggests that in tumors that express both TAp73 and mutant p53 (typically at very high levels as a result of deficient mdm-2–mediated degradation), the function of TAp73 and TAp63 might be inactivated. Moreover, these functional interactions define a network that could result in a "two-birds-with-one-stone" effect for at least some inactivating p53 mutations. If this occurs in primary human tumors, it might have far-reaching consequences because 1) it argues for a transdominant inhibition of the tumor suppressor function of TAp73 isoforms during tumor development, 2) it could be the underlying mechanism for the gain-of-function activity of certain p53 mutants, and 3) it might further increase chemoresistance in cancer therapy of established tumors. p53 is exceptional among tumor suppressors in that it selects for the overexpression of missense mutants rather than for loss of expression as most other suppressor genes do. This gain-of-function results in increased tumorigenicity compared to p53 null parental cells, increased resistance to cancer agents, and increased genomic instability as a result of abrogation of the mitotic

spindle checkpoint (Dittmer *et al.,* 1993). Conceivably, p63 also participates in this network. However, it should be noted that some p53 mutants clearly are recessive toward TAp73 (e.g., p53His283 and p53Tyr277) (Gaiddon *et al.,* 2001) and do not interfere with its action.

With respect to p63, tumor-derived p53 mutants can associate with p63 through their core domains. This interaction impairs transcriptional activity of p63 and could contribute in promoting tumorigenesis and in conferring selective survival advantage to cancer cells (Strano *et al.,* 2000).

Promoter competition by ΔNp73 at TAp73/p53 response elements is another transdominant mechanism (Kartasheva *et al.,* 2002; Stiewe *et al.,* 2002a). It is conceivable that ΔNp73 or ΔNp63 homo-oligomers might have a stronger affinity to certain target gene promoters than wild-type p53. In those cases, p53 inhibition could occur as a result of competition at the level of target gene access. In the wtp53-containing ovarian carcinoma cell line A2780, coexpression of increasing amounts of either TAp73α, β, γ, or ε inhibits specific DNA binding and transcriptional activity of p53 in the absence of hetero-oligomer formation (Vikhanskaya *et al.,* 2000).

In short, the biological consequences of deregulated TP73 and TP63 expression might be diametrically different depending on the isoform stoichometry (ΔNp73 p63 versus TAp73/63) and presence or absence of mutant p53.

An autoregulatory feedback loop exists between p53, TAp73, and ΔNp73. Both p53 and TAp73 regulate ΔNp73 levels by binding to the P2 promoter and inducing its transcription. A p73-specific responsive element was mapped within the P2 region (Nakagawa *et al.,* 2002). This generates a negative feedback loop analogous to the p53-MDM2 loop that in turn negatively regulates the activity of p53 and p73 (Grob *et al.,* 2001). ΔNp73 blocks p53 and TAp73 activity through hetercomplexes formation (Nakagawa *et al.*, 2002; Stiewe *et al.*, 2002a; Zaika *et al.*, 2002) or through promoter competition (Kartasheva *et al.,* 2002; Stiewe *et al.,* 2002a) and thus contributes to the termination of the p53/p73 response in cells that do not undergo apoptosis.

p73 and Chemosensitivity

Endogenous p73 protein levels increase in response to cisplatin and adriamycin (Costanzo *et al.*, 2002). Although originally thought to respond only to a limited spectrum, it is now clear that TAp73 (α more than β) is induced by a wider variety of chemotherapeutic agents (adriamycin, cisplatin, taxol, and etoposide) in different tumor cell lines (Bergamaschi *et al.*, 2003; Irwin *et al.*, 2003). Accumulation of p73 is the result of increased transcription and increased protein stabilization and leads to induction of apoptotic target genes such as *AIP1* (apoptosis-induced protein). Conversely, blocking TAp73 function (either by the inhibitory p73DD fragment or by p73 siRNA) leads to enhanced chemoresistance, which is independent of the p53 gene status. Of note, although the presence of p73 is essential for p53 to induce apoptosis in fibroblasts (Flores *et al.*, 2002), p73 can induce apoptosis in cells that lack functional p53 (Irwin *et al.*, 2003). This confirms the importance of p73 in the response to chemotherapeutic agents (Bergamaschi *et al.*, 2003).

In cell culture, overexpression of anti-apoptotic p73 isoforms can also block chemotherapy-induced apoptosis in wtp53 tumor cells (Zaika *et al.,* 2002). Moreover, overproduction of certain p53 mutants can block p73 function and chemotherapy-induced apoptosis (Di Como *et al.,* 1999). This effect is most strongly linked to the arginine 72 polymorphism of the p53 gene (Bergamaschi *et al.,* 2003; Irwin *et al.*, 2003; Marin *et al.,* 2000) and is mediated by stable heteroligomers involving the DNA binding domains. Bergamaschi *et al.* have used different cell lines forced to express a series of p53 mutants either as Arg (72R) or Pro (72P) versions at codon 72. Only Arg mutants correlated with chemoresistance. These data were mirrored in a series of patients with polymorphic head and neck cancer with the same p53 mutants: 72R patients showed poor response to chemotherapy and shorter survival (Bergamaschi *et al.,* 2003). Conversely, downmodulation of endogenous p53 mutants enhances chemosensitivity in p53-defective mutant cells (Irwin *et al.,* 2003). Consequently, a promising therapeutic approach includes the use of small interfering RNA (siRNA) specifically directed against particular p53 mutants, which might restore chemosensitivity of tumor.

Potential Application of p63/p73 in Gene Therapy of p53 Inactivated Tumors

Some authors suggest the use of p73β in gene therapy as a substitute for p53. For example, cervical cancers caused by HPV are resistant to p53 gene therapy, possibly because HPV E6 protein degrades p53 by ubiquitin-mediated proteolysis. However, p73β is resistant to HPV E6–mediated proteolysis, induces apoptosis, and is a potent inhibitor of cancer colony growth *in vitro* (Prabhu *et al.,* 1998). Furthermore, colorectal cancer cells that are resistant to p53-mediated cell death undergo apoptosis after adenovirus-mediated p73β and p63γ gene transfer (Sasaki *et al.,* 2001).

Also, some pancreatic adenocarcinoma lines lacking functional wild-type p53 are completely resistant to p53-mediated apoptosis. However, p73β is able to efficiently kill these cells (Rodicker *et al.,* 2003). This p73-mediated cell death is probably mediated by p53AIP1, an important mediator of p53/p73-dependent apoptosis. Because in these particular cells p53 is not phosphorylated at Ser-46, which is essential for transcriptional activation of p53AIP1 by p53, p53AIP1 is not activated by p53.

CONCLUSIONS

Both p73 and p63 appear to play a role in cancer—but as oncogenes or as suppressor genes? Clearly, p73 plays an important role in human tumors *in vivo*. However, the current picture of p73's role in human cancer is a puzzling yin-yang, given the diametrically opposing functions of the two types of concomitantly expressed gene products as well as the inhibitory family network of interactions. However, some observations seem to fall into place now: The p53-compensatory action of TAp73 after DNA damage or oncogene deregulation in primary cells and in p53-deficient tumor cells explains the frequent overexpression of TAp73 seen in many human tumors. However, there is striking evidence that ΔTAp73/63 forms might act as oncogenes *in vivo*. ΔTAp73/63 inactivate p53, TAp73, and TAp63 in their role to induce apoptosis and cell-cycle arrest and inhibits their suppressive activity in colony formation (Zaika *et al.,* 2002). In addition, TAp73 is inactivated by dominant-negative interference from mutant p53. Moreover, ΔNp73 functions as an immortalizing oncogene. In 2003 we showed that ΔNp73 promotes immortalization of primary cells and cooperates with Ras in driving their transformation *in vivo* (Figures 19 and 20) (Petrenko *et al.,* 2003). Stiewe *et al.* have found that ΔTAp73 overexpression results in malignant transformation of NIH 3T3 fibroblasts and tumor growth in nude mice (Stiewe *et al.,* 2002b). How can we decide on the true role? We feel that ultimately the fact that TP73/63 are virtually never targeted by inactivating mutations *in vivo* strongly suggests that it is indeed the oncogenic ΔTAp73/63 forms that are the truly critical ones during tumor formation and progression.

Inactivation of the p53 tumor suppressor is the single most common genetic defect in human cancer.

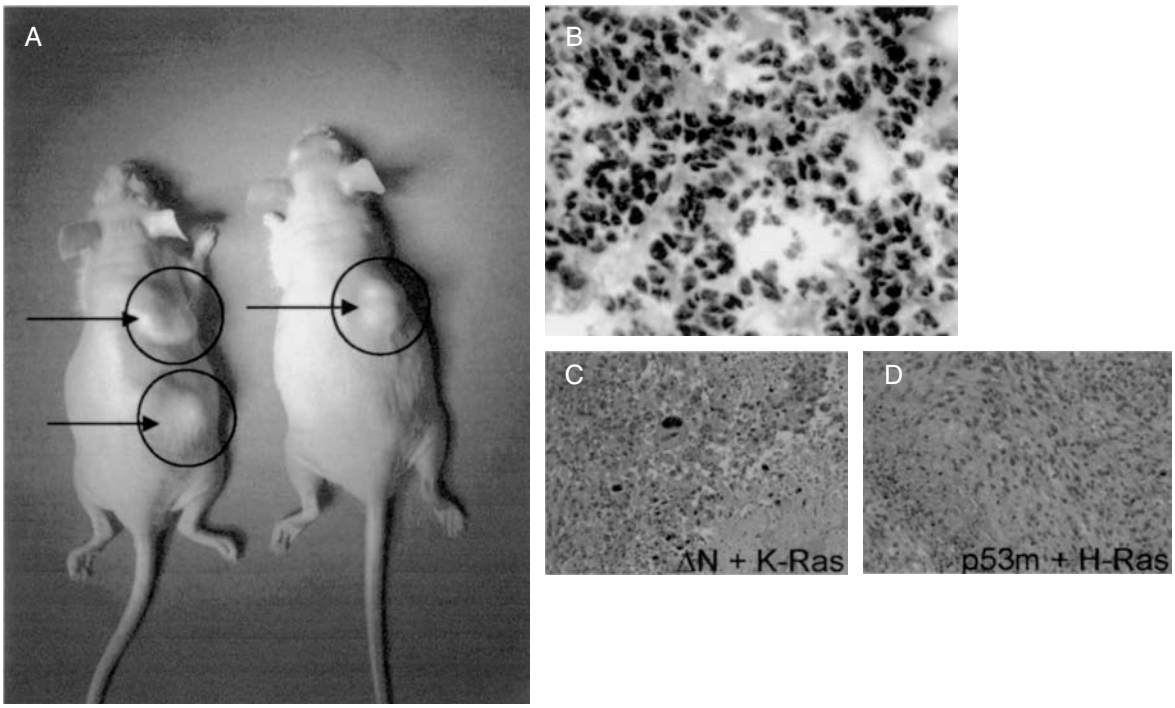

Figure 19. ΔNp73-expressing cells are tumorigenic in nude mice. **A:** Nude mice injected with ΔNp73 and oncogenic Ras-expressing mouse embryo fibroblasts (MEFs) develop tumors. **B:** Inmmunohistochemical examination shows nuclear ΔNp73 expression in tumor cells from (*A*). **C:** Histologically, ΔNp73 and Ras-coexpressing tumors from (*A*) are anaplastic fibrosarcomas and resemble fibrosarcomas produced in MEFs control cells injected with mutant p53 R175H and oncogenic Ras.

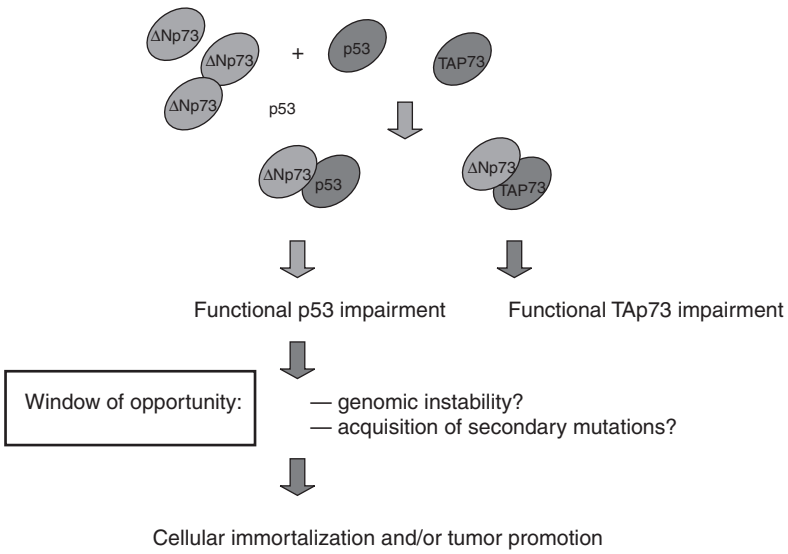

Figure 20. A proposed mechanism of the action of ΔNp73 in tumor promotion. ΔNp73 promotes immortalization of primary mouse embryo fibroblast cells by a factor of 10^3 and cooperates with oncogenic Ras in their transformation. Mechanistically, ΔNp73 counteracts the growth-restraining actions of p53 and TAp73 and creates a window of opportunity for acquisition of secondary mutations or genomic instability.

The discovery of two close structural homologs, p63 and p73, generated instant excitement and quick expectations about their biological functions. We now know that in development both genes clearly have novel, p53-independent functions, that p63 is involved in epithelial stem cell regeneration, and p73 is involved in hippocampal neurogenesis, pheromonal pathways, and ependymal cell function. To determine the role of these p53 homologs in tumor biology is still a challenge, but we have made progress. It is already clear that they are not classic Knudson-type tumor suppressors. However, the existence of inhibitory versions of both genes and intimate functional cross-talk among all family members endow these genes with both tumor suppressor and oncogenic roles. Their respective strengths determine their ultimate role in cancer.

Acknowledgment

This work is supported by the National Institutes of Health.

References

Agami, R., Blandino, G., Oren, M., and Shaul, Y. 1999. Interaction of c-Abl and p73alpha and their collaboration to induce apoptosis. *Nature 399*:809–813.

Balint, E., Bates, S., and Vousden, K.H. 1999. Mdm2 binds p73 alpha without targeting degradation. *Oncogene 18*:3923–3929.

Bergamaschi, D., Gasco, M., Hiller, L., Sullivan, A., Syed, N., Trigiante, G., Yulug, I., Merlano, M., Numico, G., Comino, A., Attard, M., Reelfs, O., Gusterson, B., Bell, A.K., Heath, V., Tavassoli, M., Farrell, P.J., Smith, P., Lu, X., and Crook, T. 2003. p53 polymorphism influences response in cancer chemotherapy via modulation of p73-dependent apoptosis. *Cancer Cell 3*:387–402.

Cai, Y.C., Yang, G.Y., Nie, Y., Wang, L.D., Zhao, X., Song, Y.L., Seril, D.N., Liao, J., Xing, E.P., and Yang, C.S. 2000. Molecular alterations of p73 in human esophageal squamous cell carcinomas: Loss of heterozygosity occurs frequently; loss of imprinting and elevation of p73 expression may be related to defective p53. *Carcinogenesis 21*:683–689.

Casciano, I., Mazzocco, K., Boni, L., Pagnan, G., Banelli, B., Allemanni, G., Ponzoni, M., Tonini, G.P., and Romani, M. 2002. Expression of DeltaNp73 is a molecular marker for adverse outcome in neuroblastoma patients. *Cell Death Differ. 9*:246–251.

Celli, J., Duijf, P., Hamel, B.C., Bamshad, M., Kramer, B., Smits, A.P., Newbury-Ecob, R., Hennekam, R.C., Van Buggenhout, G., van Haeringen, A., Woods, C.G., van Essen, A.J., de Waal, R., Vriend, G., Haber, D.A., Yang, A., McKeon, F., Brunner, H.G., and van Bokhoven, H. 1999. Heterozygous germline mutations in the p53 homolog p63 are the cause of EEC syndrome. *Cell 99*:143–153.

Chen, X., Liu, G., Zhu, J., Jiang, J., Nozell, S., and Willis, A. 2003. Isolation and characterization of fourteen novel putative and nine known target genes of the p53 family. *Cancer Biol. Ther. 2*:55–62.

Chi, S.W., Ayed, A., and Arrowsmith, C.H. 1999. Solution structure of a conserved C-terminal domain of p73 with structural homology to the SAM domain. *EMBO J. 18*:4438–4445.

Choi, H.R., Batsakis, J.G., Zhan, F., Sturgis, E., Luna, M.A., and El-Naggar, A.K. 2002. Differential expression of p53 gene family members p63 and p73 in head and neck squamous tumorigenesis. *Hum. Pathol. 33*:158–164.

Concin, N., Becker, K., Slàde, N., Erster, S., Mueller-Holzner, E., Ulmer, H., Daxenbichler, G., Zeimet, A., Zeillinger, R., Marth, C., and Moll, U.M. 2004. Transdominant Delta TAp73 isoforms are frequently up-regulated in ovarian cancer: Evidence for their role as epigenetic p53 inhibitors in vivo. *Cancer Res. 64*:2449–2460.

Corn, P.G., Kuerbitz, S.J., van Noesel, M.M., Esteller, M., Compitello, N., Baylin, S.B., and Herman, J.G. 1999. Transcriptional silencing of the p73 gene in acute lymphoblastic leukemia and Burkitt's lymphoma is associated with 5′ CpG island methylation. *Cancer Res. 59*:3352–3356.

Costanzo, A., Merlo, P., Pediconi, N., Fulco, M., Sartorelli, V., Cole, P.A., Fontemaggi, G., Fanciulli, M., Schiltz, L., Blandino, G., Balsano, C., and Levrero, M. 2002. DNA damage-dependent acetylation of p73 dictates the selective activation of apoptotic target genes. *Mol. Cell 9*:175–186.

Crook, T., Nicholls, J.M., Brooks, L., O'Nions, J., and Allday, M.J. 2000. High level expression of deltaN-p63: A mechanism for the inactivation of p53 in undifferentiated nasopharyngeal carcinoma (NPC)? *Oncogene 19*:3439–3444.

Davis, L.D., Zhang, W., Merseburger, A., Young, D., Xu, L., Rhim, J.S., Moul, J.W., Srivastava, S., and Sesterhenn, I.A. 2002. p63 expression profile in normal and malignant prostate epithelial cells. *Anticancer Res. 22*:3819–3825.

De Laurenzi, V., Costanzo, A., Barcaroli, D., Terrinoni, A., Falco, M., Annicchiarico-Petruzzelli, M., Levrero, M., and Melino, G. 1998. Two new p73 splice variants, gamma and delta, with different transcriptional activity. *J. Exp. Med. 188*:1763–1768.

Dellavalle, R.P., Walsh, P., Marchbank, A., Grayson, T.E., Su, L.J., Parker, E.R., DeGregori, J., Penheiter, K., Aszterbaum, M., Epstein, E.H. Jr., and Lee, L.A. 2002. CUSP/p63 expression in basal cell carcinoma. *Exp. Dermatol. 11*:203–208.

Di Como, C.J., Gaiddon, C., and Prives, C. 1999. p73 function is inhibited by tumor-derived p53 mutants in mammalian cells. *Mol. Cell Biol. 19*:1438–1449.

Dietz, S., Rother, K., Bamberger, C., Schmale, H., Mossner, J., and Engeland, K. 2002. Differential regulation of transcription and induction of programmed cell death by human p53-family members p63 and p73. *FEBS Lett. 525*:93–99.

Dittmer, D., Pati, S., Zambetti, G., Chu, S., Teresky, A.K., Moore, M., Finlay, C., and Levine, AJ. 1993. Gain of function mutations in p53. *Nat. Genet. 4*:42–46.

Dobbelstein, M., Wienzek, S., Konig, C., and Roth, J. 1999. Inactivation of the p53-homologue p73 by the mdm2-oncoprotein. *Oncogene 18*:2101–2106.

Dohn, M., Zhang, S., and Chen, X. 2001. p63alpha and DeltaNp63alpha can induce cell cycle arrest and apoptosis and differentially regulate p53 target genes. *Oncogene 20*:3193–3205.

Field, S.J., Tsai, F.Y., Kuo, F., Zubiaga, A.M., Kaelin, W.G. Jr., Livingston, D.M., Orkin, S.H., and Greenberg, M.E. 1996. E2F-1 functions in mice to promote apoptosis and suppress proliferation. *Cell 85*:549–561.

Fillippovich, I., Sorokina, N., Gatei, M., Haupt, Y., Hobson, K., Moallem, E., Spring, K., Mould, M., McGuckin, M.A., Lavin, M.F., and Khanna, K.K. 2001. Transactivation-deficient p73alpha (p73Deltaexon2) inhibits apoptosis and competes with p53. *Oncogene*:514–522.

Flores, E.R., Tsai, K.Y., Crowley, D., Sengupta, S., Yang, A., McKeon, F., and Jacks, T. 2002. p63 and p73 are required for p53-dependent apoptosis in response to DNA damage. *Nature 416*:560–564.

Fomenkov, A., Huang, Y.P., Topaloglu, O., Brechman, A., Osada, M., Fomenkova, T., Yuriditsky, E., Trink, B., Sidransky, D., and Ratovitski, E. 2003. P63 alpha mutations lead to aberrant splicing of keratinocyte growth factor receptor in the Hay-Wells syndrome. *J. Biol. Chem. 278*:23906–23914.

Gaiddon, C., Lokshin, M., Ahn, J., Zhang, T., and Prives, C. 2001. A subset of tumor-derived mutant forms of p53 down-regulate p63 and p73 through a direct interaction with the p53 core domain. *Mol. Cell Biol. 2l*:1874–1887.

Gong, J.G., Costanzo, A., Yang, H.Q., Melino, G., Kaelin, W.G. Jr., Levrero, M., and Wang, J.Y. 1999. The tyrosine kinase c-Abl regulates p73 in apoptotic response to cisplatin-induced DNA damage. *Nature 399*:806–809.

Grob, T.J., Novak, U., Maisse, C., Barcaroli, D., Luthi, A.U., Pirnia, F., Hugli, B., Graber, H.U., De Laurenzi, V., Fey, M.F., Melino, G., and Tobler, A. 2001. Human delta Np73 regulates a dominant negative feedback 1oop for TAp73 and p53. *Cell Death Differ. 8*:1213–1223.

Gu, J., Chen, D., Rosenblum, J., Rubin, R.M., and Yuan, Z.M. 2000. Identification of a sequence element from p53 that signals for Mdm2-targeted degradation. *Mol. Cell Biol. 20*:1243–1253.

Herranz, M., Santos, J., Salido, E., Fernandez-Piqueras, J., and Serrano, M. 1999. Mouse p73 gene maps to the distal part of chromosome 4 and might be involved in the progression of gamma-radiation-induced T-cell lymphomas. *Cancer Res. 59*:2068–2071.

Hibi, K., Trink, B., Patturajan, M., Westra, W.H., Caballero, O.L., Hill, D.E., Ratovitski, E.A., Jen, J., and Sidransky, D. 2000. AIS is an oncogene amplified in squamous cell carcinoma. *Proc. Natl. Acad. Sci. USA 97*:5462–5467.

Irwin, M., Marin, M.C., Phillips, A.C., Seelan, R.S., Smith, D.I., Liu, W., Flores, E.R., Tsai, K.Y., Jacks, T., Vousden, K.H., and Kaelin, W.G., Jr. 2000. Role for the p53 homologue p73 in E2F-1-induced apoptosis. *Nature 407*:645–648.

Irwin, M.S., Kondo, K., Marin, M.C., Cheng, L.S., Hahn, W.C., and Kaehin, W.G. 2003. Chemosensitivity linked to p73 function. *Cancer Cell 3*:403–410.

Ishida, S., Yamashita, T., Nakaya, U., and Tokino, T. 2000. Adenovirus-mediated transfer of p53-related genes induces apoptosis of human cancer cells. *Jpn. J. Cancer Res. 21*:174–180.

Ishimoto, O., Kawahara, C., Enjo, K., Obinata, M., Nukiwa, T., and Ikawa, S. 2002. Possible oncogenic potential of DeltaNp73: A newly identified isoform of human p73. *Cancer Res. 62*:636–641.

Jost, C.A., Marin, M.C., and Kaelin, W.G., Jr. 1997. p73 is a simian [correction of human] p53-related protein that can induce apoptosis. *Nature 389*:191–194.

Kaghad, M., Bonnet, H., Yang, A., Creancier, L., Biscan, J.C., Valent, A., Minty, A., Chalon, P., Lelias, J.M., Dumont, X., Ferrara, P., McKeon, F., and Caput, D. 1997. Monoallelically expressed gene related to p53 at 1p36, a region frequently deleted in neuroblastoma and other human cancers. *Cell 90*:809–819.

Kartasheva, N.N., Contente, A., Lenz-Stoppler, C., Roth, J., and Dobbelstein, M. 2002. p53 induces the expression of its antagonist p73 Delta N, establishing an autoregulatory feedback loop. *Oncogene 21*:4715–4727.

Koga, F., Kawakami, S., Kumagai, J., Takizawa, T., Ando, N., Arai, G., Kageyama, Y., and Kihara, K. 2003. Impaired Delta Np63 expression associates with reduced beta-catenin and aggressive phenotypes of urothelial neoplasms. *Br. J. Cancer 88*:740–747.

Kovalev, S., Marchenko, N., Swendeman, S., LaQuaglia, M., and Moll, U.M. 1998. Expression level, allelic origin, and mutation analysis of the p73 gene in neuroblastoma tumors and cell lines. *Cell Growth Differ. 9*:897–903.

Lissy, N.A., Davis, P.K., Irwin, M., Kaelin, W.G., and Dowdy, S.F. 2000. A common E2F-1 and p73 pathway mediates cell death induced by TCR activation. *Nature 407*:642–645.

Mai, M., Yokomizo, A., Qian, C., Yang, P., Tindall, D.J., Smith, D.I., and Liu, W. 1998. Activation of p73 silent allele in lung cancer. *Cancer Res. 58*:2347–2349.

Marin, M.C., Jost, C.A., Irwin, M.S., DeCaprio, J.A., Caput, D., and Kaelin, W.G., Jr. 1998. Viral oncoproteins discriminate between p53 and the p53 homolog p73. *Mol. Cell Biol. 18*:6316–6324.

Marin, M.C., Jost, C.A., Brooks, L.A., Irwin, M.S., O'Nions, J., Tidy, J.A., James, N., McGregor, J.M., Harwood, C.A., Yulug, I.G., Vousden, K.H., Allday, M.J., Gusterson, B., Ikawa, S., Hinds, P.W., Crook, T., and Kaelin, W.G., Jr. 2000. A common polymorphism acts as an intragenic modifier of mutant p53 behaviour. *Nat. Genet. 25*:47–54.

Matheny, K.E., Barbieri, C.E., Sniezek, J.C., Arteaga, C.L., and Pietenpol, J.A. 2003. Inhibition of epidermal growth factor receptor signaling decreases p63 expression in head and neck squamous carcinoma cells. *Laryngoscope 113*:936–939.

Mills, A.A., Zheng, B., Wang, X.J., Vogel, H., Roop, D.R., and Bradley, A. 1999. p63 is a p53 homologue required for limb and epidermal morphogenesis. *Nature 398*:708–713.

Minty, A., Dumont, X., Kaghad, M., and Caput, D. 2000. Covalent modification of p73alpha by SUMO-1. Two-hybrid screening with p73 identifies novel SUMO-1-interacting proteins and a SUMO-1 interaction motif. *J. Biol. Chem. 275*:36316–36323.

Moll, U.M., Erster, S., and Zaika, A. 2001. p53, p63 and p73—solos, alliances and feuds among family members. *Biochim. Biophys. Acta. 1552*:47–59.

Nakagawa, T., Takahashi, M., Ozaki, T., Watanabe Ki, K., Todo, S., Mizuguchi, H., Hayakawa, T., and Nakagawara, A. 2002. Autoinhibitory regulation of p73 by Delta Np73 to modulate cell survival and death through a p73-specific target element within the Delta Np73 promoter. *Moll. Cell Biol. 22*:2575–2585.

Nakagawa, T., Takahashi, M., Ozaki, T., Watanabe, K., Hayashi, S., Hosoda, M., Todo, S., and Nakagawara, A. 2003. Negative autoregulation of p73 and p53 by DeltaNp73 in regulating differentiation and survival of human neuroblastoma cells. *Cancer Lett. 197*:105–109.

Ng, S.W., Yiu, G.K., Liu, Y., Huang, L.W., Palnati, M., Jun, S.H., Berkowitz, R.S., and Mok, S.C. 2000. Analysis of p73 in human borderline and invasive ovarian tumor. *Oncogene 19*:1885–1890.

Nomoto, S., Haruki, N., Kondo, M., Konishi, H., and Takahashi, T. 1998. Search for mutations and examination of allelic expression imbalance of the p73 gene at 1p36.33 in human lung cancers. *Cancer Res. 58*:1380–1383.

Novak, U., Grob, T.J., Baskaynak, G., Peters, U.R., Aebi, S., Zwahlen, D., Tschan, M.P., Kreuzer, K.A., Leibundgut, E.O., Cajot, J.F., Tobler, A., and Fey, M.F. 2001. Overexpression of the p73 gene is a novel finding in high-risk B-cell chronic lymphocytic leukemia. *Ann. Oncol. 12*:981–986.

Nozell, S., Wu, Y., McNaughton, K., Liu, G., Willis, A., Paik, J.C., and Chen, X. 2003. Characterization of p73 functional domains necessary for transactivation and growth suppression. *Oncogene 22*:4333–4347.

Nylander, K., Coates, P.J., and Hall, P.A. 2000. Characterization of the expression pattern of p63 alpha and delta Np63 alpha in benign and malignant oral epithelial lesions. *Int. J. Cancer 87*:368–372.

Osada, M., Ohba, M., Kawahara, C., Ishioka, C., Kanamaru, R., Katoh, I., Ikawa, Y., Nimura, Y., Nakagawara, A., Obinata, M., and Ikawa, S. 1998. Cloning and functional analysis of human p51, which structurally and functionally resembles p53. *Nat. Med. 4*:839–843.

Park, B.J., Lee, S.J., Kim, J.I., Lee, S.J., Lee, C.H., Chang, S.G., Park, J.H., and Chi, S.G. 2000. Frequent alteration of p63 expression in human primary bladder carcinomas. *Cancer Res. 60*:3370–3374.

Park, J.S., Kim, E.J., Lee, J.Y., Sin, H.S., Namkoong, S.E., and Um, S.J. 2001. Functional inactivation of p73, a homolog of p53 tumor suppressor protein, by human papillomavirus E6 proteins. *Int. J. Cancer 91*:822–827.

Parsa, R., Yang, A., McKeon, F., and Green, H. 1999. Association of p63 with proliferative potential in normal and neoplastic human keratinocytes. *J. Invest. Dermatol. 113*:1099–1105.

Pellegrini, G., Dellambra, E., Golisano, O., Martinelli, E., Fantozzi, I., Bondanza, S., Ponzin, D., McKeon, F., and De Luca, M. 2001. p63 identifies keratinocyte stem cells. *Proc. Natl. Acad. Sci. USA 98*:3156–3161.

Petrenko, O., Zaika, A., and Moll, U.M. 2003. deltaNp73 facilitates cell immortalization and cooperates with oncogenic Ras in cellular transformation in vivo. *Mol. Cell Biol. 23*:5540–5555.

Pignatelli, M., Luna-Medina, R., Perez-Rendon, A., Santos, A., and Perez-Castillo, A. 2003. The transcription factor early growth response factor-1 (EGR-1) promotes apoptosis of neuroblastoma cells. *Biochem. J. 373*:739–746.

Pozniak, C.D., Radinovic, S., Yang, A., McKeon, F., Kaplan, D.R., and Miller, F.D. 2000. An anti-apoptotic role for the p53 family member, p73, during developmental neuron death. *Science 289*:304–306.

Prabhu, N.S., Somasundaram, K., Satyamoorthy, K., Herlyn, M., and El-Deiry, W.S. 1998. p73beta, unlike p53, suppresses growth and induces apoptosis of human papillomavirus E6-expressing cancer cells. *Int. J. Oncol.13*:5–9.

Ratovitski, E.A., Patturrajan, M., Hibi, K., Trink, B., Yamaguchi, K., and Sidransky, D. 2001. p53 associates with and targets Delta Np63 into a protein degradation pathway. *Proc. Natl. Acad. Sci. USA 98*:1817–1822.

Ribeiro-Silva, A., Zambelli Ramalho, L.N., Britto Garcia, S., and Zucoloto, S. 2003a. The relationship between p63 and p53 expression in normal and neoplastic breast tissue. *Arch. Pathol. Lab. Med. 127*:336–340.

Ribeiro-Silva, A., Zamzelli Ramalho, L.N., Garcia, S.B., and Zucoloto, S. 2003b. Is p63 reliable in detecting microinvasion in ductal carcinoma in situ of the breast? *Pathol. Oncol. Res. 9*:20–23.

Rodicker, F., and Putzer B.M. 2003. p73 is effective in p53-null pancreatic cancer cells resistant to wild-type TP53 gene replacement. *Cancer Res. 63*:2737–2741.

Sasaki, Y., Morimoto, I., Ishida, S., Yamashita, T., Imai, K., and Tokino, T. 2001. Adenovirus-mediated transfer of the p53 family genes, p73 and p51/p63 induces cell cycle arrest and apoptosis in colorectal cancer cell lines: Potential application to gene therapy of colorectal cancer. *Gene. Ther. 8*:1401–1408.

Schmale, H., and Bamberger, C. 1997. A novel protein with strong homology to the tumor suppressor p53. *Oncogene 15*:1363–1367.

Slade, N., Zaika, A.I., Erster, S., and Moll, U.M. 2004. Delta Np73 stabilises TAp73 proteins but compromises their function due to

inhibitory hetero-oligomer formation. *Cell Death Differ. 11*:357–360.

Stiewe, T., and Putzer, B.M. 2000. Role of the p53-homologue p73 in E2F1-induced apoptosis. *Nat. Genet. 26*:464–469.

Stiewe, T., Theseling, C.C., and Putzer, B.M. 2002a. Transactivation-deficient Delta TA-p73 inhibits p53 by direct competition for DNA binding: Implications for tumorigenesis. *J. Biol. Chem. 277*:14177–14185.

Stiewe, T., Zimmermann, S., Frilling, A., Esche, H., and Putzer, B.M. 2002b. Transactivation-deficient DeltaTA-p73 acts as an oncogene. *Cancer Res. 62*:3598–3602.

Strano, S., Munarriz, E., Rossi, M., Cristofanelli, B., Shaul, Y., Castagnoli, L., Levine, A.J., Sacchi, A., Cesareni, G., Oren, M., and Blandino, G. 2000. Physical and functional interaction between p53 mutants and different isoforms of p73. *J. Biol. Chem. 275*:29503–29512.

Tannapfel, A., Schmelzer, S., Benicke, M., Klimpfinger, M., Kohlhaw, K., Mossner, J., Engeland, K., and Wittekind, C. 2001. Expression of the p53 homologues p63 and p73 in multiple simultaneous gastric cancer. *J. Pathol. 195*:163–170.

Tannapfel, A., Wasner, M., Krause, K., Geissler, F., Katalinic, A., Hauss, J., Mossner, J., Engeland, K., and Wittekind, C. 1999. Expression of p73 and its relation to histopathology and prognosis in hepatocellular carcinoma. *J. Natl. Cancer Inst. 91*:1154–1158.

Tsao, H., Zhang, X., Majewski, P., and Haluska, F.G. 1999. Mutational and expression analysis of the p73 gene in melanoma cell lines. *Cancer Res. 59*:172–174.

Tschan, M.P., Grob, T.J., Peters, U.R., Laurenzi, V.D., Hueghi, B., Kreuzer, K.A., Schmidt, C.A., Melino, G., Fey, M.F., Tobler, A., and Cajot, J.F. 2000. Enhanced p73 expression during differentiation and complex p73 isoforms in myeloid leukemia. *Biochem. Biophys. Res. Commun. 277*:62–65.

Urist, M.J., Di Como, C.J., Lu, M.L., Charytonowicz, E., Verbel, D., Crum, C.P., Ince, T.A., McKeon, F.D., and Cordon-Cardo, C. 2002. Loss of p63 expression is associated with tumor progression in bladder cancer. *Am. J. Pathol. 161*:1199–1206.

Vikhanskaya, F., D'Incalci, M., and Broggini, M. 2000. p73 competes with p53 and attenuates its response in a human ovarian cancer cell line. *Nucleic Acids Res. 28*:513–519.

Wang, W.K., Bycroft, M., Foster, N.W., Buckle, A.M., Fersht, A.R., and Chen, Y.W. 2001. Structure of the C-terminal sterile alpha-motif (SAM) domain of human p73 alpha. *Acta. Crystallogr D. Biol. Crystallogr 57*:545–551.

Weber, A., Bellmann, U., Bootz, F., Wittekind, C., and Tannapfel, A. 2002. Expression of p53 and its homologues in primary and recurrent squamous cell carcinomas of the head and neck. *Int. J. Cancer 99*:22–28.

Weinstein, M.H., Signoretti, S., and Loda, M. 2002. Diagnostic utility of immunohistochemical staining for p63, a sensitive marker of prostatic basal cells. *Mod. Pathol. 15*:1302–1308.

Westfall, M.D., Mays, D.J., Sniezek, J.C., and Pietenpol, J.A. 2003. The Delta Np63 alpha phosphoprotein binds the p21 and 14-3-3 sigma promoters in vivo and has transcriptional repressor activity that is reduced by Hay-Wells syndrome-derived mutations. *Mol. Cell Biol. 23*:2264–2276.

Wu, M., Wang, B., Gil, J., Sabo, E., Miller, L., Gan, L., and Bunstein, D.E. 2003. p63 and TTF-1 immunostaining: A useful marker panel for distinguishing small cell carcinoma of lung from poorly differentiated squamous cell carcinoma of lung. *Am. J. Clin. Pathol. 119*:696–702.

Yang, A., Kaghad, M., Wang, Y., Gillett, E., Fleming, M.D., Dotsch, V., Andrews, N.C., Caput, D., and McKeon, F. 1998. p63, a p53 homolog at 3q27-29, encodes multiple products with transactivating, death-inducing, and dominant-negative activities. *Mol. Cell 2*:305–316.

Yang, A., Schweitzer, R., Sun, D., Kaghad, M., Walker, N., Bronson, R.T., Tabin, C., Sharpe, A., Caput, D., Crum, C., and McKeon, F. 1999. p63 is essential for regenerative proliferation in limb, craniofacial and epithelial development. *Nature 398*:714–718.

Yang, A., Walker, N., Bronson, R., Kaghad, M., Oosterwegel, M., Bonnin, J., Vagner, C., Bonnet, H., Dikkes, P., Sharpe, A., McKeon, F., and Caput, D. 2000. p73-deficient mice have neurological, pheromonal and inflammatory defects but lack spontaneous tumours. *Nature 404*:99–103.

Yuan, Z.M., Shioya, H., Ishiko, T., Sun, X., Gu, J., Huang, Y.Y., Lu, H., Kharbanda, S., Weichselbaum, R., and Kufe, D. 1999. p73 is regulated by tyrosine kinase c-Abl in the apoptotic response to DNA damage. *Nature 399*:814–817.

Zaika, A., Irwin, M., Sansome, C., and Moll, U.M. 2001. Oncogenes induce and activate endogenous p73 protein. *J. Biol. Chem. 276*:11310–11316.

Zaika, A.I., Kovalev, S., Marchenko, N.D., and Moll, U.M. 1999. Overexpression of the wild type p73 gene in breast cancer tissues and cell lines. *Cancer Res. 59*:3257–3263.

Zaika, A.I., Slade, N., Erster, S.H., Sansome, C., Joseph, T.W., Pearl, M., Chalas, E., and Moll, U.M. 2002. DeltaNp73, a dominant-negative inhibitor of wild-type p53 and TAp73, is up-regulated in human tumors. *J. Exp. Med. 196*:765–780.

Zeng, X., Chen, L., Jost, C.A., Maya, R., Keller, D., Wang, X., Kaelin, W.G., Jr., Oren, M., Chen, J., and Lu, H. 1999. MDM2 suppresses p73 function without promoting p73 degradation. *Mol. Cell Biol. 19*:3257–3266.

11

Analysis of Centrosome Amplification in Cancer

Wilma L. Lingle and Jeffrey L. Salisbury

Introduction

Centrosome Structure

Recent studies have demonstrated that centrosome abnormalities are a common feature of most cancers. *Centrosome amplification* in cancer contributes to the loss of cell and tissue architecture (i.e., anaplasia) and has been implicated in the origin of chromosome instability leading to aneuploidy. The centrosome is a fascinating organelle that resides near the cell center, hence its name (Wilson, 1925). It functions in the maintenance of cytoplasmic architecture through the nucleation and organization of microtubule arrays in interphase and mitotic cells (Palazzo, 2003). In addition to its fundamental role in microtubule organization, the centrosome may provide an important structural context for coordinating cell cycle regulation (Sluder and Hinchcliffe, 2000).

Understanding of the molecular basis for these diverse cellular functions is beginning to emerge through the careful analysis of centrosome genes and proteins and centrosome formation, structure, and organization in early embryo development in model systems such as *Drosophila,* yeast, and the nematode and in mammalian somatic cells. Centrosomes consist of three fundamental components (Figure 21): a core structure consisting of a pair of *centrioles* that serve as a centrosomal organizer, a surrounding protein lattice or matrix called *pericentriolar material* (PCM) that serves as a framework to anchor microtubule nucleation sites; and γ-*tubulin complexes* that are responsible for the nucleation of microtubules.

Centrioles are small barrel-shaped organelles (~200 nm in diameter and 400 nm in length) consisting of a cylindric array of nine triplet microtubules (Dutcher, 2001). Once during each cell cycle the centrosome doubles from one to two in a process that is initiated with centriole duplication. The centriole pair embodies an intrinsic counting mechanism that establishes the number of centrosome equivalents in the cell so that a pair of centrioles equals one and two pairs of centrioles equal two centrosome equivalents (Mazia, 1987). Studies suggest that centrosome size and organization of PCM depends on centriolar integrity (Salisbury, 2003a; Salisbury, 2003b). The PCM is structurally complex and consists of a matrix of coiled-coil proteins (Salisbury, 2003a), including pericentrin, Cep135, AKAP-450, and ninein. Several of these coiled-coil proteins act as anchors for other essential centrosome proteins and for key regulators of centrosome function. For example, γ-tubulin complexes are anchored to the centrosome by pericentrin, and protein kinase A is anchored by both pericentrin and the protein-kinase-A–anchoring protein—AKAP-450. The centriole pair duplicates during late G1 phase of the cell cycle,

Handbook of Immunohistochemistry and *in situ* Hybridization of Human Carcinomas, Volume 3: Molecular Genetics, Liver Carcinoma, and Pancreatic Carcinoma

and centrosomes increase in size through the recruitment of additional PCM. The two centrosomes of G2/M cells show a dramatic increase in microtubule nucleating activity as they begin to function as spindle poles during mitosis.

The Centrosome Cycle

The centrosome is duplicated once, and only once, during a normal cell cycle (Figure 22) to yield two centrosomes that function as the spindle poles of the dividing cell (Palazzo, 2003). The process is most clearly illustrated by the duplication of the centrioles themselves. In early G1 phase of the cell cycle the two centrioles, which originated in previous cell cycles, usually are oriented in a characteristic orthogonal arrangement relative to one another. As cells pass the G1 restriction point and commit to deoxyribonucleic acid (DNA) replication and subsequent cell division, the two centrioles separate and move a short distance away from one another (centriole disjunction) and nascent *pro*centrioles form at the proximal end and orthogonal to each preexisting centriole (Wheatley, 1982). During G2/M phase of the cell cycle, centrosome duplication is completed through a maturation process involving the recruitment of additional PCM protein, and each new centrosome, containing one old and one new centriole, functions as a spindle pole during mitosis. The presence of only two centrosomes in the cell as it enters mitosis ensures the equal segregation of sister chromatids to each daughter cell. Mitotic spindle poles also play a role in determining the position and orientation of the cleavage furrow and in exit from cytokinesis (Khodjakov and Rieder, 2001; Piel *et al.,* 2001). Although centriole duplication occurs in a semiconservative fashion in most cells, as described earlier, during development, and in certain cells under special experimental circumstances, centrioles can arise *de novo* (Dirksen, 1991; Khodjakov *et al.,* 2002).

Coordination of the Centrosome, DNA, and Cell Cycles

Progress in understanding the centrosome duplication cycle has accelerated. Several emerging lines of evidence suggest that, in addition to its function as a microtubule-organizing center, the centrosome may be a focal point for the convergence of cell cycle pathways implicating this organelle in the control of cell cycle progression. Centrosome duplication is strictly coordinated with the process of DNA replication, mitosis, and cell division (Sluder and Hinchcliffe, 2000). The control of centrosome duplication is tightly coupled to cell cycle progression through two pathways of regulation. The first of these regulatory pathways operates through activity of the G1/S and G2/M cell cycle regulators, including cyclin-dependent kinase (CDK) cyclin A and E, which coordinate the cell, centrosome, and DNA cycles (Sluder and Hinchcliffe, 2000). The second control pathway involves the p53-mediated G1/S and G2/M cell cycle checkpoints that monitor DNA integrity and arrest centrosome duplication through the induction of $p21^{waf1}$ synthesis and consequent inhibition of the CDK/cyclins.

The key stages of cell cycle progression are governed by the subcellular location and periodic activation and subsequent inactivation of the serine/threonine cyclin-dependent protein kinases (CDKs) (Pines, 1999). Evidence suggesting a direct role for the CDKs in regulating the mitotic activity of centrosomes first came to

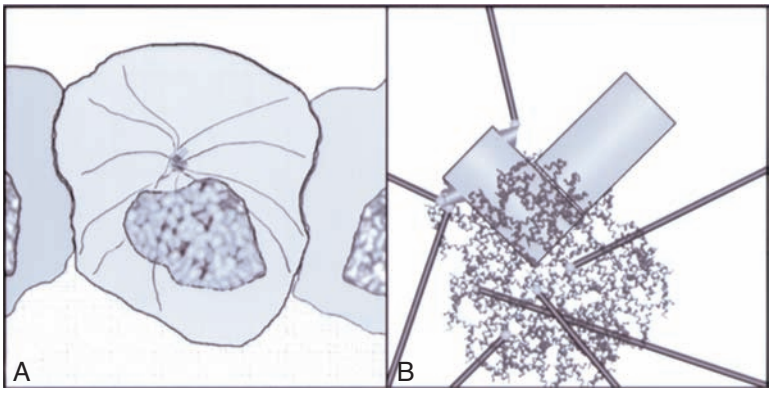

Figure 21. Centrosome structure. **A:** Diagram representing a prototypical epithelial cell showing the position of its nucleus and centrosome with associated microtubules. **B:** The centrosome consists of three fundamental structural elements: a pair of centrioles, a pericentriolar matrix or lattice, and microtubule-nucleating sites.

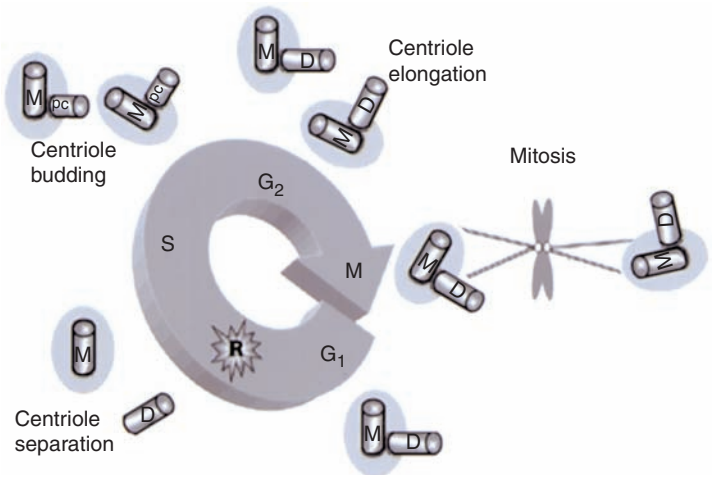

Figure 22. Diagram illustrating the centrosome and cell cycles. Cells are born in G1 with a centrosome containing a pair of centrioles. Centrosome duplication is initiated at about the time of G_1/S transition and by the time of mitosis two centrosomes (i.e., spindle poles) each contain a pair of centrioles.

light from studies on the localization of cyclin B and CDK1 ($p34^{cdc2}$) at the centrosome during G2/M phase and from experiments using *Xenopus* cell free extracts that implicated cyclins A and B in the control of microtubule dynamics (Bailly *et al.,* 1992). More recently, the direct involvement of CDK2 activity in regulation of centrosome duplication was established. Both centrosome duplication and DNA replication are dependent on CDK2 activation and are blocked by the CDK2 inhibitors butyrolactone I and roscovitine (Keezer and Gilbert, 2002).

CDK2/cyclin E activity was subsequently identified as a key regulator of the centrosome cycle because centrosome duplication was blocked by the small protein inhibitors of CDK2, $p21^{waf1}$, or p27, or by immunodepletion of CDK2 or cyclin E, and centrosome duplication was restored by excess purified CDK2/cyclin E (Hinchcliffe *et al.,* 1999). Separation of the centriole pair (centriole disjunction), an early event in the centrosome duplication cycle, was shown to be dependent on CDK2/cyclin E activity, suggesting that a CDK-mediated phosphorylation event regulates centriole pair cohesion (Lacey *et al.,* 1999). Additional protein phosphorylation events play key roles in controlling centrosome behavior and function during the cell cycle (Fry *et al.,* 2000). Centrosome protein phosphorylation increases dramatically at the onset of mitosis and falls precipitously at the metaphase/anaphase transition (Lutz *et al.,* 2001). It is important to note that several centrosome-associated kinases and target substrates implicated in the regulation of the centrosome cycle become altered during the development of centrosome amplification in cancer (Katayama *et al.,* 2001). Finally, centrosome duplication also depends on the phosphorylation status of retinoblastoma tumor suppressor retinoblastoma (Rb), which governs the availability of the E2F transcription factor to promote S-phase progression (Meraldi *et al.,* 1999). Taken together these findings establish two mechanisms by which DNA replication and centrosome duplication are coordinated during the cell cycle: Both DNA replication and centrosome duplication are controlled by the Rb pathway and depend on downstream transcriptional consequences of E2F activity, and both processes require CDK2/cyclin activation.

The Centrosome and DNA Cycles Can Be Uncoupled

In certain cycling cells, multiple rounds of centrosome duplication can occur when DNA replication is blocked; thus, the centrosome cycle is not strictly dependent on DNA replication *per se* (Balczon *et al.,* 1995). However, recent evidence suggests that uncoupling of the centrosome and DNA cycles can occur only in cells that are defective in G1/S checkpoint controls. Several studies show that loss of p53 function and certain gain-of-function p53 mutations result in deregulation of centrosome duplication and lead to functionally amplified centrosomes. The tumor suppressor protein p53 is involved in the control of centrosome duplication through activation of the G1/S checkpoint and transcriptional regulation of several downstream targets including the CDK inhibitor $p21^{Waf1}$ (Harper *et al.,* 1993). This inhibitor blocks centrosome duplication through inhibition of CDK2/ cyclin E activity.

Moreover, reduced activity of $p21^{waf1}$ by antisense expression in human cell lines resulted in centrosome amplification (Mantel *et al.,* 1999). Although introduction of wild-type p53 into $p53^{-/-}$ mouse embryonic fibroblasts reestablished centrosome homeostasis, overexpression of $p21^{waf1}$ only partially restored control of centrosome duplication in p53-null fibroblasts (Tarapore *et al.,* 2001).

Other control pathways and downstream targets of p53 may also play a role in the control of centrosome homeostasis. For example, p53 mutations and cyclin E overexpression act synergistically to further increase the frequency of centrosome amplification in cultured cells and in tumors (Mussman *et al*., 2000). Taken together, these observations suggest that an imbalance between negative and positive cell cycle regulators could accelerate centrosome defects seen in the development of cancer.

It is important to emphasize that during cancer progression, centrosome amplification and genomic instability can also develop independently of loss of p53 function, suggesting the presence of alternative mechanisms leading to disregulation of centrosome homeostasis (Lingle *et al.,* 2002). Mutations in the *BRCA1* and *BRCA2* tumor-suppressor genes associated with the development of familial breast and ovarian cancers also have been implicated in the loss of checkpoint control of the centrosome cycle (Deng and Brodie, 2000). The BRCA1 protein localizes at the centrosome during mitosis, and the hypophosphorylated form of BRCA1 coimmunoprecipitates with γ-tubulin, a centrosomal component essential for nucleation of microtubules (Xu *et al.,* 1999). Mouse embryo fibroblasts carrying gene-targeted deletions in *BRCA1* or *BRCA2* showed a defective G2/M checkpoint function, amplified centrosomes, aberrant mitoses, and aneuploidy (Xu *et al.,* 1999). The *GADD45* gene, a downstream transcriptional product of the p53 pathway, has also been implicated in both DNA damage repair and activation of the G2/M checkpoint. Cells lacking *GADD45* expression show centrosome amplification, mitotic spindle defects, and chromosomal instability (Hollander *et al.,* 1999). These studies show that centrosome amplification can develop through alternative pathways that converge on G1/S and G2/M checkpoint regulators.

Evidence for a Centrosome-Based Cell Cycle Checkpoint

Studies suggest that these regulatory mechanisms may reside at the centrosome itself (Sluder and Hinchcliffe, 2000). This concept is based on several independent observations. The first is that ablation of centrosomes by microsurgery or laser treatment resulted in cell cycle arrest at G1 prior to the onset of DNA replication (Hinchcliffe *et al.,* 2001); the second is that signaling-kinase anchoring motifs are present in proteins of PCM (Diviani and Scott, 2001); and the third is key cell cycle regulators, including the tumor suppressor proteins p53, BRCA-1 and -2, the cyclin/CDKs, and the anaphase-promoting complex/cyclosome, localize (albeit, some only transiently) within centrosome PCM. To summarize, centrosome ablation arrests the cell cycle and many important regulators of cell cycle progression reside in the centrosome. These observations suggest a mechanism by which key regulators may act locally within the structural context of the centrosome to coordinate steps critical for cell cycle progression and together suggest the existence of a centrosome-based cell cycle checkpoint.

Centrosome Amplification in Cancer

Centrosome defects have been implicated in the origin of mitotic abnormalities and the development of aneuploidy in cancer (Brinkley, 2001). Recent studies implicate centrosome defects in the origin of chromosomal instability and the pathogenesis of cancer (Lingle *et al.,* 1998; Lingle *et al.,* 2002). Centrosome defects (i.e., centrosome amplification) are characteristic of many solid tumors. The term "centrosome amplification" designates centrosomes that contain more than four centrioles (i.e., "supernumerary centrioles"), centrosomes that appear significantly larger than normal as defined by the staining of structural centrosome components in excess of that seen in the corresponding normal tissue or cell type, and/or when more than two centrosomes are present within a cell (Lingle *et al.,* 1998; Lingle and Salisbury, 1999). Figure 23 illustrates the ultrastructure of an amplified centrosome with nine centriole profiles in a human breast tumor cell. In addition, amplified centrosomes also show protein hyperphosphorylation and altered functional properties such as an increased microtubule-nucleating capacity (Lingle *et al.,* 1998). These centrosome abnormalities have been implicated as a potential cause for the loss of cell and tissue architecture seen in cancer (i.e., anaplasia) through altered centrosome function in microtubule nucleation and organization and to result in chromosome missegregation during mitosis as a consequence of an increased rate of multipolar spindle formation (Lingle *et al.,* 1998; Lingle *et al.,* 2002).

Centrosome Amplification, Aneuploidy, and Chromosomal Instability

A key question: Does centrosome amplification lead to chromosomal instability and aneuploidy, or is

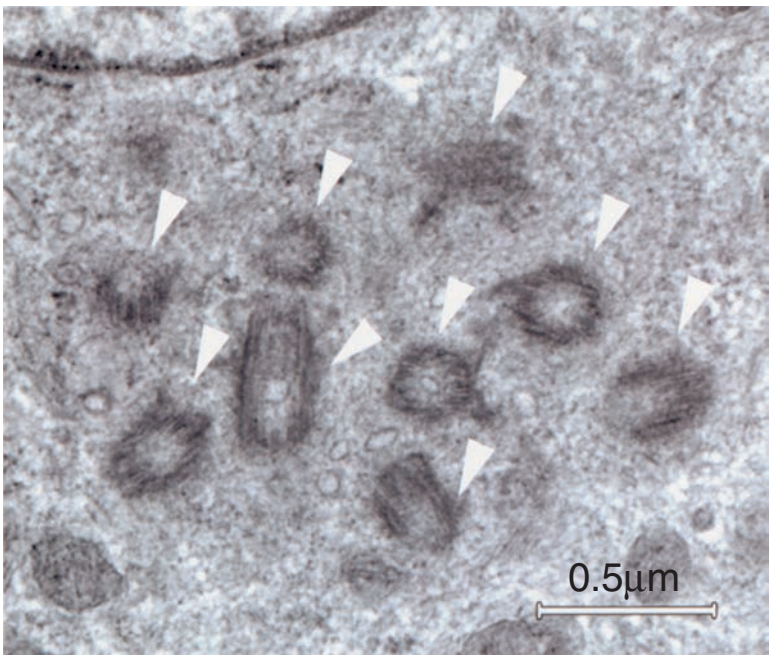

***Figure* 23.** Electron micrograph of an amplified centrosome. This section shows nine centriole profiles (arrowheads) of an amplified centrosome of a cell in a human breast tumor. Normal cells typically have two or four centrioles. Bar = 0.5 µm.

centrosome amplification a consequence of aneuploidy? Aneuploidy is characterized as the *state* of an abnormal karyotype, having gains and/or losses of whole chromosomes. Aneuploidy occurs early in the development of many tumor types, suggesting that it may play a role in both tumorigenesis and tumor progression. Indeed, aneuploidy is present in the great majority of malignant tumors, in contrast to benign tumors, which are most often diploid. Aneuploidy can be distinguished from the persistent generation of chromosomal variations, termed "chromosomal instability" (CIN), which reflects the rate of change in karyotype (Lengauer *et al.,* 1997). Quantitative analysis of CIN can be determined as the percentage of cells with a chromosome number different from the modal chromosome number. Thus, tumors may show either "stable aneuploidy" (low CIN) or "unstable aneuploidy" (high CIN). Unstable karyotypes may lead to phenotypic heterogeneity in cancer, reflecting the persistent generation of new chromosomal variations (Lingle *et al.,* 2002).

The development of aneuploidy may be a consequence of centrosome amplification, which can lead to the formation of multipolar spindles and mis-segregate sister chromatids during mitosis (and, as a result, lead to high CIN). Chromosomal instability occurs exclusively in aneuploid tumors and tumor-derived cell lines, in contrast to diploid tumors, which contain centrosomes that are functionally and structurally normal (Lingle *et al.,* 1998; Lingle *et al.,* 2002). The degree of genomic instability in aneuploid tumors parallels the degree of centrosome abnormalities in cell lines from breast, pancreas, prostate, colon, and cervix tumors; from short-term culture of mouse mammary tumors; and from SV40 ST overexpressing fibroblasts (D'Assoro *et al.,* 2002). When tissues were examined, centrosome abnormalities were higher in high-grade prostate tumors and high-grade cervical tumors than in low-grade tumors. In prostate cancer, centrosome amplification has been implicated in the development of abnormal mitoses and CIN facilitating progression to advanced stages of the disease (Pihan *et al.,* 2001; Skyldberg *et al.,* 2001).

Strong support for a direct mechanistic link between centrosome amplification and CIN is suggested by the significant linear correlation between centrosome amplification and the rate of change in karyotype (CIN) seen in human breast tumors (Lingle *et al.,* 2002). Although such correlation alone does not necessarily imply cause and effect, these observations have led many authors to propose the hypothesis that centrosome amplification is the primary cause of genomic instability observed in most tumors (Lingle *et al.,* 2002). As discussed earlier, Boveri (1914) first recognized these features of cancer cells nearly a century ago and proposed that centrosome defects could lead to mitotic

and subsequent chromosomal abnormalities. An alternative hypothesis has been proposed that claims chromosomal instability seen in cancer cells is caused by aneuploidy, i.e., that aneuploidy itself destabilizes the karyotype and thus initiates CIN leading to widespread heterogeneity in tumor cell phenotypes (Duesberg and Rasnick, 2000).

Several independent lines of evidence support the proposition that centrosome abnormalities drive genomic instability. In a study of human breast tumors, all specimens of ductal carcinoma *in situ* examined showed significant centrosome amplification, suggesting that centrosome amplification is an early event that occurs prior to invasion in breast tumors (Lingle *et al.,* 2002). Furthermore, cells transfected to express the human papilloma virus (HPV) E7 oncoprotein undergo centrosome amplification before developing nuclear morphology associated with aneuploidy (Duensing *et al.,* 2001). Finally, in a xenograft model of pancreatic cancer, metastatic foci showed a higher incidence of centrosome amplification than did the primary xenograft, and abnormal centrosome numbers were accompanied by a higher frequency of abnormal mitoses (Shono *et al.,* 2001).

Taken together, these studies underscore the importance of proper coordination of the centrosome and cell cycles and illustrate the potential for severe consequences of failure of proper regulation of these processes. They also suggest that centrosome amplification may be an early event in tumorigenesis that can drive CIN and lead to genotypic and phenotypic diversity of cells within a tumor. The following sections present methods used in our laboratories to assess structural and functional centrosome characteristics that accompany centrosome amplification in cancer.

Methods for Analysis of Centrosome Amplification in Cancer

Sample Procurement

Human tumor tissues should be collected according to an Institutional Review Board–approved protocol. It is useful to recruit a pathologist as a collaborator who can review all of the specimens in your study to confirm specific pathologies and to ensure consistent grading of the specimens. Prior exposure to chemotherapeutic or radiation therapy before surgery should be noted because these treatments themselves may cause centrosome anomalies. Tissue specimens are frozen in liquid nitrogen immediately after surgery and stored at −70°C until use or formalin fixed and paraffin embedded for later sectioning. Cultured cells should be seeded onto clean sterile glass coverslips, and cultured for 48 hr.

Morphological and Structural Methods

Centrosome Size and Number in Tissue Sections

Centrosome size can be determined in paraffin or frozen tissue sections using immunofluorescence labeling and confocal microscopy for measurements (Figure 24 A–B). The advantage of using tissue sections is that most tissues contain fibroblasts, which, as will be detailed later, can be used to normalize centrosome size so that meaningful comparisons can be made between tissue preparations and different slides. Antibodies against γ-tubulin, centrin, and pericentrin work well in cold methanol-fixed frozen sections, and anti-γ-tubulin (Sigma Chemicals, St. Louis, MO) works consistently in formalin-fixed paraffin sections.

Protocol for Immunolabeling

1. Incubate sections in blocking buffer (phosphate buffer saline [PBS], pH 7.2, 5% normal goat serum, 1% glycerol, 0.1% bovine serum albumin [BSA], 1% fish skin gelatin, and 0.04% sodium azide) for 30 min.
2. Incubate sections for 60 min in primary antibodies labeled with Zenon probes (Molecular Probes, Inc., Eugene, OR) according to the manufacturer's instructions.
3. Wash with PBS 3× for 5 min each.
4. Frozen section only (paraffin sections proceed to **Step 5**) postfix with 4% formaldehyde for 3 min, and wash with PBS 2× for 3 min each.
5. Stain nuclei with Hoechst 33342 (1 μg/ml) for 5 min.
6. Water rinse.
7. Air-dry for 5 min.
8. Mount coverslip with Prolong (Molecular Probes, Inc.) antifade medium.

For paraffin sections, once the slides are deparaffinated, antigen retrieval using pH 6 ethylenediamine tetra-acetic acid (EDTA) in a vegetable steamer for 30 min precedes **Step 1** above. After the mountant has set, usually overnight, the slides can be observed and analyzed using a Zeiss LSM 510 or equivalent confocal microscope using a 100X high N.A. objective lens.

Protocol for Confocal Analysis of Centrosome Size and Number

1. Configure the lasers and detectors for excitation and detection of Hoechst 33342 (364 excitation, blue emission) and Alexafluor 448 (448 excitation, green emission) and/or Alexafluor 568 (568 excitation, red emission).
2. Select pinholes equal to 1 Airey unit for each optical path.

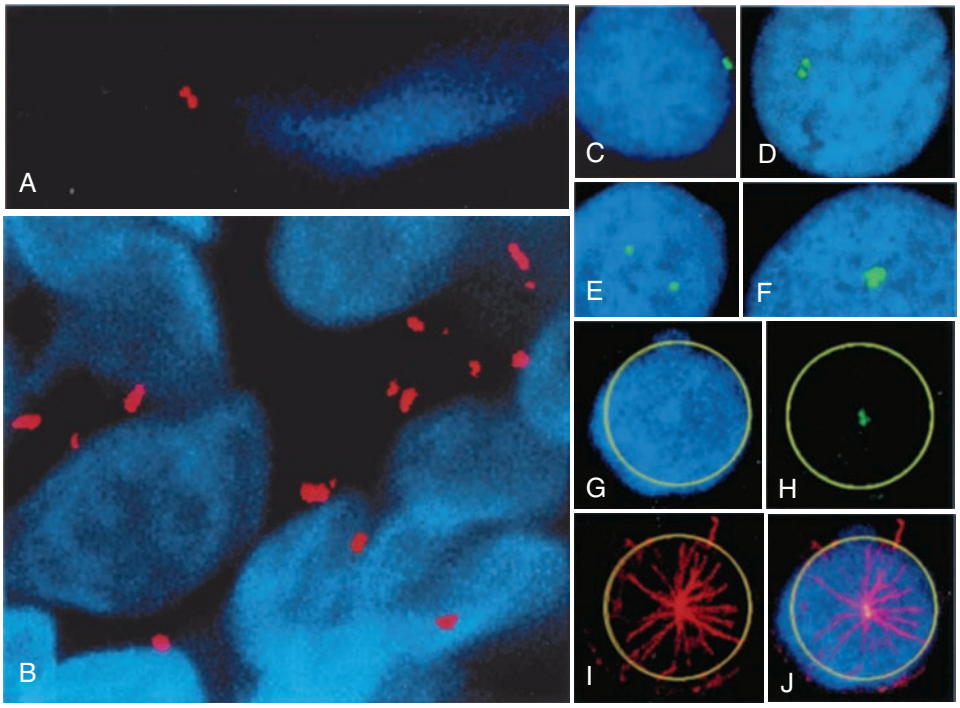

Figure 24. Analyses of centrosome characteristics. **A, B:** Determination of centrosome size and number. A paraffin section of a breast tumor showing maximum-intensity projection images of the centrosome of a fibroblast in **A,** and amplified centrosomes in a field of tumor cells in **B.** This preparation was stained with an antibody against the centrosome protein γ-tubulin (*red*) and Hoechst 33342 dye for DNA (*blue*). The red centrosome signals have been converted into pseudobinary images to allow determination of the area of the signal from each centrosome. The fibroblast centrosome in **A** has the typical bilobed shape characteristic of γ-tubulin–labeled centrosomes in normal, nonmalignant cells. In the region containing tumor cells **B,** most of the 14 centrosomes associated with this group of 11 nuclei are visibly larger than the centrosome in *A*. Therefore, this group of cells has centrosomes amplified slightly in both number and size.
C–F: Centrosome separation/duplication. These tissue culture cells have been stained using anti-γ-tubulin monoclonal antibodies tagged with Zenon Alexafluor 488 probes. The resulting centrosome signals can be categorized as **C:** single normal-sized centrosome, **D:** adjacent normal pair of centrosomes, **E:** separated normal pair of centrosomes, or **F:** a single amplified centrosome. Nuclei are stained with Hoechst 33342 dye.
G–H: Microtubule regrowth assay. This cell has been subjected to cold-induced depolymerization of its native-microtubules (MTs) followed by 2 minutes at 25°C to allow for MT regrowth prior to fixation and immunolabeling for α-tubulin (*red*) and γ-tubulin (*green*). The overlay circle was centered over the green centrosome signal and adjusted in diameter to extend just to the edge of the longest unbroken MT. The number and length of the regrown MTs can be determined from these images.

3. Set up for Z stack collection of 3–9 optical sections spaced at 0.5 μm intervals. The number of sections depends on the thickness of the tissue section but should be kept constant for a given experiment.

4. Place the slide on the microscope and focus on a fibroblast centrosome.

5. Set the digital zoom at 2X and the line averaging at 4.

6. Set laser power and detection parameters so that the resulting signal is saturated or nearly saturated only at the centrosome. (**Note:** Because this procedure is designed to measure area rather than signal intensity, saturated or nearly saturated signal is optimal.)

7. Collect a Z stack and make a maximum intensity projection of the stack.

8. Open the brightness and contrast window, select the color of the centrosome signal, and maximize both brightness and contrast to create a pseudobinary image of the centrosome. No other labeling should be seen with these settings. If other labeling is present, go back

to the detection settings and decrease detector gain slightly before collecting the image again. You may need to select a fresh fibroblast centrosome if photobleaching has occurred during these setup steps.

9. Open the measurement window and select area measurement.

10. Select the channel in which the centrosome signal was collected and adjust the slider down slightly so that everything but the centrosome signal is masked out.

11. Using the overlay function, draw a circle 3 μm diameter around the centrosome.

12. Select the area button to obtain the area of the centrosome signal inside the circle. It should be between 0.3 and 1.3 μm^2. If the value is less than 0.3 μm^2, return to the collection parameters in **Step 6** and increase the detector gain and/or amplitude and repeat the process. If the value is greater than 1.3 μm^2, repeat the collection parameters in **Step 6** and decrease the detector gain and/or amplitude and repeat the process. Once a value within the correct range is obtained, copy and paste the value into a spreadsheet. These steps establish the correct collection parameters for the particular slide under observation. From this point onward, do not alter the settings. You are now ready to use identical parameters to measure 4 additional fibroblast centrosomes, and then proceed to measure centrosomes in normal epithelial and tumor cells.

13. Focus on epithelial cells of interest.

14. Set the digital zoom at 2X.

15. Collect a Z stack and make a maximum intensity projection of the stack.

16. Open the brightness and contrast window, select the color of the centrosome signal, and maximize both brightness and contrast to create a pseudobinary image of the centrosome.

17. Open the histogram window and select area measurement.

18. Select the channel in which the centrosome signal was collected and adjust the low threshold slider down slightly so that everything but the centrosome signal is masked out.

19. Using the overlay function, draw a circle ~3 μm diameter around the first centrosome in the image. The diameter of the circle is not critical; just make sure that it includes the entire centrosome signal and excludes any autofluorescence your sample may have.

20. Select the area button to obtain the area of the centrosome signal inside the circle.

21. Copy and paste the value into a spreadsheet.

22. Repeat **Steps 19–21** for each centrosome in the image.

23. Count the number of the nuclei in the field and enter the number in the spreadsheet.

24. Repeat **Steps 13–23** until at least 50 nuclei have been counted for that tissue section.

25. Repeat **Steps 1–24** for each new tissue section.

Once the measurements have been collected, you should have a spreadsheet for each tissue analyzed. For each tissue, calculate the average and standard deviation of the fibroblast centrosome size. A standard deviation less than 15% of the average value is indicative of adequate specimen preparation and signal collection. Divide 1 by the average value to get a normalization factor. Determine the average value for the epithelial cell centrosomes and multiply it by the normalization factor to determine the normalized value. This normalized value can then be compared to normalized values from other tissues. This analysis assumes that fibroblast centrosome size is consistent between tissues.

Centrosome Number in Tissues and Cultured Cells

A much simpler analysis using only a subset of the steps described earlier can be used to calculate the number of centrosomes per cell. In cultured cells, this analysis can also be used to categorize centrosomes labeled for γ-tubulin according to the number of γ-tubulin spots per cell and the spacing of paired spots. Proceed with "Immunolabeling Protocol," as described earlier. In the "Confocal Analysis Protocol," follow **Steps 1–7,** except use a digital zoom of 1 instead of 2. Collect representative images with a total of at least 50 nuclei per sample. For tissues, count the number of centrosomes in each image and the number of nuclei in each field to determine the average number of centrosomes per nucleus. For cultured cells, the number of labeled centrosomes can be counted for each individual cell and each centrosome can be scored as follows: 1) a single normal-sized spot, 2) a separated normal pair, 3) a single amplified spot, or 4) multiple spots (Figure 24 C–F). This scoring method is difficult to apply to tissue sections because it is not always possible to assign each centrosome to a nucleus; nevertheless, it is useful for the analysis of centrosome characteristics and for comparison with cell cycle kinetics established in parallel experiments.

Functional Assay for Microtubule Nucleation and Growth

Live Cell Microtubule Regrowth Assay

This assay assesses an important parameter of centrosome functional in living cultured cells—their ability to regrow microtubules (MTs) after MT depolymerization (Figure 24 G–J). Native MTs are first depolymerized by cold treatment, then the specimen is returned to a temperature that supports MT polymerization, and the number and length of newly polymerized MTs are measured at intervals after recovery. The resulting MT asters are also characterized. Cells are cultured on

sterile 12-mm-diameter glass coverslips placed in the wells of 24-well tissue culture dishes. Let the cells grow to 80% confluence before starting the following protocol.

Protocol for MT Regrowth

1. Aspirate the growth medium from each well and rinse with microtubule stabilizing buffer (MTSB: 1% Triton X-l00, 10 mM Pipes, pH 7.2, 2 mM EGTA, 1 mM $MgSO_4$).
2. Aspirate the MTSB and add cold growth medium diluted with one part cold MTSB. Place culture dishes on ice and store for 30 min in the refrigerator. For the control, proceed directly to **Step 5.**
3. Aspirate cold solution from each well and replace with warm medium/MTSB filling the well half full. Start timing the regrowth immediately after adding the warm solution for each time point. Place plates in a 25°C incubator.
4. At each time point, aspirate the liquid and replace with 0.1% of Triton (prewarmed at 25°C). Incubate for *exactly* 1 min at room temperature.
5. Aspirate Triton and add −20°C methanol to the top of the wells. Place in the freezer for 10 min.
6. Remove the coverslips from the culture dishes and place them cell side up on a paper towel.
7. Let air-dry for at least 10 min.
8. Proceed with the "Protocol for lmmunolabeling," using primary antibodies against γ-tubulin and α-tubulin.

Protocol for Confocal Analysis of MT Regrowth

1. Follow **Steps 1–5** of the "Protocol for Confocal Analysis of Centrosome Size and Number," with the exception of taking single optical sections instead of Z sections.
2. Image cells for γ-tubulin labeled centrosomes and α-tubulin–labeled MTs.
3. Using the overlay function, draw a circle centered on the centrosome and extend the circle's perimeter to the end of the longest unbroken MT of the MT aster.
4. Display the circumference of the circle and enter that value into a spreadsheet. Convert the circumference to radius to determine the length of the longest MT.
5. Count the number of MTs in the aster.
6. Score the aster as organized (MTs radiating from the center in relatively straight paths) or unorganized (MTs crisscrossing each other in a helter-skelter fashion).
7. Score the cell as having single or multiple asters.

Abnormal Mitoses

Analysis of mitotic structure is a surrogate for centrosome function in mitosis. Cells or tissue sections can be scored for the number of abnormal mitoses as a percentage of total mitoses. This can be done on paraffin sections stained hematoxylin and eosin (H&E) or stained by immunohistochemistry for Ki-67. It can also be done on cultured cells whose nuclear morphology has been adequately preserved by formaldehyde fixation and stained with Hoechst 33342 or DAPI. The first 50–100 mitotic nuclei are counted and scored for mitotic stage (prophase, prometaphase, metaphase, anaphase, telophase, or unknown) and categorized as normal bipolar or abnormal multipolar. Centrosome abnormalities are sometimes manifested as a prolongation of the time spent in prometaphase and metaphase, so a comparison of the distribution of mitotic stages between cell populations is an important part of the overall analysis of mitotic abnormalities.

CONCLUSION

In conclusion, in this chapter we have reviewed centrosome dynamics and regulation in normal cells and the origin and consequences of centrosome amplification in cancer. Methods for the quantitative assessment of amplification of centrosome structure and function in human tumors and in cultured tumor cells were also presented. These methods can serve as a starting point for investigators who are interested in persuing the role of centrosome behavior and the origin of chromosomal instability and anaplasia in the development of cancer.

Acknowledgments

This work was supported by DAMD 17-98-1-8122 and DAMD 17-01-1-0753 from the Department of Defense Breast Cancer Research Program (to WLL), by Grant CA72836 from the National Cancer Institute (to JLS), and by the Mayo Foundation.

References

Bailly, E., Pines, J., Hunter, T., and Bornens, M. 1992. Cytoplasmic accumulation of cyclin B1 in human cells: Association with a detergent-resistant compartment and with the centrosome. *J. Cell Sci. 101*:529–545.

Balczon, R., Bao, L., Zimmer, W.E., Brown, K., Zinkowski, R.P., and Brinkley, B.R. 1995. Dissociation of centrosome replication events from cycles of DNA synthesis and mitotic division in hydroxyurea-arrested Chinese hamster ovary cells. *J. Cell Biol. 130*:105–115.

Boveri, T. 1914. Zur Frage der Entstehung Maligner Tumoren. Baltimore, Jena: Fischer Verlag (1929 English translation by M. Boveri reprinted as *The Origin of Malignant Tumors,* Williams and Wilkins Co., Baltimore).

Brinkley, B.R. 2001. Managing the centrosome numbers game: From chaos to stability in cancer cell division. *Trends Cell Biol. 11*:18–21.

D'Assoro, A.B., Lingle, W.L., and Salisbury, J.L. 2002. Centrosome amplification and the development of cancer. *Oncogene 21*:6146–6153.

Deng, C.X., and Brodie, S.G. 2000. Roles of BRCA1 and its interacting proteins. *Bioessays 22*:728–737.

Dirksen, E.R. 1991. Centriole and basal body formation during ciliogenesis revisited. *Biol. Cell. 72*:31–38.

Diviani, D., and Scott, J.D. 2001. AKAP signaling complexes at the cytoskeleton. *J. Cell Sci. 114*:1431–1437.

Duensing, S., Duensing, A., Crum, C.P., and Munger, K. 2001. Human papillomavirus type 16 E7 oncoprotein-induced abnormal centrosome synthesis is an early event in the evolving malignant P\phenotype. *Cancer Res. 61*:2356–2360.

Duesberg, P., and Rasnick, D. 2000. Aneuploidy, the somatic mutation that makes cancer a species of its own. *Cell Motil. Cytoskel. 47*:81–107.

Dutcher, S. 2001. Motile organelles: The importance of specific tubulin isoforms. *Curr. Biol. 11*:R419–R422.

Fry, A.M., Mayor, T., and Nigg, E.A. 2000. Regulating centrosomes by protein phosphorylation. *Centrosome Cell Replic. Early Develop. 49*:291–312.

Harper, J.W., Adami, G.R., Wei, N., Keyomarsi, K., and Elledge, S.J. 1993. The p21 Cdk-interacting protein Cip1 is a potent inhibitor of G1 cyclin-dependent kinases. *Cell 75*: 805–816.

Hinchcliffe, E.H., Li, C., Thompson, E.A., Maller, J.L., and Sluder, G. 1999. Requirement of Cdk2-cyclin E activity for repeated centrosome reproduction in Xenopus egg extracts [see comments]. *Science 283*:851–854.

Hinchcliffe, E.H., Miller, F.J., Cham, M., Khodjakov, A., and Sluder, G. 2001. Requirement of a centrosomal activity for cell cycle progression through G1 into S phase. *Science 291*:1547–1550.

Hollander, M.C., Sheikh, M.S., Bulavin, D.V., Lundgren, K., Augeri-Henmueller, L., Shehee, R., Molinaro, T.A., Kim, K.E., Tolosa, E., Ashwell, J.D., Rosenberg, M.P., Zhan, Q., Fernandez-Salguero, P.M., Morgan, W.F., Deng, C.X., and Fornace, A.J., Jr. 1999. Genomic instability in Gadd45a-deficient mice. *Nat. Genet. 23*:176–184.

Katayama, H., Zhou, H., Li, Q., Tatsuka, M., and Sen, S. 2001. Interaction and feedback regulation between STK15/BTAK/Aurora-A kinase and protein phosphatase 1 through mitotic cell division cycle. *J. Biol. Chem. 276*:46219–46224.

Keezer, S.M., and Gilbert, D.M. 2002. Sensitivity of the origin decision point to specific inhibitors of cellular signaling and metabolism. *Exp. Cell Res. 273*:54–64.

Khodjakov, A., and Rieder, C.L. 2001. Centrosomes enhance the fidelity of cytokinesis in vertebrates and are required for cell cycle progression. *J. Cell Biol. 153*:237–242.

Khodjakov, A., Rieder, C.L., Sluder, G., Cassels, G., Sibon, O., and Wang, C.-L. 2002. De novo formation of centrosomes in vertebrate cells arrested during S phase. *J. Cell Biol. 158*:1171–1181.

Lacey, K.R., Jackson, P.K., and Stearns, T. 1999. Cyclin-dependent kinase control of centrosome duplication. *Proc. Natl. Acad. Sci. USA. 96*:2817–2822.

Lengauer, C., Kinzler, K., and Vogelstein, B. 1997. Genetic instability in colorectal cancers. *Nature 386*:623–627.

Lingle, W.L., Barrett, S.L., Negron, V.C., D'Assoro, A.B., Boeneman, K., Liu, W., Whitehead, C.M., Reynolds, C., and Salisbury, J.L. 2002. Centrosome amplification drives chromosomal instability in breast tumor development. *Proc. Natl. Acad. Sci USA 99*:1978–1983.

Lingle, W.L., Lutz, W.H., Ingle, J.N., Maihle, N.J., and Salisbury, J.L. 1998. Centrosome hypertrophy in human breast tumors: Implications for genomic stability and cell polarity. *Proc. Natl. Acad. Sci. USA 95*:2950–2955.

Lingle, W.L., and Salisbury, J.L. 1999. Altered centrosome structure is associated with abnormal mitoses in human breast tumors. *Am. J. Pathol. 155*:1941–1951.

Lutz, W., Lingle, W.L., McCormick, D., Greenwood, T.M., and Salisbury, J.L. 2001. Phosphorylation of centrin during the cell cycle and its role in centriole separation preceding centrosome duplication. *J. Biol. Chem. 276*:20774–20780.

Mantel, C., Braun, S.E., Reid, S., Henegariu, O., Liu, L., Hangoc, G., and Broxmeyer, H.E. 1999. p21(cip-1/waf-1) deficiency causes deformed nuclear architecture, centriole overduplication, polyploidy, and relaxed microtubule damage checkpoints in human hematopoietic cells. *Blood 93*:1390–1398.

Mazia, D. 1987. The chromosome cycle and the centrosome cycle in the mitotic cycle. *Int. Rev. Cytol. 100*:49–92.

Meraldi, P., Lukas, J., Fry, A., Bartek, J., and Nigg, E. 1999. Centrosome duplication in mammalian somatic cells requires E2F and Cdk2-cyclin A. *Nature Cell Biol. 1*:88–93.

Mussman, J.G., Horn, H.F., Carroll, P.E., Okuda, M., Tarapore, P., Donehower, L.A., and Fukasawa, K. 2000. Synergistic induction of centrosome hyperamplification by loss of p53 and cyclin E overexpression. *Oncogene 19*:1635–1646.

Palazzo, R.E. 2003. Centrosome and spindle pole body dynamics: A review of the EMBO/EMBL Conference on Centrosomes and Spindle Pole Bodies, Heidelberg, September 13-17, 2002. *Cell Motil. Cytoskel. 54*:148–154.

Piel, M., Nordberg, J., Euteneuer, U., and Bornens, M. 2001. Centrosome-dependent exit of cytokinesis in animal cells. *Science 291*:1550–1553.

Pihan, G.A., Purohit, A., Wallace, J., Malhotra, R., Liotta, L., and Doxsey, S.J. 2001. Centrosome defects can account for cellular and genetic changes that characterize prostate cancer progression. *Cancer Res. 61*:2212–2219.

Pines, J. 1999. Four-dimensional control of the cell cycle. *Nat. Cell Biol. 1*:E73–E79.

Salisbury, J. 2003a. Centrosomes: Coiled-coils at the cell center. *Curr. Biol. 13*:R88–R90.

Salisbury, J.L. 2003b. Centrosome size is controlled by centriolar SAS-4. *Trends Cell Biol. 13*:340–343.

Shono, M., Sato, N., Mizumoto, K., Maehara, N., Nakamura, M., Nagai, E., and Tanaka, M. 2001. Stepwise progression of centrosome defects associated with local tumor growth and metastatic process of human pancreatic carcinoma cells transplanted orthotopically into nude mice. *Lab. Invest. 81*:945–952.

Skyldberg, B., Fujioka, K., Hellstrom, A.C., Sylven, L., Moberger, B., and Auer, G. 2001. Human papillomavirus infection, centrosome aberration, and genetic stability in cervical lesions. *Mod. Pathol. 14*:279–284.

Sluder, G., and Hinchcliffe, E.H. 2000. The coordination of centrosome reproduction with nuclear events during the cell cycle. *Curr. Top. Devel. Biol. 49*:267–289.

Tarapore, P., Horn, H.F., Tokuyama, Y., and Fukasawa, K. 2001. Direct regulation of the centrosome duplication cycle by the p53- p2lWafl/Cipl pathway. *Oncogene 20*:3173–3184.

Wheatley, D. 1982. *The Centriole: A Central Enigma of Cell Biology.* Amsterdam, Elsevier Biomedical Press.

Wilson, E.B. 1925. *The Cell in Development and Heredity.* New York, Macmillan Company.

Xu, X., Weaver, Z., Linke, S.P., Li, C., Gotay, J., Wang, X.W., Harris, C.C., Ried, T., and Deng, C.X. 1999. Centrosome amplification and a defective G2-M cell cycle checkpoint induce genetic instability in BRCA1 exon 11 isoform-deficient cells. *Mol. Cell 3*:389–395.

II

Liver Carcinoma

1

Liver Carcinoma

M.A. Hayat

The liver is unique in that it responds to physical or chemical injury by the process of regeneration. Although injured tissues and organs are capable of repairs, only the liver possesses the capability of replenishing lost functional volume. Nevertheless, parts of the liver, and the liver as a whole, can succumb to a number of genetic and epigenetic alterations. In the United States in 2004 a total of 1,368,030 new cancer cases and 563,700 deaths from cancer are expected; in the same year, 18,920 new liver cancer cases and 14,270 deaths from the disease are expected. In the United States the survival rate of patients with liver cancer is ~5 years and only 6%.

Because tumors and tumor-like lesions are common in the liver, it is necessary to differentiate between benign lesions and those that can give rise to a metastatic condition. The benign and malignant natures of hepatic tumors and tumor-like lesions are classified in Table 9. Hepatocellular adenoma and local nodular hyperplasia are the two most common benign neoplasms of the liver, occurring predominantly in women.

Primary liver carcinomas are classified as hepatocellular carcinoma (HCC), intrahepatic cholangiocarcinoma (combined HCC), and cholangiocarcinoma. The biological behavior and clinicopathologic features of the third type show that it is not simply a combination of the first two types. In fact, consistent differences of genetic alterations have been observed at different loci in HCC and intrahepatic cholangiocarcinoma (Koo *et al.,* 2003). Because HCC amounts to ~90% of primary liver cancer, it is emphasized in this chapter.

Hepatocellular Carcinoma

The primary hepatocellular neoplasms include hepatocellular adenoma, HCC, and hepatoblastoma. Of these neoplasms, HCC is the most common; it is one of the most common cancers in the world, affecting more than 500,000 people annually, and 5-year mortality exceeds 95%. Worldwide, 4% of all malignant tumors are HCC. It is the seventh most frequent cancer in males and the ninth in females. It is estimated that worldwide more than 1 million patients die of HCC annually. The number of fatalities caused by liver diseases in the United States is given in Table 10. Most patients with the disease die within weeks, or at most a few months, after diagnosis.

This malignancy exhibits uneven distribution geographically, with areas of Africa and Southeast Asia having incidences approximately tenfold higher than the average found in other parts of the world. Chronic hepatitis B virus (HBV) infection is the predominant risk factor for HCC in the high-incidence regions. The United States and Europe have much lower HCC rates, with increases in recent years attributed to hepatitis C

Handbook of Immunohistochemistry and *in situ* Hybridization of Human Carcinomas, Volume 3: Molecular Genetics, Liver Carcinoma, and Pancreatic Carcinoma

Table 9. Classification of Hepatic Tumors and Tumor-like Lesions

	Benign	Malignant
Epithelial	Hepatocellular adenoma	Hepatocellular carcinoma
	Bile duct adenoma	Cholangiocarcinoma
	Cystadenoma	Mucinous cystadenocarcinoma
	Biliary papillomatosis	Combined hepatocellular carcinoma-cholangiocarcinoma
		Hepatoblastoma
Mesenchyma	Hemangioma	Angiosarcoma
	Lymphangioma	Epithelioid haemangioendothelioma
	Infantile hemangioendothelioma	
	Angiomyolipoma	Embryonal sarcoma
	Solitary fibrous tumor	Other sarcomas
Miscellaneous		Lymphoma
		Germ-cell tumors
Tumor-like lesions	Focal nodular hyperplasia	
	Bile duct hamartoma	
	Mesenchymal hamartoma	
	Nodular regenerative hyperplasia/partial nodular transformation	
	Localized steatosis	
	Inflammatory pseudotumor	

After Clouston (2004).

virus (HCV) infection. The average age of onset of HCC is much younger in Africa and Asia, with a median of 40–50 years of age compared with 55–65 years of age in the United States. The average incidence of HCC in Africa and Asia is ~10–30 versus 1–3 per 100,000 persons each year in Western countries. The male to female ratio of HCC is ~5:1 in the HBV-endemic regions compared with 2:1 in the United States and Europe.

At least some of the causes of HCC are known, so its prevention is possible. The background of most HCCs is chronic hepatitis and/or liver cirrhosis. The risk of HCC increases in parallel to the progression of hepatic fibrosis associated with liver cirrhosis. Liver cirrhosis plays a particularly central role in hepatocarcinogenesis caused by chronic HBV or HCV infection. More than 50% of HCCs are the result of persistent (as opposed to transient) HBV infection, and ~25% are the result of persistent HCV (Pisani *et al.,* 1997). In North America, 52% of patients with HCC have positive tests for HBV surface antigen. The role of these viruses in HCCs is discussed later.

Table 10. Number of fatalities caused by liver diseases in the United States (1999)

Liver cell carcinoma	12,383
Alcoholic liver disease	11,958
Acute hepatitis C	3181
Bile duct carcinoma	2552
Acute hepatitis B	703
Chronic hepatitis C	582
Primary biliary cirrhosis	414
Acute hepatitis A	134
Chronic hepatitis B	129

Genetics of Hepatocellular Carcinoma

Carcinogenesis is a multiple-step process with molecular events in each stage of disease progression. The development of HCC is an example of the multistage process. Although early HCC is curable in most cases by surgical resectioning, the asymptomatic feature of HCC progression results in poor prognosis and a 5-year survival. Therefore, early diagnosis based on molecular genetic studies of tumorigenesis should improve the clinical management and treatment of this cancer. The molecular mechanisms of hepatocarcinogenesis are beginning to be understood.

Numerous genetic and/or epigenetic changes responsible for HCC have been identified. Multiple cancer-related genes are involved in hepatocarcinogenesis. In fact, a variety of genes and their products are responsible for the initiation, progression, and metastasis of cancers such as HCC. Approximately 20 genes carrying somatic mutations have been identified in HCC. Genetic alterations occurring in HCC include *p53* mutation, inactivation of *PTEN* and *p16* genes, Smad4 overexpression,

and hypermethylation on chromosome 16. Some other genes involved in HCC are beta-catenin, *Axin, M6P/1GF2R,* and tumor-suppressor gene Rb (retinoblastoma) (Chaubert *et al.,* 1997; de la Coste *et al.,* 1998; de Souza *et al.,* 1995; Hofseth *et al.,* 2002; Okuda *et al.,* 1996). Chromosomal aberrations in cancer cells reflect functional loss or gain in these genes, which, in turn, contributes to cancer formation and progression. Table 11 shows a number of biomarkers for HCC. Another important phase in this process is the balance between cell proliferation and cell death (apoptosis).

The genetic changes involved in HCC can be divided into at least four different pathways, although each pathway seems to be involved in a limited number of tumors. These pathways are as follows: (1) the p53 pathway involved in the DNA damage response, (2) the retinoblastoma pathway involved in the control of the cell cycle, (3) the transforming growth factor-β pathway involved in growth inhibition and apoptosis, and (4) the antigen-presenting cell beta-catenin pathway implicated in cell–cell adhesion and signal transduction (Gross-Goupil *et al.,* 2003). Loss of heterozygosity is also associated with HCC (Laurent-Puig *et al.,* 2001).

As stated earlier, hepetocarcinogenesis involves multiple mutations with distinctive pathogenetic and clinicopathologic significance. This hypothesis was tested by Pang *et al.* (2003) by evaluating *TP53* (*p53*) gene mutation in surgically resected HCC tumor specimens

Table 11. Biomarkers for Hepatocellular Carcinoma

Adenomantous polyposis coli gene	Morin *et al.* (1997)
[a]AIB1	Wang *et al.* (2002)
[a]Aldose reductase-like protein	Zeindl-Eberhart *et al.* (2004)
Axin 1 and Axin 2 genes	Ishizaki *et al.* (2004)
[a]Beta-catenin gene	Ishizaki *et al.* (2004)
Bcl-2	Garcia *et al.* (2002)
[a]Carcinoembryonic antigen	Kitagawa *et al.* (2002)
[a]Caveolin	Yerian *et al.* (2004)
[a]CD10	Borscheri *et al.* (2001)
[a]CD34 antigen	Salizzoni *et al.* (2003)
[a]CD40	Schmilovitz-Weiss *et al.* (2004)
CDK N2B (p15)	Pang *et al.* (2003)
CDKN2A (p16)	Pang *et al.* (2003)
[a]Cellular retinol-binding protein-1	Schmitt-Graff *et al.* (2003)
cFos	Mikula *et al.* (2003)
c-Jun	Komoda *et al.* (2002)
[a]C-myc	Raidl *et al.* (2004)
c-Myb	Yang *et al.* (2001)
[a]Cyclooxygenase-2 enzyme	Leng *et al.* (2003)
Cyclin D1	Zhang *et al.* (2002)
[a]Cytokeratin	Grassi *et al.* (2004)
[a]DNA binding-1 (Id-1) protein	Lee *et al.* (2003)
[a]E-cadherin	Herath *et al.* (2000)
Estrogen receptor-alpha	Iavarone *et al.* (2003)
Fetal growth factor insulin growth factor 2	Zatkova *et al.* (2004)
Galectin-1	Kondoh *et al.* (2003)
[a]Glutathione transferase (GST-π)	Yusof *et al.* (2003)
[a]Glypican	Midorikawa *et al.* (2003)
Glypican-3 protein	Hippo *et al.* (2004)
HCAP1 gene	Wan *et al.* (2004)
[a]HCCA1	Zeng *et al.* (2002)
[a]HCCA2	Wang *et al.* (2001)
Heat shock protein 70	Takashima *et al.* (2003)
[a]Hepatitis Bx antigen	Lian *et al.* (2003)
[a]Hepatocyte growth factor/MET receptor	Schoedel *et al.* (2003)
[a]Hepatoma-derived growth factor	Okuda *et al.* (2003)
[a]Her-2/neu	Potti *et al.* (2003)
Inhibitor-1 messenger ribonucleic acid (mRNA)	Aleem *et al.* (2003)
Insulin-like growth factor-binding protein-2	Ranke *et al.* (2003)
Integrin α vβ3	Kikkawa *et al.* (2002)
[a]Liver-specific ZP domain-containing protein	Xu *et al.* (2003)

continued

Table 11. Biomarkers for Hepatocellular Carcinoma—Cont'd

[a]LKB/STK11 gene	Kim *et al.* (2004)
Mad gene	Mauleon *et al.* (2004)
Mitochondrial DNA	Wong *et al.* (2004)
[a]MOC31	Morrison *et al.* (2002)
[a]$p21^{WAF1/CIP1}$	Qin and Ng (2001)
[a]$p27^{KIP1}$	Qin and Ng (2001)
[a]p53	Anzola *et al.* (2003)
[a]p62	Lu *et al.* (2001)
[a]p73	Tannapfel *et al.* (1999)
Phosphatidylethanolamine N-methyltransferase	Tessitore *et al.* (2003)
PIG11 gene	Ricketts *et al.* (2003)
PLA2G13	Smith *et al.* (2003)
PLAG1 oncogene	Zatkova *et al.* (2004)
[a]PTEN gene	Hu *et al.* (2003)
Rbl protein	Edamoto *et al.* (2003)
[a]RCAS1	Noguchi *et al.* (2001)
Ribosomal protein L36a (RPL44)	Kim *et al.* (2003)
SIAHI gene	Matsuo *et al.* (2003)
[a]Smad4	Kitamura and Ninomiya (2003)
[a]Squamous cell carcinoma antigen	Pontisso *et al*. (2004)
[a]Survivin	Moon and Tarnawski (2003)
Telomerase reverse transcriptase	Masutomi *et al.* (2002)
Tetraspanin CO-029	Kanetaka *et al.* (2003)
[a]Thyroid transcription factor-1	Pan *et al.* (2004)
[a]TP53	Szymanska *et al.* (2004)
[a]Transforming growth factor-β1	Hyashi *et al.* (2004)
Vascular endothelial growth factor	Cascinu *et al.* (2003)
[a]X-linked inhibitor of apoptosis	Shiraki *et al.* (2003)

[a]These biomarkers have been identified with immunohistochemisty and/or *insitu* hybridization.

using polymerase chain reaction (PCR)-single-strand conformation polymorphism-sequencing, and *CDKN2B* (*p15*) and *CDKN2A* (*p16*) gene methylation by methylation-specific PCR. They also tested genetic imbalances in such specimens by using comparative genomic hybridization. Based on the results of this correlative study, they proposed a model of the genetic alterations in hepatocarcinogenesis (Figure 25). In this model HBV is the predominant predisposing factor, which may synergize with aflatoxin to increase *TP53* gene mutation. Amplifications of 17q, 1q, 6p, 10p, and 20p result in enhanced tumor invasiveness, and deletions of 1p, 11q, 4q, and 14q lead to increased rate of tumor growth.

In summary, as is true in the case of other solid carcinomas, hepatocarcinogenesis is a multistage process that occurs as a result of mutations in oncogenes and tumor-suppressor genes. Loss of heterozygosity (LOH) as well as replication errors are the phenotypes of genetic instability, which have been used as tools for detecting alterations in the oncogenes and tumor-suppressor genes. The inactivation of tumor-suppressor genes is caused by the intragenic mutation of the genes or by the loss of one allele in the appropriate chromosomal region (Koo *et al.,* 2003). Regions with high LOH frequencies are important for identifying the negative regulators of tumor growth. DNA mismatch repair is also an important mechanism for maintaining the fidelity of the genomic DNA. Defective mismatch repairs are implicated in a variety of tumor types. A large number of genes and molecular pathways are involved in HCC, which are discussed next.

Biomarkers for Hepatocellular Carcinoma

The development of cancer is a relatively slow multistep process; therefore, it often takes several years to become clinically manifested. During tumor progression, cancer cells acquire multiple alterations that render them increasingly competent to establish metastatic lesions in specific organs. However, primary tumors may already contain a gene(s) expression profile that is strongly predictive of metastasis and poor survival, thus challenging the notion that metastatic ability is acquired only late during tumor progression.

Presently, techniques that possess the sensitivity and specificity to detect a tumor at its earliest stage are lacking. Because reduction of cancer mortality is dependent partly on the early detection, the importance

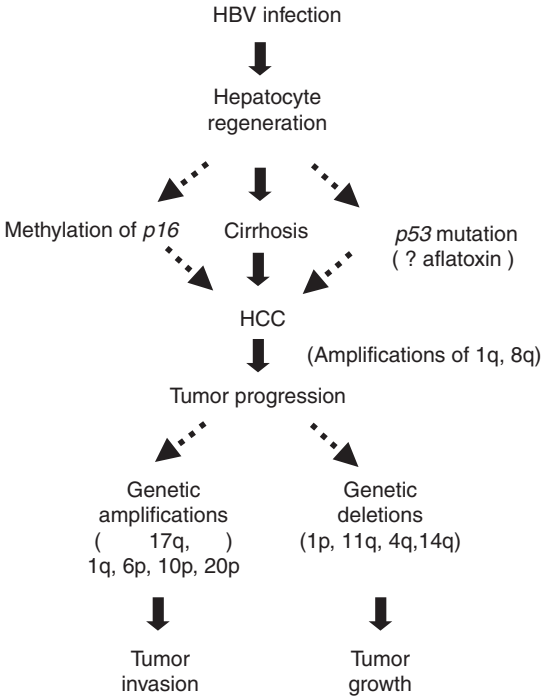

Figure 25. A model of the genetic alterations in hepatocarcinogenesis. Hepatitis B virus (HBV) is the predominant predisposing factor that may synergize with aflatoxin to increase *TP53* gene mutation. Chronic HBV infection leads to cirrhosis, and the associated liver cell regeneration enhances abnormal methylation of the *CDKN2A* gene, resulting in deregulation of cell cycle control. Amplification of chromosomes 1q and 8q is most common in tumors and may lead to overexpression of putative protooncogenes that contributes to tumorigenesis. Amplification of 17q, 1q, 6p, 10p, and 20p results in enhanced tumor invasiveness, and deletion of 1p, 11q, 4q, and 14q leads to increased tumor growth rate. After Pang *et al.* (2003).

of such detection of neoplasia is obvious. Early detection of tumor development also facilitates accurate clinical decisions such as risk assessment, monitoring course of disease, and positive or negative response to therapy. Thus, through early detection, longer disease-free survival, longer overall survival, and improved quality of life for the patient can be achieved. Early detection of certain tumor types can be achieved by detecting specific biomarkers.

Biomarkers are molecular signatures of a cellular phenotype that facilitate early cancer detection, pathologic grading and staging, and risk assessment to help in the development and use of molecularly targeted therapies tailored to the patient and to increase the rate of survival as a result of early detection or improved therapies. In other words, tumor markers can help in at least six areas: 1) screening (finding cancer early), 2) diagnosis (is it really a cancer?), 3) prognosis (how will the cancer behave?), 4) monitoring (how is the treatment working?), 5) predicting a response (will a drug be effective?), and 6) surveillance (will the patient need more treatment?). Because early detection and effective prevention represent the most promising clinical approaches, the identification of biomarkers to stratify patients into different risk groups would be a potential strategy for clinical trials.

One of the main reasons for lack of specific markers to achieve exact prognosis of HCC is that it is a very heterogeneous tumor entity and multiple changes at the cellular and subcellular levels occur during tumor development and progression. The molecular mechanisms responsible for HCC include aneuploidy and multiple genetic alterations. For example, mutations of *p53, Rb,* beta-catenin, and insulin-like growth factor 1 occur in HCC, whereas *C-myc* and cyclin D1 are frequently overexpressed; LOH is also associated with the inactivation of tumor-suppressor genes. In addition, several growth factors, including transforming growth factor and a large number of molecular biological factors, are implicated in the development of HCC. Moreover, alpha fetoprotein is associated with the invasiveness of HCC (Qin and Tang, 2002). Coleman has also discussed molecular mechanisms involved in human hepatocarcinogenesis in Chapter 2 of Part 2 in this volume.

Although the clinical value of early detection of tumor markers cannot be ignored, the prognostic power of a marker depends on the fundamental understanding of the specific disease process and their clinical use. It should also be noted that markers are molecules detectable in the primary tumor tissue, metastatic lesions, blood, or body fluids of patients with cancer. If possible, molecular diagnosis should precede clinical diagnosis. Ideally, the clinical diagnosis should correlate with the molecular diagnosis, and the former should be reversed if necessary.

Detailed immunohistochemical and *in situ* hybridization methods for the identification and functional role of the following markers in hepatocellular carcinoma are presented in Part 2 of this volume: *p21, p53, ZBP-89, PTEN, Bcl-2, Bcl-xL, Gaddh45 beta,* deoxyribonucleic acid (DNA) topoisomerase, DNA methyltransferases, hepatitis B surface antigen, and *EBAG9/RCAS1*. Most of the well-known genes (biomarkers) and their products involved in hepatocellular carcinoma are discussed next. Although most of them have not been used as yet for molecular diagnosis, they have been successfully used for conventional diagnosis.

Aldose Reductase-like Protein

Misprogramming of genetic information in cancer is reflected by quantitative and/or qualitative protein alterations. Such alterations represent tumor markers that are

useful in diagnosing human tumors, including HCC and may also help in understanding the mechanisms of tumor induction and development. Thus, proteomic protocols are valuable tools to identify proteins associated with cancer, including HCC. Members of the aldo-keto reductase (AKR) superfamily are involved in carcinogenic processes. One such member is human aldose reductase-like protein-1 (hARLP-1), which is present at elevated amounts in HCC and is discussed next.

The AKR superfamily includes several main enzyme families, the members of which are monomeric cytoplasmic proteins; most of them catalyze the nicotinamide adenine dinucleotide phosphate (NADPH)-dependent reduction of a large variety of xenobiotics and endogenous aldehydes and ketones and metabolize a wide range of substrates. They also play a role in carcinogenesis. The hARLP-1 messenger ribonucleic acid (mRNA) has been expressed in human HCC (Cao *et al.,* 1998). A novel antibody directed against common parts of the hARLP-1 has revealed positive activity in human HCC (Zeindl-Eberhart *et al.,* 2004). Thus, hARLP-1 is a strong candidate for use as an independent immunohistochemical diagnostic marker of human HCC, although it requires further testing.

Beta-Catenin

Beta-catenin is one of the key downstream effectors in the Wnt signaling pathway that plays an important role in various human cancers. Mutations at the serine and/or threonine residues near the NH_2 terminus in the *β-catenin* gene prevent their phosphorylation by the adenomatous polyposis coli (APC)-axin-glycogen synthase kinase 3β complex and subsequent degradation through the ubiquitin-proteasome pathway (Behrens *et al.,* 1998).

Beta-catenin plays important roles not only in cell–cell adhesion but also in the Wnt signaling pathway. The Wnt signaling pathway is conserved in various species and plays significant roles in development, cellular proliferation, and differentiation. It is well established that deregulation of the Wnt signaling pathway results in accumulation of β-catenin, which subsequently interacts with T-cell factor/lymphocyte enhancing– binding factor and activates their transcriptional activity (Morin *et al.,* 1997). Activating mutations in the *β-catenin* gene that result in the production of a stable form of the protein have also been identified in various malignant tumors as well as in HCC (De La Coste *et al.,* 1998).

Harada *et al*. (2004) have constructed a new transgenic mouse strain in which an activated H-*ras* protein is expressed on Cre-mediated recombination and investigated whether stabilized β-catenin can cause HCC in cooperation with activated H-*ras*. This study indicates that *β-catenin* mutations play a critical role in hepatocarcinogenesis in coordination with another oncogene (H-*ras*) and that these mice provide a convenient model to investigate early steps of hepatocarcinogenesis. Both *β-catenin* mutations and activation of H-*ras* signaling pathways, such as overexpression of transforming growth factor alpha or insulin-like growth factor II, are often found in human HCC.

Carcinoembryonic Antigen, CA19-9 and DU-PAN-2 Glycoproteins

Carcinoembryonic antigen (CEA), CA19-9, and DU-PAN-2 are glycoprotein tumor markers of the gastrointestinal tract and biliary duct system, but their serum levels are often elevated not only in patients who have chronic hepatitis or liver cirrhosis but also in those who have HCC (Maestrazi *et al.,* 1998). According to Haratake *et al.* (1995), high serum values of CA19-9 and DU-PAN-2 should indicate the mixed type of HCC. One study reports the presence of CEA in the trabecular type of HCC and that of CA19-9 and DU-IAN-2 in cholangiolar areas in the mixed type of HCC (Kitagawa *et al.,* 2002). However, further detailed immunohistochemical studies are needed to confirm the expression of these glycoproteins in HCC.

CCND1

CCND1, the cyclin D1 gene, located on chromosome 11q13, is involved in transition from G_1 to S phase, regulates cell cycle progression, and is associated with CDK4 and CDK6. Cyclins control the cell cycle by regulating the activity of CDK and commonly are altered in human malignant tumors. The HBV DNA integrates into an intron of the *cyclin A* gene, giving rise to a hybrid cDNA encoding an HBV/cyclin A fusion protein, suggesting the importance of cyclins in hepatocarcinogenesis.

Compelling evidence indicates that *CCND1* is involved in the formation and progression of malignancies. Studies indicate that the CCND1 genotype influences genetic susceptibility to HCC and its relationship to clinical outcomes of HCC (Zhang *et al.,* 2002). Such an influence requires further investigation in a larger study. This gene itself may be an important target for chemopreventive strategies in HCC and other malignant tumors.

Cyclooxygenase-2

Cyclooxygenases (COXs) are key enzymes in the conversion of arachidonic acid to prostaglandins and other eicosanoids. Two isoforms of COX have been

identified, COX-1 and COX-2. COX-1 is expressed constitutively in most tissues and is responsible for maintaining basic physiologic functions, such as cytoprotection in the stomach and vasodilation in kidney. COX-2 is not constitutively expressed and is induced by a variety of stimuli such as cytokines, hormones, mitogens, tumor promoters, and growth factors (Williams *et al.,* 1999). These causative factors explain the up-regulation of COX-2 in various inflammatory diseases and human cancers.

Several studies have demonstrated the up-regulation of COX-2 in transfection experiments of oncogenes such as *src* and *ras,* suggesting that up-regulation of COX-2 is a general phenomenon in carcinogenesis (Subbaramaiah *et al.,* 1996). Indeed, COX-2 mRNA and its protein product are expressed in human carcinomas, including colon cancer, gastric cancer, and squamous cell cancer (e.g., Ristimaki *et al.,* 1997).

Hepatocellular carcinoma often arises from chronic inflammatory liver diseases. Mediators of inflammation, such as prostaglandins, are also involved in its pathogenesis. However, the role of COX-2–controlled prostaglandin metabolism in hepatocarcinogenesis warrants further investigation.

The role of COX-2 in HCC is complex. Immunohistochemical studies have demonstrated the direct role of COX-2 in the growth control of human liver cancer cells (Leng *et al.,* 2003). This study also provides the evidence for the involvement of serine/threonine protein kinase B (Akt) activation in COX-2–mediated HCC cell growth. Some information is available about whether COX-2 is involved in the entire process of human hepatocarcinogenesis. In advanced HCC (usually consists of moderately and/or poorly differentiated HCC components), COX-2 does not play a major role in promoting dedifferentiation of the hepatocellular tumor (Koga *et al.,* 1999). Histologically, well-differentiated HCC expresses significant levels of COX-2, whereas less differentiated HCC expresses little or no COX-2. Because COX-2 regulates the production of vascular endothelial growth factor (VEGF), it is suggested that COX-2 plays a promoting role in tumor angiogenesis through the COX-2/VEGF system (Cianchi *et al.,* 2001). Studies also indicate that selective COX-2 inhibitors with COX-independent properties potentially suppress hepatocarcinogenesis (Koga, 2003). Immunohistochemical studies have demonstrated that COX-2 is related to HCC, whose histology is well-differentiated (Shiota *et al.,* 1999). Another immunohistochemical analysis suggests that COX-2 plays a role in the early stages of hepatocarcinogenesis, but not in the advanced stages, and consequently is related to HCC dedifferentiation (Koga *et al.,* 1999).

Glypican-3

Glypican-3 (GPC-3) is a heparin sulfate proteoglycan that is associated with an apoptotic effect. Silencing of GPC-3 has been demonstrated in several types of cancers, including ovarian, breast, and lung cancers (e.g., Xiang *et al.,* 2001). Overexpression of GPC-3 mRNA in HCC has been reported (Midorikawa *et al.,* 2003). Hippo *et al.* (2004) delineated the usefulness of soluble GPC-3 (sGPC-3) as highly sensitive to early-stage HCC. They have also demonstrated the complementarity of sGPC-3 and another HCC marker, alpha fetoprotein (AFP). In well-differentiated or moderately differentiated HCC, sGPC-3 is superior to AFP in sensitivity, and a combination measurement of both of these markers improves overall sensitivity. Another advantage of sGPC-3 is that the membrane-anchored portion is a potential target for antibody therapy. Further investigation into the clinical aspects of GPC-3 in HCC is warranted.

Hepatitis B XAntigen

Hepatitis B Xantigen (HB XAg) is a potentially promiscuous *trans*activating protein. This protein binds to and alters the function of transcription factors such as OCT-1, ATF-2, CREB, TBP, and other elements of the transcription machinery (e.g., Haviv *et al.,* 1996). It may also repress gene expression by binding to and inactivating the tumor-suppressor *p53* gene (Ueda *et al.,* 1995). The expression of other genes and proteins is also suppressed or down-regulated by HB XAg; these molecules include p55, p21, and Sui, all of which negatively regulate hepatocellular growth and survival. It is also known that HB XAg stimulates several cytoplasmic signal transduction pathways (e.g., mitogen-activated protein kinase [MAPK]) that promote cell growth and/or promote cell survival in the presence of apoptotic stimuli.

Information is available regarding the natural effectors of HB XAg, which contribute to the development of HCC. Up-regulated gene clone 11 (URG11) is one of such effectors, the expression of which is up-regulated by HB XAg (Lian *et al.,* 2003). The URG11 is a natural effector of HB XAg that promotes the development of HCC. *In situ* hybridization method has demonstrated that URG11 is strongly expressed in the chronically infected liver compared with uninfected liver tissues (Lian *et al.,* 2003). The expression of another effector, URG4, is also stimulated by HB XAg; the former also promotes the development of HCC (Tufan *et al.,* 2002).

Although the mechanism responsible for stimulating the expression of URG11 by HB XAg is not fully

known, calcium is thought to play a role in this process. It has been shown that HB XAg triggers the release of intracellular calcium from the endoplasmic reticulum and/or mitochondria, which in turn activates the cytosolic calcium-dependent proline-rich tyrosine kinase-2 (Bouchard *et al.,* 2001). This tyrosine kinase activates *ras* signaling. It would be interesting to find out if this pathway contributes to the HB XAg-triggered alterations in host gene expression, which are responsible for hepatocellular transformation at the molecular level.

HER-2/*neu*

In contrast to PTEN, HER-2/*neu* protein overexpression is rare in patients with advanced HCC. Immunohistochemical studies indicate that anti-HER-2/neu antibodies play only a limited role in the treatment of this carcinoma (Hsu *et al.,* 2002). Another recent fluorescence *in situ* hybridization (FISH) and immunohistochemical study also indicates that neither HER-2/*neu* gene amplification nor overexpression of its protein product can be regarded as a useful prognostic factor in HCC (Vlasoff *et al.,* 2002). However, according to Nakopoulou *et al.* (1994), 21 out of 71 HCC tissues analyzed by immunohistochemistry (IHC) showed staining for HER-2/*neu* protein. In addition, HER-2/*neu* protein overexpression was reported in the cytosol of advanced HCC, using enzyme-linked immunosorbent assay (ELISA) (Heinze *et al.,* 1999). Nevertheless, sufficient evidence is available indicating that the amplification and overexpression of this gene and protein are not important prognostic factors for patients with advanced or metastatic HCC.

Inhibitor of Differentiation and DNA Binding Protein

Inhibitor of differentiation and DNA binding (Id) proteins are transcription factors that belong to a group of helix–loop–helix proteins devoid of the DNA binding domain. As a result, these proteins function as dominant inhibitors of basic helix–loop–helix transcription factors by forming transcriptionally inactive heterodimers. Four Id genes (Id-1 through Id-4) play a role in cell growth and differentiation. Typically, these proteins are overexpressed in actively proliferating cells, while down-regulated as a prerequisite for exit from cell cycle and differentiation (Norton, 2000).

The Id family member Id-1 has been implicated in regulating cellular life span, immortalization, and delayed senescence in mammalian cells (Lundberg *et al.,* 2000). Overexpression of this protein has been reported in a number of tumor types, including breast, prostate, pancreatic, cervical, and colorectal adenocarcinomas. Overexpression of Id-1 is also correlated with patients' poor clinical outcome and mitotic index in several human cancers. This and other evidence supports the important role Id-1 plays not only in tumorigenesis but also in tumor progression.

Another effect of Id-1 is that it opposes Ets-mediated activation of $p16^{INK4a}$ via Ras-Raf-MEK signaling (Ohtani *et al.,* 2001). The $p16^{INK4A}$/retinoblastoma (RB) pathway is down-regulated in various human tumors including HCC, either through loss of $p16^{INK4A}$ or RB function or through down-regulated expression of cyclin D or cdk4 (Tannapfel *et al.,* 2001). *In vivo* and *in vitro* data provide evidence supporting the overexpression of Id-1 in HCC and its role in HCC cell proliferation (Lee *et al.,* 2003). The Id-1–induced HCC proliferation occurs through inactivation of $pl6^{INK4a}$/pRB pathway as shown by the evidence of decreased $p16^{INK4a}$ expression and activation of CDK and RB in the five Id-1 transfectants (Lee *et al.,* 2003). In conclusion, Id-1 is overexpressed in HCC tissues both at mRNA and protein levels. Overexpression of Id-1 protein is correlated with proliferating cell nuclear antigen. Hepatocellular carcinoma tissues showing low Id-1 protein expression also have a lower Id-1 mRNA level and higher $p16^{INK4A}$ expression.

LKB1 Gene

The LKB1 (STK11) gene encodes a serine/threonine kinase and resides on chromosome 19p13.3 at a distance of 190 kb proximal to D19S886. The gene is thought to play a role in the cell cycle and apoptotic pathways. Heterozygous LKB1 (±) mice have been shown to develop not only gastrointestinal polyps but also HCCs (Nakau *et al.,* 2002). A growing body of evidence suggests that inactivation of LKB1 is responsible for the development of HCC and that genetic alteration of this gene may also be associated with the development of sporadic forms of HCC. Somatic mutations of the *LKB1* and *p53* genes have been detected in HCC (Kim *et al.,* 2004). This and other evidence suggests that mutations of the *LKB1* or *p53* genes may provide the HCC cell with protection from p53-dependent apoptosis. These mutations may also play a role in tumor-progression in a subset of HCCs. Additional studies are needed to confirm the tumor-suppressing role of LKB1 in the development or progression of HCC.

Metastatic Tumor Antigen1

Metastatic tumor antigen 1 (MTA1) is a component of the nucleosome remodeling and histone deacetylation (NURD) complex, which is associated with adenosine

triphosphate (ATP)-dependent chromatin remodeling and histone deacetylase activity (Toh *et al.,* 2000). This antigen functions in conjunction with other components of NURD to mediate transcriptional repression and facilitates the association of repressor molecules with the chromatin. MTA1 is normally expressed only at low levels in various tissues. It has been shown that MTA1 enhances migration, invasion, and anchorage-independent survival of immortalized human keratinocytes (Mahoney *et al.,* 2002). This and other studies suggest that MTA1 is an indicator for assessing the potential aggressiveness of various tumors.

Involvement of estrogen receptor in the pathogenesis of HCC has been suggested, and anti-estrogen therapy has been reported to improve survival of patients with inoperable HCC (Martinez-Ceresco *et al.,* 1991). There is potential negative regulation between MTA1 and estrogen receptor. Immunohistochemical studies demonstrate that the MTA1 expression is closely related to vascular invasion and the growth of HCC (Moon *et al.,* 2004). Moreover, MTA1 inhibits translocation of estrogen receptor-α to the nucleus in human HCC cells; such movement tends to promote tumor progression.

Mitogen-Activated Protein Kinase

MAPK cascades are universal signal transduction modules that function in a wide variety of biological response mechanisms. The MAPK pathway consists of a series of protein kinases including c-Jun N-terminal kinase (JNK). The JNK signaling pathway and c-Jun are implicated in the regulation of diverse cellular functions such as proliferation differentiation, transformation, and apoptosis (Leppa and Bohmann, 1999).

c-Jun functions both as an executor of death signals and as a protector of cells from cell death, depending on cell types and environmental conditions. It is essential for normal hepatogenesis. Accordingly, c-Jun functions differently between normal and HCC tissues. A 2002 study indicates that the JNK signaling pathway and c-Jun play a negative role in cell survival and proliferation in HCC cells (Komoda *et al.,* 2002). Thus, c-Jun might be considered a tool for gene therapy for HCC.

17p

Deletion of 17p is one on the most frequent chromosomal alterations in HCC detected by both comparative genomic hybridization (CGH) and LOH (Guan *et al.,* 2000; Nose *et al.,* 1993). Allelic loss of 17p often coincides with the mutation of tumor-suppressor gene *TP53* at 17p13.1. However, in some cases, loss of the 17p allele occurs at a high frequency at 17p13.3 region distal to *TP53,* with relatively low *TP53* mutations. Studies by Katiyar *et al.* (2000) indicate that mutations in this gene may not play a direct role in the development of HCC. A 2003 study also suggests that 17p13.3 may harbor another tumor-suppressor gene that plays an important role in HCC development (Guan *et al.,* 2003).

p53

In recent years we have gained a better understanding of the genetic and environmental interactions and mechanisms associated with the development of primary liver cancer. The *p53* tumor-suppressor gene (*TP53*) plays a major role in hepatocarcinogenesis. Inactivation of this gene, located at chromosome 17p13.1, is one of the most common abnormalities in HCC and many other cancers. It encodes a 393 amino acid nuclear phosphoprotein that binds specific DNA sequences in the human genome. The *p53* gene is of critical importance for the regulation of cell cycle and maintenance of genomic integrity. Alterations in the genome or function of *p53* are important events in hepatocarcinogenesis. Frequent loss of one allele and mutations in the remaining allele occur in HCC (Hsu *et al.,* 1991).

Wild-type *p53* is polymorphic at residue 72 in exon 4, where a single base change causes a substitution of proline for arginine in the transactivation domain. The frequency of the proline variant has been studied as a potential risk factor for HCC and other cancers (Yu *et al.,* 1999). Using PCR and PCR-single strand conformation polymorphism, Anzola *et al.* (2003) suggested that the frequent loss of the proline allele in HVC-associated carcinogenesis of the liver plays some role in hepatocarcinogenesis. However, according to Okuda (2002), in the HVB-associated HCC, codon 249 mutation in the *p53* gene seems more related to exposure to aflatoxin B1 than to hepatocarcinogenesis itself. Aflatoxin B1 is a primary dietary risk factor for HCC.

PTEN

PTEN (phosphatase and tensin homologous on chromosome 10) is a well-known tumor-suppressor gene located on chromosome 10q23. It has dual specificity, dephosphorylating both lipid and protein substrates, and is associated with cellular growth, apoptosis, and tumorigenesis. Somatic mutations of *PTEN* are common in many types of cancer cell lines and primary tumors, including breast, prostate, gliomas, melanoma, thyroid, and endometrial cancers. Inactivation of this gene is a common event in advanced stages of diverse human malignancies, including HCC. Immunohistochemical studies demonstrate that reduced *PTEN* expression levels are involved in the pathogenesis of HCC (Hu *et al.,* 2003).

Decreased *PTEN* expression is correlated with tumor progression, high α fetoprotein(AFP) levels, and p53 overexpression. Accordingly, loss of *PTEN* protein following mutation of this gene is an indicator of poor prognosis in patients with HCC. Allele loss and *PTEN* mutations at 10q23 occur with HCC with a high frequency (30–50%).

Univariate analysis reveals that *PTEN* expression is an independent prognostic factor for patient survival. The overall survival is longer for the patients with HCC with high PTEN protein expression than for those with low PTEN expression. It is also known that a significant positive correlation exists between low PTEN protein expression in the HCC and increased expression of iNOS and COX-2 in the surrounding liver tissue. PTEN negatively regulates carcinoma cell growth by controlling Akt/PKB signaling pathway, whereas Akt/PKB can induce iNOS and COX-2 expression (see references in Tan *et al.,* 2002). Accordingly, down-regulation of PTEN might result in concomitant up-regulation of iNOS and COX-2 in the surrounding liver tissue through the resulting Akt up-regulation. Further studies are warranted to clarify *in vivo* tumor suppressive function of Akt signaling in HCC and establish the role of PTEN in HCC for an effective therapeutic guideline. The collaboration of PTEN with hepatitis B or C viruses and insulin-like growth factor-2 (IGF-2) with regard to the inhibition of cell growth is explained next.

An immunohistochemical study clearly demonstrates down-regulation of PTEN in the HCV-positive cirrhotic hepatocarcinogenesis (Rahman *et al.,* 2001). Hepatitis B virus plays an essential role in IGF-2 activation during the formation of HCC (Park *et al.,* 2001). Overexpression of PTEN in hepatoma cells inhibits IGF-2 expression and cell growth by blocking MAPK and MEK and PKC protein activation in a PTEN protein phosphatase activity-dependent manner (Kang-Park *et al.,* 2003). This study, in contrast to another study (Weng *et al.,* 2001), indicates that only the protein phosphatase activity is needed in IGF-2 inactivation. In conclusion, PTEN blocks Sp1 phosphorylation in response to HBVx by inactivating PKC, MAPK, and MEK, which eventually down-regulates IGF-2 expression; thus inhibiting cell growth during the formation of HCC.

Smad4

Smad4 mutations have been reported in HCC. Smad4 at the genetic level is associated with loss of mRNA transcripts and subsequent loss of protein expression. Smad4 protein overexpression is present in a subset of HCC and is strongly correlated with immunostaining of the transforming growth factor beta (TGF-β). Immunohistochemical labeling of the Smad4 protein closely mirrors gene status. Loss of immunolabeling in this case indicates biallelic gene inactivation. Activation or dysregulation of the TGF-β signaling pathway in HCCs appears to explain the up-regulation of the *Smad4* tumor-suppressor gene in a subset of HCCS (Torbenson *et al.,* 2002). Studies using complementary DNA (cDNA) microarrays have also shown overexpression of Smad4 in HCC (Xu *et al.,* 2001). In other words, increased immunostaining of these two proteins is associated with enhanced mitosis and a worse nuclear grade. In contrast, hepatic adenomas only rarely show increased staining of TGF-β2 receptor and none show Smad4 staining (Torbenson *et al.,* 2002).

Squamous Cell Carcinoma Antigen

Squamous cell carcinoma antigen (SCCA) is a serine protease inhibitor physiologically found in the spinous and granular layers of normal squamous epithelium but usually expressed in neoplastic cells of epithelial origin (Kato, 1996). Both SCCA1 and SCCA2, the two isoforms, protect neoplastic cells from apoptotic death, involving caspase-3 activity and/or upstream proteases. These isoforms are derived from two highly homologous tandemly arrayed genes, and their promoter regions have been identified on chromosome 18g21.3 (Hamada *et al.,* 2001).

In vivo experiments demonstrate that SCCA1 can promote tumor growth (Suminami *et al.,* 2000). Immunohistochemical studies have demonstrated the presence of serpin protein in the cytoplasm of HCC surgical tumor tissues, whereas the activity of this protein was not detectable in normal human liver tissue (Pontisso *et al.,* 2004).

Use of cDNA Microarray

A major obstacle in the treatment of HCC is intrahepatic recurrence, which occurs in 30–50% of patients who undergo hepatic resection. Therefore, such recurrence limits the potential of surgery for HCC. Identification of gene expression patterns that accompany HCC may allow elucidation of the mechanisms that underlie this cancer and provide important molecular markers for early diagnostic purposes. This approach enables deeper insight into the molecular basis of disease and provides an extensive list of potential early-onset molecular markers for improved diagnosis and therapy. Large-scale gene-expression profiling of human tissue is possible using cDNA microarray technology to discover target

genes that are useful in the identification of potential therapeutic interventions and/or diagnostic probes. In other words, genotyping makes it possible to screen broadly for mutations that lead to an elevated risk for HCC. Thus, differential gene expression can identify high-risk groups and prevent the disease or slow its progression.

Xiao *et al.* (2001) have used cDNA microarrays containing 1176 genes for exploring the gene-expression profiles in HCC and surrounding liver tissue for identifying novel genes differentially expressed in HCC and for exploring their potential roles in clinical diagnosis. They identified CD10 up-regulation at the mRNA level in the HCC as compared to nonneoplastic liver tissue. (CD10 is a type II integral membrane glycoprotein that is routinely used in the differential diagnosis of B-cell lymphomas.) The up-regulation of CD10 mRNA level was among the highest differentially regulated genes found in this study. The reliability of these data was validated by semiquantitative reverse transcriptase polymerase chain reaction (RT-PCR). Based on this evidence, CD10 antigen can be used as a useful diagnostic marker for HCC. It should be noted, however, that presently it is not known whether the increased expression of CD10 in HCCs has any role in carcinogenesis or simply represents aberrant expression in transformed cells.

Using high-density oligonucleotide microarrays, Iizuka *et al.* (2002) have found distinct differences in gene-expression pattern between HBV-positive HCCs and HCV-positive HCCs. In a 2003 study, Iizuka *et al.* applied the statistical pattern recognition (SSPR) system in conjunction with high-density oligonucleotide microarrays for accurate prediction of early intrahepatic recurrence of HCC. They succeeded in profiling gene expression of HBV and HCV HCCs in patients with and without liver cirrhosis. In this study 89 genes were expressed differentially between HBV HCCs associated with liver cirrhosis and those not associated with liver cirrhosis. Thus, HBV HCC can be classified into two types based on the gene expression profile, i.e., tumors associated with liver cirrhosis and those not associated with liver cirrhosis. The expression of the *HSPA1B* gene (which functions as a molecular chaperone in response to various stresses) is down-regulated in the HCV HCC not associated with liver cirrhosis versus that associated with liver cirrhosis. This system, independent of known prognostic variables, can serve as a new method for characterizing the metastatic potential of HCC.

Using microarray analysis on a genomic scale, Li *et al.* (2002) have identified 38 up-regulated and 36 down-regulated genes in HCC specimens. In another study, gene-profile analysis was used by Midorikawa *et al.* (2002) for identifying the altered expression of genes in HCC samples; the top 30 up-regulated and top 30 down-regulated genes were identified. In this study 12 genes were up-regulated and 4 were down-regulated, in asscociation with dedifferentiation from well-differentiated HCC to moderately differentiated HCC. These and other similar studies provide a quantitative view of the changes that accompany liver cancer at the genomic level and enable deeper insight into the molecular basis of disease. These studies can provide potential early-onset molecular markers for improved diagnosis.

Use of Proteomics

Although a small subset of patients with HCC qualify for surgical intervention, many patients with advanced HCC have little chance of survival. Unfortunately, the diagnosis of HCC usually occurs at late stages in the disease when there are few effective treatment options and the prognosis for patients with HCC is very poor. The extremely poor prognosis of HCC is largely the result of a high rate of recurrence and metastasis. This feature of HCC underscores the need to develop an accurate molecular profiling model to improve diagnosis and identify therapeutic targets for the treatment of patients with HCC with metastases. Indeed, early detection of the disease will allow more timely and possibly effective treatment of this devastating cancer.

Advances in the fields of genomics and proteomics are leading to the discovery of new molecular targets for therapy, biomarkers for early detection, and new end points for therapeutic efficacy and low toxicity. Genomics-based protocols include the measurements of expression of full sets of mRNA, such as differential display, serial analysis of gene expression, and large-scale gene expression arrays. Many of these methods are discussed in this volume and other volumes of this series of handbooks.

The proteomic approach can be used to test whether changes in the amount of certain serum polypeptides or changes in their posttranslational modifications predict the onset of HCC. Comparatively, proteomics technologies allow for identification of the protein changes caused by the disease process in a relatively accurate manner. These techniques allow the study of the proteome that is the total protein complement of a genome. Thus, the inherent advantage of proteomics is that the identified protein is itself the biological end point. For effective prognostic evaluation of HCC, the identification and characterization of protein profiles are important because the initiation and malignant progression of cancers result from the accumulation and combining effects of many changes in the protein expression.

Advances in the standardization of two-dimensional gel electrophoresis (2-DE) coupled with computerized image analysis permit reproducible resolution of thousands of polypeptides per run. The 2-DE is commonly used to discover and identify cancer-associated proteins (Klose and Kobalz, 1995). In combination with mass spectroscopy, 2-DE can be a powerful method for separation and subsequent identification of proteins of interest. Ciphergen's ProteinChip technology can be used to find proteomic signatures that are specific for peripheral and central tumor areas as well as for nontumorous hepatic tissue (Melle *et al.,* 2004). These various regions can be detected only in microdissected tissues.

The 2-DE approach is the mainstay of most proteomic analyses because of its simplicity, reliability, high information content, and ready accessibility to investigators. This approach has been used for studies of liver cancer using cell lines, tissues, and sera at both the cellular and subcellular levels (Park *et al.,* 2002; Steel *et al.,* 2001). These studies have provided information on carcinogenesis, liver cirrhosis, and drug toxicity. Ding *et al.* (2004) used 2-DE technique for studying complex events associated with HCC metastasis. In this study, image analysis of silver-stained 2-DE gels revealed 56 protein spots, showing significant differential expression in MHCC97-H and MHCC97-L cells (Student's t-test, $P < 0.05$). These cells are human HCC cell strains with high and low spontaneous metastasis potentials, which have been established from the parental cell line MHCC97. These cells provide good models for comparative proteome analysis of HCC metastasis-associated proteins. The results of this study provide the basis for searching for potential markers for HCC prognosis and yield some clues to elucidate the mechanism of HCC metastasis.

Other recently introduced proteomics technologies, such as protein chips, and immunodetection amplified by T7 RNA polymerase (which has single-cell resolution), are expected to find novel diagnostic markers for early detection and treatment of HCC (Seow *et al.,* 2001). Although other approaches, such as isotope-coded affinity tags (Gygi *et al.,* 1999), surface enhanced laser desorption/ionization-based protein chips (Hutchens and Yip, 1993), and a multidimensional protein identification technique (Link *et al.,* 1999), are available, 2-DE–based proteomics presently is the most commonly used method. This approach is noninvasive and may detect the on set of serious liver disease as early as possible (Steel *et al.,* 2001).

Role of Virus in Hepatocellular Carcinoma

Persistent viral infection is the most important cause of HCC worldwide. Two viruses, HBV and HCV, cause a vast majority of HCCs. Individuals chronically infected with HBV or HCV are at high risk for the development of HCC, with disease progression occurring relentlessly over many years. Persistent HBV infection occurs primarily as a result of infection in the first 5 years of life, whereas most HCV infection occurs in adult life. Thus, primary liver cancer in younger individuals (younger than 50 years of age) is attributable to HBV infection in more than 75% of the patients.

However, some types of HCCs are associated with normal liver function during continuous HBV or HCV virus infection. Thus, how liver cirrhosis affects HBV- or HCV-related hepatocarcinogenesis is not fully known. A full understanding of the effects of liver cirrhosis on this malignancy will provide patients suffering from chronic HBV or HCV infections with effective therapy.

Although it is not yet fully understood how hepatitis viruses are involved in human hepatocarcinogenesis, accumulated evidence suggests that HBV encodes an oncogenic *HBx* gene that functions as a transactivator, up-regulating the expression of multiple genes such as *c-myc* and *c-jun* (Yen, 1996). In addition, serial analysis of gene expression demonstrates that *HBx* regulates protein synthesis, gene transcription, and protein degradation (Wu *et al.,* 2002). Another study demonstrates that the core protein of HCV induces HCC in transgenic mice (Moriya *et al.,* 1998). This study points to an oncogenic role of the HCV core protein in hepatocarcinogenesis. The HCV core protein also activates nuclear factor Kappa B via both the inflammatory and the proliferation processes (Tai *et al.,* 2000). Another role of this core protein is the activation of STAT3, leading to cellular transformation (Yoshida *et al.,* 2002) (see also individual hepatitis viruses). These findings suggest therapeutic priority of eradication of these viruses to prevent virus-related HCC development.

Hepatitis B Virus

With 300 million carriers, chronic HBV infection is a major public health problem worldwide. The prevalence of chronic carriers of HBV is much higher than that in carriers of HCV. Persistent HBV infection results in chronic liver injury, including inflammation, hepatitis, liver regeneration, liver fibrosis, and cirrhosis, which predispose the person to HCC. In fact, such a large portion of chronic cases progresses to HCC that is one of the most common malignancies worldwide. It may take 20–30 years for a carrier to develop HCC. The HBV infection rates of 10–25% are the result of vertical transmission from mothers to infants or horizontal spread within families to children younger than the age of 10. The risk of HCC in a chronic HBV carrier

is increased by a factor of 100 as compared to a noninfected individual, and the estimated lifetime risk of HCC in males infected at birth is 50%.

Various clinicopathologic features of HCC, such as the number and size of the liver tumors and the clinical stage of coexisting cirrhosis, are linked to the survival rates of patients (Stuart *et al.,* 1996). The serum level of HBV-DNA is also correlated with progression of the disease. In addition, viral load is a useful prognostic marker for HBV-related patients with HCC (Ohkubo *et al.,* 2002). Patients with less favorable course appear to clear the virus poorly or to have a greater level of virus production. In patients with HBV variants, progressive liver damage occurs in parallel with relatively high levels of viremia (Kajiya *et al.,* 2001). This and other evidence suggests that clearance of the infected virus could have beneficial effects on hepatocarcinogenesis. For example, treatment with type-1 interferon clears the virus, inhibiting the development of HCC in patients with chronic HBV infection (Lin *et al.,* 1999).

Because not all HBV-related HCCs occur on a background of liver cirrhosis, the implication is that HBV (a DNA virus) may have some intrinsic hepatocarcinogenic properties. In fact, the hepatitis B core antigen is also the target antigen for host immune response. During chronic HBV infection, this gene is expressed in the nucleus, in the cytoplasm, or in both of the infected hepatocytes. Patients with cytoplasmic distribution of this gene in hepatocytes usually have active hepatitis (Chu *et al.,* 1995).

According to Seow *et al.* (2001), HBVx protein influences the development of liver cancer by promoting the survival and growth of transformed hepatocytes. Through transactivation of cellular genes and induction of signaling pathways, this protein may lead to changes in cell cycle progression and/or regulation as shown by the ability of this protein in inducing cell cycle progression in Chang liver cells (Benn and Schneider, 1995). An alternative mechanism in which HBVx protein can contribute to hepatocarcinogenesis is through its ability to inhibit DNA repair.

Mutations of HBV DNA affect the course of HBV infection. A mutation in the core region of HBV DNA might be related to exacerbation of hepatitis, whereas a mutation in the precore region results in severe hepatitis (Ehata *et al.,* 1991; Kojima *et al.,* 1999). Mutations of the core promoter region at nucleotides 1762 and 1764 are associated with severe liver injury (Lindh *et al.,* 1999). Using laser-assisted microdissection, Kawai *et al.* (2003) have shown that the core promoter mutations at nucleotides 1762 and 1764 are more prevalent in hepatocytes exhibiting cytoplasmic hepatitis B core antigen expression than in hepatocytes showing this antigen in the nucleus. Although subcellular location of this core antigen in hepatocytes has been reported to be regulated by the cell cycle, it still remains unclear whether the intracellular shift of this antigen is the cause or the result of the cell cycle. The antigen could shift from cytoplasm to the nucleus by diffusion. Additional studies are required to clarify the mechanism underlying the intracellular shift of the antigen in hepatocytes.

Hepatitis C Virus

The increasing incidence of HCC in developed countries is caused by HCV infection. It is estimated that 3% of the world population are HCV carriers. Approximately 170 million people worldwide are infected with HCV, of whom ~2 million reside in Japan. Infection with HCV leads to serious consequences such as liver cirrhosis and HCC. The growing incidence of HCC is expected to reach a plateau by 2015 and then to start to decrease.

Although parenteral transmission is the major route of infection by HCV, ~50% of chronic carriers of this virus do not show prior exposure to any known risk factors discussed in this chapter. Once acutely infected, ~80–85% of these individuals will become chronically infected. In at least 20% of those with chronic HCV infection, liver cirrhosis will develop during the first 10 years (Seow *et al.,* 2001). Whether HCV is directly carcinogenic remains uncertain. HCV is an RNA virus and the integration of its nucleic acid sequences into the host genome seems less likely. However, several *in vitro* studies have demonstrated that the core protein of this virus promotes cell growth through repression of p53 transcription and inhibits apoptosis (Ray *et al.,* 1997).

Risk Factors

Epidemiologic and experimental evidence has shown that HCC, like other cancers, has multistage origins. Risk factors for HCC can be divided into environmental factors, including biological and chemical agents, and genetic factors (Table 12). Genetic factors, such as metabolic disorders, DNA repair defects, and other altered susceptibility factors, contribute to the development of HCC. The major biological agents are HBV and HCV. Chronic HBV and HCV infections contribute to the HCC development in more than 80% of the HCC cases worldwide. Chemical agents involved include cigarette smoking, heavy alcohol consumption, vinyl chloride, polycyclic aromatic hydrocarbons, and nitrosamines. These causative agents are implicated in various molecular events including stimulation of signaling transduction pathway.

Table 12. Risk Factors That Contribute to the Development of Hepatocellular Carcinoma

Infectious agents	Hepatitis B virus,[a] hepatitis C virus (HCV)[a]
Pathology	Chronic liver disease (macronodular cirrhosis),[a] neonatal hepatitis[b]
Dietary	Long-term aflatoxin consumption,[a] dietary iron overload,[b] low vegetable intake,[b] chronic alcoholism[b]
Hormone related	Oral contraceptives (female),[b] anabolic steroids,[b] elevated serum levels of testosterone[b]
Other environmental	Vinyl chloride,[a] cigarette smoking,[b] inorganic arsenic ingestion,[b] radioactive thorium dioxide (thorotrast) exposure,[b] pesticides (?)
Genetic associations	Hereditary tyrosinemia,[a] α_1-antitrypsin deficiency,[a] idiopathic hemochromatosis,[a] porphyria (HCV),[b] Wilson's disease,[b] genetic polymorphisms of cytochrome P450 2E1 and 2D6 and arylamine N-acetyltransferase 2 (involved in detoxification),[b] L-myc,[b] mutations in glutathione *S*-transferase,[d] familial aggregation[e]
Other	Elevated transforming growth factor α,[a] age (>50),[a] gender (male),[b] elevated expression of *neu* oncoprotein,[b] low serum retinol (?)

[a] Strong association with the development of HCC.

[b] Weak or inconsistent association with the development of heptocellular carcinoma HCC.

[c] Cirrhosis, but not the underlying genetic mutation(s), appears to be the major risk factor associated with the development of HCC.

[d] A dose-response relationship between AFB exposure and HCC has been documented in HBV carriers with a GST null genotype.

[e] Familial aggregation of HCC may result from environmental agents such as HBV or HCV infections, although a genetic basis for HCC susceptibility in such families has not been excluded.

After Feitelson *et al.* (2002).

Aflatoxin B is a primary dietary risk factor. Aflatoxins are fungal toxins that commonly contaminate maize, ground nuts, and some other crops. They play an important part in modifying the risk of liver cancer associated with HBV (Hall, 2003). After being metabolized in the liver the toxin can bind to guanine in DNA, resulting in mutations (e.g., in codon 249 of the *TP53* tumor-suppressor gene). The adverse effect of combined exposure to persistent HBV infection and dietary aflatoxin on liver has been shown (Qian *et al.,* 1994). Hepatitis B vaccination in infancy dramatically reduces this persistent infection.

Treatment of Hepatocellular Carcinoma

Tremendous efforts are being made to improve the survival rate of patients with HCC. A number of treatments for HCC are being tried. Nonsurgical treatments have been attempted, including transcatheter arterial chemoembolization (Nakamura *et al.,* 1989), transcatheter arterial embolization (Yamada *et al.,* 1983), percutaneous ethanol injection (Ebara *et al.,* 1990), and radiofrequency ablation (Curley *et al.,* 2000). A 2004 comparative study indicates that transcatheter arterial embolization has a higher antitumor effect than that of transcatheter arterial infusion chemotherapy in patients with HCC, but even the former does not significantly improve the survival of patients (Ikeda *et al.,* 2004). Systemic or hepatic arterial infusion chemotherapy has also been attempted for patients unable to undergo other nonsurgical or surgical treatment because they have advanced HCC (Urabe *et al.,* 1998). Systemic chemotherapy is also hampered by impaired hepatic function and hyperspleenism resulting from underlying cirrhosis in most patients (Venook, 1994). However, these treatments have not necessarily contributed to improvement in prognosis. The avoidance of liver dysfunction is the most important factor in selecting a therapeutic modality. Identification of noncytotoxic agents to help treat this disease is urgent.

Hepatectomy (removal of the liver, whole or in part) remains one of the primary treatments for HCC with relatively high curability. Cadaveric or living-related liver transplantation is a treatment option (Mazzaferro *et al.,* 1996). Liver transplantation, as a result of progress in surgical techniques and the establishment of medical ethics, is a better treatment option. However, the shortage of organs and rapid recurrence of HCC in the transplanted liver limit the potential usefulness of this option. Indeed, surgery with curative intent is feasible for only a small number of patients.

Interferon treatment trials are in progress to demonstrate its chemopreventive potential against HCC at both initial hepatocarcinogenesis and recurrent HCC (Shiratori *et al.,* 2003), although the precise mechanism for its tumor-suppressive effect remains unclear. Another treatment being explored in secondary chemoprevention is acyclic retinoids that induce apoptosis and differentiation in hematopa cells (Nakamura *et al.,* 1996). The hope is that treatment with an acyclic retinoid might eradicate malignant clones produced in the liver with HCV-associated chronic hepatitis or cirrhosis.

Another approach to target HCC is to use a specific inhibitor of an overexpressed molecular marker. This approach is exemplified by the use of nonsteroidal antiinflammatory drugs (NSAIDs) against COX-2 (Koga, 2003). The COX-2 enzyme is overexpressed in many types of malignant tumors and promotes them through a wide range of signal pathways, such as Akt/PKB and VEGF. The presence of COX-2 in the cytoplasm of the human HCC cells has been demonstrated using IHC

(Koga, 2003). The anti-tumor effects of COX-2 inhibitors can be enhanced in combination with conventional anti-cancer agents. Such an approach was used for inhibiting growth of human lung cancer cells (Hida *et al.,* 2002).

Gene therapy is a potential future treatment strategy for HCC. It can be most effectively delivered via the hepatic artery (Takikawa *et al.,* 2003). However, gene therapy trials were postponed after one patient died in a clinical trial of transarterial injection of adenoviral vectors (Eliot, 1999). To resume systemic gene therapy a marker is required, which would be specific for HCC tumor cells without damaging nontumorous liver cells. Takikawa *et al.* (2003) developed a specific gene transduction system with enhanced gene expression using the AFP promoter and a transcriptional activator for gene therapy for HCC. Approximately 80% of HCCs produce AFP at increased levels. This gene transcription method using the AFP promoter/enhancer is advantageous because of its high specificity. However, AFP is weak and so the gene expression using this promoter is not sufficiently strong for *in vitro* experiments as well as for clinical trials. Therefore, the gene expression of the AFP promoter is enhanced by a transcriptional activator.

The risk of HCC can also be reduced by eliminating exposure to aflatoxins. This strategy is effective at an individual level by modifying the diet, but it is not practical in less developed countries because selection of food is not feasible. Although chemopreventive agents, such as oltipraz and chlorophyllin, are available to combat harmful aflatoxin metabolities in the body, their use is not a viable option in less developed countries. Genetic modification of crops to enhance fungal resistance is a promising method (Wild and Hall, 2000).

Two main reasons account for the difficulty in achieving a curative treatment of HCC. One reason is the multicentric occurrence of HCC in the liver with HBV- or HCV-associated chronic hepatitis or cirrhosis, and the other reason is the often severely deteriorated liver function at the time of HCC treatment. Unfortunately, most patients with advanced disease die within a relatively short time.

Hepatoblastoma

Hepatoblastoma is a common hepatic tumor in children, with most cases occurring before 2 years of age. It is a malignant neoplasm, primarily in the liver, and is composed of tissue resembling embryonal or fetal hepatic epithelium or mixed epithelial and mesenchymal tissues. Most of these tumors are sporadic, but some familial inherited disorders (e.g., Beckwith-Wiedemann syndrome and familial adenomatous) are associated with an increased risk of developing hepatoblastoma (Perilongo and Shafford, 1999). Recurrent chromosomal imbalances using conventional karyotyping of tumor cells have been reported (Nagata *et al.,* 1999). Comparative genomic hybridization has revealed the significance of genetic alterations of nonrandom chromosomal regions, including 1q, 2q, 4q, 8q, and 20q, in the development of hepatoblastoma (Gray *et al.,* 2000). Loss of heterozygosity and frequent mutation of the β-catenin in hepatoblastoma have also been reported to be the genetic basis for the pathogenesis of this embryonal tumor (Albrecht *et al.,* 1994; Wei *et al.,* 2000).

Nagata *et al.* (2003) compared the gene expression profiles of nondiseased liver and hepatoblastoma tumor using a high-density oligonucleotide DNA array. In this study 133 genes were differentially expressed between these two groups. Some genes regulating cell division and tumor cell growth were differentially expressed between these two types of specimens. A DNA repair gene (*MUTYH*) and 26 other genes (*NAP1L1, STMN1, CCNG2,* and *CDC7L1*) showed increased expression in the hepatoblastoma tumor. These four cell cycle-regulating genes are mapped to the chromosomal region 1q21-q32, and can be molecular targets for diagnostic and therapeutic use in this embryonal type of tumor.

References

Albrecht, S., von Schweinitz, D., Waha, A., Kraus, J.A., von Deimling, A., and Pietsch, T. 1994. Loss of maternal alleles on chromosome arm 1lp in hepatoblastoma. *Cancer Res. 54*:5041–5044.

Aleem, E., Flohr, T., Thielmann, H.W., Bannasch, P., and Mayer, D. 2003. Protein phosphatase inhibitor-1 mRNA expression correlates with neoplastic transformation of epithelial liver cells and progression of hepatocellular carcinomas. *Intern. J. Oncol. 24*:869–877.

Anzola, M., Cuevas, N., López-Martinez, M., Saiz, A., Burgos, J.J., and Martinez de Pancorbo, M. 2003. Frequent loss of p53 codon 72 Pro variant in hepatitis C virus-positive carriers with hepatocellular carcinoma. *Cancer Lett. 193*:199–205.

Behrens, J., Jerchow, B.A., Wurtele, M., Grimm, J., Asbrand, C., Wirtz, R., Kuhl, M., Wedlich, D., and Birchmeier, W. 1998. Functional interaction of an axin homolog, conductin with beta-catenin, APC, and GSK3beta. *Science 280*:596–599.

Benn, J., and Schneider, R.J. 1995. Hepatitis B virus HBX protein deregulates cell cycle check point controls. *Proc. Natl. Acad. Sci. U.S.A. 92*:11215–11219.

Borscheri, N., Roessner, A., and Röcken, C. 2001. Canalicular immunostaining of neprilysin (CD 10) as a diagnostic marker for hepatocellular carcinomas. *Am. J. Surg. Pathol. 25*:1297–1303.

Bouchard, M.J., Wang, L.H., and Schneider, R.J. 2001. Calcium signaling by HBx protein in hepatitis B virus DNA replication. *Sci. Lett. 327*:2376–2378.

Cao, D., Fan, S.T., and Chung, S.S. 1998. Identification and characterization of a novel human aldose reductase-like gene. *J. Biol. Chem. 273*:11429–11435.

Cascinu, S., Graziano, F., Catalano, V., Barni, S., Giordani, P., Baldelli, A.M., Staccoli, M.P., Rossi, C., Brenna, A., Valenti, A., Muretto, P., and Catalano, G. 2003. Vascular endothelial growth factor and p53 expression in liver and abdominal metastases from colon cancer. *Tumor Biol. 24*:77–81.

Chaubert, P., Gayer, R., Zimmermann, A., Fontolliet, C., Stamm, B., Shaw, P., and Bosman, F. 1997. Germ-line mutations of the p16INK4(MTS1) gene occur in a subset of patients with hepatocellular carcinoma. *Hepatology 25*:1376–1381.

Chu, C.M., Sheen, I.S., Yeh, C.T., Hsieh, S.Y., Tsai, S.I., and Liaw Y.F. 1995. Serum levels of interferon-alpha and -gamma in acute and chronic hepatitis B virus infection. *Dig. Dis. Sci. 40*:2107–2112.

Cianchi, F., Cortesini, C., Bechi, P., Fantappie, O., Masserini, L., Vannacci, A., Sardi, I., Baroni, G., Boddi, V., Mazzanti, R., and Masini, E. 2001. Up-regulation of angiogenesis in human colorectal cancer. *Gastroenterology 121*:1339–1347.

Clouston, A. 2004. An approach to the surgical pathology of tumors and tumor-like conditions of the liver. *Pathology 36*:5–18.

Curley, S.A., Izzo, F., Ellis, L.M., Nicholas, V.J., and Vallone, P. 2000. Radiofrequency ablation of hepatocellular cancer in 110 patients with cirrhosis. *Ann. Surg 232*:381–391.

de la Coste, A., Romagnolo, B., Billuart, P., Renard, C.A., Buendia, M.A., Soubrane, O., Fabre, M., Chelly, J., Beldjord, C., Kahn, A., and Perret, C. 1998. Somatic mutations of the β-catenin gene are frequent in mouse and human hepatocellular carcinomas. *Proc. Natl. Acad. Sci. U.S.A. 95*:8847–8851.

DeSouza, A.T., Hankins, G.R., Washington, M.K., Orton, T.C., and Jirtle, R.L. 1995. M6P/IGF2R gene is mutated in human hepatocellular carcinomas with loss of heterozygosity. *Nat. Genet. 11*:447–449.

Ding, S.-J., Li, Y., Shao, X.-X., Zhou, H., Zeng, R., Tang, Z.-Y., and Xia, Q.-C. 2004. Proteome analysis of hepatocellular carcinoma cell strains, MHCC97-H and MHCC97-L, with different metastasis potentials. *Proteomics 4*:982–994.

Ebara, M., Ohto, M., Sugiura, N., Okuda, K., Kondo, F., and Kondo, K. 1990. Percutaneous ethanol injection for the treatment of small hepatocellular carcinoma: Study of 95 patients. *J. Gastroenterol. Hepatol. 5*:616–626.

Edamoto, Y., Hara, A., Biernat, W., Terracciano, L., Cathomas, G., Riehle, H.M., Matsuda, M., Fujii, H., Scoazec, J-Y., and Ohgaki, H. 2003. Alterations of RB1, p53, and Wnt pathways in hepatocellular carcinomas associated with hepatitis C, hepatitis B and alcoholic liver cirrhosis. *Inter. J. Cancer 106*:334–341.

Ehata, T., Omata, M., Yokosuka, O., Hosoda, K., and Ohto, M. 1991. Amino acid residues of core region of hepatitis B virus. Asymptomatic carriers versus patients with liver disease. *J. Gastroenterol. Hepatol. 6*:292–296.

Eliot. L.A., and Jamali, F. 1999. Pharmacokinetics and pharmacodynamics of nifedipine in untreated and atorvastatin-treated hyperlipidemic rats. *J. Pharmacol. Exp. Ther. 291*:188–193.

Feitelson, M.A., Sun, B., Tufan, N.L.S., Liu, J., Pan, J., and Lian, Z. 2002. Genetic mechanisms of hepatocarcinogenesis. *Oncogene 21*:2593–2604.

Garcia, E.J., Lawson, D., Cotsonis, G., and Cohen, C. 2002. Hepatocellular carcinoma and markers of apoptosis (bcl-2, bax, bcl-x): Prognostic significance. *Appl. Immunohistochem. Mol. Morphol. 10*:210–217.

Grassi, A., Sucsa, M., Ferri, S., Gabusi, E., D'Errico, A., Farina, G., Maccariello, S., Zauli, D., Bianchi, F.B., and Ballardini, G. 2004. Detection of the M30 neoepitope as a new tool to quantify liver apoptosis. *Am. J. Clin. Pathol. 121*:211–219.

Gray, S.G., Kytola, S., Matsunaga, T., Larsson, C., and Ekström, T.J. 2000. Comparative genomic hybridization reveals population-based genetic alterations in hepatoblastomas. *Br. J. Cancer 83*:1020–1025.

Gross-Goupil, M., Riou, P., Emile, J., Saffroy, R., Azoulay, D., Lacherade, I., Receveur, A., Piatier-Tonneau, D., Castaing, D., Debuire, B., and Lemoine, A. 2003. Analysis of chromosomal instability in pulmonary or liver metastases and matched primary hepatocellular carcinoma after orthotopic liver transplantation. *Int. J. Cancer 104*:745–751.

Guan, X.Y., Fang, Y., Sham, J.S., Kwong, D.L., Zhang, Y., Liang, Q., Li, H., Zhou, H., Trent, J.M. 2000. Recurrent chromosome alterations in hepatocellular carcinoma detected by comparative genomic hybridization. *Genes Chromosomes Cancer 29*:110–116.

Guan, X.Y., Sham, J.S.T., Tai, L.-S., Fang, Y., Li, H., and Liang, Q. 2003. Evidence for another tumor suppressor gene at 17p13.3 distal to TP53 in hepatocellular carcinoma. *Cancer Genet. Cytogenet. 140*:45–48.

Gygi, S.P., Rist, B., Gerber, S.A., Turecek, F., Gelb, M.H., and Aebersold, R. 1999. Quantitative analysis of complex protein mixtures using isotope-coded affinity tags. *Nat. Biotechnol. 17*:994–999.

Hall, A.J. 2003. Liver cancer in low and middle income countries. *Br. Med. J. 326*:994–995.

Hamada, K., Shinomiya, H., and Asano, Y. 2001. Molecular cloning of human squamous cell carcinoma antigen gene and characterization of its promoter. *Biochem. Biophys. Acta. 1518*:124–131.

Harada, N., Oshima, H., Katoh, M., Tamai, Y., Oshima, M., and Taketo, M. 2004. Hepatocarcinogenesis in mice with β-catenin and Ha-Ras gene mutations. *Cancer Res. 64*:48–54.

Haratake, J., and Hashimoto, H. 1995. An immunohistochemical analysis of 13 cases with combined hepatocellular and cholangiocellular carcinoma. *Liver 15:*9–15.

Haviv, I., Vaizel, D., and Shaul, Y. 1996. pX, the HBV-encoded coactivator, interacts with components of the transcription machinery and stimulates transcription in a TAF-independent manner. *EMBO J. 15*:3413–3420.

Hayashi, H., Kohno, H., Ono, T., Yamanoi, A., Dhar, D.K., Ueda, S., Rahman, M.A., Kubota, H., and Nagasue, N. 2004. Transforming growth factor-β1 induced hepatocyte apoptosis. *Acta Oncol. 43:*91–97.

Heinze, T., Jonas, S., Karstem, A., and Neuhaus, P. 1999. Determination of the oncogenes p53 and c-erB2 in the tumor cytosols of advanced hepatocellular carcinoma (HCC) and correlation to survival time. *Anticancer Res. 19*:2501–2503.

Herath, N.I., Kew, M.C., Whitehall, V.L.J., Walsh, M.D., Jess, J.R., Khanna, K.K., Young, J., Powell, L.W., Leggett, B.A., and Macdonald, G.A. 2000. p73 is up-regulated in a subset of hepatocellular carcinomas. *Hepatology 31*:601–605.

Hida, T., Kozaki, K., Ito, H., Miyaishi, O., Tatematsu, Y., Suzuki, T., Matsuo, K., Sugiura, T., Ogawa, M., Takahashi, T., and Takahashi, T. 2002. Significant growth inhibition of human lung cancer cells both in vitro and in vivo by the combined use of a selective cyclooxygenase 2 inhibitor, JTE-522, and conventional anticancer agents. *Clin. Cancer Res. 8*:2443–2447.

Hippo, Y., Watanabe, K., Watanabe, A., Midorikawa, Y., Yamamoto, S., Ihara, S., Tokita, S., Iwanari, H., Ito, Y., Nakano, K., Nezu, J.-I., Tsunoda, H., Yoshino, T., Ohizumi, I., Tsuchiya, M., Ohnishi, S., Makuuchi, M., Hamakubo, T., Kodama, T., and Aburatani, H. 2004. Identification of soluble NH_2-terminal fragment of glypican-3 as a serological marker for early-stage hepatocellular carcinoma. *Int. J. Oncol. 24*:2418–2423.

Hofseth, L.J., Hussain, S.P., Wang, X.W., and Harris, C.C. 2002. Hepatocellular cancer: Molecular biology and genetics. In Kelson, D.P., Daly, J.M., Kern, S.E., Lerin, B., and Tapper, J.E., (eds) *Gastrointestinal Oncology: Principles and Practice.* Philadelphia: Lippincott Williams and Wilkins, 539–558.

Hsu, C., Huang, C.-L., Hsu, H.-C., Lee, P.-H., Wang, S.-J., and Cheng, A.-L. 2002. HER-2/neu overexpression is rare in hepatocellular carcinoma and not predictive of anti-HER-2/neu regulation of cell growth and chemosensitivity. *Cancer 94*:415–420.

Hsu, I.C., Metcalf, R.A., Sun, T., Welsh, J.A., Wang, N.J., and Harris, C.C. 1991. Mutational hot spot in p53 gene in human hepatocellular carcinomas. *Nature 350*:427–428.

Hu, T.H., Huang, C.C., Lin, P. R., Chang, H.W., Ger, L.P., Lin, Y.W., Changchien, C.S., Lee, C.M., and Tai, M.H. 2003. Expression and prognostic role of tumor suppressor gene PTEN/MMAC1/TEP1 in hepatocellular carcinoma. *Cancer 97:*1929–1940.

Iavarone, M., Lampertico, P., Seletti, C., Donato, M.F., Ronchi, G., Del Ninno, E., and Colombo, M. 2003. The clinical and pathogenetic significance of estrogen receptor-β expression in chronic liver diseases and liver carcinoma. *Cancer 98*: 529–534.

Iizuka, N., Oka, M., Yamada-Okabe, H., Mori, N., Tamesa, T., Okada, T., Takemoto, N., Tangoku, A., Hamada, K., Nakayama, H., Miyamoto, T., Uchimura, S., and Hamamoto, Y. 2002. Comparison of gene expression profiles between hepatitis B virus and hepatitis C virus infected hepatocellular carcinoma by oligonucleotide nieroarrray data on the basis of a supervised learning method. *Cancer Res. 62*:3939–3944.

Ikeda, M., Maeda, S., Shibata, J., Muta, R., Ashihara, H., Tanaka, M., Fujiyama, S., and Tomita K. 2004. Transcatheter arterial chemotherapy with and without embolization in patients with hepatocellular carcinoma. *Oncology 66*:24–31.

Ishizaki, Y., Ikeda, S., Fujimori, M., Shimizu, Y., Kurihara, T., Itamoto, T., Kikuchi, A., Okajima, M., and Asahara, T. 2004. Immunohistochemical analysis and mutational analyses of β-catenin, Axin family APC genes in hepatocellular carcinomas. *Int. J. Oncol. 24*:1077–1108.

Kajiya, Y., Hamasaki, K., Nakata, K., Miyazoe, S., Takeda, Y., Higashi, S., Ohkubo, K., Ichikawa, T., Nakao, K., Kato, Y., Eguchi, K. 2001. A long-term follow-up analysis of serial core promoter and precore sequences in Japanese patients chronically infected by hepatitis B virus. *Dig. Dis. Sci. 46*:509–515.

Kanetaka, K., Sakamoto, M., Yamamoto, Y., Takamura, M., Kanematsu, T., and Hirohashi, S. 2003. Possible involvement of tetraspanin CO-029 in hematogenous intrahepatic metastasis of liver cancer cells. *J. Gastroenterol. Hepatol*. *18*:1309–1314.

Kang-Park, S., Lee, Y.I., and Lee, Y.I., 2003. PTEN modulates insulin-like growth factor II (IGF-II)-mediated signaling; the protein phosphatase activity of PTEN downregulates IGF-II expression in hepatoma cells. *FEBS Lett. 545*:203–208.

Katiyar, S., Dash, B.C., Thakur, V., Guptan, R.C., Sarin, S.K., and Das, B.C. 2000. P53 tumor suppressor gene mutations in hepatocellular carcinoma patients in India. *Cancer 88*: 1565–1573.

Kato, H. 1996. Expression and function of squamous cell carcinoma antigen. *Anticancer Res. 16*:2149–2153.

Kawai, K., Horiike, N., Michitaka, K., and Onji, M. 2003. The effects of hepatitis B virus core promoter mutations on hepatitis B core antigen distribution in hepatocytes as detected by laser-assisted microdissection. *J. Hepatology 38*:635–641.

Kikkawa, H., Kaihou, M., Horaguchi, N., Uchida, T., Imafuku, H., Takiguchi, A., Yamazaki, Y., Koike, C., Kuruto, R., Kakiuchi, T., Tsukada, H., Takada, Y., Matsuur, N., and Oku, N. 2002. Role of integrin αvβ3 in the early phase of liver metastasis: PET and IVM analyses. *Clin. Exp. Metast. 19*:717–725.

Kim, C.J., Cho, Y.G., Park, J.Y., Kim, T.Y., Lee, J.H., Kim, H.S., Lee, J.W., Song, Y.H., Nam, S.W., Lee, S.H., Yoo, N.J., Lee, J.Y., and Park, W.S. 2004. Genetic analyses of the LKB1/ STK11 gene in hepatocellular carcinoma. *Euro. J. Cancer 40*:136–141.

Kim, J.-H., You, K.-R., Kin, I.H., Cho, B.-H., Kim, C.-Y., and Kim, D.-G. 2003. Over-expression of the ribosomal protein L36a gene is associated with cellular proliferation in hepatocellular carcinoma. *Hepatology 39:*129–138.

Kitagawa, Y., Iwai, M., Muramatsu, A., Tanaka, S., Mori, T., Harada, Y., Okanoue, T., and Kashima, K. 2002. immunohistochemical localization of CEA, CA19-9 and DU-PAN-2 in hepatitis C virus-infected liver tissues. *Histopathology 40*:472–479.

Kitamura, Y., and Ninomiya, H. 2003. Smad expression of the hepatic stellate cells in liver cirrhosis *in vivo* and hepatic stellate cell line *in vitro*. *Pathol. Intern. 53*:18–26.

Klose, J., and Kobalz, U. 1995. Two-dimensional electrophocesis of proteins: Are updated protocol and implications for a functional analysis of the genome. *Electrophocesis 16:*1034–1059.

Koga, H. 2003. Hepatocellular carcinoma: Is there a potential for chemoprevention using cyclooxygenase-2 inhibitors? *Cancer 98*:661–667.

Koga, H., Sakisaka, S., Ohishi, M., Kawaguchi, T., Taniguchi, E., Sasatomi, K., Harada, M., Kusaba, T., Tanaka, M., Kimura, R., Nakashima, Y., Nakashima, O., Kojiro, M., Kurohiji, T., and Sata, M. 1999. Expression of cyclooxygenase-2 in human hepatocellular carcinoma: Relevance to tumor dedifferentiation. *Hepatology 29*:688–699.

Kojima, N., Horiike, N., Michitaka, K., and Onji, M. 1999. In situ detection of mutated hepatitis B virus in microdissected, formalin-fixed liver tissues from patients with chronic hepatitis B. *J. Hepatol. 30*:359–365.

Komoda, F., Shino, Y., Hirano, T., Okutomi, Y., Okamoto, H., Hayashi, Y., Suyama, T., Ebara, M., Saisho, H., and Shirasawa, H. 2002. MEKK1 induces c-Jun complexes that act as negative regulators for cell survival and proliferation of HCC cells. *Int. J. Oncol. 21*:553–559.

Konda, N., Hada, A., Shuda, M., Arai, M., Arai, M., Matsubara, O., Kimura, F., Watkatsuki, T., and Yamamoto, M. 2003. Activation of galactin-1 gene in human hepatocellular carcinoma involves methylation-sensitive complex formations at the transcriptional upstream and downstream elements. *Int. J. Oncol. 23*: 1575–1583.

Kondoh, N., Hada, A., Ryo, A., Shuda, M., Arai, M., Matsubara, O., Kimura, F., Watkatsuki, T., and Yamamoto, M. 2003. Activation of galactin-1 gene in human hepatocellular carcinoma involves methylation–sensitive complex formations at the transcriptional upstream and downstream elements. *Int. J. Oncol. 23*:1575–1583.

Koo, S.H., Ihm, C.H., Kwon, K.C., Lee, J.S., Park, J.W., and Kim, J.W. 2003. Microsatellite alterations in hepatocellular carcinoma and intrahepatic cholangiocarcinoma. *Cancer Genet. Cytogenet. 146*:139–144.

Laurent-Puig, P., Legoix, P., Bluteau, O., Belghito, J., Franco, D., and Binot, F. 2001. Genetic alterations associated with hepatocellular carcinomas define distinct pathways of hepatocarcinogenesis. *Gastroenterology 120*:1763–1773.

Lee, T.K., Man, K., Ling, M.-T., Wang, X.-H., Wong, Y.-C., Lo, C.-M., Poon, R.T.P., Ng, I.O.-L., and Fan, S.-Y., 2003. Over expression of Id-1 induces cell proliferation in hepatocellular carcinoma through inactivation of $p16^{INK4a/RB}$ pathway. *Carcinogenesis 24*:1729–1736.

Leng, J., Han, C., Demetris, A.J., Michalopoulos, G.K., and Wu, T. 2003, Cyclooxygenase-2 promotes hepatocellular carcinoma cell growth through AKT activation: Evidence for AKT inhibition in celecoxib-induced apoptosis. *Hepatology 38*:756–768.

Leppa, S., and Bohmann, D. 1999. Diverse functions of JNK signaling and c-Jun in stress response and apoptosis. *Oncogene 18*:6158–6162.

Li, Y., Li, Y., Tang, R., Xu, H., Qiu, M., Chen, Q., Chen, J., Fu, Z., Ying, K., Xie, Y., and Mao, Y. 2002. Discovery and analysis of hepatocellular carcinoma genes using cDNA microarrays. *J. Cancer Res. Clin. Oncol. 128*:369–379.

Lian, Z., Liu, J., Li, L., Li, X., Tufan, N.L.S., Clayton, M., Wu, M.-C., Wang, H.-Y., Arbuthnot, P., Kew, M., and Feitelson, M.A. 2003. Upregulated expression of unique gene by hepatitis Bx antigen promotes hepatocellular growth and tumorigenesis. *Neoplasia 5*:229–244.

Lin, S.M., Sheen, I.S., Chien, R.N., Chu, C.M., and Liaw, Y.F. 1999. Long-term beneficial effect of interferon therapy in patients with chronic hepatitis B virus infection. *Hepatology 29*:971–975.

Lindh, M., Savage, K., Rees, J., Garwood, L., Horal, P., Norkrans, G., and Dhillon, A.P. 1999. HBeAg immunostaining of liver tissue in various stages of chronic hepatitis B. *Liver 19*:294–298.

Link, A.J., Eng, J., Schieltz, D.M., Carmack, E., Mize, G.J., Morris, D.R., Garvik, B.M., and Yates, J.R. 3rd. 1999. Direct analysis of protein complexes using mass spectrometry. *Nat. Biotechnol. 17*:676–682.

Lu, M., Nakamura, R.M., Dent, E.D., Zhang, J.-Y., Nielsen, F.C., Christiansen, J., Chan, E.K., and Tan, E.M. 2001. Aberrent expression of fetal RNA-binding protein p62 in liver cancer and liver cirrhosis. *Am. J. Pathol. 159*:945–953.

Lundberg, A.S., Hahn, W.C., Gupta, P., and Weinberg, R.A. 2000. Genes involved in senescence and immortalization. *Curr. Opin. Cell Biol. 12*:705–709.

Maestrazi, S., Przemioslo, R., Mitchell, H., and Sherwood, R.A. 1998. The effect of benign and malignant liver disease on the tumor markers CA19-9 and CEA. *Ann. Clin. Biochem. 35*:99–103.

Mahoney, M.G., Simpson, A., Jost, M., Noe, M., Kari, C., Pepe, D., Choi, Y.W., Uitto, J., and Rodeck, U. 2002. Metastasis-associated protein (MTA)1 enhances migration, invasion, and anchorage-independent survival of immortalized human keratinocytes. *Oncogene 21*:2161–2170.

Martinez-Ceresco, F.J., Enriquez, J., and Thomas, A. 1991. Tamoxifen improves survival in patients with advanced hepatocellular carcinoma. *J. Hepatol. 13*:S51.

Masutomi, K., Kaneko, S., Yasukawa, M., Arai, K., Murakami, S., and Kobayashi, K. 2002. Identification of serum anti-human telomerase reverse transcriptase (hTERT) auto-antibodies during progression to hepatocellular carcinoma. *Oncogene 21*:5946–5950.

Matsuo, K., Satoh, S., Okabe, H., Nomura, A., Maeda, T., Yamaoka, Y., and Ikai, I. 2003. SIAH1 inactivation correlates with tumor progression in hepatocellular carcinomas. *Genes Chromosomes Cancer 36*:283–291.

Mauleon, I., Lombard, M.-N., Munoz-Alonso, J., Canelles, M., and Lean, J. 2004. Kinetics of myc-max-mad gene expression during hepatocellular proliferation *in vivo*: Differential regulation of mad family and stress-mediated introduction of c-myc. *Mol. Carcinog. 39*:85–90.

Mazzaferro, V., Ragalia, E., Doci, R., Andreola, S., Pulvirenti, A., Bozzetti, F., Montalto, F., Ammatuna, M., Morabito, A., and Gennari, L. 1996. Liver transplantation for the treatment of small hepatocellular carcinoma in patients with cirrhosis. *N. Engl. J. Med. 334*:693–699.

Melle, C., Kaufmann, R., Hommann, M., Bleul, A., Driesch, D., Ernst, G., and Eggeling, F. 2004. Proteomic profiling in microdissected hepatocellular carcinoma tissue using protein chip technology. *Int. J. Oncol. 24*:1–7.

Midorikawa, Y., Tsutsumi, S., Taniguchi, H., Ishii, M., Kobune, Y., Kodama, T., Makuuchi, M., and Aburatani, H. 2002. Identification of genes associated with dedifferentiation of hepatocellular carcinoma with expression profiling analysis. *Jpn. J. Cancer Res. 93*:636–643.

Midorikawa, Y., Ishikawa, S., Iwanari, H., Imamura, T., Sakomoto, H., Miyazono, K., Kodoma, T., Makuuchi, M., and Aburatani, H. 2003. Glypican-3, overexpressed in hepatocellular carcinoma, modulates EGF2 and BMP-7 signaling. *Int. J. Cancer 103*:455–456.

Mikula, M., Gotzmann, J., Fischer, A.N.M., Wolschek, M.F., Thallinger, C., Schulte-Hermann, R., Beng, H., and Mikulits, W. 2003. The proto-oncogene c-Fos negatively regulates hepatocellular tumorigenesis. *Oncogene 22*:6725–6738.

Moon, W.S., Chang, K., and Taranawski, A.S. 2004. Overexpression of metastatic tumor antigen 1 in hepatocellular carcinoma: Relationship to vascular invasion and estrogen receptor-α. *Hum. Pathol. 35*:424–429.

Moon, W.S., and Tarnawski, A.S. 2003. Nuclear translocation of surviving in hepatocellular carcinoma: A key to cancer cell growth. *Hum. Pathol. 34*:1119–1126.

Morin, P.J. 1999. Beta-catenin signaling and cancer. *Bioessays 21*:1021–1030.

Morin P.J., Sparks, A.B., Korinek, V., Barker, N., Clevers, H., Vogelstein, B., Kinzler, K.W. 1997. Activation of beta-catenin-Tcf signaling in colon cancer by mutations in beta-catenin or APC. *Science 275*:1787–1790.

Moriya, K., Fujie, H., Shintani, Y., Yotsuyanagi, H., Tsutsumi, T., Ishibashi, K., Matsuura, Y., Kimura, S., Miyamura, T., and Koike, K. 1998. The core protein of hepatitis C virus induces hepatocellular carcinoma in transgenic mice. *Nat. Med. 4*:1065–1067.

Morrison, C., Marsh, W., and Frankel, W.L. 2002. A comparison of CD10 to p CEA, MOC-31, and hepatocyte for the distinction of malignant tumors in the liver. *Mod. Pathol. 15*:1279–1287.

Nagata, T., Mugishima, H., Schichino, H., Suzuki, T., Chin, M., Koshinaga, S., Inoue, M., and Harada, K. 1999. Karyotypic analyses of hepatoblastoma. Report of two cases and review of the literature suggesting chromosomal loci responsible for the pathogenesis of this disease. *Cancer Genet. Cytogenet. 114*:42–50.

Nagata, T., Takahashi, Y., Ishii, Y., Asai, S., Nishida, Y., Murata, A., Koshinaga, T., Fukuzawa, M., Hamazaki, M., Asami, K., Ito, E., Ikeda, H., Takamatsu, H., Koike, K., Kikuta, A., Kuroiwa, M., Watanabe, A., Kosaka, Y., Fujita, H., Miyake, M., and Mugishima, H. 2003. Transcriptional profiling in hepatoblastomas using high-density oligonucleotide DNA array. *Cancer Genet. Cytogenet. 145*:152–160.

Nakamura, H., Hashimoto, T., Oi, H., and Sawada, S. 1989. Transcatheter oily chemoembolization of hepatocellular carcinoma. *Radiology 170*:783–786.

Nakamura, N., Shidoji, Y., Moriwaki, H., and Muto, Y. 1996. Apoptosis in human hepatoma cell line induced by 4,5-didehydrogeranylgeranoic acid (acrylic retinoid) via down-regulation of transforming growth factor-alpha. *Biochem. Biophys. Res. Commun. 219*:100–104.

Nakau, M., Miyashi, H., Seldin, M.F., Imamura, M., Oshima, M., and Taketo, M.M. 2002. Hapatocellular carcinoma caused by

loss of heterozygosity in Lkb 1 gene knockout mice. *Cancer Res. 62*:4549–4553.

Nakopoulou, L., Stefanaki, K., Filaktopoulos, D., and Giannopoulou, I. 1994. C-erb-B-2 oncoprotein and epidermal growth factor receptor in human hepatocellular carcinoma: An immunohistochemical study. *Histol. Histopathol. 9*: 677–682.

Noguchi, K.I., Enjoji, M., Nakamuta, M., Nakashima, M., Nishi, H., Choi, I., Toguchi, K.I., Kotoh, K., Shimada, M., Sugimachi, K., Tsuneyoshi, M., Nawata, H., and Watanabe, T. 2001. Expression of a tumor associated antigen RCAS1 in hepatocellular carcinoma. *Cancer Lett. 168*:197–202.

Norton, J.D. 2000. ID helix-loop-helix proteins in cell growth, differentiation and tumorigenesis. *J. Cell Sci. 113*:3897–3905.

Nose, H., Imazeki, F., Ohto, M., and Omata, M. 1993. p53 gene mutations and 17p allelic deletions in hepatocellular carcinoma from Japan. *Cancer 72*:355–360.

Ohkubo, K., Kato, Y., Ichikawa, T., Kajiya, Y., Takeda, Y., Higashi, S., Hamasaki, K., Nakao, K., Nakata, K., Eguchi, K. 2002. Viral load is a significant prognostic factor for hepatitis B virus-associated hepatocellular carcinoma. *Cancer 94*:2663–2668.

Ohtani, N., Zebedee, Z., Huot, T.J., Stinson, J.A., Sugimoto, M., Ohashi, Y., Sharrocks, A.D., Peters, G., and Hara, E. 2001. Opposing effects of Ets and Id proteins on p16INK4a expression during cellular senescence. *Nature 409*:1067–1070.

Okuda, K., Nakamura, Y., and Miyazaki, M. 2002. Cholangiocarcinoma: Recent progress. Part 2: Molecular pathology and treatment. *Gastroenterol. Hepatol. 17*:1056–1063.

Okuda, T., Hirohashi, K., Kinoshita, H., Wakasa, K., and Sakurai, M. 1996. Characteristic histologic features of human hepatocellular carcinoma with mutant p53 protein. *World J. Surg. 20*:215–220.

Okuda, Y., Nakamura, H., Yoshida, K., Enomoto, H., Uyama, H., Hirotani, T., Funamoto, M., Ito, H., Everett, A.D., Hada, T., and Kawase, I. 2003. Hepatoma-derived growth factor induces tumorigenesis *in vivo* through both direct angiogenic activity and induction of vascular endothelial growth factor. *Cancer Sci. 94*:1034–1041.

Pan, C.-C., Chen, P.C-h., Tsay, S-H., and Chiang, H. 2004. Cytoplasmic immunoreactivity for thyroid transcription factor-1 in hepatocellular carcinoma. *Am. J. Clin. Pathol. 121*:343–349.

Pang, A., Ng, I.O., Fan, S.T., and Kwong, Y.L. 2003. Clinicopathologic significance of genetic alterations in hepatocellular carcinoma. *Cancer Genet. Cytogenet. 146*:8–15.

Park, K.S., Kim, H., Kim, N.G., Cho, S.Y., Choi, K.H., Seong, J.K., and Paik, Y.K. 2002. Proteomic analysis and molecular characterization of tissue ferritin light chain in hepatocellular carcinoma. *Hepatology 35*:1459–1466.

Park, Y.N., Chae, K.J., Kim, Y.B., Park, C., and Theise, N. 2001. Apoptosis and proliferation in hepatocarcinogenesis related to cirrhosis. *Cancer 92*:2733–2738.

Peng, C.Y., Tsai, S.L., Yeh, C.T., Hung, S.P., Chen, M.F., Chen, T.C., Chu, C.M., and Liaw, Y.F. 2000. Genetic alterations of p73 are frequent but may occur in early stage hepatocellular carcinoma. *Anticancer Res. 20*:1487–1492.

Perilongo, G., and Shafford, E.A. 1999. Liver tumours. *Eur. J. Cancer 35*:953–958.

Pisani, P., Parkin, D.M., Munoz, N., and Ferlay, J. 1997. Cancer and infection: Estimates of the attributable fraction in 1990. *Cancer Epidemiol. Biomarkers Prev. 6*:387–400.

Pontisso, P., Calabrese, F., Benvegnu, L., Lise, M., Belluco, C., Ruvoletto, M.G., Falco, S.De., Marino, M., Valente, M., Nitti, D., Gatta, A., and Fassina, G. 2004. Overexpression of squamous cell carcinoma antigen variants in hepatocellular carcinoma. *Br. J. Cancer 90*:833–837.

Potti, A., Ganti, A.K., Tendulkar, K., Chitajallu, S., Sholes, K., Koch, M., and Kargas S. 2003. HER-2/neu and CD117 (C-kit) overexpression in hepatocellular and pancreatic carcinoma. *Anticancer Res. 23*:2671–2674.

Qian, G.S., Ross, R.K., Yu, M.C., Yuan, J.M., Gao, Y.T., Henderson, B.E., Wogan, G.N., and Groopman, J.D. 1994. A follow-up study of urinary markers of aflatoxin exposure and liver cancer risk in Shanghai, People's Republic of China. *Cancer Epidemiol. Biomarkers Prev. 3*:3–10.

Qin, L.F., and Ng, I.-O. 2001. Expression of $p27^{KIP1}$ and $p21^{WFI/CIP1}$ in primary hepatocellular carcinoma: Clinicopathologic correlation and survival analysis. *Hum. Pathol. 32*:778–784.

Qin, L.X., and Tang, Z.Y. 2002. The prognostic significance of clinical and pathological features in hepatocellular carcinoma. *World J. Gastroenterol. 8*:193–199.

Rahman, M.A., Dhar, D.K., Yamaguchi, E., Maruyama, S., Sato, T., Hayashi, H., Ono, T., Yamanoi, A., Kohno, H., and Nagasue, N. 2001. Coexpression of inducible nitric oxide synthase and COX-2 in hepatocellular carcinoma and surrounding liver: Possible involvement of COX-2 in the angiogenesis of hepatitis C virus-positive cases. *Clin. Cancer Res. 7*:1325–1332.

Rahman, M.A., Kyriazanos, I.D., Ono, T., Yamanoi, A., Kohno, H., Tsuchiya, M., and Nagasue, N. 2002. Impact of PTEN expression on the outcome of hepatitis C virus-positive cirrhotic hepatocellular carcinoma patients: Possible relationship with COX II and inducible nitric oxide synthase. *Int. J. Cancer 100*:152–157.

Raidl, M., Pirker, C., Schulte-Hermann, R., Aubele, M., Kandioler-Eckersberger, D., Wrba, F., Micksche, M., Berger, W., and Grasl-Kraupp, B. 2004. Multiple chromosomal abnormalities in human liver (pre)neoplasia. *J. Hepatol. 40*:660–668.

Ranke, M.B., Maier, K.P., Schweizer, R., Stadler, B., Schleicher, S., Elmlinger, M.W., and Flehmig, B. 2003. Pilot study of elevated levels of insulin-like growth factor-binding protein-2 as indicators of hepatocellular carcinoma. *Horm. Res. 60*:174–180.

Ray, R.B., Steele, R., Meyer, K., and Ray, R. 1997. Transcriptional repression of p53 promoter by hepatitis C virus core protein. *J. Biol. Chem. 272*:10983–10986.

Ricketts, S.L., Carter, J.C., and Coleman, W.B. 2003. Identification of three 11p11.2 candidate liver tumor suppressors through analysis of known human genes. *Mol. Carcinog. 36*:90–99.

Ristimaki, A., Honkane, N., Jancala, H., Sippionen, P., and Harkonne, M. 1977. Expression of cyclooxygenase-2 in human gastric carcinoma. *Cancer Res. 57*:1276–1280.

Salizzoni, M., Romagnoli, R., Lupo, F., David, E., Mirabella, S., Cerutti, E., and Ottobrelli, A. 2003. Microscopic vascular invasion detected by anti-CD34 immunohistochemistry as a predictor of recurrence of hepatocellular carcinoma after liver transplantation. *Transplantation 76*:844–848.

Sato, M., Watanabe, Y., Ueda, S., Iseki, S., Abe, Y., Sato, N., Kimura, S., Okubo, K., and Onji, M. 1996. Microwave coagulation therapy for hepatocellular carcinoma. *Gastroenterology 110*:1507–1514.

Schmilovitz-Weiss, H., Belinki, A., Pappo, O., Sulkes, J., Melzer, E., Kaganovski, E., Kfir, B., Tur-Kaspa, R., Klein, T., and Ben-Ari, Z. 2004. Role of circulating soluble CD40 as an apoptotic marker in liver disease. *Apoptosis 9*:205–210.

Schmitt-Graff, A., Ertelt, V., Allgaier, H.P., Koelble, K., Olschewski, M., Nitschke, R., Bochaton-Piallat, M.L., Gabbiani, G., and Blum, H.E. 2003. Cellular retinol-binding protein-1 in

hepatocellular carcinoma correlates with beta-catenin, Ki-67 index, and patient survival. *Hepatology 38*:470–480.

Schoedel, K.E., Tyner, V.Z., Kim, T.-H., Michalopoulos, G.K., and Mars, W.M. 2003. HGF, MET, and matrix-related proteases in hepatocellular carcinoma, fibrolamellar variant, cirrhotic and normal liver. *Mod. Pathol. 16*:14–21.

Seidenfeld, J., Korn, A., and Aronson, N. 2002. Radiofrequency ablation of unresectable primary liver cancer. *J. Am. Coll. Surg. 4*:813–828.

Seki, T., Tamai, T., Nakagawa, T., Imamura, M., Nishimura, A., Yamashiki, N., Ikeda, K., and Inoue, K. 2000. Combination therapy with transcatheter arterial chemoembolization and percutaneous microwave coagulation therapy for hepatocellular carcinoma. *Cancer 89*:1245–1251.

Seow, T.K., Liang, R.C.M.Y., Leow, C.K., and Chung, M.C.M. 2001. Hepatocellular carcinoma: From bedside to proteomics. *Proteomics 1*:1249–1263.

Shiina, S., Teratani, T., Obi, S., Hamamura, K., Koike, Y., and Omata, M. 2001. Percutaneous ethanol injection therapy for liver tumors. *Eur. J. Ultrasound 13*:95–106.

Shiota, G., Okubo, M., Noumi, T., Oyama, K., Takano, Y., Yashima, K., Kishimoto, Y., and Kawasaki, H. 1999. Cyclooxygenase-2 expression in hepatocellular carcinoma. *Hepato-gastroenterology 46*:407–412.

Shiraki, K., Sugimoto, K., Yamanaka, Y., Yamaguchi, Y., Saitou, Y., Ito, K., Yamamoto, N., Yamanaka, T., Fujikawa, K., Murata, K., and Nakano, T. 2003. Overexpression of X-linked inhibitor of apoptosis in human hepatocellular carcinoma. *Int. J. Mol. Med. 12*:705–708.

Shiratori, Y., Shina, S., Teratani, T., Imamura, M., Obi, S., Sato, S., Koike, Y., Yoshida, H., and Omata, M. 2003. Interferon therapy after tumor ablation improves in patients with hepatocellular carcinoma associated with hepatitis C virus. *Ann. Intern. Med. 138*:299–306.

Smith, M.W., Yue, Z.N., Geiss, G.K., Sadovnikova, N.Y., Carter, V.S., Boix, L., Lazaro, C.A., Rosenberg, G.B., Bumgarner, R.E., Fausto, N., Bruix, J., and Katze, M.G. 2003. Identification of novel tumor markers in hepatitis C virus-associated hepatocellular carcinoma. *Cancer Res. 63*:859–864.

Steel, L.F., Mattu, T.S., Mehta, A., Hebestreit, H., Dwek, R., Evans, A.A., London, W.T., and Block, T. 2001. A proteomic approach for the discovery of early detection markers of hepatocellular carcinoma. *Disease Markers 17*:179–189.

Stuart, K.E., Anand, A.J., and Jenkins, R.L. 1996. Hepatocellular carcinoma in the United States. Prognostic features, treatment outcome, and survival. *Cancer 77*:2217–2222.

Subbaramaiah, K., Telang, N., Ramonetti, J.T., Araki, R., DeVito, B., Weksler, B.B., and Dannenberg, A.J. 1996. Transcription of cyclooxygenase-2 is enhanced in transformed mammary epithelial cells. *Cancer Res. 56*:4424–4429.

Suminami, Y., Nagashima, S., Vujanovic, N.L., Hirabayashi, K., Kato, H., and Whiteside, T.L. 2000. Inhibition of apoptosis in human tumor cells by the tumor-associated serpin, SCC antigen. *Br. J. Cancer 82*:981–989.

Szymanska, K., Lesi, O., O.A., Kirk, G.D., Sam, O., Taniere, P., Scoazec, J.-Y., Mendy, M., Friesen, M.D., Whittle, H., Montesano, R., and Hainaut, P. 2004. Ser-249 T53 mutation in tumor and plasma DNA of hepatocellular carcinoma patients form a high incidence in the Gambia, West Africa. *Int. J. Cancer 110*:373–379.

Tai, D.I., Tsai, S.L., Chen, Y.M., Chuang, Y.L., Peng, C.Y., Sheen, I.S., Yeh, C.T., Chang, K.S., Huang, S.N., Kuo, G.C., and Liaw, Y.F. 2000. Activation of nuclear factor kappa B in hepatitis C virus infection: Implications for pathogenesis and hepatocarcinogenesis. *Hepatology 31*:656–664.

Takashima, M., Kuramitsu, Y., Yokoyama, Y., Iizuka, N., Toda, T., Sakaida, I., Okita, K., Oka, M., and Nakamura, K. 2003. Proteomic profiling of heat shock protein 70 family members as biomarkers for hepatitis C virus-related hepatocellular carcinoma. *Proteomics 3*:2487–2493.

Takikawa, H., Mafune, K., Hamada, H., Nettelbeck, D.M., Muller, R., Makuuchi, M., and Kaminishi M. 2003. An advanced strategy of enhanced specific gene expression for hepatocellular carcinoma. *Int. J. Oncol. 22*:1051–1056.

Tan, C., Mui, A., and Dedhar, S. 2002. Integrin-linked kinase regulates inducible nitric oxide synthase and cyclooxygenase-2 expression in a NF-kappa B-dependent manner. *J. Biol. Chem. 277*:3109–3116.

Tannapfel, A., Busse, C., Weinans, L., Benicke, M., Katalinic, A., Geissler, F., Hauss, J., and Wittekind, C. 2001. INK4a-ARF alterations and p53 mutations in hepatocellular carcinomas. *Oncogene 20*:7104–7109.

Tannapfel, A., Wasner, M., Krause, K., Geissler, F., Katalinic, A., Hauss, J., Engeland, K., and Wittekind, C. 1999. Expression of p73 and its relation to histopathology and prognosis in hepatocellular carcinoma. *J. Natl. Cancer Inst. 91*:1154–1158.

Tessitore, L., Marengo, B., Vance, D.E., Papotti, M., Mussa, A., Daidone, M.G., and Costa, A. 2003. Expression of phosphatidylethanolamine N-methyltransferase in human hepatocellular carcinomas. *Oncology 65*:152–158.

Toh, Y., Kuninaka, S., Endo, K., Oshiro, T., Ikeda, Y., Nakashima, H., Baba, H., Kohnoe, S., Okamura, T., Nicolson, G.L., and Sugimachi, K. 2000. Molecular analysis of a candidate metastasis-associated gene, MTA1: Possible interaction with histone deacetylase 1. *J. Exp. Clin. Cancer Res. 19*: 105–111.

Torbenson, M., Marinopoulos, S., Dang, D.T., Choti, M., Ashfaq, R., Maitra, A., Boitnott, J., and Wilentz, R.E. 2002. Smad4 overexpression in hepatocellular carcinoma is strongly associated with transforming growth factor beta II receptor immunolabeling. *Hum. Pathol. 33*:871–876.

Tufan, N.L.S., Lian, Z., Liu, J., Pan, J., Arbuthnot, P., Kew, M., Clayton, M.M., and Feitelson, M.A. 2002. Hepatitis B xantigen stimulates expression of a novel cellular gene, URG4, that promotes hepatocellular growth and survival. *Neoplasia 4*:355–368.

Ueda, H., Ullrich, S.J., Ngo, L., Feitelson, M.A., and Jay, G. 1995. Functional inactivation but not structural mutation of p53 causes liver cancer. *Nat. Genet. 9*:41–47.

Urabe, T., Kanekors, S., Matsushita, E., Unoura, M., and Kobayashi, K. 1998. Clinical pilot study of intrahepatic arterial chemotherapy with methotrexate, 5-fluorouracil, cisplatin and subcutaneous interferon-alpha-2b for patients with locally advanced hepatocellular carcinoma. *Oncology 55*:39–47.

Venook, A.P. 1994. Treatment of hepatocellular carcinoma: Too many options? *J. Clin. Oncol. 12*:1323–1334.

Vlasoff, D.M., Baschinsky, D.Y., De Young, B.R., Morrison, C.D., Nuovo, G.J., and Frankel, W.L. 2002. C-erb B2 (Her2/neu) is neither overexpressed nor amplified in hepatic neoplasms. *Appl. Immunohistochem. Mol. Morphol. 10*:237–241.

Wan, D., He, M., Wang, J., Qui, X., Zhou, W., Luo, Z., Chen, J., and Gu, J. 2004. Two variants of the human hepatocellular carcinoma associated HCAPI gene and their effect on the growth of the human liver cancer cell line Hep3B. *Genes Chromosomes Cancer 39*:48–58.

Wang, Z.X., Wang, H.Y., and Wu, M.C. 2001. Identification and characterization of a novel human hepatocellular carcinoma-associated gene. *Br. J. Cancer 85*:1162–1167.

Wang, Y., Wu, M.C., Sham, J.S., Zhang, W., Wu, W.Q., and Guan, X-Y. 2002. Prognostic significance of c-myc and AIB1 amplification in hepatocellular carcinoma. *Cancer 95*:2346–2352.

Wei, Y., Fabre, M., Branchereau, S., Gauthier, F., Perilongo, G., and Buendia. M.A. 2000. Activation of β-catenin in epithelial and mesenchymal hepatoblastomas. *Oncogene 19*:498–504.

Weng, L.P., Brown, J.L., and Eng, C. 2001. PTEN coordinates G(1) arrest by down-regulating cyclin Dl via its protein phosphatase activity and up-regulating p27 via its lipid phosphatase activity in a breast cancer model. *Hum. Mol. Genet. 10*:599–604.

Wild, C.P., and Hall, A.J. 2000. Primary prevention of hepatocellular carcinoma in developing countries. *Mutation Res. 462*:381–393.

Williams, C.S., Mann, M., and DuBois, R.N. 1999. The role of cyclooxygenases in inflammation, cancer, and development. *Oncogene 18*:7908–7916.

Wong, L.J., Tan, D.J., Bai, R.K., Yeh, K.T., and Chang, J. 2004. Molecular alterations in mitochondrial DNA of hepatocellular carcinomas: Is there a correlation with clinicopathological profile? *J. Med. Genet. 41*:e65.

Wu, C.G., Forgues, M., Siddique, S., Farnsworth, J., Valerie, K., and Wang, X.W. 2002. Sage transcript profiles of normal primary human hepatocytes expressing oncogenic hepatitis B virus X protein. *FASEB J. 16*:1665–1667.

Xiang, Y.Y., Ladeda, V., and Filmus, J. 2001. Glypican-3 expression is silenced in human breast cancer. *Oncogene 20*:7408–7412.

Xiao, S.Y., Wang, H.L., Hart, J., Fleming, D., and Beard, M.R. 2001. cDNA arrays and immunohistochemistry identification of CD10/CALLA expression in hepatocellular carcinoma. *Am. J. Pathol. 159*:1415–1421.

Xu, X.R., Huang, J., Xu, Z.G., Qian, B.Z., Zhu, Z.D., Yan, Q., Cai, T., Zhang, X., Xiao, H.S., Qu, J., Liu, F., Huang, Q.H., Cheng, Z.H., Li, N.G., Du, J.J., Hu, W., Shen, K.T., Lu, G., Fu, G., Zhong, M., Xu, S.H., Gu, W.Y., Huang, W., Zhao, X.T., Hu, G.X., Gu, J.R., Chen, Z., and Han, Z.G. 2001. Insight into hepatocellular carcinogenesis at transcriptome level by comparing gene expression profiles of hepatocellular carcinoma with those of corresponding noncancerous liver. *Proc. Natl. Acad. Sci. U.S.A. 98*:15089–15094.

Xu, Z.G., Du, J.J., Zhang, X., Cheng, Z.H., Ma, Z.Z., Xiao, H.S., Yu, L., Wang, Z.Q., Li, Y.Y., Huo, K.K., and Han, Z.G. 2003. A novel liver-specific zona pellucida domain containing protein that is expressed rarely in hepatocellular carcinoma. *Hepatology 38*:735–744.

Yamada, R., Sato, M., Kawabata, M., Nakatsuka, H., Nakamura, K., and Takashima, S. 1983. Hepatic artery embolization in 120 patients with unresectable hepatoma. *Radiology 148*:399–401.

Yang, H., Huang, Z.Z., Wang, J., and Lu, S.C. 2001. The role of c-Myb and Sp1 in the up-regulation of methionine adenosyltransferase 2A gene expression in human hepatocellular carcinoma. *FASEB J. 15*:1507–1516.

Yen, T.S.B. 1996. Hepadnaviral X protein: Review of recent progress. *J. Biomed. Sci. 3*:20–30.

Yerian, L.M., Anders, R.A., Tretiakova, M., and Hart, J. 2004. Caveolin and thrombospondin expression during hepatocellular carcinogenesis. *Am. J. Surg. Pathol. 28*:357–364.

Yoshida, T., Hanada, T., Tokuhisa, T., Kosai, K., Sata, M., Kohara, M., and Yoshimura, A. 2002. Activation of STAT3 by the hepatitis C virus core protein leads to cellular transformation. *J. Exp. Med. 96*:641–653.

Yu, M.W., Yang, S.Y., Chiu, Y.H., Chiang, Y.C., Liaw, Y.F., and Chen, C.J. 1999. A p53 genetic polymorphism as a modulator of hepatocellular carcinoma risk in relation to chronic liver disease, familial tendency, and cigarette smoking in hepatitis B carriers. *Hepatology 29*:697–702.

Yusof, Y.A., Yan, K.L., and Hussain, S.N. 2003. Immunohistochemical expression of pi class glutathione S-transferase and alpha-fetoprotein in hepatocellular carcinoma and chronic liver disease. *Anal. Quant. Cytol. Histol. 25*:332–338.

Zatkova, A., Rouillard, J.-M., Hartmann, W., Lamb, B.T., Kuick, R., Eckart, M., Schweinitz, D.V., Koch, A., Fonatsch, C., Pietsch, T., Hanash, S.M., and Wimmer, K. 2004. Amplification and overexpression of the IGF2 regular PLAGI in the hepatoblastoma. *Genes Chromosomes Cancer 39*:126–137.

Zhang, Y.-J., Chen, S.-Y., Chen, C.-J., and Santella, R.M. 2002. Polymorphisms in cyclin D1 gene and hepatocellular carcinoma. *Mol. Carcinogenesis 33*:125–129.

Zeindl-Eberhart, E., Haraida, S., Liebmann, S., Jungblut, P.R., Lamer, S., Mayer, D., Jager, G., Chung, S., and Rabes, H.M. 2004. Detection and identification of tumor-associated protein variants in human hepatocellular carcinomas. *Hepatology 39*:540–549.

Zeng, J.Z., Wang, H.Y., Chen, Z.J., Ullrich, A., and Wu, M.C. 2002. Molecular cloning and characterization of a novel gene which is highly expressed in hepatocellular carcinoma. *Oncogene 221*:4932–4943.

2

Mechanisms of Human Hepatocarcinogenesis: An Overview

William B. Coleman

Introduction

The primary hepatocellular neoplasms include hepatocellular adenoma, hepatocellular carcinoma (HCC), and hepatoblastoma. Together, these neoplasms constitute a clinically important group of human cancers that are diagnostically and therapeutically challenging. Of these primary liver neoplasms, HCC is the most common. Early detection and diagnosis of HCC is inefficient in the absence of well-known risk factors and appropriate surveillance (Bruix *et al.,* 2004), and most currently available treatments for this tumor are ineffective (Llovet *et al.,* 2003). Consequently, HCC is nearly uniformly fatal (Jemal *et al.,* 2004; Parkin *et al.,* 2001). Clinical and basic research on mechanisms of hepatocarcinogenesis has produced a tremendous amount of information about the pathologic settings in which HCC develops and the major etiologic factors that are responsible. Recent progress has begun to unravel the molecular pathogenesis of HCC in response to specific etiologic factors (Buendia, 2000; Feitelson *et al.,* 2002; Grisham, 2002; Thorgeirsson and Grisham, 2002). The accumulated evidence suggests that HCC emerges through a multistep process (with well-characterized histopathologic manifestations), in which HCC develops in the context of the pathologic liver (chronic hepatitis and/or cirrhosis), from aberrant cells contained in dysplastic hepatocyte nodules or adenomatous hyperplasia (Feitelson *et al.,* 2002). However, in the absence of an obvious genetic predisposition for HCC development, the identification of critical genes and genetic pathways has been difficult, precluding the elucidation of the rate-limiting steps in multistage hepatocarcinogenesis (Buendia, 2000).

Epidemiology of Hepatocellular Carcinoma

Cancers of the liver and intrahepatic bile ducts are relatively rare in the United States, with 18,920 new diagnoses and 14,270 deaths in 2004 (Jemal *et al.,* 2004). This represents ~1.3% of all new cancer diagnoses and 2.5% of cancer-related deaths in the United States (Jemal *et al.,* 2004). In contrast, liver cancer occurs at high incidence when the world population is considered. In 1990 there were 437,000 new cases of liver cancer worldwide, representing 5.4% of all

Handbook of Immunohistochemistry and *in situ* Hybridization of Human Carcinomas, Volume 3: Molecular Genetics, Liver Carcinoma, and Pancreatic Carcinoma

cancers and making it the fifth leading cause of cancer incidence (Parkin *et al.,* 1999a). Deaths attributed to liver cancer for the same year totaled 427,000, which represents 8.2% of all cancer deaths and makes it the fourth leading site for cancer mortality (Parkin *et al.,* 1999a). In 2000 the worldwide incidence of liver cancer increased, with 564,000 new cases and 549,000 deaths, representing 5.5% (fifth leading site) of new cases and 8.8% of all cancer deaths (third leading cause of cancer-related deaths) (Parkin, 2001; Parkin *et al.,* 2001).

The prevalence of primary liver cancer varies greatly among world regions. The highest incidence of liver cancer worldwide is found in China, where men exhibit an incidence rate of ~36 cases per 100,000 population (Mathers *et al.,* 2002; Parkin *et al.,* 1999a). High rates of liver cancer incidence are found throughout large portions of Asia and Africa, with much lower incidence rates for this tumor found in Europe and the Americas (Mathers *et al.,* 2002). Early studies called attention to the extremely high incidence of hepatocellular carcinoma among black males in Mozambique (Berman, 1951; Higginson, 1963), which demonstrates the highest incidence worldwide at 113 cases per 100,000 population (Munoz and Bosch, 1987). In fact, the incidence of this tumor among black Mozambican males aged 25–34 years is more than 500-fold higher than the incidence for comparably aged white males in the United States and United Kingdom (Higginson, 1963; Munoz and Linsell, 1982). These statistics strongly suggest that factors related to genetic background and/or environmental exposure contribute significantly to the incidence of this tumor among world populations.

There has been a dramatic increase in HCC incidence among Japanese men during the last 30 years (Okuda *et al.,* 1987). Likewise, significant increases in HCC have been reported in the United States (El-Serag and Mason, 1999; Parkin *et al.,* 2001), the United Kingdom (Taylor-Robinson *et al.,* 1997), and France (Deuffic *et al.,* 1998). These increases in the incidence of HCC may reflect significant changes in risk factors or environmental exposures in affected populations. It has been suggested that the increased incidence of HCC in Japan, Europe, and the United States is related to increased incidence of HCV infection (Bruix *et al.,* 2004). Migration of individuals from one world region to another can affect their relative risk for development of HCC. Indians who migrate to Singapore or parts of China acquire incidence rates of HCC that are similar to those of the native population and significantly increased from that of their home country (Bosch, 1997). In contrast, migrants from world regions with high risk for HCC development to regions of low risk for HCC demonstrate a decline in HCC incidence with successive generations (Parkin *et al.,* 1999b). These observations suggest that exposure to environmental factors are more important contributors to HCC risk than population-based genetic factors or susceptibilities.

Liver cancer affects men more often than women. The ratio of male to female incidence in the United States is ~2:1, and worldwide it is ~2.4:1 (Jemal *et al.,* 2004). However, in high-incidence countries or world regions, the male to female incidence ratio can be as high as 8:1 (Simonetti *et al.,* 1991; Stevens *et al.,* 1984). This consistent observation suggests that sex hormones and/or their receptors may play a significant role in the development of primary liver tumors. Some investigators have suggested that HCCs overexpress androgen receptors (Eagon *et al.,* 1991), and that androgens are important in the promotion of abnormal liver cell proliferation (Carr and Van Thiel, 1990). In fact, anecdotal evidence suggests that therapeutic exposure of patients to androgenic–anabolic steroids increases the chances of HCC development (Johnson *et al.,* 1972). Conversely, some investigators suggest that female hormones (or their metabolites) are protective against development of HCC (Lui *et al.,* 2000). In addition to the strong linkage between gender and development of HCC, there is evidence that the progression of the disease is less severe in women and that their long-term survival is much better than that of affected men (El-Serag *et al.,* 2001). Others have suggested that the male predominance of liver cancer is related to the tendency for men to drink and smoke more heavily than women and the fact that men are more likely to develop cirrhosis (Lai *et al.,* 1987).

Natural History of Hepatocellular Carcinoma

Hepatocarcinogenesis is a continuous and slowly unfolding process that leads from the initial genetic and epigenetic alterations in one or a few hepatocytes to the acquisition of a neoplastic phenotype by one or a few cells with the capacity to grow autonomously and to metastasize to distant sites outside the liver. The descriptive natural history of HCC, including the pathologic tissue patterns and clinical course, provides a framework for attempting to trace the sequence of molecular genetic alterations that drive its development. Hepatocellular carcinoma is strongly associated with chronic liver diseases, including chronic hepatitis and cirrhosis (Grisham, 1997; Grisham, 2002). In fact, the majority of cases of primary hepatocellular carcinoma worldwide develop in cirrhotic livers, most commonly nonalcoholic posthepatitic cirrhosis (Grisham, 1997; Grisham, 2002; Okuda and Okuda, 1999).

Chronic Hepatitis

Chronic hepatitis is a prolonged inflammatory condition of the liver that is characterized by the presence of an inflammatory cell infiltrate, hepatocyte necrosis and death, and accelerated proliferation of residual hepatocytes to replace cells lost to injury and death. The inflammatory cells of chronic hepatitis consists of a mixture of B and T lymphocytes, dendritic cells, plasma cells, and macrophages (Simpson *et al.,* 1997). These cells infiltrate the connective tissue of the portal tracts and may also invade the adjacent lobular parenchyma. Lymphocytes and macrophages accumulate in the chronically inflamed liver as a result of increased expression of chemotactic cytokines by endothelial cells of the portal vessels and interlobular sinusoids (Simpson *et al.,* 1997). The inflammatory cell infiltrate of chronic hepatitis express numerous cytokines, including chemotactic cytokines of the CC and CXC types, and immunomodulatory cytokines, including tumor necrosis factor alpha (TNFα), various interleukins, and various interferons (Simpson *et al.,* 1997). The chemotactic cytokines recruit additional inflammatory cells and induce higher levels of expression by endothelial cells of adhesion molecules and receptors for inflammatory cell ligands.

The immunomodulatory cytokines stimulate both inflammatory cells and resident liver cells, including hepatocytes, to secrete cytokines, growth factors, and proteases, which stimulates destruction and repair of liver tissue. Where the inflammatory cells (infiltrate) touch the lobular parenchyma, cytotoxic T lymphocytes surround individual hepatocytes or small groups of hepatocytes; many of these hepatocytes die as a result of activation of death-signaling pathways mediated by Fas receptor or TNF1 receptor (Kagi *et al.,* 1996). The resulting persistent hepatocyte cell death produces a pathologic pattern in the liver that is characterized by zone 1 (periportal) necrosis. Residual hepatocytes are stimulated to proliferate by the loss of cells and as a result of direct stimulation by cytokines and growth factors produced by inflammatory cells.

Cirrhosis

Cirrhosis is a diffuse form of hepatic fibrosis resulting from severe, long-standing hepatitis with extensive necrosis (Anthony *et al.,* 1978). In the cirrhotic liver, the normal hepatic architecture is destroyed by fibrous septa that encompass regenerative nodules of hepatocytes (Conn, 1975). Thus, the normally continuous liver parenchyma is dissected and subdivided into nodular aggregates of varying size, each of which is segregated by encircling bands (septa) of collagenous connective tissue (Anthony *et al.,* 1978). Several general pathologic features characterize cirrhosis: 1) the hepatic parenchyma is separated into nodular aggregates of regenerative hepatocytes that vary in size; 2) the entire liver is involved and normal parenchymal structure is destroyed by septa of connective tissue; and 3) both afferent and efferent arms of the liver vasculature are consumed by connective tissue septa (Conn, 1975).

Two major morphologic types of cirrhosis are recognized, termed micronodular cirrhosis and macronodular cirrhosis. In micronodular cirrhosis, regenerative hepatocyte nodules are scarcely larger than the size of a normal lobular unit of parenchyma, and are separated by thin connective tissue septa. However, the nodules show none of the landmarks observed in the normal liver, such as portal tracts or central veins. Macronodular cirrhosis is characterized by the presence of large irregular nodules that may contain portal tracts and efferent vessels. This form of cirrhosis may result from multilobular necrosis and formation of scars surrounding an area of parenchyma larger than a single lobule. In addition, micronodular cirrhosis can progress to the macronodular form through persistent regeneration and expansion of existing nodules.

The functional consequences of cirrhosis reflect the obstruction of normal blood flow through the liver (Conn, 1975). In the cirrhotic liver, the connective tissue septa preclude the normal passage of blood via the sinusoids through the formation of shunts from the portal triads to the central vein. The decreased hepatic function observed in with cirrhosis patients is the direct result of the rerouting of blood around the parenchyma. In addition to decreased liver function, portal hypertension results from the obstruction of liver blood flow secondary to regenerative nodules impinging on the hepatic veins. Complications from portal hypertension include bleeding from gastroesophageal varices, formation of ascites, and development of splenomegaly (Conn, 1975).

Cirrhosis is a result of chronic hepatitis, and most hepatocellular carcinoma occurs in the setting of cirrhosis in humans. Despite the observation that cirrhosis is not an obligate precursor lesion for HCC development (Romeo and Colombo, 2002), cirrhosis of any morphologic type or etiology is associated with increased risk for development of the disease (Johnson and Williams, 1987). However, the magnitude of excess risk for development of HCC reflects the specific etiology of cirrhosis (Johnson and Williams, 1987), suggesting that the nature of the causative agent may be determinant (Grisham, 1997).

Hepatocellular carcinoma develops annually in 5–8% of the population affected by cirrhosis related to chronic hepatitis C virus (HCV) infection (IARC, 1994c). A similar level of risk is associated with cirrhosis resulting from hemochromatosis (Johnson and Williams, 1987). In contrast, risk for development of HCC is less for patients with hepatitis B virus (HBV)-related cirrhosis (IARC, 1994c). Likewise, alcoholic cirrhosis and cirrhosis associated with certain genetic diseases (e.g., Wilson's disease and α1-antitrypsin deficiency) are accompanied by an even smaller risk for HCC (IARC, 1988). Nonalcoholic fatty liver disease (or nonalcoholic steatohepatitis) can result in development of cirrhosis (Zafrani, 2004), and in these patients there is an increased risk for HCC as well (Bugianesi *et al.,* 2002).

Phenotypic Alterations and Dysplasia

In the setting of simultaneous hepatocellular necrosis and proliferation, nodular aggregates of hepatocytes may develop in either cirrhotic or noncirrhotic livers that are affected by chronic hepatitis. These nodular aggregates of hyperplastic hepatocytes may express a variety of aberrant metabolic phenotypes before obvious genomic abnormalities occur. Alterations in the metabolic phenotype of a few hepatocytes, evidenced by the occurrence of foci of phenotypically altered hepatocytes, are one of the earliest morphologic changes detected in hepatocytes during the process of hepatocarcinogenesis (Uchida *et al.,* 1981). Phenotypically altered hepatocytes express and store various metabolic products, such as glycogen, lipid, and iron (Bannasch, 1996). Three major types of phenotypically altered hepatocytes have been identified: 1) glycogen-storing, 2) mixed-cell type, and 3) basophilic (Su *et al.,* 1997). Phenotypically altered hepatocytes occur in 76% (84/111) of cirrhotic livers, in 91% (29/32) of cirrhotic livers containing HCC, and in 70% (55/79) of cirrhotic livers without HCC (Su *et al.,* 1997).

Glycogen-storing (clear-cell) foci were found to be smaller than mixed-cell foci, which were often associated with larger hepatocyte nodules and the development of small-cell (dysplastic) change (Su *et al.,* 1997). Glycogen-storing foci contain hepatocytes with the earliest preneoplastic alterations, whereas mixed-cell foci (containing both glycogen-storing and basophilic hepatocytes) represent more advanced lesions. Hyperplastic hepatocyte foci composed of cells with small-cell change appear to be the direct precursors of dysplastic nodules (Sugitani *et al.,* 1998), which exhibit a higher probability of undergoing malignant transformation (Terasaki *et al.,* 1998). Numerous studies of preneoplastic alterations in human livers have reported morphologic changes associated with hepatocyte dysplasia and suggested that dysplastic lesions are important in the evolution of HCC (Altmann, 1994). Further, prospective studies have shown that the presence of dysplastic hepatocytes in cirrhotic livers is correlated with increased risk for HCC (Borzio *et al.,* 1995).

Emergence and Progression of Hepatocellular Carcinoma

Development of HCC occurs in or near (and presumably from) dysplastic hepatocytes contained within either small foci or larger nodules (Okuda *et al.,* 2001). Liver cell dysplasia refers to morphologic alterations of hepatocytes, including cellular enlargement with a normal nuclear to cytoplasmic ratio, nuclear pleomorphism with hyperchromasia, and multinucleation (Anthony, 1973; Pollice *et al.,* 1988). Regenerative hepatocyte nodules containing dysplastic cells in cirrhotic livers have been referred to as atypical adenomatous hyperplasia, macroregenerative nodules, or dysplastic nodules (Paradis *et al.,* 1998). Nodular aggregates of hepatocytes in cirrhotic livers range in size from less than 3 mm to greater than 5 cm in diameter, with size primarily reflecting the cause and chronicity of the cirrhotic process (Anthony *et al.,* 1973). Similar nodules (with or without dysplastic hepatocytes) can also occur in noncirrhotic livers that are the affected by chronic hepatitis (Theise *et al.,* 1993). HCC can also occur in the setting of chronic hepatitis in the absence of cirrhosis but is always accompanied by hyperplastic nodules and foci of dysplastic hepatocytes. In Alaskan natives chronically infected with HBV (who are often infected with HBV at young ages) (McMahon *et al.,* 1985), HCC usually occurs in livers affected by chronic inflammation and mild fibrosis but lacking frank cirrhosis (McMahon *et al.,* 1990). Furthermore, dysplastic hepatocytes can also develop as a focal lesion that is not contained in a regenerative hepatocyte nodule (Sugitani *et al.,* 1998).

Etiology of Hepatocellular Carcinoma in Humans

The etiology of human HCC is clearly multifactorial (Hassan *et al.,* 2002). Numerous causative factors have been identified that are suggested to contribute to the development of HCC in humans, including exposure to naturally occurring carcinogens, industrial chemicals, pharmacologic agents, and various pollutants (Grisham, 1997). Furthermore, viral infection, genetic disease, and lifestyle factors (e.g., alcohol consumption) contribute to

the risk for development of HCC (Grisham, 1997). The major human hepatocarcinogens that have been identified are the hepatotropic viruses HBV and HCV (IARC, 1994c). Another major hepatocarcinogenic risk for humans is the dietary consumption of aflatoxins in food grains contaminated with *Aspergillus flavus* and related fungi (IARC, 1994a). Consumption of alcoholic beverages (ethanol exposure) poses a carcinogenic risk to humans, with liver as the major target organ (IARC, 1988). In addition, several chemicals, complex chemical mixtures, industrial processes, and therapeutic drugs are recognized as potentially hepatocarcinogenic in humans (Vainio and Wilbourn, 1993). Some genetically determined liver disorders are associated with elevated risk for development of HCC (Wang *et al.,* 2002). In common among all of these etiologic factors is the risk for development of chronic hepatitis and cirrhosis.

Hepatitis Viruses

Numerous studies have shown a strong correlation between HBV infection and increased incidence of HCC (Ganem and Prince, 2004). More recently, an association between chronic HCV infection and HCC has been recognized (El-Serag, 2002). Chronic infection with either HBV or HCV results in greatly increased risk for development of HCC in humans (100-fold to 200-fold) compared to individuals who are not infected (IARC, 1994c). These associations led to the suggestion that these viruses might contain transforming oncogenes. However, the evidence suggests that this is not necessarily the case. Rather, the pathologic consequences of infection by HBV and/or HCV frequently include development of chronic hepatitis and cirrhosis (Block *et al.,* 2003), and these pathologic states are the settings in which HCC occurs most often in humans (Bailey and Brunt, 2002). Thus, infection by HBV and/or HCV may contribute to the risk of development of HCC by setting up a predisposing condition in the chronically injured liver.

Aflatoxins

The most well-studied hepatocarcinogen is a natural chemical carcinogen known as aflatoxin B_1, which is produced by the *Aspergillus flavus* mold (IARC, 1994a, 1994b). This mold grows on rice or other grains (including corn) that are stored without refrigeration in hot and humid parts of the world. Ingestion of food that is contaminated with *Aspergillus flavus* mold results in exposure to potentially high levels of aflatoxin B_1 (Grisham, 1995). Aflatoxins are toxic to the liver in humans and numerous animal species (Wild and Turner, 2002; Zimmerman, 1999). The effects of these compounds are dose-related and demonstrate some dependency on age and sex. Aflatoxin B_1 is a potent, direct-acting liver carcinogen in humans, and chronic exposure leads inevitably to development of HCC (IARC, 1994b).

Methods for accurately measuring human exposures to aflatoxins have been difficult to develop. Nonetheless, epidemiologic evidence suggests that rates of HCC are highest in populations that are exposed to the greatest levels of aflatoxin (Munoz and Bosch, 1987). Aflatoxin-DNA adducts have been exploited as a molecular biomarker of aflatoxin exposure (Groopman *et al.,* 1994). Using this biomarker in a prospective study of 18,000 men in Shanghai, a significant increase in risk for development of HCC was noted in individuals who demonstrated urinary excretion of aflatoxin–DNA adducts (Qian *et al.,* 1994; Ross *et al.,* 1992). The acute and chronic effects of aflatoxin exposure have not been well documented in humans, but in animal studies these exposures resulted in hepatocyte necrosis and steatohepatitis with acute exposure and fibrosis and cirrhosis with chronic exposure (Munoz and Bosch, 1987).

Ethanol Consumption and Smoking

Chronic alcohol (ethanol) consumption is associated with an elevated risk for HCC (Nalpas *et al.,* 1995). However, alcohol is not directly carcinogenic to the liver (IARC, 1988); rather, it is thought that the chronic liver damage produced by sustained alcohol consumption (hepatitis and cirrhosis) may contribute secondarily to liver tumor formation (Lieber, 1990; Simonetti *et al.,* 1992). In fact, >80% of hepatocellular carcinoma in alcoholics occurs in cirrhotic livers (Nalpas, 1994). Furthermore, ethanol appears to potentiate the hepatocarcinogenicity of chronic HBV and chronic HCV infection (Nalpas *et al.,* 1995). Other lifestyle factors may also contribute to risk for development of HCC, including tobacco smoking (Doll, 1996). However, some epidemiologic studies find no association between cigarette smoking and risk for development of HCC (Tanaka *et al.,* 1992).

Hepatotoxic Drugs and Chemicals

Several chemicals, complex chemical mixtures, industrial processes, and/or therapeutic agents have been associated with development of HCC in exposed human populations (Grisham, 1997). These include therapeutic exposure to the radioactive compound thorium dioxide (Thoratrast) for the radiologic imaging of blood vessels (Andersson *et al.,* 1994) and exposures to high levels of certain industrial chemicals, such as vinyl chloride monomer (Du and Wang, 1998), in the workplace. Furthermore, specific occupations are

associated with slightly elevated risk for HCC, including asphalt workers and farmers exposed to pesticides (Austin *et al.,* 1987). Pharmacologic exposure to anabolic steroids and estrogens can lead to development of liver cancer (Vainio and Wilbourn, 1993). Other agents are occasionally associated with development of HCC in humans, including ingestion of inorganic arsenic compounds (Chen *et al.,* 1992).

Genetic Diseases of the Liver

Several genetic diseases that result in liver pathology can increase the risk of development of HCC (Grisham, 1997). These genetic conditions include hemochromatosis (Deugnier and Turlin, 2001), hereditary tyrosinemia (Russo *et al.,* 2001), glycogen storage diseases (Bianchi, 1993), Wilson's disease (Wilkinson *et al.,* 1983), α1-antitrypsin deficiency (Propst *et al.,* 1994), and others (Grisham, 1997). Most of these genetic liver diseases are related to inborn errors of metabolism that result in the accumulation of metabolic products in hepatocytes (Hadchouel, 1994). Liver damage resulting from this abnormal accumulation of metabolic products leads to chronic hepatitis and cirrhosis. Hereditary predisposition to HCC (in the absence of genetic liver disease) has been suggested based on the observation of tumor clusters in families (Alberts *et al.,* 1991). However, such familial clustering of HCC could reflect common exposures of family members to environmental risks factors such as HBV infection or aflatoxin exposure (Grisham, 1997).

Cellular Pathogenesis of Hepatocellular Carcinoma

Development of HCC is typically in the pathologic setting of chronic hepatitis or cirrhosis. As such, chronic hepatitis and cirrhosis represent significant preneoplastic conditions of the liver. A number of cellular alterations characterize the hepatocytes of the regenerative nodules that are found in these livers. These changes, including increased cellular proliferation and development of monoclonal cell populations, have been documented in preneoplastic liver, and they persist in HCC (Grisham, 2002).

Development of Monoclonal Hepatocyte Populations in Preneoplastic and Neoplastic Liver

A monoclonal cell population is defined as one that develops through multiple cycles of cell proliferation from a single progenitor cell. The importance of monoclonality in carcinogenesis relates to the accumulation of genetic changes in an emerging population of cells. Genetic alterations affecting the original progenitor cell will be passed to its progeny, and development of additional genetic alterations can result in the outgrowth of new clonal subpopulations. The clonality of regenerative hepatocyte nodules in cirrhotic livers has been addressed in several studies using various molecular techniques (Grisham, 2002). Of the methods used, analysis of the chromosomal integration of HBV deoxyribonucleic acid (DNA) into the genomic DNA of infected hepatocytes appears to be the most sensitive and specific but depends on integration of the viral genome. In the livers of patients chronically infected with HBV, the integration of viral DNA in nonneoplastic hepatocytes suggests clonal expansion in regenerative hepatocyte nodules (Tanaka *et al.,* 1988). Furthermore, molecular analysis of regenerative hepatocyte nodules in HBV-related cirrhosis determined that subsets (6–31%) of these nodules are monoclonal (Yasui *et al.,* 1992). Likewise, using molecular techniques, a significant fraction (43%) of hepatocyte nodules in HCV-related cirrhosis has been shown to be monoclonal (Aihara *et al.,* 1994). The monoclonality of hepatocyte nodules in the preneoplastic liver extends from regenerative hepatocyte nodules to more progressive lesions, including dysplastic nodules. Dysplastic hepatocytes in HBV-infected livers have been shown to be monoclonal using various molecular techniques (Aihara *et al.,* 1996). These observations demonstrate that monoclonal populations of hepatocytes (often phenotypically altered or dysplastic) occur in preneoplastic liver before the involved hepatocytes display characteristics of neoplastic transformation. Repetitive clonal proliferation from one progenitor (parent) cell facilitates the accumulation of genetic alterations in a large population of progeny cells (Grisham, 2002).

Monoclonal populations of hepatocytes (regenerative and/or dysplastic) have been shown in preneoplastic livers (chronic hepatitis and cirrhosis). In a few studies, neoplastic lesions have been shown to reflect clonal outgrowths from a monoclonal population of nonneoplastic hepatocytes. Identical HBV DNA integration patterns were observed between HCC and adjacent nontumorous liver in one study (Shafritz *et al.,* 1981). Similarly, the HBV integration pattern of hepatocytes contained in a dysplastic nodule was shown to be identical to that of a small HCC arising within the dysplastic nodule (Tsuda *et al.,* 1988). These observations suggest that monoclonal hepatocyte populations represent preneoplastic lesions with potential to undergo neoplastic transformation to give rise to HCC and that dysplastic lesions may represent the direct precursor for HCC.

A number of studies have evaluated the monoclonality of HCC. Nearly all (105/109, 95%) small HCCs examined (using HBV integration or other molecular techniques) have been shown to be monoclonal (Yamamoto *et al.,* 1999). However, with increasing size of the HCC resulting from continued cell proliferation, new genetically distinct subpopulations of tumor cells emerge. The clonal divergence that accompanies increasing size of HCC has been demonstrated through DNA fingerprint analysis (Sirivatanauksorn *et al.,* 1999a, 1999b). HCCs less than 6 mm in diameter (mean = 4.7 mm) were found to be monoclonal, whereas HCCs greater than 6 mm in diameter (mean = 15.4 mm) were composed of multiple genetically divergent cell populations (clones) (Sirivatanauksorn *et al.,* 1999a).

Increased Hepatocyte Proliferation in Preneoplastic and Neoplastic Liver

In the normal liver, the rates of cell proliferation and cell death are negligible and in near balance, reflecting the facts that hepatocytes are long lived and that there is very little cellular turnover in the adult. However, cell death and cell proliferation are both significantly increased in chronic hepatitis and cirrhosis (Shimizu *et al.,* 1988). In the normal liver, less than 0.5% of hepatocytes are proliferative as evidenced by bromodeoxyuridine (BrdU) labeling index (Tarao *et al.,* 1990), whereas regenerative hepatocytes in cirrhotic livers exhibit BrdU labeling indices that are more than 8-fold that of normal liver (Tarao *et al.,* 1993). The increased cell proliferation that occurs in pathologic livers reflects increases in the proliferation of regenerative hepatocytes as well as foci of phenotypically altered hepatocytes (Su *et al.,* 1997).

In nodular lesions that also contained dysplastic hepatocytes, further increases in cell proliferation were noted (Su *et al.,* 1997). Corresponding increases in cell density accompany the increased rates of cell proliferation in preneoplastic liver lesions (Le Bail *et al.,* 1995). High rates of hepatocyte proliferation correlate with increased risk for HCC (Borzio *et al.,* 1998; Tarao *et al.,* 1994). In preneoplastic liver (involving chronic hepatitis or cirrhosis), greatly increased rates of hepatocyte proliferation are accompanied by increased rates of cell death (apoptosis) (Tannapfel *et al.,* 1999). However, rates of proliferation always exceed rates of apoptosis, resulting in expansion of aberrant cell populations (Grisham, 2002; Schulte-Hermann *et al.,* 1998; Thorgeirsson *et al.,* 1998).

Compared to normal liver and to preneoplastic liver lesions, HCC demonstrates high rates of cellular proliferation. BrdU labeling indices of HCC have been shown to be 28-fold higher than for normal livers (Tarao *et al.,* 1989). However, HCCs do not exhibit uniformly high rates of cell proliferation. Rather, there appears to be an inverse correlation between cell proliferation rate and the histologic differentiation of the tumor (Sugitani *et al.,* 1998). Well-differentiated tumors exhibit BrdU labeling indices that are 18-fold higher than those of normal livers and 2.5-fold higher than those of cirrhotic livers (Tarao *et al.,* 1993). Moderately differentiated HCCs display BrdU labeling indices that are 24-fold higher than those of normal livers and 3-fold higher than those of cirrhotic livers. In contrast, poorly differentiated HCC exhibit BrdU labeling indices that are 42-fold higher than those of normal livers and 5-fold higher than those of cirrhotic livers (Tarao *et al.,* 1993). Increasing tumor grade has also been shown to be associated with higher rates of cellular proliferation in HCC (Hino *et al.,* 1996; Kubo *et al.,* 1998). Furthermore, several studies suggest that larger (more advanced) tumors have dramatically increased rates of cellular proliferation compared with early tumors (Tiniakos and Brunt, 1999).

Mechanisms Governing Increased Hepatocyte Proliferation in Preneoplastic and Neoplastic Liver

Usually HCC develops in the pathologic liver (involving either chronic hepatitis or cirrhosis), in which hepatocytes proliferate continuously and at higher rates than in nondiseased liver. The proliferative tissue microenvironment of the preneoplastic liver is characterized by elevated expression of several mitogenic factors for hepatocytes, including growth factors and their receptors, proinflammatory cytokines, and hormones. A comprehensive review of these mitogenic signaling molecules in HCC has recently appeared (Grisham, 2002).

The major growth factors in HCC include transforming growth factor α (TGFα), insulin-like growth factor-2 (IGF-2), and hepatocyte growth factor (HGF) (Grisham, 2002). Normal hepatocytes do not express TGFα, but TGFα is expressed by hepatocytes in chronic hepatitis and cirrhosis (Castilla *et al.,* 1991), with the greatest expression in nodular lesions containing dysplastic hepatocytes (Morimitsu *et al.,* 1995; Park *et al.,* 1995). TGFα expression is immunohistochemically detectable in a significant fraction of HCCs (Kiss *et al.,* 1997; Nalesnik *et al.,* 1998), and expression levels do not correlate with tumor differentiation (Morimitsu *et al.,* 1995).

The cognate receptor for TGFα is the epidermal growth factor receptor (EGFR), which is expressed at similar levels in HCC and hepatocytes of nontumorous

liver (Kiss *et al.,* 1997). Furthermore, coordinate expression of EGFR and TGFα in HCC has been shown (Yamaguchi *et al.,* 1995), suggesting the establishment of an autocrine mechanisms for self-sustaining cellular growth stimulation (Grisham, 2002). The concentration of IGF-2 increases significantly in cirrhotic livers (>threefold) and HCC (>ninefold) compared to normal livers (Cariani *et al.,* 1990). Similarly, immunohistochemical staining of pathologic livers has identified overexpression of IGF-2 in chronic hepatitis, cirrhosis, and HCC (Sohda *et al.,* 1997a).

The IGF-2 protein generally co-localizes with proliferative cells of HCC (Sohda *et al.,* 1997b), suggesting a correlation between autocrine expression of IGF-2 and cellular proliferation in those tumors (Grisham, 2002). IGF-2 signaling is mediated by the IGF-1 receptor and the insulin receptor. Both of these receptors are ubiquitously expressed in normal cells and tissues, but no studies have been reported that describe their expression in HCC (Grisham, 2002). Hepatocyte growth factor is not expressed by normal hepatocytes (Ljubimova *et al.,* 1997; Okano *et al.,* 1999) but is expressed by the neoplastic hepatocytes of many HCCs (Okano *et al.,* 1999). However, the elevated levels of HGF in neoplastic hepatocytes of HCC is thought to reflect uptake and accumulation of the growth factor (Kiss *et al.,* 1997), rather than autocrine synthesis (Noguchi *et al.,* 1996). The HGF receptor c-met is expressed by normal hepatocytes and the neoplastic cells of HCC (Chen *et al.,* 1997; Kiss *et al.,* 1997). Elevated c-met expression has been correlated with both increased cell proliferation in HCC (D'Errico *et al.,* 1996) and with poorer differentiation of tumors in some studies (Boix *et al.,* 1994). Expression or overexpression of c-met in neoplastic hepatocytes in the presence of HGF (autocrine or paracrine) might drive tumor cell proliferation as a result of increased mitogenic stimulation. In the case of each of these major growth factor/receptor pathways (TGFα/EGFR, IGF-2/IGFIR, HGF/c-met) in HCC, the cognate receptors are expressed (or thought to be) by the neoplastic hepatocytes, and the growth factor is produced in autocrine fashion or is available through paracrine signaling pathways.

The inflammatory cells that infiltrate the liver in chronic hepatitis and cirrhosis represent a rich source for production of proinflammatory cytokines (Simpson *et al.,* 1997). In addition, the expression of certain cytokines and cytokine receptors can be induced in cells of the liver, including hepatocytes (Simpson *et al.,* 1997). Cytokines exert various effects in the liver, including mediating inflammation and immune responses (Andus *et al.,* 1991). In addition, specific cytokines are required for activation of hepatocyte proliferation, especially TNFα and interleukin 6 (IL6) (Taub, 1999; Webber, 1999). It has been suggested that these cytokines may play a role in the regulation of cellular proliferation leading to and following the development of HCC (Grisham, 2002). However, the significance and specific role of these cytokines in human hepatocarcinogenesis has not yet been elucidated.

Molecular Pathogenesis of Hepatocellular Carcinoma

The molecular mechanisms that govern neoplastic transformation of hepatocytes leading to HCC have been extensively studied in humans (Grisham, 2002; Llovet *et al.,* 2003; Nishida *et al.,* 2003) and rodent models (Grisham, 1997; Sell, 2003). The major molecular features of HCC include aneuploidy and chromosomal aberrations, activation of positive mediators of cellular proliferation (including classic cellular protooncogenes), and inactivation of negative mediators of cellular proliferation (including classic tumor-suppressor genes). Both genetic and epigenetic mechanisms play significant roles in the molecular pathogenesis of HCC. The molecular mechanisms of hepatocarcinogenesis have been comprehensively reviewed (Grisham, 2002; Suriawinata and Xu, 2004; Thorgeirsson and Grisham, 2002).

Genomic Alterations in Hepatocellular Carcinoma

The genomic alterations documented in human HCC include aberrations in chromosome structure, aneuploidy and abnormal chromosome numbers, allelic losses, and microsatellite instability. Approximately 40% of HCCs exhibit an aneuploid DNA content and numeric chromosomal abnormalities (Mise *et al.,* 1998). Aneuploidy has also been documented in dysplastic lesions (Terris *et al.,* 1997), suggesting that the genetic abnormalities may represent a significant determinant of neoplastic transformation in the liver. Further, aneuploidy has been shown in some studies to increase with decreasing differentiation of HCC, suggesting that continued genomic instability accompanies tumor progression (Mise *et al.,* 1998). Karyotype analysis has been performed on a limited number of HCCs using cells taken directly from the neoplasm and cultured for short periods (Bardi *et al.,* 1998; Parada *et al.,* 1998). Most HCC-derived cells were aneuploid with increased numbers of chromosomes and contained numerous structurally altered abnormal chromosomes as well. Approximately half of the HCCs examined contained a subtetraploid

chromosome number (64–99 chromosomes per cell), whereas the remainder were near diploid. Among these studies of HCC, structural alteration of chromosome 1 was most frequently reported (Parada *et al.,* 1998). Chromosomal regions most frequently involved in structural rearrangements included 1p11, 1p22, 1p32, 1p34, 1p36, 1q10, 1ql2, 1q25, 6q13-q15, 6q22-q25, 8q10, 16q24, and 17p11 (Grisham, 2002).

Comparative genomic hybridization has been used in a number of studies to examine gains and losses of chromosome arms in HCC (Balsara *et al.,* 2001; Chang *et al.,* 2002). Chromosomal gains have been described in HCC involving 1p, 4q, 5p, 6q, 8p, 9p, 10q, 11q, 12q, 16q, 17p, and 19p. In some cases, significant gains were observed, suggestive of gene amplification. Chromosomal losses involving 1q, 6p, 8q, 11q, 17q, and 20q also occur in HCC. Some studies have addressed the possibility that specific genetic aberrations occur in HCC related to a specific etiologic agent. In one study, chromosomes 4q, 8p, and 16q were affected in HBV-related HCC, whereas 11q was affected in HCV-related HCC (Wong *et al.,* 2000a), suggesting that specific genetic abnormalities can be attributed to specific etiologic agents or mechanisms. However, other investigators conclude that no such association exists (Tornillo *et al.,* 2000). Furthermore, it appears that the most commonly affected chromosome across all studies is 1q, which is affected in HCC of all etiologies at high frequency (Grisham, 2002).

More recent studies have used spectral karyotyping to examine chromosomal rearrangements in primary HCC and derived cell lines (Pang *et al.,* 2000; Wong *et al.,* 2000b). These analyses identified aberrant chromosomes involving 1p13-q21, 8p12-q21, 17p11-q12, 17q22, and 19p10-q13.1 (Wong *et al.,* 2000b). These studies also noted that HCC of larger size (more advanced) contained increasing numbers of chromosomal abnormalities, suggesting continued genomic evolution as tumors progress. Spectral karyotyping also identified novel chromosomal breakpoints involving numerous pericentromeric chromosomal regions (Wong *et al.,* 2000b). These breakpoints could be important for large-scale chromosomal deletions (involving chromosome arms) that are recognized through allelotyping studies.

The development of HCC involves numerous chromosomal alterations (Thorgeirsson and Grisham, 2002). Comprehensive allelotyping of HCC has been performed by several groups of investigators using large numbers of polymorphic microsatellite markers spanning the entire genome with an average spacing of markers of ~20 cM (Grisham, 2002). Additional allelotyping studies have appeared, but many examined only a few chromosomal arms or used very few markers per chromosomal arm. When the most comprehensive of these studies are considered, there is very good agreement on the fraction of allelic loss in HCC and the identification of specific chromosomal arms that demonstrate significant allelic losses during hepatocarcinogenesis and tumor progression. The mean fractional allelic loss per HCC was 13–24%, and ranged from 0–43% (Grisham, 2002). Recurring allelic losses affecting more than 30% of all HCCs examined have been documented on a number of chromosome arms, including 1p, 1q, 4q, 5q, 6q, 8p, 8q, 9p, 13q, 14q, 16p, 16q, and 17p, but the frequency of loss of heterozygosity (LOH) involving loci on these chromosome arms is rarely more than 60% (Grisham, 2002; Thorgeirsson and Grisham, 2002). Nonetheless, allelic imbalance of 60–85% involving 4q, 8p, 9p, and 16q has been identified in some studies (Coleman, 2003).

In theory, the chromosomal regions affected by deletion (LOH) may harbor genes with tumor-suppressor activity. In fact, several well-known tumor-suppressor genes reside on chromosome arms that are frequently affected by regional chromosomal deletions, such as *p53* at 17p and *Rb1* at 13q (Boige *et al.,* 1997; Nagai *et al.,* 1997; Piao *et al.,* 1998). These observations suggest that chromosomal losses can be exploited to infer the location of important tumor-suppressor genes that are subject to inactivation through this mechanism. Furthermore, the diversity of chromosomal aberrations supports the suggestion that multiple genes and molecular pathways contribute to the development of HCC. Studies of gene expression in HCC support this suggestion (Shirota *et al.,* 2001).

Microsatellite instability is a specific form of genomic instability that is characterized by mutational alteration of simple repetitive sequences, including both expansions (insertional mutagenesis) and contractions (deletional mutagenesis), usually resulting in frameshift mutations (Coleman and Tsongalis, 2002). The molecular defects responsible for microsatellite instability in human tumors involve the genes that encode the proteins required for normal mismatch repair (Peltomaki, 2003). A limited number of studies have examined microsatellite instability in HCC. When all studies are combined, 25/218 (11%) HCCs demonstrated microsatellite alterations involving at least one locus (Coleman, 2003). However, with application of more stringent criteria (microsatellite alterations involving at least two loci), 25/88 (28%) of hepatocellular carcinomas exhibit microsatellite instability (Coleman, 2003). Microsatellite instability involving a small number of loci was noted in two comprehensive allelotyping studies of a large number of HCCs (Boige *et al.,* 1997; Sheu *et al.,* 1999). More recent studies have suggested that microsatellite

instability affects only ~7% of loci investigated (Kawai *et al.,* 2000). Other studies have failed to identify microsatellite instability in HCC (Kawate *et al.,* 1999b; Piao *et al.,* 2000; Rashid *et al.,* 1999; Wang *et al.,* 2001).

Comprehensive studies of the mutation status of mismatch repair genes have not been performed for HCC. However, there is evidence that mismatch repair genes (including *hMSH2* and *hMLH1*) are affected by loss of heterozygosity in HCC that exhibits microsatellite instability (Macdonald *et al.,* 1998). In addition, *hMSH2* has been shown to be mutated in some HCCs that display microsatellite instability (Yano *et al.,* 1999). These studies suggest that microsatellite instability may be mechanistically involved with the molecular pathogenesis of a subset of HCC. In fact, in some cases microsatellite instability may precede the development of HCC, as has been documented in preneoplastic cirrhotic livers (Tsopanomichalou *et al.,* 1999) and in nontumorous liver adjacent to HCC (Salvucci *et al.,* 1999). Microsatellite instability could contribute to the pathogenesis of HCC through the inactivation of critical genes for growth control, regulation of apoptosis, or some other pathway (Coleman and Tsongalis, 2002). In support of this suggestion, microsatellite alterations involving the *TGFβRII, M6P/IGFIIR,* and *BAX* genes have been documented in one case study of HCC (Yakushiji *et al.,* 1999).

Cellular Protooncogenes and Hepatocarcinogenesis

The setting for HCC is the hyperproliferative liver associated with chronic hepatitis and cirrhosis. The repetitive proliferation of regenerative hepatocytes (and progressive lesions) is promoted by the presence of numerous mitogenic growth factors and cytokines. However, neoplastic transformation of hepatocytes is accompanied by perturbation of the numerous intracellular signaling pathways leading to the acquisition of autonomous and unregulated cellular proliferation. These signaling pathways involve a number of positive mediators of cellular proliferation, including the protein products of the c-*ras* gene family, c-*myc,* c-*fos,* various cyclins and cyclin-dependent kinases, and others (Grisham, 2002).

Microarray-based studies of HCC and preneoplastic livers have resulted in the development of molecular signatures for this tumor and have potentially identified useful markers for disease initiation or progression (Kim *et al.,* 2004; Smith *et al.,* 2003). A comprehensive review of all these positive mediators of hepatocellular growth is beyond the scope of this review. Rather, the contributions of several cellular protooncogene products to hepatocarcinogenesis is considered, including the c-*ras* family, c-myc, and cyclin D1.

The expression of p21 ras is up-regulated in HCC (Radosevich *et al.,* 1993; Tang *et al.,* 1998; Tiniakos *et al.,* 1993) and in preneoplastic livers (chronic hepatitis and cirrhosis), especially dysplastic hepatocytes (Nonomura *et al.,* 1987) and HBV-infected cells (Tiniakos *et al.,* 1989). Increased levels of expression of c-H-*ras* and c-K-*ras* have been documented in HCC, as well as some preneoplastic liver lesions (Tang *et al.,* 1998). Similarly, some studies have shown c-N-*ras* to be overexpressed in HCC (Gu *et al.,* 1986; Zhang *et al.,* 1987). However, other studies failed to detect overexpression of c-H-*ras* or c-K-*ras* in HCC (Himeno *et al.,* 1988). These findings may suggest that overexpression of a single member of the c-*ras* family is necessary for hepatocarcinogenesis, irrespective of which member of the family is up-regulated. Overexpression of c-*ras* family members may reflect amplification of the corresponding gene (Gu *et al.,* 1986; Zhang *et al.,* 1987). Very few point mutations in the c-*ras* genes have been documented in HCC (Leon and Kew, 1995), suggesting that mutational activation of c-*ras* does not play a significant role in hepatocarcinogenesis. Nonetheless, the overexpression of p21 ras protein in nearly all HCCs examined (Tang *et al.,* 1998) suggests that the ras mitogen-activated protein kinase (MAPK) pathway is hyperactive in these neoplasms (Grisham, 2002).

The nuclear transcription factor c-myc is overexpressed in ~50% of HCCs (Gan *et al.,* 1993; Saegusa *et al.,* 1993), and the c-*myc* messenger ribonucleic acid (mRNA) is overexpressed in more than 90% of HCCs (Zhang *et al.,* 1990). In some studies, the level of c-myc protein overexpression was 15-fold that of adjacent nontumorous liver (Arbuthnot *et al.,* 1991). The level of expression of c-myc protein is also increased in chronic hepatitis (Tiniakos *et al.,* 1993) and cirrhosis (Gan *et al.,* 1993; Tiniakos *et al.,* 1989). Increased levels of expression of c-myc in HCC (and preneoplastic liver) may in part be a result of up-regulation of the MAPK pathway in hyperproliferative liver (Grisham, 2002). However, c-*myc* gene amplification and hypomethylation also contribute significantly to the overexpression of c-*myc* in HCC. The c-*myc* gene was found to be hypomethylated in 55% (15/27) of HCCs examined (Kaneko *et al.,* 1985; Nambu *et al.,* 1987). In addition, hypomethylation of c-myc was detected in a significant percentage of cirrhotic livers adjacent to HCC (Kaneko *et al.,* 1985; Nambu *et al.,* 1987), suggesting that hypomethylation of c-*myc* may reflect an early alteration leading to c-*myc* dysregulation in hepatocarcinogenesis. The c-*myc* gene was amplified in 31% (50/163) of HCCs evaluated (Kawate *et al.,* 1999a). However, c-*myc* gene

amplification was not detected in preneoplastic lesions associated with HCC (Lee *et al.,* 1988).

The cyclins and cyclin-dependent kinases regulate the transit of cells through the cell cycle. Overexpression of these proteins can lead to unregulated cell cycle progression and uncontrolled cellular proliferation. Cyclin D1 protein is overexpressed in a significant fraction (~40%) of HCCs (Ito *et al.,* 1999). The overexpression of cyclin D1 is related to amplification of the *cyclin D1* gene and overexpression of its mRNA in some cases (Ito *et al.,* 1998).

Tumor-Suppressor Genes and Hepatocarcinogenesis

A number of tumor-suppressor genes and other negative mediators of cellular proliferation have been implicated in the molecular pathogenesis of HCC (Elmore and Harris, 1998). These tumor suppressor genes and tumor-suppressor–like genes include *p*53, retinoblastoma 1 (*Rb1), p73*, *mdm2,* adenomatous polyposis coli *(APC), β-catenin, E-cadherin,* phosphatase and tensin homolog deleted on chromosome ten *(PTEN), BRCA1,* fragile histidine triad *(FHIT),* and several others (Buendia, 2000; Grisham, 2002). A comprehensive review of all of these genes is beyond the scope of this chapter. Therefore, in the following sections the contributions of *p53* and *Rb1* to hepatocarcinogenesis is reviewed.

The *p53* tumor-suppressor gene product is a multifunctional protein that is involved with numerous cellular processes, including cell cycle control, genomic stability and DNA repair, and apoptosis (Harris, 1996; Ko and Prives, 1996). The p53 protein is functionally inactivated in the majority of human cancers through one of several genetic or epigenetic processes, including mutation, allelic deletion, or interaction with inactivating proteins (Harris, 1996; Hollstein *et al.,* 1991). In HCC, *p53* is frequently the target of chromosomal deletion (LOH) involving 17p. A review of a large number of studies showed LOH at the *p53* gene in ~41% of HCCs examined (Grisham, 2002). A few studies have suggested that deletion of the *p53* gene occurs early in hepatocarcinogenesis as evidenced by loss of heterozygosity of the *p53* gene in nodular lesions of chronic hepatitis and cirrhosis (Tsopanomichalou *et al.,* 1999).

The frequency of *p53* deletion was found to increase with increasing size of HCC, suggesting that loss of this gene is associated with tumor progression (Hsu *et al.,* 1994). Similarly, loss of heterozygosity of the *p53* gene is associated with higher tumor grade in HCC (Tanaka *et al.,* 1993). Mutation of the *p53* gene occurs in conjunction with loss of heterozygosity of the *p53* locus in HCC, with most of the mutations following within the highly conserved region of the gene that includes exons 5–9 (Hainaut *et al.,* 1998). A summary of numerous studies of *p53* mutation in HCC suggests that mutations occur in ~27% (547/2029) of these tumors (Grisham, 2002). However, the *p53* mutation frequency and mutational spectrum varies greatly in affected populations from various world regions (Buendia, 2000; Szymanska and Hainaut, 2003), possibly reflecting specific exposures and risk factors.

Point mutation of codon 249 of the *p53* gene represents a hotspot for gene mutation in the liver, accounting for ~30% of *p53* mutations in HCC (Grisham, 2002). This mutation, which results in a G to T transversion (AGG to AGT, arginine to serine), was first recognized in patients from Qidong, China (Hsu *et al.,* 1991) but has also been recognized in HCCs from Africa and North America (Bressac *et al.,* 1991; Ozturk, 1991; Soini *et al.,* 1996). The *p53* codon 249 mutation has been attributed to exposure to aflatoxin B_1 (Puisieux *et al.,* 1991). The mutational spectrum of the *p*53 gene in HCC differs significantly between geographic areas with high aflatoxin exposure and those with low exposures (Oda *et al.,* 1992). Mutation of the *p53* gene can result in overexpression of the protein product (through stabilization of the protein) or lack of expression of the protein, depending on the nature of the mutation. Similarly, stabilization of the p53 protein can be effected through interaction with p53-binding proteins. The p53 protein is known to complex with the HBV X antigen (Feitelson, 1998), which can increase levels of the protein in cells while inactivating it.

Inappropriate overexpression of mdm2 could also result in the sequestration and functional inactivation of p53 protein, although studies to show this directly in HCC are lacking (Grisham, 2002). Overexpression of p53 protein has been described in HCC, as well as preneoplastic liver lesions, including dysplastic hepatocytes and regenerative hepatocyte nodules in cirrhotic liver (Zhao *et al.,* 1994). In some studies, overexpression of p53 protein was noted in a higher percentage of more advanced HCCs (Qin *et al.,* 1997), suggesting that p53 abnormalities may be associated with tumor progression.

Like *p*53, the *Rb1* gene product is a multifunctional protein that plays a central role in cell cycle control (Smolinski, 2002). The *Rb1* gene is deleted in a significant percentage of HCCs (~30–40%) (Coleman, 2003). In individual studies, the frequency of LOH at the *Rb1* locus was as high as 73% (Ashida *et al.,* 1997). In some studies, investigators examined LOH at the *Rb1* locus using specific probes that flank this gene, producing evidence suggesting that deletion of the *Rb1* gene is a frequent event in HCC (Kuroki *et al.,* 1995; Zhang *et al.,* 1994). Deletion of *Rb1* (LOH)

usually is accompanied by loss of expression of pRb (Zhang *et al.,* 1994). Deletion of *Rb1* has also been documented in nonneoplastic cirrhotic liver adjacent to HCC lacking this gene (Ashida *et al.,* 1997). In contrast, cirrhotic nodules adjacent to HCCs that exhibit no loss of *Rb1* also retain both *Rb1* alleles (Ashida *et al.,* 1997). These observations suggest that deletion of *Rb1* is an early event in hepatocarcinogenesis, occurring in preneoplastic cirrhotic livers. However, others have shown that HCCs that show loss of heterozygosity for *Rb1* can be closely associated with preneoplastic cirrhotic nodules that retain both *Rb1* alleles (Kuroki *et al.,* 1995). This study, as well as others (Murakami *et al.,* 1991; Zhang *et al.,* 1994), suggests that deletion of *Rb1* may be a late genetic alteration in HCC, associated with tumor progression.

CONCLUSIONS AND PERSPECTIVE

The major risk factors and etiologic agents responsible for development of HCC in humans have been identified, characterized, and described, including chronic infection with HBV or HCV, exposure to aflatoxin B_1, and cirrhosis of any etiology (including alcoholic cirrhosis and cirrhosis associated with genetic liver diseases). Both chronic hepatitis and cirrhosis represent major preneoplastic conditions of the liver because the majority of HCCs arise in these pathologic settings. Hepatocarcinogenesis represents a linear and progressive, albeit slow, process in which successively more aberrant monoclonal populations of hepatocytes evolve. Regenerative hepatocytes in focal lesions in the inflamed liver (chronic hepatitis or cirrhosis) give rise to hyperplastic hepatocyte nodules, and these progress to dysplastic nodules, which are thought to be the direct precursor of HCC. In most cases, the neoplastic transformation of hepatocytes results from accumulation of genetic damage during the repetitive cellular proliferation that occurs in the injured liver in response to paracrine growth factor and cytokine stimulation. HCCs exhibit numerous genetic abnormalities, including chromosomal deletions, rearrangements, aneuploidy, gene amplifications, and mutations, as well as epigenetic alterations, including modification of DNA methylation. These genetic and epigenetic alterations together activate positive mediators of cellular proliferation, including protooncogenes and their mitogenic signaling pathways, and inactivate negative mediators of proliferation, including tumor-suppressor and cell-cycle control genes, resulting in cells with autonomous growth potential. However, HCCs exhibit a high degree of genetic heterogeneity, suggesting that multiple molecular pathways may be involved in the genesis of subsets of liver cancers. Nonetheless, comprehensive elucidation of the specific genes and molecular pathways involved in progression from preneoplastic lesions to frank neoplasia in the protracted process of hepatocarcinogenesis will facilitate development of new strategies for prevention and therapy. Identification of molecular pathways that drive the proliferation of neoplastic hepatocytes may enable development of drugs that can specifically target and kill those cells. Alternatively, chemopreventive agents may be developed that will impede the malignant conversion of dysplastic hepatocytes, impeding development of HCC in high-risk patients. Until molecular-based therapies of these sorts can be developed, the best hope for significant reductions in the worldwide incidence of HCC will require development of more effective anti-viral treatments or implementation of improved (more effective) strategies for preventing HBV and HCV infection.

References

Aihara, T., Noguchi, S., Sasaki, Y., Nakano, H., and Imaoka, S. 1994. Clonal analysis of regenerative nodules in hepatitis C virus-induced liver cirrhosis. *Gastroenterology 107*:1805–1811.

Aihara, T., Noguchi, S., Sasaki, Y., Nakano, H., Monden, M., and Imaoka, S. 1996. Clonal analysis of precancerous lesion of hepatocellular carcinoma. *Gastroenterology 111*:455–461.

Alberts, S.R., Lanier, A.P., McMahon, B.J., Harpster, A., Bulkow, L.R., Heyward, W.L., and Murray, C. 1991. Clustering of hepatocellular carcinoma in Alaska Native families. *Genet. Epidemiol. 8*:127–139.

Altmann, H.W. 1994. Hepatic neoformations. *Pathol. Res. Pract. 190*:513–577.

Andersson, M., Vyberg, M., Visfeldt, J., Carstensen, B., and Storm, H.H. 1994. Primary liver tumors among Danish patients exposed to Thorotrast. *Radiat. Res. 137*:262–273.

Andus, T., Bauer, J., and Gerok, W. 1991. Effects of cytokines on the liver. *Hepatology 13*:364–375.

Anthony, P.P. 1973. Liver cell dysplasia: A premalignant condition. *J. Pathol. 109*:Pxvii.

Anthony, P.P., Ishak, K.G., Nayak, N.C., Poulsen, H.E., Scheuer, P.J., and Sobin, L.H. 1978. The morphology of cirrhosis. Recommendations on definition, nomenclature, and classification by a working group sponsored by the World Health Organization. *J. Clin. Pathol. 31*:395–414.

Arbuthnot, P., Kew, M., and Fitschen, W. 1991. c-fos and c-myc oncoprotein expression in human hepatocellular carcinomas. *Anticancer Res. 11*:921–924.

Ashida, K., Kishimoto, Y., Nakamoto, K., Wada, K., Shiota, G., Hirooka, Y., Kamisaki, Y., Itoh, T., and Kawasaki, H. 1997. Loss of heterozygosity of the retinoblastoma gene in liver cirrhosis accompanying hepatocellular carcinoma. *J. Cancer Res. Clin. Oncol. 123*:489–495.

Austin, H., Delzell, E., Grufferman, S., Levine, R., Morrison, A.S., Stolley, P.D., and Cole, P. 1987. Case-control study of hepatocellular carcinoma, occupation, and chemical exposures. *J. Occup. Med. 29*:665–669.

Bailey, M.A., and Brunt, E.M. 2002. Hepatocellular carcinoma: Predisposing conditions and precursor lesions. *Gastroenterol. Clin. North Am. 31*:641–662.

Balsara, B.R., Pei, J., De Rienzo, A., Simon, D., Tosolini, A., Lu, Y.Y., Shen, F.M., Fan, X., Lin, W.Y., Buetow, K.H.,

London, W.T., and Testa, J.R. 2001. Human hepatocellular carcinoma is characterized by a highly consistent pattern of genomic imbalances, including frequent loss of 16q23.1-24.1. *Genes Chromosomes Cancer 30*:245–253.

Bannasch, P. 1996. Pathogenesis of hepatocellular carcinoma: Sequential cellular, molecular, and metabolic changes. *Prog. Liver Dis. 14*:161–197.

Bardi, G., Rizou, H., Michailakis, E., Dietrich, C., Pandis, N., and Heim, S. 1998. Cytogenetic findings in three primary hepatocellular carcinomas. *Cancer Genet. Cytogenet. 104*:165–166.

Berman, C. 1951. *Primary Carcinoma of the Liver.* London: Lewis.

Bianchi, L. 1993. Glycogen storage disease I and hepatocellular tumours. *Eur. J. Pediatr. 152 Suppl 1*:S63–70.

Block, T.M., Mehta, A.S., Fimmel, C.J., and Jordan, R. 2003. Molecular viral oncology of hepatocellular carcinoma. *Oncogene 22*:5093–5107.

Boige, V., Laurent-Puig, P., Fouchet, P., Flejou, J.F., Monges, G., Bedossa, P., Bioulac-Sage, P., Capron, F., Schmitz, A., Olschwang, S., and Thomas, G. 1997. Concerted nonsyntenic allelic losses in hyperploid hepatocellular carcinoma as determined by a high-resolution allelotype. *Cancer Res. 57*:1986–1990.

Boix, L., Rosa, J.L., Ventura, F., Castells, A., Bruix, J., Rodes, J., and Bartrons, R. 1994. c-met mRNA overexpression in human hepatocellular carcinoma. *Hepatology 19*:88–91.

Borzio, M., Bruno, S., Roncalli, M., Mels, G.C., Ramella, G., Borzio, F., Leandro, G., Servida, E., and Podda, M. 1995. Liver cell dysplasia is a major risk factor for hepatocellular carcinoma in cirrhosis: A prospective study. *Gastroenterology 108*:812–817.

Borzio, M., Trere, D., Borzio, F., Ferrari, A.R., Bruno, S., Roncalli, M., Colloredo, G., Leandro, G., Oliveri, F., and Derenzini, M. 1998. Hepatocyte proliferation rate is a powerful parameter for predicting hepatocellular carcinoma development in liver cirrhosis. *Mol. Pathol. 51*:96–101.

Bosch, F.X. 1997. Global epidemiology of hepatocellular carcinoma. In: Okuda, K., Tabor, E., (eds.) *Liver Cancer.* New York: Churchill Livingstone, 13–28.

Bressac, B., Kew, M., Wands, J., and Ozturk, M. 1991. Selective G to T mutations of p53 gene in hepatocellular carcinoma from southern Africa. *Nature 350*:429–431.

Bruix, J., Boix, L., Sala, M., and Llovet, J.M. 2004. Focus on hepatocellular carcinoma. *Cancer Cell 5*:215–219.

Buendia, M.A. 2000. Genetics of hepatocellular carcinoma. *Semin. Cancer Biol. 10*:185–200.

Bugianesi, E., Leone, N., Vanni, E., Marchesini, G., Brunello, F., Carucci, P., Musso, A., De Paolis, P., Capussotti, L., Salizzoni, M., and Rizzetto, M. 2002. Expanding the natural history of nonalcoholic steatohepatitis: From cryptogenic cirrhosis to hepatocellular carcinoma. *Gastroenterology 123*:134–140.

Cariani, E., Seurin, D., Lasserre, C., Franco, D., Binoux, M., and Brechot, C. 1990. Expression of insulin-like growth factor II (IGF-II) in human primary liver cancer: mRNA and protein analysis. *J. Hepatol. 11*:226–231.

Carr, B.I., and Van Thiel, D.H. 1990. Hormonal manipulation of human hepatocellular carcinoma. A clinical investigative and therapeutic opportunity. *J. Hepatol. 11*:287–289.

Castilla, A., Prieto, J., and Fausto, N. 1991. Transforming growth factors beta 1 and alpha in chronic liver disease. Effects of interferon alfa therapy. *N. Engl. J. Med. 324*:933–940.

Chang, J., Kim, N.G., Piao, Z., Park, C., Park, K.S., Paik, Y.K., Lee, W.J., Kim, B.R., and Kim, H. 2002. Assessment of chromosomal losses and gains in hepatocellular carcinoma. *Cancer Lett. 182*:193–202.

Chen, C.J., Chen, C.W., Wu, M.M., and Kuo, T.L. 1992. Cancer potential in liver, lung, bladder and kidney due to ingested inorganic arsenic in drinking water. *Br. J. Cancer 66*:888–892.

Chen, Q., Seol, D.W., Carr, B., and Zarnegar, R. 1997. Co-expression and regulation of Met and Ron proto-oncogenes in human hepatocellular carcinoma tissues and cell lines. *Hepatology 26*:59–66.

Coleman, W.B. 2003. Mechanisms of human hepatocarcinogenesis. *Curr. Mol. Med. 3*:573–588.

Coleman, W.B., and Tsongalis, G.J. 2002. The role of genomic instability in the development of human cancer. In: Coleman, W.B., Tsongalis, G.J. (eds). *The Molecular Basis of Human Cancer.* Totowa: Humana Press, 115–142.

Conn, H.O. 1975. Cirrhosis. In: Schiff, L. (ed.). *Diseases of the Liver, Fourth Edition.* Philadelphia: J.B. Lippincott Company, 833–939.

D'Errico, A., Fiorentino, M., Ponzetto, A., Daikuhara, Y., Tsubouchi, H., Brechot, C., Scoazec, J.Y., and Grigioni, W.F. 1996. Liver hepatocyte growth factor does not always correlate with hepatocellular proliferation in human liver lesions: Its specific receptor c-met does. *Hepatology 24*:60–64.

Deuffic, S., Poynard, T., Buffat, L., and Valleron, A.J. 1998. Trends in primary liver cancer. *Lancet 351*:214–215.

Deugnier, Y., and Turlin, B. 2001. Iron and hepatocellular carcinoma. *J. Gastroenterol. Hepatol. 16*:491–494.

Doll, R. 1996. Cancers weakly related to smoking. *Br. Med. Bull. 52*:35–49.

Du, C.L., and Wang, J.D. 1998. Increased morbidity odds ratio of primary liver cancer and cirrhosis of the liver among vinyl chloride monomer workers. *Occup. Environ. Med. 55*:528–532.

Eagon, P.K., Francavilla, A., DiLeo, A., Elm, M.S., Gennari, L., Mazzaferro, V., Colella, G., Van Thiel, D.H., and Strazl, T.E. 1991. Quantitation of estrogen and androgen receptors in hepatocellular carcinoma and adjacent normal human liver. *Dig. Dis. Sci. 36*:1303–1308.

Elmore, L.W., and Harris, C.C. 1998. Hepatocellular carcinoma. In: Vogelstein, B., Kinzler, K.W. (eds.). *The Genetic Basis of Human Cancer.* New York: McGraw-Hill, 681–689.

El-Serag, H.B., Mason, A.C. 1999. Rising incidence of hepatocellular carcinoma in the United States. *N. Engl. J. Med. 340*:745–750.

El-Serag, H.B., Mason, A.C., and Key, C. 2001. Trends in survival of patients with hepatocellular carcinoma between 1977 and 1996 in the United States. *Hepatology 33*:62–65.

El-Serag, H.B. 2002. Hepatocellular carcinoma and hepatitis C in the United States. *Hepatology 36*:S74–83.

Feitelson, M.A. 1998. Hepatitis B x antigen and p53 in the development of hepatocellular carcinoma. *J. Hepatobiliary Pancreat. Surg. 5*:367–374.

Feitelson, M.A., Sun, B., Satiroglu Tufan, N.L., Liu, J., Pan, J., and Lian, Z. 2002. Genetic mechanisms of hepatocarcinogenesis. *Oncogene 21*:2593–2604.

Gan, F.Y., Gesell, M.S., Alousi, M., and Luk, G.D. 1993. Analysis of ODC and c-myc gene expression in hepatocellular carcinoma by in situ hybridization and immunohistochemistry. *J. Histochem. Cytochem. 41*:1185–1196.

Ganem, D., and Prince, A.M. 2004. Hepatitis B virus infection—Natural history and clinical consequences. *N. Engl. J. Med. 350*:1118–1129.

Grisham, J.W. 1995. Liver. In: Craighead, J.E. (ed.). *Pathology of Environmental and Occupational Disease.* St. Louis: Mosby, 491–509.

Grisham, J.W. 1997. Interspecies comparison of liver carcinogenesis: Implications for cancer risk assessment. *Carcinogenesis 18*:59–81.

Grisham, J.W. 2002. Molecular genetic alterations in primary hepatocellular neoplasms: Hepatocellular adenoma, hepatocellular carcinoma, and hepatoblastoma. In: Coleman, W.B., Tsongalis, G.J. (eds.). *The Molecular Basis of Human Cancer.* Totowa: Humana Press, 269–346.

Groopman, J.D., Wogan, G.N., Roebuck, B.D., and Kensler, T.W. 1994. Molecular biomarkers for aflatoxins and their application to human cancer prevention. *Cancer Res. 54*:1907s–1911s.

Gu, J.R., Hu, L.F., Cheng, Y.C., and Wan, D.F. 1986. Oncogenes in human primary hepatic cancer. *J. Cell. Physiol. Suppl. 4*:13–20.

Hadchouel, M. 1994. Metabolic liver diseases and liver carcinoma. In: Brechot, C. (ed.). *Primary Liver Cancer: Etiological and Progression Factors.* Boca Raton: CRC Press, 79–86.

Hainaut, P., Hernandez, T., Robinson, A., Rodriguez-Tome, P., Flores, T., Hollstein, M., Harris, C.C., and Montesano, R. 1998. IARC Database of p53 gene mutations in human tumors and cell lines: Updated compilation, revised formats and new visualisation tools. *Nucleic Acids Res. 26*:205–213.

Harris, C.C. 1996. Structure and function of the p53 tumor suppressor gene: Clues for rational cancer therapeutic strategies. *J. Natl. Cancer Inst. 88*:1442–1455.

Hassan, M.M., Hwang, L.Y., Hatten, C.J., Swaim, M., Li, D., Abbruzzese, J.L., Beasley, P., and Patt, Y.Z. 2002. Risk factors for hepatocellular carcinoma: Synergism of alcohol with viral hepatitis and diabetes mellitus. *Hepatology 36*:1206–1213.

Higginson, J. 1963. The geographical pathology of primary liver cancer. *Cancer Res. 23*:1624–1633.

Himeno, Y., Fukuda, Y., Hatanaka, M., and Imura, H. 1988. Expression of oncogenes in human liver disease. *Liver 8*:208–212.

Hino, N., Higashi, T., Nouso, K., Nakatsukasa, H., and Tsuji, T. 1996. Apoptosis and proliferation of human hepatocellular carcinoma. *Liver 16*:123–129.

Hollstein, M., Sidransky, D., Vogelstein, B., and Harris, C.C. 1991. p53 mutations in human cancers. *Science 253*:49–53.

Hsu, H.C., Peng, S.Y., Lai, P.L., Sheu, J.C., Chen, D.S., Lin, L.I., Slagle, B.L., and Butel, J.S. 1994. Allelotype and loss of heterozygosity of p53 in primary and recurrent hepatocellular carcinomas. A study of 150 patients. *Cancer 73*:42–47.

Hsu, I.C., Metcalf, R.A., Sun, T., Welsh, J.A., Wang, N.J., and Harris, C.C. 1991. Mutational hotspot in the p53 gene in human hepatocellular carcinomas. *Nature 350*:427–428.

International Agency for Research on Cancer (IARC). 1988. IARC Monographs on the Evaluation of Carcinogenic Risks to Humans. Vol. 44. *Alcohol Drinking.* Lyon, France: IARC Scientific Publications.

International Agency for Research on Cancer (IARC). 1994a. IARC Monographs on the Evaluation of Carcinogenic Risks to Humans. Vol. 56. *Some Naturally Occurring Substances: Food Items and Constituents, Heterocyclic Aromatic Amines, and Mycotoxins.* Lyon, France: IARC Scientific Publications.

International Agency for Research on Cancer (IARC). 1994b. IARC Monographs on the Evaluation of Carcinogenic Risks to Humans. Vol. 58. *Aflatoxins.* Lyon, France: IARC Scientific Publications.

International Agency for Research on Cancer (IARC). 1994c. IARC Monographs on the Evaluation of Carcinogenic Risks to Humans. Vol. 59. *Hepatitis Viruses.* Lyon, France: IARC Scientific Publications.

Ito, Y., Sasaki, Y., Horimoto, M., Wada, S., Tanaka, Y., Kasahara, A., Ueki, T., Hirano, T., Yamamoto, H., Fujimoto, J., Okamoto, E., Hayashi, N., and Hori, M. 1998. Activation of mitogen-activated protein kinases/extracellular signal-regulated kinases in human hepatocellular carcinoma. *Hepatology 27*:951–958.

Ito, Y., Matsuura, N., Sakon, M., Miyoshi, E., Noda, K., Takeda, T., Umeshita, K., Nagano, H., Nakamori, S., Dono, K., Tsujimoto, M., Nakahara, M., Nakao, K., Taniguchi, N., and Monden, M. 1999. Expression and prognostic roles of the G1-S modulators in hepatocellular carcinoma: p27 independently predicts the recurrence. *Hepatology 30*:90–99.

Jemal, A., Tiwari, R.C., Murray, T., Ghafoor, A., Samuels, A., Ward, E., Feuer, E.J., and Thun, M.J. 2004. Cancer statistics, 2004. *CA Cancer J. Clin. 54*:8–29.

Johnson, F.L., Lerner, K.G., Siegel, M., Feagler, J.R., Majerus, P.W., Hartmann, J.R., and Thomas, E.D. 1972. Association of androgenic-anabolic steroid therapy with development of hepatocellular carcinoma. *Lancet 2*:1273–1276.

Johnson, P.J., and Williams, R. 1987. Cirrhosis and the aetiology of hepatocellular carcinoma. *J. Hepatol. 4*:140–147.

Kagi, D., Ledermann, B., Burki, K., Zinkernagel, R.M., and Hengartner, H. 1996. Molecular mechanisms of lymphocyte-mediated cytotoxicity and their role in immunological protection and pathogenesis in vivo. *Annual Rev. Immunol. 14*:207–232.

Kaneko, Y., Shibuya, M., Nakayama, T., Hayashida, N., Toda, G., Endo, Y., Oka, H., and Oda, T. 1985. Hypomethylation of c-myc and epidermal growth factor receptor genes in human hepatocellular carcinoma and fetal liver. *Jpn. J. Cancer Res. 76*:1136–1140.

Kawai, H., Suda, T., Aoyagi, Y., Isokawa, O., Mita, Y., Waguri, N., Kuroiwa, T., Igarashi, M., Tsukada, K., Mori, S., Shimizu, T., Suzuki, Y., Abe, Y., Takahashi, T., Nomoto, M., and Asakura, H. 2000. Quantitative evaluation of genomic instability as a possible predictor for development of hepatocellular carcinoma: Comparison of loss of heterozygosity and replication error. *Hepatology 31*:1246–1250.

Kawate, S., Fukusato, T., Ohwada, S., Watanuki, A., and Morishita, Y. 1999a. Amplification of c-myc in hepatocellular carcinoma: Correlation with clinicopathologic features, proliferative activity and p53 overexpression. *Oncology 57*:157–163.

Kawate, S., Takenoshita, S., Ohwada, S., Mogi, A., Fukusato, T., Makita, F., Kuwano, H., and Morishita, Y. 1999b. Mutation analysis of transforming growth factor beta type II receptor, Smad2, and Smad4 in hepatocellular carcinoma. *Int. J. Oncol. 14*:127–131.

Kim, J.W., Ye, Q., Forgues, M., Chen, Y., Budhu, A., Sime, J., Hofseth, L.J., Kaul, R., and Wang, X.W. 2004. Cancer-associated molecular signature in the tissue samples of patients with cirrhosis. *Hepatology 39*:518–527.

Kiss, A., Wang, N.J., Xie, J.P., and Thorgeirsson, S.S. 1997. Analysis of transforming growth factor (TGF)-alpha/epidermal growth factor receptor, hepatocyte growth Factor/c-met, TGF-beta receptor type II, and p53 expression in human hepatocellular carcinomas. *Clin. Cancer Res. 3*:1059–1066.

Ko, L.J., and Prives, C. 1996. p53: Puzzle and paradigm. *Genes Develop. 10*:1054–1072.

Kubo, K., Matsuzaki, Y., Okazaki, M., Kato, A., Kobayashi, N., and Okita, K. 1998. The Fas system is not significantly involved in apoptosis in human hepatocellular carcinoma. *Liver 18*:117–123.

Kuroki, T., Fujiwara, Y., Nakamori, S., Imaoka, S., Kanematsu, T., and Nakamura, Y. 1995. Evidence for the presence of two tumour-suppressor genes for hepatocellular carcinoma on chromosome 13q. *Br. J. Cancer 72*:383–385.

Lai, C.L., Gregory, P.B., Wu, P.C., Lok, A.S., Wong, K.P., and Ng, M.M. 1987. Hepatocellular carcinoma in Chinese males and females. Possible causes for the male predominance. *Cancer 60*:1107–1110.

Le Bail, B., Belleannee, G., Bernard, P.H., Saric, J., Balabaud, C., and Bioulac-Sage, P. 1995. Adenomatous hyperplasia in cirrhotic livers: Histological evaluation, cellular density, and proliferative activity of 35 macronodular lesions in the cirrhotic explants of 10 adult French patients. *Human Pathol. 26*:897–906.

Lee, H.S., Rajagopalan, M.S., and Vyas, G.N. 1988. A lack of direct role of hepatitis B virus in the activation of ras and c-myc oncogenes in human hepatocellular carcinogenesis. *Hepatology 8*:1116–1120.

Leon, M., and Kew, M.C. 1995. Analysis of ras gene mutations in hepatocellular carcinoma in southern African blacks. *Anticancer Res. 15*:859–861.

Lieber, C.S. 1990. Interaction of alcohol with other drugs and nutrients. Implication for the therapy of alcoholic liver disease. *Drugs 40*:23–44.

Ljubimova, J.Y., Petrovic, L.M., Wilson, S.E., Geller, S.A., and Demetriou, A.A. 1997. Expression of HGF, its receptor c-met, c-myc, and albumin in cirrhotic and neoplastic human liver tissue. *J. Histochem. Cytochem. 45*:79–87.

Llovet, J.M., Burroughs, A., and Bruix, J. 2003. Hepatocellular carcinoma. *Lancet 362*:1907–1917.

Lui, W.Y., Lin, H.L., Chau, G.Y., Liu, T.Y., and Chi, C.W. 2000. Male predominance in hepatocellular carcinoma: New insight and a possible therapeutic alternative. *Med. Hypotheses 55*:348–350.

Macdonald, G.A., Greenson, J.K., Saito, K., Cherian, S.P., Appelman, H.D., and Boland, C.R. 1998. Microsatellite instability and loss of heterozygosity at DNA mismatch repair gene loci occurs during hepatic carcinogenesis. *Hepatology 28*:90–97.

Mathers, C.D., Shibuya, K., Boschi-Pinto, C., Lopez, A.D., and Murray, C.J. 2002. Global and regional estimates of cancer mortality and incidence by site: I. Application of regional cancer survival model to estimate cancer mortality distribution by site. *BMC Cancer 2*:36.

McMahon, B.J., Alward, W.L., Hall, D.B., Heyward, W.L., Bender, T.R., Francis, D.P., and Maynard, J.E. 1985. Acute hepatitis B virus infection: Relation of age to the clinical expression of disease and subsequent development of the carrier state. *J. Infect. Dis. 151*:599–603.

McMahon, B.J., Alberts, S.R., Wainwright, R.B., Bulkow, L., and Lanier, A.P. 1990. Hepatitis B-related sequelae. Prospective study in 1400 hepatitis B surface antigen-positive Alaska native carriers. *Arch. Intern. Med. 150*:1051–1054.

Mise, K., Tashiro, S., Yogita, S., Wada, D., Harada, M., Fukuda, Y., Miyake, H., Isikawa, M., Izumi, K., and Sano, N. 1998. Assessment of the biological malignancy of hepatocellular carcinoma: Relationship to clinicopathological factors and prognosis. *Clin. Cancer Res. 4*:1475–1482.

Morimitsu, Y., Hsia, C.C., Kojiro, M., and Tabor, E. 1995. Nodules of less-differentiated tumor within or adjacent to hepatocellular carcinoma: Relative expression of transforming growth factor-alpha and its receptor in the different areas of tumor. *Human Pathol. 26*:1126–1132.

Munoz, N., and Bosch, X. 1987. Epidemiology of hepatocellular carcinoma. In: Okuda, K., Ishak, K.G. (ed.). *Neoplasms of the Liver.* New York: Springer-Verlag, 3–19.

Munoz, N., and Linsell, A. 1982. Epidemiology of primary liver cancer. In: Correa, P., Haenszel, W. (eds.). *Epidemiology of Cancer of the Digestive Tract.* The Hague: Martinus Nijhoff, 161–195.

Murakami, Y., Hayashi, K., Hirohashi, S., and Sekiya, T. 1991. Aberrations of the tumor suppressor p53 and retinoblastoma genes in human hepatocellular carcinomas. *Cancer Res. 51*:5520–5525.

Nagai, H., Pineau, P., Tiollais, P., Buendia, M.A., and Dejean, A. 1997. Comprehensive allelotyping of human hepatocellular carcinoma. *Oncogene 14*:2927–2933.

Nalesnik, M.A., Lee, R.G., and Carr, B.I. 1998. Transforming growth factor alpha (TGFalpha) in hepatocellular carcinomas and adjacent hepatic parenchyma. *Human Pathol. 29*:228–234.

Nalpas, B. 1994. Alcohol and hepatocellular carcinoma. In: Brechot, C. (ed). *Primary Liver Cancer: Etiological and Progression Factors.* Boca Raton: CRC Press, 231–245.

Nalpas, B., Feitelson, M., Brechot, C., and Rubin, E. 1995. Alcohol, hepatotropic viruses, and hepatocellular carcinoma. *Alcohol Clin. Exp. Res. 19*:1089–1095.

Nambu, S., Inoue, K., and Saski, H. 1987. Site-specific hypomethylation of the c-myc oncogene in human hepatocellular carcinoma. *Jpn. J. Cancer Res. 78*:695–704.

Nishida, N., Nishimura, T., Ito, T., Komeda, T., Fukuda, Y., and Nakao, K. 2003. Chromosomal instability and human hepatocarcinogenesis. *Histol. Histopathol. 18*:897–909.

Noguchi, O., Enomoto, N., Ikeda, T., Kobayashi, F., Marumo, F., and Sato, C. 1996. Gene expressions of c-met and hepatocyte growth factor in chronic liver disease and hepatocellular carcinoma. *J. Hepatol. 24*:286–292.

Nonomura, A., Ohta, G., Hayashi, M., Izumi, R., Watanabe, K., Takayanagi, N., Mizukami, Y., and Matsubara, F. 1987. Immunohistochemical detection of ras oncogene p21 product in liver cirrhosis and hepatocellular carcinoma. *Am. J. Gastroenterol. 82*:512–518.

Oda, T., Tsuda, H., Scarpa, A., Sakamoto, M., and Hirohashi, S. 1992. p53 gene mutation spectrum in hepatocellular carcinoma. *Cancer Res. 52*:6358–6364.

Okano, J., Shiota, G., and Kawasaki, H. 1999. Expression of hepatocyte growth factor (HGF) and HGF receptor (c-met) proteins in liver diseases: An immunohistochemical study. *Liver 19*:151–159.

Okuda, K., Fujimoto, I., Hanai, A., and Urano, Y. 1987. Changing incidence of hepatocellular carcinoma in Japan. *Cancer Res. 47*:4967–4972.

Okuda, K., and Okuda, H. 1999. Primary liver cell carcinoma. In: Bircher, J., Benhamou, J.P., McIntyre, N., Rizzetto, M., and Rodes, J. (eds.). *Oxford Textbook of Clinical Hepatology, Second Edition.* New York: Oxford University Press, 1491–1530.

Okuda, T., Wakasa, K., Kubo, S., Hamada, T., Fujita, M., Enomoto, T., Haba, T., Hirohashi, K., and Kinoshita, H. 2001. Clonal analysis of hepatocellular carcinoma and dysplastic nodule by methylation pattern of X-chromosome-linked human androgen receptor gene. *Cancer Lett. 164*:91–96.

Ozturk, M. 1991. p53 mutation in hepatocellular carcinoma after aflatoxin exposure. *Lancet 338*:1356–1359.

Pang, E., Wong, N., Lai, P.B., To, K.F., Lau, J.W., and Johnson, P.J. 2000. A comprehensive karyotypic analysis on a newly developed hepatocellular carcinoma cell line, HKCI-1, by spectral karyotyping and comparative genomic hybridization. *Cancer Genet. Cytogenet. 121*:9–16.

Parada, L.A., Hallen, M., Tranberg, K.G., Hagerstrand, I., Bondeson, L., Mitelman, F., and Johansson, B. 1998. Frequent rearrangements of chromosomes l, 7, and 8 in primary liver cancer. *Genes Chromosomes Cancer 23*:26–35.

Paradis, V., Laurendeau, I., Vidaud, M., and Bedossa, P. 1998. Clonal analysis of macronodules in cirrhosis. *Hepatology 28*:953–958.

Park, B.C., Huh, M.H., and Seo, J.H. 1995. Differential expression of transforming growth factor alpha and insulin-like growth factor II in chronic active hepatitis B, cirrhosis and hepatocellular carcinoma. *J. Hepatol. 22*:286–294.

Parkin, D.M., Pisani, P., and Ferlay, J. 1999a. Global cancer statistics. *CA Cancer J. Clin. 49*:31,33–64.

Parkin, D.M., Pisani, P., and Ferlay, J. 1999b. Estimates of the worldwide incidence of 25 major cancers in 1990. *Int. J. Cancer 80*:827–841.

Parkin, D.M. 2001. Global cancer statistics in the year 2000. *Lancet Oncol. 2*:533–543.

Parkin, D.M., Bray, F., Ferlay, J., and Pisani, P. 2001. Estimating the world cancer burden: Globocan 2000. *Int. J. Cancer 94*:153–156.

Peltomaki, P. 2003. Role of DNA mismatch repair defects in the pathogenesis of human cancer. *J. Clin. Oncol. 21*:1174–1179.

Piao, Z., Park, C., Park, J.H., and Kim, H. 1998. Allelotype analysis of hepatocellular carcinoma. *Int. J. Cancer 75*:29–33.

Piao, Z., Kim, H., Malkhosyan, S., and Park, C. 2000. Frequent chromosomal instability but no microsatellite instability in hepatocellular carcinomas. *Int. J. Oncol. 17*:507–512.

Pollice, L., Ricco, R., Russo, S., Maiorano, E., Pagniello, G., and Delfino-Pesce, V. 1988. Hepatocellular dysplasia: Imunohistochemical and morphometrical evaluation. *Appl. Pathol. 6*:73–81.

Propst, T., Propst, A., Dietze, O., Judmaier, G., Braunsteiner, H., and Vogel, W. 1994. Prevalence of hepatocellular carcinoma in alpha-1-antitrypsin deficiency. *J. Hepatol. 21*:1006–1011.

Puisieux, A., Lim, S., Groopman, J., and Ozturk, M. 1991. Selective targeting of p53 gene mutational hotspots in human cancers by etiologically defined carcinogens. *Cancer Res. 51*:6185–6189.

Qian, G.S., Ross, R.K., Yu, M.C., Yuan, J.M., Gao, Y.T., Henderson, B.E., Wogan, G.N., and Groopman, J.D. 1994. A follow-up study of urinary markers of aflatoxin exposure and liver cancer risk in Shanghai, People's Republic of China. *Cancer Epidemiol. Biomarkers Prev. 3*:3–10.

Qin, G., Su, J., Ning, Y., Duan, X., Luo, D., and Lotlikar, P.D. 1997. p53 protein expression in patients with hepatocellular carcinoma from the high incidence area of Guangxi, Southern China. *Cancer Lett. 121*:203–210.

Radosevich, J.A., Gould, K.A., Koukoulis, G.K., Haines, G.K., Rosen, S.T., Lee, I., and Gould, V.E. 1993. Immunolocalization of ras oncogene p21 in human liver diseases. *Ultrastruct. Pathol. 17*:1–8.

Rashid, A., Wang, J.S., Qian, G.S., Lu, B.X., Hamilton, S.R., and Groopman, J.D. 1999. Genetic alterations in hepatocellular carcinomas: Association between loss of chromosome 4q and p53 gene mutations. *Br. J. Cancer 80*:59–66.

Romeo, R., and Colombo, M. 2002. The natural history of hepatocellular carcinoma. *Toxicology 181–182*:39–42.

Ross, R.K., Yuan, J.M., Yu, M.C., Wogan, G.N., Qian, G.S., Tu, J.T., Groopman, J.D., Gao, Y.T., and Henderson, B.E. 1992. Urinary aflatoxin biomarkers and risk of hepatocellular carcinoma. *Lancet 339*:943–946.

Russo, P.A., Mitchell, G.A., and Tanguay, R.M. 2001. Tyrosinemia: A review. *Pediatr. Develop. Pathol. 4*:212–221.

Saegusa, M., Takano, Y., Kishimoto, H., Wakabayashi, G., Nohga, K., and Okudaira, M. 1993. Comparative analysis of p53 and c-myc expression and cell proliferation in human hepatocellular carcinomas—An enhanced immunohistochemical approach. *J. Cancer Res. Clin. Oncol. 119*:737–744.

Salvucci, M., Lemoine, A., Saffroy, R., Azoulay, D., Lepere, B., Gaillard, S., Bismuth, H., Reynes, M., and Debuire, B. 1999. Microsatellite instability in European hepatocellular carcinoma. *Oncogene 18*:181–187.

Schulte-Hermann, R., Hufnagl, K., Low-Baselli, A., Rossmanith, W., Wagner, A., Ruttkay-Nedecky, B., Bursch, W., Mullauer, L., Parzefall, W., and Grasl-Kraupp, B. 1998. Apoptosis and hepatocarcinogenesis. *Digestion 59*:64–65.

Sell, S. 2003. Mouse models to study the interaction of risk factors for human liver cancer. *Cancer Res. 63*:7553–7562.

Shafritz, D.A., Shouval, D., Sherman, H.I., Hadziyannis, S.J., and Kew, M.C. 1981. Integration of hepatitis B virus DNA into the genome of liver cells in chronic liver disease and hepatocellular carcinoma. Studies in percutaneous liver biopsies and postmortem tissue specimens. *N. Engl. J. Med. 305*:1067–1073.

Sheu, J.C., Lin, Y.W., Chou, H.C., Huang, G.T., Lee, H.S., Lin, Y.H., Huang, S.Y., Chen, C.H., Wang, J.T., Lee, P.H., Lin, J.T., Lu, F.J., and Chen, D.S. 1999. Loss of heterozygosity and microsatellite instability in hepatocellular carcinoma in Taiwan. *Br. J. Cancer 80*:468–476.

Shimizu, A., Tarao, K., Takemiya, S., Harada, M., Inoue, T., and Ono, T. 1988. S-phase cells in diseased human liver determined by an in vitro BrdU-anti-BrdU method. *Hepatology 8*:1535–1539.

Shirota, Y., Kaneko, S., Honda, M., Kawai, H.F., and Kobayashi, K. 2001. Identification of differentially expressed genes in hepatocellular carcinoma with cDNA microarrays. *Hepatology 33*:832–840.

Simonetti, R.G., Camma, C., Fiorello, F., Politi, F., D'Amico, G., and Pagliaro, L. 1991. Hepatocellular carcinoma. A worldwide problem and the major risk factors. *Dig. Dis. Sci. 36*:962–972.

Simonetti, R.G., Camma, C., Fiorello, F., Cottone, M., Rapicetta, M., Marino, L., Fiorentino, G., Craxi, A., Ciccaglione, A., and Giuseppetti, R. 1992. Hepatitis C virus infection as a risk factor for hepatocellular carcinoma in patients with cirrhosis. A case-control study. *Ann. Intern. Med. 116*:97–102.

Simpson, K.J., Lukacs, N.W., Colletti, L., Strieter, R.M., and Kunkel, S.L. 1997. Cytokines and the liver. *J. Hepatol. 27*:1120–1132.

Sirivatanauksorn, Y., Sirivatanauksorn, V., Bhattacharya, S., Davidson, B.R., Dhillon, A.P., Kakkar, A.K., Williamson, R.C., and Lemoine, N.R. 1999a. Evolution of genetic abnormalities in hepatocellular carcinomas demonstrated by DNA fingerprinting. *J. Pathol. 189*:344–350.

Sirivatanauksorn, Y., Sirivatanauksorn, V., Bhattacharya, S., Davidson, B.R., Dhillon, A.P., Kakkar, A.K., Williamson, R.C., and Lemoine, N.R. 1999b. Genomic heterogeneity in synchronous hepatocellular carcinomas. *Gut 45*:761–765.

Smith, M.W., Yue, Z.N., Geiss, G.K., Sadovnikova, N.Y., Carter, V.S., Boix, L., Lazaro, C.A., Rosenberg, G.B., Bumgarner, R.E., Fausto, N., Bruix, J., and Katze, M.G. 2003. Identification of novel tumor markers in hepatitis C virus-associated hepatocellular carcinoma. *Cancer Res. 63*:859–864.

Smolinski, K.N., and Meltzer, S.J. 2002. Inactivation of negative growth regulators during neoplastic transformation. In: Coleman, W.B., Tsongalis, G.J. (eds.). *The Molecular Basis of Human Cancer.* Totowa: Humana Press, 81–111.

Sohda, T., Kamimura, S., Iwata, K., Shijo, H., and Okumura, M. 1997a. Immunohistochemical evidence of insulin-like growth factor II in human small hepatocellular carcinoma with hepatitis C virus infection: Relationship to fatty change in carcinoma cells. *J. Gastroenterol. Hepatol. 12*:224–228.

Sohda, T., Oka, Y., Iwata, K., Gunn, J., Kamimura, S., Shijo, H., Okumura, M., and Yun, K. 1997b. Co-localisation of insulin-like growth factor II and the proliferation marker MIB1 in hepatocellular carcinoma cells. *J. Clin. Pathol. 50*:135–137.

Soini, Y., Chia, S.C., Bennett, W.P., Groopman, J.D., Wang, J.S., DeBenedetti, V.M., Cawley, H., Welsh, J.A., Hansen, C., Bergasa, N.V., Jones, E.A., DiBisceglie, A.M., Trivers, G.E., Sandoval, C.A., Calderon, I.E., Munoz Espinosa, L.E., and Harris, C.C. 1996. An aflatoxin-associated mutational hotspot at codon 249 in the p53 tumor suppressor gene occurs in hepatocellular carcinomas from Mexico. *Carcinogenesis 17*:1007–1012.

Stevens, R.G., Merkle, E.J., and Lustbader, E.D. 1984. Age and cohort effects in primary liver cancer. *Int. J. Cancer 33*:453–458.

Su, Q., Benner, A., Hofmann, W.J., Otto, G., Pichlmayr, R., and Bannasch, P. 1997. Human hepatic preneoplasia: Phenotypes and proliferation kinetics of foci and nodules of altered hepatocytes and their relationship to liver cell dysplasia. *Virchows Arch. 431*:391–406.

Sugitani, S., Sakamoto, M., Ichida, T., Genda, T., Asakura, H., and Hirohashi, S. 1998. Hyperplastic foci reflect the risk of multicentric development of human hepatocellular carcinoma. *J. Hepatol. 28*:1045–1053.

Suriawinata, A., and Xu, R. 2004. An update on the molecular genetics of hepatocellular carcinoma. *Semin. Liver Dis. 24:* 77–88.

Szymanska, K., and Hainaut, P. 2003. TP53 and mutations in human cancer. *Acta Biochim. Pol. 50*:231–238.

Tanaka, K., Hirohata, T., Takeshita, S., Hirohata, I., Koga, S., Sugimachi, K., Kanematsu, T., Ohryohji, F., and Ishibashi, H. 1992. Hepatitis B virus, cigarette smoking and alcohol consumption in the development of hepatocellular carcinoma: A case-control study in Fukuoka, Japan. *Int. J. Cancer 51*:509–514.

Tanaka, S., Toh, Y., Adachi, E., Matsumata, T., Mori, R., and Sugimachi, K. 1993. Tumor progression in hepatocellular carcinoma may be mediated by p53 mutation. *Cancer Res. 53*:2884–2887.

Tanaka, Y., Esumi, M., and Shikata, T. 1988. Frequent integration of hepatitis B virus DNA in noncancerous liver tissue from hepatocellular carcinoma patients. *J. Med. Virol. 26*:7–14.

Tang, Z., Qin, L., Wang, X., Zhou, G., Liao, Y., Weng, Y., Jiang, X., Lin, Z., Liu, K., and Ye, S. 1998. Alterations of oncogenes, tumor suppressor genes and growth factors in hepatocellular carcinoma: With relation to tumor size and invasiveness. *Chinese Med. J. 111*:313–318.

Tannapfel, A., Geissler, F., Kockerling, F., Katalinic, A., Hauss, J., and Wittekind, C. 1999. Apoptosis and proliferation in relation to histopathological variables and prognosis in hepatocellular carcinoma. *J. Pathol. 187*:439–445.

Tarao, K., Shimizu, A., Harada, M., Kuni, Y., Ito, Y., Tamai, S., Iimori, K., Sugimasa, Y., Takemiya, S., and Okamoto, T. 1989. Difference in the in vitro uptake of bromodeoxyuridine between liver cirrhosis with and without hepatocellular carcinoma. *Cancer 64*:104–109.

Tarao, K., Shimizu, A., Harada, M., Ohkawa, S., Tamai, S., Ito, Y., Kuni, Y., Takemiya, S., and Okamoto, T. 1990. Increased DNA synthetic potency of hepatocytes in cirrhotic patients may indicate a super-high risk for hepatocellular carcinoma. *Jpn. J. Med. 29*:373–378.

Tarao, K., Ohkawa, S., Shimizu, A., Harada, M., Nakamura, Y., Okamoto, N., Ito, Y., Tamai, S., Iimori, K., and Sugimasa, Y. 1993. DNA synthesis activities of hepatocytes from noncancerous cirrhotic tissue and of hepatocellular carcinoma (HCC) cells from cancerous tissue can predict the survival of hepatectomized patients with HCC. *Cancer 71*:3859–3863.

Tarao, K., Ohkawa, S., Shimizu, A., Harada, M., Nakamura, Y., Ito, Y., Tamai, S., Hoshino, H., Inoue, T., and Kanisawa, M. 1994. Significance of hepatocellular proliferation in the development of hepatocellular carcinoma from anti-hepatitis C virus-positive cirrhotic patients. *Cancer 73*:1149–1154.

Taub, R. 1999. IL-6 and liver growth regulation. In: Fleig, W.E. (ed.). *Normal and Malignant Liver Cell Growth.* Dordrecht: Kluwer Academic Publishers, 68–74.

Taylor-Robinson, S.D., Foster, G.R., Arora, S., Hargreaves, S., and Thomas, H.C. 1997. Increase in primary liver cancer in the UK, 1979-94. *Lancet 350*:1142–1143.

Terasaki, S., Kaneko, S., Kobayashi, K., Nonomura, A., and Nakanuma, Y. 1998. Histological features predicting malignant transformation of nonmalignant hepatocellular nodules: A prospective study. *Gastroenterology 115*:1216–1222.

Terris, B., Ingster, O., Rubbia, L., Dubois, S., Belghiti, J., Feldmann, G., Degott, C., and Henin, D. 1997. Interphase cytogenetic analysis reveals numerical chromosome aberrations in large liver cell dysplasia. *J. Hepatol. 27*:313–319.

Theise, N.D., Lapook, J.D., and Thung, S.N. 1993. A macroregenerative nodule containing multiple foci of hepatocellular carcinoma in a noncirrhotic liver. *Hepatology 17*:993–996.

Thorgeirsson, S.S., Teramoto, T., and Factor, V.M. 1998. Dysregulation of apoptosis in hepatocellular carcinoma. *Semin. Liver Dis. 18*:115–122.

Thorgeirsson, S.S., and Grisham, J.W. 2002. Molecular pathogenesis of human hepatocellular carcinoma. *Nature Genet. 31:* 339–346.

Tiniakos, D., Spandidos, D.A., Kakkanas, A., Pintzas, A., Pollice, L., and Tiniakos, G. 1989. Expression of ras and myc oncogenes in human hepatocellular carcinoma and non-neoplastic liver tissues. *Anticancer Res. 9*:715–721.

Tiniakos, D., Spandidos, D.A., Yiagnisis, M., and Tiniakos, G. 1993. Expression of ras and c-myc oncoproteins and hepatitis B surface antigen in human liver disease. *Hepatogastroenterology 40*:37–40.

Tiniakos, D.G., and Brunt, E.M. 1999. Proliferating cell nuclear antigen and Ki-67 labeling in hepatocellular nodules: A comparative study. *Liver 19*:58–68.

Tornillo, L., Carafa, V., Richter, J., Sauter, G., Moch, H., Minola, E., Gambacorta, M., Bianchi, L., Vecchione, R., and Terracciano, L.M. 2000. Marked genetic similarities between hepatitis B virus-positive and hepatitis C virus-positive hepatocellular carcinomas. *J. Pathol. 192*:307–312.

Tsopanomichalou, M., Kouroumalis, E., Ergazaki, M., and Spandidos, D.A. 1999. Loss of heterozygosity and microsatellite instability in human non-neoplastic hepatic lesions. *Liver 19*:305–311.

Tsuda, H., Hirohashi, S., Shimosato, Y., Terada, M., and Hasegawa, H. 1988. Clonal origin of atypical adenomatous hyperplasia of the liver and clonal identity with hepatocellular carcinoma. *Gastroenterology 95*:1664–1666.

Uchida, T., Miyata, H., and Shikata, T. 1981. Human hepatocellular carcinoma and putative precancerous disorders: Their enzyme histochemical study. *Arch. Pathol. Lab. Med. 105*:180–186.

Vainio, H., and Wilbourn, J. 1993. Cancer etiology: Agents causally associated with human cancer. *Pharmacol. Toxicol. 72*:4–11.

Wang, G., Zhao, Y., Liu, X., Wang, L., Wu, C., Zhang, W., Liu, W., Zhang, P., Cong, W., Zhu, Y., Zhang, L., Chen, S., Wan, D., Zhao, X., Huang, W., and Gu, J. 2001. Allelic loss and gain, but not genomic instability, as the major somatic mutation in primary hepatocellular carcinoma. *Genes Chromosomes Cancer 31*:221–227.

Wang, X.W., Hussain, S.P., Huo, T.I., Wu, C.G., Forgues, M., Hofseth, L.J., Brechot, C., and Harris, C.C. 2002. Molecular pathogenesis of human hepatocellular carcinoma. *Toxicology 181–182*:43–47.

Webber, E.M., Yamada, Y., Bruix, J., Pierce, R.H., and Fausto, N. 1999. Initiation of liver regeneration by tumour necrosis factor. In: Fleig, W.E. (ed.). *Normal and Malignant Liver Cell Growth.* Dordtrecht: Kluwer Academic Publishers, 56–67.

Wild, C.P., and Turner, P.C. 2002. The toxicology of aflatoxins as a basis for public health decisions. *Mutagenesis 17*:471–481.

Wilkinson, M.L., Portmann, B., and Williams, R. 1983. Wilson's disease and hepatocellular carcinoma: Possible protective role of copper. *Gut 24*:767–771.

Wong, N., Lai, P., Pang, E., Fung, L.F., Sheng, Z., Wong, V., Wang, W., Hayashi, Y., Perlman, E., Yuna, S., Lau, J.W., and Johnson, P.J. 2000a. Genomic aberrations in human hepatocellular carcinomas of differing etiologies. *Clin. Cancer Res. 6*:4000–4009.

Wong, N., Lai, P., Pang, E., Leung, T.W., Lau, J.W., and Johnson, P.J. 2000b. A comprehensive karyotypic study on human hepatocellular carcinoma by spectral karyotyping. *Hepatology 32*:1060–1068.

Yakushiji, H., Mukai, S., Matsukura, S., Sato, S., Ogawa, A., Sasatomi, E., and Miyazaki, K. 1999. DNA mismatch repair deficiency in curatively resected sextuple primary cancers in different organs: A molecular case report. *Cancer Lett. 142*:17–22.

Yamaguchi, K., Carr, B.I., and Nalesnik, M.A. 1995. Concomitant and isolated expression of TGF-alpha and EGF-R in human hepatoma cells supports the hypothesis of autocrine, paracrine, and endocrine growth of human hepatoma. *J. Surg. Oncol. 58*:240–245.

Yamamoto, T., Kajino, K., Kudo, M., Sasaki, Y., Arakawa, Y., and Hino, O. 1999. Determination of the clonal origin of multiple human hepatocellular carcinomas by cloning and polymerase chain reaction of the integrated hepatitis B virus DNA. *Hepatology 29*:1446–1452.

Yano, M., Asahara, T., Dohi, K., Mizuno, T., Iwamoto, K.S., and Seyama, T. 1999. Close correlation between a p53 or hMSH2 gene mutation in the tumor and survival of hepatocellular carcinoma patients. *Int. J. Oncol. 14*:447–451.

Yasui, H., Hino, O., Ohtake, K., Machinami, R., and Kitagawa, T. 1992. Clonal growth of hepatitis B virus-integrated hepatocytes in cirrhotic liver nodules. *Cancer Res. 52*:6810–6814.

Zafrani, E.S. 2004. Non-alcoholic fatty liver disease: An emerging pathological spectrum. *Virchows Arch. 444*:3–12.

Zhang, X., Xu, H.J., Murakami, Y., Sachse, R., Yashima, K., Hirohashi, S., Hu, S.X., Benedict, W.F., and Sekiya, T. 1994. Deletions of chromosome 13q, mutations in Retinoblastoma 1, and retinoblastoma protein state in human hepatocellular carcinoma. *Cancer Res. 54*:4177–4182.

Zhang, X.K., Huang, D.P., Chiu, D.K., and Chiu, J.F. 1987. The expression of oncogenes in human developing liver and hepatomas. *Biochem. Biophys. Res. Commun. 142*:932–938.

Zhang, X.K., Huang, D.P., Qiu, D.K., and Chiu, J.F. 1990. The expression of c-myc and c-N-ras in human cirrhotic livers, hepatocellular carcinomas and liver tissue surrounding the tumors. *Oncogene 5*:909–914.

Zhao, M., Zhang, N.X., Laissue, J.A., and Zimmermann, A. 1994. Immunohistochemical analysis of p53 protein overexpression in liver cell dysplasia and in hepatocellular carcinoma. *Virchows Arch. 424*:613–621.

Zimmerman, H.J. 1999. *Hepatotoxicity: The Adverse Effects of Drugs and Other Chemicals on the Liver. Second Edition.* Philadelphia: Lippincott Williams & Wilkins.

3

Genes Involved in Hepatocellular Carcinoma

Andrea Tannapfel

Introduction

Hepatocellular carcinoma (HCC) accounts for 80–90% of all liver cancers and is one of the most frequently occurring carcinomas worldwide. Clinical and molecular medical analyses yielded a considerable amount of information about liver carcinogenesis. Many genes undergo somatic aberrations with a tendency to cluster at genes involved in cell cycle regulation, in the p53 and Wnt/catenin pathways of signal transduction and cellular adhesion and also in the transforming growth factor-beta (TGF-β)/insulin-like growth factor (IGF) axis. Because HCC may arise in cirrhotic and noncirrhotic livers, one may speculate that different pathways in hepatocarcinogenesis may exist. Recent results of high-output gene analysis using complementary deoxyribonucleic acid (cDNA) microarrays support the idea of different genetic alterations in HCC with or without cirrhosis. However, molecular diagnosis of HCC has—until now—been of limited clinical value in routine surgical pathology. There are no specific markers with diagnostic sensitivity to exclude other types of liver tumors.

As is true in other types of cancers, the etiology and carcinogenesis of HCC is multifactorial and multistage. The multistep process of HCC may be divided into several steps: chronic liver injury, which produces inflammation, cell death, cirrhosis, and regeneration; epigenetic/genetic DNA damage; dysplasia; and HCC (Figure 26). In general, specific genetic or epigenetic changes have been identified for some of these stages. These genetic changes include gene amplification (leading to activation of protooncogenes), gene deletion or mutation (leading to inactivation of tumor-suppressor genes), and reactivation of telomerase activity. The high number of genes involved in HCC may indicate that different etiologic factors affect different sets of genes in hepatocytes. This etiologically defined genetic heterogeneity of HCC results in the phenotypic heterogeneity of these tumors. In other words, distinct but related genetic pathways are altered during hepatocarcinogenesis as a result of different etiologic factors. Given the facts that 60–80% of all HCCs arise in liver cirrhosis and that the risk of development of HCC increases up to 1–5% per year in patients with cirrhosis, cirrhotic nodules are apparently premalignant lesions of HCC, and they may already contain genetic aberrations (Tannapfel *et al.,* 2002; WHO 2000). Because a number of somatic gene and protein changes have been investigated in HCC, we discuss the main regulatory pathways that are altered in HCC. It is emphasized that these pathways are related one to another, and the genetic events should not be considered as independent and separate pathways. Furthermore, because of the etiologic heterogeneity, differences in the

Handbook of Immunohistochemistry and *in situ* Hybridization of Human Carcinomas, Volume 3: Molecular Genetics, Liver Carcinoma, and Pancreatic Carcinoma

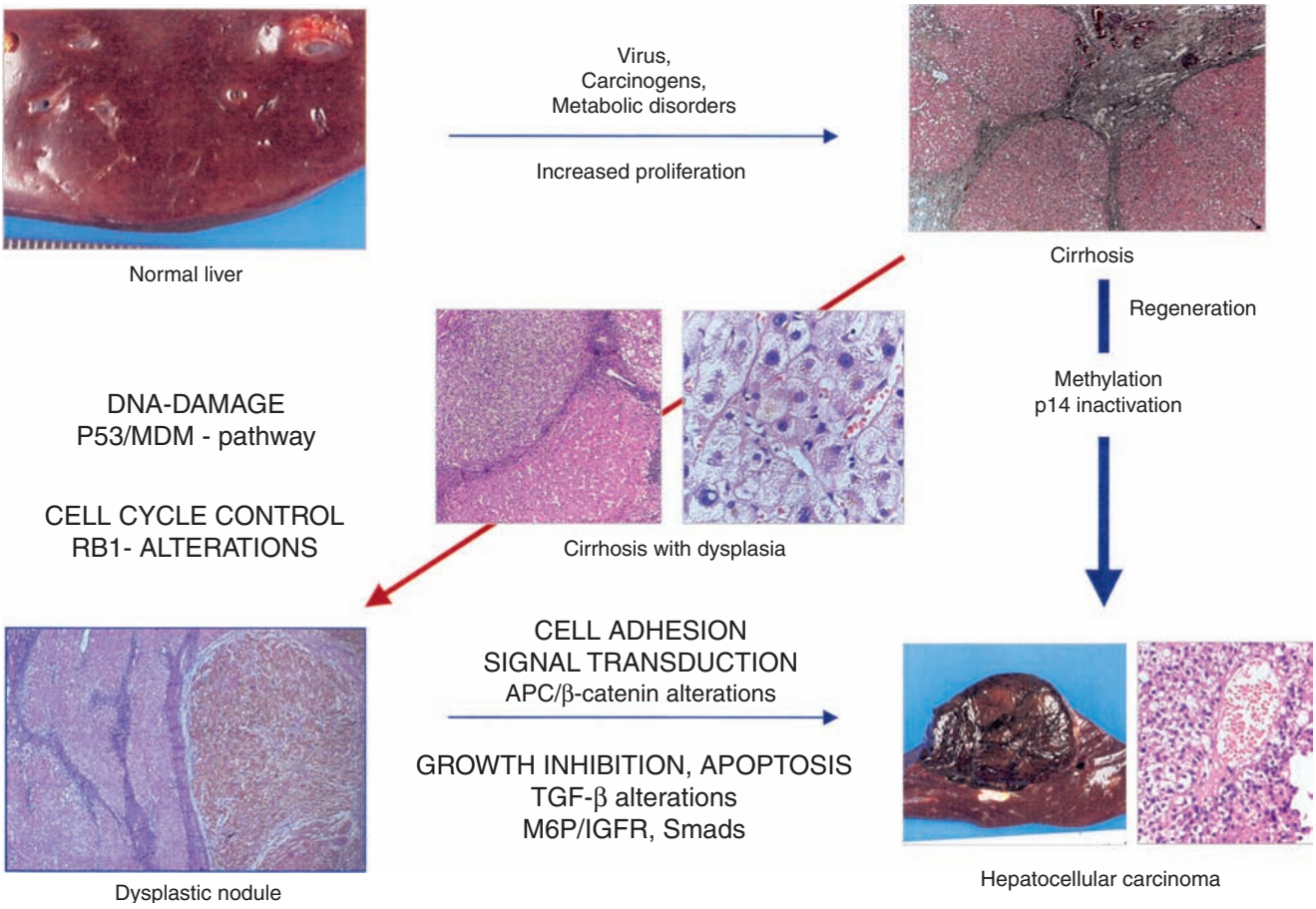

Figure 26. Multistage process of carcinogenesis (Modified according to Tannapfel *et al.,* 2002).

genetic alterations of HCC arising in cirrhosis compared to those without cirrhosis will be described.

Allelic Imbalance and Microsatellite Instability

Chromosomal instability is characterized by allelic losses and aneuploidy. Most of the genes mutated in HCC are tumor-suppressor genes, and frequent allelic losses (loss of heterozygosity [LOH]) leading to the biallelic inactivation have been described. By comparative genomic hybridization, chromosomes 1q, 8q, and 17q showed gene dosage increase, whereas chromosomes 1p, 4q, 8p, 9p, 13q, 16p, 16q, and 17p showed gene dosage loss. Consistently, frequent LOH, or more comprehensive allelic imbalance (AI), was observed on chromosomes 1p, 4q, 6p, 8p, 13q, 16q, and 17p by whole-genome allelotyping. The chromosome regions with gene dosage increase may contain critical oncogenes, whereas those with gene dosage loss may contain tumor-suppressor genes. For chromosomes 17p, 13q, 9p, 6q, and 16p, LOH could be related to p53, retinoblastoma 1 (RB1), p16, and IGF2R inactivation, respectively (Feitelson *et al.,* 2002).

Although the genes causing chromosomal instability or AI remain unknown, microsatellite instability (MSI) is caused by inactivation of a DNA mismatch repair gene (predominantly hMLH1 or hMSH2). It has been shown that most tumors in patients with hereditary nonpolyposis colorectal cancer (HNPCC) harbor MSI. This phenotype was linked to defects in the DNA mismatch repair genes MSH2 and MLH1 located on chromosomes 2 and 3. In HCC these chromosomal regions are not frequently affected by allelic losses. Furthermore, no mutation in the repeated sequences in *Bax, IGF-IIR,* or *MLH* genes (a hallmark of MSI) has been detected so far in HCC (Enomoto *et al.,* 2001). These findings indicate that, in contrast to AI, defective mismatch repair does not contribute significantly to hepatocellular carcinogenesis.

Cell Cycle Regulation

The RB gene is one of the best-studied tumor-suppressor genes in HCC. Mutations of RB are observed in ~15% of HCC. At chromosome 13q, where RB is located, LOH is frequently observed in HCC with a prevalence of 25–48%. An overexpression of cyclins has been observed in ~10–13% of all HCC. Cyclin D1, for example, is a known oncogene and a key regulator of cell cycle progression. Amplification of the cyclin D1 gene and its overexpression has been associated with aggressive forms of HCC. It has been shown in a transgene mouse model that overexpression of cyclin D1 is sufficient to initiate hepatocellular carcinogenesis. The transduction of anti-sense cyclin D1 inhibits tumor growth in a xenograft hepatoma model (Deane *et al.,* 2001). Correcting alterations that have occurred in the G1-phase regulatory machinery may therefore provide a novel weapon to prevent and treat HCC.

Signaling through the mitogen-activated protein kinase (MAPK) cascade is transduced by guanosine triphosphate (GTP) loading of RAS leading to the activation of RAF kinase. In mammalian cells, there are three isoforms of RAF: A-*RAF,* B-*RAF,* and C-*RAF.* Although all three of the RAF isoforms share a common function with respect to MEK phosphorylation, studies have shown that these proteins might be differentially activated by oncogenic *ras* (Davies *et al.,* 2002). In 2003 we described that activating B-*RAF* mutations may play a role in the carcinogenesis of cholangiocarcinoma of the liver, but not in HCC (Tannapfel *et al.,* 2003).

Inactivation of p16, either as a result of LOH at chromosome 9p or *de novo* methylation of the promoter, is detected in up to 60% of all HCC examined; p14 alterations were found in ~15% of HCC (Tannapfel *et al.,* 2001). Our observations demonstrate that the INK4a-ARF/p53-pathway was disrupted in 86% of HCC, either by p53 mutations or by INK4a-ARF inactivation. It is interesting that an inverse relationship between p53 and p14 existed in our patients: Inactivation of p14 was nearly restricted to tumors with wild-type p53. Thus, the loss of p14 and mutations of p53 could be mutually exclusive events, suggesting that they may be functionally equivalent in hepatocarcinogenesis (Tannapfel *et al.,* 2002). The overall frequency of 9p21 alterations, including deletion and methylation, was 78%. Silencing of INK4a-ARF gene products (coding for critical regulators of cell cycle progression) is therefore one of the most frequent genetic defects in HCC.

p53 and Homologues

The *p53* tumor-suppressor gene is frequently mutated in human cancers. Additionally, in many cancers, p53 function is altered through binding to viral oncoproteins or abrogation of p53 degradation by mdm-2/hdm-2 in concert with p14, as described earlier. The identification of two homologues, p63 and p73, revealed that p53 is a member of a family of related transcription factors. In contrast to *p53, p63* and *p73* genes are rarely mutated in human cancer (Tannapfel *et al.,* 1999a). In HCC, p53 mutations were found in ~30% of HCC worldwide. The frequency of all p53 mutations varies between 20% in North America and 67% in Africa. Up to now, all reported mutations (mostly missense leading to stabilization of protein) are somatic, indicating that germline p53 mutations appear not to predispose for HCC. Both the frequency and the type of mutations are different depending on the geographic location and etiology of the tumors (Feitelson *et al.,* 2002; Weihrauch *et al.,* 2000).

Specific-specific p53 mutations have been identified in several studies, linking the mutation pattern to suspected etiologic factors. A selective guanine-to-thymine transversion mutation in codon 249 (AGG to AGT [transversion underlined] leading to an arginine-to-serine substitution) of the p53 gene has been identified as a "hotspot" mutation for HCC. Epidemiologic and experimental evidence have suggested that in HCC this mutation is strongly associated with exposure to aflatoxin B1 in combination with a high level of chronic hepatitis B virus infection in the population. The presence of this "hotspot" mutation in HCC is extremely low in patients in Europe, United States, Japan, and Australia; only three mutations (one in Europe and two in Japan) were identified among 664 patients with HCC. Patients who have not been exposed to aflatoxin B1 or hepatitis virus have a lower prevalence of p53 gene mutations, indicating other genes involved in the process of hepatocarcinogenesis (Buendia, 2000).

For p73 and p63, no specific mutations have been described so far. However, an overexpression of p73 (wild type) has been described in a subset of HCC, indicating a poor prognosis of these patients. According to our data, p53 mutations in a given tumor are neither related to absence nor presence of p73 or p63 (Pützer *et al.,* 2003; Tannapfel *et al.,* 1999b).

Wnt Pathway: APC, β-Catenin, Axin 1, and E-Cadherin

Adenomatous polyposis coli (APC) protein has been thought to function as a tumor suppressor through its involvement in the Wnt/β-catenin signaling pathway.

The APC/β-catenin pathway is highly regulated and includes molecules such as GSK3, CBP, Groucho, Axin, Conductin, and TCF. Furthermore, c-MYC and cyclin D1 have been identified as key transcriptional targets of this pathway, indicating a broad overlap between several tumor-permissive pathways. Wnt proteins are involved in a large number of events during tumor development, not only in HCC but also in other types of cancers. Activation of the Wnt pathway can be caused by β-catenin mutation or by an inactivating mutation of the *axin* gene. In HCCs, somatic mutations of β-catenin were observed in 19–26%, mostly missense mutations and interstitial deletions of exon 3. These mutations that occur at the N-terminal region of β-catenin lead to a nuclear accumulation of aberrant β-catenin proteins that stimulate the activity of other transcription factors. Axin, an important regulator of β-catenin, is mutated in ~10% of HCC, leading to an activation of the Wnt pathway. However, mutations in the *axin* gene were identified only in HCC that lacked mutations in the *β-catenin* gene (Chen *et al.,* 2002). It has been shown that transduction of the wild-type *Axin* gene (AXIN1) induces apoptosis in HCC cells, indicating that Axin 1 may be an effective growth suppressor of hepatocytes (Taniguchi *et al.,* 2002).

Somatic APC mutations are rare events in HCC, but it has been reported that biallelic inactivation of the APC gene contributed to the development of HCC in a patient with familial adenomatous polyposis (FAP) and a known germline mutation of the *APC* gene at codon 208. E-cadherin, the cytoplasmic anchor protein of β-catenin, is rarely mutated in HCC. However, loss of function because of LOH or *de novo* methylation occurred in ~30% of all HCCs (Feitelson, 2002; Tannapfel *et al.,* 2002).

Alterations of the Transforming Growth Factor-β/Insulin-like Growth Factor-Axis

Both growth inhibition and apoptosis are induced by TGF-β in hepatocytes; TGF-β initiates signaling through heteromeric complexes of transmembrane type I and type II serine/threonine kinase receptors. Activated TGF-β type I receptor phosphorylates receptor-regulated Smads (2 and 3). However, genetic alterations of the TGF-β pathway are mediated by mutations of the *Smad2* and *Smad4* genes, which occur in ~10% of all HCCs. Mutations of the TGF-β receptor (TGF-β1RII) gene itself are detected in patients with HCC and may also abrogate TGF-β signaling.

A potent activator of TGF-β is the mannose-6-phosphate/insulin-like growth factor 2 receptor (M6P/IGF2R). This receptor suppresses cell growth through binding to the IGF2 and latent complex of TGF-β. The deregulation of the IGF axis, including the autocrine production of IGFs, IGF-binding proteins (IGFBPs), IGFBP proteases, and the expression of the IGF receptors (IGFR), has also been identified in the development of HCC. Mutations of the M6P/IGF2R and LOH have been reported in ~30% of patients in North America with HCC. However, a recently published study from Japan failed to identify relevant alterations of the M6P/IGF2R gene. Increased expression of IGF-II, IGF-I receptor, alterations of IGFBP production, and the proteolytic degradation of IGFBPs result in an excess of bioactive IGFs. The previously mentioned defective function of the IGF degrading M6P/IGF2R may further potentiate the mitogenic effects of IGFs in the development of HCC (for review, see Bissell, 2001).

PTEN/MMAC1/TEP1 (PTEN) is a tumor-suppressor gene that is located on chromosome band 10q23.3. Alterations, mainly mutations but also LOH, of PTEN have been reported in ~10% of HCCs. It has been demonstrated that PTEN significantly reduced IGF secretion and also expression of secretory and cellular vascular endothelial growth factor (VEGF) proteins in HCC cell lines and could therefore inhibit tumorigenicity (Buendia, 2000). Taken together, these findings demonstrate that several genes of the complex growth regulatory TGF-β/IGF pathway could be altered during hepatocellular carcinogenesis. The situation is further complicated as a result of the observation that activation of TGF-β and IGF signaling is observed even in liver cirrhosis and that complex interactions may exist between hepatitis virus particles in a preneoplastic stage (Enomoto *et al.,* 2001).

Distinct Hepatocarcinogenic Pathways in Hepatocellular Carcinoma with or without Cirrhosis?

A number of genetic alterations have been described in HCC, and more than 20 genes within at least four carcinogenesis pathways have been shown to be altered in HCC. One of the most frequently affected genes in HCC is *p53,* and the INK4a-ARF pathway is most frequently altered in HCCs. However, the prevalence of genetic alterations described in the literature showed a considerable variance (Okabe *et al.,* 2001). This may be explained by different etiologic factors (hepatitis B or C virus, aflatoxin intake) leading to liver cirrhosis, which is present in up to 90% of all HCCs in high-incidence areas. In contrast, in low-incidence areas (e.g., Western Europe) the incidence of HCC in a cirrhotic liver is much lower (~60%). In the current literature, these differences have not been discussed in detail, which may be because of a lack of patients having HCC without cirrhosis. Recent advances in DNA

sequencing technology and the development of gene expression arrays have provided more powerful tools to study the expression of thousands of genes in HCC in a single experiment (Gozuacik *et al.,* 2001; Kim *et al.,* 2001; Wu *et al.,* 2001, and in this volume). Gene expression arrays are created by depositing unique cDNA fragments on a nylon filter or on glass slides. The filter is then hybridized with labeled cDNA from HCC tissue of interest. The readout is performed by high-throughput (phospho)imagers. Using this new technique in combination with bioinformatics, the first results indicate two different "genetic makeups" for HCC, depending on whether they arise in cirrhosis or in noncirrhotic liver. Despite our small number of patients (a total of 210), a trend toward a lower rate of p53 mutations (and p73 expression), higher prevalence of β-catenin mutations, p14 inactivation, and global gene methylation were observed in HCC without cirrhosis. Evidently, further studies on a larger number of patients are necessary to define distinct pathways of hepatocarcinogenesis more precisely (Laurent-Puig *et al.,* 2001).

Molecular Markers in the Differential Diagnosis of Hepatocellular Carcinomas

The main differential diagnosis in liver nodules is benign liver tumors (focal nodular hyperplasia, liver cell adenoma, dysplastic nodules) and primary and secondary liver cancer. The histologic appearance of tumorlike nodules is, at least in most cases, typical, and the differential diagnosis is relatively easy in everyday practice. However, the differential diagnosis of liver cell adenoma (LCA) versus well-differentiated HCC may cause problems, at least in fine-needle biopsies. Molecular markers are of limited value in this setting because there are no clear "cutoff" data to differentiate between LCA and HCC. In LCA, genetic alterations are also present, e.g., hypermethylation of $p16^{INK4a}$ (Tannapfel *et al.,* 2002). β-catenin and p53 mutations may occur in a subset of LCA, making these markers unsuitable for differential diagnosis (Chen *et al.,* 2002). It may be difficult to exclude metastases from primary liver tumors in some cases. When there is doubt about the hepatocyte origin of the tumor, further evidence can be gained by immunohistochemical analysis of (polyclonal) carcinoembryonic antigen, liver cell cytokeratins 8 and 18, albumin, or fibrinogen. *In situ* hybridization may show albumin messenger ribonucleic acid in the tumor cells as evidence for hepatocellular origin. To exclude primary cholangiocarcinoma of the liver, immunohistochemical analysis of biliary cytokeratins 7 and 19, and epithelial membrane antigen may be useful because these markers are negative in HCC. The specificity of alpha feto protein (AFP) is high, but, unfortunately, the sensitivity of AFP staining in HCC tumor tissue is low. The expression pattern may be weak, and a specific staining may be detected only in ~30% of all HCCs. The proliferative activity of HCC is not of special value in the differential diagnosis of HCC. The expression of Ki-67 (MIB1) or proliferating cell nuclear antigen correlates with histologic grade of differentiation. In general, the proliferation rate in liver cirrhosis and LCA may be as high as in well-differentiated HCC (Tannapfel *et al.,* 1999a; Tannapfel *et al.,* 1999b).

Other proteins, such as p27, thrombospondin, MMPs, TGF-α and -β, cathepsin B, inhibin, or CD44 have also been shown to be expressed in HCC (Buendia, 2000; Tannapfel *et al.,* 2000). However, they are of limited value in routine surgical pathology because they are not specifically expressed in HCC.

References

Bissell, D.M. 2001. Chronic liver injury, TGF-beta, and cancer *Exp. Mol. Med. 33*:179–90.

Buendia, M.A. 2000. Genetics of hepatocellular carcinoma. *Semin. Cancer Biol. 10*:185–200.

Chen, Y.W., Jeng, Y.M., Yeh, S.H., and Chen, P.J. 2002. P53 gene and Wnt signaling in benign neoplasms: Beta-catenin mutations in hepatic adenoma but not in focal nodular hyperplasia. *Hepatology 36*:927–935.

Davies, H., Bignell, G.R., Cox, C., Stephens, P., Edkins, S., Clegg, S., Teague, J., Woffendin, H., Garnett, M.J., Bottomley, W., Davis, N., Dicks, E., Ewing, R., Floyd, Y., Gray, K., Hall, S., Hawes, R., Hughes, J., Kosmidou, V., Menzies, A., Mould, C., Parker, A., Stevens, C., Watt, S., Hooper, S., Wilson, R., Jayatilake, H., Gusterson, B.A., Cooper, C., Shipley, J., Hargrave, D., Pritchard-Jones, K., Maitland, N., Chenevix-Trench, G., Riggins, G.J., Bigner, D.D., Palmieri, G., Cossu, A., Flanagan, A., Nicholson, A., Ho, J.W., Leung, S.Y., Yuen, S.T., Weber, B.L., Seigler, H.F., Darrow, T.L., Paterson, H., Marais, R., Marshall, C.J., Wooster, R., Stratton, M.R., and Futreal, P.A. 2002. Mutations of the BRAF gene in human cancer. *Nature 417*:949–954.

Deane, N.G., Parker, M.A., Aramandla, R., Diehl, L., Lee, W.J., Washington, M.K., Nanney, L.B., Shyr, Y., and Beauchamp, R.D. 2001. Hepatocellular carcinoma results from chronic cyclin D1 overexpression in transgenic mice. *Cancer Res. 61*:5389–5395.

Enomoto, A., Esumi, M., Yamashita, K., Takagi, K., Takano, S., and Iwai, S. 2001. Abnormal nucleotide repeat sequence in the TGF-betaRII gene in hepatocellular carcinoma and in uninvolved liver tissue. *J. Pathol. 195*:349–354.

Feitelson, M.A., Sun, B., Satiroglu Tufan, N.L., Liu, J., Pan, J., and Lian, Z. 2002. Genetic mechanisms of hepatocarcinogenesis. *Oncogene 21*:2593–2604.

Gozuacik, D., Murakami, Y., Saigo, K., Chami, M., Mugnier, C., Lagorce, D., Okanoue, T., Urashima, T., Brechot, C., and Paterlini-Brechot, P. 2001. Identification of human cancer-related genes by naturally occurring hepatitis B virus DNA tagging. *Oncogene 20*:6233–6240.

Graveel, C.R., Jatkoe, T., Madore, S.J., Holt, A.L., and Farnham, P.J. 2001. Expression profiling and identification of novel genes in hepatocellular carcinomas. *Oncogene 20*:2704–2712.

Kim, M.Y., Park, E., Park, J.H., Park, D.H., Moon, W.S., Cho, B.H., Shin, H.S., and Kim, D.G. 2001. Expression profile of nine novel genes differentially expressed in hepatitis B virus-associated hepatocellular carcinomas. *Oncogene 20*:4568–4575.

Laurent-Puig, P., Legoix, P., Bluteau, O., Belghiti, J., Franco, D., Binot, F., Monges, G., Thomas, G., Bioulac-Sage, P., and Zucman-Rossi, J. 2001. Genetic alterations associated with hepatocellular carcinomas define distinct pathways of hepatocarcinogenesis. *Gastroenterology 120*:1763–1773.

Okabe, H., Satoh, S., Kato, T., Kitahara, O., Yanagawa, R., Yamaoka, Y., Tsunoda, T., Furukawa, Y., and Nakamura, Y. 2001. Genome-wide analysis of gene expression in human hepatocellular carcinomas using cDNA microarray: Identification of genes involved in viral carcinogenesis and tumor progression. *Cancer Res. 61*:2129–2137.

Püzer, B.M., Tuve, S., Tannapfel, A., and Stiewe, T. 2003. Increased DeltaN-p73 expression in tumors by upregulation of the E2F1-regulated, TA-promoter-derived DeltaN′-p73 transcript. *Cell Death Differ. 10*:612–614.

Taniguchi, K., Roberts, L.R., Aderca, I.N., Dong, X., Qian, C., Murphy, L.M., Nagorney, D.M., Burgart, L.J., Roche, P.C., Smith, D.I., Ross, J.A., and Liu, W. 2002. Mutational spectrum of beta-catenin, AXIN1, and AXIN2 in hepatocellular carcinomas and hepatoblastomas. *Oncogene 21*:4863–4871.

Tannapfel, A., Benicke, M., Weinans, L., Katalinic, A., Uhlmann, D., Hauss, J., and Wittekind, Ch. 2001. INK4a-ARF alterations and p53 mutations in hepatocellular carcinomas. *Oncogene 20*:7104–7109.

Tannapfel, A., Busse, C., Geissler, F., Witzigmann, H., Hauss, J., and Wittekind, Ch. 2002. INK4a-ARF alterations in liver cell adenoma. *Gut 51*:253–258.

Tannapfel, A., Geissler, F., Köckerling, F., Katalinic, A., Hauss, J., and Wittekind, Ch. 1999a. Apoptosis and proliferation in relation to histopathological variables and prognosis in hepatocellular carcinoma. *J. Pathol. 187*:439–445.

Tannapfel, A., Grund, D., Katalinic, A., Uhlmann, D., Köckerling, F., Haugwitz, U., Wasner, M., Hauss, J., Engeland, K., and Wittekind, Ch. 2000. Decreased expression of p27 protein is associated with advanced tumor stage in hepatocellular carcinoma. *Int. J. Cancer 89*:350–355.

Tannapfel, A., Sommerer, F., Benicke, M., Katalinic, A., Uhlmann, D., Witzigmann, H., Hauss, J., and Wittekind, C. 2003. Mutations of the BRAF gene in cholangiocarcinoma but not in hepatocellular carcinoma. *Gut 52*:706–712.

Tannapfel, A., Wasner, M., Krause, K., Geissler, F., Katalinic, A., Hauss, J., Mössner, J., Engeland, K., and Wittekind, Ch. 1999b. Expression of p73 and its relation to histopathology and prognosis in hepatocellular carcinoma. *J. Natl. Cancer Inst. 91*:1154–1158.

Tannapfel, A., and Wittekind, Ch. 2002. Genes involved in hepatocellular carcinoma: Deregulation in cell cycling and apoptosis. *Virchows Arch. 440*:345–352.

Weihrauch, M., Lehnert, G., Köckerling, F., Wittekind, Ch., and Tannapfel, A. 2000. p53 mutation pattern in hepatocellular carcinoma in workers exposed to vinyl chloride. *Cancer 88*:1030–1036.

WHO: Pathology and Genetics: Hamilton, S.R., and Aaltonen, L.A. 2000. *Tumours of the Digestive System.* Lyon: IARC Press.

Wu, C.G., Salvay, D.M., Forgues, M., Valerie, K., Farnsworth, J., Markin, R.S., and Wang, X.W. 2001. Distinctive gene expression profiles associated with hepatitis B virus x protein. *Oncogene 20*:3674–3682.

4

Role of *p53* and *ZBP-89* in Hepatocellular Carcinoma

George G. Chen, Paul B.S. Lai, and Juanita L. Merchant

Introduction

Hepatocellular carcinoma (HCC) is one of the most common cancers in Africa and Asia, especially in sub-Saharan Africa, Southeast Asia, and China. Unlike in Western countries, ~90% of HCC in Asia is associated with hepatitis B virus (HBV) infection instead of hepatitis C virus (HCV) infection. According to the *Cancer Incidence and Mortality in Hong Kong* issued by the Hong Kong Cancer Registry of Hospital Authority, HCC is the second leading cause of cancer death in Hong Kong, with the crude mortality rate of 32.7 per 100,000 in men and 10.5 in women (Hong Kong Cancer Registry, 2000). Surgical resection of tumor is still the most effective treatment for HCC. However, ~70% of patients will die from recurrent tumor within 5 years after liver tumor resection. Furthermore, most patients with HCC are unresectable at the time of diagnosis because of widespread intrahepatic or extrahepatic involvement or limited hepatic reserves resulting from coexisting advanced cirrhosis. The median survival for patients with unresectable tumor is less than 3 months. Searching an early detection of cancer and a novel treatment for HCC has been challenging scientists and clinicians for years, and a reliable early detection tool and an effective remedy are yet to be established.

Over the past two decades, a great deal of effort has been made to reveal how HBV contributes to the development of HCC and how to prevent its formation. It is now known that HBV contains four overlapping open-reading frames that encode the structural and nonstructural viral proteins. Among them, the x protein (HBx) has been shown to play a central role in HBV infection and a causative role in liver oncogenesis (Andrisani and Barnabas, 1999). There is evidence for an important role of HBx in the expression and replication of viral deoxyribonucleic acid (DNA). Furthermore, transfection experiments have suggested that HBx can transform NIH3T3 immortalized fibroblasts and differentiate murine hepatocytes *in vitro* (Feitelson and Duan, 1997). The HBx gene is frequently integrated into the cellular genome and expressed in HCC (Feitelson and Duan, 1997; Koike *et al.,* 1994) and interferes with various tumor suppressor genes and other molecules related to cell proliferation and growth, such as p53, insulin-like growth factor 1, nuclear factor kappa B, and Bid (Chen *et al.,* 2001; Huo *et al.,* 2001; Lian *et al.,* 2001; Stuver *et al.,* 2000).

The p53 tumor suppressor gene is the most frequent target for genetic alterations in human cancer. The wild-type p53 protein can exert a variety of anti-proliferative effects, including induction of cell cycle arrest and

Handbook of Immunohistochemistry and *in situ* Hybridization of Human Carcinomas, Volume 3: Molecular Genetics, Liver Carcinoma, and Pancreatic Carcinoma

apoptosis. These effects are usually evident in cells exposed to DNA damage and other types of stress, which impinge on the otherwise latent p53 protein and cause its accumulation and biochemical activation (Blagosklonny 2002; Hickman *et al.,* 2002). The therapeutic efficacy of anti-cancer agents depends strongly on their ability to trigger apoptosis in target tumor cells. Many physical and chemical DNA damaging agents used routinely in cancer therapy are potent apoptosis inducers via the p53-related pathway (Blagosklonny, 2002). Given the documented contribution of p53 to radiation-induced apoptosis (Pruschy *et al.,* 2001), it is conceivable that cells maintaining functional p53 will be more prone to be killed by many anti-cancer agents. Numerous subsequent basic and clinical studies have provided further support for this notion (Blagosklonny 2002; Ferreira *et al.,* 1999). However, accumulation of certain mutant p53 may also enhance the sensitivity of tumor cells to chemotherapy (Kandioler-Eckersberger *et al.,* 2000; Kielb *et al.,* 2001; Trepel 1997). For example, paclitaxel or other DNA-damaging agents have been shown to be more effective against cancer cells with p53 mutations than those without. The mechanism responsible for the sensitivity of cancer cells with p53 mutations to therapeutic agents is unknown. However, wild-type p53 may enhance chemosensitivity by promoting apoptosis via transcription-independent mechanisms as well as transcriptional activation of proapoptotic genes such as Bax and transcriptional repression of antiapoptotic genes such as Bcl-2 (Srinivas *et al.,* 2000). Drug-induced suicide mediated by the CD95/CD95 ligand system may also involve the p53-controlled pathway (Muller *et al.,* 1998).

ZBP-89 is a four zinc-finger transcription factor that regulates the expression of several genes related to cell growth through binding to GC-rich DNA elements (Law *et al.,* 1998). It can function at the transcriptional level to regulate the expression of several genes and exert a negative effect on cell proliferation. Altered expression of ZBP-89 has been documented in malignant cells, and the inhibitory mechanism of ZBP-89 is now known to involve activation of $p21^{waf1}$ and stabilization of p53 (Bai and Merchant, 2000; 2001). It has been suggested that ZBP-89 stabilizes p53 through direct protein contact, which leads to retention of p53 in the nucleus (Bai and Merchant, 2001).

MATERIALS

1. ABC reagent (ABC-HRP or ABC-AP) (Vector Laboratories, Ltd., Peterborough, U.K.).

2. Antibodies: 1) normal serum (goat, rabbit or horse) for blocking; 2) primary antibody (monoclonal or polyclonal): rabbit polyclonal ZBP-89 antibody, which was raised against amino acids 1-521 of rat ZBP-89 (Taniuchi *et al.,* 1997), mouse anti-p53 antibody (Santa Cruz Biotechnology, Santa Cruz, CA); 3) secondary antibody (rabbit anti-mouse, goat anti-rabbit, etc.).

3. Antibody diluent: phosphate buffer saline (PBS) containing 0.1% bovine serum albumin (BSA) and 0.1% sodium azide. Store antibody at 4°C at working dilution.

4. Avidin/biotin blocking kit (Vector Laboratories, Ltd., Peterborough, U.K.).

5. BCIP/NBT substrate (Vector Laboratories, Ltd., Peterborough, U.K.).

6. Blocking serum: 1000 µl of blocking serum consists of 900 µl PBS, 100 µl of goat or rabbit or horse serum, and 4 drops of avidin D.

7. Citrate buffer, 0.01 M, (pH 6.0): 1) 1.05 g citric acid; 2) 2M NaOH. Dissolve citric acid in 450 ml distilled water and add enough NaOH until pH 6.0 is reached, then top up to 500 ml.

8. Diaminobenzidine tetrahydrochloride (DAB). To make a stock, take 5 g of DAB and add 100 ml distilled water. Using a magnetic stirrer, stir for 30 min in a fume hood until completely dissolved; then aliquot into small tubes and store at −20°C.

9. DPX mountant (Fisher Scientific, Pittsburgh, PA).

10. ECL kit: available from Amersham Biosciences (Piscataway, NJ).

11. Ethanol: 100%, 98%, 95%, and 70%.

12. Formalin: 10% neutral buffered.

13. Gill's hematoxylene (Fisher Scientific, Pittsburgh, PA).

14. Hematoxylene (Fisher Scientific, Pittsburgh, PA).

15. Hydrogen peroxide (Sigma, St Louis, MO): stock solution: 30% aqueous (w/v), stored at 4°C.

16. Levamisole solution (l00X) (Vector Laboratories, Ltd., Peterborough, U.K.).

17. Lysis buffer: 30 mM Tris-HCl, 150 mM NaCl, 1 mM PMSF, 1% Triton X-l00, 10% glycerol, and a protease inhibitor cocktail.

18. Methanol 70% in PBS.

19. NovaRED (Vector Laboratories, Ltd., Peterborough, U.K.).

20. OCT embedding medium (Vector Laboratories, Ltd., Peterborough, U.K.).

21. PBS/BSA solution: add 1–2 mg thimerosal merthiolate and 0.1 g BSA in 1 L PBS, and use a stirrer to dissolve both.

22. PBS: 1) 8.7 g sodium chloride; 2) 0.272 g potassium dihydrogen phosphate; and 3) 1.136 g disodium hydrogen phosphate. Dissolve all salts separately in distilled water, then mix, make up to 1 L, and check pH is 7.2.

23. Protein A-Sepharose (Sigma, St Louis, MO).
24. SDS-PAGE buffer (2X) (Sigma, St Louis, MO).
25. Thimerosal merthiolate (Vector Laboratories, Ltd., Peterborough, U.K.).
26. Xylene (Vector Laboratories, Ltd., Peterborough, U.K.).

METHODS

Handling of Liver Tissues

1. Wear gloves and use universal precautions when handling fresh tissue samples.
2. Liver tissue samples are normally collected at the time of surgical resection of tumors. After collection, samples should immediately stored in liquid nitrogen (−160°C) until use.
3. Liver tissues can be snap frozen by placing them in histocassettes or cryogenic tubes and dropping these cassettes or tubes in liquid nitrogen. Tissues can be stored indefinitely in liquid nitrogen. Alternatively, and preferably for reliable immunohistochemical staining, fresh tissue can be placed on a clean chuck layered with OCT embedding medium and cold embedded in a precooled cryostat. Freshly embedded tissue generally sections better than snap-frozen tissue, which is subsequently embedded. Tissues can be snap frozen in OCT for better histology, but keep in mind that OCT might interfere with molecular biology techniques requiring snap-frozen tissue. Therefore, snap freeze in OCT only if the tissue will be used for histology. Otherwise, cut liver tissue in half and snap freeze it with and without OCT respectively.
4. Fix overnight fresh liver tissue or thawed tissue (from liquid nitrogen) in 10% neutral buffered formalin. Larger tissue sections require a longer period of time; the time of fixation will affect the characteristics of sectioning the tissue (crumbling or cracking of the tissue) and possibly antigen recognition.
5. After carrying out tissue processing through graded alcohol, xylene, and paraffin, the tissue is subjected to paraffin emedding. Tissue is sectioned at 4 µm thick and is adhered to the microscope slide previously treated with 3-aminopropyltriethoxysilane.

Immunohistochemical Staining of p53 or ZBP-89

1. Deparaffinization:
   a) Incubate 2–3× in xylene for 3 min each.
   b) Incubate 3× in 100% ethanol for 1 min each.
   c) Hydrate by placing in 95% and 70% ethanol for 1 min each.
   d) Place in tap water 2× for 2 min each.
2. Antigen retrieval:
   a) Place the slides in the container containing citrate buffer and boil for 20 min using a microwave oven.
   b) Leave at room temperature for 20 min to cool.
3. Rinsing
   a) Rinse with distilled or Milliq water for 5 min, then wash with H_2O_2 + methanol solution (2 ml 30% H_2O_2 + 200 ml methanol) for 20–30 min.
   b) Rinse with distilled water for 5 min.
   c) Rinse with PBS for 5 min.
4. Equilibrate in PBS/BSA solution for ~5 min.
5. Blocking:
   a) Wipe off excess liquid and surround the tissue with PAP PEN.
   b) Add 100 µl of blocking serum to each slide.
   c) Incubate at room temperature for 30 min.
6. Application of primary antibody:
   a) Appropriately dilute primary antibody to a working concentration.
   b) Add 4 drops of biotin for 1 ml of primary antibody.
   c) Add 100 µl of primary antibody (with biotin) to each slide.
   d) Incubate for 1 hr at room temperature or overnight at 4°C.
   e) Tap off excess antibody and rinse slides in PBS/BSA solution for at least 5 min.
7. Application of secondary antibody (rabbit immunoglobulin G, or IgG)
   a) Apply 100 µl of biotinylated secondary antibody (appropriate dilution in PBS) for 30 min at room temperature.
   b) Rinse slides in PBS/BSA solution for at least 5 min.
8. Application of ABC-HRP reagent:
   a) Add 20 µl of solution A (avidin DH) and 20 µl of solution B (biotinylated horseradish peroxidase H) to 1000 µl PBS/BSA solution and let it sit for at least 30 min at room temperature.
   b) Apply 100 µl of the previously mentioned ABC reagent for each slide and leave for 30 min at room temperature.
   c) Rinse in PBS/BSA solution for 5 min at room temperature. Do not dry the slides.
9. Application of DAB or NovaRED:
   a) Apply 100 µl of DAB or NovaRED to each slide for equal time (each for 5 min).
   b) Rinse in PBS or distilled water.

10. Counterstaining:
    a) Counterstain with Gill's hematoxylin for 1 or 2 min.
    b) Rinse in tap water until cleared from blue color (usually need 2 rinses).

11. Dehydration:
    a) Place the slide in different concentrations of ethanol, starting with 70% ethanol for 1 min. Followed by 98% for 1 min and 100% 3× each for 1 min.
    b) Incubate with xylene 2× for 3 min. Do not dry the slides.

12. Mounting:
    a) Place the slides down with the section facing upward.
    b) Add a drop of the DPX mount.
    c) Cover the section with coverslip.

Dual-Immunohistochemical Staining to Detect ZBP-89 and p53 in the Same Cell

1. Stain the first antigen (ZBP-89) following **Steps 1–9** listen in *Immunohistochemical staining of p53 or ZBP-89.*

2. Add 100 µl of blocking serum to each slide and incubate at room temperature for 30 min.

3. Application of the second primary antibody (anti-p53):
    a) Appropriately dilute primary antibody to a working concentration.
    b) Add 4 drops of biotin for 1 ml of primary antibody.
    c) Add 100 µl of primary antibody to each slide.
    d) Incubate for 1 hr at room temperature or overnight at 4°C.
    e) Tap off excess antibody and rinse slides in PBS/BSA solution for at least 5 min.

4. Application of secondary antibody (horse anti-mouse IgG):
    a) Apply 100 µl of secondary antibody (appropriate dilution in PBS) for 30 min at room temperature.
    b) Rinse slides in PBS/BSA solution for at least 5 min.

5. Application of ABC-AP reagent
    a) Add 20 µl of solution A (avidin DH) and 20 µl of solution B (biotinylated horseradish peroxidase H) to 1000 µl PBS/BSA solution and let it sit for at least 30 min at room temperature.
    b) Apply 100 µl of the previously mentioned ABC reagent for each slide and leave for 30 min at room temperature.
    c) Rinse in PBS/BSA solution for 5 min at room temperature. Do not dry the slides.

6. Application of BCIP/NBT substrate and levamisole solution (l00X):
    a) Add one drop of levamisole solution (l00X) to 5 ml of BCIP/NBT substrate solution.
    b) Apply 100 µl BCIP/NBT/levamisole to each slide for equal time (each for 20 min). Incubation time with BCIP/NBT/levamisole may need to be adjusted according to the degree of the molecule staining because too strong staining of the second antigen may affect the first antigen detection.
    c) Rinse in PBS or water.

7. Follow **Steps 10–12** listed in *Immunohistochemical staining of p53 or ZBP-89.*

Co-Immunoprecipitation of p53 and ZBP-89

1. Harvest cells, wash with PBS 1×, and transfer cells into microcentrifuge tubes.
2. Lyse cell samples in 1 ml lysis buffer for 10 min at 4°C with pipetting cells up and down extensively.
3. Spin down cell extracts at 14,000 rpm for 10 min at 4°C.
4. Add 10 µg of anti-p53 antibody to 1 ml of extract.
5. Incubate with end-over-end mixing for 2 hr at 4°C.
6. Add 50 µl protein A-Sepharose and incubate with end-over-end mixing for 1 hr at 4°C.
7. Wash immunoprecipates 3× with 1 ml of lysis buffer.
8. Add 50 µl of 2 X SDS-PAGE buffer and boil for 5 min.
9. Load onto a SDS-PAGE gel.
10. Western Blot to transfer proteins to membranes.
11. Probe the membrane with ZBP-89 antibody and detect signals using the ECL kit.

Notes:

1. Protocols for immunohistochemistry vary widely as a result of the differences between antigens and their recognition by antibody. Some epitopes are destroyed by the high temperatures and organic solvents used for paraffin embedding, whereas others cannot survive freezing and thawing. Each fixative is effective with a different mechanism, which may either help to uncover the epitope or may destroy it or make it less accessible. Some antibodies may even adhere to the blocking agent used, so that it causes rather than eliminates background.

2. Negative control: The simplest negative control is the absence of expression in tissues, in which the molecule of interest is known not to be expressed. A better negative control is the elimination of the signal by preincubating the antibody with an excess of the peptide or protein with which it is raised. A Western Blot can suggest specificity of the interaction if only one band is seen;

nonetheless, the difficulty of optimizing conditions for a Western Blot should demonstrate the possibility that conditions in the immunohistochemistry reaction are less than optimal. However, there can also be doubts as to whether the antigen is visualized everywhere; in particular, one must determine whether the fixation protocol used actually permeabilizes the nuclear membrane to a sufficient degree for nuclear antigens to be fully visible.

3. Positive control: Cells or tissues known to express the protein molecule of interest can be used as positive control.

4. If there is a high level of background staining, try one of the following solutions:

a) Dilute the primary antibody further, or reduce the antibody incubation time. The following problems are often caused by the use of excess antibody: 1) staining is excessively dark; 2) staining occurs throughout the section rather than in expected areas of antigen localization; 3) staining appears to fade, float, or leach off the section during or after substrate reaction; 4) color develops immediately after addition of substrate; and 5) particles of dye are scattered across the section after staining.

b) Reduce substrate staining time. In some instances prolonged staining also inhibits nuclear counterstaining.

c) Raise the pH, or increase the ionic strength of diluent buffers. Sodium chloride (0.1–0.5 M) added to the buffer diluent reduces nonspecific binding on endothelia and collagen fibers.

d) Apply blocking protein before applying primary antibody. The blocking protein should be of the same species used in the link or enzyme labeled antibody diluent and should not be used in the primary antibody diluent.

e) The addition of ethylene glycol, Tween 20, or other detergent to the antibody diluent and washes will help remove unbound antibodies and artifacts that contribute to nonspecific binding as well as remove excess dye from the section.

f) Try an alternative enzyme system, such as alkaline phosphatase, horseradish peroxidase, or β-galactosidase.

g) Factors related to tissue preparation and fixation are as follows: 1) Inadequate penetration of fixative can produce nonspecific staining. 2) Overfixation can destroy antigens contained within the tissue. 3) Tissue that has dried out can exhibit artifact and nonspecific staining. 4) Incomplete removal of paraffin from tissue sections will result in artifacts. 5) Poor dehydration causes smudging of the stain. 6) Thick sections may prevent adequate penetration of primary antibody, producing false reactions or uneven staining over the tissue surface.

RESULTS AND DISCUSSION

In human tumors, the majority of p53 gene alterations are missense mutations, often within the conserved DNA binding core domain of the protein (Ferreira, 1999; Ikawa *et al.,* 1999). The primary selective advantage of such mutations may well be the elimination of cellular wild-type p53 activity. However, at variance with the observations for several other tumor-suppressor genes, cells with p53 mutations typically maintain expression of full-length mutant protein, often at markedly elevated levels. This suggests that at least certain mutant forms of p53 may possess a gain of function. Multiple types of p53 mutations are known to possess distinct biological features, e.g., mutants deficient for transcriptional activation, but competent for induction of apoptosis, and vice versa (Wang and Harris, 1996). Many studies have shown that p53 is frequently mutated in human HCC and is correlated with advanced tumor grade, progression, therapy, and survival (Heinze *et al.,* 1999; Honda *et al.,* 1998; Jeng *et al.,* 2000; Katiyar *et al.,* 2000). It is believed that p53 may also play a role in recurrent HCC, which is the major factor contributing to the high mortality of HCC. Therefore, understanding the role of p53 in recurrent tumor may provide useful molecular information that can be of therapeutic significance. Very few reports have addressed the p53 status in recurrence of HCC. In our experiment, we found that mutations in the p53 gene were detected in 48.5% of recurrent HCC. Exon 7 of p53 gene may be considered a prevalent site of p53 mutation because it accounts for 44% of all alterations found (Figure 27). The distribution of p53 mutation in recurrent HCC is detailed in Figure 28.

The p53 nuclear import or retention is essential for its normal function in growth inhibition or induction of apoptosis (Knippschild *et al.,* 1996; Stewart and Pietenpol, 2001). A defect in the regulation of p53 nuclear import or export may result in tumorigenesis. Dysfunctional transportation of p53 between the nucleus and cytoplasm is known to occur in a subset of human tumors, and in such a situation p53 is sequestered either in the cytoplasm or in the nucleus (Bosari *et al.,* 1995; Lee *et al.,* 1999). In normal cells, wild-type p53 protein is kept at a low concentration by rapid degradation. Therefore, wild-type p53 protein is usually undetected or detected at very low levels.

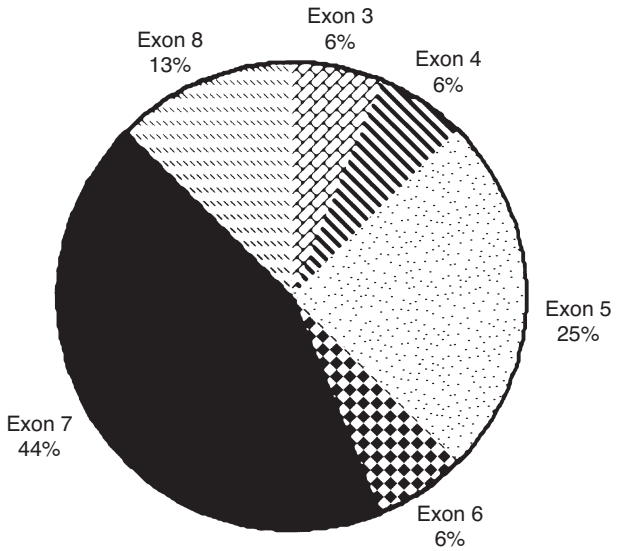

Figure 27. The distribution of p53 mutations in the different exons.

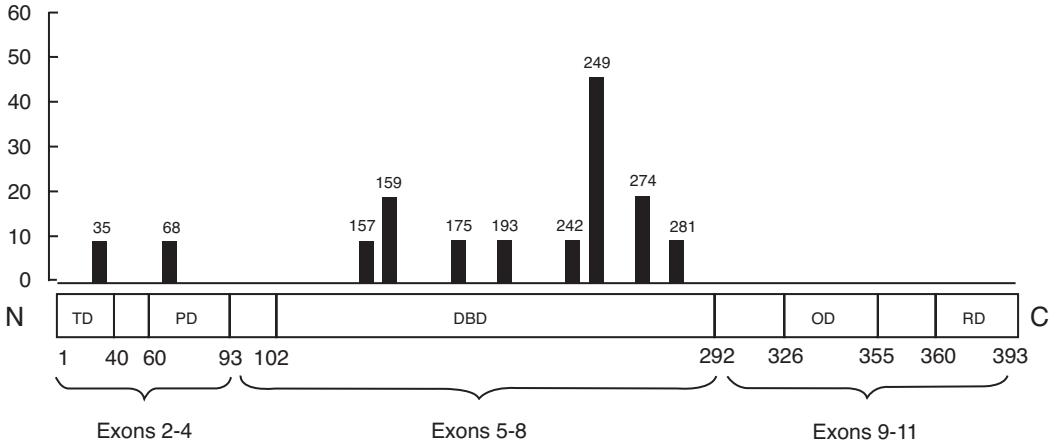

Figure 28. Schematic outline of human p53 protein and p53 mutations in hepatocellular carcinoma (HCC). The upper part of the diagram shows the position and frequency of the mutations found in recurrent HCC. The numbers indicate amino acid residue positions. TD, transactivation domain; PD, PXXP domain involved in apoptosis; DBD, sequence-specific DNA-binding domain with the residues that contact DNA; OD, oligomerization domain; RD, regulatory domain.

However, when there are mutations within the p53 gene, they result in a dysfunctional protein product with a prolonged half-life that enables them to accumulate in the cell. Accumulation of p53 protein either in the cytoplasm or in the nucleus is considered a pathologic index (Stewart and Pietenpol, 2001). In the case of recurrent HCC, nearly 58% (19/33) of patients showed nuclear localization of p53 protein and ~9% (3/33) are positive for p53 protein in the cytoplasm. Figure 29 shows the result of immunohistochemical staining of p53 and ZBP-89 in liver tissues of patients with HCC. Accumulation of p53 protein in the nucleus occurs in the cells either with or without a mutant p53 gene, whereas cytoplasmic p53 protein exists in all recurrent HCC with mutant p53 gene.

Mechanisms responsible for the sequestration of a particular mutant p53 protein in the nucleus or the cytoplasm are very complicated and not yet completely known. The nuclear localization signals are located within the carboxyl terminus of p53 (amino acids 293–393) (Stewart and Pietenpol, 2001). Mutations in this nuclear signal region can affect the nuclear import or export of p53. However, none of the mutations detected in the HCC study are within this nuclear signal region. ZBP-89 protein can stabilize p53 through a direct protein contact leading to its retention in the nucleus (Bai and Merchant, 2001). ZBP-89 can be co-localized with p53 in the nucleus in about 63% (12/19) of HCC positive for the nuclear p53 protein, suggesting that ZBP-89 may play a role in the nuclear accumulation of p53 protein in a subset of HCC. Indeed, ZBP-89 is able to bind wild-type p53 and some forms of p53 mutants, as demonstrated by co-immunoprecipitation experiments. Mutation in N-terminal of p53 nonbinding domains retains the binding ability to ZBP-89, whereas mutation in DNA binding domain (after codon 175) abolishes the direct interaction between ZBP-89 and p53. These p53 mutations may thus eliminate ZBP-89-mediated stabilization of p53 (Bai and Merchant, 2001).

In agreement with co-immunoprecipitation experiments, ZBP-89 is found to be co-localized not only with the wild-type p53 but also with mutant one. This further confirms that the ZBP-89-interaction domain in some mutant p53 remains intact. The co-localization of ZBP-89 and p53 in the nucleus may be clinically significant in certain types of patients who possess a functional p53. Figure 30 shows the proposed interaction between p53 and ZBP-89 in HCC cells. The function of p53 protein depends on the nuclear localization (Stewart and Pietenpol, 2001). With accumulation of p53 protein in the nucleus, tumor cells are liable to undergo apoptosis and thus more susceptible to radiotherapy and chemotherapy (Lowe *et al.,* 1994; McIlwrath *et al.,* 1994).

In conclusion, by co-localizing p53 protein, the expression of ZBP-89 may be clinically significant and may define a subgroup of recurrent HCC that is more suitable to receive radiotherapy and chemotherapy.

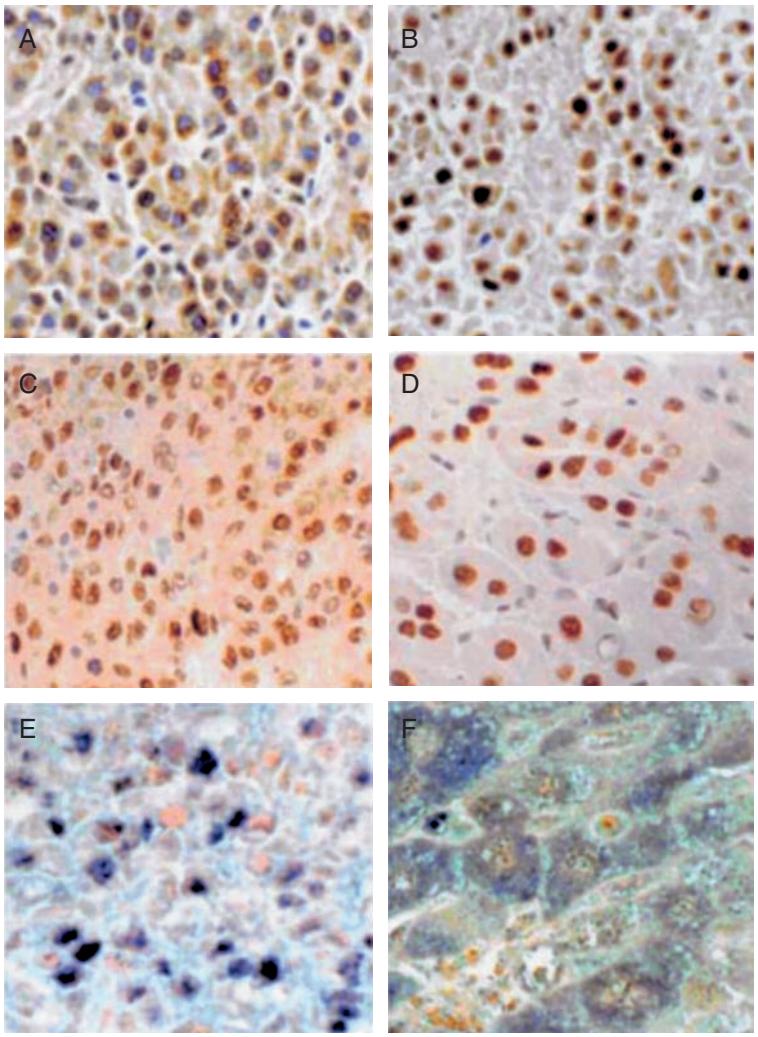

Figure 29. Immunohistochemical analysis of p53 and ZBP-89 in liver tissues obtained from recurrent hepatocellular carcinoma (HCC) with or without mutations in p53. **A:** Expression of ZBP-89 in recurrent HCC with mutant p53 gene. ZBP-89 stained brown. **B:** Expression of ZBP-89 in recurrent HCC with wild-type p53 gene. ZBP-89 stained brown. **C:** Expression of p53 in recurrent HCC with mutant p53 gene. p53 stained brown. **D:** Expression of p53 in recurrent HCC with wild-type p53 gene. p53 stained brown. **E:** Coexpression of ZBP-89 and p53 in recurrent HCC with wild-type p53 gene. ZBP-89 stained brown and p53 blue. **F:** Coexpression of ZBP-89 and p53 in recurrent HCC with mutant p53 gene. ZBP-89 stained brown and p53 blue.

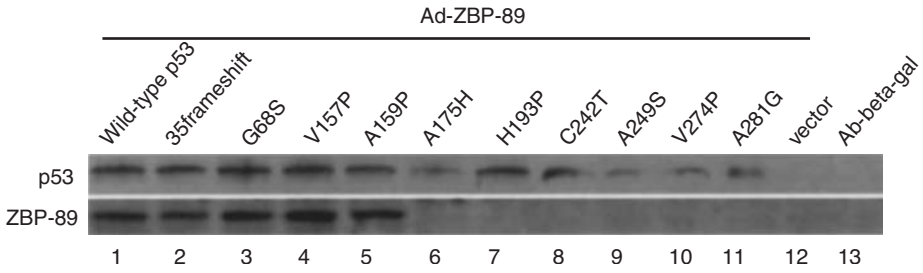

Figure 30. Proposed interaction between p53 and ZBP-89.

References

Andrisani, O.M., and Barnabas, S. 1999. The transcriptional function of the hepatitis B virus X protein and its role in hepatocarcinogenesis (Review). *Int. J. Oncol. 15*:373–379.

Bai, L., and Merchant, J.L. 2000. Transcription factor ZBP-89 cooperates with histone acetyltransferase p300 during butyrate activation of p2lwaf1 transcription in human cells. *J. Biol. Chem. 275*:30725–30733.

Bai, L., and Merchant, J.L. 2001. ZBP-89 promotes growth arrest through stabilization of p53. *Mol. Cell. Biol. 21*: 4670–4683.

Blagosklonny, M.V. 2002. p53: An ubiquitous target of anticancer drugs. *Int. J. Cancer 98*:161–166.

Bosari, S., Viale, G., Roncalli, M., Graziani, D., Borsani, G., Lee, A.K., and Coggi, G. 1995. p53 gene mutations, p53 protein accumulation and compartmentalization in colorectal adenocarcinoma. *Am. J. Pathol. 147*:790–798.

Chen, G.G., Lai, P.B., Chan, P.K., Chak, E.C., Yip, J.H., Ho, R.L., Leung, B.C., and Lau, W.Y. 2001. Decreased expression of Bid in human hepatocellular carcinoma is related to hepatitis B virus X protein. *Eur. J. Cancer 37*:1695–1702.

Feitelson, M.A., and Duan, L.X. 1997. Hepatitis B virus X antigen in the pathogenesis of chronic infections and the development of hepatocellular carcinoma. (Review) *Am. J. Pathol. 150*:1141–1157.

Ferreira, C.G., Tolis, C., and Giaccone, G. 1999. p53 and chemosensitivity. *Ann. Oncol. 10*:1011–1021.

Heinze, T., Jonas, S., Karsten, A., and Neuhaus, P. 1999. Determination of the oncogenes p53 and C-erb B2 in the tumour cytosols of advanced hepatocellular carcinoma (HCC) and correlation to survival time. *Anticancer Res. 19*: 2501–2503.

Hickman, E.S., Moroni, M.C., and Helin, K. 2002. The role of p53 and pRB in apoptosis and cancer. *Curr. Opin. Genet. Dev. 12*:60.

Honda, K., Sbisa, E., Tullo, A., Papeo, P.A., Saccone, C., Poole, S., Pignatelli, M., Mitry, R.R., Ding, S., Isla, A., and Davies, A., and Habib, N.A. 1998. p53 mutation is a poor prognostic indicator for survival in patients with hepatocellular carcinoma undergoing surgical tumour ablation. *Br. J. Cancer 77*: 776–782.

Hong Kong Cancer Registry, Hospital Authority. 2000. Highlights on Cancer Statistics 2000 (www3.ha.org.hk/cancereg/data/2000.pdf)

Huo, T.I., Wang, X.W., Forgues, M., Wu, C.G., Spillare, E.A., Giannini, C., Brechot, C., and Harris, C.C. 2001. Hepatitis B virus X mutants derived from human hepatocellular carcinoma retain the ability to abrogate p53-induced apoptosis. *Oncogene 20*:3620–3628.

Ikawa, S., Nakagawara, A., Ikawa, Y., 1999. p53 family genes: Structural comparison, expression and mutation. *Cell Death Different. 6*:1154–1161.

Jeng, K.S., Sheen, I.S., Chen, B.F., and Wu, J.Y. 2000. Is the p53 gene mutation of prognostic value in hepatocellular carcinoma after resection? *Arch. Surg. 135*:1329.

Kandioler-Eckersberger, D., Ludwig, C., Rudas, M., Kappel, S., Janschek, E., Wenzel, C., Schlagbauer-Wadl, H., Mittlbock, M., Gnant, M., Steger, G., and Jakesz, R. 2000. TP53 mutation and p53 overexpression for prediction of response to neoadjuvant treatment in breast cancer patients. *Clin. Cancer Res 6*:50–56.

Katiyar, S., Dash, B.C., Thakur, V., Guptan, R.C., Sarin, S.K., and Das, B.C. 2000. p53 tumor suppressor gene mutations in hepatocellular carcinoma patients in India. *Cancer 88*:1565–1573.

Kielb, S.J., Shah, N.L., Rubin, M.A., and Sanda, M.G. 2001. Functional p53 mutation as a molecular determinant of paclitaxel and gemcitabine susceptibility in human bladder cancer. *J. Urol. 166*:482–487.

Knippschild, U., Milne, D., Campbell, L., and Meek, D. 1996. p53 N-terminus-targeted protein kinase activity is stimulated in response to wild type p53 and DNA damage. *Oncogene 13*: 1387–1393.

Koike, K., Moriya, K., Iino, S., Yotsuyanagi, H., Endo, Y., Miyamura, T., and Kurokawa, K. 1994. High-level expression of hepatitis B virus HBx gene and hepatocarcinogenesis in transgenic mice. *Hepatology 19*:810–819.

Law, G.L., Itoh, H., Law, D.J., Mize, G.J., Merchant, J.L., and Morris, D.R., 1998. Transcription factor ZBP-89 regulates the activity of the ornithine decarboxylase promoter. *J. Biol. Chem. 273*:19955–19964.

Lee, K.C., Crowe, A.J., and Barton, M.C. 1999. p53-mediated repression of alpha-fetoprotein gene expression by specific DNA binding. *Mol. Cell Biol. 19*:1279–1288.

Lian, Z., Liu, J., Pan, J., Satiroglu Tufan, N.L., Zhu, M., Arbuthnot, P., Kew, M., Clayton, M.M., and Feitelson, M.A. 2001. A cellular gene up-regulated by hepatitis B virus-encoded X antigen promotes hepatocellular growth and survival. *Hepatology 34*: 146–157.

Lowe, S.W., Bodis, S., McClatchey, A., Remington, L., Ruley, H.E., Fisher, D.E., Housman, D.E., and Jacks, T. 1994. p53 status and the efficacy of cancer therapy *in vivo. Science 266*:807–810.

McIlwrath, A.J., Vasey, P.A., Ross, G.M., and Brown, R. 1994. Cell cycle arrests and radiosensitivity of human tumor cell lines: Dependence on wild-type p53 for radiosensitivity. *Cancer Res. 54*:3718–3722.

Muller, M., Wilder, S., Bannasch, D., Israeli, D., Lehlbach, K., Li-Weber, M., Friedman, S.L., Galle, P.R., Stremmel, W., Oren, M., and Krammer, P.H. 1998. p53 activates the CD95 (APO-l/Fas) gene in response to DNA damage by anticancer drugs. *J. Exp. Med. 188*:2033–2045.

Pruschy, M., Rocha, S., Zaugg, K., Tenzer, A., Hess, C., Fisher, D.E., Glanzmann, C., and Bodis, S. 2001. Key targets for the execution of radiation-induced tumor cell apoptosis: The role of p53 and caspases. *Int. J. Rad. Oncol. Biol. Physics 49*:561–567.

Srinivas, G., Kusumakumary, P., Nair, M.K., Panicker, K.R., and Pillai, M.R. 2000. Mutant p53 protein, Bcl-2/Bax ratios and apoptosis in paediatric acute lymphoblastic leukaemia. *J. Cancer Res. Clin. Oncol. 126*:62–67.

Stewart, Z.A., and Pietenpol, J.A. 2001. p53 Signaling and cell cycle checkpoints. *Chem. Res. Toxicol. 14*:243–263.

Stuver, S.O., Kuper, H., Tzonou, A., Lagiou, P., Spanos, E., Hsieh, C.C., Mantzoros, C., and Trichopoulos, D. 2000. Insulin-like growth factor 1 in hepatocellular carcinoma and metastatic liver cancer in men. *Int. J. Cancer 87*:118–121.

Taniuchi, T., Mortensen, E.R., Ferguson, A., Greenson, J., and Merchant, J.L. 1997. Overexpression of ZBP-89, a zinc finger DNA binding protein, in gastric cancer. *Biochem. Biophys. Res. Comm. 233*:154–160.

Trepel, M., Scheding, S., Groscurth, P., Horny, H.P., Malipiero, U., Brugger, W., Dichgans, J., and Weller, M. 1997. A new look at the role of p53 in leukemia cell sensitivity to chemotherapy. *Leukemia 11*:1842–1849.

Wang, X.W., and Harris, C.C. 1996. TP53 tumour suppressor gene: Clues to molecular carcinogenesis and cancer therapy. *Cancer Surv. 28*:169–196.

5

Role of Immunohistochemical Expression of PTEN in Hepatocellular Carcinoma

Ming-Hong Tai

Introduction

Hepatocellular carcinoma (HCC) is one of the most prevalent cancers worldwide with 600,000 estimated new cases annually and almost as many deaths (Pisani *et al.,* 1999; Thorgeirsson and Grisham, 2002). Despite advances in surgical and adjuvant therapy, the long-term survival for patients with HCC remains poor, underscoring the demands for development of diagnostic and treatment strategies. Epidemiologic studies have shown that HCC is frequently associated with infection of hepatitis B virus (HBV) or hepatitis C virus (HCV), exposure to aflatoxin B1, and alcohol intake. Although HBV vaccination shows promising results in reducing the incidence of HBV-related HCC, the recent spread of HCV will lead to a substantial increase in HCC incidence worldwide, including developed countries.

Liver carcinogenesis is a multifactorial and multistep process that involves activation of oncogenes or inactivation of tumor-suppressor genes during different stages of HCC progression. The activation of oncogenes or inactivation of tumor-suppressor genes usually occurs as a consequence of chromosomal or epichromosomal abnormalities. Chromosomal abnormalities in HCC were poorly defined. Mutation of one allele or loss of heterozygosity (LOH) has been reported on chromosome 1p, 4q, 5q, 8p, 10q, 11p, 13q, 16q, 17p, and 22q in HCC. Several tumor suppressor genes are known to participate in the progression of HCC, including the *p53* gene on chromosome 17q13, retinoblastoma (*Rb*) gene on chromosome 13q14, and *adenomatous polyposis coli* (*APC*) gene on chromosome 5q21. Studies of allelotyping and comparative genomic hybridization also characterized a handful of genes that are consistently found mutated in HCC including *WT1, p16, p14, SOCS1, FHIT, AXIN1,* and *p53* genes (Pineau *et al.,* 2003; Thorgeirsson, 2003). Among them, *p53* and *AXIN1* genes are inactivated by somatic mutations in 30% and 5% of HCC cases, respectively. In contrast, *p16* and *SOCS1* are silenced through promoter hypermethylation in more than 50% of cases. Finally, β-catenin, the protooncogene found to be mutated in liver cancer, is activated in 20% of the HCC samples.

Allelic loss or LOH of chromosome 10q was identified in HCC (Piao *et al.,* 1998), suggesting the presence of tumor-suppressor gene(s) on chromosome 10q for HCC. Screening of homozygous deletions in hepatobiliary tumor cell lines revealed that several tumor suppressor genes, not known for their roles in HCC, may participate in liver carcinogenesis (Pineau *et al.,* 2003). One of these genes is *PTEN,* a phosphatase and tensin homolog deleted in chromosome 10, which is located on chromosome 10q. Moreover, loss of PTEN

Handbook of Immunohistochemistry and *in situ* Hybridization of Human Carcinomas, Volume 3: Molecular Genetics, Liver Carcinoma, and Pancreatic Carcinoma

allele was found in 20–30% of HCC cases (Fujiwara *et al.,* 2000; Kawamura *et al.,* 1999). The involvement of PTEN in HCC was also supported by a gene-knockout study (Podsypanina *et al.,* 1999), in which $PTEN^{+/-}$ heterozygous mice exhibited neoplasms in multiple organs including liver adenoma.

PTEN, also known as mutated in multiple advanced cancers (MMAC1) or transforming growth factor-beta (TGF-β)-regulated and epithelia cell-enriched (TEP1), is located on human chromosome 10q23 (Li and Sun, 1997; Li *et al.,* 1997; Steck *et al.,* 1997). Mutation of the PTEN gene is a common event in advanced stage of diverse human cancers, occurring in about 70% of glioblastoma, 50% of endometrial carcinoma, 50% of prostate carcinoma, and 30% of melanoma (Maehama and Dixon, 1999). In addition, germline mutations in PTEN are associated with the dominantly inherited Cowden and Bannayan-Zonana syndromes (Murata *et al.,* 1999; Sutphen *et al.,* 1999), which are characterized by the formation of multiple benign tumors and by the increased risk of malignant breast and thyroid tumors. The 403-amino acid PTEN protein encodes dual-specificity phosphatase and has at least two biochemical functions: lipid phosphatase and protein phosphatase activity. The two major substrates for PTEN are phosphatidylinositol triphosphate (PIP3) phospholipids and protooncogene Akt. Both are important signal transducers for growth, survival, and proliferation of cells (Di Cristofano and Pandolfi, 2000). The lipid phosphatase activity of PTEN decreases intracellular PtdIns(3,4,5)P3 level and downstream Akt activity. Cell cycle arrest at G1/S is at least partially moderated by PTEN through the up-regulation of the cyclin-dependent kinase inhibitor p27. In addition, agonist-induced apoptosis is mediated by PTEN, through the up-regulation of proapoptotic machinery involving caspases and BID and the down-regulation of anti-apoptotic proteins such as Bcl-2. The protein phosphatase activity of PTEN is apparently less central to its involvement in tumorigenesis. It is involved in the inhibition of focal adhesion formation, cell spreading and migration, and the inhibition of growth factor-stimulated mitogen-activated protein kinase (MAPK) signaling (Gu *et al.,* 1999; Tamura *et al.,* 1999). Therefore, the combined effects of the loss of PTEN lipid and protein phosphatase activity may result in aberrant cell growth and escape from apoptosis, as well as abnormal cell spreading and migration.

Cumulative evidences indicate that PTEN interacts with and regulates the expression of several tumor-suppressor genes including *p27* (Di Cristofano *et al.,* 2001), *p21* (Wu *et al.,* 2000), and *p53* (Stambolic *et al.,* 2001; Yeon *et al.,* 2003). Statistic analysis in HCC specimens indeed unveils an inverse correlation between p53 overexpression and PTEN loss (Hu *et al.,* 2003), which suggests that PTEN loss frequently occurs in hepatoma cells with mutant *p53*. The prognostic role of structural abnormality in *p53* gene for HCC has been extensively deciphered (Ng *et al.,* 1995). The loss of PTEN alleles appears to be related to the lack of functional p53, which normally maintains chromosomal stability. A p53-binding element was identified in the promoter region of *PTEN* gene (Stambolic *et al.,* 2001), indicating that p53 may activate PTEN gene expression. In a recent report, protooncogene Akt is activated in liver cells stably expressing HBV x protein (HBx) because HBx disrupted p53-mediated PTEN transcription (Chung *et al.,* 2003). However, PTEN inhibits PI3K/Akt signaling and promotes degradation of Mdm2, thereby increasing the cellular content and transactivation of the p53 (Mayo *et al.,* 2002). It was reported that PTEN reconstitution induced the transactivation of p53 and increased the expression of p53 target genes such as p21 and insulin-like growth factor binding protein 3 in glioma cells (Su *et al.,* 2003). Similarly, chronic alcohol exposure increased levels of PTEN with concomitant inhibition of Akt/PI3K signaling and increased level of nuclear p53 (Yeon *et al.,* 2003). Together with findings in HCC, these data strongly indicate that PTEN loss and p53 mutation may cooperatively contribute to liver carcinogenesis.

Immunohistochemical Protocols for PTEN Staining of Paraffin Sections

PTEN Antibodies for Immunohistochemical Analysis

Polyclonal PTEN antibodies for immunohistologic studies were available from our laboratory on request (Hu *et al.,* 2003) or purchased from commercial vendors such as Neo Markers (Fremont, CA) (Rahman *et al.,* 2002) and Cell Signaling Technology Inc. (Beverly, MA).

MATERIALS

1. Buffer solutions:

   a. 1X phosphate buffer saline (PBS) containing 0.1% Tween (PBS/T): Dissolve 8 g NaCl, 0.2 g KCl, 1.44 g Na_2PO_4, and 0.24 g KH_2PO_4 in 800 ml distilled water (dH_2O). Adjust pH to 7.4 with HCl. Add 1 ml Tween-20 (Sigma; St. Louis, MO) and adjust the volume to 1 L. Store at room temperature.

   b. 1X Tris buffered saline containing 0.1% Tween 20 (TBS/T): Dissolve 2.42 g Tris and 8.0 g

NaCl in 800 ml dH_2O. Adjust the pH to 7.6 with HCl. Add 1 ml Tween 20 and adjust the volume to 1 L. Store at room temperature.

2. Solutions for antigen retrieval:
   a. 10 mM sodium citrate buffer: To prepare 1 L, add 2.94 g sodium citrate to 1 L dH_2O. Adjust pH to 6.0.
   b. 1 mM ethylenediamine tetra-acetic acid (EDTA) solution: To prepare 1 L, add 0.372 g EDTA (Sigma; St. Louis, MO) to 1 L dH_2O. Adjust pH to 8.0.
   c. 10 mM Tris: To prepare 1 L, add 1.21 g Tris to 1 L dH_2O and adjust PH to 7.5 with HCl.

3. 3% Hydrogen peroxide: Add 10 ml 30% dH_2O_2 to 90 ml dH_2O for final working solution.

4. Blocking solution: 5% horse serum or goat serum (Vector Laboratories, Inc.; Burlingame, CA) in PBS.

5. PicTure-plus polymer detection system (Zymed; South San Francisco, CA; Cat. No. 87-9943): Prepare according to manufacturer's instructions 30 min before use.

6. Diaminobenzidine (DAB) reagent (Vector Laboratories, Inc.; Burlingame, CA; Cat. No. SK-4100): Prepare according to manufacturer's instructions.

METHODS

1. Deparaffinize/hydrate sections:
   a. Incubate sections in three washes of xylene for 5 min each.
   b. Incubate sections in two washes of 100% ethanol for 10 min each.
   c. Incubate sections in two washes of 95% ethanol for 10 min each.

2. Wash sections 2× in dH_2O for 5 min each.

3. Wash sections in PBS for 5 min.

4. For antigen unmasking, heat sections in 10 mM sodium citrate buffer, pH 6.0, for 1 min at full power, followed by 9 min at medium power in microwave. Be sure to keep slides fully immersed in buffer and maintain temperature at or just below boiling. Cool slides for 20 min after antigen unmasking.

5. Wash sections in dH_2O 3× for 5 min each.

6. Incubate sections in 1% hydrogen peroxide for 10 min.

7. Wash sections in dH_2O 3× for 5 min each.

8. Wash section in PBS for 5 min.

9. Block each section with 100–400 µl blocking solution for 1 hr at room temperature.

10. Remove blocking solution and add 100–400 µl PTEN primary antibody (1:100 diluted antibody in blocking solution) to each section. Incubate for 1 hr at room temperature or overnight at 4°C.

11. Remove antibody solution and wash sections in PBS 3× for 5 min each.

12. Add 100–400 µl secondary antibody, diluted in blocking solution, to each section. Incubate for 30 min at room temperature.

13. Remove secondary antibody solution and wash sections 3× with PBS for 5 min each.

14. Add 100–400 µl PicTure-plus polymer detection system to each section and incubate for 30 min at room temperature.

15. Remove polymer detection system and wash sections 3× in PBS for 5 min each.

16. Add 100–400 µl DAB reagent to each section and monitor staining closely.

17. As soon as the section turns brown, immerse slides in dH_2O.

18. Counterstain sections in hematoxylin for 10 sec.

19. Wash sections in dH_2O 2× for 5 min each.

20. Dehydrate sections:
   a. Incubate sections in 95% ethanol 2× for 10 sec each.
   b. Repeat in 100% ethanol, incubating sections 2× for 10 sec each.
   c. Repeat in xylene, incubating sections 2× for 10 sec each.

21. Mount coverslips.

RESULTS AND DISCUSSION

The role of PTEN expression during liver carcinogenesis has been investigated by immunohistochemical approaches in HCC specimens (Hu *et al.,* 2003; Rahman *et al.,* 2002; Wan *et al.,* 2003). The representative pattern of PTEN immunostaining in HCC specimens is shown in Figure 31. Immunostaining by PTEN is detected in hepatocytes, hepatoma cells, and cells in bile ducts, but it is not observed in infiltrating mononuclear cells or sinusoidal lining cells (Hu *et al.,* 2003; Rahman *et al.,* 2002; Wan *et al.,* 2003). By comparison with adjacent noncancerous regions, the intensities of PTEN immunostaining were significantly lower in tumor tissues than that in nontumor tissues (Figure 31A). Decreased PTEN immunostaining is identified in 30–60% of resected HCC specimens, particularly in the advanced ones. This finding was also confirmed by Western Blot analysis (Tai *et al.,* unpublished data).

The PTEN immunostaining is localized in cytoplasm as well as nucleus of cells in HCC samples. The cytoplasmic PTEN staining was diffused, whereas the nuclear PTEN staining was localized primarily in the nucleoli and nuclear membrane (Hu *et al.,* 2003). The loss of cytoplasmic PTEN staining in tumor tissues

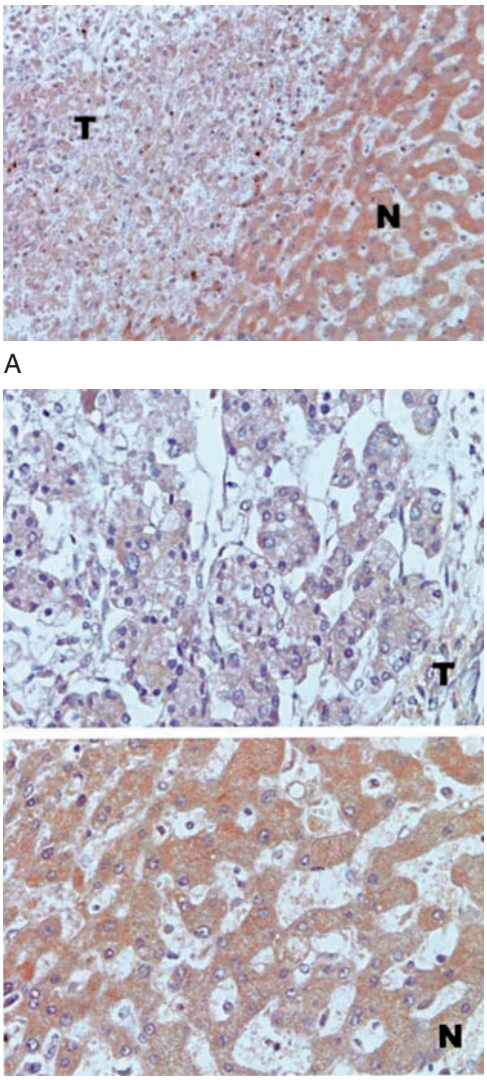

Figure 31. PTEN expression in clinical specimens of hepatocellular carcinoma. **A:** Differential PTEN expression between tumor and noncancerous tissues. T, tumor region; N, noncancerous region. X100. **B:** Loss of cytoplasmic PTEN staining in HCC specimens. Comparison was made between tumor (*upper panel*) and noncancerous (*lower panel*) regions to reveal the disappearance of PTEN immunostaining in cytoplasm. 200X.

was particularly noticeable when compared with their nontumor counterparts (Figure 29B). Although exclusion of nuclear PTEN staining was observed in pancreatic (Perren *et al.,* 2000) and thyroid cancers (Gimm *et al.,* 2000), the reduced PTEN expression was found mainly in cytoplasm of cells in HCC specimens (Dong-Dong *et al.,* 2003; Hu *et al.,* 2003; Rahman *et al.,* 2002; Wan *et al.,* 2003).

The mechanism underlying PTEN inactivation in HCC remains unclear. It can be inactivated through a wide range of mechanisms (Dahia *et al.,* 1999), including somatic mutations, hemizygous deletions, promoter methylation (Yu *et al.,* 2002), decreased transcription or translation, increased protein degradation or phosphorylation (Vazquez *et al.,* 2001), and differential subcellular compartmentalization (Gimm *et al.,* 2000; Perren *et al.,* 2000). Somatic mutation in the PTEN gene rarely occurs in HCC, which is found in less than 5% of HCC specimens (Fujiwara *et al.,* 2000; Kawamura *et al.,* 1999; Yao *et al.,* 1999; Yeh *et al.,* 2000). Given that PTEN loss was found in 30–60% of HCC cases, gene mutation is likely not the primary cause for PTEN inactivation in HCC. Allelic loss was the primary pathway for PTEN inactivation in many types of cancers (Marsh *et al.,* 1998; Suzuki *et al.,* 1998). The frequency of loss of flanking markers around PTEN allele in HCC was determined at 27% (25 in 89 cases) (Kawamura *et al.,* 1999) and 32% (12 in 37 cases) (Fujiwara *et al.,* 2000), respectively. Thus, allele loss may account for a significant fraction of HCC cases with PTEN loss. However, the involvement of other mechanisms for PTEN inactivation in HCC remains to be elucidated.

Statistical analysis was performed to characterize the correlation between PTEN expression and clinicopathologic parameters of patients with HCC in immunohistochemical studies (Dong-Dong *et al.,* 2003; Hu *et al.,* 2003; Rahman *et al.,* 2002; Wan *et al.,* 2003) to delineate the role of PTEN expression during liver carcinogenesis. It has been found that PTEN expression correlates with tumor grades, advanced stages, high serum alpha-fetoprotein (AFP) level, lymph node metastasis (Dong-Dong *et al.,* 2003), tumor recurrence, and poor prognosis of patients with HCC (Hu *et al.,* 2003; Rahman *et al.,* 2002). By Cox's hazards model, two of these studies further indicate that PTEN expression is an independent prognostic factor for survival of patients with HCC (Hu *et al.,* 2003; Rahman *et al.,* 2002).

Infection with HBV or HCV is involved in the pathogenesis of HCC. An unusually high frequency (63.1%) of PTEN down-regulation was observed in HCV-positive HCC specimens with concomitant up-regulation of inducible nitric oxide synthase (iNOS) and cyclooxygenase II (COX II) (Rahman *et al.,* 2002). Besides, HBx protein modulates PTEN expression through inhibition of p53 activities in HBx-transfected liver cells (Chung *et al.,* 2003). These results implicate the status of viral infection might influence the PTEN expression in patients with HCC. However, statistical analysis failed to identify significant association between PTEN expression and viral infection or the status of cirrhosis.

In conclusion, inactivation of tumor-suppressor gene PTEN is a common event in the advanced stage

of diverse human cancers. Although PTEN mutations rarely occur in HCC, loss of PTEN allele or LOH is observed in 20–30% of HCC specimens. The prognostic role of PTEN inactivation in HCC has been explored. Immunohistochemical analysis reveals prominent reduction of PTEN immunostaining, PTEN loss, in 30–60% of HCC specimens, particularly the advanced ones. PTEN loss correlates with advanced tumor stages, high serum AFP level, tumor recurrence, and poor prognosis of patients with HCC. Above all, PTEN loss is associated with the status of p53 mutation in hepatoma cells, suggesting that functional loss of PTEN and p53 may cooperatively contribute to liver carcinogenesis.

References

Chung, T.W., Lee, Y.C., Ko, J.H., and Kim, C.H. 2003. Hepatitis B virus X protein modulates the expression of PTEN by inhibiting the function of p53, a transcriptional activator in liver cells. *Cancer Res. 63*:3453–3458.

Dahia, P.L., Aguiar, R.C., Alberta, J., Kum, J.B., Caron, S., Sill, H., Marsh, D.J., Ritz, J., Freedman, A., Stiles, C., and Eng, C. 1999. PTEN is inversely correlated with the cell survival factor Akt/PKB and is inactivated via multiple mechanisms in haematological malignancies. *Hum. Mol. Genet. 8*:185–193.

Di Cristofano, A., De Acetis, M., Koff, A., Cordon-Cardo, C., and Pandolfi, P.P. 2001. Pten and p27KIP1 cooperate in prostate cancer tumor suppression in the mouse. *Nat. Genet. 27*: 222–224.

Di Cristofano, A., and Pandolfi, P.P. 2000. The multiple roles of PTEN in tumor suppression. *Cell 100*:387–390.

Dong-Dong, L., Xi-Ran, Z., and Xiang-Rong, C. 2003. Expression and significance of new tumor suppressor gene PTEN in primary liver cancer. *J. Cell Mol. Med. 7*:67–71.

Fujiwara, Y., Hoon, D.S., Yamada, T., Umeshita, K., Gotoh, M., Sakon, M., Nishisho, I., and Monden, M. 2000. PTEN/MMAC1 mutation and frequent loss of heterozygosity identified in chromosome 10q in a subset of hepatocellular carcinomas. *Jpn. J. Cancer Res. 91*:287–292.

Gimm, O., Perren, A., Weng, L.P., Marsh, D.J., Yeh, J.J., Ziebold, U., Gil, E., Hinze, R., Delbridge, L., Lees, J.A., Mutter, G.L., Robinson, B.G., Komminoth, P., Dralle, H., and Eng, C. 2000. Differential nuclear and cytoplasmic expression of PTEN in normal thyroid tissue, and benign and malignant epithelial thyroid tumors. *Am. J. Pathol. 156*:1693–1700.

Gu, J., Tamura, M., Pankov, R., Danen, E.H., Takino, T., Matsumoto, K., and Yamada, K.M. 1999. Shc and FAK differentially regulate cell motility and directionality modulated by PTEN. *J. Cell Biol. 146*:389–404.

Hu, T.H., Huang, C.C., Lin, P.R., Chang, H.W., Ger, L.P., Lin, Y.W., Changchien, C.S., Lee, C.M., and Tai, M.H. 2003. Expression and prognostic role of tumor suppressor gene PTEN/MMAC1/TEP1 in hepatocellular carcinoma. *Cancer 97*: 1929–1940.

Kawamura, N., Nagai, H., Bando, K., Koyama, M., Matsumoto, S., Tajiri, T., Onda, M., Fujimoto, J., Ueki, T., Konishi, N. 1999. PTEN/MMAC1 mutations in hepatocellular carcinomas: Somatic inactivation of both alleles in tumors. *Jpn. J. Cancer Res. 90*:413–418.

Li, D.M., and Sun, H. 1997. TEP1, encoded by a candidate tumor suppressor locus, is a novel protein tyrosine phosphatase regulated by transforming growth factor beta. *Cancer Res. 57*:2124–2129.

Li, J., Yen, C., Liaw, D., Podsypanina, K., Bose, S., Wang, S.I., Bigner, S.H., Giovamella, B.C., Ittmann, M., Tycko, B., Hibshoosh, H., Wigler, M.H., Parsons, R., Puc, J., Miliaresis, C., Rodgers, L., and McCombie, R. 1997. PTEN, a putative protein tyrosine phosphatase gene mutated in human brain, breast, and prostate cancer. *Science 275*:1943–1947.

Maehama, T., and Dixon, J.E. 1999. PTEN: A tumour suppressor that functions as a phospholipid phosphatase. *Trends Cell Biol. 9*:125–128.

Marsh, D.J., Dahia, P.L., Coulon, V., Zheng, Z., Dorion-Bonnet, F., Call, K.M., Little, R., Lin, A.Y., Eeles, R.A., and Goldstein, A.M. 1998. Allelic imbalance, including deletion of PTEN/MMACI, at the Cowden disease locus on 10q22-23, in hamartomas from patients with Cowden syndrome and germline PTEN mutation. *Genes Chromosomes Cancer 21*:61–69.

Mayo, L.D., Dixon, J.E., Durden, D.L., Tonks, N.K., and Donner, D.B. 2002. PTEN protects p53 from Mdm2 and sensitizes cancer cells to chemotherapy. *J. Biol. Chem. 277*:5484–5489.

Murata, J., Tada, M., Sawamura, Y., Mitsumori, K., Abe, H., and Nagashima, K. 1999. Dysplastic gangliocytoma (Lhermitte-Duclos disease) associated with Cowden disease: Report of a case and review of the literature for the genetic relationship between the two diseases. *J. Neurooncol. 41*:129–136.

Ng, I.O., Lai, E.C., Chan, A.S., and So, M.K. 1995. Overexpression of p53 in hepatocellular carcinomas: A clinicopathological and prognostic correlation. *J. Gastroenterol. Hepatol. 10*:250–255.

Perren, A., Komminoth, P., Saremaslani, P., Matter, C., Feurer, S., Lees, J.A., Heitz, P.U., and Eng, C. 2000. Mutation and expression analyses reveal differential subcellular compartmentalization of PTEN in endocrine pancreatic tumors compared to normal islet cells. *Am. J. Pathol. 157*:1097–1103.

Piao, Z., Park, C., Park, J.H., and Kim, H. 1998. Allelotype analysis of hepatocellular carcinoma. *Int. J. Cancer 75*:29–33.

Pineau, P., Marchio, A., Nagamori, S., Seki, S., Tiollais, P., and Dejean, A. 2003. Homozygous deletion scanning in hepatobiliary tumor cell lines reveals alternative pathways for liver carcinogenesis. *Hepatology 37*:852–861.

Pisani, P., Parkin, D.M., Bray, F., and Ferlay, J. 1999. Estimates of the worldwide mortality from 25 cancers in 1990. *Int. J. Cancer 83*:18–29.

Podsypanina, K., Ellenson, L.H., Nemes, A., Gu, J., Tamura, M., Yamada, K.M., Cordon-Cardo, C., Catoretti, G., Fisher, P.E., and Parsons, R. 1999. Mutation of Pten/Mmac1 in mice causes neoplasia in multiple organ systems. *Proc. Natl. Acad. Sci. USA 96*:1563–1568.

Rahman, M.A., Kyriazanos, I.D., Ono, T., Yamanoi, A., Kohno, H., Tsuchiya, M., and Nagasue, N. 2002. Impact of PTEN expression on the outcome of hepatitis C virus-positive cirrhotic hepatocellular carcinoma patients: Possible relationship with COX II and inducible nitric oxide synthase. *Int. J. Cancer 100*:152–157.

Stambolic, V., MacPherson, D., Sas, D., Lin, Y., Snow, B., Jang, Y., Benchimol, S., and Mak, T.W. 2001. Regulation of PTEN transcription by p53. *Mol. Cell. 8*:317–325.

Steck, P.A., Pershouse, M.A., Jasser, S.A., Yung, W.K., Lin, H., Ligon, A.H., Langford, L.A., Baumgard, M.L., Hattier, T., and Davis, T. 1997. Identification of a candidate tumour suppressor gene, MMAC1, at chromosome 10q23.3 that is mutated in multiple advanced cancers. *Nat. Genet. 15*:356–362.

Su, J.D., Mayo, L.D., Donner, D.B., and Durden, D.L. 2003. PTEN and phosphatidylinositol 3′-kinase inhibitors up-regulate p53 and block tumor-induced angiogenesis: Evidence for an effect

on the tumor and endothelial compartment. *Cancer Res. 63*:3585–3592.

Sutphen, R., Diamond, T.M., Minton, S.E., Peacocke, M., Tsou, H.C., and Root, A.W. 1999. Severe Lhermitte-Duclos disease with unique germline mutation of PTEN. *Am. J. Med. Genet. 82*:290–293.

Suzuki, A., de la Pompa, J.L., Stambolic, V, Elia, A.J., Sasaki, T., del Barco Barrantes, I., Ho, A., Wakeham, A., Itie, A., Khoo, W. 1998. High cancer susceptibility and embryonic lethality associated with mutation of the PTEN tumor suppressor gene in mice. *Curr. Biol. 8*:1169–1178.

Tai, M.H., Lin, P.R., Hu, T.H., Huang, C.C., Liang, H.T., Lin, Y.W., and Chen, J.L. Suppression of hepatocellular carcinoma by PTEN gene delivery: Role of bystander effect (submitted).

Tamura, M., Gu, J., Danen, E.H., Takino, T., Miyamoto, S., and Yamada, K.M. 1999. PTEN interactions with focal adhesion kinase and suppression of the extracellular matrix-dependent phosphatidylinositol 3-kinase/Akt cell survival pathway. *J. Biol. Chem. 274*:20693–20703.

Thorgeirsson, S.S. 2003. Hunting for tumor suppressor genes in liver cancer. *Hepatology 37*:739–741.

Thorgeirsson, S.S., and Grisham, J.W. 2002. Molecular pathogenesis of human hepatocellular carcinoma. *Nat. Genet. 31*:339–346.

Vazquez, F., Grossman, S.R., Takahashi, Y, Rokas, M.V., Nakamura, N., and Sellers, W.R. 2001. Phosphorylation of the PTEN tail acts as an inhibitory switch by preventing its recruitment into a protein complex. *J. Biol. Chem. 276*:48627–48630.

Wan, X.W., Jiang, M., Cao, H.F., He, Y.Q., Liu, S.Q., Qiu, X.H., Wu, M.C., and Wang, H.Y. 2003. The alteration of PTEN tumor suppressor expression and its association with the histopathological features of human primary hepatocellular carcinoma. *J. Cancer Res. Clin. Oncol. 129*:100–106.

Wu, R.C., Li, X., and Schonthal, A.H. 2000. Transcriptional activation of p21WAF1 by PTEN/MMAC1 tumor suppressor. *Mol. Cell Biochem. 203*:59–71.

Yao, Y.J., Ping, X.L., Zhang, H., Chen, F.F., Lee, P.K., Ahsan, H., Chen, C.J., Lee, P.H., Peacocke, M., Santella, R.M., and Tsou, H.C. 1999. PTEN/MMAC1 mutations in hepatocellular carcinomas. *Oncogene 18*:3181–3185.

Yeh, K.T., Chang, J.G., Chen, Y.J., Chen, S.T., Yu, S.Y., Shih, M.C., Perng, L.I., Wang, J.C., Tsai, M., and Chang, C.P. 2000. Mutation analysis of the putative tumor suppressor gene PTEN/MMAC1 in hepatocellular carcinoma. *Cancer Invest. 18*:123–129.

Yeon, J.E., Califano, S., Xu, J., Wands, J.R., and De La Monte, S.M. 2003. Potential role of PTEN phosphatase in ethanol-impaired survival signaling in the liver. *Hepatology 38*:703–714.

Yu, J., Ni, M., Xu, J., Zhang, H., Gao, B., Gu, J., Chen, J., Zhang, L., Wu, M., Zhen, S., and Zhu, J. 2002. Methylation profiling of twenty promoter-CpG islands of genes which may contribute to hepatocellular carcinogenesis. *BMC Cancer 2*:29.

6

The Potential Role of Bcl-2 and Protein Expression in Hepatocellular Carcinomas: A Clinicopathologic Study

Dimitrios Kardamakis, Athanassios C. Tsamandas, Thomas Makatsoris, Vassiliki Zolota, Charalambos Gogos, Cristine Kalogeropoulou, Chrisoula Karatza, Theodore Petsas, Dionissios Karavias, and Dionissis S. Bonikos

Introduction

Today it is widely accepted that development and progress of a malignant tumor is the combined result of cell proliferation and apoptosis (Salakou *et al.,* 2001, 2002). Apoptosis is a morphologically distinct, gene-directed form of cell death characterized by cytoplasmic fragmentation and nuclear condensation and contributes to both physiologic and pathologic processes (Cummings *et al.,* 1997). In the liver, apoptosis and apoptosis-related proteins contribute to intrahepatic bile duct development; previous studies have demonstrated the expression of apoptosis-related proteins in normal and diseased human liver, including instances of acute and chronic hepatitis (Columbano *et al.,* 1985; Tsamandas *et al.,* 2002).

One of the oncogenes involved in the apoptotic process is Bcl-2. It is a gene located at chromosome 18q21, and it was first described in studies regarding t_j chromosome translocation in B-cell leukemia (Cleary and Sklar, 1985). Subsequently, it was detected in other malignant tumors such as carcinoma of the gastrointestinal tract (Bronner *et al.,* 1995). Bcl-2 encodes a 26-kD protein located mainly in the outer mitochondrial membrane but also in the nuclear envelope, perinuclear membrane, and endoplasmic reticulum. It blocks programmed cell death without affecting cellular proliferation (Hockenbery *et al.,* 1991). More specifically it has emerged as a key regulator of apoptosis because it can protect cells from death induced by a number of injuries including radiation, chemotherapy, or growth factor deprivation. Bcl-2 has been detected

Handbook of Immunohistochemistry and *in situ* Hybridization of Human Carcinomas, Volume 3: Molecular Genetics, Liver Carcinoma, and Pancreatic Carcinoma

in the long-lived, self-renewing populations of stem cells that line the basement membrane of several epithelia, including skin, colon, and prostate, but not in the terminally differentiated cells found at the surface of those epithelia, which are believed to die by apoptosis (Hockenbery *et al.,* 1991). In the liver, Bcl-2 presence has been reported in areas of cholangiolar proliferation, and less in hepatocytes in patients with cirrhosis resulting from hepatitis C (Terada and Nakanuma, 1995). In addition, Bcl-2 expression was shown in periportal hepatocytes of the bile duct–ligated rat, where it is believed to protect metaplastic hepatocytes from cholestasis-induced apoptotic death (Kurosawa *et al.,* 1997).

Regarding Bcl-2 expression in liver malignant tumors there is a disagreement among previous reports. Other authors have reported that Bcl-2 protein expression should be considered a reliable marker in the differential diagnosis between hepatocellular carcinomas (HCCs) (which are Bcl-2 negative) and cholangiocarcinomas and liver metastatic adenocarcinomas (which are Bcl-2 positive) (Charlotte *et al.,* 1994). Other studies have demonstrated a low degree expression of Bcl-2 protein in HCC (Zhao *et al.,* 1994). A previous study showed that Bcl-2 messenger ribonucleic acid (mRNA) presence detected by *in situ* hybridization (ISH) was more frequent in HCCs compared to Bcl-2 protein expression and suggested that in the absence of a well-demonstrated posttranscriptional control of Bcl-2, ISH is a possible alternative method for assessing the expression of Bcl-2 mRNA in HCCs (Fiorentino *et al.,* 1999). This study has investigated Bcl-2 mRNA and protein expression in HCCs and analyzed possible differences in their expression.

MATERIALS AND METHODS

Patients

The study comprised 35 surgical specimens of primary HCCs, resected from an equal number of patients, for therapeutic reasons, at the Department of Surgery, University of Patras School of Medicine, Rion University Hospital, Patras, Greece, between 1994 and 1999. This material represented a group of patients for whom archival tissue and adequate data on pathologic finding and clinical follow-up were readily available. Nine patients underwent chemoembolization of the neoplastic masses before surgery.

The study included 21 men and 14 women, aged 43–59 years (median 51 years). The slides and pathology report for each patient, obtained from the files of the Pathology Department, were reviewed to confirm the histologic type pathologic grading according to Edmondson criteria (Craig *et al.,* 1988). In addition, in each case the pathologic stage according to TNM classification was recorded. In 28 cases the HCC was developed on the background of a cirrhotic liver resulting from chronic hepatitis B (n = 18) and chronic hepatitis C (n = 10). Patients were followed up for a 27–108 (median 62)-month period.

In situ Hybridization for Bcl-2 mRNA Detection

In this study, for Bcl-2 mRNA detection purposes, a standard nonradioactive ISH method was performed on one selected paraffin block from each case that included neoplastic and nonneoplastic (cirrhotic or noncirrhotic) tissues, using the Hybridization/Detection Complete System (IH-60002 [IHD-0052]: Ultra Sensitivity, Maxim Biotech, Inc. [MBI], San Francisco, CA).

MATERIALS

1. Fixative: 10% Neutral formalin.
2. Materials and reagents included in the Hybridization/Detection Complete System. All these reagents were supplied by MBI. These were as follows:
   a. Biotinylated Housekeeping (GAPDH) Gene Probe: blue, 1 vial, 1 ml
   b. Proteinase K: brown, 1 vial, 4 mg
   c. DNase and RNase-free Dilution Buffer: 1 vial, 2 ml
   d. Hybridization solution: white, 1 vial, 6 ml
   e. Protein block (20X): 1 bottle, 50 ml
   f. RNase A (15 µg/ml): purple, 1 vial, 6 ml
   g. Mouse Anti-Biotin Linker 1: green, 1 vial, 6 ml
   h. Biotin-Goat Anti-Mouse Ig Linker 2: yellow, 1 vial, 6 ml
   i. Streptavidin-AP Conjugate: red, 1 vial, 6 ml
   j. Substrate brown: 1 vial, 6 ml
   k. Detergent wash buffer (20X:) 1 bottle, 100 ml
3. Microscope slides (polylysine, microscopic slides, US Pat. 4481246, 4624882, Menzel-Glaser, Braunschweig, Germany).
4. Test and positive control tissue (supplied with the biotinylated probe SP-10043 [bcl-1001/bcl-1002], MBI).
5. Distilled H_2O.
6. Coverslips.
7. Xylene.
8. Ethanol.
9. Tris buffer (pH: 7.6): 6.1 g Tris in 1000 ml distilled water and 37 ml 1 N HCl.
10. Tris buffered saline (TBS) buffer: 1800 ml NaCl and 200 ml Tris (TR 0423, Scharlau, Germany).

11. Counterstain: Nuclear fast red (S1963, Dako, Carpinteria, CA).
12. Human Bcl-2 biotinylated deoxyribonucleic acid (DNA) probe: Cat. No.: SP-10043 (BCL-1001/BCL-1002), MBI). (Alignment on database: M14745).
13. Mounting medium: Entellan, neu, rapid mounting media for microscopy, (1.07961.0500, Merck, Germany).

Preparation of the Reagents According to Manufacturer's Instructions (Hybridization/Detection Complete System [IH-60002 (IHD-0052)]: Ultra Sensitivity, MBI)

Proteinase K

10 X Concentration Proteinase K Solution

1. Warm the Dnase (RNase-free) dilution buffer before use to avoid precipitation.
2. Add the entire contents (2 ml) of the DNase dilution buffer vial to the vial containing the lyophilized Proteinase K powder (4 mg).
3. Mix gently.
4. Divide the resulting 10X concentrated Proteinase K solution into small aliquots, and store any portion that is not to be used immediately at −20°C.

1X Proteinase K Solution

1. Remove aliquot(s) of 10X concentration Proteinase K solution from the freezer and allow them to thaw.
2. Dilute this solution 10-fold with distilled water as follows: 1 part of 10X concentration solution and 9 parts of water.

Protein Block Buffer

1. Dilute 50 ml of 20X concentrated Protein Block buffer into 1000 ml distilled water. Store the 1X Protein Block buffer when not in use at 4°C.

Detergent Wash Buffer

1. Dilute 50 ml of 20X concentrated detergent wash buffer into 1000 ml of distilled water.
2. Store the 1X detergent wash buffer that is not used at room temperature.

METHODS

Tissue Preparation

1. Fix liver tissue in 10% neutral formalin for 16 hr.
2. Embed the tissues in paraffin.
3. Cut serial tissue sections 4 μm thick, being careful to prevent RNAase contamination, and float them in a protein-free water bath.
4. Position the sections on the microscope slides with polylysine carefully to prevent RNAase contamination.
5. Deparaffinize sections overnight at 37°C.
6. Deparaffinize sections in xylene for 20 min.
7. Hydrate sections through graded alcohols:
   a. 100% ethanol for 2 min.
   b. 100% ethanol for 2 min.
   c. 96% ethanol for 1 min.
   d. 80% ethanol for 1 min.
   e. 70% ethanol for 1 min.
8. Rinse sections with distilled water for 5 min.
9. Dry sections at 37°C for 5 min.
10. Add Proteinase K for 15 min at 37°C.
11. Wash with detergent for 5 min.
12. Rinse with distilled water for 1 min.
13. Dehydrate slides in the following:
   a. 70% ethanol for 1 min.
   b. 80% ethanol for 1 min.
   c. 96% ethanol for 1 min.
   d. 100% ethanol for 1 min.
14. Dry at 37°C for 5 min.

Hybridization Protocol

1. Place 1 drop of the working DNA probe/hybridization solution (10-fold dilution of the probe in hybridization solution) on the tissue section. Place a coverslip over each slide. Be careful to avoid trapping any air bubbles.
2. Place the slides with coverslips in an oven at 95°C for 10 min to denature the secondary structure of RNA.
3. Place the slides in a humidity chamber and incubate at 37°C for 8 hr to allow hybridization of the probe with the target nucleic acid.
4. Soak the slides in 1X detergent wash at 37°C until the coverslips fall off. Be careful not to tear the tissue.
5. Place 1–2 drops of RNase A (15 μg/ml) on tissue section.
6. Place slides in humidity chamber. Incubate at 37°C for 30 min.
7. Wash the slide with Protein Block (prewarmed) at 37°C for 3 min., 3X. 1X, 3–5 min.
8. Protein Block (2X) for 3–5 min at 37°C.
9. Carefully wipe excess buffer from around the tissue section.
10. Place 1–2 drops of Linker 1 (green) on tissue section.
11. Place slides in humidity chamber. Incubate at 37°C for 40 min.
12. Tap off excess reagent. Rinse slides in detergent wash buffer for 5 min.
13. Carefully wipe off excess buffer from around the tissue section.
14. Put 1–2 drops of Linker 2 (yellow) on tissue section.

15. Place slides in humidity chamber and incubate at 37°C for 20 min.
16. Tap off excess reagent.
17. Rinse slides in detergent wash buffer for 5 min.
18. Carefully wipe off excess buffer from around the tissue section.
19. Place 1–2 drops of conjugate (red) on tissue section.
20. Place slides in humidity chamber. Incubate at 37°C for 20 min.
21. Tap off excess reagent.
22. Rinse slides in detergent wash buffer for 5 min.
23. Carefully wipe excess buffer from around the tissue section.
24. Place 1–2 drops of substrate (brown) on tissue section.
25. Incubate at room temperature for ~10 min or until color development is complete.
26. Tap off excess reagent.
27. Rinse slides in 2–3 changes of distilled water.
28. Counterstain and mount.
    a. Counterstain: Nuclear Fast Red for 10 min. Monitor under light microscope for color development (blue color).
    b. Rinse with distilled water for 5 min.
    c. Dehydrate through graded alcohols: 70%, 80%, 96%, and 100% (twice) for 1 min in each.
    d. Xylene, twice for 1 min each.
    e. Mount using Entellan.

Cytoplasmic staining for Bcl-2 is considered positive. For positive control tissues, we used paraffin sections from human tonsils. To confirm that the positive stain was specific, the slides were processed in an identical way and hybridized with probes known to be complementary to sequences in the test sections (human genomic DNA probes) (positive-control probes). These control probes were similar in length and GC content to the test probe. For negative control purposes, the slides were processed in the same way but hybridized with heterologous probes. The latter were not complementary to any sequence in the test tissues (plant genomic DNA probe). These negative control probes were similar in length and GC content to the Bcl-2 probe.

Immunohistochemistry for Bcl-2 and Hepatocyte Protein

MATERIALS

1. Fixative: 10% neutral formalin.
2. Microscope slides.
3. Distilled H_2O.
4. Coverslips.
5. Xylene.
6. Ethanol.
7. Tris buffer.
8. Hydrogen peroxide (30%).
9. Sodium citrate.
10. Albumin bovine fraction V, fatty acid–free lyophil, (13257, Serva, Germany).
11. Mouse monoclonal anti-bcl2 antibody, clone 124 (code No M0887, Dako, Carpinteria, CA).
12. Mouse monoclonal anti-hepatocyte antigen, clone OCH1ES, (code No M7158, Dako) to confirm the hepatocytic origin of the tumors.
13. Super-sensitive Ready-to-Use Detection kit (Catalog No QP900-CL, Biogenex, San Ramon, CA).
14. Chromogen: diaminobenzidine (DAB) tablets (Sigma Fast DAB, St Louis, MO).
15. Counterstain: Harris hematoxylin, Papanikolaou 1a, solution (1.09253.2500, Merck).
16. Mounting medium: Entellan, neu, rapid mounting media for microscopy (1.07961.0500, Merck).

Preparation of Solutions

1. Sodium citrate solution (pH 6): 500 ml distilled water, 1.05 g sodium citrate.
2. Tris buffer (pH: 7.6): 6.1 g Tris in 1000 ml distilled water and 37 ml 1N HCl.
3. Tris buffered saline (TBS buffer): 1800 ml NaCl and 200 ml Tris.
4. Solution for endogenous peroxidase consumption: 98 ml methanol, 2 ml H_2O_2.
5. Dilution solutions (for primary antibodies and other reagents) and blocking serum: 30 ml TBS and 0.3 g albumin.
6. Chromogen solution: 100 ml Tris, 2 ml DAB, 100 µl H_2O_2.

Protocol (Methods)

Tissue Preparation and Immunohistochemistry for Bcl-2 and Hepatocyte Antigen Protein

1. Fix the liver tissue in 10% neutral formalin for 16 hr.
2. Embed the tissues in paraffin.
3. Cut serial tissue sections 4 µm thick, and float them in a protein-free water bath.
4. Position the sections on the microscope slides with polylysine.
5. Deparaffinize sections overnight at 37°C.
6. Dewax sections into xylene for 20 min.
7. Hydrate sections through graded alcohols.
   a. 100% ethanol for 2 min.
   b. 100% ethanol for 2 min.

c. 96% ethanol for 1 min.
d. 80% ethanol for 1 min.
e. 70% ethanol for 1 min.

8. Rinse sections with distilled water for 5 min.
9. Antigen retrieval: Place sections in sodium citrate solution and heat them in a microwave oven at 750 W, 3× for 5 min each. Every 5 min the levels of the solutions are checked by adding sodium citrate, if necessary.
10. Rinse sections with distilled water for 5 min.
11. Incubate the sections with H_2O_2 for endogenous peroxidase blocking for 20 min in the dark.
12. Rinse sections with distilled water for 5 min.
13. Carefully wipe excess buffer from around the tissue section.
14. Add blocking serum and incubate the sections within a humidity chamber for 20 min.
15. Carefully tap serum from around the tissue sections, and, without rinsing them with TBS, place the primary antibody (Bcl-2 in dilution 1:40 or hepatocyte antigen in dilution 1:50). Incubate the sections within a humidity chamber at 37°C for 1 hr.
16. Rinse with TBS, 3× for 5 min each.
17. Carefully wipe excess buffer from around the tissue sections and place the Link (biotynilated anti-immunoglobulins Super-sensitive Ready-to-Use Detection kit). Incubate the sections within a humidity chamber for 20 min at room temperature.
18. Rinse with TBS, 3× for 5 min each.
19. Carefully wipe excess buffer from around the tissue sections and place the Label (enzyme-conjugated streptavidin Super-sensitive Ready-to-Use Detection kit). Incubate the sections within a humidity chamber for 20 min at room temperature.
20. Rinse with TBS, 3× for 5 min each.
21. Rinse with Tris buffer for 5 min.
22. Place the sections within chromogen solution for 4–5 min.
23. Monitor the color development (brown color) under a light microscope.
24. Rinse with water for 1 min.
25. Rinse with distilled water for 5 min.
26. Counterstain with Harris' hematoxylin for 2 min.
27. Rinse with water.
28. Dehydration through graded alcohols: 70% 1 min, 80% 1 min, 96% 1 min, 100% 1 min, and 100% 1 min.
29. Xylene, 2× for 1 min each.
30. Mount using Entellan.

As positive controls, paraffin sections from human tonsils were used. For negative control purposes, the same streptavidin–biotin technique was used in tissue sections in which 1% bovine serum albumin (BSA) in PBS was substituted for the primary antibody. Cytoplasmic staining for Bcl-2 and hepatocyte antigen was positive.

Morphometric Analysis

Quantitative analysis of the percentage of hepatocytes (neoplastic or nonneoplastic) that displayed positive ISH stain for Bcl-2 mRNA was performed as previously described (Salakou *et al.,* 2001, 2002; Tsamandas *et al.,* 2002, 2003), which is as follows: all tissue sections were scanned at a low power, and areas with positive stain were chosen. Thereafter, a 10 × 10 microscope grid at 400X magnification was applied on the sections and both the number of positive stained cells and the total number of cells (at least 500 cells) were determined by visual inspection of six different fields per section. For each field a percentage value for each marker was obtained by dividing the positive-stained cells by the total number of cells included in the grid. It should be noted that the variance in cell counts from field to field in the same section was less than 10%. The average of these scores was then taken. The sections were scored blindly to the clinical profile of the patients. Presence of Bcl-2 mRNA or oncoprotein within cholangiolar cells or lymphocytes was reported as positive or negative.

Statistical Analysis

Results were reported as mean ± standard deviation. Intergroup comparisons regarding 1) correlation of tumor features (histologic type, grade, and stage) with staining results and 2) correlation of staining results between different groups (neoplastic versus nonneoplastic and cirrhotic or noncirrhotic liver) were performed using one-way analysis of variance (ANOVA). When the equal-variance test or normality test failed, the Kruskall-Wallis nonparametric test was applied. To address the problem of multiple comparisons, these tests (ANOVA and Kruskall-Wallis) were followed by a *post hoc* Bonferroni test. Data were analyzed using the SPSS for Windows (SPSS, Inc., Chicago, IL). Significance was defined as $p < 0.05$.

RESULTS

Conventional Pathology

In all 35 cases the immunostain for hepatocyte antigen was positive in neoplastic and nonneoplastic hepatocytes and confirmed the origin of the tumors. According to Edmondson criteria, 20 tumors were grade I, 11 were grade II, and 4 were grade III. In 25 cases the tumor exhibited mainly a microtrabecular/microglandular pattern, whereas in the remaining 10 the histologic pattern was more solid and less

microtrabecular/microacinar. According to TNM classification, 4 cases were stage I, 11 were stage II, and 20 were stage III.

In situ Hybridization for Bcl-2 mRNA

Bcl-2 mRNA was present within neoplastic hepatocytes in 25/35 (70%) instances and was present in all 35 cases within hyperplastic cholangioles of the surrounding the tumor fibrous tissue (Figure 32A) and lymphocytes. The 25 cases that were positive for hepatocytic Bcl-2 mRNA were further analyzed (regarding histologic type, grade, stage, and prior chemoembolization) as follows: 1) 18/25 tumors displayed a microtrabecular/microacinar pattern, whereas 7 tumors had a solid pattern; 2) 14/25 tumors were of grade I, 8/25 of grade II, and 3/25 of grade III; 3) 3/25 tumors were of stage I, 8/15 of stage II, and 14/25 of stage III.

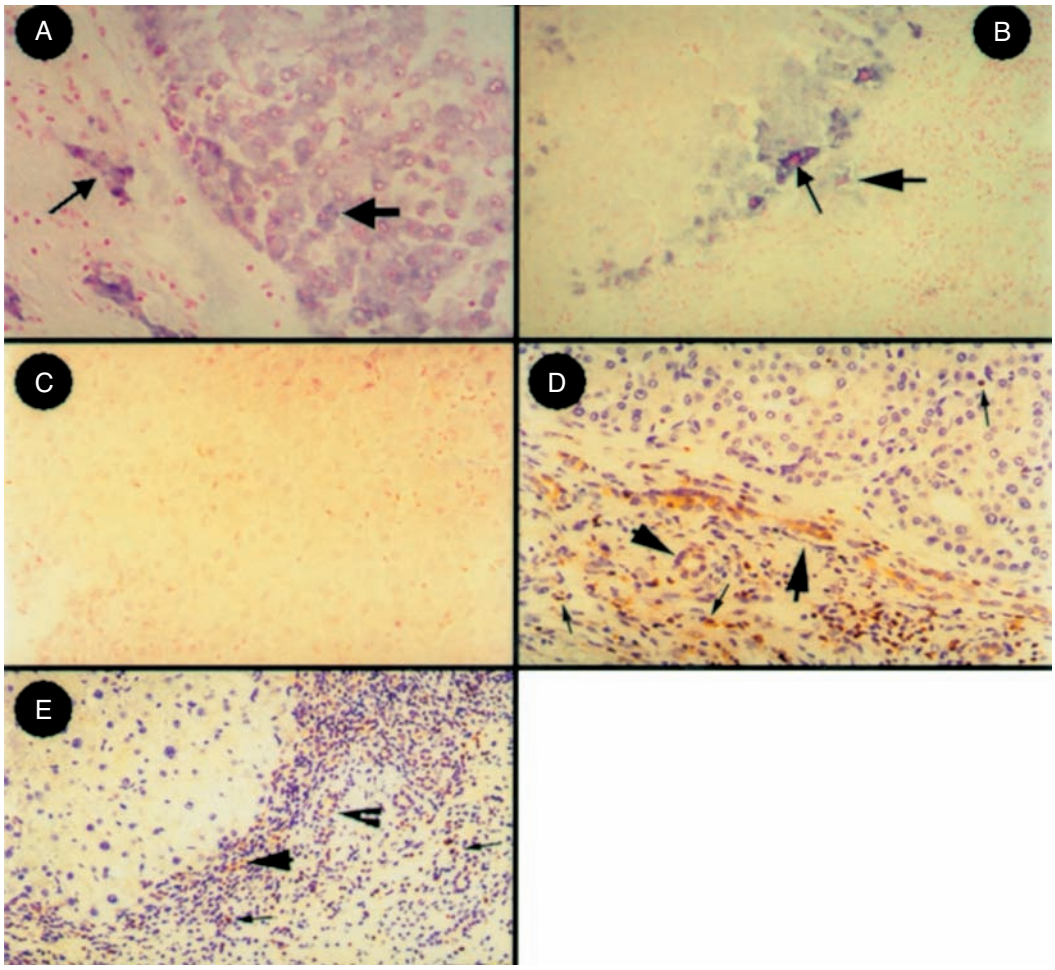

Figure 32. A: *In situ* hybridization histochemistry (digoxigenin) showing messenger ribonucleic acid for Bcl-2 within hepatoma cells (*thick arrow*) and hyperplastic cholangioles (*thin arrow*) in a case of hepatocellular carcinoma (*Left:* X250, *Right:* X400).
B: *In situ* hybridization histochemistry (digoxigenin) showing messenger ribonucleic acid for Bcl-2 within hepatocytes near the edge of fibrous tissue (*thin arrow*) and a cholangiole (*thick arrow*) in a section that shows nonneoplastic cirrhotic area of the liver (X250).
C: *In situ* hybridization histochemistry (digoxigenin) using the negative control (sense) probe for Bcl-2 in a case of hepatocellular carcinoma (X400).
D: Immunohistochemistry for Bcl-2 oncoprotein in a case of hepatocellular carcinoma. Septal and intratumoral lymphocytes (*thin arrows*) and septal cholangioles (*thick arrows*) display positive stain. Neoplastic hepatocytes are negative (streptavidin-biotin peroxidase X400).
E: Immunohistochemistry for Bcl-2 oncoprotein in a section from a nonneoplastic cirrhotic area of the liver. Septal lymphocytes (*thin arrows*) and cholangioles (*thick arrows*) display positive stain. Hepatocytes are negative (*Left:* streptavidin-biotin peroxidase X250; *Right:* streptavidin-biotin peroxidase X400).

In 6/25 cases, chemoembolization was administered before treatment, whereas in 19/25 no chemoembolization was given. In the liver parenchyma adjacent to the tumor (cirrhotic or noncirrhotic), Bcl-2 mRNA was present in hepatocytes near the edge of the fibrous tissue and in hyperplastic cholangioles (Figure 32B). These results are in disagreement with a previous study that reported that Bcl-2 mRNA is not present in nonneoplastic hepatocytes adjacent to HCC (Fiorentino *et al.,* 1999). When the negative control (sense) probe was used, no staining was present (Figure 32C).

Immunohistochemistry for Bcl-2 Oncoprotein

In cases of HCCs, Bcl-2 protein was present only in hyperplastic cholangioles and intratumoral or septal lymphocytes in all 35 instances. In no one case, did normal or neoplastic hepatocytes display positivity for Bcl-2 protein (Figure 32D). In the surrounding the tumor nonneoplastic (cirrhotic or noncirrhotic) liver, Bcl-2 protein was expressed within lymphocytes in portal tracts, lobules, and bands of fibrous tissue and cholangioles of interface area. Hepatocytes and interlobular bile ducts of portal tracts were negative for Bcl-2 protein and mRNA (Figure 32E).

Statistical Analysis

Bcl-2 mRNA expression was higher in neoplastic hepatocytes compared to nonneoplastic ones (either in cirrhotic or noncirrhotic parenchyma, 43.5 ± 2.32 versus 30.4 ± 1.05, $p < 0.001$ and 43.5 ± 2.32 versus 20.77 ± 1.02, $p < 0.001$, respectively). In addition, Bcl-2 mRNA expression within periportal or periseptal hepatocytes was higher in cirrhotic compared to noncirrhotic, nonneoplastic liver parenchyma (30.4 ± 1.05 versus 20.77 ± 1.02, $p < 0.001$). No significant relations were found between hepatocytic Bcl-2 mRNA expression and 1) tumor histologic type (microtrabecular/microacinar, 46 ± 1.0 versus solid pattern, 42 ± 0.8, $p > 0.05$); 2) grade (grade I, 44 ± 0.9 versus grade II, 47 ± 0.3 versus grade III, 41 ± 0.6, $p > 0.05$); and 3) tumor stage (stage I, 44 ± 0.1 versus stage II, 46 ± 0.2, versus stage III, 40 ± 0.7, $p > 0.05$). In addition, no significant difference regarding hepatocytic Bcl-2 mRNA expression was observed between cases with previous chemotherapy and cases without chemotherapy (42 ± 0.3 versus 43 ± 0.1, $p > 0.05$).

DISCUSSION

This study demonstrates that in cases of HCC, Bcl-2 oncoprotein is actively produced 1) from neoplastic and nonneoplastic hepatocytes and 2) from cholangiolar epithelial cells. The finding of Bcl-2 mRNA expression from nonneoplastic hepatocytes in cases of HCC is in disagreement with those of a previous study in which Bcl-2 mRNA was present only in hepatoma cells (Fiorentino *et al.,* 1999). The difference between the two studies may be attributed to different methods and reagents used by the investigators.

In the past it was reported that Bcl-2 is expressed in the liver by cholangiocytes and not by hepatocytes and that this could be used as a diagnostic tool to differentiate HCCs from cholangiocarcinomas (Charlotte *et al.,* 1994). However, a more recent study showed that Bcl-2 mRNA is expressed in both hepatocellular and cholangiocarcinomas, and thus it can not be used as a differential marker (Fiorentino *et al.,* 1999). In addition, in the liver it has never been conclusively shown that Bcl-2 really does have prognostic value or gives an indication about response to chemotherapy (Fiorentino *et al.,* 1999).

Previously, Bcl-2 protein was detected in HCC in low percentages (3–20%) (Fiorentino *et al.,* 1999). More specifically, in the study by Zhao *et al.* (1994), Bcl-2 expression was mainly cytoplasmic, whereas a paranuclear and a nuclear expression was also observed. The nuclear Bcl-2 expression is somewhat peculiar because Bcl-2 oncoprotein mainly is located in the mitochondria, endoplasmic reticulum, and nuclear membranes (Hockenbery *et al.,* 1990, Krajewski *et al.,* 1993). The present study did not demonstrate any Bcl-2 protein positivity in the hepatocytes. This difference could be attributed to the sensitivity of the immunohistochemical technique. However, we used a well-controlled immunohistochemical technique and the internal positive controls (intratumoral lymphocytes) displayed strong cytoplasmic immunohistochemical staining for Bcl-2.

The striking difference observed between Bcl-2 mRNA and protein expression in this study could be attributed to a disorder of posttranscriptional regulation of the Bcl-2 gene. This mechanism has not been yet fully elucidated (Harigai *et al.,* 1996). In this study the absence of Bcl-2 protein and the presence of Bcl-2 mRNA suggest that Bcl-2 may be actively produced in HCCs, but its protein product is not expressed within the neoplastic cells. We, therefore, speculate that a mechanism operating at the posttranscriptional level (e.g., associated with the 3′ untranslated region) prevents this mRNA from being translated into protein in cases of HCC. Thus, in contrast to other epithelial neoplasms, Bcl-2 does not play a relevant role in HCC progression.

Another interesting finding is that Bcl-2 mRNA expression was not correlated with tumor grade or the histologic type of HCC (microacinar, microtrabecular, solid). In a previous study (Lee, 1997), Bcl-2 expression

in experimentally induced HCCs was correlated with basophilic appearance of hepatocytes; this was not demonstrated in our study. Thus, we are unable to state whether the tumors expressing Bcl-2 represent a distinct subset of human HCC. However, Bcl-2 mRNA expression was significantly higher in neoplastic compared to nonneoplastic hepatocytes. This increase in Bcl-2 active production by hepatocytes may correlate with the development of HCC, given the anti-apoptotic/oncogenic potential of Bcl-2.

The finding that Bcl-2 mRNA was present in nonneoplastic hepatocytes in HCC instances, combined with the results of a previous study (Frommel *et al.,* 1999), implies that the presence of this oncogene may be correlated with the development of HCC that may accompany cases of cirrhosis as a result of chronic hepatitis B or C. Down-regulation of the gene may play a role in liver cell differentiation and turnover by committing them to apoptosis, whereas abnormal expression of Bcl-2 may lead to the accumulation of long-living cells and finally to tumor development. A deregulated expression of Bcl-2 gene in neoplastic cells may transform them and increase their resistance to apoptosis. This hypothesis is further supported by the fact that Bcl-2 provides survival advantage to progenitor and effector cells in some tissues (Hockenbery *et al.,* 1991); thus, its expression in cholangiolar epithelial cells may be correlated with a prolonged survival of these cells. Therefore, Bcl-2 expression in the periportal hepatocytes may be an additional indication of presence of liver stem cells and especially of oval cells that represent a progeny of the hepatic cell compartment, which is constituted by the terminal ductule cells connecting the canals of Herring with the bile canaliculi and/or a distinct population of periductal cells (Hsia *et al.,* 1992). Previously we demonstrated that in cases of chronic hepatitis type B or C, oval cell expression is related to the progress of fibrosis and coexistence of HCC (Tsamandas *et al.,* 2001). Thus, we speculate that Bcl-2 expression in the cholangioles may be related to the presence of liver progenitor cells that differentiate to ductular epithelial cells and to the development of HCC. However, further research is warranted to confirm this possibility.

In conclusion, this study shows that in HCCs, Bcl-2 gene is frequently present but its protein product is absent. This suggests a posttranslational mechanism of Bcl-2 protein degradation indicating that Bcl-2 does not play a substantial role in the development and progress of HCC. Further studies are warranted to detect the exact disorder on posttranscriptional and posttranslational regulation mechanisms of the Bcl-2 gene during the development and progress of HCC.

References

Bronner, M.P., Culin, C., Reed, J.C., and Furth, E.E. 1995. The bcl-2 protooncogene and the gastrointestinal epithelial tumor progression model. *Am. J. Pathol. 146*:20–26.

Charlotte, F., L'Hermine, A., Martin, N., Geleyn, Y., Nollet, M., Gaulard, P., and Zafrani, E.S. 1994. Immunohistochemical detection of Bcl-2 protein in normal and pathologic human liver. *Am. J. Pathol. 144*:460–465.

Cleary, M.L., and Sklar, J. 1985. Nucleotide sequence of a t(14;18) chromosomal breakpoint in follicular lymphoma and demonstration of a breakpoint-cluster region near a transcriptionally active locus on chromosome 18. *Proc. Natl. Acad. Sci. USA 82*:7439–7443.

Columbano, A., Ledda-Columbano, G.M., Coni, P.P., Faa, G., Liguori, C., Santa Cruz, G., and Pani, P. 1985. Occurrence of cell death (apoptosis) during the involution of liver hyperplasia. *Lab. Invest. 52*:670–675.

Craig, J.R., Peters, R.L., and Edmondson, H.A. 1988. Tumors of the liver and intrahepatic bile ducts.

Cummings, M.C., Winterford C.M., and Walker N.I. 1997. Apoptosis. *Am. J. Surg. Pathol. 21*:88–101.

Fiorentino, M., D'Errico, A., Altimari, A., Barozzi, C., and Grigioni, W.F. 1999. High levels of BCL-2 messenger RNA detected by *in situ* hybridization in human hepatocellular and cholangiocellular carcinomas. *Diagn. Mol. Pathol. 8*:189–194.

Frommel, T.O., Yong, S., and Zarling, E.J. 1999. Immunohistochemical evaluation of Bcl-2 gene family expression in liver of hepatitis C and cirrhotic patients: A novel mechanism to explain the high incidence of hepatocarcinoma in cirrhotics. *Am. J. Gastroenterol. 94*:178–182.

Harigai, M., Miyashita, T., Hanada, M., and Reed, J.C. 1996. A cis-acting element in the bcl-2 gene that controls expression through translational mechanisms. *Oncogene 12*:1369–1374.

Hockenbery, D., Nunez, G., Milliman, C., Schreiber, R.D., and Korsmeyer, S.J. 1990. Bcl-2 is an inner mitochondrial membrane protein that blocks programmed cell death. *Nature 348*:334–336.

Hockenbery, D.M., Zutter, M., Hickey, W., Nahm, M., and Korsmeyer, S.J. 1991. Bcl-2 protein is topographically restricted in tissues characterized by apoptosic cell death. *Proc. Natl. Acad. Sci. USA 88*:6961–6965.

Hsia, C.C., Evarts, R.P., Nakatsukasa, H., Marsden, E.R., and Thorgeirsson, S.S. 1992. Occurrence of oval-type cells in hepatitis B-virus associated human hepatocarcinogenesis. *Hepatology 16*:1327–1333.

Krajewski, S., Tanaka, S., Takayama, S., Schibler, M.J., Fenton, W., and Reed, J.C. 1993. Investigations of the subcellular distribution of the bcl-2 oncoprotein: Residence in the nuclear envelope, endoplasmic reticulum and outer mitochondrial membranes. *Cancer Res. 53*:4701–4714.

Kurosawa, H., Que, F.G., Roberts, L.R., Fesmier, P.J., and Gores, G.J. 1997. Hepatocytes in the bile duct-ligated rat express Bcl-2. *Am. J. Physiol. 272*:G1587–1593.

Lee, G.H. 1997. Correlation between Bcl-2 expression and histopathology in diethylnitrosamine-induced mouse hepatocellular tumors. *Am. J. Pathol. 151*:957–961.

Salakou, S., Tsamandas, A.C., Bonikos, D.S., Papapetropoulos, T., and Dougenis, D. 2001. The potential role of bcl-2, bax and Ki67 expression in thymus of patients with myasthenia gravis, and their correlation with clinicopathologic parameters. *Eur. J. Cardiothorac. Surg. 20*:712–721.

Salakou, S., Tsamandas, A.C., Tsimbri, E., Dougenis, D., Bonikos, D.S., and Papapetropoulos, T. 2002. Bcl-2 and Bax and

p53 expression in thymous of patients with myasthenia gravis and their correlation with clinicopathologic parameters. *J. Neurol. Sci. 199(S1)*:P621.

Terada, T., and Nakanuma, Y. 1995. Detection of apoptosis and expression of apoptosis-related proteins during human intrahepatic bile-duct development. *Am. J. Pathol. 146*:67–74.

Tsamandas, A.C., Thomopoulos, K., Zolota, V., Kourelis, T., Karatzas, T., Ravazoula, P., Tepetes, K., Petsas, T., Karavias, D., Karatza, C., Bonikos, D.S., and Gogos, C. 2003. The potential role of bcl-2 and bax mRNA and protein expression in chronic hepatitis type B and C. A clinicopathologic study. *Mod. Pathol. 16*:1273–1288.

Tsamandas, A.C., Gogos, C., Kourelis, T., Ravazoula, P., Tepetes, K., Petsas, T., and Karavias, D. 2001. Oval hepatocytes express alpha-fetoprotein and correlate with disease severity and presence of hepatocellular carcinoma in cases of chronic hepatitis type B or C. *Hepatology 34*:392A.

Tsamandas, A.C., Thomopoulos, K., Gogos, C., Tepetes, K., Kourelis, T., Ravazoula, P., Petsas, T., Bonikos, D.S., Karatza, C., and Karavias, D.D. 2002. Expression of bcl-2 oncoprotein in cases of acute and chronic viral hepatitis type B and type C. A clinicopathologic study. *Dig. Dis. Sci. 47*: 1618–1624.

Zhao, M., Zhang, N.X., Economou, M., Blaha, I., Laissue, J.A., and Zimmermann, A. 1994. Immunohistochemical detection of bcl-2 protein in liver lesions: bcl-2 is expressed in hepatocellular carcinomas but not in liver cell dysplasia. *Histopathology 25*:237–245.

7

The Detection and Clinical Aspect of Immunohistochemical Analysis of Bcl-xL Protein in Hepatocellular Carcinoma

Jota Watanabe and Fumiki Kushihata

Introduction

Apoptosis is the mechanism that eliminates unwanted or potentially harmful cells to maintain ontogenesis, morphogenesis, and homeostasis (Carson and Ribeiro, 1993; Kerr *et al.,* 1972). In addition to increased cell proliferation, inhibition of apoptosis plays a major role in the development of cancer (Grasl-Kraupp *et al.,* 1997), and cancer initiation and progression occur when apoptosis is inhibited. It is well known that apoptosis is controlled by the Bcl-2 family of proteins, along with a variety of anti-apoptotic (e.g., Bcl-2 and Bcl-xL) and proapoptotic (e.g., Bax and Bcl-xS) factors present in homodimeric or heterodimeric forms (Gross *et al.,* 1999). The onset of apoptosis is triggered by changes in both the intracellular content and localization of anti-apoptotic and proapoptotic Bcl-2 family proteins (Charlotte *et al.,* 1994). Although Bcl-2 expression has been observed in both normal and cancerous human liver cells, Bcl-xL expression has not been elucidated. In the present study, we investigated the relationship between Bcl-xL and hepatocellular carcinoma (HCC) using surgical specimens.

MATERIALS AND METHODS

Patients

Primary HCC tissues were obtained from 33 patients (age 60.85 ± 9.84 [mean ± SD], range 36 to 77 years; male to female ratio, 23:10) who underwent surgical resection at our unit from 1993 to 1998. Informed consent was obtained from all patients. Of the patients, 14 were infected with hepatitis B virus (HBV), 10 were infected with hepatitis C virus (HCV), and 5 were infected with both HBV and HCV; 2 of the patients had no previous history of hepatitis, 19 had chronic hepatitis (CH), and 12 had liver cirrhosis (LC). The patients were subdivided into groups based on whether the HCC was extensively (well) (n = 6), moderately (n = 24), or poorly (n = 3) differentiated. We used International Union Against Cancer (UICC) TNM classification and stage grouping. Many of the tumors were very large; 12 patients had tumors more than 50 mm in diameter.

Tissue samples from seven patients with HCC who underwent hepatic resection in 2000 were obtained and frozen. Western Blot analysis was performed. Normal liver samples representing nontumor tissue were obtained

Handbook of Immunohistochemistry and *in situ* Hybridization of Human Carcinomas, Volume 3: Molecular Genetics, Liver Carcinoma, and Pancreatic Carcinoma

from three patients who underwent resection for hepatic metastases resulting from colon carcinoma. No patients had a history of hepatitis infection.

Western Blot Analysis

Specimens (each weighing 300 µg) from the cancerous region of the tumor, and from a noncancerous region of the liver of the seven patients with HCC, were frozen in liquid nitrogen immediately after hepatectomy and used for Western Blot analysis. The specimens were immersed in 10 volumes of lysis buffer (250 mM sucrose in 10 mM Tris-NaCl, pH 7.5). The samples were disrupted using a Polytron homogenizer and centrifuged at 10,000 rpm for 4 min at 4°C. The protein concentrations in the supernatants were measured using the Lowry method. We used 15 µg on each lane accurately. The samples were electrophoresced on 15% polyacrylamide gels and then transferred to PVDF (polyvinylidene fluoride) membranes (Hybond-P, Amersham Pharmacia Biotech, Bucks, UK). The membranes were blocked with 5% skim milk in Tris-buffered saline (20 mM Tris, 500 mM NaCl, pH 7.5) at 4°C overnight. We used anti-Bcl-X rabbit polyclonal antibody (Transduction Laboratories, Lexington, KY). After a secondary antibody was added, an ECL Western Blotting Kit (Amersham Pharmacia Biotech) was used for detection and the blots were visualized on Hyperfilm (Amersham Pharmacia Biotech). The level of Bcl-xL was calculated as the relative value to a commercial positive control (Transduction Laboratories) serially diluted five times on the same membranes. We quantified the uptake using NIH Image (for the U.S. National Institutes of Health) using the data from all blots and comparing them with the results for normal livers.

Immunohistochemical Staining

Tissue from patients with HCC was fixed in formalin and embedded in paraffin, and 4-µm-thick sections were prepared. The paraffin was removed in xylene three times, after which the tissues were rehydrated through a graded ethanol series ranging from 60% to 100%. The samples were treated in a microwave oven for 30 min. We used anti-Bcl-X rabbit polyclonal antibody (Transduction Laboratories) as in the Western Blot analysis. Then we incubated them with peroxidase-labeled polymer-conjugated antibody in the Envision System (Teckmate Horizon System, Dako A/S, DK-2600 Glostrup, Denmark) (Shibayama and Koizumi, 1996). The final reaction product was visualized with diaminobenzidine (DAB). Nuclear staining was carried out using hematoxylin. A negative control slide was included in each batch, in which the first antibody was replaced with normal serum. Immunopositive reactions were observed under a light microscope. Three independent observers analyzed the Bcl-xL immunoreaction under light microscopy. Estimates were scored using the following arbitrary range: (–) negative overexpression of cells compared to noncancerous cells; (+) positive overexpression compared to noncancerous cells.

Immuno-Electron Microscopy

The remaining HCC tissue was fixed in 4% paraformaldehyde–0.1% glutaraldehyde in 0.1 M phosphate buffer (pH 7.4). The tissue was cut into 50-µm sections with a microslicer. The sections were immunostained with anti-Bcl-X rabbit polyclonal antibody (Transduction Laboratories) and were subjected to a modified version of the cobalt-glucose oxidase–DAB method. The sections were postfixed with 1% osmium tetroxide, dehydrated in a graded series of ethanol, double stained with 1% uranyl acetate in 70% ethanol and lead citrate, transferred to propylene oxide, and embedded in epoxy resin. Ultrathin sections were cut with a Reichert ultramicrotome (Leica, Chicago, IL) and observed by electron microscopy (Hitachi H-800, Japan). Control sections were incubated with primary antiserum adsorbed with an excess of Bcl-xL and then processed as described earlier.

RESULTS

Western Blot of Bcl-xL

Western Blot analysis was used to confirm the expression of Bcl-xL in HCC. Figure 33 shows the findings from a representative case. Bcl-xL was strongly overexpressed in normal liver, whereas that in the noncancerous part of the patients who had underlying liver disease (HBV or HCV) was weak and, again, that in HCC was strong. The data from the seven patients with HCC were quantified using NIH image and revealed significantly greater expression of Bcl-xL in tumor versus nontumor tissue ($p = 0.016$).

Immunohistochemical Staining

In all cases, Bcl-xL was expressed in the cytoplasm of liver cells in both normal liver regions (Figure 34A) and cancerous liver regions. In nonparenchymal regions, immunostaining in the portal veins and arteries of Glisson's capsule was weak, whereas immunoreactivity was seen in the cytoplasm of bile duct cells. Positive reactions were also seen in many nonparenchymal cells in Glisson's capsule (Figure 34B);

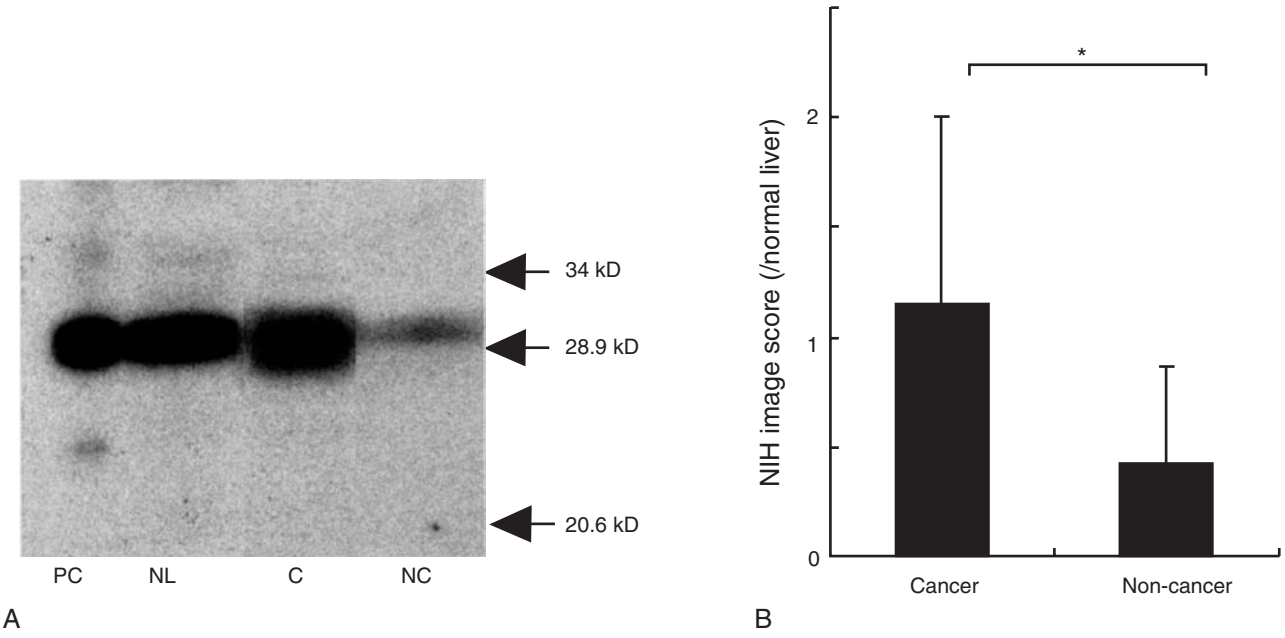

Figure 33. Western Blot analysis was performed to confirm expression of Bcl-xL in hepatocellular carcinoma (HCC). **A:** The findings from a representative case are shown. Bcl-xL was expressed in cancerous and noncancerous tissue, but expression was greater in cancerous tissue. **B:** Quantification of uptake with National Institutes of Health Image using data from seven patients with HCC revealed significantly greater expression of Bcl-xL in cancerous versus noncancerous tissue (*: $p = 0.016$, Mann-Whitney U-test.) (The values are expressed mean ± SD. PC, positive control; NL, normal liver; C, cancer; NC, noncancer.)

these were thought to be immature cell components derived from bile duct cells (Krajewski *et al.,* 1994). In most cases, Bcl-xL immunoreactivity was stronger in the cancerous regions than in the noncancerous regions (Figure 34C). Pretreatment of the Bcl-xL antiserum with Bcl-xL eliminated all immunoreactivity (Figure 34D). The level of expression in specimens from 21/33 (63.6%) patients was stronger in cancerous than in noncancerous regions. Elevated Bcl-xL immunoreactivity, apparent as granular patterning in magnified images, was present in the cytoplasm of hepatocytes in the margins of liver tumors that included many cancer cells. The level of Bcl-xL immunoreactivity was lower in patients with LC than in patients without cirrhosis. In some cases, the immunoreactivity was stronger in the margins of the tumors than in the central regions. Bcl-xL staining was stronger in the cytoplasm of residual tumor cells in nonnecrotic areas after transcatheter arterial embolization (TAE). Immunoreactive spots appeared in both the cytoplasm and nuclei of cells in tumor margins.

Immuno-Electron Microscopy

Immuno-electron microscopy demonstrated Bcl-xL immunoreactivity within hepatocytes and stringlike cells mainly in the cytoplasm, but not in fibroblasts or endothelial cells in normal liver specimens. Under high magnification, immunoreactivity was seen homogeneously in the cytoplasm and densely in the mitochondria (data not shown). Immuno-electron microscopy demonstrated strongly positive areas of immunoreactivity for Bcl-xL, particularly in the cytoplasm in cancerous specimens. These sites were mainly around the mitochondria but not in the nucleus, centriole, or endoplasmic reticulum.

DISCUSSION

Bcl-xL first identified in 1993 (Boise *et al.,* 1993), belongs to the Bcl-2 family, and has anti-apoptotic activity. It has been proposed that Bcl-xL modulates apoptosis by controlling mitochondrial membrane permeability and regulating the release of cytochrome c (Tsujimoto and Shimizu, 2000). During liver regeneration induced by partial hepatectomy, Bcl-2 is not detected, whereas hepatocytes express Bcl-xL at G1 phase (Tzung *et al.,* 1997), and hepatocyte growth factor strongly induces Bcl-xL expression and inhibits massive hepatocyte apoptosis (Kosai *et al.,* 1999). The introduction of Bcl-2 into liver cancer cells by genetic manipulation partially suppressed Fas-induced apoptosis *in vitro* (Takahashi *et al.,* 1999). Therefore, we speculated that both in hepatocytes and HCC cells, Bcl-xL

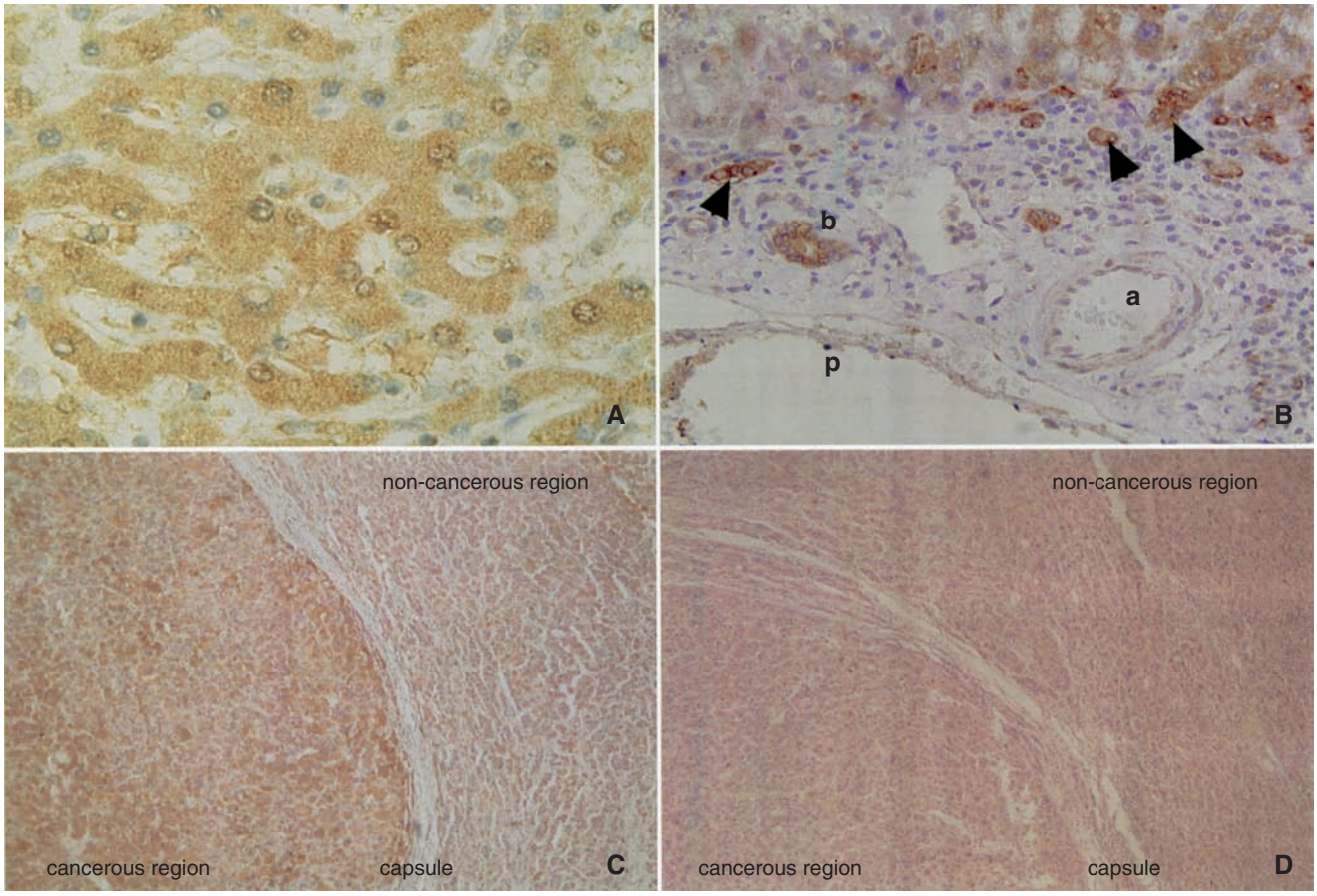

***Figure* 34. A:** Bcl-xL was expressed in the cytoplasm of liver cells in normal liver regions (magnification: A 400X). **B:** Positive reactions were also seen in many nonparenchymal cells (arrows) in Glisson's capsule. (a, artery; p, portal vein; b, bile duct.) (Magnification: B 200X.) **C:** Bcl-xL immunoreactivity was stronger in the cancerous regions than in the non-cancerous regions (magnification: C 40X). **D:** Pretreatment of the Bcl-xL antiserum with Bcl-xL eliminated all immunoreactivity (magnification: D 40X).

is the functional anti-apoptotic protein of the Bcl-2 family.

In this study, we demonstrated that Bcl-xL was overexpressed in liver tumors. Bcl-xL was localized mainly in the cytoplasm and mitochondria of both normal and cancer cells. It is interesting that Bcl-xL expression was also found in the nuclei of liver cancer cells in the tumor margins. This suggests that Bcl-xL participates in the progression of liver cancer cells. This hypothesis is also supported by the finding that Bcl-xL contributes to liver tissue regeneration. From a clinical perspective, it is of interest to note that Bcl-xL expression was stronger in the cytoplasm of residual tumor cells in nonnecrotic areas after TAE. This implies that residual tumor cells acquire resistance to the ischemic stress of TAE and get the higher grade of malignancy. Radical resection is therefore advisable in these cases.

Using immuno-electron microscopy, we suggest that Bcl-xL is localized around the mitochondria of HCC cells. Studies suggest that apoptosis signal transduction in HCC cells primarily takes place via mitochondria. As Bcl-2 family members have their effect upstream from the point of irreversible cellular damage, they play a pivotal role in deciding whether a cell will live or die at the level of the mitochondria (Li *et al.,* 1998; Yin *et al.,* 1999). Our findings demonstrate that Bcl-xL also plays an important role in controlling apoptosis in HCC cells in addition to liver regeneration (Tzung *et al.,* 1997; Watanabe *et al.,* 2002).

One of the biological characteristics of tumor cells is their ability to "escape from immune surveillance," which is in essence an "escape from apoptosis" (Nagao *et al.,* 2000; Tatsumi *et al.,* 1997). This molecular mechanism, in addition to interference with the inactivation mechanism of tumor immunity in patients with cancer,

involves the resistance of the target tumor cells to apoptosis (Nagao *et al.,* 1999; Shin *et al.,* 1998). By clinicopathologic analysis, we found a significant negative correlation between Bcl-xL overexpression and both overall and disease-free survival (Watanabe *et al.,* 2004). This implies that Bcl-xL overexpressed HCC has not always high-grade malignancy itself but also the resistance to apoptosis-induced therapy such as postoperative chemotherapy. Bcl-xL is a new prognostic factor for HCC. Determination of Bcl-xL overexpression should set a new standard in the postoperative evaluation of patients with HCC, which has high possibility for recurrence.

In conclusion, Bcl-xL overexpression was found in the majority of surgically removed HCC specimens. Bcl-xL overexpression was found mainly in the cytoplasm of liver cancer cells. It was especially dense in the mitochondria, but it was also found in the nuclei of some liver cancer cells, suggesting that Bcl-xL is involved in the progression of HCC.

References

Boise, L.H., Gonzalez-Garcia, M., Postema, C.E., Ding, L., Lindsten, T., Turka, L.A., Mao, X., Nunez, G., and Thompson, C.B. 1993. bcl-x a bcl-2-related gene that functions as a dominant regulator of apoptotic cell death. *Cell 74*:597–608.

Carson, D.A., and Ribeiro, J.M. 1993. Apoptosis and disease. *Lancet 341*:1251–1254.

Charlotte, F., L'Hermine, A., Martin, N., Geleyn, Y., Nollet, M., Gaulard, P., and Zafrani, E.S. 1994. Immunohistochemical detection of bcl-2 protein in normal and pathological human liver. *Am. J. Pathol. 144*:460–465.

Grasl-Kraupp, B., Ruttkay-Nedecky, B., Mullauer, L., Taper, H., Huber, W., Bursch, W., and Schulte-Hermann, R. 1997. Inherent increase of apoptosis in liver tumors: Implications for carcinogenesis and tumor regression. *Hepatology 25*:906–912.

Gross, A., McDonnell, J.M., and Korsmeyer, S.J. 1999. Bcl-2 family members and the mitochondria in apoptosis. *Genes Dev. 13*:1899–1911.

Kerr, J.F., Wyllie, A.H., and Currie, A.R. 1972. Apoptosis: A basic biological phenomenon with wide ranging implications in tissue kinetics. *Br. J. Cancer 26*:239–257.

Kosai, K., Matsumoto, K., Funakoshi, H., and Nakamura, T. 1999. Hepatocyte growth factor prevents endotoxin-induced lethal hepatic failure in mice. *Hepatology 30*:151–159.

Krajewski, S., Krajewski, M., Shabaik, A., Wang, H.G., Irie, S., Fong, L., and Reed, J.C. 1994. Immunohistochemical analysis of in vivo patterns of Bcl-X expression. *Cancer Res. 54*:5501–5507.

Li, H., Zhu, H., Xu, C.J., and Yuan, J. 1998. Cleavage of BID by caspase 8 mediates the mitochondrial damage in the fas pathway of apoptosis. *Cell 94*:491–501.

Nagao, M., Nakajima, Y., Hisanaga, M., Kayagaki, N., Kanehiro, H., Aomatsu, Y., Ko, S., Yagita, H., Yamada, T., Okumura, K., and Nakano, H. 1999. The alteration of Fas receptor and ligand system in hepatocellular carcinomas: How do hepatoma cells escape from the host immune surveillance in vivo? *Hepatology 30*:413–421.

Nagao, M., Nakajima, Y., Kanehiro, H., Hisanaga, M., Aomatsu, Y., Ko, S., Tatekawa, Y., Ikeda, N., Kanokogi, H., Urizono, Y., Kobayashi, T., Shibaji, T., Kanamura, T., Ogawa, S., and Nakano, H. 2000. The impact of interferon gamma receptor expression on the mechanism of escape from host immune surveillance in hepatocellular carcinoma. *Hepatology 32*:491–500.

Shibayama, E., and Koizumi, H. 1996. Cellular localization of the Trk neurotrophin receptor family in human non-neuronal tissue. *Am. J. Pathol. 148*:1807–1828.

Shin, E.C., Shin, J.S., Park, J.H., Kim, J.J., Kim, H., and Kim, S.J. 1998. Expression of Fas-related genes in human hepatocellular carcinomas. *Cancer Lett. 134*:155–162.

Takahashi, M., Saito, H., Okuyama, T., Miyashita, T., Kosuga, M., Sumisa, F., Yamada, M., Ebimura, H., and Ishii, H. 1999. Overexpression of Bcl-2 protects human hepatoma cells from Fas-antibody-mediated apoptosis. *J. Hepatol. 31*:315–322.

Tatsumi, T., Takehara, T., Katayama, K., Mochizuki, K., Yamamoto, M., Kanto, T., Sasaki, Y., Kasahara, A., and Hayashi, N. 1997. Expression of costimulatory molecules B7-1(CD80) and B7-2(CD86) on human hepatocellular carcinoma. *Hepatology 25*:1108–1114.

Tsujimoto, Y., and Shimizu, S. 2000. Bcl-2 family: Life-or-death switch. *FEBS Lett. 466*:6–10.

Tzung, S.P., Fausto, N., and Hockenbery, D.M. 1997. Expression of Bcl-2 family during liver regeneration and identification of Bcl-x as a delayed early response gene. *Am. J. Pathol. 150*:1985–1995.

Watanabe, J., Kushihata, F., Honda, K., Mominoki, K., Matsuda, S., and Kobayashi, N. 2002. Bcl-xL overexpression in human hepatocellular carcinoma. *Int. J. Oncol. 21*:515–519.

Watanabe, J., Kushihata, F., Honda, K., Sugita, A., Tateishi, N., Mominoki, K., Matsuda, S., and Kobayashi, N. 2004. Prognostic significance of Bcl-xL in human hepatocellular carcinoma. *Surgery 135*:604–612.

Yin, X.M., Wang, K., Gross, A., Zhao, Y., Zinkel, S., Klocke, B., Roth, K.A., and Korsmeyer, S.J. 1999. Bid-deficient mice are resistant to Fas-induced hepatocellular apoptosis. *Nature 400*:886–891.

8

Growth Arrest DNA Damage-Inducible Gene *45* β in Human Hepatocellular Carcinoma

Yun Yen

Introduction

Epidemiology of Liver Cancer

Worldwide hepatocellular carcinoma (HCC) is the fifth most common cancer and is becoming the third highest cause of cancer deaths. Moreover, HCC is the most common cancer in some geographic areas, particularly in the Far East, South Sahara, and southern Europe. Epidemiologic data suggest that the incidence of HCC is increasing in the United States from 1.4/100,000 in 1976 to 2.4/100,000 in 1995, (El-Serag, 2002), and the annual rate of new cases is 17,300. The increase in HCC is expected to continue as a result of the increase in hepatitis B virus (HBV) and hepatitis C virus (HCV) (Wands, 2004). Hepatitis viral B and C infections are common—350 and 170 million cases worldwide, respectively—and important causes of cirrhosis (Madhava *et al.,* 2002). Approximately 15% of patients with HBV become chronic carriers, whereas 60% of individuals infected with HCV become chronically affected by the disease; of these individuals, significant numbers, 25–30%, become cirrhotic and die of end-stage liver disease of HCC.

Chronic alcoholism is also a major cause of cirrhosis, accounting for 61% of patients with cirrhosis in an HCC surveillance study in Belgium (Lieber *et al.,* 1986; Prior, 1988; Tuyns, 1990). Aflatoxin contamination of foods is a common source of hepatocarcinogens in some parts of the world. It has been shown that a combination of liver toxins, such as alfatoxin and HBV, can increase the risk of developing HCC (Driver *et al.,* 1987). Hemochromatosis increases the risks for HCC twofold (Takada *et al.,* 1986). Diabetes mellitus is considered a risk factor for HCC; however, a large Veterans Administration study found that when other factors such as HBV and HCV are taken into account, in a multivariate analysis diabetes increased the risks for HCC only in the presence of other risk factors (Maher, 1990).

The overall survival for HCC is low: less than 10% at 5 years after diagnosis. Only 30% of patients are considered resectable, and the recurrence rate after surgical treatment is considerably high, in the order of 40–50% depending on the initial stage of disease (Hakulinen *et al.,* 1974). Adjuvant chemotherapy to prevent recurrences benefits 20–30% of the resected patients (Kono *et al.,* 1987).

Hepatitis, Liver Cirrhosis, and Liver Cancer

Despite recent advances in diagnostic and therapeutic management, prognosis of HCC still remains poor. Many risk factors, such as viral hepatitis, alcohol abuse, biliary disease, metabolic disorders, drugs, and toxins

Handbook of Immunohistochemistry and *in situ* Hybridization of Human Carcinomas, Volume 3: Molecular Genetics, Liver Carcinoma, and Pancreatic Carcinoma

are related to carcinogenesis of HCC. These risk factors result in hepatocellular injury and replacement of normal acini by nodules. Regenerative hyperplasias of fibrous tissue and acini nodules profoundly disturb the hepatic parenchymal structure and vascular network, which can directly or indirectly contribute to carcinogenesis as a final stage of liver disease (Austin, 1991; Okuda *et al.,* 1994; Yu *et al.,* 1991). Therefore, carcinogenesis and the development of HCC constitute a long and complex course related to hepatocyte damage and the repair process, which involve multiple oncogenes and tumor-suppressor genes. Molecular markers, which accurately reflect the process of hepatocarcinogenesis from liver injury to cirrhosis and progressing to liver cancer, may become useful surrogate or intermediate end points in prevention trials or markers associated with treatment response of HCC and eventual prognosis.

Double-stranded deoxyribonucleic acid (DNA) of HBV is often incorporated into the host DNA contributing to chromosomal instability (Jensen, 1979). The HBV X protein interacts with p53 and also with AFB1 throughout p52 and other nucleotide excision repair genes (Hirayama, 1989; Lam *et al.,* 1982). The HBV X gene functions as a transactivator and up-regulates several cellular genes such as *c-myc* and *c-jun* (Benvgenù *et al.,* 1994). Worldwide, HCV is half as prevalent as HBV; however, the rate of cirrhosis conversion is higher, up to 30% (Okuda, 1992). The HCV is a ribonucleic acid (RNA) virus, it does not use cellular DNA synthesis for replication, and consequently it does not integrate into the host genome. Findings support the nonimmune mechanism of liver injury (Yamauchi *et al.,* 1993).

Liver fibrosis progressing to cirrhosis with incremental risks for HCC has a latency period of 5–15 years and is the common pathologic process for several initiators such as alfatoxin, HBV, and HCV. The liver extracellular matrix and the hepatic stellate cells (HSC) are generally inconspicuous elements of the liver parenchyma. The pathway to liver fibrosis can begin with the activation of HSC. The HSC activators can be numerous: lipid peroxidation with reactive oxygen species, altered fibronectin, proinflammatory cytokines, platelet-derived growth factor (PDGF), transforming growth factor-beta 1, (TGF-β1), endothelin-1, and others (Raynal *et al.,* 1991).

Hepatocarcinogenesis

The majority of patients with HCC present with a precedence of liver injury and cirrhosis from hepatitis B and C, alfatoxin, alcohol, and liver storage disease such as hemochromatosis. These factors can also be magnified by the host genetic predisposition. The pathogenesis on the molecular and genetic scale can evolve over 1 to 3 decades and involves mechanisms common to other cancers and a few more specific to the liver (Yin *et al.,* 1992).

The p53 gene is an important tumor suppressor gene mutated in several cancers. Mutations of p53 have been found in the range of 50% of HCC and were associated with lower survival and higher recurrence rates (Hsu *et al.,* 1991; Murakami *et al.,* 1991). The HBV X protein interacts with p53 in the up-regulation of cell cycle signals (Feitelson *et al.,* 1993; Murakami *et al.,* 1991). Chromosomal instability associated with the inactivation of elements of the Wnt/β-catenin signaling system is closely associated with progression of neoplasia in the liver (Nishida *et al.,* 1993).

Insulin growth factors play important roles in diverse cellular functions including cell growth and survival. Insulin growth factor-2 (IGF-2) is physiologically expressed at high levels in several fetal tissues such as the liver, kidney, and skeletal muscle. In the adult, hepatocytes essentially have no (IGF-2) activity; however, the situation is reversed in HCC, in which IGF-2 is highly expressed. In addition, focal expression can be seen in premalignant hepatic neoplasia (Kaufmann and Kaufman, 1993). Insulin-like growth factor binding protein-1 (IGFBP-1) is a physiologic regulator of the mitogenic activity of IGF. Induction of IGFBP-1 has been found to inhibit hepatic preneoplasia in the transgenic mouse model (Fausto, 1991).

Transforming growth factor-β (TFG-β) is actively produced by Kupffer and hepatic stellate cells in reaction to several injury signals such as steatosis, HCV, and HBV. It stimulates fibrosis and is an important early factor in the process of cirrhosis (Alexandrow and Moses, 1995; Raynal *et al.,* 1991). The TGF-β is a potent inhibitor of epithelial cell growth and yet is produced by HCC and modulates the tumor growth by the autocrine mechanism. The signal switch from inhibition to stimulation occurred during the carcinogenic steps involving its receptors (Michalopoulos, 1990; Morimitsu *et al.,* 1995).

Vascular endothelial growth factor (VEGF) and other angiogenic factors are up-regulated by hypoxia, which is brought on by the inflammatory response of early liver injury and the ensuing stromal tissue reaction (Fausto, 1991). Hypoxia-inducible factor interacts with VEGF and other hypervascularity and nodular regeneration characteristics of cirrhosis.

Aflatoxin B1 (AFB1) is produced by *Aspergillus flavus* and related fungi when grown on improperly stored foods. This is an endemic food contaminant in many parts of the world, especially in the Asia. When converted to the epoxide form it reacts readily with guanine to form several forms of DNA adducts (Foster *et al.,* 1983). The intercalated adducts cause

chromosomal instability, the nature of which can depend on the site of adduct formation. As an example, p53 hotspot mutation at codon 249 in HCC is commonly associated with AFB1. Association of HBV with AFB1 increases the incidence of HCC, possibly through the binding of HBx protein on the terminus of p53 (Aguilar *et al.,* 1993; Austin, 1991).

The Down-Regulation of *GADD45β* Gene Is Associated with Liver Cell Malignant Transformation

Epidemiologic and molecular studies show that loss of DNA repair capacity is associated with specific hereditary tumor types. For example, mismatch repair defects are associated with hereditary nonpolypsis colon cancer and nucleotide excision repair defects and found in xeroderma pigmentosum (Fornace *et al.,* 1999). Because the liver is a very important metabolic organ in humans, hepatocytes are readily damaged by things such as chemical agents, viral infections, or accumulated metabolic products. In many cases, HCC is known to result from environmental exposures such as hepatitis virus, alfatoxin, alcohol, or other *in vivo* or *in vitro* genotoxins. However, the data to support a role for DNA damage in hepatocarcinogenesis still are quite limited (Goodman *et al.,* 1993; Vorce and Goodman, 1989). The human HCC-prone disorders, such as liver cirrhosis, share a very close relationship with genotoxic DNA damage and mutations of known DNA repair genes. DNA damage and repair defects that lead to increased tumorogenesis involve multiple factors. Defects in p53, p21, cyclins, or growth-suppression genes such as the GADD45 gene family could be involved (Fornace *et al.,* 1988; Fornace *et al.,* 1999).

The GADD45β (MyD118) gene was first identified as a myeloid differentiation primary response gene that is activated in the mouse myeloid leukemia cell line M1 by interleukin-6 (IL-6) on induction of terminal differentiation and associated with growth arrest and apoptosis. It has been known that GADD45β plays a role in negative growth control including inhibition of cellular growth and apoptotic cell death (Nakayama *et al.,* 1999; Smith *et al.,* 1994; Takekawa *et al.,* 1998). Overexpression of GADD45β has been known to inhibit cell growth of the human carcinoma cell (Nakayama *et al.,* 1999). GADD45β was also found to be a primary response gene to the growth inhibitory and apoptotic cytokine TGF-β, which induces M1 cells for growth arrest and apoptosis uncoupled from differentiation (Zhan *et al.,* 1994). Blocking GADD45β expression in M1 cells by GADD45β antisense RNA was found to compromise TGF-β–mediated apoptosis. Ectopic expression of Bcl-2 in M1 cells, which blocked TGF-β–induced apoptosis, resulted in reduced levels of GADD45β transcription (Nakayama *et al.,* 1999). In contrast, deregulated expression of either c-myc or c-myb in M1 cells, which accelerated TGF-β–induced apoptosis, markedly elevated the level of GADD45β transcription (Abdollahi *et al.,* 1991). Taken together, these findings are consistent with GADD45β being a positive modulator of TGF-β–induced apoptosis (Liebermann and Hoffman, 1998). Other studies have shown that ectopic expression of GADD45β in a variety of human tumor cell lines or in NIH3T3 fibroblasts negatively regulated cellular growth resulting in suppression of colony formation (Liebermann and Hoffman, 1998).

It was shown that GADD45β encode for nuclear proteins that interact with proliferating cell nuclear antigen (PCNA), as well as with p21 (Qiu *et al.,* 2003; Zhang *et al.,* 1999). More recently it became clear that GADD45β also interacts with several other cellular proteins, including the core histones, the stress-inducible MTK1/MEKK4 kinase, and Cdk1. How this multitude of interactions modulates the functions of GADD45β in negative growth control has not been established.

In one study, it was found that GADD45β was underexpressed in HCC consistently and significantly when compared to matched nonneoplastic liver tissue using the microarray assay, the immunohistochemistry (IHC), and the quantitative real-time polymerase chain reaction (PCR) analyses. Furthermore, we observed that downregulation of GADD45β was strongly correlated with differentiation and high nuclear grade of HCC. The IHC study of multiple human cancer tissues revealed that GADD45β was highly expressed in other human cancer tissues and the decreased expression was specific to HCC (Reddy *et al.,* 2003). Our result suggested that defective expression of GADD45β might lead to insufficient DNA repair, lack of a proper response to DNA damage, failure to inhibit atypical cell growth and arrest cell cycle, and it may trigger apoptosis. In this scenario, under chronic genotoxic stress, the failure to initiate DNA repair and control growth may contribute to liver carcinogenesis. Thus, the lack of GADD45β expression may play an important role in HCC carcinogenesis.

GADD45 Gene Family Involves Program Cell Death When the Cell Is Damaged by Genotoxins

Currently, three members of GADD45 gene family, GADD45α, GADD45β, and GADD45γ, have been identified based on the extensive region of conserved sequence and induction following DNA damage and/or other environmental stresses (Kearsey *et al.,* 1995; Zhang *et al.,* 1999). It has been reported that GADD45α,

a 165-amino acid nuclear protein whose expression is p53-dependent, is required for the activation of a G2/M checkpoint induced by either ultraviolet (UV) radiation or alkylating agents (Fornace *et al.,* 1999; Heinemeyer *et al.,* 1999). GADD45α was originally identified on the basis of a rapid induction in Chinese hamster ovarian cells after UV irradiation (Goodman *et al.,* 1993). Induction of GADD45α also was observed following treatment with many other types of DNA-damaging agents, including various environmental stresses, hypoxia, radiation genotoxic drugs, and growth factor withdrawal (Fornace *et al.,* 1988).

In mammalian cells, two additional family members with extensive sequence homology, GADD45β and GADD45γ, were identified based on the extensive region of conserved sequence and induction following DNA damage and/or other environmental stresses (Nakayama *et al.,* 1999; Selvakumaran *et al.,* 1994; Zhang *et al.,* 1999). The control regions of these proteins share more than 80% sequence homology with GADD45α. Similar to p53-deficient cells, cells from GADD45α-deficient mice show genomic instability, including chromosome abnormalities and centrosome amplification (Fornace *et al.,* 1999). It is known that GADD45α binds to PCNA, $p21^{waf1}$, and Cdc2 (Heinemeyer *et al.,* 1999; Hwang *et al.,* 1999; Zhang *et al.,* 1999). In addition, GADD45α can directly inhibit the kinase activity of the Cdc2 cyclin B1 complex by physically interacting with Cdc2 (Fornace *et al.,* 1988).

Increased expression of GADD45α in primary human fibroblasts arrests cells at the G2-M boundary (Zhan *et al.,* 1999). The GADD45α-mediated G2/M arrest is dependent on wild-type p53 but does not require $p21^{waf1}$ (Zhang *et al.,* 1999). Moreover, only GADD45α is able to induce a G2/M arrest and to inhibit the Cdc2 cyclin B1 kinase, whereas neither GADD45β and GADD45γ have such activity (Zhang *et al.,* 1999). These data indicate that additional functions may be associated with GADD45β. Although GADD45β and GADD45α share extensive sequence similarity and so far appear to have very similar biologic and biochemical effects, the individual family members display distinct patterns of gene expression in the organs of adult mice and human tissues (Zhang *et al.,* 1999). This finding suggests that GADD45β and the other members of the gene family have tissue-specific regulatory functions in normal adult tissues in addition to their roles in responses to genotoxic stress. The molecular basis of the unique pattern of expression of the GADD45β gene and the regulation of the human GADD45β gene in liver disease needs to be further elucidated. Our proposal makes it possible to gain a deeper understanding of the function and evolution of GADD45β and the SAMe in gene regulation and the response to alcohol stress in liver disease.

MATERIALS AND METHODS

RNA Isolation, cRNA Preparation, and Microarray Hybridization

For gene expression microarray analysis, six cases of fresh HCC tissues, coupled with nonneoplastic liver tissues from each individual, were obtained from City of Hope National Medical Center and St. Vincent Hospital. Tissue samples were cut into small pieces and snap frozen in liquid nitrogen immediately. All the samples were submitted for routine pathology evaluation and diagnosis confirmation. Frozen tissue (100 mg) was homogenized, and total RNA was extracted using TRIzol (Life Technologies, Rockville MD). Poly-A messenger RNA (mRNA) was then isolated from l mg of total RNA using Oligotex mRNA Spin-Column mini kit (Qiagen, Valencia, CA), according to the manufacturer's recommended protocol. Double-stranded complementary DNA (cDNA) was created using the SuperScript Choice System (Life Technologies). A T7-oligonucleotide was used to primer synthesis of first-strand cDNA from poly-A mRNA. The cDNA was purified by PLG spin column, and precipitated with 0.5 volumes 7.5 M ammonia acetate and 2.5 volumes 100% ethanol. cDNA (2 μg) was used to synthesize cRNA *in vitro* using T7 RNA polymerase and four biotin-labeled ribonucleotides. After incubation at 37°C for 5 hr, the labeled cRNA was purified by RNeasy Mini kit (Qiagen). The RNA was tested at every step by separation in a 1.2% morpholino propane sulfonic acid/formaldehyde agarose gel, and the amount was estimated based on the OD 260/280 reading; RNA was stored in diethyl pyrocarbonate water with l0 mM dithiothreitol and RNasin 1 U/ml in −70°C. The biotinylated cRNA was hybridized to the Affymetrix HU95A oligonuleotide probe microarray gene chip (Affymetrix, Santa Clara, CA) for 16 hr at 45°C, which represented 12,588 full-length human genes and oligo expression sequence tag (EST) sequences. The pattern of gene expression in the microarray was confirmed in four separate samples.

Microarray Analyses

All the analyses were performed at the Microarray Core Facility, Children's Hospital Los Angeles. Fluorescence intensities from biotinylated probes were detected with streptavidin-phycoerythrin (Molecular Probes, Eugene, OR), and quantitative scanning was performed using the HP Agilgent 2200 confocal scanner.

The data were analyzed using Affymetrix Microarray Software Suite (v.4.0). The average difference values representing perfect match–mismatch for each gene were normalized after scaling the total chip intensities to an average of 1500 units. The data were further analyzed by GeneSpring software (Silicon Genetics, Redwood City, CA). The comparison of the hybridization efficiency and its complementary sequence was used to determine the presence of target gene. A single reference sample composed of a pool of DNA from HCC and nonneoplastic liver tissue was used throughout all hybridizations. Mismatch probes were used for specificity control, and both the background and cross-hybridization signals were extracted directly. Measurement values were extracted for signal intensities as normalized ratios of sample versus reference, which represented the relative mRNA for each gene in each sample compared with the common reference.

Defective spots, ones that were substandard on the scanned imager or had negative values after background was subtracted, were first excluded. To minimize the effects of measurement variations introduced by artificial sources during experiments, we only included spots that had significant signals in both channels. The significance cutoff for the signal/background ratio is 1.4. For each spot, the median ratio was used in subsequent analyses. Spots representing housekeeping genes were used to normalize the entire slide so that all slides could be compared directly. For each sample, at least two hybridizations were carried out. The average of median ratios from replicates was calculated for each spot. We then used 2.0 SD as our cutoff for the determination of expression outlines.

Immunohistochemical Study of GADD45β, GADD45α, and Mutant p53 Protein

Paraffin sections were deparaffinized in xylene and rehydrated in a graded alcohol series followed by blocking in 1:20 normal horse serum. The primary goat anti-human polyclonal GADD45β antibody (200 μg/ml, Santa Cruz Biotechnology) was used irretrievably in a 1:8000 dilution in a humid container overnight and washed 3 times (5 min each) with phosphate buffer saline plus 0.2% Tween (PBST). The slides were then incubated with biotinylated anti-goat immunoglobulin antibody (Vector Laboratories, Burlingame CA) at a dilution of 1:200 followed by 3 washes (5 min each) of PBST. Then, after a 45-min incubation with AB Complex (Vector Elite Kit, 1:200 dilution) and 3 washes, DAB (0.05 g DAB and 100 μl 30% H_2O_2 in 100 ml PBS) and 1% copper sulfate were applied for 5 and 10 min, respectively. Each slide was counterstained with Mayer's hematoxylin. To examine the relationship between GADD45β and mutant p53, the primary mouse anti-human p53 protein mutant forms monoclonal antibody (NCL-p53-DO7, 1:300 dilation, NovoCASTRA Laboratories, Newcastle upon Tyne, United Kingdom) was used for IHC study, which represents the multiple mutant forms p53 mutant protein; the method of staining was conducted, as described earlier. For all IHC studies, PBS was used as a negative control. Granular cytoplasmic stain was accessed as positive. The evaluation of staining intensity was performed by three independent observers.

Genomic GADD45β Promoter Sequence and Binding Elements Involved in Transcription Regulation

Understanding the regulation of GADD45β may reveal the relationship between DNA-damage repair and the process of hepatocarcinogenesis. Several strategies were designed to understand the mechanism of GADD45β regulation. It is generally accepted that changes in transcription regulatory pathways could be essential to the process of malignant transformation of cells. Therefore, we focused on the elucidation of the GADD45β transcriptional regulation and seeking agents to up-regulate GADD45β as a possible hepatoprotective and therapeutic treatment. Two important GADD45β promoter regions identified by deletion analysis were shown to contain binding sites for nuclear factor (NF)-κB and E2F-1 predicted by the TRANSFAC database (Heinemeyer *et al.,* 1999). Up-regulation of GADD45β in response to SAMe and oxaliplatin was demonstrated by Northern Blot and quantitative real-time PCR.

The role of NF-κB in SAMe-mediated induction of GADD45β expression was confirmed by gel shift, enzyme-linked immunosorbent assay (ELISA) and Western Blot. The E2F-1 binding site was also located in the promoter region and shown to be important for promoter activity; it could be induced by oxaliplatin treatment. It is interesting that E2F-1 failed to show any response to SAMe, whereas NF-κB could be induced by oxaliplatin. Non-HCC cells, such as KB and PC3 cells, also did not demonstrate SAMe-mediated induction of GADD45β expression, suggesting that this mechanism may be specific to HCC. More recently, we identified the hypermethylation status in the area around the third NF-κB binding site. Methylation-specific PCR and sequencing of the sodium bisulfite–treated DNA from HepG2 and clinical HCC samples revealed a high percentage of hypermethylation in this area. Comparatively, the nonneoplastic liver tissues demonstrated very low levels of methylation. These findings suggested the complicated structure of GADD45β promoter and multiple regulation mechanism, which involved

NF-κB, E2F-1, and hypermethylation. Our results provided a deeper understanding to the molecular mechanism of GADD45β down-regulation in HCC.

NF-κB is a pleiotropic transcription factor that regulates the expression of various genes. It was first discovered as one of the B-cell proteins interacting with the immunoglobulin κ light-chain gene enhancer (Leonardo *et al.,* 1999). The NF-κB family consists of p65 (RelA), p50 (NF-κB1), c-Rel (Rel), p52 (NF-κB2), and RelB, which can form homodimers and heterodimers with each other (Baldwin *et al.,* 1996). Both transcriptional and posttranscriptional regulation of GADD45β has been reported (Tanaka *et al.,* 1995). The three NF-κB elements at GADD45β promoter we described here have also been identified by another group and shown to form complexes with NF-κB *in vitro.* Their data support the direct participation of NF-κB in the induction of GADD45β (Jin *et al.,* 2002). Activation of NF-κB occurs when various stimuli trigger signal transduction pathways that lead to activation of IκB kinase. Phosphorylation of IκBα and IκBβ by IκB kinase initiates polyubiquitination and rapid degradation by the proteasome, allowing NF-κB to enter the nucleus (Ballard *et al.,* 1992).

Accumulation of NF-κB in the nucleus and DNA binding are necessary for positive regulation of gene expression (Baldwin, 2001). Therefore, degradation of IκBα is very important for NF-κB function. It has been reported that the hepatoprotective action of SAMe may be mediated through the modulation of nitric oxide production. That report also showed that SAMe could accelerate the resynthesis of IκBα and blunt the activation of NF-κB, which is different from our results (Majano *et al.,* 2001). However, normal rat hepatocytes were used in their study, whereas human HCC cell-line HepG2 was examined in our study. The disparity between normal and cancer cells may explain the different effects observed for SAMe. In future work we will examine the hepatoprotective and chemopreventive effect of SAMe in normal human liver cells and any differences from those found in cancerous human liver cells. Meanwhile, we noticed that GADD45α and GADD45γ could not be induced by NF-κB, contrary to the regulation of GADD45β (Baldwin, 1996). In our previous study, we showed that expression of GADD45α was the same in both HCC and nontumor liver tissues (Qiu *et al.,* 2003). These findings suggest that, in HCC, different mechanisms may be involved in regulation of GADD45α and GADD45β, and these differences may be important for HCC malignant transformation.

In addition to the NF-κB binding sites, we identified an E2F-1 binding site on the GADD45β promoter that was shown to be important for promoter activity. Deletion of the negative regulation area (–520/–470), which is adjacent to the E2F-1 binding region, nearly peaked GADD45β promoter activity. Therefore, this negative regulation area may be the main regulator of GADD45β expression. However, our results showed that the negative regulation area and E2F-1 site showed no response to SAMe treatment, suggesting that only NF-κB plays a specific role in SAMe-mediated up-regulation of GADD45β. The key to the puzzle may be back at the CpG islands located in the negative regulation area, which cannot be modulated by SAMe in *in vitro* luciferase activity assay.

These findings further suggested the complicated structure of GADD45β promoter and multiple roles of SAMe in gene regulation. We are examining the role of methylation in the GADD45β regulation by SAMe on this area. In deeper consideration, the possibility of the existence of a balance among NF-κB, E2F-1, and the negative regulation area in promoter of GADD45β or the existence of a provocation to impede biological functions need further exploration.

p53 Tumor-Suppressor Gene Involved in Liver Disease and HCC Development

The p53 tumor-suppressor gene is the gene most commonly mutated in liver cirrhosis and cancers (Hsu *et al.,* 1991; Murakami *et al.,* 1991). Wild-type p53 protein regulates cell growth and suppresses tumor formation through two distinct pathways: p53 can initiate the arrest of mitosis at any of several checkpoints, or it can initiate apoptosis (programmed cell death) (Yin *et al.,* 1992). These events are mediated by intermediate proteins induced by p53 such as p2l of cell cycle arrest and GADD45 gene family of apoptosis (Marshal, 1991). In HCCs, mutations of p53 are common (Nishida *et al.,* 1993). In some geographic locations, they have a pattern that is unique among human cancers, with 30 to 50% being G to T transversions at codon 249; in cancers other than HCC, p53 mutations are commonly found at a variety of different codons (Bressac *et al.,* 1991). As with many other human cancers, p53 mutations may be late occurrences in carcinogenesis of the liver in some circumstances (Murakami *et al.,* 1991).

The function of normal p53 can be inactivated when p53 protein becomes bound by viral or other stress as alcohol or other genotoxins, in the absence of a p53 mutation (Moll *et al.,* 1992; Yuwen *et al.,* 1995). For instance, the oncoproteins of HBV X protein can form stable complexes with wild-type p53 and either prevent its normal function or induce its degradation (Feitelson *et al.,* 1993; Wang *et al.,* 1990). Levels of p53 in cells are regulated, at least in part, by an autocrine feedback system involving the cellular protein mdm2 under normal conditions; the levels of wild-type p53 and mdm2

inversely regulate each other (Kaufmann and Kaufman, 1993). When mdm2 is amplified as a result of genostress, p53 function is interrupted. When the mdm2 protein binds to p53, p53-directed transactivation is inhibited. Other cellular proteins such as TGF-β in the liver have been identified that bind to p53 and may play a role in its regulation; abnormal expression of TGF-β could contribute to carcinogenesis of liver cells (Alexandrow *et al.,* 1995; Morimitsu *et al.,* 1995).

Under physiologic conditions of wild-type p53 even under partial (2/3) hepatectomy, the cell cycle of the hepatocyte is tightly controlled (Fausto, 1991; Michalopoulos, 1990). To pass through the cell cycle requires the p53 successive activation of different cyclin-dependent protein kinases (cdk) and its inhibitors (Biggs and Kraft, 1995; Carr, 1996; Nigg, 1995; Strauss *et al.,* 1995). Such molecular processes act as key regulators of the cell cycle in liver cell growth, arrest, or apoptosis (Morgan, 1995). There are known checkpoints in G1 phase that help prevent genetic damage induced by toxins, such as alcohol, generally by repairing damaged DNA before proceeding further through the cell cycle (Strauss *et al.,* 1995). There is also evidence that attenuation or loss of the cell cycle checkpoint response and the inability to delay cell cycle progression in response to DNA damage are associated with enhanced sensitivity to toxic agents and genetic instability, contributing to HCC progression (Murray, 1994; Wang *et al.,* 1990).

The p53-associated DNA damage repair pathway constitutes a very complicated network, and the GADD45 gene family has been reported to be a downstream effector of p53 required for cell cycle arrest following DNA damage (Smith *et al.,* 1994). GADD45β plays an important role in this network by interacting with PCNA, p21 (Zhang *et al.,* 1999), the core histones, the stress-inducible MTK1/MEKK4 kinase, and Cdk1 (Zhang *et al.,* 1999), but how this multitude of interactions modulates negative growth control has not been established. In our previous study, low expression of GADD45β in HCC cells was associated with mutant p53. These results support the viewpoint that normal p53 function is involved in the regulation of this gene. The suppression of GADD45β led to dysfunction of damage recognition, cell cycle arrest, and apoptosis initiation, all of which are important in carcinogenesis. Based on these observations, we hypothesize that suppression of GADD45β may be p53-dependent, supporting the involvement of p53 in hepatocarcinogenesis. Therefore, in a multistage model of liver carcinogenesis, changes in GADD45β expression may compromise growth control mechanisms, making cells susceptible to malignant transformation by additional cellular events. Figure 35 shows p53 mutant protein associated with down-expression of GADD45β in HCC specimens, using IHC.

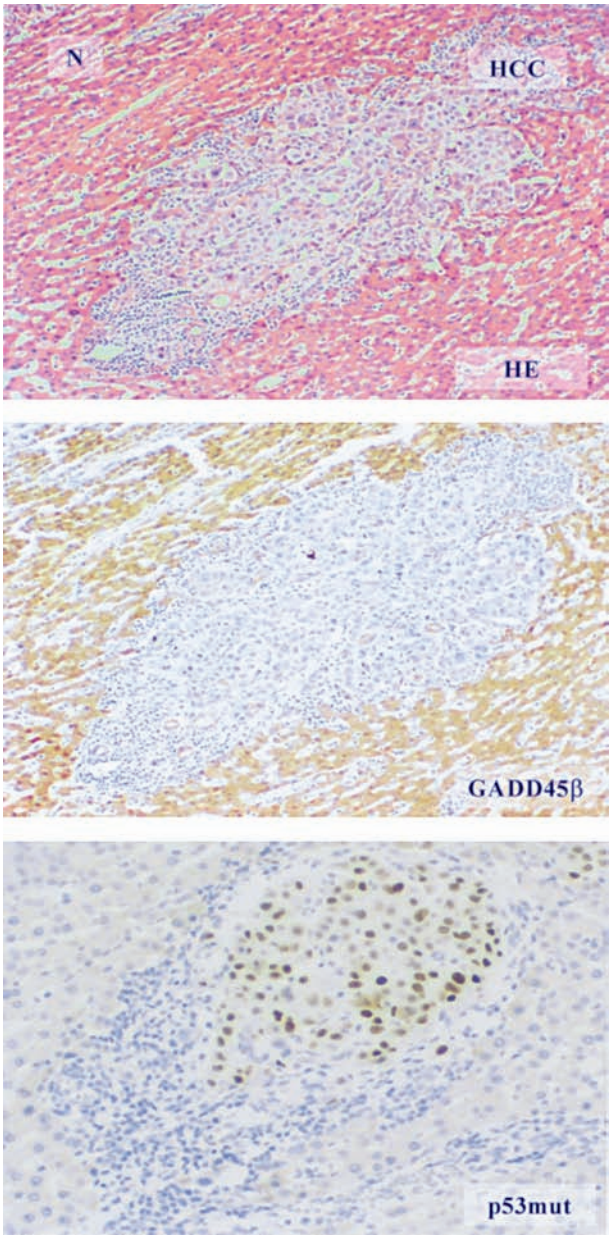

Figure 35. The p53 mutant protein associated with down-expression of *GADD45β* in hepatocellular carcinoma (HCC) samples. The relationship between p53 mutation and *GADD45β* expression in HCC tissues is shown by immunohistochemistry (IHC) (200X). The **top panel** is hematoxylin and eosin stained. N indicates normal liver tissue and HCC indicates liver cancer tissue. *GADD45β* is stained in the **middle panel,** whereas the **bottom panel** is stained with an antibody specific for mutant p53. Mutant p53 staining appears as a black tint in the nucleus of HCC cells, whereas *GADD45β* staining appears only in the normal tissue.

References

Abdollahi, A., and Lord, K.A., Hoffman-Leibermann, B., and Leibermann, D.A. 1991. Sequence and expression of a cDNA encoding MyDl18: A novel myeloid differentiation primary response gene induced by multiple cytokines. *Oncogene 6*: 165–167.

Aguilar, F., Hussin, S.P., and Cerutti, P. 1993. Aflatoxin B1 induces the trhasversion of G-T in codon 249 of the p53 tumor suppressor gene in human hepatocytes. *Proc. Natl. Acad. Sci. USA 90*:8586–8590.

Alexandrow, M.G., and Moses, H.L. 1995. Transforming growth factor beta and cell cycle regulation. *Cancer Res. 55*: 12452–12457.

Austin, H. 1991. The role of tobacco use and alcohol consumption in the etiology of hepatocellular carcinoma. In Tabor E, Di Bisceglie AM, Purcell RH (eds). *Etiology, Pathology, and Treatment of Hepatocellular Carcinoma in North America.* the Woodlands, TX:Portfolio Pub Co.

Baldwin, A.S. 2001. Control of oncogenesis and cancer therapy resistance by the transcription factor NF-KappaB. *J. Clin. Invest*. *107*:241–246.

Baldwin, Jr., A. 1996. The NF-kB proteins: New discoveries and insights. *Annu. Rev. Immunol*. *14*:694–781.

Ballard, D.W., Dixon, E.P., Peffer, N.J., Bogerd, H., Doerre, S., Stein, B., and Green, W.C. 1992. The 65-Kda subunit of human NF-kB functions as a potent transcriptional activator and a target for v-rel-mediated repression. *Proc. Natl. Acad. Sci. USA 89*:1875–1879.

Benvegnù, L., Fattovich, G., and Noventa, F., et al. 1994. Concurrent hepatitis B and C virus infection and risk of hepatocellular carcinoma in cirrhosis. A prospective study. *Cancer 74*:2442–2448.

Biggs, J.R., and Kraft, A.S. 1995. Inhibitors of cyclin-dependent kinase and cancer. *J. Mol. Med. 73*:509–514.

Bressac, B., Kew, M., Wands, J., and Ozturk, M. 1991. Selective G to T mutations of p53 gene in hepatocellular carcinoma from southern Africa. *Nature 350*:429–431.

Carr, A.M. 1996. Checkpoints taken the next step. *Science 271*: 314–315.

Driver, H.E., and Swann, P.F. 1987. Alcohol and human cancer. *Anti-Cancer Res*. *7*:309–320.

El-Serag, H.B. 2002. Hepatocellular carcinoma: An epidemiologic view. *J. Clin. Gastroenterol. 35(5 Suppl 2)*:S72–S78.

Fausto, N. 1991. Growth factors in liver development, regeneration and carcinogenesis. *Prog*. *Growth Factor Res. 3*:219–234.

Feitelson, M.A., Zhu, M., Duan, L.X., and London, W.T. 1993. Hepatitis B x antigen and p53 are associated *in vitro* and in liver tissues from patients with primary hepatocellular carcinoma. *Oncogene 8*:1109–1117.

Fornace, A.J., Jr., Jackman, J., Hollander, M.C., Hoffman-Liebermann, B., and Liebermann, D.A. 1999. Genotoxic-stress-response genes and growth-arrest genes. GADD, MyD, and other genes induced by treatment eliciting growth arrest. *Ann. N.Y. Acad. Sci. 663*:139–153.

Fornace, Jr., A.J., Alamo, I., Jr., and Hollander, M.C. 1988. DNA damage-inducible transcripts in mammalian cells. *Proc. Natl. Acad. Sci. USA 85*:8800–8804.

Foster, P.L., Eisenstadt, E., and Miller, J.H. 1983. Base substitution mutations induced by metabolically activated aflatoxin B1. *Proc. Natl. Acad. Sci. USA 80*:2695–2698.

Goodman, J.I., and Counts, J.L. 1993. Hypoemthylation of DNA: A possible nongenotoxic mechanism underlying the role of cell proliferation in carcinogenesis. *Environ. Health Prospect 5*: 169–172.

Hakulinen, T., Lehtimaki, L., Lehronen, M., and Teppo, L. 1974. Cancer mortality two male cohorts with increased alcohol consumption. *J. Natl. Cancer Inst. 52*:1711–1714.

Heinemeyer, T., Chen, X., Karas, H., Kel, A.E., Kel, O.V., Liebich, I., Meinhardt, T., Reuter, I., Schacherer, F., and Wingender, E. 1999. Expanding the TRASFAC database towards an expert system of regulatory molecular mechanisms. *Nucelic Acids Res. 27*:318–322.

Hirayama, T. 1989. A large-scale cohort study on risk factors for primary liver cancer, with special reference to the role of cigarette smoking. *Cancer Chemother*. *Pharmacol. 23(Suppl)*: S114–S117.

Hsu, I.C., Metcalf, R.A., and Sun, T., 1991. Mutational hotspot in the p53 gene in human hepatocellular carcinomas. *Nature 350*:427–428.

Hwang, B.J., Ford, J.M., Hanawalt, P.C., and Chu, G. 1999. Expression of the p48 xeroderma pigmentosum gene is p53-dependent and is involved in global genomic repair. *Proc. Natl. Acad. Sci. USA 96*:424–428.

Jensen, O. 1979. Cancer morbidity and causes of death among Danish brewery workers. *Int. J. Cancer 23*:454–463.

Jin, R., De Smaele, E., Zarreroin, F., Nguyen, D.U., Papa, S., Jones, J., Cox, C., Gelinas, C., and Franzoso, G. 2002. Regulation of the GADD45β promoter by NF-kappB. *DNA Cell Biol. 21*:491–503.

Kaufmann, W.K., and Kaufman, D.G. 1993. Cell cycle control, DNA repair and initiation of carcinogenesis. *FASEB J. 7*:1188–1191.

Kearsey, J.M., Coates, P.J., Prescott, A.R., Warbrick, E., and Hall, P.A. 1995. GADD45 is a nuclear cell cycle regulated protein which interacts with p21 C1p1. *Oncogene 11*:1675–1683.

Kono, S., Ikeda, M., and Tokudome, S. 1987. Cigarette smoke alcohol and cancer mortality: A cohort study of male Japanese physicians. *Jpn. J. Cancer Res. (Gann) 78*:1323–1328.

Lam, K., Yu, M., Leung, J., and Henderson, B. 1982. Hepatitis B virus and cigarette smoking: Risk factors for hepatocellular carcinoma in Hong Kong. *Cancer Res. 42*:5246–5248.

Leonardo, M.J., and Baltimore, D. 1999. NF-kappa B: A pleiotropic mediator of inducible and tissue-specific gene control. *Cell 58*:227–229.

Lieber, C.S., Garro, A., Leo, M.A., and Mak, K.M. 1986. Alcohol and cancer. *Hepatology 6*:1005–1019.

Liebermann, D.A., and Hoffman, B. 1998. MyD genes in negative growth control *Oncogene 17*:3319–3329.

Madhava, V., Burgess, C., and Drucker, E. 2002. Epidemiology of chronic hepatitis C virus infection in sub-Saharan Africa. *Infect. Dis. 2*:293–302.

Maher, J.J. 1990. Hepatic fibrosis caused by alcohol. *Semin. Liver Dis. 10*:66–74.

Majano, P.L., Garcia-Monzon, C., Garcia-Trevijano, E.R., Corrales, F.J., Camara, J., Ortiz, P., Mato, J.M., Avila, M.A., and Moreno-Otero, R. 2001. S-Adenosylmethionine modulates inducible nitric oxide synthase gene expression in rat liver and isolated hepatocytes. *J. Hepatol. 35*:692–699.

Marshal, C.J., 1991. Tumor suppressor genes. *Cell 64*:313–326.

McMahon, G., David, E.F., and Humber, L.J. 1990. Characterization of c-Ki-ras and N-ras oncogenes in aflatoxin B1-induced rat liver tumors. *Proc. Natl. Acad. Sci. USA 87*:1104–1108.

Michalopoulos, G.K. 1990. Liver regeneration: Molecular mechanisms of growth control. *FASEB J. 4*:176–187.

Moll, U.M., Riou, G., and Levine, A.J. 1992. Two distinct mechanisms alter p53 in breast cancer: mutation and nuclear exclusion. *Proc. Natl. Acad. Sci. USA 89*:7262–7266.

Morgan, D.O. 1995. Principles of CDK regulation. *Nature 374*:131–234.

Morimitsu, Y., Hsia, C.C., Kojiro, M., and Tabor, E. 1995. Nodules of less-differentiated tumor within or adjacent to hepatocellular carcinoma: Relative expression of transforming growth factor-a and its receptor in the different areas of tumor. *Human Pathol. 26*:1126–1132.

Murakami, Y., Hayashi, K., Hirohashi, S., and Sekiya, T. 1991. Aberrations of the tumor suppressor p53 and retinoblastoma genes in human hepatocellular carcinoma. *Cancer Res. 51*:5520–5525.

Murray, A.W. 1994. The genetics of cell cycle checkpoints. *Curr. Opin. Genet. Dev. 5*:5–11.

Nakayama, K., Hara, T., Hibi, M., Hirano, T., Miyuajima, A. 1999. A noel oncostatin M-inducible gene OIG37 forms a gene family with MyD118 and GADD45 and negatively regulates cell growth. *Biol. Chem. 274*:24766–24772.

Nigg, E.A. 1995. Cyclin-dependent protein kinases: Key regulators of the eukaryotic cell cycle. *Bioessays 17*:471–480.

Nishida, N., Fukuda, Y., and Kokuryu, H. 1993. Role and mutational heterogeneity of the p53 gene in hepatocellular carcinoma. *Cancer Res. 53*:368–372.

Okuda, K. 1992. Hepatocellular carcinoma recent progress. *Hepatology 5*:948–963.

Okuda, K., and Ohnishi, K. 1994. The role of viral infections in alcoholic liver disease. In alcoholic liver disease: *Pathology and Pathogenesis*. 2nd ed. Edward Arnold, London, pp. 147–159.

Prior, P. 1988. Long-term cancer risk in alcoholism. *Alcohol 23*: 163–171.

Qiu, W.H., David, D., Zhou, B.S., Chu, P.G., Zhang, B.H., Wu., M.C., Xiao, J.C., Han, T.Q., Zhu, Z.G., Wang, T.X, Liu, X.Y., Lopez, R., Frankel, P., Jong, A., and Yen, Y. 2003. Down-regulation of growth arrest DNA damage-inducible gene 45 b expression is associated with human hepatocellular carcinoma. *Am. J. Patho. 6*:1961–1974.

Raynal, S., Jullien, P., and Pawrence, D.A. 1991. *Toxicology 70*:293–302.

Selvakumaran, M., Lin, H.K., Sjin, R.T., Reed, J.C., Liebermann, D.A., and Hoffman, B. 1994. The novel primary response geen MyD118 and the proto-oncogenes myb, myc, and bcl-2 modulate transforming growth factor b1-inducted apoptosis of myeloid leukemia cells. *Mol. Cell. Biol. 14*:2352–2360.

Smith, M.L., Chen, I.T., Zhan, Q., Bae, I., Chen, C.Y., Gilmer, T.M., Kastan, M.B., O'Connor, P.M., and Fornance, A.J., Jr. 1994. Interaction of the p53-regulated protein GADD45 with proliferating cell nuclear antigen. *Science 266*:1376–1380.

Strauss, M., Lukaas, K., and Bartek, J. 1995. Unrestricted cell cycling and cancer. *Nat. Med. 1*:1245–1246.

Takada, A., Nei, J., Takase, S., and Matsuda, Y. 1986. Effect of ethanol on experimental hepatocarcinogenesis. *Hepatology 6*:65–72.

Tanaka, K., Hirohata, T., and Fukuda, K., 1995. Risk factors in hepatocellular carcinoma among Japanese women. *Cancer Causes Control 6*:91–98.

Tuyns, A.J. 1990. Alcohol and cancer. *Proc. Nutr. Soc. 49*:145–151.

Vorce, R.L., and Goodman, J.L. 1989. Altered methylation of ras oncogenes in benzidine-induced B6C3F1 mouse liver tumors. *Toxicol. Appl. Pharmacol. 100*:398–410.

Wands, J.R. 2004. Prevention of hepatocellular carcinoma. *New Engl. J. Med. 351*:1566–1569.

Wang, J., Chenivesse, X., Heglein, B., and Bréchot, C. 1990. Hepatitis B virus integration in a cyclin A gene in hepatocellular carcinoma. *Nature 343*:555–557.

Yamauchi, M., Nakahara, M., and Maezawa, Y., 1993. Prevalence of hepatocellular carcinoma in patients with alcoholic cirrhosis and prior exposure to hepatitis C. *Am. J. Gasteroenterol. 88*:39–43.

Yin, Y., Tainsky, M.A., and Bischoff, F.Z. 1992. Wild-type p53 restores cell cycle control and inhibits gene amplification in cells with mutant p53 alleles. *Cell* 70:937–948.

Yu, M., Tong, M., Govindarajan, S., and Henderson, B. 1991. Nonviral risk factors for hepatocellular carcinoma in low-risk population, the non-Asians of Los Angeles County, California. *J. Natl. Cancer Inst. 83*:1820–1826.

Yuwen, H., Kazachkov, Y., Mortimitsu, Y., and Tabor, E. 1995. Identification of two p53-binding proteins using a recombinant vaccinia virus containing the wild-type human p53 gene. *Biochem. Bio. Res. Comm. 213*:986–993.

Zhan, Q., Antinore, M.L., Wang, X.W., Carrier, F., Smith, M.L., Harris, C.C., and Forance, A.J., Jr. 1999. Association with Cdc2 and inhibition of Cdc2/Cyclin B1 kinase activity by the p52-regulated protein GADD45. *Oncogene 18*:2892–2900.

Zhan, Q., Lord, K.A., Alamo, I., Jr., Hollander, M.C., Carrier, F., Ron, D., Kohn K.W., Hoffman, B., Liebermann, D.A., Forance, A.J., Jr. 1994. The GADD and MyD genes define a novel set of mammalian genes encoding acidic proteins that synergistically suppress cell growth. *Mol. Cell. Biol. 14*:2361–2371.

Zhang, W., Bae, I., Krishnaraju, K., Azam, N., Fan, W., Smith, K., Hoffman, B., and Leibermann, D.A. 1999. CR6: A third member in the MyD118 and GADD45 gene family which functions in negative growth control. *Oncogene 18*:4899–4907.

9

Immunohistochemical Detection of DNA Topoisomerase IIα in Hepatocellular Carcinoma

Susumu Ohwada, Akira Watanuki, Tetsuhiro Nakano, and Toshio Fukusato

Introduction

Deoxyribonucleic acid (DNA) topoisomerase II (topo II), which is encoded by a gene on chromosome 17q21–22 (Tsai-Pflugfelder *et al.,* 1988), is a major scaffold protein of mitotic chromosomes. Topo II is present in the interphase nuclear matrix and is essential for many vital biological processes, especially negative supercoiling of DNA organized as a superhelix, a process that is necessary for the replication, recombination, and transcription of nuclear DNA. The amount and stability of topo II within eukaryotic cells undergo significant cell-cycle–dependent alterations, with more of the protein associated with actively growing cells and less with the stationary phase. This enzyme acts by generating and then resealing breaks in double-stranded DNA, which are necessary for the segregation of chromosomes at the end of mitosis (Uemura *et al.,* 1987). Topo II is needed for complete condensation of chromosomes, regulating the G2 checkpoint mechanism (Downes *et al.,* 1994). Topo II has two isoforms in mammalian cells: topo IIα (170 kDa) and topo IIβ (180 kDa) (Watt and Hickson, 1994). Whereas topo IIβ levels are relatively constant throughout the cell cycle, topo IIα expression is low in G1, increases in S phase, and is maximal in G2/M phase, which is consistent with the association of this isoform with DNA replication, mitosis, and cell proliferation (Woessner *et al.,* 1991). Accordingly, topo II serves as a target that mediates the cytotoxicity of several anti-neoplastic agents, including etoposide, doxorubicin, and mitoxantron (Fry *et al.,* 1991). Therefore, topo II is considered a specific marker of cell proliferation, and it plays an important role in malignant tumors. Previous clinical studies have also shown that topo II expression reflects biological behavior in human cancers, such as lung carcinomas, breast carcinomas, uterine cervical squamous lesions, and malignant nonbrainstem glioma. This chapter describes the immunohistochemical detection of topo IIα and the association between its expression in hepatocellular carcinoma (HCC) and various clinicopathologic features, proliferative activity, and tumor-suppressor gene *p53* abnormalities (Watanuki *et al.,* 2002).

MATERIALS

HCC specimens from 70 patients (53 men, 17 women; mean age: 59.3 years, range: 34 to 72) who underwent curative liver resection were examined. Specimens were fixed in 10% formalin at room temperature and embedded in paraffin. All the tumors were diagnosed

Handbook of Immunohistochemistry and *in situ* Hybridization of Human Carcinomas, Volume 3: Molecular Genetics, Liver Carcinoma, and Pancreatic Carcinoma

histologically and graded using Edmondson's scale. Tumors were also grouped according to size as <3 cm (n = 28) and ≥3 cm (n = 42). Of patients, 54 (77%) had hepatitis C virus (HCV) infection, 14 (20%) had hepatitis B virus (HBV) infection, and two had joint HCV and HBV infections. When recurrence was noted, each patient received the best combination of treatments appropriate for that individual, i.e., transarterial chemoembolization, microwave coagulation therapy, and percutaneous ethanol injection therapy for intrahepatic recurrence and radiation therapy for bone metastasis. The follow-up interval ranged from 2 to 105 months, with a median of 28.5 months.

Antibodies

Monoclonal antibody 8D2 of the IgG2b subtype recognizes human topo IIα exclusively and was kindly provided by Kikuchi *et al*. Details of the cloning and production of this antibody have been reported. Monoclonal antibody MIB-1 (Immunotech, Marseille, France) is a mouse monoclonal antibody that recognizes the Ki-67 antigen. Monoclonal antibody DO-7 (Novocastra Laboratories, Newcastle-upon-Tyne, UK) recognizes both wild-type and mutant forms of human p53 protein under either denaturing or nondenaturing conditions.

Mouse immunoglobulin G2 was used as a negative control and was purchased from Dako (Glostrup, Denmark).

METHODS

1. Tissue sections of HCC (3 μm thick) were dewaxed in xylene and rehydrated in graded ethanol.
2. After washing, the tissue sections were incubated in 0.02% trypsin-phosphate buffer saline (PBS) solution at 37°C for 30 min.
3. The tissue sections were then heated in 1 mM citric acid buffer solution (pH 6.0) at 90°C for 15 min (5-min exposures from three different angles) in a microwave processor (H2800, Energy Beam Sciences, Inc., Agawan, MA) to retain the antigenicity recognized by the three antibodies and were left at room temperature for 30 min.
4. Endogenous peroxidase activity was blocked by the addition of 3% aqueous H_2O_2 for 20 min, and nonspecific antibody binding was blocked by adding normal horse serum for 20 min.
5. The tissue sections were incubated with primary antibodies at room temperature for 60 min. The working dilutions of these antibodies in PBS were 1:200 for 8D2, 1:50 for MIB-1, and 1:100 for DO-7.
6. An avidin–biotin–peroxidase complex method including biotinylated anti-mouse immunoglobulin as the secondary antibody was used according to the manufacturer's instructions (Elite ABC KIT, Mouse IgG, VECTASTAIN, Vector Laboratories, Burlingame, VT).
7. To produce color, 0.02% diaminobenzidine–PBS solution with 0.01% H_2O_2 was used.
8. The sections were counterstained with Meyer's hematoxylin for 3 sec and mounted.
9. Human tonsillar mucosa and lymphatic tissues were used as a positive control for 8D2 and MIB-1, and human colonic carcinoma was used for DO-7 immunostaining.
10. More than 1,000 HCC nuclei were counted in the same areas, not at random, and the percentage of positive nuclei was considered in terms of a topo IIα labeling index (topo IIα LI) and Ki-67 labeling index (Ki-67 LI) per high-power field (400X).
11. Strong nuclear staining for topo IIα or Ki-67 was scored as positive. Overexpression of p53 was considered positive when more than 50% of the nuclei were stained.

RESULTS

Immunohistochemical Detection and Labeling Index of Topo IIα

All 70 HCC samples showed positive, but heterogeneous, staining for 8D2 (topo IIα antibody) both in terms of staining intensity and the percentage of positive nuclei, whereas few nuclei of adjacent noncancerous hepatocytes were stained (Figure 36A). The mean topo IIα LI was 14.1 ± 15.1% (mean ± SD) and ranged from 0.2 to 55.6, and the median topo IIα labeling index (LI) was 9.9%. The 70 HCCs were divided equally into two groups with either more or less than the median value of the topo IIα LI. The topo IIα LI did not correlate with age, gender, hepatitis B or C viral status, cirrhotic state, tumor size, the number of satellite nodules, International Union Against Cancer (UICC) stage, fibrous capsule, capsular invasion, or Edmondson's scale. However, it did show a significant association with the serum α-fetoprotein (AFP) level ($p < 0.05$) and with vein involvement ($p < 0.05$).

Relationship between Topo IIα and Other Prognostic Factors (Ki-67 and p53)

The nuclei of many HCC cells were stained with varying intensity and showed heterogeneous distribution of the MIB-1 antibody (Figure 36B). The pattern of topo IIα expression was similar to that of Ki-67,

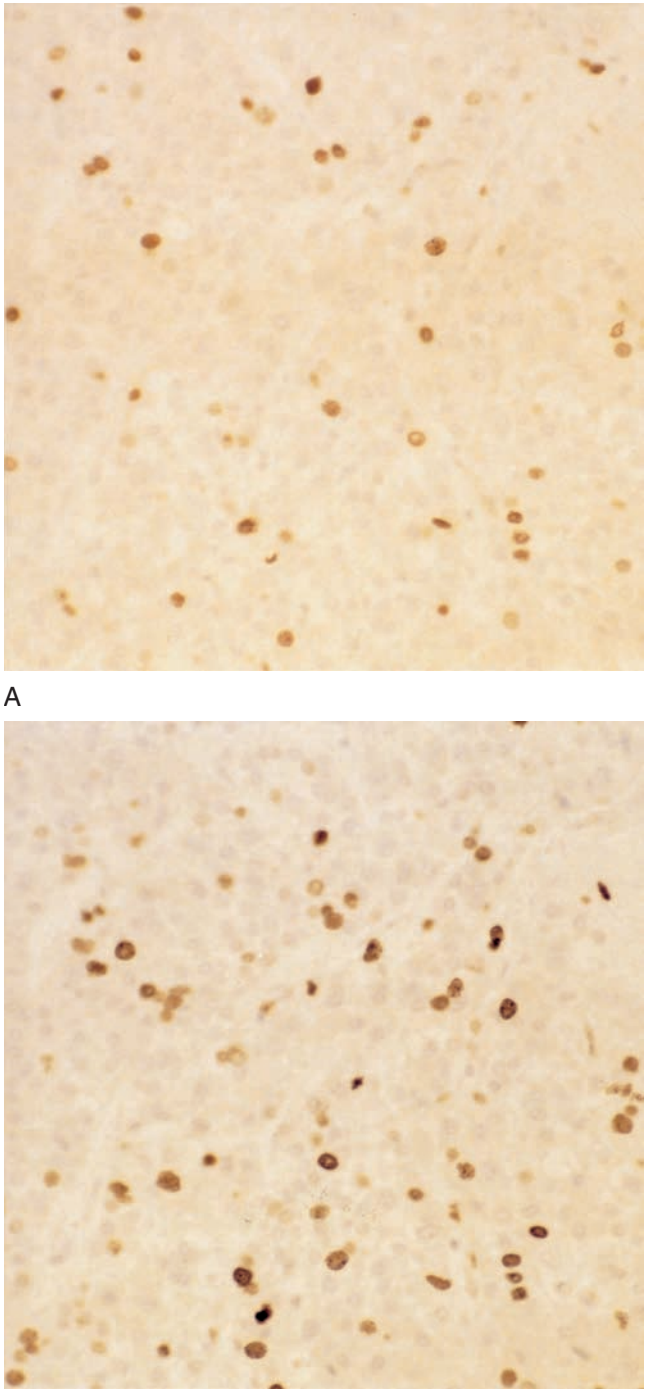

A

B

***Figure* 36.** Immunohistochemistry of topo IIα using monoclonal antibody 8D2 (**A**) and Ki-67 monoclonal antibody MIB-1 (**B**). The nuclei of hepatocellular carcinoma cells were positively stained for both topo IIα and Ki-67. There were fewer nuclei positive for topo IIα than for Ki-67.

although nuclei positive for topo IIα were less intensely stained than those positive for Ki-67. In general, the nuclei positive for Ki-67 were also positive for topo IIα. Conversely, nuclei that were negative for Ki-67 were essentially unstained by topo IIα antibody in the serial sections. The mean Ki-67 LI was 25.6 ± 22.5 (mean ± SD) and ranged from 0.5 to 82.5, and the median Ki-67 LI was 19.3%. Topo IIα expression was significantly linked to MIB-1 antibody labeling of the Ki-67 nuclear antigen ($r = 0.806$, $p < 0.001$).

Of the 70 HCC samples, 17 (24%) were positive for p53 by immunostaining. Of the patients positive for p53 HCC, 15 had a high topo IIα LI. Topo IIα overexpression was associated with p53 positivity, and p53-negative HCC had a lower mean topo IIα LI. The mean topo IIα LI was significantly higher in p53-positive HCC (25.6 ± 7.4) than in p53-negative HCC (10.3 ± 12.3) ($p < 0.01$).

Topo IIα Labeling Index and Survival

The topo IIα LI did not correlate with hepatitis B or C viral status, tumor size, the number of satellite nodules, UICC stage, capsular invasion, or Edmondson's scale with any prognostic significance. Patients with a lower topo IIα LI had significantly longer disease-free survival ($p < 0.05$) and a longer cumulative survival period ($p < 0.05$).

DISCUSSION

Topo IIα-positive nuclei for monoclonal antibody 8D2 were widely distributed in the HCC cells, with very few in adjacent noncancerous tissues. Topo IIα overexpression was associated with vein involvement and the serum alpha fetoprotein (AFP) level, although topo IIα expression was not linked with disease extent (stage or lymph node status). High topo IIα, high Ki-67 immunoexpression, and p53 protein overexpression were all correlated with earlier cancer-related death. This observation is in line with the hypothesis that topo IIα overexpression reflects not only the proliferative activity of these cells but also qualitative alterations in topo IIα expression caused by malignant transformation.

Topo IIα expression is closely related to other indicators of high malignant potential: MIB-1, p53, and c-erbB2 (Bredel, 2001). Ki-67 expression is an independent prognostic indicator for patients with HCC after resection. A close correlation between topo IIα expression and the Ki-67 staining (MIB-1) index is seen in HCC. Ki-67 is a useful marker of proliferation, but some loss of immunoreactivity may occur when sections are left for a long time, as exemplified by a

particular case of Ki-67 staining. The Ki-67 antigen is degraded during prolonged storage, making it very unreliable for determining proliferative activity. By contrast, topo IIα antigen is more stable. The examination of serial sections also revealed that topo IIα-positive cells were nearly always positive for Ki-67, although there were more Ki-67-positive cells than topo IIα-positive cells. Unlike Ki-67, which can be detected at all phases of the cell cycle (Gerdes *et al.,* 1984), topo IIα is not expressed during phase G1 (Hsiang *et al.,* 1988; Uemura *et al.,* 1987). Poorly differentiated HCC showed more Ki-67 immunoreactivity than did well- or moderately differentiated HCC (Watanuki *et al.,* 1998). Similarly, topo IIα was more positive in poorly differentiated HCC. Nevertheless, the differentiation status may be responsible for some of the differences in positivity between Ki-67 and topo IIα. Topo IIα may have more specificity for a particular proliferation state than Ki-67.

The cell cycle–regulated promoter determines the level of topo IIα messenger ribonucleic acid. In normal cells, topo IIα expression varies throughout the cell cycle; it is low in G1, increases in S, and peaks in G2/M (Adachi *et al.,* 1997), and the overexpression of topo IIα varies inversely with the doubling time (McPherson and Goldenberg, 1998). In malignant cells, the expression of topo IIα is both higher according to, and less dependent on, the proliferation state of the cell. The expression of topo IIα is significantly higher in the S/G2/M phase of the cell cycle than in the G0/G1 phase in both DNA diploid and DNA nondiploid tumors, but more than 50% of topo IIα-positive cells are in the G0/G1 phase. The topo II promoter region contains two GC boxes (a potential SP1 binding site), five inverted CCAAT elements (ICEs), and an activating transcription factor (ATF) site (Hochhauser *et al.,* 1992). In particular, ICEs are reported to be functionally important for the transcriptional regulation of the *topo II* gene (Ng *et al.,* 1995).

Experimental studies show that topo II expression is regulated by p53 (Wang *et al.,* 1997) and *ras* protein (Chen *et al.,* 1999). Wild-type p53 functions as a transcriptional repressor of topo IIα expression, possibly via a functional interaction with specific ICEs. Wild-type *p53*-induced inhibition of *topo IIα* gene expression could prevent the production of *topo IIa* at the level required to progress through a G2/M checkpoint. Inactivation of wild-type p53 reduces the normal regulatory suppression of topo IIα and contributes to abortive cell cycle checkpoints, accelerated cell proliferation, and alterations in genomic stability associated with neoplasia (Wang *et al.,* 1997; Yuwen *et al.,* 1997). The mean topo IIα LI was significantly higher in p53-positive HCC than in p53-negative HCC, suggesting that the overexpression of topo IIα induced by mutant p53 causes more aggressive carcinogenesis. p53 overexpression is closely related to proliferative activity and a negative prognosis in HCC (Watanuki *et al.,* 1998), and mutation of the *p53* gene in HCC is an unfavorable prognostic factor related to recurrence. Further, the progression of human HCC is putatively related to various cell cycle regulators of cyclin-dependent kinases (Cdks). In particular, topo IIα expression indicates a level of enzymatic activity that contributes to cell proliferation, and this suggests a worse prognosis for patients with curatively resected HCC.

Enhanced topo IIα levels are associated with overexpression of the c-erbB2 oncogene in breast cancers (Park *et al.,* 2003) and high-grade gliomas (Bredel, 2001). The close proximity of the *topo IIα* gene to the c-erbB2 gene locus on chromosome 17q21–q22 has led to speculation that there is a mechanism causing aberrant coexpression of these two proteins. Furthermore, a low level of topo II-binding protein 1 (TopBP1) specifically disrupts the regulation of Chk1 kinase, but not Chk2 kinase, resulting in only partial abrogation of the G2/M checkpoint (Yamane *et al.,* 2003). In addition, oncogenic *ras* stimulates the topo IIα promoter independently of normal cell cycle regulation via both the mitogen-activated protein kinase or extracellular signal-regulated (ERK) (MEK)/ERK and stress-associated protein kinase (SAPK) signaling pathways (Chen *et al.,* 1999). Then, topo II overexpression inhibits p53-triggered apoptosis, leading to unrestricted cell growth, even in the presence of wild-type p53 (Yuwen *et al.,* 1997). By contrast, Epstein-Barr virus–encoded nuclear antigen 1 (EBNA1) significantly increases topo IIα protein expression in HER2/neu-overexpressing ovarian cancer, indicating that up-regulation of topo IIα enhances sensitivity to topo II-targeting anticancer drugs (Chuang *et al.,* 2003). The response to chemotherapy is increased in breast cancer cases with co-amplification of HER2 and topo II. Furthermore, significant expression of topo IIα in the G0/G1 phase of the cell cycle may have clinically important implications for the treatment efficacy of topo II inhibitors. Topo II amplification may play a role in determining the chemosensitivity of various cancers. Understanding these relationships may lead to strategies for optimizing chemotherapy and increasing the precision of tumor cell targeting to overcome drug resistance and consequent chemotherapy failure.

The pathologic features of tumors, such as tumor size, invasion of the portal or hepatic vein, and satellite nodules, are presently the best predictive factors of recurrence. The proliferative index, *p53* mutations, and the expression of cell cycle–related genes have also been proposed as negative predictors of biological

behavior, and it has been proposed that p27 is an independent predictor of clinical recurrence (Ito *et al.,* 1999). Topo IIα overexpression appears to be linked to a potentially aggressive tumor phenotype and may play a role in determining chemosensitivity. Assessment of topo IIα levels may complement information obtained from tumor morphology, thereby improving the accuracy of predicting patient prognosis.

In conclusion, the immunohistochemical detection of the nuclear enzyme DNA topo IIα and the biological significance of its expression in human HCC are described. The nuclei of tumor cells in HCC tissues were positive for topo IIα, although there was a wide range in the LI: the mean and median topo IIα LI were 14.1 ± 15.1 and 9.9%, respectively. Cases with a lower topo IIα LI had significantly better disease-free and cumulative survival than cases with a higher topo IIα LI. Topo IIα expression was significantly linked to Ki-67 nuclear antigen labeling using MIB-1 antibody ($r = 0.806$, $p < 0.001$). The mean topo IIα LI was significantly higher in p53-positive HCC cases (25.6 ± 7.4) than in p53-negative cases (10.3 ± 12.3). Topo IIα overexpression appears to be linked to a potentially aggressive tumor phenotype and may complement the information obtained from tumor morphology as a means of improving the accuracy of predicting patient prognosis.

References

Adachi, N., Kobayashi, M., and Koyama, H. 1997. Cell cycle-dependent regulation of the mouse DNA topoisomerase IIalpha gene promoter. *Biochem. Biophys. Res. Commun. 230*:105–109.

Bredel, M. 2001. Anticancer drug resistance in primary human brain tumors. *Brain Res. Rev. 35*:161–204.

Chen, G., Templeton, D., Suttle, D.P., and Stacey, D.W. 1999. Ras stimulates DNA topoisomerase II alpha through MEK: A link between oncogenic signaling and a therapeutic target. *Oncogene 18*:7149–7160.

Chuang, T.C., Lee, Y.J., Liu, J.Y., Lin, Y.S., Li, J.W., Wang, V., Law, S.L., and Kao, M.C. 2003. EBNA1 may prolong G(2)/M phase and sensitize HER2/neu-overexpressing ovarian cancer cells to both topoisomerase II-targeting and paclitaxel drugs. *Biochem. Biophys. Res. Commun. 307*:653–659.

Downes, C.S., Clarke, D.J., Mullinger, A.M., Gimenez-Abian, J.F., Creighton, A.M., and Johnson, R.T. 1994. A topoisomerase II-dependent G2 cycle checkpoint in mammalian cells. *Nature 372*:467–470.

Fry, A.M., Chresta, C.M., Davies, S.M., Walker, M.C., Harris, A.L., Hartley, J.A., Masters, J.R., and Hickson, I.D. 1991. Relationship between topoisomerase II level and chemosensitivity in human tumor cell lines. *Cancer Res. 51*:6592–6595.

Gerdes, J., Lemke, H., Baisch, H., Wacker, H.H., Schwab, U., and Stein, H. 1984. Cell cycle analysis of a cell proliferation-associated human nuclear antigen defined by the monoclonal antibody Ki-67. *J. Immunol. 133*:1710–1715.

Hochhauser, D., Stanway, C.A., Harris, A.L., and Hickson, I.D. 1992. Cloning and characterization of the 5′-flanking region of the human topoisomerase II alpha gene. *J. Biol. Chem. 267*:18961–18965.

Hsiang, Y.H., Wu, H.Y., and Liu, L.F. 1988. Proliferation-dependent regulation of DNA topoisomerase II in cultured human cells. *Cancer Res. 48*:3230–3235.

Ito, Y., Matsuura, N., Sakon, M., Miyoshi, E., Noda, K., Takeda, T., Umeshita, K., Nagano, H., Nakamori, S., Dono, K., Tsujimoto, M., Nakahara, M., Nakao, K., Taniguchi, N., and Monden, M. 1999. Expression and prognostic roles of the G1-S modulators in hepatocellular carcinoma: p27 independently predicts the recurrence. *Hepatology 30*:90–99.

Kato, S., and Kikuchi, A. 1998. DNA topoisomerase: the key enzyme that regulates DNA super structure. *Nagoya J. Med. Sci. 61*:11–26.

McPherson, J.P., and Goldenberg, G.J. 1998. Induction of apoptosis by deregulated expression of DNA topoisomerase IIalpha. *Cancer Res. 58*:4519–4524.

Ng, S.W., Eder, J.P., Schnipper, L.E., and Chan, V.T. 1995. Molecular cloning and characterization of the promoter for the Chinese hamster DNA topoisomerase IIalpha gene. *J. Biol. Chem. 270*:25850–25858.

Park, K., Kim, J., Lim, S., and Han, S. 2003. Topoisomerase II–alpha (topoII) and HER2 amplification in breast cancers and response to preoperative doxorubicin chemotherapy. *Eur. J. Cancer 39*:631–634.

Tsai-Pflugfelder, M., Liu, L.F., Liu, A.A., Tewey, K.M., Whang-Peng, J., Knutsen, T., Huebner, K., Croce, C.M., and Wang, J.C. 1988. Cloning and sequencing of cDNA encoding human DNA topoisomerase II and localization of the gene to chromosome region 17q21-22. *Proc. Natl. Acad. Sci. USA 85*:7177–7181.

Uemura, T., Ohkura, H., Adachi, Y., Morino, K., Shiozaki, K., and Yanagida, M. 1987. DNA topoisomerase II is required for condensation and separation of mitotic chromosomes in S. pombe. *Cell 50*:917–925.

Wang, Q., Zambetti, G.P., and Suttle, D.P. 1997. Inhibition of DNA topoisomerase II alpha gene expression by the p53 tumor suppressor. *Mol. Cell Biol. 17*:389–397.

Watanuki, A., Ohwada, S., Fukusato, T., Kawate, S., Makita, F., and Morishita, Y. 1998. Low MIB-1 labeling index in anti-HCV positive hepatocellular carcinoma. *Int. J. Oncol. 13*:1017–1022.

Watanuki, A., Ohwada, S., Fukusato, T., Makita, F., Yamada, T., Kikuchi, A., and Morishita, Y. 2002. Prognostic significance of DNA topoisomerase IIalpha expression in human hepatocellular carcinoma. *Anticancer Res. 22*:1113–1119.

Watt, P.M., and Hickson, I.D. 1994. Structure and function of type II DNA topoisomerases. *Biochem. J. 303 (Pt 3)*:681–695.

Woessner, R.D., Mattern, M.R., Mirabelli, C.K., Johnson, R.K., and Drake, F.H. 1991. Proliferation- and cell cycle-dependent differences in expression of the 170 kilodalton and 180 kilodalton forms of topoisomerase II in NIH-3T3 cells. *Cell Growth Differ. 2*:209–214.

Yamane, K., Chen, J., and Kinsella, T.J. 2003. Both DNA topoisomerase II-binding protein 1 and BRCA1 regulate the G2-M cell cycle checkpoint. *Cancer Res. 63*:3049–3053.

Yuwen, H., Hsia, C.C., Nakashima, Y., Evangelista, A., and Tabor, E. 1997. Binding of wild-type p53 by topoisomerase II and overexpression of topoisomerase II in human hepatocellular carcinoma. *Biochem. Biophys. Res. Commun. 234*:194–197.

10

Role of Immunohistochemical Expression of DNA Methyltransferases in Hepatocellular Carcinoma

Mi Sun Choi, Dong Eun Song, and Eunsil Yu

Introduction

The methylation of deoxyribonucleic acid (DNA) is an epigenetic modification that is involved in the control of gene expression of mammalian cells (Singal and Ginder, 1999). In mammalian cells, approximately 3–5% of the cytosine residues in genomic DNA are present as 5-methylcytosine, 70–80% of which are found in CpG dinucleotides-rich regions, termed "CpG islands" (Bird, 1986; Ehrlich *et al.,* 1982). In normal cells, CpG methylation patterns in the genome can be maintained precisely through DNA replication and mitosis via the action of DNA methyltransferases (Dnmts) (Reik *et al.,* 1999). In cancer cells, genomewide hypomethylation is a general phenomenon (Gama-Sosa *et al.,* 1983); however, specific CpG island sequences are hypermethylated (Baylin *et al.,* 1998; Jones and Laird, 1999). Such aberrant methylation of CpG islands is one of the most consistent epigenetic mechanisms of gene expression in human cancers (Jones and Laird, 1999). Hypermethylation of tumor-suppressor genes causes gene inactivation leading to functional impairment (Momparler and Bovenzi, 2000). Furthermore, aberrant DNA methylation facilitates gene mutation (Shen *et al.,* 1992) or is closely associated with allelic loss (Chen *et al.,* 1998).

The enzymatic methylation machinery is composed of three catalytically active Dnmts; Dnmt1, Dnmt3a, and Dnmt3b. Dnmt1 is the most abundant Dnmt; it is targeted to replication foci and has a 10–40-fold preference for hemimethylated DNA substrates (Pradhan *et al.,* 1999). It seems to be the main enzyme responsible for copying methylation pattern after each round of DNA replication (Robertson *et al.,* 1999). However, studies of Dnmt1-deficient embryonic stem cells have revealed that other enzymes must exist for *de novo* methylation after the wave of global demethylation that occurs during early embryonic development (Lei *et al.,* 1996; Shay and Bacchetti, 1997). Independently encoded new Dnmts such as Dnmt2 (Yoder and Bestor, 1998), Dnmt3a, and Dnmt3b (Okano *et al.,* 1998) have been identified. Dnmt3a and Dnmt3b are essential for embryonic development and responsible for the *de novo* methylation during the

Handbook of Immunohistochemistry and *in situ* Hybridization of Human Carcinomas, Volume 3: Molecular Genetics, Liver Carcinoma, and Pancreatic Carcinoma

embryogenesis and tumorigenesis (Bird, 1999; Xie *et al.,* 1999).

It has been noted that Dnmts are overexpressed in tumorigenic cells (Kautiainen and Jones, 1986) and in a few types of human tumors (De Marzo *et al.,* 1999; Sun *et al.,* 1997). Increased levels of Dnmt1 messenger ribonucleic acid (mRNA) are known to be dependent on cell proliferation (Goto *et al.,* 1994; Szyf *et al.,* 1991) and seem to be regulated by a post-transcriptional mechanism such as differential mRNA stability in normal somatic cells (Robertson *et al.,* 2000). Thus, the increase of Dnmt1 enzymatic activity might not be always correlated with the Dnmt1 mRNA levels in cancer cells. Dnmt3a and 3b are differentially expressed in normal and tumor cells. Dnmt3b mRNA levels were nearly undetectable, whereas Dnmt3a mRNA levels were less sensitive to cell cycle alterations and maintained at a slightly higher level in tumor cell lines compared to normal cell strains (Robertson *et al.,* 2000). However, contrasting results on the expression of Dnmts and a clue as to the decreased methylation of CpG dinucleotides have been reported in human colon cancers (Chuang *et al.,* 1997; Eads *et al.,* 1999).

In the development of human hepatocellular carcinomas (HCCs), the average levels of Dnmt1 and Dnmt3a mRNA were significantly higher in non-cancerous liver tissues showing chronic hepatitis or cirrhosis and much higher in HCCs than in histologically normal liver tissues (Saito *et al.,* 2001). Nagai *et al.* (2003) also demonstrated the increased levels of Dnmt1 and Dnmt3b mRNA in HCCs than in nontumorous liver tissue. Although higher mRNA levels of Dnmts are confirmed in HCCs, it is still necessary to clarify whether the increased mRNA levels of Dnmts lead to protein overexpression in HCCs. To directly evaluate the expression of Dnmts in multistep hepatocarcinogenesis, Choi *et al.* (2003) first investigated the protein expression of Dnmt1 and Dnmt3a in the 59 cases of surgically resected liver specimens by immunohistochemical analysis. Cases included 9 low-grade dysplastic nodules (DNs), 24 high-grade DNs, and 41 HCCs. Diagnosis of DNs and HCCs was made according to the previously described criteria (International Working Party, 1995). Thirteen cases of HCCs arose within the high-grade DNs, representing the early stage of HCCs, and 28 cases were advanced HCCs. Nonneoplastic livers displayed cirrhotic nodules (CNs) in 47 cases and chronic hepatitis in 9 cases and were unremarkable in 3 cases. Furthermore, an HCC cell line and a hepatoblastoma cell line were investigated for the expression of Dnmt1 and Dnmt3a by immunofluorescent staining technique.

MATERIALS

59 cases of surgically resected liver specimens with nodular lesions
- 9 low-grade DNs
- 24 high-grade DNs
- 41 HCCs
  - 13 cases of HCCs arising within the high-grade DNs
  - 28 cases of advanced HCCs
    - Nonneoplastic livers
    - 47 liver cirrhosis
    - 9 chronic hepatitis
    - 3 unremarkable liver

For Immunohistochemical Staining

- Xylene
- Ethanol
- Tap water
- 3% hydrogen peroxide
- 0.01 M sodium citrate buffer (pH 6.0)
- 10% normal goat serum
- Tris-buffer saline (TBS) (pH 7.4)
- Primary mouse monoclonal antibodies for Dnmt1 (IMG-261, 60B1220) (IMGENEX, San Diego, CA) 1:125 and Dnmt3a (IMG-268, 64B1446), IMGENEX) 1:125
- Biotinylated anti-mouse antibody
- Streptavidin–horseradish peroxidase conjugate (Dako LSAB kit; Dako, Los Angeles, CA) with diaminobenzidine
- Harris's hematoxylin
- Distilled water
- Mounting media

For Cell Culture and Immunofluorescent Staining

- Dulbeco's modified essential medium
- 10% fetal calf serum
- 5% CO_2 incubator
- Round coverslips measuring 12 mm in diameter
- 24-well culture plates
- 2% paraformaldehyde
- 0.2% Triton X
- Primary mouse monoclonal antibody for Dnmt1 (IMG-261, 60B1220) (IMGENEX) 1:125 and Dnmt3a (IMG-268, 64B1446) (IMGENEX, San Diego, CA), 1:125
- Fluorescein isothiocyanate–conjugated anti-mouse antibody
- 0.5 mg/ml bisbenzimide (Hoechst 33258, Sigma St. Louis, MO)

Phosphate buffer saline (PBS) (pH 7.4)
Mounting media (Vector)

METHODS

Immunohistochemical Staining

1. Mount paraffin sections (4–6 μm thick) onto poly-L-lysine-coated glass slides.
2. Bake the slides in an oven at 60°C for 15 min.
3. Deparaffinize the slides in xylene.
4. Rehydrate the slides in graded ethanol.
5. Wash the slides in tap water.
6. Incubate the slides with 3% H_2O_2 for blocking the endogeneous peroxidase activity.
7. Place the slides in a steam cooker filled with 0.01 M sodium citrate buffer (pH 6.0) for antigen retrieval.
8. Cool the slides in 0.01 M sodium citrate buffer (pH 6.0) solution at room temperature.
9. Treat the slides with 10% normal goat serum for 10 min to block nonspecific protein binding.
10. Wash the slides with TBS 3× for 2 min each.
11. Apply mouse monoclonal antibodies for Dnmt1 (IMG-261, 60B1220, (IMGENEX, 1:125) and Dnmt3a (IMG-268, 64B1446, IMGENEX 1:125) to the slides for 1 hr.
12. Wash the slides with TBS 3× for 2 min each.
13. Apply a biotinylated anti-mouse antibody for 1 hr.
14. Wash the slides with TBS 3× for 2 min each.
15. Apply a streptavidin–horseradish peroxidase conjugate (Dako LSAB kit; Dako) with diaminobenzidine.
16. Wash the slides with distilled water.
17. Counterstain with Harris hematoxylin for 3–5 min.
18. Dehydrate and mount.

Cell Culture and Immunofluorescent Staining

1. Culture HepG2 (human hepatoblastoma cell line) and Hep3B (human hepatocellular carcinoma cell line) in Dulbeco's modified essential medium with 10% fetal calf serum in 5% CO_2 incubator at 37°C.
2. Plate cells of 2× 10^5/ml on round coverslips measuring 12 mm in diameter, and culture in 24-well culture plates.
3. Wash the cultured cells with 70–80% confluency in TBS, and fix the cells in 2% paraformaldehyde for 20 min.
4. Wash the cells 3×, in TBS, and penetrate the cells in 0.2% Triton X for 10 min.
5. Wash the cells 3×, and incubate the cells in the Dnmt1 (IMG-261, 60B1220, IMGENEX, 1:125) and Dnmt3a (IMG-268, 64B1446, IMGENEX, 1:125) antibodies for 1 hr.
6. Wash the cells 3×, in TBS, and incubate the cells in fluorescein isothiocyanate–conjugated anti-mouse antibody for 30 min.
7. Stain the cells for DNA with 0.5 mg/ml bisbenzimide (Hoechst 33258, Sigma) in PBS for 5 min with no washing.
8. Wash the cells in tap water, and mount with Fluoromount (Vector Laboratories, Inc., Burlingame, VT).

RESULTS AND DISCUSSION

Genomewide hypomethylation and aberrant methylation of specific gene loci are characteristics of human cancers including HCCs (Lin *et al.,* 2001). Dnmts are the most important proteins involved in such abnormal methylation processes. Thus, the transcript levels of Dnmts have been analyzed in various types of human cancers including HCC (De Marzo *et al.,* 1999; Nagai *et al.,* 2003; Robertson *et al.,* 1999; Saito *et al.,* 2001). However, their protein expressions rarely have been examined in primary human cancers such as colon and prostate cancers because of the lack of specific antibodies for Dnmts (De Marzo *et al.,* 1999; Patra *et al.,* 2002). We could use recently developed and commercially available monoclonal antibodies for Dnmt1 and Dnmt3a to examine the expression of Dnmts in multistep hepatocarcinogenesis from nonneoplastic liver tissues, through precancerous dysplastic lesions to neoplastic liver tissues.

Immunolocalization of Dnmts has not been described even in cultured cells. Thus, we first analyzed the expression of Dnm1 and Dnmt3a in two liver cancer cell lines, Hep3B and HepG2, by the immunofluorescent staining as a positive control. Diffuse and granular staining for Dnmt1 was exclusively observed in the nucleus of cells in interphase, and cells in metaphase showed localization of Dnmt1 in chromosomes. The expression of Dnmt3a was similar to that of Dnmt1; however, a few cells displayed granular cytoplasmic stainability as well as nuclear staining.

Expression of Dnmts rarely has been reported in human tissues. De Marzo *et al.* (1999) detected Dnmt1 expression only in the nucleus of various normal human tissues and colon cancer tissues using a polyclonal antibody that they had developed. However, on the basis of the immunolocalization characteristics of Dnmt1 and Dnmt3a in cultured cells, we evaluated both nuclear and cytoplasmic immunopositivity in liver tissues using the scoring system according to the staining intensity (0–3): 0, negative; 1, mild; 2, moderate; and 3, severe; and the proportion of positive cells (0–4): 0, negative; 1, positive cells in ≤10% of cells; 2, positive

cells in >10% and ≤1/3 of cells; 3, positive cells in >1/3 and ≤2/3 of cells; and 4, positive cells in >2/3 of cells. Two scores were added in each case, and the expression was graded as negative (0), weak positive (score 1 and 2), intermediate positive (score 3–5), and strong positive (score 6 and 7).

In our study (Choi *et al.,* 2003), immunoreactivity for Dnmt1 in liver tissue sections was evident only in nuclei of liver cells and sinusoidal lymphocytes. Immunopositivity for Dnmt1 was sequentially increased through the multistep hepatocarcinogenesis. Of nonneoplastic liver tissues 42 of 59 (71.2%) showed no immunoreactivity, 12 of 59 (20.3%) displayed weak; and 5 of 59 (8.5%) showed intermediate immunopositivity. In 9 cases of low-grade DNs, the immunoreactivity for Dnmt1 was not detectable in 5 cases (55.6%) and weak in 4 cases (44.4%). In 24 cases of high-grade DNs, the immunoreactivity for Dnmt1 was not detectable in 9 cases (37.5%) and weak in 15 cases (62.5%). In 13 cases of HCCs arising in DNs, the immunoreactivity for Dnmt1 was weak in 8 cases (61.5%), intermediate in 4 cases (30.8%), and strong in 1 case (7.7%). The increase in Dnmt1 immunoreactivity in HCCs in DNs was statistically significant compared with the Dnmt1 immunoreactivity in nonneoplastic livers ($p < 0.0001$), low-grade DNs ($p = 0.0028$), and high-grade DNs ($p = 0.004$). In 28 cases of advanced HCCs, the immunoreactivity for Dnmt1 was weak in 4 cases (14.3%), intermediate in 14 cases (50.0%), and strong in 10 cases (35.7%). There was a statistically significant difference in the Dnmt1 nuclear immunoreactivity between advanced HCC and HCC in DN ($p = 0.0031$).

The nuclear immunopositivity for Dnmt1 (28.8%) of 59 nonneoplastic liver tissues with either chronic hepatitis or liver cirrhosis was compatible with the previous report that the level of Dnmt1 mRNA was significantly higher in chronic hepatitis and cirrhosis than that in normal liver tissues, adjacent to HCC (Saito *et al.,* 2001). There was no significant difference of immunoreactivity between nonneoplastic liver tissues and DNs, but the immunopositivity for Dnmt1 was significantly increased in HCCs in DNs and advanced HCCs. These results indicate that Dnmt1 may play an important role in the early stage of HCC development. Furthermore, the degree of Dnmt1 expression was even stronger in advanced HCCs compared with HCCs arising in DNs. This result further suggests that Dnmt1 is also involved in the progression of HCCs. In addition, Saito *et al.* (2003) subsequently reported that the increased expression of Dnmt1 in human HCCs was significantly correlated with the malignant potential and poor prognosis.

However, Dnmt3a immunopositivity was detected both in the nucleus and the cytoplasm of cells in liver tissues as in cultured cells. Nuclear immunoreactivity for Dnmt3a was not detected in any cases of nonneoplastic livers and low-grade DNs. In 7 of 24 cases (29.2%) of high-grade DN and in 7 of 13 cases (53.8%) of HCC in DNs, weak to intermediate nuclear immunopositivity for Dnmt3a was displayed. In advanced HCCs, 11 of total 28 cases (39.3%) showed variable degrees of nuclear immunoreactivity for Dnmt3a. Although the number of cases that displayed nuclear immunoreactivity for Dnmt3a was lower in advanced HCC, compared with that in HCCs in DNs (39.7% versus 53.8%), the staining intensity was stronger and the number of positive tumor cells was higher in advanced HCCs than in HCCs arising in DNs. The difference of nuclear Dnmt3a immunopositivity was not statistically significant between cases with low-grade DN and high-grade DN, between cases with high-grade DN and HCC in DN, and between cases with HCC in DN and advanced HCC. However, there was a statistically significant difference between low-grade DN and HCC in DN ($p = 0.0146$) or advanced HCC ($p = 0.0494$).

The degree of nuclear Dnmt3a expression was generally lower compared with that of Dnmt1, and the increase of nuclear Dnmt3a immunopositivity was not statistically significant between high-grade DNs and HCCs. However, nuclear Dnmt3a and Dnmt1 may cooperate to silence genes in the early stage of hepatocarcinogenesis, as suggested by Rhee *et al.,* (2002). Interaction of Dnmt3a with other nuclear proteins involved in cell cycle or proliferation should be studied further to elucidate the functional role of Dnmt3a in human hepatocarcinogenesis.

In addition to the nuclear immunoreactivity, cytoplasmic immunopositivity was also present for Dnmt3a. In 59 cases of nonneoplastic liver, the cytoplasmic immunoreactivity for Dnmt3a was diffusely strong in 58 cases (98.3%) and intermediate in 1 case (1.7%). In 9 cases of low-grade DNs, the cytoplasmic immunoreactivity for Dnmt3a was strong in 8 cases (88.9%) and weak in 1 case (11.1%). In high-grade DNs, the cytoplasmic immunoreactivity for Dnmt3a was significantly decreased compared with those of nonneoplastic liver and low-grade DNs. More than 50% of total cases with high-grade DN showed no detectable or weak cytoplasmic immunoreactivity for Dnmt3a, and only 4 cases (16.7%) displayed strong cytoplasmic immunopositivity for Dnmt3a. Of 13 cases of HCCs in DNs, the cytoplasmic immunoreactivity for Dnmt3a was not detectable in 5 cases (38.5%), weak in 7 cases (53.8%), and strong in only 1 case (7.7%). Sequential decrease of cytoplasmic immunoreactivity for Dnmt3a through the multistep hepatocarcinogenesis was statistically significant between each type of liver tissues except for advanced HCCs. In cases with advanced HCCs, the cytoplasmic

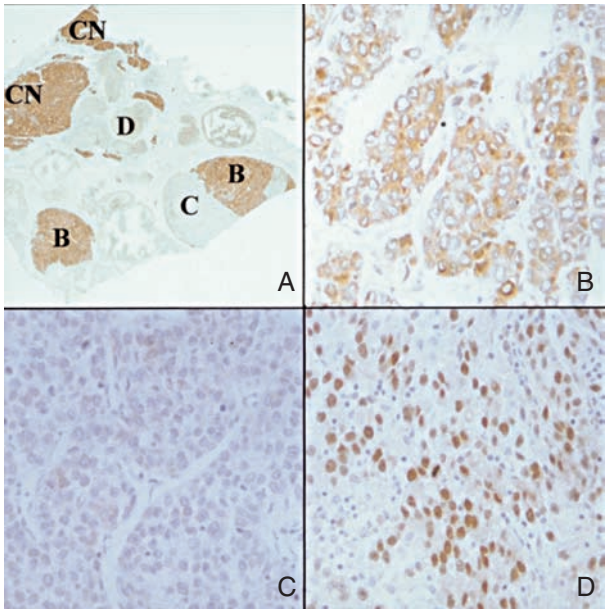

Figure 37. Expression of deoxyribonucleic acid (DNA) methyltransferase3a in a representative case of advanced hepatocellular carcinoma (HCC) by immunohistochemical staining. **A:** Both nuclear and cytoplasmic immunoreactivities are heterogeneous in area to area of the same tumor section. CN, cirrhotic nodule. **B:** In some areas of HCC, nuclear immunoreactivity is absent in tumor cells, whereas moderate cytoplasmic immunopositivity is present. **C:** Other areas of the same tumor are negative for Dnmt3a both in the nucleus and in the cytoplasm. **D:** Some HCC cells display strong nuclear staining with no cytoplasmic staining (original magnification, 100X).

expression of Dnmt3a was generally weak and quite variable (Figure 37). Thus, there was no statistical significance in the cytoplasmic immunoreactivity for Dnmt3a between HCC cases in DNs and advanced HCC cases.

The cytoplasmic immunoreactivity for Dnmt3a can be attributable to either the presence of Dnmt3a in the cytoplasm or a cross-reactivity to another proteins. However, the sequential decrease of cytoplasmic immunoreactivity for Dnmt3a and concurrent increase of nuclear Dnmt3a in high-grade DNs and HCCs arising in DNs suggest that nucleocytoplasmic shuttling of Dnmt3a may be involved in the development of HCCs, and the nuclear expression of Dnmt3a is closely related to DNA methylation. Furthermore, heterogeneity of Dnmt3a expression in the cytoplasm as well as in the nucleus of advanced HCCs suggests that a progressive dysregulation of Dnmt3a expression is involved in the late stage of human hepatocarcinogenesis and may contribute much more to the abnormal CpG islands methylation patterns of dysplastic hepatocytes and HCC cells, as in the case of Dnmt1 in human colon cancers (De Marzo *et al.,* 1999). In the diagnostic point of view, the significant decrease of cytoplasmic immunoreactivity for Dnmt3a in HCCs in DNs can be useful for the diagnosis of carcinoma development from DNs.

In conclusion, it is suggested that nuclear Dnmt1 and Dnmt3a play important roles in the early stage of multistep human hepatocarcinogenesis and dysregulation of Dnmt3a is involved in the progression of HCC. Furthermore, the decreased cytoplasmic immunoreactivity for Dnmt3a in high-grade DNs and HCCs arising in DNs compared with the surrounding DNs can be applied in the diagnosis of precancerous lesions such as high-grade DNs and well-differentiated HCCs in the needle biopsy specimens.

References

Baylin, S.B., Herman, J.G., Graff, J.R., Vertino, P.M., and Issa, J.P. 1998. Alterations in DNA methylation: A fundamental aspect of neoplasia. *Adv. Cancer Res*. *72*:141–196.

Bird, A.P. 1986. CpG-rich islands and the function of DNA methylation. *Nature 321*:209–213.

Bird, A. 1999. DNA methylation de novo. *Science 286*:2287–2288.

Chen, R.Z., Pettersson, U., Beard, C., Jackson-Grusby, L., and Jaenisch, R. 1998. DNA hypomethylation leads to elevated mutation rates. *Nature 395*:89–93.

Choi, M.S., Shim, Y.H., Hwa, J.Y., Lee, S.K., Ro, J.Y., Kim, J.S., and Yu, E. 2003. Expression of DNA methyltransferases in multistep hepatocarcinogenesis. *Hum. Pathol. 34*:11–17.

Chuang, L.S., Ian, H.I., Koh, T.W., Ng, H.H., Xu, G., and Li, B.F. 1997. Human DNA-(cytosine-5) methyltransferase-PCNA complex as a target for p21WAF1. *Science 277*:1996–2000.

De Marzo, A.M., Marchi, V.L., Yang, E.S., Veeraswamy, R., Lin, X., and Nelson, W.G. 1999. Abnormal regulation of DNA methyltransferase expressing during colorectal carcinogenesis. *Cancer Res*. *59*:3855–3860.

Eads, C.A., Danenberg, K.D., Kawakami, K., Saltz, L.B., Danenberg, P.V., and Laird, P.W. 1999. CpG island hypermethylation in human colorectal tumors is not associated with DNA methyltrasferase overexpression. *Cancer Res*. *59*: 2302–2306.

Ehrlich, M., Gama-Sosa, M.A., Huang, L.H., Midgett, R.M., Kuo, K.C., McCune, R.A., and Gehrke, C. 1982. Amount and distribution of 5-methylcytosine in human DNA from different types of cells. *Nucleic Acids Res*. *10*: 2709–2721.

Gama-Sosa, M.A., Slagel, V.A., Trewyn, R.W., Oxenhandler, R., Kuo, K.C., Gehrke, C.W., and Ehrlich, M. 1983. The 5-methylcytosine content of DNA from human tumors. *Nucleic Acids Res*. *11*:6883–6894.

Goto, K., Numata, M., Komura, J.I., Ono, T., Bestor, T.H., and Kondo, H. 1994. Expression of DNA methyltransferase gene in mature and immature neurons as well as proliferating cells in mice. *Differentiation 56*:39–44.

International Working Party. 1995. Terminology of nodular hepatocellular lesions. *Hepatology 22*:983–993.

Jones, P.A., and Laird, P.W. 1999. Cancer epigenetics comes of age. *Nat. Genet*. *21*:163–167.

Kautiainen, T.L., and Jones, P.A. 1986. DNA methyltransferase levels in tumorigenic and nontumorigenic cells in culture. *J. Biol. Chem*. *261*:1594–1598.

Lei, H., Oh, S.P., Okano, M., Juttermann, R., Goss, K.A., Jaenisch, R., and Li, E. 1996. De novo DNA cytosine methyltransferase activities in mouse embryonic stem cells. *Development 122*:3195–3205.

Lin, C.H., Hsieh, S.Y., Sheen, I.S., Lee, W.C., Chen, T.C., Shyu, W.C., and Liaw, Y.F. 2001. Genome-wide hypomethylation in hepatocellular carcinogenesis. *Cancer Res. 61*:4238–4243.

Momparler, R., and Bovenzi, V. 2000. DNA methylation and cancer. *J. Cell Physiol*. *183*:145–154.

Nagai, M., Nakamura, A., Makino, R., and Mitamura, K. 2003. Expression of DNA (5-cytosin)-methyltransferase (DNMTs) in hepatocellular carcinomas. *Hepatol. Res*. *26*:186–191.

Okano, M., Xie, S., and Li, E. 1998. Cloning and characterization of a family of novel mammalian DNA (cytosine-5) methyltranferases. *Nat. Genet*. *19*:219–220.

Patra, S.K., Patra, A., Zhao, H., and Dahiya, R. 2002. DNA methyltransferase and demethylase in human prostate cancer. *Mol. Carcinogenesis 33*:163–171.

Pradhan, S., Bacolla, A., Wells, R.D., and Roberts, R.J. 1999. Recombinant human DNA (cytosine-5) methyltransferase. I. Expression, purification, and comparison of de novo and maintenance methylation. *J. Biol. Chem*. *274*:33002–33010.

Reik, W., Kelsey, G., and Walter, J. 1999. Dissecting de novo methylation. *Nat. Genet*. *23*:380–382.

Rhee, I., Bachman, K.E., Park, B.H., Jair, K.W., Yen, R.W., Schuebel, K.E., Cul, H., Feinberg, A.P., Lengauer, C., Kinzler, K.W., Baylin, S.B., and Vogelstein, B. 2002. DNMT1 and DNMT3b cooperate to silence genes in human cancer cells. *Nature 416*:552–556.

Robertson, K.D., Uzvolgyi, E., Liang, G., Talmadge, C., Sumegi, J., Gonzales, F.A., and Jones, P.A. 1999. The human DNA methyltransferases (DNMTs) 1, 3a and 3b: Coordinate mRNA expression in normal tissues and overexpression in tumors. *Nucleic Acids Res*. *27*:2291–2298.

Robertson, K.D., Keyomarsi, K., Gonzales, F.A., Velicescu, M., and Jones, P.A. 2000. Differential mRNA expression of the human DNA methyltransferases (DNMTs) 1, 3a and 3b during the G_0/G_1 to S phase transition in normal and tumor cells. *Nucleic Acid Res*. *28*:2108–2113.

Saito, Y., Kanai, Y., Sakamoto, M., Saito, H., Ishii, H., and Hirohashi, S. 2001. Expression of mRNA for DNA methyltrasferases and methyl-CpG-binding proteins and DNA methylation status on CpG islands and pericentromeric satellite regions during human hepatocarcinogenesis. *Hepatology 33*: 561–568.

Saito, Y., Kanai, Y., Nakagawa, T., Sakamoto, M., Saito, H., Ishii, H., and Hirohashi, S. 2003. Increased protein expression of DNA methyltransferase (DNMT1) is significantly correlated with the malignant potential and poor prognosis of human hepatocellular carcinomas. *Int. J. Cancer 105*:527–532.

Shay, J.W., and Bacchetti, S. 1997. A survey of telomerase activity in human cancer. *Eur. J. Cell Biol. 33*:787–791.

Shen, J.C., Rideout, W.M 3rd, and Jones, P.A. 1992. High frequency mutagenesis by a DNA methyltransferase. *Cell 71*: 1073–1080.

Singal, R., and Ginder, G.D. 1999. DNA methylation. *Blood 93*: 4059–4070.

Sun, L., Hui, A.M., Kanai, Y., Sakamoto, M., and Hirohashi, S. 1997. Increased DNA methyltransferase expression is associated with an early stage of human hepatocarcinogenesis. *Jpn. J. Cancer Res*. *88*:1165–1170.

Szyf, M., Bozovic, V., and Tanigawa, G. 1991. Growth regulation of mouse DNA methyltransferase gene expression. *J. Biol. Chem. 266*:10027–10030.

Xie, S., Wang, Z., Okano, M., Nogami, M., Li, Y., He, W.W., Okumura, K., and Li, E. 1999. Cloning, expression and chromosome locations of the human DNMT3 gene family. *Gene 236*:87–95.

Yoder, J.A., and Bestor, T.H. 1998. A candidate mammalian DNA methyltransferase related to pmt1p of fission yeast. *Hum. Mo1. Genet*. *7*:279–284.

11

Role of Hepatitis B Surface Antigen in Hepatocarcinogenesis

Xin-Yuan Guan, Sze-Hang Lau, and Yi Wang

Introduction

Hepatitis B Virus and Hepatocellular Carcinoma

Hepatocellular carcinoma (HCC) is one of the most common human malignant neoplasms. It is the fifth most common cancer and the third cause of cancer death in the world (Parkin *et al.,* 2001). The prognosis of HCC is very poor with or without therapeutic intervention. The overall 5-year survival rate worldwide is estimated at only ~3%, mainly because of late diagnosis.

Although the molecular pathogenesis of HCC remains elusive, the etiologic association between hepatitis B virus (HBV) infection and hepatocarcinogenesis has been well established (Thorgeirsson and Grisham, 2002). There are an estimated 387 million HBV carriers worldwide, and geographic distribution of HBV carriers match well with HCC incidences. Epidemiologic studies have demonstrated that the risk of developing HCC among HBV carriers is 100-fold higher than among noncarriers and the death rate from HCC is between 10 and 25% (Block *et al.,* 2003; Montalto *et al.,* 2002).

Inside the virion, the HBV genome exists as a partially double-stranded deoxyribonucleic acid (DNA) molecule. The 3.2-kb DNA genome of HBV encodes proteins from four partially overlapping opening reading frames (ORFs): S-ORF, C-ORF, P-ORF, and X-ORF. The S-ORF is divided into three coding regions: preS1, preS2, and S, which encode the hepatitis B surface antigens (HBsAg). By using different in-frame translation initiation sites, large hepatitis B surface antigen (LHBs) encompassing the preS1-, preS2-, and S-regions; middle hepatitis B surface antigen (MHBs), containing the preS2- and S-domains; and small hepatitis B surface antigen (SHBs), encompassing the S-region, can be synthesized. The HBsAg polypeptides are important for HBV infection and are an important target for diagnosis and vaccine development. The C-ORF encodes the nucleocaspid protein hepatitis B core antigen (HBcAg) and soluble hepatitis B e antigen (HBeAg). The P-ORF encodes the polymerase for viral replication, and the X-ORF encodes the hepatitis Bx protein (HBx). HBx also affects cell cycle checkpoints, cell death, and carcinogenesis, but the exact mechanisms remain elusive (Murakami, 2001).

Hepatitis B Virus Integration and Hepatocarcinogenesis

Viral DNA integration has been considered to play an important role in the hepatocellular carcinogenesis because the integration of HBV in the host genome was observed in ~80–90% of HBV-related HCC cases. From our previous findings, integrated HBV sequence

Handbook of Immunohistochemistry and *in situ* Hybridization of Human Carcinomas, Volume 3: Molecular Genetics, Liver Carcinoma, and Pancreatic Carcinoma

existed in most tumors (19/23 cases, 83%) but only in 1/23 (4%) nontumor tissue samples (Wang *et al.,* 2002). In contrast, the free replicative viral form of HBV was detected more frequently in nontumor tissue (14/23 cases, 61%) than that in tumor tissue (3/23 cases, 13%). Unlike the woodchuck hepatitis virus (WHV), which caused more than 80% cases of animal liver tumors through *cis*-activating myc oncogene family (Buendia *et al.,* 1992), the HBV integration site in human genome has been demonstrated as a random event (Wang *et al.,* 2004).

Although the exact mechanism(s) of how HBV integration causes carcinogenic changes in liver is still under debate, it is believed that several direct or indirect interactions between HBV and host factors (e.g., inflammatory or genetic factors) may contribute to the long-term susceptibility of HCC development. Integration of HBV DNA into host genomic DNA may play an important role in the development of HCC through the following ways: 1) induction of chromosomal instability—HBV DNA insertion can directly induce chromosome rearrangements, deletions, translocations, and duplications, which result in host chromosomal DNA instability; 2) *trans*activation of cellular genes—HBV encodes at least two transcriptional activators, surface protein LHBs/MHBs, and HBx, and transactivation of cellular oncogenes by integration of HBV DNA seems to be an important step in the development of HCC (Stockl *et al.,* 2003); 3) escape from immune-mediated elimination— BsAg is the major target of immune response, and absence or decreased expression of HBsAg could make the host hepatocyte escape from immune-mediated elimination and thus contribute to the process of hepatocarcinogenesis (Carman *et al.,* 1996); and 4) C-terminal truncated X protein—3′-deleted X gene and consequent C-terminal truncated X protein caused by HBV integration has been frequently detected in HCC, and it may lead to cell proliferation and transformation (Wang *et al.,* 2004).

Role of Hepatitis B Surface Antigen and Hepatocellular Carcinoma

The expression level of HBsAg in HCC tumor cells was contradictory in previous studies. In our study, the expression of HBsAg is significantly lower in HCCs (11/138 cases, 8%) than that in surrounding nontumor liver tissue (103/138 cases, 75%) (Wang *et al.,* 2002). The decreased HBsAg expression in HCC might be caused by the loss of partial or whole sequence of the S gene during the HBV integration. Besides, mutation of the HBV S gene was frequently detected in HCC and most of these mutations occurred within the antigenic "a" determinant, with the presence of a glycine–arginine substitution at codon 145 (Oon *et al.,* 1999). Deletions and mutations of the S gene may induce "antibody escape" and cause the deficient recognition of monoclonal antibody to the HBsAg (Imazeki *et al.,* 1987).

It is well-known that HBsAg is the major target of both the humoral and the cellular immune response and is often related to chronic immune-mediated liver cell injury (Carman *et al.,* 1996). Absence or decreased expression of HBsAg could make the host hepatocyte escape from immune-mediated elimination and thus contribute to the process of hepatocarcinogenesis (Carman *et al.,* 1996). In addition, truncated HBs protein may use protein kinase C (PKC)-dependent and reactive oxygen-intermediate–mediated pathways for cellular signal transduction and may thereby drive the infected hepatocyte toward malignancy (Hildt *et al.,* 2002).

Detection of Hepatitis B Surface Antigen in Hepatocellular Carcinoma

Because HBVs protein plays important roles in HCC development, detection of HBsAg expression and HBV integration in HCC tissue may lead to additional insight into the hepatocarcinogenesis related to HBV. In this chapter, two frequently used methods will be introduced: detection of HBsAg expression by immunohistochemistry (IHC) using anti-HBsAg antibody and identification of HBV integration by Southern blot analysis.

MATERIALS

Immunohistochemistry

Reagents

1. 2% working solution of 3-aminopropyltriethoxy silane (APES): Dilute 1 vol of APES (Dako, Glostrup, Denmark) with 49 vol of acetone.
2. Xylene.
3. Graded ethanol (70%, 80%, 95%, and 100%) in distilled water (dH_2O).
4. Phosphate-buffered saline (PBS, pH 7.2): Dissolve 8 g NaCl, 0.2 g KCl, 1.44 g Na_2HPO_4, and 0.24 g KH_2PO_4 in 800 ml dH_2O. Adjust pH to 7.4 with HCl and then adjust the volume to 1 L with dH_2O. Store at room temperature.
5. 0.3% hydrogen peroxide in methanol (v/v): Mix 1 ml 30% hydrogen peroxide with 99 ml methanol.
6. 0.01 M citrate buffer (pH 6.0): Dissolve 2.1 g citric acid and 1.04 g NaOH in 800 ml dH_2O. Adjust the volume to 1 L with dH_2O.
7. Nonimmune rabbit serum (Dako).
8. Mouse Anti-HBsAg monoclonal antibody 3E7 (Dako).

9. EnVision Kit (contains HRP Labelled Polymer conjugated to antibodies to mouse immunoglobulins) (Dako).

10. Diaminobenzidine solution (DAB): Dissolve thoroughly 40 mg DAB in 100 ml 0.05 M Tris-HCl (pH 7.6), filter, and store the solution in dark. Add 100 µl 30% H_2O_2 and mix well before use.

11. Hematoxylin.

12. 75% ethanol with 1% HCl (EtOH-1%HCl): Add 1 vol 1 N HCl into 99 vol 75% ethanol.

13. Resinous mounting media (e.g., DPX Mounting Medium from ProSciTech, Queensland, Australia).

Special Equipment

1. Coplin jar.
2. Heat-proof slide holder.
3. Moist chamber.

Southern Blot Analysis

DNA Preparation from Tissue

1. 5 M sodium chloride: Dissolve 292.2 g NaCl in 800 ml dH_2O and adjust the final volume to 1 L with dH_2O.

2. 0.5 M Tris (pH 8.0): Dissolve 60.6 g Tris base in 800 ml dH_2O. Adjust pH to 8.0 with HCl and then adjust the volume to 1 L with ddH_2O.

3. 0.5 M ethylenediamine tetraacetic acid (EDTA) (pH 8.0): Dissolve 186.1 g disodium ethylenediaminetetraacetate•$2H_2O$ in 800 ml dH_2O. Adjust pH to 8.0 with NaOH and then adjust the volume to 1 L with dH_2O.

4. 10% sodium dodecyl sulfate (SDS): Dissolve 100 g sodium dodecyl sulfate in 800 ml dH_2O. Adjust pH to 7.2 and then adjust the volume to 1 L with dH_2O.

5. Cell lysis buffer (100 mM NaCl, 20 mM Tris-HCl, 10 mM EDTA, 0.5% SDS): Add 2 ml 5 M NaCl, 4 ml 0.5 M Tris (pH 8.0), 2 ml 0.5 M EDTA, and 5 ml 10% SDS into 80 ml dH_2O. Adjust the volume to 100 ml with dH_2O.

6. Proteinase K Stock (20 mg/ml): Dissolve 0.2 g proteinase K in 10 ml dH_2O. Aliquot and store at −20°C.

7. Buffer-saturated phenol.

8. Chloroform.

9. Isopropanol.

10. TE buffer (10 mM Tris, 1 mM EDTA), pH 8.0: Add 2 ml 0.5 M Tris and 0.2 ml 0.5 M EDTA into 97.8 ml dH_2O.

11. RNase A Stock (10 mg/ml): Dissolve 0.1 g DNase-free RNase A in 10 ml 0.01 M sodium acetate (pH 5.2). Heat to 100°C for 15 min, adjust the pH to 7.0 by adding 0.1 volume of 1 M Tris (pH 7.4), and store in aliquots at −20°C.

Probe Preparation

1. Polymerase chain reaction (PCR) primers for HBV S gene: forward primer (5′-ATCACATCAGGATTCCTAGG) and reverse primer (5′-TGGTAACAGCGGTATAAAGG).

2. PCR reaction mixture (final concentration): 10 mM Tris-HCl (pH 8.4), 2 mM $MgCl_2$, 50 mM KCl, 0.2 mM each dNTP, 0.4 µM each of forward and reverse primers, 2 U/50 µl Taq Polymerase.

3. Agarose.

4. 10 × TBE (tris-borate-EDTA): Dissolve 108 g Tris and 55 g boric acid in 800 ml dH_2O. Add 40 ml 0.5 M EDTA (pH 8.0) and adjust the volume to 1 L with dH_2O.

5. GENECLEAN Kit (Qbiogene, Irvine, CA).

Southern Blotting

1. High-concentration Eco *RI* (50 U/µl) enzyme and 10 × Reaction Buffer 3 (Amersham Biosciences, Piscataway, NJ).

2. 3 M Sodium acetate (pH 5.2): Dissolve 408.1 g sodium acetate•$3H_2O$ in 800 ml dH_2O. Adjust pH to 5.2 with glacial acetic acid and then adjust the volume to 1 L with dH_2O.

3. 1.5 M sodium hydroxide: Dissolve 60 g NaOH in 1 L dH_2O.

4. Denaturation solution (0.5 M NaOH, 1.5 M NaCl): Mix 1/3 each of 4.5 M NaCl, 1.5 M NaOH, and dH_2O.

5. 1.5 M Tris-Cl (pH 7.0): Dissolve 181.7 g Tris base in 800 ml dH_2O. Adjust pH to 7.0 with HCl and then adjust the volume to 1 L dH_2O.

6. Neutralization solution (0.5 M Tris-Cl, pH 7.0, 1.5 M NaCl): Mix 1/3 each of 1.5 M Tris-Cl (pH 7.0), 4.5 M NaCl, and dH_2O.

7. Uncharged nylon membrane.

Hybridization

1. Random Primers DNA Labeling System (Invitrogen, Carlsbad, CA).

2. G-50 Sephadex columns for radiolabeled DNA purification (Roche, Basel, Switzerland).

3. 6000 Ci/mmol [α^{32}P] dCTP (Amersham Biosciences).

4. 50 × Denhardt's solution (USB).

5. Formamide.

6. 20 × saline-sodium chloride (SSC): Dissolve 175.3 g NaCl and 88.2 g sodium citrate in 800 ml dH_2O. Adjust pH to 7.0 and then adjust the volume to 1 L dH_2O.

7. Hybridization solution: Mix well with 30 ml 20 × SSC, 10 ml 50 × Denhardt's solution, 5 ml 10% SDS, 50 ml 100% formamide, and 5 ml dH_2O.

8. 10 mg/ml Sheared DNA (Resgen, Carlsbad, CA).
9. Washing solution I (2 × SSC, 0.1% SDS): Add 100 ml 20 × SSC, 10 ml 10% SDS to 890 ml dH_2O.
10. Washing solution II (0.2 × SSC, 0.1% SDS): Add 10 ml 20 × SSC and 10 ml 10% SDS to 980 ml dH_2O.

METHODS

Immunohistochemistry

The following protocols are routinely used in the author's laboratory, but optimization must be performed in each laboratory to achieve the best results. All steps are performed at room temperature unless otherwise stated. For safety, perform steps involving organic solvents (e.g., deparaffinization) in a chemical fume hood.

Section Preparation and Deparaffinzation

The HCC specimen and its surrounding nontumor liver tissue are collected at the time of surgical resection, fixed in buffered formalin, dehydrated, and embedded in paraffin according to routine procedures.

1. For greater tissue attachment, put the slides into 2% APES working solution for 30 sec. Drain the slides and then rinse the slides with dH_2O to remove the excess APES. Dry the slides in a fume hood with circulation.
2. Cut 5-μm section of the paraffin block with a microtome. Float the tissue section onto sterile dH_2O in a water bath and mount the tissue section onto an APES-treated slide.
3. Air-dry briefly and bake the slide for 10 min at 63°–75°C depending on the melting point of the paraffin. Unused slides can be stored at room temperature or at 4°C in the dark.
4. The section is then deparaffinized by placing the slide 3× in xylene for 5 min each.
5. Rehydrate tissue by passing the slide through 100%, 95%, and 80% ethanol, 3× each for 5 min each time.
6. Wash the slide in dH_2O for 5 min.
7. Wash the slides 3× in PBS for 5 min.

Immunohistochemistry

1. Immerse the slide in 0.3% H_2O_2-methanol to block endogenous peroxidase activity. Incubate the slide at room temperature for 10 min, and then rinse the slide 3× in PBS for 3 min.
2. Boil appropriate amount of 0.01 M citrate buffer in a microwavable container. Place the slide in a heat-proof slide holder and immerse it completely in the boiling buffer for 15 min. After the slide cools down, rinse it 3× in PBS for 5 min each.
3. Add 100 μl nonimmune animal serum onto the slide and incubate the section at room temperature for 20 min.
4. Discard the serum gently and add 100 μl mouse anti-HBsAg monoclonal antibodies 3E7 (dilution in 1:100 with antibody diluted liquid). The slide is incubated at 4°C overnight in a moist chamber.
5. Wash the slide 3× in PBS for 5 min each. Add 100 μl Labelled Polymer, HRP (EnVision Kit) and incubate the slide at 37°C for 45 min.
6. Wash the slide 3× in PBS for 5 min each. Immerse the slide in freshly prepared DAB solution for 5–10 min. Observe the color intensity by visual inspection or view under microscope. Stop the reaction by rinsing the slide with dH_2O.
7. Counterstain the slide with hematoxylin for 3–5 min. Immerse the slide in 1% HCl-ethanol for 5 sec and then immerse the slide in dH_2O for at least 30 min.
8. Dehydrate the section with graded alcohol by passing the slide through 70%, 80%, and 95% ethanol for 5 min each and absolute ethanol for 10 min.
9. Immerse the slide 2× in xylene for 5 min each. Mount the slide with neutral resin. Capture the image by microscope.

Southern Blot Analysis

DNA Preparation from Tissue

1. Homogenize tissue sample in PBS by a homogenizer.
2. Centrifuge at 3000 g for 5 min to collect the homogenized tissue pellet. Aspirate the supernatant. Add ~10 volumes (w/v) of cell lysis buffer into the cell pellet. Mix gently until a homogenized cell suspension appears.
3. Add proteinase K to a final concentration of 100 μg PK/ml, mix well, and incubate at 55°C overnight.
4. Add equal volume of buffer-saturated phenol, mix by inverting the tubes slowly for 5–10 min, and centrifuge at 3000 g for 10 min. Transfer the upper aqueous layer into a new 15-ml tube.
5. Add equal volumes of chloroform using glass pipette. Mix briefly by inverting tubes for a few times, and centrifuge at 3000 g for 10 min. Transfer the upper aqueous to a new 15-ml tube.
6. Add equal volumes of isopropanol, mix well, and leave at room temperature briefly. Transfer the DNA (white mass) into a 1.5-ml tube by using a glass Pasteur

pipette, and dry the DNA pellet by air-drying or with a vacuum dryer (avoid overdrying of genomic DNA).

7. Dissolve the DNA in 100 µl tris-EDTA (TE) buffer. Digest ribonucleic acid (RNA) overnight at 37°C by RNase A treatment (final concentration of 500 µg/ml RNase A).

Probe Preparation

1. A regular PCR reaction is performed in 50 µl PCR reaction mixture with 50 ng genomic DNA from HBV-positive liver tissue as a template. Perform 30-cycle reaction at 94°C for 1 min, 60°C for 1 min, and 72°C for 1 min, with a final elongation time of 5 min at 72°C.

2. Visualize 5 µl of the amplified PCR product in a 1% (w/v) agarose gel under 0.5× TBE buffer stained with ethidium bromide. The expected size of the PCR product is 642 bp.

3. Purify the PCR product with GENECLEAN Kit following the manufacturer's protocol.

Southern Blotting

1. Digest 10 µg genomic DNA overnight at 37°C with restriction enzyme Eco*RI* (5-10 U Eco*RI* per microgram DNA) in 100 µl dH_2O.

2. Visualize cleavage efficiency by running 1–2 µl on 1% agarose gel.

4. Concentrate Eco*RI*-cut DNA by precipitation. Add 1/10 volume 3 M sodium acetate and 2.5 volume cooled absolute ethanol. Precipitate the product for 2 hours at −20°C. Recover DNA by centrifugation at maximum speed for 20 min at 4°C. Discard the supernatant. The pellet is washed with 300 µl 75% ethanol and air-dried. Dissolve the DNA in 10 µl dH_2O.

5. Separate the digested DNA fragments by electrophoresis in 1% agarose gel at 30 V overnight. Stain the gel with ethidium bromide and place a ruler alongside as a size reference.

6. Denature the DNA fragments by soaking gel in an excess of denaturation solution for 45 min, and shake gently at room temperature.

7. Neutralize the denatured DNA by soaking the gel in an excess of neutralization solution for 30 min, and shake gently at room temperature.

8. Prewet the uncharged nylon membrane with dH_2O, and assemble the transfer apparatus as described (Sambrook *et al.,* 1989). Pour 6× SSC into the blotting reservoir, cover the apparatus with cling film, and allow the DNA transfer to proceed overnight.

9. Mark the orientation of the blot, and immobilize the transferred DNA by ultraviolet (UV)-crosslinking. Proceed to prehybridization or save the membrane in a dessicated environment until use.

Hybridization

1. Before hybridization, prewet the membrane in distilled water. Prewarm the hybridization solution in 42°C. Place the membrane into prewarmed 8 ml hybridization solution.

2. Denature sheared DNA by boiling for 5 min and then put it on ice for 5 min. Add 80 µl denatured sheared DNA (100 µg sheared DNA/ml hybridization solution).

3. Prehybridize the membrane at 42°C for 6 hr.

4. Label the S gene probe by random priming using [α^{32}P] dCTP (Random Primers DNA Labeling System, GibcoBRL, Gaithersburg, MD) following the manufacturer's protocol.

5. Remove unlabeled [α^{32}P] dCTP by using Sephadex G-50 column according to the manufacturer's protocol. Denature the labeled HBsAg probe by boiling for 5 min and then put the denatured probe on ice for 5 min. Transfer the labeled probe into the hybridization solution and hybridize the probe to target DNA overnight at 42°C.

6. Pull out the hybridization solution after hybridization. Wash the membrane in 100 ml washing solution I at 42°C for 10 min. Discard the washing solution.

7. Wash the membrane in 100 ml washing solution I at 55°C for 20 min. Discard the washing solution.

8. Wash the membrane 2× in 100 ml washing solution II at 55°C for 20 min each. Discard the washing solution.

9. Place the membrane on a 3 mm paper, and cover the membrane with cling film. Expose the membrane to X-ray film overnight at −80°C. Determine the size of the fragment with reference to the gel photo.

RESULTS AND DISCUSSION

Detection of Hepatitis B Surface Antigen Expression by Immunohistochemistry

Cellular or tissue antigens can be identified with IHC by means of antibody–antigen interaction, and IHC involves a series of methodologies. Factors affecting the performance of an IHC experiment include the type and duration of fixation, antigen-retrieval method, quality and quantity of antibodies, and the detection system being used. Fresh tissue samples can be sectioned by cryostat immediately or stored as formalin-fixed and paraffin-embedded (FFPE) blocks. Ideally, tissues should be fixed with a faithful retention of cell morphology and minimal masking of epitopes. For maximal

sensitivity and minimal background, unmasking of antigens should be done in optimized chemical composition, temperature, pH value, and duration. New antibodies need to be titrated. Suitable positive and negative controls should be included for each IHC experiment to avoid false-positive and false-negative results.

For the detection of HBsAg expression by IHC, appropriate positive and negative controls should be included. We suggest using HBV-positive and HBV-negative HCC cases as controls. A positive result is recorded if the cytoplasm displays brown particles (Figure 38). Our previous study showed that the expression frequency of HBsAg was significantly lower in HCC as compared with its surrounding nontumor liver tissues, which would act as a useful marker for early HCC detection (Wang *et al.,* 2002).

Detection of Hepatitis B Virus Integration by Southern Blot Analysis

As reported previously, expression of HBsAg is more frequently detected in nontumor liver tissue surrounding HCC cells. The low frequency of HBsAg expression in HCC tissue could be associated with HBV integration (Wang *et al.,* 2002). Southern Blot analysis can be used to detect the integration of HBV. Single or multiple integration sites as well as the free replicative virus form (FRV) of HBV can be detected simultaneously. The size of the FRV form of HBV is ~3 kb, whereas the size of integrated HBV varies dramatically and usually is larger than 3 kb.

In Chinese patients who are HBV-positive and have HCC, integrated and FRV forms of HBV frequently are observed in HCC tissue and its surrounding nontumor liver tissue, respectively. In our previous study, HBV integration was more frequently detected in HCC samples (3/40, 7.5%) (Wang *et al.,* 2004). In contrast to the integration, the FRV form was detected more frequently in nontumor tissues than in HCCs. The high frequency of detected HBV integrants in HCC suggests the important role of HBV integration in HCC development and its association with HBsAg expression. Further study of the integrated HBV may help to explain the association between HBV integration and carcinogenesis in HCC.

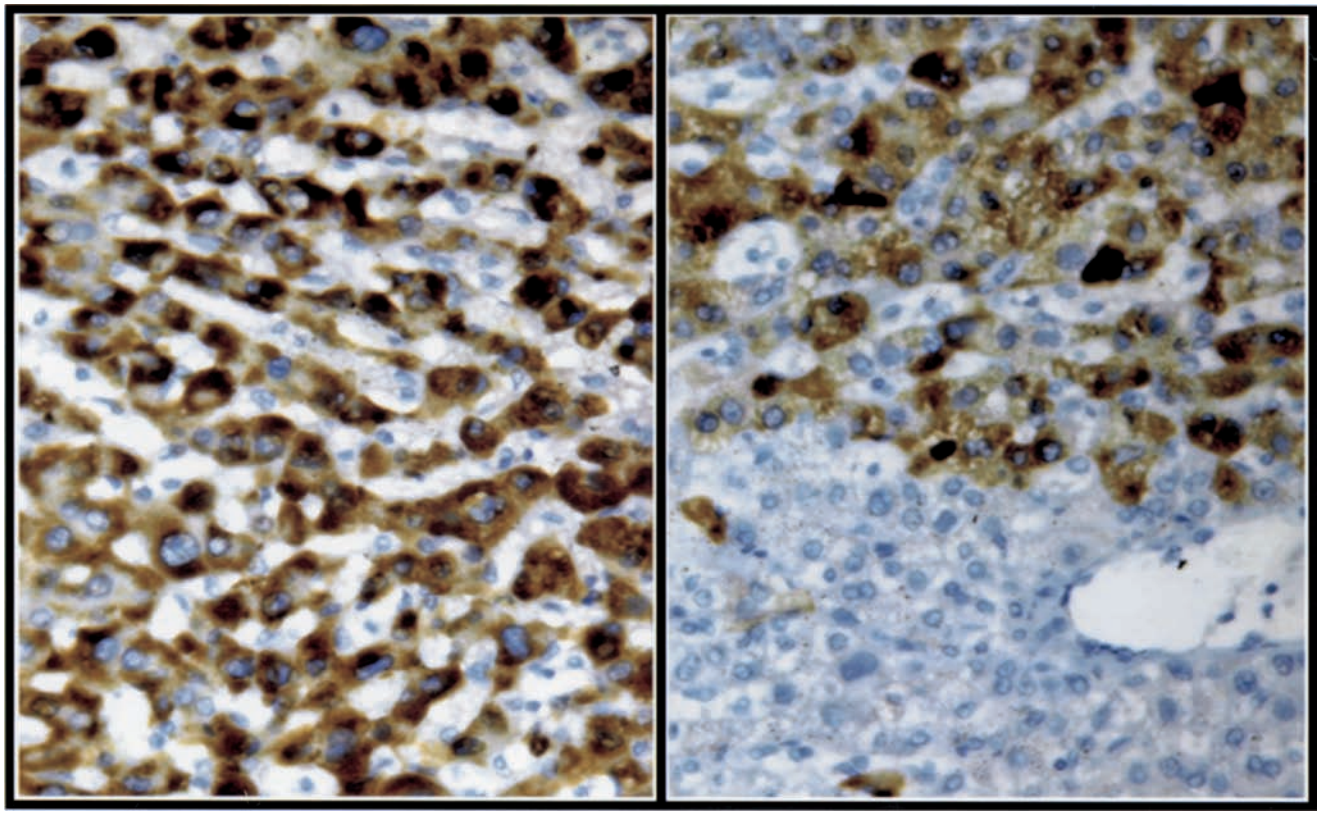

Figure 38. Examples of hepatitis B surface antigen (HBsAg) positive staining detected by anti-HBsAg antibody. **A:** Positive cytoplasmic staining (*brown color*) is observed in liver tissue from a patient with hepatitis B infection. **B:** Expression of HBV S protein is detected in adjacent nontumor liver tissue but not in tumor tissue of an hepatocellular carcinoma.

References

Block, T.M., Mehta, A.S., Finamel, C.J., Jordan, R. 2003. Molecular viral oncology of hepatocellular carcinoma. *Oncogene 22(33)*:5093–5107.

Buendia, M.A. 1992. Hepatitis B viruses and hepatocellular carcinoma. *Adv. Cancer Res. 59*:167–226.

Carman, W.F., Tratwein, C., van Deursen, F.J., Colman, K., Dornan, E., McIntyre, G., Waters, J., Kliem, V., Muller, R., Thomas, H.C., and Manns, M.P. 1996. Hepatitis B virus envelope variation after transplantation with and without hepatitis B immune globulin prophylaxis. *Hepatology 24*:489–493.

Hildt, E., Munz, B., Saher, G., and Hofschneider, P.H. 2002. The PreS2 activator MHBs(t) of hepatitis B virus activates c-raf-1/Erk2 signaling in transgenic mice. *EMBO J. 21(4)*: 525–535.

Imazeki, F., Yaginuma, K, Omata, M., Okuda, K., Kobayashi, M., and Koike, K. 1987. RNA transcripts of hepatitis B virus in hepatocellular carcinoma. *Hepatology 7(4)*:753–757.

Montalto, G., Cervello, M., Giannitrapani, L., Dantona, F., Terranova, A., and Castagnetta, L.A. 2002. Epidemiology, risk factors, and natural history of hepatocellular carcinoma. *Ann. NY Acad. Sci. 963*:13–20.

Murakami, S. 2001. Hepatitis B virus X protein: A multifunctional viral regulator. *J. Gastroenterol. 36(10)*:651–660.

Oon, C.J., Chen, W.N., Zhao, Y., Teng, S.W., and Leong, A.L. 1999. Detection of hepatitis B surface antigen mutants and their integration in human hepatocellular carcinoma. *Cancer Lett. 136(1)*:95–99.

Parkin, D.M., Bray, F.I., and Devesa, S.S. 2001. Cancer burden in the year 2000. The global picture. *Eur. J. Cancer. 37(8)*: S4–S66.

Sambrook, J., Fritsch, E.F., Maniortis, T. 1989. *Molecular Cloning: A Laboratory Manual,* 2nd ed. Cold Spring Harbor, NY: Cold Spring Harbor Laboratory Press, 9.31–9.57.

Stockl, L., Berting, A., Malkowski, B., Foerste, R., Hofschneider, P.H., and Hildt, E. 2003. Integrity of c-Raf-1/MEK signal transduction cascade is essential for hepatitis B virus gene expression. *Oncogene 22*:2604–2610.

Thorgeirsson, S.S., and Grisham, J.W. 2002. Molecular pathogenesis of human hepatocellular carcinoma. *Nat. Genet. 31(4):*339–346.

Tiollais, P., Pourcel, C., and Dejean, A. 1985. The hepatitis B virus. *Nature 317*:489–495.

Wang, Y., Wu, M.-C., Sham, J.S.T., Tai, L-S., Fang, Y., Wu, W.-Q., Xie, D., and Guan, X-Y. 2002. Different expression of hepatitis B surface antigen between hepatocellular carcinoma and its surrounding liver tissue detected by tissue microarray. *J. Pathol. 197*:610–616.

Wang, Y., Lau, S.H., Sham, J.S.T., Wu, M.-C., Wang, T., Guan, X.-Y. 2004. Characterization of HBV integrants in 14 hepatocellular carcinomas: Association of truncated X gene and hepatocellular carcinogenesis. *Oncogene 23*:142–148.

12

Immunohistochemical Detection of Host Gene Products Up-Regulated by Hepatitis B Virus X Antigen and Their Putative Roles in Hepatocellular Carcinoma

Mark A. Feitelson, Jie Liu, Zhaorui Lian, Jingbo Pan, N. Lale Tufan, and Marcia M. Clayton

Introduction

The pathogenesis of hepatitis B virus (HBV) infection is variable (Eddleston, 1990; Feitelson, 1989), with most patients experiencing subclinical infections characterized only by seroconversion to virus antibodies. Others develop acute, resolving infections, characterized by a peak of viremia and liver damage that are transient, followed by clearance of virus and seroconversion to viral antibodies. Approximately 90% of infants and 5–10% of adults infected with HBV become chronic carriers, and although the majority of adult carriers are asymptomatic, 10–30% of carriers develop chronic liver diseases (CLDs), which include hepatitis. The latter may progress to cirrhosis (end-stage liver disease) and hepatocellular carcinoma (HCC). Among the most common tumor types worldwide, HCC has an estimated 250,000 new cases yearly (Feitelson, 1986). Early detection and surgical resection are often curative, although these patients are at risk for recurrence at a later time. A major problem with HCC is that most people with small tumors are asymptomatic, and by the time symptoms appear and they are diagnosed, the tumors are often multinodular and inoperable, with less than a 6-month life expectancy.

Hepatocarcinogenesis, like the development of other tumors, is multistep (Feitelson *et al.,* 2002). Accordingly, many studies have compared genetic and epigenetic changes in tumor with nontumor tissue, hoping to identify tumor-specific markers. These studies have examined deoxyribonucleic acid (DNA) methylation, polyploidy, loss of heterozygosity, and point mutations in important genes that regulate cell growth and survival (Feitelson *et al.,* 2002; Sheu, 1997). More recently, many labs have conducted microarray and related procedures, which have provided a wealth of

Handbook of Immunohistochemistry and *in situ* Hybridization of Human Carcinomas, Volume 3: Molecular Genetics, Liver Carcinoma, and Pancreatic Carcinoma

molecular-based data in gene expression profiles that distinguish tumor from nontumor tissue (Cheung *et al.,* 2002; Okabe *et al.,* 2001; Paradis *et al.,* 2003). In many cases, however, it is difficult to determine whether the changes that distinguish tumor from nontumor represent cause or effect. In addition, it is likely that many of the changes in gene expression that distinguish tumor from nontumor are likely to represent genes that are involved in tumor progression and not in the early stages of tumor formation. In addition, microarray analysis does not readily distinguish between changes that occur in hepatocytes that are related to carcinogenesis from those changes that occur in other cell types or are associated with variable inflammatory responses in the liver. It is likely that some of these studies will identify molecular changes that represent important steps in identifying whether a nodule is tumor or nontumor, but getting to early changes in the liver that significantly contribute to the risk of tumor formation still represents a major challenge in the field.

The facts that the carrier state and CLD are among the most important risk factors for the development of HCC, and that the relative risk of carriers with CLD developing HCC is more than 100-fold that of noncarriers (Beasley and Hwang, 1984), suggests a very close relationship between HBV and this tumor type. It is interesting that HBV-like viruses in nature, such as the woodchuck hepatitis virus (WHV), are also associated with nearly 100% of tumor incidence among woodchucks that are carriers of the virus and that have CLD (Tennant and Gerin, 2001). Careful experimental manipulation of WHV-infected woodchucks to exclude other known hepatocarcinogens strongly suggests that WHV is a complete carcinogen (Popper *et al.,* 1987) and implies that WHV (and HBV, by extension) make a genetic contribution to HCC. It turns out that this genetic contribution is the HBV and WHV encoded X antigen (HB XAg for HBV and WH XAg for WHV) (Feitelson and Duan, 1997). Many studies have now shown that HB XAg is a *trans*activating protein that may alter patterns of host gene expression that are important to the appearance of the transformed phenotype (Feitelson and Duan, 1997; Henkler and Koshy, 1996). HB XAg is not a DNA-binding protein; instead it functions by binding to transcription factors in the nucleus and, perhaps more commonly, by activating a variety of signal transduction pathways in the cytoplasm. There is also some evidence that HB XAg may act post-translationally by inhibiting the normal turnover of proteins by blocking ubiquitin-mediated degradation of proteins in the proteasome (Zhang *et al.,* 2000). Although the expression of several host proteins appears to be up-regulated by HB XAg, most notably insulin-like growth factor II and the insulin-like growth factor receptor I (Feitelson and Duan, 1997), it is not clear which pathways and which effectors mediate early changes in hepatocellular phenotype that are responsible for HB XAg-triggered malignant transformation.

During the early stages of chronic infection, there is evidence that HB XAg helps to support virus gene expression and replication (Bouchard *et al.,* 2001). With each bout of CLD, however, fragments of HBV DNA randomly integrate into the host chromosomes (Matsubara and Tokino, 1990). Over time, the number of integration events increases. Characterization of the integrated viral sequences has shown that many produce functional HB XAg (Schluter *et al.,* 1994), so that over time, the levels of intracellular HB XAg increase. Virus replication often slowly declines over many years, with intrahepatic HB XAg increasingly acting on cellular instead of viral genes. The correlation between HB XAg staining and the intensity of CLD suggests that HB XAg is widely expressed in the liver where preneoplastic and neoplastic foci eventually develop (Jin *et al.,* 2001; Wang *et al.,* 1991a,b). Hence, the question becomes: Do the actions of HB XAg on patterns of host gene expression under these circumstances represent early events in multistep carcinogenesis?

MATERIALS AND METHODS

Cell Lines and Culture

HepG2 cells, a differentiated cell line derived from a human hepatoblastoma (Aden *et al.,* 1979; Knowles *et al.,* 1980), were cultured on type-1 rat tail collagen (Becton Dickinson, Franklin Lakes, NJ) coated tissue culture dishes or plates. Cells were grown in Earle's MEM supplemented with 10% heat-inactivated fetal calf serum (FCS), 100 μM MEM nonessential amino acids, 1 mM sodium pyruvate, and standard concentrations of penicillin plus streptomycin. The retrovirus packaging cell line PA317 (Danos, 1991) was also grown on plastic dishes in the same medium.

Plasmids

The retroviral vector plasmid, pSLXCMVneo, was used to clone the HBV X gene (Valenzuela *et al.,* 1980) or the bacterial chloramphenicol acetyltransferase (CAT) gene sequences for these studies, as described (Duan *et al.,* 1995; Vile, 1991). Briefly, pSLXCMV-CAT was constructed by inserting a 726 bp *Hind*III-*Bam*HI fragment containing the CAT gene into the *Hpa*I-*Bg*III site of the pSLXCMV polylinker. pSLXCMV-FlagX was constructed by inserting a 920-bp *Mlu*I-*Bg*III fragment of Flag-HBx DNA into the

*Mlu*I-*Bg*III site of the pSLX-CMV polylinker. In both cases, the recombinant proteins were expressed under control of the cytomegalovirus (CMV) immediate-early promoter. The rationale for using the FLAG epitope in the HB X-containing construct is that it provided an alternative way to detect HB XAg polypeptides in HepG2 cells using anti-FLAG. Additional details of the procedures used for the preparation and use of recombinant retroviruses have been published (Cepko, 1992; Danos, 1991; Vile, 1991). Recombinants were used to transform HB101. Miniprepreps were prepared, and the DNA was used for sequence analysis at the DNA sequencing facility of Thomas Jefferson University.

Preparation of Recombinant Retroviruses and Infection of HepG2 Cells

Approximately 1×10^6 PA317 cells/100-mm dish were transfected using standard calcium phosphate precipitation using 15 µg of pSLXCMV-FLAGX or 15 µg of pSLXCMV-CAT. At 24, 48, and 72 hr after transfection, the medium was removed and processed through a 0.45-µm filter to remove PA317 cells. Filtered supernatants were used immediately for infection of HepG2 cells, as described in Duan *et al.* (1995). The virus was also quantitated by infection of NIH3T3 cells with different dilutions of PA317 cell culture supernatant, followed by G418 selection for 7 days and then by visual inspection of the number of colonies. Recombinant retrovirus-enriched supernatant (5 ml) was used to infect 1×10^6 target HepG2 cells/100 mm dish in the presence of polybrene (8 µg/ml) for 24 hr. Fresh virus supernatant was added after 24 hr and again after 48 hr so that the cells were exposed to virus for a total of 72 hr. All of these infections were carried out in log-phase cultures. HepG2 cultures that received at least 5×10^5 CFU/ml of virus were then passaged at 1:2 and selected by incubation in G418 (800 µg/ml; GIBCO/BRL, Grand Island, NY) for 14 days to maximize the fraction of cells producing HB XAg or CAT. G418 colonies were then expanded in normal growth medium and used for analysis.

Detection of CAT Activity and HB XAg Polypeptide in HepG2 Cells

The CAT assays were performed essentially as described (Wang *et al.,* 1994). Briefly, 5×10^6 HepG2CAT cells in a 100-mm dish were lysed by addition of 0.9 ml of 1X reporter lysis buffer (Promega, Madison, WI) for 15 min and harvested by scraping. Cells were pelleted, and 180 µl of cell lysate was used for a standard CAT assay. After incubation with ^{14}C-chloramphenicol, acetylated forms were separated by thin-layer chromatography. To detect HB XAg (a 17-kDa polypeptide), lysates prepared from 5×10^6 HepG2X cells were assayed by Western Blot using a mixture of rabbit anti-x peptide antibodies, as described in Feitelson and Clayton (1990). Horseradish peroxidase (HRP)–conjugated goat anti-rabbit immunoglobulin (Ig) (Accurate, Westbury, NY) and ECL substrate (Amersham, Piscataway, NJ) were used for detection.

Polymerase Chain Reaction, Select Complementary DNA Subtraction, Cloning, Sequencing, and Identification of a Complementary DNA from Putative HB XAg Effectors

The differences in gene expression that distinguish HepG2X from HepG2CAT cells were determined by using a commercially available subtraction hybridization kit (the polymerase chain reaction [PCR]-select complementary DNA [cDNA] subtraction kit from Clontech, Palo Alto, CA) according to the instructions provided by the manufacturer. Whole-cell ribonucleic acid (RNA) was extracted separately from HepG2X and HepG2CAT cells using the Qiagen RNeasy RNA kit (QIAGEN, Inc., Valencia, CA), and the quality of the extraction was determined by assaying for 18S and 28S rRNAs by agarose gel electrophoresis and ethidium bromide staining. The PCR-select cDNA subtraction was carried out by reverse transcriptase (RT)-PCR starting with 2 µg of polyA$^+$ RNA isolated from the HepG2X and HepG2CAT cell lines. Adaptors were then ligated to a fraction of *Rsa*-1 digested cDNA generated by RT-PCR. The cDNA was subjected to two rounds of subtractive hybridization against the PCR products from the cells in which the comparison was being made. The resulting products, now enriched for differentially expressed genes, were PCR amplified using primers that matched the sequence of the adaptors (in the Clontech Advantage cDNA PCR kit). Following agarose gel electrophoresis, the unique fragments were then eluted from the gels (using the QIAGEN gel extraction kit) and cloned into pT7Blue(R) T vector (Novagen, Madison, WI). Positive clones were selected by blue–white phenotype. Recombinant DNA was isolated from minipreps of individual clones, digested by *Rsa* I to check insert size, and then both strands were individually analyzed by sequence analysis in the DNA-sequencing facility at the Kimmel Cancer Institute of Thomas Jefferson University. The sequences obtained were then compared to those in GenBank using the FASTA command in the GCG software package for homology to known genes (Benson *et al.,* 1997).

Patient Samples

The 23 paired tumor (HCC)/nontumor (surrounding liver) samples came from as many Chinese patients who had undergone surgery for the removal of their tumors. Most patients lived in and around Xi'an and were treated at the Fourth Military Medical University. All patients were hepatitis B serum antigen (HBsAg) positive in serum. Formalin-fixed and paraffin-embedded tissues, fresh frozen blocks, and −80°C snap-frozen paired liver and tumor samples from individual patients were collected from most patients, used for diagnostic purposes, and were then made available for these studies. Analogous pieces of uninfected human liver from two individuals were available to serve as controls.

Cloning of Full-Length cDNA from Up- and Down-Regulated Genes and Identification of the Encoded Products

The full-length cDNA clone contained the up-regulated genes (URG) 4 (URG4), URG7, and URG11. URG12 and the down-regulated gene (DRG) 2 (DRG2) sequences were obtained by 5′ and 3′ rapid amplification of cDNA ends (RACE) PCR using the Marathon cDNA Amplification Kit (Clontech, Palo Alto, CA). Briefly, one 3′ and one 5′ gene specific primers were synthesized. Human placental cDNA was a template for PCR, using these primers together with an adaptor primer to get the 3′ or 5′ cDNA-specific products in separate amplification reactions. The products were cloned into pT7Blue(R) T vector (Novagen, Inc., Madison, WI) and sequenced. The appropriate 3′ and 5′ gene specific fragments were then digested with suitable restriction enzymes and cloned into pcDNA3 (Invitrogen, Carlsbad, CA) at the chosen site(s), and the integrity of the full-length clone was verified by DNA sequencing.

Preparation and Use of Antisera

The full-length cDNAs from URG4, URG7, URG11, URG12, and DRG2 were used to deduce the corresponding amino acid sequence using the TRANSLATE program. The amino acid sequences of each protein were then subjected to analysis in the PEPTIDESTRUCTURE and PLOTSTRUCTURE programs to identify hydrophilic peptides likely to be on the surface of each protein that would be suitable candidates for solid-phase peptide synthesis. Accordingly, appropriate peptides were made in the Peptide Synthesis Facility at the Kimmel Cancer Center of Thomas Jefferson University. These are listed in Table 13. Peptides were individually coupled by virtue of their free cysteine sulfhydryl (either in the peptide sequence or added to the carboxy-terminus) to keyhole limpet hemocyanin (KLH; Sigma Chemical Co., St. Louis, MO) using the coupling agent m-maleimidobenzyol-N-hydroxysuccinimide ester (MBS; Pierce Chemical Co., Rockford, IL), and antibodies were raised in New Zealand rabbits (2 rabbits/peptide), as described (Feitelson *et al.,* 1988). Antisera were initially characterized in specific enzyme-linked immunosorbent assays (ELISAs) prior to use in Western Blot analysis and immunohistochemical staining as outlined later in the chapter.

Table 13. Peptides Used for Raising Antibodies

Protein	Peptide	Sequence (N → C terminus)	Amino Acids	Dilution used for Western	Dilution used for IHC	Reference
URG4	a	CEECQKAKDRMERITRKIKDSDAY	457–480	1:1000	1:4000	Tufan *et al.,* 2002
	b	SVPGPRPRDKRQLLDPPGC	817–834	1:1000	1:4000	
URG7	a	GVWNQTEPEPAATSC	12–25	1:500	1:5000	Lian *et al.,* 2001
	b	HHHGRGYLRMSPLFK	56–70	1:500	1:5000	
URG11	a	PCPELACPREEWRLGP	254–269	1:600	1:9000	Lian *et al.,* 2003
	b	DPSRSPHSTSSFPRGSSATSCDSR	568–591	1:600	1:9000	
	c	HPPDGSFSTFHDGPQPLEDPC	611–630	1:600	1:9000	
URG12 (S15a)	a	KSINNAEKRGKRQC	12–23	1:500	1:2000	Lian *et al.,* 2004
	b	DHEEARRKHTGGKC	112–124	1:500	1:2000	
DRG2 (Sui1)	a	DDYDKKKLVKAFKKKFAC	52–69	1:2000	1:2000	Lian *et al.,* 1999
	b	EHPEYGEVIQLQGDQRKNIC	75–94	1:2000	1:2000	
HB XAg		LPAMSTTDLEAYFKDC	100–115	1:500	1:500	Feitelson and Clayton, 1990

IHC, immunohistochemistry.

Western Blot

Confluent cultures of cells were lysed, as outlined later. Protein concentration was determined using the BioRad Protein Assay reagent (Bio-Rad, Hercules, CA), and 100 μg of protein lysate were loaded onto each lane and then analyzed by sodium dodecyl sulfate/polyacrylamide gel electrophoresis (SDS/PAGE). Proteins were electroblotted onto polyvinylidene fluoride (PVDF) membranes, which were then blocked with 5% nonfat milk overnight at room temperature. For Western Blot analysis, a mixture of primary antibodies against a single protein (see Table 13) was used. Preimmune serum was used as a negative control. Western Blots for β-actin were performed as an internal (sample loading) control using commercially available antibody (Ab-1; Oncogene Research Products, Cambridge, MA), as described by Tufan *et al.* (2002). Horseradish peroxidase conjugated goat anti-rabbit Ig (Accurate, Westbury, NY) and ECL substrate (Amersham, Piscataway, NJ) were used for detection.

Detailed Protocols

Preparation of Cell Lysates

1. Remove medium and wash cells thoroughly with phosphate buffer saline (PBS).
2. Put 1 ml of ice-cold cell-lysis buffer in a 100-mm dish. (Cell lysis buffer: 50 mM Tris-HCl, 150 mM NaCl, pH 8.0, 1% NP-40, 0.1 mM phenylmethylsulfonyl fluoride [PMSF], 0.2 mM ethylenediamine tetraacetic acid [EDTA]).
3. Scrape plate with a rubber policeman. Pass the lysate through the 21-gauge needle to shear the DNA.
4. Microcentrifuge cell lysate at 12,500 rpm for 10 min at 4°C. Keep all lysates on ice for immediate use or store at –20°C.

Electrophoresis

1. Mix 40–60 μg of whole-cell lysate with an equal volume of 2X SDS gel-loading buffer (100 mM Tris-HCl, pH 6.8, 200 mM dithiothreitol, 4% SDS, 0.2% bromophenol blue, 20% glycerol).
2. Place the sample in a boiling water bath for 5 min.
3. Load samples onto a 12% SDS-polyacrylamide gel. Note that the molecular weights for URG4, URG7, URG11, and URG12 (S15a) are 104 kDa, 11 kDa, 68 kDa, and 14 kDa, respectively (Lian *et al.,* 2001; Lian *et al.,* 2003; Lian *et al.,* 2004; Tufan *et al.,* 2002).

The separating gel (10 ml of a 12% gel) is made by adding the following in sequential order: distilled water (3.15 ml), 1 M Tris-HCl (pH 8.8) (3.75 ml), acrylamide/bis (40% stock, 37.5:1) (3 ml), and 10% ammonium persulfate (freshly prepared for each gel) (50 μl). Mix gently, but thoroughly, degas under vacuum, and then add 10% SDS (w/v; 100 μl) and finally TEMED (7 μl). Mix gently and pour within gel mold to desired height. Gently overlay with distilled water and allow to polymerize (15–20 mm). When the stacking gel is to be poured (see later), remove the water from the top of the running gel.

The stacking gel (10 ml of a 4% gel) is made by adding the following in sequential order: distilled water (7.675 ml), 1 M Tris-HCl (pH 6.8) (1.25 ml), acrylamide/bis (40% stock, 37.5:1) (0.975 ml), and 10% ammonium persulfate (freshly prepared for each gel) (50 μl). Mix gently but thoroughly, degas under vacuum, and then add 10% SDS (w/v; 100 μl) and finally TEMED (10 μl). Mix and pour on top of the separating gel until the level reaches the top of the teeth in the comb. Polymerization should take 15–20 min. Remove the comb, rinse the wells with running buffer (25 mM Tris base, 200 mM glycine, 0.1% SDS), fill the top and bottom half-cells with running buffer, and then underlay the samples in each well below the running buffer.

Note: Make sure that no air bubbles lodge between the gel and the running buffer.

4. Run the gel using constant voltage (100 V) for 1.5–2.0 hr until the bromophenol blue reaches the bottom of the resolving gel.
5. Transfer proteins from the gel to PVDF membranes by constant current 100 mA (20–30 V) in the transfer buffer (40 mM glycine, 50 mM Tris base, 0.04% SDS, 20% methanol, pH 8.3) for 1–2 hr using an electroblotting apparatus (Bio-Rad).

Immunoblotting

1. Block nonspecific binding by incubating membrane in 5% nonfat dry milk for 1 hr at room temperature.
2. Incubate primary antibody (at the dilutions listed in Table 13) in buffer (0.05 M Tris-HCl, 0.15 M NaCl, 5% nonfat dry milk, pH 7.6) at 4°C overnight.
3. Rinse and wash the membrane in fresh changes of wash buffer (0.05 M Tris-HCl, 0.15 M NaCl, 0.1% Tween 20, pH 7.6). Quick rinses: 1× for 15 min, and 2× for 5 min each.
4. Incubate membrane in HRP-labeled second antibody diluted 1:1600 (HRP-labeled anti-rabbit Ig)

in buffer (0.05 M Tris-HCl, 0.15 M NaCl, pH 7.6) for 1 hr at room temperature.

5. Repeat washing as in **Step 3**.

6. Incubate membrane in an equal volume of detection reagent 1 and detection reagent 2 provided by the manufacturer (Amersham/Pharmcia Biotech; ECL Western Blot-detection reagents). Drain off detection reagent and wrap blots in cling film. Expose and develop with X-ray film (1 sec to 3 min) to reveal the band of interest.

Tissue Staining

Immunohistochemical staining was performed on slides prepared from formalin-fixed and paraffin-embedded tissues (Wang *et al.,* 1991a,b) using the Vectastain Elits avidin–biotin complex kit according to manufacturer's instructions (Vector Laboratories, Burlingame, CA) with minor modifications (Tufan *et al.,* 2002). A mixture of rabbit antibodies raised against one of the proteins in Table 13 were used as primary antibodies. Biotinylated anti-rabbit Ig was used as secondary antibody, and diaminobenzidine (DAB) was used as substrate for detection. Preimmune serum or preincubation of primary antibodies with an excess of the corresponding synthetic peptide(s) (25 μg of each peptide for 1 hr at 37°C) served as controls. For HB XAg staining, uninfected liver was used as an additional control (Wang *et al.,* 1991a,b). Immunohistochemistry (IHC) was evaluated independently by two pathologists counting stained and total hepatocytes in 5 random fields per slide by light microscopy at a magnification of 200.

Embedding

Each tissue sample is placed inside a labeled cassette. The lid is snapped into place and then processed as follows: 50% ethanol for 30 min, 80% ethanol (2×)[a] for 30 min each, 90% ethanol (2×)[a] for 30 min each, 100% ethanol (2×)[a] for 30 min each, 100% ethanol/xylene (1:1 v/v) for 30 min, xylene (2×)[a] for 30 min each, and paraffin (2×)[a,b] for 30 min each.

Immunostaining Protocol for Tissue

1. Rehydrate each of the slides sequentially as follows: xylene (2×) for 10 min each, 100% ethanol (2×) for 5 min each, 95% ethanol for 5 min, 85% ethanol for 5 min, and running water for 5 min.

2. Incubate slides with 0.1% trypsin in 0.1% $CaCl_2$ (pH 7.8, preheated to 37°C) at room temperature for 10 min.

3. Rinse gently with distilled water or buffer solution (0.05 M Tris-HCl, 0.15 M NaCl, pH 7.6).

4. Block the endogenous peroxidase in the tissue by adding 1% H_2O_2 (from 30% H_2O_2 stock Fisher Scientific, Cat No. 001823) to each tissue slide at room temperature for 15 min.

5. Rinse gently with running water and then gently blow dry slides.

6. Add 1% bovine serum albumin (BSA) in buffer (0.05 M Tris-HCl, 0.15 M NaCl, pH 7.6) to the tissue samples for 20 min at room temperature.

7. Add primary antibody or negative control (preimmune serum) (same dilution as primary antibody). Tap off excess buffer and wipe the slides (but do not dry). Incubate slides with primary antibody overnight at 4°C in a humidified chamber.

8. Rinse each slide gently with washing buffer (0.05 M Tris-HCl, 0.15 M NaCl, pH 7.6) 2× for 5 min each.

9. Incubate each sample in peroxidase-labeled polymer (Dako Envision+ Cat No. K4010, Glostrup, Denmark) for 30 min at room temperature.

10. Add the substrate by washing slides as in **Step 8**. Add prepared liquid DAB-chromogen solution (Dako, Cat No. K3467) to cover specimens. Incubate for 2–10 min.

11. To counterstain, immerse slides in a bath of hematoxylin (Sigma, Hematoxylin Solution, Cat No. GHS-2-16) 15 times (dip in and out). Rinse gently with running tap water for 5 min. Decolorize by putting slides in 70% ethanol containing 1% HCl for a 1 sec and then quickly transferring slides to running tap water for 10 min.

12. Dehydrate the samples through alcohol to xylene as follows: 85% ethanol for 5 min, 95% ethanol for 5 min, 100% ethanol for 5 min, 100% ethanol for 5 min, and xylene (2×) for 5 min each.

13. For mounting, cover specimens by microscope cover glass (Fisher Scientific, Cat No. 12-545E, Hampton, NH) with mounting medium (Stephens Scientific, Cat No. 8310-4, Canada) and view by light microscopy.

RESULTS

The optimization of a staining procedure for any antigen requires that the dilution of the primary, and sometimes secondary, antibody be calibrated. If the dilution of secondary antibody is not known (i.e., if the

[a]Each incubation is in a fresh batch of reagent.

[b]Tissue Prep Paraffin, melting point 56–57°C (Fisher Cat No. T565).

second antibody is not supplied in a kit), the tissue of interest (in this case, liver) needs to be stained with increasing dilutions of secondary antibody, followed by substrate, until a dilution is found in which no signal is observed. Using this dilution, the same thing is done with preimmune serum. The dilution of preimmune or control serum that yields a completely negative staining signal is the working dilution in which the primary antibody should be used. When this optimization was done, it is likely that the staining patterns achieved represented a true positive result. Figure 39, for example, shows immunohistochemical staining for URG4 and for HB XAg on consecutive tissue sections from formalin-fixed and paraffin-embedded samples of HCC (Figure 39A and 39B, respectively) and surrounding nontumor liver (Figure 39D and 39E, respectively). In this case, staining of another consecutive section of tumor (Figure 39C) or nontumor (Figure 39F) with preimmune serum ensures the specificity of the staining in each case. Because independent data suggested that URG4 was up-regulated by HBV (Tufan *et al.,* 2002), this was further tested by staining sections from uninfected livers with anti-URG4 (Figure 39G) or preimmune serum (Figure 39H). The comparative staining intensity of Figure 39G compared to Figure 39A and Figure 39D suggest that URG4 is up-regulated in diseased liver and in tumor cells. Another important control that was used to confirm the specificity of staining involved preincubation of the primary antibody with 25 μg of corresponding antigen (in this case, URG4 or HB XAg synthetic peptide[s]) for 1 hr at 37°C prior to staining). Although the data for this are not shown here, the successful blocking of an antibody by immunizing antigen suggests that the staining is specific.

Another important measure of specificity, and a way that expression levels could be quantitated, is to perform Western Blots on lysates from tissue or tissue culture cells. An example of such a blot is shown in Figure 40 for tissue culture cells. In this case, an *in vitro* translated URG4 polypeptide was used as a positive control to verify that immunoreactivity occurred at the appropriate band location on the gel (Figure 40, lane 4). When an equivalent amount of total protein from different cell lines was loaded onto each well, and Western Blot analysis was performed, the results were directly comparable by gel scanning and normalization of the URG4 bands in each lane to the intensity of β-actin in each corresponding lane. The assumption here is that the expression of β-actin, a housekeeping gene, is insensitive to the introduction of HB XAg or exogenous URG4 and therefore serves as a loading control for each lane. The experiment here shows that if the levels of URG4 in HepG2 cells transfected with empty plasmid is taken as 1.0 (Figure 40, lane 1), then the introduction of HB XAg results in a 2.1-fold increase in URG4 expression (Figure 40, lane 2). In comparison, HepG2 cells stably transfected with an expression vector encoding URG4 results in increased expression about 5.5-fold higher than HepG2 cells transfected with empty vector. However, the levels of URG4 in HepG2.2.15 cells, which replicate HBV, are approximately 2.4-fold higher than in control cells (Figure 40, lane 5), suggesting that HB XAg made in the context of virus replication also stimulates the expression of URG4. Similar experiments with URG7, URG11, and URG12 also show that they are specifically up-regulated in HB XAg-positive compared to HB XAg-negative cells and in the livers of carriers with chronic liver disease.

DISCUSSION

The observations that HB XAg supports HBV replication (Bouchard *et al.,* 2001), that the X region of HBV DNA integrates into host DNA over the years in parallel with each bout of liver disease and accompanying regeneration (Jin *et al.,* 2001; Matsubara and Tokino, 1990), and that HB XAg accumulates in the livers of such patients (Wang *et al.,* 1991a,b) suggest that HB XAg is expressed many years before the development of the tumor. If HB XAg alters the expression of host gene products, and these alterations are important to the pathogenesis of HCC, then changes in HB XAg-positive compared to HB XAg-negative cells should reveal early changes in host gene expression that contribute to the early pathogenesis of HCC. The finding of up-regulated URG4 in peritumor liver tissue is consistent with it being an early marker of hepatocarcinogenesis (Tufan *et al.,* 2002). Very similar results were obtained with URG7, URG11, and S15a (Lian *et al.,* 2001; Lian *et al.,* 2003; Lian *et al.,* 2004), suggesting that the staining patterns observed with these proteins indentify early steps in multistep carcinogenesis. Given that each of these markers is up-regulated and co-stains with HB XAg in the great majority of the livers examined, it is possible that they may serve as prognostic indicators of tumor development in needle-biopsy samples from patients with chronic liver disease. This information would be very important, especially in countries with millions of carriers, in distinguishing carriers who will develop cancer from those who will not develop tumors. In addition, these markers may be useful in following the course of treatment among patients who are chronically infected because successful treatment may not only reduce the risk of HCC development but also the up-regulated expression of these multiple markers in the liver.

The ability to specifically stain for these proteins and to quantitate their levels by Western Blot will

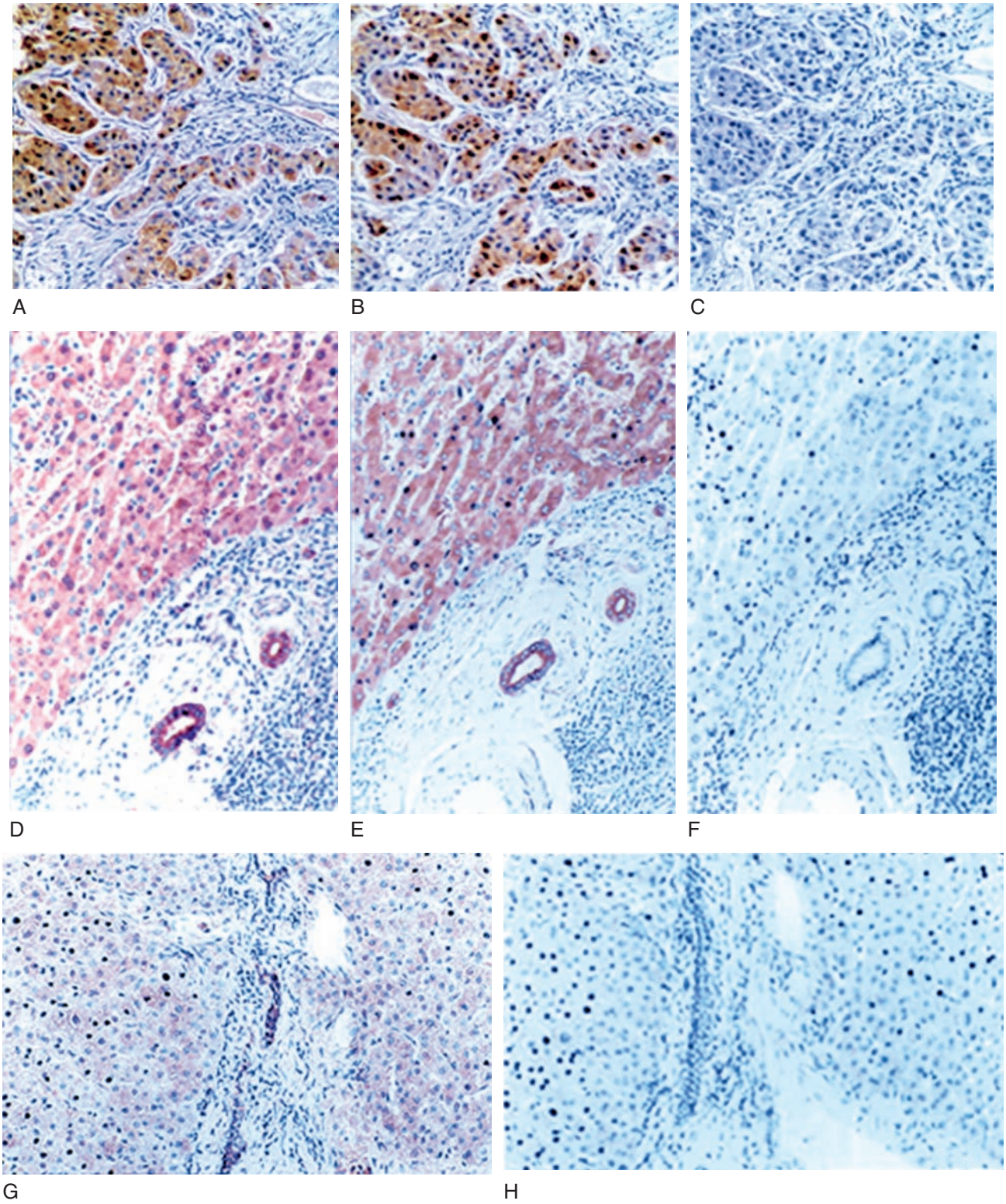

Figure 39. Immunohistochemical staining for URG4 and HB XAg (Tufan *et al.,* 2002). **A:** Anti-URG4 staining of hepatocellular carcinoma (HCC) tissue from a hepatitis B virus (HBV) carrier. **B:** Anti-HBx staining of a consecutive section from the same patient as in panel A. **C:** Preimmune rabbit serum used to stain a consecutive section from the same patient as in panel A. **D:** Anti-URG4 staining of nontumor liver tissue from an HBV carrier. **E:** Anti-HBx staining of a consecutive section from the same patient as in panel D. **F:** Preimmune rabbit serum used to stain a consecutive section from the same patient as in panel D. **G:** Anti-URG4 used to stain an uninfected liver. **H:** Preimmune rabbit serum used to stain a consecutive section of the same uninfected liver. Magnification in all panels 200X.

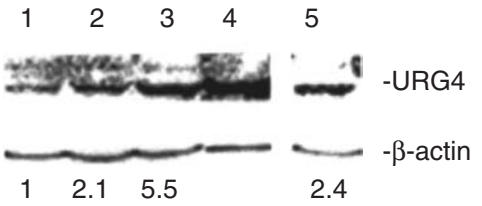

Figure 40. Western Blot with anti-URG4 was conducted on protein isolated from HepG2-pcDNA3 (lane 1), HepG2-pcDNA3-HBx (lane 2), HepG2-pcDNA3-URG4 (lane 3), and HepG2.2.15 (lane 5) (Tufan *et al.,* 2002). A pcDNA3-URG4 *in vitro* translation sample (lane 4) was used as a positive control. The numbers below the lanes are the relative amounts of URG4 protein in the Western Blot upon gel scanning and normalized by comparison with the corresponding β-actin loading control shown below each sample.

contribute significantly to their functional characterization. For example, overexpression of URG4, URG11, and S15a in HepG2 cells is associated with increased cell growth in culture, increased growth in soft agar, and accelerated tumor growth when such cells are transplanted into nude mice (Lian *et al.,* 2003; Lian *et al.,* 2004; Tufan *et al.,* 2002). This suggests that these proteins act as positive growth regulators or, in some cases, oncoproteins. Overexpression of URG7, however, provides resistance of HepG2 cells to killing by anti-Fas (Lian *et al.,* 2001), suggesting that URG7 overexpression promotes hepatocellular survival in the face of ongoing and persistent immune responses aimed at eliminating virus-infected cells. These techniques will also be very useful in elucidating the mechanism(s) whereby these proteins work in the infected hepatocyte. As this information is accumulated, it will be possible to assess whether one or more of these markers are good candidates for therapeutic intervention. Hence, the development of specific antibody markers to HB XAg-triggered changes in gene expression that correlate with altered hepatocellular phenotype has a wide range of applications in both the basic science of the host-virus relationship and in translational research.

In summary, chronic HBV infection is associated with the development of CLDs, including chronic hepatitis, cirrhosis, and HCC. A protein encoded by HBV, known as X antigen, or HB XAg, contributes importantly to the development of HCC. As a *trans*activating protein, HB XAg contributes to the development of HCC, at least in part by up-regulating the expression of host genes that promote cell growth and survival, while it turns off genes that keep cell growth in check. To identity these genes, subtraction hybridization was conducted on RNAs from HB XAg-positive compared to HB XAg-negative cells. The results revealed a list of cellular gene products that were expressed at elevated levels in HB XAg-positive hepatocytes from HBV carriers who developed HCC. These markers consistently showed elevated levels of expression in peritumor hepatocytes but often lower levels in adjacent HCC cells. *In vitro* characterization of these proteins showed they stimulated hepatocellular growth and survival, as well as promoted tumorigenesis, suggesting that they were early markers of HCC. The staining patterns for these proteins suggest that they will be useful as prognostic markers in tumor development and will help to distinguish carriers who are at high risk for HCC. This will permit early identification and intervention, which will invariably save lives.

References

Aden, D.P., Fogel, A., Plotkin, S., Damjanov, I., and Knowles, B.B. 1979. Controlled synthesis of HBsAg in a differentiated human liver carcinoma-derived cell line. *Nature 282*:615–616.

Beasley, R.P., and Hwang, L.Y. 1984. Epidemiology of hepatocellular carcinoma. In Vyas, G., Dienstag, J.L., and Hoofnagle, J. (eds) *Viral Hepatitis and Liver Disease.* New York: Grune & Stratton, Inc., 209–224.

Benson, D.A., Boguski, M.S., Lopman, D.J., and Ostell, J. 1997. GenBank. *Nucleic Acids Res. 25*:1–6.

Bouchard, M.J., Wang, L.H., and Schneider, R.J. 2001. Calcium signaling by HBx protein in hepatitis B virus DNA replication. *Science 294*:2376–2378.

Cepko, C. 1992. Overview of the retrovirus transduction system. Transduction of genes using retrovirus vectors. In Ausubel, F.M. (ed) *Current Protocols in Molecular Microbiology*. Chichester, England: Wiley-Interscience, 9.10.1–9.10.7.

Cheung, S.T., Chen, X., Guan, X.Y., Wong, S.Y., Tai, L.S., Ng, I.O.L., So, S., and Fan, S.T. 2002. Identify metastasis-associated gene in hepatcellular carcinoma through clonality delineation for multinodular tumor. *Cancer Res. 62*:4711–4721.

Danos, O. 1991. Construction of retroviral packaging cell lines. In Collins, M. (ed) *Methods in Molecular Biology, Practical Molecular Virology: Viral vectors for gene expression.* Clifton, NJ: Human Press, Inc., 17–27.

Duan, L.X., Zhu, M., Bagasra, O., and Pomerantz, R.J. 1995. Intracellular immunization against HIV-1 infection of human T lymphocytes: Utility of anti-rev single-chain variable fragments. *Human Gene Ther. 6*:1561–1573.

Eddleston, A.L.W.F. 1990. Overview of HBV pathogenesis. In Hollinger, F.B., Lemon, S.M., and Margolis, H. (eds) *Viral Hepatitis and Liver Disease.* Philadelphia: Williams & Wilkins, 234–237.

Feitelson, M.A. 1986. HBV and cancer. In Notkins A.L., and Oldstone, M.B.A. (eds) *Concepts in Viral Pathogenesis.* New York: Springer-Verlag, Inc., 269–275.

Feitelson, M.A. 1989. HBV gene products as immunological targets in chronic infection. *Mol. Biol. Med. 6*:367–393.

Feitelson, M.A., and Clayton, M.M. 1990. X antigen polypeptides in the sera of hepatitis B virus-infected patients. *Virology 177*:367–371.

Feitelson, M.A., and Duan, L.X. 1997. Hepatitis B virus x antigen in the pathogenesis of chronic infections and the development of hepatocellular carcinoma. *Am. J. Pathol. 150*:1141–1157.

Feitelson, M.A., Millman, I., Duncan, G.D., and Blumberg, B.S. 1988. Presence of antibodies to the polymerase gene product(s)

of hepatitis B and woodchuck hepatitis virus in natural and experimental infections. *J. Med. Virol. 24*:121–136.

Feitelson, M.A., Sun, B., Tufan, N.L., Liu, J., Pan, J., and Lian, Z. 2002. Genetic mechanisms of hepatocarcinogenesis. *Oncogene 21*:2593–2604.

Henkler, F., and Koshy, R. 1996. Hepatitis B virus transcriptional activators: Mechanisms and possible role in oncogenesis. *J. Viral. Hepat. 3*:109–121.

Jin, Y.M., Yun, C., Park, C., Wang, H.J., and Cho, H. 2001. Expression of hepatitis B virus X protein is closely correlated with the high periportal inflammatory activity of liver diseases. *J. Viral. Hepat. 8*:322–330.

Knowles, B.B., Howe, C.C., and Aden, D.P. 1980. Human hepatocellular carcinoma cell lines secrete the major plasma proteins and hepatitis B surface antigen. *Science 209*:497–499.

Lian, Z., Liu, J., Li, L., Li, X., Arbuthnot, P., Kew, M., and Feitelson, M.A. 2004. Human S15a is an effector which is up regulated by HBV X protein. *Mol. Carcinog. 40*:34–46.

Lian, Z., Liu, J., Li, L., Li, X., Tufan, N.L.S., Clayton, M.M., Wu, M.C., Wang, H.Y., Arbuthnot, P., Kew, M., and Feitelson, M.A. 2003. Up-regulated expression of a unique gene by hepatitis B x antigen promotes hepatocellular growth and tumorigenesis. *Neoplasia 5*:229–244.

Lian, Z., Liu, J., Pan, J., Tufan, N.L.S., Zhu, M., Arbuthnot, P., Kew, M., Clayton, M.M., and Feitelson, M.A. 2001. A cellular gene upregulated by hepatitis B virus encoded X antigen promotes hepatocellular growth and survival. *Hepatology 34*:146–157.

Lian, Z., Pan, J., Liu, J., Zhu, M., Arbuthnot, P., Kew, M.C., and Feitelson, M.A. 1999. The translation initiation factor, SUI1, may be a target of hepatitis B x antigen in hepatocarcinogenesis. *Oncogene 18*:1677–1687.

Matsubara, K., and Tokino, T. 1990. Integration of HBV DNA and its implications for hepatocarcinogenesis. *Mol. Biol. Med. 7*:243–260.

Okabe, H., Satoh, S., Kato, T., Kitahara, O., Yanagawa, R., Yamaoka, Y., Tsunoda, T., Furukawa, Y., and Nakamura, Y. 2001. Genome-wide analysis of gene expression in human hepatocellular carcinomas using cDNA microarray: Identification of gene involved in viral carcinogenesis and tumor progression. *Cancer Res. 61*:2129–2137.

Paradis, V., Bieche, I., Dargere, D., Laurendeau, I., Laurent, C., Sage, P.B., Degott, C., Belghiti, J., Vidaud, M., and Bedossa, P. 2003. Molecular profiling of hepatocellular carcinomas (HCC) using a large-scale real-time RT-PCR approach. Determination of a molecular diagnostic index. *Am. J. Pathol. 163*:733–741.

Popper, H., Roth, L., Purcell, R.H., Tennant, B.C., and Germ, J.L. 1987. Hepatocarcinogenicity of the woodchuck hepatitis virus. *Proc. Natl. Acad. Sci. USA 84*:866–870.

Schluter, V., Meyer, M., Hofschneider, P.H., Koshy, R., and Caselmann, W.H. 1994. Integrated hepatitis B virus X and 3′ truncated preS/S sequences derived from human hepatomas encode functionally active transactivators. *Oncogene 9*:3335–3344.

Sheu, J.-C. 1997. Molecular mechanism of hepatocarcinogenesis. *J. Gastroenterol. Hepatol. 12(Suppl)*:S309–S318.

Tennant, B.C., and Gerin, J.L. 2001. The woodchuck model of hepatitis B virus infection. *Ilar J. 42*:89–102.

Tufan, N.L.S., Lian, Z., Liu, J., Pan, J., Arbuthnot, P., Kew, M., Clayton, M.M., and Feitelson, M.A. 2002. HB XAg stimulates expression of a novel cellular gene, URG4, that promotes hepatocellular growth and survival. *Neoplasia 4*:355–368.

Valenzuela, P., Quiroga, M., Zaldivar, J., Gray, P., and Rutter, W.J. 1980. The nucleotide sequence of the hepatitis B viral genome and the identification of the major viral genes. In Fields, B.N., Jaenisch, R., and Fox, C.F. (eds) *Animal Virus Genetics.* San Diego:Academic Press, 57–70.

Vile, R. 1991. The retroviral life cycle and the molecular construction of retrovirus vectors. In Collins, M. (ed) *Methods in Molecular Biology. Practical Molecular Virology: Viral Vectors for Gene Expression.* Clifton, NJ: Humana Press, Inc., 1–15.

Wang, X.W., Forrester, K., Yeh, H., Feitelson, M.A., Gu, J.-R., and Harris, C.C. 1994. Hepatitis B virus X protein inhibits p53 sequence-specific DNA binding, transcriptional activity and association with ERCC3. *Proc. Natl. Acad. Sci. USA 91*:2230–2234.

Wang, W., London, W.T., and Feitelson, M.A. 1991a. Hepatitis B x antigen in hepatitis B virus carrier patients with liver cancer. *Cancer Res. 51*:4971–4977.

Wang, W., London, W.T., Lega, L., and Feitelson, M.A. 1991b. Hepatitis B x antigen in liver from carrier patients with chronic hepatitis and cirrhosis. *Hepatology 14*:29–37.

Zhang, Z., Torii, N., Furusaka, A., Malayaman, N., Hu, Z., and Liang, T.J. 2000. Structural and functional characterization of interaction between hepatitis B virus X protein and the proteasome complex. *J. Biol. Chem. 275*:15157–15165.

13

Distinction between Well-Differentiated Hepatocellular Carcinoma and Benign Hepatocellular Nodular Lesions, Using Fine-Needle Aspiration Biopsy

Aileen Wee

Introduction

Hepatocellular carcinoma (HCC) is gaining clinical importance because of its increasing worldwide incidence. It is the fifth most common cancer in the world, with more than 1 million deaths annually. It is no longer a disease of developing countries associated with hepatitis B virus (HBV) infection or aflatoxin exposure. Hepatitis C virus (HCV)-related cases are on the rise. Percutaneous radiologically guided hepatic fine-needle aspiration biopsy (FNAB) is widely performed. The diagnosis of HCC is not difficult with optimal specimen procurement and processing, combined cytohistologic approach, judicious use of ancillary techniques, close clinicopathologic correlation, and trained expertise (Wee and Sampatanukul, 2004). The sensitivity of hepatic FNAB diagnosis of malignancy is about 85% (range, 67–100%), whereas the specificity approaches 100% (Hertz *et al.,* 2000). However, distinguishing a highly well-differentiated HCC (WD-HCC) from benign hepatocellular nodular lesions can be extremely challenging. Immunohistochemistry (IHC) has an adjunctive role in enhancing the yield and precision of cytodiagnosis of such lesions.

The FNAB material is routinely made into smears that are air-dried and stained with Diff-Quik or May-Grunwald-Giemsa (MGG) or fixed immediately in 95% ethanol and stained by the Papanicolaou method. Any particulate fragments/microbiopsy cores should be retrieved, fixed in 10% buffered formalin, and processed into cell blocks for histologic sections. Cell blocks allow for evaluation of architecture (reticulin framework and trabecular thickness), pigments (bile, lipochrome, and iron), and small-cell change; they also provide material for further stains. Many studies have attested to the improved diagnostic yield and accuracy of FNAB using the combined cytohistologic approach (Longchampt *et al.,* 2000).

Handbook of Immunohistochemistry and *in situ* Hybridization of Human Carcinomas, Volume 3: Molecular Genetics, Liver Carcinoma, and Pancreatic Carcinoma

What Are the Diagnostic Problems and Pitfalls?

In HBV-prevalent populations, the cytologic differentiation of HCC from other focal hepatic lesions is almost as frequent as with metastases. This is particularly so when hepatitis B surface antigen (HBsAg) carriers with chronic liver disease are routinely screened for the early detection of HCC by serum alpha-fetoprotein (AFP) estimation and ultrasonography or computed tomography scanning. When associated with cirrhosis, HCC can present as solitary mass, multifocal lesions, or diffuse disease. Smaller and smaller lesions (<2 cm diameter) are being increasingly detected by improved imaging techniques and subjected to FNAB for tissue characterization. There is difficulty separating small HCCs from regenerative/dysplastic nodules radiologically. Table 14 lists the histologic entities that are likely to pose diagnostic dilemmas and pitfalls in FNAB material of well-differentiated hepatocellular nodular lesions.

Serum AFP evaluation, although fairly specific, shows poor sensitivity for the diagnosis of HCC regardless of tumor size or degree of differentiation. About half of histologically confirmed HCCs have normal serum AFP levels. The value of AFP as a screening and diagnostic tool has to be reevaluated, especially for small lesions.

Histologically, HCCs are known to be heterogeneous. Classic HCCs are graded as well-, moderately, or poorly differentiated based on nuclear features (Ishak *et al.,* 2001). Architectural patterns can comprise trabecular-sinusoidal, pseudoacinar, and/or solid areas. Currently used histologic criteria for the diagnosis of malignant transformation in hepatocellular nodules are as follows: 1) loss of reticulin framework and thickening of trabeculae, 2) sinusoidal capillarization, 3) increasing number of arterioles, 4) cellular pleomorphism/heterogeneity, 5) "clonal" growth patterns, 6) pseudoacinar formation, and 7) mitotic activity (Quaglia *et al.,* 2001). Some of these details are not forthcoming in cytologic material.

Table 14. Well-Differentiated Hepatocellular Nodular Lesions

Macroregenerative nodule in cirrhosis
Dysplastic nodule (low- and high-grade)
Focal nodular hyperplasia
Liver cell adenoma
Well-differentiated hepatocellular carcinoma
Focal fatty alteration
Focal nodular hyperplasia with fatty change
Liver cell adenoma with fatty change
Well-differentiated hepatocellular carcinoma with fatty change

The morphologic diagnosis of HCC is complicated by two divergent problems at the ends of the spectrum. At the highly WD-HCC end, the hepatocytic histogenesis is obvious but proof of malignancy may be lacking (Wee *et al.,* 1994). This dilemma is compounded by the fact that HCCs tend to occur in a cirrhotic background together with regenerative/macroregenerative/dysplastic nodules (Ferrell *et al.,* 1993). Another diagnostic challenge occurs when mass lesions in noncirrhotic livers—such as focal nodular hyperplasia (FNH), liver cell adenoma (LCA), or WD-HCC—have to be distinguished cytologically from each other and from surrounding hepatocytes. This is not withstanding the suspicion of nonrepresentative sampling.

One must also be cognizant of the fact that neoplastic cells in WD-HCC and LCA can undergo fatty metamorphosis without associated steatosis in the adjacent parenchyma (Wee *et al.,* 1991). These true neoplasms must be differentiated from focal fatty alteration as well as diffuse steatosis. An interesting observation that adds to the diagnostic pitfalls is that small HCCs, which tend to be well-differentiated, are prone to fatty change as a result of insufficient development of tumor vessels—the fat disappears as the the tumor grows and gains angiogenic competence.

With the use of advanced imaging techniques in high-risk populations, nodules suspicious of malignancy as well as nonmalignant nodules are being detected. Some may be precursor lesions exhibiting architectural and cytologic atypia insufficient for an outright diagnosis of HCC although suggestive of a premalignant state. Current concepts of how these premalignant lesions develop and how HCC may arise within them affect the accuracy of the pathologic diagnosis of hepatocellular nodules (Theise, 1995). The incompleteness and inadequacies of evaluation of hepatocellular nodules by a technique such as FNAB cannot be ignored given the focality of proliferative clones of atypical cells within apparently benign nodules and the shortcomings of pure morphologic interpretation.

To add to this dilemma is the increasing evidence that the histopathology of HCC changes as the lesion enlarges. Small HCCs tend to be well-differentiated as compared to the heterogeneity exhibited by larger tumors. Critical reappraisal of the current histopathologic criteria for the diagnosis of small HCCs is necessary in the face of ever-increasing demands for tissue characterization of radiologically guided biopsies of small suspicious nodules. The window of opportunity for effective therapy of HCC is limited because the diagnosis is usually made late in the course of the disease. There is an urgency to develop improved diagnostic parameters and modalities to widen this therapeutic opportunity.

This chapter gives an overview of nomenclature of hepatocellular nodular lesions, changing concepts in the evolution of HCC and its precursor lesions, current pathologic criteria for diagnosis of such nodules, cytologic parameters in the FNAB categorization of well-differentiated hepatocellular nodules, diagnostic problems and pitfalls, and the adjunctive role of special stains and IHC.

Fine-Needle Aspiration Biopsy

Normal Liver, Cirrhosis, and Steatosis

The procedure FNAB of normal liver is usually not very cellular but may include microbiopsy cores of intact parenchyma. The cell picture is polymorphic, comprising hepatocytes, bile-duct epithelial clusters, and endothelial and Kupffer cells. The hepatocytes occur singly, in short cords or monolayered sheets, and typically exhibit some degree of anisocytosis and anisokaryosis. The polygonal cells have well-defined cell borders, ample granular cytoplasm, a central round nucleus, well-delineated nuclear membrane, distinct nucleolus, and granular chromatin. The nuclear-cytoplasmic ratio, on eyeballing the diameters of the nucleus and the cell, is one-third or less. In cirrhosis, binucleated hepatocytes and cords that are one or two cells thick are frequent. Regenerating hepatocytes may be smaller or larger than normal cells with prominent nucleoli. Those hepatocytes exhibiting large cell change (see "Dysplastic Nodule" on this page) have correspondingly enlarged nuclei, thus maintaining the normal nuclear-cytoplasmic ratio.

Lipochrome pigment is seen as black cytoplasmic granules with Giemsa stain. The presence of lipochrome and iron within hepatocytes is nearly always associated with benign processes. The hepatocytes may also contain fat, bile, and Mallory bodies. In steatosis, the hepatocytes are enlarged by the presence of lipid-laden cytoplasmic vacuoles. In macrovesicular fatty change, the nucleus is pushed to one side of the cell. Empty-looking bubbles of various sizes abound in Giemsa-stained smears.

The bile-duct epithelial clusters usually consist of sheets of regular cuboidal cells with a honeycomb appearance. The cells have indistinct cell borders, scanty pale cytoplasm, and oval nuclei with inconspicuous nucleoli. Larger ducts are represented by strips of columnar cells with basal nuclei imparting a picket-fence look. The cuboidal cell clusters from small bile ducts should be distinguished from proliferating bile ductules. These ductular cells sometimes bear a vague resemblance to hepatocytes with more granular cytoplasm ("hepatocellular metaplasia"). They represent regenerative activity at the hepatocellular–stromal interface from a proliferation of stem cells that normally reside in the canals of Hering.

Elongated, comma-shaped Kupffer cell nuclei and spindly endothelial cell nuclei are scattered among the hepatocytes. Some inflammatory cells are not unexpected in cirrhotic aspirates. Flat sheets of mesothelial cells with a uniform, pavement-like appearance may be present. Particulate fragments are very thick when smeared, consisting of cores of intact liver parenchyma with innumerable endothelial cells intimately admixed with hepatocytes.

Benign Hepatocellular Nodular Lesions

There are a number of benign focal hepatocellular lesions that can mimic WD-HCC.

Macroregenerative Nodule

Most regenerative lesions occur in a background of cirrhosis. When multiacinar regenerative nodules are distinctively larger than most cirrhotic nodules of the same liver, they are called macroregenerative nodules (MRN) (>5 mm in diameter) (IWP, 1995). They contain several portal tracts and two cells–thick cords of regenerating hepatocytes bordered by endothelial cells. The FNAB specimens are polymorphic, comprising hepatocytes, bile-duct epithelial clusters, and endothelial and Kupffer cells. The hepatocytes are dispersed or in short cords, and they display cellular polymorphism and binucleation but no cytologic atypia. Lipochrome and iron pigments may be detected. Pseudoacinar formation and hepatocytic multinucleation are not seen. Without the benefit of architectural details, it is almost impossible to discern any appreciable cytologic difference between intralesional and extralesional hepatocytes. Stromal fragments from cirrhotic fibrous septa and proliferating bile-ductular epithelial clusters may be evident in the background. The diagnostic challenge arises when foci of cytologic atypia in keeping with large- or small-cell change are encountered within the nodules. The possibility of malignant transformation has to be considered because HCCs can arise in MRNs.

Dysplastic Nodule

The term "liver cell dysplasia" has now been superseded by the terms "large cell change" and "small cell change" to replace large- and small-cell dysplasia, respectively (Ishak *et al.,* 2001). However, the terms "dysplastic foci" and "dysplastic nodule" still exist (IWP, 1995). Dysplastic lesions are currently defined histologically by the presence of topographically recognizable subpopulations of hepatocytes exhibiting cytoplasmic and nuclear variations of large- or small-cell change.

"Dysplastic foci" consist of clusters of atypical hepatocytes less than 1 mm in diameter, without accompanying portal tracts. "Dysplastic nodules" are larger than 1 mm diameter and can exhibit neoangiogenesis and sinusoidal capillarization. Hepatocytes exhibiting large- and small-cell change are common in cirrhosis. Morphometric studies suggest that small-cell change is more sinister biologically and may be the putative precancerous lesion in humans. Of patients with cirrhosis, 5–40% have HCC and foci of carcinoma may be found in one-third of dysplastic nodules.

Dysplastic nodules can be subdivided into low-grade (MRN without significant atypia but cytologic features suggesting clonality) and high-grade (MRN with atypia or borderline) types (Ferrell *et al.,* 1993). In the former, the hepatocytes show minimal atypia with a slight increase in nuclear–cytoplasmic ratio; the cords are one to two cells thick; and large- and/or small-cell change may be present. Separation from MRN may be problematic. High-grade dysplastic nodules show a higher degree of pleomorphism, cytoplasmic basophilia, cords more than two cells thick, and pseudoacinar formation. Distinguishing a high-grade dysplastic nodule from WD-HCC can be difficult based on currently available diagnostic modalities in routine use. Invasion of stroma and portal tracts is highly suggestive of malignancy—a feature lost in smears. Some dysplastic nodules display "nodule-in-nodule" lesions. These subnodules, with or without distinctive cellular changes, exhibit greater proliferative rates than the surrounding dysplastic parenchyma. They show expansile growth, and their presence should upgrade the whole dysplastic nodule to a high-grade lesion.

Aspirates from dysplastic nodules are not excessively cellular and typically contain a mixed population of dissociated hepatocytes, biliary epithelial and clusters, and endothelial and Kupffer cells. The hepatocytes exhibit varying degrees of cytologic atypia corresponding to large- or small-cell change. In the former, both the nucleus and cell are proportionately bigger; hence, the nuclear-cytoplasmic ratio is still one-third or less, despite the acquisition of thick nuclear membrane, nuclear hyperchromatism, prominent nucleolus, and coarse granular chromatin. Hepatocytic multinucleation may be present. In small-cell change, the hepatocytes assume a more regular appearance accompanied by a slight increase in nuclear-cytoplasmic ratio, closely mimicking highly WD-HCC.

The reticulin framework may be focally decreased, but the cords should not be more than two to three cells thick. Histologic examination allows for recognition of foci of small- or large-cell change, which is not possible on smears alone. Immunohistochemical studies can lend light to the vascular profile of the nodules.

Focal Nodular Hyperplasia

The condition FNH is a nonneoplastic, multinodular, hepatocellular lesion arising in normal liver. It can occur in all age groups and usually presents incidentally. Pregnancy and oral contraceptive use are not considered risk factors (Ishak *et al.,* 2001). It is characterized by a central stellate scar containing malformed blood vessels surrounded by regenerating hepatocytes arranged in cords that are one to two cells thick. Proliferating bile ductules, in addition to the normal complement of bile ducts, are present at the interface between hepatocytes and scar tissue. Pseudoacinar formation and multinucleated hepatocytes are usually not evident. The reticulin framework is essentially intact.

Typical aspirates are fairly cellular, comprising dispersed and short cords of regenerating hepatocytes admixed with ductular epithelial clusters and endothelial and Kupffer cells. Stromal fragments from the scar are rarely included (Ruschenburg and Droese, 1989). Depending on whether the hepatocellular, ductular, or stromal component predominates, and on the degree of regenerative atypia, FNH can be mistaken for WD-HCC, adenocarcinoma, or spindle-cell neoplasm, respectively. This diagnostic pitfall can be avoided if one is alert to the mixed-cell picture in the aspirate.

Variations and coexisting lesions of other hepatocellular nature as well as an array of vascular abnormalities have been documented in FNH (Bioulac-Sage *et al.,* 2001). Atypical features in variant lesions include lack of central scar, presence of portal vein, and telangiectactic changes. Multiple lesions have been reported (Nguyen *et al.,* 1999). Because FNH can coexist with more sinister lesions, it is imperative that clinicians are aware that when multiple lesions are present it cannot be assumed that all of them are of a similar nature. FNH can also exhibit fatty change mimicking other benign hepatocellular lesions that undergo similar change. Atypical FNH is difficult to distinguish from LCA. Furthermore, FNH can coexist with LCA and liver cell adenomatosis. There is no real management dilemma if the lesions are deemed benign. However, if there is suspicion of sampling error, further diagnostic procedures may be required.

Liver Cell Adenoma

The condition LCA is a rare benign tumor of hepatocytes usually associated with use of oral contraceptives or anabolic/androgenic steroids (Ishak *et al.,* 2001). Encountered principally in women of reproductive age, this lesion is usually solitary and hypervascular, arising in normal liver. Rarely, there are reports of liver cell adenomatosis.

The tumor is characterized by proliferation of rather monotonous hepatocytes accompanied by unpaired blood vessels and is devoid of bile ducts. The hepatocytes are arranged in cords that are one to two (and occasionally three) cells thick. The cells may be smaller, larger, or of the same size as normal hepatocytes; depicting some variation in nuclear size but no cytologic atypia or increase in nuclear-cytoplasmic ratio. Lipochrome pigment, bile, glycogen, fat, hyaline, and Mallory bodies may be present. Multinucleated tumor giant cells are not seen. Pseudoacini, if seen, are sparse. The reticulin framework is generally well-developed.

Aspirates contain three-dimensional, cohesive groupings of benign hepatocytes as well as hepatocytes occurring singly or in short cords with sinusoidal endothelium. Bile-duct epithelial clusters are conspicuous by their absence. Some of the hepatocytes may show fatty change or appear pale and vacuolated as a result of glycogen. The nuclei are relatively small, round, and regular, and there is no increase in nuclear-cytoplasmic ratio. The cytologic features are extremely difficult to distinguish from a highly WD-HCC, so much so that the cytodiagnosis is usually worded as "hepatocellular neoplasm that is highly suggestive of but not diagnostic of LCA," based purely on cytomorphologic grounds (Wee and Nilsson, 2003).

The disease LCA can mimic FNH; both lesions can be steatotic and coexist in the same liver. Dysplastic hepatocytes and foci of HCC have been reported, suggesting malignant transformation of LCA. Much caution should be exercised when rendering a diagnosis of LCA in an adult whose history lacks exogenous hormone usage—a highly WD-HCC is more likely even in a noncirrhotic liver.

Focal Fatty Alteration

Nodular fatty alterations of the liver may be subcapsular and wedge-shaped or occur as single or multiple discrete lesions with scalloped borders. They may mimic metastatic disease radiographically and thereby be subjected to FNAB (Zeppa *et al.,* 2002). Aspirates are polymorphic, comprising hepatocytes with clear cytoplasmic vacuoles, admixed with bile-duct epithelial clusters and endothelial and Kupffer cells. The first impression is nonrepresentative sampling from diffuse steatosis. Recognition of this entity with accurate needle placement in the nodule can establish the diagnosis and obviate the need for further tissue confirmation. It is, however, prudent to pay close attention to the nuclear details and nuclear–cytoplasmic ratio because the clear-cell variant of HCC and fatty change in WD-HCC or LCA can produce similar-looking hepatocytes.

Well-Differentiated Hepatocellular Carcinoma

About one-third of classic HCCs constitute WD-HCCs, with the highly well-differentiated lesions accounting for only a few cases at this end of the spectrum (Wee and Nilsson, 2003). They generally have narrow trabeculae with the malignant hepatocytes tending toward the small side. Small HCCs (< 3 cm diameter) are usually well differentiated and not necessarily vascular, making distinction from a high-grade dysplastic nodule with small-cell change difficult.

Cytodiagnosis of Classic Hepatocellular Carcinoma

Table 15 lists well-established criteria for the cytodiagnosis of classic HCC (Cohen *et al.,* 1991; Longchampt *et al.,* 2000). The smears are hypercellular with a granular, well-spread-out appearance of the tumor clusters on naked eye inspection. The irregular, cohesive clusters of malignant hepatocytes have arborescent, tonguelike projections of broad trabeculae (≥3 cells thick) that may be wrapped by peripheral endothelium. Rows of transgressing endothelium course through larger aggregates and are best appreciated in Giemsa-stained smears, which highlight the basement membrane material a pink color. Epithelial cohesiveness is the general rule. However, in cases in which trabeculae are less than five cells thick, there is a paucity of intact trabeculae. In fact, an increasing tendency to dissociation is noted in very WD-HCCs (Figure 41). Bile-duct epithelial clusters, if present, are few and far apart, intermingling with dispersed regenerating hepatocytes from the likely cirrhotic background. Reactive hepatocytes on the same smear are usually

Table 15. Cytologic Features in Hepatocellular Carcinoma

Granular spread on naked eye inspection
Hypercellularity
Hepatocytic appearance
Epithelial cohesiveness
Trabeculae (>2 cells thick)
Peripheral and transgressing endothelial cells (sinusoidal capillarization)
Pseudoacini
Increased nuclear–cytoplasmic ratio
Atypical naked nuclei
Tumor giant cells
Bile
Cytoplasmic vacuoles (fat, glycogen)
Intracytoplasmic inclusions (Mallory, hyaline, and pale bodies)
Intranuclear inclusions
Abnormal vasculature (unpaired arteries)
Necrosis
Inflammatory cells
Lack of bile-duct epithelium

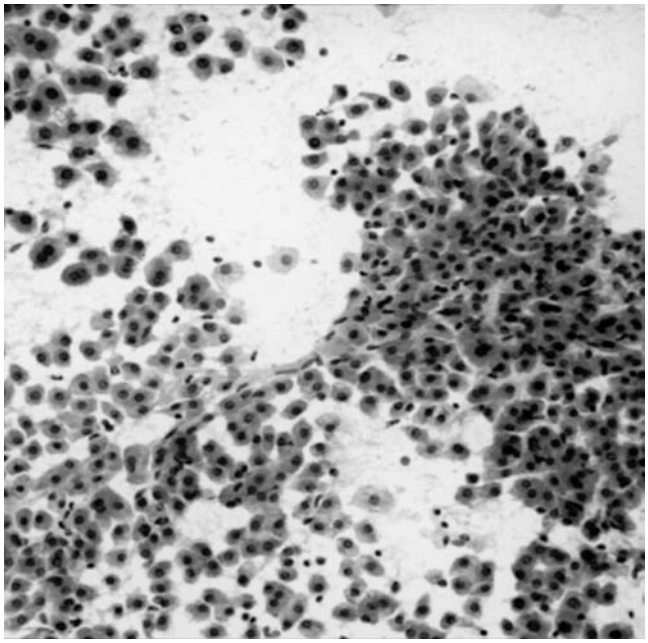

Figure 41. Fine-needle aspiration biopsy of well-differentiated hepatocellular carcinoma. Hypercellular smear shows loosely cohesive clusters and dissociated well-differentiated hepatocytes with transgressing endothelial cells running across the field. Note the well-defined cell borders, dense and monotonous cytoplasm, round and centrally located nuclei with well-delineated nuclear membrane, slightly increased nuclear–cytoplasmic ratio, and distinct nucleolus. Binucleated hepatocytes are prominent. There is minimal cytologic atypia. The hepatocytes tend to be on the small side, exhibiting cellular monomorphism and nuclear crowding. (Papanicolaou).

topographically separated from tumor aggregates, providing the subtle contrast in the different cell populations. Kupffer cells are observed more frequently in MRN than in WD-HCC.

Pseudoacini containing bile or pale secretions are common. In the midst of thick tumor fragments, these spaces are visible as dark, circular gaps surrounded by rosettes of polygonal malignant hepatocytes—quite unlike true acini rimmed by columnar cells with basal nuclear palisading and brush borders. Slightly curved rows of cohesive cells representing disrupted pseudoacini can also be seen issuing from the periphery of larger aggregates.

WD-HCC cells may be smaller, larger, or of the same size as normal hepatocytes. Hepatocytic characteristics, such as polygonal cells with well-defined cell borders, ample granular cytoplasm, a round and centrally located nucleus, well-delineated nuclear membrane, prominent nucleolus, and finely but irregularly granular chromatin, are obvious. What is characteristic of many WD-HCCs is the lack of anisocytosis and anisokaryosis, both of which are seen in less-differentiated HCCs and benign aspirates. Instead, the tumor cells are conspicuous by their small size, monotony, and subtle increase in nuclear–cytoplasmic ratio, all contributing to the impression of nuclear crowding. Mitotic figures are rare.

Atypical naked hepatocytic nuclei may be present. Although naked nuclei can be found in benign aspirates, atypical ones are seen only in HCC. This can be a useful criterion to distinguish WD-HCC from benign aspirates; the crux of the matter is the ability to discern subtle nuclear atypia. A problem may arise with the small-cell type of HCC, where the naked nuclei may be mistaken for those of carcinoid or other small, round, cell tumors. Carcinoid tumor cells have round nuclei with finely stippled chromatin and inconspicuous nucleoli.

Binucleated hepatocytes are common. Multinucleated tumor giant cells showing nuclear feature kinship with the company they keep can be found even in WD-HCC, albeit rarely and only after much scrutiny of the smears. A single multinucleated hepatocytic giant cell in a sea of well-differentiated hepatocytes favors malignancy (Wee *et al.,* 1994). This is a very helpful discriminant feature, being largely absent from LCA, FNH, and regenerative nodules except for dysplastic nodules.

The tumor cells may contain bile; iron pigment is lacking. Intracytoplasmic fat and glycogen vacuoles are common. It is important to reiterate that fatty change is not unusual in small HCCs and that it can be confined to the tumor without associated steatosis. Intracytoplasmic inclusions include hyaline, pale, and Mallory bodies. Intranuclear cytoplasmic inclusions are not specific.

Unpaired arteries should be searched for in cell-block material (Wee *et al.,* 1991). Reticulin is typically deficient or virtually absent in HCCs (de Boer *et al.,* 2000). Tumor necrosis, with or without inflammatory cellular infiltrate, is uncommon in small lesions but may be extensive in infarcted tumors or those treated with transarterial chemoembolization.

Cytohistologic Features Predictive of Hepatocellular Carcinoma

With the use of stepwise logistic regression analysis, three cytologic features were identified as predictive of HCC with a sensitivity of 100% and specificity of 87% (Cohen *et al.,* 1991). They are increased nuclear–cytoplasmic ratio, trabeculae more than two cells thick, and atypical naked hepatocytic nuclei. Another study selected four cytologic features

as predictive of HCC: increased nuclear-cytoplasmic ratio, cellular monomorphism, nuclear crowding, and lack of bile duct cells. The study also selected four histologic features: increased nuclear–cytoplasmic ratio, decreased Kupffer cells, cellular monomorphism, and increased trabeculae thickness (Longchampt *et al.,* 2000).

Cytodiagnosis of Highly Well-Differentiated Hepatocellular Carcinoma

This category of highly WD-HCCs is diagnostically very challenging. The diagnostic dilemma is encountered even at the histologic level, let alone on cytologic grounds. The subtle atypia and narrow trabeculae (one to three cells thick) with great tendency to dissociation, forming dispersed cells and short cords with no discernible peripheral endothelium, make distinction from benign hepatocellular lesions almost impossible. Takenaka *et al.* (1999), in their analysis of HCC and cirrhosis, established six new cytologic criteria for the diagnosis of highly WD-HCC and developed an M-score to separate WD-HCC from regenerating hepatocytes. These parameters include well-defined cytoplasmic borders, scant cytoplasm, monotonous cytoplasm, thick cytoplasm, eccentric nuclei, and increased nuclear-cytoplasmic ratio.

A similar study to evaluate these parameters (Wee and Nilsson 2003) found that WD-HCC cells were generally smaller with fairly well-defined cytoplasmic borders (52%), decreased cytoplasm (100%), thick (52%) and monotonous (48%) cytoplasm, eccentric nuclei (62%), and slightly increased nuclear–cytoplasmic ratio (100%). However, more benign hepatocytes displayed well-defined cytoplasmic borders (73%), with thick (41%) and monotonous (14%) cytoplasm. The nuclei were generally centrally located. The results of the M-scores, which were based on the total number of cytologic parameters observed out of the six with higher scores for malignant cases, were not so consistent and clear-cut—about half of the benign aspirates and WD-HCCs obtained scores of 2 or 3.

Other cytologic features observed were that the nuclei in WD-HCC were round with thick nuclear membranes (90%), nuclear contour irregularities (33%), large nucleoli (62%), multiple nucleoli (38%), irregular chromatin density (29%), and abnormal chromatin pattern (24%). There were multiple nuclei in 19% and atypical naked nuclei in 62%. Most of the nuclei in the regenerating hepatocytes were central and round, with thick nuclear membranes (60%) but no irregular nuclear contours. There were more cells with large nucleoli (86%) but less with multiple nucleoli or chromatin abnormalities (10%). Multinucleated giant-cell transformation was absent, whereas naked nuclei were observed in 14%.

Ancillary Studies

The diagnostic issues one has to grapple with when faced with aspirates from a focal hepatic lesion composed of well-differentiated hepatocytes are as follows:

1. Is the sample representative of the lesion?
2. Are the hepatocytes malignant (i.e., from HCC) or benign?
3. If benign, are they neoplastic (i.e., from LCA) or nonneoplastic hepatocytes?
4. If nonneoplastic, are they intralesional (from FNH, dysplastic nodule, or MRN) or extralesional hepatocytes (i.e., from cirrhosis or normal liver; with or without steatosis)?

With limited amounts of material, appropriate utilization is crucial. It is always prudent to anticipate that special stains and immunostains may have to be performed to clinch the diagnosis. Save the larger fragments or retrieve some of the bigger particulate granules from the smeared material for preparation of cell blocks. Results of ancillary studies must always be viewed in light of the larger perspective of the case.

Special Stains

Reticulin

Studying the reticulin framework on cell-block sections stained with Gomori's method is a cheap, simple, and particularly useful way of trying to distinguish WD-HCC from benign hepatocellular nodules. Normal reticulin, present in regenerating/hyperplastic lesions, consists of thick fibers that are regular and fairly parallel, outlining narrow cords (Bergman *et al.,* 1997). All HCCs have deficient or virtually absent reticulin; this is especially so when the trabeculae are broad (de Boer *et al.,* 1999, 2000). This feature can be reasonably demonstrated in small amounts of tissue. The dilemma arises when the malignant lesion has cords that are less than three cells thick. The reticulin in LCAs may or may not be well developed.

Periodic Acid-Schiff with and without Diastase

The periodic acid-Schiff (PAS) pair of stains is usually performed to distinguish epithelial mucin, which is PAS-positive and diastase-resistant, from diastase-labile glycogen, which is likely to be present in both benign and malignant hepatocytes. Mucin, if detected within cytoplasmic vacuoles, implies glandular differentiation. Adenocarcinomatous elements among HCC cells increase the possibility of a combined hepatocellular-cholangiocarcinoma. Diastase-resistant, PAS-positive, alpha-l-antitrypsin globules and fibrinogen can also be exhibited by HCCs.

Iron

Iron appears as dark-brown cytoplasmic granules in Papanicolaou-stained smears and black granules with Giemsa stain. It can be confirmed with Perls' Prussian blue method. The presence of iron pigment in well-differentiated hepatocytes implies benignity.

Fat

Cytoplasmic vacuoles may contain lipid, which can be confirmed with Oil Red O staining of fresh or formalin-fixed tissue. The detection of fat in well-differentiated hepatocytes does not in any way favor benignity. It has been increasingly appreciated that fatty change can be confined solely to the neoplastic lesion and that small HCCs are prone to fatty change resulting from angiogenic incompetence.

Immunohistochemistry

A whole battery of antibodies is available for the comparative immunohistochemical study of liver tumors, but the diagnostic utility varies with the sensitivity and specificity of the antibody as well as the amount of material available. A panel of useful antibodies for the study of HCC and related lesions includes AFP, polyclonal carcinoembryonic antigen (*p*CEA), CD10, Hep Par 1, cytokeratins (CK 7, 8, 18, 19, and 20; CAM 5.2; AE1/AE3), and CD34 (Table 16). Monoclonal CEA (*m*CEA) is usually negative. Markers of cell proliferation, such as proliferating cell nuclear antigen (PCNA) and Ki67, and monoclonal antibody to p53 tumor suppressor gene are not routinely used. Because the issue here is not the confirmation of histogenesis but the ascertainment of malignancy, the antibody panel should comprise at least AFP, *p*CEA, and CD34.

Table 16. Antibody Stains in Study of Hepatocellular Carcinoma

Antibody	Immunostaining Results (%) (Overall, range)	
Alpha-fetoprotein	50	(20–75)
Monoclonal carcinoembryonic antigen	<5	(0–5)
Polyclonal carcinoembryonic antigen	70	(60–95)
Canalicular pattern		
Diffuse cytoplasmic pattern		
CD 10	68	
Hep Par 1	80–100	(40–100)
CAM 5.2	>90	(90–95)
AE1/AE3	20	(5–33)
CK8	Usually positive	
CK18	Usually positive	
CK7	15	(0–25)
CK19	10	(0–20)
CK20	20	(10–30)
CD34	>80	
Alpha-1-antitrypsin	50	(10–80)
Vimentin	5	(0–10)
PCNA	>15	
Ki67	30	(15–50)
p53 gene product	35	(19–59)

Alpha-Fetoprotein

This tumor marker was considered fairly specific but not sensitive for HCCs. However, apart from germ-cell tumors, there is a growing list of AFP-producing hepatoid/nonhepatoid tumors that arise in extrahepatic sites and nonhepatocellular tissues such as gastrointestinal carcinomas, small- and large-cell carcinomas of lung, and carcinomas from urinary and female genital tracts (Wee *et al.,* 2003). The sensitivity of AFP is about 50% (range, 20–75%) (Goldstein and Silverman, 2002; Lau *et al.,* 2002). Tissue AFP immunoreactivity is seen in malignant hepatocytes but not in regenerating, hyperplastic, or benign neoplastic hepatocytes. Staining of the tumor can be patchy and minimal. Positivity has been reported to correlate with HCC grade but not with tumor size; the poorly differentiated tumors have the lowest reactivity rate and the lowest number of cells staining (5–20%). The sensitivity is particularly low at both ends of the histologic spectrum. In this context, AFP often proves to be of little help in the distinction of highly WD-HCC from benign hepatocellular lesions. Although AFP-positive hepatocytes imply malignancy, AFP-negative hepatocytes do not preclude malignancy.

Monoclonal Carcinoembryonic Antigen

There is hardly any staining of HCCs with *m*CEA (range, 0–5%). If present, it is only detectable extremely focally and in the higher grades of HCC (Maeda *et al.,* 1996). Biliary epithelium shows cytoplasmic immunoreactivity.

Polyclonal Carcinoembryonic Antigen

This antibody cross-reacts with biliary glycoprotein I. In normal liver, *p*CEA stains bile canaliculi and ductal epithelium but not hepatocytes. The normal *p*CEA canalicular staining pattern consists of a delicate plexiform network of fine tubules imparting a "chicken-wire" appearance (Wee *et al.,* 1997). Biliary epithelial cells show diffuse cytoplasmic and brush border reactivity. The canalicular patterns in cirrhosis and MRNs are normal. FNH may show focal decrease in canaliculi. This deficiency is more evident in LCA.

HCCs show an overall *p*CEA positivity rate of 70% (range, 60–95%) (Goldstein and Silverman, 2002; Lau *et al.,* 2002). There are two patterns of staining—canalicular pattern and a diffuse cytoplasmic staining

of the tumor cells. In the context of carcinomas, a canalicular pattern is specific for HCC. The canalicular pattern ranges from fewer tubules to irregular, tortuous tubules and cystically dilated pseudoacini. There is an inverse correlation with tumor grade—75% of WD-HCCs show *p*CEA canalicular staining compared to 70% and 25–50% of moderately and poorly differentiated HCCs, respectively. Prominent pseudoacinar formation is usually not evident in benign lesions, including LCA; its presence is suspicious of malignancy. Diffuse cytoplasmic staining of hepatocytes is seen in 50% of HCCs. The results correlate with tumor grade—less than 5% of better differentiated HCCs stain, whereas 20% of poorly differentiated lesions are positive.

CD10

Also called Neprilysin, CD10 is a cell membrane metallopeptidase that participates in the postsecretory processing of neuropeptidase and peptide hormones. Apart from hematopoietic malignancies and a whole host of carcinomas, CD10 is expressed in both normal and neoplastic liver, where it exhibits a similar canalicular staining pattern to *p*CEA (Lau *et al.,* 2002; Morrison *et al.,* 2002). It is, hence, a highly specific marker for hepatocytic differentiation. Comparative studies show that the sensitivity of CD10 reactivity in HCCs (68.3%) is far better than AFP (23.8%) but less than *p*CEA (95.2%) (Borscheri *et al.,* 2001).

Hep Par 1

The diagnostic utility of hepatocyte paraffin 1 monoclonal antibody, Hep Par 1, in labeling cells of hepatocellular origin has been of great interest. This immunostain has been touted as a sensitive marker for hepatocytic differentiation and is now part of the armamentarium used in the immunohistochemical distinction of HCC from cholangiocarcinoma and metastatic carcinomas (Chu *et al.,* 2002; Fan *et al.,* 2003; Lau *et al.,* 2002; Siddiqui *et al.,* 2001; Zimmerman *et al.,* 2001). There is also a high correlation between Hep Par 1 immunoreactivity and albumin *in situ* hybridization. However, it is not specific. Not all Hep Par 1-positive tumors are of hepatocellular origin or arise in the liver. Hepatoid carcinomas from various extrahepatic sites may be the actual primary lesions (Wee *et al.,* 2003).

Normal/regenerating hepatocytes show diffuse 100% Hep Par 1 positivity. There is a uniformly intense, coarse granular cytoplasmic appearance with no discernible localization toward the canalicular surface. Bile-duct epithelium and stromal cells are negative. Variations in Hep Par 1 staining occur when there is fatty, clear-cell (glycogen), or oncoctyic change. Fat vacuoles push the Hep Par 1–positive granules to the periphery of the cells. In glycogen-laden hepatocytes, the granules are more dispersed. Oncocytic hepatocytes tend to exhibit a less intense but more densely packed, somewhat homogeneous, granular look with this antibody.

Macroregenerative and dysplastic nodules as well as FNH and LCA tend to exhibit 100% Hep Par 1 positivity, albeit with some variation in the intensity of staining. It has been reported that about 80–100% of HCCs (range, 40–100%) stain with Hep Par 1 (Siddiqui *et al.,* 2001; Zimmerman *et al.,* 2001). Although 100% of classic HCCs may stain with Hep Par 1, the extent can range from 100% positive cells in WD-HCCs to less than 5% in some poorly differentiated cases, with much variability within the Hep Par 1-positive areas (personal experience). In addition to a similar inverse correlation with tumor grade, other studies also report an association with growth patterns (Chu *et al.,* 2002).

Hep Par 1 does not distinguish WD-HCCs from benign hepatocellular lesions. However, because hepatocellular masses, neoplastic or nonneoplastic, tend to show variations in the intensity and expression of Hep Par 1 in contrast to the strikingly uniform and intense expression in normal/regenerating hepatocytes, this antibody can still contribute to delineating whether or not hepatocytes encountered in small specimens are lesional.

Cytokeratins (CK 7, 8, 18, 19, and 20; CAM 5.2; AE1/AE3)

Mature hepatocytes stain with low molecular weight keratins such as CK8 and 18 and diffusely and strongly with CAM 5.2. They do not stain with CK7, CK19, CK20, or AE1/AE3. Embryonal hepatocytes contain CK8, CK18, and CK19; however, CK19 expression is lost by the 10th week of gestation. Cirrhotic nodules, MRN, FNH, and LCA, have the same cytokeratin profile as normal hepatocytes. In addition, a variable number of hepatocytes adjacent to fibrous septa acquire biliary phenotype by staining with CK7, CK19, and AE1/AE3. These cells represent hepatocyte metaplasia with bile-ductular configuration—reflecting bipotential progenitor cells in human liver regeneration.

CAM 5.2 staining has been reported in 90–95% of HCCs, either diffusely cytoplasmic, membranous, or both (Goldstein *et al.,* 2002). It is the most reliable cytokeratin antibody for HCCs because it stains the highest number of HCC cells of all grades with the strongest intensity.

AE1/AE3 positivity has been reported in 20% of HCCs (range, 5–33%) (Goldstein *et al.,* 2002). The number of positive cases and the number of positive cells per lesion are influenced by tumor grade. Few WD-HCCs are positive compared to 33% of poorly

differentiated lesions. The staining is patchy and isolated and not related to growth patterns. AE1/AE3 negativity weakly favors a diagnosis of HCC if it is used in the context of an antibody panel to distinguish one type of carcinoma from HCC. Benign hepatocellular lesions and WD-HCCs lack AE1/AE3 reactivity.

About 15% (range, 0–25%) of HCCs stain with CK7 (Maeda *et al.,* 1996). CK7 positivity is related to the degree of HCC differentiation—the poorly differentiated tumors yielding the highest percentage of positive cases. CK19 positivity rate is in the region of 10% (range, 0–20%), with mostly focal staining (Lau *et al.,* 2002; Maeda *et al.,* 1996). There is a similar relationship, as in CK7, between HCC grade and number of positive cells. CK20 positivity has been noted in 20% of HCCs (range, 10–30%), with mostly weak and patchy staining (Maeda *et al.,* 1996). Generally, HCCs show no CK20 staining.

Endothelial Markers (CD34, CD31, Factor VIII-Related Antigen, *Ulex Europeus*)

Although hepatocytes themselves, benign or malignant, do not stain with these endothelial markers, these antibodies can be used as discriminant ancillary immunohistochemical markers to distinguish HCC from other carcinomas and from benign hepatocellular masses (Gottschalk-Sabag *et al.,* 1998; Kong *et al.,* 2000). The human hematopoietic progenitor cell antigen, CD34, is an intercellular adhesion protein found in normal endothelium. It is negative in normal hepatic sinusoids. The immunostain highlights regions of sinusoids where the endothelial cells have lost their unique characteristics and have acquired the phenotype of capillary endothelial cells. This process of capillarization involves loss of sinusoidal fenestrae, deposition of basement membrane material (Type IV collagen and laminin), and an increase in CD34 expression. Sinusoidal capillarization occurs in HCCs, even in the small WD-HCCs.

CD34 shows diffuse sinusoidal reactivity in HCCs (82.5%) (de Boer *et al.,* 2000); this is especially helpful in the context of small WD-HCCs. The trabeculae and acini are invested with an encircling endothelial cell layer, even in the absence of well-defined sinusoids. However, significant diffuse sinusoidal CD34 reactivity can occur in LCA (71%) (Figure 42) and FNH (44%), with at least 50% of the masses showing staining (Kong *et al.,* 2000). In cirrhosis and dysplastic nodules, staining is minimal to absent and focal in distribution, mostly confined to the periportal/periseptal regions.

All this implies that caution is advised in the use of these vascular antibodies. The encirclement pattern of CD34-positive endothelial cells around malignant hepatocytes is a useful adjuvant staining pattern favoring an HCC diagnosis, especially in cytologic specimens. CD34 shows the strongest reaction in HCC and stains the fewest endothelial cells in cirrhotic sinusoids. However, one must confine the examination of this marker to the presence or absence of endothelial cells around malignant cells because sinusoids adjacent to metastatic carcinomatous nodules also undergo capillarization with consequent CD34 expression. CD34 reactivity, if used as a criterion for diagnosis, can potentially lead to a false-positive diagnosis of malignancy, especially with small amounts of tissue. A reticulin stain can be used in conjunction with CD34. In benign hepatocellular nodules, be it neoplastic or hyperplastic, the reticulin framework should be intact even in the presence of CD34 positivity (de Boer *et al.,* 2000).

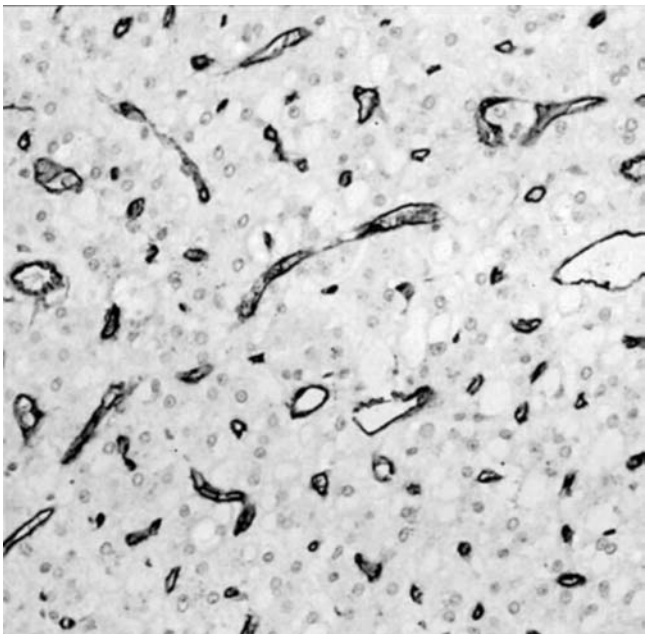

Figure 42. Resection specimen of liver cell adenoma. The tumor shows diffuse sinusoidal CD34 immunoreactivity highlighting the capillarization process. The hepatocytes have normal nuclear-cytoplasmic ratio and are arranged in trabeculae that are generally two cells thick. (Immunostain.)

Other Immunostains

Other immunostains that may be of use are outlined in the following paragraphs.

Smooth Muscle Actin

Generally HCCs are considered hypervascular tumors. However, this is not necessarily so with small HCCs (< 3 cm diameter). The number of intratumoral

arterioles or unpaired arteries increases with enlarging size and increasing dedifferentiation of the HCC. These vessels are sometimes visible as three-dimensional, folded tubular structures with cigar-shaped nuclei of smooth muscle cells. They can be demonstrated in cell-block sections with immunostaining for smooth muscle actin if there is sufficient material.

Alpha-1-Antitrypsin

About 50% of HCCs stain with alpha-1-antitrypsin (A1-AT) (range, 10–80%). The majority of positive cases show extensive staining (Goldstein *et al.,* 2002). A1-AT is also found in numerous other tumors. Hence, it is of no discriminant value.

Vimentin

Vimentin stains up Kupffer cells as spider- or star-shaped cells with multiple elongated and slender cytoplasmic processes, providing a new clue to cytologic diagnosis of primary and metastatic HCC by FNAB (Sharifi *et al.,* 2000). Normal hepatocytes do not stain; HCCs show minimal or no staining with only about 5% (range, 0–10%) exhibiting some staining and almost all occurring in high-grade lesions (Maeda *et al.,* 1996).

Cell Proliferation Markers (PCNA, Ki67)

The marker PCNA is an auxiliary protein of DNA polymerase delta expressed by cycling cells. Its immunolocalization in paraffin sections is an index of cell proliferation. Normal/regenerative livers are either completely negative or minimally immunoreactive (<5% positive nuclei) (Ojanguren *et al.,* 1993). Most WD-HCCs exhibit more than 15% positive nuclei. The PCNA-labeling indices of HCC show a close correlation with histologic findings and biologic behavior. Small-cell change is a small round focus having a proliferative activity similar to that of better-differentiated HCCs. Cell proliferative activity is also noted to be increased in some LCAs. Absent or minimal PCNA immunoreactivity seems to be a useful adjuvant to discriminate normal/regenerating liver from HCC.

The monoclonal antibody, Ki67, reacts with a nuclear protein expressed in the G1, G2, S, and M phases of the cell cycle (Grigioni *et al.,* 1989). The Ki67 scores (positive cells/total neoplastic cells) seem to correlate with the histologic type of hepatocellular nodules. In the HCC group, the proportion of labeled nuclei ranged from 15–50%, showing a good correlation with degree of differentiation. The benign lesions showed a very low growth fraction, similar to that of normal/cirrhotic tissue. The use of the Ki67 score seems to offer useful information about the biological behavior of some liver masses and may aid in the separation of LCA from HCC.

p53 Gene Product

The incidence of mutations of the p53 tumor suppressor gene in HCCs is variable, depending on the etiology. Expression of p53 was reported in 35% of HCCs (range, 19–59%). There appears to be a correlation of p53 overexpression with histologic grades, especially in the less-differentiated areas, implying that overexpression of the presumed mutant p53 may have contributed to dedifferentiation during the development of the HCC. No correlation, however, was noted with tumor size or vascular invasion. There was no expression in benign aspirates (Ojanguren *et al.,* 1995). Immunostaining with a monoclonal antibody to p53 may have some value in enhancing the precision of making a cytodiagnosis of malignancy.

CONCLUSIONS

Several benign hepatocellular nodular lesions can mimic WD-HCC, especially at the highly well-differentiated end of the spectrum. This poses a diagnostic challenge not only on the cytologic level but at the histologic front as well. A multidisciplinary approach to FNAB diagnosis should reduce the number of indeterminate reports.

- **Close clinicopathologic correlation is mandatory.** A history of HBV/HCV infection, alcoholism, chronic liver disease, or oral contraceptive or anabolic/androgenic steroid usage is helpful. A significantly elevated serum AFP is highly suggestive of HCC if other AFP-producing tumors have been ruled out. Imaging findings may be contributory.
- **Stepwise combined cytohistologic assessment is highly recommended.** FNAB diagnosis of hepatocellular nodules calls for attention to architectural and cytologic details in smears/cell blocks. The most specific architectural criteria in smears are broad trabeculae, well-defined capillaries transgressing tissue fragments, and solid cores of hepatocytes rimmed by peripheral endothelium. The most valuable architectural criteria in cell blocks are trabeculae more than two cells thick and reduced or absent reticulin framework. Unpaired vessels, diffuse sinusoidal CD34 reactivity, and abnormal *p*CEA canalicular patterns are helpful. The most useful cytologic features in the smears are a well-spread-out granular appearance on naked eye inspection; hypercellularity; small and monotonous well-differentiated hepatocytes with slightly increased nuclear-cytoplasmic ratio, nuclear crowding, and tendency to dissociate; transgressing sinusoidal

capillaries with visible basement membrane; and lack of bile-duct epithelial clusters.

- **Use of a discriminant panel of special and immunostains is complementary.** The panel of antibodies should include *p*CEA, CD34, and perhaps AFP. Reticulin stain should be part of the routine assessment of cell blocks because it distinguishes more consistently between benign and malignant hepatocellular lesions.
- **Trained expertise goes without saying.** Despite this, there will always be a small residual group of cases that cannot be resolved satisfactorily even to the most well-trained eye. The final diagnosis in the combined cytohistologic report may be worded as either "a hepatocellular neoplasm, unable to distinguish a highly WD-HCC from a LCA" or "a benign hepatocellular lesion, either a MRN associated with cirrhosis or FNH." If the aspirate is suboptimal and the clinical data are wanting, then it may come down to a cytodiagnosis of "benign hepatocellular lesion, MRN, FNH, or LCA." Under such ambiguous circumstances, one can only recommend surgical resection of the mass with wide margins for diagnostic and therapeutic purposes.

References

Bergman, S., Graeme-Cook, F., and Pitman, M.B. 1997. The usefulness of the reticulin stain in the differential diagnosis of liver nodules on fine-needle aspiration biopsy cell block preparations. *Mod. Pathol. 10*:1258–1264.

Bioulac-Sage, P., Balabaud, C., and Wanless, I.R. 2001. Diagnosis of focal nodular hyperplasia: Not so easy. *Am. J. Surg. Pathol. 25*:1322–1325.

Borscheri, N., Roessner, A., and Rocken, C. 2001. Canalicular immunostaining of neprilysin (CD10) as a diagnostic marker for hepatocellular carcinomas. *Am. J. Surg. Pathol. 25*:1297–1301.

Chu, P.G., Ishizawa, S., Wu, E., and Weiss, L.M. 2002. Hepatocyte antigen as a marker of hepatocellular carcinoma: An immunohistochemical comparison to carcinoembryonic antigen, CD 10, and alpha-fetoprotein. *Am. J. Surg. Pathol. 26*:978–988.

Cohen, M.B., Haber, M.M., Holly, E.A., Ahn, D.K., Bottles, K., and Stoloff, A.C. 1991. Cytologic criteria to distinguish hepatocellular carcinoma from nonneoplastic liver. *Am. J. Clin. Pathol. 95*:125–130.

de Boer, W.B., Segal, A., Frost, F.A., and Sterrett, G.F. 1999. Cytodiagnosis of well differentiated hepatocellular carcinoma: Can indeterminate diagnoses be reduced? *Cancer 87*:270–277.

de Boer, W.B., Segal, A., Frost, F.A., and Sterrett, G.F. 2000. Can CD 34 discriminate between benign and malignant hepatocytic lesions in fine-needle aspirates and thin core biopsies? *Cancer 90*:273–278.

Fan, Z., Van De Rijn, M., Montgomery, K., and Rouse, R.V. 2003. Hep Par 1 antibody stain for the differential diagnosis of hepatocellular carcinoma: 676 tumors tested using tissue microarrays and conventional tissue sections. *Mod. Pathol. 16*:137–144.

Ferrell, L., Crawford, J., Dhillon, A., Scheuer, P., and Nakanuma, Y. 1993. Proposal for standardized criteria for the diagnosis of benign, borderline, and malignant hepatocellular lesions arising in chronic advanced liver disease. *Am. J. Surg. Pathol. 17*:1113–1123.

Goldstein, N.S., and Silverman, J.F. 2002. Immunohistochemistry of the gastrointestinal tract, pancreas, bile ducts, gallbladder, and liver. In Dabbs, D.J. (ed). *Diagnostic Immunohistochemistry.* New York: Churchill Livingstone, 374–378.

Gottschalk-Sabag, S., Ron, N., and Glick, T. 1998. Use of CD34 and factor VIII to diagnose hepatocellular carcinoma on fine needle aspirates. *Acta Cytol. 42*:691–696.

Grigioni, W.F., D'Errico, A., Bacci, F., Gaudio, M., Mazziotti, A., Gozzetti, G., and Mancini, A.M. 1989. Primary liver neoplasms: Evaluation of proliferative index using MoAb Ki67. *J. Pathol. 158*:23–29.

Hertz, G., Reddy, V.B., Green, L., Spitz, D., Massarani-Wafai, R., Selvaggi, S.M., Kluskens, L., and Gattuso, P. 2000. Fine-needle aspiration biopsy of the liver: A multicenter study of 602 radiologically guided FNA. *Diagn. Cytopathol. 23*:326–328.

International Working Party. 1995. Terminology of nodular hepatocellular lesions. *Hepatology 22*:983–993.

Ishak, K.G., Goodman, Z.D., and Stocker, J.T. 2001. Tumors of the liver and intrahepatic bile ducts. In *Atlas of Tumor Pathology,* 3rd series, Fascicle 31. Armed Forces Institute of Pathology, Washington, DC, 199–230.

Kong, C.S., Appenzeller, M., and Ferrell, L.D. 2000. Utility of CD34 reactivity in evaluating focal nodular hepatocellular lesions sampled by fine needle aspiration biopsy. *Acta Cytol. 44*:218–222.

Lau, S.K., Prakash, S., Geller, S.A., and Alsabeh, R. 2002. Comparative immunohistochemical profile of hepatocellular carcinoma, cholangiocarcinoma, and metastatic adenocarcinoma. *Hum. Pathol. 33*:1175–1181.

Longchampt, E., Patriache, C., and Fabre, M. 2000. Accuracy of cytology vs. microbiopsy for the diagnosis of well-differentiated hepatocellular carcinoma and macroregenerative nodule. Definition of standardized criteria from a study of 100 cases. *Acta Cytol. 44*:515–523.

Maeda, T., Kajiyama, K., Adachi, E., Takenaka, K., Sugimachi, K., and Tsuneyoshi, M. 1996. The expression of cytokeratins 7, 19, and 20 in primary and metastatic carcinomas of the liver. *Mod. Pathol. 9*:901–909.

Morrison, C., Marsh, W., Jr., and Frankel, W.L. 2002. A comparison of CD10 to pCEA, MOC-31, and Hepatocyte for the distinction of malignant tumors in the liver. *Mod. Pathol. 15*:1279–1287.

Nguyen, B.N., Flejou, J.F., Teris, B., Belghiti, J., and Degott, C. 1999. Focal nodular hyperplasia of the liver: A comprehensive pathologic study of 305 lesions and recognition of new histologic forms. *Am. J. Surg. Pathol. 23*:1441–1454.

Ojanguren, I., Ariza, A., Castella, E.M., Fernandez-Vasalo, A., Mate, J.L., and Navas-Palacios, J.J. 1995. p53 immunoreactivity in hepatocellular adenoma, focal nodular hyperplasia, cirrhosis and hepatocellular carcinoma. *Histopathology 26*:63–68.

Ojanguren, I., Ariza, A., Llatjos, M., Castella, E., Mate, J.L., and Navas-Palacios, J.J. 1993. Proliferating cell nuclear antigen expression in normal, regenerative, and neoplastic liver: A fine-needle aspiration cytology and biopsy study. *Hum. Pathol. 24*:905–908.

Quaglia, A., Bhattacharjya, S., and Dhillon, A.P. 2001. Limitations of the histopathological diagnosis and prognostic assessment of hepatocellular carcinoma. *Histopathology 38*:167–174.

Ruschenburg, I., and Droese, M. 1989. Fine needle aspiration cytology of focal nodular hyperplasia of the liver. *Acta Cytol. 33*:857–860.

Sharifi, S., Hayek, J., Khettry, U., and Nasser, I. 2000. Immunocytochemical staining of Kupffer and endothelial cells in fine needle aspiration cytology of hepatocellular carcinoma. *Acta Cytol. 44*:7–12.

Siddiqui, M.T., Saboorian, M.H., Gokaslan, S.T., and Ashfaq, R. 2001. Diagnostic utility of the HepPar1 antibody to differentiate hepatocellular carcinoma from metastatic carcinoma in fine-needle aspiration samples. *Cancer (Cancer Cytopathol.) 96*:49–52.

Takenaka, A., Kaji, I., Kasugai, H., Sasaki, Y., Ishiguro, S., Wada, A., Horai, T., Otani, T., and Ishikawa, H. 1999. Usefulness of diagnostic criteria for aspiration cytology of hepatocellular carcinoma. *Acta Cytol. 43*:610–616.

Theise, N.D. 1995. Macroregenerative (dysplastic) nodules and hepatocarcinogenesis: Theoretical and clinical considerations. *Semin. Liver Dis. 15*:360–371.

Wee, A., Nilsson, B., Chan-Wilde, C., and Yap, I. 1991. Fine needle aspiration biopsy of hepatocellular carcinoma: Some unusual features. *Acta Cytol. 35*:661–670.

Wee, A., Nilsson, B., Tan, L.K.A., and Yap, I. 1994. Fine needle aspiration biopsy of hepatocellular carcinoma: Diagnostic dilemma at the ends of the spectrum. *Acta Cytol. 38*:347–354.

Wee, A., and Nilsson, B. 2003. Highly well differentiated hepatocellular carcinoma and benign hepatocellular lesions: Can they be distinguished on fine needle aspiration biopsy? *Acta Cytol. 47*:16–26.

Wee, A., and Nilsson, B. 1997. *p*CEA canalicular immunostaining in fine needle aspiration biopsy diagnosis of hepatocellular carcinoma. *Acta Cytol. 41*:1147–1155.

Wee, A., Thamboo, T.P., and Thomas, A. 2003. Alpha-fetoprotein-producing liver carcinomas of primary extrahepatic origin: Fine needle aspiration biopsy experience in 2 cases. *Acta Cytol. 47*:799–808.

Wee, A., and Sampatanukul, P. 2004. Fine needle aspiration cytology of the liver: Diagnostic algorithms. A Southeast Asian perspective. Bangkok, Thailand: Year Book Publisher. Available at http://cai.md.chula.ac.th/pichet.

Zeppa, P., Anniciello, A., Vetrani, A., and Palombini, L. 2002. Fine needle aspiration biopsy of hepatic focal fatty change: A report of two cases. *Acta Cytol. 46*:567–570.

Zimmerman, R.L., Burke, M.A., Young, N.A., Solomides, C.C., and Bibbo, M. 2001. Diagnostic value of hepatocyte paraffin 1 antibody to discriminate hepatocellular carcinoma from metastatic carcinoma in fine needle-aspiration biopsies of the liver. *Cancer (Cancer Cytopathol.) 93*:288–291.

14

Immunohistochemical Detection of EBAG9/RCAS1 Expression in Hepatocellular Carcinoma

Taku Aoki, Hiroshi Imamura, Masatoshi Makuuchi, and Satoshi Inoue

Introduction

Identification of EBAG9/RCAS1

Estrogen receptor–binding fragment-associated gene 9 (*EBAG9*) is an estrogen-responsive gene that has been isolated from a CpG island library of MCF-7 human breast cancer cells by the genomic binding-site cloning method (Watanabe *et al.,* 1998). The complementary deoxyribonucleic acid (cDNA) of human EBAG9 encodes an open reading frame (ORF) of 213 amino acids. An estrogen-responsive element (ERE) is located in the 5′ flanking region of the EBAG9 gene, and its transcript is directly up-regulated by estrogen (Tsuchiya *et al.,* 2001; Watanabe *et al.,* 1998).

The receptor-binding cancer antigen expressed on SiSo cells (RCAS1) was originally isolated as the antigen recognized by 22-1-1 antibody against human uterine adenocarcinoma cell line SiSo (Sonoda *et al.,* 1996) and was later found to be identical to EBAG9 (EBAG9/RCAS1) (Nakashima *et al.,* 1999). Based on *in vitro* observation, RCAS1 has been assumed to act as a ligand for a putative receptor present on normal peripheral lymphocytes, such as T, B, and natural killer (NK) cells. RCAS1 has also been found to inhibit the growth of activated $CD3^+$ T lymphocytes and NK cells and to induce apoptotic cell death (Nakashima *et al.,* 1999). Based on these observations, it has been speculated that EBAG9/RCAS1 is involved in the escape of tumor cells from immune system action.

EBAG9/RCAS1 Expression in Normal Tissue and Cancer Tissue

Two antibodies have been used to assess the expression of EBAG9/RCAS1 in various tissues and cell lines. The first is the 22-1-1 monoclonal antibody established by cell fusion between mouse myeloma cells and spleen cells derived from mice immunized with human uterine cervical adenocarcinoma cell line, SiSo (Sonoda *et al.,* 1996). Immunoreactivity to this antibody has been detected in normal human tissues, such as uterine endometrial glands (Sonoda *et al.,* 2000), goblet cells of bronchi and bronchioles (Iwasaki *et al.,* 2000; Izumi *et al.,* 2001), and gastric mucosa (Kubokawa *et al.,* 2001). Immunoreactivity has also been reported in various cancer tissues, including cancer of the uterus (Kaku *et al.,* 1999; Sonoda *et al.,* 1996; Sonoda *et al.,* 1998; Sonoda *et al.,* 2000), ovary (Sonoda *et al.,* 1996), lung (Iwasaki *et al.,* 2000; Izumi *et al.,* 2001; Oizumi *et al.,* 2002), stomach (Kubokawa *et al.,* 2001), skin (Takahashi *et al.,* 2001), gallbladder (Oshikiri *et al.,* 2001), esophagus (Nakakubo *et al.,* 2002), pancreas (Hiraoka *et al.,* 2002), bile duct

(Enjoji *et al.,* 2002; Suzuoki *et al.,* 2002), and liver (Noguchi *et al.,* 2001).

We raised a rabbit polyclonal anti-EBAG9 antibody against a glutathione-*S*-transferase (GST)-EBAG9 fusion protein (Tsuchiya *et al.,* 2001), and the antibody has been shown to react with human and mouse EBAG9 and yield a 32-kD band in Western Blot analysis. The intensity of the band has been shown to be reduced by prior incubation of the antibody with recombinant EBAG9 protein (Suzuki *et al.,* 2001). Immunostaining with this polyclonal antibody has shown that EBAG9 is expressed in various tissues from normal mice, including liver (Tsuchiya *et al.,* 2001), and tissues from normal humans, such as mammary gland tissue (Suzuki *et al.,* 2001) and prostate tissue (Takahashi *et al.,* 2003). EBAG9 has also been shown to be widely distributed in human breast cancer and prostate cancer (Suzuki *et al.,* 2001; Takahashi *et al.,* 2003).

Because the reports referred to earlier have documented that expression of EBAG9/RCAS1 is more remarkable in cancer tissues than in normal tissues, EBAG9/RCAS1 has attracted attention as a potential cancer-associated antigen. Its expression is generally thought to be related to tumor invasiveness and to be associated with poor patient prognosis in cancer of the uterus (Kaku *et al.,* 1999), lung (Iwasaki *et al.,* 2000; Izumi *et al.,* 2001; Oizumi *et al.,* 2002), gallbladder (Oshikiri *et al.,* 2001), esophagus (Nakakubo *et al.,* 2002), pancreas (Hiraoka *et al.,* 2002), bile duct (Suzuoki *et al.,* 2002), and prostate (Takahashi *et al.,* 2003).

Stepwise Evolution of Hepatocellular Carcinoma and EBAG9/RCAS1 Expression in Hepatocellular Carcinoma

Hepatocellular carcinoma (HCC) is one of the most common malignancies worldwide, ranking 5th in frequency in the world (Parkin *et al.,* 2001). Although HCC is more prevalent in Asia and Africa, its incidence is on the rise in Western countries (El-Serag and Mason, 1999; El-Serag *et al.,* 2003; Taylor-Robinson *et al.,* 1997). The condition HCC has the unique characteristic of developing and progressing in a typical multistep manner—that is, from early HCC (Liver Cancer Study Group of Japan, 2000; Takayama *et al.,* 1998), through early-advanced HCC, to advanced HCC (Kojiro and Nakashima, 1999). Most early HCCs are small, well-differentiated nodules with low proliferative activity, but when they progress to a more advanced stage, they transform into moderately to poorly differentiated cancers and undergo a rapid increase in size. During this process (tumor dedifferentiation and proliferation), HCCs acquire malignant potential as reflected by intrahepatic metastasis and vascular invasion (see later discussion). This transformation occurs nonuniformly within a given tumor nodule, resulting in the simultaneous presence of well-differentiated and moderately to poorly differentiated lesions within the same nodule. This produces what histologists refer to as a "nodule-in-nodule" or "mosaic" appearance (Kojiro and Nakashima, 1999). As mentioned earlier, HCC frequently invades blood vessels, especially the portal system, resulting in intrahepatic metastasis. Many previous reports have documented vascular invasion and intrahepatic metastasis as unfavorable prognostic factors.

In this chapter, we describe immunohistochemical detection of EBAG9/RCAS1 expression in noncancerous liver tissue and in HCC tissue, especially the methodologic aspects. We used a rabbit polyclonal anti-EBAG9 antibody (Tsuchiya *et al.,* 2001). In view of the pathologic features of HCC and the results of previous studies on EBAG9/RCAS1 as a cancer marker, we paid particular attention to the multistep evolution of HCC, including the following: 1) process of tumor dedifferentiation, 2) cancer proliferative activity, and 3) ability to metastasize. The overall results have previously been reported by our group elsewhere (Aoki *et al.,* 2003).

MATERIALS

Liver Samples

Samples of HCC tissue and adjacent noncancerous liver tissue from 143 cases of HCC were analyzed immunohistochemically. Testing for hepatitis B virus surface antigen was positive in 23 patients, and testing for anti-hepatitis C virus (HCV) antibody was positive in 100 patients. The liver tissue was obtained during surgery in our department between October 1994 and December 1998. Ten liver biopsy specimens obtained for preoperative evaluation of potential liver transplant donors, and 10 liver biopsy specimens obtained to assess patients who were serologically anti-HCV antibody positive were also made available for the analysis as noncancerous samples. The biopsy specimens from the patients who were HCV antibody positive were kindly provided by Dr. Jyunichi Fukushima (Department of Pathology, Teikyo University School of Medicine, Tokyo, Japan).

Materials for Immunohistochemistry

1. 10% formalin for fixation.
2. Xylene: for dewaxing.
3. Ethanol: diluted to 50%, 70%, 90%, and 95% with distilled water.

4. Tris-buffered saline (TBS): 6.06 g TRIZMA Base and 8.77 g NaCl; brought to a volume of 1 L with deionized distilled water and adjusted to pH 7.6 with HCl.

5. 10 mM Na-citrate solution (pH 6.0): 2.10 g citric acid brought to a volume of 1 L with deionized distilled water and adjusted to pH 6.0 with 6 M NaOH.

6. 0.3% hydrogen peroxide (H_2O_2) in 100% methanol: 150 ml of 100% methanol was mixed with 1.5 ml of 30% H_2O_2.

7. Fetal calf serum (FCS): stored at −20°C.

8. Primary antibody: rabbit polyclonal anti-EBAG9 antibody (Tsuchiya *et al.,* 2001) diluted 1:40 in 10% FCS-TBS or normal rabbit immunoglobulin (IgG) diluted 1:800 in 10% FCS-TBS.

9. Envision (Dako, Glostrup, Denmark; for rabbit polyclonal antibody).

10. 3,3′-diaminobenzidine tetrahydrochloride (DAB) working solution mixed with Tris-HCl (pH 7.5) and 0.02% H_2O_2.

11. 50% Mayer's hematoxylin: for counterstaining.

METHOD

Liver Tissue Preparation

Resected liver specimens were fixed in 10% formalin, cut into blocks, and embedded in paraffin. They were then sliced into 4-μm sections and mounted on glass slides.

Protocol for EBAG9/RCAS1 Immunostaining

1. Dip the slides in xylene for 3 min 3×.
2. Dip the slides in 100% ethanol for 3 min 2×.
3. Dip the slides in 95% ethanol for 3 min 2×.
4. Rinse the slides in TBS for 5 min.
5. Dip the slides in 10 mM Na-citrate solution (pH 6.0) and then heat them in an autoclave at 125°C for 5 min.
6. Rinse the slides in TBS for 5 min. at room temperature.
7. Block endogenous peroxide by dipping the slides in 0.3% hydrogen peroxide (H_2O_2) in 100% methanol for 30 min.
8. Rinse the slides in TBS for 5 min 3×.
9. Block nonspecific binding by incubating the sections in 10% FCS-TBS for 30 min in a moist chamber.
10. Incubate the sections in primary antibody (rabbit polyclonal antibody for EBAG9) or control rabbit IgG diluted in 10% FCS-TBS in a moist chamber at 4°C overnight.
11. Wash the slides quickly in TBS 3× at room temperature.
12. Rinse the slides in TBS for 5 min.
13. Incubate the sections in Envision (Dako; for rabbit polyclonal antibody) for 1 hr in a moist chamber at room temperature.
14. Rinse the slides in TBS for 5 min 3× at room temperature.
15. Visualize the staining with 3,3′-DAB: apply the working solution and stop the reaction as soon as adequate color develops (usually 2–3 min).
16. Counterstain the sections in 50% Mayer's hematoxylin.
17. Wash the slides in tap water for 5 min.
18. Dip the slides in graded ethanol solutions (50%, 70%, 90%, and 100%) and then in xylene (each for 3 min).
19. Place coverslips on the sections. They are now ready for final examination under a light microscope.

RESULTS AND DISCUSSION

EBAG9 Expression in Normal and Chronically Diseased Liver

Noncancerous hepatocytes, including hepatocytes from normal liver, chronic HCV-related hepatitis, or cirrhotic liver, displayed a low but significant level of EBAG9 immunoreactivity (Figure 43a). High-power magnification revealed punctate staining concentrated specifically near the cell membrane bordering adjacent hepatocytes (not shown). The distribution of the EBAG9 staining was homogeneous and regular throughout the tissue, suggesting that it becomes localized in the cells.

EBAG9/RCAS1 has been detected in various normal human tissues, e.g., uterine endometrial glands (Sonoda *et al.,* 2000), goblet cells of bronchi and bronchioles (Iwasaki *et al.,* 2000; Izumi *et al.,* 2001), mammary glands (Suzuki *et al.,* 2001), and gastric mucosa (Kubokawa *et al.,* 2001), suggesting that EBAG9/RCAS1 is expressed and secreted by gland cells. Thus, the polarity of EBAG9/RCAS1 expression in noncancerous liver tissue suggests that it is related to some physiologic function, e.g., glandular secretion, in normal liver tissue.

EBAG9 Expression in Hepatocellular Carcinoma

EBAG9 Expression at the Cell Level

The EBAG9 immunoreactivity of HCC cells varied. Some exhibited weak immunoreactivity, similar to that of noncancerous hepatocytes (enhancement-negative cells) (Figure 43b), whereas others displayed enhanced immunoreactivity (enhancement-positive cells)

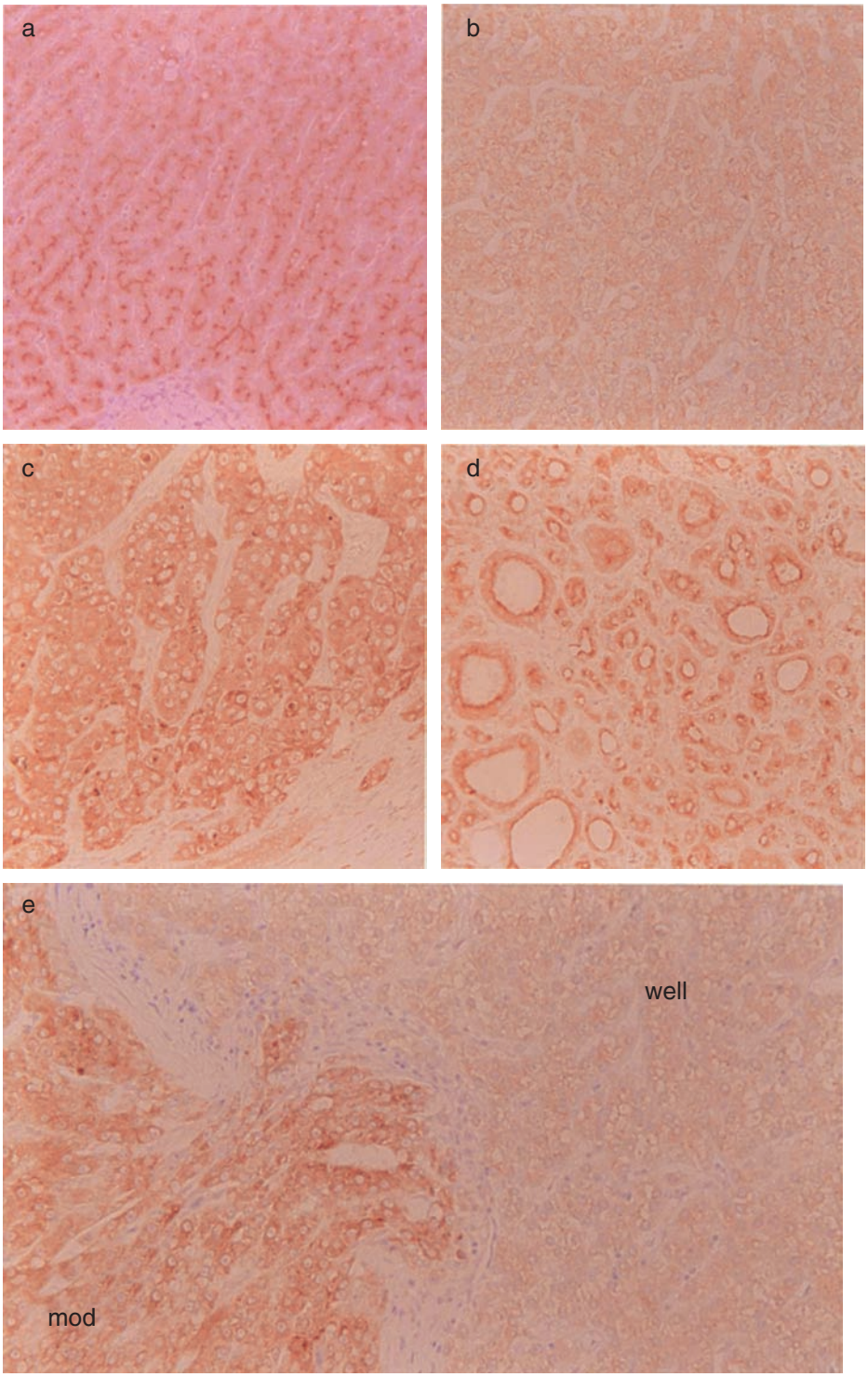

Figure 43. **a:** Normal liver tissue showing weak EBAG9 immunoreactivity. The staining pattern is homogeneous and regular throughout the tissue (200X). **b:** A well differentiated hepatocellular carcinoma (HCC) classified as EBAG9-negative. The pattern of expression is similar to the pattern in noncancerous tissue (200X). **c:** An EBAG9-positive case of moderately differentiated HCC (trabecular type) (200X). Immunoreactivity is detected over the entire surface of the cancer cells and in their cytoplasm. **d:** Pseudoglandular type of moderately differentiated HCC displaying intense expression on the apical surface of the cells (200X). **e:** A tumor with a "nodule-in-nodule" appearance showing intense staining in the interior, moderately differentiated region ("mod"), contrasting with weak staining in the outer, well-differentiated region ("well") (100X).

(Figure 43c). The staining pattern in enhancement-negative cancer cells showed regular distribution of EBAG9-positive granules, similar to the pattern in noncancerous hepatocytes. By contrast, in the majority of enhancement-positive cells there was intense staining over the entire surface of the cell as well as in the cytoplasm. Coarse, thickened granules were dispersed throughout the cytoplasm, and the regularity of the granule distribution noted in the noncancerous hepatocytes was lost. This finding was consistent with observations in the cells of invasive ductal carcinoma of the breast showing that normal mammary gland cells expressed EBAG9/RCAS1 only on their apical surface, whereas carcinoma cells exhibit enhanced expression without a polar distribution (Suzuki *et al.,* 2001). The apical surfaces of the pseudoglands stained strongly in the pseudoglandular type of moderately differentiated HCC (Figure 43d).

Intranodular Distribution of Enhanced EBAG9 Immunoreactivity

The proportion and distribution of enhancement-positive cancer cells were highly variable from nodule to nodule (range 5–100%). It is interesting that, "nodule-in-nodule" tumors, i.e., those consisting of a combination of well-differentiated lesion and a less-differentiated lesion, displayed different immunoreactivity in the two regions, with the less-differentiated intensely immunoreactive region contrasting clearly with the weakly immunoreactive well-differentiated region (Figure 43e).

Semiquantitative Classification of EBAG9 Expression in Hepatocellular Carcinoma Sections

Based on the observations described earlier, HCC section was classified in a semiquantitative manner as follows:

1. Negative (−): sections in which all the cancer cells were identified as enhancement-negative.
2. Borderline (±): sections in which 1–5% of the malignant cells were enhancement-positive, or, sections showing uniformly positive but very weak immunoreactivity.
3. Positive (+): sections in which more than 5% of enhancement-positive cancerous cells.

As a result, 35 of the 143 sections examined (24.5%) were classified as negative, 24 (16.8%) as borderline, and 84 (58.7%) as positive.

Correlation between EBAG9 Expression and Pathologic Variables

For purposes of analysis, the borderline group and negative group were combined and compared with the positive group. The relationship between EBAG9 immunoreactivity and various clinicopathologic parameters was analyzed by comparing the EBAG9-positive group (n = 84) with the EBAG9-negative/borderline group (n = 59), as shown in Table 17. Enhanced EBAG9 immunoreactivity was more frequently observed in the less-differentiated tumors (P = 0.01), and EBAG9 immunoreactivity was significantly correlated with the Ki-67 labeling index. However, there was no significant correlation between enhanced EBAG9 expression and tumor invasiveness (Kosuge *et al.,* 1993; intrahepatic metastasis and/or vascular invasion) (P = 0.86). No other clinical or pathologic variables were significantly correlated with enhanced EBAG9 expression, and no significant correlation was established between enhanced EBAG9 expression and disease-free survival evaluated by the Kaplan-Meier method and log-rank test (P = 0.17) (Figure 44).

EBAG9/RCAS1 Expression in the Process of Stepwise Hepatocellular Carcinoma Progression

Our results showed that enhanced EBAG9/RCAS1 expression is closely correlated with degree of tumor differentiation and increased Ki-67 labeling index. Ki-67 is now widely used as a marker of cell proliferation, including in human studies (Gerdes *et al.,* 1984; Scholzen and Gerdes, 2000). Thus, our findings suggest that enhanced EBAG9/RCAS1 expression is associated with HCC tumor progression as represented by dedifferentiation and proliferation. It is interesting that, tumors showing a "nodule-in-nodule" appearance displayed intense expression in the less-differentiated region and weak expression in the more highly differentiated region (Figure 43e), suggesting that enhancement of EBAG9/RCAS1 expression parallels tumor dedifferentiation.

In contrast to a previous report (Noguchi *et al.,* 2001), EBAG9/RCAS1 was unassociated with tumor metastasis in our series. All of our results lead us to conclude that EBAG9/RCAS1 is closely associated with tumor dedifferentiation and proliferation but not with tumor metastasis. In other words, EBAG9/RCAS1 appears to be more related to growth of the primary tumor than to development of tumor metastases. Our results therefore imply that enhanced EBAG9/RCAS1 expression is an intermediate event in the multistep progression of HCC and is unrelated to the final event, which is characterized by the frequent occurrence of vascular invasion and resultant intrahepatic metastasis. Because enhanced EBAG9 expression was not significantly associated with patient disease-free survival, EBAG9 may not be a prognostic factor in patients with HCC. Nevertheless, we consider it to be of value as a

Table 17. Association between EBAG9 Immunoreactivity and Clinicopathologic Parameters

Parameters	Number of Patients	Intensity of EBAG9 Immunoreactivity Negative/Borderline (%)	Positive (%)	*P*
Age (years)[a]		62.2±11.6	61.8±10.6	.44
<65	75	28 (37.3)	47 (62.7)	
≥65	68	31 (45.6)	37 (54.4)	.39
Sex				
Male	107	40 (37.4)	67 (62.6)	
Female	36	19 (52.8)	17 (47.2)	.12
HBsAg				
+	23	10 (43.5)	13 (56.5)	
–	120	49 (40.8)	71 (59.2)	.82
HCV Ab				
+	100	42 (42.0)	58 (58.0)	
–	43	17 (39.5)	26 (60.5)	.85
Child-Turcotte-Pugh Score				
A	110	43 (39.1)	67 (60.9)	
B	33	16 (48.5)	17 (51.5)	.42
AFP (ng/ml)[b]		51 [2-436000]	55 [2-69000]	.57
≤20	48	17 (35.4)	31 (64.6)	
>20	95	42 (44.2)	53 (55.8)	.37
DCP (AU/ml)[b]		62.5 [11-80000]	76.0 [10-77520]	.10
≤62.5	76	36 (47.4)	40 (52.6)	
>62.5	67	23 (34.3)	44 (65.7)	.12
Degree of tumor differentiation				
Well	25	16 (64.0)	9 (36.0)	
Moderately/poorly	118	43 (36.4)	75 (63.6)	.01
Tumor size (cm)[a]		2.8 [0.8-15.5]	3.4 [1.0-16.0]	.29
≤2.0	38	20 (52.6)	18 (47.4)	
>2.0	105	39 (37.1)	66 (62.9)	.12
Tumor number				
Solitary	79	35 (44.3)	44 (55.7)	
Multifocal	64	24 (37.5)	40 (62.5)	.49
IM and/or VI				
Positive	58	23 (39.6)	35 (60.3)	
Negative	85	36 (42.4)	49 (57.6)	.86
Fibrous capsular formation/infiltration				
Positive/positive	79	30 (38.0)	49 (62.0)	
Positive/negative	27	13 (48.1)	14 (51.9)	
Negative	37	16 (43.2)	21 (56.8)	.62
Background liver disease				
Liver fibrosis	5	1 (20.0)	4 (80.0)	
Chronic hepatitis	40	13 (32.5)	27 (67.5)	
Liver cirrhosis	98	45 (45.9)	53 (54.1)	.21
	143	59 (41.3)	84 (58.7)	

[a]Data expressed as average ± SD

[b]Data expressed as median value [range]

HBsAg, HBsAg-positive; HCV Ab, HCV Ab-positive; AFP, alpha-fetoprotein; DCP, des-γ-carboxy prothrombin; IM, intrahepatic metastasis; VI, vascular invasion

Cited from Reference Aoki *et al.,* 2003 with permission.

pathologic marker of a specific stage of HCC tumor progression.

In conclusion, we observed weak but discretely localized expression of EBAG9/RCAS1 in noncancerous normal and chronically diseased liver tissue, suggesting that EBAG9/RCAS1 is expressed in a positionally regulated fashion. We also found enhanced expression in about half of the HCCs examined, and we found that the enhanced expression was characterized by loss of the localized staining pattern. Enhanced EBAG9/RCAS1 expression was correlated with tumor dedifferentiation and proliferation and not with metastasis.

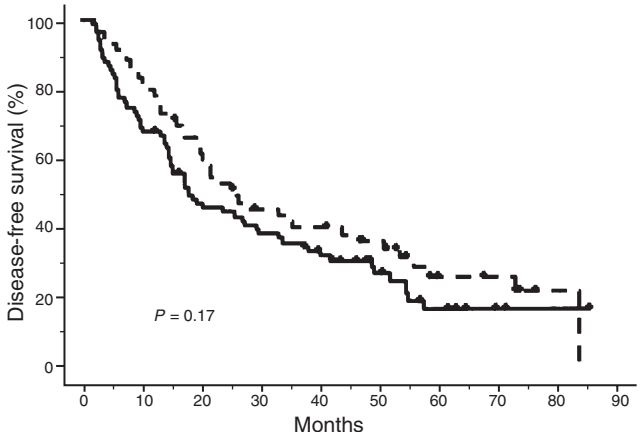

Figure 44. The Kaplan-Meier curves for disease-free survival in the EBAG9-positive group (*solid line, n* = 84) and EBAG9-negative/borderline group (*broken line, n* = 59). There is no significant difference between the two groups ($P = 0.17$).

Future investigation of EBAG9/RCAS1 function should help clarify the mechanism of HCC progression.

References

Aoki, T., Inoue, S., Imamura, H., Fukushima, J., Takahashi, S., Urano, T., Hasegawa, K., Ogushi, T., Ouchi, Y., and Makuuchi, M. 2003. EBAG9/RCAS1 expression in hepatocellular carcinoma: Correlation with tumour dedifferentiation and proliferation. *Eur. J. Cancer 39*:1552–1561.

Enjoji, M., Nakashima, M., Nishi, H., Choi, I., Oimomi, H., Sugimoto, R., Kotoh, K., Taguchi, K., Nakamuta, M., Nawata, H., and Watanabe, T. 2002. The tumor-associated antigen, RCAS1 can be expressed in immune-mediated diseases as well as in carcinomas of biliary tract. *J. Hepatol. 36*:786–792.

El-Serag, H.B., and Mason, A.C. 1999. Rising incidence of hepatocellular carcinoma in the United States. *N. Engl. J. Med. 340*:745–750.

El-Serag, H.B., Davila, J.A., Peterson, N.J., and McGlynn, K.A. 2003. The continuing increase in the incidence of hepatocellular carcinoma in the United States: An update. *Ann. Intern. Med. 139*:817–823.

Gerdes, J., Lemke, H., Baisch, H., Wacker, H.H., Schwab, U., and Stein, H. 1984. Cell cycle analysis of a cell proliferation-associated human nuclear antigen defined by the monoclonal antibody Ki-67. *J. Immunol. 133*:1710–1715.

Hiraoka, K., Hida, Y., Miyamoto, M., Oshikiri, T., Suzuoki, M., Nakakubo, Y., Shinohara, T., Itoh, T., Shichinohe, T., Kondo, S., Kasahara, N., and Katoh, H. 2002. High expression of tumor-associated antigen RCAS1 in pancreatic ductal adenocarcinoma is an unfavorable prognostic marker. *Int. J. Cancer 99*:418–423.

Iwasaki, T., Nakashima, M., Watanabe, T., Yamamoto, S., Inoue, Y., Yamanaka, H., Matsumura, A., Iuchi, K., Mori, T., and Okada, M. 2000. Expression and prognostic significance in lung cancer of human tumor-associated antigen RCAS1. *Int. J. Cancer 89*:488–493.

Izumi, M., Nakanishi, Y., Yoshino, I., Nakashima, M., Watanabe, T., and Hara, N. 2001. Expression of tumor-associated antigen RCAS1 correlates significantly with poor prognosis in nonsmall cell lung carcinoma. *Cancer 92*:446–451.

Kaku, T., Sonoda, K., Kamura, T., Hirakawa, T., Sakai, K., Amada, S., Ogawa, S., Kobayashi, H., Nakashima, M., Watanabe, T., and Nakano, H. 1999. The prognostic significance of tumor-associated antigen 22-1-1 expression in adenocarcinoma of the uterine cervix. *Clin. Cancer Res. 5*:1449–1453.

Kojiro, M., and Nakashima, O. 1999. Histopathologic evaluation of hepatocellular carcinoma with special reference to small early stage tumors. *Semin. Liver Dis. 19*:287–296.

Kosuge, T., Makuuchi, M., Takayama, T., Yamamoto, J., Shimada, K., and Yamasaki, S. 1993. Long-term results after resection of hepatocellular carcinoma: Experience of 480 cases. *Hepato-gastroenterol. 40*:328–332.

Kubokawa, M., Nakashima, M., Yao, T., Ito, K., Harada, N., Nawata, H., and Watanabe, T. 2001. Aberrant intracellular localization of RCAS1 is associated with tumor progression of gastric cancer. *Int. J. Oncol. 19*:695–700.

Liver Cancer Study Group of Japan. 2000. *The General Rules for the Clinical and Pathological Study of Primary Liver Cancer.* 4th ed. Tokyo: Kanehara & Co. Ltd., 28–34.

Nakakubo, Y., Hida, Y., Miyamoto, M., Hashida, H., Oshikiri, T., Kato, K., Suzuoki, M., Hiraoka, K., Ito, T., Morikawa, T., Okushiba, S., Kondo, S., and Katoh, H. 2002. The prognostic significance of RCAS1 expression in squamous cell carcinoma of the oesophagus. *Cancer Lett. 177*:101–105.

Nakashima, M., Sonoda, K., and Watanabe, T. 1999. Inhibition of cell growth and induction of apoptotic cell death by the human tumor-associated antigen RCAS1. *Nat. Med. 5*:938–942.

Noguchi, K., Enjoji, M., Nakamuta, M., Nakashima, M., Nishi, H., Choi, I., Taguchi, K., Kotoh, K., Shimada, M., Sugimachi, K., Tsuneyoshi, M., Nawata, H., and Watanabe, T. 2001. Expression of a tumor-associated antigen RCAS1 in hepatocellular carcinoma. *Cancer Lett. 168*:197–202.

Oizumi, S., Yamazaki, K., Nakashima, M., Watanabe, T., Hommura, F., Ogura, S., Nishimura, M., and Dosaka-Akita, H. 2002. RCAS1 expression: A potential prognostic marker for adenocarcinoma of the lung. *Oncology 62*:333–339.

Oshikiri, T., Hida, Y., Miyamoto, M., Hashida, H., Katoh, K., Suzuoki, M., Nakakubo, Y., Hiraoka, K., Shinohara, T., Itoh, T., Kondo, S., and Katoh, H. 2001. RCAS1 as a tumour progression marker: An independent negative prognostic factor in gallbladder cancer. *Br. J. Cancer 85*:1922–1927.

Parkin, D.M., Bray, F., Ferlay, J., and Pisani, P. 2001. Estimating the world cancer burden: GLOBOCAN 2000. *Int. J. Cancer 94*:153–156.

Scholzen, T., and Gerdes, J. 2000. The Ki-67 protein: From the known and the unknown. *J. Cell Physiol. 182*:311–322.

Sonoda, K., Nakashima, M., Kaku, T., Kamura, T., Nakano, H., and Watanabe, T. 1996. A novel tumor-associated antigen expressed in human uterine and ovarian carcinomas. *Cancer 77*:1501–1509.

Sonoda, K., Kaku, T., Kamura, T., Nakashima, M., Watanabe, T., and Nakano, H. 1998. Tumor-associated antigen 22-1-1 expression in the uterine cervical squamous neoplasias. *Clin. Cancer Res. 4*:1517–1520.

Sonoda, K., Kaku, T., Hirakawa, T., Kobayashi, H., Amada, S., Sakai, K., Nakashima, M., Watanabe, T., and Nakano, H. 2000. The clinical significance of tumor-associated antigen RCAS1 expression in the normal, hyperplastic, and malignant uterine endometrium. *Gynecol. Oncol. 79*:424–429.

Suzuki, T., Inoue, S., Kawabata, W., Akahira, J., Moriya, T., Tsuchiya, F., Ogawa, S., Muramatsu, M., and Sasano, H. 2001.

EBAG9/RCAS1 in human breast carcinoma: A possible factor in endocrine-immune interactions. *Br. J. Cancer 85*:1731–1737.

Suzuoki, M., Hida, Y., Miyamoto, M., Oshikiri, T., Hiraoka, K., Nakakubo, Y., Shinohara, T., Itoh, T., Okushiba, S., Kondo, S., and Katoh, H. 2002. RCAS1 expression as a prognostic factor after curative surgery for extrahepatic bile duct carcinoma. *Ann. Surg. Oncol. 9*:388–393.

Takahashi, H., Iizuka, H., Nakashima, M., Wada, T., Asano, K., Ishida-Yamamoto, A., and Watanabe, T. 2001. RCAS1 antigen is highly expressed in extramammary Paget's disease and in advanced stage squamous cell carcinoma of the skin. *J. Dermatol. Sci. 26*:140–144.

Takahashi, S., Urano, T., Tsuchiya, F., Fujimura, T., Kitamura, T., Ouchi, Y., Muramatsu, M., and Inoue, S. 2003. EBAG9/RCAS1 expression and its prognostic significance in prostatic cancer. *Int. J. Cancer 106*:310–315.

Takayama, T., Makuuchi, M., Hirohashi, S., Sakamoto, M., Yamamoto, J., Shimada, K., Kosuge, T., Okada, S., Takayasu, K., and Yamasaki, S. 1998. Early hepatocellular carcinoma as an entity with a high rate of surgical cure. *Hepatology 28*:1241–1246.

Taylor-Robinson, S.D., Foster, G.R., Arora, S., Hargreaves, S., and Thomas, H.C. 1997. Increase in primary liver cancer in the UK, 1979–94. *Lancet 350*:1142–1143.

Tsuchiya, F., Ikeda, K., Tsutsumi, O., Hiroi, H., Momoeda, M., Taketani, Y., Muramatsu, M., and Inoue, S. 2001. Molecular cloning and characterization of mouse EBAG9, homolog of a human cancer associated surface antigen: Expression and regulation by estrogen. *Biochem. Biophys. Res. Commun. 284*:2–10.

Watanabe, T., Inoue, S., Hiroi, H., Orimo, A., Kawashima, H., and Muramatsu, M. 1998. Isolation of estrogen-responsive genes with a CpG island library. *Mol. Cell Biol. 18*:442–449.

15

Hepatocellular Carcinoma of Differential Viral Origin: Analysis by Oligonucleotide Microarray

Norio Iizuka, Hisafumi Yamada-Okabe, Yoshihiko Hamamoto, and Masaaki Oka

Introduction

With an estimated 564,000 new cases registered in 2000 (Parkin *et al.,* 2001), hepatocellular carcinoma (HCC) is one of the most common cancers, and it represents a major international health problem because its incidence is increasing in many countries (Okuda, 2000). The major risk factors for development of HCC are well known. Among these risk factors, hepatitis B and C virus (HBV and HCV) infections are highly correlated with the pathogenesis of HCC (Llovet *et al.,* 2003; Okuda, 2000); most HCC cases are attributable to infection with one of these two viruses. Given that there are ~400 million HBV carriers and ~170 million HCV carriers throughout the world (Cohen, 1999; Conjeevaram and Lok, 2003), elucidation of the molecular mechanism of hepatitis virus–mediated HCC would greatly benefit medical practice worldwide.

The HBV strain is a partially double-stranded hepatotropic deoxyribonucleic acid (DNA) virus belonging to the Hepadnaviridae family (Szabo *et al.,* 2004). It is generally accepted that the majority of HBV-related HCCs contain the HBV DNA sequence integrated into the cellular chromosomal DNA (Okuda, 2000), suggesting that viral integration may act as a random insertional mutagen, which leads to or contributes to secondary chromosomal rearrangements such as inversions, translocations, or deletions. The hepadnaviral genome contains four promoters, two enhancers, and two transactivating elements. Among these, it has been shown that the HBx protein is related to the development of HCC in transgenic mice (Kim *et al.,* 1991), suggesting that HBV plays a direct carcinogenic role in HCC.

The HCV strain is a pesti-like and flavi-like virus that possesses a single-stranded (ribonucleic acid) RNA as genome. The HCV genome encodes a single polyprotein precursor of ~3000 amino acids (Choo *et al.,* 1989) that is cleaved by both host and viral proteases, generating at least 10 individual proteins, core, El, E2, p7, NS2, NS3, NS4A, NS4B, NS5A, and NS5B (Clarke, 1997; Simmonds, 2001). Among these, the HCV core protein is associated with the development of HCC in transgenic mice (Moriya *et al.,* 1998); however, there is little inflammation in the surrounding liver tissues in this model, and its features are likely to differ from those of human hepatocarcinogenesis. In addition, HCV itself has less direct influence on hepatocarcinogenisis than does HBV, because HCV is not capable of inducing integration of its genome into the host chromosomal DNA. Thus, despite intense research efforts in this field, a number of important issues related to HBV- and HCV-mediated disease progression remain unclear.

DNA microarray analysis is a state-of-the art, high-throughput technology that has ushered in a new era in

Handbook of Immunohistochemistry and *in situ* Hybridization of Human Carcinomas, Volume 3: Molecular Genetics, Liver Carcinoma, and Pancreatic Carcinoma

the medical sciences (DeRisi *et al.,* 1996; Golub *et al.,* 1999; Schena *et al.,* 1995). Many studies using this technology have detected pathogenesis-related genes in human HCCs (Smith *et al.,* 2003; Xu *et al.,* 2001a). These studies may contribute to our understanding of the molecular basis of HCC; however, there are many problems such as sample bias, differences in algorithms, and differences in DNA microarrays used. In particular, patients with HCC have various backgrounds and divergent clinical courses, resulting in much heterogeneity among tumor samples examined (Figure 45). Unlike *in vitro* studies with cell lines, in analyzing the transcriptome in human HCC tissues, it is crucial to take interpatient heterogeneity into consideration. With this in mind, we have used a supervised learning method to identify molecular signatures related to the pathogenesis of HCC (Figure 45) (Iizuka *et al.,* 2002; Iizuka *et al.,* 2003a; Iizuka *et al.,* 2003b, Okada *et al.,* 2003).

In our studies, we have identified distinct differences in gene expression patterns between HBV positive HCCs (B-type HCCs) and HCV-positive HCCs (C-type HCCs) (Iizuka *et al.,* 2002; Iizuka *et al.,* 2003a). More recently, we analyzed gene expression profiles of HBV- and HCV-negative HCCs (non-B, non-C HCCs) with similar microarrays and compared the gene expression patterns of non-B, non-C HCCs with those of B- and C-type HCCs using a supervised learning method (Iizuka *et al.,* 2004a). The results of these studies provide a framework to better understand the pathogenesis of HCCs of differential viral origins and to provide

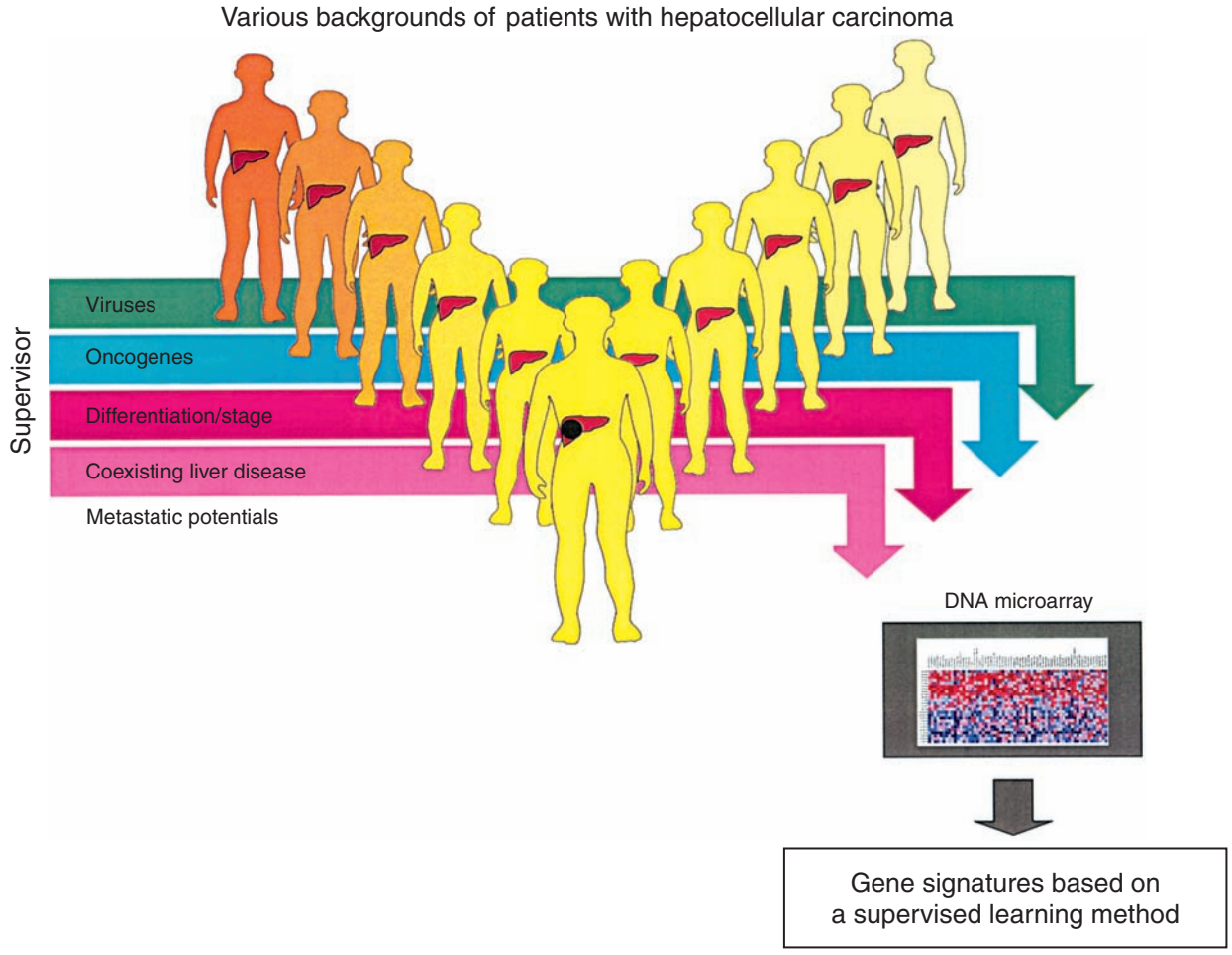

Figure 45. Gene selection based on various backgrounds between patients with hepatocellular carcinoma (HCC). Patients with HCC have various backgrounds and divergent clinical course, resulting in much heterogeneity between tumor samples examined. Unlike *in vitro* study with cell lines, in analyzing transcriptome in human cancer tissues, it is crucial to take this interpatient heterogeneity into consideration. With this concept in mind, we have used a supervised learning method (the Fisher ratio and random permutation test; see the Materials and Methods section) to identify molecular signature related to the background.

additional markers and molecular targets for the diagnosis and treatment of each type of HCC. The molecular basis of HCCs of differential viral origins is discussed with respect to molecular profiling.

MATERIALS AND METHODS

Hepatocellular Carcinoma Samples

We used 56 HCC samples to analyze the levels of expression of approximately 6000 genes by DNA microarray (Iizuka *et al.,* 2002; Iizuka *et al.,* 2003a; Iizuka *et al.,* 2004a). Surgical specimens were obtained from 56 patients who underwent surgical treatment for HCC at Yamaguchi University Hospital between May 1997 and August 2000. Written informed consent was obtained from all patients before surgery. The study protocol was approved by the Institutional Review Board for Human Use at Yamaguchi University School of Medicine. Histopathologic diagnosis of HCC was made after surgery in each case. Of the 56 patients, 14 were positive for serum HBs antigen (Ag) (B-type HCC), 31 were positive for HCV antibody (Ab) (C-type HCC), and 11 were negative for both HBsAg and HCV Ab (non-B, non-C HCC).

Control Liver Samples

Six nontumorous liver samples (Iizuka *et al.,* 2004b) were obtained from patients who underwent hepatic resection for benign liver tumor or metastatic liver tumor, which derive from gastrointestinal cancer. Liver function of each of these six patients was shown to be normal, and the liver of each was shown to be histopathologically normal. All six patients were seronegative for both HBsAg and HCV Ab.

Sample Preparation

All tumorous and nontumorous liver samples from each patient were immediately divided into several sections (~125 mm^3) after resection (Iizuka *et al.,* 2002; Iizuka *et al.,* 2003a). One section was fixed in 10% formalin, embedded in paraffin, and stained with hematoxylin-eosin for pathologic diagnosis. Another was frozen in liquid nitrogen for complementary DNA (cDNA) microarray analysis and stored at –80°C until use. All specimens were suspended in Sepasol-RNAI (Nacalai Tesque, Tokyo, Japan) and homogenized twice with a Polytron (5 sec at maximum speed). After extraction with chloroform and precipitation by EtOH, the total RNA was purified with the use of an RNeasy Mini Kit (QIAGEN, Tokyo, Japan) according to the manufacture's instructions. The quality of the total RNA was judged from the ratio of 28S to 18S ribosomal RNAs after agarose gel electrophoresis.

Complementary DNA Synthesis and *in vitro* Translation for Labeled Complementary RNA Probe

The cDNA was synthesized with the reverse SuperScript Choice System (Invitrogen Life Technologies, Carlsbad, CA) according to the manufacturer's instructions. Purified total RNA (5 μg) was hybridized with an oligo-dT primer containing the sequences for the T7 promoter and 200 units of Super ScriptII reverse transcriptase and incubated at 42°C for 1 hr. The resulting cDNA was extracted with phenol/chloroform and purified with Phase Lock Gel Light (Eppendorf, Tokyo, Japan). The cRNA was also synthesized with the use of a MEGAscript T7 kit (Ambion, Austin, TX) with the cDNA as a template according to the manufacturer's instructions. Approximately 5 μg of the cDNA was incubated with T7 polymerase, 7.5 mM each of adenosine triphosphate (ATP) and guanosine triphosphate (GTP), 5.625 mM each of cytidine triphosphate (CTP) and uridine triphosphastase (UTP), and 1.875 mM each of Bio-11-CTP and Bio-16-UTP (Roche Biochemicals, Tokyo, Japan) at 37°C for 6 hr. Mononucleotides and short oligonucleotides were removed by column chromatography on a CHROMA SPIN +STE-100 column (Clontech, Tokyo, Japan).

Gene Expression Analysis by High-Density Oligonucleotide Array

Gene expression patterns were examined by high-density oligonucleotide array (HuGeneFL array, Affymetrix, Santa Clara, CA). For hybridization to oligonucleotides on the chips, the cRNA was fragmented at 95°C for 35 min in a buffer containing 40 mM Tris-acetate (pH 8.1), 100 mM potassium acetate, and 30 mM magnesium acetate. Hybridization was performed in 200 μl of buffer containing 0.1 M 2-(*N*-morpholino) ethanesulfonic acid (MES) (pH 6.7), 1 M NaCl, 0.01% Triton X-100, 20 μg herring sperm DNA, 100 μg acetylated bovine serum albumin, 10 μg fragmented cRNA, and biotinylated-control oligonucleotides at 45°C for 12 hr. After being washed with a buffer containing 0.01 M MES (pH 6.7), 0.1 M NaCl, and 0.001% Triton X-100, the chips were incubated with biotinylated anti-streptavidin antibody and stained with streptavidin R-phycoerythrin (Molecular Probes, Eugene, OR) as described in the instruction manual (Affymetrix) to increase hybridization signals. Each pixel intensity was collected by a laser scanner (Affymetrix), and the

expression levels and reliability (Present/Absent call) of each cDNA were calculated with software (Affymetrix GeneChip version 3.3 and Affymetrix Microarray Suite version 4.0). For statistical analysis of gene expression in tumors and normal tissues, StatView 4.5 was used to perform Mann-Whitney U-tests.

Procedure for Gene Selection

We filtered genes to compare the three types of HCC (B-, C-, non-B, and non-C types) as follows. First, we investigated all genes whose mean average difference in one type of HCC (e.g., B-type) was more than double that in another type of HCC (e.g., C-type or non-B, non-C type). Subsequently, we selected genes that showed average expression levels of >20 (arbitrary units from Affymetrix) in both groups in each comparison. This filtering yielded 169, 283, and 157 genes comparing B-type HCC versus C-type HCC; non-B, non-C HCC versus B-type HCC; and non-B, non-C HCC versus C-type HCC, respectively. We then ranked the selected genes in order of decreasing magnitude of the Fisher ratio in each comparison. For example, the Fisher ratio to evaluate separability between B- and C-type HCCs is calculated as follows. The Fisher ratio for gene i is given by:

$$\mathrm{F}(i) = \frac{(\mu_{BT}(i) - \mu_{CT}(i))^2}{P(BT)\sigma^2_{BT}(i) + P(CT)\sigma^2_{CT}(i)}$$

where $\mu_{BT}(i)$ and $\sigma^2_{BT}(i)$ are the sample mean and sample variance, respectively, of the expression levels of gene i for the samples in B-type HCC (BT). $P(BT)$ is the *a priori* probability of *BT*. The Fisher ratio measures the difference between two means normalized by the average variance. Thus, the Fisher ratio represents the ability of a gene to discriminate the two types of HCC. As a final step, we ranked D selected genes by the Fisher ratio as follows:

$$F(i_1) > F(i_2) > \cdots > F(i_D)$$

To decide how many genes should be considered, we used a random permutation test (Iizuka *et al.,* 2002; Iizuka *et al.,* 2003a). In this test, sample labels were randomly permutated between each group, and the Fisher ratio for each gene was computed again. This random permutation of sample labels was repeated 1000 times. The Fisher ratios generated from the actual data were then assigned P values based on the distribution of the Fisher ratios from the randomized data. From the distribution of these Fisher ratios, the top 83 genes with Fisher ratios >0.40 were considered to show statistically significant differences in expression ($P < 0.05$) between B-type HCC and C-type HCC. In the same manner, we selected the top 112 genes with Fisher ratios >0.64 ($P < 0.05$) between non-B, non-C HCC and B-type HCC and the top 64 genes with Fisher ratios >0.48 ($P < 0.05$) between non-B, non-C HCC and C-type HCC. Finally, gene expression data from tumor tissues were compared with those from the six nontumorous liver specimens.

Statistical Analysis

Fisher's exact test and ANOVA (analysis of variance) with Fisher's PLSD (protected least-significant difference) test were used to analyze differences in patient and tumor characteristics among patients with non-B, non-C HCC; B-type HCC; and C-type HCC. $P < 0.05$ was considered to be significant.

RESULTS AND DISCUSSION

Clinicopathologic Characteristics of the Three Types of Hepatocellular Carcinomas

Patients with B-type HCC were significantly younger than patients with C-type HCC and patients with non-B, non-C HCC ($P < 0.01$ for both by ANOVA with Fisher's PLSD test). All 11 patients with non-B, non-C HCC were male. This frequency was significantly higher than that of B-type HCC ($P < 0.05$ by Fisher's exact test). We found no significant differences in other clinicopathologic features or tumor characteristics among the three groups.

Genes Selected in Each Comparison

Our gene selection yielded 83, 112, and 64 genes with expression levels that differed significantly for B-type HCC versus C-type HCC; non-B, non-C HCC versus B-type HCC; and non-B, non-C HCC versus C-type HCC. Of the 83 discriminatory genes for B-type versus C-type HCC, 31 showed increased expression and 52 showed decreased expression in B-type HCC compared to that in C-type HCC. Of the 112 discriminatory genes for non-B, non-C versus B-type HCC, 49 showed increased expression and 63 showed decreased expression in non-B, non-C HCC compared to that in B-type HCC. Of the 64 discriminatory genes for non-B, non-C versus C-type HCC, 43 showed increased expression and 21 showed decreased expression in non-B, non-C HCC compared to that in C-type HCC. Levels of expression of 12 genes in non-B, non-C HCC differed significantly from those in both B- and C-type HCCs. Likewise, levels of expression of 27 genes were specific to B-type HCC, and levels of expression of 6 genes were specific to C-type HCC. In addition, an interferon-inducible gene, *IFI27*, was expressed

differentially in all three types of HCC. Thus, using a supervised learning method, we successfully profiled genes that characterize HCCs of differential viral origin. Characteristic features are summarized in the following.

Molecular Features of B-type Hepatocellular Carcinoma

Expression of imprinted genes (*H19* and *IGF2*) was up-regulated in B-type HCC in comparison to expression in C-type HCC. In addition, *H19* expression was up-regulated in B-type HCC in comparison to non-B, non-C HCC. *H19* and *IGF2* are located close to each other on chromosome 11p15.5, and they are regulated by the loss of imprinting. Graveel *et al.* (2001) reported altered expression levels of several genes in a diethylnitrosamine-induced hepatocarcinogenesis model as determined by DNA microarray analysis. Among the genes listed in that report, up-regulation of *H19* expression in mouse HCC corresponded to characteristic features of B-type HCC in our series. *H19* is an untranslated gene, and its biological function remains unclear. IGF2 is a known autocrine growth factor for many malignant tumors (Sohda *et al.,* 1998).

Expression of *H19* and *IGF2* is reported to be coordinately up-regulated in HCC (Sohda *et al.,* 1998). Our study showed up-regulated expression of these genes specifically in B-type HCC, suggesting that up-regulation of the *IGF-2* pathway plays an important role in the pathogenesis of B-type HCC but not of C-type HCC or non-B, non-C HCC. Our 2003 study (Iizuka *et al.,* 2003a) confirmed and extended this finding. Namely, among the cases of B-type HCC, *IGF2* expression was up-regulated in tumors arising from noncirrhotic liver but not from cirrhotic liver. Because *IGF2* is an imprinted gene, its up-regulated expression in B-type HCC patients without liver cirrhosis (LC) may be caused by an epigenetic mechanism. Notably, *IGFBP3*, a putative negative regulator of the IGF signal pathway, showed down-regulated expression in B-type HCC patients without LC (Iizuka *et al.,* 2003a). Taken together, the data suggest that stimulation of the IGF signal pathway plays a central role in the development of B-type HCC, particularly when it arises from noncirrhotic liver.

The expression levels of many detoxification-related genes (*NNMT, UGT2B7, CYP2E, ADHIB, AKR1D1,* and *metallothionein*) were decreased in B-type HCC in comparison to levels in the other types of HCC, and nontumorous liver contained higher levels of the messenger RNA (mRNA) for these genes. The results for *CYPIIE* were consistent with those obtained in a previous microarray study (Okabe *et al.,* 2001). *ADH* and *CYP* family genes are also reported to be down-regulated in HCC in comparison to expression in nontumorous liver tissue (Xu *et al.,* 2001b). Thus, it is likely that blockade of the detoxification system is a common pathway during carcinogenesis or progression of HCC. Moreover, markedly reduced levels of detoxification-related genes in B-type HCC suggest that HBV-infected liver could be more susceptible than HCV-infected liver and nonvirus-infected liver to various xenobiotics or carcinogens.

Other characteristic features of B-type HCC include the down-regulated expression of genes related to the immune response including inflammation. The majority of HBV-related HCCs contain the HBV DNA sequence integrated into the cellular chromosomal DNA (Okuda, 2000), supporting the concept of a direct carcinogenic effect on infected liver. For example, it has been reported that the HBx protein alone is related to the development of HCC in transgenic mice (Kim *et al.,* 1991). In this regard, development of HBV-induced HCC depends less on inflammation of the liver than does development of HCV- or nonvirus-induced HCC. As a result, it appears that the relatively decreased expression of genes related to immune response is a hallmark of B-type HCC.

B-type HCC showed lower expression levels of several metabolism-related genes (*ABAT*, *GYS2*, and *TAT*) than did the other types of HCC. By contrast, the levels of expression of *acid phosphatase 5* (*ACP5*), which is known to play a role in the differentiation of normal human monocytes to macrophages (Lord *et al.,* 1990), were higher than in the other types of HCC. The role of this gene product in the development of HCC remains unclear. Because serum ACP5 activity may be a useful marker for the early detection of the metastasis of breast cancer cells to bone (Halleen, 2003), *ACP5* may serve as a surrogate marker for metastasis caused by B-type HCC.

Molecular Features of C-type Hepatocellular Carcinoma

The most intriguing feature of C-type HCC was the increase in expression levels of many immune response-related genes. In keeping with a previous study (Okabe *et al.,* 2001), we found up-regulation of the NK receptor in C-type HCC versus B-type HCC. Among the 52 genes up-regulated in C-type HCC. *C15, IFI27, C6,* and *OAS1* showed the larger Fisher ratios, suggesting that C-type HCC is closely related to the immune response, particularly to inflammation. Thus, regarding immune response–related genes, C-type HCC showed expression patterns opposite those of B-type HCC. Additionally, C-type HCC showed higher expression levels of interferon-inducible genes than the other types of HCC. For example, interferon-inducible genes (*IFI27, OAS1, IFI15,* and *IFIT4*) showed up-regulated expression in C-type

HCC by more than twofold and 1.5-fold versus B-type HCC and nontumorous liver, respectively. *IFI27, IFIT1, IFIT4,* and *IFI15* expression was also up-regulated in C-type HCC by more than twofold versus non-B, non-C HCC. Because interferon (IFN) is induced by double-stranded RNA species, it is reasonable that up-regulation of these IFN-inducible genes is the consequence of the generation of double-stranded RNA by infection with HCV. Accumulated evidence has also shown that IFNs are effective not only for cancer prevention but also for treatment of developing HCC when combined with anticancer agents such as 5-fluorouracil (Leung, 1999). Considering that IFN pathways are exclusively involved in C-type HCC, our present data indicate that IFN therapy may exert its anti-tumor activity preferentially in C-type HCC.

It is interesting that only six genes were specific to C-type HCC and that the number was smaller than that for B-type and non-B, non-C HCCs . Although this result may be in part a result of a difference in sample size of each type of HCC, it is logical to assume that many pathways are involved in HCV-related hepatocarcinogenesis. The HCV is an RNA virus that is not reverse-transcribed to DNA and the HCV genome does not integrate into the cellular genome. It contributes to carcinogenesis by causing inflammation such as chronic hepatitis or LC (Okuda, 2000). Our previous profiling data (Iizuka *et al.,* 2003a) showed that the number of genes whose expression differed significantly between tumors arising from noncirrhotic and cirrhotic livers was 89 in B-type HCC; in contrast, it was only 8 in C-type HCC. Thus, the idea that HCV-related carcinogenesis depends on many pathways may explain the heterogeneity among patients with C-type HCC, resulting in a small number of genes whose expression is commonly altered in this type of HCC. The time lag between HCV infection and cancer development can be several decades. HCV-associated tumors usually arise in older people and are almost always associated with cirrhosis. Thus, it is apparent that C-type HCC is closely related to chronic inflammation (Shimotohno, 2000), suggesting that the immune response–related genes identified here may serve as molecular targets for chemoprevention and for treatment of C-type HCC.

Molecular Features of Non-B, Non-C Hepatocellular Carcinoma

As mentioned earlier, the occurrence of most HCCs can be explained by either HBV or HCV infection. However, some types of HCC may be the result of other factors such as aflatoxin Bl or alcoholic or non-alcoholic steatohepatitis (NASH), which have attracted a great deal of attention as inducers or coinducers of HCC. Occult HBV infection is also related to HCC with negative HBV and HCV serology. Thus, the non-B, non-C HCC samples used here are likely to have resulted from various etiologic factors. Our gene selection yielded 112 and 64 genes whose expression levels differed significantly in comparing non-B, non-C HCC versus B-type HCC and non-B, non-C HCC versus C-type HCC, respectively. Expression of 12 genes was specific to non-B, non-C HCC, suggesting that HCC can be classified into three types according to viral origin. Thus, our profiling data yield a new paradigm for HCC. Although recent developments in DNA microarray technology have yielded a number of gene expression profiles related to subclasses of HCC, there have been no studies that examined the molecular characteristics of HCC without HBV or HCV.

Comparison of non-B, non-C HCC and B- or C-type HCC enabled us to identify target genes specific to this type of HCC. Expression of protease inhibitor genes such as *SERPINB1* and *neutrophil lipocalin* was markedly higher in non-B, non-C HCC than in B- and C-type HCCs and in nontumorous livers. Because tumor growth in a tissue is restricted by extracellular protease/protease inhibitor interactions (Bratt, 2000), these two genes could be molecular targets for non-B, non-C HCC. It is interesting that expression of *RPSS3* and *FURIN,* which promote proteolysis and peptidolysis, was lower in non-B, non-C HCC than in the other two types of HCC. The protein encoded by *FURIN* belongs to the subtilisin-like proprotein convertase family. Some of its substrates include proparathyroid hormone, transforming growth factor beta 1 precursor, proalbumin, and membrane type-1 matrix metalloproteinase. Thus, altered activity of proteolysis and peptidolysis is a hallmark of non-B, non-C HCC.

Expression of *CYR61* in non-B, non-C HCC differed significantly from that in B- and C-type HCCs. Expression of *ITGAM* and *CTGF* was up-regulated in non-B, non-C HCC in comparison to expression in C-type HCC. ITGAM is an adhesion receptor for *CYR61* (*CCN1*) and *CTGF* (*CCN2)* gene products expressed on peripheral blood monocytes (Schober *et al.,* 2002). Thus, changes of these three genes may reflect changes in stromal cells specific to the pathogenesis of non-B, non-C HCC.

NQO1 expression was up-regulated significantly in non-B, non-C HCC versus B- and C-type HCCs. *NQO1* encodes a xenobiotic-metabolizing enzyme that detoxifies quinones derived from the oxidation of phenolic metabolites of benzene (Smith, 1999). Benzene derivatives have been reported to cause liver cancer in rodent models (Ito *et al.,* 1975). Up-regulation of *NQO1* expression in HCC has also been reported

(Strassburg *et al.,* 2002). Some environmental carcinogens induce expression of this gene (Jaiswal, 2000); therefore, it is likely that these *NQO1*-related carcinogens promote the pathogenesis of non-B, non-C HCC more strongly than they promote that of B- and C-type HCCs.

There were significant differences in sex and age between patients with non-B, non-C HCC and patients with B-type HCC in the present study. Such differences actually exist among patients with HCC with distinct etiologic backgrounds, and they will yield more divergent results if DNA chip technology is applied to larger sample sizes. Further studies are needed to clarify how differences or biases in patient backgrounds (e.g., sex, age, duration of viral infection, alcohol consumption) affect gene selection, and clarification of these complicated features in individual patients with HCC will aid in the development of personalized medicines.

References

Bratt, T. 2000. Lipocalins and cancer. *Biochim. Biophys. Acta 1482*:318–326.

Choo, Q.L., Kuo, G., Weiner, A.J., Overby, L.R., Bradley, D.W., and Houghton, M. 1989. Isolation of a cDNA clone derived from a blood-borne non-A, non-B viral hepatitis genome. *Science 244*:359–362.

Clarke, B. 1997. Molecular virology of hepatitis C virus. *J. Gen. Virol. 78*:2397–2410.

Cohen, J. 1999. The scientific challenge of hepatitis C. *Science 285*:26–30.

Conjeevaram, H.S., and Lok, A.S. 2003. Management of chronic hepatitis B. *J. Hepatol. 38*:S90–S103.

DeRisi, J., Penland, L., Brown, P.O., Bittner, M.L., Meltzer, P.S., Ray, M., Chen, Y., Su, Y.A., and Trent, J.M. 1996. Use of a cDNA microarray to analyse gene expression patterns in human cancer. *Nat. Genet. 14*:457–460.

Golub, T.R., Slonim, D.K., Tamayo, P., Huard, C., Gaasenbeek, M., Mesirov, J.P., Coller, H., Loh, M.L., Downing, J.R., Caligiuri, M.A., Bloomfield, C.D., and Lander, E.S. 1999. Molecular classification of cancer: Class discovery and class prediction by gene expression monitoring. *Science 286*:531–537.

Graveel, C.R., Jatkoe, T., Madore, S.J., Holt, A., and Land Farnham, P.J. 2001. Expression profiling and identification of novel genes in hepatocellular carcinomas. *Oncogene 20*: 2704–2712.

Halleen, J.M. 2003. Tartrate-resistant acid phosphatase 5B is a specific and sensitive marker of bone resorption. *Anticancer Res. 23*:1027–1029.

Iizuka, N., Oka, M., Yamada-Okabe, H., Mori, N., Tamesa, T., Okada, T., Takemoto, N., Tangoku, A., Hamada, K., Nakayama, H., Miyamoto, T., Uchimura, S., and Hamamoto, Y. 2002. Comparison of gene expression profiles between hepatitis B virus- and hepatitis C virus-infected hepatocellular carcinoma by oligonucleotide microarray data on the basis of a supervised learning method. *Cancer Res. 62*:3939–3944.

Iizuka, N., Oka, M., Yamada-Okabe, H., Mori, N., Tamesa, T., Okada, T., Takemoto, N., Hashimoto, K., Tangoku, A., Hamada, K., Nakayama, H., Miyamoto, T., Uchimura, S., and Hamamoto, Y. 2003a. Differential gene expression in distinct virologic types of hepatocellular carcinoma: Association with liver cirrhosis. *Oncogene 22*:3007–3014.

Iizuka, N., Oka, M., Yamada-Okabe, H., Nishida, M., Maeda, Y., Mori, N., Takao, T., Tamesa, T., Tangoku, A., Tabuchi, H., Hamada, K., Nakayama, H., Ishitsuka, H., Miyamoto, T., Hirabayashi, A., Uchimura, S., and Hamamoto, Y. 2003b. Oligonucleotide microarray for prediction of early intrahepatic recurrence of hepatocellular carcinoma after curative resection. *Lancet 361*:923–929.

Iizuka, N., Oka, M., Yamada-Okabe, H., Hamada, K., Nakayama, H., Mori, N., Tamesa, T., Okada, T., Takemoto, N., Matoba, K., Takashima, M., Sakamoto, K., Tangoku, A., Miyamoto, T., Uchimura, S., and Hamamoto, Y. 2004a. Molecular signature in three types of hepatocellular carcinoma with different viral origin by oligonucleotide microarray. *Int. J. Oncol. 24*:565–574.

Iizuka, N., Oka, M., Hamamoto, Y., Mori, N., Tamesa, T., Okada, T., Takemoto, N., Matoba, K., Takashima, M., Sakamoto, K., Tangoku, A., Miyamoto, T., Uchimura, S., Nakayama, H., Hamada, K., and Yamada-Okabe, H. 2004b. Altered levels of cytochrome P450 genes in hepatitis B or C virus-infected liver identified by oligonucleotide microarray. *Cancer Genom. Proteom. 1*:53–58.

Ito, N., Nagasaki, H., Aoe, H., Sugihara, S., and Miyata, Y. 1975. Development of hepatocellular carcinomas in rats treated with benzene hexachloride. *J. Natl. Cancer. Inst. 54*:801–805.

Jaiswal, A.K. 2000. Regulation of genes encoding NAD(P)H: Quinone oxidoreductases. *Free Radic. Biol. Med. 29*:254–262.

Kim, C.M., Koike, K., Saito, I., Miyamura, T., and Jay, G. 1991. HBx gene of hepatitis B virus induces liver cancer in transgenic mice. *Nature 351*:317–320.

Leung, T.W., Patt, Y.Z., Lau, W.Y., Ho, S.K., Yu, S.C., Chan, A.T., Mok, T.S., Yeo, W., Liew, C.T., Leung, N.W., Tang, A.M., and Johnson, P.J. 1999. Complete pathological remission is possible with systemic combination chemotherapy for inoperable hepatocellular carcinoma. *Clin. Cancer Res. 5*:1676–1681.

Llovet, J.M., Burroughs, A., and Bruix, J. 2003. Hepatocellular carcinoma. *Lancet 362*:1907–1917.

Lord, D.K., Cross, N.C.P, Bevilacqua, M.A., Rider, S.H., Gorman, P.A., Groves,V., Moss, D.W., Sheer, D., and Cox, T.M. 1990. Type 5 acid phosphatase: Sequence, expression and chromosomal localization of a differentiation-associated protein of the human macrophage. *Eur. J. Biochem. 189*:287–293.

Moriya, K., Fujie, H., Shintani, Y., Yotsuyanagi, H., Tsutsumi, T., Ishibashi, K., Matsuura, Y., Kimura, S., Miyamura, T., and Koike, K. 1998. The core protein of hepatitis C virus induces hepatocellular carcinoma in transgenic mice. *Nat. Med. 4*:1065–1067.

Okabe, H., Satoh, S., Kato, T., Kitahara, O., Yanagawa, R., Yamaoka, Y., Tsunoda, T., Furukawa, Y., and Nakamura, Y. 2001. Genome-wide analysis of gene expression in human hepatocellular carcinomas using cDNA microarray: Identification of genes involved in viral carcinogenesis and tumor progression. *Cancer Res. 61*:2129–2137.

Okada, T., Iizuka, N., Yamada-Okabe, H., Mori, N., Tamesa, T., Takemoto, N., Tangoku, A., Hamada, K., Nakayama, H., Miyamoto, T., Uchimura, S., Hamamoto, Y., and Oka, M. 2003. Gene expression profile linked to p53 status in hepatitis C virus-related hepatocellular carcinoma. *FEBS Lett. 555*: 583–590.

Okuda, K. 2000. Hepatocellular carcinoma. *J. Hepatol. 32*:225–237.

Parkin, D.M., Bray, F.I., and Devesa, S.S. 2001. Cancer burden in the year 2000: The global picture. *Eur. J. Cancer 37*:S4–S66.

Schena, M., Shalon, D., Davis, R.W., and Brown, P.O. 1995. Quantitative monitoring of gene expression patterns with a complementary DNA microarray. *Science 270*:467–470.

Schober, J.M., Chen, N., Grzeszkiewicz, T.M., Jovanovic, I., Emeson, E.E., Ugarova, T.P., Ye, R.D., Lau, L.F., and Lam, S.C.

2002. Identification of integrin alpha (M) beta(2) as an adhesion receptor on peripheral blood monocytes for Cyr61(CCN1) and connective tissue growth factor (CCN2): Immediate-early gene products expressed in atherosclerotic lesions. *Blood 99*:4457–4465.

Shimotohno, K. 2000. Hepatitis C virus and its pathogenesis. *Semin. Cancer Biol. 10*:233–240.

Simmonds, P. 2001. The origin and evolution of hepatitis viruses in humans. *J. Gen. Virol. 82*:693–712.

Smith, M.T. 1999. Benzene, NQO1, and genetic susceptibility to cancer. *Proc. Natl. Acad. Sci. USA 96*:7624–7626.

Smith, M.W., Yue, Z.N., Geiss, G.K., Sadovnikova, N.Y., Carter, V.S., Boix, L., Lazaro, C.A., Rosenberg, G.B., Bumgarner, R.E., Fausto, N., Bruix, J., and Katze, M.G. 2003. Identification of novel tumor markers in hepatitis C virus-associated hepatocellular carcinoma. *Cancer Res. 63*:859–864.

Sohda, T., Iwata, K., Soejima, H., Kamimura, S., Shijo, H., and Yun, K. 1998. In situ detection of insulin-like growth factor II (IGF2) and H19 gene expression in hepatocellular carcinoma. *J. Hum. Genet. 43*:49–53.

Strassburg, A., Strassburg, C.P., Manns, M.P., and Tukey, R.H. 2002. Differential gene expression of NAD(P)H: Quinone oxidoreductase and NRH: Quinone oxidoreductase in human hepatocellular and biliary tissue. *Mol. Pharmacol. 61*:320–325.

Szabo, E., Paska, C., Kaposi, Novak, P., Schaff, Z., and Kiss, A. 2004. Similarities and differences in hepatitis B and C virus induced hepatocarcinogenesis. *Pathol. Oncol. Res.10*:5–11.

Xu, L., Hui, L., Wang, S., Gong, J., Jin, Y., Wang, Y., Ji, Y., Wu, X., Han, Z., and Hu, G. 2001a. Expression profiling suggested a regulatory role of liver-enriched transcription factors in human hepatocellular carcinoma. *Cancer Res. 61*:3176–3181.

Xu, X.R., Huang, J., Xu, Z.G., Qian, B.Z., Zhu, Z.D., Yan, Q., Cai, T., Zhang, X., Xiao, H.S., Qu, J., Liu, F., Huang, Q.H., Cheng, Z.H., Li, N.G., Du, J.J., Hu, W., Shen, K.T., Lu, G., Fu, G., Zhong, M., Xu, S.H., Gu, W.Y, Huang, W., Zhao, X.T., Hu, G.X., Gu, J.R., Chen, Z., and Han, Z.G. 2001b. Insight into hepatocellular carcinogenesis at transcriptome level by comparing gene expression profiles of hepatocellular carcinoma with those of corresponding noncancerous liver. *Proc. Natl. Acad. Sci. USA 98*:15089–15094.

III

Pancreatic Carcinoma

1

Pancreatic Carcinoma: An Introduction

M.A. Hayat

Introduction

The pancreas is composed of two major compartments: 1) the exocrine pancreas, which consists of the digestive enzyme-producing acinar cells and ducts that conduct these enzymes to the intestines, and 2) the endocrine pancreas, composed of the hormone-producing cells in the islets of Langerhans. All of these cells arise developmentally from a common endodermally derived pancreas progenitor cell. Tumors arise in the pancreas with the features of the three major cell types of the pancreas: the acinar cells, endocrine cells, and the pancreatic duct cells.

According to the American Cancer Society, an estimated 1,268,000 new cases of cancer were diagnosed in the year 2001, and an estimated 553,400 Americans died from cancer. Pancreatic cancer now ranks fourth and fifth as a cause of cancer death in men and women, respectively, with an estimated incidence of 31,860 cases in the year 2004, and 31,270 deaths. More than 50,000 Europeans are also estimated to die of the disease annually. Pancreatic cancer is highly aggressive and characterized by extensive local invasion and early formation of metastases, which occur mainly in the regional lymph nodes and liver. The overall prognosis for this cancer remains grim, with a 5-year survival rate of only 4%. The mortality rate is nearly identical to the incidence rate, affirming the poor prognosis of this disease.

Unfortunately, more than 90% of patients with pancreatic cancer present with metastatic disease or advanced local disease and are precluded from a curative surgical resection. However, surgical resection remains the only hope for cure, although only 5% of patients are candidates at the time of presentation because of the biologically aggressive nature of these tumors (Cowgill and Muscarella, 2003). Even in this group of patients, only 25% can hope to survive for 5 years. Although adjuvant chemotherapy and radiation may allow for some increases in survival, the effectiveness of these treatments is uncertain. In fact, chemotherapy has not resulted in a significant survival benefit, and the 5-year survival rate with this treatment is <1–3% in the United States (Ahlgren, 1996), with a median survival of 4.1 months. The risk of pancreatic cancer in certain individuals can approach 50%. Considering these data, it is apparent that new molecular targets are needed for the prevention and treatment of pancreatic cancer.

Although pancreatic tumor is manifested most often in a solid, infiltrating pattern, cystic and solid/cystic variants are not uncommon. Even when confined to the pancreas, adenocarcinoma usually carries an unfavorable prognosis because a diagnosis is usually not established until an advanced tumor stage. In these cases, palliative surgery, often associated with significant

Handbook of Immunohistochemistry and *in situ* Hybridization of Human Carcinomas, Volume 3: Molecular Genetics, Liver Carcinoma, and Pancreatic Carcinoma

morbity, and/or chemotherapy is usually required (Rampy *et al.,* 2001). Because of the deep retroperitoneal location of the pancreas, a less invasive alternative method for establishing a diagnosis of pancreatic carcinoma is computed tomography (CT)-guided core biopsy or fine-needle aspiration (FNA) biopsy. Percutaneous image-guided FNA is thought to be the most suitable method for tissue diagnosis of this disease before surgery (Chang *et al.,* 1994). Selected types of pancreatic tumors are summarized later.

The knowledge of molecular alterations in pancreatic cancer has increased significantly during the last decade. For example, alterations have been identified in the *K-ras, p16, p35, DPC4 (Smad 4), COX-2,* and *KAl1* genes (Caldas *et al.,* 1994; Friess *et al.,* 1998; Hahn *et al.,* 1996; Tucker *et al.,* 1999; Yamaguchi *et al.,* 2000). In addition, increased expression of growth factors, growth factor receptors, and cytokines has been identified in pancreatic cancer specimens; one example is neurokinin-1 receptor that stimulates pancreatic cancer cell growth (Friess *et al.,* 2003). This *in situ* hybridization and immunohistochemical study suggests a link between the neural system and pancreatic cancer. The role of these and other genes in this cancer is further discussed later in this chapter.

Pancreatic Adenocarcinomas

Adenocarcinomas of ductal origin histologically account for ~85–90% of all pancreatic tumors. The World Health Organization recognizes several histomorphologic variants of ductal adenocarcinomas, including mucinous noncystic carcinoma, signet ring carcinoma, adenosquamous carcinoma, undifferentiated (anaplastic) carcinoma, undifferentiated carcinoma with osteoclast-like giant cells, and mixed ductal-endocrine carcinoma (Hamilton and Aaltonen, 2000). These variants are in addition to the classic tubuloglandular ductal adenocarcinomas. Clear-cell carcinoma of the pancreas is characteristically rich in glycogen and poor in mucin. A unique case of infiltrating ductal adenocarcinomas with predominantly clear cell morphology was reported by Ray *et al.* (2004). They suggest that it should be regarded as a rare variant of pancreatic ductal adenocarcinoma.

Pancreatic adenomacarcinoma presents a particular challenge in clinical management because of very poor response to current therapeutic modalities. An understanding of the genetic regulatory pathways involved in this malignancy may provide the necessary targets for therapy. Special efforts have been made to analyze potential precursor lesions of the ductal adenocarcinoma to gain insights into the development of this malignant tumor. An accumulation of inherited and acquired genetic defects results in the neoplastic transformation and progression of this and other carcinomas. Some of the genetic defects occurring in pancreatic adenocarcinoma are summarized next.

Pancreatic adenocarcinoma has activating mutations in the *K-ras2* oncogene in >90% of cases, as well as loss of the *INK4A* locus that encodes p16 tumor suppressor protein (Bardeesy and DePinho, 2002). In addition, *DPC4, TP53,* and *MADH4* tumor suppressor genes are functionally inactivated in ~50% of the cases. These genes may also be affected in precursor lesions. Crnogorac-Jurcevic *et al.* (2003) have listed 29 genes that were up-regulated fourfold or more in pancreatic adenocarcinoma specimens, using complementary deoxyribonucleic acid (cDNA) arrays method. They have also listed 46 genes that were down-regulated at least fourfold or more in similar specimens, using the same method. These data were confirmed by serial analysis of gene expression (www.ncbi.nlm.nih.gov/SAGE) database and digital differential display (www.ncbi.nlm.nih.gov/Uni.Gene).

The molecular information discussed earlier has been integrated into a tumor progression model that is based on the recently proposed classification of putative ductal adenocarcinoma precursor lesions, i.e., pancreatic intraepithelial neoplasia (PanIN) grades 1–3, and even in normal-appearing duct epithelium obtained from carcinoma-associated tissue or from nonneoplastic pancreas (Lüttges *et al.,* 1999). They also report noninvolvement of *K-ras* mutations in apoptotic activity in low-grade PanINs, although such mutations may have an effect on proliferation in PanIN-1 and PanIN-2.

Pancreatic adenosquamous carcinoma (PASC) is a rare variant of ductal adenocracinoma and is characterized histologically by variable proportions of classic, often mucin-producing glandular epithelium and malignant squamous epithelium (Rahemtullah *et al.,* 2003). Like classic ductal adenocarcinomas, PASC carries a poor prognosis. It usually represents a high-grade tumor and demonstrates features of both glandular and squamous differentiation. A specific diagnosis of PASC is feasible when aspirates show evidence of both squamous and glandular differentiation. The diagnosis of PASC and its distinction from squamous cell carcinoma and ductal adenocarcinomas can be made using FNA biopsy (Rahemtullah *et al.,* 2003).

Mucinous Tumors of the Pancreas

Pancreatic neoplasms associated with significant amounts of extracellular mucin production include mucin-producing ductal adenocarcinoma, mucinous

cystic neoplasm (MCN), and intraductal papillary mucinous tumor (IPMT). Ductal adenocarcinoma is the most common of these tumor types and often develops in older people. It presents as a firm, ill-defined mass usually involving the head of the pancreatic gland (Recine *et al.,* 2003). Ductal adenocarcinoma associated with significant mucin production differs from conventional ductal adenocarcinoma.

The MCNs are classified as mucinous cystadenomas, borderline mucinous tumors, or mucinous cystadenocarcinomas, depending on the degree of atypia of the mucinous epithelium lining the cystic spaces. They are uncommon tumors, representing 2–5% of all pancreatic tumors, and occur predominantly in middle-aged women, with a peak incidence in the fourth and fifth decades (Wilentz *et al.,* 2000). Most often MCNs are found in the body and tail of the pancreatic gland and represent unilocular or multilocular cystic masses filled with thick mucoid material and surrounded by an ovarian type of stroma. The cystic mass does not communicate with the pancreatic duct system (Recine *et al.,* 2003).

The IPMTs are characterized by dilation of the main pancreatic duct or its branches, which are filled with mucus and lined by papillary proliferation of the epithelial lining encompassing varying degrees of atypia (Recine *et al.,* 2004). Unlike MCNs, IPMTs are more common in men and occur mainly in the sixth and seventh decades of life.

Intraductal Papillary Mucinous Tumors

The IPMTs are classified as adenoma, borderline, or malignant based on the degree of epithelial dysplasia present. Malignant IPMTs are further subclassified into noninvasive and invasive. In the IPMT, dilated pancreatic ducts and ductules are lined by tall columnar mucin-producing neoplastic epithelial cells. Pathologic and clinical features of IPMTs are entirely different from those of the pancreatic duct cell carcinoma. The prognosis is usually good but depends on the presence of invasive carcinoma. Operative strategy should be based on routine frozen sections of the surgical margin and perioperative endoscopic examination of the Wirsung duct with staged intraductal biopsies when technically feasible (Gigot *et al.,* 2001).

Some information is available regarding the genetic alterations that occur in the IPMTs. A number of examples are presented later. Using polymerase chain reaction (PCR)-based microsatellite analysis, loss of heterozygosity was detected at chromosomal sites 6q, 8p, 9p, 17p, and 18q in IPMT, suggesting that targeted genetic inactivation may occur at these loci (Fujii *et al.,* 1997). *DPC4* (*MADH4, SMAD4*) is a tumor-suppressor gene on chromosome 18q. This gene is genetically inactivated in ~55% of pancreatic adenocarcinomas (Moskaluk *et al.,* 1997). However, immunohistochemical studies demonstrate that *DPC4* inactivation, detected as loss of DPC4 protein expression, is an infrequent event in IPMT (Iacobuzio-Donahue *et al.,* 2000). This evidence contrasts with the important role that DPC4 inactivation has been shown to play in the progression of conventional pancreatic ductal adenocarcinoma. The difference in DPC4 protein expression between IPMT and ductal carcinomas suggests a fundamental genetic difference in tumorigenesis of these two types of pancreatic tumors.

Pancreatic Neuroendocrine Tumors

Pancreatic neuroendocrine tumors (PNTs) represent less than 10% of all pancreatic tumors. Routine histologic examination is usually not predictive of their behavior. These tumors are diagnosed at an advanced stage because they usually manifest few symptoms except when there is a hormone syndrome associated with them (Mignon, 2000). Although infrequent, PNTs can cause acute pancreatitis even in patients younger than 50 years (Griñó *et al.,* 2003).

Capella *et al.* (1995) have classified neuroendocrine tumors of the pancreas, lung, and gut to assess tumor prognosis in terms of the degree of differentiation and the predominant cell type as well as tumor size; the presence or absence of a clinical syndrome; and the degree of local, vascular, and/or metastatic involvement. Histologic and immunohistochemical studies confirm this classification, which is very useful in routine practice for predicting the behavior of PNT (Heymann *et al.,* 2000).

Acinar Cell Carcinomas

Acinar cell carcinomas (ACCs) are rare neoplasms of the exocrine pancreas, comprising less than 1% of primary pancreatic tumors. The ACCs are distinct from the more common pancreatic ductal adenocarcinomas. The prognosis of ACCs is poor because the majority of patients show evidence of metastatic disease either at or subsequent to diagnosis; the mean survival is ~18 months after diagnosis.

Genetic alterations, such as *K-ras* oncogene and *p53* and *DPC4* tumor-suppressor genes, have been either absent or only rarely present in ACCs, although aneuploidy and ACC allelotype are present (Hsueh and Kuo, 1992; Rigaud *et al.,* 2000). Allelic loss on chromosome 11p is the most common genetic alteration in the ACC

(Abraham *et al.,* 2002). In contrast, activation of *K-ras* oncogene and inactivation of *DPC4* and *p53* are common in conventional pancreatic ductal adenocarcinomas. This difference indicates that ACC is genetically distinct from pancreatic ductal adenocarcinomas. It is interesting to note that morphologic, immunohistochemical, and clinical features of ACC overlap with those of another rare pancreatic neoplasm, pancreatoblastoma (Abraham *et al.,* 2002).

Biomarkers for Pancreatic Cancer

It is established that gene mutations confer increased risk of cancer. The majority of mutations found in tumor cells occur in signal transduction pathways that ultimately regulate transcription factors involving a large number of genes and their transcription patterns. Therefore, abnormalities in gene expression are characteristic of neoplastic tissues. Adenocarcinomas are correlated with specific sequential genetic mutations. Although the total accumulation of mutations is the principal factor in most cancers, the causative mutations in tumor-suppressor genes and oncogenes occur in a specific order. However, cancer is an exceedingly complex disease that refers to conditions that emerge as a result of the interaction of genes and environment. Genes impart susceptibility or protection, which is neither necessary nor sufficient for disease to develop. Environmental factors are required, and these can promote, delay, or prevent disease. Not only gene–enviroment interactions but also gene–gene interactions (e.g., p53-mdm 2) play a role in complex disease genetics.

Despite improved diagnostic and therapeutic modalities, pancreatic cancer still has a very poor prognosis with a 5-year survival rate of less than 5%. Pancreatic cancer is usually advanced at the time of presentation, but the detection of premalignant pancreatic lesions and earlier detection of malignant pancreatic lesions should improve the clinical outcome of the disease. It is known that pancreatic cancer progression from normal ductal and ductular epithelium to cancer results from a series of lesions (termed PanIN). Recognition of biomarkers in early pancreatic neoplastic ductal lesions can provide effective new diagnostic and treatment approaches.

Advances in molecular genetics have resulted in a significant increase in current knowledge regarding the genetic events associated with pancreatic tumorigenesis. Further characterization of the molecular changes associated with tumor initiation and progression will elucidate the essential cellular pathways responsible for maintaining noncancerous states. Such information will identify novel, effective, therapeutic and diagnostic strategies. Molecular characterization of tumors will also provide clinically useful information for guiding further therapy after surgical resections.

Like most other cell types, pancreatic cells experience a constant barrage of mutations. Many of such mutations are irrelevant unless the function of a critical gene is lost or an oncogene is activated. In other words, sequential accumulations of genetic alterations including the activation of oncogene and the inactivation of tumor-suppressor genes play a central role in the development of cancer. Somatic inactivation of a tumor-suppressor gene is usually caused by an intragenic mutation in one allele of the gene with subsequent loss of chromosomal region that spans the second allele. Such an affected cell has growth advantage over normal cells with subsequent clonal expansion. It has been clear that up-regulation and/or down-regulation of certain genes initiates pancreatic cancer. Detailed immunohistochemical and *in situ* hybridization methods for analyzing the following markers for pancreatic cancers are presented in Part III of this volume: *K-ras* protooncogene, p27 protein, cyclooxygenase-2, synaptic vesicle protein, activated stat3 protein, transcription factor E2F-1, maspin, chromogranins, DUSP6/MKP-3, carbohydrate antigens, mucins, mast cells, and endocrine cells.

The pancreas can contain several different types of tumors with distinct genetic profiles and clinical behavior. Table 18 shows most of such types and the presence of certain mutations in each type. Furthermore, genetic alterations are not always the same in different areas of the pancreatic tumor or in the sites with same histologic dysplasia in each tumor. This means that the tumor is hetrogenous, and the pattern of association of histologic features with genetic alterations differs from tumor to tumor.

Importance of Biomarkers

Although pancreatic cancer is fairly well-characterized at the histopathologic level, the molecular mechanisms leading to cell transformation are beginning to be elucidated. Identification of key players in the process of

Table 18. Types of Pancreatic Tumors and their Mutations

Tumor Types	Mutations
Acinar cell carcinoma	APC/β-catenin
Ductal adenocarcinoma	KRAS, SMAD, TP53, CDKN1A
Pancreatic endocrine tumors	MEN1
Serous cystadenoma	VHL

cellular transformation is a crucial step toward our understanding of pancreatic cancer progression and toward the development of new, effective cancer therapies. There is an urgent need for determining such players (pancreatic cancer biomarkers). The use of inherited genetic markers to evaluate pancreatic cancer outcome could enhance our ability to identify those persons who are more likely to develop clinically significant pancreatic cancer and to intervene in these persons to reduce morbidity resulting from this disease.

Biomarkers are molecules detectable in the primary tumor, metastatic lesions, blood, or bodily fluids of patients with cancer, providing diagnostic, prognostic, or predictive information. The detection of clinically useful tumor markers whose expression predicts tumor stage or clinical outcome is an important priority in cancer research. The identification of markers is a major advance in the understanding of cancer because their alterations result in a high predisposition to malignancy. The elucidation of the effect of candidate tumor markers can be used to derive biological insight regarding the mechanisms underlying tumor initiation and progression. Furthermore, early detection of a marker can lead to prevention of certain cancers.

Another important advantage of detecting markers is to elucidate their behavior when tumors are exposed to the stress of cytotoxic therapy.

Proportions of cells expressing a particular marker profile in a heterogeneous tumor can change in response to this stress (Crane *et al.,* 2003). The question is: Will identifying or targeting altered marker expression in response to cytotoxic therapy be of prognostic or therapeutic value? Such information is available with regard to some markers. For example, the short half-life of the p53 protein is substantially increased following genotoxic stress such as irradiation- and chemically induced DNA damage. It has been shown that radiation-induced DNA damage causes *p53* to arrest the cell cycle in G_1 or (depending on cell type and external stimuli) triggers apoptosis (Ko and Prives, 1996).

Ideally, a tumor marker should have clinical utility in the management of cancer. For a marker to be clinically relevant, it must be notably overexpressed or underexpressed in the majority of the tumor samples of a given histology. For a marker to have prognostic significance, it should also show expression alterations concordant with tumor stage or clinical outcome. A number of prognostic biomarkers for pancreatic cancer, with varying degrees of specificity, have been determined. Most of these markers, including those at the experimental stage, are summarized later and enumerated in Table 19. Although most of them have not demonstrated clinical utility as yet, most have proved to be useful for diagnosis, whereas some require further testing. The expression

Table 19. Pancreatic Carcinoma Biomarkers

[a]ADAM 9	Grützmann *et al.* (2004)
[a]Alpha$_6$β1- INTEGRIN	Sawai *et al.* (2003)
[a] Amylin	Rotondo *et al.* (2003)
Basic fibroblast growth factor	Mentula *et al.* (2003)
[a]Bcl-2	Lüttges *et al.* (2003)
[a]Beta catenin	Watanabe *et al.* (2003)
BRCA2	Hahn *et al.* (2003)
BRAF	Ishimura *et al.* (2003)
Carbohydrate antigens 19-9	Ziske *et al.* (2003)
[a]Cartilage oligomeric matrix protein	Liao *et al.* (2003b)
CDKN2A	Rozenblum *et al.* (1997)
[a]Chromogranin A/B	Lukinius *et al.* (2003); this volume
[a]CD 117	Potti *et al.* (2003)
CFTR gene	Gomez-Lira *et al.* (2003)
[a]Claudin 4	Nichols *et al.* (2004)
[a]c-Myc	Lewis *et al.* (2003)
[a]CXCR 4	Mori *et al.* (2004)
[a]Cyclin D1	Maitra *et al.* (2003)
[a]Cyclooxygenase-2	Okami *et al.* (2003); this volume
[a]Cystein-rich secretory protein-3 (CRISP-3)	Liao *et al.* (2003)
Cystic fibrosis transmembrane conductance regulator	Lee *et al.* (2003)
[a]Cytokeratin	Du *et al.* (2003)
[a]DPC4	Maitra *et al.* (2003)

continued

Table 19. Pancreatic Carcinoma Biomarkers—Cont'd

[a]Epidermal growth factor	Xiong and Abbruzzese (2002)
[a]Epidermal growth factor receptor (Egfr)	Bruell *et al.* (2003)
[a]Heat shock protein-70	Sagol *et al.* (2002)
[a]HER-2/neu	Potti *et al.* (2003)
[a]Hypoxia-inducible factor-1α	Kitada *et al.* (2003)
Id protein	Lee *et al.* (2004)
[a]Ink4a/Arf	Aguirre *et al.* (2003)
[a]Integrin α 6β1	Sawai *et al.* (2003)
[a]Interleukin-1α	Sawai *et al.* (2003)
[a]Interleukin-8 (IL-8)	Kuwada *et al.* (2003)
[a]Interleukin-8 receptors (CXCR 1/2)	Kuwada *et al.* (2003)
[a]Keratin	Du *et al.* (2003)
KOC gene	Mueller *et al.* (2002)
[a]K-ras	Aguirre *et al.* (2003); in this volume
[a]MAGE-1	Sato *et al.* (2003)
[a]Maspin	Ohike *et al.* (2003); this volume
[a]Metastatis-associated gene 1 (MTA1)	Hofer *et al.* (2004)
[a]Microvascular density	Tan *et al.* (2004)
[a]Mitogen-activated protein kinase 2 (MEK2)	Tan *et al.* (2004)
[a]MMP2	Iacobuzio-Donahue *et al.* (2002b)
[a]MUC1, MUC2	Adsay *et al.* (2002)
[a]Neurokinin-1 receptor	Friess *et al.* (2003)
NF–κB	Satoh *et al.* (2003)
Nuclear factor Kappa B	Chang *et al.* (2003)
Nuclear factor Kappa B	Satoh *et al.* (2003)
Osteopontin	Koopman *et al.* (2004)
[a]p16	Maitra *et al.* (2003)
[a]p21	Hermanová *et al.* (2003)
[a]p27	Juuti *et al.* (2003); this volume
[a]p53	Lüttges *et al.* (2003)
Peroxisome proliferator–activated receptor gamma	Sasaki *et al.* (2001)
[a]Polyoma virus middle T antigen	Lewis *et al.* (2003)
[a]PS2 protein	Sagol *et al.* (2002)
PSTI	Hirota *et al.* (2003)
[a]Rad 51	Maacke *et al.* (2002)
[a]S100A4	Rosty *et al.* (2002)
[a]S100A6	Shekouh *et al.* (2003)
S100P	Crnogorac-Jurcevic *et al.* (2003)
[a]SERPINE2 (protease nexin I)	Buchholz *et al.* (2003)
[a]Smad 4	Maitra *et al.* (2003)
[a]Small intestinal mucin antigen	Yamasaki *et al.* (2004)
Soluble DNA in the circulating blood	Moriyama *et al.* (2002)
SPINK 1	Gomez-Lira (2003)
[a]STK 11/LKB 11	Sahin *et al.* (2003)
Stromal cell-derived factor-1	Mori *et al.* (2004)
[a]Synaptic vesicle protein	Jakobsen *et al.* (2002)
[a]Synaptophysin	Lewis *et al.* (2003)
Telomerase	Murakami *et al.* (2002)
[a]Telomere	van Heek *et al.* (2002)
[a]Topoisomerase II alpha	Maitra *et al.* (2003)
Transforming growth factor	Ramachandra *et al.* (2002)
Transforming growth factor beta 1	
[a]Trefoil factor family (TFF1-3)	Terris *et al.* (2002)
[a]Trypsin	Du *et al.* (2003)
[a]Tuberin	Francalanci *et al.* (2003)
Vascular endothelial growth factor	Karayiannakis *et al.* (2003)
[a]Vascular endothelial growth factor receptor neuropilin -1	Parikh *et al.* (2003)
VHL gene	Mohr *et al.* (2000)

[a]These biomarkers have been identified with immunochemistry or *in situ* hybridization.

of most of them can be assessed with reliability in formalin-fixed and paraffin-embedded pancreatic tissue specimens, using immunohistochemistry (IHC) or flourescence *in situ* hybridization (FISH). The protocols of IHC and FISH for some of these markers are detailed in chapters of Part III of this volume. It should be noted that some of these markers (e.g., *p53, BRCA2*, and *HER-2*) are involved not only in pancreatic cancer but also in other cancers such as breast cancer and ovarian cancer. Despite the multitargets of a biomarker, immunohistochemical specificity can be obtained by using monoclonal antibodies.

The identification of tumor markers, however, is not a simple biological problem. Unlike clonal cell cultures, the molecular analysis of human tissue specimens necessarily involves heterogeneous cell populations whose messenger ribonucleic acid (mRNA) composition is proportionally complex. Similarly, the variability in gene expression from one individual tissue sample to another is substantial and may obscure common patterns of gene expression that are predictive of clinical outcome. Furthermore, because a gene may be responsible for a variety of tumor types, its value as an independent prognostic factor is considerably diminished. For example, *p53* amplification is not likely to be an independent marker for pancreatic cancer. Mutations of *p53* occur not only in pancreatic cancer but also in many other cancers including endometrial and ovarian cancers. Genes exert different effects in different populations (genetic heterogeneity). Therefore, identifying the targets, developing target-specific interventions, and validating biological effects of an intervention are daunting tasks. Molecular target expression is certainly a dynamic phenomenon. Nevertheless, the future of oncology undoubtedly involves the detection, validation, and targeting of tumor-specific molecules. In fact, cancer risk assessment has developed into a distinct discipline.

The question is: To what extent it is possible to predict phenotypes from genotypes? This can be accomplished relatively easily for monogenic diseases such as genetic disorders of hemoglobin (e.g., thalassemias), muscular dystrophy (muscle weakness), cystic fibrosis, Gaucher's disease, and familial adenomatous polyposis. In contrast, attempts to identify the genes in the multigenic diseases are fraught with difficulty. These diseases include diabetes and asthma. A wide variety of approaches is being used to dissect the genetic factors in these diseases. Many different classes of genetic markers have been used, including candidate genes, microsatellite DNA, and single nucleotide polymorphisms (SNPs). Some of these approaches are detailed in this and other volumes of the series. A closely integrated partnership between the clinical and basic biomedical sciences is needed.

The era of molecular medicine for cancer has dawned. Progress in cancer prevention and early cancer detection will be delayed by the failure to adopt a critical and nondogmatic approach to the pathogenesis of cancer. The advent of DNA chip technology will catalyze the development of revised paradigms. Specifically, modern genomics will allow cancers to be grouped within pathogenic pathways on the basis of shared gene expression profiles.

Biomarkers

Most of the well-known genes (biomarkers) and their products involved in pancreatic cancer are discussed next. A large number of up-regulated and down-regulated genes in pancreatic adenocarcinoma specimens is also presented by Crnogorac-Jurcevic *et al.* (2003).

ADAM9

ADAM9 is a member of the large family of proteases that are type I transmembrane proteins with both metalloproteinase and disintegrin–containing extracellular domains. The ADAMs are involved in modulating cell–cell and cell–matrix interactions (Amour *et al.,* 2002). ADAM9 is one of the genes that is overexpressed in pancreatic ductal adenocarcinomas, in comparison with normal pancreatic tissues. Overexpression of this gene also occurs in prostate, breast, and liver cell carcinomas. ADAM9 may exert its action via its disintegrin domain, its metalloproteinase domain, or both. Various matrix metalloproteinases (e.g., MMP2 and MMP9) have been described as being overexpressed in pancreatic ductal adenocarcinomas and seem to play an important role in the progression of this carcinoma (Bloomston *et al.,* 2002).

Immunohistochemical studies demonstrate that ADAM9 is overexpressed in pancreatic ductal adenocarcinomas but not in endocrine tumors or ACCs (Grützmann *et al.,* 2004). Pancreatic ductal adenocarcinomas showing cytoplasmic ADAM9 expression correlate with poor tumor differentiation as well as with shorter overall survival than in cases showing only an apical membranous staining pattern. Cytoplasmic ADAM9 overexpression is thought to be a useful diagnostic marker and could be used as a potential target in the treatment of pancreatic ductal adenocarcinomas.

BRAF

BRAF is a member of the RAS-RAF-MEK-ERK-MAP kinase growth signal transduction system. The three RAF genes (BRAF is one of them) code for

cytoplasmic serine/threonine kinases, which are regulated by binding to RAS. Regarding these three RAF genes, BRAF somatic missense mutations are found in 66% of malignant melanomas and at a lower frequency in a wide range of human cancers (Davies *et al.,* 2002). All mutations are found within the kinase domain, with a single substitution (V599E) accounting for 80%. Mutated BRAF proteins also have elevated kinase activity and could transform NIH3T3 cells. Mutated K-ras constitutively activates the RAF-MEK-ERK-MAP kinase system, which is linked to cell growth stimulation. Because up to 90% of pancreatic cancers show active *K-ras* mutation (codon 12), activation of the RAS-RAF-MEK-ERK-MAP kinase pathway may be critically important for pancreatic cells to be transformed to cancer cells (Ishimura *et al.,* 2003). In fact, BRAF V599E mutation is an important mutation in pancreatic cancers, provided *K-ras* codon 12 mutation is also present.

BRCA2

BRCA2 is a tumor-suppressor gene that participates in DNA damage repair. There is an increased risk of pancreatic cancer development in patients with germline BRCA2 mutations. Goggins *et al.* (1996) evaluated 41 pancreatic adenocarcinomas, and 15 demonstrated loss of heterozygosity at BRCA2, and 4 harbored mutations. Germline BRCA2 mutations were responsible for 7.3% of inactivating events, including that both germline (hereditary) and sporadic (nonhereditary) events play a role in pancreatic cancer development.

Extensive studies have been carried out to elucidate the comparative role of BRCA2 germline mutations and sporadic mutations in families with familial pancreatic cancer. The term familial pancreatic cancer is applied to families with at least two first-degree relatives with pancreatic ductal adenocarcinoma but that do not fulfill the criteria for other familial cancer syndromes. The risk for pancreatic carcinoma developing among first-degree relatives of a patient with pancreatic cancer is estimated to be 18-fold in people with two affected family members and as high as 57-fold in people with three or more affected family members (Tersmette *et al.,* 2001).

The majority of pancreatic cancer cases are sporadic. It is estimated that ~10% of patients with pancreatic cancer may have an inherited form of the disease. To study the relationship between BRCA2 germline mutations and familial pancreatic cancer, Hahn *et al.* (2003) identified 26 European families in which at least two first-degree relatives had a histologically confirmed diagnosis of pancreatic ductal adenocarcinoma. They sequenced genomic DNA isolated from peripheral blood lymphocytes obtained from these family members to identify germline mutations in BRCA2. This study supports an important role for BRCA2 germline mutations in a subpopulation of families with familial pancreatic cancer. Based on this and other studies, it is recommended that BRCA2 mutation analysis be included in molecular genetic testing and counseling strategies in families with at least two first-degree relatives affected with ductal adenocarcinoma of the pancreas.

Cartilage Oligomeric Matrix Protein

Cartilage oligomeric matrix protein (COMP) is a member of the thrombospondin family of extracellular glycoproteins. This protein is found in articular nasal cartilage, tracheal cartilage, and tendons. In the growth plate, COMP is primarily observed in the proliferative region, indicating a role in cell growth and matrix development (Shen *et al.,* 1995). Immunohistochemical and *in situ* hybridization studies have been carried out for investigating COMP mRNA and protein in normal pancreatic tissues, chronic pancreatic tissues, and cultured pancreatic cancer cells (Liao *et al.,* 2003a). (Chronic pancreatitis is an inflammatory disease of the pancreas characterized histomorphologically by progressive development of fibrosis and atrophy of the pancreatic parenchyma.) These studies indicate that COMP is preferentially expressed in degenerating acinar cells in chronic pancreatitis and in chronic pancreatitis-like areas in pancreatic cancer, suggesting a potential role of this gene in the course of acinar cell degeneration and dedifferentiation.

Although COMP is not a disease-specific marker for chronic pancreatitis, because it is also present in chronic pancreatitis-like changes in pancreatic cancer tissues, the marker may serve as an important progression marker to monitor the activity of tissue destruction in chronic pancreatitis. The role of another matrix component, integrin, in pancreatic cancer is also discussed in this chapter.

CDKN2A

Loss of CDKNA2 tumor-suppressor gene and its function, as a result of mutation, deletion, or promoter hypermethylation, occurs in 80–90% of sporadic pancreatic adenocarcinomas (Rozenblum *et al.,* 1997). Loss of heterozygosity occurs at chromosome 9q21. The inheritance of mutant CDKN2A alleles confer a 13-fold increased risk of pancreatic cancer. Loss of this gene is seen in moderately advanced lesions that show features of dysplasia. The tumor-suppressor locus at 9q21 encodes two tumor suppressors: INK4A and ARF via distinct first exons and alternative reading

frames in shared downstream exons (Sherr, 2001). Many pancreatic cancers sustain loss of both the INK4A and ARF transcripts. INK4A is thought to be the more important pancreatic-cancer suppressor at this locus. Loss of INK4A usually occurs only in later stages of pancreatic neoplasia (Bardeesy and DePinho, 2002). Because INK4A is implicated in the cellular response to DNA damage *in vivo* (Schmitt *et al.,* 2002), the absence of INK4A might contribute to the chemoresistance of pancreatic adenocarcinoma.

Cyclooxygenase-2

Most pancreatic neoplasms are adenocarcinomas, which are the most lethal malignancies. Cyclooxygenase-2 (COX-2) is expressed in adenocarcinomas of the human pancreas. Quantitative reverse transcription (RT)-PCR, immunoblotting, and IHC have been used for assessing the expression of COX-2 in this tumor (Tucker *et al.,* 1999). This study showed an increase of ~60-fold in the level of COX-2 mRNA in the pancreatic cancer compared to that in the adjacent nontumorous tissue. Also, COX-2 protein was commonly present in the adenocarcinoma of the pancreas but was absent in the nontumorous pancreatic tissue. It means that COX-2 is up-regulated in pancreatic cancer. Mutations in the *Ki-ras* oncogene are common in pancreatic cancer. Levels of COX-2 are increased in *Ras*-transformed epithelial cells (Subbaramaiah *et al.,* 1996). Therefore, activation of the *Ras* pathways contributes to the up-regulation of COX-2 in this cancer. These results suggest that COX-2 may be a target for the prevention or treatment of pancreatic cancer. It should be noted that COX-2 expression is also up-regulated in a variety of other human cancers, including colon, lung, gastric, and esophageal cancer. Biological consequences of such up-regulation include inhibition of apoptosis, increase in metastatic potential, and promotion of angiogenesis.

Cysteine-Rich Secretory Protein-3

Human cysteine-rich secretory protein-3 (CRISP-3: SGP28) is the third member of the cysteine-rich secretory protein family. This protein has been detected in several types of human tissues, with predominance in the pancreas, prostate, and salivary gland (Kratzschmar *et al.,* 1996). The distribution of CRISP-3 in gastrointestinal tissues is predominantly in the pancreas. *In situ* hybridization and immunohistochemical analysis reveal high levels of CRISP-3 in acinar cells differentiating into small proliferating ductal cells in chronic pancreatitis and chronic pancreatitis-like lesions in pancreatic cancer, suggesting a role of this protein in the pathophysiology of chronic pancreatitis (Liao *et al.,* 2003). In contrast, CRISP-3 expression is weak to absent in the cytoplasm of cancer cells as well as in acinar cells and ductal cells in pancreatic cancer tissues and normal pancreatic tissues.

In vivo studies have shown that CRISP-3 is under androgen control in the salivary gland (Haendler *et al.,* 1993). Studies of the androgen profile in patients with chronic pancreatitis and pancreatic cancer have revealed that serum testosterone, dihydrotestosterone, and androstanediol glucuronide levels are significantly lower in patients with pancreatic cancer compared to patients with chronic pancreatitis (Jansa *et al.,* 1996). This changed androgen profile might contribute to the differential expression of CRISP-3 in chronic pancreatitis and pancreatic cancer.

Cystic Fibrosis Transmembrane Conductance Regulator

Cystic fibrosis transmembrance conductance regulator (CFTR) gene is associated with a wide spectrum of respiratory and pancreatic disorders as well as classically defined cystic fibrosis. Several mutations of CFTR, such as F508del, G542X, and N1303K, are associated with severe cystic fibrosis phenotypes and display high disease penetrance. Many other mutations of CFTR are associated with monosymptomatic diseases of lung, pancreas, or vas deferens, which show partial penetrance. Recent studies indicate that CFTR mutations of M470V- Q1352H, IVS8T_5-M470V, and E217G are associated with bronchiectasis and chronic pancreatitis (Lee *et al.,* 2003). Defects in CFTR-dependent ion transport are an important aggravating factor in the disease development or progression in addition to other genetic and environmental factors. Mutations of CFTR gene are not independent markers for the diagnosis of chronic pancreatitis.

DPC4

DPC4 (Smad 4) tumor-suppressor gene is deleted in 50% of pancreatic cancers (Hahn *et al.,* 1996). For further details, see Smad 4 in this chapter.

Epidermal Growth Factor Receptor

The human epidermal growth factor receptor (EGFR), a 170-kDa transmembrane glycoprotein, is a member of a family of tyrosine kinase receptors that are characterized by an extracellular domain, a transmembrane region, and a cytoplasmic domain. The EGFR was one of the first cellular molecules identified to

play a fundamental role in the regulation of cell proliferation, differentiation, and tumorigenesis. It is also involved in tumor angiogenesis, a critical step in the progression of pancreatic tumors as well as other tumors. The activity of angiogenesis depends on the net effects of stimulatory and inhibitory factors secreted by the tumor and its microenvironment. The EGFR is one of these stimulatory factors.

The EGFR has the ability of transforming normal cells to a neoplastic phenotype when it is expressed at a high level or when an activation mutation is introduced into it. It is known that overexpression of this receptor accompanied by production of one or more of its ligands is a characteristic feature of a large number of human epithelial tumors, including tumors of the pancreas, brain, urinary bladder, prostate, lung, breast, ovaries, and head and neck. Changes in the expression and activity of the EGFR correlate with continued proliferation of many types of malignant cells. Clinical studies have shown that coexpression of EGFR and epidermal growth factor (EGF) or transforming growth factor (TGF)-α is associated with increased tumor size, advanced clinical stage, and decreased survival of patients (Yamanaka *et al.,* 1993). Both EGF and TGF-α are potent inducers of vascular endothelial growth factor (VEGF), the most effective angiogenesis stimulator in human cancer.

Because EGFR is a tumor-associated surface antigen and rarely is expressed on normal tissue cells, it presents an appropriate target for immunotherapy. Blockade of EGFR not only abrogates its effect on cell proliferation but also inhibits angiogenesis. Therefore, such blockade provides a novel strategy for the treatment of cancer, including pancreatic carcinoma. This strategy comprises the application of monoclonal antibodies, immunotoxins, and tyrosine kinase inhibitors. The selectivity of the monoclonal antibodies for the pancreatic tumor does not seem to affect normal cells expressing EGFR. Currently, several phase II and III clinical trials with EGFR inhibitor IMC-C225 are under way, justifying the EGFR as a suitable target for therapy of pancreatic carcinoma (Bruell *et al.,* 2003). Xiong and Abbruzzese (2002) have also used IMC-C225 in combination with gemcitabine for patients with advanced pancreatic cancer in a phase II clinical trial. This therapy induced apoptosis and suppressed proliferation of tumor cells.

It should be noted that immunohistochemical expression of EGFR and TGF-α, either alone or in concert, does not show any correlation with size, functional status, secretory profile, or biological behavior in the pancreatic endocrine tumors (Srivastava *et al.,* 2001). Hence, expression of these factors cannot be used as a marker of malignancy in this group of pancreatic tumors.

Some information is available regarding the use of immunotoxins. It is known that the chimeric (mouse/human) anti-EGFR is very effective in suppressing the growth of pancreatic tumors. Bruell *et al.* (2003) have demonstrated the elimination of the metastatic pancreatic cancer cell line L3.6 pl *in vitro* after incubation with the recombinant anti-EGFR immunotoxin 425(scFv)-ETA. The use of this immunotoxin in *in vivo* studies in a mouse model is awaited.

Hypoxia-Inducible Factor-1 Alpha

Growth of malignant epithelial tumors is limited to only several square millimeters in the absence of neoangiogenesis because of insufficient oxygen and glucose diffusion from blood vessels. Neoangiogenesis and cellular adaptation to hypoxia are therefore essential events for cancer progression. One of the key factors involved in this adaptation is hypoxia-inducible factor-1 alpha (HIF-1α). This is a basic helix–loop–helix–Per–AHR/Arnt–Sim homology sequence transcription factor that plays a major role in cellular oxygen homeostasis (Iyer *et al.*, 1998). This factor transactivates genes whose protein products function either to increase O_2 availability or to allow metabolic adaptation to O_2 deprivation. These genes include VEGF and insulin-like growth factor 2. Protein products of these genes are implicated in tumor progression, and overexpression of HIF-1α has been demonstrated in a variety of human malignancies. Overexpression of HIF-1α has been reported in pancreatic carcinoma *in vivo* and *in vivo* (Akakura *et al.,* 2001; Zhong *et al.,* 1999).

Kitada *et al.* (2003) have investigated the expression of HIF-1α protein in primary and metastatic pancreatic cancer tissues using IHC. This study has demonstrated a significant association between HIF-1α expression and certain clinicopathologic parameters (cell proliferation, microvessel density, tumor size, and advanced TNM stage) known to be prognostic factors in pancreatic carcinoma. It is concluded that HIF-1α can be used as a therapeutic target in pancreatic ductal carcinoma.

Id Protein

Id proteins are members of a family of basic helix–loop–helix (bHLH) transcription factors lacking the DNA-binding domain and are inhibitors of differentiation. Therefore, they act as dominant negative regulators of HLH proteins by forming transcriptionally inactive Id-bHLH protein complexes (Riechmann and Sablitzky, 1995). Id proteins play important roles in the regulation of cell differentiation during neurogenesis, lymphoiesis, and angiogenesis (Lee *et al.,* 2004). Their functions also include promotion of cell growth and cell cycle progression and apoptotic induction (Norton, 2000). Id proteins, in addition, can induce cell

proliferation, increase DNA synthesis, and immortalize mammalian cells in association with other oncogenes.

Id protein overexpression has been found in a number of primary human cancers including cervical, breast, prostate, skin, and pancreatic cancers (e.g., Maruyama *et al.,* 1999). Moreover, Id-1 protein is an essential factor in the promotion of G1/S cell-cycle transition in certain cancers by inactivating p16 and increasing cDK4 activity/RB (Ouyang *et al.,* 2002a). Several lines of evidence strongly suggest that these proteins have a potential role in the aggressiveness of malignant tumors and formation of tumor angiogenesis. It has been demonstrated that Id-I is significantly overexpressed in pancreatic cancer but not in chronic pancreatitis, suggesting that this protein may be associated with the enhanced proliferative potential of pancreatic cancer cells (Maruyama *et al.,* 1999). Immunohistochemical studies have demonstrated overexpression of Id-1 in human primary pancreatic cancer, which is closely related to tumor angiogenesis (Lee *et al.,* 2004). Thus, Id-1 can be used as a target molecule for antiangiogenic drug design in pancreatic cancer treatment.

Integrin

Transmembrane receptors of the integrin family mediate dynamic cell-adhesion processes. Integrins can mediate signaling entering the cell or leaving the cell, these signals play principal roles in various aspects of tumor biology, such as growth, differentiation, invasion, and metastasis formation (Dedhar and Hannigan, 1996). Increased expression of laminin-binding integrins or decreased expression of fibronectin-binding integrins is correlated with aggressive growth and metastatic potential in several types of tumors, including human pancreatic carcinoma (Vogelmann *et al.,* 1999).

It is also known that human metastatic pancreatic cancer cells express interleukin-1α (IL-1α) mRNA (Yamamoto, 1999). Immunohistochemical studies have demonstrated that enhanced integrin $\alpha_6\beta_1$ levels by IL-lα signaling is an important determinant of metastasis formation in pancreatic cancer (Sawai *et al.,* 2003). Expression of both integrin $\alpha_6\beta_1$ and IL-1α is increased in pancreatic cancer, and both play important roles in metastasis formation. Such expression might provide valuable prognostic information for treatment strategies. The role of another component of extracellular matrix, cartilage oligomeric matrix protein, in pancreatic cancer is also discussed in this chapter.

Interleukin-8

Interleukin-8 (IL-8) is a member of the CXC chemokine family and has a wide range of proinflammatory effects. This protein is expressed in normal cells such as monocytes and fibroblasts as well as several types of tumor cells, including pancreas cancer cells (Shi *et al.,* 1999). Two receptors for IL-8, CXCR1 and CXCR2, have been identified. Both receptors bind to IL-8 with high affinity. The role of these receptors in pancreatic cancer is presented later.

The protein IL-8 can act multifunctionally to induce angiogenesis and proliferation of pancreatic carcinoma (Takamori *et al.,* 2000). Immunohistochemical and RT-PCR analysis have shown overexpression of IL-8 and its receptors in pancreatic cancer (Kuwada *et al.,* 2003). This study also suggests that IL-8 regulates matrix metalloproteinase in supernatants of the PANC-1 human pancreatic cancer cell lines. A Vectastain Elite ABC kit was used to perform IHC; antibodies used were a rabbit polyclonal antibody (1:100 dilution) for IL-8 and a rabbit polyclonal antibody (1:200 dilution) for CXCR1 and CXCR2.

KOC

KOC is one of the differentially expressed genes in pancreatic cancer. It encodes a protein with four K-homologous (KH) domains, which are overexpressed in pancreatic cancer (Mueller-Pillasch *et al.,* 1997). These domain-containing proteins are involved in fundamental biological processes such as development, cell growth, differentiation, and carcinogenesis (Ross *et al.,* 1997). KOC is thought to play a role in the regulation of tumor cell proliferation by interfering with transcriptional or posttranscriptional processes. Mueller *et al.* (2002) have used the KOC assay for detecting malignant cells in aspirates of fluids containing ascites, liver fluid, cerebrospinal fluid, and pancreatic and mediastinal cysts. This assay could be useful to facilitate screening for malignant disease and to improve the diagnostic accuracy of fine-needle aspirates.

K-*ras* Gene

One of the most frequent types of protooncogene activation is the *ras* protooncogene activation. The family of these genes has three well-characterized members (H-*ras*, K-*ras*, and N-*ras*). The K-*ras* protooncogene located at chromosome 12p codes for a 21-kDa guanosine triphosphate (GTP) binding protein (p21 *ras*) that is involved in the signal transduction of activated tyrosine kinase cell membrane receptors to downstream signal cascades (Bos, 1989). Activation of this gene usually results from point mutations at codons 12, 13, or 16, causing the oncogenic *ras* protein to be in a permanently active GTP-bound state. In fact, *ras* group of proteins functions as a part of the membrane-associated

signal-transduction pathway of GTP-binding proteins. Once activated, these proteins code for key mediators in a number of pathways regulating cell growth and differentiation. In other words, *ras* functions as a molecular switch in a network of intracellular signaling pathways, mainly controlling cell differentiation or proliferation.

Ras-activating mutations result in constitutive signaling, stimulating not only cell proliferation but also apoptosis inhibition. However, according to Lüttges *et al.* (2003), K-*ras* mutations are not involved in apoptotic activity. They suggested that in PanIN there is a relationship between K-*ras* mutations and proliferation but not between mutated K-*ras* and apoptosis or apoptotic markers. Cells carrying K-*ras* mutations therefore may not be eliminated but persist as dormant cells until an additional genetic hit triggers further malignant transformation. Alterations of the apoptotic pathway are thought to be late events in pancreatic cancerogenesis. According to these scientists, molecular pathology and epidemiologic studies suggest that wild-type K-*ras* carcinomas of the pancreas may arise through a genetic pathway distinct from that involved in carcinomas that harbor a K-*ras* mutation only.

Nevertheless, oncogene *ras* mutations are one of the fundamental initiating events in several types of cancers, including pancreatic carcinoma. In fact, K-*ras* is the most commonly altered gene in pancreatic cancers. High frequencies of *K-ras* gene mutation in the adenomas, borderline tumors, and carcinomas of mucin-producing tumors of the pancreas indicate that this mutation is a common and early event in these tumors (Sakai *et al.,* 2000). At diagnosis, pancreatic tumors show the highest prevalence of K-*ras* mutations of all human cancers, ranging from 75–85% (Gress, 2000). K-*ras* point mutations are found in ~90–95% of all pancreatic ductal adenocarcinomas and represent the earliest known genetic alterations in premalignant or precursor lesions. K-*ras* mutations are involved in the entire progression of pancreatic carcinogenesis, including early and late stages. Almost all K-*ras* mutations occur in codon 12 (Alguacil *et al.,* 2003).

Because up to 90% of pancreatic cancers show active K-*ras* mutation, activation of the RAS-RAF-MEK-ERK-MAP kinase pathway is critically important for pancreatic cells to be transformed to cancer cells. This pathway mediates cellular responses to growth signals (Kolch, 2000). It is concluded that K-*ras* oncogene is strongly associated with the tumorigenesis of pancreatic cancers, because mutations of this gene at codon 12 are detected at a level (up to 90%) higher than in other cancers. Accumulated evidence indicates that K-*ras* mutations play an important role in the development of premalignant stages not only in the pancreas but also in other cancers such as stomach cancer. This information can be translated into effective chemopreventive and therapeutic strategies.

Although K-*ras* mutations are important initiating events, inactivation of the *Rb-1, p16*, and *p53* tumor-suppressor genes, as well as the *Smad* genes, are also important in pancreatic tumor development and progression, which are discussed later in this chapter. Unlike ductal adenocarcinoma, pancreatic acinar carcinomas frequently contain alterations in the *APC* or *CTNNB1* genes, which lead to deregulated Wnt signaling but do not harbor mutations in the K-*ras, p16, p53,* and *Smad* genes (Abraham *et al.,* 2002; Bardeesy and DePinho, 2002). Indeed, it has been suggested that the mutation in K-*ras* may require combination with inactivation of one or more of these genes to induce cancer (Brembeck *et al.,* 2003). Thus, pancreatic adenocarcinomas arise in ductal epithelial cells and undergo a carefully orchestrated program of genetic alterations that arise in premalignant lesions. In other words, multiple oncogene types are involved in this cancer and many other cancer types in a coordinated way. As an example of coordination, the relationship of the *p53* gene with the K-*ras* gene is presented next.

A relationship between alterations in K-*ras* genes and those in *p53* genes has been reported in the pancreatic tumors. Both of these alterations occur, for example, in the intraductal stage of mucin-producing tumors of the pancreas, and the latter is superimposed on the former during the course of tumor progression (Sakai *et al.,* 2000). With regard to the distribution of K-*ras* mutation and loss of heterozygosity (LOH) of *p53* gene, the former is distributed widely throughout the tumor, whereas the latter appears only in some limited areas of the tumor. The specificity of K-*ras* mutations is relatively easy to detect because they are generally limited to one codon (codon 12), whereas the detection of *p53* is more difficult because of its multiple sites of mutations. A stepwise increase in the frequency of codon 12 mutations correlates with the stage of neoplastic evolution to cancer. With respect to clonal progression, certain clones with K-*ras* gene mutations gain a growth advantage to form a tumor, and then a selected subclone harboring alteration of a different gene (e.g., LOH of *p53* gene) obtains a further growth advantage.

A relationship has also been reported between K-*ras* mutations and serum organochlorine compounds in pancreatic cancer (Porta *et al.,* 1999). However, these results require replication before their acceptance as a diagnostic tool for this cancer. Similarly, the measurement of markers, such as carcinoembryonic antigen, cancer-associated carbohydrate antigen, and pancreatic oncofetal antigen, in the pancreatic juice is not useful in the diagnostic modalities of this cancer.

Also, the detection of point mutations in the K-*ras* gene at codon 12 even in pure pancreatic juice has little or no specificity for pancreatic neoplasms (personal communication, Hitoshi Kondo).

Additional information regarding the functional relevance of Ras proteins in pancreatic cancer has been obtained by studying the effect of these proteins on transforming growth factor beta (TGFβ). Such information is meaningful because overexpression of TGFβ and its receptor (TGFβR) as well as inactivating mutations of TGFβ pathway components (e.g., Smad 4 and TGFβ2) have been described in pancreatic cancer (Goggins *et al.,* 1996). Expression profiling analyses have been used for studying the relevance of *Ras*-signaling events in the TGFβ1-mediated transcriptional phenotype of the pancreatic cancer cell line PANC-1 (Fensterer *et al.,* 2004). These cells have a functional TGFβ pathway with an intact TGFβR system and wild-type *Smad* 4, which react to TGFβ1 treatment by a moderate inhibition of cell growth (Giehl *et al.,* 2000).

Comparative studies have shown significant differences in the overall frequency of K-*ras* mutations in pancreatic cancer among persons of different ethnicities (Dong *et al.,* 1999). In addition, the effect of these mutations in terms of poor prognosis of this cancer differs depending on the ethnicity of the patient. For example, the frequency of K-*ras* point mutations is lower in Chinese patients than in Japanese patients, but is similar to that in White patients. The primary reason for these differences is different lifestyles of individuals of different ethnicities in different countries.

Maspin

Maspin protein is related to the serpin family of protease inhibitors. Protease inhibitors have the ability to prevent tumor invasion and metastasis by inhibiting degradation of extracellular matrix proteinase (Liotta *et al.,* 1991). Accumulated functional evidence demonstrates that maspin blocks tumor metastasis *in vitro* (e.g., Cher *et al.,* 2003). It has been shown that maspin expression is lost at the critical transition from noninvasive to invasive breast and prostate carcinomas (Chen *et al.,* 2003). Maspin also suppresses tumor progression by enhancing cellular sensitivity to apoptotic stimuli. Cellular, molecular, and biochemical studies demonstrate an essential role of Bax in the proapoptotic effect of maspin (Liu *et al.,* 2004). Bax is up-regulated in maspin-transfected prostate and breast tumor cells. The link between maspin and Bax up-regulation explains the loss of maspin-expressing tumor cells in invasive breast and prostate carcinomas.

Maspin is down-regulated but not mutated in cancer cells. Down-regulation of maspin is also involved in carcinomas other than breast and prostate cancers. Oh *et al.* (2002) have investigated the usefulness of maspin as an adjunct diagnostic marker in various pancreatic neoplasms. This immunohistochemical study showed that all of the pancreatic ductal adenocarcinomas were positive for maspin, although a significant correlation between the maspin expression and the clinical stage was not determined. In contrast, nonneoplastic pancreatic parenchyma and chronic pancreatitis lacked maspin expression. This and other studies suggest that maspin may be of importance in the pathobiology of pancreatic neoplasms with epithelial origin, especially pancreatic tumors that are composed of mucin-producing cells. Using IHC of maspin may be useful in separating ductal adenocarcinoma from ACC, pancreatic endocrine tumor, solid-pseudopapillary tumor, and chronic pancreatitis, particularly in needle biopsy specimens. It is suggested that maspin may be used as a modifier for apoptosis-based cancer therapy.

Metastasis-Associated Gene 1

The metastasis-associated gene (*MTA1*) is mapped to the center of a 1.6 Mb region of human chromosome 14q 31.2 and encodes a protein of 715 amino acids with a calculated molecular mass of 80.8 kDa. Enhanced expression of MTA1 mRNA is found in a variety of human cancerous tissues and carcinoma cell lines, including colorectal, gastric, and esophageal (e.g., Toh *et al.,* 1999). Comparative analyses reveal differential expression of this mRNA in nonmetastatic and metastatic tumors, pointing toward a role of MTA1 in enhancing the metastatic potential of malignant tumor cells (Nicolson *et al.,* 2003). Immunofluorescence studies also demonstrate enhanced expression of MTA1, which triggers the development of motile, invasive pancreatic carcinoma cells by altering the organization of the cellular cytoskeleton (Hofer *et al.,* 2004). Thus, enhanced expression of MTA1 is thought to be of considerable importance to understand the malignancy of pancreatic neoplasms.

Microvascular Density

A brief comment on the role of microvascular density, a marker for tumor angiogenesis, in pancreatic cancer is given later. It is known that the process of angiogenesis is essential for tumor growth and is important for the tumor capacity to metastasize. Routinely, IHC is used to measure the angiogenic activity. This technique has shown that high microvascular density is correlated with decreased survival rate in several types of cancers. Microvascular density has also been demonstrated to be a valuable indicator of

overall and relapse-free survival in patients with pancreatic adenocarcinoma and may therefore be useful for prognostic evaluation and treatment of patients with pancreatic ductal carcinoma (Fujioka *et al.,* 2001).

The prognostic value of microvascular density in pancreatic neuroendocrine tumors has also been investigated. Tan *et al.* (2004) have evaluated microvascular density in these tumors and correlated it with clinicopathologic features and patient outcome for determining whether this information is a useful prognostic indicator for these patients. In their study, 25 pancreatic neuroendocrine tumors from archival files resected between 1981 and 2000 were studied. According to this study, microvascular density in pancreatic neuroendocrine tumors is not correlated with the patient outcome and is not a useful prognostic indicator in these patients. These results suggest that factors other than the number of microvessels are important in determining pancreatic neuroendocrine tumor behavior. However, most tumors, including these tumors, are highly vascularized.

Mucins

Mucins are a group of genes that transcribe for glycoproteins (MUC1-9) and that are differentially expressed in various tumor types. Epithelial mucins (MUC1, MUC2, and MUC5) are frequently overexpressed in epithelial cancers, particularly those arising in the gastrointestinal tract and pancreas. MUC1 (mammary-type mucin) is a membrane-associated glycoprotein detected in most epithelial tissues and is highly expressed in the pancreas and breast. MUC2 is an intestinal-type secretory mucin, expressed in goblet cells of the intestine. The expression of MUC1 is commonly observed in invasive pancreatic adenocarcinoma at both the transcript and protein levels, whereas MUC2 expression is a marker of the indolent pathway (Adsay *et al.,* 2002).

The differential expression of mucins described earlier is important in differentiating pancreatic invasive ductal carcinoma (IDC) from pancreatic intraductal papillary mucinous tumor (IPMT) because patients with IDC show poor outcome of radical surgery. However, patients with IPMT can be cured by appropriate surgery and a considerable number can survive without surgery. Patients with IPMT, however, sometimes show invasive proliferation and poor outcome. Thus, it is important to know which subtype of IPMT has a high potential for malignancy and needs surgical treatment. Such subtype can be determined by targeting the type of mucin present.

Immunohistochemical and *in situ* hybridization studies have been carried out for differentiating malignant pancreatic tumors from benign (Nakamura *et al.,* 2002). Invasive ductal carcinoma usually showed positive MUC1 and negative MUC2 expression, whereas IPMT was negative for MUC1 and positive for MUC2. This information is of value in assessing the biological behavior of the IPMTs and their potential for malignancy and improved surgical management. This and other evidence indicates that a dichotomy in carcinogenesis exists in the pancreas in the forms of IDC and IPMT.

A uniform nomenclature and standardized diagnostic criteria for pancreatic precursor lesions have been adopted, and the accepted terminology is now PanIN, the precursors of ductal adenocarcinoma. The PanINs are small incidental duct lesions that progress to invasive ductal adenocarcinomas. Immunohistochemical labeling with MUC1 and MUC2 antibodies has been performed on PanINs, intraductal papillary mucinous neoplasms, ductal carcinoma, and colloid carcinomas (Adsay *et al.,* 2002). This study indicates that colloid carcinomas are MUC2 positive, whereas this labeling pattern is reverse for ductal adenocarcinomas that are rich in MUC1 and poor in MUC2. Because these two pathways often lead to different types of invasive carcinomas, they are an invaluable model for the study of pancreatic carcinogenesis.

A high-throughput tissue microarray study demonstrates that molecular abnormalities in pancreatic cancer are not random; they can usually be stratified into early changes (expression of MUC5 and prostate stem antigen, or loss of p16), intermediate changes (expression of D1), and late changes (expression of p53, proliferation antigens, MUC1, mesothelin, or loss of Smad4/Dpc4) (Maitra *et al.,* 2003). Invasive pancreatic adenocarcinoma, once established, is almost always fatal, and, therefore, the systematic identification and targeting of molecular abnormalities in the precursor lesions of invasive cancer is one of the strongest avenues for combating this lethal disease.

Neurokinin-1 Receptor

Neurokinin-1 receptor (NK-1R) belongs to the class of seven transmembrane domain receptors that interact with intracellular effector systems via guanine nucleotide-binding regulatory proteins (G-proteins) (Quartara and Maggi, 1997). Neurokinin-1 receptor is up-regulated in human pancreatic cancer, and pancreatic cancer cell growth is stimulated by the neurotransmitter substance P (SP). The expression of NK-1R mRNA and protein in human pancreatic cancer specimens has been investigated by quantitative RT-PCR, *in situ* hybridization, IHC, and Western Blot analysis and compared with normal controls (Friess *et al.,* 2003). This study indicates that the NK-1R pathway is activated in human pancreatic cancer and has the potential to contribute to cancer cell growth.

Nuclear Factor Kappa B

Nuclear factor kappa B (NF-kB) is a member of the Rel family of transcriptional regulatory proteins, including p50 and p52. The untethered NF-kB translocates to the nucleus and binds to the specific *cis*-elements located in the promoters of various genes, including adhesion molecules, enzymes, cytokines, and chemokines. The activation of NF-kB has been shown to involve multiple immune and inflammatory mechanisms (Mariagrazia *et al.,* 1993). Many experimental studies have implicated the activation of NF-kB as an important step in the pathogenesis of acute pancreatitis and the development of systemic complications (Chen *et al.,* 2002).

Considerable evidence indicating that the expression of NF-kB in peripheral blood mononuclear cells (PBMCs) is increased in pathologic conditions such as sepsis, trauma, inflammation, and diabetes mellitus is available (e.g., Arnalich *et al.,* 2000). Such expression level might therefore serve as an indicator of clinical severity. It has been shown the NF-kB is activated in experimental pancreatitis models and that there are quantitative differences in the degree of NF-kB expression between the macrophoges from rats with severe pancreatitis and those from rats with mild pancreatitis (Satoh *et al.,* 1999). In 2003, it was demonstrated that NF-kB is involved in the clinical course of acute pancreatitis (Satoh *et al.,* 2003). In this study it was suggested that altered features of NF-kB in PBMCs may predispose patients to a higher risk of serious systemic complications if these altered features are prolonged.

A brief comment on the development of acute pancreatitis is in order. The natural course of severe acute pancreatitis constitutes two phases: The early phase is characterized by multiple organ failure, chiefly during the first 2 to 3 weeks after the onset, and the late phase is dominated by septic complications, mostly later than 3 weeks from the onset (Beger *et al.,* 1986). A relationship between an impaired immune reaction and susceptibility to bacterial infection has been suggested (Satoh *et al.,* 2002). An immune disorder is thought to be present even in the early phase of acute pancreatitis and continues for a long time in the patients who develop sepsis in the later clinical course. Elucidation of immunologic status during acute pancreatitic may contribute to the development of an effective approach for improving the prognosis of the disease (Satoh *et al.,* 2003).

Osteopontin

Osteopontin (OPN), a glycoprotein normally produced by osteoblasts, arterial smooth muscle cells, various epithelia, activated T cells, and macrophages, is secreted into most body fluids (O'Brien *et al.,* 1994). As a member of the small integrin family, OPN is able to bind to extracellular matrix proteins. It functions as a signaling molecule, either in the soluble form or as an immobilized cell-adhesion protein. The functions most likely related to tumorigenesis include facilitation of anchorage-independent growth in transformed cells, stimulation of migration and invasion, binding and activation of matrix metalloproteinases, protection from apoptosis, enhancement of metastatic ability, and direct stimulation of cancer cell proliferation and progression (for references, see Koopmann *et al.,* 2004).

In clinical studies, OPN has been associated with decreased survival in patients with cancer, increased metastatic potential, and advanced disease stage. Using global gene expression technology, OPN was identified as overexpressed (7.9-fold) in pancreatic cancer (Iacobuzio-Donahue *et al.,* 2002a). Because of the secreted nature of the OPN, it was evaluated as a serum marker of pancreatic adenocarcinomas (Koopmann *et al.,* 2004). This ISH study has shown strong OPN mRNA in tumor-infiltrating macrophages in pancreatic adenocarcinomas, compared with normal pancreatic tissues. This and other studies demonstrate that serum OPN has a diagnostic potential as a marker for pancreatic adenocarcinomas.

p16

The *p16* gene product is a 16-Kd protein that inhibits formation of cyclin D/CDK4 complexes. Loss of p16 function results in the release of activated transcription factors and progression of the cell cycle through the G1/S checkpoint. Frequent alterations of p16 occur in a number of human malignancies, and mechanisms of inactivation include homozygous deletion, mutation, and aberrant methylation of 5′ CpG islands (Cowgill and Muscarella, 2003). It is known that 5′ CpG island methylation of pancreatic cancers exhibits abrogation of the Rb/p16 tumor-suppressive pathway by potentially inactivating *p16* gene alterations (Schutte *et al.,* 1997). This evidence and immunohistochemical results indicate a significant role for *p16* inactivation in pancreatic cancer.

p21$^{WAF1/C1P1}$

p21 is an inhibitor of cyclin-dependent kinase and acts to prevent protein retinoblastoma (pRb) phosphorylation by inhibiting activation of cyclin E/cdk2 complexes that are required for Rb phosphorylation. Expression of *p21* is regulated by a number of signaling molecules, including *p53* and *K-ras.* However, an agreement on the role of these two genes in the induction of *p21* in pancreatic cancer is lacking. Some studies

indicate that *p21* is induced by wild-type *p53* but not mutant *p53* (El-Deiry *et al.,* 1994). Other studies report that *p21* expression in pancreatic adenocarcinoma may be induced by a *p53*-independent pathway (DiGiusseppe *et al.,* 1995). Immunohistochemical studies have demonstrated that overexpression of p21 is an early event in the development of PanIN (Hermanová *et al.,* 2003). Overexpression of *p2l* increases progressively from normal ducts through the spectrum of PanIN lesions in resection specimens of chronic pancreatitis and invasive carcinoma.

Activating mutations of *K-ras* are known to increase intracellular levels of *p21* in experimental models (Kivinen *et al.,* 1999). However extensive immunohistochemical and PCR-restriction fragment length polymorphism (PCR-RFLP) studies indicate the absence of activating *K-ras* mutations in specimens containing normal ducts and PanIN lesions that overexpressed *p21* (Hermanová *et al.,* 2003). An alternative pathway to explain the activation of *p21* is the overexpression of HER-2/neu that is detected in a significant proportion of PanIN lesions and pancreatic carcinomas (Novotny *et al.,* 2000). The role of HER-2/neu biomarker in pancreatic cancer is discussed elsewhere in this chapter.

p27

The p27/Kip 1 protein belongs to the family of proteins called cyclin-dependent kinase inhibitors (CDKIs). It prevents progression of the cell cycle from G1 phase into S phase by binding to and inhibiting the cyclin E/Cdk2 complex. Because p27 also interacts with various other cyclin complexes, it is designated as a universal CDKI. The highest levels of *p27* expression occur during the quiescent G0 and prereplicative G1 phases.

Neoplastic cells progress rapidly through the cell cycle, often ignoring the mechanisms that control cell division. Cyclin-dependent kinases (CDKs) play an important role in cell cycle control. They form cyclin-CDK complexes that facilitate entry into the S phase. The CDKs are bound and inactivated by various proteins, including p27, thus reducing cell proliferation. In this role, p27 is a potential tumor suppressor, and its levels are reduced in many tumor types, including pancreatic ductal adenocarcinomas. In this cancer, a loss of p27 expression is correlated with high tumor grade, advanced clinical stage, and aggressive character of the disease. The prognostic value of p27 is discussed later.

Immunohistochemical expression of p27 and its prognostic value in a series of 147 human pancreatic ductal adenocarcinomas has been investigated (Juuti *et al.,* 2003). This study demonstrated loss of p27 expression, which was associated with poor prognosis in stages 1 and 2 of pancreatic adenocarcinoma. The 5-year survival for patients negative for p27 was only 3.6% compared with 20% for patients positive for p27. Another immunohistochemical study has analyzed the relationships among p27 expression, pathologic features, and clinical outcome in resected pancreatic ductal adenocarcinomas from 46 European patients and in associated lymph node metastases from 13 patients (Feakins and Ghaffar, 2003). The extent of p27 expression (the percentage of cells expressing p27) was lower in carcinomas than in non-neoplastic ductal epithelia. No significant difference was seen between the extent of p27 expression in lymph node metastases and their corresponding primary tumors, and p27 expression did not correlate with patient gender.

p53

The *p53* tumor-suppressor gene is ubiquitous in the discussion of biomarkers for human cancers. It is inactivated in 40–75% of pancreatic cancers. The protein product of the *p53* gene responds to cellular DNA damage. Like *p16,* it tends to block the progression of cells through the G1 phase of the cell cycle. This protein also mediates cell death or apoptosis by detecting irreversible DNA damage within a cell. Interactions of p53 with many regulatory pathways have been identified, which are highly complex. In pancreatic cancer the primary mechanism of p53 inactivation is thought to be mutation because homozygous deletions have not been observed (Cowgill and Muscarella, 2003). Mutated p53 protein inhibits wild-type p53, and biallelic inactivation may not be necessary for loss of function. Alterations of p53 are associated with K-ras mutations, suggesting a cooperative effects in tumorigenesis (Kalthoff *et al.,* 1993).

Rad51

In the DNA repair pathway, recombinational processes function to maintain genetic stability, but if this process is deregulated or enhanced, genomic instability and malignant transformation can result (Maacke *et al.,* 2002). Rad51 is one of the key enzymes of homologous recombination and repairs DNA double-strand breaks. Overexpression of wild-type Rad51 is correlated with histologic grading of invasive ductal breast carcinoma as well as with human pancreatic adenocarcinoma (Maacke *et al.,* 2000a; Maacke *et al.,* 2000b). Because overexpression of Rad51 is restricted to tumor cells, it is a tumor-specific antigen. This antigen has been localized in pancreatic adenocarcinoma using monoclonal antibody 1 G8 and IHC (Maacke *et al.,* 2002).

S100P

S100P belongs to the family of S100 Ca-binding proteins. *S100* genes are small (9–12 kD), displaying 30–50% homology within the group. The *S100P* gene is located on 4p16. The functions of the S100 proteins are multiple, including interaction with cytoskeletal elements leading to dysfunction in microtubule assembly and increased motility and invasion (Donato, 2001). S100 proteins are of major interest owing to their differential expression in a variety of tumors and their putative involvement in the metastatic process (Ilg *et al.,* 1996). The IHC (using anti-S100P monoclonal antibody) of S100P protein has been carried out and correlated S100P expression with the level of its transcript detected on cDNA arrays to determine the site of protein expression (Crnogorac-Jurcevic *et al.,* 2003). This study suggests specific increase of S100P at both RNA and protein levels almost exclusively in pancreatic adenocarcinoma. In addition, this protein is highly elevated in intraductal papillary mucinous tumors, pointing to the involvement of the S100P gene in early stages of pancreatic tumor development (Terris *et al.,* 2002). This evidence suggests a potential value of S100P for diagnostic and disease-monitoring purposes.

S100A6

S100A6 is a low molecular mass (10 kDa) Ca^{2+} binding protein. It belongs to a family of S100 proteins, members of which are expressed in a cell- and tissue-specific manner. These proteins are implicated in a variety of diseases, including cancer development and metastasis. Immunohistochemical analysis of a pancreatic cancer tissue array has revealed that the normal ductal cells in 83% of cases were devoid of detectable cytoplasmic S100A6, whereas more than half lacked nuclear S100A6 (Shekouh *et al.,* 2003). The level of S100A6 expression was weak or intermediate in the normal ducts that exhibited staining. Well-differentiated tumors showed slightly more cytoplasmic staining but similar nuclear staining.

In contrast, moderately and poorly differentiated pancreatic cancers showed both a greater frequency and a higher intensity of S100A6 expression. This pattern of staining indicates that this protein is potentially involved in pancreatic cancer progression. Microarray technology has also identified Sl00A6 as highly expressed at the RNA level in this cancer (Crnogorac-Jurcevic *et al.,* 2003) . This proteomic approach can uncover changes in protein expression that correlate with the malignant pancreatic phenotype. The exact function of S100A6 and the mechanism(s) underlying its overexpression in pancreatic cancer cells are not known.

Serine Proteinase Inhibitor

SERPINE2 (protease nexin I) is an extracellular serine proteinase inhibitor with activity toward trypsin, thrombin, plasmin, uPA, and other serine proteinases. This inhibitor plays a central role in a physiologic process of invasion—namely, neurite outgrowth during embryogenesis and nerve regeneration (Zurn *et al.,* 1988). The mechanism by which SERPINE2 exerts its effect on the invasiveness of tumor cells is derived from the observation that SERPINE2-expressing tumors, especially highly invasive specimens, contain significantly higher amounts of extracellular matrix (ECM) components organized in prominent fibrous bundles than their non–SERPINE2-expressing counterparts (Pupa *et al.,* 2002). It is known that the ECM, depending on its cellular context, can actively regulate growth, death, adhesion, cell migration, invasion, gene expression, and differentiation in neighboring cells. Invasive cancer cells benefit in many ways from inducing specific changes in the ECM composition in and around the tumor. Immunohistochemical studies demonstrate that SERPINE2 overexpression enhances the invasive potential of pancreatic cancer cells in nude mice xenografts by altering ECM production and organization within the tumors (Buchholz *et al.,* 2003). This experimental system provides the opportunity to model the desmoplastic reaction of pancreatic cancer and represents a new tool for studying tumor–stroma interactions.

Smad 4

The Smad signal inhibits the growth of most epithelial cells. Impairment of the Smad pathway causes escape from growth inhibition and leads to the promotion of cell proliferation, thereby contributing to carcinogenesis. Several genetic or epigenetic alterations of the components of the Smad pathway have been identified in several human cancers (Wang *et al.,* 2000). Mutations or deletion of the Smad gene have been detected in ~50% of all pancreatic cancers. (Smad gene was originally designated as the tumor-suppressor gene that DPC4 deleted in pancreatic carcinoma, locus 4.) Many pancreatic cancer cell lines also have impaired TGFβ-Smad signaling owing to a functionally inactivated Smad 4 (Ijichi *et al.,* 2001).

Stk11 Gene

Stk 11 (LKB11) mediates cell cycle arrest through induction of the cyclin-dependent kinase inhibitor $p21^{WAF1}$, through a p53-dependent process. The Stk11 protein also interacts with brahma-related gene-1

(BRG1) and ATPase that is associated with SW1/SNF chromatin-remodeling complexes. Exogenous expression of BRG1 induces cell cycle arrest and senescence (Tiainen *et al.,* 2002). The tumor-suppressor function of Stk11 is related to its ability to affect the cell cycle proliferation. It is also known that germline mutations of Stk11 gene located on distal chromosome 19p cause Peutz-Jeghers syndrome (PJS). This syndrome is an autosomal-dominant disorder characterized by hamartomatous polyps in the gastrointestinal tract and pigmented macules of the lips and buccal mucosa. The syndrome is also associated with an increased risk of developing cancers, including pancreatic cancer (Su *et al.,* 1999). Somatic mutations of Stk11 are involved in a small proportion of sporadic pancreatic adenocarcinomas, intraductal papillary mucinous neoplasms, and biliary adenocarcinomas.

An antibody specific for the protein product of the Stk11 gene has been used for characterizing its distribution in pancreatobiliary neoplasms (Sahin *et al.,* 2003). This study included a large series of pancreatic (n = 56) and biliary (n = 38) neoplasms with known Stk11 gene status. The inactivation of Stk11 was observed in 7% of pancreatic adenocarcinomas and 27% of intraductal papillary mucinous neoplasms. This difference suggests genetic disparity in the pathogenesis of these closely related neoplasms. Because IHC has the advantage of detecting genetic abnormalities irrespective of the mechanism of gene inactivation, immunohistochemical analysis of the abrogation of Stk11 expression may be a valid surrogate for genetic analysis of this mutation in cancer.

Telomerase

Telomerase is an enzyme involved in the *de novo* synthesis of telomere at chromosomal ends. Telomerase is activated in various human malignant tumors, including lung, gastric, and colorectal tumours (Shay and Bacchetti, 1997). This enzyme has also been detected in the pancreatic cancer but not in benign tumors or precancerous lesions (Hiyama *et al.,* 1997). It has also been detected in some types of normal cells, especially in proliferative stem cells and activated lymphocytes (Hiyama *et al.,* 1997). To avoid the false-positive results by contaminating lymphocytes, Murakami *et al.* (2002) have detected telomerase activity in the pure pancreatic juice that was obtained preoperatively by endoscopic retrograde pancreatic juice aspiration; the juice was analyzed by telomeric repeat amplification protocol (TRAP) assay. This study was carried out when a 52-year-old man complained of abdominal pain and was diagnosed with malignant IPMT of the pancreas. This malignancy is difficult to diagnose by imaging examination. It is concluded that detection of telomerase activity of the pure pancreatic juice can be useful to distinguish benign from malignant IPMT preoperatively.

Transforming Growth Factor Beta 1

The gene *TGFβ1* plays a dual role in pancreatic carcinogenesis. In early phases of carcinogenesis, *TGFβ1* is a potent mediator of antiproliferative effects such as cell-cycle arrest and growth inhibition. In later stages, this factor contributes to tumor progression by inducing cell spreading, migration, angiogenesis, and tumor cell invasion (Akhurst and Derynck, 2001). One of the main mechanisms responsible for this dual role is thought to be the introduction of an epithelial-mesenchymal transdifferentiation (EMT) of epithelial tumor cells. During this transdifferentiation, the epithelial phenotype is lost and a mesenchymal phenotype is acquired that is associated with enhanced invasiveness and metastasis (Janda *et al.,* 2002).

The *Ras* pathway is implicated in mediating these effects of TGFβ1 on tumor cell morphology. It has been shown that TGFβ1 causes reversible and time-dependent EMT in TGFβ1-responsive pancreatic cancer cell lines that harbor activating mutations of the *Ras2* oncogene (Ellenrieder *et al.,* 2001). Expression-profiling analyses have been used for studying the functional relevance of Ras proteins to the TGFβ1-mediated transcriptional phenotype of the pancreatic cancer cell line PANG-1 (Fensterer *et al.,* 2004). This study indicates that in these cells *Ras*-dependent signal-transduction pathways are intimately involved in the induction of EMT following TGFβ1 stimulation. It is known that TGFβ1 activates several signaling pathways such as the RAS-RAF-MEK-MAPK pathway in addition to Smad-dependent signal transduction (Janda *et al.,* 2002).

Vascular Endothelial Growth Factor

The VEGF is a potent angiogenic peptide with specific mitogenic activity on endothelial cells. It is the best characterized of the angiogenic factors and has been associated with increased angiogenesis and poor prognosis in patients with a variety of solid tumors, including pancreatic carcinoma. Members of the VEGF family mediate both vascular permeability and endothelial cell proliferation through three tyrosine kinase receptors: VEGFR receptor-3 (VEGFR-3; Flt-4). The VEGF exists in four isoforms generated by alternative mRNA splicing. The shorter isoforms ($VEGF_{121}$ and $VEGF_{165}$) are secreted peptides that may act as diffusible agents with $VEGF_{165}$ being the predominant soluble isoform, whereas the longer isoforms

($VEGF_{189}$ and $VEGF_{206}$) are bound to the extracellular matrix (Houck *et al.,* 1991).

The VEGF affects not only endothelial cells but also tumor cells. Up-regulation of VEGF and its receptors at both mRNA and protein levels has been demonstrated in pancreatic ductal carcinoma cell lines and in human pancreatic cancer tissues (Itakura *et al.,* 2000). Furthermore, tissue VEGF expression is an independent prognostic marker for early recurrence after curative resection of the pancreatic tumor (Niedergethmann *et al.,* 2002).

Immunohistochemical and immunofluorescent studies demonstrate that the VEGF receptor neuropilin-1 (NRP-1) is associated with human pancreatic adenocarcinoma but not with nonmalignant pancreatic tissue (Parikh *et al.,* 2003). Regulation of NRP-1 expression is thought to be involved, at least in part, in VEGF-dependent signaling pathways. This receptor is also involved in the potential mechanism by which EGF affects the growth of pancreatic carcinoma (Parikh *et al.,* 2003).

Soluble forms of VEGF are also detectable in the serum from patients with various types of adenocarcinomas, often correlating with tumor stage, microvessel density, and tumor VEGF expression (Yamamoto *et al.,* 1996). Karayiannakis *et al.* (2003) also report that patients with pancreatic cancer have significantly higher serum VEGF levels compared with healthy controls, with a significant association between serum VEGF levels, disease stage, and the presence of both lymph node and distant metastases. Serum levels of VEGF decrease markedly after radical resection of the tumor. Elevated preoperative serum VEGF level is an important prognostic factor for patient survival, although not independent of tumor stage. These findings suggest that serum VEGF concentrations tend to reflect pancreatic cancer progression, and their determination may be clinically useful.

Validity of Biomarkers in Clinical Practice

Tumor markers are usually proteins associated with a malignancy, which might be clinically usable in patients with cancer. A tumor marker can be detected in a solid tumor; in circulating tumor cells in peripheral blood; in lymph nodes; in bone marrow; or in other body fluids such as urine, stool, and ascites. Screening for early diagnosis via marker detection generally results in lower mortality for diseases such as breast cancer and cervical cancer. Many malignancies, including pancreatic cancer, however, are still diagnosed after the metastatic process has already begun, indicating poor prognosis.

A tumor marker can be used to define a particular disease entity; in this case it can be used for diagnosis, staging, or population screening (Lindblom and Liljegren, 2000). In addition, markers can be used to detect the presence of occult metastatic disease, to monitor response to treatment, or to detect a recurrent disease. Markers can also be used as targets for therapeutic intervention in clinical trials.

Although biomarkers are being introduced into clinical decisionmaking at an increasing rate, the basic understanding of the underlying molecular mechanisms and their clinical use is not always clear. Some aspects of such molecular mechanisms, including molecular pathways, are explained in this volume. Caution is warranted in the use of biomarkers because only a few guidelines have been established to standardize a biomarker for a specific type of cancer. The guidelines will help to interpret the data correctly to reach correct clinical decisionmaking.

Hayes *et al.* (1996) have proposed a tumor marker utility grading system, a framework to evaluate clinical utility of tumor markers. In support of this proposal, the editor of the *International Journal of Biomarkers* has suggested a checklist for designing studies using biomarkers (Gion *et al.,* 1999). More recently, Sweep *et al.* (2003) have discussed in detail various factors that may play a role in discordant test results; these factors include method of specimen collection (FNA, core biopsy, or large biopsy obtained during surgery), source of tissue (fresh or frozen), storage (duration, temperature, or freeze-thawing cycles), and processing (e.g., differences in antibody specificity or affinity used in different test kits and reference materials provided with the kits). For detailed information on the factors that affect antigen retrieval, the reader is referred to Hayat (2002).

The size of the tissue specimen is also important because of the heterogeneity of tumors. Subclonal diversity results in a heterogeneous tumor. Because of this, sampling bias may occur, leading to different test results if different areas of a tumor are examined. The necessity of including a standardized, detailed Materials and Methods section in scientific publications cannot be overemphasized. This requirement is fulfilled uniformally in various chapters in this volume. The major question that remains is how and when to transfer technologies from the research setting to the clinic (translational research). This question is answered by the type of biomarker, its relevancy to a certain malignancy, and the demand by both the patient and the clinician.

References

Abraham, S.C., Wu, T.T., Hruban, R.H., Lee, J.H., Yeo, C.J., Conlon, K., Brennan, M., Cameron, J.L., and Klimstra, D.S.

2002. Genetic and immunohistochemical analysis of pancreatic acinar cell carcinoma: Frequent allelic loss on chromosome 1lp and alterations in the APC/beta-catenin pathway. *Am. J. Pathol. 160*:953–962.

Adsay, N.V., Merati, K., Andea, A., Sarkar, F., Hruban, R.H., Wilentz, R.E., Goggins, M., Iocobuzio-Donahue, C., Longnecker, D.S., and Klimstra, D.S. 2002. The dichotomy in the preinvasive neoplasia to invasive carcinoma sequence in the pancreas: Differential expression of MUC1 and MUC2 supports the existence of two separate pathways of carcinogenesis. *Mod. Pathol. 15*:1087–1095.

Aguirre, A.J., Bardeesy, N., Sinha, M., Lopez, L., Tuveson, D.A., Horne, J., Redston, M.S., and DePinho, R.A. 2003. Activated Kras and Ink4a/Arf deficiency cooperate to produce metastatic pancreatic ductal adenocarcinoma. *Genes Dev. 17*:3112–3126.

Ahlgren, J.D. 1996. Epidemiology and risk factors in pancreatic cancer. *Semin. Oncol. 23*:241–250.

Akakura, N., Kobayashi, M., Horiuchi, I., Suzuki, A., Wang, J., Chen, J., Niizeki, H., Kawamura, K.I., Hosokawa, M., and Asaka, M. 2001. Constitutive expression of hypoxia-inducible factor-1α renders pancreatic cancer cell resistant to apoptosis induced by hypoxia and nutrient deprivation. *Cancer Res. 61*: 6548–6554.

Akhurst, R.J., and Derynck, R. 2001. TGF-beta signaling in cancer—a double-edged-sword. *Trends Cell Biol. 11*:S44–S52.

Alguacil, J., Porta, M., Kauppinen, T., Malats, N., Kogevinas, M., and Carrato, A. 2003. Occupational exposure to dyes, metals, polycyclic aromatic hydrocarbons and other agents and K-ras activation in human exocrine pancreatic cancer. *Int. J. Cancer. 107*:635–641.

Amour, A., Knight, C.G., English, W.R., Webster, A., Slocombe, P.M., Knauper, V., Docherty, A.J., Becherer, J.D., Blobel, C.P., and Murphy, G. 2002. The enzymatic activity of ADAM8 and ADAM9 is not regulated by TIMPs. *FEBS. Lett. 524*:154–158.

Arnalich, F., Garcia-Palomero, E., Lopez, J., Jimenez, M., Madero, R., Renart, J., Vazquez, J.J., and Montiel, C. 2000. Predictive value of nuclear factor-kappa B activity and plasma cytokine levels in patients with sepsis. *Infect. Immunol. 68*:1942–1945.

Bardeesy, N., and DePinho, R.A. 2002. Pancreatic cancer biology and genetics. *Nature Rev. Cancer 2*:897–909.

Beger, H.G., Bittner, R., Block, S., and Buchler, M. 1986. Bacterial contamination of pancreatic necrosis: A prospective study. *Gastroenterology 91*:433–438.

Bloomston, M., Zervos, E.E., and Rosemurgy, A.S. 2002. Matrix metalloproteinase and their role in pancreatic cancer: A review of preclinical studies and clinical trials. *Ann. Surg. Oncol. 9*:668–674.

Bos, J.L. 1989. Ras oncogenes in human cancer: A review. *Cancer Res. 49*:4682–4689.

Brembeck, F.H., Schreiber, F.S., Deramaudt, T.B., Craig, L., Rhoades, B., Swain, G., Grippo, P., Stoffers, D.A., Silberg, D.G., and Rustgi, A.K. 2003. The mutant K-ras oncogene causes pancreatic periductal lymphocytic infiltration and gastric mucous neck cell hyperplasia in transgenic mice. *Cancer Res. 63*:2005–2009.

Bruell, D., Stocker, M., Huhn, M., Redding, N., Kupper, M., Schumacher, P., Paetz, A., and Bruns, C.J., Haisma, H.J., Fischer, R., Finnern, R., and Barth, S. 2003. The recombinant anti-EGF receptor immunotoxin 425(scFv)-ETA' suppresses growth of a highly metastatic pancreatic carcinoma cell line. *Int. J. Oncol. 23*:1179–1186.

Buchholz, M., Biebl, A., Neebetae, A., Wagner, M., Iwamura, T., Leder, G., Adler, G., and Gress, T.M. 2003. SERPINE2 (protease nexin I) promotes extracellular matrix production and local invasion of pancreatic tumors in vivo. *Cancer Res. 63*: 4945–4951.

Caldas, C., Hahn, S.A., deCosta, L.T., Redston, M.S., Schutte, M., Seymour, A.B., Weinstein, C.L., Hruban, R.H., Yeo, C.J., and Kern, S. 1994. Frequent somatic mutations and homozygous deletions of the p16 (MTS1) gene in pancreatic adenocarcinoma. *Nat. Genet. 8*:27–32.

Capella, C., Heitz, P.U., Hofler, H., Solcia, E., and Kloppel, G. 1995. Revised classification of neuroendocrine tumours of the lung, pancreas and gut. *Virchows Arch. 425*:547–560.

Chang, I., Kim, S., Kim, J.Y., Cho, N., Kim, Y.H., Kim, H.S., Lee, M.K., Kim, K.W., and Lee, M.S. 2003. Nuclear factor κB protects pancreatic β-cells from tumor necrosis factor-alpha-mediated apoptosis. *Diabetes 52*:1169–1175.

Chang, K.J., Albers, C.G., Erickson, R.A., Butler, J.A., Wuerker, R.B., and Lin, F. 1994. Endoscopic ultrasound-guided fine needle aspiration of pancreatic carcinoma. *Am. J. Gastroenterol. 89*:263–266.

Chen, J.M., Montier. T., and Ferec, C. 2001. Molecular pathology and evolutionary and physiological implications of pancreatitis-associated cationic trypsinogen mutations. *Hum. Genet. 109*: 245–252.

Chen, X., Ji, B., Han, B., Ernst, S.A., Simone, D., and Logsdon, C.D. 2002. NF-kappaB activation in pancreas induces pancreatic and systemic inflammatory response. *Gastroenterology 122*:448–457.

Chen, Z., Fa, Z., McNeal, J.E., Nolly, R., Caldwell, M.C., Mahadevappa, M., Zhang, Z., Warrington, T.A., and Stamey, T.A. 2003. Hespin and maspin are inversely expressed in laser capture microdissectioned prostate cancer. *J. Urol. 169*:1316–1319.

Cher, M.L., Biliran, H.R., Bhagat, S., Meng, Y., Che, M., Locket, J., Abrams, J., Friedman, R., Zachareas, M., and Sheng, S. 2003. Maspin expression inhibits osteolysis, tumor growth, and angiogenesis in a model of prostate cancer bone metastatis. *Proc. Natl. Acad. Sci. USA 100*:7847–7852.

Cowgill, S.M., and Muscarella, P. 2003. The genetics of pancreatic cancer. *Am. J. Surg. 186*:279–286.

Crane, C.H., Thames, H.D., and Hamilton, S.R. 2003. Will identifying and targeting altered marker expression in response to cytotoxic therapy be of prognostic or therapeutic value? *J. Clin. Oncol. 21*:3381–3382.

Crnogorac-Jurcevic, T., Missiaglia, E., Blaveri, E., Gangeswaran, R., Jones, M., Terris, B., Costello, E., Neoptolemos, J.P., and Lemoine, N.R. 2003. Molecular alterations in pancreatic carcinoma: Expression profiling shows that dysregulated expression of S100 genes is highly prevalent. *J. Pathol. 201*:63–74.

Davies, H., Bignell, G.R., Cox, C., Stephens, P., Edkins, S., Clegg, S., Teague, J., Woffendin, H., Garnett, M.J., Bottomley, W., Davis, N., Dicks, E., Ewing, R., Floyd, Y., Gray, K., Hall, S., Hawes, R., Hughes, J., Kosmidou, V., Menzies, A., Mould, C., Parker, A., Stevens, C., Watt, S., Hooper, S., Wilson, R., Jayatilake, H., Gusterson, B.A., Cooper, C., Shipley, J., Hargrave, D., Pritchard-Jones, K., Maitland, N., Chenevix-Trench, G., Riggins, G.J., Bigner, D.D., Palmieri, G., Cossu, A., Flanagan, A., Nicholson, A., Ho, J.W., Leung, S.Y., Yuen, S.T., Weber, B.L., Seigler, H.F., Darrow, T.L., Paterson, H., Marais, R., Marshall, C.J., Wooster, R., Stratton, M.R., and Futreal, P.A. 2002. Mutations of the BRAF gene in human cancer. *Nature 417*:949–954.

Dedhar, S., and Hannigan, G.E. 1996. Integrin cytoplasmic interactions and bidirectional transmembrane signaling. *Curr. Opin. Cell Biol. 8*:657–669.

DiGiusseppe, J.A., Redston, M.S., Yeo, C.J., Kern, S.E., and Hruban, R.H. 1995. p53-independent expression of the cyclin-dependent kinase inhibitor p21 in pancreatic carcinoma. *Am. J. Pathol. 147*:884–888.

Donato, R. 2001. S100: A multigenic family of calcium-modulated proteins of the EF-hand type with intracellular and

extracellular functional roles. *Int. J. Biochem. Cell Biol. 33*: 637–668.

Dong, M., Nio, Y., Tamura, K., Song, M.-M., Guo, K.-J., Guo, R.-X., and Dong, Y.-T. 1999. K-ras point mutation and p53 expression in human pancreatic cancer: A comparative study among Chinese, Japanese, and Western patients. *Cancer Epidemiol. Biomark. Prev. 9*:279–284.

Du, E., Katz, M., Weidner, N., Yoder, S., Moossa, A.R., and Shabaik, A. 2003. Ampullary pancreatoblastoma in an elderly patient: A case report and review of the literature. *Arch. Pathol. Lab. Med. 127*:1501–1505.

El-Deiry, W.S., Harper, J.W., O'Connor, P.M., Velculescu, V.E., Canman, C.E., Jackman, J., Pietenpol, J.A., Burrell, M., Hill, D.E., and Wang, Y. 1994. WAF1/CIP1 is induced in p53-mediated G1 arrest and apoptosis. *Cancer Res. 54*:1169–1164.

Ellenrieder, V., Hendler, S.F., Boeck, W., Seufferlein, T., Menke, A., Ruthland, C., Adler, G., and Gress, T.M. 2001. Transforming growth factor beta 1 treatment leads to an epithelial-mesenchymal transdifferentiation of pancreatic cancer cells requiring extracellular signal-regulated kinase-2 activation. *Cancer Res. 61*:4222–4228.

Feakins, R.M., and Ghaffar, A.H. 2003. $p27^{kip1}$ expression is reduced in pancreatic carcinoma but has limited prognostic value. *Hum. Pathol. 34*:385–390.

Fensterer, H., Giehl, K., Buchholz, M., Ellenrieder, V., Buck, A., Kestler, H.A., Adler, G., Gierschik, P., and Gress, T.M. 2004. Expression profiling of the influence of RAS mutants on the TGFB1-induced phenotype of the pancreatic cancer cell line PANC-1. *Genes Chromosomes Cancer 39*:224–235.

Francalanci, P., Diomedi-Camassei, F., Purificato, C., Santorelli, F.M., Giannotti, A., Dominici, C., Inserra, A., and Boldrini, R. 2003. Malignant pancreatic endocrine tumor in a child with tuberous sclerosis. *Am. J. Surg. Pathol. 27*:1386–1389.

Friess, H., Guo, X.Z., Berberat, P., Graber, H.U., Zimmermann, A., Korc, M., and Buchler, M.W. 1998. Reduced KAI1 expression in pancreatic cancer is associated with lymph node and distant metastases. *Int. J. Cancer. 79*:349–355.

Friess, H., Zhu, Z., Liard, V., Shi, X., Shrikhande, S.V., Wang, L., Lieb, K., Korc, M., Palma, C., Zimmermann, A., Reubi, J.C., and Buchler, M.W. 2003. Neurokinin-1 receptor expression and its potential effects on tumor growth in human pancreatic cancer. *Lab. Invest. 83*:731–742.

Fujii, H., Inagaki, M., Kasai, S., Miyokawa, N., Tokusashi, Y., Gabrielson, E., and Hruban, R.H. 1997. Genetic progression and heterogeneity in intraductal papillary-mucinous neoplasms of the pancreas. *Am. J. Pathol. 151*:1447–1454.

Fujioka, S., Yoshida, K., Yanagisawa, S., Kawakami, M., Aoki, T., and Yamazaki, Y. 2001. Angiogenesis in pancreatic carcinoma. *Cancer 92*:1788–1797.

Giehl, K., Seidel, B., Gierschik, P., Adler, G., and Menke, A. 2000. TGF-beta1 represses proliferation of pancreatic carcinoma cells which correlates with Smad4-independent inhibition of ERK activation. *Oncogene 19*:4531–4541.

Gigot, J.F., Deprez, P., Sempoux, C., Descamps, C., Metairie, S., Glineur, D., and Gianello, P. 2001. Surgical management of intraductal papillary mucinous tumors of the pancreas: The role of routine frozen section of the surgical margin, intraoperative endoscopic staged biopsies of the Wirsung duct, and pancreaticogastric anastomosis. *Arch. Surg. 136*: 1256–1262.

Gion, M., Boracchi, P., Biganzoli, E., and Daidone, M.G. 1999. A guide for reviewing submitted manuscripts (and indications for the design of translational research studies on biomarkers). *Int. J. Biol. Markers 14*:123–133.

Goggins, M., Schutte, M., Lu, J., Moskaluk, C.A., Weinstein, C.L., Petersen, G.M., Yeo, C.J., Jackson, C.E., Lynch, H.T., Hruban, R.H., and Kern, S.E. 1996. Germline *BRCA2* gene mutations in patients with apparently sporadic pancreatic carcinomas. *Cancer Res. 56*:5360–5364.

Gomez-Lira, M., Bonamini, D., Castellani, C., Unis, L., Cavallini, G., Assael, B.M., and Pignatti, P.F. 2003. Mutations in the SPINK1 gene in idiopathic pancreatitis Italian patients. *Eur. J. Hum. Genet. 11*:543–546.

Gress, T.M. (ed). 2000. *Molecular Pathogenesis of Pancreatic Cancer.* Amsterdam: IOS Press.

Griñó, P., Martinez, J., Griñó, E., Carnicer, F., Alonso, S., Perez-Berenguer, H., and Perez-Mateo, M. 2003. Acute pancreatitis secondary to pancreatic neuroendocrine tumors. *J. Pancreas 4*:103–110.

Grützmann, R., Lüttges, J., Sipos, B., Ammerpohl, O., Dobrowolski, F., Alldinger, I., Kersting, S., Ockert, D., Koch, R., Kalthoff, H., Schackert, H.K., Saeger, H.D., Kloppel, G., and Pilarsky, C. 2004. ADAM9 expression in pancreatic cancer is associated with tumour type and is a prognostic factor in ductal adenocarcinoma. *Br. J. Cancer 90*:1053–1058.

Haendler, B., Kratzschmar, J., Theuring, F., and Schleuning, W.D. 1993. Transcripts for cysteine-rich secretory protein-1 (CRISP-1; DE/AEG) and the novel related CRISP-3 are expressed under androgen control in the mouse salivary gland. *Endocrinology 133*:192–198.

Hahn, S.A., Greenhalf, B., Ellis, I., Sina-Frey, M., Rieder, H., Korte, B., Gerdes, B., Kress, R., Ziegler, A., Raeburn, J.A., Campra, D., Grützmann, R., Rehder, H., Rothmund, M., Schmiegel, W., Neoptolemos, J.P., and Bartsch, D.K. 2003. BRCA2 germline mutations in familial pancreatic carcinoma. *J. Natl. Cancer Inst. 95*:214–221.

Hahn, S.A., Schutte, M., Hoque, A.T., Moskaluk, CA., da Costa, L.T., Rozenblum, E., Weinstein, C.L., Fischer, A., Yeo, C.J., Hruban, R.H., and Kern, S.E. 1996. DPC4, a candidate tumor suppressor gene at human chromosome 18q21.1. *Science 271*: 350–353.

Hamilton, S.R., Aaltonen, L.A. (eds.) 2000. *Pathology and Genetics of Tumours of the Digestive* System, Vol. 2. World Health Organization Classification of Tumours. Lyon, France: IARC Press, 221–250.

Hayat, M.A. 2002. *Microscopy, Immunohistochemistry, and Antigen Retrieval Methods*. New York and London: Kluwer Academic/Plenum Publishers.

Hayes, D.F., Bast, R.C., Desc, C.E., Fritsche, H., Kemeny, N.E., Jessup, J.M., Locker, G.Y., MacDonald, J.S., Mennel, R.G., Norton, L., Ravdin, P., Taube, S., and Winn, R.J. 1996. Tumor marker utility grading system: A framework to evaluate clinical utility of tumor markers. *J. Natl. Cancer Inst. 88:* 1456–1466.

Hermanová, M., Lukas, Z., Kroupova, I., Kleibl, Z., Novotny, J., Nenutil, R., Pazourkova, M., Brazdil, J., Kren, L., and Dite, P. 2003. Relationship between K-ras mutation and the expression of p21 WAF1/CIP1 and p53 in chronic pancreatitis and pancreatic adenocarcinoma. *Neoplasma 50*:319–325.

Heymann, M.F., Joubert, M., Nemeth, J., Franc, B., Visset, J., Hamy, A., le Borgne, J., le Neel, J.C., Murat, A., Cordel, S., and le Bodic, M.F. 2000. Prognostic and immunohistochemical validation of the capella classification of pancreatic neuroendocrine tumours: An analysis of 82 sporadic cases. *Histopathology 36*:421–432.

Hirota, M., Kuwata, K., Ohmuraya, M., and Ogawa, M. 2003. From acute to chronic pancreatitis: The role of mutations in the pancreatic secretory trypsin inhibitor gene. *J. Pancreas 4*: 83–88.

Hiyama, E., Hiyama, K., Ohtsu, K., Yamaoka, H., Ichikawa, T., Shay, J.W., and Yokoyama, T. 1997. Telomerase activity in neuroblastoma: Is it a prognostic indicator of clinical behaviour? *Eur. J. Cancer 33*:1932–1936.

Hofer, M.D., Menke, A., Genze, F., Gierschik, P., and Giehl, K. 2004. Expression of MTA1 promotes motility and invasiveness of PANC-1 pancreatic carcinoma cells. *Br. J. Cancer 90*: 455–462.

Houck, K.A., Ferrara, N., Winer, J., Cachianes, G., Li, B., and Leung, D.W. 1991. The vascular endothelial factor family: Identification of fourth molecular species and characterization of alternate splicing of RNA. *Mol. Endocrinol. 5*:1806–1814.

Hsueh, C., and Kuo, T.T. 1992. Acinar cell carcinoma of the pancreas. Report of two cases with complex histomorphologic features causing diagnostic problems. *Int. J. Pancreatol. 12*:305–313.

Iacobuzio-Donahue, C.A., Maitra, A., Shen-Ong, G.L., van Heek, T., Ashfaq, R., Meyer, R., Walterm, K., Bergm, K., Hollingsworth, M.A., Cameron, J.L., Yeo, C.J., Kern, S.E., Goggins, M., and Hruban, R.H. 2002a. Discovery of novel tumor markers of pancreatic cancer using global gene expression technology. *Am. J. Pathol.160*:1239–1249.

Iacobuzio-Donahue, C.A., Ryu, B., Hruban, R.H., and Kern, S.E. 2002b. Exploring the host desmoplastic response to pancreatic carcinoma: Gene expression of stromal and neoplasmtic cells at the site of primary invasion. *Am. J. Pathol. 160*:91–99.

Iacobuzio-Donahue, C.A., Wilentz, R.E., Argani, P., Yeo, C.J., Cameron, J.L., Kern, S.E., and Hruban, R.H. 2000. Dpc4 protein in mucinous cystic neoplasms of the pancreas: Frequent loss of expression in invasive carcinomas suggests a role in genetic progression. *Am. J. Surg. Pathol. 24*:1544–1548.

Ijichi, H., Ikenoue, T., Kato, N., Mitsuno, M., Togo, G., Kato, J., Kanai, F., Shiratori, Y., and Omata, M., 2001. Systematic analyses of the TGF-beta-Smad signaling pathway in gastrointestinal cancer cells. *Biochem. Biophys. Res. Commun. 289*:350–357.

Ijichi, H., Otsuka, M., Tateishi, K., Ikenoue, T., Kawakami, T., Kanai, F., Arakawa, Y., Seki, N., Shimizu, K., Miyazono, K., Kawabe, T., and Omata, M. 2004. Smad4-independent regulation of p21/WAF1 by transforming growth factor-β. *Oncogene 23*:1043–1051.

Ilg, E.C., Schafer, B.W., and Heizmann, C.W. 1996. Expression pattern of S100 calcium-binding proteins in human tumors. *Int. J. Cancer 68*:325–332.

Ishimura, N., Yamasawa, K., Rumi, M.A., Kadowaki, Y., Ishihara, S., Amano, Y., Nio, Y., Higami, T., and Kinoshita, Y. 2003. BRAF and K-ras gene mutations in human pancreatic cancers. *Cancer Lett. 199*:169–173.

Itakura, J., Ishiwata, T., Shen, B., Kornmann, M., and Korc, M. 2000. Concomitant over-expression of vascular endothelial growth factor and its receptors in pancreatic cancer. *Int. J. Cancer 85*:27–34.

Iyer, N.V., Kotch, L.E., Agni, F., Leung, S.W., Laughner, E., Wenger, R.H., Gassmann, M., Gearhart, E.J.D., Lawler, A.M., Yu, A.Y., and Semenza, G.L. 1998. Cellular and developmental control of O_2 homeostatis by hypoxia-inducible factor 1 alpha. *Genes Dev. 12*:149–162.

Jakobsen, A.M., Ahlman, H., Wangberg, B., Kolby, L., Bengtsson, M., and Nilsson, O. 2002. Expression of synaptic vesicle protein 2 (SV2) in neuroendocrine tumours of the gastrointestinal tract and pancreas. *J. Pathol.196*:44–50.

Janda, E., Lehmann, K., Killisch, I., Jechlinger, M., Herzig, M., Downward, J, Beug, H., and Grunert, S. 2002. Ras and TGF[beta] cooperatively regulate epithelial cell plasticity and metastasis: Dissection of Ras signaling pathways. *J. Cell Biol.156*:299–313.

Jansa, R., Prezeij, J., Kocijancic, A., Osredkar, J., and Ferlic, F. 1996. Androstanediol glucuronide in patients with pancreatic cancer and in those with chronic pancreatitis. *Horm. Metab. Res. 28*:381–383.

Juuti, A., Nordling, S., Louhimo, J., Lundin, J., von Boguslawski,. K., and Haglund, C. 2003. Loss of p27 expression is associated with poor prognosis in stage I-II pancreatic cancer. *Oncology 65*:371–377.

Kalthoff, H., Schmiegel, W., Roeder, C., Kasche, D., Schmidt, A., Lauer, G., Thiele, H.G., Honold, G., Pantel, K., and Riethmuller, G. 1993. p53 and K-RAS alterations in pancreatic epithelial cell lesions. *Oncogene 8*:289–298.

Karayiannakis, A.J., Bolanaki, H., Syrigos, K.N., Asimakopoulos, B., Polychronidis, A., Anagnostoulis, S., and Simopouios, C. 2003. Serum vascular endothelial growth factor levels in pancreatic cancer patients correlate with advanced and metastasic disease and poor prognosis. *Cancer Lett. 194*:119–124.

Kitada, T., Seki, S., Sakaguchi, H., Sawada, T., HIrakawa, K., and Wakasa, K. 2003. Clinicopathological significance of hypoxia-inducible factor-1α expression in human pancreatic carcinoma. *Histopathology 43*:550–555.

Kivinen, L., Tsubarim, M., Haapajarvi, T., Datto, M.B., Wang, X.F., and Laiho, M. 1999. Ras induces p21Cip1/Waf1 cyclin kinase inhibitor transcriptionally through Sp1-binding sites. *Oncogene 18*:6252–6261.

Ko, L.J., and Prives, C. 1996. p53: Puzzle and paradigm. *Genes Dev. 10*:1054–1072.

Kolch, W. 2000. Meaningful relationships: The regulation of the Ras/Raf/MEK/ERK pathway by protein interactions. *Biochem. J. 351*:289–305.

Koopman, J., Fedarko, N.S., Jain, A., Maitra, A., Iacobuzio-Donahue, C., Rahman, A., Hruban, R.H., Yeo, C.J., and Goggins, M. 2004. Evaluation of osteopontin as biomarker for pancreatic adenocarcinoma. *Cancer Epidemiol. Biomark. Prev. 13*:487–491.

Kuwada, Y., Sasaki, T., Morinaka, K., Kitadai, Y., Mukaida, N., and Chayama, K. 2003. Potential involvement of IL-8 and its receptors in the invasiveness of pancreatic cancer cells. *Int. J. Oncol. 22*:765–771.

Kratzschmar, J., Haendler, B., Eberspaecher, U., Roosterman, D., Donner, P., and Schleuning, W.D. 1996. The human cysteine-rich secretory protein (CRISP) family. Primary structure and tissue distribution of CRISP-2 and CRISP-3. *Eur. J. Biochem. 236*:827–836.

Lee, J.H., Choi, J.H., Namkung, W., Hanrahan, J.W., Chang, J., Song, S.Y., Park, S.W., Kim, D.S., Yoon, J.H., Suh, Y., Jang, I.J., Nam, J.H., Kim, S.J., Cho, M.O., Lee, J.E., Kim, K.H., and Lee, M.G. 2003. A haplotype-based molecular analysis of CFTR mutations associated with respiratory and pancreatic diseases. *Hum. Mol. Genet. 12*:2321–2332.

Lee, K.T., Lee, Y.W., Lee, J.K., Choi, S.H., Rhee, J.C., Paik, S.S., and Kong, G. 2004. Overexpression of Id-1 is significantly associated with tumor angiogenesis in human pancreas cancers. *Br. J. Cancer 90*:1198–1203.

Lewis, B.C., Klimstra, D.S., and Varmus, H.E. 2003. The c-myc and PyMT oncogenes induce different tumor types in a somatic mouse model for pancreatic cancer. *Genes Dev. 17*:3127–3138.

Lewis, E.H., Nashid, N., Ludwig, M.E., and Cartun, R.C. 2002. New onset visual disturbances in a 37-year old female with metastatic carcinoma from unknown origin. *J. Histotechnol. 25*:279–281.

Liao, Q., Kleeff, J., Xiao, Y., Di Cesare, P.E., Korc, M., Zimmermann, A., Buchler, M.W., and Friess, H. 2003a. COMP is selectively up-regulated in degenerating acinar cells in chronic pancreatitis and in chronic-pancreatitis-like lesions in pancreatic cancer. *Scand. J. Gastroenterol. 38*:207–215.

Liao, Q., Kleef, J., Xiao, Y., Guweidhil, A., Schambony, A., Töpfer-Petersen, E., Zimmermann, A., Büchler, M.W., and Friess, H. 2003b. Preferential expression of cystein-rich secretory protein-3 (CRISP-3) in chronic pancreatitis. *Histol. Histopathol. 18*:1–9.

Lindblom, A., and Liljegren, A. 2000. Tumor markers in malignancies. *Br. Med. J. 320*:424–427.

Liotta, L.A., Steeg, P.S., and Stetler-Stevenson, W.G. 1991. Cancer metastasis and angiogenesis: An imbalance of positive and negative regulation. *Cell 64*:327–336.

Liu, J., Yin, S., Reddy, N., Spencer, C., and Sheng, S. 2004. Bax mediates the apoptosis-sensitizing effect of maspin. *Cancer Res. 64*:1703–1711.

Lukinius, A., Stridsberg, M., and Wilander, E. 2003. Cellular expression and specific intragranular localization of chromogranin A, chromogranin B, and synaptophysin during ontogeny of pancreatic islet cells: an ultrastructural study. *Pancreas 27*:38–46.

Lüttges, J., Schlehe, B., Menke, M.A.O.H., Vogel, L., Henne-Bruns, D., and Kloppel, G. 1999. The K-ras mutation pattern in pancreatic ductal adenocarcinoma is usually identical to that in associated normal, hyperplastic and metaplastic duct epithelium. *Cancer 85*:1703–1710.

Lüttges, J., Neumann, S., Jesnowski, R., Borries, V., Lohr, M., and Kloppel, G. 2003. Lack of apoptosis in PanIN-1 and PanIN-2 lesions associated with pancreatic ductal adenocarcinoma is not dependent on K-ras status. *Pancreas 27*:e57–e62.

Maacke, H., Jost, K., Opitz, S., Miska, S., Yuan, Y., Hasselbach, L., Lüttges, J., Kalthoff, H., and Stürzbecher, H.W. 2000a. DNA repair and recombination factor Rad 51 is over-expressed in human pancreatic adenocarcinoma. *Oncogene 19*: 2791–2795.

Maacke, H., Opitz, S., Jost, K., Hamdorf, W., Krüger, S., Feller, A., Lopens, A., Diedrich, K., Schwinger, E., and Stürzbecher, H.W. 2000b. Over-expression of wild-type Rad 51 correlates with histological grading of invasive ductal breast cancer. *Int. J. Cancer 88*:907–913.

Maacke, H., Hundertmark, C., Miska, S., Voss, M., Kalthoff, H., and Stürzbecher, H.W. 2002. Autoantibodies in sera of pancreatic cancer patients identify recombination factor Rad51 as a tumour-associated antigen. *J. Cancer Res. Clin. Onco1. 128*:219–222.

Maitra, A., Adsay, N.V., Argani, P., Iacobuzio-Donahue, C., De Marzo, A., Cameron, J.L., Yeo, C.J, and Hruban, R.H. 2003. Multicomponent analysis of the pancreatic adenocarcinoma progression model using a pancreatic intraepithelial neoplasia tissue microarray. *Mod Pathol. 16*:902–912.

Mariagrazia, G., Jason, J.S., and Michael, J.L. 1993. NF-kB Rel:participants in multiform transcriptional regulatory system. *Int. Rev. Cytol. 143*:1–62.

Maruyama, H., Kleef J., Wildi, S., Friess, H., Buchler, M.W., Israel, M.A., and Korc, M. 1999. Id-1 and Id-2 are overexpressed in pancreatic cancer and in dysplastic lesions in chronic pancreatitis. *Am. J. Pathol. 155*:815–822.

Mentula, P., Kylanpaa, M.L., Kemppainen, E., Eklund, K.K., Orpana, A., Puolakkainen, P., Haapiainen, R., and Repo, H. 2003. Serum levels of mast cell tryptase, vascular endothelial growth factor and basic fibroblast growth factor in patients with acute pancreatitis. *Pancreas 27*:e29–e33.

Mignon, M. 2000. Natural history of neuroendocrine enteropancreatic tumors. *Digestion 62*:51–58.

Mohr, V.H., Vortmeyer, A.O., Zhuang, Z., Libutti, S.K., Walther, M.M., Choyke, P.L., Zbar, B., Linehan, W.M., and Lubensky, I.A. 2000. Histopathology and molecular genetics of multiple cysts and microcystic (serous) adenomas of the pancreas in von Hippel-Lindau patients. *Am. J. Pathol. 157*:1615–1621.

Mori, T., Doi, R., Koizumi, M., Toyoda, E., Ito, D., Kami, K., Masui, T., Fujimoto, K., Tamamura, H., Hiramatsu, K., Fujii, N., and Imamura, M. 2004. CXCR4 antagonist inhibits stromal cell-derived factor 1-induced migration and invasion of human pancreatic cancer. *Mol. Cancer Ther. 3*:29–37.

Moriyama, H., Matsubara, N., Kanbara, T., Mori, M., Matsuoka, J., Yoshino, T., Takakura, N., Shimizu, K., and Takaka, N. 2002. Allelic imbalance and microsatellite instability in plasma DNA released from polyclonal pancreatic adenocarcinoma. *Int. J. Oncol. 21*:949–956.

Moskaluk, C.A., Hruban, R.H., Schutte, M., Lietman, A.S., Smyrk, T., Fusaro, L., Fusaro, R., Lynch, J., Yeo, C.T., Jackson. C.E., Lynch, H.T., and Kern, S.E. 1997. Genomic sequencing of DPC4 in the analysis of familial pancreatic carcinoma. *Diagn. Mol. Pathol. 6*:85–90.

Mueller, F., Bommer, M., Lacher, U., Ruhland, C., Stagge, V., Adler, G., Gress, T.M., and Seufferlein, T. 2002. KOC is a novel molecular indicator of malignancy. *Br. J. Cancer 88*: 699–701.

Mueller-Pillasch, F., Lacher, U., Wallrapp, C., Micha, A., Zimmerhackl, F., Hameister, H., Varga, G., Friess, H., Buchler, M., Beger, H.G., Vila, M.R., Adler, G., and Gress, T.M. 1997. Cloning of a gene highly over-expressed in cancer coding for a novel KH-domain containing protein. *Oncogene 14*:2729–2733.

Murakami, Y., Yokoyama. T., Hiyama, E., Yokoyama, Y., Kanehiro, T., Uemura, K., Sasaki, M., Morifuji, M., and Sueda, T. 2002. Successful pre-operative diagnosis of malignant intraductal papillary mucinous tumor of the pancreas by detecting telomerase activity. *Int. J. Gastrointest. Cancer. 31*:117–121.

Nakamura, A., Horinouchi, M., Goto, M., Nagata, K., Sakoda, K., Takao, S., Imai, K., Kim, Y.S., Sato, E., and Yonezawa, S. 2002. New classification of pancreatic intraductal papillary-mucinous tumour by mucin expression: Its relationship with potential for malignancy. *J. Pathol.197*:201–210.

Nichols, L.S., Ashfaq, R., and Iacobuzio-Donahue, C.A. 2004. Claudin 4 protein expression in primary and metastasic pancreatic cancer: Support for use as a therapeutic target. *Am. J. Clin. Pathol.121*:226–230.

Nicolson, G.L., Nawa, A., Toh, Y., Taniguchi, S., Nishimori, K., and Moustafa, A. 2003. Tumor metastasis-associated human MTA1 gene and its MTA1 protein product: Role in epithelial cancer cell invasion, proliferation and nuclear regulation. *Clin. Exp. Metastasis 20*:19–24.

Niedergethmann, M., Hildenbrand, R., Wostbrock, B., Hartel, M., Sturm, J.W., Richter, A., and Post, S. 2002. High expression of vascular endothelial growth factor predicts early recurrence and poor prognosis after curative resection for ductal adenocarcinoma of the pancreas. *Pancreas 25*:122–129.

Norton, J.D. 2000. ID helix-loop-helix proteins in cell growth, differenciation and tumorigenesis. *J. Cell Sci. 113*:3897–3905.

Novotny, J., Kleiby, Z., Vedralova, J., Kolarova, M., Petruzelka, L., Janku, F., and Matous, B. 2000. C-erbB2 expression and K-ras mutations in pancreatic cancer. Correlation with clinical course and pathological characteristics. *Klin. Onkol. 13*:167–170.

O'Brien, E.R., Garvin, M.R., Stewart, D.K., Hinohara, T., Simpson, J.B., Schwartz, S.M., and Giachelli, C.M. 1994.

Osteopontin is synthesized by macrophage, smooth muscle, and endothelial cells in primary and restinotic human coronary atherosclerotic plaques. *Arterioscler. Thromb. 14*:1648–1656.

Oh, Y.L., Song, S.Y., and Ahn, G. 2002. Expression of maspin in pancreatic neoplasms: Applications of maspin immunohistochemistry to the differential diagnosis. *Appl. Immunohistochem. Mol. Morphol. 10*:62–66.

Ohike, N., Maass, N., Mundhenke, C., Biallek, M., Zhang, M., Jonat, W., Lüttges, J., Morohoshi, T., Klöppel, G., and Nagasaki, K. 2003. Clinicopathological significance and molecular regulation of maspin expression in ductal adenocarcinoma of the pancreas. *Cancer Lett. 199*:193–200.

Okami, J., Nakamori, S., Hiraoka, N., Tsujie, M., Hayashi, N., Yamamoto, H., Fujiwara, Y., Nagano, H., Dono, K., Umeshita, K., Sakon, M., and Monden, M. 2003. Suppression of pancreatic cancer cell invasion by a cyclooxygenase-2-specific inhibitor. *Clin. Exp. Metastasis 20*:577–584.

Ouyang, X.S., Wang, X., Lee, D.T., Tsao, S.W., and Wong Y.C. 2002a. Overexpression of Id-1 in prostate cancer. *J. Urol. 167*:2598–2602.

Parikh, A.A., Liu, W.B., Fan, F., Stoeltzing, O., Reinmuth, N., Bruns, C.J, Bucana, C.D., Evans, D.B., and Ellis, L.M. 2003. Expression and regulation of the novel vascular endothelial growth factor receptor neuropilin-1 by epidermal growth factor in human pancreatic carcinoma. *Cancer 98*:720–729.

Porta, M., Malats, N., Jariod, M., Grimalt, J.O., Rifa, J., Carrato, A., Guarner, L., Salas, A., Santiago-Silva, M., Corominas, J.M., Andreu, M., and Real, F.X. 1999. Serum concentrations of organochlorine compounds and K-ras mutations in exocrine pancreatic cancer. *Lancer 354*:2125–2129.

Potti, A., Ganti, A.K., Tendulkar, K., Chitajallu, S., Sholes, K., Koch, M., and Kargas, S. 2003. HER-2/neu and CD117 (C-kit) overexpression in hepatocellular and pancreatic carcinoma. *Anticancer Res. 23*:2671–2674.

Pupa, S.M., Menard, S., Forti, S., and Tagliabue, E. 2002. New insights into the role of extracellular matrix during tumor onset and progression. *Cell Physiol. 192*:259–267.

Quartara, L., and Maggi, C.A. 1997. The tachykinin NK1 receptor. Part I: Ligands and mechanisms of cellular activation. *Neuropeptides 31*:537–563.

Rahemtullah, A., Misdraji, J., and Pitman, M.B. 2003. Adenosquamous carcinoma of the pancreas. *Cancer (Cancer Cytopathol.) 99*:372–378.

Ramachandra, M., Atencio, I., Rahman, A., Vaillancourt, M., Zou, A., Avanzini, J., Wills, K., Bookstein, R., and Shabram, P. 2002. Restoration of transforming growth factor beta signaling by functional expression of smad4 induces anoikis. *Cancer Res. 62*:6045–6051.

Rampy, B.A., Waxman, I., Xiao, S.Y., and Logrono, R. 2001. Serous cystadenoma of the pancreas with papillary features: A diagnostic pitfall on fine-needle aspiration biopsy. *Arch. Pathol. Lab. Med. 125*:1591–1594.

Ray, S., Lu, Z., and Rajindiran, S. 2004. Clear cell ductal carcinoma of pancreas. *Arch. Pathol. Lab. Med. 128*:693–696.

Recine, M., Kaw, M., Evans, D.B., and Krishnamurthy, S. 2004. Fine-needle aspiration cytology of mucinous tumors of the pancreas. *Cancer (Cancer Cytol.) 102*:92–99.

Riechmann, V., and Sablitzky, F. 1995. Mutually exclusive expression of two dominant-negative helix-loop-helix (dnHLH) genes, Id4 and Id3, in the developing brain of the mouse suggests distinct regulatory roles of these dnHLH proteins during cellular proliferation and differentiation of the nervous system. *Cell Growth Differ. 6*:837–843.

Rigaud, G., Moore, P.S., Zamboni, G., Orlandini, S., Taruscio, D., Paradisi, S., Lemoine, N.R., Kloppel, G., and Scarpa, A. 2000. Allelotype of pancreatic acinar cell carcinoma. *Int. J. Cancer. 88*:772–777.

Ross, A.F., Oleynikov, Y., Kislauskis, E.H., Taneja, K.L., and Singer, R. H. 1997. Characterization of a beta-actin mRNA zipcode-binding protein. *Mol. Cell Biol. 17*:2158–2165.

Rosty, C., Ueki, T., Argani, P., Jansen, M., Yeo, C.J., Cameron, J.L., Hruban, R.H., and Goggins, M. 2002. Overexpression of S100A4 in pancreatic ductal adenocarcinomas is associated with poor differentiation and DNA hypomethylation. *Am. J. Pathol. 160*:45–50.

Rotondo, F., Vidal, S., Bell, D., Horvath, E., Kovacs, K., Scheithauer, B.W., and Lloyd, R.V. 2003. Immunohistochemical localization of amylin in human pancreas, thyroid, pituitary and their tumors. *Acta Histochem. 105*:303–307.

Rozenblum, E., Schutte, M., Goggins, M., Hahn, S.A., Panzer, S., Zahurak, M., Goodman, S.N., Sohn, T.A., Hruban, R.H., Yeo, C.J., and Kern, S.E. 1997. Tumor suppressor pathways in pancreatic carcinoma. *Cancer Res. 57*:1731–1734.

Sagol, O., Tuna, B., Coker, A., Karademir, S., Obuz, F., Astarcioglu, H., Kupelioglu, A., Astarcioglu, I., and Topalak, O. 2002. Immunohistochemical detection of pS2 protein and heat shock protein-70 in pancreatic adenocarcinomas. Relationship with disease extent and patient survival. *Pathol. Res Pract. 198*:77–84.

Sahin, F., Maitra, A., Argani, P., Sato, N., Maehara, N., Montgomery, E., Goggins, M., Hruban, R.H., and Su, G.H. 2003. Loss of Stk11/Lkb1 expression in pancreastic and biliary neoplasms. *Mod. Pathol. 16*:686–691.

Sakai, Y., Yanagisawa, A., Shimada, M., Hidaka, E., Seki, M., Tada, Y., Harada, T., Saisho, H., and Kato, Y. 2000. K-ras gene mutations and loss of heterozygosity at the *p53* gene locus relative to histological characteristics of mucin-producing tumors of the pancreas. *Hum. Pathol. 31*:795–803.

Sasaki, T., Fujimoto, Y., Tsuchida, A., Kawasaki, Y., Kuwada, Y., and Chayama, K. 2001. Activation of peroxisome proliferator-activated receptor gamma inhibits the growth of human pancreatic cancer. *Pathobiology 69*:258–265.

Sato, N., Maitra, A., Fukushima, N., van Heek, N.T., Matsubayashi, H., Iacobuzio-Donahue, C.A., Rosty, C., and Goggins, M. 2003. Frequent hypomethylation of multiple genes overexpressed in pancreatic ductal adenocarcinoma. *Cancer Res. 63*:4158–4166.

Satoh, A., Masamune, A., Kimura, K., Kaneko, K., Sakai, Y., Yamagiwa, T., Satoh, M., Kikuta, K., Asakura, T., and Shimosegawa, T. 2003. Nuclear factor kappa B expression in peripheral blood mononuclear cells of patients with acute pancreatitis. *Pancreas 26*:350–356.

Satoh, A., Miura, T., Satoh, K., Masamune, A., Yamagiwa, T., Sakai, Y., Shibuya, K., Takeda, K., Kaku, M., and Shimosegawa, T. 2002. Human leukocyte antigen-DR expression on peripheral monocytes as a predictive marker of sepsis during acute pancreatitis. *Pancreas 25*:245–250.

Satoh, A., Shimosegawa, T., Fujita, M., Kimura, K., Masamune, A., Koizumi, M., and Toyota, T. 1999. Inhibition of nuclear factor-kappaB activation improves the survival of rats with taurocholate pancreatitis. *Gut 44*:253–258.

Sawai, H., Funahashi, H., Yamamoto, M., Okada, Y., Hayakawa, T., Tanaka, M., Takeyama, H., and Manabe, T. 2003. Interleukin-1 alpha enhances integrin alpha6β1 expression and metastatic capability of human pancreatic cancer. *Oncology 65*:167–173.

Schmitt, C.A., Fridman, J.S., Yang, M., Lee, S., Baranov, E., Hoffman, R.M., and Lowe, S.W. 2002. A sensecence program

controlled by p53 and p16 (INK4a) contributes to the outcome of cancer therapy. *Cell 109*:335–346.

Schutte, M., Hruban, R.H., Geradts, J., Maynar, R., Hilgers, W., Rabindran, S.K., Moskaluk, C.A., Hahn, S.A., Schwarte-Waldhoff, I., Schmiegel, W., Baylin, S.B., Kern, S.E., and Herman, J.G. 1997. Abrogation of the Rb/p16 tumor-suppressive pathway in virtually all pancreatic carcinomas. *Cancer Res. 57*:3126–3130.

Shay, J.W., and Bacchetti, S. 1997. A survey of telomerase activity in human cancer. *Eur. J. Cancer 33*:787–791.

Shekouh, A.R., Thompson, C.C., Prime, W., Campbell, F., Hamlett, J., Herrington, C.S., Lemoine, N.R., Crnogorac-Jurcevic, T., Buechler, M.W., Friess, H., Neoptolemos, J.P., Pennington, S.R., and Costello, E. 2003. Application of laser capture microdissection combined with two-dimensional electrophoresis for the discovery of differentially regulated proteins in pancreatic ductal adenocarcinoma. *Proteomics 3*:1988–2001.

Shen, Z., Heinegard, D., and Sommarin, Y. 1995. Distribution and expression of cartilage oligomeric matrix protein and bone sialoprotein show marked changes during rat femoral head development. *Matrix Biol. 14*:773–781.

Sherr, C.J. 2001. The INK4a/ARF network in tumour suppression. *Nat. Rev. Mol. Cell Biol. 2*:731–737.

Shi, Q., Abbruzzese, J.L., Huang, S., Fidler, I.J., Xiong, Q., and Xie, K. 1999. Constitutive and inducible interleukin 8 expression by hypoxia and acidosis renders human pancreatic cancer cells more tumorigenic and metastatic. *Clin. Cancer Res. 5*:3711–3721.

Srivastava, A., Alexander, J., Lomakin, I., and Dayal, Y. 2001. Immunohistochemical expression of transforming growth factor alpha and epidermal growth factor receptor in pancreatic endocrine tumors. *Hum. Pathol. 32*:1184–1189.

Su, G.H., Huban, R.H., Bansal, R.K., Bo, G.S., Tang, D.J., Shekher, M.C., Westerman, M., Entius, M.M., Goggins, M., Yeo, C.J., and Kern, S.E. 1999. Germline and somatic mutations of the STK11/LKB1 Peutz-Jeghers gene in pancreatic and biliary cancers. *Am. J. Pathol. 15*:1835–1840.

Subbaramaiah, K., Telang, N., Ramonetti, J.T., Araki, R., DeVito, B., Weksler, B.B., and Dannenberg, A.J. 1996. Transcription of cyclooxygenase-2 is enhanced in transformed mammary epithelial cells. *Cancer Res. 56*:4424–4429.

Sweep, F.C., Fritsche, H.A., Gion, M., Klee, G.G., and Schmitt, M. 2003. EORTC-NCI Working Group. Considerations on development, validation, application, and quality control of immuno (metric) biomarker assays in clinical cancer research: An EORTC-NCI working group report. *Int. J. Oncol. 23*:1715–1726.

Takamori, H., Oaes, Z.G., Hoch, O.C., Burger, M., and Schraufstatter, I.U. 2000. Autocrine growth effect of IL8 and GROalpha on a human pancratic cancer cell line, Capan-1. *Pancreas 2*:52–55.

Tan, X., Egami, H., Kamohara, H., Ishikawa, S., Kurizaki, T., Yoshida, N., Tamori, Y., Takai, E., Hirota, M., and Ogawa, M. 2004. Involvement of the mitogen-activated protein kinase kinase 2 in the induction of cell dissociation in pancreatic cancer. *Int. J. Oncol. 24*:65–73.

Terris, B., Blaveri, E., Crnogorac-Jurcevic, T., Jones, M., Missiaglia, E., Ruszniewski, P., Sauvanet, A., and Lemoine, N. 2002. Characterization of gene expression profiles in intraductal papillary-mucinous tumors of the pancreas. *Am. J. Pathol. 106*:1745–1754.

Tersmette, A.C., Petersen, G.M., Offerhaus, G.J., Falatko, F.C., Brune, K.A., Goggins, M., Rosenblim, E., Wilentz, R.E., Yeo, C.J., Cameron, J.L., Kern, S.E., and Hruban, R.H. 2001. Increased risk of incident pancreatic cancer among first-degree relatives of patients with familial pancreatic cancer. *Clin. Cancer Res. 17*:738–744.

Tiainen, M., Vaahtomeri, K., Ylikorkala, A., and Makela, T.P. 2002. Growth arrest by the LKB1 tumor suppressor: Induction of p21(WAF1/CIP1). *Hum. Mol. Genet. 1*:1497–1504.

Toh, Y., Kuwano, H., Mori, M., Nicolon, G.L, and Sugimachi, K. 1999. Overexpression of metastasis-associated MTA1 mRNA invasive oesophageal carcinomas. *Br. J. Cancer 7*:1723–1726.

Truninger, K., Kock, J., Wirth, H.P., Muellhaupt, B., Arnold, C., von Weizsacker, F., Seifert, B., Ammann, R.W., and Blum, H.E. 2001. Trypsinogen gene mutations in patients with chronic or recurrent acute pancreatitis. *Pancreas 22*:18–23.

Tucker, O.N., Dannenberg, A.J., Yang, E.K., Zhang, F., Teng, L., Daly, J.M., Soslow, R.A., Masferrer, J.L., Woerner, B.M., Koki, A.T., and Fahey, T.J. 1999. Cyclooxygenase-2 expression is up-regulated in human pancreatic cancer. *Cancer Res. 59*:987–990.

van Heek, N.T., Meeker, A.K., Kern, S.E., Yeo, C.J., Lillemoe, K.D., Cameron, J.L., Offerhaus, G.J., Hicks, J.L., Wilentz, R.E., Goggins, M.G., De Marzo, A.M., Hruban, R.H., and Maitra, A. 2002. Telomere shortening is nearly universal in pancreatic intraepithelial neoplasia. *Am. J. Pathol. 161*:1541–1547.

Vogelmann, R., Kreuse, E.D., Adler, G., and Lutz, M.P. 1999. Integrin alpha6beta1 role in metastatic behavior of human pancreatic carcinoma cell. *Int. J. Cancer 8*:791–795.

Wang, D., Kanuma, T., Mizunima, H., Takama, F., Ibuki, Y., Wake, N., Mogi, A., Shitara, Y., and Takenoshita, S. 2000. Analysis of specific gene mutations in transforming growth factor-beta signal transduction pathway in human ovarian cancer. *Cancer Res. 60*:4507–4512.

Watanabe, I., Hasebe, T., Sasaki, S., Konishi, M., Inoue, K., Nakagohri, T., Oda, T., Mukai, K., and Kinoshita, T. 2003. Advanced pancreatic ductal cancer: Fibrotic focus and beta-catenin expression correlate with outcome. *Pancreas 26*:326–333.

Wilentz, R.E., Albores-Saavedra, J., and Hruban, R.H. 2000. Mucinous cystic neoplasms of the pancreas. *Semin. Diagn. Pathol. 17*:31–42.

Xiong, H.Q., and Abbruzzese, J.L. 2002. Epidermal growth factor receptor-targeted therapy for pancreatic cancer. *Semin. Oncol. 29*:31–37.

Yamaguchi, K., Chijiiwa, K., Torato, N., Kinoshita, M., and Tanaka, M. 2000. Ki-ras codon 12 point and P53 mutations: A molecular examination of the main tumor, liver, portal vein, peripheral arterial blood and para-aortic lymph node in pancreatic cancer. *Am. J. Gastroenterol. 8*:1939–1945.

Yamamoto, M. 1999. Differential expression of interleukin-1alpha (IL-1alpha) messenger RNA in metastatic and non-metastatic human pancreatic carcinoma cell lines and effect of Il-1alpha on cell invasion (in Japanese). *J. Nagoya City Univ. Med. Assoc. 50*:31–44.

Yamamoto, Y., Toi, M., Kondo, S., Matsumoto, T., Szuki, H., Kitamura, M., Tsuruta, K., Taniguchi, T., Okamoto, A., Mori, T., Yoshida, M., Ikeda, T., and Tominaga, T. 1996. Concentrations of vascular endothelial growth factor in the sera of normal controls and cancer patients. *Clin. Cancer Res. 2*:821–826.

Yamasaki, H., Ikeda, S., Okajima, M., Miura, Y., Asahara, T., Kohno, N., and Shimamoto, F. 2004. Expression and localization of MUC1, MUC2, MUC5AC and small intestinal mucin antigen in pancreatic tumors. *Int. J. Oncol. 24*:107–113.

Yamanaka, Y., Friess, H., Kobrin, M.S., Buchler, M., Beger, H.G., and Korc, M. 1993. Coexpression of epidermal growth factor receptor and ligands in human pancreatic cancer is associated

with enhanced tumor aggressiveness. *Anticancer Res. 13*: 565–569.

Zhong, H., Marzo, A.M., Laughter, E., Lim, M., Hilton, D.A., Zagzag, D., Buechler, P., Isacc, W.B., Semenza, G.L., and Simons, J.W. 1999. Overexpression of hypoxia-inducible factor 1 alpha in common human cancers and their metastases. *Cancer Res. 59*:5830–5835.

Ziske, C., Schlie, C., Gorschluter, M., Glasmacher, A., Mey, U., Strehl, J., Sauerbruch, T., and Schmidt-Wolf, I.G. 2003. Prognostic value of CA 19-9 levels in patients with inoperable adenocarcinoma of the pancreas treated with gemcitabine. *Br. J. Cancer 89*:1413–1417.

Zurn, A.D., Nick, H., and Monard, D. 1988. A glia-derived nexin promotes neurit outgrowth in cultured chick sympathetic neurons. *Dev. Neurosci. 10*:17–24.

2

Detection of Genomic Imbalances in Endocrine Pancreatic Tumors Using Comparative Genomic Hybridization

Jianming Zhao, Aurel Perren, and Paul Komminoth

Introduction

Endocrine pancreatic tumors (EPTs) are neoplasms with an annual clinically recognized incidence of approximately 5 cases per 1 million people. The majority of clinically discovered EPTs are functionally active, leading to a recognizable clinical syndrome resulting from a hormone-excess state. These tumors are called functioning EPTs. Other endocrine tumors of the pancreas that do not cause a distinct clinical syndrome are nonfunctioning. The malignancy rate varies widely in these tumors, being dependent on tumor types defined by hormonal secretion: <10% in insulinomas, 40–70% in VIPomas, 50–80% in glucagonomas, 60–90% in gastrinomas, >70% in somatostatinomas, and 60–90% in nonfunctioning tumors (Jensen, 1999). In contrast to the poor prognosis of the exocrine tumors originating from the pancreas, EPTs usually grow in a more indolent fashion and tend to be associated with a longer survival. The most common sites of metastatic dissemination are regional lymph nodes and the liver. The presence of metastases, especially in the liver, is the most important survival determinant. According to published reports, the 5-year survival rate is 20–50% in patients with liver metastases compared to 65–100% in those without liver metastases (Madeira *et al.,* 1998; Stabile and Passaro, 1985; Weber *et al.,* 1995).

Traditional histologic and morphologic assessments of primary EPTs without clear invasion or metastasis are not reliable for predicting malignant behavior. Studies to detect genetic changes in EPTs have shed light on their molecular background. Some inherited syndromes are reported to be associated with the development of EPT, including the multiple endocrine neoplasia type 1 (MEN1) syndrome and the von Hippel-Lindau (VHL) syndrome. In patients with MEN1, more than 80% develop EPT (Jensen, 1998). In contrast, only 12–17% of patients with VHL suffer from EPT (Libutti *et al.,* 1998). The susceptibility gene for both diseases has been identified. The *MEN1* gene has been mapped to the chromosomal locus 11q13 and *VHL* to 3q25. Previous molecular studies have shown somatic mutations of the *MEN1* gene in a subset of sporadic EPTs (Gortz *et al.,* 1999; Zhuang *et al.,* 1997). Other genes such as *P16/CDKN2A*, *DPC4/SMAD4*, and *HER-2/NEU* have also been implicated in the development of EPT

Handbook of Immunohistochemistry and *in situ* Hybridization of Human Carcinomas, Volume 3: Molecular Genetics, Liver Carcinoma, and Pancreatic Carcinoma

(Bartsch *et al.,* 1999; Evers *et al.,* 1994; Ruas and Peters, 1998); however, none of these genes are convincingly linked to the pathogenesis of EPT, especially sporadic EPT.

Tumorigenesis is believed to be a multistep process, involving an accumulation of genetic changes that results in the acquisition of the properties of tumorous growth. Comprehensive identification of genetic changes in a tumor could facilitate the discovery of genetic events responsible for the tumor initiation and progression. In past years, powerful technologies such as comparative genomic hybridization (CGH) and microarray methods have been developed for genomewide survey of genetic alterations (Kallioniemi *et al.,* 1992; Liotta and Petricoin, 2000). The technology CGH is a useful tool to examine an entire genome for changes in deoxyribonucleic acid (DNA) sequence copy number. Unlike classical cytogenetic methods, CGH analysis does not require cell culture to obtain metaphases from patients. It also does not need a previous knowledge of genetic aberrations or a complex series of loci-specific probes, as used in fluorescence *in situ* hybridization (FISH) analysis. In CGH, only genomic DNA that is extracted from tumor cells is used as probe. Therefore, solid tumors and archived materials, i.e., formalin-fixed and paraffin-embedded tumor samples, can be analyzed for comprehensive genomic imbalances. This technology has been widely used to screen for genomic alterations in a variety of tumors (Forozan *et al.,* 1997; Knuutila *et al.,* 1998; Knuutila *et al.,* 1999). Here we summarize the results of our CGH studies on endocrine pancreatic tumors (Speel *et al.,* 1999; Speel *et al.,* 2001; Zhao *et al.,* 2001). A new statistic evaluation is made for the CGH data from a total of 102 EPTs investigated in our laboratory. The CGH results highlight important genomic imbalances involved in EPT development and thereby provide a significant insight into the molecular background of these tumors.

MATERIALS

1. 20 mg/ml proteinase K, store at –20°C.
2. Digestion buffer: 10 mM Tris, 25 mM ethylenediamine tetraacetic acid (EDTA), 100 mM NaCl and 0.5% sodium dodecyl sulfate (SDS) (pH 8.0).
3. 25:24:1 phenol/chloroform/isoamyl alcohol.
4. 3 M sodium acetate, adjust pH to 5.2 with 100% acetic acid.
5. 20X saline-sodium citrate (SSC) (pH 5.3).
6. Denaturation solution: 70% formamide in 2X SSC (pH 7.0–7.5). Cover and store at 4°C. Discard after 7 days.
7. Hybridization buffer: 10 g dextran sulfate, 50 ml formamide, and 10 ml 20X SSC; bring volume to 100 ml with purified water (pH 7.0).
8. Ethanol solutions (70%, 85%, and 100%): Dilute 100% ethanol v/v with purified water to 70% and 85% ethanol.
9. Wash solution: 50% formamide in 2X SSC (pH 7.0).
10. Stock PN wash solution (phosphate-buffered NP-40 stock solution): 13.8 g sodium dihydrogen phosphate × 2 H_2O ($NaH_2PO_4 \times 2H_2O$) and 1 ml Nonidet P 40 (NP-40); bring volume to 1 L with purified water.
11. PN wash solution: 17.8 g disodium hydrogen phosphate × 2 H_2O ($Na_2HPO_4 \times 2H_2O$) and 1 ml NP-40; bring volume to 950 ml with purified water; adjust pH to 8.0 with ca. 50 ml stock PN wash solution.
12. 100 mg/ml 4,6-diamidino-2-phenylindole (DAPI; stock): 1 mg DAPI, add 2–3 drops of methanol to dissolve and then add 10 ml purified water; store up to 1 year at –20°C.
13. 0.1–0.2 µg/ml DAPI: 1–2 µl DAPI stock solution in 1 ml phenylendiamin antifade mounting medium.
14. DNA polymerase I (10 U/µl), store at –20°C.
15. 10X enzyme mix: 0.5 units/µl DNA polymerase I, 0.0075 units/µl DNase I, 50 mM Tris-HCl (pH 7.5), 5 mM magnesium acetate, 1 mM β-mercaptoethanol, 0.1 mM phenymethylsulfonyl fluoride, 50% (v/v) glycerol, and 100 µg/ml nuclease-free bovine serum albumin (BSA).
16. 10X nucleotide mix: 0.2 mM each dCTP, dGTP, and dATP; 0.2 mM $MgCl_2$, 100 mM β-mercaptoethanol, 500 mM Tris-HCl (pH 7.8), and 100 µg/ml nuclease-free BSA.
17. Human Cot-1 DNA: 1 mg/ml, store at –20°C.
18. D-5000 Puregene DNA isolation kit (Gentra Systems, Minneapolis, MN), used for isolation DNA from frozen samples. This kit contains cell lysis solution, protein precipitation solution, ribonuclease (RNase) A solution, and DNA hydrate solution.
19. Following reagents used for CGH are available from the Vysis company (Vysis, Downers Grove, IL): SpectrumRed dUTP, SpectrumGreen dUTP, SpectrumRed total human male or female genomic DNA, SpectrumGreen total human male or female genomic DNA, unlabeled or SpectrumGreen MPG 600 (control DNA, extracted from an immortalized female breast cancer cell line of known passage number and predefined genetic abnormalities), and normal human lymphocyte metaphase slides (the lymphocytes are derived from karyotypically normal male donors).

METHODS

DNA Extraction from Frozen Tumor Sample

Extraction of genomic DNA from frozen tissues by using the D-5000 Puregene DNA isolation kit according to manufacturer's protocol.

1. Select representative areas containing more than 80% of tumor cells, based on the hematoxylin and eosin (H&E)–stained slides prepared from frozen samples using a cryostat technique.
2. Homogenize 10–20 mg of frozen tissue in 600 µl cooled cell lysis solution in a 1.5-ml microcentrifuge tube.
3. Add 3 µl proteinase K solution (20 mg/ml).
4. Incubate lysate at 55°C for 3 hr to overnight.
5. Add 3 µl RNase A solution to degrade ribonucleic acid (RNA).
6. Mix the sample by gently inverting the tube several times, and then incubate 15 min at 37°C.
7. Add 200 µl protein precipitation solution.
8. Vortex vigorously to mix well.
9. Centrifuge for 3 min at 14,000 rpm. The precipitated proteins will form a tight pellet.
10. Pour the supernatant containing DNA into a clean 1.5-ml tube.
11. Add 600 µl 100% isopropanol.
12. Invert the tube gently until the white threads of DNA form a visible clump.
13. Centrifuge for 1 min at 14,000 rpm to pellet DNA.
14. After removing the supernatant, add 600 µl 70% ethanol and vortex.
15. Centrifuge for 1 min at 14,000 rpm. Carefully pour off the ethanol.
16. Dry the pellet for 3 min under a vacuum at room temperature.
17. Add 100 µl DNA hydrate solution or purified water and heat at 65°C for 1 hr to disperse the DNA.
18. Measure the DNA concentration with the spectrophotometer.

DNA Extraction from Paraffin-Embedded Tumor Material

1. Microdissect representative tumor samples from 5 to 10 sections of 10 µm thick unstained tissue specimen using PALM Robot-MicroBeam (P.A.L.M. Lit., Bernried, Germany) and scrape the samples under a stereomicroscope (Stemi DV4, Zeiss, Germany) at 10X–40X magnification.
2. Collect the sample in a 1.5-ml tube containing 500 µl 100% ethanol.
3. Centrifuge for 5 min at 14,000 rpm and remove ethanol.
4. Add 1 ml xylol, heat for 10 min at 55°C, and then centrifuge for 5 min at 14,000 rpm.
5. Repeat **Step 4** 2×.
6. Add 1 ml 100% ethanol, vortex, and keep 15 min at room temperature.
7. Centrifuge for 2 min at 14,000 rpm and then remove ethanol.
8. Repeat **Step 6** and **Step 7.**
9. Add 1 ml digestion buffer and vortex to disperse the sample.
10. Transfer the sample into a clean 15-ml centrifuge tube and add 25 µl proteinase K (20 mg/ml).
11. Incubate in a water bath at 55°C for overnight to 3 days, and add 25 µl proteinase K every day during the time of digestion.
12. After the tissue sample is completely digested, purify DNA by using standard phenol-chloroform extraction and quantify by spectrophotometer.

DNA Labeling by Nick Translation

1. Add the following components into a 1.5-ml microcentrifuge tube: 5 µl 10X nucleotide mix, 2 µg tumor genomic DNA, 1 µl SpectrumGreen dUTP, 1 µl DNA Polymerase I, and 3–5 µl 10X enzyme mix; add purified water to 50 µl of a total reaction volume.
2. Incubate for 75 min in a water bath at 15°C.
3. Keep for 15 min at 75°C to stop the reaction.

Probe Mix Preparation

1. Combine the following components in a 1.5-ml microcentrifuge tube: 10 µl (400 ng) SpectrumGreen-labeled tumor DNA, 1 µl (100 ng) SpectrumRed total human genomic reference DNA, and 10 µl (10 µg) Human Cot-1 DNA.

Note: The reference DNA should be sex-matched to the tumor DNA.

2. Add 2.1 µl (0.1 volume) 3 M sodium acetate and 52.5 µl (2.5 volume) of 100% ethanol. Mix contents, briefly spin tube, and leave 30 min at –20°C.
3. Centrifuge for 30 min at 12,000 rpm at 4°C to precipitate DNA.
4. Remove the supernatant carefully and dry the pellet for 3 min under a vacuum at room temperature.
5. Dissolve the pellet in 10 µl hybridization buffer.
6. Denature the probe mix for 5 min in a water bath at 75°C.
7. Leave 30 min in water bath at 37°C to preanneal the probe.

Hybridization

1. Mark hybridization areas on the underside of the metaphase slide using a diamond-tipped scribe.
2. Immerse slide into the denaturation solution at 73±1°C for 3–5 min.
3. Dehydrate slide for 2 min each in 70%, 85%, and 100% ethanol.
4. Dry slide by touching the bottom edge and wiping the underside with a paper towel.
5. Place slide on a slide warmer, previously warmed to 37°C, to allow remaining ethanol to evaporate.

6. Add 10 µl of the denatured probe mix on the marked area of the slide.
7. Immediately mount a clean coverslip (18 × 18 cm) and seal with rubber cement.
8. Incubate for 3 days at 37°C in a sealed humidified box.

Post-Hybridization Wash and Counterstain

1. After removing the rubber-cement seal and the coverslip on a 37°C slide warmer, immerse slide immediately into the wash solution at 45°C in a water bath for 10 min.
2. Rinse slide 2× as in **Step 1.**
3. Place slide into 2X SSC at 45°C for 5 min, then rinse 2× in 2X SSC at room temperature for 5 min each.
4. Immerse slide into the PN wash solution for 5 min.
5. Repeat **Step 4.**
6. Rinse 2× in water for 5 min each.
7. Air-dry slide in darkness.
8. Place 20 µl DAPI solution on slide to counterstain and immediately mount a clean coverslip (24 × 46 mm).

Visualization and Analysis

The CGH digital images are collected using a cooled charge-coupled device (CCD) camera (Microimager 1400; Xillix Technologies, Vancouver, Canada) attached to a Zeiss Axioskop microscope that is equipped with a filter set specific for DAPI, SpectrumRed (Texas Red), and SpectrumGreen (FITC, fluorescein isothiocyanate) and connected to a computer. The software program QUIPS (Vysis) is used to calculate average green-to-red ratio profiles for each chromosome.

At least six observations per autosome and three observations per sex chromosome are included in each analysis. Chromosomal gains and losses are defined if the fluorescence ratio values are above 1.2 or below 0.8. Amplification is assumed at chromosomal regions where a green-to-red ratio exceeds 1.5. Gains at the G-C-rich regions of 1p32-pter, 16p, 19, and 22 are excluded from the analysis to avoid false-positive results. For scoring of genetic alterations, chromosome changes are scored by chromosomal arm. A loss and a gain on one arm are scored as two changes, whereas two separate losses (or gains) on the same arm are scored as one change.

Statistics

The following statistical methods are used for CGH data analyses:

1. Contingency table analysis, to compare frequencies of genomic alterations in different groups of tumors.
2. Student's t-test and ANOVA, to determine significance in the number of genomic alterations between two groups and in more than two groups, respectively.
3. Percent concordance, to measure the concordance between the primary tumors and the corresponding metastases for the CGH alterations, as described by Waldman *et al.* (2000).
4. Probabilistic model, to determine the probability of clonal relationship (CR) between the primary tumors and the corresponding metastases for the CGH alterations, as previously described (Zhao *et al.,* 2001).

RESULTS AND DISCUSSION

Common Regions of Chromosomal Gains and Losses

Genomic imbalances resulting from chromosomal gains and losses are common in EPT. Genetic aberrations were detected in 36 of 44 (82%) unselected EPTs (Speel *et al.,* 1999), in 27 of 38 (71%) small EPTs with a diameter of 2 cm or less (Speel *et al.,* 2001) and all metastases (Zhao *et al.,* 2001). Compiled CGH data from 102 EPTs reveal genomic imbalances in 82 (80%) tumors. The overall number of chromosome arm aberrations per tumor ranges from 0 to 36 (mean, 9.2). Prevalent chromosomal regions in which alterations are found in more than 25% of tumors include 2q (25.5%), 3p (26.5%), 3q (26.5%), 5q (26.5%), 6q (38.2%), 7q (39.2%), 9q (30.4%), 11p (32.4%), 11q (36.3%), 12q (25.5%), 13q (25.5%), 14q (28.4%), 17q (36.3%), 20q (27.5%), Xp (29.4%), Xq (33.3%), and Y (28.4%). Chromosomal losses (range, 0–17; mean, 4.8) are slightly more frequent than gains (range, 0–19; mean, 4.4), and amplifications are rare. Frequent DNA copy number losses occur at 3p, 3q, 6q, 11p, and 11q, with the highest frequency of losses on 6q and 11q (35.3% each). Prevalent gains of DNA copy number involve the chromosomal regions of 5q, 7q, 9q, 14q, 17q, and 20q with the highest frequency of gains on chromosomes 7q (38.2%) and 17q (36.3%).

Genetic Changes in Association with Tumor Size and Malignant Outgrowth

The number of detected genetic aberrations is clearly associated with tumor size. Many more genetic alterations occur in large tumors (diameter >2 cm) than in small ones (diameter ≤2 cm). The average number of chromosomal aberrations per tumor identified in large and small EPTs is 12.2 and 2.9 ($P < 0.0001$), respectively. In addition, the vast majority of large EPTs display genomic imbalances. Currently, tumor size is one of the important diagnostic parameters for

distinguishing benign from malignant EPTs. Well-differentiated EPTs are classified as benign if they are 2 cm or less in size, confined to the pancreas and not angioinvasive (Kloppel, 1997). In contrast, EPTs with a size of more than 2 cm are generally considered at risk of malignancy, with the exception of insulinomas. The CGH findings provide a supportive evidence for the clinical diagnosis.

An increased number of genetic alterations correlates well with the malignant behavior in EPT. Malignant EPTs harbor a higher number of chromosomal alterations, when compared to benign EPTs (mean, 12.0 versus 3.6; $P < 0.0001$). Moreover, all tumors that have already metastasized show extensive chromosomal aberrations. Strikingly, almost all of the chromosomal losses and gains are more often identified in the malignant tumors. Significant differences between the two groups are revealed for losses of 2q, 3p, 3q, 6p, 6q, 10p, 10q, 11p, 15q, 16q, and 21q and for gains of 4p, 4q, 5p, 5q, 7p, 7q, 12q, 14q, 17p, 17q, and 20q. These chromosomal regions might contain candidate genes associated with EPT progression from a benign or a low-grade neoplasm to a high-grade (malignant) tumor. Of note is that gains of chromosome 4 and losses of 6q are often detectable in small tumors, albeit at a significantly lower frequency. Similarly, the common losses of 11q and gains of 9q also seem to be early events in the development of EPT. These alterations occur frequently not only in the advanced primary/metastatic tumors but also in clinically benign EPTs.

Losses of 11q are of particular interest because the *MEN1* gene has been mapped to this chromosomal region. Loss of heterozygosity (LOH) at the *MEN1* locus and mutations of the gene are reported in both benign and malignant EPTs regardless of whether they are associated with MEN1 (Hessman *et al.,* 1999; Zhuang *et al.,* 1997). Nevertheless, some studies suggest that one or more EPT-relevant tumor-suppressor genes may exist distal to the *MEN1* locus on 11q (Chakrabarti *et al.,* 1998; Stumpf *et al.,* 2000). The long arm of chromosome 9, where DNA copy number gains are frequently detected in EPTs, harbors several putative oncogenes including *ABL* and *VAV2* (located at 9q34). However, the significance of these genes in the EPT initiation and development remains to be clarified.

Comparative Genomic Hybridization Findings in Primary Tumors and Metastases

Our tumor collection for the CGH analysis includes 17 matched primary tumor and metastasis pairs that are obtained from 17 patients. Chromosomal alterations are detected in all of the 17 primary and metastatic tumor pairs. Losses and gains of DNA sequence copy number occur equally often in each of the tumor groups. No amplifications are evident in the tumors. The total number of chromosomal aberrations is higher in the metastases (mean, 17.3) than in the primary EPTs (mean, 12.5). The most frequent losses in the 17 metastases involve 2p (41%), 2q (41%), 3p (47%), 3q (41%), 6q (47%), 10p (47%), 11p (53%), and 11q (53%). Prevalent chromosomal gains detected in the metastases include 4p (53%), 4q (53%), 5p (47%), 5q (59%), 7p (59%), 7q (71%), 9q (41%), 12q (47%), 14q (47%), 17q (53%), 18q (41%), and 20q (41%). These chromosomal aberrations are also detected in the corresponding primary tumors, but with a lower frequency. These results clearly indicate a progression of genomic imbalances in cells of the metastases.

The median percent concordance for the tumor pairs is 67% (range, 0–100%; 95% confidence interval = 52–83%). Pairwise analysis reveals that the primary and metastatic tumors share at least four genomic changes in 15 of 17 tumor pairs. Similar results are also obtained from the probabilistic model analysis. The 15 tumor pairs that have a high percent concordance of genetic changes also display a high probability (>0.95) for a clonal relationship between the primary tumor and the corresponding metastasis. Of the 17 tumor pairs, 10 show more chromosomal changes in the metastasis than in the primary tumor, whereas 4 exhibit equal genomic alterations in the primary tumors and their metastases. The high probability for shared genomic alterations in primary EPTs and corresponding metastases suggest that the asynchronous metastatic lesions originated from the sites of primary tumors rather than from newly arising lesions. Genomic imbalances accumulated in these metastases might harbor crucial genetic alterations contributing to dissemination of tumor cells.

Comparative Genomic Hybridization Differences in Endocrine Pancreatic Tumor Subtypes

Major differences in chromosomal aberrations are observed between nonfunctioning and functioning EPTs. Genomic alterations are significantly more frequent in nonfunctioning EPTs than in functioning EPTs (mean, 12.8 versus 5.9, $P = 0.0005$). The average number of chromosomal gains and losses differs significantly in the two tumor groups, i.e., mean gain, 6.7 versus 2.6 ($P < 0.0001$) and mean loss, 6.1 versus 3.3 ($P < 0.01$).

Nonfunctioning EPTs account for 24–67% of all pancreatic neuroendocrine tumors (Eriksson *et al.,* 1989). These tumors usually present late with local symptoms resulting from compression or invasion of pancreatic or peripancreatic structures. Therefore, many of these tumors are large (>5 cm in diameter) at

the time of diagnosis. The detected genomic imbalances in nonfunctioning tumors involve many chromosomes. Frequent chromosomal gains occurring in nonfunctioning EPTs include 4p (40%), 5p (36%), 5q (32%), 7p (40%), 7q (56%), 9q (36%), 12q (40%), 14q (48%), 17q (48%), 20q (48%), and Xq (28%). Chromosomal losses mainly involve 2q (32%), 3p (36%), 3q (28%), 6q (56%), 8q (32%), 10p (28%), 10q (32%), 11p (52%), and 11q (48%). Almost all of these chromosomal aberrations are significantly more frequent in these tumors than in functioning EPTs, with the exception of 9q. Most of these changes involve entire chromosomes or chromosomal arms and are generally enriched in clinically malignant tumors. Corresponding to the CGH results, LOH studies have revealed a variety of allelic imbalances in these tumors (Barghorn *et al.,* 2001; Gortz *et al.,* 1999). Somatic mutations of several genes have also been identified in nonfunctioning tumors, such as *MEN1* (locus at 11q13) and *PTEN* (10q23.3) (Perren *et al.,* 2000; Wang *et al.,* 1998).

Functioning EPTs, in general, display fewer genomic imbalances compared with nonfunctioning tumors. This could be explained by the fact that functioning tumors are usually discovered at early stages because of clinical symptoms caused by an excessive secretion of hormone. However, the majority of functioning EPTs are benign insulinomas that harbor the lowest number of genomic imbalances when compared with other types of EPTs. The average number of genetic alterations (ANGC) in a series of 8 benign insulinomas is 2.8, whereas the ANGC in 25 malignant insulinomas is 12.6. In our sets of 8 glucagonomas, 10 VIPomas, and 9 gastrinomas, the ANGC is 9.3, 7, and 4.7, respectively. It is striking that the most frequently occurring aberrations are different in the functioning EPT subtypes. For instance, 9q gains occur frequently in malignant insulinomas and gastrinomas, but they are rare in glucagonomas and VIPomas. Losses of 11q are prevalent in glucagonomas and VIPomas but less common in the other functioning EPTs including malignant insulinomas. Losses of 3q are most frequently present in malignant insulinomas (75%), followed by glucagonomas (37.5%). In strong contrast to these tumors, no 3q losses occur in the other functioning EPTs. Losses of chromosome 6 are frequent in malignant insulinomas and glucagonomas; however, they are rare in other functioning tumors.

Insulinoma is the most frequent tumor of all functioning EPTs, and the majority of insulinomas are benign. There are marked differences in genetic alterations between benign and malignant insulinomas (mean, 2.5 versus 12.3; $P = 0.0001$). In malignant insulinomas, prevalent losses of chromosomal material are present at 2p, 2q (50%, each), 6q (75%), and 3q (75%), whereas common gains involve 12q, 17q, and Xp (50%, each). These genetic alterations are rare in benign insulinomas, indicating a clear association with malignant behavior. Other genetic changes commonly occurring in malignant insulinomas, such as 11q loss and gains of 1p and 9q, are also frequently detected in benign insulinomas and even in small insulinoms (diameter ≤2 cm), suggesting an involvement of these alterations in early stage of the tumor development. These CGH findings correspond well with LOH results with regard to 11q loss. Allelic losses of 11q13 (the locus of *MEN1*) is reported in up to 40% of insulinomas (Hessman *et al.,* 1998, 1999; Moore *et al.,* 2001; Wang *et al.,* 1998; Zhuang *et al.,* 1997). However, somatic mutations of the *MEN1* gene appear to be rare when compared with the other endocrine tumor types.

Other less frequently encountered types of functioning EPTs, i.e., gastrinomas, glucagonomas, and VIPomas, exhibit no significant differences in the average number of genomic alterations. In gastrinomas, frequent genomic changes include losses of 3p and gains of 9q, 7q, 17q, and 22q with the highest occurrence of 9q gain (44%). In glucagonomas, frequent chromosomal gains and losses involve many different chromosomes. Most strikingly, gains of chromosomes 7 and 17 are present in up to 50% of these tumors. In VIPomas, the most frequent aberration is loss of 11q (50%). Other common alterations include losses of 11p, Xq, Y, and 13q and gains of 17q and 7q.

Taken together, the average number of chromosomal losses and gains is clearly associated with tumor size and malignant behavior. Genomic imbalances increase with the progression of endocrine pancreatic tumors. Some genetic aberrations such as 9q gain and 6q and 11q losses are frequently detectable in small, benign tumors, representing early genetic changes in the EPT development. The majority of other detected chromosomal gains and losses are enriched in advanced malignant EPTs. Pairwise analysis reveals a high probability for a clonal relationship between the primary tumor and the corresponding metastasis, suggesting a clonal tumor progression in these malignancies. Genetic alterations differ in EPT subtypes, indicating that the tumor type-specific genetic aberrations may contribute to the development of subtypes of EPTs via separate molecular pathways.

Acknowledgment

The authors thank Parvin Saremaslani, Sonja Schmid, and Claudia Bonvin for excellent technical assistance; Ernst J.M. Speel for his experimental work; and Philipp U. Heitz and Jürgen Roth for continuous support. This work is supported by grants of the Swiss Cancer League (SKL-997-02-2000) and the Swiss National Science Foundation (NF 31-618845-00).

References

Barghorn, A., Speel, E.J., Farspour, B., Saremaslani, P., Schmid, S., Perren, A., Roth, J., Heitz, P.U., and Komminoth, P. 2001. Putative tumor suppressor loci at 6q22 and 6q23-q24 are involved in the malignant progression of sporadic endocrine pancreatic tumors. *Am. J. Pathol. 158*:1903–1911.

Bartsch, D., Hahn, S.A., Danichevski, K.D., Ramaswamy, A., Bastian, D., Galehdari, H., Barth, P., Schmiegel, W., Simon, B., and Rothmund, M. 1999. Mutations of the DPC4/Smad4 gene in neuroendocrine pancreatic tumors. *Oncogene 18*:2367–2371.

Chakrabarti, R., Srivatsan, E.S., Wood, T.F., Eubanks, P.J., Ebrahimi, S.A., Gatti, R.A., Passaro, E., Jr., and Sawicki, M.P. 1998. Deletion mapping of endocrine tumors localizes a second tumor suppressor gene on chromosome band 11q13. *Genes Chromos. Cancer 22*:130–137.

Eriksson, B., Oberg, K., and Skogseid, B. 1989. Neuroendocrine pancreatic tumors: Clinical findings in a prospective study of 84 patients. *Acta Oncol. 28*:373–377.

Evers, B.M., Rady, P.L., Sandoval, K., Arany, I., Tyring, S.K., Sanchez, R.L., Nealon, W.H., Townsend, C.M., Jr., and Thompson, J.C. 1994. Gastrinomas demonstrate amplification of the HER-2/neu proto-oncogene. *Ann. Surg. 219*:596–601.

Forozan, F., Karhu, R., Kononen, J., Kallioniemi, A., and Kallioniemi, O.P. 1997. Genome screening by comparative genomic hybridization. *Trends Genet. 13*:405–409.

Gortz, B., Roth, J., Krahenmann, A., de Krijger, R.R., Muletta-Feurer, S., Rutimann, K., Saremaslani, P., Speel, E.J., Heitz, P.U., and Komminoth, P. 1999. Mutations and allelic deletions of the MEN1 gene are associated with a subset of sporadic endocrine pancreatic and neuroendocrine tumors and not restricted to foregut neoplasms. *Am. J. Pathol. 154*:429–436.

Hessman, O., Lindberg, D., Einarsson, A., Lillhager, P., Carling, T., Grimelius, L., Eriksson, B., Akerstrom, G., Westin, G., and Skogseid, B. 1999. Genetic alterations on 3p, 11q13, and 18q in nonfamilial and MEN1-associated pancreatic endocrine tumors. *Genes Chromos. Cancer 26*:258–264.

Hessman, O., Lindberg, D., Skogseid, B., Carling, T., Hellman, P., Rastad, J., Akerstrom, G., and Westin, G. 1998. Mutation of the multiple endocrine neoplasia type 1 gene in nonfamilial, malignant tumors of the endocrine pancreas. *Cancer Res. 58*:377–379.

Jensen, R.T. 1998. Management of the Zollinger-Ellison syndrome in patients with multiple endocrine neoplasia type 1. *J. Intern. Med. 243*:477–488.

Jensen, R.T. 1999. Pancreatic endocrine tumors: Recent advances. *Ann. Oncol. 10*:170–176.

Kallioniemi, A., Kallioniemi, O.P., Sudar, D., Rutovitz, D., Gray, J.W., Waldman, F., and Pinkel, D. 1992. Comparative genomic hybridization for molecular cytogenetic analysis of solid tumors. *Science 258*:818–821.

Kloppel, G. 1997. Classification of neuroendocrine tumors. *Verh. Dtsch. Ges. Pathol. 81*:111–117.

Knuutila, S., Aalto, Y., Autio, K., Bjorkqvist, A.M., El-Rifai, W., Hemmer, S., Huhta, T., Kettunen, E., Kiuru-Kuhlefelt, S., Larramendy, M.L., Lushnikova, T., Monni, O., Pere, H., Tapper, J., Tarkkanen, M., Varis, A., Wasenius, V.M., Wolf, M., and Zhu, Y. 1999. DNA copy number losses in human neoplasms. *Am. J. Pathol. 155*:683–694.

Knuutila, S., Bjorkqvist, A.M., Autio, K., Tarkkanen, M., Wolf, M., Monni, O., Szymanska, J., Larramendy, M.L., Tapper, J., Pere, H., El-Rifai, W., Hemmer, S., Wasenius, V.M., Vidgren, V., and Zhu, Y. 1998. DNA copy number amplifications in human neoplasms: Review of comparative genomic hybridization studies. *Am. J. Pathol. 152*:1107–1123.

Libutti, S.K., Choyke, P.L., Bartlett, D.L., Vargas, H., Walther, M., Lubensky, I., Glenn, G., Linehan, W.M., and Alexander, H.R. 1998. Pancreatic neuroendocrine tumors associated with von Hippel Lindau disease: Diagnostic and management recommendations. *Surgery 124*:1153–1159.

Liotta, L., and Petricoin, E. 2000. Molecular profiling of human cancer. *Nat. Rev. Genet. 1*:48–56.

Madeira, I., Terris, B., Voss, M., Denys, A., Sauvanet, A., Flejou, J.F., Vilgrain, V., Belghiti, J., Bernades, P., and Ruszniewski, P. 1998. Prognostic factors in patients with endocrine tumours of the duodenopancreatic area. *Gut 43*:422–427.

Moore, P.S., Missiaglia, E., Antonello, D., Zamo, A., Zamboni, G., Corleto, V., Falconi, M., and Scarpa, A. 2001. Role of disease-causing genes in sporadic pancreatic endocrine tumors: MEN1 and VHL. *Genes Chromos. Cancer 32*:177–181.

Perren, A., Komminoth, P., Saremaslani, P., Matter, C., Feurer, S., Lees, J.A., Heitz, P.U., and Eng, C. 2000. Mutation and expression analyses reveal differential subcellular compartmentalization of PTEN in endocrine pancreatic tumors compared to normal islet cells. *Am. J. Pathol. 157*:1097–1103.

Ruas, M., and Peters, G. 1998. The p16INK4a/CDKN2A tumor suppressor and its relatives. *Biochim. Biophys. Acta 1378*: F115–177.

Speel, E.J., Richter, J., Moch, H., Egenter, C., Saremaslani, P., Rutimann, K., Zhao, J., Barghorn, A., Roth, J., Heitz, P.U., and Komminoth, P. 1999. Genetic differences in endocrine pancreatic tumor subtypes detected by comparative genomic hybridization. *Am. J. Pathol. 155*:1787–1794.

Speel, E.J., Scheidweiler, A.F., Zhao, J., Matter, C., Saremaslani, P., Roth, J., Heitz, P.U., and Komminoth, P. 2001. Genetic evidence for early divergence of small functioning and nonfunctioning endocrine pancreatic tumors: Gain of 9Q34 is an early event in insulinomas. *Cancer Res. 61*:5186–5192.

Stabile, B.E., and Passaro, E., Jr. 1985. Benign and malignant gastrinoma. *Am. J. Surg. 149*:144–150.

Stumpf, E., Aalto, Y., Hoog, A., Kjellman, M., Otonkoski, T., Knuutila, S., and Andersson, L.C. 2000. Chromosomal alterations in human pancreatic endocrine tumors. *Genes Chromos. Cancer 29*:83–87.

Waldman, F.M., DeVries, S., Chew, K.L., Moore, D.H., 2nd, Kerlikowske, K., and Ljung, B.M. 2000. Chromosomal alterations in ductal carcinomas in situ and their in situ recurrences. *J. Natl. Cancer Inst. 92*:313–320.

Wang, E.H., Ebrahimi, S.A., Wu, A.Y., Kashefi, C., Passaro, E., Jr., and Sawicki, M.P. 1998. Mutation, of the MENIN gene in sporadic pancreatic endocrine tumors. *Cancer Res. 58*:4417–4420.

Weber, H.C., Venzon, D.J., Lin, J.T., Fishbein, V.A., Orbuch, M., Strader, D.B., Gibril, F., Metz, D.C., Fraker, D.L., and Norton, J.A. 1995. Determinants of metastatic rate and survival in patients with Zollinger-Ellison syndrome: A prospective long-term study. *Gastroenterology 108*:1637–1649.

Zhao, J., Moch, H., Scheidweiler, A.F., Baer, A., Schaffer, A.A., Speel, E.J., Roth, J., Heitz, P.U., and Komminoth, P. 2001. Genomic imbalances in the progression of endocrine pancreatic tumors. *Genes Chromos. Cancer 32*:364–372.

Zhuang, Z., Vortmeyer, A.O., Pack, S., Huang, S., Pham, T.A., Wang, C., Park, W.S., Agarwal, S.K., Debelenko, L.V., Kester, M., Guru, S.C., Manickam, P., Olufemi, S.E., Yu, F., Heppner, C., Crabtree, J.S., Skarulis, M.C., Venzon, D.J., Emmert-Buck, M.R., Spiegel, A.M., Chandrasekharappa, S.C., Collins, F.S., Burns, A.L., Marx, S.J., and Lubensky, I.A. 1997. Somatic mutations of the MEN1 tumor suppressor gene in sporadic gastrinomas and insulinomas. *Cancer Res. 57*:4682–4686.

3

Molecular Detection of Micrometastases in Pancreatic Cancer

Marco Niedergethmann, Stefanie Knob, and Stefan Post

Introduction

Despite advances in surgical oncology, local recurrence and distant metastases are the major problems in treating pancreatic cancer. Only 25% of all pancreatic cancers are resectable, and only patients who have been curatively resected (R0) enjoy a favorable outcome (Richter *et al.,* 2003). However, the survival after surgery still remains poor. Most surgeons and oncologists treating pancreatic cancer believe that local recurrence represents the growth of residual tumor (Pantel *et al.,* 2000). Despite histologically confirmed curative resection (no residual tumor: R0) and tumor-free lymph nodes, most patients will suffer from postoperative local recurrence or distant metastases (Trede *et al.,* 2001). Occult dissemination of tumor cells beyond resection margins is of paramount importance for prognosis. This is impressively shown by a 50% recurrence rate within 2 years after surgery for pancreatic cancer (Richter *et al.,* 2003; Trede *et al.,* 2001).

In recent years, numerous new techniques to detect minimal residual disease (MRD), including immunohistochemical and molecular assays, have been introduced to reveal the accurate resection status (R0 versus R1) and enrich the routine histopathology (Niedergethmann *et al.,* 2002). These techniques detect micrometastases and disseminated tumor cells not only in lymph nodes that had appeared tumor free in routine histology but also in body compartments such as bone marrow, peritoneal cavity, and blood (Vogel *et al.,* 2001). From the current data, it has been concluded that routine histopathology often underestimates the true tumor stage. It is well known that micrometastases of a diameter of 3 cells are diagnosed only in 1% based on serial 5-μm sections (Keene and Demeure, 2001). Diagnosing micrometastases with routine histopathology can be accomplished only on extensive serial sections and extensive lymph node dissection, which are not useful in pancreatic cancer. However, occult metastases can be more easily detected by immunohistochemical or molecular methods designed to recognize certain tumor-associated antigens, lineage-specific markers, or distinct tumor-related gene mutations. Immunohistochemical methods use antibodies against a variety of epithelial cell markers such as cytokeratins, CA 19.9, carcinoembryonic antigen (CEA), or Ber-Ep 4. These markers are

Handbook of Immunohistochemistry and *in situ* Hybridization of Human Carcinomas, Volume 3: Molecular Genetics, Liver Carcinoma, and Pancreatic Carcinoma

often not specific because nonmalignant cells are also able to express them and thus might deliver false-positive results. It has been demonstrated that CA 19.9 antibodies can be detected in 60% of regional lymph nodes dissected as a result of chronic pancreatitis (Ridwelski *et al.,* 2001). As in histopathology, the limiting factor is the analysis of tissue in stepwise serial sections and not as a whole specimen.

As shown in other gastrointestinal malignancies, specific genetic disorders, e.g., mutations, can be used in pancreatic cancer to detect micrometastases in different body compartments (Pantel and von Knebel-Doeberitz, 2000). According to various analyses, mutated K-*ras* gene has been found in a range from 70% to 95% of pancreatic adenocarcinomas, and the site of mutation is restricted to codon 12 of the K-*ras* gene (Almoguera *et al.,*1988; Löhr *et al.,* 2000). Therefore, mutant K-*ras* is one of the most promising genetic alterations in ductal adenocarcinoma to detect malignant cells by molecular techniques. In several studies, micrometastases have been detected at the molecular level by sensitive polymerase chain reaction (PCR) and restriction fragment length polymorphism (RFLP) assays for the detection of mutant codon 12 K-*ras* allele (Banerjee *et al.,* 1997; Niedergethmann *et al.,* 2002).

Nevertheless, it has been discussed whether micrometastases are of prognostic significance or if these are only "dormant" tumor cells arrested in G0-phase (Pantel and von Knebel-Doeberitz, 2000; Keene *et al.,* 2001). This chapter attempts to answer these questions and provides detailed information of immunohistochemical and molecular methods to detect lymph node micrometastases in pancreatic cancer.

The following investigations were carried out with 69 specimens of resected ductal pancreatic adenocarcinomas (Department of Surgery, University-Hospital Mannheim). In all cases, corresponding paraaortic lymph nodes were obtained by *en bloc* dissection from the suprarenal paraaortic region. All cases had tumor-free margins. We used nine surgical specimens of patients diagnosed for adenomas of Vater's papilla ($n = 4$), chronic pancreatitis ($n = 4$), and one cystadenoma with corresponding paraaortic lymph nodes as controls. Normal pancreatic tissue served as a negative control for each individual subject. Tumor, normal tissue, and paraaortic lymph nodes were used for histopathology and immunohistochemistry, and extended deoxyribonucleic acid (DNA) investigations were prepared. Each paraaortic lymph node was divided into two portions, one of which was formalin-fixed and paraffin-embedded for immunohistochemistry, and the other one was stored frozen at −80°C until PCR analysis.

MATERIALS

Immunohistochemistry for Pan-Cytokeratin

1. Buffered formalin (4%): 100 ml phosphate buffer saline (PBS) buffer (PBS-buffer: 200 g Natriumhydrogenphosphat, 325 g Dinatiumhydrogenphosphat, bring volume to 5 L with distilled water), 100 ml formalin (37%), bring volume to 800 ml with distilled water.
2. Paraffin wax.
3. Microtome.
4. Xylene.
5. Alcohol 100%, 96%, and 80%.
6. Brood-cupboard.
7. 0.1% Trypsine solution: 100 mg trypsine, 100 mg calciumchloride, bring volume to 100 ml with distilled water.
8. Deionized water.
9. Blocking-solution (Zymed, Bad Homburg, Germany).
10. Primary anti-pan-cytokeratin antibody (Zymed; NCC-pan-ck, dilution 1:50).
11. Tris-buffered saline (TBS) (pH 7.6): 6.055 g Tris buffer, 8.52 g NaCl, 37 ml 1 N HCl, bring volume to 1 L with distilled water, 0.5 ml Tween 20.
12. Secondary biotinylated antibody (Zymed).
13. Streptavidin-labeled immunoalkaline phosphatase (Zymed, Bad Homburg, Germany).
14. Substrate-chromogen-mixture (SCM): 0.121 g Tris-buffer and 0.5 ml 1 N HCl, bring volume to 10 ml distilled water, 2 mg Naphtol AS-MX Phosphat, 2.4 mg Levamisole hydrochloride, and 10 mg Fast Red TR Salt.
15. Hematoxylin.
16. Kaiser's glycerine gelatin (Merck, Darmstadt, Germany).

Molecular Detection by Mutated K-Ras

1. Human pancreatic adenocarcinoma cell line Pa-Tu-8902 (DSMZ: German Department of Human and Animal Cell Cultures, Mainz, Germany).
2. QIAamp DNA mini Kit (Qiagen, Hilden, Germany).
3. Photometer.
4. Thermocycler.
5. 0.5-ml tubes (for PCR) and 1.5-ml/2-ml tubes (for DNA extraction) (Eppendorf, Hamburg, Germany).
6. Thermocycler (Perkin-Elmer Inc., Norfolk, VA).
7. 25 mM $MgCl_2$.
8. 5 mM of each dNTP (deoxyribonucleotide-triphosphate).
9. 0.3 µM 3′-primer (5′-GTC CTG CAC CAG AAA TAT TGC-3′) and 5′-primer (5′-ACT GAA TAT AAA CTT GTG GTA GTT GGA CCT-3′) (MWG Biotech AG, Ebersberg, Germany).

10. Two units of *Taq* polymerase in PCR-buffer containing 500 mM KCl, 15 mM $MgCl_2$, and 100 mM Tris-HCl (Amersham Pharmacia Biotech, Freiburg, Germany).
11. Ampermeter.
12. Agarose (ultra PURE, Paisley, UK).
13. Tris-acetat-ethylenediamine tetraacetic acid (TAE)-buffer: dilution 1:10 (Sigma Aldrich Chemie, Steinheim, Germany).
14. Ethidium bromide (Invitrogen Corporation, Paisley, Scotland).
15. Electrophoresis-box.
16. Loading buffer (Invitrogen Corporation, Paisley, Scotland).
17. DNA-ladder (Invitrogen Corporation, Paisley, Scotland).
18. Gel documentation system (Bio-Rad Laboratories GmbH, München, Germany).
19. Endonuclease *Mva* I system containing *Mva* I and incubation-buffer (Roche, Mannheim, Germany).

METHODS

Immunohistochemistry for Pan-Cytokeratin

1. Fix tissue blocks in 4% buffered formalin for 24 hr and embed in paraffin.
2. Cut serial sections of 5 µm thickness of paraaortal lymph nodes with microtome.
3. Deparaffinizing and rehydration: Rinse the samples for 5 min in xylene, then for 2 mm in 100% alcohol; repeat the procedure with 96% alcohol and 80% alcohol.
4. Dry the samples for 12 hr in brood-cupboard at 37°C.
5. Incubate the samples for 40 min in 0.1% trypsine solution at 37°C for antigen retrieval.
6. Rinse sections in deionized water for 5 min.
7. For immunohistological detection the biotin-streptavidin-amplified indirect immunoalkaline phosphatase method (Zymed, Bad Homburg, Germany) was used (as described in manufacturer's instructions).
8. Add 100 µl of blocking solution to each sample and incubate for 15 min at room temperature; rinsing is not necessary.
9. Thereafter, the primary anti-pan-cytokeratin antibody is applied (100 µl) for 1 hr at room temperature.
10. Control sections are incubated with TBS instead of the primary antibody.
11. Rinse all samples for 5 min in TBS.
12. The sections are incubated for 10 min with the secondary biotinylated antibody (100 µl).
13. Rinse the samples for 5 min in TBS.
14. Streptavidin-labeled immunoalkaline phosphatase is added for 10 min (2 drops or 100 µl).
15. Rinse the samples for 5 min in TBS.
16. The SCM-staining is applied for 30 min at room temperature.
17. Sections are washed in tap water.
18. Counterstain the samples with hematoxylin for 1–3 min at room temperature, and mount them in Kaiser's Glycerine Gelatin.

Molecular Detection by Mutated K-Ras

1. The human pancreatic adenocarcinoma cell line Pa-Tu-8902 from DSMZ (German Department of Human and Animal Cell Cultures) serves as a positive control.
2. Distilled water without tissue is used as an internal negative control.
3. For DNA extraction, the scheme of the QIAamp DNA mini Kit is used (as described in manufacturer's instructions).
4. After DNA extraction, the optical density (OD) at 260 and 280 nm, respectively, is measured.
5. Aliquots corresponding to 200 ng of genomic DNA are submitted to PCR.
6. The PCR is performed using 0.5 ml tubes and a thermocycler.
7. Reactions are carried out in a total volume of 50 µl containing final concentrations of 20 µl aliquot of genomic DNA; 5 µl PCR buffer (see earlier steps); 1 µl 25 mM $MgC1_2$; 2 µl with 5 mM of each dNTP; 3 µl 0.3 µM of each 3′- and 5′-primer, respectively; 0.4 µl with 2 units of *Taq* polymerase; and 15.6 µl distilled water.
8. Experiments using the technique of mismatch PCR are carried out starting with an initial step for denaturation at 95°C for 5 min; then, 35 cycles are run including denaturing at 95°C for 45 sec, annealing at 59°C for 45 sec, and DNA synthesis at 72°C for 90 sec, followed by a final step at 72°C for 10 min. The primers used are leading to a PCR product of 147 base pairs (bp) in length.
9. Successful PCR is shown by ethidium bromide agarose gel (2%) electrophoresis.
10. Bring 1 g agarose in 50 ml TAE buffer, and heat the solution until agarose is completely dissolved.
11. Add 2.5 µl ethidium bromide after 2 min cooling of the solution.
12. Pour the solution into the electrophoresis box and bring into the gel-comb.
13. After cooling for 30 min at room temperature, fill TAE buffer until complete coverage of the gel is obtained.
14. After, bring 10 µl DNA aliquot and 2 µl loading buffer into the gel-pouch.
15. Fill reference line with 5 µl DNA ladder and 2 µl loading buffer.

16. To run gel, use ampermeter (70–100 V) for 1 hr. Digital analysis is recommended.

17. After electrophoresis digest, aliquots of genomic DNA with restriction endonuclease *Mva* I according to the manufacturer's instructions (Roche, Mannheim, Germany).

18. Reactions are carried out in a total volume of 20 µl containing final concentrations of 10 µl DNA aliquot after PCR, 1 µl Mva I, 2 µl incubations buffer, and 7 µl distilled water; incubate the aliquots for 5 hr at 37°C.

19. Analyze PCR again in ethidium bromide agarose gel electrophoresis (2%) as described in **Steps 9–12,** then fill in 20 µl aliquot with 3 µl loading buffer into the gel-pouch and run gel using ampermeter (70–100 V) for 90 min.

20. Each individual sample is analyzed in triplicate manner.

RESULTS

Immunohistochemical Examination

Using the pan-cytokeratin, antibody-positive immunoreaction of single or grouped carcinoma cells within the lymphoreticular tissue of the nodes was found. Positive immunoreactivity was observed in 5 out of 69 specimens (7.2%). As a consequence, these five cases were diagnosed for micrometastases in paraaortic lymph nodes. In Figure 46 a strong cytoplasmic immunoreaction of carcinoma cells within the lymphoreticular tissue of a paraaortic node is demonstrated. No positive staining was found except in cancer cells. In comparison, using routine histology with hematoxylin and eosin staining, one could find occult tumor cells in paraaortic lymph nodes only in 3 of 69 specimens (4%).

Molecular Detection of Micrometastases

The use of the described mismatch primers results in amplification of a 147-bp product. A restriction site for *Mva* I is created in wild-type (wt), but not in mutated K-*ras* using the 5′-primer, whereas 3′-primer inserts a restriction site in both, serving as an internal control for a successful *Mva* I digestion. Thus, a wild-type allele, is detected by the appearance of a 107-bp band, whereas in cells harboring K-*ras* mutations, an additional band of 136 bp can be visualized. Forty-two of 69 (61%) ductal adenocarcinomas harboring the K-*ras* mutation in primary tumor were identified, visualized by appearence of the additional 136-bp band after *Mva* I digestion and subsequent gel electrophorsis. In the control specimen K-*ras* mutation was found in 1 of 4 (25%) adenomas of Vater's papilla but in no other case of the control group. In addition, no mutation was detected in all individual negative controls (normal pancreatic tissue). In pancreatic adenocarcinoma specimen, 12 cases (12/69, 17.4%) showed mutant K-*ras* gene in corresponding paraaortic lymph nodes. Therefore, in subjects with K-*ras*–positive primary tumors, micrometastases could be found in 29% (12/42). Immunohistological staining was able to detect tumor cells in lymph nodes in only five of these subjects. Mutated K-*ras*, an indicator for tumor-cell DNA, that is found in paraaortic lymph nodes, can be set equivalent with micrometastases. There was no mutated K-*ras* found in paraaortic lymph node specimen of the control group.

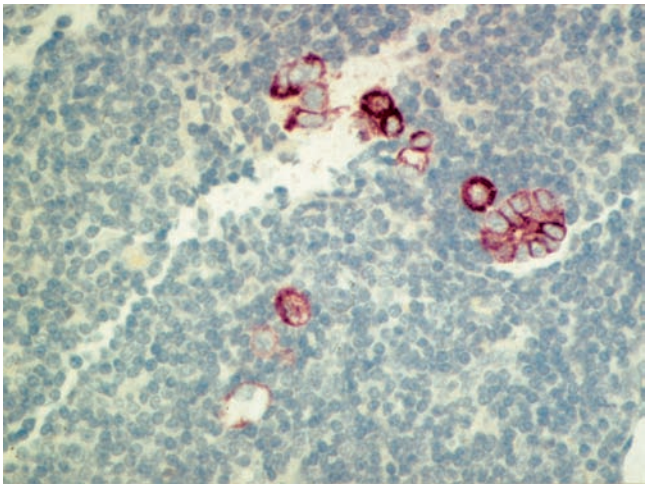

Figure 46. Occult tumor cells in a paraaortic lymph node of a patient with pancreatic adenocarcinoma after curative pancreatico-duodenectomy: Positive immunoreactions of carcinoma cells within the lymphoreticular tissue of a paraaortic node using anti-pan-cytokeratin antibodies; counterstained with hematoxylin (magnification: 200X).

DISCUSSION

Ductal adenocarcinoma of the pancreas is associated with the worst 5-year survival rate of any form of gastrointestinal cancer, even after curative resection (Hartel *et al.,* 2002; Richter *et al.,* 2003). However, until now, the question of why some patients die within a few months after curative resection because of metastases or local recurrence, whereas others enjoy a more favorable outcome has not been sufficiently answered. We argue that the present histologic sectioning may lack sufficient sensitivity for assessing lymph nodes and surgical resection margins for tumor involvement and minimal residual cancer, respectively.

Therefore, highly sensitive methods have been investigated to assess patients with other types of

gastrointestinal cancers for minimal residual disease (Vogel *et al.,* 2001) In 2001, PCR-based assays were used for detecting MRD in histologically negative lymph nodes from patients with gastric and colorectal cancer (Keene and Demeure, 2001). For pancreatic cancer, it has been suggested that immunohistochemical antibodies be used against epithelial- or tumor-associated antigens, such as cytokeratin (CK) or CEA in various body compartments for the detection of occult micrometastases at the time of surgery (Niedergethmann *et al.,* 2002). One group suggested combining routine histopathology with CK immunohistology for detection of MRD after surgery because the latter method increases the sensitivity for micrometastases (Ridweiski *et al.,* 2001).

Because mutant K-*ras* is the most evident genetic alteration in pancreatic adenocarcinoma, several investigators have performed analyses for this gene as a marker for occult tumor cells, e.g., in stool, blood, or tissue specimens (Tada *et al.,* 1991). It has been demonstrated that detection of K-*ras* mutation in regional and paraaortic lymph nodes is superior to routine pathologic examination, and it has been suggested that using this for prognostic reevaluation (Demeure *et al.,* 1998). Tamagawara *et al.* (1997) could reveal that evidence of MRD in regional lymph nodes by detection of mutant K-*ras* was a predictive marker for recurrence in patients with pancreatic adenocarcinoma.

From our investigations the following conclusions can be drawn: 1) patients with positive K-*ras* mutations in paraaortic lymph nodes will have a significantly worse prognosis than those without, 2) K-*ras* positive paraaortic lymph nodes are an independent prognostic marker after curative resection, and 3) patients with K-*ras* mutations in paraaortic lymph nodes will suffer significantly earlier from recurrent cancer (Niedergethmann *et al.,* 2002).

A summary of recent methods to detect minimal residual disease in pancreatic cancer is given in Table 20. With the described method one could find K-*ras* mutations in a similar range, as described by other authors

Table 20. Minimal Residual Disease in Pancreatic Adenocarcinoma: Summary of Detection Methods and Prognostic Implications

Author/year	Patients [n]	Compartment	Method	Marker	Detection of Micrometastases (%)	Prognostic Correlation
Ando 1997	15	Paraaortic LN	PCR	K-*ras* (DNA)	42	n.a.
Bilchik 2000	33	Blood	PCR	MET, Gal-Nac-T, βhCG	94	n.a.
Demeure 1998	29	Reg. LN	PCR	K-*ras* (DNA)	68	+
Funaki 1998	3	Blood	PCR	CEA (mRNA)	100	n.a.
Hosch 1997	18	Reg. LN	IHC	Ber-EP4	72	+
Niedergethmann 2002	69	Paraaortic LN	Histology	Hematoxylin and eosin	4	+
			IHC	Cytokeratin (pan CK)	7	+
			PCR	K-*ras* (DNA)	17	+ (IPF)
Ridwelski 2000	15	Reg. LN	IHC	Cytokeratin (AE1, AE3)	100	n.a.
Roder 1999	48	Bone marrow	IHC	Cytokeratin (CKKL- 1, CK2, A45-B/B3)	52	+
Tamagawara 1997	12	Reg. LN	PCR	K-*ras* (DNA)	83	+
Vogel 1999	80	Bone marrow	IHC	CA19.9, C1P83, Ra96,	38 (BM)	+
		Peritoneum		Kl–1	39 (P)	
Warshaw 1991	40	Peritoneum	Cytology	–	30	+
Yamada 2000	25	Reg. LN	IHC	K-ras (DNA)	52	+
Yamaguchi 2000	31	Paraaortic LN	PCR	K-ras, P53 (DNA)	33	+
Z'graggen 2001	105	Blood	IHC	Cytokeratin (AE1, AE3)	26	–
		Bone marrow			24	–

BM; bone marrow; IHC; immunohistochemistry; IPF; independent prognostic factor (multivariate analysis); P; peritoneal cavity; Paraaortic LN; paraaortic lymph nodes; PCR, Polymerase chain reaction; n.a.; not applicable; Reg. LN; regional lymph nodes.

(Demeure *et al.,* 1998; Tamagawa *et al.,* 1997). Minimal residual disease in paraaortic lymph nodes after curative resection can be detected in 7% by cytokeratin immunohistochemistry and in 17% by the PCR-based assay to detect mutant K-*ras*, underlining the sensitivity of the presented molecular detection system. In comparison, in routine histology with hematoxylin and eosin staining, occult tumor cells in those lymph nodes can only be diagnosed in 4%. Therefore, we believe, in accordance with other authors (Demeure *et al.,*1998; Tamagawa *et al.,* 1997; Yamada *et al.,* 2000), that the identification of K-*ras* mutations for the detection of MRD in lymph nodes is superior to the morphologic approach of the pathologic examination and that cancer cells may have already spread to lymph nodes that were histologically diagnosed as negative.

In conclusion, the routine, stepwise sectioning pathologic examination lacks the detection of micrometastases in many patients, whereas PCR-based assays to screen for mutated K-*ras* analyzes tumor cell DNA of the whole sample reveals a higher sensitivity. This can enrich the routine histopathologic examination in resectable pancreatic cancer and might precisely identify the "real" tumor stage.

References

Almoguera, C., Shibata, D., Forrester, K., Martin, J., Arnheim, N., and Perucho, M. 1988. Most human carcinomas of the exocrine pancreas contain mutant c-K-ras genes. *Cell 53*:549–555.

Ando, N., Nakao, A., Nomoto, S., Takeda, S., Kaneko, T., Kurokawa, T., Nonami, T., and Takagi, H. 1997. Detection of mutant K-ras in dissected paraaortic lymph nodes of patients with pancreatic adenocarcinoma. *Pancreas 15*:374–378.

Banerjee, S.K., Makdisi, W.F., Weston, A.P., and Campbell, D.R. 1997. A two-step enriched nested PCR technique enhances sensitivity for detection of codon 12 K-ras mutations in pancreatic adenocarcinoma. *Pancreas 15*:16–24.

Bilchik, A., Miyashiro, M., Kelley, M., Kuo, C., Fujiwara, Y., Nakamori, S., Monden, M., and Hoon, D.S. 2000. Molecular detection of metastatic pancreatic carcinoma cells using a multimarker reverse transcriptase-polymerase chain reaction assay. *Cancer 88*:1037–1044.

Demeure, M.J., Doffek, K.M., Komorowski, R.A., and Wilson, S.D. 1998. Adenocarcinoma of the pancreas: Detection of occult metastases in regional lymph nodes by a polymerase chain reaction based assay. *Cancer 83*:1328–1334.

Elsässer, H.P., Lehr, U., Agricola, B., and Kern, H.F. 1993. Structural analysis of a new highly metastatic cell line PaTu 8902 from a primary human pancreatic adenocarcinoma. *Virch. Arch. B Cell Pathol. 64*:201–207.

Funaki, N.O., Tanaka, J., Hosotani, R., Kogire, M., Suwa, H., Imamura, M. 1998. Quantitative analysis of carcinoembryonic antigen messenger RNA in peripheral venous blood and portal blood of patients with pancreatic ductal adenocarcinoma. *Clin. Cancer Res. 4*:855–860.

Hartel, M., Niedergethmann, M., Farag-Soliman, M., Sturm, J.W., Richter, A., Trede, M., and Post, S. 2002. Benefit of venous resection for ductal adenocarcinoma of the pancreatic head. *Eur. J. Surg. 168*:707–712.

Hosch, S.B., Knoefel, W.T., Metz, S., Stoecklein, N, Niendorf, A., Broelsch, C.E., and Izicki, J.R. 1997. Early lymphatic tumor cell dissemination in pancreatic cancer: Frequency and prognostic significance. *Pancreas 15*:152–159.

Keene, S.A., and Demeure, M.J. 2001. The clinical significance of micrometastases and molecular metastases. *Surgery 129*:1–5.

Löhr, M., Maisonneuve, P., and Lowenfels, A.B. 2000. K-Ras mutations and benign pancreatic disease. *Int. J. Pancreatol. 27*:93–103.

Niedergethmann, M., Rexin, M., Hildenbrand, R., Knob, S., Sturm, J.W., Richter, A., and Post, S. 2002. Prognostic implications of routine, immunohistological, and molecular staging in resectable pancreatic adenocarcinoma. *Am. J. Surg. Pathol. 26*:1578–1587.

Pantel, K., and von Knebel-Doeberitz, M. 2000. Detection and clinical relevance of micrometastatic cancer cells. *Curr. Opin. Oncol. 12*:95–101.

Richter, A., Niedergethmann, M., Hartel, M., Sturm, J.W., Lorenz, D., Trede, M., and Post, S. 2003. Longterm results of partial pancreaticoduodenectomy for ductal adenocarcinoma of the pancreatic head: A 25-year experience. *World J. Surg. 27*:324–329.

Ridwelski, K., Meyer, F., Fahlke, J., Kasper, U., Roessner, A., and Lippert, H. 2001. Value of cytokeratin and Ca 19-9 antigen in immunohistological detection of disseminated tumor cells in lymph nodes in pancreas carcinoma. *Chirurg 72*:920–926.

Roder, J.D., Thorban, S., Pantel, K., and Siewert, J.R. 1999. Micrometastases in bone marrow: Prognostic indicators for pancreatic cancer. *World J. Surg. 23*:888–891.

Tada, M., Omata, M., and Otho, M. 1991. Clinical application of ras gene mutation for diagnosis of pancreatic adenocarcinoma. *Gastroenterology 100*:233–238.

Tamagawa, E., Ueda, M., Sugano, K., Mukai, K., Ogata, S., and Kitajima, M. 1997. Pancreatic lymph nodal and plexus micrometastasis detected by enriched polymerase chain reaction and nonradioisotopic single-trans conformation polymorphism analysis: A new predictive factor for recurrent pancreatic carcinoma. *Clin. Cancer Res. 3*:2143–2149.

Trede, M., Richter, A., and Wendl, K. 2001. Personal observations, opinions, and approaches to cancer of the pancreas and the periampullary area. *Surg. Clin. North Am. 81*:595–610.

Vogel, I., Kruger, U., Marxsen, J., Soeth, E., Kalthoff, H., Henne-Bruns, D., Kremer, B., and Juhl, H. 1999. Disseminated tumor cells in pancreatic cancer patients detected by immunocytology: A new prognostic factor. *Clin. Cancer Res. 5*:593–599.

Vogel, I., and Kalthoff, H. 2001. Disseminated tumour cells: Their detection and significance for prognosis of gastrointestinal and pancreatic carcinomas. *Virch. Arch. 439*:109–117.

Warshaw, A.L. 1991. Implications of peritoneal cytology for staging of early pancreatic cancer. *Am. J. Surg. 161*:26–29.

Yamada, T., Nakamori, S., Ohzato, H., Higaki, N., Aoki, T., Oshimda, S., Shiozaki, K., Okami, J., Hayashi, N., Nagano, H., Dono, K., Umeshita, K., Sakon, M., and Monden, M. 2000. Outcome of pancreatic cancer patients based on genetic lymph node staging. *Int. J. Oncol. 16*:1165–1171.

Yamaguchi, K., Chijiiwa, K., Torato, N., Kinoshita, M., and Tanaka, M. 2000. Ki-ras codon 12 point and P53 mutations: A molecular examination of the main tumor, liver, portal vein, peripheral arterial blood and para-aortic lymph node in pancreatic cancer. *Am. J. Gastroenterol. 95*:1939–1945.

Z'graggen, K., Centeno, B.A., Fernandez-del Castillo, C., Jimenez, R.E., Werner, J., and Warshaw, A.L. 2001. Biological implications of tumor cells in blood and bone marrow of pancreatic cancer patients. *Surgery 129*:537–546.

4

K-ras Protooncogene in Human Pancreatic Cancer

Ming Dong and Kejian Guo

Introduction

Pancreatic Cancer

The incidence of pancreatic cancer has risen markedly during the last half-century. In 1997, pancreatic cancer is the fifth leading cause of adult deaths from cancer and causes approximately 27,000 deaths per year in the United States. Pancreatic cancer as a unique and heterogeneous disease is difficult to study. We have yet to define all of the molecular processes that cause or accompany the pathogenesis of malignant diseases of the pancreas, and we are hampered by a poor understanding of the molecular aspects of normal cell differentiation and development of the pancreas. The origin and nature of cells that are transformed in pancreatic cancer are not well defined. Yet we have little understanding of whether these differences portend differences in prognosis or require distinct treatments. Clinically, pancreatic tumors display insidious growth properties. The lack of anatomic barriers to protect against local infiltration and the biologic propensity to invade the lymphatics, nerves, and large vessels result in rapid progression of the tumor, and these are nearly insurmountable obstacles to achieve a complete surgical eradication of this tumor. However, pancreatic tumors are undetectable at early stages and display a high degree of resistance to both conventional chemotherapy and radiation therapy. Clearly evident symptoms of pancreatic cancer are not present until the disease is advanced, fewer than 15% of patients with pancreatic cancer are potential candidates for a curative resection, 65% of patients with pancreatic cancer die within 6 months of the time of diagnosis, and about 90% die within 1 year. Only 4% of patients will survive for 5 years after diagnosis (Rosenberg, 2000).

Although the cause and mechanism of development of human pancreatic cancers are still unclear, the effects of the activation of protooncogenes on the occurrence, development, and prognosis of this disease have been followed widely with interest. It is clear that tumor formation is initiated via the conversion of normal cellular genes, called protooncogenes, into oncogenes. The biological function of protooncogenes is not to cause cancer. These genes encode proteins that are part of the signal transduction pathways, which control normal cellular growth and differentiation. The activated protooncogenes result in a change in the amino acid sequence of the protein, which plays an important role in carcinogenesis. Factors of activation include point mutation, chromosome rearrangement, and gene amplification.

Handbook of Immunohistochemistry and *in situ* Hybridization of Human Carcinomas, Volume 3: Molecular Genetics, Liver Carcinoma, and Pancreatic Carcinoma

K-*ras* Protooncogene

It was reported that the human genome contains c-Ha-*ras* and c-Ki-*ras* in the 1980s (Chang *et al.,* 1982). Consequently, structure and organization of the K-*ras* protooncogene were clarified (McGrath *et al.,* 1983). The *ras* family contains three members: K-*ras*, N-*ras*, and H-*ras*. The K-*ras* gene is located at 12p12.1 (McBride *et al.,* 1983; O'Connell *et al.,* 1985; Popescu *et al.,* 1985), H-*ras* at 11p15.5 (Junien *et al.,* 1984), and N-*ras* at 1p13.2 (McBride *et al.,* 1983; Mitchell *et al.,* 1995). Although they have different genetic structures, they all code for proteins of 189 amino acid residues, generically designated 21-kDa proteins. The $p21^{ras}$-encoded proteins bind the guanosine diphosphate (GDP) and guanosine triphosphate (GTP) with high affinity and possess a low intrinsic GTPase activity. The *ras* gene bound to GTP is maintained in an active configuration that triggers other enzymatic second messengers, leading to nuclear signals and resulting in cellular division and proliferation. The mutated *ras* protooncogene is not able to convert GTP to inactive guanosine diphosphate (GDP), resulting in a constitutively active *ras* protein product, unregulated cellular proliferation signals, and susceptibility to transformation.

Of the *ras* family, K-*ras* is the most frequently mutated member in human tumors, especially in human pancreatic cancer. Point mutation at its hot-spot codon 12, 13, 59, and 61 within domains responsible for GTP binding and hydrolysis activate *ras* proteins to their oncogenic form and block the ability of the GTPase activity to be stimulated by GAP (Adari *et al.,* 1988; Barbacid, 1987; Calés, *et al.,* 1988; Trahey and McCormick, 1987). Accordingly, $p21^{ras}$-encoded proteins, normal or oncogenic, play a central role in human carcinogenesis. A low level of $p21^{ras}$-encoded proteins may be expressed in some normal tissues. Overexpression of this protein usually is proposed to be an abnormality of K-*ras* gene function and has been reported in various human cancers, including breast cancer (Rundle *et al.,* 2002), colorectal cancer (Karelia *et al.,* 2001), lung cancer (Harada *et al.,* 1992), head and neck cancer (Yarbrough *et al.,* 1994), bladder cancer (Miao *et al.,* 1991), and pancreatic cancer (Song *et al.,* 2000). The *ras* gene mutations were frequently found in 30% of other human cancers, including breast cancer (Miyakis *et al.,* 1988), colorectal cancer (Doolittle *et al.,* 2001; Voice *et al.,* 1999), prostate cancer (Konishi *et al.,* 1997), ovarian cancer (Varras *et al.,* 1999), lung cancer (Rosell *et al.,* 1993; Voice *et al.,* 1999), head and neck cancer (Yarbrough *et al.,* 1994), and leukemia (Voice *et al.,* 1999). The abnormalities of K-*ras* gene are implicated as an early event in pancreatic cancer in both nitrosamine-induced hamster models (Sugio *et al.,* 1996) and humans (Pellegata *et al.,* 1994; Tada *et al.,* 1996). Because a review reported that 75–95% of human pancreatic cancer harbors K-*ras* gene mutation (Dong *et al.,* 2000) and harbors a high prevalence of mutations at codon 12 of the K-*ras* gene (Almoguera *et al.,* 1988; Caldas and Kern, 1995), most analysis was restricted to codon 12 of the K-*ras* gene.

Currently, immunohistochemistry (IHC), single-strand conformation polymorphism (SSCP), Dot Blot hybridization, and direct deoxyribonucleic acid (DNA) sequencing are commonly used to screen and identify expression and mutations of the K-*ras* gene.

METHODS

Immunohistochemistry

Reagents

1. Phosphate buffer saline (PBS): 7.75 g sodium chloride, 1.50 g K_2HPO_4, 0.20 g KH_2PO_4; bring volume to 1 L with deionized glass distilled water, pH 7.6.
2. 0.3% H_2O_2: 1 ml 30% H_2O_2 in 99 ml methanol.
3. 0.21% citrate buffer: 2.l0 g citric acid [C_3H_4 (OH) (COOH) $3{\cdot}H_2O$, MW: 210.14]; bring volume to 1 L with ddH_2O, pH 6.0, adjusted by 4 N NaOH.
4. 10% of normal rabbit serum.
5. Pepsin.
6. Saponin.
7. Diaminobenzidine.
8. Hematoxylene.

Protocol

1. Five-micrometer slides were deparaffinized in xylene 5 min 3× and then rehydrated in 100% alcohol, 10 min 2× and 95% alcohol, 10 min 2×.
2. Chose one of following methods for pretreatments:
   a. Microwave oven: Place slides in 0.21% citrate buffer, pH 6.0. Heat at 800 W, 5 min 3×.
   Allow slides to cool in the buffer at room temperature for 40 min.
   b. Pepsin: Incubate slides in 0.1% pepsin in 0.01 N HCl at room temperature for 15 min.
   c. Saponin: Place slides in 0.05% saponin in ddH_2O at room temperature for 30 min.
3. Block endogenous peroxidase with 0.3% H_2O_2 in methanol for 15 min. PBS 5 min 3×.
4. Mark slides with Dako pen, drying up to 1 min. PBS 5 min 3×.
5. Blocking of nonspecific binding of antibodies with 10% of normal rabbit serum at room temperature for 10 min.
6. Add primary antibody prediluted with PBS at desired concentration (e.g., c-K-*ras* [Ab-1] at

5–10 µg/ml), in a moist chamber at room temperature for 2 hr or at 4°C overnight. PBS 5 min 3×.

7. Add biotinylated second antibody at room temperature for 20 min. PBS 5 min 3×.

8. Apply streptavidin peroxidase at room temperature for 10 min. PBS 5 min 3×.

9. Incubate slides with diaminobenzidine at room temperature for 5–15 min. Rinse in distilled water for 5 min 2×.

10. Apply hematoxylene for 40 sec and put slides in flowing water for 30 min (or methyl green for at least 2 hr, or possibly overnight at room temperature).

11. Graded alcohol: 95% alcohol 5 min and 100% alcohol, 5 min 2×.

12. Xylene: 5 min 3×.

13. Mounting cover glass.

The results of this method are shown in Figure 47.

Dot Blot Hybridization

Reagents

1. Xylene.
2. Ethanol.
3. SS-Phenol.
4. Chloroform.
5. Isoamyl alcohol.
6. Proteinase K (10 mg/ml).
7. Ribonuclease (RNase) A (10 mg/ml).
8. 0.5 Methylenediamine tetraacetic acid $(EDTA)_2$ Na ($C_{10}H_{14}N_2O_8Na_2 \cdot 2H_2O$, MW: 372.24): 186.12 g EDTA, about 20.0 g NaOH (adjusted to pH 8.0); bring volume to 1 L with deionized glass distilled water (autoclave).
9. 1 M TrisHCl (pH 7.8): 121.11 g TrisHCl; bring volume to 1 L with deionized glass distilled water.
10. 3 M Na-acetate (adjust to pH 7.4 with acetic acid): 408.1 g Na-acetate; bring volume to 1 L with deionized glass distilled water (autoclave).
11. Tris EDTA (TE) (10 mM TrisHCl, 1 mM EDTA): 1.211 g TrisHCl (MW: 121.11), 0.3722 g EDTA (MW: 372.24); bring volume to 1 L with deionized glass distilled water, pH 8.0 (autoclave).
12. Lysis buffer (10 mM TrisHCl, 10 mM EDTA, 150 mM NaCl, 0.5% sodium dodecyl sulfate [SDS], pH 8.0): 0.12111 g TrisHCl, 0.37224 g EDTA, 0.8766 g NaCl, 5 m1 of 10% SDS (pH 7.2), 1 ml proteinase K (from 10 mg/ml); bring volume to 100 ml with deionized glass distilled water.
13. Proteinase K store buffer (10 mM TrisHCl, 5 mM EDTA, 0.5% SDS, pH 8.0): 0.5 ml 1 M TrisHCl (pH 7.8), 0.5 ml 0.5 M EDTA (pH 8.0), 2.5 ml 10% SDS (pH 7.2); bring volume to 46.5 ml with deionized glass distilled water.
14. RNase A store buffer (10 mM TrisHCl pH 7.5, 15 mM NaCl): 0.12111 g TrisHCl (MW: 121.11), 0.08766 g NaCl (formula weight [FW] 58.44); bring volume to 100 ml with deionized glass distilled water (adjust pH to 7.5 with 1 mM HCl).

Preparation before using:

a. 10 mg/ml RNase A in RNase A store buffer.
b. Heat to 100°C for 15 min.
c. Cool slowly. Store at −20°C.

15. PBS for washing cell lines: 8.0 g NaCl, 0.2 g KCl, 3.0 g TrisHCl, 0.015 g phenol red; bring volume to 1 L with deionized glass distilled water (adjust pH to 7.4 with HCl, and autoclave).
16. Tris-buffered saline (TBS) (25 mM TrisHCl) for washing cell lines: 8.0 g NaCl, 0.2 g KCl, 1.44 g Na_2HPO_4, 0.24 g KH_2PO_4; bring volume to 1 L with deionized glass distilled water (adjust pH to 7.4 with HCl, and autoclave).
17. 2N NaOH (autoclave).
18. 8 mM NaOH: 0.4 ml 2 M NaOH, 99.6 ml deionized glass distilled water.
19. 1 M HEPES Buffer (free acid).

Part One: Lysis of Tissues

For Formalin-Fixed and Paraffin-Embedded Samples

1. Prepare six consecutive 5-micrometer sections from the cancer tissues.
2. Take 3 sections of them in 2 tubes, respectively.
3. Add 1 ml xylene in 2 tubes, respectively (mixed by sterilized glass stick).
4. Centrifuge at 12,000 rpm for 3 min at room temperature.
5. Descant supernatant (repeat **Steps 3–5**).
6. Add 1 ml 100% ethanol (mixed).
7. Centrifuge at 12,000 rpm for 3 min at room temperature.
8. Descant suspension (repeat **Steps 6–8**).
9. Dry precipitation in vacuum for 5–10 min or in air for 30–60 min.
10. Add 300 µl of lysis buffer (contained 50–100 µg/ml proteinase K) for 1 sample: 297 µl lysis buffer, 3 µl of 10 mg/ml proteinase K.
11. Oscillate 24–36 hr at 37°C, add 50 µl of 1 mg/ml proteinase K (diluted with TE buffer, pH 8.0) per 12 hr (total 3×).

*Dispensation of 1 sample: 5 µl of 10 mg/ml proteinase K and 45 µl TE.

For Fresh Tissues

1. Drop freshly excised tissue into liquid nitrogen.
2. Blend at top speed until the tissue is ground to a powder.

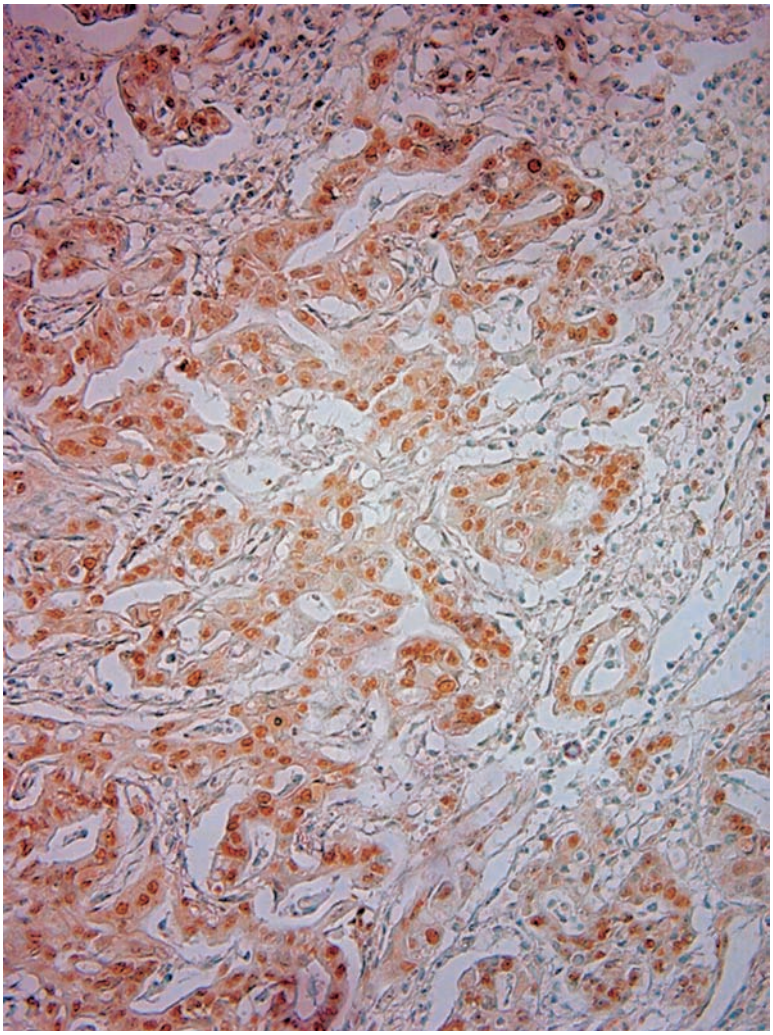

Figure 47. Immunostaining of K-*ras* p21 with anti-K-*ras* p21 mouse monoclonal immunoglobulin G (Ab-1, Oncogene Science, Inc., Uniondale, NY) in primary invasive ductal carcinoma of the pancreas (original magnification 200X).

3. Add a small amount of the powdered tissue to 10 volumes of lysis buffer.

4. Incubate at 65°C for 15 min and then incubate at 37°C with slight shaking until all of the tissue is in solution (approximately 1–24 hr).

For Cell Growing in Monolayers

1. Cells were washed twice with ice-cold PBS or TBS.

2. Scrape the cells into approximately 0.5 ml of TBS or PBS.

3. Transfer the cell suspension to a centrifuge tube stored on ice. Add 1 ml of TBS or PBS and recover the cells by centrifugation at 1500 g (5000 rpm) for 10 min at 4°C.

4. Resuspend the cells in 5–10 volumes of ice-cold TBS or PBS and repeat the centrifugation at the same conditions mentioned previously.

5. Resuspend the cells in TE, pH 8.0, at a concentration of 5×10^7/ml.

6. Add 10 volumes of lysis buffer.

7. Incubate at 65°C for 15 min and then incubate at 37°C with slight shaking overnight.

For Cells Growing in Suspension

1. Recover the cells by centrifugation at 1500 g (5000 rpm) for 10 min at 4°C.

2. Resuspend the cells in a volume of ice-cold TBS or PBS equal to the volume of original culture.

3. Recover the cells by recentrifugation, and repeat the washing procedure.

4. Resuspend the cells in TE, pH 8.0, at a concentration of 5×10^7/ml.

5. Add 10 volumes of lysis buffer.

6. Incubate at 65°C for 15 min and then incubate at 37°C with slight shaking overnight.

Part Two: Extraction of Genomic DNA by Phenol/Chloroform

1. Add equal volumes (450 µl) phenol, chloroform, and isoamyl alcohol in proportion of 25:24:1, and mix at 20–40 rpm by Rotator for 40–60 min at room temperature.
2. Centrifuge at 12,000 g (13,500 rpm) at 4°C for 5 min.
3. Transfer supernatant (above 400–450 µl) to a fresh tube (repeat **Steps 1–2** for 3–5× until no impurity is seen between the aqueous and organic phases).
4. Add equal volumes (400–450 µl) of chloroform and isoamyl alcohol in proportion of 24:1 at 20–40 rpm by a Rotator at room temperature for 40–60 min.
5. Centrifuge at 12,000 g (13,500 rpm) at 4°C for 5 min.
6. Transfer supernatant (above 400–450 µl) to a new tube (repeat **Steps 4–6**, 2×).
7. Add 1/10 previous volume (above 450 µl) of 3 M Na-acetate, pH 7.4, and 2.5 previous volumes of –20°C ethanol, mixed.
8. Store at –80°C for 30 min or at –20°C for at least 12 hr to precipitate DNA.
9. Centrifuge at 12,000 g (13,500 rpm) at 4°C for 10 min.
10. Descant supernatant and add 1.5 ml of 75% ethanol.
11. Centrifuge at 12,000 g (13,500 rpm) 4°C for 10 min.
12. Descant supernatant and dry precipitation in vacuum for 5–10 min or in air for 30–60 min.
13. Dissolve DNA in 449.1 µl of TE, pH 8.0, or incubate at 37°C with slight shaking overnight, if dissolution is different.

Part Three: Free of RNA with RNase A

1. Add 0.9 µl of 10 mg/ml RNase A in 449.1 µl of previous volume (finally working concentration of RNase A is 20 µg/ml).
2. Store at 37°C for 30–60 min quietly.
3. Repeat Part Two **Steps 1–13**.
4. Add 50 µl TE, pH 8.0 (1 µl TE can dissolute DNA of 1–5 × 10^6 cells) and store at –20°C.

Part Four: Dot Blot Oligonucleotide Hybridization

Reagents

1. Denaturating solution (0.4 M NaOH, 25 mM EDTA, pH 9.3): l00 ml 1 M NaOH, 2.3265 g EDTA; bring volume to 250 ml with deionized glass distilled water.
2. Neutralizing solution (1.5 M NaCl, 0.5 M TrisHCl, 1 mM EDTA, pH 7.2): 87.66 g NaCl, 60.55 g TrisHCl, 2 ml EDTA (from 0.5 M EDTA); bring volume to 1 L with deionized glass distilled water (adjust to pH 7.2 with HCl).
3. 2 M TrisHCl, pH 7.4: 242.2 g TrisHCl: bring volume to 1 L with deionized glass distilled water (adjust to pH 7.4 with HCl).
4. TE, pH 8.0: 0.3028 g TrisHCl (MW: 121.1), 0.0931 g EDTA (MW: 372.24); bring volume to 250 ml with deionized glass distilled water (adjust to pH 8.0 with HCl).
5. 20× saline-sodium citrate (SSC): 88.2 g trisodium citrate dihydrate, 175.3 g NaCl; bring volume to 1 L with deionized glass distilled water (adjust to pH 7.0 with NaOH).
6. 5 × SSC, 0.1% SDS.
7. 1 × SSC, 0.1% SDS.
8. Buffer 1 (0.15 M NaCl, 0.1 M TrisHCl): 8.77 g NaCl, 12.l g TrisHCl; bring volume to 1 L with deionized glass distilled water (adjust to pH 7.5 with HCl).
9. Buffer 2 (0.4 M NaCl, 0.1 M TrisHCl): 23.4 g NaCl, 12.l g TrisHCl; bring volume to 1 L with deionized glass distilled water (adjust to pH 7.5 with HCl).
10. Proportion of hybridization buffer (HB) is shown in Table 21.
11. Proportion of 0.5% blocking solution (BS) in Buffer 1.
12. 0.5% bovine serum albumin (BSA) solution in Buffer 2.
13. 0.18% Na_2SO_3: 1.8 g Na_2SO_3; bring volume to 1 L with deionized glass distilled water.
14. 0.5% SDS (pH 7.2).

Table 21. Proportion of hybridization buffer in various working volumes

	100 ml	80 ml	60 ml	40 ml	20 ml
5 × SSC	25 ml	20 ml	15 ml	10 ml	5 ml
0.1% HB	0.1 g	0.08 g	0.06 g	0.04 g	0.02 g
0.02% SDS	200 µl	160 µl	l20 µl	80 µl	40 µl
0.5% Blocking liquid	5 ml	4 ml	3 ml	2 ml	1 ml
ddH2O	69.8 ml	55.84 ml	41.8 ml	27.92 ml	13.96 ml

15. Oligonucleotide Probes (TaKaRa Corp., Kyoto, Japan): CGT (Arginine), GAT (aspartic acid), AGT (serine), GCT (alanine), GTT (valine), TGT (cysteine), and GGT (glycine).

16. ECL 3′-oligolabeling and detection system protocols (Amersham International, Plc., Buckinghamshire, U.K.).

Protocol according to the manufacturer's instructions of ECL 3′-oligolabeling and detection system kit

Oligonucleotide Labeling

1. Place the required tubes from the labeling components, excluding the enzyme, on ice to thaw.

2. To a 1.5-ml conical polypropylene tube, on ice, add the labeling reaction components in the following order:

Oligonucleotide (100×10^{-12} moles) *X* µl (generally 100 µl, 6.6 ng/µl, when probe length = 20 mer, 1 pmol = 6.6 ng)

Fluorescein-11-dUTP	10 µl
Cacodylate buffer	16 µl
Water (supplied)	*Y* µl
Terminal transferase	16 µl
Total	160 µl (final concentration 4.125 ng/µl or 0.625 pmol/µl)

The volumes corresponding to *X* and *Y* should be adjusted so that the total reaction volume is 160 µl.

*It is recommended that the oligonucleotide is dissolved (or diluted) in sterile distilled water; the water supplied with the labeling system can be used. The weight corresponding to 100×10^{-12} moles of an oligonucleotide is dependent on the length of the sequence is shown in Table 22.

3. Mix gently by pipetting up and down in the pipette tip.

4. Incubate the reaction mixture at 37°C for 60–90 min.

5. If desired, the reaction can be checked using the rapid labeling assay.

6. Store labeling probe on ice for immediate use or place at –15°C to –30°C for long-term storage. Do not store in a frost free freezer.

Table 22. Number of base and corresponding amount

Number of Base	Amount (ng)
15	500
20	660
30	1000
50	1660

Reactions ranging from $25–250 \times 10^{-2}$ moles have been undertaken.

Preparation of Membrane

1. Make marker on membrane of hybridization according to probes and then prewet an Amersham Hybond-N nylon membrane with 20 × SSC solution.

2. Load 20 µl DNA sample of the polymerase chain reaction (PCR) mixture to 100 µl of denaturation solution for DNA denaturation and then heat the DNA at 95°C for 2 min.

3. Place the reaction mixture on ice and add 100 µl for 2 M TrisHCl, pH 7.4.

4. Place the membrane of hybridization on Dot Blot well, Electrophoresis AE-6190 (ATTO Corporation, Tokyo, Japan).

5. Blot DNA samples of PCR products, respectively.

6. Wash wells with 100 µl TE, pH 8.0, respectively.

7. Take water and air bubble out with Genopirator Pump AE-6680p (TAAO Corporation, Japan).

8. Fix DNA on the membrane of hybridization by Ultra-violet radiation bioinstrument, DNA-FIX DF-20M (ATTO Corporation) at 0.160 J or 160 mJ/cm^2 2×.

Hybridization

1. Place blots into the HB and prehybridize at the required temperature (56°C), for a minimum of 30 min, in a shaking water bath.

2. Add the labeled oligonucleotide probes to the HB used for the prehybridization step at a final concentration of 5–10 ng/ml (or 0.76–1.52 picomolar) and hybridize at the required temperature (56°C) for 60–90 min in a shaking water bath.

3. Remove the blots from the HB, and place in a clear container. Cover with an excess of 5 × SSC, 0.1% SDS, and incubate at room temperature for 5 min with constant agitation. (This step is done 2×).

4. Discard the wash solution. Place blots in a clear container and cover with an excess of appropriate prewarmed stringency wash buffer. For many systems a suitable wash buffer would contain 1 × SSC, 0.1% SDS, and incubate at the desired temperature of 60°C (55–65°C) (typically 42–50°C) for 15 min in a shaking water bath. (This step is done 2×).

5. Place the filters in a clear container and rinse with 2 ml of Buffer 1 for each cm^2 of membrane for 1 min.

6. Discard Buffer 1 and replace with BS. Incubate for at least 30 min.

*The amount of diluted liquid block solution prepared should be equivalent to 0.25 ml/cm^2 of membrane.

7. Rinse blots briefly in 2 ml of Buffer 1 for each square centimeter of membrane for 1 min.

8. Dilute the anti-fluorescein HRP conjugate 1000-fold in Buffer 2 containing 0.5% (w/v) BSA, and incubate the blots in the diluted antibody conjugate solution for 30 min.

*The amount of diluted antibody conjugate solution prepared should be equivalent to 0.25 ml/cm^2 of membrane.

9. Place filters in a clean container and rinse with 2 ml of Buffer 2 for each cm^2 of membrane for 5 min 4×.

10. Mix equal volumes of detection solution 1 and detection solution 2 (add solution 2 to solution 1 in order by gentle shaking) to give sufficient reagent to cover the blot (0.125 ml/cm^2 is recommended) for signal generation and detection.

11. Drain the excess buffer from washed blots and place them on a sheet of Cling film DNA side up. Add the detection buffer directly to the blots on the side carrying the DNA and incubate for precisely 1 min at room temperature. Do not allow the membrane to dry out.

12. Drain off excess detection buffer and wrap blots in cling film. Gently smooth out air pockets.

13. Place the blots DNA side up in the film cassette. Work as quickly as possible; minimize the delay between incubating the blots in substrate and exposing them to film.

14. Switch off the lights and place a sheet of autoradiography film (Hyperfilm-ECL is recommended) on top of the blots. Close the cassette.

15. Expose the film for the required length of time and develop as recommended for the film type.

*In general, exposure times will vary from 1–10 min for high-target applications and 10–60 min for lower target applications.

16. Develop the exposed film for 4 min and fix for 4 min.

Washing DNA Membrane for Using Again

1. Sink membrane in 0.18% Na_2SO_3 for 5 min.

2. Sink membrane in 0.5% SDS (pH 7.2) at 65°C for 1 hr.

Single-Strand Conformation Polymorphism (PCR-SSCP)

Reagents

1. 0.5 M $EDTA_2Na$: 18.16 g $EDTA_2Na$ (MW: 372.24), about 2.0 g NaOH; bring volume to 100 ml with deionized glass distilled water, pH 8.0.

2. Loading buffer: 95% formamide, 0.05% bromophenol blue, 0.05% xylene cyanol FF, 20 mM EDTA.

3. 5X TBE: 54.45 g TrisHCl (final concentration 45 mmol/L), 27.823 g boric acid (final concentration 45 mmol/L), 3.722 g $EDTA_2Na$ (final concentration 1 mmol/L); bring volume to 1 L with deionized glass distilled water (autoclave).

4. 30% Poly-acrylamide (acrylamide:bisacrylamide = 37.5:1 or 29:1) (w/w) 100 ml (heat up to 37°C).

5. Glycerol (molecular biological grade).

6. Polyacrylamide gel for 25 ml (see Table 23).

10% ammonium persulfate: 100 mg ammonium persulfate plus 1 ml ddH_2O, adjust up to pH 8.0. Polytime is about 40–60 min.

7. Fixing or stopping buffer: 10% acetic acid.

8. Staining buffer: 1 g silver nitrate, 1.5 ml formaldehyde (from 37%); bring volume to 1 L with deionized glass distilled water.

9. Developing buffer: 30.0 g Na_2CO_3, 2 mg $Na_2S_2O_35H_2O$, 1.5 ml formaldehyde (from 37%); bring volume to 1 L with deionized glass distilled water.

10. 50X TAE-buffer: 242 g TrisHCl, 57.1 ml acetic acid (CH_3COOH), 18.612 g EDTA (MW: 372.24) (pH 8.0 by acetic acid); bring volume to 1 L with deionized glass distilled water. Working concentration: 1X final concentration equals 40 mM Tris-Ace, 1 mM EDTA, 1 mg EtBr/L-TAE).

Add 10–50 µl (10 mg/ml) of ethidium bromide into 1 L of 1 × TAE-buffer (working concentration is 0.5 µg/ml).

11. Dilution of 1 kb or 50 bp DNA ladder (1 µg/µl): 50 µl 1kb of DNA ladder (1 µg/µl), 100 µl 10× Blue Juice Gel Loading Buffer (GIBCOBRL), 2.5 µl 4 M NaCl, 347.5 µl TE, pH 8.0. The ladder was adjusted at final concentration: 0.1 µg/µl ladder; 20 mM NaCl.

Table 23. Polyacrylamide gel in various concentrations for 25 ml

Final concentration	6%	8%	10%	12%	14%
30% polyacrylamide	5 ml	6.65 ml	8.33 ml	10 ml	11.65 ml
ddH_2O	12.82 ml	11.l7 ml	9.49 ml	7.83 ml	6.18 ml
5 × TBE	5 ml	5 ml	5 ml	5 ml	5 ml
Glycerol	2 ml	2 ml	2 ml	2 ml	2 ml
TEMED	8.75 µl	8.75 µl	8.75 µl	8.75 µl	8.75 µl
10% Ammonium persulfate	175 µl	175 µl	175 µl	175 µl	175 µl

12. 10× Blue Juice Gel Loading Buffer (GIBCO-BRL, 2000): 65% sucrose, 10 mM TrisHCl (pH 7.5), 10 mM EDTA, 0.3% (w/v) Bromophenol Blue.

13. Usage (ladder:DNA sample):

Agarose gel at any concentration: 1:4 (5X).

Polyacrylamide gel: 1:9 (less than 1× avoiding the bands to "smile" slightly).

14. 5× SDS Sample Loading Buffer (Funakoshi): 0.25 M TrisHCl (pH 6.8), 10% SDS, 0.5 M dithiothreitol (DTT), 0.5% Bromophenol Blue, 50% Glycerol.

15. Store buffer for 1 kb or 50 bp of DNA ladder (1 μg/μl): 10 mM TrisHCl (pH 7.5), 50 mM NaCl, 0.1 mM EDTA.

Protocol

1. 3 μl (0.5–1 μg) of genomic DNA was subjected to PCR-SSCP in total volume of 50 μl of PCR reaction buffer.

2. Run PCR under the following conditions: Denaturation at 94°C for 1 min, annealing at 55°C for 45 sec, and extension at 72°C for 2 min (a total of 35 cycles). After the last cycle, the extension was continued for an additional 7 min at 72°C.

3. Add 2–4 μl of PCR product into 20–40 μl of loading buffer, heat at 95°C for 5 min, and chill on ice for 5 min.

4. 3 μl of previous sample was electrophoresced on 8% polyacrylamide gel at 200 V and 40 mA for 2–3 hr at 4°C.

5. Staining the gel:

Rinse the gel in 10% acetic acid shakily for 20 min, and then wash the gel with H_2O for 2 min 3×.

Stain the gel in 0.1% silver nitrate for 30 min, and then wash the gel in H_2O for 20 sec.

Incubate the gel in developing buffer for 2–5 min.

Transfer the gel in 10% acetic acid for 5 min to stop development.

6. Dry the gel:

Rinse the gel in ddH_2O for 30 min shakily (change ddH_2O per 10 min).

Rinse the gel in 50% ethanol or dry-solution shakily for desired time (4–20 min).

Dry the gel at room temperature for 1–2 days.

7. Photography.

The results of this method are shown in Figure 48.

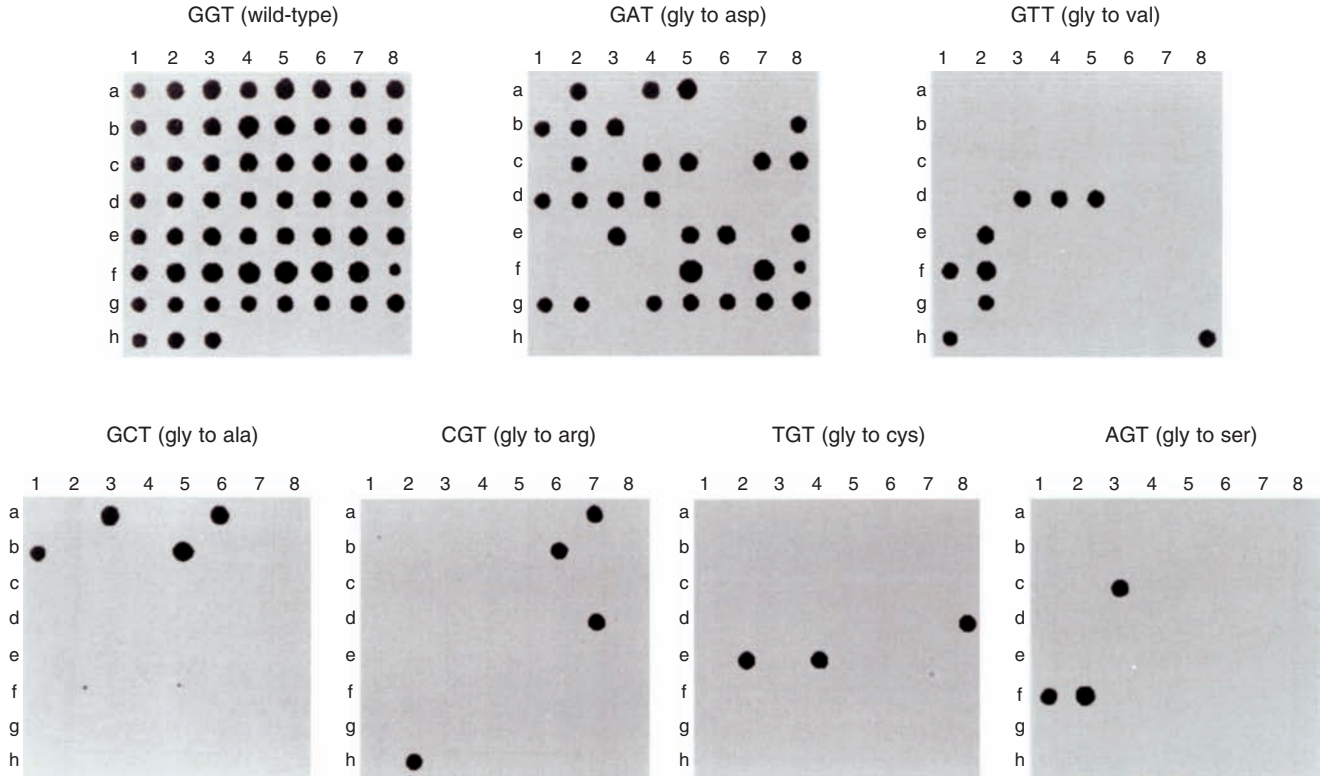

Figure 48. The results of Dot Blot hybridization. A total of seven blots, each containing the same polymerase chain reaction product at the same position, have been hybridized using wild or mutant oligonucleotide probes. h8 is a positive control for GTT. (Dong *et al.,* 2000)

DNA Auto Sequencing by ABI 310 Systems

Reagents

1. Low Gelling Agarose (Sigma Chemical Co., St. Louis, MO).
2. MicroconTM-100-Colums (TaKaRa, Tokyo, Japan).
3. QIAquick Gel Extraction Kit (QIAGEN, Valencia, CA).
4. BigDye Terminator Cycle Sequencing FS Ready Reaction Kit (PE Applied Biosystems, Perkin-Elmer Japan Co., Ltd, Osaka, Japan).
5. Template Suppression Reagent (TSR).
6. 5× SDS Sample Loading Buffer (Funakoshi): 0.25 M TrisHCl, pH 6.8, 10% SDS, 0.5 M DTT, 0.5% Bromophenol Blue, 50% Glycerol.
7. Store buffer for 1 kb or 50 bp of DNA ladder (1 µg/µl): 10 mM TrisHCl (pH 7.5), 50 mM NaCl, 0.1 mM EDTA.

Protocol According to the Manufacturer's Instructions of ABI 310 Systems

1. PCR mixture and running conditions are similar with PCR-SSCP.
2. The PCR product was electrophoresed in 1% agarose gel at 50 V for 40 min for confirming products.
3. Concentrate and purify PCR product using Micropure-EZ-Columns and MicroconTM-100-Columns (Millipore Corporation, Bedford, MA).

Using Micropure-EZ with Microcon: Place Micropure-EZ reservoir into a MicroconTM-100-Columns and then into a vial. Add sample (up to 250 µl) into the Micropure-EZ reservoir. Cap assembly and centrifuge 3–15 min. Remove Micropure-EZ and discard. If buffer exchange is required, add wash buffer to Microcon sample reservoir and spin again. If only sample concentration is desired, proceed to **Step 4.** Invert Microcon into a new filtrate vial; spin briefly to recover sample. If the Microcon membrane appears dry, add 10–20 µl of an appropriate buffer to sample reservoir and vortex briefly.

Using Microcon independently: Add 500 µl of ddH_2O or 0.1 N NaOH into sample reservoir and spin at 12 Kg (14,000 rpm) for 2 min to remove glycerin in microcon ultrafiltration membrane. Pipette PCR product into sample reservoir (0.5 ml maximum volume), load 400–450 µl of ddH_2O onto the column, seal with attached cap, and spin at 3000 g (7000 rpm) in a fixed-angle centrifuge for 10–12 min. Remove the waste receptacle and attach the collection vial. Add 14 µl of ddH_2O into sample reservoir, invert the column, and then spin at 270 g (3000 rpm) for 2 min for recovery of samples. This should yield approximately 10 µl of sample. Add desired volume of ddH_2O or TE to bring the purified PCR fragments to the original volume.

Using Micropure-EZ independently: Place Micropure-EZ into vial; pipette the sample (up to 250 µl) into the Micropure-EZ reservoir. Close cap. Place device in a microcentrifuge and spin at full speed (12,000–14,000 g) for 60 sec. Spin time will depend on the sample volume. For example, a 50-µl sample will pass in less than 30 sec when spun at 14,000 g. Filtrate contains purified DNA. To maximize DNA recovery, add 5–10 µl of TE buffer or water to the Micropure-EZ reservoir and then spin for 30 sec. The Micropure-EZ reservoir may now be discarded. Cap vial to store sample.

4. Extension for auto sequencing: 8 µl Terminator Ready Reaction Mix, 2 µl (1.6 pmol/µl) primer (forward or reverse), 2 µl (5 ng of purified K-*ras* PCR product), deionized water quantum sufficit (up to total volume 20 µl), 40 µl light mineral oil.

Note: The amount of PCR product to use in sequencing will depend on the length and purity of the PCR product of the target gene.

Control sample: 0.5 µl (from 200 ng/µl) pGEM 3Zf(+) (dsDNA), 4 µl (from 0.8 pmol/µl) M13 (–21) (forward), 7.5 µl (up to total volume 20 µl) deionized water, 8 µl Terminator Ready Reaction Mix, 40 µl light mineral oil.

5. When cycle sequencing on DNA Thermal Cycle 480, the conditions of extension PCR: denaturation at 96°C for 30 sec, annealing at 50°C for l5 sec, extension at 60°C for 4 min (total of 25 cycles and soak at 4°C until ready to purify. If G+C is more than 70%, heat the sample at 98°C for 5 min to denature).

6. Spin the PCR product, and then purify extended PCR products with the ethanol method: Pipette entire contents of each extension reaction into a 1.5-ml microcentrifuge tube. Add l6 µl of ddH_2O and 64 µl of 95% ethanol. Close the tubes and vortex briefly. Leave the tubes at room temperature for 15 min to precipitate the extension products. Place the tubes in a microcentrifuge and mark their orientations. Spin the tubes for 20 min at maximum speed at room temperature and then proceed to the next step immediately. Carefully aspirate the supernatants with a separate pipette tip for each sample and discard. Pellets may or may not be visible. Add 250 µl of 70% ethanol to the tubes and vortex them briefly. Place the tubes in the microcentrifuge in the same orientation as in **Step 5** and spin for 10 min at maximum speed at room temperature. Aspirate the supernatants carefully as in **Step 6.** Dry the samples in a vacuum centrifuge for 10–15 min or to dryness. (Alternatively, place the tubes with the lids open in a heat block or thermal cycler at 90°C for 1 min.)

7. Denaturing and loading the sample in 20 µl of TSR, vortex thoroughly, and spin the samples. At room

temperature, samples in TSR are stable for a maximum of 48 hr, and samples in TSR can be frozen for several weeks.

8. Heat the samples at 95°C for 2 min to denature, then chill on ice.

9. Vortex thoroughly and spin the samples again. Place on ice or keep frozen until ready to load on the instrument.

10. Transfer the samples to 0.5-ml sample tubes and cover with a tube septum.

11. Load the samples for auto sequencing on ABI Prism 310 Genetic Analyzer (Foster, CA).

Sequencing on ABI Prism 310 Genetic Analyzer

1. Preparing the Sample Sheet

In the ABI Prism 310 Data Collection Software, select New from the file menu. Click Sequence Smpl Sheet 48 or 96 Tube (match the type of tray used in the autosampler). The Sample Sheet window appears. The number in the first column corresponds to the location of the sample in the autosampler tray. Put Sample Names in the second column. Select Dye Set/Primer and Matrix files through the pop-up menus.

Note: The first time you run sequencing reactions under new conditions, any matrix file can be used for the run. After the run, you must make a matrix file for the new conditions. Enter any additional comments that you want to link to the samples. Open the file pull-down menu, and select Save As. Name the Sample Sheet, and press Return to save it in the Sample Sheet folder.

2. Fill out an Injection List to start a run.

In the ABI Prism 310 Data Collection Software, select New from the file menu. The same boxes of icons are displayed. Select Sequence Injection List. Click the arrow in the Sample Sheet field to display a pop-up menu of Sample Sheets stored in the Sample Sheet folder; select a Sample Sheet. The Injection List is automatically filled in with information from the selected Sample Sheet. Select a module from the Module pop-up menu.

3. Running and Monitoring Sample

During the run, four ways can be used for monitoring the run. From the window menu, select one of the following: status, log, raw data, and electrophoresis history. Running time is up to the length of PCR products (about 2.5 hr/sample).

Control conditions on ABI PrismTM 310 Genetic Analyzer:

Volt: 12.2 kv
A: 3.0 µA
Gel temperature: 50°C (10–70°C)
Laser power MW: 9.8

The results of this method are shown in Figure 49.

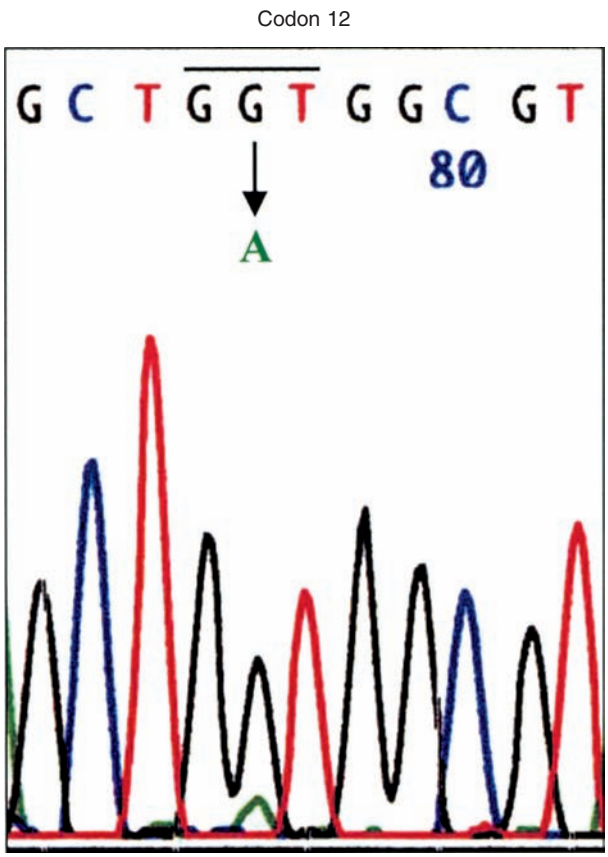

Figure 49. Partial sequence of K-*ras* gene shows a G to A transition at the second nucleotide of codon 12 in exon 1 with a GGT (glycine) to GAT (aspartic acid) substitution.

RESULTS AND DISCUSSION

IHC is commonly used to assess overexpression of K-*ras* protein. The nuclear staining of tumor cells was considered as positive, and, furthermore, it may be scored according to the intensity, distribution, and pattern. SSCP analysis is wildly used for screening K-*ras* gene mutation. However, the length of the PCR products could limit the sensitivity of SSCP, especially if they are longer than 300 base pairs (Suzuki *et al.,* 1991). In addition, SSCP cannot localize substitutions of K-*ras* gene mutations. Genomic DNA could be analyzed for the presence of K-*ras* mutations by Dot Blot hybridization with allele-specific oligonucleotide probes. Dot Blot hybridization is usually used to detect large samples. The intensity of exposure is dependant on conditions of experiment and the numbers of mutated DNA copies. Direct DNA sequencing is used to confirm K-*ras* gene mutation. However, the sequencing data may contain heterogeneous components, probably because the genomic DNA contained normal stroma and the PCR products were not cloned before the sequencing.

Another cause may be that not all of the tumor cells harbored K-*ras* gene mutation.

K-*ras* mutation has been involved in pancreatic carcinogenesis, but the effect of K-*ras* mutation on clinicopathologic parameters, such as age, sex, TNM stage, histologic grade, site of tumor, and prognosis of the patients with pancreatic cancer, remains controversial. Most studies indicate no relationships between K-*ras* mutations and the parameters noted earlier. However, one study indicated that K-*ras* mutation was significantly associated with TNM tumor stage and a poor prognosis in pancreatic cancer in Spain (Castells *et al.,* 1999). Another study indicated that a double mutation compared to a single mutation of the K-*ras* gene was significantly related to a poor prognosis in pancreatic cancer in Japan (Song *et al.,* 1996). A previous report suggested that the TGT and AGT mutation of the codon 12 K-*ras* gene might mean a low potential for malignant transformation in pancreatic cancer (Tada *et al.,* 1996). However, the same results were not found in another study (Dong *et al.,* 2000). These controversial conclusions indicated that K-*ras* mutations alone have been involved in pancreatic carcinogenesis and might have a weak influence on the biological behaviors of pancreatic cancer. To date, more than 1000 mutations of genes have been identified in human tumors (Frebourg and Friend, 1993), but only a few of them have been studied and confirmed in pancreatic cancer. This might be one of the reasons for the controversial results noted earlier. In addition, these controversial conclusions from different countries might be the result of the differences of K-*ras* gene components in various populations with pancreatic cancer (Dong *et al.,* 2000).

Pancreatic tumors are heterogeneous in genetics, and independent pathways and simultaneous tumorigenesis may exist within the same organ. Because some mutations exist in benign and also in malignant conditions, it is an important challenge to define the molecular characteristics of significant versus nonsignificant lesions. Thus, analysis of heterogeneous types of gene expressions may provide a better insight into the biological role of gene interaction with pancreatic carcinogenesis. Previous studies indicated that pancreatic carcinogenesis was associated with multiple cancer-related genes, including K-*ras, p53, p16,* and *DPC4* genes. Mutations in more than two of them were present in up to 76% of cases of pancreatic cancer (Rozenblum *et al.,* 1997). Of them, *p53* gene controls the G1-S checkpoint and promotes the correct repair of DNA damage (Hickman 1992; Hickman *et al.,* 1992). The loss of its safeguard function induced by mutation may be a key factor in human carcinogenesis. Allelic deletions in p16 were found in 27–95% of human pancreatic cancer. Inactivation of *p16* could lead to unregulated cell growth (Gerdes *et al.,* 2002). The *DPC-4* gene is inactivated in about 50% of pancreatic cancer cases (Hahn *et al.,* 1996) and belongs to the group of *Smad* genes that mediate the signal transduction of the transforming growth factor-beta (TGF-β) family. Inactivation of Smad proteins can result in loss of the growth-inhibitory effects of TGF-β1, which plays a central role in the pathogenesis of pancreatic cancer. Thus, pancreatic cancer cell growth, despite TGF-β1 overexpression, may be supported by defects in DPC-4 or the TGF-β-receptor II. Furthermore, the loss of Smad4/DPC4 expression along with the inhibition of Smad2/3 expression through the ras protein can lead to the resistance of epithelial cells against the growth-inhibitory and antiproliferative function of TGF-β1 (Calonge and Massague, 1999). It is especially worth noting that DNA miroarrays allow the measurement of expression levels for thousands of genes, perhaps all genes of a cell or an organism, with a number of different experimental conditions. The dynamic patterns of genes expressed under different conditions may reveal possible states and trajectories of carcinogenesis. However, the data with high-level noise from microarray are currently important issues.

Pancreatic cancer is a major contributor to cancer-related death in developed countries. Activity of K-*ras* protooncogene, as the early molecular events, plays a crucial role in pancreatic carcinogenesis. The methods noted earlier allow both detection of extremely small amounts of mutated K-*ras* gene and screening strategies, thereby increasing the number of patients with pancreatic cancer able to undergo curative surgical procedure.

References

Adari, H., Lowy, D., Willumsen, B.M., Der, C.J., and McCormick, F. 1988. Guanosine triphosphatase activating protein (GAP) interacts with the p21 ras effector binding domain. *Science 240*:518–521.

Almoguera, C., Shibata, D., Forrester, K., Martin, J., Arnheim, N., Perucho, M. 1988. Most human carcinomas of the exocrine pancreas contain mutant c-Ki-ras genes. *Cell 53*:549–554.

Barbacid, M. 1987. ras genes. *Annu. Rev. Biochem. 56*:779–827.

Caldas, C., and Kern, S.E. 1995. K-ras mutation and pancreatic carcinoma. *Int. J. Pancreatol. 18*:1–6.

Calés, C., Hancock, J.F., Marshall, C.J., and Hall, A. 1988. The cytoplasmic protein GAP is implicated as the target for regulation by the ras gene product. *Nature 332*:548–551.

Calonge, M.J., and Massague, J. 1999. Smad4/DPC4 silencing and hyperactive Ras jointly disrupt transforming growth factor-beta antiproliferative responses in colon cancer cells. *Biol. Chem. 274*:J33637–33643.

Castells, A., Puig, P., Mora, J., Boadas, J., Boix, L., Urgell, E., Sole, M., Capella, G., Lluis, F., Fernandez-Cruz, L., Navarro, S., and Farre, A. 1999. K-ras mutations in DNA extracted from the plasma of patients with pancreatic carcinoma: Diagnostic utility and prognostic significance. *J. Clin. Oncol. 17*:578–584.

Chang, E.H., Gonda, M.A., Ellis, R.W., Scolnick, E.M., and Lowy, D.R. 1982. Human genome contains four genes homologous to transforming genes of Harvey and Kirsten murine sarcoma viruses. *Proc. Natl. Acad. Sci. USA 79*:4848–4852.

Dong, M., Nio, Y., Tamura, K., Song, M., Guo, K., Guo, R., and Dong, Y. 2000. Ki-ras point mutation and p53 expression in human pancreatic cancer: A comparative study among Chinese, Japanese, and Western patients. *Cancer Epidemiol. Biomark. Prev. 9*:279–284.

Doolittle, B.R., Emanuel, J., Tuttle, C., and Costa, J. 2001. Detection of the mutated K-Ras biomarker in colorectal carcinoma. *Exp. Mol. Pathol. 70*:289–301.

Frebourg, T., and Friend, S.H. 1993. The importance of p53 gene alterations in human cancer: Is there more than circumstantial evidence? *J. Natl. Cancer Inst. 85*:1554–1557.

Gerdes, B., Ramaswamy, A., Ziegler, A., Lang, S.A., Kersting, M., Baumann, R., Wild, A., Moll, R., Rothmund, M., and Bartsch, D.K. 2002. p16INK4a is a prognostic marker in resected ductal pancreatic cancer: An analysis of pl6INK4a, p53, MDM2, an Rb. *Ann. Surg. 235*:51–59.

Hahn, S.A., Schutte, M., Hoque, A.T., Moskaluk, C.A., da Costa, LT, Rozenblum, E., Weinstein, C.L., Fischer, A., Yeo, C.L., Hruban, R.H., and Kern, S.E. 1996. DPC4, a candidate tumour suppressor gene at human chromosome 18q21.1. *Science 271*:350–353.

Harada, M., Dosaka-Akita, H., Miyamoto, H., Kuzumaki, N., and Kawakami, Y. 1992. Prognostic significance of the expression of ras oncogene product in non-small cell lung cancer. *Cancer 69*:72–77.

Hickman, J.A. 1992. Apoptosis induced by anticancer drugs. *Cancer Metastasis Rev. 11*:121–139.

Hickman, J.A., Beere, H.M., Wood, A.C., Waters, C.M., and Parmar, R. 1992. Mechanisms of cytotoxicity caused by antitumour drugs. *Toxicol. Lett.* 64-65 Spec No:553–561.

Junien, C., Huerre, C., Despoisse, S., Gilgenkrantz, S., and Lenoir, G.M. 1984. c-Ha-ras1 is not deleted in del(11p13) Wilms' tumor (WAGR) and maps to 11p15.1-11p15.5. (Abstract) *Cytogenet. Cell Genet. 37*:503.

Karelia, N.H., Patel, D.D., Desai, N.S., Mehta, H.V., Yadav, P.K., Patel, S.M., Kothari, K.C., and Shah, P.M. 2001. Prognostic significance of DNA aneuploidy and *p21 ras* oncoprotein expression in colorectal cancer and their role in determination of treatment modalities. *Int. J. Biol. markers. 16*:97–104.

Konishi, N., Hiasa, Y., Tsuzuki, T., Tao, M., Enomoto, T., and Miller, G.J. 1997. Comparison of ras activation in prostate carcinoma in Japanese and American men. *Prostate 30*:53–57.

McBride, O.W., Swan, D.C., Tronick, S.R., Gol, R., Klimanis, D., Moore, D.E., and Aaronson, S.A. 1983. Regional chromosomal localization of N-ras, K-ras-1, K-ras-2 and myb oncogenes in human cells. *Nucleic Acids Res. 11*:8221–8236.

McGrath, J.P., Capon, D.J., Smith, D.H., Chen, E.Y., Seeburg, P.H., Goeddel, D.V., and Levinson, A.D. 1983. Structure and organization of the human Ki-ras proto-oncogene and a related processed pseudogene. *Nature 304*:501–506.

Miao, T.J., Wang, Z., and Sang, N. 1991. Correlation between the expression of the P21 ras oncogene product and the biological behavior of bladder tumors. *Eur. Urol. 20*:307–310.

Mitchell, E.L.D., Jones, D., White, G.R.M., Varley, J.M., and Santibanez Koref, M.F. 1995. Determination of the gene order of the three loci CD2, NGFB, and NRAS at human chromosome band 1p13 and refinement of their localisation at the subband level by fluorescence in situ hybridization. *Cytogenet. Cell Genet. 70*:183–185.

Miyakis, S., Sourvinos, G, and Spandidos D.A. 1988. Differential expression and mutation of the ras family genes in human breast cancer. *Biochem. Biophys. Res. Commun. 20:251*: 609–612.

O'Connell, P., Leppert, M., Hoff, M., Kumlin, E., Thomas, W., Cai, G., Law, M., White, R. 1985. A linkage map for human chromosome 12. (Abstract) *Am. J. Hum. Genet. 37*:A169.

Pellegata, N.S., Sessa, F., Renault, B., Bonato, M., Leone, B.E., Solcia, E., and Ranzani, G.N. 1994. K-ras and p53 gene mutations in pancreatic cancer, ductal and nonductal tumors progress through different genetic lesion. *Cancer Res. 54*:1556–1560.

Popescu, N.C., Amsbaugh, S.C., DiPaolo, J.A., Tronick, S.R., Aaronson, S.A., and Swan, D.C. 1985. Chromosomal localization of three human ras genes by in situ molecular hybridization. *Somat. Cell Mol. Genet. 11*:149–155.

Rosell, R., Li, S., Skacel, Z., Mate, J.L., Maestre, J., Canela, M., Tolosa, E., Armengol, P., Barnadas, A., and Ariza, A. 1993. Prognostic impact of mutated K-ras gene in surgically resected non-small cell lung cancer patients. *Oncogene 8*:2407–2412.

Rosenberg, L. 2000. Pancreatic cancer: A review of emerging therapies. *Drug 59*:1071–1089.

Rozenblum, E., Schutte, M., Goggins, M., Hahn, S.A., Panzer, S., Zahurak, M., Goodman, S.N., Sohn, T.A., Hruban, R.H., Yeo, C.J., and Kern, S.E. 1997. Tumor-suppressive pathways in pancreatic carcinoma. *Cancer Res. 57*:1731–1734.

Rundle, A., Tang, D., Brandt-Rauf, P., Zhou, J., Kelly, A., Schnabel, F., and Perera, F.P. 2002. *Cancer Lett. 185*:71–78.

Song, M.M., Nio, Y., Dong, M., Tamura, K., Furuse, K., Tian, Y.L., He, S.G., and Shen, K. 2000. Comparison of K-ras point mutations at codon 12 and p21 expression in pancreatic cancer between Japanese and Chinese patients. *J. Surg. Oncol. 75*:176–185.

Song, M.M., Nio, Y., Sato, Y., Tamura, K., and Furuse, K. 1996. Clinicopathological significance of Ki-ras point mutation and p21 expression in benign and malignant exocrine tumors of human pancreas. *Int. J. Pancreatol. 20*:85–93.

Sugio, K., Gazdar, A.F., Albores-Saavedra, J., and Kokkinakis, D.M. 1996. High yields of K-ras mutations in intraductal papillary mucinous tumors and invasive adenocarcinomas induced by N-nitroso (2-hydroxypropyl) (2-oxopropyl) amine in the pancreas of female Syrian hamster. *Carcinogenesis (Lond). 17*:303–309.

Suzuki, Y., Sekiya, T., and Hayashi, K. 1991. Allele-specific polymerase chain reaction: A method for amplification and sequence determination of a single component among a mixture of sequence variants. *Anal. Biochem. 192*:82–84.

Tada, M., Ohashi, M., Shiratori, Y., Okudaira, T., Komatsu, Y., Kawabe, T., Yoshida, H., Machinami, R., Kishi, K., and Omata, M. 1996. Analysis of K-ras gene mutation in hyoerplastic duct dells of the pancreas without pancreatic disease. *Gastroenterol. 110*:227–231.

Trahey, M., and McCormick, F. 1987. A cytoplasmic protein stimulates normal N-ras p21 GTPase, but does not affect oncogenic mutants. *Science 238*:542–545.

Varras, M.N., Sourvinos, G., Diakomanolis, E., Koumantakis, E., Flouris, G.A., Lekka-Katsouli, J., Michalas, S., and Spandidos, D.A. 1999. Detection and clinical correlations of ras gene mutations in human ovarian tumors. *Oncology 56*:89–96.

Voice, J.K., Klemke, R.L., Le, A., and Jackson, J.H. 1999. Four human ras homologs differ in their abilities to activate Raf-1, induce transformation, and stimulate cell motility. *J. Biol. Chem. 274*:17164–17170.

Yarbrough, W.G., Shores, C., Witsell, D.L., Weissler, M.C., Fidler, M.E., and Gilmer, T.M. 1994. ras mutations and expression in head and neck squamous cell carcinomas. *Laryngoscope 104*:1337–1347.

5

Altered Expression of p27 Protein in Pancreatic Carcinoma

Norio Sawabu and Hiroyuki Watanabe

Introduction

In mammals, the cell division cycle is governed directly by cyclin-dependent kinases (CDKs). The CDKs are controlled by a variety of regulatory proteins, including cyclins, kinases, phosphatases, and CDK inhibitors. A CDK inhibitor, p27 negatively regulates cell cycle progression from G1 to S phase by binding to the cyclin D-CDK4 and E-CDK2 complexes and thus reduces cell proliferation (Polyak *et al.,* 1994; Toyoshima *et al.,* 1994). It is up-regulated by cytokins, including transforming growth factor-beta (TGF-β).

Although mutations of the *p27* gene have not been demonstrated in human carcinomas, unlike those of *p16* or *p53* gene, loss of p27 expression or down-regulation of p27 proteins induced by enhanced proteasomal degradation have been shown in many human carcinomas. The *p27* gene also may have other roles, including promotion of apoptosis, regulation of drug resistance in solid tumors, and mediation of cell differentiation.

Low p27 expression may be a poor prognostic factor for various carcinomas, including those of the colon, stomach, gall bladder, esophagus, breast, and prostate, although some subsequent studies have not confirmed its prognostic value. There have been, to our knowledge, only three reports on immunohistochemical analysis of p27 expression in human pancreatic carcinomas, including our study (Feakins *et al.,* 2003; Hu *et al.,* 2000; Lu *et al.,* 1999). In this chapter, we demonstrate procedures of immunohistochemical analysis of the p27 protein and discuss the relationship among p27 expression, pathologic features, and clinical outcome.

MATERIALS

1. Tris-buffered saline (TBS): 0.05 M/L Tris-HCl, 0.15 M/L NaCl (pH 7.6).
2. 1% Bovine serum albumin (BSA): 1 g BSA and 100 ml TBS buffer; add BSA to buffer by stirring.
3. Primary antibody: rabbit polyclonal antibody against p27 protein, C-19 (Santa Cruz Biotechnology, Santa Cruz, CA) diluted in TBS with 1% BSA.
4. Biotinylated secondary antibody: biotinylated swine anti-rabbit immunoglobulins (Dako Corp., Carpinteria, CA), diluted TBS with 1% BSA.
5. Horseradish peroxidase–labeled streptavidin (Dako Corp.) diluted in TBS.

Handbook of Immunohistochemistry and *in situ* Hybridization of Human Carcinomas, Volume 3: Molecular Genetics, Liver Carcinoma, and Pancreatic Carcinoma

METHODS

Immunohistochemical Staining Using Streptavidin-Biotin Complex Method

1. All surgical specimens were fixed in 10% formalin and embedded in paraffin.
2. The resulting blocks were cut at 5-µm-thick serial sections and mounted on glass slides.
3. For deparaffinization, sections were placed in xylene 3× for 10 min each.
4. The sections were placed in 99% ethanol 2× for 5 min each and then placed in distilled water.
5. The sections were incubated with 3% hydrogen peroxide solution for 5 min at room temperature, rinsed in distilled water, and placed in TBS for 5 min at room temperature.
6. The sections were incubated with blocking serum containing carrier protein (10% normal swine serum) and 15 mM sodium azide for 5 min at room temperature to block nonspecific binding; then the sections were tapped off.
7. The sections were incubated overnight at 4°C with rabbit polyclonal antibody against p27 protein, C-19 (Santa Cruz Biotechnology), diluted at 4% with TBS.
8. The sections were rinsed in TBS and treated with TBS 3× for 5 min each.
9. Immunohistochemical staining was done using the streptavidin-biotin complex method with a commercial kit, SLAB (Dako Corp.) as follows:
   a. Incubate the sections for 10 min in biotinylated swine anti-rabbit immunoglobulins (Dako Corp.,) diluted in TBS containing 1% BSA.
   b. Rinse as in **Step 8.**
   c. Incubate the sections for 10 min in horseradish peroxidase–labeled streptavidin (Dako Corp.) diluted at 1% withTBS.
   d. Rinse as in **Step 8.**
   e. Incubate the sections for 10 min in 0.1 M/L acetate buffer with 3% AEC (3-amino-9-ethyl carbazole) substrate chromogen (Dako Corp.) and 0.3% hydrogen peroxide.
   f. Rinse the sections in distilled water and place them in distilled water.
10. Counterstain the sections with hematoxylin solution for 1 min at room temperature, and wash them with running water for 5 min.
11. The sections were tapped off thoroughly and mounted using an aqueous medium.
12. For negative controls, the primary antibody was omitted.
13. Lymphocytes in each section served as positive internal controls.

RESULTS AND DISCUSSION

The staining pattern of p27 protein in tumor cells was divided into three types: 1) staining only in the cytoplasm, 2) Staining only in the nucleus, and 3) Staining in both the cytoplasm and the nucleus. However, immunoreactivity for the p27 protein only in the nucleus or in both cytoplasm and nucleus was considered to be positive. In each tumor, at least 20 high-power fields and a minimum of 1000 tumor cells were examined. The percentage extent of p27 expression was determined by dividing the number of stained tumor cells by the number of tumor cells in all fields and multiplying the result by 100. In our study, scores representing the percentage of tumor cells stained were as follows: strong staining, >50% of cellular nuclei; intermediate staining, 5–50% of cellular nuclei; and no staining, <5% of cellular nuclei. The majority of peritumoral and intratumoral lymphocytes showed strong immunocytochemical staining for p27, and thus staining for p27 in the lymphocytes is used for positive control. Pancreatic islet cells showed more extensive staining than ductal epithelium, whereas acinar cells showed less extensive staining.

Our study, in which most of the pancreatic specimens were obtained from Chinese patients, showed <5% p27 expression in 66% of pancreatic duct adenocarcinoma cases (Hu *et al.,* 2000), whereas another Japanese study showed <1% expression in 56% of adenocarcinoma cases (Lu *et al.,* 1999). In the study using tumors from European patients, there was <1% p27 expression in 15% of tumors and <5% expression in 41% of tumors (Feakins *et al.,* 2003). These data suggest that reduced expression of p27 is less prevalent in tumors from European patients than in those from Asian patients, although methodologic differences might be partly responsible for the discrepancy.

Expression of p27 may correlate with the stage and grade of various carcinomas. In pancreatic duct adenocarcinoma, p27 loss correlated with high stage in two Japanese studies but not in the European study. Reduced expression of p27 was more frequent in poorly or moderately differentiated than in well-differentiated tumor in two studies, as shown in Figure 50A and 50B, but not in the other study. The inconsistences suggest that association between p27 expression and pathologic features are weak. However, in the two Japanese studies, a high incidence of positive staining for p27 has been reported in pancreatic cytoadenocarcinoma or mucin-producing pancreatic carcinoma, which are well known as having low malignant characters. This result may partly explain why most of the pancreatic cytoadenocarcinoma or mucin-producing pancreatic carcinoma have a low malignant behavior and a good prognosis.

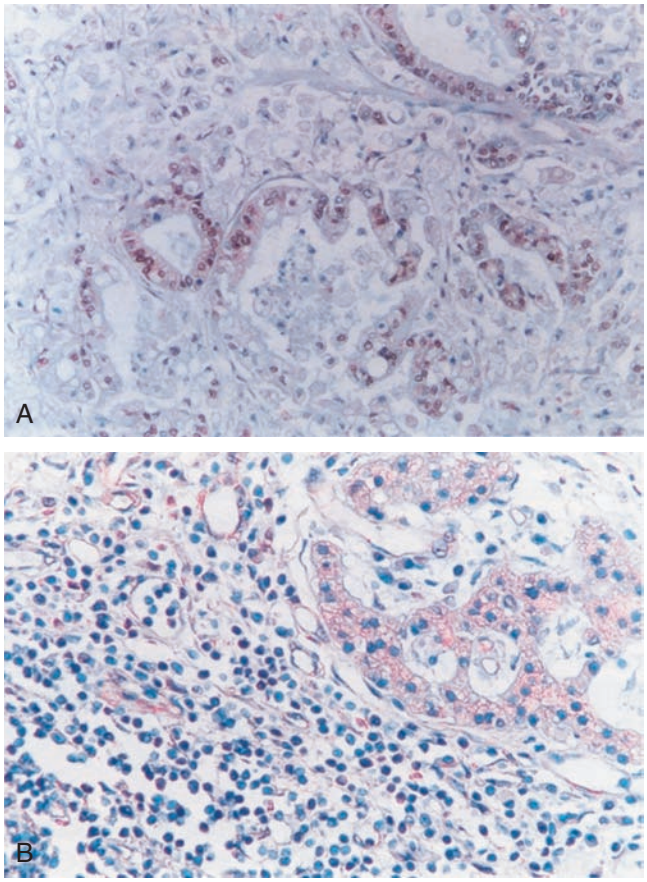

Figure 50. Immunohistochemical staining of p27 protein in tissues of pancreatic adenocarcinoma. **A:** Strong staining is observed in well-differentiated carcinoma (100X). **B:** A case of moderately differentiated carcinoma shows no staining, but some stromal cells are positive for p27 protein (200X).

Low p27 expression was a strong independent negative prognostic indicator for pancreatic adenocarcinoma in the Japanese study (Lu *et al.,* 1999) but was a weak prognostic indicator in the European study (Feakins *et al.,* 2003), despite the use of the same antibody and a similar immunohistochemical procedure. The reasons for this discrepancy are unclear. Additional larger scale studies consisting of many patients are needed to explore how this molecular marker is useful for evaluating the biological aggressiveness and predicting prognosis of the pancreatic carcinoma. These data suggest that loss of p27 expression is a common event in advanced stage of pancreatic adenocarcinoma, and, moreover, this alteration may contribute to the progression of this malignant disease.

References

Feakins, R.M., and Ghaffar, A.H. 2003. p21 Kip 1 expression is reduced in pancreatic carcinoma but has limited prognostic value. *Hum. Pathol. 34*:385–390.

Hu, Y.X., Watanabe, H., Li, P., Wang, Y., Yamaguchi, Y., and Sawabu, N. 2000. An immunohistochemical analysis of p27 expression in human pancreatic carcinomas. *Pancreas 21*: 226–230.

Lu, C.D., Morita, S., Ishibashi, T., Hara, H., Isozaki, H., and Tanigawa, N. 1999. Loss of p27 Kip 1 expression independently predicts poor prognosis for patients with resectable pancreatic adenocarcinoma. *Cancer 85*:1250–1260.

Polyak, K., Lee, M.H., Erdjument-Bromage, H., Koff, A., Roberts, J.M., Tempst, P., and Massague, J. 1994. Cloning of p27 Kip 1, a cyclin-dependent kinase inhibitor and a potential mediator of extracellular antimitogenic signals. *Cell 78*:59–66.

Toyoshima, H., and Hunter, T. 1994. p27, a novel inhibitor of GI cyclin-Cdk protein kinase activity, is related to p21. *Cell 78*: 67–74.

6

The Role of *DUSP6/MKP-3* in Pancreatic Carcinoma

Toru Furukawa and Akira Horii

Introduction

The long arm of chromosome 12 (12q) harbors frequently hemizygously deleted regions in human pancreatic cancer cells (Kimura *et al.,* 1996). In a study of 40 tissues with primary pancreatic ductal adenocarcinoma, the two smallest regions of overlap (SROs) were found (one at 12q21 and the other at 12q22-q23.1), and their frequencies of loss of heterozygosity (LOH) were 67.5% and 60%, respectively (Kimura *et al.,* 1998). Moreover, the loss of 12q is associated with a poor survival of patients (Yatsuoka *et al.,* 2000). These results strongly indicate the possibility of the existence of tumor-suppressor genes for pancreatic cancer at 12q. To detect such putative tumor-suppressor genes, bacterial artificial chromosome (BAC) contigs were created for cloning the deleted regions, and expression sequence tags (ESTs) were mapped (Youssef *et al.,* 2001). Then, the ESTs were deduced into full-length complementary deoxyribonucleic acid (cDNAs) by cDNA library screening. In the course of these studies, *DUSP6/MKP-3* was found to be one of the candidate tumor-suppressor genes that resides at 12q21-q22 (Furukawa *et al.,* 1998).

Primary Function of *DUSP6/MKP-3*

DUSP6/MKP-3 was first identified in 1996 by Groom *et al.* and Muda *et al.* (Groom *et al.,* 1996; Muda *et al.,* 1996) as a new class of dual-specificity phosphatase. It shares highly homologous sequences of carboxyl terminal active phosphatase domain and cdc25-like amino terminal domain with MKP-1 and MKP-2. DUSP6/MKP-3 specifically binds and dephosphorylates extracellular signal-regulated kinase 2 (ERK2) (Groom *et al.,* 1996; Muda *et al.,* 1996). ERK is a key effector mitogen-activated protein kinase (MAPK) involved in the RAS-GTP (guanosine triphosphate) signal transduction pathway (Hunter 1995). Active RAS-GTP mediated by signals from growth factor-receptor tyrosine kinase recruits and stimulates RAF-1, which leads to activation of MEK (MAP2K1) and ERK by subsequent phosphorylation. Activated ERK translocates into the nucleus and, in turn, activates various transcription factors, resulting in cell growth and differentiation (Hunter, 1995). DUSP6/MKP-3 can act on phosphothreonine or phosphotyrosine residues for dephosphorylation in the sequence of Thr-Glu-Tyr of active ERK2. Specific and

Handbook of Immunohistochemistry and *in situ* Hybridization of Human Carcinomas, Volume 3: Molecular Genetics, Liver Carcinoma, and Pancreatic Carcinoma

tight binding of DUSP6/MKP-3 to ERK2 is mediated through its amino terminal domain, and the binding results in a sufficient activation of the carboxyl terminal phosphatase domain (Farooq *et al.,* 2001; Nichols *et al.,* 2000). The crystal structure of DUSP6/MKP-3 indicates that it forms an active shallow pocket comprising the phosphatase domain, which can fit phosphorylated active residues of ERK2 (Stewart *et al.,* 1999). DUSP6/MKP-3 is primarily expressed in the cytosol (Groom *et al.,* 1996; Muda *et al.,* 1996). The very strict specificity for ERK2 and localization of DUSP6/MKP-3 in the cytosol are unusual characteristics that differ greatly from those of other MAPK phosphatases such as MKP-1 and MKP-2. MKP-1 and MKP-2 have less substrate specificity than DUSP6/MKP-3; they can catalyze p38 and JNK/SAPK (c-Jun N-terminal kinase/stress-activated protein kinase), other MAPK members pertaining to stress response, as well as ERK (Groom *et al.,* 1996; Guan and Butch 1995; Keyse and Emslie 1992). MKP-1 and MKP-2 are expressed predominantly in the nucleus (Groom *et al.,* 1996; Guan and Butch 1995). The cytosolic expression of DUSP6/MKP-3 may contribute to making it an effective inactivator for ERK by retaining it in the cytoplasm and preventing it from translocation into the nucleus where the target effectors reside (Brunet *et al.,* 1999). These evidences indicate that DUSP6/MKP-3 is a specific inactivator of ERK in a negative feedback loop manner. However, despite the evidences indicating DUSP6/MKP-3 as the important regulator of ERK, an essential physiologic role in mammalian cells remains to be clearly established. From pathologic aspects, one of a few clues reported is that MKP-3/DUSP6 plays a role in tumor necrosis factor-alpha (TNF-α)–induced endothelial injury by participating in proteolytic degradation of Bcl-2, which triggers apoptotic cell injury (Dimmeler *et al.,* 1999).

DUSP6/MKP-3 resides in l2q, one of the regions with frequent LOH in primary pancreatic cancer tissues (Kimura *et al.,* 1996), so the possibility of abrogation needed to be considered. We investigated its primary genomic structure, alterations in genomic DNA sequence, and expression in cultured pancreatic cancer cells and primary pancreatic cancer tissues.

MATERIALS

1. Ethanol and xylene.
2. 0.01 M phosphate buffer saline (PBS): 4.5 g $NaH_2PO_4 \cdot 2H_2O$, 32.3 g $Na_2HPO_4 \cdot 12H_2O$, 80.0 g NaCl; bring volume to 10 L with deionized distilled water.
3. 1 M Tris-HCl (pH 7.6): 121.1 g Tris base; bring volume to 1 L with deionized distilled water; adjust pH to 7.6 with concentrated HCl. Sterilize by autoclave.
4. Normal rabbit serum (Dako Japan Co., Tokyo, Japan).
5. Anti-MKP-3 C-20 antibody (Santa Cruz Biotechnology Inc., Santa Cruz, CA).
6. Biotinylated anti-goat immunoglobulin (IgG) (H+L) antibody (Vector Laboratories Inc., Burlingame, CA).
7. Streptavidin solution (Nichirei, Tokyo, Japan).
8. Chromogen solution: dissolve 20 mg 3,3′-diaminobenzidine tetrahydrochloride (DAB) (Sigma, St. Louis, MO) in 100 ml 0.05 M Tris-HCl pH 7.6); filtration with 3 MM paper (Whatman International Ltd., Maidman, U.K.). Add 17 µl 30 % H_20_2 immediately before use.

METHODS

Immunohistochemistry Using the Indirect Peroxidase Method

1. Prepare tissue sections 4 µm thick using microtome.
2. Deparaffinize sections in 100% xylene with three changes for 1 min each.
3. Hydrate sections with washing in 100% ethanol 2× and 95% ethanol 2× for 1 min each. Then wash in deionized distilled water for 5 min.
4. Wash the sections 3× for 5 min each with PBS.
5. Block endogenous peroxidase by incubating the sections in 0.3% H_2O_2/PBS for 30 min at room temperature.
6. Wash the sections 6× for 5 min each with PBS.
7. Incubate the sections in 10% normal rabbit serum/PBS for 30 min at room temperature.
8. Prepare primary antibody solution by diluting the anti-MKP-3 antibody to 1:100 in 10% normal rabbit serum/PBS.
9. Drain excess fluid from the sections and apply the primary antibody solution on them. Incubate overnight at 4°C in humid chambers.
10. Wash the sections 6× for 5 min each with PBS.
11 Prepare secondary antibody solution by diluting the biotinylated anti-goat IgG (H+L) antibody to 1:50 in 10% normal rabbit serum/PBS.
12. Drain excess fluid from the sections and apply the secondary antibody solution on them. Incubate for 30 min at room temperature.
13. Wash the sections 6× for 5 min each with PBS.
14. Drain excess fluid from the sections and apply streptavidine solution on them. Incubate for 30 min at room temperature.
15. Wash the sections 6× for 5 min each with PBS.
16. Rinse the sections with 0.05 M Tris-HCl (pH 7.6).

17. Incubate the sections in the chromogen solution for optimal time.
18. Wash the sections with running tap water.
19. Rinse the sections in deionized distilled water.
20. Counterstain with standard hematoxyline.
21. Wash with water, dehydrate with ethanol and xylene, and mount coverglass.

RESULTS AND DISCUSSION

Inactivation of DUSP6/MKP-3 in the Pancreatic Cancer

The genomic structure of the gene was determined; the gene consists of three exons with two introns. Reverse transcription polymerase chain reaction (RT-PCR) revealed two forms of transcripts: one with three exons termed *DUSP6-Full,* and the other with in-frame skipping of exon 2, termed *DUSP6-ALT* (Furukawa *et al.,* 1998). Nucleotide sequencing analysis to search for possible function-affecting alterations was performed in 24 kinds of cultured pancreatic cancer cell lines, which detected no significant alterations. To check for epigenetic inactivation or splicing alterations affecting function of the protein product, gene expressions were analyzed in the cells by RT-PCR; the expressions were markedly reduced, and the fraction of the *DUSP6-Full* was markedly reduced in most of the cells with some expression of the gene (Furukawa *et al.,* 1998). The cultured pancreatic cancer cells lacking expression of DUSP6/MKP-3 tended to show constitutive active ERK (Furukawa *et al.,* 2003). To further characterize the epigenetic inactivation of DUSP6/MKP-3, gene expressions were analyzed in primary pancreatic cancer tissues by immunohistochemistry. In a study of 46 pancreatic cancer tissues, the intensity of staining was evaluated in cells of invasive carcinoma and in the ductal epithelial cells, which were classified as normal, mild dysplasia, or severe dysplasia/carcinoma *in situ.* The results indicated that DUSP6/MKP-3 was overexpressed in cells of mild dysplasia as well as in cells of severe dysplasia/carcinoma *in situ,* but it was underexpressed in cells of invasive carcinoma, and it was especially abolished in carcinoma cells of the poorly differentiated type (Figure 51) (Furukawa *et al.,* 2003). These results suggest that DUSP6/MKP-3 is specifically inactivated in an epigenetic manner in invasive carcinoma of the pancreas.

What is the impact of inactivation of DUSP6/MKP-3 on the pathologic process of pancreatic cancer? Most primary pancreatic cancer cells, i.e., 80–90% of them, harbor the gain-of-function mutation in *KRAS2* (Almoguera *et al.,* 1988). *KRAS2* encodes RAS, a central signal mediator upstream of MAPK cascades.

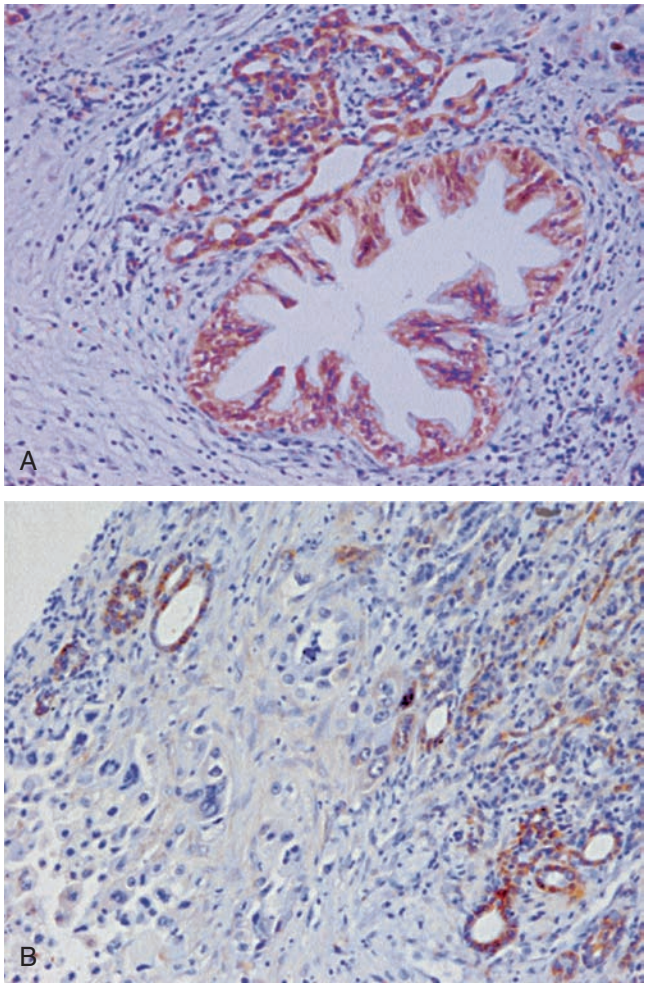

Figure 51. Immunohistochemistry of DUSP6/MKP-3 in primary pancreatic cancer tissues. DUSP6/MKP-3 is overexpressed in severely dysplastic/*in situ* carcinoma cells **(A)**, but underexpressed in invasive carcinoma cells **(B)**.

Although the RAS acts as a molecular switch of downstream signal cascades, the mutated *KRAS2* generates a constitutively active RAS, and it is supposed to hyperstimulate the downstream cascades including RAF-MEK-ERK. In the negative feedback loop, the hyperactivated ERK induced by mutated RAS would activate DUSP6/MKP-3, which can suppress the excessively activated ERK. However, abrogation of DUSP6/MKP-3 may result in loss of the feedback loop and lead to prolonged hyperactivation of ERK and subsequent signal cascades, which could contribute to uncontrolled cell growth and cellular oncogenesis. From these points of view and based on the results of studies in cultured cells and primary tissues of pancreatic cancer, DUSP6/MKP-3 potentially acts as a tumor suppressor, especially under the activated RAS phenotype. Moreover, DUSP6/MKP-3 could act as a gatekeeper

for pancreatic carcinogenesis. Growing evidence indicates that the pancreatic ductal dysplastic cells correspond to precursor lesions of common invasive ductal adenocarcinoma (Furukawa *et al.,* 1994). They harbor mutated *KRAS2* in high frequency, even in cells of mild dysplasia (Yanagisawa *et al.,* 1993). The overexpression of DUSP6/MKP-3 in dysplastic cells supposed to harbor mutated *KRAS2* suggests that DUSP6/MKP-3 is up-regulated by hyperactivation of ERK induced by mutated RAS and thus suppressing its overdrive, which could prevent cells from going to a more malignant, (i.e., invasive) phenotype.

Growth Suppressive Effect of DUSP6/MKP-3

One important question that emerged is whether recovery of expression of DUSP6/MKP-3 in pancreatic cancer cells would suppress ERK activity and stop or retard propagation of the cells. To resolve this question, a replication defective adenovirus expressing exogenous DUSP6/MKP-3 was constructed and used for transfection experiments. The result indicated that overexpression of DUSP6/MKP-3 in cultured pancreatic cancer cells, induced by the adenoviral infection, not only retarded cellular growth but also induced apoptosis (Furukawa *et al.,* 2003). This experiment, although the exogenous expression was fairly overdosed compared to that of the physiologic level, illustrates that DUSP6/MKP-3 is a growth suppressor for pancreatic cancer cells.

Although DUSP6/MKP-3 has emerged as a growth suppressor for pancreatic cancer cells, other MKP phosphatases appear to express different phenotypes. Liao *et al.* (2003) demonstrated that MKP-1, one of the major MAPK phosphatases showing a broad substrate specificity and nuclear expression, was expressed constitutively throughout pancreatic cancer tissues and pancreatic intraepithelial neoplasia, the latter of which corresponded to ductal dysplastic cells. They also showed that down-regulation of MKP-1 by antisense construct resulted in decreased anchorage-dependent and anchorage-independent growth of pancreatic cancer cells and decreased tumorigenecity in a nude mice tumor model. Yip-Schneider *et al.* (2001) indicated that some of the cultured pancreatic cancer cells show weak expressions of activated ERK, and they claimed that overexpression of MKP-2 was a reason for the down-regulation in such cells.

CONCLUSION AND FUTURE PERSPECTIVES

DUSP6/MKP-3 is inactivated epigenetically in some invasive pancreatic cancer cells, whereas it is fairly well-expressed in precancerous dysplastic cells. Exogenous overexpression of DUSP6/MKP-3 induces suppression of cell growth and apoptosis in cultured pancreatic cancer cells, especially in those that reveal constitutively activated ERK *in vitro*. From these observations, DUSP6/MKP-3 is suggested to play a significant role in tumor-suppressive pathways in pancreatic cancer. This tumor-suppressive function should be fully investigated *in vivo,* especially with a gene inactivation system under an activated RAS phenotype. Still unresolved questions include the following: How is DUSP6/MKP-3 inactivated in the invasive cancer? What is the role of LOH frequently observed in 12q, the region harboring *DUSP6/MKP-3?* How is apoptosis induced by exogenous overexpression of DUSP6/MKP-3? What can this system teach us about possible inactivation in other types of cancers with mutated RAS, which is one of the major oncogenic proteins involved in many types of human cancer? What are the therapeutic implications of DUSP6/MKP-3 for pancreatic cancer? Thus, the roles of MAPK and MKP in the pathologic processes of pancreatic cancer still present important challenges for future work.

Acknowledgment

We are grateful to Dr. Barbara Lee Smith Pierce (the Academic Director of Life Sciences for the University of Maryland Asian Division) for editorial work in the preparation of this chapter.

References

Almoguera, C., Shibata, D., Forrester, K., Martin, J., Arnheim, N., and Perucho, M. 1988. Most human carcinomas of the exocrine pancreas contain mutant *c-K-ras* genes. *Cell 53*:549–554.

Brunet, A., Roux, D., Lenormand, P., Dowd, S., Keyse, S., and Pouyssegur, J. 1999. Nuclear translocation of p42/p44 mitogen-activated protein kinase is required for growth factor-induced gene expression and cell cycle entry. *EMBO J. 18*:664–674.

Dimmeler, S., Breitschopf, K., Haendeler, J., and Zeiher, A.M. 1999. Dephosphorylation targets Bcl-2 for ubiquitin-dependent degradation: A link between the apoptosome and the proteasome pathway. *J. Exp. Med. 189*:1815–1822.

Farooq, A., Chaturvedi, G., Mujtaba, S., Plotnikova, O., Zeng, L., Dhalluin, C., Ashton, R., and Zhou, M.M. 2001. Solution structure of ERK2 binding domain of MAPK phosphatase MKP-3: Structural insights into MKP-3 activation by ERK2. *Mol. Cell 7*:387–399.

Furukawa, T., Chiba, R., Kobari, M., Matsuno, S., Nagura, H., and Takahashi, T. 1994. Varying grades of epithelial atypia in the pancreatic ducts of humans. Classification based on morphometry and multivariate analysis and correlated with positive reactions of carcinoembryonic antigen. *Arch. Pathol. Lab. Med. 118*:227–234.

Furukawa, T., Sunamura, M., Motoi, F., Matsuno, S., and Horii, A. 2003. Potential tumor suppressive pathway involving DUSP6/MKP-3 in pancreatic cancer. *Am. J. Pathol. 162*:1807–1815.

Furukawa, T., Yatsuoka, T., Youssef, E.M., Abe, T., Yokoyama, T., Fukushige, S., Soeda, E., Hoshi, M., Hayashi, Y., Sunamura, M.,

Kobari, M., and Horii, A. 1998. Genomic analysis of DUSP6, a dual specificity MAP kinase phosphatase, in pancreatic cancer. *Cytogenet Cell Genet*. *82*:156–159.

Groom, L.A., Sneddon, A.A., Alessi, D.R., Dowd, S., and Keyse, S.M. 1996. Differential regulation of the MAP, SAP and RK/p38 kinases by Pyst1, a novel cytosolic dual-specificity phosphatase. *EMBO J*. *15*:3621–3632.

Guan, K.L., and Butch, E. 1995. Isolation and characterization of a novel dual specific phosphatase, HVH2, which selectively dephosphorylate the mitogen-activated protein kniase. *J*. *Biol*. *Chem*. *270*:7197–7203.

Hunter, T. 1995. Protein kinases and phosphatases: The yin and yang of protein phosphorylation and signaling. *Cell 80*:225–236.

Keyse, S.M., and Emslie, E.A. 1992. Oxidative stress and heat shock induce a human gene encoding a protein-tyrosine phosphatase. *Nature 359*:644–647.

Kimura, M., Abe, T., Sunamura, M., Matsuno, S., and Horii, A. 1996. Detailed deletion mapping on chromosome arm 12q in human pancreatic adenocarcinoma: Identification of a I-cM region of common allelic loss. *Genes Chromosom Cancer 17*:88–93.

Kimura, M., Furukawa, T., Abe, T., Yatsuoka, T., Youssef, E.M., Yokoyama, T., Ouyang, H., Ohnishi, Y., Sunamura, M., Kobari, M., Matsuno, S., and Horii, A. 1998. Identification of two common regions of allelic loss in chromosome arm 12q in human pancreatic cancer. *Cancer Res*. *58*:2456–2460.

Liao, Q., Guo, J., Kleeff, J., Zimmermann, A., Buchler, M.W., Korc, M., and Friess, H. 2003. Down-regulation of the dual-specificity phosphatase MKP-l suppresses tumorigenicity of pancreatic cancer cells. *Gastroenterology 124*:1830–1845.

Muda, M., Boschert, U., Dickinson, R., Martinou, J.C., Martinou, I., Camps, M., Schiegel, W., and Arkinstall, S. 1996. MKP-3, a novel cytosolic protein-tyrosine phosphatase that exemplifies a new class of mitogen-activated protein kinase phosphatase. *J*. *Biol*. *Chem*. *271*:4319–4326.

Nichols, A., Camps, M., Gillieron, C., Chabert, C., Brunet, A., Wilsbacher, J., Cobb, M., Pouyssegur, J., Shaw, J.P., and Arkinstall, S. 2000. Substrate recognition domains within extracellular singal-regulated kinase mediate binding and catalytic activation of mitogen-activated protein kinase phosphatase-3. *J*. *Biol*. *Chem*. *275*:24613–24621.

Stewart, A.E., Dowd, S., Keyse, S.M., and McDonald, N.Q. 1999. Crystal structure of the MAPK phosphatase Pyst1 catalytic domain and implications for regulated activation. *Nat*. *Struct*. *Biol*. 6:174–181.

Yanagisawa, A., Ohtake, K., Ohashi, K., Hori, M., Kitagawa, T., Sugano, H., and Kato, Y. 1993. Frequent c-Ki-ras oncogene activation in mucous cell hyperplasias of pancreas suffering from chronic inflammation. *Cancer Res*. *53*:953–956.

Yatsuoka, T., Sunamura, M., Furukawa, T., Fukushige, S., Yokoyama, T., Inoue, H., Shibuya, K., Takeda, K., Matsuno, S., and Horii, A. 2000. Association of poor prognosis with loss of l2q, 17p, and 18q, and concordant loss of 6q/l7p and 12q/l8q in human pancreatic ductal adenocarcinoma. *Am*. *J*. *Gastroenterol*. *95*:2080–2085.

Yip-Schneider, M.T., Lin, A., and Marshall, M.S. 2001. Pancreatic tumor cells with mutant K-ras suppress ERK activity by MEK-dependent induction of MAP kinase phosphatase-2. *Biochem*. *Biophys*. *Res*. *Commun*. *280*:992–997.

Youssef, E.M., Kaneko, K., Yatsuoka, T., Hayashi, Y., Hoshi, M., Horii, A., and Furukawa, T. 2001. Human BAC contig covering the deleted region in pancreatic cancer at l2q21. *DNA Seq*. *11*:541–546.

7

Expression of Carbohydrate Antigens in Pancreatic Cancer

Makoto Osanai

Introduction

In the past generation, the incidence of pancreatic cancer has increased from less than 5 per 100,000 to between 11 and 12 per 100,000 people in the population (DiMagno, 1996). In developed countries, the annual age-adjusted incidence rates range from 8.0 to 12.0 per 100,000 males and from 4.5 to 7.0 per 100,000 females (Solcia *et al.,* 1997). Incidence rates from most third-world countries range from 1.0 to 2.5 per 100,000 people. It is noteworthy that pancreatic cancer has an extremely poor prognosis and is usually diagnosed after there has been local invasion or metastasis, and as a result, treatment is seldom effective. A previous study reported that median survival after diagnosis is 4–8 months and overall survival is less than 1% (DiMagno, 1996). Although resecting the tumor improves the median survival to 17–20 months, the actual average of resection rates is 10.7% (Gudjionsson, 1987) and 5-year survival remains less than 10% (DiMagno, 1996).

Most pancreatic neoplasms are malignant, but benign forms or tumors with various malignant potentials also occur. The most common tumor type in the pancreas is ductal adenocarcinoma and its variants, comprising 85–90% of cases. These carcinomas vary in their differentiation with markedly altered architecture and typically are accompanied by the dense proliferation of stromal fibrous tissue. Less than 10% of the exocrine pancreatic tumors are benign or uncertain. Approximately 75% of all pancreatic carcinomas occur in the head of the organ, whereas ~25% occur in the body and tail regions. Histologic classification of tumors originating from the exocrine pancreas and the location of occurrence have both clinical and prognostic significance.

The histogenesis of the pancreatic neoplasm remains unclear; however, a number of animal models have suggested plausible mechanisms for development. Animal models using rodents have indicated that proliferative lesions of the ductal cells are likely to be the origin of most ductal carcinomas. Intraductal papillary hyperplasia and intraductal hyperplasia with various degrees of atypia may arise from the ductal cells. Similarly, proliferative lesions of the acinar cells give rise to acinar cell carcinoma showing a partial phenotype of ductal cell, indicating that malignant transformation and metaplastic change occur simultaneously in acinar cells. It remains to be clarified whether this pathway is involved in the histopathogenesis of human pancreatic cancer, and it has yet to be confirmed that any single factor or carcinogen is responsible for the development of pancreatic cancers in humans.

Usually, patients suspected of having pancreatic cancer are diagnosed based on their symptoms, routine blood analyses such as hematology and chemistry, and a series of radiographic image studies. After these routine tests, plasma will be examined for specific tumor markers. In some patients who required further

Handbook of Immunohistochemistry and *in situ* Hybridization of Human Carcinomas, Volume 3: Molecular Genetics, Liver Carcinoma, and Pancreatic Carcinoma

examination to diagnose the pancreatic malignancy, pathologic or cytologic examination or both would be used in the next line of clinical examinations. However, no specific and sensitive serologic marker for tumors has been identified as a routine diagnostic or screening test for pancreatic cancer. To date, clinically available serologic tests mainly include carcinoembryonic antigen (CEA), carbohydrate antigen (CA) 19-9, and DU PAN-2. Although these tests have ranged in sensitivity from 50–70%, and CA 19-9 has been proved to be useful as a pancreatic tumor maker and is widely used in clinical settings with a sensitivity of 76% and a specificity of 87% (Gupta *et al.,* 1985), none of the tests satisfactorily detect the lesion at early stages of development. Elevated levels of serologic markers are also detected in benign diseases, including acute and chronic pancreatitis, and cholangitis. If further examination was performed using biopsy specimens, it is widely believed that even experienced pathologists gave different diagnostic results in some selected cases. Moreover, immunohistochemistry (IHC) testing of these samples is of limited diagnostic value. For example, immunostaining for markers such as CA 19-9 may yield positive results not only in neoplastic cells but also in normal ductal epithelial cells. None of these markers can be used satisfactorily to differentiate between primary pancreatic carcinomas and carcinomas originating from other organs.

Here, the author presents a case diagnosed as adenocarcinoma arising from gastric heterotopic pancreas and describes the role of CA 19-9 in immunohistochemical staining and its diagnostic significance and limited use in the diagnostic procedures in patients with pancreatic carcinomas. In addition, the roles and characters of major CAs that are available to clinical laboratories are described. As a result of these limited preexisting diagnostic tools, the author examined the possible clinical application for genetic analyses based on the detection of specific genetic alterations over the course of pancreatic carcinogenesis, which would be a highly specific and sensitive method when compared with the currently available immunohistochemical techniques.

MATERIALS

Immunohistochemistry

1. Fixative: 10% phosphate-buffered formalin, pH 7.4.

2. Phosphate buffer saline (PBS, 10X stock solution): 77.5 g NaCl, 15.0 g K_2HPO_4, 2.0 g KH_2PO_4; dissolve the salt completely and bring volume to 1 L. The pH of this solution should be 7.4–7.6, and it should be stored at room temperature.

3. PBS (1X working solution): 10X PBS stock solution, 100 ml; distilled water, 900 ml.

4. Primary antibody: CA 19-9 (1:50–200, M3517, Dako, Tokyo, Japan). In a preliminary experiment, the appropriate dilution for this antibody must be determined for each slide.

5. Permanent mounting media.

6. 3% solution of hydrogen peroxide: 30% hydrogen peroxide, 1 part; absolute methanol, 9 parts.

7. 0.1% solution of trypsin: Trypsin (Sigma, Japan) should be dissolved in 1X PBS solution, pH 7.4 at 4°C.

8. Hematoxylin for counterstaining.

9. EnVision/HRP (horseradish peroxidase) (diaminobenzidine, or DAB) kit (Dako, Japan): Peroxidase-conjugated enhanced polymer one-step staining system. Dako has developed a technology that enables the coupling of a large number of molecules to a dextran-based polymer. This unique chemistry permits binding of a large number of enzyme molecules (e.g., HRP) to a secondary antibody via the dextran backbone. The major benefits are as follows: 1) increased sensitivity, 2) minimal nonspecific background staining, and 3) reduction in the total number of assay steps compared with conventional techniques.

10. Histofine DAB kit (Nichirei, Japan): DAB, 3,3′-diaminobenzidine as a chromogen substrate. This kit gives high sensitivity and low background activity.

11. Moist (humidified) chamber: All immunoreactions and the color reaction should be performed in this chamber, because drying results in salt precipitation produces artifacts.

12. Staining rack or coplin jar.

Polymerase Chain Reaction

1. Double-distilled water (DDW): Autoclave the distilled water that has been run through a Millipore Q filter system (Billerica, MA).

2. Primer: Each oligonucleotide should be synthesized by a specialized company. Nucleotide sequences are shown in Figure 52.

3. Taq deoxyribonucleic acid (DNA) polymerase (Takara, Shiga, Japan): 10X polymerase chain reaction (PCR) buffer and dNTP (deoxynucleotide triphosphate) mixture of satisfactory quality are provided with the enzyme.

4. Pipette, pipette tip, 1.5 mL microcentrifuge tube, and 0.2 mL microtube for PCR: PCR microtube is uniquely designed for the PCR machine. Use the appropriate tube and check before the experiments to determine whether your machine needs mineral oil overlying the PCR reaction mixture. Failure to use the required mineral oil overlay will result in the vaporization of samples or unsatisfactory amplification.

A

Oligonucleotide of K-*ras* codon 12 for MASA	K-*ras* codon 12
Sense (5'-3')	
Set 1	
ACTTGTGGTAGTTGGAGCTA	AGT
ACTTGTGGTAGTTGGAGCTC	CGT
ACTTGTGGTAGTTGGAGCTT	TGT
Set 2	
CTTGTGGTAGTTGGAGCTGA	GAT
CTTGTGGTAGTTGGAGCTGC	GCT
CTTGTGGTAGTTGGAGCTGT	GTT
Antisense (5'-3')	
CTCATGAAAATGGTCAGAGAAACC	

B

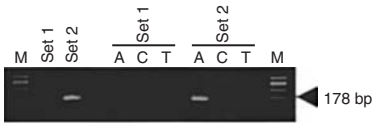

Figure 52. Mutant allele-specific amplification (MASA) analysis of K-*ras* mutation at codon 12. **A:** Primer sets used in this study. Set 1, primers for the first base mutation; set 2, primers for the second base mutation. **B:** Agarose gel electrophoresis shows a mutant specific band with primer set 2 and the transition for GGT to GAT. Lane l, sense set 1; Lane 2, sense set 2; Lanes 3–5, each mutant primer in the first base instead of set 1; Lanes 6–8, each mutant primer in the second base instead of set 2. M, molecular size marker; bp, base pairs.

4. Agarose: Electrophoresis grade should be prepared.
5. 5X TBE (Tris-Bolate-EDTA [ethylenediamine tetra-acetic acid]) buffer (stock solution): Tris Base, 54 g; boric acid, 27.5 g; 0.5 M EDTA pH 8.0, 20 ml. Bring volume to 1 L.
6. 0.5X TBE buffer (working solution): 5X TBE buffer stock solution, 100 ml; distilled water, 900 ml.
7. Ethidium bromide (EtBr): 10 mg/ml.
8. Loading buffer: 0.25% bromophenol blue, 0.25% xylene cyanol FF in 40% (w/v) sucrose in water.
9. Thermal cycler and ultraviolet (UV) illuminator.

METHODS

Hematoxylin and Eosin Staining

1. Tissue samples were fixed in 10% phosphate-buffered formalin overnight (generally more than 20 hr).
2. Fixed samples were embedded in paraffin.
3. The slides were stained with hematoxylin and eosin (H&E) in a standard procedure.

Immunohistochemistry

l. Cut paraffin sections at 4 or 5 μm and mount on silanized slides.
2. Positive control must be run along with each antibody each time immunohistochemical staining is performed.
3. Negative control also must be run by substituting the appropriate diluent solution for the primary antibody (e.g., PBS).
4. Dry overnight in a drying oven maintaining a temperature of 40–45°C.
5. Deparaffinize by treatment with xylene: Immerse the slides in xylene. After 3 min, take out and shake off the excess xylene from the slides. Repeat 3× for at least 3 min in each series using fresh xylene.
6. Immerse the slides in 100% ethanol. After 3 min, take out and shake off the excess ethanol in the slides. Repeat 3× for at least 3 min in each series with fresh 100% ethanol.
7. Treat them 2× with 95% ethanol in a similar manner as described in **Step 6.**
8. Rehydration: After excess ethanol is shaken off, immerse slides in PBS for 5 min.
9. Treat the slides with a fresh 3% solution of hydrogen peroxide in methanol for 15 min at RT. Hydrogen peroxide is used as the first blocking solution to inhibit the endogenous peroxidase activity of the tissues.
10. Rinse the slides in PBS 3× for 5 min each time.
11. Digest the slides in 0.1% trypsin solution for 10 min at 37°C to unmask most antigens.
12. Rinse well, as in **Step 10.**
13. Rinse well again in PBS working solution.
14. Remove excess fluid from the slides with cotton gauze to prevent dilution of the antiserum in the subsequent step; however, the tissue must not be allowed to dry from this step so as to avoid generation of artifacts.
15. Put the blocking serum on the slides and incubate for 10 min.
16. Tap off the excess solution on the slides. *Do not* rinse off.
17. Apply a couple of drops of primary antibody diluted in PBS to completely cover the sections and incubate at room temperature for 1 hr in the humidified chamber.
18. Wash the slides well, as in **Step 10.** Place the slides in PBS and leave at room temperature for 10 min.
19. Wipe areas around the sections on the slides carefully.
20. Place a few drops of Bottle 3 provided as part of the EnVision kit onto each section. Incubate section for 30–60 min. Bottle 3 content is a mixture of HRP-conjugated goat anti-mouse polyclonal antibody and goat anti-rabbit polyclonal antibody bound to the dextran polymer reagent.
21. Rinse the slides well, as in **Step 10.**
22. Wipe areas around the section on the slides carefully and apply histofine DAB as the chromogen substrate (prepared according to the manufacturer's instructions) to completely cover the sections. Incubate for 10 min in the humidified chamber.
23. Rinse well, as in **Step 10.**

24. Wash the slides in two changes of distilled water.
25. Counter-staining: Immerse slides in hematoxylin for 15 min.
26. Wash them well in running water for 15 min.
27. Dehydrate the sections in a graded series of alcohol and clear in xylene.
28. Mount with permanent mounting media.

Genetic Analysis for Detecting Point Mutations of K-*ras* at Codon 12

1. All pipette tips and tubes must be autoclaved for 20–30 min at 121°C.
2. Extraction of DNA from 1-µm-thick paraffin-embedded tissue specimens: The most important thing for the PCR reaction is the quality and quantity of the DNA template, which does not always need to be high in certain situations. A crude lysate prepared by simple boiling in DDW may provide template DNA of adequate quality and quantity for successful amplification. In this context, we generally used 1-µm-thick samples cut from paraffin-embedded tissue specimens. If these are unavailable, the tiny debris or improperly cut sections are sufficient. However, excess amounts of paraffin debris are not acceptable because they inhibit the enzymatic activity in PCR reactions.
   a. Suspend the 1-µm-thick paraffin-embedded tissue specimen in DDW and pellet down in a centrifuge at no less than 10,000X g for 10 min at room temperature.
   b. Resuspend in 25–100 µl DDW and transfer to a 1.5-ml microcentrifuge tube.
   c. Incubate for 5 min in boiling water.
   d. Transfer the tube immediately to ice and incubate for 3–5 min. This crude lysate contains DNA of sufficient quality and quantity for the following PCR reaction.
3. Set up a 20-µl reaction mixture in a 0.2-ml microcentrifuge tube: 1 µl, template DNA (crude lysate); 2 µl, 5 µM each primer; 2 µl, 10X PCR buffer; 1.6 µl, dNTP mixture (2.5 mM each dNTP: dCTP, dATP, dGTP and dTTP); 11.3 µl, DDW.
4. Add 0.1 µl Taq DNA polymerase.
5. (Option) The reaction mixture in **Step 3** and **Step 4** must be on ice to reduce the incidence of primer-dimmer artifacts.
6. Spin down briefly in a benchtop centrifuge.
7. Run the PCR reactions in a thermalcycler using the following profile:
   a. Initial denaturation: 94°C for 5 min.
   b. Denaturation, 94°C for 30 sec; annealing, 55°C for 30 sec. (The annealing temperature is dependent on your primer design. If you use a different primer set, the optimal annealing temperature for your primers is Tm −5°C.); extension, 72°C for 45 sec.
   c. Repeat step b for 30–35 cycles.
   d. Cycling should conclude with a final extension at 72°C for 10 min.
   e. Store at 4°C.
8. Add 2 µl 10X loading buffer in each sample.
9. Electrophorese on 2.0% agarose gel containing 100 µg/ml EtBr at 100 V for approximately 30 min in 0.5X TBE electrophoresis buffer.
10. Obtain results under UV illumination.

RESULTS

This section describes a case of adenocarcinoma presumably arising from a gastric heterotopic pancreas and considers the morphologic and immunohistochemical features along with genetic analysis to examine its histogenesis (Osanai *et al.,* 2001). Although heterotopic pancreas in the stomach is a relatively common congenital condition, the risk of malignant transformation is believed to be extremely low.

This unusual lesion was seen in a 57-year-old Japanese female. She was in good general health, and all laboratory tests including tumor marker examinations such as CEA, CA 19-9, and DU PAN-2 were within normal limits. Clinical examinations including X-ray image studies and biopsy specimens confirmed the final diagnosis as advanced adenocarcinoma of the stomach. After the sequential diagnostic procedures, a total gastrectomy was performed on the patient.

Gross features of the surgically resected specimen included an irregular ulcerated mass (~12.5 × 9 cm) that extended from the angle to the body in the lesser curvature of the stomach. This invasive tumor was exposed to the serosal membrane and adhered tightly to the perigastric soft tissue, but the resected surgical margins were determined to be negative for neoplastic cells.

Microscopically, the heterotopic pancreas was located broadly within the submucosal and muscular layers of the stomach. The surface epithelium over the tumor was intact except in the region of ulceration. Nontumorous heterotopic pancreatic tissue demonstrated the elements of a normal pancreas: ducts and acini (Heinrich type II). The tumor showed mixed patterns of trabecular and solid neoplastic cell proliferation with poor ductal differentiation and moderately differentiated glandular structures. Most of the dilated ducts showed papillary hyperplasia with focal intestinal metaplasia and also demonstrated lesions in transition to malignancy where adjacent to obviously malignant lesions. These transitional lesions were classified as duct cell dysplasia or carcinoma *in situ.* Invasion of the

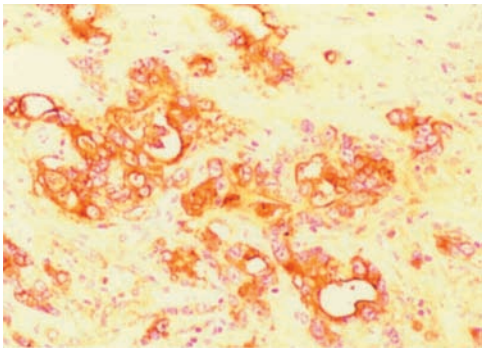

Figure 53. The tumor shows mixed patterns of solid neoplastic cell proliferation and moderately differentiated glandular structures. Immunohistochemical staining demonstrates that CA 19-9 has strong and widespread positive immunoreactivity in the ductal epithelium of tumor tissue with ductal differentiation. (Final magnification 200X.)

lymphatic and vascular vessels was frequently observed in histologic specimens.

We performed immunohistochemical staining using various antibodies. In areas of the tumor with ductal differentiation, CA19-9 (Figure 53), transmembrane glycoprotein tumor antigen mucin (MUC) 1 and cytokeratin 19 exhibited a strong, widespread positive immunoreactivity in ductal epithelium. Alpha 1-antitrypsin and alpha 1-antichimotrypsin were also strongly reactive in the ductal luminal surface. Insulin staining revealed approximate positivity rates of 50–60% for cells in neoplastic duct epithelial cytoplasm. Whereas cells positive for CEA, MUC2, and cytokeratin 20 were scattered focally in the ducts, staining for MUC 5AC, glucagon, and p53 was faint or negative.

Because the incidence of point mutation in K-*ras* codon 12 (KRM) in patients with pancreatic carcinoma and biliary tract carcinoma has been reported to be high (75–100%) (Almoguera *et al.,* 1988), we attempted to identify KRM in this case by the mutant allele-specific amplification (MASA) method as described by Takeda *et al.* (1993). Although no band was present with primer set 1, primer set 2 generated a mutant-specific band suggesting that our case was positive for KRM (Figure 52). We performed further analysis to identify the mutational type in this case and found the transition of GGT (Gly) to GAT (Asp), which is the most common mutational change in KRM observed in the patients with pancreatic carcinomas.

These findings provide evidence that the tumor in our clinical case originated from heterotopic pancreatic tissue rather than gastric epithelium. This patient had multiple liver metastatic lesions and inoperable local recurrence 13 months after the operation. She became cachexic and died of peritonitis carcinomatosa.

DISCUSSION

Heterotopic (ectopic, aberrant) pancreas has been found frequently in the gastrointestinal tract, especially in the antrum of the stomach; however, malignant change in heterotopic pancreas is extremely rare (Guillou *et al.,* 1994). There are few reports detailing cases of gastric carcinoma that have presumably arisen from heterotopic pancreatic tissue in the gastric wall. The significance of this unusual lesion is its potential confusion with conventional adenocarcinoma arising from gastric epithelium. Such confusion may occur if the presence of pancreatic tissue cannot be verified. The well-differentiated cell structure and predominantly submucosal lesion of gastric heterotopic pancreas make it an infertile soil for neoplastic transformation (Hickman *et al.,* 1981). Because surface irritation may not be a significant factor for carcinogenesis in submucosal sites, it is not clear why neoplastic formation may occur in this restricted location.

With regard to immunohistochemical findings, the staining pattern of this tumor resembled that of adenocarcinoma arising from an orthotopic pancreas, rather than that of adenocarcinoma arising from gastric epithelium. The positive immunoreactivity for CA 19-9, cytokeratin 19, and insulin support the speculation that the tumor cells may have arisen from the duct epithelium or acinar cells in the heterotopic pancreas. Immunohistochemical staining for insulin confirmed the production of insulin by the neoplastic cells and acinar cells in the nontumorous heterotopic pancreatic tissue. The occurrence of endocrine cells in ductal neoplasm is reasonable if the neoplasm is originated from primitive, multipotent cells that have the capacity to differentiate in several directions. In the concept of multistep carcinogenesis, the presence of a subclone of the cells sharing characteristics distinct from the neighboring cells is not difficult to envisage. It is plausible that, like the orthotopic pancreas, ductal cells of the heterotopic pancreas have the potential to differentiate into acinar and islet cells.

Although these findings may be correct in terms of the histologic origin of the tumor, no definite diagnostic immunoreactivity could be established by using preexisting antibodies. Therefore, we applied genetic analysis to identify KRM for the purpose of confirming our diagnosis and speculating on its possible histogenesis. Pancreatic carcinoma has the highest incidence of KRM among various human cancer tissues. Many investigators have reported the presence of KRM in this carcinoma at higher rates, ranging from 75% to 100% (Almoguera *et al.,* 1988). Moreover, the KRM found in our study is the most common type of change observed in the patients with pancreatic carcinoma.

In contrast, published studies have shown that the incidence of KRM in gastric cancer ranges from 0% to 28% (Jiang *et al.,* 1989). The reason for the difference in the occurrence of KRM between the two types of cancer is not known. It is interesting that the genetic change often seen in pancreatic carcinoma is not common in gastric carcinoma, indicating that KRM may be a "hot spot" for pancreatic carcinoma and a very convenient genetic tumor marker for clinical application. However, it should be noted that the findings of previous studies suggest that KRM is not specific to pancreatic cancer. Results from this study support the conclusion that the adenocarcinoma observed in our case developed from gastric heterotopic pancreas.

It is clear from the diagnostic procedure that there are limitations in diagnosing pancreatic cancer by conventional pathologic examination. It is necessary to combine the results of various examinations such as the physical status of the patient, blood tests including tumor markers, various imaging examinations, and pathologic examinations. When attempting to make a diagnosis, the clinical pathologist must play a central role in evaluating the clinical samples from the patients with suspected pancreatic cancer and in contributing to the development of useful immunohistochemical techniques that use antibodies very specific to pancreatic cancer.

Modern IHC has evolved from the pioneering work of Köhler and Milstein (1975), who made it possible to produce unlimited quantities of monoclonal antibodies with the hybridoma technique. Immunohistochemical staining uses antibodies to distinguish between cells based on antigenic differences. These differences are based on the different cellular phenotypes of interest. With the development of this method, IHC has had a significant and fundamental impact on the practice of surgical pathology (Cote and Taylor, 1996). Next, scientists looked for cell-specific antigens because the success of IHC is dependent on the specificity of antibodies for the target antigens. Many scientists have tried to identify antibodies that react with antigens of interest in very specific manner; however, researchers have been unable to identify tumor-specific antigens that meet the strict criteria. In the last few decades, a number of chemically valuable antibodies with satisfactory specificity to certain neoplastic cells have been identified and characterized, which has been useful for clinical applications. These antibodies have been termed "tumor-associated antigens (TAAs)" (Juhl *et al.,* 1996). The TAAs were known to express in the cell membrane of the target cells and are measurable as tumor markers in the serum of patients. A subgroup of TAAs is CA, which are detectable with monoclonal antibodies (mAbs). These mAbs react with cell-surface mucins in neoplastic pancreatic cells.

Cell-surface mucins in neoplastic pancreatic cells are high molecular weight (MW) glycoproteins with oligosaccharide residue on their protein backbone. These mucins are synthesized and secreted from the glandular epithelium, and there is a report that the glycosylation of mucins is altered in cancers (Osako *et al.,* 1993). One of the epitopes on a mucin glycoprotein is CA, in which carbohydrate epitopes on mucin antigen are recognized with its oligosaccharides residue by mAbs.

CA 19-9

The CA 19-9 antigen was isolated by a mAb that is specific for cells of human carcinoma of the colon as determined by the direct binding of antibody to thin-layer chromatograms of total lipid extracts of tissues (Magnani *et al.,* 1981). The binding of this antibody to antigen is inhibited by the serum of most patients with advanced colorectal carcinoma but not by the serum of normal individuals, patients with inflammatory bowel diseases, or most patients with other malignancies. CA 19-9 consists of a migratory mucin-like glycoprotein (monosialoganglioside) expressed on the cell membrane. Because the epitope has components similar to the Lewis^a blood-group antigen (Magnani *et al.,* 1981), CA 19-9 cannot detect patients who are sialyl Lewis^a blood group-negative, who account for ~5% of the general population.

CA 19-9 appears to have a great value as a pancreatic tumor maker and is widely used in clinical diagnosis (initially described by Del Villano *et al.,* 1983 and Ricolleau *et al.,* 1983). Immunohistochemical staining of pancreatic cancer has shown that 86% of tumors express CA 19-9 antigen (Juhl *et al.,* 1996) and immunoreactivity is predominantly found in the luminal contents and along the luminal borders. The clinical significances of this TAA comes from the fact that elevated concentrations of serum CA 19-9 can be found in patients with pancreatic cancer. This marker is expressed in more than 80% of ductal adenocarcinomas and tumor cells of the serous cystadenomas and acinar cell carcinomas, and sensitivity was 76% (Gupta *et al.,* 1985), which seems to be higher than the sensitivity of other TAAs, such as CEA. However, CA 19-9 may also be detected in various other gastrointestinal and extragastrointestinal malignancies, in transitional lesions of obvious pancreatic malignancy (Zamora *et al.,* 2001), and in a number of benign diseases including chronic inflammatory diseases such as chronic pancreatitis and obstructive jaundice and even in smokers (Hammarström, 1985).

In contrast, Steinberg (1990) reported that CA 19-9 is a TAA synthesized by normal pancreatic acinar and ductal cells and occurs in large quantities within normal

pancreatic juice. These results suggest that CA 19-9 is not pathognomonic of pancreatic cancer because most patients demonstrate elevated concentrations of this marker in serum and pancreatic juice and CA 19-9 stains the epithelium of normal pancreatic ducts, particularly in chronic pancreatitis (Solcia *et al.,* 1997). This observation demonstrates that the testing for CA 19-9 may be of no clinical value to diagnose a pancreatic malignancy; however, clinical trials indicate that the kinetics of CA 19-9 are comparable to conventional imaging procedures and may serve as an early indicator of patient outcome following surgery or chemotherapy. This suggests that the testing of CA 19-9 kinetics may help to reduce the number of costly imaging procedures (Heinemann *et al.,* 1999). In addition, a previous study of patients with pancreatic malignancy showed that the combination of the CA 19-9 assay in the serum and the cytologic study of aspirated materials obtained by percutaneous fine-needle aspiration of the pancreas increases the diagnostic rate to 100% (Tatsuta, 1985).

The peculiar histogenesis of the pancreas has received much attention. It is well known that three different main cell lineages are found in the human pancreas: the duct cell, the acinar cell, and the endocrine cell. These cells originate from the common prototype epithelium (protodifferentiated cells) developed in the fetal pancreas (Githens, 1993). Some protodifferentiated cells may exist even in adulthood within the ductal epithelium and may retain the capacity to regenerate and differentiate into duct, acinar, or islet cells, and pancreatic neoplasm is thought to originate from primitive, multipotential cells that have the capacity to differentiate in several directions. In fact, animal experiments have demonstrated that islet cells can regenerate even in the adult from ductal cells when islet cells are injured with various insults (Githens, 1988). The cellular phenotype of the various tumors arising from these cell lineages is believed to reflect their origin and differentiation from one of these cell types. Although IHC can be used to separate and categorize tumors occurring from pancreatic tissue, CA 19-9 is not pathognomonic for differential diagnosis of pancreatic tumors because the CA 19-9 antibody is known to crossreact with a variety of other cellular phenotypes. This phenomenon can be easily explained by the accumulated evidences that many types of pancreatic cells can produce this specific TAA.

Over the course of multistep carcinogenesis, a number of subclones have accumulated genetic alterations spontaneously and lead to the characteristic heterogeneity of malignant tumors. In this context, it is not surprising to discover the presence of cells sharing partial characteristics with each of these three types of cell lineages. Given the fact that the ductal cells of the adult pancreas have a potential to differentiate into acinal cells and islet cells (transdifferentiation), IHC using only CA 19-9 antibody would be unable to differentiate between cell types as a result of this chimeric property of tumor cells. Unless we can improve or revolutionalize our diagnostic strategies, the exact clonal origin of the tumor cell cannot be determined distinctly and we would not understand the overall view of the histogenesis of pancreatic cancer, which is implicated in the quality of the surgical pathology.

An increasing number of studies have reported the usefulness of new CAs; however, none of these markers have proved superior to CA 19-9. In addition, their uses as tumor and tissue markers for pancreatic cancer are limited by their lack of tumor and tissue specificity, and even a combination of positive markers does not increase this sensitivity. Furthermore, although the effectiveness of other possible combinations of CAs remains to be elucidated, limited application of these antibodies may lead to no clinical improvement in the diagnosis of pancreatic malignancy.

DU PAN-2

DU PAN-2 is a human pancreatic adenocarcinoma–associated mucin-like antigen defined by the murine mAb DU PAN-2. The epitope defined by this mAb is thought to be expressed on glandular cell secretory products that exhibit molecular microheterogeneity in structure (Lan *et al.,* 1985). This epitope is predominantly found in pancreatic and hepatobiliary malignancies, but it is also expressed in normal ductal cells in the pancreas (Juhl *et al.,* 1996). The combination of serologic analyses of CA 19-9 and DU PAN-2 has been shown to be a useful diagnostic tool for pancreatic carcinomas (Solcia *et al.,* 1997).

Span-1

Span-1 is a high MW, mucin-like glycoprotein identified as a human pancreatic cancer–associated antigen, which was produced from spleen cells of mice immunized against the human pancreatic cancer cell line, Capan-2 (Yuan *et al.,* 1985). It reacts preferentially with cancerous and normal human pancreatic tissue, and it is also found in colonic and stomach carcinomas. This mAb is known to crossreact with CA 19-9 and CA 50.

CA 15-3

The CA 15-3 TAA is found in a variety of adenocarcinomas including ductal adenocarcinoma of the pancreas and malignant mucinous cystic neoplasms. Expression of the CA 15-3 protein is reported to coincide with malignant transformation in pancreatic

mucinous cystic neoplasms and has proved useful in the differentiation between benign and malignant pancreatic mucinous cysts (Rubin *et al.,* 1994).

CA 50

The CA-50 ganglioside antigen present in the COLO 205 cell line has been characterized as sislosylfucosyllactotetraosylceramide, which is the sialylated Lewis[a] pentaglycosylceramide (Nilsson *et al.,* 1985). Because CA 50 is also present in patients who are Lewis[a] blood group-negative (~5%) and who therefore cannot have the CA 19-9 antigen, a combination of CA 50 and CA 19-9 may be useful for accurate diagnosis of pancreatic neoplasm. Studies using a mAb against the CA-50 ganglioside have demonstrated CA 50 to be a minor component in many different carcinomas.

CA 72-4

A high MW, mucin-like, human tumor–associated glycoprotein (TAG-72), CA 72-4 is expressed in a wide variety of human gastrointestinal carcinomas, including pancreatic carcinomas (Ching *et al.,* 1993; Byrne *et al.,* 1990). Antibodies against this TAA can detect aberrant glycosylation of structural and secretary glycoconjugates in epithelial cancer cells and has proved to be a sensitive and specific tumor marker for the pancreas. CA 72-4 also has been well studied in gastric cancer as a tumor marker, and one study indicates that CA 72-4 is a reliable tumor marker of disease stage and activity in gastric cancer with a specificity and sensitivity of 95% and 0.94, respectively (Byrne *et al.,* 1990).

CA 125

The glycoprotein CA 125 is a higher MW mucin that is predominantly associated with ovarian carcinomas (Kabawat *et al.,* 1983) but has also been detected in other carcinomas including pancreatic carcinomas (Mattes *et al.,* 1990) and in normal lung tissue (Noumen *et al.,* 1986) and breast milk (Hanisch *et al.,* 1985). The use of CA 125 in combination with CEA has been shown to reliably distinguish malignant cystic pancreatic tumors and potentially premalignant mucinous cystic neoplasms from pseudocysts and serous cystadenomas (Lewandrowski *et al.,* 1993).

CA 242

The epitope recognized by CA 242 has been shown to be a sialated carbohydrate structure situated on the same macromolecules as CA 50, but it is completely unique from the latter (Röthlin *et al.,* 1993). The CA 50 mAb reacts with serum samples from pancreatic cancer and has a sensitivity of 66.2% (90% specificity level). The use of CA 242 alone does not improve on the sensitivities reached with CA 19-9 and CA 50, but in combination with these antibodies it results in higher sensitivity and specificity (Röthlin *et al.,* 1993).

CA 494

The CA 494 antigen is another epitope on the same mucin on which CA 19-9 and CA 50 are located. A mAb, BW 494, initially isolated from BALB/c mice immunized with a human colon cancer cell line, defines the CA 494 antigen and has been shown to have a high immunohistochemical binding capacity for pancreatic ductal carcinomas (Friess *et al.,* 1993). The sensitivity of CA 494 for pancreatic cancer is 90%, whereas the specificity for chronic pancreatitis is 94%.

PAM4

The epitope PAM4 is a murine mAb directed against a pancreatic cancer–derived mucin that reacts with greater than 80% of the human pancreatic carcinomas and is nonreactive with normal pancreatic tissue (Gold *et al.,* 1995). This epitope is distinct from that of CA 19-9, DU PAN-2, Span-1, and Lewis antigens. Its high specificity has proved useful for diagnostic and therapeutic approaches.

CAM 17-1

The assay for the CAM 17-1 mAb is an enzyme-linked immunoassay that uses lectin wheatgerm agglutinin as a capture agent (Yiannakou *et al.,* 1997). The lectin binds to *N*-acetylglucosamine or sialic acid, components of oligosaccharides that are abundant on mucins. Thus, CAM 17-1 has an advantage over CA 19-9 because its epitope is ubiquitous. The sensitivity and specificity in patients with pancreatic cancer were 86% and 91%, respectively. Use of this assay in combination with ultrasonography identified 94% of the patients with pancreatic tumors and 100% of those with resectable tumors.

TKH2

The sialyl-Tn antigen, a disaccharide antigen found on mucin proteoglycan, was detected by immunohistochemical studies using the mAb TKH2. This antigen is expressed on colon epithelial cells in a cancer-associated fashion (Ogata *et al.,* 1995). TKH2 detects the tumor-associated sialylated antigens, and these sialylated epitopes can be expressed in different gastrointestinal epithelial cells and cancer tissues including carcinomas of the colon, stomach, and pancreas.

A10

A10 is an immunoglobulin M (IgM) mAb raised against murine Ehrlich tumor cells that has been demonstrated to inhibit their growth. It recognizes an undefined carbohydrate epitope that is carried on a high MW cell-surface glycoprotein (Medina *et al.,* 1999). A10 mAb reacts strongly with most human colon adenocarcinomas but not with normal colon. A10 is also reactive with a selected variety of adenocarcinomas including pancreatic adenocarcinomas and nonmalignant ductal cells of the pancreas.

Studies using human pancreatic cancer tissue and human pancreatic cancer cell lines have identified some characteristic genetic alterations associated with the development of this disease, indicating that accumulation of some oncogenic activation is associated with the tumor phenotype. The most common molecular abnormality in pancreatic cancer is the point mutations in the codon 12 of the K-*ras* oncogene, located on chromosome 12p13. This mutation occurs in 70–90% of ductal adenocarcinomas, which is higher than rates observed in either acinal (8%) or endocrine tumors (0%) (Almoguera *et al.,* 1988; Solcia *et al.,* 1997). The alternative common changes are deletions or mutations that occur in many codons of the *p53* tumor-suppressor gene (40–60% of ductal cancers and 8% of endocrine tumors) (Solcia *et al.,* 1997). Preneoplastic ductal lesions and invasive adenocarcinoma have been shown to harbor mutations in genes including *p53* (Boschman *et al.,* 1994), *p16* (Moskaluk *et al.,* 1997), and activated telomerase (Suehara *et al.,* 1997). Activation of epidermal growth factor (EGF), EGF receptor (EGFR), and *HER-2/neu* protooncogene pathways in concert with transforming growth factor-alpha (TGF-α) expression have a role in the pathogenesis of pancreatic cancer by forming an autocrine growth-stimulating mechanism (Smith *et al.,* 1987). Other genetic alterations associated with pancreatic malignancies are as follows: *bcl-2* gene family and its corresponding proteins, Smad4, retinoblastoma (Rb), TGF-β, p15, p21, fibroblast growth factor (FGF), insulin-like growth factor (IGF), vascular endothelial growth factor (VEGF), and multidrug resistance gene (MDR) (see review by Wolff *et al.,* 2000). A number of chromosomal examinations have identified the rearrangement and allelic loss in chromosome 1p, 1q, 6q, 12p, 16q, 17p, and 18q (Solcia *et al.,* 1997).

To date, no clear correlation between prognosis or disease-free survival and these genetic changes have been established. It is worth noting here that these genetic changes are not always specific and diagnostic for pancreatic carcinogenesis. For example, K-*ras* codon 12 mutations are also observed in other malignancies such as gastrointestinal cancers and cancers in the hepatobiliary tract and pancreas. These cancers are also indistinguishable by IHC alone.

In summary, because there is no antibody available as an immunohistochemical marker "specific" to pancreatic neoplastic cells, IHC testing is of limited diagnostic value. Some CAs, such as CA 19-9, however, appear to have great value as pancreatic tumor markers. They have served 1) to identify that ~86% of malignant tumors express the CA 19-9 antigen, 2) for patient follow-up, and 3) as the predictor of patient response over the course of treatment by measuring the kinetics of serum CA 19-9 concentrations. Use of the CA 19-9 assay in combination with other tumor markers, medical imaging, and cytohistologic studies increases the diagnostic rate for pancreatic cancer. The clinical application of genetic analyses specific for pancreatic malignancy is a promising approach both for establishing an accurate diagnosis and for the understanding of novel characteristics of pancreatic cancer.

References

Almoguera, C., Shibata, D., Forrester, K., Martin, J., Arnheim, N., and Perucho, M. 1988. Most human carcinomas of the exocrine pancreas contain mutant c-K-*ras* genes. *Cell*. *53*:549–554.

Boschman, C.R., Stryker, S., Reddy, J.K., and Rao, M.S. 1994. Expression of p53 protein in precursor lesions and adenocarcinoma of human pancreas. *Am. J. Pathol. 145*:1291–1295.

Byrne, D.J., Browning, M.C.K., and Cuschieri, A. 1990. CA72-4: A new tumour marker for gastric cancer. *Br. J. Cancer 77*:1010–1013.

Ching, C.K., Holmes, S.W., Holmes, G.K.T., and Long, R.G. 1993. Comparison of two sialosyl-Tn binding monoclonal antibodies (MLS102 and B72.3) in detecting pancreatic cancer. *Gut 34*: 1722–1725.

Cote, R.J., and Taylor, C.R. 1996. Immunohistochemistry and related marking techniques. In Damjanov, I., and Linder, J., (ed) *Anderson's Pathology,* 10th edition. Philadelphia: Mosby, 136–175.

Del Villano, B.C., Brennan, S., Brock, P., Bucher, C., Liu, V., McClure, M., Rake, B., Space, S., Westrick, B., Schoemaker, H., and Zurawski, V.R. 1983. Radio-immunometric assay for a monoclonal antibody-defined tumor marker CA 19-9. *Clin. Chem. 29*:549–552.

DiMagno, E.P. 1996. Carcinoma of the pancreas. In Bennett, J.C., and Plum, F., (eds), Cecil textbook of medicine, 20th edition, Philadelphia: W.B. Saunders Company, 736–738.

Friess, H., Büchler, M., Auerbach, B., Weber, A., Malfertheiner, P., Hammar, K., Madry, N., Greiner, S., Bosslet, K., and Beger, H.G. 1993. CA 494: A new tumor marker for the diagnosis of pancreatic cancer. *Int. J. Cancer 44*:759–763.

Githens, S. 1988. The pancreatic duct cell: Proliferative capabilities, specific characteristics, metaplasia, isolation, and culture. *J. Pedistr. Gastroenterol. Nutr. 7*:486–506.

Githens, S. 1993. Differentiation and development of the pancreas in animals. In Go, V.L.W. (ed), *The Pancreas: Biology, Pathobiology, and Disease,* New York: Raven Press, 21–55.

Gold, D.V., Alisauskas, R., and Sharkey, R.M. 1995. Targeting of xenografted pancreatic cancer with a new monoclonal antibody, PAM4. *Cancer Res. 55*:1105–1110.

Gudjonsson, B. 1987. Cancer of the pancreas. *Cancer 60*:2284–2303.

Guillou, L., Nordback, P., Gerber, C., and Schneider, R.P. 1994. Ductal adenocarcinoma arising in heterotopic pancreas situated in hiatal hernia. *Arch. Pathol. Lab. Med. 118*:568–571.

Gupta, M., Arciaga, R., Bocci, L., Tubbs, R., Bukowski, R., and Deodhar, S. 1985. Measurement of a monoclonal antibody-defined antigen (CA 19-9) in the sera of patients with malignant and nonmalignant diseases. *Cancer 56*:277–283.

Hammarström, S. 1985. Chemistry and immunology of CEA, CA 19-9 and CA 50. Holmgren, J. (ed), *Tumor Marker Antigens*. Lund: Studentlitteratur 32–49.

Hanisch, F.G., Uhlenbruck, G., Dienst, C., Stottrop, M., and Hippauf, E. 1985. CA125 and CA 19-9: Two cancer associated sialosaccharide antigens on a mucous glycoprotein from human milk. *Eur. J. Biochem. 149*:323–330.

Heinemann, V., Schermuly, M.M., Stieber, P., Schulz, L., Jüngst, D., Wilkowski, R., and Schalhorn, A. 1999. CA 19-9: A predictor of response in pancreatic cancer treated with gemcitabine and cisplatin. *Anticancer Res. 19*:2433–2436.

Hickman, D.M., Frey, C.F., and Carson, J.W. 1981. Adenocarcinoma arising in heterotopic pancreas. *West. J. Med. 135*:57–62.

Jiang, W., Kahn, S., Guillem, J.G., Ku, S., and Weinstein, I.B. 1989. Rapid detection of ras oncogenes in human tumors: Applications to colon, esophageal, and gastric cancer. *Oncogene 4*:923–928.

Juhl, H., Schmiegel, W., and Kalthoff, H. 1996. Clinical applications of cancer-associated antigens. In Neoptolemos, J.P., and Lemoine, N.R. (eds), *Pancreatic Cancer: Molecular and Clinical* Advances. London: Blackwell Science, 214–223.

Kabawat, S.E., Bast, R.C., Welch, W.R., Knapp, R.C., and Colvin, R.B. 1983. Immunopathologic characterization of a monoclonal antibody that recognizes common surface antigens of human ovarian tumors of serous, endometrioid, and clear cell types. *Am. J. Clin. Pathol. 79*:98–104.

Köhler, G., and Milstein, C. 1975. Continuous cultures of fused cells secreting antibody of predefined specificity. *Nature 256*:495–497.

Lan, M.S., Finn, O.J., Fernsten, P.D., and Metzgar, R.S. 1985. Isolation and properties of human pancreatic adenocarcinoma-associated antigen, DU-PAN-2. *Cancer Res. 45*:305–310.

Lewandrowski, K.B., Southern, J.F., Pins, M.R., Compton, C.C., and Warshaw, A.L. 1993. Cyst fluid analysis in the differential diagnosis of pancreatic cysts. *Ann. Surg. 217*:41–47.

Magnani, J.L., Brockhaus, M., Smith, D.F., Ginsburg, V., Blaszczyk, M., Mitchell, K.F., Steplewski, Z., and Koprowski, H. 1981. A monosialoganglioside is a monoclonal antibodydefined antigen of colon carcinoma. *Science 212*:55–56.

Mattes, M.J., Major, P.P., Goldenberg, D.M., Dion, A.S., Hutter, R.V.P., and Klein, K.M. 1990. Pattern of antigen distribution in human carcinomas. *Cancer Res. 50*:880s–884s.

Medina, M., Vélez, D., Asenjo, J.A., Egea, G., Real, F.X., Gil, J., and Subiza, J. 1999. Human colon adenocarcinomas express a MUC1-associated novel carbohydrate epitope on core mucin glycans defined by a monoclonal antibody (A10) raised against murine Ehrlich tumor cells. *Cancer Res. 59*:1061–1070.

Moskaluk, C.A., Hruban, R.H., and Kern, S.E. 1997. p16 and K-ras gene mutations in the intraductal precursors of human pancreatic adenocarcinoma. *Cancer Res. 57*:2140–2143.

Nilsson, O., Månsson, J.E., Lindholm, L., Holmgren, J., and Svennerholm, L. 1985. Sialosyllactotetraosylceramide, a novel ganglioside antigen detected in human carcinomas by a monoclonal antibody. *FEBS Lett. 182*:398–402.

Noumen, E.J., Pollet, D.E., Eerdekens, M.W., Hendrix, P.G., Briers, T.W., and DeBroe, M.E. 1986. Immunohistochemical localization of placental alkaline phosphatase, carcinoembryonic antigen and cancer antigen 125 in normal and neoplastic human lung. *Cancer Res. 46*:866–876.

Ogata, S., Ho, I., Chen, A., Dubois, D., Maklansky, J., Singhal, A., Hakomori, S., and Itskowitz, S.H. 1995. Tumor-associated sialylated antigens are constitutively expressed in normal human colonic mucosa. *Cancer Res. 55*:1869–1874.

Osako, M., Yonezawa, S., Siddiki, B., Huang, J., Ho, J.J.L., Kim, Y.S., and Sato, E. 1993. Immunohistochemical study of mucin carbohydrates and core proteins in human pancreatic tumors. *Cancer 71*:2191–2199.

Osanai, M., Miyokawa, N., Tamaki, T., Yonekawa, M., Kawamura, A., and Sawada, N. 2001. Adenocarcinoma arising in gastric heterotopic pancreas: Clinicopathological and immunohistochemical study with genetic analysis of a case. *Pathol. Int. 51*:549–554.

Ricolleau, G., Kremer, M., Curtet, C., Fumoleau, P., Douillard, J.Y., Le Mevel, B., Le Bodic, L., and Chatal, J.F. 1983. Intérêt diagnostique comparé au radio-immunodosage de I'antigène carcino-embryonnaire et de I'antigène CA 19-9 isolé par un anticorps monoclonal. *Gastroentérol. Clin. Biol. 7*:25A.

Röthlin, M.A., Joller, H., and Largiadér, F. 1993. CA242 is a new tumor marker for pancreatic cancer. *Cancer 71*:701–707.

Rubin, D., Warshaw, A.L., Southern, J.F., Pins, M., Compton, C.C., and Lewandrowski, L.B. 1994. Expression CA 15.3 protein in the cyst contents distinguishes benign from malignant pancreatic mucinous cyst neoplasms. *Surgery 115*:52–55.

Smith, J.J., Derynck, R., and Korc, M. 1987. Production of transforming growth factor alpha in human pancreatic cancer cells: Evidence for a superagonist autocrine cycle. *Proc. Natl. Acad. Sci. USA 84*:7567–7570.

Solcia, E., Capella, C., and Klöppel, G. 1997. Atlas of tumor pathology. Third series. Fascicle 20. In Rosai, J., (ed), *Tumor of the Pancreas.* Washington, DC: Armed Forces Institute of Pathology. 64–88.

Steinberg, W. 1990. The clinical utility of the CA 19-9 tumor associated antigen. *Am. J. Gastroenterol. 85*:350–355.

Suehara, N., Mizumoto, K., Muta, T., Tominaga, Y., Shimura, H., Kitajima, S., Hamasaki, N., Tsuneyoshi, M., and Tanaka, M. 1997. Telomerase elevation in pancreatic ductal carcinoma compared to nonmalignant pathological states. *Clin. Cancer Res. 3*:993–998.

Takeda, S., Ichii, S., and Nakamura, Y. 1993. Detection of K-ras mutation in sputum by mutant allele specific amplification (MASA). *Hum Mutat. 2*:112–117.

Tatsuta, M., Yamamura, H., Iishi, H., Ichii, M., Noguchi, S., Yamamoto, R., and Okuda, S. 1985. Values of CA 19-9 in the serum, pure pancreatic juice and aspirated pancreatic material in the diagnosis of malignant pancreatic cancer. *Cancer 56*:2669–2673.

Wolff, R.A., Abbruzzese, J.L., and Evans, D.B. 2000. *Cancer medicine,* 5th edition, Hamilton, Ontario, Canada: B.C. Decker Inc., 1436–1464.

Yiannakou, J.Y., Newland, P., Calder, F., Kingnorth, A.N., and Rhodes, J.N. 1997. Prospective study of CAM 17-1/WGA mucin assay for serological diagnosis of pancreatic cancer. *Lancet 349*:389–392.

Yuan, S.Z., Ho, J.J.L., Yuan, M., and Kim, Y.S. 1985. Human pancreatic cancer-associated antigens detected by murine monoclonal antibodies. *Cancer Res. 45*:6179–6187.

Zamora, C., Sahel, J., Cantu, D.G., Heyries, L., Bernard, J.P., Bastid, C., Payan, M.J., Sielezneff, I., Familiari, L., Sastre, B., and Barthet, M. 2001. Intraductal papillary and mucinous tumors (IPMT) of the pancreas: Report of a case series and review of the literature. *Am. J. Gastroenterol. 96*:1441–1447.

8

Role of Mucins in Pancreatic Carcinoma

Genevieve M. Monges and Marie-Pierre A. Mathoulin-Portier

Introduction

Mucins (MUCs) are heavily glycosilated, high molecular weight (MW) glycoproteins, many of which are synthesized by specialized mucus-producing epithelial cells. These molecules are widely synthesized and expressed by epithelial cells of the gastrointestinal, respiratory, and genitourinary tracts (Gendler and Spicer, 1995). They serve mainly to lubricate and protect mucosal ducts. Some of these proteins may also be involved in regulating cell multiplication and differentiation, modulating cell adhesion, promoting metastasis, and modulating immune reactions (Ringel and Lohr, 2003). An aberrant expression profile is observed in various malignancies. The MUC expression pattern will represent potential diagnostic markers for detection of pancreatic cancer and specific discrimination between pancreatic cancer and benign pancreatic diseases. These peptides therefore represent a potential target for tumor immunotherapy (Heukamp *et al.,* 2001).

Since 1987, eight types of mucin-encoding genes (*MUC* genes) have become well known and have been identified on various chromosomes (Moniaux *et al.,* 2001). These include *MUC1-4, MUC5B, MU5C, MUC6,* and *MUC7.* Two others, *MUC8* and *MUC9,* have also been described, but their characterization is as yet incomplete. Partial complementary deoxyribonucleic acid (cDNA) sequences for *MUC11* and *MUC12* have been published. MUC13 was identified as a cell-surface mucin expressed by epithelial cells and hematopoietic cells (Williams *et al.,* 2001) MUC16 is the most recent member of the MUC protein family. It was characterized from a cDNA sequence encoding a mucin that has long been known as the ovarian cancer marker: CA125 (Yin *et al.,* 2002). They are VNTR genes (genes with a variable number of tandem repeats), from which the major peptide domain produced consists of tandem-repeat amino acid sequences. Because these genetic sequences are unstable, they show a high level of interindividual polymorphism. This raises the question as to whether this has consequences in terms of genetic predisposition to mucosal disorders. These genes code for high MW proteins (mucins), which contain high levels of threonine and serine. It has been suggested that the qualitative and quantitative changes found to occur in these mucins in several types of cancer may be the result of alterations in the pattern of glycosylation occurring in these molecules. Previous reports have described the heterogeneous and anomalous glycans associated with mucins of tumors. Because MUC1 is the mucin that has been studied the most, the immunohistochemical techniques will be described in detail for this mucin only.

Handbook of Immunohistochemistry and *in situ* Hybridization of Human Carcinomas, Volume 3: Molecular Genetics, Liver Carcinoma, and Pancreatic Carcinoma

Expression of MUC1 on a cell surface was detected using three monoclonal antibodies (MAbs) raised against the tandem repeat sequence: MAb H23 (Tsarfaty *et al.,* 1990) (specific for the epitope APDTR within the repeat array); MAb 12C10, specific for MUC1, exact epitope unknown; and MAb 1G5 (epitope APDTRP within the tandem repeat). The specificity of the three monoclonal antibodies has already been established (Balloul *et al.,* 1994; Tsarfaty *et al.,* 1990).

MATERIALS

1. Formaldehyde 40% (1/3) in alcohol 80% (2/3).
2. Paraffin for embedding.
3. Capillary Gap microscope slides (Dako, Glostrup, Germany, with blue painting areas), coverslips.
4. Phosphate buffer saline (PBS) Dulbecco's (10X) diluted to 10%.
5. Antibody diluent ready to use (Dako).
6. Primary antibody diluted in diluent: H23 (1/500).
7. Hydrogen peroxide (30%), diluted 3% in distilled water.
8. Blocking serum: buffer 1 (Dako kit) ready-to-use, containing carrier protein, detergent, and preservative.
9. Link, biotinylated secondary antibody (AB2) ready-to-use. Biotinylated anti-mouse and anti-rabbit immunoglobulins in buffered solution, containing carrier protein and sodium azide.
10. Streptavidine peroxidase (horseradish peroxidase, or HRP) ready-to-use. Streptavidine conjugated to HRP in buffered solution, containing carrier protein and preservative.
11. Chromogenic substrate (AEC), ready-to-use. Buffered solution of hydrogen peroxide and 3-amino-9-ethylcarbazole.
12. Mayer's hematoxylin ready-to-use, filtered before use.
13. Aqueous mounting media.

METHODS

Fixation: specimens are fixed in formaldehyde-alcohol overnight, then they are treated including automat overnight until embedding in paraffin wax.

Sections: sections 4 μm thick are applied to special slides and baked overnight at 60°C.

Deparaffinization:

Histolemon: 3 × 10 min

Ethanol: 3 × 5 min

Normal water: 10 min

Immunostaining: at room temperature.

Do not forget positive and negative control slides.

1. Rinse the slides in distilled water.
2. Hydrogen peroxide 3%: 5 min.
3. Rinse in PBS: 2 × 3 min.
4. At this step surround the sections with a special pencil.
5. Apply blocking serum: 10 min (buffer 1, Dako).
6. At this point do not rinse the slides; clear the buffer.
7. Incubate at room temperature for 1 hr with primary antibody (AB2).
8. Rinse in PBS: 2 × 2 min.
9. Link, biotinylated secondary antibody (AB2): 25 min.
10. Rinse in PBS: 2 × 2 min.
11. Streptavidine peroxidase (HRP): 25 min.
12. Rinse in PBS: 2 × 2 min.
13. Chromogenic substrate (AEC): ≃10 min, but at this step control the revelation.
14. Rinse in PBS: 5 min. Then rinse in distilled water: 5 min.
15. Counterstain nuclei with hemathoxylin filtered: 1 min.
16. Tissue sections should be mounted with aqueous mounting medium.

DISCUSSION

Normal pancreases seem to express predominantly MUC1 and MUC6. MUC1 is a member of the membrane-bound mucins, involved in the renewal and differentiation of the epithelium, in the modulation of cell adhesion, and in cell signaling (Mensdorff-Pouilly *et al.,* 2000). The product of the MUC1 gene (apomucin of the mammary type) is the best known of all the MUC gene products. It has been identified in normal pancreatic tissue as well as in a large number of pancreatic adenocarcinomas (Monges *et al.,* 1999). Overexpression of MUC1 can lead to the presence of the protein in serum, where it can be readily assayed using a technique described for the diagnosis and surveillance of pancreatic carcinoma (Kotera *et al.,* 1994). It has also been established that, in patients with pancreatic adenocarcinomas, T-lymphocytes are present that recognize a specific MUC1 epitope. This finding shows that these patients have acquired an immune reaction against MUC-1 protein. Based on all these data, research is under way to develop and test vaccination and active immunotherapeutic procedures (Balloul *et al.,* 1994). The mucin MUC6 is a secreted gel-forming mucin, a member of the group of mucins

including MUC2, MUC5AC, and MUC5B, located within the 11p15 chromosomal locus. Of the other MUCs, MUC2 and MUC4, which are usually undetectable in normal pancreas, seem to play important roles—MUC2 in intraductal papillary mucinous neoplasms (IPMN) and MUC4 as a marker for pancreatic adenocarcinoma.

MUC1 in Pancreatic Adenocarcinomas

The *MUC1* gene codes for a membrane glycoprotein that is present in most epithelial cells. It is located on chromosome 1q21-24, and its genomic structure has been almost completely determined. Its major peptide domain consists of VNTR sequences each of 20 amino acids. This is the main MUC gene expressed in the normal pancreas, but abnormally high levels have also been observed in neoplastic epithelial cells from patients with breast, ovarian, pancreatic, and (to a lesser extent) colonic carcinomas (Ringel and Lohr, 2003).

The initial work on MUC1 concentrated on the MUC1 expression profile in the normal and tumoral pancreatic tissue. The work has subsequently examined MUC1 expression in the different stages of dysplasia PaNIn (pancreatic intraepithelial neoplasia) I, II, and III.

Gene product expression of MUC1 has been explored by several methods, including immunohistochemistry (IHC), *in situ* hybridization, and Northern Blot analysis, and the results obtained have shown excellent agreement between the methods. The mucin has been detected using each of these methods in normal ductal and acinar cells as well as in exocrine pancreatic carcinoma. The results obtained in our previous study (Monges *et al.,* 1999), by using IHC on the normal exocrine pancreas, showed positive staining by anti-MUC1 antibodies of the ductal, acinar, and centroacinar cells, further confirming the *in situ* hybridization data published (Balague *et al.,* 1995). Various patterns of immunohistochemical staining have been described so far by authors using various anti-MUC1 antibodies, ranging from simple apical membrane staining to dense, diffuse cytoplasmic labeling. The patterns of immunostaining described depend on the antibodies used Balague *et al.* (1995) used anti-MUC1 antibodies BC1 and BC2 and reported that ductal cells were labeled only apically, whereas cytoplasmic labeling was observed in normal acinar cells and in tumor cells. With all the antibodies used in our study, all the normal pancreatic cells, including those of both ductal and acinar origin, showed the same pattern of strictly apical immunostaining. The pattern of staining obtained on chronic pancreatic tissue was practically identical with that obtained with normal tissue, apart from occasional patches of basolateral membrane labeling, instead of the strictly apical distribution obtained with the duct cells. Completely different results were obtained with the ductal adenocarcinomas, which showed a cytoplasmic pattern of immunoreactivity in 38 cases out of the 39 studied with the antibody H23. Only two acinar cell tumors were studied in this experimental series. In both cases, MUC1 protein was expressed and the immunolabeling was again cytoplasmic. In our study (Monges *et al.,* 1999), the most commonly expressed epitope was that recognized by the monoclonal antibody H23.

In mucinous cystadenoma the pattern is identical to normal ductal cells. In mucinous cystadenocarcinoma the pattern is identical to pancreatic adenocarcinoma, with abrupt zones of modification between the nontransformed zones and the zones with malignant transformation (Figure 54 and Figure 55). Pancreatic carcinoma is associated with enormous diagnostic problems, especially when the diagnosis is performed on a fine-needle aspiration biopsy. Based on the conspicuous and consistent differences observed between the patterns of immunostaining obtained in malignant tumors and nonmalignant pancreatic disease, it should be possible to achieve more accurate diagnosis. To assist diagnostics on microbiopsies and monolayer cytology, we use the monoclonal antibody H23.

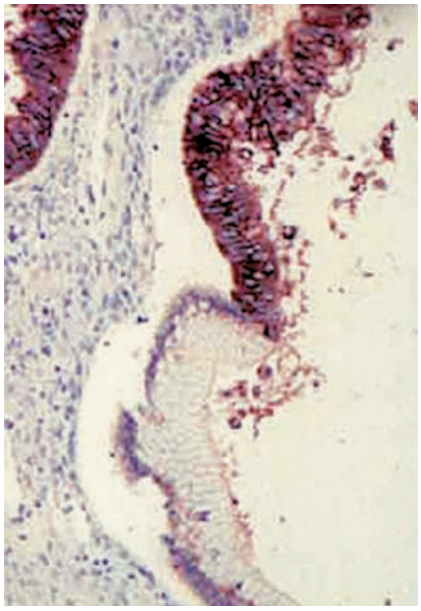

Figure 54. Mucinous cystadenoma and mucinous cystadenocarcinoma. (HES, 400X.)

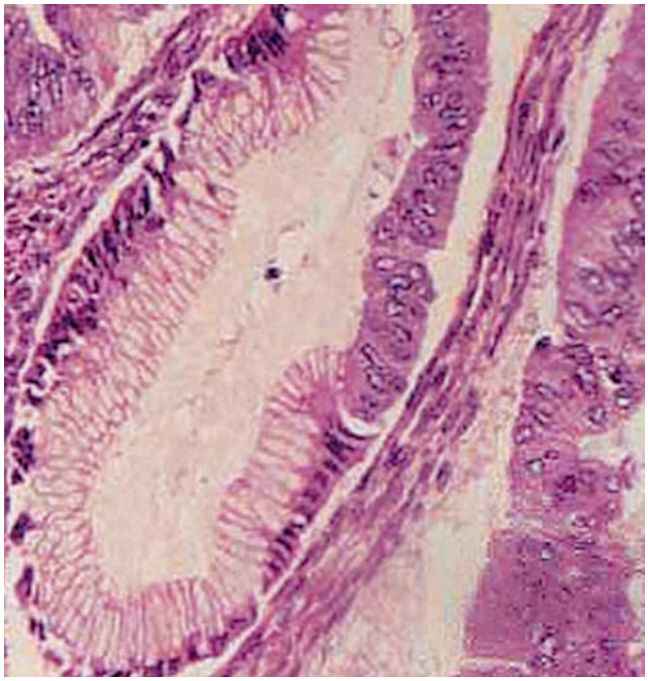

Figure 55. Mucinous cystadenoma and mucinous cystadenocarcinoma mucin1: H23 immunostaining. (400X.)

Previous studies of the possible correlation between MUC1 expression and long-term survival have mostly been carried out on breast carcinoma and have yielded contradictory results. Some authors have claimed that a correlation exists between MUC1 expression and a fairly favorable prognosis. MUC1 may serve as a marker of differentiation in breast cancer. For the pancreas, the results are contradictory concerning the prognostic value of this marker. Other studies have shown that MUC1 can contribute to changes in intercellular adhesion and, thus, to invasive processes and to the development of metastases (Satoh *et al.,* 2000). The mucin MUC1 is known to have an inhibitory role in cell–cell and cell–stroma interactions as well as in immunoresistance of tumor cell calls and is a marker of the aggressive pathway of pancreatic intraepithelial neoplasia (PanIN) to ductal carcinoma (Adsay *et al.,* 2002).

Changes in the expression of the MUC1 gene product may occur for several reasons, such as aberrant glycosylation, deficient glycosylation, or an anomalous expression of the gene coding for MUC1. An aberrant or defective process of glycosylation could lead to a decrease in the amount of mature glycoprotein available, to an accumulation of abnormal products, and hence to inappropriate compartmentation of these products. An anomalous expression of the gene, consisting of either a complete lack of expression or an overexpression of the protein in the cytoplasm of the neoplastic cells, could also be responsible. These mechanisms might also account for the alterations in cell adhesion cited earlier.

Moreover, a cytotoxic T-lymphocyte response to MUC1 has been observed in patients with breast, ovarian, and pancreatic carcinoma. Met-mice (an animal model for pancreatic cancer) mimic the human condition and are an excellent model with which to elucidate the native immune responses that develop during tumor progression and to develop effective anti-tumor vaccine strategies (Mukherjee *et al.,* 2000).

In the study of Kotera *et al.* (1994), 16.7% of the patients with adenocarcinoma of the pancreas were found to show humoral immunity to MUC1 protein. Research is under way to develop and test appropriate immunization and active immunotherapeutic strategies. In our study, 97% of the patients with pancreatic adenocarcinomas were found to express MUC1 protein at the cellular level; hence, such patients might in the future benefit from immunization against MUC1 protein or from active immunotherapy.

MUC1 in Pancreatic Adenocarcinomas and Precursor Lesions

According to the studies about the relationship between hyperplastic, dysplastic epithelial lesions and ductal adenocarcinoma there is increasing knowledge about the expression of MUC1 in adenocarcinoma and the precursory lesions. The present ductal pancreatic cancer model is based on the concept of intraepithelial neoplasia and describes a series of lesions termed PanIN. Three grades of PanINs are determined: PanIN I, PanIN II, and PanIN III. The distinctions are based on architectural and morphologic criteria and cytologic atypia. Overexpression of MUC1 has been observed in all stages of PanINs (Andrianifahanana *et al.,* 2001; Kim *et al.,* 2002) indicating the early occurrence of MUC1 in the development of DACs. Overexpression is correlated to the degree of PanIN (Adsay *et al.,* 2002).

MUC1 and MUC2 in Intraductal Papillary Mucinous Neoplasms

The IPMN are large, intraductal tumors with ductal dilatation, often associated with colloid carcinoma, which has a much better prognosis than ductal carcinomas: 5-year survival >55% versus 15% for ductal carcinoma. Adsay *et al.* (2002) showed that the expression of MUC1 is infrequent in IPMN (20%) and in colloid carcinoma (0%). However, MUC2 is very frequently observed in these two pathologies and absent in the PanINs and the adenocarcinomas, as if there were a dichotomy between these two groups of entities.

The expression of MUC1 and MUC2 reflects aggressive or indolent phenotypes in pancreatic cancer.

Yonezawa *et al.* (2002), found that for IPMN with carcinomatous change showing invasive growth, the invasive areas acquired a characteristic of MUC1 expression. The IPMN with poor outcome showed a pattern of MUC1 (+), MUC2 (–), and MUC5AC (+ or –); in contrast, IPMN with a favorable outcome showed the pattern MUC1 (–), MUC2 (+), and MUC5AC (+).

For Suda *et al.* (2000) and Terris *et al.* (2002), the mucin expression profile supports the existence of two types of invasive tumor associated with IPMN: a colloid and an ordinary form, differing in the pattern of MUCs expression and in the outcome of the tumor. The mucin profile of noninvasive and invasive mucinous cystic neoplasm of the pancreas is comparable. Noninvasive mucinous cystic neoplasms were all negative for MUC1 and positive for MUC5AC regardless of the degree of cellular atypia. Only in cases with an invasive component was MUC1 expression observed (Luttges *et al.,* 2002).

MUC4 in Pancreatic Adenocarcinomas

The mucin MUC4 is usually undetectable in normal pancreas. The Andrianifahanana *et al.* (2001) study using reverse transcription-polymerase chain reaction demonstrates a *de novo* expression of MUC4 in pancreatic adenocarcinoma and cell lines. The mucin MUC4 displayed a differential expression that was specific for pancreatic carcinoma. This tumor-associated mucin could be used to discriminate between pancreatic carcinoma and pancreatitis. Furthermore, the MUC 4 expression profile observed in pancreatic cell lines may suggest a link between the level of MUC4 messenger ribonucleic acid and the tumor cell differentiation stage. These findings may affect the development of highly specific techniques that allow the detection of the MUC4 antigen in the circulation, which in turn may represent a significant step toward the diagnosis of pancreatic carcinoma at its earliest stage of development.

Further studies on the biological characterization of MUC1, MUC2, and MUC4 should yield valuable information that may help elucidate mechanisms underlying human pancreatic carcinogenesis and may facilitate the design of therapeutic strategies.

References

Adsay, N.V., Merati, K., Andea, A., Sarkar, F., Hruban, R.H., Wilentz, R.E., Goggins, M., Iacobuzio-Donahue, C., Longnecker, D.S., and Klimstra, D.S. 2002. The dichotomy in the preinvasive neoplasia to invasive carcinoma sequence in the pancreas: Differential expression of MUC1 and MUC2 supports the existence of two separate pathways of carcinogenesis. *Mod. Pathol. 15*:1087–1095.

Andrianifahanana, M., Moniaux, N., Schmied, B.M., Ringel, J., Friess, H., Hollingsworth, M.A., Buchler, M.W., Aubert, J.P., and Batra, S.K. 2001. Mucin (MUC) gene expression in human pancreatic adenocarcinoma and chronic pancreatitis: A potential role of MUC4 as a tumor marker of diagnostic significance. *Clin. Cancer Res. 7*:4033–4040.

Balague, C., Audie, J.P., Porchet, N., and Real, F.X. 1995. *In situ* hybridization shows distinct patterns of mucin gene expression in normal, benign, and malignant pancreas tissues. *Gastroenterology 109*:953–964.

Balloul, J.M., Acres, R.B., Geist, M., Dott, K., Stefani, L., Schmitt, D., Drillien, R., Spehner, D., and McKenzie, I. 1994. Recombinant MUC1 vaccinia virus: A potential vector for immunotherapy of breast cancer. *Cell Mol. Biol.* (Noisy.-le-grand) *40* Suppl 1: 49–59.

Gendler, S.J., and Spicer, A.P. 1995. Epithelial mucin genes. *Annu. Rev. Physiol. 57*:607–634.

Heukamp, L.C., van der Burg, S.H., Drijfhout, J.W., Melief, C.J., Taylor-Papadimitriou, J., and Offringa, R. 2001. Identification of three non-VNTR MUC1-derived HLA-A*0201-restricted T-cell epitopes that induce protective anti-tumor immunity in HLA-A2/K(b)-transgenic mice. *Int. J. Cancer 91*:385–392.

Kim, G.E., Bae, H.I., Park, H.U., Kuan, S.F., Crawley, S.C., Ho, J.J., and Kim, Y.S. 2002. Aberrant expression of MUC5AC and MUC6 gastric mucins and sialyl Tn antigen in intraepithelial neoplasms of the pancreas. *Gastroenterology 123*:1052–1060.

Kotera, Y., Fontenot, J.D., Pecher, G., Metzgar, R.S., and Finn, O.J. 1994. Humoral immunity against a tandem repeat epitope of human mucin MUC-1 in sera from breast, pancreatic, and colon cancer patients. *Cancer Res. 54*:2856–2860.

Luttges, J., Feyerabend, B., Buchelt, T., Pacena, M., and Kloppel, G. 2002. The mucin profile of noninvasive and invasive mucinous cystic neoplasms of the pancreas. *Am. J. Surg. Pathol. 26*:466–471.

Mensdorff-Pouilly, S., Snijdewint, F.G., Verstraeten, A.A., Verheijen, R.H., and Kenemans, P. 2000. Human MUC1 mucin: A multifaceted glycoprotein. *Int. J. Biol. Markers 15*:343–356.

Monges, G.M., Mathoulin-Portier, M.P., Acres, R.B., Houvenaeghel, G.F., Giovannini, M.F., Seitz, J.F., Bardou, V.J., Payan, M.J., and Olive, D. 1999. Differential MUC1 expression in normal and neoplastic human pancreatic tissue: An immunohistochemical study of 60 samples. *Am. J. Clin. Pathol. 112*:635–640.

Moniaux, N., Escande, F., Porchet, N., Aubert, J.P., and Batra, S.K. 2001. Structural organization and classification of the human mucin genes. *Front Biosci. 6*:D1192–D1206.

Mukherjee, P., Ginardi, A.R., Madsen, C.S., Sterner, C.J., Adriance, M.C., Tevethia, M.J., and Gendler, S.J. 2000. Mice with spontaneous pancreatic cancer naturally develop MUC-1-specific CTLs that eradicate tumors when adoptively transferred. *J. Immunol. 165*:3451–3460.

Ringel, J., and Lohr, M. 2003. The MUC gene family: Their role in diagnosis and early detection of pancreatic cancer. *Mol. Cancer 2*:9.

Satoh, S., Hinoda, Y., Hayashi, T., Burdick, M.D., Imai, K., and Hollingsworth, M.A. 2000. Enhancement of metastatic properties of pancreatic cancer cells by MUC1 gene encoding an anti-adhesion molecule. *Int. J. Cancer 88*:507–518.

Suda, K., Nobukawa, B., Yamasaki, S., Suzuki, F., Shimizu, H., and Takase, M. 2000. Pre-existing histological type and developmental mechanism of mucinous noncystic carcinoma of pancreas. *Pathol. Oncol. Res. 6*:125–129.

Terris, B., Dubois, S., Buisine, M.P., Sauvanet, A., Ruszniewski, P., Aubert, J.P., Porchet, N., Couvelard, A., Degott, C., and Flejou, J.F. 2002. Mucin gene expression in intraductal papillary-mucinous pancreatic tumours and related lesions. *J. Pathol. 197*:632–637.

Tsarfaty, I., Hareuveni, M., Horev, J., Zaretsky, J., Weiss, M., Jeltsch, J.M., Garnier, J.M., Lathe, R., Keydar, I., and Wreschner, D.H. 1990. Isolation and characterization of an expressed hypervariable gene coding for a breast-cancer-associated antigen. *Gene 93*:313–318.

Williams, S.J., Wreschner, D.H., Tran, M., Eyre, H.J., Sutherland, G.R., and McGuckin, M.A. 2001. Muc13, a novel human cell surface mucin expressed by epithelial and hemopoietic cells. *J. Biol. Chem. 276*:18327–18336.

Yin, B.W., Dnistrian, A., and Lloyd, K.O. 2002. Ovarian cancer antigen CA125 is encoded by the MUC16 mucin gene. *Int. J. Cancer 98*:737–740.

Yonezawa, S., Nakamura, A., Horinouchi, M., and Sato, E. 2002. The expression of several types of mucin is related to the biological behavior of pancreatic neoplasms. *J. Hepatobiliary Pancreat. Surg*. 9:328–341.

9

Immunohistochemical Detection of Cyclooxygenase-2 in Pancreatic Ductal Adenocarcinomas and Neuroendocrine Tumors

Nobuyuki Ohike, Gunter Kloppel, and Toshio Morohoshi

Introduction

Cyclooxygenase (COX) is a rate-limiting enzyme involved in the conversion of arachidonic acid to prostaglandin H_2, which is the precursor of several molecules, including prostaglandins, prostacyclin, and thromboxanes. It consists of at least two related but unique isoforms, COX-1 and COX-2. The *COX-1* gene is located on chromosome regions 9q32-q33.3, and *COX-2* maps to 1q25.2-q25.3. The two proteins show structural and enzymatic similarities, both having a molecular weight of approximately 70 kDa and sharing more than 60% identity at the amino acid level. Nevertheless, they serve distinct functions. *COX-1* is constitutively expressed in a large number of human tissues to mediate house keeping, physiological functions such as vascular homeostasis, gastroprotection, and absorption of sodium and water in the kidney. *COX-2* is an immediate, early-response gene whose expression is induced by growth factors, tumor promoters, cytokines, and other inflammatory mediators. Its overexpression, in fact, has been demonstrated in several human inflammatory diseases e.g., *Helicobacter pylori*–infectious gastritis (Sawaoka *et al.,* 1998), inflammatory bowel disease (Singer *et al.,* 1998), chronic hepatitis (Kondo *et al.,* 1999), Hashimoto's thyroiditis (Cornetta *et al.,* 2002), and rheumatoid arthritis (Kang *et al.,* 1996). Recent studies have highlighted the potential role of *COX-2* in tumorigenesis. Epidemiologic studies indicate that administration of nonsteroidal anti-inflammatory drugs (NSAIDs) that inhibit both *COX-1* and *COX-2* expression reduces the risk for developing many types of human tumors. Oshima *et al.* (1996) showed that the formation of intestinal polyps in $Apc^{\Delta 716}$ knockout mice was dramatically suppressed by crossing these animals with COX-2 knockout mice. COX-2 overexpression has been found in a variety of carcinomas and several effects of COX-2 have been proposed, including inhibition of apoptosis, stimulation of invasiveness and proliferative activity, and facilitation of neovascularization. Epidermal growth factor (EGF), transforming growth factor beta (TGF-β), and their receptors as well as inducible nitric oxide synthase (iNOS) emerge as significant COX-2–inducers, not only in inflammation but also in carcinogenesis.

Handbook of Immunohistochemistry and *in situ* Hybridization of Human Carcinomas, Volume 3: Molecular Genetics, Liver Carcinoma, and Pancreatic Carcinoma

Overexpression of *COX-2* is also observed in premalignant lesions such as adenoma of the colon (Eberhart *et al.,* 1994; Hao *et al.,* 1999) and stomach (Lim *et al.,* 2000), Barrett's esophagus (Wilson *et al.,* 1998), dysplasia of the head and neck (Nathan *et al.,* 2001) and esophagus (Shamma *et al.,* 2000), prostatic intraepithelial neoplasia (Uotila *et al.,* 2001), endometrial hyperplasia (Fujiwaki *et al.,* 2002), and pulmonary atypical alveolar epithelium (Wolff *et al.,* 1998). This suggests that *COX-2* may be involved in early cellular changes leading to the development of several types of carcinoma. Inhibitors of *COX-2* could therefore play a role in chemoprevention of such cancers in a broad range.

Pancreatic ductal adenocarcinoma (PDAC) accounts for 85–90% of all pancreatic neoplasms and is currently the fifth leading cause of cancer death in Western countries. Because there are no suitable markers for early diagnosis, in the majority of patients PDAC is diagnosed at a stage that is not curable by cancer-directed surgery. Unfortunately, it is also barely affected by any other form of cancer-directed therapy, i.e., chemotherapy, radiation therapy, or immunotherapy. To achieve better insight into the disease mechanism, it is important to understand the molecular characteristics of PDAC. It has repeatedly been shown that distinct genes such as the K-*ras* gene and the tumor-suppressor genes *p53, p16,* and *DPC4/SMAD4* are frequently altered in PDAC, and may therefore be essential for its tumorigenesis. Further genetic studies have demonstrated that some cancer-related genes such as vascular endothelial growth factor (VEGF), *Her-2/neu, c-Myc, Rad51, maspin,* and *COX-2* are overexpressed in pancreatic cancer cells. The identification and characterization of these genes will lead to a better understanding of PDAC pathogenesis and provide therapeutic strategies. Especially notable is *COX-2,* because the *COX-2* inhibitors have been demonstrated to inhibit proliferation and induce apoptosis in human pancreatic carcinoma cells (Ding *et al.,* 2000; Molina *et al.,* 1999) and in PDAC in Syrian golden hamsters (Takahashi *et al.,* 1990). Interestingly, pancreatic islets are among the few tissues that constitutively express *COX-2*. However, only a few studies have been done on *COX-2* expression in pancreatic endocrine tumors (PETs) (Ohike and Morohoshi, 2001; Okami *et al.,* 2002).

Here, we reconfirmed *COX-2* expression in 28 PDACs and 20 PETs immunohistochemically using the EnVision ChemMate method. EnVision is a very sensitive detection method for routine immunohistochemistry (IHC) (Sabattini *et al.,* 1998) and is a two-step staining technique in which the primary antibody is followed by a polymeric conjugate in sequential steps. The polymeric conjugate consists of a large number of peroxidase and secondary antibody molecules bound directly to an activated dextran backbone.

MATERIALS

1. Tissue sections: Tumor tissues were fixed in 10% formalin and embedded in paraffin, and the paraffin block sections were cut at into 3-µm thick sections and placed on silane-coated glass slides for immunohistochemical staining.
2. 10 mM citrate buffer: 0.36 g citrate acid·1 H_2O and 2.44 g trisodium citrate·2 H_2O were dissolved in distilled water and made up to 1 L solution.
3. TBS (Tris-buffered saline: 6.06 g trisaminomethane and 3.40 ml HCl) was added to distilled water and the volume was brought up to 1 L with distilled water.
4. TBS containing 0.1% Tween-20 (TBS-T) and 5 ml Tween-20 were added to 5 L of TBS.
5. Primary antibody: Anti-human *COX-2* rabbit polyclonal antibody (IBL, Gunma, Japan) diluted at 1:200 with antibody diluent (DakoCytomation, Kyoto, Japan).
6. Blocking reagent (DakoCytomation).
7. Visualization system: HRP conjugated dextran polymer reagent (DakoCytomation).
8. Chromogen: 3,3-diaminobenzidine tetrahydrochloride (DAB) (DakoCytomation).

METHODS

(ChemMate EnVision working procedure)

1. Bake tumor tissue sections for 30 min at 65°C in incubater, deparaffinize in xylene, and rehydrate through ethanol.
2. Rinse the sections in water.
3. For antigen retrieval, pretreat the sections by microwaving (960 W) for 10 min in 10 mM citrate buffer that has been microwaved for 10 min.
4. Quench the endogeneous peroxidase activity by adding a few drops of 0.3% H_2O_2 onto the sections, and incubate in moisture chamber for 6 min.
5. Rinse the sections with TBS-T, and immerse the sections in TBS-T for 5 min.
6. Add a drop of the blocking reagent onto the sections in order to prevent nonspecific background staining, and place in moisture chamber for 5 min.
7. Tap off the excess blocking reagent and wipe slide; incubate with primary antibody in moisture chamber for 30 min at room temperature.
8. Rinse the sections with TBS-T, and immerse in TBS-T for 5 min.
9. Incubate the sections with dextran polymer reagent (ChemMate, EnVision) in moisture chamber for 30 min at room temperature.
10. Rinse the sections with TBS-T, and immerse in TBS-T for 5 min.

11. Develop the sections with Liquid DAB chromogen in moisture chamber for 10 min at room temperature.
12. Rinse with water.
13. Counterstain lightly with hematoxylin, and rinse in water for 5 min.
14. Dehydrate through ethanol and clear through xylene.
15. Coverslip the sections and mount.

The *COX-2* immunostaining was evaluated as negative, weakly positive, moderately positive, or strongly positive. The cases were then divided into high expressers (i.e., when at least 10% of tumor cells were moderately to strongly positive) and low expressers. We evaluated the *COX-2* expression in relationship to a number of clinicopathological features. Additional immunohistochemical studies used antibodies to Ki-67 (Dako), p53 (Oncogene Research Products, Boston, MA), and DPC4 (Santa Cruz Biotechnology, Santa Cruz, CA). All statistical evaluations were carried out using Student's t-test and χ^2 test for independence (2×2 contingency table). Statistical significance was tested at a probability level of 0.05.

RESULTS AND DISCUSSION

All PDACs showed cytoplasmic staining for COX-2 of variable extent (Figure 56). Of PDACs, 19/28 (67.9%) were classified as high expressers and 9 were low expressers. So far, several authors have reported *COX-2* overexpression in PDACs by Western Blot, reverse transcription polymerase chain reaction (RT-PCR), and IHC, and the frequency of *COX-2* immunohistochemical overexpression ranges from 53% to 90% (Koshiba *et al.,* 1999; Maitra *et al.,* 2002; Merati *et al.,* 2001; Molina *et al.,* 1999; Okami *et al.,* 1999). Tucker *et al*. (1999) showed a more than 60-fold increase in COX-2 messenger ribonucleic acid (mRNA) expression in PDAC tissues in parallel with up-regulation of the COX-2 protein. These findings indicate that COX-2 up-regulation is a frequent event in PDACs.

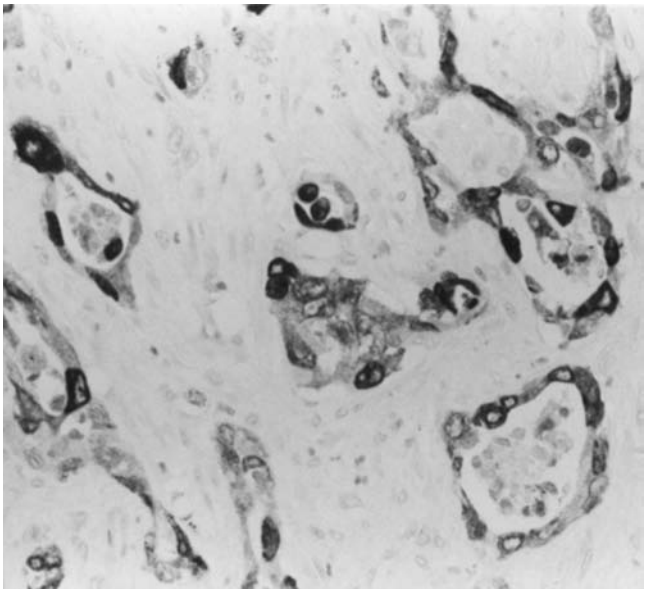

Figure 56. Invasive ductal adenocarcinoma with strong cytoplasmic staining for COX-2. Note negatively stained surrounding cells. COX-2 immunostaining, 70X.

Okami *et al.* (1999) did not find any significant differences between high expressers and low expressers among clinicopathological parameters, including age, sex, location, histological grade, nodal involvement, metastasis, and stage. We also found no correlation between COX-2 expression and sex, size, location, histological grade, and Ki-67-labeling index (data are not described) except patients' age (high and low expressers; average ages 66.5 and 59.3 years, $p = 0.046$). Therefore COX-2 expression does not seem to be affected by clinicopathological features. Merati *et al.* (2001), however, showed that COX-2 overexpression was significantly related to perineural invasion and was more common in the glandular component than in the solid component.

Our investigation revealed a close relationship between COX-2 expression and abnormalities in *p53* (high and low expressers; 17/19 and 5/9, $p = 0.04$) and DPC4 (15/19 and 4/9, $p = 0.07$). Recent genetic analyses have indicated that the tumorigenesis of PDAC is a complex, multistep process involving the progressive accumulation of alterations in oncogenes such as K-*ras* and tumor-suppressor genes such as *p16, p53,* and *DPC4.* Moreover, the accumulation of genetic changes correlates with increasing grade of dysplasia of pancreatic intraepithelial neoplasias (PanINs), which are considered precursor lesions of PDAC (Lüttges *et al.,* 2001). Since significant COX-2 expression is observed in PanINs (Maitra *et al.,* 2002), it is possible that COX-2 contributes to the carcinogenesis of PDAC via PanINs and may be interrelated with the previously mentioned cancer-associated genes. Overexpression of COX-2 in premalignant lesions is also observed in intraductal papillary-mucinous neoplasms (Aoki *et al.,* 2002; Koshiba *et al.,* 1999; Niijima *et al.,* 2002), where the hypothesis of the adenoma-carcinoma developmental sequence is widely accepted.

PETs, particularly insulinomas, usually show benign behavior, but some can metastasize widely. The diagnosis of malignancy and the prognostic assessment are difficult, because the histological appearance of PETs does not correlate with their biological behavior. A new World Health Organization classification provides three categories: 1) tumors with benign behavior;

2) tumors with uncertain behavior (borderline lesions); and 3) carcinomas (low-grade or high-grade malignancy) based on tumor size, angioinvasion, metastasis, mitotic index, Ki-67-LI, and the hormone produced (Solcia *et al.,* 2000). Like PDACs, PETs showed heterogeneous and cytoplasmic staining for COX-2 in almost all cases (Figure 57), and 13/20 (65%) were high expressers. Further, based on the WHO classification, the 13 high expressers included 3 of 4 borderline lesions and all malignant tumors (10 cases), while the low expressers consisted of 1 borderline lesion and all benign tumors (6 cases). Moreover, the 13 high expressers showed significantly large tumor size, frequent angioinvasion and metastasis, and a high Ki-67 labeling index compared to the low expressers (detailed data have been described in a previous report [Ohike and Morohoshi, 2001]). Therefore, COX-2 may be a potential marker that indicates the malignant behavior of PET. A corresponding result in neuroendocrine tumors has been found in pheochromocytomas (Salmenkivi *et al.,* 2001). Okami *et al.* (2002), however, showed that COX-2 might well play a role in the endocrine function of PETs, but that its expression is unrelated to its biological behavior. They proposed that, to elucidate whether *COX-2* expression is associated with tumor development and malignant potential, further examinations on more cases focusing on *COX-2* expression in stromal cells as well as tumor cells are required.

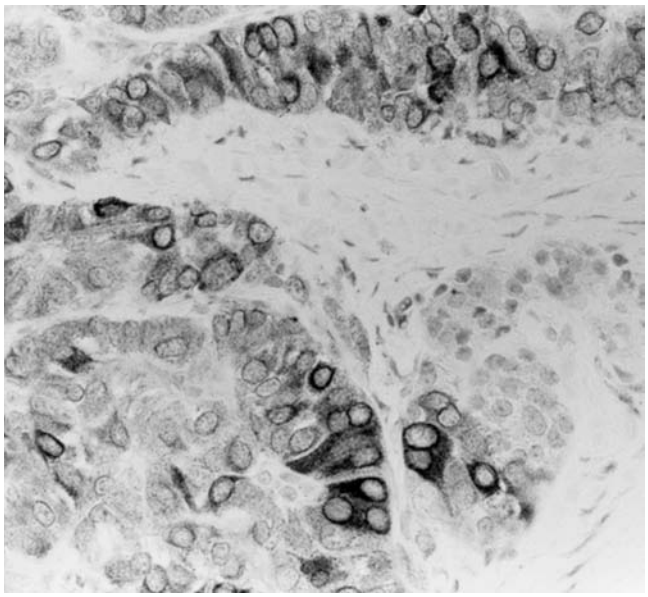

Figure 57. Endocrine tumor with strong cytoplasmic staining for COX-2, especially at the marginal area. The tumor cells can be distinguished from weakly positive islet cells and negative stromal cells. COX-2 immunostaining, 100X.

The surrounding islet cells, acinar cells, duct cells, or stromal cells showed weak or negative COX-2 expression in most cases of PDAC and PET, and only occasionally exhibited strong expression. However, the significance of intense *COX-2* expression in tumor-surrounding stromal cells remains unclear. *COX-2* was also found to be involved in nonneoplastic diseases such as chronic pancreatitis (Schlosser *et al.,* 2002) and diabetes mellitus (Luo *et al.,* 2002). Thus, tumor-associated pancreatitis may also have an influence on *COX-2* expression in PDAC-associated stromal cells.

In conclusion, this study showed that *COX-2* overexpression is a frequent event in PDACs and PETs, when studied with the EnVision ChemMate method, which is a very sensitive, easy detection system for routine IHC. For both tumors, *COX-2* seems to be somehow related to their progression from premalignant lesions to definite carcinomas and *COX-2* inhibitors might therefore be effective chemopreventive agents.

References

Aoki, T., Nagakawa, Y., Tsuchida, A., Kasuya, K., Kitamura, K., Inoue, K., Ozawa, T., Koyanagi, Y., and Itoi, T. 2002. Expression of cyclooxygenase-2 and vascular endothelial growth factor in pancreatic tumors. *Oncol. Rep. 9*:761–765.

Cornetta, A.J., Russell, J.P., Cunnane, M., Keane, W.M., and Rothstein, J.L. 2002. Cyclooxygenase-2 expression in human thyroid carcinoma and Hashimoto's thyroiditis. *Laryngoscope 112*:238–242.

Ding, X.Z., Tong, W.G., and Adrian, T.E. 2000. Blockade of cyclooxygenase-2 inhibits proliferation and induces apoptosis in human pancreatic cancer cells. *Anticancer Res. 20*: 2625–2631.

Eberhart, C.E., Coffey, R.J., Radhika, A., Giardiello, F.M., Ferrenbach, S., and DuBois, R.N. 1994. Up-regulation of cyclooxygenase 2 gene expression in human colorectal adenomas and adenocarcinomas. *Gastroenterology 107*:1183–1188.

Fujiwaki, R., Iida, K., Kanasaki, H., Ozaki, T., Hata, K., and Miyazaki, K. 2002. Cyclooxygenase-2 expression in endometrial cancer: Correlation with microvessel count and expression of vascular endothelial growth factor and thymidine phosphorylase. *Hum. Pathol. 33*:213–219.

Hao, X., Bishop, A.E., Wallace, M., Wang, H., Willcocks, T.C., Maclouf, J., Polak, J.M., Knight, S., and Talbot, I.C. 1999. Early expression of cyclo-oxygenase-2 during sporadic colorectal carcinogenesis. *J. Pathol. 187*:295-301.

Kang, R.Y., Freire-Moar, J., Sigal, E., and Chu, C.Q. 1996. Expression of cyclooxygenase-2 in human and an animal model of rheumatoid arthritis. *Br. J. Rheumatol. 35*:711–718.

Kondo, M., Yamamoto, H., Nagano, H., Okami, J., Ito, Y., Shimizu, J., Eguchi, H., Miyamoto, A., Dono, K., Umeshita, K., Matsuura, N., Wakasa, K., Nakamori, S., Sakon, M., and Monden, M. 1999. Increased expression of COX-2 in nontumor liver tissue is associated with shorter disease-free survival in patients with hepatocellular carcinoma. *Clin. Cancer Res. 5*:4005–4012.

Koshiba, T., Hosotani, R., Miyamoto, Y., Wada, M., Lee, J.U., Fujimoto, K., Tsuji, S., Nakajima, S., Doi, R., and Imamura, M. 1999. Immunohistochemical analysis of cyclooxygenase-2 expression in pancreatic tumors. *Int. J. Pancreatol. 26*:69–76.

Lim, H.Y., Joo, H.J., Choi, J.H., Yi, J.W., Yang, M.S., Cho, D.Y., Kim, H.S., Nam, D.K., Lee, K.B., and Kim, H.C. 2000. Increased expression of cyclooxygenase-2 protein in human gastric carcinoma. *Clin. Cancer Res. 6*:519–525.

Luo, C., Kallajoki, M., Gross, R., Mulari, M., Teros, T., Ylinen, L., Makinen, M., Laine, J., and Simell, O. 2002. Cellular distribution and contribution of cyclooxygenase (COX)-2 to diabetogenesis in NOD mouse. *Cell Tissue Res. 310*:169–175.

Lüttges, J., Galehdari, H., Brocker, V., Schwarte-Waldhoff, I., Henne-Bruns, D., Klöppel, G., Schmiegel, W., and Hahn, S.A. 2001. Allelic loss is often the first hit in the biallelic inactivation of the p53 and DPC4 genes during pancreatic carcinogenesis. *Am. J. Pathol. 158*:1677–1683.

Maitra, A., Ashfaq, R., Gunn, C.R., Rahman, A., Yeo, C.J., Sohn, T.A., Cameron, J.L., Hruban, R.H., and Wilentz, R.E. 2002. Cyclooxygenase 2 expression in pancreatic adenocarcinoma and pancreatic intraepithelial neoplasia: An immunohistochemical analysis with automated cellular imaging. *Am. J. Clin. Pathol. 118*:194–201.

Merati, K., said Siadaty, M., Andea, A., Sarkar, F., Ben-Josef, E., Mohammad, R., Philip, P., Shields, A.F., Vaitkevicius, V., Grignon, D.J., and Adsay, N.V. 2001. Expression of inflammatory modulator COX-2 in pancreatic ductal adenocarcinoma and its relationship to pathologic and clinical parameters. *Am. J. Clin. Oncol. 24*:447–452.

Molina, M.A., Sitja-Arnau, M., Lemoine, M.G., Frazier, M.L., and Sinicrope, F.A. 1999. Increased cyclooxygenase-2 expression in human pancreatic carcinomas and cell lines: Growth inhibition by nonsteroidal anti-inflammatory drugs. *Cancer Res. 59*: 4356–4362.

Nathan, C.A., Leskov, I.L., Lin, M., Abreo, F.W., Shi, R., Hartman, G.H., and Glass, J. 2001. COX-2 expression in dysplasia of the head and neck: Correlation with elF4E. *Cancer 92*:1888–1895.

Niijima, M., Yamaguchi, T., Ishihara, T., Hara, T., Kato, K., Kondo, F., and Saisho, H. 2002. Immunohistochemical analysis and in situ hybridization of cyclooxygenase-2 expression in intraductal papillary-mucinous tumors of the pancreas. *Cancer 94*:1565–1573.

Ohike, N., and Morohoshi, T. 2001. Immunohistochemical analysis of cyclooxygenase (COX)-2 expression in pancreatic endocrine tumors: Association with tumor progression and proliferation. *Pathol. Int. 51*:770–777.

Okami, J., Nakamori, S., Yamamoto, H., Sakon, M., Tsujie, M., Hayashi, N., Nagano, H., Dono, K., Umeshita, K., Ishikawa, O., Ohigashi, H., and Monden, M. 2002. An immunohistochemical study of cyclooxygenase (COX)-2 expression in endocrine tumors of the pancreas. *J. Exp. Clin. Cancer Res. 21*:569–576.

Okami, J., Yamamoto, H., Fujiwara, Y., Tsujie, M., Kondo, M., Noura, S., Oshima, S., Nagano, H., Dono, K., Umeshita, K., Ishikawa, O., Sakon, M., Matsuura, N., Nakamori, S., and Monden, M. 1999. Overexpression of cyclooxygenase-2 in carcinoma of the pancreas. *Clin. Cancer Res. 5*:2018–2024.

Oshima, M., Dinchuk, J.E., Kargman, S.L., Oshima, H., Hancock, B., Kwong, E., Trzaskos, J.M., Evans, J.F., and Taketo, M.M. 1996. Suppression of intestinal polyposis in Apc delta716 knockout mice by inhibition of cyclooxygenase 2 (COX-2). *Cell 87*:803–809.

Sabattini, E., Bisgaard, K., Ascani, S., Poggi, S., Piccioli, M., Ceccarelli, C., Pieri, F., Fraternali-Orcioni, G., and Pileri, S.A. 1998. The EnVision++ system: A new immunohistochemical method for diagnostics and research: Critical comparison with the APAAP, ChemMate, GSA, LABC, and SABC techniques. *J. Clin. Pathol. 51*:506–511.

Salmenkivi, K., Haglund, C., Ristimaki, A., Arola, J., and Heikkila, P. 2001. Increased expression of cyclooxygenase-2 in malignant pheochromocytomas. *J. Clin. Endocrinol. Metab. 86*:5615–5619.

Sawaoka, H., Kawano, S., Tsuji, S., Tsuji, M., Sun, W., Gunawan, E.S., and Hori, M. 1998. *Helicobacter pylori* infection induces cyclooxygenase-2 expression in human gastric mucosa. *Prostaglandins Leukot. Essent. Fatty Acids 59*:313–316.

Schlosser, W., Schlosser, S., Ramadani, M., Gansauge, F., Gansauge, S., and Beger, H.G. 2002. Cyclooxygenase-2 is overexpressed in chronic pancreatitis. *Pancreas 25*:26–30.

Shamma, A., Yamamoto, H., Doki, Y., Okami, J., Kondo, M., Fujiwara, Y., Yano, M., Inoue, M., Matsuura, N., Shiozaki, H., and Monden, M. 2000. Up-regulation of cyclooxygenase-2 in squamous carcinogenesis of the esophagus. *Clin. Cancer Res. 6*:1229–1238.

Singer, II., Kawka, D.W., Schloemann, S., Tessner, T., Riehl, T., and Stenson, W.F. 1998. Cyclooxygenase 2 is induced in colonic epithelial cells in inflammatory bowel disease. *Gastroenterology 115*:297–306.

Solcia, E., Klöppel, G., and Sobin, L.H. 2000. Endocrine tumours of the pancreas. In Solcia, E., Klöppel, G., and Sobin, L.H., (eds) *Histological Typing of Endocrine Tumours: International Histological Classification of Tumours*. Heidelberg, Germany: World Health Organization, 56–60.

Takahashi, M., Furukawa, F., Toyoda, K., Sato, H., Hasegawa, R., Imaida, K., and Hayashi, Y. 1990. Effects of various prostaglandin synthesis inhibitors on pancreatic carcinogenesis in hamsters after initiation with N-nitrosobis(2-oxopropyl) amine. *Carcinogenesis 11*:393–395.

Tucker, O.N., Dannenberg, A.J., Yang, E.K., Zhang, F., Teng, L., Daly, J.M., Soslow, R.A., Masferrer, J.L., Woerner, B.M., Koki, A.T., and Fahey, T.J. 3rd. 1999. Cyclooxygenase-2 expression is up-regulated in human pancreatic cancer. *Cancer Res. 59*:987–990.

Uotila, P., Valve, E., Martikainen, P., Nevalainen, M., Nurmi, M., and Harkonen, P. 2001. Increased expression of cyclooxygenase-2 and nitric oxide synthase-2 in human prostate cancer. *Urol. Res. 29*:23–28.

Wilson, K.T., Fu, S., Ramanujam, K.S., and Meltzer, S.J. 1998. Increased expression of inducible nitric oxide synthase and cyclooxygenase-2 in Barrett's esophagus and associated adenocarcinomas. *Cancer Res. 58:*2929–2934.

Wolff, H., Saukkonen, K., Anttila, S., Karjalainen, A., Vainio, H., and Ristimaki, A. 1998. Expression of cyclooxygenase-2 in human lung carcinoma. *Cancer Res. 58*:4997–5001.

10

Immunohistochemical Detection of Activated Stat3 Protein in Pancreatic Cancer

Suyun Huang, Weida Gong, and Keping Xie

Introduction

Pancreatic cancer is the fifth most common cause of cancer death in the Western World and is a leading cause of cancer death worldwide (Wei *et al.,* 2003b). The American Cancer Society estimated that there would be 30,700 new cases of pancreatic cancer and 30,000 deaths from pancreatic cancer in the year 2003 in the United States alone (ACS, 2003). The current 5-year survival rate is approximately 1–2%, and the median survival time after diagnosis is 4–6 months. The prominent cause of death in patients with pancreatic adenocarcinoma is metastatic disease. Unfortunately, patients usually have metastatic disease that is locally advanced or involving the lymph nodes, liver, lungs, or peritoneum at the time of diagnosis (Wei *et al.,* 2003a). The aggressive nature of metastatic pancreatic adenocarcinoma is caused by the activation of various oncogenes and inactivation of various tumor-suppressor genes, as well as abnormalities in growth factors and their receptors, which together affect the downstream signal transduction pathways involved in the control of cell growth and differentiation (Xie, 2001). These perturbations confer a tremendous growth advantage on pancreatic cancer cells. One of these transduction pathways is the Stat3 (signal transducer and activator of transcription 3) signal transduction pathway, which is the focus of this chapter.

Stat3 is one of seven Stat proteins that have been identified (Bromberg, *et al.,* 1999), which represent a unique group of proteins that are key mediators of various cytokine signaling pathways that control cellular growth, differentiation, development, and survival (Bowman *et al.,* 2000). The Stat proteins are inactive as transcription factors in the absence of specific receptor stimulation and are located in the cytoplasm of unstimulated target cells. They are activated rapidly in response to receptor-ligand coupling and are recruited to the intracellular domain of the receptor through specific binding of the Stat Src-homology 2 (SH2) domains to receptor phosphotyrosine residues. Stat proteins are then phosphorylated in tyrosine and serine residues. The phosphorylation is mediated most often by the cytokine receptor Janus-associated kinases (JAKs) or growth factor receptor tyrosine kinases. Once phosphorylated, the Stats form homodimers or heterodimers,

Handbook of Immunohistochemistry and *in situ* Hybridization of Human Carcinomas, Volume 3: Molecular Genetics, Liver Carcinoma, and Pancreatic Carcinoma

enter the nucleus, and lead to increased transcriptional initiation, thereby altering the expression of specific target genes and affecting the downstream production of those genes (Darnell, 1997).

Stat3, a member of the JAK-Stat signaling pathway, is ubiquitously expressed in most tissues as a latent transcription factor (Darnell, 1997). Stat3 was first identified as a deoxyribonucleic acid (DNA)-binding factor that selectively interacts with an enhancer element in the promoter of acute-phase genes from interleukin (IL)-6–stimulated hepatocytes (Zhong *et al.,* 1994). The gene that encodes *Stat3* is located on chromosome 17q21, and it encodes a 92-kD protein. Structurally, Stat3 is similar to other Stat proteins, in that it has a conserved amino-terminus involved in tetramerization, a DNA-binding domain with a sequence specific for a palindromic interferon-gamma (IFN-γ)–activated sequence (GAS) element very similar to that of Stat1, an SH2 domain involved in receptor recruitment and Stat dimerization, and a carboxy-terminal transactivation domain.

Stat3 is activated by many cytokines and growth factors, including epidermal growth factor, platelet-derived growth factor, and IL-6 (Zhong *et al.,* 1994); it also is activated by oncogenic proteins such as Src and Ras (Yu *et al.,* 1995). On activation, Stat3 is phosphorylated on tyrosine residues (Tyr705) by activated JAK kinases in receptor complexes; this leads to the formation of homodimers and heterodimers and their translocation to the nucleus, where they regulate transcription. Tyrosine phosphorylation is required for Stat3 dimerization, nuclear translocation, and DNA binding. Stat3 can also be phosphorylated in the serine residue in the C-terminal transcriptional domain, which has been found to enhance the transcriptional activity of Stat3 (Decker and Kovarik, 2000). There is also evidence that serine phosphorylation serves a negative function, but the mechanism involved is unclear.

The biological functions of Stat3 are very broad. For example, Stat3 plays a crucial role in the regulation of cell proliferation, survival, apoptosis, and differentiation. In normal cells and in animals, ligand-dependent activation of the Stat3 is a transient process, lasting for several minutes to several hours. In contrast, in many cancer cell lines and tumors, the Stat3 protein is persistently activated. In particular, constitutively activated Stat3 protein has been found in various types of tumors, including leukemia and cancers of the breast, head and neck, melanoma, prostate, and pancreas (Grandis *et al.,* 2000; Scholz *et al.,* 2003; Wei *et al.,* 2003b).

Studies have revealed that altered Stat3 could contribute to oncogenesis (Bromberg *et al.,* 1999). For example, Stat3 activation has not only been observed in cells transformed *in vitro* with v-*src* and v-*abl* oncogenes (Yu *et al.,* 1995), but this activation also is demonstrated to be required for v-*src* to mediate cellular transformation. Further, Stat3 activation has been demonstrated to be sufficient to mediate cellular transformation. Overexpression of the constitutively activated Stat3 mutant (Stat3-C) into immortalized NIH 3T3 fibroblasts induced cellular transformation and tumor formation in nude mice (Bromberg *et al.,* 1999), providing genetic evidence that Stat3 has oncogenic potential. Moreover, it has been observed that the level of Stat3 activation correlates with the stages of human malignancies.

In terms of its effects in tumor cells, Stat3 activation has been found to prevent apoptosis and enhance cell proliferation in many human tumor cells by regulating genes that encode proteins involved in cell growth and apoptosis, including cyclin Dl, C-Myc, Bcl-x_L, and Mcl-1 (Bromberg *et al.,* 1999). Conversely, the blocking of constitutive Stat3 signaling results in the growth inhibition and apoptosis of Stat3-positive tumor cells *in vitro* and *in vivo*. These results therefore further suggest that Stat3 functions as an oncogene and plays a critical role in transformation and tumor progression.

Several lines of evidence indicate that the constitutive activation of Stat3 contributes to malignant transformation and the progression of human pancreatic cancer (Scholz *et al.,* 2003; Wei *et al.,* 2003b). Specifically, the prevalence of activated Stat3 in nontransformed pancreatic tissue, chronic pancreatitis, and pancreatic adenocarcinoma has been analyzed. All carcinoma samples analyzed expressed activated Stat3, whereas ductal epithelium from nontransformed pancreatic tissue obtained from the resection margins of pancreatic tumors or tissue obtained from patients with chronic pancreatitis showed negligible or no activated Stat3 expression (Scholz *et al.,* 2003). Moreover, most pancreatic cancer cell lines examined have shown constitutively activated Stat3 (Scholz *et al.,* 2003; Wei *et al.,* 2003b). Further incriminating Stat3 in the oncogenesis of pancreatic cancer was the finding that the blockade of the activated Stat3 inhibited pancreatic cancer cell growth *in vitro* and *in vivo* (Scholz *et al.,* 2003; Wei *et al.,* 2003b). The mechanisms for this inhibition could be the result in part of the down-regulation of Bc1-x_L expression caused by the inhibition of Stat3 activation in pancreatic cancer cells. Furthermore, the finding that activated Stat3 directly regulates the promoter of the angiogenic molecule vascular endothelial growth factor (VEGF) gene is another clue to Stat3's role in the development of pancreatic cancer. This was shown by the fact that the blockade of activated Stat3 by ectopically expressed dominant-negative Stat3 significantly inhibited VEGF expression, and

hence angiogenesis and the growth and metastasis of human pancreatic cancer cells (Wei *et al.,* 2003b). These results therefore collectively show that the activation of the Stat3 signaling pathway is critical for pancreatic tumor progression and that Stat3 activation may constitute both a diagnostic and prognostic marker as well as a molecular target for therapeutic interventions.

In the current study, we examined the expression of activated Stat3 in human pancreatic cancers using a phosphotyrosine-specific Stat3 antibody (p-Stat3 [Tyr-705]). As noted earlier, the tyrosine phosphorylation of Stat3 constitutes an early event in the activation of this transcription factor and is required for its dimerization and DNA-binding activity. Of particular importance, the constitutive tyrosine phosphorylation of Stat3 is necessary for this transcription factor to exert its oncogenic effect (Bromberg *et al.,* 1999). Therefore, this phosphotyrosine-specific Stat3 antibody exclusively detects activated Stat3 and, for this reason, has been used in numerous studies (Bartoli *et al.,* 2000).

MATERIALS

1. Formalin-fixed and paraffin-embedded primary pancreatic adenocarcinoma specimens and normal pancreatic tissue specimens.
2. Xylene.
3. Ethanol.
4. Distilled H_2O (dH_2O).
5. Phosphate buffer saline (PBS): 100 mg of anhydrous calcium chloride, 200 mg of potassium chloride, 200 mg of monobasic potassium phosphate, 100 mg of magnesium chloride 6 H_2O; 8 g of sodium chloride, and 2.16 g of dibasic sodium phosphate 7 H_2O; bring volume to 1 L with dH_2O, and adjust pH to 7.5.
6. 50 mM Tris buffer: 0.6 g of Tris(hydroxymethyl)aminomethane in 100 mL of dH_2O; adjust pH to 7.6 using HCl.
7. 10 mM Sodium citrate buffer: add 2.94 g of sodium citrate to 1 L of dH_2O, and adjust pH to 6.0.
8. Trypsin (Invitrogen Corporation, Carlsbad, CA).
9. 3% H_2O_2 in methanol: add 9 ml of 30% H_2O_2 to 92 ml of methanol.
10. Blocking solution: 5% bovine serum albumin (BSA) and 5% normal horse serum (Jackson Immunoresearch Laboratories, Inc., West Grove, PA) in PBS.
11. Primary antibody: a polyclonal rabbit antibody against activated Stat3 (Phospho-Stat3 [Tyr-705]; Cell Signaling Technology, Inc., Beverly, MA). Phospho-Stat3 (Tyr705) antibody detects endogenous levels of Stat3 only when phosphorylated at tyrosine 705. This antibody does not appreciably cross-react with the corresponding phosphotyrosines of other Stat proteins. Polyclonal antibodies are produced by immunizing rabbits with a synthetic phosphopeptide (KLH coupled) corresponding to residues around Tyr705 of Stat3. Antibodies are purified by protein A and peptide-affinity chromatography.
12. Secondary antibody: peroxidase-conjugated anti-rabbit immunoglobulin (IgG) (Jackson Immunoresearch Laboratories, Inc.).
13. Diaminobenzidine (DAB) solution: dissolve 50 mg of DAB (3,3-diaminobenzidine tetrahydrochloride; Sigma) in 99.5 ml of PBS and add 0.5 ml of 30% H_2O_2; use immediately because solution is good for only 20 min.
14. Hematoxylin (Biogenex Laboratories, San Ramon, CA).
15. Universal mount (Research Genetics, Huntsville, AL).

METHODS

Tissue Slide Preparation

1. Standard tissue sections (5 μm thick) of specimens were cut and mounted on glass slides.
2. Air-dry the slides overnight at room temperature.

Deparaffinization

1. Heat the section slides at 60°C for 30 min.
2. Incubate the section slides in xylene for 6 min at room temperature. Repeat the step 1×.

Rehydration

1. Rinse the slides with 100% ethyl alcohol (ETOH) 2× for 2 min each.
2. Rinse the slides with 95% ETOH 2× for 1 min each.
3. Rinse the slides with 80% ETOH for 1 min
4. Rinse the slides with 50% ETOH for 1 min.
5. Rinse the slides with PBS 2× for 2 min each.

Antigen Retrieval

1. Immerse the slides in 10 mM sodium citrate buffer (pH 6.0).
2. Heat the slides in a microwave oven for 1 min at high power, followed by 19 min at medium power.
3. Cool the slides for 20 min after antigen unmasking.

Tissue Digestion

1. Incubate sections with 0.025% trypsin in 50 mM Tris buffer (pH 7.6) for 5 min at 37°C.
2. Rinse slides with PBS 3× for 2 min each and continue the immunostaining.

Immunostaining Procedure

1. Use paper towel to wipe around the tissue on each slide.
2. Draw a circle with a Pap pen around tissue on each slide.
3. Place all slides in a humidified chamber (care must be taken to prevent tissue from drying out).
4. Quench endogenous peroxidase by placing slides in 3% H_2O_2 methanol for 15 min.
5. Rinse the slides with PBS 3× for 5 min each.
6. Incubate each slide with 300 µl of blocking solution for 1 hr at room temperature.
7. Remove blocking solution and add 200 µl of diluted primary antibody (diluted 1:50 in blocking solution) to each slide. Incubate the slides overnight at 4°C.
8. Rinse as in **Step 2.**
9. Incubate each slide with 300 µl of blocking solution for 1 hr at room temperature.
10. Remove blocking solution and add diluted secondary antibody (anti-rabbit IgG, 1:500 diluted in blocking solution). Incubate the slides with the antibody for 2 hr.
11. Rinse as in **Step 2.**
12. Add 150 µl of DAB solution to each slide. At this point, the slides may be examined under a bright-field microscope to monitor the staining quality. Positive staining is shown by the finding of a reddish-brown precipitate in the nucleus.
13. As soon as the section turns brown, immerse slides into dH_2O.
14. Rinse the slides with dH_2O 3× for 5 min each.
15. Counterstain slides with hematoxylin for 10 sec.
16. Rinse the slides briefly with dH_2O.
17. Rinse the slides with PBS for 1 min.
18. Rinse the slides with dH_2O 2× for 5 min each.
19. Mount the slides with universal mount and place on hot plate (65°C) for 30 min to dry the slides.
20. The slides are now ready for final examination under a bright-field microscope.

Specimen Analysis

1. The sections were examined by a pathologist who was blinded to the clinical characteristics of the patients.
2. The intensity of staining of activated Stat3 was evaluated by a digital image analysis system (Sony 3CD color video camera, Sony, Tokyo, Japan) and personal computer equipped with the Optimas Image Analysis software program (Optimas Corp., Bothell, WA).
3. The intranuclear staining of tumor cells was considered to indicate the presence of constitutively activated Stat3.
4. Immunohistochemistry (IHC) staining results were classified into three groups depending on the percentage of cells with positively stained nuclei, as follows: negative (<10%), weakly positive (10%–24%), and strongly positive (≥25%). Specifically, if less than 10% of tumor cells showed a nuclear staining pattern, the slide was classified as negative. When the percentage of positive tumor cells was between 10–25%, the slide was classified as weak positive. When the percentage of positive tumor cells was equal or more than 25%, the slide was classified as strong positive.

RESULTS AND DISCUSSION

We determined the degree of expression of activated Stat3 in a panel of human pancreatic adenocarcinoma specimens (20 cases) and in normal pancreatic tissue specimens (10 cases) obtained from subjects who did not have cancer, as shown by IHC analyses using an anti-phospho-Stat3 (Tyr705) antibody. This antibody exclusively detects activated Stat3 and does not cross-react with latent Stat3. Fifteen of the 20 (75%) pancreatic adenocarcinomas strongly expressed phosphorylated Stat3 in the foci of pancreatic adenocarcinoma (Figure 58A). The Stat3 staining was mainly localized in the nuclei of the pancreatic cancer epithelial cells. In contrast, among 10 normal pancreatic tissues, analysis of the immunohistochemical staining showed either negligible or negative expression of activated Stat3 (Figure 58B). These results therefore showed that Stat3 is highly activated in pancreatic tumor tissue but not in normal pancreatic tissue. Consistent with the data, several studies have shown that majority of human pancreatic cancer cell lines highly express constitutive activated Stat3 (Scholz *et al.,* 2003; Wei *et al.,* 2003b).

The mechanisms responsible for the overexpression of activated Stat3 in pancreatic tumors are largely unknown. It is known that Stat3 is activated by various cytokines and growth factors, including epidermal growth factor and fibroblast growth factor, and by oncogenic proteins such as Src and Ras. Significantly, these molecules are also often overexpressed in pancreatic cancers (Xie, 2001). For example, the epidermal growth factor receptor (EGFR) is overexpressed in approximately 90% of human pancreatic cancers (Friess *et al.,* 1999; Xie, 2001). Further, either an EGFR-specific antagonist or a neutralizing antibody were observed to suppress constitutive Stat3 DNA-binding activity in human pancreatic cancer cells (Scholz *et al.,* 2003). Because these experiments were performed without exogenous growth factors and cytokines, they clearly identified autocrine or paracrine EGFR signaling as a major upstream stimulus of Stat3 activation in

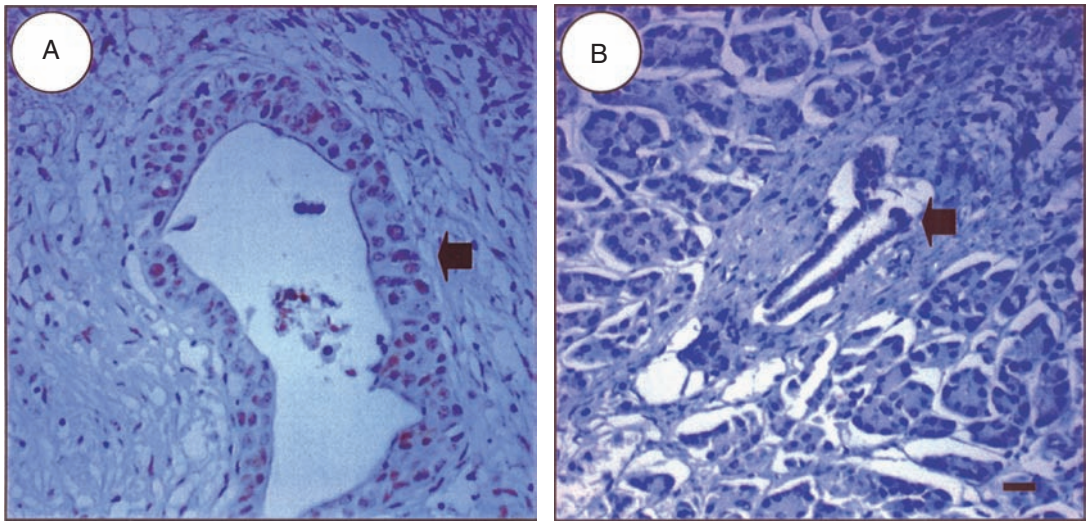

Figure 58. Activated Stat3 protein expression in human pancreatic tissue. Tissue sections were prepared from formalin-fixed and paraffin-embedded specimens of human pancreatic adenocarcinoma **(A)** and adjacent normal pancreas tissue **(B)**. Immunohistochemical staining was performed using a specific anti-phospho-Stat3 antibody. Of note is that the normal pancreas cells were negative for Stat3, whereas the majority of the tumor cells were positive for Stat3 in nuclei *(arrows).* Calibration bar, 40 μm.

human pancreatic cancer cells. Several groups have additionally observed the overexpression and activation of tyrosine kinase Src in most human pancreatic ductal adenocarcinoma, raising the possibility that the activation of Src contributes to the constitutive activation of Stat3 in pancreatic cancers (Coppola, 2000; Lutz *et al.,* 1998). The activation of the K-*ras* oncogene is also a common genetic alteration in pancreatic cancers (Friess *et al.,* 1999). It therefore seems that the constitutive activation of Stat3 in pancreatic cancers is a result of the previously mentioned aberrant epigenetic and genetic alterations that occur during malignant transformation.

Because of its central position downstream in the signaling pathways from growth factors, cytokines, and oncogenic protein tyrosine kinases, aberrant Stat3 activity is a key mediator in the development and progression of tumors. Stat3 executes its roles in the processes through transcriptional regulation of several important target genes. For example, activated Stat3 has been shown to regulate the expression of the anti-apoptotic regulatory proteins Bcl-x_L and Mcl-1 (Yu *et al.,*1995), thereby preventing the apoptosis of tumor cells. It is interesting that, both Bcl-x_L and Mcl-l proteins have been detected in pancreatic cancer tissue. Specifically, Bcl-x_L is up-regulated early in tumor development, and this persists throughout pancreatic carcinogenesis (Greten *et al.,* 2002). Moreover, Stat3 activation induces increased Bcl-x_L expression in pancreatic cancer cells (Greten *et al.,* 2002). Conversely, the inhibition of Stat3 transcription factor leads to Bcl-x_L down-regulation and induces apoptosis in pancreatic cancer cells. Of further note, in a clinical study, the enhanced expression of Bcl-x_L in pancreatic cancer was found to be associated with shorter patient survival. Stat3 also contributes to cancer cell proliferation by regulating the cyclin Dl, C-*Myc*, and *p21*^{WAF1} genes. In particular, constitutively activated Stat3 has been found to transcriptionally up-regulate cyclin D1 expression (Bromberg *et al.,* 1999); indeed, this gene is overexpressed in 85% of invasive pancreatic carcinomas (Poch *et al.,* 2001). The C-*Myc* gene that is also regulated by *Stat3* is commonly deregulated in pancreatic cancer and may be involved in early neoplastic development and progression (Schleger *et al.,* 2002). Furthermore, activated Stat3 regulation of p21^{WAF1} expression in pancreatic cancer cells could be a cell-type–specific regulatory event (Scholz *et al.,* 2003). Inhibition of activated Stat3 led to a delay in the G1/S-phase progression of pancreatic cancer cells, which was caused by selective inhibition of p21^{WAF1} expression (Scholz *et al.,* 2003).

More recently, we have demonstrated that Stat3 may contribute to the angiogenesis of pancreatic tumors by regulating the expression of VEGF (Wei *et al.,* 2003b), a key mediator of tumor angiogenesis. Like other solid tumors, the growth and metastasis of pancreatic adenocarcinoma is dependent on angiogenesis, the formation of new blood vessels from a preexisting network of capillaries (Folkman, 1997; Shi *et al.,* 2001). Of the numerous angiogenic factors discovered so far, VEGF, also known as vascular

permeability factor, has been identified as a key mediator of tumor angiogenesis. Indeed, the level of VEGF was noted to be significantly elevated in biopsy specimens of human pancreatic adenocarcinoma (Itakura *et al.,* 1997), as it has in human tumor biopsy specimens of various other cancers (Itakura *et al.,* 1997). Physiologically, the pancreas is a highly vascularized organ, and the VEGF level is quite high in the islets of normal pancreas but relatively low in the pancreatic ductal epithelial cells. However, significantly elevated expression of VEGF is found in biopsy specimens of human pancreatic adenocarcinoma (Itakura *et al.,* 1997).

The mechanism of VEGF expression and its regulation in human pancreatic cancer are mostly unknown. We have shown that the overexpression of VEGF in human pancreatic cancer cells is the result of elevated Stat3 activity (Wei *et al.,* 2003b). This was shown by several findings. First, we found that both human pancreatic cancer cells and human pancreatic cancer specimens have constitutively activated Stat3 and that its activation directly correlated with the level of VEGF expression. In addition, the overactivation of Stat3 correlated directly with increased blood vessel density. Further experiments of ours indicated that Stat3 regulates VEGF expression by directly interacting with the VEGF promoter via a Stat3 response element or elements on the VEGF promoter. Our data also indicated that VEGF can be excessively up-regulated as a result of the constitutive overactivation of Stat3. Conversely, the blockade of activated Stat3 by ectopically expressed dominant-negative Stat3 in human pancreatic cancer cells significantly down-regulated the constitutive expression of VEGF. Furthermore, the inhibition of activated Stat3 suppressed tumor angiogenesis, tumor growth, and metastasis *in vivo* (Wei *et al.,* 2003b). Taken together, these studies therefore provide evidence that activated Stat3 in human pancreatic cancer cells regulates the expression of genes related to cell survival, cell proliferation, and tumor angiogenesis. Tumor cell proliferation, survival, angiogenesis, and invasion are essential for tumor growth and metastasis; to that end, activated Stat3 is a critical transcription factor in human pancreatic cancer tumor development and progression.

In summary, activated Stat3 is overexpressed in human pancreatic cancers as compared with normal pancreatic tissues. Stat3 has also been found to be constitutively activated in the human pancreatic cancer cell lines examined. Stat3 may contribute to human pancreatic cancer development and progression by collectively affecting the expression of genes related to cell survival, cell cycle control, and angiogenesis, such as the genes that encode Bcl-x_L, $p21^{WAF1}$, and VEGF. In turn, these results suggest that activated Stat3 might serve as both a molecular marker for the early detection of human pancreatic cancer and a prognostic indicator for use in determining the aggressiveness of the disease. It might also serve as a target for therapy, as indicated by the fact that the blockade of activated Stat3 significantly inhibited VEGF expression, angiogenesis, and the metastasis of human pancreatic cancer cells. Thus, targeting of Stat3 signaling may represent a novel approach to controlling the angiogenesis, growth, and metastasis of human pancreatic cancer.

Acknowledgment

The laboratory research work was supported in part by a Research Scholar Grant CSM-106659 from the American Cancer Society and a Research Grant from the Brain Tumor Society (S. H.).

References

American Cancer Society 2003. *Cancer Facts and Figures.* Atlanta: American Cancer Society.

Bartoli, M., Gu, X., Tsai, N.T., Venema, R.C., Brooks, S.E., Marrero, M.B., and Caldwell, R.B. 2000. Vascular endothelial growth factor activates STAT proteins in aortic endothelial cells. *J. Biol. Chem. 275*:33189–33192.

Bowman, T., Garcia, R., Turkson, J., and Jove, R. 2000. STATs in oncogenesis. *Oncogene 19*:2474–2488.

Bromberg, J.F., Wrzeszczynska, M.H., Devgan, G., Zhao, Y., Pestell, R.G., Albanese, C., and Darnell, J.E., Jr. 1999. Stat3 as an oncogene. *Cell 98*:295–303.

Brown, L.F., Detmar, M., Claffey, K., Nagy, J.A., Feng, D., Dvorak, A.M., and Dvorak, H.F. 1997. Vascular permeability factor/vascular endothelial growth factor: A multifunctional angiogenic cytokine. In Goldberd, I.D., and Rosen, E.M., (eds), *Regulation of Angiogenesis,* Basel: Birkhauser Verlag 233–269.

Campbell, C.L., Jiang, Z., Savarese, D.M., and Savarese, T.M. 2001. Increased expression of the interleukin-11 receptor and evidence of STAT3 activation in prostate carcinoma. *Am. J. Pathol. 158*:25–32.

Coppola, D. 2000. Molecular prognostic markers in pancreatic cancer. *Cancer Control 7*:421–427.

Darnell, J.E., Jr. 1997. STATs and Gene Regulation. *Science 277*:1630–1635.

Decker, T., and Kovarik, P. 2000. Serine phosphorylation of Stats. *Oncogene 19*:2628–2637.

Ducy, P., Amling, M., Takeda, S., Priemel, M., Schilling, A.F., Beil, F.T., Shen, J., Vinson, C., Rueger, J.M., and Karsenty, G. 2000. Leptin inhibits bone formation through a hypothalamic relay: A central control of bone mass. *Cell 100*:197–207.

Folkman, J. Angiogenesis and angiogenesis inhibition: An overview. 1997. *EXS 79*:1–8.

Friess, H., Guo, X.Z., Nan, B.C., Kleeff, O., and Buchler, M.W. 1999. Growth factors and cytokines in pancreatic carcinogenesis. *Ann. N. Y. Acad. Sci. 880*:110–121.

Grandis, J.R., Drenning, S.D., Zeng, Q., Watkins, S.C., Melhem, M.F., Endo, S., Johnson, D.E., Huang, L., He, Y., and Kim, J.D. 2000. Constitutive activation of stat3 signaling abrogates apoptosis in squamous cell carcinogenesis in vivo. *Proc. Natl. Acad. Sci. USA 97*:4227–4232.

Greten, F.R., Weber, C.K., Greten, T.F., Schneider, G., Wagner, M., Adler, G., and Schmid, R.M. Dec. 2002. Stat3 and NF-kappaB activation prevents apoptosis in pancreatic carcinogenesis. *Gastroenterology 123*:2052–2063.

Itakura, J., Ishiwata, T., Friess, H., Fujii, H., Matsumoto, Y., Buchler, M.W., and Korc, M. 1997. Enhanced expression of vascular endothelial growth factor in human pancreatic cancer correlates with local disease progression. *Clin. Cancer Res. 3*:1309–1316.

Lutz, M.P., Esser, I.B., Flossmann-Kast, B.B., Vogelmann, R., Luhrs, H., Friess, H., Buchler, M.W., and Adler, G. 1998. Overexpression and activation of the tyrosine kinase Src in human pancreatic carcinoma. *Biochem. Biophys. Res. Commun. 243*:503–508.

Poch, B., Gansauge, F., Schwarz, A., Seufferlein, T., Schnelldorfer, T., Ramadani, M., Beger, H.G., and Gansauge, S. 2001. Epidermal growth factor induces cyclin Dl in human pancreatic carcinoma: Evidence for a cyclin D1-dependent cell cycle progression. *Pancreas 23*:280–287.

Schleger, C., Verbeke, C., Hildenbrand, R., Zentgraf, H., and Bleyl, U. 2002. c-MYC activation in primary and metastatic ductal adenocarcinoma of the pancreas: Incidence, mechanisms, and clinical significance. *Mod. Pathol.15*:462–469.

Scholz, A., Heinze, S., Detjen, K.M., Peters, M., Welzel, M., Hauff, P., Schirner, M., Wiedenmann, B., and Rosewicz, S. 2003. Activated signal transducer and activator of transcription 3 (STAT3) supports the malignant phenotype of human pancreatic cancer. *Gastroenterology 125*:891–905.

Shi, Q., Le, X., Peng, Z., Tang, H., Xiong, Q., Wang, B., Li, X.-C., Abbruzzese, J.L., and Xie, K. 2001. Constitutive Sp1 activity is essential for differential constitutive expression of vascular endothelial growth factor in human pancreatic adenocarcinoma. *Cancer Res. 61*:4143–4154.

Wei, D., Xiong, H.Q., Abbruzzese, J.L., and Xie, K. 2003a. Experimental animal models of pancreatic carcinogenesis and metastasis. *Intl. J. Gastrointestinal Cancer 33*:43–60.

Wei, D., Le, X., Zheng, L., Wang, L., Frey, J.A., Gao, A.C., Peng, Z., Huang, S., Xiong, H.Q., Abbruzzese, J.L., and Xie, K. 2003b. Stat activation regulates the expression of vascular endothelial growth factor and human pancreatic cancer angiogenesis and metastasis. *Oncogene 22*:319–329.

Xie, K., 2001. Interleukin-8 and human cancer biology. *Cytokine Growth Factor Rev. 12*:375–391.

Yu, C.L., Meyer, D.J., Campbell, G.S., Lamer, A.C., Carter-Su, C., Schwartz, J., and Jove, R. 1995. Enhanced DNA-binding activity of a Stat3-related protein in cells transformed by the Src oncoprotein. *Science 269*:81–83.

Zhong, Z., Wen, Z., and Darnell, J.E., Jr. 1994. Stat3: A STAT family member activated by tyrosine phosphorylation in response to epidermal growth factor and interleukin-6. *Science 264*:95–98.

11

The Role of Transcription Factor E2F-1 in Pancreatic Ductal Carcinoma

Kazuto Yamazaki

Introduction

The transcription factor E2F-1 was the first cloned and is the better-characterized member of the E2F family. E2F-1 forms a complex with unphosphorylated retinoblastoma protein (pRb), lying within a pocket formed by the C-terminal domain. The pRb phosphorylation results in the release of E2F-1 from this pocket. This exposes the transactivation domain of E2F-1, which then initiates transcription of some set of genes required for deoxyribonucleic acid (DNA) synthesis (Dyson, 1997; Nevins, 1998).

This pRb pathway, converging many upstream stimulatory and inhibitory signals, is one of the most frequent targets of genetic alterations in human neoplasms, including pancreatic ductal carcinoma (Rozenblum *et al.,* 1997). In this means, we investigated E2F-1 expression immunohistochemically and analyzed its status and possible role. In addition, several cell cycle regulators in this pathway can be detected immunohistochemically and have been reported as biomarkers of tumor proliferation and adverse prognosis (Gansauge *et al.,* 1997). Thus, we also analyzed the feasibility of E2F-1 expression as a biomarker of tumor proliferation, prognosis or both in pancreatic ductal carcinomas.

MATERIALS

Fifty-four surgically resected specimens of pancreatic ductal adenocarcinoma were used. Tissue sections were fixed in 10% buffered formalin for 24–48 hr and embedded in paraffin. Tumor-free pancreatic tissues from the same patients were used as controls. To assess the relevance of E2F-1 expression and clinical outcome, we calculated the disease-associated survival time in each case.

METHODS

Paraffin-embedded tissue was cut into serial sections (4 μm) and mounted on 2% 3-aminopropyltriethoxysilane-coated slides. Briefly, after deparaffinization in xylene and rehydration through a series of graded ethanol, each section was heated in an autoclave for 10 min in 0.01 M citrate buffer (pH 7.0) for antigen retrieval. Antigen retrieval using a microwave or autoclave in citrate buffer (pH 6.0) resulted in insufficient contrast of positive staining of E2F-1 immunostaining. Endogenous peroxidase activity was blocked by immersion in 3% hydrogen peroxide in methanol for 30 min. The sections were then incubated from 4 hr to overnight with specific primary antibodies. These were

Handbook of Immunohistochemistry and *in situ* Hybridization of Human Carcinomas, Volume 3: Molecular Genetics, Liver Carcinoma, and Pancreatic Carcinoma

diluted with Protein Block Serum-Free-Ready-to-Use (Dako, Carpinteria, CA) at 1:100 with anti-human E2F-1 monoclonal antibody (KH95, Santa Cruz Biotechnology, Santa Cruz, CA), which was thought to recognize and react with amino acids 342–386 of E2F-1 (Helin *et al.,* 1993). Proliferative activity was also measured immunohistochemically using an antibody against Ki-67 antigen (MIB-1, Immuno-tech, Marseilles, France; dilution, 1:100). After the sections had been washed with phosphate buffer saline (PBS), biotinylated anti-mouse immunoglobulin (Ig) was applied for 30 min at room temperature. After the sections had been washed again with PBS, peroxidase-conjugated streptavidin solution was applied for 30 min and visualized using Liquid DAB (diaminobenzidine) + Substrate-Chromogen System (Dako, Carpinteria, CA) according to manufacturer's instruction. Counterstaining was performed with Mayer's hematoxylin. Five representative fields were examined for each specimen, and more than 1000 tumor cells (200 for each field) were counted under the microscope with a high-power (200X) objective. Only a nuclear stain was counted as positive. The percentage of positive tumor cells was recorded as the positivity index (PI, number of positive cells per 100 tumor cells) for E2F-1 or MIB-1 staining. Active stromal fibroblast or lymphocyte, which occasionally showed nuclear staining for each staining, was used as internal positive controls. Sections incubated with normal mouse IgG instead of primal antibodies were used as negative controls for both.

RESULTS AND DISCUSSION

In this study, E2F-1 immunostaining revealed positive signals localized mainly in tumor cell nuclei, in contrast to negative expressions in nonneoplastic pancreatic ductal cells. Although the mechanism of increased E2F-1 expression in this series is not studied, one possible explanation is that E2F-1 expression is up-regulated in transcriptional level, such as in gastric carcinomas (Suzuki *et al.,* 1999).

In this study, we found a statistically significant correlation between E2F-1 PI (ranged from 3.8 to 71.4) and histologic grades of tumor differentiation (P = 0.0133), *i.e.,* E2F-1 PI is higher in less-differentiated carcinomas. Furthermore, there was positive correlation between E2F-1 PI and the percentage of MIB-1 PI (r = 0.763; $P < 0.0001$), and the patients with higher E2F-1 PI (E2F-1 PI ≥ 38.0 = median) showed significantly shorter disease-associated survival time in 49 R0 resection cases (n = 49, P = 0.015). Studies show similar result as ours in non–small cell lung carcinomas and breast carcinomas (Gorgoulis *et al.,* 2002; Zhang *et al.,* 2000).

During the past decade, a large number of studies revealed the regulation of G1/S transition and the control of cell proliferation by modulating the activity of the transcription factor E2F-1 (Degregori *et. al.,* 1995; Johnson *et al.,* 1993; Singh *et al.,* 1994). Furthermore, investigations have shown that overexpression of E2F-1 in transgenic mice promotes tumorigenesis (Pierce *et al.,* 1998; Pierce *et al.,* 1999). However, the pRb pathway has been shown to be associated with an anti-tumor mechanism through the induction of apoptosis that is largely mediated by E2F1 in several systems, either in association with p53 or p73 (Irwin *et al.,* 2000; Wu *et al.,* 1994). In addition, E2F-1 knockout mice develop

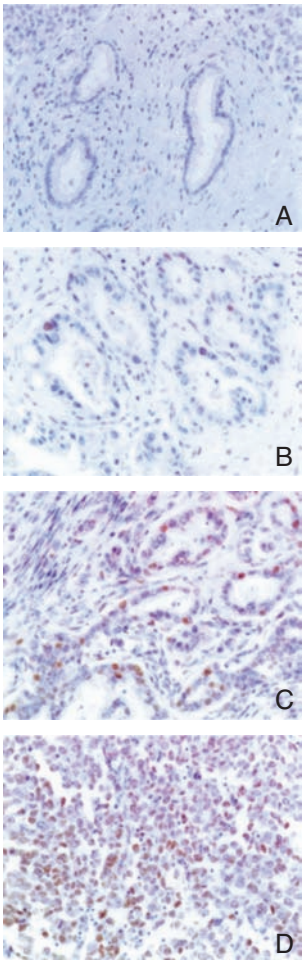

Figure 59. Immunohistochemistry for E2F-1 **(A)** in nonneoplastic pancreas tissues, showing occasional positive nuclear staining in active stromal fibroblasts and lymphocytes. Poor nuclear stainings were seen in ductal cells. Immunohistochemistry for E2F-1 in well-differentiated adenocarcinoma **(B),** showing sparse nuclear staining. Moderately differentiated **(C)** and poorly differentiated **(D)** adenocarcinoma, showing dense nuclear staining.

a broad range of tumors (Yamasaki *et al.,* 1996; Yamasaki *et al.,* 1998). Despite this paradoxical role of E2F-1, our data seem to support the view that E2F-1 acts as an effector of tumor cell proliferation.

Reports have shown a hypothetical model for E2F-1 promoting tumor cell proliferation in the background of a defective p53 pathway (Gorgoulis *et al.,* 2002; Pan *et al.,* 1998). Deregulation of the pRb/E2F-1 network should stimulate both cell proliferation and p53-dependent and/or p53-independent apoptosis. However, in case of dysfunctional apoptotic pathways, increased E2F-1 expression results in tumor cell proliferation. Because the p53 pathway, as well as pl6/pRb pathway, is mostly abrogated in pancreatic ductal carcinomas (Rozenblum *et al.,* 1997), it is conceivable that p53-dependent, E2F-1–derived apoptosis might be largely defective in this series. The results of this immunohistochemical method are shown in Figure 59.

In conclusion, our study showed E2F-1 expression is up-regulated and increased E2F-1 positivity has significantly raised growth indexes and is associated with poor patient outcome as far as pancreatic ductal carcinoma is concerned.

References

Degregori, J., Leone, G., Ohtani, K., Miron, A., and Nevins, J.R. 1995. E2F1 accumulation bypasses a G1 arrest resulting from the inhibition of G1 cyclin-dependent kinase activity. *Genes. Dev. 9*:2873–2887.

Dyson, N. 1998. The regulation of E2F by pRB-family proteins. *Genes Dev. 12*:2245–2262.

Gorgoulis, V.G., Zacharatos, P., Mariatos, G., Kotsinas, A., Bouda, M., Kletsas, D., Asimacopoulos, P.J., Agnantis, N., Kittas, C., and Papavassiliou, A.G. 2002. Transcription factor E2F-1 acts as a growth-promoting factor and is associated with adverse prognosis in non-small cell lung carcinomas. *J. Pathol. 198*:142–156.

Gansauge, S., Gansauge, F., Ramadani, M., Stobbe, H., Rau, B., Harada, N., and Beger, H.G. 1997. Overexpression of cyclin D1 in human pancreatic carcinoma is associated with poor prognosis. *Cancer Res. 57*:1634–1637.

Helin, K., Wu, C.L., Fattaey, A.R., Lees, J.A., Dynlacht, B.D., Ngwu, C., and Harlow, E. 1993. Heterodimerization of the transcription factors E2F-1 and DP-1 leads to cooperative transactivation. *Genes. Dev. 7*:1850–1861.

Irwin, M., Martin, M.C., Phillips, A.C., Seelan, R.S., Smith, D.I., Liu, W., Flores, E.R., Tsai, K.Y., Jacks, T., Vousden, K.H., and Kaelin, W.G., Jr. 2000. Role for the p53 homologue p73 in E2F-1-induced apoptosis. *Nature 407*:645–648.

Johnson, D.G., Schwarz, J.K., Cress, W.D., and Nevins, J.R. 1993. Expression of transcription factor E2F-1 induces quiescent cells to enter S phase. *Nature 365*:349–352.

Linder, S., Parrado, C., Falkmer, U.G., Blasjo, M., Sundelin, P., and von Rosen, A. 1997. Prognostic significance of Ki-67 antigen and p53 protein expression in pancreatic duct carcinoma: A study of the monoclonal antibodies MIB-1 and DO-7 in formalin-fixed paraffin-embedded tumour material. *Br. J. Cancer 76*:54–59.

Nevins, J.R. 1998. Toward an understanding of the functional complexity of the E2F and retinoblastoma families. *Cell Growth Differ. 9*:585–593.

Pan, H., Yin, C., Dyson, N.J., Harlow, E., Yamasaki, L., and van Dyke, T. 1998. Key roles for E2F1 in p53-dependent apoptosis and in cell division within developing tumors. *Mol. Cell 2*:283–292.

Pierce, A.M., Gimenez-Conti, I.B., Schneider-Broussard, R., Martinez, L.A., Conti, C.J., and Johnson, D.G. 1998. Increased E2F1 activity induces skin tumors in mice heterozygous and nullizygous for p53. *Proc. Natl. Acad. Sci. USA 95*:8858–8863.

Pierce, A.M., Schneider-Broussard, R., Gimenez-Conti, I.B., Russell, J.L., Conti, C.J., and Johnson, D.G. 1999. E2F1 has both oncogenic and tumor-suppressive properties in a transgenic model. *Mol. Cell. Biol. 19*:6408–6414.

Rozenblum, E., Schutte, M., Goggins, M., Hahn, S.A., Panzer, S., Zahurak, M., Goodman, S.N., Sohn, T.A., Hruban, R.H., Yeo, C.J., and Kern, S.E. 1997. Tumor-suppressive pathways in pancreatic carcinoma. *Cancer Res. 57*:1731–1734.

Singh, P., Wong, S.H., and Hong, W. 1994. Overexpression of E2F-1 in rat embryo fibroblasts leads to neoplastic transformation. *EMBO J. 13*:3329–3338.

Suzuki, T., Yasui, W., Yokozaki, H., Naka, K., Ishikawa, T., and Tahara, E. 1999. Expression of the E2F family in human gastrointestinal carcinomas. *Int. J. Cancer 81*:535–538.

Wu, X., and Levine, A.J. 1994. p53 and E2F-1 cooperate to mediate apoptosis. *Proc. Natl. Acad. Sci. USA 91*:3602–3606.

Yamasaki, L., Bronson, R., Williams, B.O., Dyson, N.J., Harlow, E., and Jacks, T. 1998. Loss of E2F-1 reduces tumorigenesis and extends the lifespan of Rb1(+/–)mice. *Nat. Genet. 18*:360–364.

Yamasaki, L., Jacks, T., Bronson, R., Goillot, E., Harlow, E., and Dyson, N.J. 1996. Tumor induction and tissue atrophy in mice lacking E2F-1. *Cell 85*:537–548.

Zhang, S.Y., Liu, S.C., Al-Saleem, L.F., Holloran, D., Babb, J., Guo, X., and Klein-Szanto, A.J. 2000. E2F-1: A proliferative marker of breast neoplasia. *Cancer Epidemiol. Biomarkers Prev. 9*:395–401.

12

Role of Immunohistochemical Expression of Chromogranins in Pancreatic Endocrine Tumors

Noriko Kimura, Monika Pilichowska, and Takayoshi Toyota

Introduction

Pancreatic endocrine tumors produce and secrete various peptide hormones that induce hormone-related syndromes. For instance, excessive production of gastrin mediates the Zollinger-Ellison syndrome; insulin causes hypoglycemia; and glucagon induces the "glucagonoma syndrome," which is characterized by necrolytic migratory erythema, diabetes, and diarrhea. The Verner-Morrison syndrome, which is brought about by high circulating levels of vasoactive intestinal peptide (VIP), produces severe secretory diarrhea. The "somatostatinoma syndrome" is associated with gallbladder dysfunction and gallstones, diarrhea with or without steatorrhea, and impaired glucose tolerance (Tomassetti *et al.,* 2001). Cushing's syndrome, which results from an ectopic adrenocorticotropic hormone (ACTH)-producing tumor of the pancreas, is also noteworthy. The diagnosis of functioning tumors is established by the measurement of the specific tumor marker in the plasma. Specific markers for pancreatic endocrine tumors include insulin, gastrin, glucagon, VIP, somatostatin, serotonin, and ACTH. The immunohistochemical study of peptide hormones is important for the pathologic diagnosis of pancreatic endocrine tumors. Le Bodic *et al.* (1996) have reported an immunohistochemical study of the 100 pancreatic endocrine tumors: 7 were unclassified, 10 were plurihormonal, and 83 produced a predominant hormonal secretion (with 50–90% of the same cell type). Those included 37 glucagonomas, 27 insulinomas, 11 pancreatic polypeptide (PP)-cell tumors, one gastrinoma, and one VIP-cell tumor (Le Bodic *et al.,* 1996).

In addition to the peptide hormones, general markers for the diagnosis of pancreatic endocrine tumors are available. Among these, plasma chromogranin A (CGA) has proved to be of great value for diagnosing functioning and nonfunctioning tumors and is considered the most sensitive general marker (Tartaglia *et al.,* 2003). Chromogranins are a family of water-soluble, acidic glycoproteins that are present in almost all endocrine, neuroendocrine, and neuronal tissue. This family comprises five members: chromogranin A (CGA), chromogranin B (CGB)/secretogranin I, secretogranin II/chromogranin C, 7B2, and NESP55. The molecules of human CGA and CGB are 48,000 and 76,000 Daltons, respectively. The role of chromogranins has been assumed to be the formation of neuroendocrine granules by aggregating with amines, nucleotides, calcium, and other peptides (Helle and Aunis, 2000).

Antisera against CGA and CGB and secretogranin II are used for analyzing the bovine pancreas by immunoblotting and immunohistochemistry (IHC). In IHC, CGA is found in all pancreatic endocrine cell types with

Handbook of Immunohistochemistry and *in situ* Hybridization of Human Carcinomas, Volume 3: Molecular Genetics, Liver Carcinoma, and Pancreatic Carcinoma

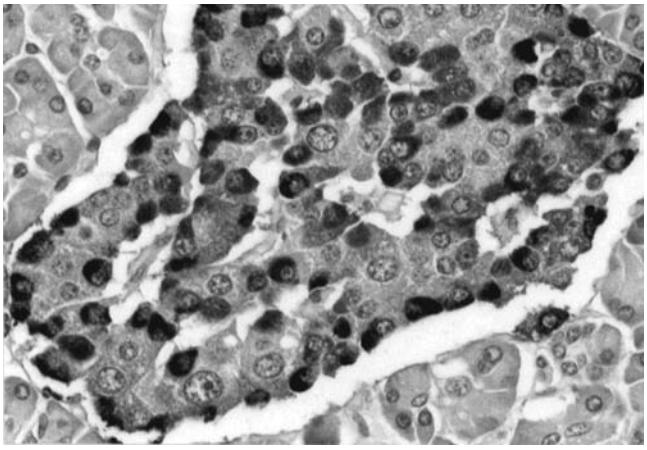

Figure 60. Immunostaining of chromogranin A in normal human pancreatic islet. Stronger staining is observed in the outer cells of the islet. (Counterstained with hematoxylin; original magnification 400X).

the exception of most PP-producing cells (Figure 60). For chromogranin B, only a faint immunostaining is obtained. For secretogranin II, A and B cells are faintly positive, whereas the majority of PP cells exhibit a strong immunostaining for this antigen (Yoshie *et al.,* 1987). For pathologic diagnosis of the pancreatic endocrine tumors, CGA is the most effective general tumor marker independent of the previously mentioned peptide hormones; however, CGB is expressed less (Kimura *et al.,* 2000; Lloyd *et al.,* 1988). Unlike pancreatic endocrine tumors, CGB is a useful marker for some rectal, ovarian, or testicular carcinoids (Kimura *et al.,* 2000). When tumors with endocrine tumor-like histology show no immunoreactivity for CGA, immunohistochemical study of CGB is highly recommended.

MATERIALS AND METHODS

For immunostaining of CGA, pancreatic endocrine tumor tissues are fixed in 10% buffered formalin and embedded in paraffin. Chromogranins in neuroendocrine granules are usually well-preserved, and it is worthwhile to examine the immunohistochemical staining for pathologic diagnosis even in poorly fixed tissues.

For hormone or chromogranin immunostaining, antigen-retrieval pretreatments should be avoided. The antibodies for CGA and CGB are commercially available. Thin sections of 3 μm are suitable for immunostaining. Immunohistochemical procedures using various kits such as the avidin-biotin method, streptavidin-biotin method, amino acid polymer method, or dextran polymer method, are available.

The procedures should be followed according to the manufacturer's manual. For example, CGA staining is given here. After dewaxing, the sections are immersed in ethanol. Endogenous peroxidase activity is blocked with 0.03% hydrogen peroxide in methanol for 10 min. After washing with phosphate buffer saline (PBS), the sections are incubated with normal goat serum for 10 min to decrease nonspecific staining. The sections are incubated for 18 hr at 4°C with rabbit polyclonal antibody for human CGA (Dako, Glostrup Germany; 1:1500). After washing, the sections are incubated with biotinylated anti-rabbit goat immunoglobulin (IgG) for 30 min. After washing with PBS, the sections are incubated with streptavidin-biotin peroxidase complex for 30 min. After washing with PBS, the sections are incubated in 0.33% 3,3′-diaminobenzidine tetrahydrochloride in 0.1 M Tris buffer and 0.02% hydrogen peroxide mixture for 10 min. Counterstaining is performed with hematoxylin or methylgreen. A normal pancreas section is simultaneously stained as positive control. For negative control, normal rabbit serum is incubated instead of CGA antibody. The streptavidin-biotin peroxide complex method is applied using a Histofine SAB-PO kit (Nichirei, Tokyo).

RESULTS AND DISCUSSION

All pancreatic endocrine tumors examined are positive for CGA (Kimura *et al.,* 2000). The marker CGA is diffusely stained in cytoplasm (Figure 61). Immunoreactive intensity of CGA is usually weaker in endocine tumors than that of normal pancreatic islets

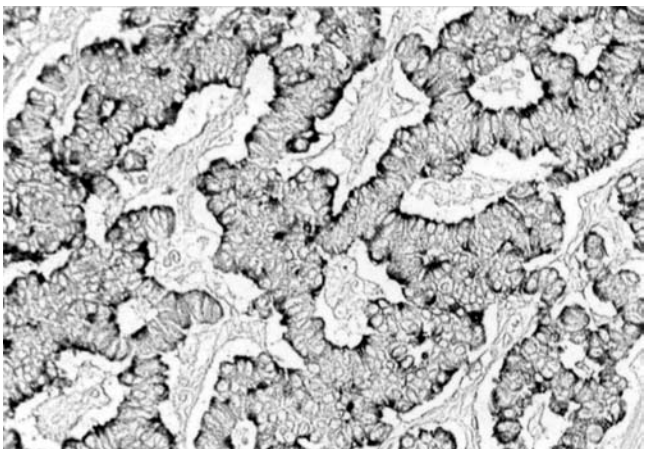

Figure 61. Pancreatic endocrine tumor, adrenocorticotropin hormone–producing type with trabecular arrangement, shows strong immunoreactivity of chromogranin A at the subnuclear regions. (Counterstained with methylgreen; original magnification 200X).

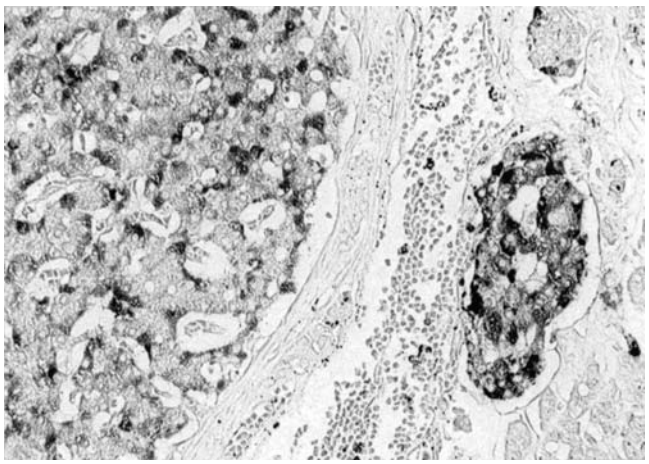

Figure 62. Immunoreactive intensity of chromogranin A is usually weaker in endocrine tumor cells (*left side*) than in normal pancreatic islet cells (*right side*). (Counterstained with methyl green; original magnification 200X).

(Figure 62). CGA is used as the tumor marker of first choice for pancreatic endocrine tumors both for IHC and as a serum marker. Then, any peptide hormones should be examined depending on the symptom or syndromes of patients with tumors.

The amino acid sequences of chromogranins have many dibasic sites that, in theory, can still be processed. Actually, sequence homology between the middle portion of chromogranin A and pancreastatin was revealed, and it formulated prohormone concept for the chromogranins (Eiden, 1987). Since then, numerous novel peptides have been described, some of them with biological activity (Helle, 2000). Human pancreastatin (PST) is deduced to be a 52-residue peptide amide that is present as residues 250–301 of human chromogranin A as a sequence homologous of porcine pancreastatin.

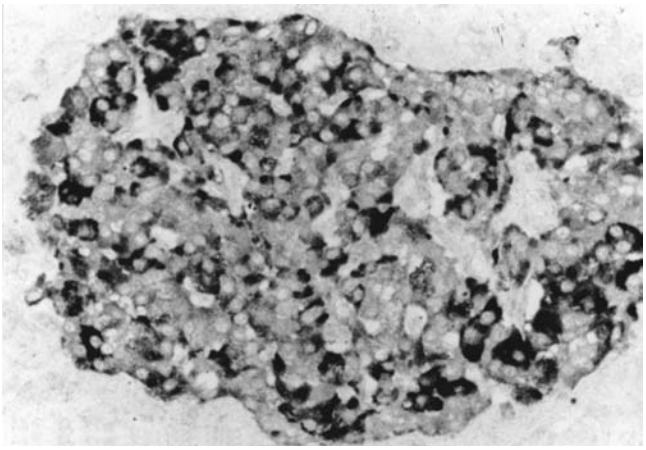

Figure 63. Immunohistochemical staining of pancreastatin in normal pancreatic islet of human. There are many immunoreactive cells. (Counterstained with methyl green; original magnification 400X).

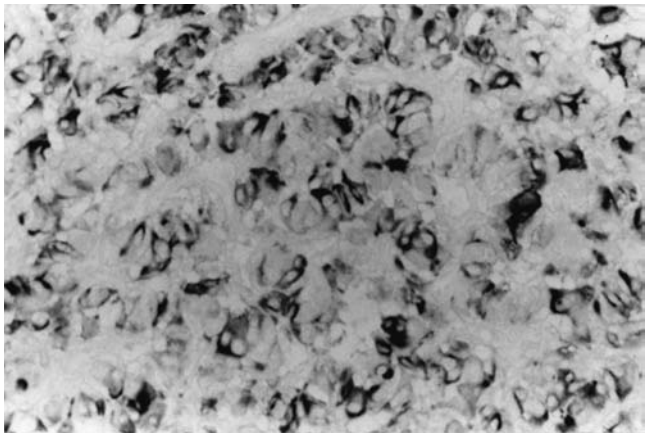

Figure 64. Immunoreactivity to pancreastatin is observed in pancreatic endocrine tumor. (Counterstained with methyl green; original magnification 400X).

Human PST is reported to suppress insulin release (Funakoshi *et al.,* 1989), and a significant increase of plasma PST has been observed in some patients with pancreatic islet tumors (Tateishi *et al.,* 1989). Double immunostaining of PST and pancreatic hormones in human pancreas showed PST immunoreactivity in all pancreatic endocrine cells, including insulin, glucagon, somatostatin, and PP cells (Kimura *et al.,* 1995) (Figure 63). PST is also detected in pancreatic endocrine tumors (Figure 64). Other chromogranin-derived peptide hormones detected in the pancreatic endocrine tumors are chromacin (the midportion fragment CGA 176-195) in insulinomas (Portel-Gomes *et al.,* 2001) and WE-14 (Curry *et al.,* 2000). Neuroendocrine secretory protein 55 (NESP55) is another novel member of the chromogranin family. Jakobsen *et al.* (2003) showed that 14 out of 25 pancreatic endocrine tumors expressed NESP55. Advances in the study of novel peptides, especially of region-specific antibodies to fragments of chromogranins, could lead to further characterization of pancreatic endocrine tumors.

For the treatment of pancreatic endocrine tumors, especially metastatic endocrine tumors, a somatostatin analog is effective. The presence of somatostatin receptor, especially types 2 and 5, should be confirmed before treatment (Kimura *et al.,* 1999). The immunohistochemical study of somatostatin receptor combined with chromogranins can contribute greatly to the diagnosis and treatment of patients with pancreatic endocrine tumors.

References

Curry, W.J., Norlen, P., Barkatullah, S.C., Johnston, C.F., Hakanson, R., and Hutton, J.C. 2000. Chromogranin A and its derived peptides in the rat and porcine gastro-entero-pancreatic system: Expression, localization and characterization. *Adv. Exp. Med. Biol. 482*:205–213.

Eiden, L.E. 1987. Is chromogranin A a prohormone? *Nature 325*:301.

Funakoshi, A., Jimi, A., Yasunami, Y., Tateishi, K., Funakoshi, S., Tamamura, H., and Yajima, H. 1989. Bioactivity of human pancreastatin and its localization in pancreas. *Biochem. Biophys. Res. Commun. 159*:913–918.

Helle, K.B. 2000. The chromogranins: Historical perspectives. *Adv. Exp. Med. Biol. 482*:3–20.

Helle, K.B., and Aunis, D. 2000. A physiological role for the granins as prohormones for homeostatically important regulatory peptides? A working hypothesis for future research. *Adv. Exp. Med. Biol. 482*:389–397.

Jakobsen, A.M., Ahlman, H., Kolby, L., Abrahamsson, J., Fischer-Colbrie, R., and Nilsson, O. 2003. NESP55, a novel chromogranin-like peptide, is expressed in endocrine tumors of the pancreas and adrenal medulla but not in ileal carcinoids. *Br. J. Cancer 88*:1746–1754.

Kimura, N., Funakoshi, A., Aunis, D., Tateishi, K., Miura, W., and Nagura, H. 1995. Immunohistochemical localization of chromostatin and pancreastatin, chromogranin A-derived bioactive peptides, in normal and neoplastic neuroendocrine tissues. *Endocr. Pathol. 6*:35–43.

Kimura, N., Pilichowska, M., Okamoto. H., Kimura. I., and Aunis, D. 2000. Immunohistochemical expression of chromogranins A and B, prohormone convertases 2 and 3, and amidating enzyme in carcinoid tumors and pancreatic endocrine tumors. *Mod. Pathol. 13*:140–146.

Kimura, N., Pilichowska, M., Date, F., Kimura, I., and Schindler, M. 1999. Immunohistochemical expression of somatostatin type 2A receptor in neuroendocrine tumors. *Clin. Cancer Res. 5*:3483–3487.

Le Bodic, M.F., Heymann, M.F., Lecomte, M., Berger, N., Berger, F., Louvel, A., De Micco, C., Patey, M., De Mascarel, A., Burtin, F., and Saint-Andre, J.P. 1996. Immunohistochemical study of 100 pancreatic tumors in 28 patients with multiple endocrine neoplasia, type I. *Am. J. Sure. Pathol. 20*:1378–1384.

Lloyd, R.V., Cano, M., Rosa, P., Hille, A., and Huttner, W.B. 1988. Distribution of chromogranin A and secretogranin I (chromogranin B) in neuroendocrine cells and tumors. *Am. J. Pathol. 130*:296–304.

Portel-Gomes, G.M., Grimelius, L., Johansson, H., Wilander, E., and Stridsberg, M. 2001. Chromogranin A in human neuroendocrine tumors: An immunohistochemical study with region-specific antibodies. *Am. J. Surg. Pathol. 25*:1261–1267.

Tartaglia, A., Bianchini, S., and Vezzadini, P. 2003. Biochemical diagnosis of gastroenteropancreatic endocrine tumors. *Minerva Med. 94*:1–7.

Tateishi, K., Funakoshi, A., Wakasugi, H., Iguchi, H., Shinozaki, H., Abe, M., Funakoshi, S., Tamamura, H., Yajima, H., and Matsuoka, Y. 1989. Plasma pancreastatin-like immunoreactivity in various diseases. *J. Clin. Endocrinol. Metab. 69*:1305–1308.

Tomassetti, P., Migliori, M., Lalli, S., Campana, D., Tomassetti, V., and Corinaldesi, R. 2001. Epidemiology, clinical features and diagnosis of gastroenteropancreatic endocrine tumors. *Ann. Oncol.12* Suppl 2:S95–S99.

Yoshie, S., Hagn, C., Ehrhart, M., Fischer-Colbrie, R., Grube, D., Winkler, H, and Gratzl, M. 1987. Immunological characterization of chromogranins A and B and secretogranin II in the bovine pancreatic islet. *Histochemistry 87*:99–106.

13

Role of Immunohistochemical Expression of Maspin in Pancreatic Carcinoma

Young Lyun Oh and Geunghwan Ahn

Introduction

Maspin is a recently identified protein related to the serpin family of protease inhibitors (Zou *et al.,* 1994). The *maspin* gene is part of a serpin locus cluster at chromosome 18q21.3-q23 closely linked to plasminogen activator inhibitor type 2, Bcl2, the tumor-suppressor gene *DCC*, and squamous cell carcinoma antigen 1 and 2 (Sager *et al.,* 1994; Schneider *et al.,* 1995). Maspin was originally isolated from normal mammary epithelium by subtractive hybridization. In cultured human mammary myoepithelial cells, maspin is a predominantly cytoplasmic protein that associates with secretory vesicles and is present at the cell surface (Sheng *et al.,* 1996).

Maspin is down-regulated but not mutated in cancer cells (Zou *et al.,* 1994). It is also known to be a tumor suppressor that inhibits the motility, invasion, and metastasis of the breast and prostatic cancer cell lines (Sager *et al.,* 1996; Sheng *et al.,* 1996; Zou *et al.,* 1994). Maspin is also known to be part of the p53 tumor-suppressor pathway (Zou *et al.,* 2000) and acts as an inhibitor of angiogenesis (Zhang *et al.,* 2000). However, its functional mechanisms are considered to be unresolved and its role as a protease inhibitor is not clearly established.

Only a few reports of maspin expression in pancreatic neoplasm have been published (Maass *et al.,* 2001; Oh *et al.,* 2002). In our study (Oh *et al.,* 2002), we investigated the expression of maspin in 107 resected pancreatic neoplasms and nontumorous pancreatic lesions. The pancreatic tumors included were 38 ductal adenocarcinomas, 13 intraductal papillary mucinous tumors (IPMTs), 13 mucinous cystic tumors (MCTs), 16 pancreatic endocrine tumors (PETs), 10 solid-pseudopapillary tumors (SPTs), 5 serous cystadenomas, 4 pancreatoblastomas, 2 acinar cell carcinomas, 4 adenosquamous carcinomas, and 2 undifferentiated carcinomas available for assessment. The tumors were classified according to the histologic criteria outlined by the World Health Organization using hematoxylin and eosin stains of formalin-fixed and paraffin-embedded tissue. The stage was classified according to the staging manual of the American Joint Committee on Cancer.

MATERIALS

1. Xylene.
2. Ethanol.
3. Phosphate buffer saline (PBS) (pH 7.4).
4. Tris-buffered saline (TBS) (pH 7.4).

Handbook of Immunohistochemistry and *in situ* Hybridization of Human Carcinomas, Volume 3: Molecular Genetics, Liver Carcinoma, and Pancreatic Carcinoma

5. 0.01 M sodium citrate buffer (pH 6.0).
6. 30% hydrogen peroxide.
7. Absolute methanol.
8. Primary antibody (Maspin, Pharmingen, San Diego, CA; 1:3,000).
9. Antibody diluent (Dako Glostrup, Denmark).
10. Antibody/peroxidase-conjugated polymer (EnVision+, Peroxidase, Mouse, Dako).
11. Diaminobenzidene (DAB)+ chromogen (Dako).
12. Hematoxylin.
13. Distilled or deionized water.
14. Mounting media.

METHODS

1. Paraffin sections (4 μm thick) are mounted onto poly-L-lysine–coated glass slides.
2. Dry slides in an oven for 1 hr at 60°C.
3. Deparaffinize the slides in three changes of xylene.
4. Rehydrate the slides in a graded series of ethanol.
5. Wash the slides 2× in PBS.
6. Microwave 0.01 M citrate buffer of pH 6.0 for 3 min.
7. Place the slides in the citrate buffer and microwave at 97°C for 5 min.
8. Cool the slides in citrate buffer solution at room temperature for 10 min.
9. Rinse slides and place them in the TBS.
10. Incubate slides with 3% hydrogen peroxide in absolute methanol for 10 min.
11. Wash with TBS 3× for 2 min each.
12. Remove excess liquid from around specimen.
13. Apply primary antibody against Maspin (Pharmingen; 1:3,000) to slides and incubate in moist chamber at room temperature for 1 hr.
14. Rinse with TBS 3× for 2 min each.
15. Apply EnVision+, Peroxidase, Mouse (Dako) for 30 min.
16. Rinse with TBS 3× for 2 min each.
17. Apply substrate-chromogen solution (DAB) for 3–5 min.
18. Rinse well with distilled water.
19. Counterstain with hematoxylin.
20. Dehydrate and mount.

RESULTS AND DISCUSSION

The cells were considered positive if granular cytoplasmic/nuclear or cytoplasmic staining was observed. The staining was evaluated using the "quick score," where estimation was made of both the proportion and intensity of the cells stained. The proportions were scored as 0 (0), 1 (less than 1/100 of tumor cells), 2 (1/100–1/10 of tumor cells), 3 (1/10–1/3 of tumor cells), 4 (1/3–2/3 of tumor cells), and 5 (more than 2/3 of tumor cells), whereas the intensity was assigned as 0, no staining; 1, weak; 2, moderate; and 3, strong staining. For statistical analysis, the tumors were divided into no (total score of 0), low (total score of 5 or less), and high (total score of 6 or more) expressers.

All cases of ductal adenocarcinomas expressed maspin, of which 30 (78.9%) were classified as high expressers (Figure 65) and 8 (21.1%) were low expressers. The majority of tumor cells showed strong cytoplasmic expressions that occasionally accompany nuclear staining. There was no statistical difference between the maspin expression (low versus high) and clinicopathologic parameters including histologic grade, lymph node metastasis, or stage. However, the staining score for maspin was positively correlated with the tumor size ($p = 0.004$). Four cases of adenosquamous carcinoma exhibited high expressions for maspin in both areas of the adenocarcinoma and squamous carcinoma. In two cases of undifferentiated carcinoma, there was low expression in the glandular area but not in the sarcomatous area.

All 13 IPMTs were stained with maspin, as were 11 of the 13 MCTs. Staining patterns were variable and heterogeneous. All six cases of intraductal papillary mucinous carcinoma and two of the three IPMTs of borderline malignant potential expressed high levels of maspin, whereas all four cases of intraductal papillary mucinous adenoma showed a low level of maspin expression. All three cases of mucinous cystic carcinoma, three out of four MCTs of borderline malignant potential, and one out of six mucinous cystadenoma were high maspin expressers. Maspin was expressed more frequently in the dysplastic epithelium. The invasive component of intraductal papillary mucinous carcinoma and mucinous cystic carcinoma showed strong immunoreactivity for maspin. It is interesting that,

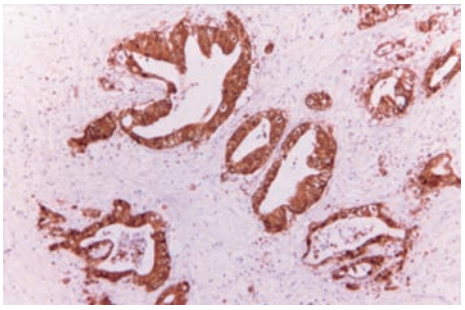

Figure 65. High expression of maspin in ductal adenocarcinoma (200X).

with increasing degree of dysplasia the localization of maspin seemed to shift from nuclear/cytoplasmic staining to cytoplasmic staining that was prominently seen in ductal adenocarcinoma.

Of the four cases of pancreatoblastoma, one case displayed a high expression for maspin in the glandular and solid portion with squamoid nests, whereas three cases showed focal immunoreactivity for maspin in the solid squamoid cell nests. In the case with a high expression, tumor cells were more pleomorphic with frequent mitosis than those with low expression.

None of the PETs were positive for maspin. One case, which was originally diagnosed as ductal adenocarcinoma and negative for maspin, showed a strong immunoreaction for chromogranin and was reclassified as PET. Some cases of PET that showed vascular invasion, adjacent organ involvement, or metastasis, however, were still negative for maspin. In addition, two cases of acinar cell carcinoma were also negative. These data are not surprising in view of the report by Pemberton *et al.* (1997), which showed that maspin expression was associated almost exclusively with epithelia in many of the human tissues. Our data confirmed the observation that maspin expression may be involved in the tumor of epithelial differentiation but not in endocrine and acinar cell differentiation.

Another interesting observation in our study was the absence of immunoreactivity for maspin in serous cystadenoma and SPT. There are two possible explanations for the lack of maspin expression in these neoplasms. In our experience maspin was focally expressed in the main and interlobular duct epithelium with mucinous cytoplasm but not in the intralobular, intercalated, or centroacinar cells of normal pancreatic tissue. The ductal epithelium of the pancreas is divided into two compartments: the mucinous cells lining the main and interlobular ducts and the ductulocentroacinar (intralobular) compartments. Ductal adenocarcinoma, MCT, and IPMT are closely related to the former, whereas serous cystadenoma and SPT are related to the latter compartment. It is therefore possible that maspin expression may be up-regulated in the neoplasms of the main and interlobular duct origin. However, the absence of maspin expression might be caused by their minimal malignant potential.

In normal pancreatic parenchyma and chronic pancreatitis adjacent to the tumor, maspin expression was rarely seen in the interlobular and the main duct epithelium but not in the intralobular, intercalated or centroacinar cells. Acinar and islet cells were negative for maspin in all cases.

In our study, all of the pancreatic ductal adenocarcinomas were positive for maspin, and the carcinomatous portion of IPMT and MCT showed high expression for maspin in contrast to the reduced or no maspin expression in the advanced breast and prostate cancers. Maass *et al.* (2001) also demonstrated this conflicting expression of maspin in pancreatic cancer. They observed a strong cytoplasmic reaction in 23 of 24 pancreatic ductal adenocarcinomas, but they saw negative staining in normal pancreas by immunohistochemistry using a monoclonal antimaspin antibody (Pharmingen). In their study, there was no correlation between the staining intensity and the histologic grade or stage of the tumors. They also reported that more than half of the pancreatic cancer cell lines expressed maspin messenger ribonucleic acid (mRNA) and suggested that up-regulated maspin mRNA expression is translated into protein in pancreatic cancer cells.

Pemberton *et al.* (1997) also could not detect maspin mRNA expression in intralobular duct epithelia of the pancreas by Northern Blot. However, they observed maspin staining in intralobular duct epithelia of the pancreas using affinity-purified polyclonal anti-maspin immunoglobulin G. We thought that this discrepancy of maspin staining in normal pancreas might be caused by different characteristics of the antimaspin antibody.

Of note, Pemberton *et al.* (1997) observed that proliferating epithelial cells at the base of the crypts in the stomach stained strongly with maspin in comparison with surface epithelium. In their study on breast and prostate, myoepithelial cells and basal cells exhibited much stronger staining than adjacent luminal epithelium. Based on these observations, they suggested that maspin down-regulation may be a normal event in cell differentiation and that maspin contributes to the maintenance of normal architecture. However, to date the function and significance of maspin expression in pancreatic cancer is unknown and further investigation is needed.

The up-regulated cytoplasmic maspin expression in pancreatic tumors can be interpreted in several aspects. Maass *et al.* (2001) suggested that the maspin gene could be one of possible genes involved in pancreatic carcinogenesis because the *maspin* gene is mapped on chromosome 18q21.3 in close proximity to the *DCC* and *DPC4/SMAD4* genes and losses of chromosome 18q including *DCC* and *DPC4/SMAD4* are the most frequently identified genetic alterations in pancreatic cancer. However, the cytoplasmic expression of maspin can be speculated as an inactive or nonfunctional form in pancreatic cancers.

In summary, maspin may play an important role in the carcinogenesis of pancreatic neoplasm with epithelial origin, especially for pancreatic tumor composed of mucin-producing cells. Maspin immunostaining may also be a useful adjunctive marker for differentiating ductal adenocarcinoma from SPT, PET, acinar cell carcinoma, and chronic pancreatitis.

References

Maass, N., Hojo, T., Ueding, M., Luttges, J., Kloppel, G., Jonat, W., and Nagasaki, K. 2001. Expression of the tumor suppressor gene maspin in human pancreatic cancers. *Clin. Cancer Res. 7*:812–817.

Oh, Y.L., Song, S.Y., and Ahn, G. 2002. Expression of maspin in pancreatic neoplasms: Application of maspin immunohistochemistry to the differential diagnosis. *Appl. Imunohistochem. Mol. Morphol. 10*:62–66.

Pemberton, P.A., Tipton, A.R., Pavloff, N., Smith, J., Erickson, J.R., Mouchabeck, Z.M., and Kiefer, M.C. 1997. Maspin is an intracellular serpin that partitions into secretory vesicles and is present at the cell surface. *J. Histochem. Cytochem. 45*:1697–1706.

Sager, R., Sheng, S., Anisowicz, A., Sotiropoulou, G., Zou, Z., Stenman, G., Swisshelm, K., Chen, Z., Hendrix, M.J., Pemberton, P., Rafidi, K., and Ryan, K. 1994. RNA genetics of breast cancer: Maspin as paradigm. *Cold Spring Harb. Symp. Quant. Biol. 59*:537–546.

Sager, R., Sheng, S., Pemberton, P., and Hendrix, M.J. 1996. Maspin: A tumor suppressing serpin. *Curr. Top. Microbiol. Immunol. 213*:51–64.

Schneider, S.S., Schick, C., Fish, K.E., Miller, E., Pena, J.C., Treter, S.D., Hui, S.M., and Silverman, G.A. 1995. A serine proteinase inhibitor locus at 18q21.3 contains a tandem duplication of the human squamous cell carcinoma antigen gene. *Proc. Natl. Acad. Sci. USA 92*:3147–3151.

Sheng, S., Carey, J., Seftor, E.A., Dias, L., Hendrix, M.J., and Sager, R. 1996. Maspin acts at the cell membrane to inhibit invasion and motility of mammary and prostatic cancer cells. *Proc. Natl. Acad. Sci. USA 93*:11669–11674.

Zhang, M., Volpert, O., Shi, Y.H., and Bouck, N. 2000. Maspin is an angiogenesis inhibitor. *Nat. Med. 6*:196–199.

Zou, Z., Anisowicz, A., Hendrix, M.J., Thor, A., Neveu, M., Sheng, S., Rafidi, K., Seftor, E., and Sager, R. 1994. Maspin, a serpin with tumor-suppressing activity in human mammary epithelial cells. *Science 263*:526–529.

Zou, Z., Gao, C., Nagaich, A.K., Connell, T., Saito, S., Moul, J.W., Seth, P., Appella, E., and Srivastava, S. 2000. p53 regulates the expression of the tumor suppressor gene maspin. *J. Biol. Chem. 275*:6051–6054.

14

Role of Mast Cells in Pancreatic Carcinoma

Irene Esposito, Frank Bergmann, Markus W. Büchler, and Helmut Friess

Introduction

Mast cells play a key role in immediate hypersensitivity (type I) immune reactions. Binding of a specific antigen to two adjacent immunoglobulin E (IgE) molecules expressed on mast cell plasma membrane ("cross-linking") initiates the process of degranulation, which is the release of preformed mediators of the inflammatory reaction contained in mast cell granules (e.g., histamine, adenosine, heparin, various proteases). At the same time, the synthesis of new mediators (e.g., prostaglandins, leukotrienes, cytokines, and growth factors) is initiated. Through this and other IgE-independent mechanisms (e.g., under the stimulation of the anaphylotoxins C3a and C5a, dextran, basic peptides and physical agents), mast cells exert their function as major cell mediators of the allergic reactions (Schulman, 1993). At the same time, they are also involved in acute and, at a higher level, chronic fibrogenic inflammatory processes in which they directly induce fibrosis through the production of fibroblast growth factor (FGF), platelet-derived growth factor (PDGF), and transforming growth factor-β (Krishnaswamy *et al.,* 2001). The differentiation of mast cells from bone marrow precursors and their proliferation is promoted by stem cell factor (SCF), which binds to c-kit, a type-3 tyrosine–kinase receptor (Gurish and Boyce, 2002). Mast cell precursors complete their maturation at peripheral sites, under the influence of the specific local microenvironment (Kitamura *et al.,* 1993). There are many cellular sources of SCF: fibroblasts, endothelial cells, the basal cells of the epidermis, and various tumor cells. Mast cells can also produce SCF and stimulate their own growth in an autocrine way (Mierke *et al.,* 2000; Zhang *et al.,* 1998).

Role of Mast Cells in Nonpancreatic Tumors

Studies have provided evidence that mast cells play an important yet controversial role in the pathogenesis of human neoplasms. The accumulation of mast cells at the tumor infiltrative borders was first described by Westphal in 1891 (Westphal, 1891). More recently it has been demonstrated that mast cells can produce and release growth factors, proangiogenetic factors, and lytic enzymes, which might influence local tumor growth and invasion. The number of infiltrating mast cells has been found to be associated with the intratumoral microvessel density and to be directly correlated with the presence of lymph node metastases in lung adenocarcinoma (Takanami *et al.,* 2000). It also correlates with a worse prognosis in non-Hodgkin's lymphoma (Molin *et al.,* 2002). Furthermore, metastatic melanomas show a higher number of vascular endothelial

Handbook of Immunohistochemistry and *in situ* Hybridization of Human Carcinomas, Volume 3: Molecular Genetics, Liver Carcinoma, and Pancreatic Carcinoma

growth factor (VEGF)-positive mast cells at the tumor periphery when compared with nonmetastatic tumors (Toth-Jakatics *et al.,* 2000). The expression of VEGF and other proangiogenic factors (tryptase, basic fibroblast growth factor [bFGF]) by peritumoral mast cells has been also described in squamocellular larynx cancer (Sawatsubashi *et al.,* 2000) and esophageal cancer (Elpek *et al.,* 2001). In breast cancer the production of the serin-proteases tryptase and chymase by mast cells has been related to the tumor's invasive ability (Kankkunen *et al.,* 1997). In contrast, the number of mast cells has been found to be correlated with a shallower penetration of gastric cancer cells into the gastric walls and with a lower number of lymph node metastases in patients with gastric cancer (Jiang *et al.,* 2002).

Role of Mast Cells in Pancreatic Cancer

Pancreatic cancer is an aggressive disease with a dismal prognosis (Greenlee *et al.,* 2000). In its classic ductal histotype pancreatic cancer appears as a "scirrhous" tumor, characterized by well-to-moderately differentiated neoplastic glands embedded in a dense stroma. The onset of pancreatic adenocarcinoma can be preceded by a chronic inflammatory condition, chronic pancreatitis, which has been recognized as a definite risk factor for the development of pancreatic cancer (Malka *et al.,* 2002). This risk increases with the duration of the disease and is particularly high in patients affected by hereditary pancreatitis, who develop the disease at a young age (Lowenfels *et al.,* 2000). In 2001, using deoxyribonucleic acid (DNA)-array technology, the expression patterns of 5600 genes in pancreatic tissues were analyzed, comparing chronic pancreatitis with the normal pancreas and pancreatic cancer (Friess *et al.,* 2001). The results of this study showed that the mast cell serine-protease tryptase is overexpressed in chronic pancreatitis (11.1-fold), and to a lesser extent in pancreatic cancer (7.3-fold), when compared to the normal pancreas. Tryptase is contained in mast cell granules and is released as a preformed mediator on mast cell degranulation. It is considered a specific marker for mast cells; moreover, tryptase immunostaining can reveal the presence of mast cells with a higher sensitivity than histochemical stainings such as toluidine blue or Giemsa (Walls *et al.,* 1990). Therefore, the increased expression of tryptase messenger ribonucleic acid (mRNA) in chronic pancreatitis and pancreatic cancer in comparison with the normal pancreas might correspond to an increased number of mast cells in these disorders.

Tryptase is a proteolytic enzyme that exerts a proinflammatory activity by cleaving multiple substrates, such as prothrombin, fibrinogen, prourokinase, and neuropeptides (Harris *et al.,* 2001). In addition, tryptase acts as a signaling molecule by binding to a protein G–coupled receptor named PAR-2 (protease activated receptor-2), thus inducing different cell responses, such as vasodilation, leukocyte adhesion and extravasation, and cytokine synthesis (Cenac *et al.,* 2002). Moreover, tryptase exerts a fibroproliferative action by binding PAR-2 and then stimulating the synthesis of cyclooxygenase 2 (COX2) and prostaglandins, which ultimately leads to fibroblast proliferation (Frungieri *et al.,* 2002). The induction of angiogenesis is another important function of tryptase, which can specifically induce endothelial cell proliferation and capillary formation (Blair *et al.,* 1997). Mast cells, as the cellular source of tryptase, are therefore likely to play an active role in fundamental pathogenic aspects of chronic pancreatitis and pancreatic cancer, such as the induction of stromal cell proliferation and angiogenesis.

A further step in our analysis was the evaluation of mast cell expression (through tryptase immunostaining) in chronic pancreatitis of varying etiology. We demonstrated an increase in total mast cell number in comparison with the normal pancreas and a correlation between mast cell number and the degree of inflammation and fibrosis (Esposito *et al.,* 2001). However, the etiology of chronic pancreatitis was not related to the number of infiltrating mast cells.

In this chapter we summarize an analysis of mast cell infiltration in pancreatic cancer and of its relation to the SCF-c-kit system, which provides novel information about the biology of this disease. These data have been published in detail elsewhere (Esposito *et al.,* 2002).

MATERIALS

1. 10% formalin: 37% formalin diluted 1:10 in water.
2. Carnoy's solution: 6 parts of ethanol (absolute or 95%), 3 parts chloroform, 1 part glacial acetic acid.
3. Xylene.
4. Ethanol solutions: 99%, 95%, 70%, 50%, and 30% diluted in deionized water.
5. Tris-buffered saline (TBS) + 0.1% bovine serum albumin (BSA): combine 3.03 g Tris HCl and 8.18 g NaCl, bring volume to 1 L with distilled water, adjust pH to 7.4; add 1 g BSA.
6. Methanol.
7. Methanol/0.6% hydrogen peroxide (H_2O_2): 4 µl of 30% H_2O_2 in 200 µL methanol.
8. Primary antibodies: mouse anti-tryptase (Chemicon International, Temecula, CA) diluted 1:1000 in normal goat serum (NGS) (Kirkegaard and Perry Laboratories, Gaithersburg, MD); mouse anti-chymase (Chemicon International) diluted 1:4000 in NGS (Kirkegaard and

Perry Laboratories); goat anti-SCF (Santa Cruz Biotechnology, Santa Cruz, CA) diluted 1:100 in normal rabbit serum (NRS) (Kirkegaard and Perry Laboratories); rabbit anti-c-kit (Santa Cruz Biotechnology) diluted 1:200 in NGS (Kirkegaard and Perry Laboratories).

9. Pronase (1 mg/ml in TBS, pH 7.5).
10. Biotinylated secondary antibodies (rabbit anti-goat, goat anti-rabbit, goat anti-mouse) (Kirkegaard and Perry Laboratories).
11. Streptavidin-peroxidase complex (Kirkegaard and Perry Laboratories).
12. Diaminobenzidine (DAB): 10 µg/ml in distilled water.
13. Tris-HCl buffer: dissolve 121.1 g of Tris base in 800 ml distilled water. Adjust pH to 7.6 by adding HCl. Bring volume to 1 L.
14. DAB tetrahydrochloride solution (DAB + Tris-HCl + 0.03% H_2O_2): 200 µL DAB + 3 ml Tris-HCl buffer + 3 µl H_2O_2 30%.
15. Mayer's hematoxylin.
16. Mounting medium.

METHODS

Immunostaining Procedure

1. Fix the tissue samples immediately after surgical removal in 10% buffered formalin or in Carnoy's solution (for chymase detection because formalin fixation destroys chymase immunoreactivity) for 12–24 hr at room temperature; then embed them in paraffin and cut into 4 µm thick sections.
2. Deparaffinize in xylene (3×, 10 min each).
3. Rehydrate in descending ethanol solutions: ethanol 99% (3×, 5 min each), 95% (1×, 5 min), 70% (1×, 5 min), 50% (1×, 5 min), 30% (1×, 3 min), deionized water (1×, 3 min).
4. Rinse the sections in TBS-0.1% BSA (2×, 5 min).
5. Pretreatment: in the case of SCF immunostaining a pretreatment of the tissue sections is necessary to improve antigen retrieval. Incubate the sections with 100 µl of pronase solution for 6 min at 37°C on a warming plate.
6. Rinse the sections in TBS-0.1% BSA (1×, 5 min).
7. Quench the endogenous peroxidase activity: incubate the sections for 1 min in methanol, then for 20 min in methanol/0.6% hydrogen peroxide, then again for 1 min in methanol, and finally for 3 min in deionized water.
8. Rinse the sections in TBS-0.1% BSA (2×, 5 min).
9. Block nonspecific binding by incubating the sections in normal serum (2–3 drops) at room temperature for 30 min in a humid chamber to prevent evaporation.
10. Primary antibody: After removal of the serum, incubate the slides with the appropriate primary antibody (100 µl per section) overnight at 4°C in a humid chamber.
11. Rinse the sections in TBS-0.1% BSA (2×, 5 min).
12. Incubate with the appropriate secondary antibody (2–3 drops) at room temperature for 45 min in a humid chamber.
13. Rinse the sections in TBS-0.1% BSA (2×, 5 min).
14. Incubate with the streptavidin-peroxidase complex (2–3 drops) at room temperature for 30 min in a humid chamber.
15. Rinse the sections in TBS-0.1% BSA (2×, 5 min).
16. Color reaction: Add 100 µl of DAB solution to each section, and incubate in the dark at room temperature for a maximum of 15 min (usually 2–5 min are enough, check under the light microscope); stop the reaction in deionized water.
17. Counterstain the slides in hematoxylin (30 sec–1 min), then rinse in tap water.
18. Dehydrate the sections in ascending ethanol solutions: ethanol 50% (1×, 5 min), 70% (1×, 5 min), 95% (1×, 5 min), 99% (2×, 5 min).
19. Clear the tissue sections in xylene (3×, 5 min).
20. Mount.

To ensure antibody specificity, consecutive sections can be incubated in the absence of primary antibody or in the presence of a nonimmune serum.

Evaluation of Immunohistochemical Findings

The number of tryptase/chymase-positive mast cells is assessed by counting the stained cells in each specimen at a 200X magnification after determination of the area of the whole tissue section using a computer-assisted image analysis system. The results are expressed as number of cells/mm^2. The number of SCF and c-kit–positive mast cells is expressed as a percentage of total mast cells present in each section, by comparing two consecutive sections stained with anti-tryptase and anti-SCF or anti-tryptase and anti-c-kit, respectively. Other methods of mast cell counting have been described. For example, the tissue section can be examined at low magnification (100X) to find the areas with higher mast cell density. Then, the single cells are counted at 200X magnification in the five fields with the highest cell density and the mean value is taken as the mast cell count for that case (Kojima *et al.,* 2002). Expression of SCF and c-kit by cancer cells is quantified by counting at least 1000 cells in each tumor sample. The immunohistochemical results are scored positive when 5% of the tumor cells are immunoreactive (Arber *et al.,* 1998).

RESULTS AND DISCUSSION

Demographic and Pathologic Characteristics of the Patient Population

The patient population comprised 10 males and 16 females (median age: 69 years; range: 35–83 years) suffering from pancreatic cancer. Normal pancreas tissues were obtained through an organ donor program (n = 17; 11 male, 6 female; median age: 46 years; range: 18–77 years).

The specimens were subjected to histologic analysis; the staging and grading of the cancer specimens were assessed according to the TNM classification of the International Union Against Cancer (1997). All the tumor samples were ductal adenocarcinomas; 7 (27%) were well differentiated (G1), 14 (54%) were moderately differentiated (G2), and 5 (19%) were poorly differentiated (G3). Four tumors (15%) were in stage I, 5 (19%) were in stage II, 15 (58%) were in stage III, and 2 (8%) were in stage IV.

Mast Cell Count and Characterization in the Normal Pancreas and Pancreatic Cancer

The presence of inflammatory cells in the neoplastic tissues is considered a mechanism of host defense against cancer (Dunn *et al.,* 2002). However, it has been demonstrated that the production and release of lytic enzymes and growth factors by the inflammatory infiltrate can promote the growth and invasive capacity of the cancer cells (Bingle *et al.,* 2002). It is well known that chronic inflammatory conditions favor the development of neoplastic processes in many tissues and organs (Kuper *et al.,* 2000). Although different mechanisms can be involved in different anatomic sites, it seems that the presence of the inflammatory cells might alter the tissue environment, thus making the normal cells more susceptible to malignant transformation (Kinzler and Vogelstein, 1998). Free radicals, produced by neutrophils and activated macrophages, are among the factors that can generate this anomalous microenvironment; they induce DNA damage and can be directly mutagenic (Jackson and Loeb, 2001). The tissue damage in the context of a chronic inflammatory condition leads to the production and release of cytokines and growth factors that stimulate the regeneration of the damaged cells but at the same time induce the proliferation of genomically altered cells (Kinzler and Vogelstein, 1998). Mast cell infiltration of the tumor tissues can enhance the invasive capacity of the cancer cells essentially by promoting the angiogenic process (Norrby, 2002). In human and animal tissues two main populations of mast cells have been identified: tryptase-positive mast cells (MC_T), also known as mucosal-type mast cells, and tryptase/chymase double-positive mast cells (MC_{TC}), also named connective-tissue–type mast cells (Irani *et al.,* 1986).

In this study we used a monoclonal antibody directed against the enzyme tryptase to detect the presence and the number of mast cells in the normal pancreas and in pancreatic cancer tissues. Immunohistochemistry revealed that mast cells are found around blood vessels and nerves, in the interstitial space between acinar lobules, around the neoplastic glands, and at the infiltrative borders of the tumor (Figure 66A). The mean number of tryptase-positive cells in cancer tissues was 1.7-fold higher than in the normal pancreas ($p = 0.03$), thus confirming at a morphologic level the increased gene expression levels that resulted from the DNA-array analysis.

After chymase immunostaining of Carnoy-fixed tissue samples, the mean number of positive cells was 2.8-fold higher in pancreatic cancer than in the normal pancreas, thus indicating the presence of connective-tissue–type mast cells in pancreatic tissues as well as their accumulation in pancreatic cancer (Figure 66B).

We further characterized the pancreatic cancer–associated mast cells by staining consecutive sections with tryptase and SCF or tryptase and c-kit. Only a small percentage of the mast cells present in the normal samples or in the cancer specimens stained positive for SCF. Cytoplasmic or membrane staining for c-kit was detected in up to 18.5% of total mast cells in the normal pancreas and in up to 16% of total mast cells in pancreatic cancer.

SCF and c-kit Expression in the Normal Pancreas and Pancreatic Cancer

The acquisition of the mature phenotype by mast cells is tissue-specific and mostly regulated by the SCF–c-kit system. These two factors are produced by different kinds of tumor cells, but their role in the promotion of tumor growth is still under discussion. In some human neoplasms (e.g., lung cancers) the coexpression of SCF and c-kit by tumor cells has been interpreted as an autocrine growth-stimulating loop (Pietsch *et al.,* 1998). In other tissues, the development of malignancy is accompanied by a decrease of SCF–c-kit expression (e.g., thyreocytes, melanocytes) (Welker *et al.,* 2000). It was therefore interesting to determine the expression of these factors in the human pancreas and to explore their possible relation to the accumulation of mast cells in pancreatic cancer.

In the normal pancreas, SCF immunostaining was limited to mast cell cytoplasm. In contrast, 20% of the cancer specimens exhibited SCF-immunoreactivity in

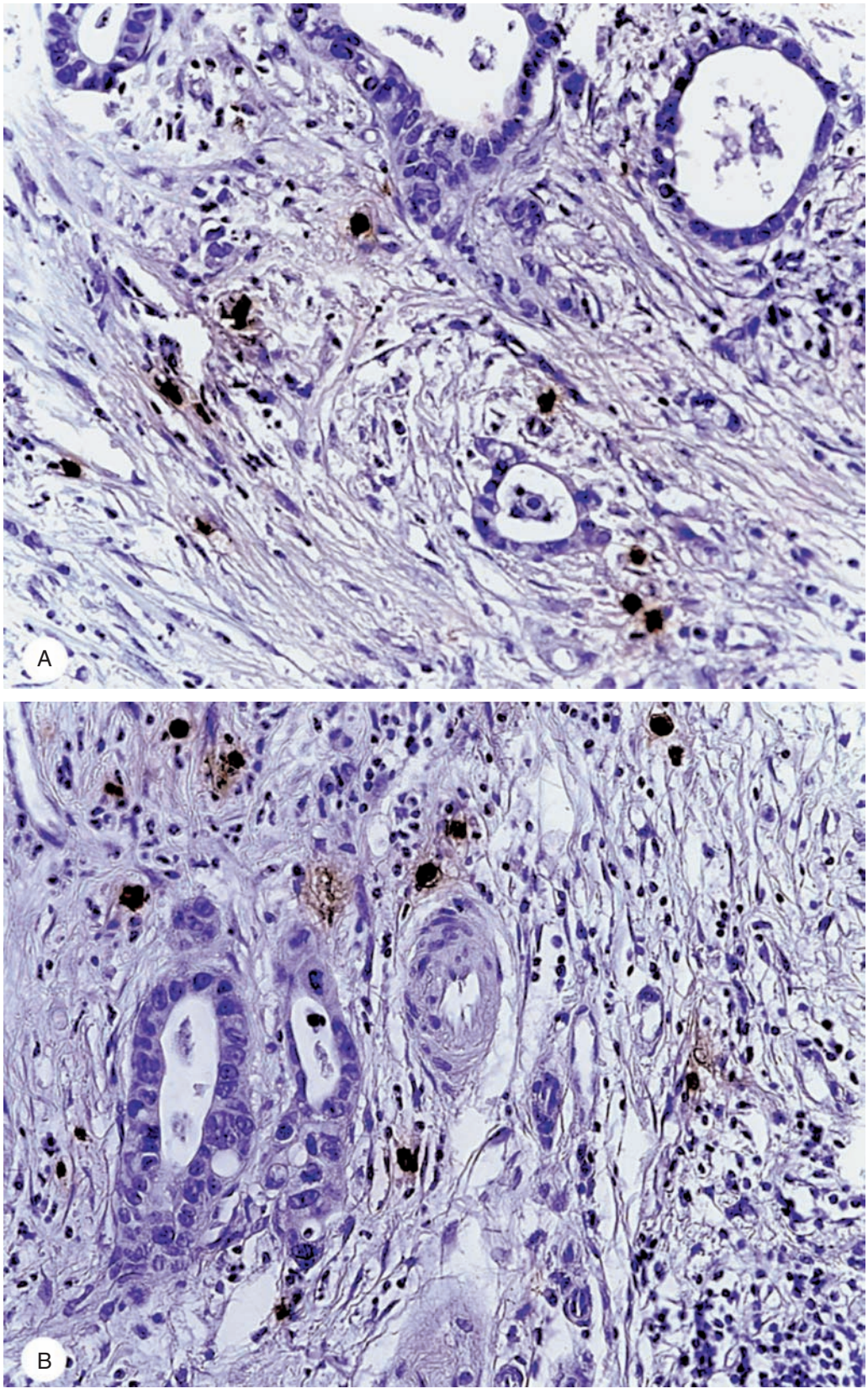

Figure 66. **A:** Tryptase immunostaining reveals with high specificity the presence of mast cells in the connective tissue that surrounds the neoplastic glands in a case of moderately differentiated pancreatic adenocarcinoma. **B:** The highly specific anti-chymase monoclonal antibody leads to the identification of chymase-positive mast cells in pancreatic cancer (260:1).

5–10% of the cancer cells. c-kit was detected in the cytoplasm or on the cell membrane of mast cells. Additionally, moderate to strong c-kit immunoreactivity was present in the cytoplasm of ductal cells of normal and hyperplastic ducts. The c-kit–positive pancreatic ducts were often surrounded by c-kit–positive and, less frequently, SCF-positive mast cells. In addition, pancreatic cancer cells frequently showed c-kit immunoreactivity (73% of the cases). No correlation was found between mast cell number, c-kit or SCF expression, and the histopathologic characteristics (grading, TNM status, stage) of the tumors.

In summary, we have shown an accumulation of mast cells in pancreatic cancer. Pancreatic mast cells belong to the connective-tissue type, they express c-kit and SCF, and they tend to accumulate around c-kit–expressing ducts. Moreover, pancreatic cancer cells frequently express c-kit, whereas SCF expression is restricted to about one-fifth of the tumor cases. Based on these results, it seems that the SCF–c-kit system does not significantly contribute to the growth of pancreatic cancer, although it is possible that SCF-positive cancer cells can recruit mast cells to the tumor mass. The reason for mast cell accumulation in pancreatic cancer is not known. It is possible that the cells represent a nonspecific inflammatory response to the tissue damage provoked by the growth of the cancer cells. However, examining larger series of pancreatic adenocarcinomas, we have found high expression of proangiogenic growth factors (VEGF, bFGF) by pancreatic mast cells and an association between the number of pancreatic cancer–associated mast cells and the angiogenetic process, measured by the assessment of the intratumoral microvessel density after CD34-immunostaining of endothelial cells (Esposito *et al.,* 2004).

In conclusion, tryptase and chymase immunostaining reveals with high specificity the presence of mast cells in pancreatic tissues, where they accumulate possibly in response to the chemotactic capacity of tumor-derived SCF. Mast cells produce and release proangiogenic growth factors (tryptase, VEGF, bFGF) that ultimately lead to tumor angiogenesis and invasion and thereby influence the prognosis of pancreatic cancer.

References

Arber, D.A., Tamayo, R., and Weiss, L.M. 1998. Paraffin section detection of the c-kit gene product (CD117) in human tissues: Value in the diagnosis of mast cell disorders. *Hum. Pathol. 29*:498–504.

Bingle, L., Brown, N.J., and Lewis, C.E. 2002. The role of tumour-associated macrophages in tumour progression: Implications for new anticancer therapies. *J. Pathol. 196*:254–265.

Blair, R.J., Meng, H., Marchese, M.J., Ren, S., Schwartz, L.B., Tonnesen, M.G., and Gruber, B.L. 1997. Human mast cells stimulate vascular tube formation: Tryptase is a novel, potent angiogenic factor. *J. Clin. Invest. 99*:2691–2700.

Cenac, N., Coelho, A.M., Nguyen, C., Compton, S., Andrade-Gordon, P., MacNaughton, W.K., Wallace, J.L., Hollenberg, M.D., Bunnett, N.W., Garcia-Villar, R., Bueno, L., and Vergnolle, N. 2002. Induction of intestinal inflammation in mouse by activation of proteinase-activated receptor-2. *Am. J. Pathol. 161*:1903–1915.

Dunn, G.P., Bruce, A.T., Ikeda, H., Old, L.J., and Schreiber, R.D. 2002. Cancer immunoediting: From immunosurveillance to tumor escape. *Nat. Immunol. 3*:991–998.

Elpek, G.O., Gelen, T., Aksoy, N.H., Erdogan, A., Dertsiz, L., Demircan, A., and Keles, N. 2001. The prognostic relevance of angiogenesis and mast cells in squamous cell carcinoma of the oesophagus. *J. Clin. Pathol. 54*:940–944.

Esposito, I., Friess, H., Kappeler, A., Shrikhande, S., Kleeff, J., Ramesh, H., Zimmermann, A., and Buchler, M.W. 2001. Mast cell distribution and activation in chronic pancreatitis. *Hum. Pathol. 32*:1174–1183.

Esposito, I., Menicagli, M., Funel, N., Bergmann, F., Boggi, U., Mosca, F., Bevilacqua, G., and Campani, D. 2004. Inflammatory cells contribute to the generation of an angiogenic phenotype in pancreatic ductal adenocarcinoma. *J. Clin. Pathol. 57*:630–636.

Esposito, I., Kleeff, J., Bischoff, S.C., Fischer, L., Collecchi, P., Iorio, M., Bevilacqua, G., Buchler, M.W., and Friess, H. 2002. The stem cell factor–c-kit system and mast cells in human pancreatic cancer. *Lab. Invest. 82*:1481–1492.

Friess, H., Ding, J., Kleeff, J., Liao, Q., Berberat, P.O., Hammer, J., and Buchler, M.W. 2001. Identification of disease-specific genes in chronic pancreatitis using DNA array technology. *Ann. Surg. 234*:769–778.

Frungieri, M.B., Weidinger, S., Meineke, V., Kohn, F.M., and Mayerhofer, A. 2002. Proliferative action of mast-cell tryptase is mediated by PAR2, COX2, prostaglandins, and PPAR gamma: Possible relevance to human fibrotic disorders. *Proc. Natl. Acad. Sci. USA 99*:15072–15077.

Greenlee, R.T., Murray, T., Bolden, S., and Wingo, P.A. 2000. Cancer statistics, 2000. *CA. Cancer J. Clin. 50*:7–33.

Gurish, M.F., and Boyce, J.A. 2002. Mast cell growth, differentiation, and death. *Clin. Rev. Allergy Immunol. 22*:107–118.

Harris, J.L., Niles, A., Burdick, K., Maffitt, M., Backes, B.J., Ellman, J.A., Kuntz, I., Haak-Frendscho, M., and Craik, C.S. 2001. Definition of the extended substrate specificity determinants for beta-tryptases I and II. J. *Biol. Chem. 276*: 34941–34947.

Irani, A.A., Schechter, N.M., Craig, S.S., DeBlois, G., and Schwartz, L.B. 1986. Two types of human mast cells that have distinct neutral protease compositions. *Proc. Natl. Acad. Sci. USA 83*:4464–4468.

Jackson, A.L., and Loeb, L.A. 2001. The contribution of endogenous sources of DNA damage to the multiple mutations in cancer. *Mutat. Res. 477*:7–21.

Jiang, Y.A., Zhang, Y.Y., Luo, H.S., and Xing, S.F. 2002. Mast cell density and the context of clinicopathological parameters and expression of p185, estrogen receptor, and proliferating cell nuclear antigen in gastric carcinoma. *World J. Gastroenterol. 8*:1005–1008.

Kankkunen, J.P., Harvima, I.T., and Naukkarinen, A. 1997. Quantitative analysis of tryptase- and chymase-containing mast cells in benign and malignant breast lesions. *Int. J. Cancer 72*:385–388.

Kinzler, K.W., and Vogelstein, B. 1998. Landscaping the cancer terrain. *Science 280*:1036–1037.

Kitamura, Y., Kasugai, T., Arizono, N., and Matsuda, H. 1993. Development of mast cells and basophils: Processes and regulation mechanisms. *Am. J. Med. Sci. 306*:185–191.

Kojima, H., Shijubo, N., and Abe, S. 2002. Thymidine phosphorylase and vascular endothelial growth factor in patients with stage I lung adenocarcinoma. *Cancer 94*:1083–1093.

Krishnaswamy, G., Kelley, J., Johnson, D., Youngberg, G., Stone, W., Huang, S.K., Bieber, J., and Chi, D.S. 2001. The human mast cell: Functions in physiology and disease. *Front. Biosci. 6*: D1109–1127.

Kuper, H., Adami, H.O., and Trichopoulos, D. 2000. Infections as a major preventable cause of human cancer. *J. Intern. Med. 248*:171–183.

Lowenfels, A.B., Maisonneuve, P., and Whitcomb, D.C. 2000. Risk factors for cancer in hereditary pancreatitis. International Hereditary Pancreatitis Study Group. *Med. Clin. North Am. 84*:565–573.

Malka, D., Hammel, P., Maire, F., Rufat, P., Madeira, I., Pessione, F., Levy, P., and Ruszniewski, P. 2002. Risk of pancreatic adenocarcinoma in chronic pancreatitis. *Gut 51*:849–852.

Mierke, C.T., Ballmaier, M., Werner, U., Manns, M.P., Welte, K., and Bischoff, S.C. 2000. Human endothelial cells regulate survival and proliferation of human mast cells. *J. Exp. Med. 192*:801–811.

Molin, D., Edstrom, A., Glimelius, I., Glimelius, B., Nilsson, G., Sundstrom, C., and Enblad, G. 2002. Mast cell infiltration correlates with poor prognosis in Hodgkin's lymphoma. *Br. J. Haematol. 119*:122–124.

Norrby, K. 2002. Mast cells and angiogenesis. *APMIS 110*:355–371.

Pietsch, T., Nicotra, M.R., Fraioli, R., Wolf, H.K., Mottolese, M., and Natali, P.G. 1998. Expression of the c-Kit receptor and its ligand SCF in non-small-cell lung carcinomas. *Int. J. Cancer 75*:171–175.

Sawatsubashi, M., Yamada, T., Fukushima, N., Mizokami, H., Tokunaga, O., and Shin, T. 2000. Association of vascular endothelial growth factor and mast cells with angiogenesis in laryngeal squamous cell carcinoma. *Virchows Arch. 436*:243–248.

Schulman, E.S. 1993. The role of mast cells in inflammatory responses in the lung. *Crit. Rev. Immunol. 13*:35–70.

Takanami, I., Takeuchi, K., and Naruke, M. 2000. Mast cell density is associated with angiogenesis and poor prognosis in pulmonary adenocarcinoma. *Cancer 88*:2686–2692.

Toth-Jakatics, R., Jimi, S., Takebayashi, S., and Kawamoto, N. 2000. Cutaneous malignant melanoma: Correlation between neovascularization and peritumor accumulation of mast cells overexpressing vascular endothelial growth factor. *Hum. Pathol. 31*:955–960.

Walls, A.F., Jones, D.B., Williams, J.H., Church, M.K., and Holgate, S.T. 1990. Immunohistochemical identification of mast cells in formaldehyde-fixed tissue using monoclonal antibodies specific for tryptase. *J. Pathol. 162*:119–126.

Welker, P., Schadendorf, D., Artuc, M., Grabbe, J., and Henz, B.M. 2000. Expression of SCF splice variants in human melanocytes and melanoma cell lines: Potential prognostic implications. *Br. J. Cancer 82*:1453–1458.

Westphal, E. 1891. Über Mastzellen. In Ehrlich P. *Farbenanalytische Untersuchungen. Zur Histologie and Klinik des Plutes: gesammelte Mitt(h)eilungen.* Berlin: Hirschwald Press, 17.

Zhang, S., Anderson, D.F., Bradding, P., Coward, W.R., Baddeley, S.M., MacLeod, J.D., McGill, J.I., Church, M.K., Holgate, S.T., and Roche, W.R. 1998. Human mast cells express stem cell factor. *J. Pathol. 186*:59–66.

15

Endocrine Cells in Invasive Ductal Adenocarcinoma of the Pancreas: An Immunohistochemical Study

Mika Sakaki and Toshiaki Sano

Introduction

Endocrine cells are frequently observed in a wide variety of ordinary adenocarcinomas. In pancreatic ductal adenocarcinomas, scattered endocrine cells have been reported to be either lined up along the base of the neoplastic glands or to lie between the neoplastic columnar cells (Kodama and Mori, 1983; Permert *et al.,* 1992; Pour *et al.,* 1993; Solcia *et al.,* 1997; Suda and Hashimoto, 1979). They should be separated from endocrine cells in mixed ductal-endocrine carcinomas in which ductal and endocrine cells, which compose at least one third to one half of tumor tissue, are intimately admixed in the primary tumors as well as in their metastasis (Solcia *et al.,* 1997). Endocrine cells in ductal adenocarcinomas might be neoplastic considering their close association with neoplastic glands (Kodama and Mori, 1983; Permert *et al.,* 1992; Pour *et al.,* 1993; Pour, 1997). However, metastases from ductal adenocarcinomas usually lack the endocrine cell population seen in the primary sites, and thus these endocrine cells may represent nonneoplastic rather than true neoplastic cells (Kloppel, 2000; Solcia *et al.,* 1997). Therefore, it has not been clearly concluded whether these endocrine cells are neoplastic.

To clarify whether endocrine cells are neoplastic, we studied the localization of the endocrine cells in the primary, invasive, and metastatic sites of pancreatic invasive ductal adenocarcinomas by immunohistochemistry (IHC) for chromogranin A (CgA), islet hormone (insulin, glucagon, and pancreatic polypeptide [PP]), serotonin, and gastrin (Sakaki *et al.,* 2002).

MATERIALS

Twenty-nine invasive ductal adenocarcinomas of the pancreas, which had been surgically resected, were collected from the University of Tokushima, Tokushima Prefecture Central, and Tokushima Municipal Civic Hospitals. The age of the 29 patients, 17 men and 12 women, ranged from 36 to 82 years, with a mean of 64.3 years. Primary sites in the pancreas were the head in 20 cases, the body in 6, and the tail in 3. Seventeen cases had metastatic lesions: lymph nodes in 15 cases, liver in 1 case, and both lymph nodes and liver in 1 case.

METHODS

For immunohistochemical study, formalin-fixed and paraffin-embedded tissues were used. The labeled streptavidin biotin (LSAB) method (Dako, Carpinteria, CA) was adopted for all reactions except for a double

Handbook of Immunohistochemistry and *in situ* Hybridization of Human Carcinomas, Volume 3: Molecular Genetics, Liver Carcinoma, and Pancreatic Carcinoma

staining of CgA and Ki-67. Monoclonal CgA antibody (clone DAK-A3, 1:100, Dako, Glostrup, Denmark) was used to detect endocrine cells in adenocarcinoma and nonneoplastic pancreatic tissue around adenocarcinomas. Cases with CgA-immunoreactive (IR) cells in adenocarcinomas were further stained with antibodies to insulin (polyclonal, 1:100, Dako, Carpinteria, CA), glucagon (polyclonal, 1:75, Dako), PP (polyclonal, 1:600, Dako), serotonin (clone 5HT-H209, 1:50, Dako) and gastrin (polyclonal, 1:500, Dako). All CgA-IR adenocarcinomas were double stained with CgA and laminin (polyclonal, 1:200, Dako) to see whether endocrine cells in neoplastic glands are located within the basal membrane of the neoplastic glands. Ten CgA-positive adenocarcinomas were also double stained with CgA and Ki-67 (clone MIB-1, 1:50, Dako). The incubation time for all primary antibodies was 30 min at room temperature. Antigen retrieval was performed by autoclave (15 min) in 10 mM/L citrate buffer, pH 6.0 for CgA, and by microwave (2× at 600 W for 6 min) for serotonin. For the double staining of CgA and laminin, CgA was applied first and cobalt-3,3′-diaminobenzidine (Co-DAB) was used as a first chromogen. For a second staining sequence, antigen retrieval was performed by proteinase K (40 μ 1/3 ml 0.05 M Tris-HCl pH 7.7, Dako) before the application of laminin, and DAB served as a second chromogen. For the double staining of CgA and Ki-67, antigen retrieval was performed by autoclave (15 min) before the application of Ki-67, and Co-DAB was used as a first chromogen. CgA was detected in a second staining sequence using the Envision method (Dako) and DAB as a second chromogen.

RESULTS

Incidence and Location of CgA-IR Cells

Of 29 cases, 24 (82.3%) had CgA-IR cells in the adenocarcinomas. Regarding the site of the tumor in the pancreas, there was no significant difference between cases with and without CgA-IR cells. However, most of the cases of well- (93.3%) or moderately (88.9%) differentiated adenocarcinomas had CgA-IR cells, whereas only 40% of cases of poorly differentiated adenocarcinomas did. Poorly differentiated adenocarcinomas were, thus, less likely to have endocrine cells ($P < 0.05$). About 70% (12/17) of cases with metastases and all cases (12/12) without metastases had CgA-IR cells in the primary tumors. There was no significant difference in incidence of CgA-IR cells between tumors with and without metastases.

CgA-IR cells in adenocarcinomas occupied a very small proportion of the adenocarcinoma cells, being less than 1% in all 24 cases. The CgA-IR cells lined up along the base of the neoplastic glands, showing a periglandular arrangement (Figure 67), or a single CgA-IR cell was at the base of the neoplastic gland. When tumor cells formed multilayered or papillary architecture, some CgA-IR cells lay between the tumor cells. In one case in which tumor cells predominantly presented papillary architecture, most of the CgA-IR cells lay between tumor cells and a few were on the luminal side. As tumor cells invaded, acini were destroyed, leaving islets. Islet cells were often broken up into small nests, cords, or single cells in the fibrous stroma and often were in contact with neoplastic glands and bordered on part of the neoplastic glands (Figure 67).

The double immunostaining for CgA and laminin revealed that CgA-IR cells along the base of the neoplastic glands were located within the basement membrane. Whether CgA-IR cells were located at the base of the neoplastic glands or between carcinoma cells, CgA-IR cells in neoplastic glands were at least visibly in contact with adjacent nontumorous islets or closely located to them in all 24 cases (Figure 67). In two cases, nests of CgA-IR cells were in the lumen of some neoplastic glands and part of the walls of the neoplastic glands were destroyed. In one of the two cases, nests were connected to the stroma and protruded into the lumen, whereas in the other case they floated in the lumen without connection to the stroma.

Tumor cells sometimes invaded the preexisting interlobular ducts and formed a front with nonneoplastic cells in the same ducts, presenting an intraductal

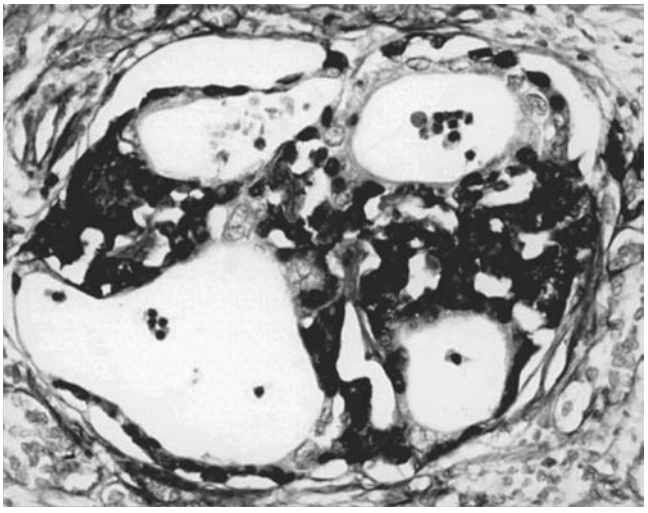

Figure 67. Chromogranin A-positive cells are lined up along the neoplastic glands and show contact with surrounding islets. 50X.

extension in three cases. The CgA-IR cells were located at the base, lay between tumor cells, or were on the luminal side. In one of the three cases, tumor cells within the duct proliferated in cribriform or papillary architecture where CgA-IR cells on the luminal side were also seen. In another case, CgA-IR cells were found in both nonneoplastic and neoplastic epithelia of the same ducts. The CgA-IR cells in the intraductal extensions showed no contact with the surrounding islets. In the remaining 21 of 24 cases, CgA-IR cells were found only in neoplastic glands.

The CgA-IR cells were recognized in nontumorous interlobular ducts near adenocarcinomas in 21 of 24 CgA-IR adenocarcinomas and in 4 out of 5 CgA-IR tumors. They were sparsely present, ranging from 1 to 10 in a duct. There were more CgA-IR cells in hyperplastic than in nonhyperplastic epithelium. Ductuloinsular-complex–like structures, which indicated that the interlobular duct was incorporated in an islet, were found in 3 CgA-IR adenocarcinomas. In 2 CgA-IR tumors of the head, a few nonneoplastic pancreatic lobules around adenocarcinomas contained more than 20% CgA-IR cells of all cells in the lobule.

Among 24 CgA-IR tumors, there were 12 cases in which adenocarcinomas invaded the adjacent tissue beyond the pancreas. In 10 cases of the head, 6 adenocarcinomas invaded to the muscularis or further into the duodenum, 1 invaded the adjacent lymph node, and 3 cases invaded both. In the 2 cases of the body or tail, 1 tumor invaded the muscularis of the stomach and the connective tissue around the spleen, whereas the other went into the subserosa of the stomach and the adjacent lymph node. When an adenocarcinoma invaded these surrounding tissues beyond the pancreas where islets were not present, there were no CgA-IR cells in the invaded site. No pancreatic tissue was recognized in the duodenum in the present cases. Three of five cases without CgA-IR cells in the adenocarcinoma had invaded sites beyond the pancreas, but no CgA-IR cells were found there.

Of 24 CgA-IR tumors, 12 had metastatic sites. Only one case showed several CgA-IR cells in a metastatic site, one regional lymph node. This was a case of poorly differentiated adenocarcinoma of the head, where the tumor cells proliferated in nests or organoid patterns and had several regional lymph nodes as metastatic sites.

Hormonal Reactivity of CgA-IR Cells

Tests of IHC for insulin, glucagon, and PP were positive in 12 of 16 cases of the head; insulin and glucagon were positive in 2 cases, and insulin and PP were positive in 2 cases. No case showed serotonin positivity. In 6 of the 8 cases of the body or tail, CgA-IR cells showed glucagon and insulin positivity. Insulin, glucagons, and PP were positive in one case and insulin, glucagons, and serotonin were positive in another case, which was the only case that showed serotonin positivity in neoplastic glands. All 24 cases showed two or three islet hormones (insulin, glucagons, and PP). Different types of hormones were recognized in the same neoplastic glands or the same cluster of neoplastic glands in 22 (91.7%) of the 24 cases. Similar to immunoreactive cells for CgA in neoplastic glands, immunoreactive cells for each of the three islet hormones were closely located to cords or nests of nontumorous islet cells, which showed the same hormonal immunoreactivity as in the neoplastic glands. Among 13 PP-IR adenocarcinomas, 12 were in the head, but only 1 was in the body. In the body case, PP cells were recognized in nontumorous islets near PP-IR cells in the neoplastic glands. The numbers of PP-IR cells were much fewer in both islets and neoplastic glands in the body than in the head. In 1 case presenting serotonin-positive cells, there were no serotonin-IR cells in nontumorous tissue around the neoplastic glands. None of the 24 cases showed gastrin positivity in neoplastic glands. In 2 cases, nests of CgA-IR cells were in the lumen of a few neoplastic glands. The nests were comprised of insulin-IR and glucagon-IR cells.

Two of three adenocarcinomas with CgA-IR cells in the intraductal extensions showed hormonal reactivity. These two were located in the head. In one case, PP-IR cells and serotonin-IR cells were in neoplastic epithelium in the duct, whereas PP-IR cells were in nonneoplastic epithelium of the same duct. The other case had serotonin-IR cells in neoplastic epithelium of the duct. In the last case in the body, CgA-IR cells were seen, but because the carcinomatous component in the duct was observed only in a specimen for HE and CgA, their hormonal activity was unknown. However, in nonneoplastic epithelia of this case, hormonal reactivity was present, which was gastrin and serotonin positivity.

CgA-IR cells were also recognized in nontumorous interlobular ducts near or at the site of invasion in 21 of 24 CgA-IR adenocarcinomas. In 19 of the 21 cases, hormonal reactivity was identified. In 14 cases, only one hormone was positive, but in the other 5 cases, two types of hormones within the same duct were identified: insulin and PP in 3 and insulin and glucagon in 2. Of the 5 CgA-negative adenocarcinomas, 4 had CgA-IR cells in nontumorous interlobular ducts. Of those 4 cases, 3 showed hormonal reactivity, but in 1 of the 3 cases only PP-IR cells were identified. In 2 CgA-IR adenocarcinomas with numerous CgA-IR cells in nontumorous lobules, these cells were PP positive.

Numerous PP-IR cells in nontumorous lobules were found in another CgA-IR adenocarcinoma, but they lacked CgA positivity.

In the metastatic lymph node with several CgA-IR cells in one case, a few of them showed serotonin reactivity. The other metastatic lymph nodes in this case showed no immunoreactivity for CgA or other hormones.

Ki-67 Positivity of CgA-IR Cells in Adenocarcinoma

Ten CgA-IR adenocarcinomas were double-stained with CgA and Ki-67. None of the CgA-IR cells at the base of neoplastic glands or between tumor cells in neoplastic glands stained with Ki-67 in all 10 cases. In 1 case, tumor cells in the intraductal extension proliferated in cribriform or papillary architecture. CgA-IR cells were at the base or on the luminal side of the duct, but they were negative for Ki-67.

DISCUSSION

Endocrine cells have been recognized in 40–80% of ductal adenocarcinomas of the pancreas (Kodama and Mori, 1983; Permert *et al.,* 1992; Pour *et al.,* 1993; Solcia *et al.,* 1997; Suda and Hashimoto, 1979) and reported to be most common in well-differentiated adenocarcinoma (Pour *et al.,* 1993). In our study, 24 (82.8%) of 29 cases had CgA-IR endocrine cells in the primary sites. These cells were located along the base of the neoplastic glands. When carcinoma cells formed multilayer or papillary architectures, some CgA-IR cells lay between tumor cells. Regardless of their arrangement, at least visually they always seem to be in contact with or near to the surrounding CgA-IR islet cells, which sometimes seemed to adhere to the neoplastic glands. Endocrine cells in neoplastic glands and those of the surrounding islets are often located together within the same basement membrane, as revealed by a double immunostaining of CgA and laminin. Interactions between islet and pancreatic adenocarcinoma have been reported. Kodama and Mori (1983) suggested interactions between carcinomatous ductal cells and islet cells in pancreatic carcinogenesis. In hamsters, normal pancreatic islets were necessary for the induction of pancreatic adenocarcinoma by a chemical carcinogen (Bell and Strayer 1983, Povoski *et al.,* 1993) and ductal adenocarcinoma arose from progenitor cells in islets (Pour, 1997). Cancer cell growth has been shown to be regulated by islet hormones such as insulin and somatostatin *in vitro* (Ding *et al.,* 2000). Conversely, an abnormality in islet composition and secretion is common in pancreatic cancer (Ding *et al.,* 1998; Permert *et al.,* 1992; Pour *et al.,* 1993). For example, beta cells of the islets adjacent to the pancreatic cancer secrete increased amounts of islet amyloid polypeptide (IAPP) *in vivo* (Permert *et al.,* 1994) and *in vitro* (Suda and Hashimoto, 1979). Ding *et al.* (1998) thought that a soluble factor from pancreatic cancer cells selectively stimulated amylin secretion from islet cells. It is understandable that tumor cells and surrounding islets were close in terms of location and that endocrine cells persisted within a basement membrane of neoplastic glands, if some interactions between neoplastic ductal and nonneoplastic adjacent islet cells existed.

Exocrine and endocrine components have the same origin in the developmental stage of human pancreas, the primitive gut endoderm, and originate from branching "protodifferentiated" epithelial cells with the features of duct cells (Peters *et al.,* 2000).

In the first phase, i.e., 13–16th gestation week (gw), small aggregates of endocrine cells grow out from pancreatic ducts, losing their contact with ducts from gw 17–20 (Peters *et al.,* 2000). Because carcinomas can show features comparable to the embryonic pancreas (Peters *et al.,* 2000; Pour *et al.,* 1993), neoplastic glands in well-differentiated carcinomas could most likely show a close relation to islets, mimicking the developmental stage of pancreas. This may be one reason why endocrine cells are frequently seen in well-differentiated adenocarcinomas. In addition, because even in well-differentiated adenocarcinoma endocrine cells were only focally seen in neoplastic glands, the close relation of endocrine cells to neoplastic glands may only be present during the limited period of neogenesis and growth of carcinomas. Rapidly growing carcinomas such as some poorly differentiated adenocarcinomas might have no chance to present endocrine cells within them. In our study, the presence of endocrine cells in carcinoma was most unlikely in the poorly differentiated carcinoma.

We found that when carcinoma invaded adjacent organs or tissues, such as the duodenum (muscularis or further), stomach, and connective tissue around the spleen where islets of pancreas were not present, endocrine cells in carcinoma were completely absent. Therefore, the existence of islet cells near cancer seems to be a key to the existence of endocrine cells in neoplastic glands. This finding, in addition to the close location of neoplastic glands and nonneoplastic islets, leads us to believe that endocrine cells in neoplastic glands may come from the surrounding nonneoplastic islet cells.

Endocrine cells have been reported to be located in the invasive edge of cancers (Permert *et al.,* 1992; Pour *et al.,* 1993) and to occur in the base of the neoplastic glands,

at different distances from the lumen and within the lumen (Permert *et al.,* 1992; Pour *et al.,* 1993). In those reports it was thought that these endocrine cells were shed and renewed, as were tumor cells and constituents of tumors, and that these findings indicated the neoplastic nature of the endocrine cells. However, the occurrence of endocrine cells on the edge of the invasion may be the result of the presence of the numerous intact or broken islets because compared to acini, islets tend to survive in carcinomatous tissue (Kodama and Mori, 1983). None of the endocrine cells, including those in neoplastic glands and those on the luminal side of the intraductal extension, showed Ki-67 positivity with double staining of Ki-67 and CgA. Even in normal pancreatic ducts, endocrine cells sometimes border the lumen and are joined to the neighboring ductal cells by tight junctions (Klimstra, 1997). Therefore, being on the luminal side does not mean that they are of a neoplastic nature. The endocrine cells on the luminal side might occur because of intricate folds of lining epithelium protruding into the lumen. In two cases here, there were nests of endocrine cells composed of insulin-positive and glucagon-positive cells, which were thought to be islets in the lumen of some neoplastic glands. It seemed that an artifact had been caused by the destruction of part of the neoplastic glands during the process of invasion to the islets. Thus, an artifact can cause nontumorous endocrine cells to be present in the lumen. Pour *et al.* (1993) reported a lack of colocation of CgA in some somatostatin or glucagon cells in tumor-associated endocrine cells and stated that this abnormality may indicate the neoplastic nature of tumor-associated endocrine cells. In one case in the present study, however, it was recognized that lack of colocation of CgA and PP positivity might indicate some effect by a carcinoma on the islets, as reported in previous articles (Ding *et al.,* 1998; Permert *et al.,* 1992; Permert *et al.,* 1994; Povoski *et al.,* 1993). We believe that the findings of Pour *et al.* are insufficient to conclude that endocrine cells in pancreatic adenocarcinoma have a neoplastic nature.

As for hormonal reactivity, all four islet hormones and amylin (IAPP), serotonin, and occasionally gastrin have been identified in endocrine cells in pancreatic carcinomas (Permert *et al.,* 1992; Pour *et al.,* 1993; Solcia *et al.,* 1997). More than one type of hormonal reactivity has been identified in some cases (Permert *et al.,* 1992). Colocation of two types of hormones within an endocrine cell has also been reported (Pour *et al.,* 1993). In our study, all 24 cases with endocrine cells in neoplastic glands showed more than one hormonal reactivity of the three islet hormones (insulin, glucagon, and PP), and in 22 (91.7%) of the 24 cases, immunoreactive cells for different types of hormones were seen within the same gland or cluster of neoplastic glands. PP-IR cells were mostly found in neoplastic glands of the head, which is consistent with previous reports (Permert *et al.,* 1992; Pour *et al.,* 1993; Solcia *et al.,* 1997). PP-IR cells in the body were seen in one case (8.1%), which has not been reported before. PP-IR cells in nontumorous islets both in the head and body were recognized near neoplastic glands. However, the number of PP-IR cells was much fewer in both islets and neoplastic glands in the body than in the head, which reflected the differences in the numbers of PP cells seen in normal pancreas in the head and body or tail. Therefore, this finding, as well as the heterogeneity in hormonal localization within the same neoplastic glands, seems to support our hypothesis that endocrine cells in neoplastic glands may originate from the surrounding islets.

In the present study, 3 cases had endocrine cells in the intraductal extensions. These endocrine cells showed no contact with adjacent islet cells, suggesting that they could be neoplastic. They could be nonneoplastic, however, because nonneoplastic endocrine cells may be left over after neoplastic cells replaced the preexisting epithelium in the ducts. In the present study, endocrine cells in nontumorous ducts near or at the site of invasion were seen in 25 of 29 cases and most of them showed hormonal reactivity. In 1 case with intraductal extensions, endocrine cells were present in both nonneoplastic and neoplastic epithelium in the same duct. Of the 3 cases with intraductal extensions, 2 showed serotonin positivity, which is not uncommon for endocrine cells in the pancreatic duct, but is not common for those in pancreatic adenocarcinoma. We are inclined to think that endocrine cells in the intraductal extension were present before the carcinomatous invasion and that they are nonneoplastic rather than neoplastic.

There has been a report stating that endocrine cells existed in the metastatic sites of pancreatic exocrine carcinomas (Eusebi *et al.,* 1981). However, the cases were actually mixed ductal-endocrine carcinomas, a different category from ductal adenocarcinoma with endocrine cells. In the present study, only one case showed several CgA-IR cells in one metastatic lymph node. Endocrine cells in the metastatic lymph node showed immunoreactivity for serotonin, whereas the endocrine cells in the primary site showed focal contact with the surrounding islets and immunoreactivity for insulin, glucagon, and PP. We think that these endocrine cells in the metastatic site are neoplastic. Other than this case, there were a few serotonin-positive cells in neoplastic glands of the body in only one case. Because islets usually do not have serotonin cells and there were no serotonin-IR cells in nontumorous tissue

near the neoplastic glands and thus there was no source of nonneoplastic endocrine cells nearby, they could be neoplastic. However, the absence of endocrine cells in metastatic sites seen in the other cases strongly supports their nonneoplastic nature.

We concluded that most endocrine cells in pancreatic ductal adenocarcinoma are nonneoplastic and are derived from the surrounding islets and that there is a possibility that endocrine cells in the intraductal extensions are preexisting nonneoplastic cells. Neoplastic endocrine cells may exist, although their frequency is low.

References

Bell, R.H., Jr., and Strayer, D.S. 1983. Streptozotocin prevents development of nitrosamine-induced pancreatic cancer in the Syrian hamster. *J. Surg. Oncol. 24*:258–262.

Ding, X., Flatt, P.R., Permert, J., and Adrian, T.E. 1998. Pancreatic cancer cells selectively stimulate islet beta cells to secrete amylin. *Gastroenterology 114*:130–138.

Ding, X.Z., Fehsenfeld, D.M., Murphy, L.O., Permert, J., and Adrian, T.E. 2000. Physiological concentrations of insulin augment pancreatic cancer cell proliferation and glucose utilization by activating MAP kinase, P13 kinase and enhancing GLUT-1 expression. *Pancreas 21*:310–320.

Eusebi, V., Capella, C., Bondi, A., Sessa, F., Vexxadini, P., and Mancini, A.M. 1981. Endocrine-paracrine cells in pancreatic exocrine carcinomas. *Histopathology 5*:599–613.

Klimstra, D.S. 1997. Pancreas. In Sternberg, S.S. (ed), *Histology for Pathologists*. Philadelphia: Lippincott-Raven Press, 630–633.

Kloppel, G. 2000. Mixed exocrine-endocrine tumors of the pancreas. *Semin. Diagn. Pathol. 17*:104–108.

Kodama, T., and Mori, W. 1983. Morphological behavior of carcinoma of the pancreas. 2. Argyrophil cells and Langerhans' islets in the carcinomatous tissues. *Acta. Pathol. Jpn. 33:*483–493.

Permert, J., Mogaki, M., Andren-Sandberg, A., Kazakoff, K., and Pour, P.M. 1992. Pancreatic mixed ductal-islet tumors: Is this an entity? *Int. J. Pancreatol. 11*:23–29.

Permert, J., Larsson, J., Westermark, G.T., Herrington, M.K., Christmanson, L., Pour, P.M., Westermark, P., and Adrian, T.E. 1994. Islet amyloid polypeptide in patients with pancreatic cancer and diabetes. *N. Engl. J. Med. 330*:313–318.

Peters, J., Jurgensen, A., and Kloppel, G. 2000. Ontogeny, differentiation and growth of the endocrine pancreas. *Virchows Arch. 436*:527–538.

Pour, P.M., Permert, J., Mogaki, M., Fujii, H., and Kazakoff, K. 1993. Endocrine aspect of exocrine cancer of the pancreas: Their patterns and suggested biologic significance. *Am. J. Clin. Pathol. 100*:223–230.

Pour, P.M. 1997. The role of Langerhans islets in pancreatic ductal adenocarcinomas. *Front Biosci. 2*:d271–282.

Povoski, S.P., Fenoglio-Preiser, C.M., Sayers, H.J., McCullough, P.J., Zhou, W., and Bell, R.H., Jr. 1993. Effect of streptozotocin diabetes on development of nitrosamine-induced pancreatic carcinoma when diabetes induction occurs after nitrosamine exposure. *Carcinogenesis 14*:961–967.

Sakaki, M., Sano, T., Hirokawa, M., Takahashi, M., and Kiyoku, H. 2002. Immunohistochemical study of endocrine cells in ductal adenocarcinomas of the pancreas. *Virchows Arch. 441*:249–255.

Solcia, E., Capella, C., and Kloppel, G. 1997. Tumors of the pancreas. In Rosai, J. (ed). *Atlas of Tumor Pathology.* Washington, DC: Armed Forces Institute of Pathology, 93–98.

Suda, K., and Hashimoto, K. 1979. Argyrophil cells in the exocrine pancreas *Acta Pathol. Jpn. 29*:413–419.

16

Fine-Needle Aspiration Biopsy of Pancreatic Adenocarcinoma

Fan Lin and Gregg Staerkel

Introduction

Pancreatic malignant tumors are the fifth most common cause of cancer death among both men and women in the United States, and the incidence of these tumors continues to increase (DeMay, 1996). Approximately 2900 Americans are diagnosed with pancreatic malignancies each year, and nearly all of them die of the disease, with an overall 5-year survival rate of less than 5% (Greenle *et al.,* 2001; Niederhuber *et al.,* 1995). Among these pancreatic malignant tumors, ductal adenocarcinoma and its variants account for 90% of the total cases (Kloppel *et al.,* 1996).

Fine-needle aspiration biopsy (FNAB) of the pancreas has become a method of choice to establish a tissue diagnosis in many institutions before chemotherapy or surgery (David *et al.,* 1998; Lin and Staerkel, 2003). The primary indication of FNAB of the pancreas is a pancreatic mass suspected as a carcinoma radiographically and clinically, in most instances. Such biopsies generally provide better diagnostic sensitivity and specificity and fewer complications such as pancreatitis and bleeding, than tissue (large core or wedge) biopsies.

An FNAB is most frequently performed with computed tomography (CT) guidance or endoscopic ultrasound (EUS) guidance preoperatively. Both of the procedures provide similar diagnostic specificity and sensitivity. The overall accuracy of FNAB of the pancreas is variable, but it increases with experience. The average sensitivity is about 80–90%, and specificity approaches 100% (Mitchell and Carney, 1985; Al-Kaisi and Siegler, 1989). In our study series of 291 cases of CT-guided FNAB of the pancreatic lesions, the diagnostic sensitivity increased to 98% if special criteria are used (Lin and Staerkel, 2003). Similar diagnostic sensitivity was also reported (David *et al.,* 1998). The main advantages of EUS-guided FNAB over CT-guided FNAB include the ability to detect smaller lesions, to identify a possible local invasion of the tumor, and to simultaneously sample the adjacent lymph node for cancer staging (Chang, 1995; Palazzo *et al.,* 1993). Intraoperative FNAB can be performed as well, which allows direct visualization or palpation of the lesion during the sampling process. As the result of this, the diagnostic sensitivity of intraoperative FNAB is more than 90%, with at least one reported series of 100%, and the specificity is usually 100% (Blandamura *et al.,* 1995).

Unfortunately, an interpretation of FNAB of the pancreas is not always straightforward. False-positive results, which are rare, and a significant number of false-negative results do occur (Glenthoj *et al.,* 1990; Hancke *et al.,* 1984; Moossa, 1982). The distinction of well-differentiated adenocarcinoma (WDA) from

Handbook of Immunohistochemistry and *in situ* Hybridization of Human Carcinomas,
Volume 3: Molecular Genetics, Liver Carcinoma, and Pancreatic Carcinoma

benign/reactive glandular epithelium represents the major diagnostic challenge (Pitman, 1999). Other diagnostic problems may include differential diagnosis of WDA from pancreatic endocrine neoplasms, acinar cell carcinoma, solid pseudopapillary tumor of the pancreas (SPTP), mucinous cystic neoplasms, serous microcystic adenoma, and metastasis.

MATERIALS

1. The specimens in this study, including 291 CT-guided FNABs of pancreatic lesions.
2. Carnoy's solution (1:6, glacial acetic acid:70% ethanol).
3. Harris Hematoxylin.
4. Ethanols (70% ethanol, 95% ethanol, 100% ethanol).
5. Eosin alcohol (EA) polychrome-modified dye.
6. Xylene.
7. Eosin.
8. Quik-Dip Solution I (100% methanol).
9. Quik-Dip Solution II.
10. Quik-Dip Solution III.
11. Plus slides.
12. Coverslips.

METHODS

Preparation of Slides

1. Direct smears are obtained from CT-guided biopsies, endoscopic-ultrasound guided biopsies, or intraoperative FNABs.
2. Two slides are recommended from each pass of the FNAB. It is recommended to have one air-dried slide for Diff-Quik stain and one ethanol (Carnoy's solution) fixed slide for Papanicolaou Quick-staining or hematoxylin-eosin stain (for intraoperative FNABs if a Papanicolaou quick-staining is not available).

Staining Methods

Papanicolaou Quick-Staining Technique

1. 10 dips in water.
2. 8 sec in Harris Hematoxylin.
3. 10 dips in water.
4. 10 dips in 95% ethanol.
5. 10 dips in 95% ethanol.
6. 2 min in EA polychrome-modified dye.
7. 10 dips in 95% ethanol.
8. 10 dips in 100% ethanol.
9. 10 dips in xylene.

Diff-Quik Stain

1. 5 sec in Quik-Dip Solution I.
2. 20 sec in Quik-Dip Solution II.
3. 20 sec in Quik-Dip Solution III.
4. Rinse slides with water.
5. Allow to air-dry.
6. Coverslip.

Hematoxylin-Eosin Stain

1. 5 sec in fixation solution (100% methanol).
2. 10 dips in water.
3. 1 min in Harris Hematoxylin.
4. 10 dips in water.
5. 10 dips in blueing solution (0.5% ammonium hydroxide).
6. 10 dips in water.
7. 10 dips in 70% ethanol.
8. 5 dips in eosin solution.
9. 10 dips in 70% ethanol.
10. 10 dips in 95% ethanol.
11. 10 dips in 100% ethanol.
12. 10 dips in xylene.
13. 10 dips in xylene.
14. Coverslip.

Cytologic Criteria for Adenocarcinoma

1. Anisonucleosis (variation in nuclear size greater than 4× within a same epithelial group).
2. Nuclear membrane irregularity.
3. Nuclear crowding/overlapping/three-dimensionality.
4. Nuclear enlargement (if more than two red blood cells).
5. Hypercellularity.
6. Gap versus confluent cell spacing.
7. Hyperchromasia.
8. Macronucleoli.
9. Mitosis.
10. Chromatin clearing.
11. Necrosis.
12. Single intact cells.

Evaluation of Fine-Needle Aspiration Biopsy Smears

Microscopic Observations at Low Magnification (40X and 100X)

1. Cellularity.
2. Epithelial group shape, architecture, and cohesiveness.
3. Background of smears, such as necrosis, inflammation, mucin, and cystic changes.
4. Nuclear enlargement.

Microscopic Observations at Intermediate Magnification (200X)

1. Architectural changes, such as nuclear crowding, loss of nuclear polarity, nuclear overlapping, three-dimensional clusters, and papillary groups.
2. Gap versus confluent cell spacing.
3. Single intact cells (pleomorphic cells, columnar cells, mucin-containing cells, plasmacytoid cells).
4. Nuclear enlargement.

Microscopic Observations at High Magnification (400X and 600X)

1. Anisonucleosis (variation in nuclear size greater than 4× within a same epithelial group).
2. Nuclear membrane irregularity.
3. Macronucleoli.
4. Mitosis.
5. Nuclear chromatin, such as salt and pepper, chromatin clearing, and hyperchromasia.

RESULTS AND DISCUSSION

The diagnostic sensitivity and specificity of FNAB of pancreatic lesions have improved greatly as a result of several articles on the cytologic criteria for the diagnosis of pancreatic malignancies (Cohen *et al.,* 1991; Mitchell and Carney, 1985; Robins *et al.,* 1995). In 1985, Mitchell and Carney published the first comprehensive study on diagnostic criteria (Mitchell and Carney, 1985). They focused on three-dimensional cellular fragments, nuclear enlargement, and nuclear membrane irregularity.

Following their publication, several modified cytologic criteria based on those of Mitchell and Carney were reported. Cohen *et al*. (1991) identified anisonucleosis (variation in nuclear size of at least three times within a same epithelial group), nuclear molding, and large nuclei as the significant cytologic features for the diagnosis of pancreatic adenocarcinoma.

Robins *et al.* (1995) were the first to propose major criteria (overlapping nuclei/crowded groups, nuclear contour irregularity, and chromatin clearing and/or clumping) and minor criteria (single epithelial cells, necrosis, mitosis, and nuclear enlargement) for pancreatic adenocarcinoma. According to these authors, the sensitivity and specificity for diagnosing pancreatic adenocarcinoma are 100% when two or more major criteria or one major and three minor criteria are identified, although these data have not been validated prospectively. In addition, they proposed that at least six groups of atypical ductal epithelial cells were needed to confirm a diagnosis. Additionally, several authors also considered single epithelial cells, necrosis, mitosis, hyperchromasia, and prominent nuclei as significant cytologic features for a diagnosis (Robins *et al.,* 1995).

It is our experience, and that of others as well, that establishing a correct diagnosis of pancreatic adenocarcinoma from FNAB specimens is generally straightforward unless the tumor is a WDA, which could be extremely difficult, and in rare instances impossible, to distinguish from reactive conditions such as chronic pancreatitis (Pitman, 1999). The previous published cytologic criteria generally apply to all grades of adenocarcinomas, but do not specifically focus on WDA. We have tried to add, redefine, and test these cytologic criteria in a large series of WDA in our article (Lin and Staerkel, 2003). In this retrospective study, 291 cases of CT-guided FNABs of pancreatic lesions were included. Available surgical specimens (84 cases) and cell blocks (131) prepared from a needle rinse solution were also reviewed. The original cytologic diagnoses were nondiagnostic in 24 (8%) cases, benign in 27 (9%), suspicious for malignancy in 15 (5%), and malignant in 225 (77%). The diagnoses among the 225 malignant cases were as follows: WDA, 74 (25%); moderately differentiated adenocarcinoma (MDA), 58 (20%); poorly differentiated adenocarcinoma (PDA), 62 (21%); mucinous adenocarcinoma, 8 (3%); neuroendocrine tumor, 12 (4%); and metastasis, 11 (4%).

We have applied 10 cytologic criteria to evaluate this group of tumors classified as WDA. These criteria included the following: 1) anisonucleosis (variation in nuclear size greater than four times within a same epithelial group), 2) nuclear membrane irregularity, 3) nuclear crowding/overlapping/three-dimensionality, 4) nuclear enlargement (if more than two red blood cells), 5) gap versus confluent cell spacing, 6) hyperchromasia, 7) macronucleoli, 8) mitosis, 9) chromatin clearing, and 10) necrosis. Our data showed that the most prevalent criteria for diagnosing WDA were anisonucleosis (97% of cases), nuclear membrane irregularity (97% of cases), nuclear crowding/overlapping/three-dimensionality (92% of cases), and nuclear enlargement (99% of cases). In contrast, the criteria of gap versus confluent cell spacing, hyperchromasia, macronucleoli, mitosis, chromatin clearing, and necrosis were seen in 38%, 36%, 14%, 22%, 14%, and 7% of WDA cases, respectively.

Six cases in the suspicious category with a subsequent histologic or clinical confirmation of adenocarcinoma met most of these criteria (67–100%). For example, anisonucleosis, nuclear membrane irregularity, nuclear crowding, and nuclear enlargement were present in 100%, 83%, 67%, and 83% of the six cases, respectively. Additionally, there were four false-negative cases in this study, all of which also exhibited many of these four criteria (50–100%) (Lin and Staerkel, 2003).

It should be emphasized that some of the nonprevalent cytologic features of WDA from this study, such as macronucleoli, mitosis, and necrosis, have been claimed as significant cytologic features for a diagnosis by some of the previous articles (Robins *et al.,* 1995). Our findings suggest that these criteria are important in diagnosing adenocarcinoma in general, but there is limited value in diagnosing WDA. We do observe these cytologic features (marked nuclear pleomorphism, single malignant cells, tumor necrosis, prominent nucleoli, and many mitoses) in less differentiated adenocarcinoma, especially in a PDA. Figure 68A demonstrates a group of benign ductal epithelium showing two-dimensional honeycombed pattern; uniform, small nuclei; smooth nuclear membrane; and inconspicuous nucleoli. In contrast, WDA with anisonucleosis, nuclear membrane irregularity, nuclear crowding, and nuclear enlargement is shown in Figures 68B and C. In Figure 68C, abundant intracytoplasmic mucin is noted, representing a case of WDA with mucin production.

Fraig *et al.* (2002) applied 10 cytologic criteria to evaluate the 33 cases of pancreatic adenocarcinoma with false-negative diagnoses. The cytologic criteria used in their study were very similar to our criteria, including the following: 1) loss of polarity, 2) nuclear enlargement, 3) nuclear membrane irregularity, 4) pleomorphism, 5) pale or granular chromatin, 6) gaps between cells versus confluence, 7) increased cellularity, 8) hyperchromasia, 9) macronucleoli, and 10) necrosis. Their results demonstrated that loss of polarity, nuclear enlargement, and nuclear membrane irregularity were the most prevalent cytologic criteria, followed by nuclear pleomorphism, chromatin pattern (pale or granular), gap versus confluence, and hypercellularity. Also, similar to our findings, hyperchromasia, macronucleoli, and necrosis were only observed in 22–27% cases.

As mentioned in the section on methods, our general approach to an FNAB smear is as follows. Scan the entire slide at low-power field, getting an overall impression of the cellularity and the background of the smear.

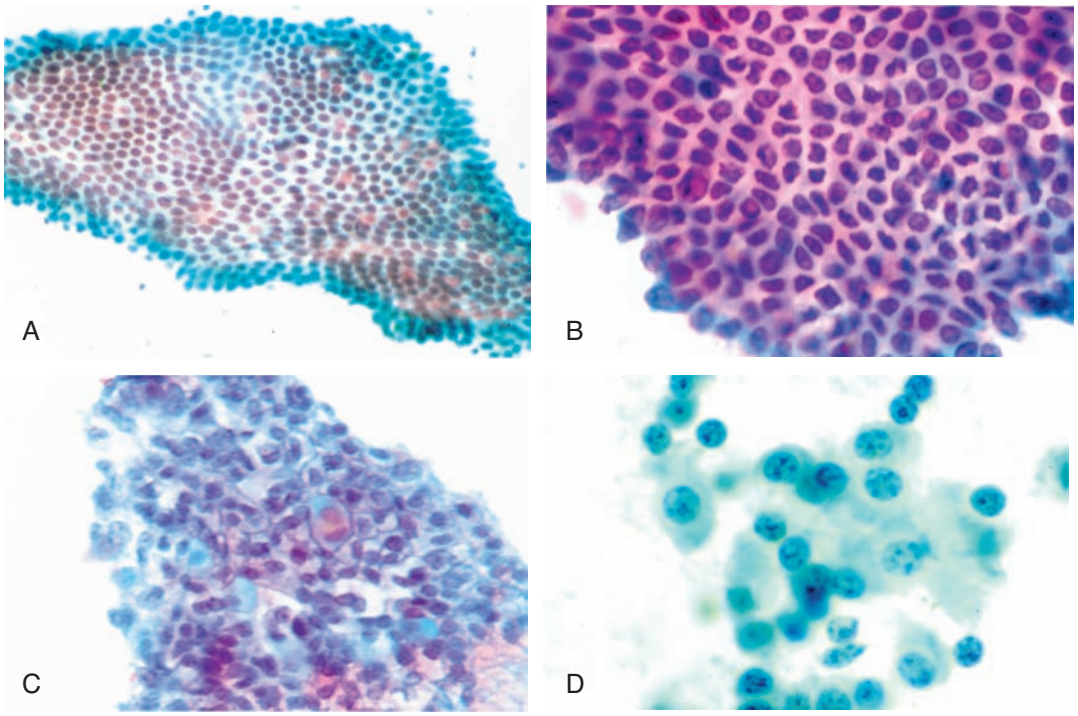

Figure 68. **A:** Benign ductal epithelium. Cohesive, flat sheet of benign ductal cells with small, uniform nuclei and smooth nuclear membranes. Papanicolaou stain, 400X. **B** and **C:** Well-differentiated adenocarcinoma of the pancreas. Nuclear crowding/loss polarity, nuclear variation, nuclear membrane irregularity, and nuclear enlargement. Intracytoplasmic nucin in part **C,** representing a case of WDA with mucin production, no mucin in the background seen. Papanicolaou stain, 600X. **D:** Pancreatic endocrine neoplasm. Loosely cohesive clusters and single cells with a salt-and-pepper nuclear chromatin pattern, abundant cytoplasm, and plasmacytoid appearance. Papanicolaou stain, 600X.

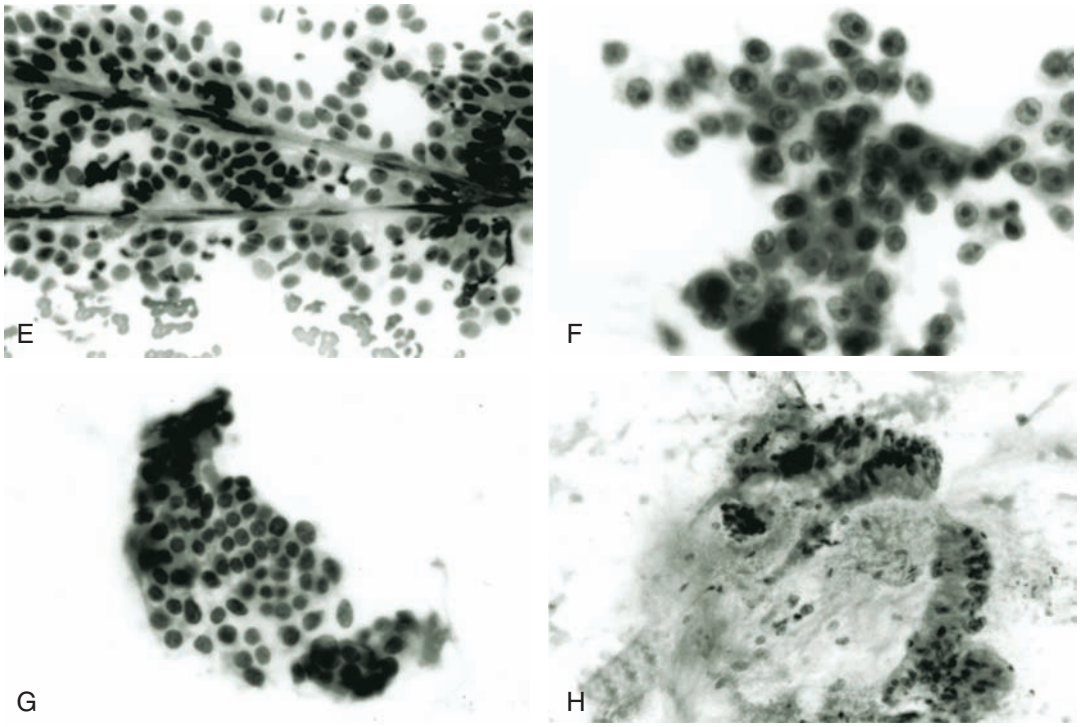

Figure 68—cont'd. E: Solid-pseudopapillary tumor of the pancreas. Papillary fronds lined by one to multiple layers of monomorphic, bland nuclei with evenly distributed nuclear chromatin and nuclear grooves. Diff-Quik stain, 400X. **F:** Acinar cell carcinoma. Loosely cohesive groups with high nuclear/cytoplasmic ratio and prominent nucleoli. Papanicolaou stain, 600X. **G:** Microcystic adenoma. Cohesive group of ductal-like cells with slight nuclear variation and nuclear membrane irregularity, in a background of clear fluid. Papanicolaou stain, 600X. **H:** Mucinous cystic neoplasm. Columnar, mucin-containing epithelial groups in a background of mucinous macrophages and mucoid material. Papanicolaou stain, 400X.

The majority of adenocarcinomas exhibit moderate to high cellularity of ductal epithelial cells.

Hypercellularity is also frequently seen from normal pancreatic tissue. However, the cellular components are groups of acinar cells and few ductal cells. Pancreatic endocrine neoplasms, solid and pseudopapillary tumor of the pancreas, and acinar cell carcinoma usually demonstrate high cellularity as well. It is important to pay attention to background of the smear, such as any necrosis (tumor or pancreatitis) inflammation (acute and chronic pancreatitis), granular debris with pigmented histiocytes (pancreatic pseudocyst), mucin (mucinous cystic neoplasms or mucinous adenocarcinoma), or clear fluid (microcystic serous adenoma). Nuclear enlargement can be easily observed at low power. As a general rule, benign ductal cells are the same size or slightly larger than red blood cells. The cytologic details of benign ductal cells would not be easily appreciated at low power. Therefore, it is almost certain that there is nuclear enlargement if you can see some of the nuclear features of these ductal epithelial groups at low magnification (4X). A hypercellular smear containing many groups of ductal cells with nuclear crowding and nuclear enlargement is suspicious for adenocarcinoma.

At intermediate magnification, pay attention to the architectural features of these epithelial groups. Loss of nuclear polarity, nuclear crowding, nuclear overlapping, and three-dimensionality are the common findings in pancreatic adenocarcinoma. The finding of papillary groups lined by one to two layers of cytologically bland epithelial cells should raise a concern of SPTP and pancreatic endocrine neoplasms. Loss of cohesion at the edge of an epithelial group can be seen in adenocarcinoma. However, the cohesive groups of ductal cells are the most consistent finding in a case of WDA. Gap cell spacing (as opposed to confluent cell spacing) means there is a distinct open space formation within a confluent sheet of epithelial cells. This feature has been observed in 38% of WDAs.

Nuclear enlargement and single intact cells should be easily identified at this magnification. Following a diligent search, a few intact malignant cells are frequently seen, even in a WDA. A few very large, well-formed columnar malignant cells, referred to as

"tombstone cells" (DeMay, 1996), may be present in a less-differentiated adenocarcinoma. If many single intact cells with bland cytomorphology are present, pancreatic endocrine neoplasms and SPTP should be included in the diagnostic considerations. Bland single columnar cells are commonly present in a mucinous tumor.

At high magnification, attention should be shifted to observe the detailed features of nuclei. Anisonucleosis is one of the most significant cytology criteria and was observed in the vast majority of WDAs in our study. Anisonucleosis was probably first introduced by Cohen *et al.* (1991) in the cytology literature for diagnosis of pancreatic adenocarcinoma, but it also served as one of the three major criteria for identifying pancreatic adenocarcinoma on frozen sections (Hyland *et al.,* 1981). We strongly suggest that anisonucleosis, variation in nuclear size greater than four times in the same epithelial group instead of three times as proposed by Cohen *et al.,* should be observed because this is somehow subjective among interobservers from our limited experience. It is our experience that small-sized nuclei tend to present in the peripheral portion of the epithelial group if anisonucleosis is seen focally.

Nuclear membrane irregularity is one of the most significant cytologic features for diagnosing WDA, and it is present in nearly all of cases of WDA in our study series, although the finding could be very focal. The degree of the nuclear membrane irregularity can range from small notch and groove to popcorn and resinoid. A combination of anisonucleosis and nuclear membrane irregularity is highly suggestive of adenocarcinoma because such combinations are nearly absent in a reactive condition. Extensive nuclear clearing or pale chromatin is a relatively unique feature for WDA if it is present. Hyperchromasia, granular chromatin, macronucleoli, and mitosis may be seen. Unfortunately, a WDA usually lacks these features.

As mentioned earlier, 90% of pancreatic malignancies are ductal carcinoma and its variants. We have discussed the cytologic features for a diagnosis of pancreatic adenocarcinoma, especially for a WDA. However, before a final diagnosis of adenocarcinoma is rendered, one should be certain to exclude the possibility of other neoplasms, such as pancreatic endocrine neoplasms, acinar cell carcinoma, SPTP, microcystic serous adenoma, mucinous cystic neoplasms, and metastasis. More importantly, a reactive condition, such as chronic pancreatitis, should be excluded as well.

Chronic Pancreatitis

Chronic pancreatitis is probably the most important nonneoplastic disease, which needs to be distinguished from adenocarcinorna of the pancreas. It may mimic pancreatic adenocarcinoma both clinically and cytologically. Clinically, obstructive jaundice, pain, and weight loss may present. A mass lesion or diffuse involvement of the pancreas may be seen radiographically. The main cytologic features include chronic inflammation, acinar atrophy, fibrosis, ductal hyperplasia, and relatively increased numbers of islet cells (DeMay, 1996). The cytologic findings largely depend on the stage of chronic pancreatitis. In the early stage, evidence of acute and chronic inflammation, fat necrosis, and granulation tissue may be the dominant features. In the late stage, as a result of an extensive acinar atrophy, the smear may be composed predominately of ductal epithelial cells, fibrosis, chronic inflammatory cells, and islet cells (Frias-Hidvegi, 1988). Squamous metaplasia has been described. Ductal epithelial proliferation associated with significant cytologic atypia may present (Pitman, 1999). The nuclear atypia more frequently show a combination of nuclear enlargement and prominent nucleoli. Marked anisonucleosis and/or nuclear membrane irregularity are rare findings. However, in some instances, the differential diagnosis from well-differentiated adenocarcinoma is virtually impossible.

If a cell block is available, some immunohistochemical markers, including clusterin, mesothelin, and prostate stem-cell antigen (PSCA), may provide some valuable information. Clusterin is a heat shock protein and has been shown to play a role in cell proliferation. A 2002 study of 8 cases of adenocarcinoma of the pancreas and 7 cases of chronic pancreatitis demonstrated a strong expression of clusterin in pancreatic duct and chronic pancreatitis and nearly absent expression in pancreatic adenocarcinoma (Jhala *et al.,* 2002). The study by McCarthy *et al.* (2003) showed that PSCA was present in 16 of the 19 pancreatic adenocarcinomas and was absent in 10 of the 11 benign lesions, with the sensitivity of 84% and specificity of 91%. They also demonstrated that mesothelin was present in 11 of the 19 cases of adenocarcinoma of the pancreas and absent in 10 of the 11 benign lesions, with a sensitivity of 68% and specificity of 91%.

Pancreatic Endocrine Neoplasms

Pancreatic endocrine neoplasms are relatively rare tumors, accounting for less than 5% of all pancreatic neoplasms. The neoplasms frequently occur in adults; they rarely occur in children. The majority of pancreatic endocrine neoplasms are functional. Nonfunctional tumors account for 15–30% of the reported cases (Kloppel and Heitz, 1993). It is important to distinguish pancreatic endocrine neoplasms from adenocarcinoma because some of the pancreatic endocrine neoplasms are benign or borderline tumors. In fact, pancreatic

endocrine neoplasms encompass a spectrum of lesions, including adenoma, borderline tumor, well-to moderately differentiated carcinomas, and poorly differentiated/undifferentiated carcinomas (Solcia *et al.,* 1997).

There are no reliable histologic criteria to predict the malignant potential of these tumors, risk of recurrence, or metastasis (Solcia *et al.,* 1997). However, tumors exceeding 2 cm in size, 0–3 mitoses/10 high-power field (HPF), and 1–5% of Ki-67 proliferation index are indicative of borderline malignant potential (Solcia *et al.,* 1997). Most low-grade (differentiated) pancreatic endocrine carcinomas are larger than 3 cm, with 1–10 mitoses/10 HPF and 1–10% of Ki-67 proliferation index (Solcia *et al.,* 1997). In contrast, poorly differentiated (undifferentiated) pancreatic endocrine carcinomas generally have more than 10 mitoses/10 HPF and greater than 10% of Ki-67 proliferation index (Solcia *et al.,* 1997). Tumors exceeding 6 cm in size usually are regarded as malignant, as documented in a large series in which 93% of malignant pancreatic endocrine tumors were of this size (Cubilla and Hajdu, 1975). Tumor necrosis is a good indicator for malignancy. However, it occurs only rarely in a differentiated pancreatic endocrine carcinoma. The unequivocal indicators for malignancy are metastasis and invasion of adjacent organs.

The FNAB specimen is usually hypercellular. It frequently consists of a 50–50 mixture of loosely cohesive clusters and single cells, as shown in Figure 68D. Acinar-like formation, perivascular tumor growth, or trabecular pattern can be seen (Al-Kaisi *et al.,* 1992; Sneige *et al.,* 1987). The neoplastic cells are typically monotonous, with focal nuclear pleomorphism (Nguyen and Rayani, 1986; Shaw *et al.,* 1990). Individual cells with well-defined cytoplasm or even a plasmacytoid appearance are the common findings. The nuclei tend to be round to oval with smooth nuclear membranes and a salt-and-pepper nuclear chromatin pattern (Al-Kaisi *et al.,* 1992; Sneige *et al.,* 1987). Binucleated and multinucleated neoplastic cells are usually seen. In less-differentiated tumors, predominated single cells with high nuclear/cytoplasmic ratio, prominent nucleoli, and mitoses are characteristic features. Immunohistochemical stains for chromogranin, neuron specific enolase (NSE), and synaptophysin may confirm the nature of neuroendocrine differentiation. As stated earlier, reliable histologic criteria, as well as cytologic criteria, to predict the malignant potential are not available (Nguyen and Rayani, 1986; Sneige *et al.,* 1987).

Solid-Pseudopapillary Tumor of the Pancreas

SPTP is an unusual low-grade malignant epithelial tumor, predominately occurring in adolescent girls and young women (Albores-Saavedra *et al.,* 1990; Pettinato *et al.,* 1992; Pettinato *et al.,* 2002). The cell origin of these neoplasms is uncertain. However, the neoplasm has been shown to express epithelial, mesenchymal, and neuroendocrine markers (Pettinato *et al.,* 1992; Pettinato *et al.,* 2002). The long-term prognosis following an adequate local surgery is generally excellent, although local recurrence or even metastasis has been reported (Cappellari *et al.,* 1990). An accurate preoperative diagnosis on FBAB specimen is crucial because it should lead to a more conservative surgery.

The FNAB specimen is highly characteristic. It is a highly cellular smear with clusters of papillary fronds and dissociated single cells, as shown in Figure 68E. The papillary fronds are composed of delicate fibrovascular core covered by one to two layers of bland neoplastic cells. The tumor cells are monomorphic, bland nuclei with evenly distributed nuclear chromatin and frequent nuclear grooves (Cappellari *et al.,* 1990; Katz and Ehya, 1990; Pettinato *et al.,* 1992; Pettinato *et al.,* 2002). Nuclear pleomorphism, mitosis, and prominent nucleoli are consistently absent (Katz and Ehya, 1990). Cytoplasmic process and hyalin globules may present (Cappellari *et al.,* 1990; Pettinato *et al.,* 2002). Foamy histiocytes, multinucleated giant cells, and cystic background are the common features. Immunoreactivity for vimentin and alpha-1 antitrypsin in all of the reported cases, and for progesterone receptor in some cases, is helpful in confirming the diagnosis (Pettinato *et al.,* 1992; Pettinato *et al.,* 2002). Focal pancytokeratin positivity can be seen from our experience and others (Pettinato *et al*., 1992; Pettinato *et al.,* 2002).

Acinar Cell Carcinoma

Acinar cell carcinoma is a rare tumor, accounting for less than 1% of all pancreatic malignancies. This tumor has been reported in a wide age distribution, from 3–90 years, with higher frequency in males. Approximately 15% of the patients may be associated with a clinical syndrome, which is characterized by extrapancreatic fat necrosis, polyarthralgia, and eosinophilia (DeMay, 1996). The FNAB specimen is usually highly cellular. It is composed of a mixture of cohesive groups and single acinar cells, as shown in Figure 68F. The neoplastic cells tend to have high nuclear/cytoplasmic ratio, irregular nuclear contour, and prominent nuclei (DeMay, 1996). Many naked nuclei may present in the background. A well-differentiated tumor may resemble benign acinar tissue. Ductal epithelial cells are usually absent. The overall cytologic features are similar to acinar cell carcinoma of the parotid gland (DeMay, 1996).

Serous Microcystic Adenoma

Serous microcystic adenoma or serous cystadenoma is an uncommon, but benign, cystic tumor, with a striking predilection for elderly women. The tumors frequently occur in the head of the pancreas, with an average size of 10 cm. The tumors are sharply demarcated, multilocular cysts and may have a central stellate scar and a sunburst type calcification on a CT scan. The FNAB specimen is usually hypocellular and characterized by the presence of few groups of ductal-like cells in a background of clear, watery fluid (Hittmair *et al.,* 1991; Laucirica *et al.,* 1992). The epithelial cell groups are usually tightly cohesive, with mild nuclear pleomorphism. Focal nuclear crowding and nuclear membrane irregularity may present, as shown in Figure 68G. Single atypical cells, marked nuclear pleomorphism, prominent nucleoli, and mitosis are not the cytologic features. Periodic acid-Schiff stain should demonstrate positive reactivity for the cytoplasmic glycogen. Mucicarmine stain for intracytoplasmic mucin is uniformly negative.

Mucinous Cystic Neoplasms

Mucinous cystic neoplasms are uncommon tumors of the pancreas, accounting for approximately 1% of total pancreatic tumors. It usually occurs in middle-age patients and is more common in females than males. The average size of tumors is 10 cm (ranging from 2–20 cm), and they are frequently located in the body or tail of the pancreas. All mucinous cystic neoplasms are currently regarded as having at least borderline malignant potential (Compagno and Oertel, 1978). However, it has been proposed that mucinous cystic tumors of the pancreas can be classified into mucinous cystadenoma, mucinous cystic tumor of borderline malignant potential, and mucinous cystadenocarcinoma, according to their grade of dysplasia (Solcia *et al.,* 1997).

An important diagnostic clue for mucinous cystic neoplasms can be appreciated grossly (Vellet *et al.,* 1988), when an FNAB specimen of pancreatic lesion contains watery or viscid mucoid material. Mucoid material tends to be metachromatic on Diff-Quick stain, but it may not be very visible on the Papanicolaou stain (DeMay, 1996). An additional unstained slide for mucicarmine stain is recommended. The cellularity of FNAB specimen is variable depending on the amount of mucin obtained or if the solid area is aspirated. The finding of columnar, mucin-containing cells is the key diagnostic feature, as illustrated in Figure 68H. The degree of architectural and nuclear atypia may be variable depending on the nature of the lesion. Papillary clusters may present (Centeno *et al.,* 1994; Gupta and Al-Ansari, 1994). Unequivocal cytologic features of malignancy are diagnostic for mucinous cystadenocarcinoma. However, mucinous cystadenocarcinoma may be noninvasive or invasive. Unfortunately, no reliable cytologic criteria are available to differentiate invasive versus noninvasive mucinous cystadenocarcinoma.

Dpc4 protein is a nuclear transcription factor and has been demonstrated in the inactivation of more than half of the infiltrating ductal adenocarcinomas of the pancreas. The study of Dpc4 expression in 36 mucinous cystic neoplasms showed that only 1 of the 7 mucinous carcinomas was positive for Dpc4, whereas 29 noninvasive mucinous cystic neoplasms were positive (Iacobuzio-Donahue *et al.,* 2000).

Metastasis

Distinction of primary ductal adenocarcinoma of the pancreas from metastatic carcinoma may be impossible. As reported in the literature, the most common sources of metastatic malignant tumors of the pancreas are lung, kidney, breast, liver, and gastrointestinal tract; sarcoma; and melanoma (DeMay, 1996). In our study, 11 cases of metastatic malignant tumors were identified, including renal (4 cases), stomach (3 cases), prostate (1 case), squamous cell carcinoma (1 case), liver (1 case), and sarcoma (1 case).

If a cell block is available, a panel of immunohistochemical markers may provide some useful information, including cytokeratin 7 (CK-7), cytokeratin 20 (CK-20), cytokeratin 17 (CK-17), thyroid transcription factor-1 (TTF-1), and estrogen receptor (ER). The most common staining profiles for these tumors are as follows: adenocarcinoma of the pancreas –CK7+, CK20–, CK17+, TTF-1–, ER–; adenocarcinoma of the lung –CK7+, CK20–, CK17–, TTF-1+; renal cell carcinoma –CK7–, CK20–, TTF-1–; and ductal carcinoma of the breast –CK7+, CK20–, ER+, TTF-1–. Metastatic renal cell carcinoma is frequently positive for RCC marker, CD-10, and P504S (Avery *et al.,* 2000; Chu and Arber, 2000; Lin *et al.,* 2004).

CONCLUSION

In summary, the majority of pancreatic lesions can be accurately diagnosed on FNAB specimens. The high diagnostic sensitivity and specificity in diagnosing adenocarcinoma of the pancreas, including WDA, can be achieved by observance of nuclear crowding/three-dimensionality, anisonucleosis, nuclear membrane irregularity, and nuclear enlargement. Other cytologic criteria, such as mitosis, necrosis, prominent nucleoli, and

hyperchromasia, which are frequently present in less-differentiated adenocarcinomas of the pancreas, are of little value in diagnosing WDA. Some immunohistochemical markers, including CK-17, clusterin, Dpc4, mesothelin, and PSCA, may provide useful information in diagnosis and differential diagnosis of pancreatic adenocarcinomas on FNAB specimens. Exploration of global gene expression of pancreatic carcinomas by complementary deoxyribonucleic acid (cDNA) microarray analysis will identify more specific genes as potentially important in diagnosis and treatment of pancreatic carcinomas.

References

Albores-Saavedra, J., Gould, E.W., Angeles-Angeles, A., and Herson, D.E. 1990. Cystic tumors of the pancreas. *Pathol. Annu. 25(2)*:19–50.

Al-Kaisi, N., and Siegler, E.E. 1989. Fine needle aspiration cytology of the pancreas. *Acta Cytol. 33*:145–152.

Al-Kaisi, N., Weaver, M.G., Abdul-Karim, F.W., and Siegler, E. 1992. Fine needle aspiration cytology of neuroendocrine tumors of the pancreas: A cytologic, immunocytochemical and electron microscopic study. *Acta Cytol. 36*:655–660.

Avery, A.K., Beckstead, J., Renshaw, A.A., and Corless, C.L. 2000. Use of antibody to RCC and CD10 in the differential diagnosis of renal neoplasms. *Am. J. Surg. Pathol. 24*:203–210.

Blandamura, S., Costantin, G., Nitti, D., and Boccato, P. 1995. Intraoperative cytology pancreatic masses: A 10-year experience. *Acta Cytol. 39*:23–27.

Cappellari, J.O., Geisinger, K.R., Albertson, D.A., Wolfman, N., and Kute, T. 1990. Malignant papillary cystic tumor of the pancreas. *Cancer 66*:193–198.

Centeno, B.A., Lewandrowski, K.B., Warshaw, A.L., Compton, C.C., and Southern, J.F. 1994. Cyst fluid cytologic analysis in the differential diagnosis of pancreatic cystic lesions. *Am. J. Clin. Pathol. 101*:483–487.

Chang, K.J. 1995. Endoscopic ultrasound-guided fine needle aspiration in the diagnosis and staging of pancreatic tumors. *Gastrointest. Endosc. Clin. North Am. 5*:723–734.

Chu, P., and Arber, D.A. 2000. Paraffin-section detection of CD10 in 505 nonhematopoietic neoplasms: Frequent expression in renal cell carcinoma and endometrial stromal sarcoma. *Am. J. Clin. Pathol. 113*:374–382.

Cohen, M.B., Egerter, D.P., Holly, E.A., Ahn, D.K., and Miller, T.R. 1991. Pancreatic adenocarcinoma: Regression analysis to identify improved cytologic criteria. *Diagn. Cytopathol. 7*:341–345.

Compagno, J., and Oertel, J.E. 1978. Mucinous cystic neoplasm of the pancreas with overt and latent malignancy (cystadenocarcinoma and cystadenoma). *Am. J. Clin. Pathol. 69*:573–580.

Cubilla, A.L., and Hajdu, S.I. 1975. Islet cell carcinoma of the pancreas. *Arch. Pathol. 99*:204–207.

David, O., Green, L., Reddy, V., Kluskens, L., Bitterman, P., Attal, H., Prinz, R., and Gattuso, P. 1998. Pancreatic masses: A multi-institutional study of 364 fine-needle aspiration biopsies with histopathologic correlation. *Diagn. Cytopathol. 19*:423–427.

DeMay, R.M. 1996. *The Art and Science of Cytopathology: Pancreas.* Chicago: ASCP Press, 1054–1069.

Fraig, M.M., Cheng, R., Hoda, R.S., Lewin, D., and Wallace, M. 2002. Reassessment of the cytologic criteria of pancreatic adenocarcinoma: Review of 33 cases with false negative diagnoses. *Mod. Pathol.15*:73A #293.

Frias-Hidvegi, D. 1988. *Guides to Clinical Aspiration Biopsy: Liver and Pancreas.* New York: Igaku-Shion.

Glenthoj, A., Sehested, M., and Trop-Pedersen, S. 1990. Ultrasonically guided histological and cytological fine needle biopsies of the pancreas: Reliability and reproducibility of diagnoses. *Gut 31*:930–933.

Greenle, R.T., Hill-Harmon, M.B., Murray, T., and Thun, M. 2001. Cancer statistics, 2001. *CA Cancer J. Clin. 51*:16–36.

Gupta, R.K., and Al-Ansari, A.G. 1994. Needle aspiration cytology in the diagnosis of mucinous cystadenocarcinoma of pancreas. *Int. J. Pancreatol. 15*:149–153.

Hancke, S., Holm, H.H., and Koch, F. 1984. Ultrasonically guided puncture of solid pancreatic mass lesions. *Ultrasound Med. Biol. 10*:613–615.

Hittmair, A., Pernthaler, H., Totsch, M., and Schmid, K.W. 1991. Preoperative fine needle aspiration cytology of a microcystic adenoma of the pancreas. *Acta Cytol. 35*:546–548.

Hyland, C., Kheir, S.M., and Kashlan, M.B. 1981. Frozen section diagnosis of pancreatic carcinoma: A prospective study of 64 biopsies. *Am. J. Surg. Pathol. 5*:179–191.

Iacobuzio-Donahue, C.A., Wilentz, R.E., Argani, P., Yeo, C.J., Cameron, J.L., Kern, S., and Hruban, R.H. 2000. Dpc4 protein in mucinous cystic neoplasms of the pancreas. *Am. J. Surg. Pathol. 24*:1544–1548.

Jhala, D.N., Jhala, N.C., El Qubeidi, M.A., Medeiros, J.L., Eltoum, I.A., and Forst, A.R. 2002. Clusterin expression in pancreatic adenocarcinoma and chronic pancreatitis. *Mod. Pathol. 15*: 288A #1195.

Katz, L.B.K., and Ehya, H. 1990. Aspiration cytology of papillary cystic neoplasm of the pancreas. *Am. J. Clin. Pathol. 94*: 328–333.

Kloppel, G., and Heitz, P.U. 1993. Pancreatic endocrine tumors in man. In Polak, J.M., (ed), *Diagnostic Histopathology of Neuroendocrine Tumors.* Edinburgh: Churchill Livingstone, 91–121.

Kloppel, G., Solcia, E., and Longnecker, D.S. 1996. *Histologic Typing of Tumors of the Exocrine Pancreas,* ed 2. Berlin: Springer-Verlag.

Laucirica, R., Schwartz, M.R., and Ramzy, I. 1992. Fine needle aspiration of pancreatic cystic epithelial neoplasms. *Acta Cytol. 36*:881–886.

Lin, F., and Staerkel, G. 2003. Cytologic criteria for well differentiated adenocarcinoma of the pancreas in fine-needle aspiration biopsy specimens. *Cancer Cytopathol. 99*:44–50.

Lin, F., Brown, R.E., Shen, T., Yang, X.J., and Schuerch, C. 2004. Immunohistochemical detection of P504S in primary and metastatic renal cell carcinomas. *Applied Immunohistochem. Mol. Morphol. 12*:153–159.

McCarthy, D.M., Maitra, A., Argani, P., Rader, A.E., Faigel, D.O., van Heek, N.T., Hurban, R.H., and Wilentz, R.E. 2003. Novel markers of pancreatic adenocarcinoma in fine needle aspiration: Mesothelin and prostate stem cell antigen labeling increases accuracy in cytologically borderline cases. *Applied Immunohistochem. Mol. Morphol. 11*:238–243.

Mitchell, M.I., and Carney, C.N. 1985. Cytologic criteria for the diagnosis of pancreatic carcinoma. *Am. J. Clin. Pathol. 83*:171–176.

Moossa, A.R. 1982. Pancreatic cancer: Approach to diagnosis, selection for surgery and choice of operation. *Cancer 50*:2689–2698.

Nguyen, G-K., and Rayani, N.A. 1986. Hyperplastic and neoplastic endocrine cells of the pancreas in aspiration biopsy. *Diagn. Cytopathol. 2*:204–211.

Niederhuber, J.E., Brennan, M.R., and Menck, H.R. 1995. The national cancer data base report on pancreatic cancer. *Cancer 76*:1671–1677.

Palazzo, L., Roseau, G., and Gayet, B. 1993. Endoscopic ultrasonography in the diagnosis and staging of pancreatic adenocarcinoma: Results of a prospective study with comparison to ultrasonography and CT scan. *Endoscopy 25*:143–150.

Pettinato, G., Di Vizio, D., Manivel, J.C., Pambuccian, S.E., Pasquale, S., and Insabato, L. 2002. Solid-pseudopapillary tumor of the pancreas: Aneoplasm with distinct and highly characteristic cytological features. *Diagn. Cytopathol. 27*:325–334.

Pettinato, G., Manivel, J.C., Ravett, C., Terracciano, L., Gould, E., Di Tuoro, A., Jaszcz W., and Albores-Saavedra, J. 1992. Papillary cystic tumor of the pancreas: A clinicopathologic study of 20 cases with cytologic, immunohistochemical, ultrastructural, and flow cytometric observations, and a review of the literature. *Am. J. Clin. Pathol. 98*:478–488.

Pitman, M.B. 1999. Fine needle aspiration biopsy of the pancreas. In Centeno, B.A., and Pitman, M.B., (eds) *Pancreatitis.* Wilburn, MA: Butterworth-Heinemann 31:51.

Robins, D.B., Katz, R.L., Evans, D.B., and Green, L. 1995. Fine needle aspiration of the pancreas: In quest of accuracy. *Acta Cytol. 39*:1–10.

Shaw, J.A., Vance, R.P., Geisinger, K.R., and Marshall, R.B. 1990. Islet cell neoplasms: A fine-needle aspiration cytology study with immunocytochemical correlations. *Am. J. Clin. Pathol. 94*:142–149.

Sneige, N., Ordonez, N.G., Veanattukalathil, S., and Samaan, N.A. 1987. Fine-needle aspiration cytology in pancreatic endocrine tumors. *Diagn. Cytopathol. 3*:35–40.

Solcia, E., Capella, C., and Kloppel, G. 1997. *Atlas of tumor pathology: Tumor of pancreas.* Washington, D.C.: Armed Forces Institute of Pathology, 41–196.

Vellet, D., Leiman, G., Mair, S., and Bilchik, A. 1988. Fine needle aspiration cytology of mucinous cystadenocarcinoma of the pancreas: Further observations. *Acta Cytol. 32*:43–48.

17

Immunohistochemical Expression of Mitogen-Activated Protein Kinase Kinase 2 in Pancreatic Cancer

Hiroshi Egami and Xiaodong Tan

Introduction

Pancreatic cancer is known to be an extremely lethal neoplasm; one reason being that pancreatic cancer itself has an extremely high potential of invasion and metastasis. It is important to establish a new therapeutic method based on anti-invasion and anti-metastasis drugs, which may contribute to ameliorating the prognosis of pancreatic cancer. Thus far, the cellular and molecular mechanisms of the invasion and metastasis of pancreatic cancer remain unclear. Detection of the factor(s) related to the differences in potential for invasion and metastasis of cancer cells could provide useful information for the development of new therapeutic methods to prevent the invasion and metastasis of pancreatic cancer.

Two hamster pancreatic cancer cell lines with different potentials for invasion and metastasis (PC-1 with a low, and PC-1.0 with a high potential of invasion and metastasis after intrapancreatic transplantation) were established from a pancreatic ductal carcinoma induced by N-nitrosobis (2-oxopropyl) amine (BOP) in a Syrian golden hamster (Egami *et al.,* 1989; Egami *et al.,* 1991; Pour *et al.,* 1991). Also, PC-1.0 cells have been found to produce a soluble proteinous factor, called dissociation factor (DF), which induces cell dissociation and cell motility of weakly invasive and rarely metastatic PC-1 cells (Hirota *et al.,* 1993; Kurizaki *et al.,* 1995).

In our study, the difference of the messenger ribonucleic acid (mRNA) expression between PC-1.0 cells and PC-1 cells was examined using the Representational Difference Analysis (RDA) method. As a result, mitogen-activated protein kinase kinase2 (MEK2) was isolated as a postulated factor, which was correlated to the potential of the invasion and metastasis of these cell lines (Ishikawa *et al.,* 2003; Tan *et al.,* 2004).

MEK2 is a key kinase in the mitogen-activated protein kinase (MAPK) signal transduction pathway, which is involved in the cellular program in diverse ways, including cell proliferation, differentiation, cell division, stress, apoptosis, and others (Balif and Blenis, 2001; Cobb, 1999; Robinson and Cobb, 2003; Walter, 2000). The kinase MEK2 has been reported to be related to the cell motility and invasiveness of several cancer cells (Krueger *et al.,* 2001; Torimura *et al.,* 2001; Ueoka *et al.,* 2000). Furthermore, inhibition of MEK activation

Handbook of Immunohistochemistry and *in situ* Hybridization of Human Carcinomas, Volume 3: Molecular Genetics, Liver Carcinoma, and Pancreatic Carcinoma

could suppress the invasion of melanoma and hepatoma cells (Abiru *et al.,* 2002; Ge *et al.,* 2002). However, there currently is no report that elucidates the involvement of MEK2 in the cancer cell dissociation as well as invasion–metastasis of pancreatic cancer.

To clarify the biological significance of MEK2 expression in relation to cell dissociation and the potential of invasion and metastasis in pancreatic cancer, the immunocytochemical expressions of MEK2 and phosphorylated-MEK (p-MEK) in hamster and human pancreatic cancer cell lines were analyzed and the immunohistochemical expression in human pancreatic cancer tissues was studied.

MATERIALS

Cell Lines

Hamster pancreatic cancer cell lines PC-1 and PC-1.0 were used. The PC-1 cell line was established from pancreatic ductal/ductular adenocarcinomas induced by BOP in a Syrian golden hamster (Egami *et al.,* 1989). The PC-1.0 cell line was established from a subcutaneous tumor produced after inoculation of the PC-1 cell (Hirota *et al.,* 1993). Two human pancreatic cancer cell lines, AsPC-1 and Capan-2 (American Tissue Culture Collection, Rockville, MD), were also used. The PC-1 and Capan-2 cells grow mainly as islandlike clonies, whereas the PC-1.0 and AsPC-1 cells exhibit a growth pattern of single cells.

Tissue Samples

All of the tissue samples were obtained at the time of surgical operation at the Department of Surgery II, Kumamoto University Hospital, from October 1989 to July 2001. Specimens were from 37 pancreatic cancers (29 tubular adenocarcinomas, 2 papillary adenocarcinomas, 1 invasive mucinous cystadenocarcinoma, 1 adenosquamous carcinoma, 2 intraductal papillary adenocarcinomas, 1 mucinous cystadenocarcinoma, and 1 peritoneal wall metastasis). The median age of the patients with pancreatic cancer was 63.5 years (range, 35–78 years). These patients included 14 males and 23 females. Histologically, these consisted of 13 well-differentiated, 20 moderately differentiated, and 4 poorly differentiated adenocarcinomas. All of the tissue samples were histologically examined, and the pathologic diagnoses were confirmed.

Antibodies

Rabbit polycolonal antibodies raised against amino acid sequences of MEK2 and p-MEK1/2 of human origins (Santa Cruz Biotechnology, Santa Cruz, CA) were used in this study. Rhodamine-labeled fluorescence secondary antibody (Santa Cruz Biotechnology) was also used in this study.

METHODS

Immunofluorescent Staining of MEK2 in Pancreatic Cancer Cell Lines

Cell Culture

All of these cell lines were incubated in RPMI-1640 (Gibco-BRL, Grand Island, NY), supplemented with 10% fetal bovine serum (Bioserum, Victoria, Australia), 100 units/ml penicillin G, and 100 μg/ml streptomycin at 37°C in a humidified atmosphere of 5% CO_2 to 95% air. The cells were serum starved overnight before the experiments.

Treatment with DF and Specific MEK1/2 Inhibitor U0126

All of the 4 cell lines mentioned earlier were planted into the FALCON CultureSlides (Becton, Dickinson and Company Franklin Lakes, NJ) and incubated for 36 hr (untreated cells). To evaluate the relationship between the expression of MEK2 and the biological characteristics of pancreatic cancer cells, the effects of DF and U0126 (CellSignaling Technology, Beverly, MA) were studied. U0126 is a specific MEK1/2 inhibitor and it can inhibit the phosphorylation of MEK2 (Favata, *et al.,* 2002). For activation study, the PC-1 cells and Capan-2 cells were added with the conditioned medium (CM) of PC-1.0 cells, which contained DF (DF-CM) at a total concentration of 40% and was incubated for 36 hr. For inhibition study, PC-1.0 and ASPC-1 cells were incubated with 10 μM at a concentration of U0126 for 36 hr. In addition, PC-1 and Capan-2 cells were incubated for another 36 hr with a treatment of 10 μM U0126 after incubation with DF-CM for 36 hr.

Fluorescent Staining

Fixation After incubation, the cells were fixed with 0.5% paraformaldehyde for 10 min at room temperature. Normally 4% paraformaldehyde is used, but the bubbles were found to be located at the peripheral sites of cells fixed with high concentrations of paraformaldehyde. Furthermore, the cell membrane was disrupted easily by the washing with phosphate buffer saline (PBS). At last, we found 0.5% was the most optimal concentration, and these cells were properly fixed.

Permeabilization The cells were washed 3× with PBS. Then the cells were permeabilized with 0.2% Triton X-100 for 3 min at room temperature.

Nonspecific Blocking The cells were washed 3× with PBS. For nonspecific blocking, the cells were incubated with 10% normal goat serum for 30 min at room temperature.

Incubation with Primary Antibodies Then for the MEK2 and p-MEK staining, the cells were incubated with polyclonal anti-MEK2 or anti-phosphorylated MEK1/2 antibodies (1:200, dilution in PBS containing 1% bovine albumin) at 4°C overnight.

Incubation with Secondary Antibodies The cell was washed 3× with PBS. Then the cells were incubated with rhodamine-labeled secondary antibody for 2 hr at room temperature. The culture slide was covered with aluminum foil to protect it from light.

Mounting The culture slide was rinsed 3× with PBS, and then the chamber was removed from the slide with the Removal Key prongs. The slide was mounted with VECTASHIELD Mounting Medium (Vector Laboratories, Burlingame, CA) and covered with aluminum foil to protect it from light. Although VECTASHIELD Mounting Medium can preserve fluorescence for weeks at 4°C, the slides were examined immediately in this study.

Analysis of Fluorescence Intensity After they were mounted, the slides were observed and fluorescent images were taken with a confocal laser scanning biological microscope (FV500-IX, Olympus, Japan). Images of six sites of the cell nucleus, cytoplasm, and whole cell were taken randomly, and the fluorescence intensity (FI) in each site was measured by using the software of Fluoview 500 (version 3.1, Olympus, Japan).

Control Slide Nonspecific rabbit immunoglobulin G (IgG) was used as negative control instead of a polyclonal anti-MEK2 or anti p-MEK1/2 antibody in this study.

Immunohistochemical Staining of MEK2 Protein in Human Pancreatic Cancer Specimens

Immunohistochemical staining was performed using the avidin-biotin-peroxidase complex technique (Vectastain Elite ABC Kit; Vector Laboratories). Other chemicals were also commercially available.

Fixation

All of the tissue specimens were fixed as soon as possible after the surgical resection in 10% formalin.

Embedment and Serial Sections

Then the tissue specimens were embedded in paraffin and cut into 5-μm serial sections.

Deparaffinization and Rehydration

Tissue sections were deparaffinized and hydrated through xylenes and graded alcohol series.

Quenching of Endogenous Peroxidase Activity

After deparaffinization and rehydration, the sections were immersed in 1.5% H_2O_2 in absolute methanol for 30 min for quenching the endogenous peroxidase activity and then washed 3× with distilled water.

Nonspecific Blocking

Next, 10% normal goat serum was added for nonspecific blocking for 30 min.

Incubation with Primary Antibodies

Without washing, the sections were then incubated with a primary antibody (1:200 diluted in PBS containing 1% bovine albumin, pH 7.4) for 2 hr at room temperature.

Incubation with Secondary Antibody

After being washed 3× in PBS, the sections were incubated with the biotinylated secondary antibody for 50 min at room temperature.

Reaction with Avidin-Peroxidase Conjugate

Sections were washed for 5 min with PBS and were subsequently incubated with avidin-peroxidase conjugate for 1 hr at room temperature.

Reaction with Diaminobenzidine and Hydrogen Peroxide

The sections were washed 3× with PBS. At last, the sections were reacted with diaminobenzidine and hydrogen peroxide (Vector Laboratories) at room temperature.

Counterstaining

After washing with PBS for 5 min, the sections were slightly counterstained with hematoxylin for 3 sec.

Mounting

After rinsing sections in tap water, the sections were mounted with VectaMount Mounting Medium (Vector Laboratories). The sections are stored at 4°C and protected from light. All the sections should be stained and examined simultaneously and as early as possible after mounting.

Immunohistochemical Evaluation

To evaluate the immunoreactivity, the immunoreactive score (IRS) proposed by Remmele and Stegner (1987) was applied with a slight modification, as follows: IRS = Staining intensity (SI) × Percentage of positive cells (PP). The SI was determined as 0, negative; 1, weak; 2,

moderate; and 3, strong. The PP was defined as 0, negative; 1, 1–30%; 2, 31–50%; 3, 51–80%; and 4, 81–100% positive cells individually. Ten visual fields from different areas of each specimen were chosen at random for the IRS evaluation, and the average IRS was calculated as a final value.

Control Slide

The control slides were prepared as follows: 1) sections were processed without a primary antibody; and 2) normal rabbit serum and nonspecific rabbit IgG were used instead of a polyclonal anti-MEK2 or p-MEK1/2 antibody.

Statistical Analysis

The differences of MEK2 or p-MEK expressions in various pancreatic cancer tissue specimens were examined by unpaired Student's t-test with the Stat View computerized program (SAS Institute, Inc., Cary, NC). A probability value of <0.05 was considered significant.

RESULTS AND DISCUSSION

A MEK2 is a 45-KDa protein and is one of two members of MEK (MEK1 and MEK2), which serves in the MAPK pathway. The MAPK pathway is one of the most important signal transduction pathways in eucaryotes. It usually is organized in a three-kinase architecture consisting of a MAPK, a MAPK activator (MAPKK), and a MAPKK activator (MAP kinase kinase kinase, MAPKKK). This signal transduction pathway could be activated by sequential phosphorylation (Schaelfer and Weber 1999). Although the relationships between MEK2 and cell proliferation, differentiation, cell division, stress, apoptosis, and others have been elucidated (Balif and Blenis, 2001; Cobb, 1999; Robinson and Cobb, 2003; Walter, 2000), the involvement of MEK2 activation in the cell dissociation and the mechanism of invasion–metastasis of pancreatic cancer are not fully understood.

The quantity and distribution of both MEK2 and p-MEK were quite different in the cell lines that had different capability of invasion and metastasis. In the present study, MEK2 (FI = 125.40 ± 11.75) and p-MEK (activated MEK) (FI = 120.00 ± 17.50) were found to be constitutively highly expressed in highly invasive pancreatic cancer cell lines (PC-1.0), which grew as single cells. Also, p-MEK mainly distributed in the nucleus in these cells. In contrast, both MEK2 (FI = 27.96 ± 7.79) and p-MEK (FI = 48.55 ± 10.72) were faintly expressed in weakly invasive pancreatic cancer cell lines (PC-1), which formed islandlike colonies. Furthermore, either MEK2 or p-MEK was mainly distributed in the cytoplasm.

High magnitude of MEK2 expression, especially activated MEK2 expression, is necessary for cell dissociation in pancreatic cancer. PC-1 cells that were incubated with the DF-CM showed an obvious dissociation of island-like colonies and a high frequency of pseudopodia formation. Simultaneously, significant induction of intracellular MEK2 expression (FI = 210.87 ± 6.65), especially p-MEK expression (FI = 213.90 ± 9.17), was observed in the nucleus of PC-1 cells. This was diametrically opposite to the expression and distribution of activated MEK in untreated PC-1 cells. Herein, MEK2 presented a translocation from cytoplasm to nuclear after activation. Because MEK2 is a molecule of 45 KDa, a molecule whose molecular weight is more than 45 KDa could not enter nuclear through diffusion. There are reports that demonstrate that the translocation to nuclear of activated MEK2 is a process of active transport (Fukuda *et al.,* 1996; Fukuda *et al.,* 1997; Lenormand *et al.,* 1993). Our current results are consistent with these reports. Furthermore, our present study provided direct evidence to support the view that MEK2 is a key kinase in the signal pathway involved in regulation of cell dissociation and MEK2 was activated through phosphorylation by upstream kinase and then translocated to nuclear. Finally, the signal was transducted into the nucleus and lead to a series of morphologic changes including cell dissociation. In our other studies, ERK2, a downstream kinase of MEK2, showed identical changes of expression after various treatments (the same as those mentioned earlier) (Tan *et al.,* 2004). The observations in this study strongly suggest that MEK2, especially the translocation of activated MEK2 into the nucleus, is closely associated with cell dissociation of pancreatic cancer *in vitro.*

Duration of MEK2 expression, especially activated MEK2 expression, is also necessary for cell dissociation in pancreatic cancer. Furthermore, by the treatment with MEK1/2 specific inhibitor U0126, the induced MEK2 and p-MEK expressions by DF-CM were significantly reduced (FI = 55.61 ± 30.32 and 50.33 ± 12.56 respectively), and the dissociated PC-1 cells were found to be aggregated and formed a cell–cell adhesion again. More interesting, PC-1.0 cells that had grown as dissociated single cells were found to be aggregated and formed islandlike colonies after U0126-treatment. Correspondingly, MEK2 (FI = 37.10 ± 15.48) and P-MEK (FI = 14.19 ± 4.08) expressions in PC-1.0 cells were almost completely suppressed. This may implicate that high magnitude and sustained expression of MEK2, especially activated MEK2 in these pancreatic cancer cells, is essential

for induction of cells dissociated in pancreatic cancer cells.

Similar changes of MEK2 and activated MEK2 expressions, as well as cell morphology, were observed in human pancreatic cancer cells. An even more important observation is that we found the different changes of the MEK2 and p-MEK expressions were also according to a different dissociate state of two human pancreatic cancer cell lines, AsPC-1 and Capan-2. The correlation of MEK2 expression and cell dissociation was consistent with that indicated in pancreatic cancer cell lines of hamster origin (PC-1.0 and PC-1). Our previous studies demonstrated that highly invasive hamster pancreatic cancer cells (PC-1.0) produce the DF, which could induce the cell dissociation of PC-1 cells (Hirota *et al.,* 1993; Kurizaki *et al.,* 1995). In this study, stronger constitutive expressions of MEK2 (FI = 79.88 ± 13.45) and p-MEK (FI = 109.32 ± 19.67) were observed in untreated AsPC-1 cells. After 36 hr of incubation with U0126, the expressions of MEK2 (FI = 10.82 ± 3.66) and p-MEK (FI = 16.24 ± 13.70) were also obviously inhibited in AsPC-1 cells. The light microscopic images showed that untreated AsPC-1 cells also grew as single cells similar to the observation in PC-1.0 cells. However, these cells aggregated and showed island-like cell colonies formation after 36 hr of incubation with U0126. Similarly, the expressions of MEK2 (FI = 12.56 ± 9.23) and p-MEK (FI = 28.45 ± 18.51) in Capan-2 cells were also extremely weak. After 36 hr of incubation with DF-CM, the expressions of MEK2 (FI = 179.71 ± 90.59) and p-MEK (FI = 135.09 ± 7.31) were significantly induced in the Capan-2 cells. In addition, after a subsequent incubation with U0126 for another 36 hr, the formerly induced expressions of MEK2 and p-MEK by DF-CM in the Capan-2 cells were apparently suppressed (FI = 22.16 ± 4.16 and 58.41 ± 27.80, respectively). The light microscopic images showed that a growth pattern of island-like cell colonies was observed in Capan-2 cells, which was similar to that of PC-1 cells. Treatment (36 hr) with DF-CM also induced significant dissociation of island-like cell colonies in Capan-2 cells, and the dissociated Capan-2 cells formed island-like cell colonies again after the subsequent incubation with U0126 for another 36 hr.

In the current work, we observed that DF could also induce the cell dissociation and the other morphologic changes of human pancreatic cancer line, Capan-2. The relevant changes of the intracellular MEK2 and p-MEK expressions were also similar to those found in hamster pancreatic cancer cell line (PC-1). Our present results suggest that MEK2, especially activated MEK2, is similarly involved in the signal transduction pathway in relation to cell dissociation even in pancreatic cancer cells of human origin.

MEK2 expression, especially activated MEK2 expression in human pancreatic cancer tissue samples, was correlated with invasion of pancreatic cancer. In nonmalignant tissues, immunostaining of MEK2 was detected neither in acinar and islet cells nor in duct/ductular cells (IRS = 0.100 ± 0.141; Figure 69A). However, the overexpressions of MEK2 were observed both in the center (IRS = 6.482 ± 2.138; Figure 69B) and the invasive front (7.768 ± 2.509; Figure 69C) of pancreatic cancer tissues. Furthermore, the expressions of MEK2 were found to be mainly distributed in the cytoplasm of cancer cells. The significant difference of the average IRS of MEK2 expression was found between the malignant and nonmalignant tissues ($P < 0.05$). However, no significant difference was observed between the average of IRS of MEK2 expression in the center and that in the invasive front of pancreatic cancer tissues ($P > 0.05$).

In nonmalignant tissues (IRS = 2.600 ± 1.058; Figure 69D), a weak immunostaining of p-MEK expression was detected in the nucleus of acinar cells, islet cells, and duct/ductular cells. In pancreatic cancer tissues, the overexpressions of p-MEK were found both in the center (IRS = 6.727 ± 1.050; Ce, upper right part of Figure 69E) and invasive front (IRS = 9.783 ± 1.508; I, lower left part of Figure 69E) of pancreatic cancer tissues. The significant difference of the average IRS of p-MEK expression was observed between the malignant and nonmalignant tissues ($P < 0.05$). Moreover, IRS of p-MEK expressions in the invasive front was significantly higher than that in the center of pancreatic cancer tissues ($P < 0.05$). In addition, p-MEK expressions were observed either in the nucleus or in the cytoplasm of cancer cells (Figure 69F) in comparison with that of MEK2.

The correlation of MEK2 and p-MEK expressions with clinicopathologic factors in pancreatic cancer was evaluated; however, because of the almost universal expressions of MEK2 and p-MEK in the pancreatic cancer cells, no significant difference in any clinical or pathologic characteristic was identified with respect to MEK2 or p-MEK expression ($P > 0.05$). The statistical analysis revealed significantly different MEK2 expressions between the malignant tissue and nonmalignant tissue. Moreover, the p-MEK expression in invasive fronts was apparently stronger than that in the center sites of pancreatic cancer tissue. As we know, tumor invasion and metastasis consists of a cascade of multiple steps, and the dissociation and release of tumor cells from the primary site is thought to be the first step of this cascade (Fincham *et al.,* 2000; Rescan *et al.,* 2001; Torimura *et al.,* 2001). The dissociation of cell–cell adhesion and increase in cell motility play an important role in tumor invasion and metastasis (Akagi *et al.,* 1997;

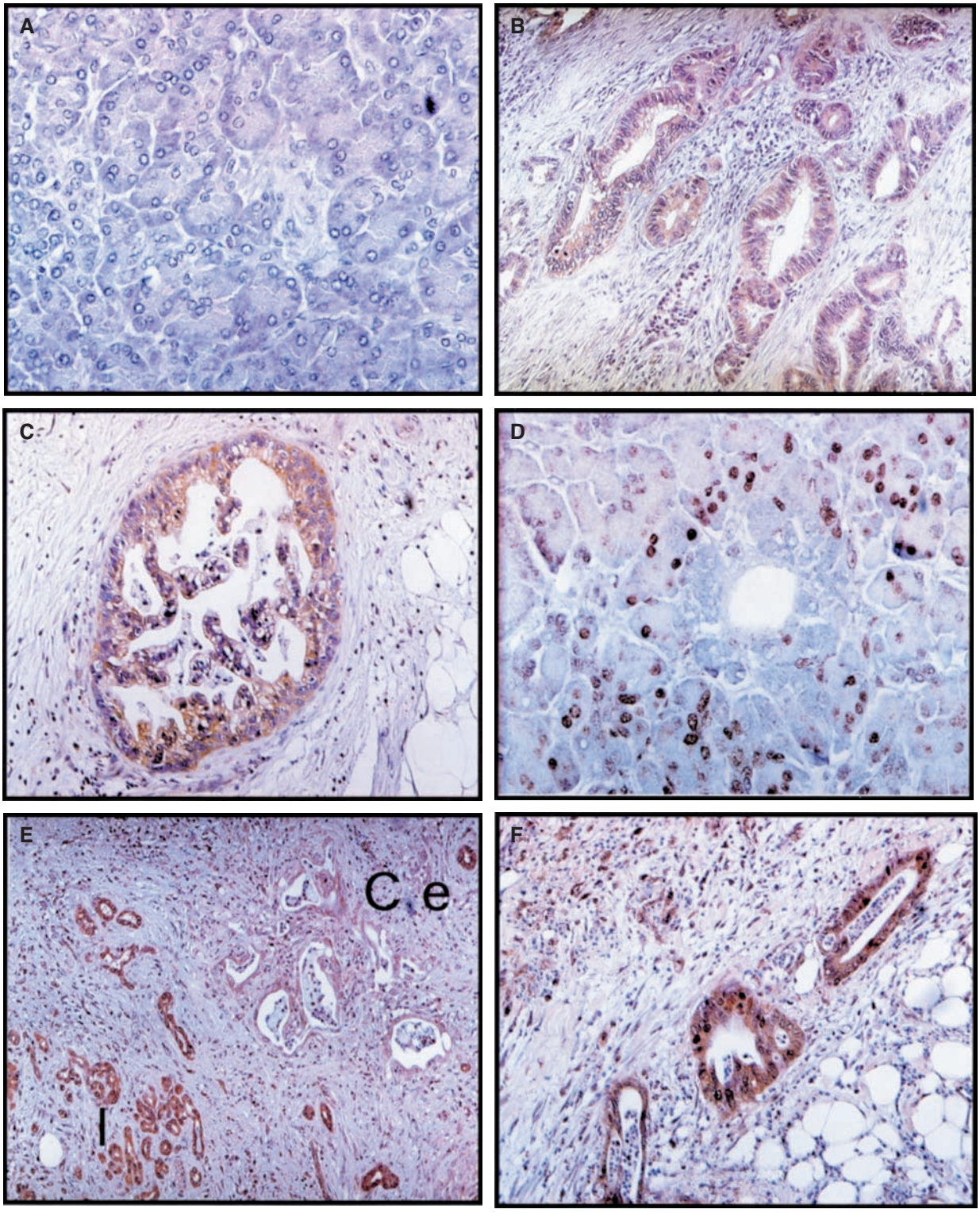

Figure 69. **A:** Expression of MEK2 (mitogen-activated protein kinase kinase2) in the nonmalignant pancreatic tissues (original magnification 100X). **B:** Expression of MEK2 in the center of pancreatic cancer tissues (original magnification 100X). **C:** Expression of MEK2 in the invasive front of pancreatic cancer tissues (original magnification 100X). **D:** Expression of p-MEK (phosphorylated-MEK) in the nonmalignant pancreatic tissues (original magnification 100X). **E:** Expression of p-MEK in the center (*Ce, upper right*) and invasive front (*I, lower left*) of pancreatic cancer tissues (original magnification 50X). **F:** Expression of p-MEK in the invasive front of pancreatic cancer tissues (original magnification 100X).

Partin *et al.,* 1989). A higher level of p-MEK expression in the invasive front of human pancreatic cancer may indicate that activation of MEK2 is even more closely related to the invasion potential of human pancreatic cancer cells *in vivo* and activated MEK2 may serve as a malignant and invasion-related marker in the diagnosis of pancreatic cancer.

Critical points in the immunohistochemical staining for MEK2 protein in human pancreatic cancer specimens. To obtain a perfect result of immunohistochemical staining, preservation of target antigen is the first and pivotal step. In this study, p-MEK protein, which is the active form of MEK, was stained immunohistochemically. Hence, it could not deny the possibility that the phosphorylation status of MEK2 could change during the preparation and fixation of the tumor. For example, during surgical resection, the vascularization may be cut off prior to removing the tumor. Therefore, in current work, the cancer tissue samples were kept cold on ice and fixed immediately after the resection.

Second, unmasking of the antigen is another important point in some cases of immunohistochemical staining. Formalin fixative can induce reversible or irreversible masking of part of target antigens as a result of the cross-linkage of proteins. The unmasking treatment can retrieve the target antigens by disrupting the steric hindrance caused by reverse intramolecular cross-linkage and intermolecular cross-linkage. We used a Serotec's Target unmasking fluid in the preliminary experiment, but there was no difference of "all or none" for MEK2 or p-MEK. Immunohistochemical staining was observed between the retrieval buffer treated sections and untreated sections, although it showed somewhat of a decrease in background staining. These results demonstrated that retrieval buffer was not necessary for MEK2 or p-MEK staining in this study.

Third, suppressing the background staining is also an important point in immunohistochemical staining. According to our experience, the following steps are critical.

1. The optimal diluted concentration of primary antibody should be determined by preliminary experiment. A high concentration of primary antibody may cause a high background staining.
2. The section should not be dried during the staining process. Otherwise, a high background staining may emerge.
3. A complete rinse of section with PBS is necessary for preventing background staining. In principle, 3× for 5 min (or 5× for 3 min) or more is needed.
4. Time for reaction with diaminobenzidine is also essential. It is especially important in the case of p-MEK staining in our current study because the difference of immunostaining intensity between the invasive front and the center site of pancreatic cancer in same section should be shown. Extended reaction time will bring a high background staining, and it will be difficult to distinguish the difference of immunostaining intensity between the invasive front and center site. The optimal time for the immunohistochemical staining of MEK2 and p-MEK in this work was found to be 5 min at room temperature.

In conclusion, the results observed in this study suggest that MEK2 is closely related to the induction and sustaining of cell dissociation in pancreatic cancer. Furthermore, MEK2 activation is probably involved in the first step of the cascade in cancer invasion and metastasis, the dissociation and release of cancer cells from the primary site. Selective inhibition of MEK2 expression and activation may contribute to the development of a new therapeutic method for pancreatic cancer. In addition, activated MEK2 can serve as a malignant and invasion-related marker in the diagnosis of pancreatic cancer.

References

Abiru, S., Nakao, K., Ichikawa, T., Migita, K., Shigeno, M., Sakamoto, M., Ishikawa, H., Hamasaki, K., Nakata, K., and Eguchi, K. 2002. Aspirin and NS-398 inhibit hepatocyte growth factor-induced invasiveness of human hepatoma cells. *Hepatology 35*:1117–1124.

Akagi, J., Egami, H., Kurizaki, T., Ohmachi, H., and Ogawa, M. 1997. Signal transduction pathway of the induction of cell motility in hamster pancreatic ductal adenocarcinoma cell. *Invas. Metast. 17*:16–25.

Balif, B.A., and Blenis, J. 2001. Molecular mechanisms mediating mammalian mitogen-activated protein kinase (MAPK) kinase (MEK)-MAPK cell survival signals. *Cell Growth Differ. 12*:397–408.

Cobb, M.H. 1999. MAP kinase pathways. *Prog. Biophys. Mol. Biol. 71*:479–500.

Egami, H., Takiyama, Y., Cano, M., Houser, W.H., and Pour, P.M. 1989. Establishment of hamster pancreatic ductal carcinoma cell line (PC-1) producing blood group-related antigens. *Carcinogenesis 10*:861–869.

Egami, H., Tomioka, T., Tempero, M., Kay, D., and Pour, P.M. 1991. Development of intrapancreatic transplantable model of pancreatic duct adenocarcinoma in syrian golden hamsters. *Am. J. Pathol. 138*:557–561.

Favata, M.F., Hriuchi, K.Y., Manos, E.J., Daulerio, A.J., Stradley, D.A., Feeser, W.S., van Dyk, D.E., Pitts, W.J., Earl, R.A., Hobbs, F., Copeland, R.A., Magolda, R.L., Scherle, P.A., and Trzaskos, J.M. 2002. Identification of a novel inhibitor of mitogen-activated protein kinase kinase. *J. Biol. Chem. 273*:18623–18632.

Fincham, V.J., James, M., Frame, M.C., and Winder, S.J. 2000. Active ERK/MAP kinase is targeted to newly forming cell-matrix adhesions by integrin engagement and v-Src. *EMBO J. 19*:2911–2923.

Fukuda, M., Gotoh, I., Gotoh, Y., and Nishida, E. 1996. Cytoplasmic localization of mitogen-activated protein kinase kinase directed by its NH2-terminal, leucine-rich short amino acid sequence, which acts as a nulear export signal. *J. Biol. Chem. 271*:20024–20028.

Fukuda, M., Gotoh, Y., and Nishida, E. 1997. Interaction of MAP kinase with MAP kinase kinase: Its possible role in the control of nucleocytoplasmic transport of MAP kinase. *EMBO J. 16*: 1901–1908.

Ge, X., Fu, Y.M., and Meadows, G.G. 2002. U0126, a mitogen-activated protein kinase kinase inhibitor, inhibits the invasion of human A375 melanoma cells. *Cancer Lett. 179*:133–140.

Hirota, M., Egami, H., Corra, S., Fujii, H., Chaney, W.G., Rizzino, A., and Pour, P.M. 1993. Production of scatter factor-like activity by a nitrosamine-induced pancreatic cancer cell line. *Carcinogenesis 14*:259–264.

Ishikawa, S., Egami, H., Kurizaki, T., Akagi, J., Tamori, Y., Yoshida, N., Tan, X., Hayashi, N., and Ogawa, M. 2003. Analysis of the factor in related to the signal transduction pathway of invasion and metastasis in pancreatic cancer. *J. Exp. Clin. Cancer Res. 22*:299–306.

Krueger, J.S., Keshamouni, V.G., Atanaskova, N., and Reddy, K.B. 2001. Temporal and quantitative regulation of mitogen-activated protein kinase (MAPK) modulates cell motility and invasion. *Oncogene 20*:4209–4218.

Kurizaki, T., Egami, H., Hirota, M., Akagi, J., Ohmachi, H., Yamamoto, S., and Ogawa, M. 1995. Characterization of cancer cell dissociation factor in a highly invasive pancreatic cancer cell line. *Cancer 75*:l554–1561.

Lenormand, P., Sardet, C., Pages, G., L'Allemain, G., Brunet, A., and Pouyssegur, J. 1993. Growth factors induce nuclear translocation of MAP kinase (p42 mapk and p44 mapk) but not their activator MAP kinase kinase (p45 mapkk) in fibroblasts. *J. Cell Biol. 122*:1079–1088.

Partin, A.W., Schoeniger, J.S., Mohler, J.L., and Coffey, D.S. 1989. Fourier analysis of cell motility: Correlation of motility with metastatic potential. *Proc. Natl. Acad. Sci. USA 86*:l254–1258.

Pour, P.M., Egami, H., and Takiyama, Y. 1991. Patterns of growth and metastases of induced pancreatic cancer in relation to the prognosis and its clinical implications. *Gastroenterology 100*:529–536.

Remmele, W., and Stegner, H.E. 1987. Recommendation for uniform definition of an immunoreactive score (IRS) for immunohistochemical estrogen receptor detection (ER-JCA) in breast cancer tissue. *Pathologe 8*:138–140.

Rescan, C., Coutant, A., Talarmin, H., Theret, N., Glaise, D., Guguen-Guillouzo, C., and Baffet, G. 2001. Mechanism in the sequential control of cell morphology and S phase entry by epidermal growth factor involves distinct MEK/ERK activations. *Mol. Biol. Cell 12*:725–738.

Robinson, M.J., and Cobb, M.H. 2003. Mitogen-activated protein kinase pathway. *Curr. Opin. Cell. Biol. 9*:180–186.

Schaelfer, H.J., and Weber, M.J. 1999. Mitogen-activated protein kinases: Specific messages from ubiquitous messengers. *Mol. Cell. Biol. 19*:2435–2444.

Tan, X., Egami, H., Ishikawa, S., Kurizaki, T., Tamori, Y., Takai, E., Hirota, M., and Ogawa, M. 2004. Relationship between the expression of extracellular signal-regulated kinase 1/2 and the dissociation of pancreatic cancer cells: Involvement of ERK1/2 in the dissociation status of cancer cells. *Int. J. Oncol. 24*:815–820.

Tan, X., Egami, H., Kamohara, H., Ishikawa, S., Kurizaki, T., Yoshida, N., Tamori, Y., Takai, E., Hirota, M., and Ogawa, M. 2004. Involvement of the mitogen-activated protein kinase kinase2 in the induction of cell dissociation in pancreatic cancer. *Int. J. Oncol. 24*:65–73.

Tan, X., Tamori, Y., Egami, H., Ishikawa, S., Kurizaki, T., Takai, E., Hirota, M., and Ogawa, M. 2004. Analysis of invasion-metastasis mechanism in pancreatic cancer: Involvement of tight junction transmembrane protein occludin and MEK/ERK signal transduction pathway in cancer cell dissociation. *Oncol. Rep. 11*: 993–998.

Torimura, T., Ueno, T., Kin, M., Harada, R., Nakamura, T., Kawaguchi, T., Harada, M., Kumashiro, R., Watanabe, H., Avraham, R., and Sata, M. 2001. Autocrine motility factor enhances hepatoma cell invasion across the basement membrane through activation of beta1 integrins. *Hepatology 34*:62–71.

Ueoka, Y., Kato, K., Kuriaki, Y., Horiuchi, S., Terao, Y., Nishida, J., Ueno, H., and Wake, N. 2000. Hepatocyte growth factor modulates motility and invasiveness of ovarian carcinomas via Ras-mediated pathway. *Br. J. Cancer 82*:89l–899.

Walter, K. 2000. Meaningful relationships: The regulation of the Ras/Raf/MEK/ERK pathway by protein interactions. *Biochem. J. 351*:289–305.

Index

D

E

F

G

H

N

Q

R

U

V

W

X

Z